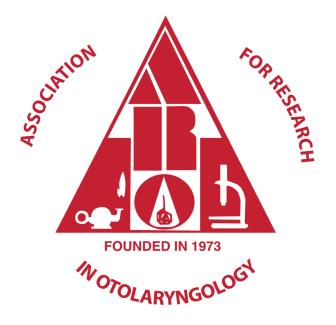
ABSTRACTS OF THE THIRTY-FOURTH ANNUAL MIDWINTER RESEARCH MEETING

ASSOCIATION FOR RESEARCH IN OTOLARYNGOLOGY



February 19 – 23, 2011 The Baltimore Marriott Waterfront Hotel Baltimore, Maryland, USA

Abstracts of the Thirty- Fourth Annual MIDWINTER Research Meeting of the

Association for Research in Otolaryngology

February 19 - 23, 2011

Baltimore, Maryland, USA

Peter A. Santi, PhD Editor

Association for Research in Otolaryngology 19 Mantua Road, Mt. Royal, NJ 08061 USA

CONFERENCE OBJECTIVES

After attending the Scientific Meeting participants should be better able to:

- 1. Understand current concepts of the function of normal and diseased ears and other head and neck structures.
- 2. Understand current controversies in research methods and findings that bear on this understanding.
- Understand what are considered to be the key research questions and promising areas of research in otolaryngology.

ISSN-0742-3152

The Abstracts of the Association for Research in Otolaryngology is published annually and consists of abstracts presented at the Annual MidWinter Research Meeting. A limited number of copies of this CD and previous books of abstracts (1978-2010) are available.

> Please address your order or inquiry to: Association for Research in Otolaryngology 19 Mantua Road Mt. Royal, NJ 08061 USA

> General Inquiry Phone (856) 423-0041 Fax (856) 423-3420 E-Mail: headquarters@aro.org

Meetings E-Mail: meetings@aro.org

This book was prepared from abstracts that were entered electronically by the authors. Authors submitted abstracts over the World Wide Web using Mira Digital Publishing's PaperCutterTM Online Abstract Management System. Any mistakes in spelling and grammar in the abstracts are the responsibility of the authors. The Program Committee performed the difficult task of reviewing and organizing the abstracts into sessions. The Program Committee Chair, Dr. Sharon Kujawa and the President, Dr. Karen Avraham constructed the final program. Mira electronically scheduled the abstracts and prepared Adobe Acrobat pdf files of the Program and Abstract Books. These abstracts and previous years' abstracts are available at: http://www.aro.org.

Citation of these abstracts in publications should be as follows: Authors, year, title, Assoc. Res. Otolaryngol. Abs.: page number.

For Example: Robert V. Shannon, 2011, Ear and Brain: Cochlear Implant Lessons for Hearing, House Ear Institute. Abs.: **775.**



General Chair Karen B. Avraham, PhD (2010-2011)

Program Organizing Committee

Sharon G. Kujawa, PhD, *Chair* (3/08-2/11) Steve D.M. Brown, PhD (3/10-2/13) M. Patrick Feeney, PhD (3/08-2/11) Stefan Heller, PhD (3/10-2/13) Keiko Hirose, MD (3/10-2/13) Jeffrey R. Holt, PhD (3/09-2/12) Bohua Hu, PhD (3/09-2/12) Douglas Oliver, PhD (3/10-2/13) Kenna D. Peusner, PhD (3/08-2/11) Alec N. Salt, PhD (3/08-2/11) Russell L. Snyder, PhD (3/08-2/11) Mitchell Steinschneider, MD, PhD (3/08-2/11) Jeremy Gene Turner, PhD (3/09-2/12) *Council Liaison:* Sharon G. Kujawa, PhD (3/08-2/11) spARO Representative: Thomas Welch

Program Publications

Peter A. Santi, PhD, Editor (2009-2012)

Animal Research Committee Rickie R. Davis, PhD, *Chair* (3/10-2/13) Kumar N. Alagramam, PhD (3/09-2/12) Byung Yoon Choi, MD, PhD (3/09-2/12) Yale E. Cohen, PhD (3/08-2/11) Robert Keith Duncan, PhD (3/08-2/11) Charles A. Miller, PhD (3/09-2/12) Suhrud M. Rajguru, PhD (3/10-2/13) Saima Riazuddin, PhD (3/10-2/13) Isabelle C. Roux, PhD (3/08-2/11) *Council Liaison:* Peter A. Santi, PhD (3/10-2/11) spARO Representative: Ann Hickox

Award of Merit Committee

M. Charles Liberman, PhD, *Chair* (3/10-2/13) Judy R. Dubno, PhD (3/10-2/13) Robert D. Frisina, PhD (3/09-2/12) Peter G. Gillespie, PhD (3/10-2/13) Edwin Rubel, PhD (3/08-2/11) Robert V. Shannon, PhD (3/10-2/13) Karen Steel, PhD (3/08-2/11) *Council Liaison*: David J. Lim, MD (3/10-2/11)

Diversity & Minority Affairs Committee

Howard W. Francis, *Chair* (3/10-2/13) Shaum P. Bhagat, PhD (3/08-2/11) Catherine E. Carr, PhD (3/09-2/12) Avril Genene Holt, PhD (3/08-2/11) Diana I. Lurie, PhD (3/09-2/12) Raju Metherate, PhD (3/10-2/13) Neeliyath A. Ramakrishnan, PhD (3/10-2/13) Xiaorui Shi, MD, PhD (3/10-2/13) *Council Liaison*: Dan H. Sanes, PhD (3/10-2/11) *spARO Representative:* Yoojin Chung, PhD

External Relations Committee

Maureen Hannley, PhD, *Chair* (3/09-2/12) Anne E. Luebke, PhD, *Chair* (3/08-2/11) Gregory I. Frolenkov, PhD (3/08-2/11) David Z.Z. He, MD, PhD (3/08-2/11) Cornelis Jan Kros, MD, PhD (3/08-2/11) Anna Lysakowski, PhD (3/08-2/11) Sunil Puria, PhD (3/08-2/11) Elba E. Serrano, PhD (3/08-2/11) Robert K. Shepherd, PhD (3/08-2/11) Mario A. Svirsky, PhD (3/10-2/13) spARO Representative: Adrian KC Lee

Finance Committee

Dennis R. Trune, PhD, MBA, *Chair* (3/10-2/13) Steven Wan Cheung, MD (3/10-2/13) Karen Jo Doyle, MD, PhD (3/10-2/13) Jean Luc Puel, PhD (3/10-2/13)

International Committee

David McAlpine, *Chair* (3/08-2/11) Joong Ho Ahn, MD, PhD, Korea (3/09-2/12) Deniz Baskent, PhD, Netherlands (3/10-2/13) Kathleen E. Cullen, PhD, Canada (3/08-2/11) James Fallon, PhD, Australia (3/10-2/13) W. Wiktor Jedrzejczak, Poland (3/10-2/13) Seiji Kakehata, MD, PhD, Japan (3/08-2/11) Khalid M. Khan, PhD, Kuwait (3/09-2/12) Goran Laurell, MD, Sweden (3/10-2/13) Hannes Maier, Germany (3/08-2/11) Rodrigo Martinez Monedero, MD, Spain (3/09-2/12) Xiaoqin Wang, PhD, USA (3/08-2/11) Azel Zine, PhD, France (3/10-2/13) *Council Liaison:* David McAlpine (3/08-2/11) spARO Representative: Simon Jones, PhD

JARO Editorial Board

Ruth Anne Eatock, PhD, Editor-in-Chief (2006-2011) Karen B. Avraham, PhD (2008-2011) Robert P. Carlyon, PhD (2010-2012) Laurel H. Carney, PhD (2010-2013) Nigel P. Cooper, PhD (2010-2013) Charles C. Della Santina, MD, PhD (2009-2012) Didier Dulon, PhD (2007-2010) Stefan Heller, PhD (2009-2012) John C. Middlebrooks, PhD (2009-2012) Jennifer Melcher, PhD (2010-2013) Tobias Moser, MD (2009-2012) Cythia F. Moss, PhD (2009-2012) Sunil Puria, PhD (2010-2013) Anthony J. Ricci, PhD (2010-2013) Barbara G. Shinn-Cunningham, PhD (2009-2012) Laurence O. Trussell, PhD (2009-2012)

Long Range Planning Committee

Dan H. Sanes, PhD, *Chair* (3/08-2/11) Carey D. Balaban, PhD (3/09-2/12) Maryline Beurg, PhD (3/08-2/11) Karina S. Cramer, PhD (3/10-2/13) Charley C. Della Santina, MD, PhD (3/09-2/12) Michael Anne Gratton, PhD (3/09-2/12) Andrej Kral, MD, PhD (3/10-2/13) Tobias Moser, MD (3/10-2/13) Bernd H. Sokolowski, PhD (3/08-2/11) Amy Donahue, PhD - *NIDCD Rep. Council Liaison:* Debra L. Tucci, MD (3/10-2/11) Chair, International Cmte: David McAlpine (3/08-2/11) spARO Representative: Jasmine M. Grimsley, PhD

Membership Committee

Virginia M. Richards, PhD, *Chair* (3/08-2/11) Colleen Le Prell, PhD (3/09-2/12) Stephane F. Maison, PhD (3/09-2/12) Mitsuya Suzuki, MD (3/09-2/12) *spARO Representative:* Jazz Bailey, PhD

Nominating Committee

Steven D. Rauch, MD, *Chair* (10-11) Didier Dulon, PhD (10-11) Ruth Anne Eatock, PhD (10-11) Yehoash Raphael, PhD (10-11) Jay T. Rubinstein, MD, PhD (10-11)

Publications Committee

Anil K. Lalwani, MD, Chair (3/10-2/13) Catherine E. Carr, PhD (3/08-2/11) Ana Belen Elgoyhen, PhD (3/09-2/12) Paul A. Fuchs, PhD (3/10-2/13) John J. Galvin (3/09-2/12) Clifford R. Hume, MD, PhD (3/08-2/11) Philip X. Joris, MD, PhD (3/10-2/13) Paul B. Manis. PhD (3/10-2/13) Elizabeth S. Olson, PhD (3/10-2/13) Alan R. Palmer, PhD (3/10-2/13) Doris Kar-Wah Wu, PhD (3/09-2/12) Eric D. Young, PhD (3/08-2/11) JARO Editor: Ruth Anne Eatock, PhD, ex officio JARO Editor: Paul B. Manis, PhD, ex officio Springer Representative: Ann Avouris, ex officio Secretary/Treasurer: Karen Jo Doyle, MD, PhD, ex officio Council Liaison: Peter A. Santi, PhD (3/10-2/11) spARO Representative: Stephen David, PhD

Travel Awards

Marlan R. Hansen, MD, Chair (3/08-2/11) Zubair M. Ahmed, PhD (3/09-2/12) Jong Woo Chung, MD (3/08-2/11) Ronna P. Hertzano, MD, PhD (3/10-2/13) Karl Kandler, PhD (3/08-2/11) Simone Kurt, PhD (3/09-2/12) Daniel Lee, MD (3/09-2/12) Ivan A. Lopez, PhD (3/08-2/11) Yunxia Wang Lundberg, PhD (3/08-2/11) Anh Nguyen-Huynh, MD, PhD (3/09-2/12) Shu-Chen Peng, PhD (3/09-2/12) Pamela Carol Roehm, MD, PhD (3/08-2/11) Alec N. Salt, PhD (3/09-2/12) Alexander A. Spector, PhD (3/10-2/13) James F. Battey, MD, PhD, NIDCD Dir ex-officio Maureen Hannley, PhD, Exec VP Rsch, ex officio spARO Representative: Judith S. Kempfle, MD

President's Message 2011

Welcome back to the East Coast! It's wonderful to be back to the Baltimore Marriott Waterfront at the Inner Harbor for the 34th Annual MidWinter Meeting of the Association for Research in Otolaryngology. The latest research and translation to the clinic will be covered in symposiums, workshops, podium and poster sessions over a period of five days. We will open the meeting with the Presidential Symposium on "Genomics and its Impact on Otolaryngology" with presentations by some of our most esteemed and favorite ARO members, and non-ARO members who are leaders in the genomics field. The Welcome Get-Together will be sponsored by Springer and for the rest of the meeting, symposium and podium sessions abound, with poster sessions remaining a highlight of ARO to spend as much time as needed to talk about results in a relaxed setting. Please join us at the ARO Business Meeting on Sunday early evening, where an update of ARO events, honors and plans for the future will be discussed. This is an opportunity to be part of this wonderful organization and play a role in its activities. An added bonus will be the scavenger hunt, where we'll be giving away an iPad, iPod Touch, iPod Nano, iPod Shuffle, Flip Video, and AMEX gift cards.

We have an exciting list of **symposiums** including: Development, Trafficking, Function and Plasticity; Prosthetic Stimulation of the Vestibular System; Molecular Regulation of Primary Sensory Cell Development; Progress and



Challenges in Implantable Auditory Prostheses: Lessons Learned from Psychophysics, Physiology and Engineering; From Synaptic Potentials to Spikes: In vivo Whole-cell Recordings in the Auditory System; Presbycusis - From Animal Models to Human Perceptual Deficits; Developmental Plasticity of the Central Auditory System: Mechanisms and Molecules; Biological Imaging in Otolaryngology: Yesterday, Today and Tomorrow; Hearing and Communication in the Global Village; and The Auditory Brain Beyond A1. Remember to submit your proposals for symposiums for ARO 2012. **Podium sessions** will include Regeneration; From Normal to Aberrant Sound Processing; Inner Ear Hair Cells: From Bundle to Synapse; Ototoxicity: Mechanisms and Protection; Genetics; Development; and Making Sense of Ambiguous Auditory Patterns. Last but not least, a number of **workshops** will provide us with the latest technology and experimental techniques in our field: Cell Type-Specific Studies Using Fluorescent Activated Cell Sorting in Neuro-Epithelia; Photonics of the Auditory and Vestibular Systems; and Research Techniques & Approaches 101, as well as on Training/Career Development and an Early Stage/New Investigator workshop.

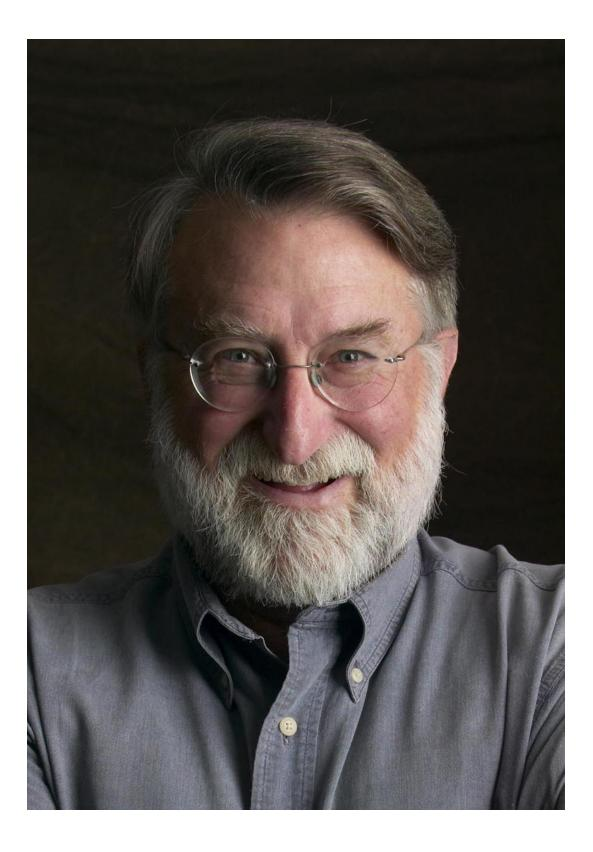
Join us for the **Presidential Lecture and Awards Ceremony** to honor the Award of Merit winner, Robert V. Shannon, on Ear and Brain: Cochlear Implant Lessons for Hearing, where we will hear about his career from Fan-Gang Zeng and Monita Chatterjee, followed by the **Awards and Honors Reception**. We have **special events** that include an exhibit of the Celebration of the 50th Anniversary of Bekesy Nobel Prize. Graduate students and post-docs – don't forget to attend the spARO Town Hall and be part of this group and learn more about their activities at ARO.

So many people are involved to make ARO the wonderful organization that it is and for an excellent meeting. A special thanks goes to Talley Management, for their superb running of the meeting. Our many committee members make ARO 'tick' and we thank you for your efforts, both during the year and at the meeting. We will part from Ruth-Anne Eatock as JARO editor and introduce our new editor, Paul Manis. We are thankful to AAO-HNSF, DRF, AAAF and the CORLAS-US group for their donations to allow more students and fellows to attend the meeting with travel funds, the exhibitors for helping support the many activities of the meeting, and for the NIH-NIDCD for making the meeting possible.

And when you're hungry or find some free time, Little Italy and Fell's Point are not far away and the Inner Harbor, a short walk from the hotel, is full of restaurants and shops. During the breaks, the National Aquarium, American Visionary Arts Museum and the Science Center are just around the corner. We will part before the closing session, dancing away at the Hair Ball with the Radiant Band, who were a huge hit two years ago. Bring your dancing shoes and watch your colleagues in another mode.

There are yet more events and we continue to want your input to make the ARO MidWinter the best possible, and scientifically crucial, meeting of the year. This meeting gives us the opportunity to be exposed to the cutting-edge research being performed in our field, interact with our colleagues, and meet old and new friends. ARO goes beyond the meeting to have its own journal, JARO, the leading journal in the subject category Otorhinolaryngology, and we encourage you to continue to send your exciting results for submission. And finally, be sure to check out our revised Web site, a resource throughout the year that continues to grow with your input. I thank you for giving me the opportunity to chair my absolute favorite meeting of the year and for the privilege to have led this organization for a term.

Karen B. Avraham President



Robert V. Shannon 2011 Award of Merit Recipient

Robert V. Shannon

2011 Recipient of the Award of Merit

Bob Shannon needs no introduction to the ARO community. In his 35-odd years as an auditory researcher, he has contributed enormously to the field, not only by advancing the science, but also – uniquely – by enhancing its soul. We take great pleasure in celebrating this singular individual, his life in research, and his many accomplishments.

Bob's life in auditory research began when he entered David Green's lab at the University of California (UC), San Diego as a shy young graduate student with a strong background in mathematics and psychology. By his own account, he was in awe of Dave and the post docs in the lab – Neal Viemeister, Walt Jesteadt, and Bill Yost, to name a few. Bob trained in auditory psychophysics and his PhD dissertation was on psychophysical measures of cochlear two-tone suppression. He went on to do post-doctoral work with Tammo Houtgast at the Institute for Perception TNO, in Soesterberg, Netherlands and additionally with Richard Thompson at the Department of Psychobiology, UC Irvine.

In 1978, Bob joined Michael Merzenich's group at UC San Francisco and began working on electrical stimulation of the deaf auditory system. During this time and his years as Cochlear Implant Co-ordinator at Boys Town National Research Hospital, Bob conducted seminal studies on characterizing basic processing of electrical stimulation – channel interaction, loudness and pitch coding, forward masking, gap detection, and amplitude modulation detection. These classical studies, conducted in the infancy of cochlear implant research, have significantly advanced our understanding of both normal and impaired auditory processing. While at Boys Town, Bob managed to reverse-engineer one of the commercial devices and reported on how to send controlled electrical pulses to the implanted electrode array. This report made it possible a "research interface" that would allow accurate stimulus control for rigorous psychophysical experiments with electric stimulation. Using this research interface and a portable computer, Bob, "the travelling psycho-electrician," has revolutionized the way that cochlear implant research was done by being able to test patients under controlled conditions anytime and anywhere from rural Utah to cosmopolitan Rome.

In 1990, Bob moved to the House Ear Institute to head the Cochlear Implant research department there. Soon, he recruited Fan-Gang Zeng, who had just completed his PhD with Chris Turner at Syracuse University, as post-doc. Their mutual discussions resulted in the development of a method to acoustically simulate the speech transmitted by a cochlear implant processor. Their noise-band vocoding work (Shannon et al., 1995, Speech recognition with primarily temporal cues. Science 270, 303-304) provided not only a way to simulate cochlear implant processing, but also found diverse applications as an elegant way to independently control the spectral and temporal-envelope information in speech. This study underscored the robustness of the human auditory system to severe degradations in speech, and paved the way for many revealing experiments conducted both by members of the Shannon and Zeng labs (most notably by Qian-Jie Fu, who trained with both, and his students) but also by other investigators world-wide. The original Shannon et al. Science paper has been cited 800 times in the 15 years since its publication, a remarkable feat in a relatively small field of research.

In addition to cochlear implants, Bob has collaborated with Derald Brackmann and William Hitselberger at House Ear Clinic, Jean Moore of House Ear Institute and Douglas McCreery at the Huntington Medical Research Institute in Pasadena CA to develop an Auditory Brainstem Implant (ABI) and a Penetrating ABI, devices which restore hearing to patients who don't have a functional auditory nerve. These devices have been of particular benefit to patients who suffer from Neurofibromatosis 2 (NF2) and have poor quality of life in addition to the problems associated with acoustic neuromas. The ABI has now been implanted in over 500 patients world-wide. In recent years, Bob has been involved with evaluation of the ABI in patients who do not have acoustic neuromas, and expanded his research horizon to include Auditory Midbrain Implants and retinal implants. He is always excited about science, always happy to be doing it, and always enthused about the newest idea that captures his imagination.

One of Bob's most important contributions to the field has been the training of graduate students and post-docs. Bob has always emphasized and encouraged independence, and those of us (e.g., Fan-Gang Zeng, Monita Chatterjee, Qian-Jie Fu, Deniz Baskent, John Galvin, Lendra Friesen, David Landsberger, Arthi Srinivasan) who have trained in his lab benefited greatly from this approach. The training did not just involve science, but as in all great labs, we learned a great deal about the process of science – the integrity that is critical to the success of research, the duty to publish federally-funded work, the importance of social interactions among scientists, and service to not only the professional community but the society and humanity in general.

The self-deprecating warmth and generosity which are a hallmark of Bob's unique personality, have endeared him to the entire community, from grateful patients to crusty senior scientists and graduate students attending their first conference. He is the center and the soul of all our conferences, radiating kindness and humor, organizing the social gatherings, making sure to have tremendous fun in every endeavor. A final distinctive feature of Bob's life in research is his strong connection to patients and their families. He is genuinely interested in helping improve their experience with the implant

and ultimately the quality of their lives. Bob has a rare ability to interact with patients and research subjects, with many of them becoming lifelong friends, and in their turn, making lasting and valuable contributions to research in his and other investigators' laboratories.

Bob has received numerous awards and honors, and is sure to receive many more in his life as a scientist. We know, however, that ARO has always been his scientific home, and that this award delights him in a very special way. We take equal delight in celebrating this award with him, and look forward to many more years of great science and interaction from this most wonderful colleague, mentor, and friend.

MONITA CHATTERJEE and FAN-GANG ZENG

Association for Research in Otolaryngology

Executive Offices 19 Mantua Road • Mt. Royal, New Jersey 08061 Phone: (856) 423-0041 • Fax: (856) 423-3420 Email: meetings@aro.org

ARO Officers for 2010-2011

President: Karen B. Avraham, PhD (2010-2011)

Tel Aviv University, Sackler School of Medicine Dept. of Human Molecular Genetics & Biochemistry Ramat Aviv Tel Aviv 69978, Israel

President Elect: Debara L. Tucci, MD (2010-2011) Duke University Medical Center Division of Otolaryngology-HNS Durham, NC 27710

Past President: Steven Rauch, MD (2010-2011) Harvard Medical School Massachusetts Eye & Ear Infirmary 243 Charles Street Boston, MA 02114

Secretary/Treasurer: Karen Jo Doyle, MD, PhD (2008-2011) University of California, Davis 6392 Harmon Drive Sacramento, CA 95831

Editor: Peter A. Santi, PhD (2009-2012) University of Minnesota Dept. of Otolaryngology Lions Research Building, Room 121 2001 Sixth Street, SE Minneapolis, MN 55455

Historian: David J. Lim, MD (1996-2012) House Ear Institute 2100 W. Third Street, Fifth Floor Los Angeles, CA 90057

Council Members

Jay T. Rubinstein, MD (2008-2011)

Virginia Merrill Bloedel Hearing Research Center University of Washington Box 357923 Seattle, WA 98195 Robin L. Davis, PhD (2009-2012) Rutgers University Cell Biology & Neuroscience 604 Allison Road

Piscataway, NJ 08854-8082

Dan H. Sanes, PhD (2010-2013) New York University Center for Neural Science 4 Washington Place New York, NY 10003

Association for Research in Otolaryngology

Executive Offices 19 Mantua Road, Mt. Royal, NJ 08061 USA Phone: (856) 423-0041 Fax: (856) 423-3420 E-Mail: headquarters@aro.org Meetings E-mail: meetings@aro.org

Past Presidents

1973-74 David L. Hilding, MD 1974-75 Jack Vernon, PhD 1975-76 Robert A. Butler, PhD 1976-77 David J. Lim, MD 1977-78 Vicente Honrubia, MD 1978-80 F. Owen Black, MD 1980-81 Barbara Bohne, PhD 1981-82 Robert H. Mathog, MD 1982-83 Josef M. Miller, PhD 1983-84 Maxwell Abramson, MD 1984-85 William C. Stebbins, PhD 1985-86 Robert J. Ruben, MD 1986-87 Donald W. Nielsen, PhD 1987-88 George A. Gates, MD 1988-89 William A. Yost, PhD 1989-90 Joseph B. Nadol, Jr., MD 1990-91 Ilsa R. Schwartz, PhD 1991-92 Jeffrey P. Harris, MD, PhD 1992-93 Peter Dallos, PhD 1993-94 Robert A. Dobie, MD 1994-95 Allen F. Ryan, PhD 1995-96 Bruce J. Gantz, MD 1996-97 M. Charles Liberman, PhD 1997-98 Leonard P. Rybak, MD, PhD 1998-99 Edwin W. Rubel, PhD 1999-00 Richard A. Chole, MD, PhD 2000-01 Judy R. Dubno, PhD 2001-02 Richard T. Miyamoto, MD 2002-03 Donata Oertel, PhD 2003-04 Edwin M. Monsell, MD, PhD 2004-05 William E. Brownell, PhD 2005-06 Lloyd B. Minor, MD Robert V. Shannon, PhD 2006-07 2007-08 P. Ashley Wackym, MD 2008-09 Paul A. Fuchs, PhD 2009-10 Steven Rauch, MD

Award of Merit Recipients

1978	Harold Schuknecht, MD
1979	Merle Lawrence, PhD
1980	Juergen Tonndorf, MD
1981	Catherine Smith, PhD
1982	Hallowell Davis, MD
1983	Ernest Glen Wever, PhD
1984	Teruzo Konishi, MD
1985	Joseph Hawkins, PhD
1986	Raphel Lorente de Nó, MD
1987	Jerzy E. Rose, MD
1988	Josef Zwislocki, PhD
1989	Åke Flóck, PhD
1990	Robert Kimura, PhD
1991	William D. Neff, PhD
1992	Jan Wersäll, PhD
1993	David Lim, MD
1994	Peter Dallos, PhD
1995	Kirsten Osen, MD
1996	Ruediger Thalmann, MD & Isolde Thalmann, PhD
1997	Jay Goldberg, PhD
1998	Robert Galambos, MD, PhD
1999	Murray B. Sachs, PhD
2000	David M. Green, PhD
2001	William S. Rhode, PhD
2002	A. James Hudspeth, MD, PhD
2003	David T. Kemp, PhD
2004	Donata Oertel, PhD
2005	Edwin W. Rubel, PhD
2006	Robert Fettiplace, PhD
2007	Eric D. Young, PhD
2008	Brian C. J. Moore, PhD
2009	M. Charles Liberman, PhD
2010	Professor Ian Russell
2011	Robert V. Shannon, PhD

ARO Abstracts

Table of Contents

Abstract Number

Presidential Symposiu	im second se	
A:	Presidential Symposium: Genomics and its Impact in Otolaryngology	1-6
Symposium		
В:	Amino Acid Transmitter Receptors: Development, Trafficking, Function and Plasticity	7-13
Podium		
C :	Regeneration I	14-26
Exhibit: Celebration of	the 50th Anniversary of Bekesy Nobel Prize	27-29
Poster		
D1:	Development I	30-43
D2:	External & Middle Ear Mechanics	44-56
D3:	External & Middle Ear Mechanics: Pathology	57-64
D4:	Outer Hair Cells & Prestin	65-83
D5:	Inner Ear Hair Cells: Mechanics and Models I	84-95
D6:	Otoacoustic Emissions I	96-107
D7:	Inner Ear Physiology I	108-125
D8:	Inner Ear: Genetic Pathology	126-139
D9:	Aging	140-154
D10:	Tinnitus	155-168
D11:	Auditory Cortex and Thalamus: Physiology	169-178
D12:	Relating Physiological Processes to Perception	179-186
D13:	Perception with Hearing Loss and Other Challenges	187-197
D14:	Auditory Prosthesis: Modeling & Simulations	198-205
D15:	Auditory Prosthesis: Optimizing Methods	206-216
D16:	Clinical Audiology I	217-230
D17:	Clinical Otolaryngology	231-242
D18:	Vestibular Receptors	243-256
NIDCD Workshops		
E:	Training/Career Development Workshop	
	Early Stage/New Investigator Workshop	
	Dissemination of Resources Derived from NIDCD Grants	
Symposium		
F:	Prosthetic Stimulation of the Vestibular System	259-269
Symposium		
G:	Molecular Regulation of Primary Sensory Cell Development	270-276
Podium		
H:	From Normal to Aberrant Sound Processing	277-291
Symposium		
l:	Progress and Challenges in Implantable Auditory Prostheses: Lessons Learned from Psychophysics, Physiology and Engineering	292-298
Symposium		
J:	From Synaptic Potentials to Spikes: In vivo Whole-cell Recordings in the Auditory System.	299-303
Workshop		
К:	Workshop: Cell Type-Specific Studies Using Fluorescent Activated Cell Sorting in Neuro-Epithelia	304-310
Poster		
L1:	Development II	311-324
L2:	Genetics I	
L3:	Otitis Media	334-343
L4:	Inner Ear Hair Cells: Transduction	344-356
L5:	Inner Ear: Mechanics and Models II	357-367
L6:	Otoacoustic Emissions II	368-378

Table of Contents

L7:	Inner Ear: Clinical Pathology	
L8:	Inner Ear: Damage	
L9:	Acoustic Trauma: Mechanisms	
L10:	Auditory Nerve I	
L11:	Cochlear Nucleus I	
L12:	Midbrain I	
L13:	Auditory Cortex and Thalamus: Pathophysiology	
L14:	Physiological Encoding of Spatial Cues	
L15:	Psychophysics: Loudness, Pitch, and More	
L16:	Auditory Prosthesis: Optical Stimulation	
L17:	Auditory Prosthesis: Bilateral Stimulation	
L18:	Clinical Vestibular	
Symposium		
M:	Presbycusis - From Animal Models to Human Perceptual Deficits	
Symposium		
N:	Developmental Plasticity of the Central Auditory System: Mechanisms and Mo	lecules 529-534
Workshop		
0:	Workshop: Photonics of the Auditory and Vestibular Systems	
Symposium		
P:	Biological Imaging in Otolaryngology: Yesterday, Today and Tomorrow	
Podium		
Q:	Inner Ear Hair Cells: From Bundle to Synapse	
Poster		
R1:	Inner Ear Hair Cells: Channels & Pumps	
R2:	Inner Ear Hair Cells: Synapses	
R3:	Regeneration Poster II	
R4:	Inner Ear Physiology II	
R5:	Ototoxicity: Mechanisms	
R6:	Prevention and Treatment Strategies	
R7:	Acoustic Trauma: Prevention	
R8:	Auditory Nerve II	
R9:	Cochlear Nucleus II	
R10:	Auditory Pathways: Brainstem - Superior Olive I	
R10:	Midbrain II	
R12:	Auditory Cortex and Thalamus: Plasticity	
R12:	Auditory Cortex and Thalamus: Flashcity	
R13:	Learning to Localize Sound.	
R15:	Auditory Prosthesis: Cognitive Effects	
R15:	Speech: Coding Strategies	
R10.	Clinical Audiology II	
R18:	Vestibular Afferents and CNS	
-	e and Awards Ceremony	
S:	Ear and Brain: Cochlear Implant Lessons for Hearing	775
S. Symposium	Ear and Brain. Cochiear implant Lessons for Hearing	
T:	Hearing and Communication in the Global Village	776 700
r. Podium	Hearing and Communication in the Global Village	
U:	Ototoxicity: Mechanisms and Protection	703 705
-	סנסנסגוכונץ. ואפטומווזסווזס מווע דוטנפטוטוו	
Workshop V:	Workshop: Research Techniques & Approaches 101	706 707
	איטוגאוטף. הפשמוכוו ופכווווענפט מ אףטוטמכוופט וטו	
Symposium W:	The Auditory Prain Payand A1	706 004
ARO Abstracts	The Auditory Brain Beyond A1 xii	Volume 34, 2011
		· ····· · · · · · · · · · · · · · · ·

Table of Contents

Podium		
X :	Genetics	16
Poster		
Y1:	Inner Ear Hair Cells: Genetics	26
Y2:	Inner Ear: Hair Cells: Life & Death827-8	36
Y3:	Regeneration Poster III	51
Y4:	Inner Ear Fluids I	37
Y5:	Cochlear Nucleus III	75
Y6:	Auditory Pathways: Brainstem - Superior Olive II) 0
Y7:	Midbrain III	98
Y8:	Ototoxicity: Prevention)5
Y9:	Hearing Loss	14
Y10:	ABR, FFR, & MRI	25
Y11:	Auditory Cortex and Thalamus: Circuitry	35
Y12:	Auditory Cortex and Thalamus: Complex Sound Processing	14
Y13:	Auditory Prosthesis: Current Steering	17
Y14:	Spatial hearing: The Precedence Effect and Beyond948-9	58
Y15:	Perception with Cochlear Implants959-9	37
Y16:	Understanding Complex Signals in Complex Scenes	33
Y17:	Speech - Cognitive Effects) 0
Y18:	Vestibular Behavior)8
Podium		
Z :	Development III	23
Podium		
AA:	Making Sense of Ambiguous Auditory Patterns	38

1 Genes and Deafness

James Battey, Jr.¹

¹National Institute on Deafness and Other Communication Disorders (NIDCD)

Dr. Battev will discuss some of the major breakthroughs in the area of genetic research since the launch of the Human Genome Project in 1990. He will explain how these breakthroughs have advanced research in hereditary hearing impairment, showing the audience how NIDCD scientists have used linkage analysis to map single gene disorders. He will discuss the importance of knockout mice, and explain how scientists plan to continue using them in new ways to advance our understanding of genetic inheritance and hearing impairment. Finally, Dr. Battey will introduce the genome-wide association studies (GWAS), designed to identify common genetic factors that influence health and disease. He will explain how GWAS are helping us understand genetically complex disorders within NIDCD's Mission, including specific language impairment, autism, and presbycusis.

2 Mechanosensory Transduction: The View from a Worm's Ear Martin Chalfie¹

¹Columbia University

The senses that allow us to touch, hear, detect acceleration, and determine body position all respond to mechanical signals. In contrast to senses such as vision, taste, and smell where the molecules that detect the sensory signals are known, the proteins underlying the mechanical senses in humans are still a mystery. For several years we have used genetics, particularly the ability to find mutants that are insensitive to gentle touch in the small round worm Caenorhabditis elegans, to find the elusive genes that encode proteins needed for mechanosensation in a set of neurons called the touch receptor neurons. Some genes are needed for the specification and differentiation of the touch receptor neurons. Others are needed for the function of these cells. We now know that the proteins encoded by several of these later genes form a membrane sensor for touch, the first such transducer to be found in any mechanosensory neuron. The sensor is quite complex, involving at least six proteins and affected by the lipid composition of the associated membrane. In addition, recent methods developed in my lab have allowed us to identify several new genes whose products appear to modulate touch sensitivity.

3 Mouse Genetics and Otolaryngology Karen Steel¹

¹Wellcome Trust Sanger Institute

Mouse mutants with hearing impairment have played a key role in understanding the molecular basis of hearing and deafness, and they continue to surprise us. Identification of the genes underlying deafness started with the collection of spontaneous mutations arising throughout the last century, mostly detected by their associated vestibular dysfunction leading to head bobbing and circling. Investigation of the effects of radiation on DNA led to further mutations affecting hearing.

However, it soon became clear that deafness was an extremely heterogeneous disorder with many genes involved in both human and mouse, and that further deaf mouse mutants could lead to more candidate genes for deafness in humans. Chemical mutagenesis using Nethyl-N-nitrosourea (ENU) was employed to create single base changes randomly in the DNA of mouse spermatogonia, and the resulting offspring were screened for dominantly-inherited deafness using the Preyer reflex. In a pan-European collaboration, we identified by positional cloning 23 of the resulting mutations in mutant lines with deafness and/or balance defects, affecting 12 genes in total. In parallel we characterised their phenotypes and found a wide range of developmental defects affecting the ear. Of the 12 genes, four were already known to be involved in deafness, four represented the first mouse mutants described for the gene, and four of the mutations identified a previously unknown role in deafness for known genes.

The NIH-funded KOMP and EC-funded EUCOMM programmes are generating large numbers of targeted ES cells, and over 7000 genes are currently available. As part of the Sanger Institute's Mouse Genetics Programme, we have used these ES cells to generate over 300 new mouse mutant lines and screened them for many disease features including hearing impairment at 14 weeks old using ABR. This screen is revealing unexpected genes involved in auditory function, and has the advantage that we know the gene involved before we start. One mutant has a severe hearing impairment, two have raised thresholds at high frequencies only, several show mild or moderate hearing impairment across all frequencies, two have highly variable thresholds amongst the mutant group, and others show normal thresholds but reduced amplitudes of response. These all represent new candidate genes for involvement in deafness in humans, including mild and moderate hearing loss.

Funded by the Wellcome Trust, MRC, EC and DRUK.

4 Rare and Common Variants in Human Genetics

David B. Goldstein¹

¹Center for Human Genome Variation Duke University There are now hundreds of confirmed common variants that associate with risk of common diseases, responses to infection, and responses to drugs. In the case of drug responses there are examples of strong effects of common variants, while for most common diseases effect sizes have proven small and it has been difficult to identify the causal variants.

Here I first contrast human traits that are and are not strongly influenced by common variants. I next review the role of rare copy number variants in schizophrenia and epilepsy and outline a framework for discovery of other kinds of rare high penetrant risk factors focusing on whole genome sequencing and evaluation of candidate variants through a combination of a) testing for cosegregation in multiplex families, b) bioinformatic analyses, and c) frequency comparison in large case control cohorts. Finally, I discuss what I see as the near term opportunities for discovery genetics for both disease predisposition and drug response.

5 Genomic Analysis of Inherited Hearing Loss: A Success Story of the Human Genome Project and an Emerging Example of Personalized Genomic Medicine Mary-Claire King¹

¹University of Washington

Discovery and characterization of the genes responsible for inherited hearing loss represents one of the most successful applications of the Human Genome Project to In this presentation, I will first biomedical research. address why genomic analysis of hearing loss has been so remarkably successful. I will focus on the roles of the phenotype itself, of family structure and the involvement of communities. interdisciplinary families and of collaborations, and of leadership in national and international scientific administration. Then I will ask how this success can be exploited for the future of hearing research and treatment of hearing loss. What results from genomics are poised now for application? What applications can we anticipate in the longer term? What more biology need we understand and technology need we develop to hasten applications to prevention and treatment of hearing loss?

6 The Evolving Management of Genetic Testing for Deafness and Its Impacts on Clinical Care Richard J. Smith¹

¹The University of Iowa

Deafness is an etiologically diverse condition that has major clinical, social and quality-of-life implications. In developed countries as the rate of acquired hearing loss secondary to environmental causes has decreased, the significance of genetic factors that lead to deafness has increased. One of the most dramatic changes over the past decade has been the ability to provide genetic testing for deafness to assist clinicians in their care of deaf and hard-of-hearing persons. This type of testing has impacted the practice of otolaryngology and has become integrated into clinical practice.

However, the extreme genetic heterogeneity of nonsyndromic hearing loss (NSHL) makes a gene-by-gene genetic testing strategy both expensive and time consuming using available methods. With the advent of targeted sequence capture and massively parallel sequencing strategies, it is now possible to interrogate all exons of all genes implicated in NSHL simultaneously. This concept has been validated and with multiplexing of samples, has made genetic testing for deafness very inexpensive.

Variants of this strategy can also be applied to massively parallel candidate gene screening to identify novel genetic causes of NSHL. This gene discovery initiative is an important requisite for personalized genomic medicine and mutation-specific therapies to treat hearing loss.

Early gene-therapy treatments are likely to target "easy-tocorrect" types of deafness with "simple-to-achieve" goals. An example would be a therapy to prevent progression of hearing loss in an adult segregating autosomal dominant NSHL that is predicted to progress to profound deafness based on genetic testing.

7 Introduction to Symposium on Amino Acid Transmitter Receptors Richard Altschuler¹

¹University of Michigan

This symposium will celebrate the memory of Dr. Robert Wenthold and his contributions as an innovator, colleague and mentor. It will focus on the areas of his interest in amino acid transmitters and their receptors, with presentations on Development, Function, Plasticity and Trafficking by leading experts in the auditory field and outside of the auditory field.

8 Glutamatergic Synapses in the Cochlear Nucleus, Do We Know All? Maria Rubio¹

¹University of Pittsburgh

Glutamate receptors mediate fast synaptic transmission in the central nervous system. In the auditory pathway, the response of auditory neurons to acoustic stimulation must accommodate rapid transmission and maximize temporal fidelity through their synaptic networks. Consistent with these demands is the observation that targets of the auditory nerve often express fast glutamate receptors in the cochlear nuclei. Hearing disorders affect auditory nerve activity and therefore the excitability of synaptic circuitries along the auditory pathway. But it is undetermined whether changes in afferent activity reorganizes auditory nerve synapses and whether or not it alters the expression and/or localization of glutamate receptors at the postsynaptic membrane. This is important considering that synapse size, and therefore the number and subunit composition of the glutamate receptor channel relate to the electrophysiological properties of the neuron. This paper will discuss different approaches to gain understanding of the anatomy and subunit composition of glutamatergic synapses in the cochlear nucleus during normal hearing and following hearing impairment.

Synaptic Transmission at Auditory Nerve Synapses in the Cochlear Nucleus Paul Manis¹

¹UNC Chapel Hill

This talk will focus on excitatory synaptic transmission at auditory nerve synapses in the cochlear nucleus. At this synapse, Bob Wenthold and his collaborators developed their evidence for glutamate as the transmitter, and elaborated much of our current understanding into the receptor subunit composition. I will put this body of work in it's historical context in both avian and mammalian systems, as well as with non-auditory synapses, and discuss the critical issues that surrounded the determination of the transmitter at that time. Finally, I will discuss subsequent work on the central auditory nerve synapses, the consequences of different kinds of hearing loss for synaptic function and possible subunit composition, and outline a number of unresolved issues.

10 Glycinergic Transmission and Cotransmission in the Auditory System

Larry Trussell¹, Pierre Apostolides¹, Yuil Kim¹, Michael Roberts¹

¹OHSU

Glycine is a major inhibitory neurotransmitter of the auditory brainstem. This conclusion derives from numerous studies beginning in the late 1970's-early 1980's, in large part from the work of Bob Wenthold. He and his colleagues developed high-quality antibodies to both the transmitter and its receptor and used these to describe the distribution of glycinergic neurons and provide evidence for some of the major glycinergic projections. The functional significance of these pathways has rightly been a subject of growing interest. Moreover, the role of GABA, another major area of Bob's early work, has also been of great interest, in part because the widespread of expression of GABA, often within glycinergic terminals, stands in contrast to the difficulty in detecting obvious GABAergic transmission . In this talk, I will focus on cartwheel cells, major glycinergic interneurons in the dorsal cochlear nucleus (DCN) which play an essential role in controlling the non-auditory input to the DCN. These cells are unique in the generation of a spike burst, termed the complex spike, which propagates both to nerve terminals and back into dendrites. At the terminals, these spikes trigger the release of glycine and GABA, which activate glycine and GABA-A receptors on fusiform and cartwheel cells. Physiological aspects of this transmission will be discussed.

11 Functional NMDA Receptors at Axonal Growth Cones of Young Hippocampal Neurons

Philip Y. Wang^{1,2}, Ronald S. Petralia², Ya-Xian Wang², Robert J. Wenthold², Stephan D. Brenowitz¹ ¹Section on Synaptic Transmission, NIDCD/NIH, ²Laboratory of Neurochemistry, NIDCD/NIH N methyl D aspartate recentor (NMDAP) function is crit

N-methyl D-aspartate receptor (NMDAR) function is critical to the development of the nervous system, though their roles at axonal growth cones remain enigmatic. We performed an examination of NMDAR localization and function at axonal growth cones of young hippocampal Our immunocytochemical data showed that neurons. native and transfected NMDAR subunits are expressed in axons and growth cones of young (days in vitro 4, DIV4) hippocampal rat neurons. Additionally, immunogold electron microscopy showed that NR1 is expressed in growth cones of postnatal day 2 (P2) rat hippocampus. Applying NMDAR agonists locally at growth cones in voltage clamped neurons induced an inward current that was inhibited by bath application of an NMDAR antagonist, DL-APV, indicating that these NMDAR are functional. In addition, calcium imaging experiments indicated that NMDARs present in growth cones mediate calcium influx. Voltage-sensitive calcium channel blockers or depletion of intracellular calcium stores had no significant effect on the calcium transients in growth cones induced by NMDA application, indicating that the observed calcium influx is primarily due to activation of NMDARs. Our findings show that functional NMDARs are targeted to axons and growth cones in young neurons, supporting their role in axonal guidance and synapse formation during neuronal development.

This work was supported by the NIDCD/NIH Intramural Research Program.

12 Molecular Mechanisms Regulating NMDA Receptor Trafficking Katherine Roche¹

¹NIH/NINDS

NMDA receptors play a critical role in neuronal development and synaptic plasticity. The subunit composition of NMDA receptors defines their functional properties and also regulates their trafficking and stabilization at synapses. NMDA receptors are tetramers composed of combinations of subunits (NR1, NR2A-D, NR3A-B). We have focused on the distinct regulation of the NR2 subunits and have shown that subunit-specific phosphorylation and protein-protein interactions regulate NMDA receptor expression at synapses. Specifically, we find that CK2 phosphorylates NR2B, but not NR2A, in response to synaptic activity. Phosphorylation of NR2B on S1480 by CK2 drives NR2B endocytosis and removal of NR2B from synapses resulting in an increase in synaptic NR2A expression. Furthermore, we identified an interplay between S1480 phosphorylation and phosphorylation of a critical tyrosine-based endocytic motif on NR2B (YEKL), providing a molecular mechanism for the observed effects of CK2 on NMDAR trafficking. During development there is an activity-dependent switch from NR2B to NR2A at cortical synapses. We also observe an increase in CK2 expression and NR2B phosphorylation over this same critical period and show that the acute activity-dependent switch in NR2 subunit composition at developing hippocampal synapses requires CK2 activity. Thus, CK2 plays a central role in determining the NR2 subunit content of synaptic NMDARs.

13 Regulation of Neurotransmitter Receptor Function and Synaptic Plasticity in the Brain Richard Huganir¹

¹Johns Hopkins University/HHMI

Neurotransmitter receptors mediate signal transduction at the postsynaptic membrane of synaptic connections between neurons in the nervous system. We have been studying the molecular mechanisms in the reculation of neurotransmitter receptor function. Recently we have tocused on glutamate receptors the major excitatory receptors in the brain Glutamate receptors can be divided into two major classes: AMPA and NMDA receptors. AMPA receptors mediate rapid excitatory synaptic transmission while NMDA receptors play important roles in neuronal plasticity and development. Studies in our laboratory have found that both AMPA and NMDA receptors are multiply phosphorylated by a variety of Phosphorylation regulates several protein kinases. functional properties of these receptors including conductance and membrane targeting. Recent studies in our lab have demonstrated that the phosphorylation of AMPA receptors is regulated during cellular models of learning and memory such as long-term potentiation (LTP) (LTD). and lona-term depression Moreover. phosphorylation of the AMPA receptor GluR1 subunit is required for the expression of these forms of plasticity and for the retention of spatial memory.

We have also been examining the mechanisms of the subcellular targeting and clustering of glutamate receptors at synapses. We have recently identified a variety of proteins that directly or indirectly interact with AMPA and NMDA receptors. We have found a novel family of proteins that we call GRIPs (Glutamate Receptor Interacting Proteins) that directly bind to the C-termini of the GluR2/3 subunits of AMPA receptors. GRIPs contain seven PDZ domains, protein-protein interaction motifs, which crosslink AMPA receptors to each other or link them to other proteins. In addition, we have found that the C-termini of GluR2 also interacts with the PDZ domain of PICK1, a protein kinase C-binding protein that is found at excitatory synapses. The GluR2 subunit also interacts with the NSF protein, a protein involved in the regulation of membrane fusion events. These AMPA receptor interacting proteins are critical in the proper membrane trafficking and synaptic targeting of these receptors. We have shown that the binding of PICK1 and GRIP is required for specific form of LTD in the cerebellum that is a cellular model for motor learning.

These studies have demonstrated that regulation of receptor function is a major mechanism for the regulation of synaptic plasticity in the nervous system and is an important determinant of animal behavior.

14 Transgenic Atoh-1 Induces Ectopic Hair Cell Production in Postnatal Mouse Cochlea

Seiji B. Shibata^{1,2}, Hideto Fukui^{1,2}, Mark A. Crumling¹, Lisa A. Beyer¹, Aaron Seidman¹, Hiu-Tung Wong¹, Yehoash Raphael¹

¹KHRI, Dept. of Otolaryngology, University of Michigan, ²Dept. of Otolaryngology, Kansai Medical University The basic helix-loop-helix gene transcription factor, Atonal homologue 1 (Atoh1) directs prosensory cells to a hair cell fate in the developing ear, and in deafened guinea pigs, transgenic Atoh1 can induce surviving supporting cells to express hair cell like features. However, it is unclear whether forced expression of Atoh1 can induce transformation of non-sensory cells in normal, post-mitotic mouse ears. Because such a model would be useful for studying the genetic pathways and processes necessary for hair cell regeneration, we investigated whether transgenic expression of Atoh1 can generate new ectopic hair cells in p5 mice. We inoculated ears with 1µl of an adenovirus carrying Atoh1 and GFP reporter genes (Ad. Atoh1-GFP) via lateral wall cochleostomy at P5 and

harvested the ears for histological assessment at P12. Control animals were inoculated with Ad. GFP or Ad.Null at the same time point. Cells with hair cell like phenotype were identified by Myosin VIIa antibody or F-actin labeling and GFP expression. Robust production of ectopic hair cells was apparent medial to the inner hair cells or between the outer hair cells, whereas no ectopic hair cells were observed in the control ears. Many, but not all ectopic hair cells were GFP positive. Our data demonstrate that transgenic expression of Atoh1 via adenovirus in post-mitotic mouse cochlea can produce ectopic hair cells in vivo. Presence of GFP-negative and Myosin VIIa-positive cells may indicate that signaling initiated by new hair cells leads to phenotypic changes in neighboring cells. Further investigation of this model may provide us information for inducing hair cell regeneration in the severely deafened adult ear in the future.

Supported by The A. Alfred Taubman Medical Research Institute, The Williams Professorship, and NIH/NIDCD grants T32-DC005356, DC-007634, DC001634 and DC05188.

15 An Inducible Atoh1 Transgenic Mouse: A Flexible Model for Testing the Potential and Limitations of Hair Cell Generation in Vivo

Michael Kelly¹, Yibo Huang^{1,2}, Alex Pan¹, Ping Chen¹ ¹Emory University, ²Fudan University

The transcription factor Atoh1 is known to be a potent hair cell differentiation factor important for cell fate decisions during the development of the inner ear sensory organs. Ectopic delivery of Atoh1 to the cochlear epithelium leads to the differentiation of new hair cells under certain conditions, making Atoh1 a gene of particular interest for hair cell regeneration strategies. In vivo delivery of Atoh1 in mammals, either by electroporation or viral vector, has been successful at generating mature and functional hair cells. However, current models of Atoh1 delivery preclude more extensive characterization of the potential and limitations of Atoh1-mediated hair cell generation.

Here, we describe a doxycycline-inducible Atoh1 transgenic mouse line for use in inner ear studies. In combination with a cre-activated TetON line and various tissue-specific cre lines, this system provides a high degree of flexibility and control to direct Atoh1 transgene expression in a temporal and cell-specific manner. By using the Foxg1-cre line to activate TetON expression throughout the cochlear epithelium, we found most cells were capable of initiating a hair cell differentiation program following induction of Atoh1 expression early in development. However, regions competent for hair cell differentiation become more defined with increasing age. Ectopic hair cells express hair cell markers, display wellformed stereocilia bundles and become innervated. Regions with ectopic hair cells display an intriguing mosaic cellular pattern of alternating sensory and non-sensory cells. Furthermore, significant cell proliferation was observed within the normally post-mitotic organ of Corti following Atoh1 transgene induction. Using a GFAP-cre line to specifically target Atoh1 transgene expression within differentiated supporting cells, we found that neonatal supporting cells can be converted into hair cells, consistent with previous reports that these cell types are competent for hair cell differentiation.

These results suggest that Atoh1 may play a more complex role than previously thought in the regulatory network that coordinates cell fate specification and cell cycle control in the organ of Corti. These results have implications for our understanding of development and inform possible regeneration strategies.

16 Inducible Overactivation of Notch1 Signaling Generates Ectopic Hair Cells in the Mouse Inner Ear

Zhiyong Liu^{1,2}, Thomas Owen^{1,3}, Jian Zuo¹ ¹St. Jude Children's Research Hospital. ²University of Tennessee Health Science Center, ³University of Bath Notch1 signaling may regulate the development of mouse inner ear hair cells (HCs) and surrounding supporting cells (SCs) by lateral induction (promoting generation of prosensory progenitor cells) and lateral inhibition (subsequently blocking them from committing into HCs). Although presence of these mechanisms is supported by loss-of-function studies, whether supernumerary or ectopic HCs can be induced given the augmented Notch1 signaling remains unclear. Here, we performed comprehensive in vivo studies of the inducible overactivation of Notch1 signaling at various ages in the developing mouse inner ear. Induction of Notch1 signaling at embryonic day 10.5 (E10.5) and E13 in a CAG $^{\rm CreER+};$ Rosa26-NICD $^{\rm loxp/+}$ mouse model showed ectopic HCs in nonsensory and supernumerary HCs in the endogenous sensory regions. Use of a lineage tracer showed that ectopic HCs were not derived from Notch1-active prosensory progenitor cells, supporting the presence of lateral induction and inhibition mechanisms. Furthermore, induction of Notch1 signaling specifically in differentiating cochlear HCs at E16 and after birth in an Atoh1 CreER+ Rosa26-NICD ^{loxp/+} model showed that although Sox2 and Prox1 were reactivated, these HCs developed normally without any detectable functional deficits. Therefore, Notch1 signaling in the mammalian inner ear is capable of generating new sensory epithelia where HCs can be further induced. Activation of Notch1 signaling, in conjunction with other signaling pathways, may be effective in regenerating HCs in damaged mammalian inner ears.

17 Inhibition of Gamma-Secretase Promotes Non-Mitotic Hair Cell Regeneration in the Adult Mouse Utricle

Justin Golub¹, Vincent Lin², Tot Bui Nguyen¹, Clifford Hume¹, Elizabeth Oesterle¹, Jennifer Stone¹ ¹University of Washington, ²University of Toronto

We examined hair cell regeneration in adult mice utricles following neomycin-induced damage in vitro. Utricles were transduced with an adenovirus encoding GFP under control of a 3' enhancer for the developmentally active prosensory gene atoh1. By 3 days post-neomycin, atoh1 transcription was reactivated in a few non-sensory supporting cells. Additional rare cells transcribing atoh1 were located in the hair cell layer and were immunoreactive for myosinVIIa, a hair cell marker. The number of atoh1-expressing cells increased by 6 days post-neomycin but did not increase significantly between 6 and 14 days post-neomycin. Similar results were obtained employing antibodies to Atoh1. Treatment with DAPT, an inhibitor of gamma-secretase required for notch activation, induced higher levels of atoh1 mRNA and protein. Moreover, significantly more atoh1-expressing cells differentiated hair cell features following DAPT treatment than controls. This effect was particularly prominent in the striolar region. Similar results were noted with TAPI, an inhibitor of a second notch targeting enzyme, TACE-1. Supporting cell cycle entry in control or DAPT-treated utricles was very rare, as demonstrated by cumulative BrdU labeling. These findings, and the observation that atoh1 did not appear to be upregulated in original hair cells after damage, suggest that a small number of hair cells were regenerated by direct conversion from supporting cells (direct transdifferentiation). This was confirmed using supporting cell-targeted adenovirus-GFP transduction during DAPT treatment. These findings show that supporting cells in the adult mouse utricle give rise to new hair cells via direct conversion and that notch signaling normally blocks this process, particularly in the striola.

18 ERBB Signaling Regulates Cochlear Supporting Cell Proliferation

Patricia White¹, Jennifer Stone², Andrew Groves³, Neil Seail⁴

¹University of Rochester School of Medicine, ²University of Washington, ³Baylor College of Medicine, ⁴House Ear Institute

Lack of cell replacement in the damaged cochlea underlies many forms of sensorineural hearing loss. Signaling pathways that might regulate proliferation in mammalian supporting cells are unknown. Here we report that ERBB signaling is necessary for cochlear supporting cell proliferation in both mammals and birds. Analysis of downstream signaling pathways suggests that phosphoinositol-3 kinase (PI3K) is the likely second messenger for Moreover, ERBB signaling appears to proliferation. function by down-regulating Cdkn1b / p27Kip1. These results suggest that endogenous signaling pathways might be used to promote proliferation in the mammalian cochlea.

19 Inner Ear Stem Cells Express Lgr5 and Are Induced to Differentiate to Hair Cells by Wnt

Fuxin Shi^{1,2}, Judith Kempfle^{1,2}, Albert Edge^{1,2}

¹Department of Otolaryngology, Harvard Medical School, ²Eaton-Peabody Laboratory, Massachusetts Eye and Ear Infirmary

Canonical Wnt activity could be detected in the developing and neonatal inner ear, using Wnt reporter mouse, BAT-GAL, and stem cell marker, Lgr5, a target of the Wnt pathway, was used to further distinguish cells that had Wnt activity. In newborn mice with GFP under the control of

the Lgr5 locus, green fluorescence was present in supporting cells: inner pillar, inner border and 3rd row of Deiter's cells. To test whether the Lgr5-positive supporting cells had stem cell properties that would lead to neurosphere formation, a single cell suspension was made from the organ of Corti and allowed to form neurospheres: the newly formed spheres were reporter-positive. Lar5positive cells sorted by flow cytometry after making a cell suspension from an Lgr5-GFP organ of Corti showed an enhanced capacity for renewal as compared to Lgr5negative spheres. Sorted Lgr5-positive cells, in addition, contained a markedly higher percentage of hair cell progenitors as shown by increased differentiation of myosin VIIa expressing cells from sorted as compared to unsorted cells (mean of 33% from sorted vs 2.5% from unsorted). Lgr5 negative cells did not give rise to hair cells. To test the hypothesis that Wnt signaling was fundamental to the expansion and differentiation of spheres, we added exogenous Wnt or forced expression of Wnt pathway molecules. Wnt3a treatment of neurospheres increased the rate of sphere self-renewal (4.3 + 0.5 spheres per original sphere per passage fromthe treated vs 1.8 + 0.3 from the control spheres). Overexpression of β -catenin by transfer of the gene with an adenovirus increased the number of myosin VIIa positive cells resulting from differentiation of inner ear stem cells.

Supported by NIDCD RO3 DC010270 and R01 DC007174.

20 Role of HMGA2 in the Mouse Inner Ear

Marco Petrillo¹, Judith Kempfle¹, Mingqian Huang¹, Albena Kantardzhieva¹, Albert Edge¹, Zheng-Yi Chen¹ ¹*MEEI*

In contrast to lower vertebrate inner ears, mammalian inner ears do not have the capacity to regenerate the sensory hair cells that are lost as a consequence of injury, disease, or genetic deafness. Hair cell regeneration through stem cells might represent one route to generating new hair cells, but genes that govern inner ear stem cell properties including self-renewal and the capacity to become hair cells have not been identified. Identification of such genes would enable us to characterize the origin of inner ear stem cells and to test the hypothesis that inner ear stem cells could be expanded in situ to generate new hair cells. We have performed microarray analysis of gene expression patterns of regenerating chick inner ear and identified differentially expressed genes. One of the upregulated genes, HMGA2, is involved in neural stem cell self-renewal. We found that HMGA2 was highly expressed in embryonic stem cells. HMGA2 was expressed in the otocyst at E10.5 based on in situ hybridization and gPCR. and the expression persisted until E16.5 with subsequent downregulation. In undifferentiated neurospheres made from the inner ear, HMGA2 was highly expressed, whereas in differentiated spheres, HMGA2 was absent. By siRNA mediated HMGA2 knockdown, proliferation of inner ear spheres was severely attenuated, indicating a role of HMGA2 in the self-renewal of undifferentiated inner ear neurospheres. Further, knockdown of HMGA2 increased expression of differentiation markers including Jag1, p27kip1 and β -III-tubulin, indicating that HMGA2 could suppress differentiation. Future experiment will examine the role of HMGA2 during development and in the expansion of inner ear stem cells in vitro and in vivo, and will examine a potential role for HMGA2 in hair cell regeneration.

21 Tympanic Border Cells Are Wnt-Responsive and Act as Progenitor Cells in the Postnatal Mouse Cochlea

Taha Jan^{1,2}, Renjie Chai¹, Zahra N. Sayyid¹, Saku T. Sinkkonen¹, Anping Xia¹, Tian Wang¹, Jared R. Levin¹, Yi Arial Zeng^{1,2}, Stefan Heller¹, Roel Nusse^{1,2}, Alan G. Cheng¹

Stanford University, ²Howard Hughes Medical Institute Previous studies have described limited proliferative capacity in the early postnatal mouse cochlea, yet little is known about the cell types that harbor such characteristics. Using 3-day-old (P3) Axin2^{LacZ/+} reporter mice, we found active canonical Wnt signaling below the basement membrane of the organ of Corti, including the tympanic border cells (TBC). These cells express markers for mesenchymal (Vimentin and Fibronectin) and epithelial cells (Pancytokeratin), active proliferation (Ki67 and PH3), but not markers for supporting cells (Prox1, P27Kip1, Sox2) or hair cells (Myosin7a). EdU injection experiments found these Axin2-expressing cells to be highly proliferative. During the first 3 postnatal weeks, there is a rapid decline in Wnt signaling, correlating with a loss of the cochlear sphere-forming capacity and a loss of proliferation and number of TBCs in vivo. To further characterize their capacity to self-renew and differentiate, Axin2-high cells isolated from P3 Axin2^{LacZ/+} cochleae via flow cytometry formed clonal colonies (~94%) in vitro. Growth factor deprivation led to differentiation of these colonies to express markers for epithelial cells (100% Pancytokeratin-positive), hair cells (6.9±1% Myosin7apositive) and supporting cells (77±3% Sox2-positive; 74±4% Jag1-positive; 15±3% Prox1-positive), while purified Wnt3a treatment promoted proliferation and expansion of isolated Axin2-high cells, and not Axin2-low cells. Cells from expanded Axin2-high populations were also able to acquire these supporting cell-like and hair celllike phenotypes. Furthermore, purified Wnt3a upregulated proliferation and Axin2 expression in cochlear explants, while treatment with Fz8CRD downregulated them. We therefore conclude that Axin2-high cells are Wntresponsive progenitor cells in the early postnatal cochlea. Supported by NIDCD P30DC010363, K08DC011043, American Otological Society, and Triological Society.

22 Postnatal Accumulation of Junctional F-Actin Is Phylogenetically Unique to Mammalian Supporting Cells, Paralleled by Cytoskeletal Stabilization, and Reversible by Cofilin Overexpression

Joseph Burns¹, Jeffrey T. Corwin² ¹University of Virginia, Department of Biomedical Engineering, ²University of Virginia, Department of Neuroscience

Marked differences exist between mammals and nonmammals in their replacement of lost hair cells (HCs). Efforts to find what impedes replacement in mammals led to identification of an unusual age-dependent reinforcement of the junctional F-actin belts in vestibular supporting cells (SCs). In chickens, such belts remain thin even in adulthood, but the belts in SCs of humans and rodents thicken dramatically with age and fill 89% of the average adult SC at the level of the junction. Between E18 and P83, ~1300% thickening of belts in mice is closely paralleled by declines in SC spreading at wound sites (r = -0.989), proliferation (r = -0.975), and generation of new HCs (r = -0.91). Here, we examined belt thickness in vestibular SCs of young and adult dogfish sharks, zebrafish, and bullfrogs, representing three vertebrate classes and >400 million years of evolutionary separation from extant birds and mammals. As in birds, the belts in all those regeneration capable species do not exhibit substantial postnatal reinforcement and are significantly thinner than those in adult mice (p<0.005, ANOVA). We hypothesized that the unique belt reinforcement in mammalian SCs would be accompanied by filament stabilization. We tested that by photobleaching belts in utricles of knock-in mice that express a GFP-actin fusion protein and measuring fluorescence recovery. By 2.5hrs after photobleaching, normalized fluorescence recovered 81.8 ± 4.5% in P0 mouse utricles, compared to just 37.7 ± 4.2% in mouse utricles >P20, suggesting that the thickened belts in older mice are highly stabilized. Next we used adenovirus to transfect actin depolymerizing factor (ADF)/cofilin in utricles from adult mice and observed marked reduction of SC belt thickness showing that junctional F-actin accumulation in the ear can be reversed. That will be used for assessing belt function and influence on regenerative capacity of SCs.

23 MicroRNA181a Is Necessary for Auditory Hair Cell Regeneration in the Avian Inner Ear

Corey Frucht¹, Joseph Santos-Sacchi¹, Dhasakumar Navaratnam¹

¹Yale University

Hair cells, the sensory transducing cells of the inner ear, regenerate in response to injury in non-mammalian vertebrates such as birds and fish but not in mammals. As yet, the molecular events underlying hair cell regeneration remain elusive. Previous work has shown that overexpression of microRNA181a (miR181a) in cultured chicken basilar papillae, the avian equivalent of the cochlea, is sufficient to stimulate proliferation with production of new hair cells. The present study

investigates the role of miR181a in hair cell regeneration after injury in explants of chicken auditory epithelia. Basilar papillae were explanted from 0-day-old chickens and transfected with either anti-miR181a, which knocks down endogenous miR181a, or a non-targeting miRNA and then cultured with 78 µM streptomycin for 48 hours to eradicate all hair cells in the epithelium. The explants were then transfected again with either anti-miR181a or a nontargeting miRNA and cultured for an additional 48 hours. Labeling with BrdU, a thymidine analog, was used to quantify proliferation. Explants exposed to streptomycin and transfected with anti-miR181a had significantly fewer BrdU-positive cells than basilar papillae treated with streptomycin and transfected with a non-targeting miRNA. Activated caspase-3 and myosin VI labeling were used to show that the pattern of hair cell death and loss, respectively, were not affected by anti-miR181a transfection. Anti-miR181a overexpression therefore seems to play an important role in the proliferative component of hair cell regeneration rather than in preventing hair cell death following ototoxic injury.

24 Transcriptome and Enhancer Networks During Hair Cell Regeneration

Yuan-Chieh Ku¹, Nicole Renaud¹, Rose Veile¹, Cynthia Helms¹, Mark Warchol¹, Michael Lovett¹

¹Washington University

Lower vertebrates can regenerate inner ear hair cells, mammals cannot. We used Next Gen RNA Sequencing (RNA-seq) to derive a comprehensive description of all mRNAs and miRNAs over a 168hr regenerative time course in vitro, following aminoglycoside treatment of avian utricles. We also identified putative enhancer elements activated during regeneration by ChIP-Seq, using an antibody to the histone deacetylase p300. From mRNAseq we detected ~15,000 genes and ~1800 transcripts that reproducibly changed by >2-fold during regeneration, compared to controls. These include previously described components of NOTCH, WNT, FGF, PAX and SOX signaling, but also many additional genes involved in interesting pathways (e.g. the MLL gene that encodes a histone methyltransferase). Fifty two avian miRNAs show >2-fold changes in expression during regeneration. These include members of the miR-182-183-96 family that have been previously implicated in inner ear function, and many new miRNA orthologs discovered in this project. We have tested several miRNAs by knock down or over expression techniques to assess their effects upon early regenerative events. For example, a knock down of miR-34c proliferation. significantly increased regenerative Components of the NOTCH signalling pathway are predicted targets of this miRNA. We have validated our dataset by qRT-PCR assays. These confirm the RNA-seq data. In our enhancer dataset there are many examples of temporal changes in activity. We correlated these with nearby gene expression changes. For example, we observed temporal changes in enhancers close to the POU4F3 gene that have been mapped in other model systems but have not previously been described in hair cell regeneration. Our three avian databases are being

compared to RNA-seq data from mouse utricles damaged by antibiotic or induced to transdifferentiate by gamma secretase inhibitors, to identify similarities and differences in regenerative programs between birds and mammals.

25 Stem Cell-Derived Sensory Progenitors Can Innervate the Early Post-Natal Sensory Epithelium in Vitro

Bryony Nayagam¹, Albert Edge², Mirella Dottori¹ ¹University of Melbourne, ²Eaton-Peabody Laboratory The focus of our research is to determine whether stem cells can be used to replace the auditory neurons (ANs) lost following deafness. In order to successfully replace ANs, stem cells must be capable of directed differentiation toward a sensory neural lineage, of organised outgrowth of processes, and of forming functional connections. We have developed an in vitro assay to test these parameters using co-cultures of cochlear explants and human embryonic stem cells (hESCs). Specifically, hESC-derived neurospheres were differentiated toward a sensory lineage using mouse fibroblast feeder cells and the small molecule, Y27632, and then co-cultured for up to 12 days with either cochlear explants isolated from early post-natal rats, or alone (n=10). Untreated neurospheres were set-up concomitantly as controls (n=12). The ENVY line of hESCs was used in all experiments as this line expresses high levels of green fluorescent protein (GFP) in all differentiated progeny, enabling discrimination of stem cells and their processes in co-cultures. hESC sensory progenitors differentiated into neurons which expressed both NF200 and peripherin, and extended processes into the explant. Significantly greater numbers of stem cellderived processes were observed growing into the explant when neurospheres were pre-treated with fibroblast feeder cells and Y27632 (p<0.001), and these GFP positive processes were often observed growing along the endogenous peripheral processes of the explant. In addition, when grown in co-culture with hair cells alone (microisolates; n=16), stem cell processes were capable of locating and growing along the rows of hair cells, however synapse formation occurred infrequently. These data illustrate that hESC-derived neural progenitors primed towards sensory neural differentiation can innervate the sensory epithelium after 12 days in culture, but are likely to require longer periods of culture in order to make mature synaptic contacts with sensory tissues.

26 Monitoring Migration and Engraftment of Mesenchymal Stem Cells in the Cochlea Using a High-Resolution Microscopic-Endoscope and MRI

Akihiro Matsuoka¹, Michael Fritsch^{2,3}, Karl Koehler³, Eri Hashino^{2,3}

¹University of California San Diego, Division of Otolaryngology-Head and Neck Surgery, ²Indiana University School of Medicine, Department of Otolaryngology-Head and Neck Surgery, ³Stark Neurosciences Institutes Monitoring transplanted stem cell delivery is of the utmost importance for developing translational strategies. Success of cell-based therapy depends upon the proper migration of transplanted stem cells to damaged areas in the cochlea. The goal of this study was to evaluate the extent of migration and engraftment of transplanted stem cells in areas of degenerated spiral ganglion neurons in the cochlea. To this end two techniques were used. A high-resolution microscopic-endoscope was used to examine real-time movements of stem cells in the modiolus and a Varian 9.4 T MRI system was used for non-invasive monitoring of manganese chloride (MnCl2)labeled stem cell engraftment in the cochlea. Mongolian gerbil subjects were deafened by ouabain. After four weeks of recovery, the animals received an intra-modiolar transplantation of mesenchymal stem cells (MSCs) labeled either with toluidine blue or MnCl2. For the toluicine bluelabeled MSCs, time lapse images were captured with a Karl-Storz model 7215AA microscopic-endoscope. The MSCs were migrating toward the osseous spiral lamina (OSL) of the modiolus. There appeared to be two different populations of MSCs; those closer to the OSL (group A) and those far away from the OSL (Group B). The mean velocity of group A (139.3 ± 89.8 um/h) was greater than group B (49.2 ± 13.1 um/h). GFP-positive MSCs were also recorded with a cooled CCD camera. GFP-positive MSCs transplanted into the modiolus were also surveyed using immunohistochemical analysis. For the MnCl2-labeled MSCs, serial coronal MRI sections at 200-um intervals were obtained throughout the gerbil head that had received a unilateral MSC injection 24 hrs prior to scanning. The MRI images revealed that the transplanted cochlea exhibited hyperintense contrasts when compared to the non-injected cochlea. These results demonstrate proof of concept of two novel imaging systems, which are complementary when monitoring stem cell movements in the cochlea in vivo.

27 Originality and Success in Science and Art, Celebration of the 50th Anniversary of Bekesy Nobel Prize

Richard Hallworth, Barbara Canlon, **David Lim**¹ ¹House Ear Institute

This is a shortened video presentation of the two part (75) seventy-five minute lecture filmed and produced by House Ear Institute in 1972. Bekesy, is also known for his primitive art collections which were donated to the Nobel Foundation in Stockholm, Sweden. In this film, he discussed his life-long love affair with both science and art. As far as we know this is his last filmed lecture, and the only one in existence. He died on June 13, 1972.

28 Georg Von Békésy and His Work Jürgen Tonndorf¹

In observance of the 50th anniversary of the award of the Nobel Prize for Physiology or Medicine to Georg von Békésy, the ARO here reproduces the text of the presentation made by Jürgen Tonndorf at the Nobel Symposium 63, Cellular Mechanisms in Hearing (En Hommage à Georg von Békésy), held at Alfred Nobel's Björkborn, Karlskoga, Sweden, 2-6 September, 1985, and printed as a supplement to Hearing Research, volume 22, in 1986.

29 Concerning the Pleasure of Observing, and the Mechanics of the Inner Ear Georg von Békésy¹

In observance of the 50th anniversary of the award of the Nobel Prize for Physiology or Medicine to Georg von Békésy, the ARO here reproduces the text of the Nobel lecture delivered by von Békésy on receiving the award, December 11, 1961.

30 Insulin-Like Growth Factor Signaling Promotes Cochlear Growth and Hair Cell Differentiation

Takayuki Okano¹, Matthew Kelley¹ ¹NIDCD/ NIH

The organ of Corti is a highly ordered cellular structure. During embryogenesis, a sequence of cellular and molecular processes, including cell proliferation, coordinated cell cycle exit, cellular differentiation, and cellular specification are required for its development. This process is presumed to be regulated by a variety of growth factors and transcription factors, but the majority of these factors have not been identified.

One potential regulator of cochlear development is the insulin-like growth factor (IGF) signaling family. IGF signaling is known to play a critical role in the determination of body size, and Woods, et al. (1996) described severe hearing loss along with growth failure in a 15-year-old boy with a homozygous mutation in the *IGF1* gene. In addition, the recent study by Sanchez-Calderon, et al. (2010) demonstrated that *Igf1* and the type 1 IGF receptor (*Igf1R*) are both expressed in the developing cochlea. These observations suggest that the IGF pathway could play a role in development of the mammalian cochlea. However, the specific effects of the IGF pathway have not been determined.

To examine the role of the IGF pathway, we analyzed cochleae from *Igf1r* mutant mice. Deletion of *Igf1r* leads to several changes in cochlear development including a shortened cochlear duct and a decrease in the total number of hair cells. In addition, the maturation of surviving hair cells was delayed as was the development of stereociliary bundles. To determine the molecular basis for these defects, inhibition of IGF signaling was replicated pharmacologically in vitro. Results indicated that IGF signaling regulates cochlear elongation and hair cell development through the PI3 kinase-Akt signaling pathway. Moreover, in vitro inhibition of the IGF1R-PI3 kinase-Akt pathway caused down-regulation of Atoh1. These results reveal a novel role for IGF signaling in inner ear development, and should provide insights regarding the factors that regulate cochlear formation.

31 The Role of Foxi3 in Establishment of the Pre-Placodal Domain and in Otic Development

Safia Khatri¹, Renee Edlund¹, Ryan Mayle¹, Andy Grove¹ ¹Baylor College of Medicine

Cranial placodes form a disparate group of sensory structures such as the lens, inner ear, nasal epithelium and distal portions of cranial sensory ganglia. All placode precursors reside in a continuous territory adjacent to the anterior neural plate called the preplacodal region (PPR). It is now well established that FGF signaling induces the otic placode - the precursor of the inner ear - from the PPR. Our laboratory has shown that only certain populations of cranial ectoderm are competent to respond to FGF signaling and that this responsiveness correlates with the expression of genes that mark the PPR. Recently, we have identified a novel forkhead transcription factor called Foxi3 that is expressed in the PPR. Foxi3 deletion in mice causes a complete morphological absence of the inner ear. We hypothesize that Foxi3 plays a central role in otic placode induction by providing inducing PPR genes and providing competence to respond to FGF signaling. To test if Foxi3 is sufficient and necessary to establish the PPR, we are electroporating full-length mouse Foxi3 or siRNA-Foxi3 in HH4-5 stage chick embryos and examining the expression of PPR genes such as DIx5, Six1, Six4 and Eva2. To test if Foxi3 provides competence to respond to FGF signaling we are culturing non-competent ectoderm electroporated with Foxi3 cDNA in FGF and will analyze the expression of otic genes.

32 The Effect of Sprouty1 and Sprouty2 Gene Dosage on Mouse Otic Placode Induction and Invagination

Katherine Shim¹, Jian Zhang¹, Amanda Mahoney Rogers¹, Kevin Wright¹

¹Medical College of Wisconsin

The otic placode is composed of the embryonic progenitors for most of the cell types of the inner ear, including the mechanosensory hair cells, supporting cells and innervating neurons. In the mouse, at 8 - 9 somite stages (s), the otic placode becomes morphologically distinct as a pseudostratified region of ectoderm on either side of the hindbrain. Multiple signaling pathways, including Fibroblast Growth Factor (FGF), Wnt, and Notch are required for induction of the otic placode. We are studying the role of the Sprouty (Spry) gene family (of which there are four murine members, Spry1 - 4) in otic placode induction. Spry genes encode antagonists of signaling downstream of receptor tyrosine kinases (RTKs), including FGF receptors. In Spry1-/-; Spry2-/- double mutants, the otic placode is enlarged, and this enlargement of the otic placode can be rescued by reducing the gene dosage of Fgf10 (Spry1-/-; Spry2-/-; Fgf10-/+ embryos). This suggests that Spry1 and Spry2 normally antagonize FGF signaling to limit the size of the otic placode. In preliminary data, we find that the otic placode is also expanded in Spry1-/+; Spry2-/- mutant embryos at 8 - 11 s, suggesting that the presence of one

functional copy of Spry1 is not sufficient to limit the size of the otic placode. Interestingly, at 17 - 19 s, whereas the otic placode remains larger in Spry1-/-; Spry2-/- double mutants, in Spry1-/+; Spry2-/- mutant embryos, the size of the otic placode is indistinguishable from controls. These preliminary data suggest that the presence of an enlarged otic placode at 8 - 11 s is not a committed genetic event, and the presence of a single functional allele of Spry1 is sufficient to rescue this early enlargement. Experiments exploring the mechanism by which a single functional copy of Spry1 can rescue the initial enlargement of the otic placode will be presented.

33 Function of Hey1 and HeyL in the Developing Mammalian Cochlea

Dean Campbell¹, Erin Golden¹, Matthew Barton¹, Angelika Doetzlhofer¹

¹Department of Neuroscience Johns Hopkins University School of Medicine

In the differentiating cochlea, lateral inhibition, mediated by Notch signaling, is critical for the stereotypical patterning of sensory hair cells and surrounding supporting cells. The best-characterized Notch effectors are Hes, and the Hes related Hey transcription factors. Recent studies revealed an important function of Hes1, Hes5, and Hey2 in auditory sensory epithelium patterning. Little is known about the function of two additional Hey factors (Hey1 and HeyL) in the developing cochlea. Based on their structural and functional similarity with Hes1, Hes5 and Hey2 we hypothesized that these factors are also involved in patterning the developing cochlea.

To investigate the function of Hey1 and HeyL in development of the cochlea, we analyzed Hey1, and HeyL mutant mice. The Hey1 and HeyL mutants had a wild-type hair cell patterning phenotype, presumably due to redundancy with Hes5, which is expressed in a similar spatial manner. To examine the functional redundancy between Hes5 and Hey1and HeyL, we analyzed Hes5, Hey1 and HeyL double and triple mutants. Our analysis revealed that both double and triple mutants had a steepened outer hair cell patterning defect when compared to the Hes5 single mutant. Further analysis revealed that ectopic supporting cells accompanied the ectopic hair cells. Preliminary BrdU incorporation studies suggest that ectopic cells result from defects in the coordination of cell cycle exit and differentiation. Furthermore we are exploring the possibility that cross regulation between these factors is used to maintain the highly specific and invariant expression pattern observed in the auditory sensory epithelium.

34 Dicer/microRNAs Function in the Development of the Mouse Inner Ear

SACHELI Rosalie¹, Priscilla Van den Ackerveken¹, Volvert Marie Laure¹, Nguyen Laurent¹, Bodson Morgan¹, Malgrange Brigitte¹, Lefebvre Philippe² ¹University of Liège, ²CHU of Liège

MicroRNAs (miRNAs) constitute a class of small, noncoding RNAs which can posttranscriptionally silence many complementary target genes by inhibiting messenger RNA translation. Although they have been found to regulate developmental and physiological processes in several organs, their role in the regulation of the cochlear transcriptome remain unknown.

We studied the role of Dicer, a ribonuclease esential for miRNA processing by conditionally deleting the Dicer gene in the mouse inner ear. In this mutant, severe morphological defects were observed together with a lot of apoptotic cells within the cochlea and the vestibule. The level of p53 also appeared to be higher in mutant mice, suggesting that loss of miRNA biogenesis induces DNA damage.

We also studied differentiation in the Dicer mutant mice and found that myosin VI positive hair cells are present while supporting cells seem to be absent. Nevertheless, cells surrounding hair cells are positive for sox2, a marker of early progenitors. We therefore hypothesized that supporting cells are not able to differentiate in the absence of miRNAs..

Altogether, these results suggest an indispensible role for Dicer and miRNAs in regulating the development and differentiation of inner ear cells.

35 Lgr5, a Wnt Target Gene, Is Expressed in the Developing and Mature Mouse Cochlea

Renjie Chai¹, Anping Xia¹, Taha Jan¹, Alan Cheng¹ ¹Department of Otolaryngology-HNS, Stanford University School of Medicine

The Wnt signaling pathway is a recurring theme in developmental biology, however, its different roles during inner ear development are just emerging. Lgr5, a member of the G-protein-coupled- receptor family, has been shown to be a Wnt target and mark adult stem cells in the gastrointestinal and integumentary systems. Although Lgr5's exact function is not known, its deficiency leads to perinatal lethality due to gastrointestinal distension. In this study, we used a knock-in reporter mouse to examine the spatiotemporal expression of Lgr5 in the cochlear duct during the late embryonic and postnatal periods. The expression of Lgr5-GFP partially overlapped with Sox2, Jagged1, and p27(Kip1), which are markers of the prosensory region. Myosin7a-expressing hair cells first appeared within the Lgr5-GFP-positive region on the floor At E18.5, outer and inner hair cells epithelium. downregulated Lgr5-GFP, while the third row of Deiters' cells, inner pillar cells, medial inner phalangeal cells and lateral GER continued to express Lgr5-GFP. By the second postnatal week, only the third row of Deiters' cells had detectable levels of Lgr5-GFP, which remained robust into adulthood. Normal development of cochlear hair cells and supporting cells was observed in the homozygous and heterozygous transgenic mouse. To validate that Lgr5 is a Wht target, we treated postnatal cochlear explants with Wnt3a or Fz8CRD to activate or inhibit Wnt signaling and found that Lqr5 expression was up- or downregulated, respectively. We conclude that Lgr5 has a dynamic expression pattern in the developing the organ of Corti. Though not essential for cochlear development, we hypothesize that Lgr5 serves as a useful readout of Wnt signaling activity in the cochlea.

Supported by Triological Society, American Otological Society, and NIDCD K08DC011043 and P30DC010363.

36 Development of Planar Cell Polarity in Mammalian Maculae

Jack Etheredge¹, Dong Qian¹, Ping Chen¹ ¹Department of Cell Biology, Emory University

Epithelial planar cell polarity (PCP) refers to the coordinated orientation of neighboring cells, resulting in a polarity axis parallel to the plane of the epithelium. The vertebrate PCP pathway consists of a set of membrane-associated proteins, and primary cilia and their associated basal bodies. The underlying mechanism in vertebrate PCP signaling, however, has yet to be revealed.

Each sensory hair cell of the inner ear contains a polarized hair bundle comprising an asymmetrically positioned primary cilium, the kinocilium, and rows of microvilliderived stereocilia of graded height. Hair cells within each inner ear organ are oriented coordinately. In particular, the hair cells in the saccule and utricle show reverse polarity along a line of polarity reversal, providing a unique opportunity to determine PCP signaling. To explore the mammalian maculae as PCP models, we established the timeline for cell proliferation, differentiation, and hair bundle formation in the mouse maculae. We further analyzed the subcellular localization of membrane associated PCP proteins, Vang-like 2 (Vangl2) and Frizzled 3 (Fz3). We found asymmetric and polarized membrane distribution of Vangl2 and Fz3. Moreover, asymmetric distribution of both Fz3 and Vangl2 precedes formation of stereocilia. Similar to published results of Pk2 polarity, confocal microscopy of embryonic day 18 (E18) embryos shows that Vangl2, or Vangl2-GFP, and Fz3 appear to colocalize on the medial edge of hair cells or the lateral edge of supporting cells of both maculae. We will further determine the precise localization of Vangl2 and Fz3 in hair cells and supporting cells to address the issue of directionality of localization within a single cell. We will also determine the polarity of basal bodies across the line of polarity reversal in the maculae to assess whether basal body polarity acts as a polarity determinant for individual cells.

37 Shift of PCP Protein Localization with Hair Cell Reorientation in the Avian Basilar Papilla

Ulrike Sienknecht¹

¹Carl von Ossietzky University Oldenburg

Coordinated alignment of hair cell stereociliary bundles is essential for mechanoreceptive function. There is striking evidence that invertebrates and vertebrates share common molecular mechanisms to control the systematic cell orientations in epithelial sheets, i.e., planar cell polarity (PCP). Core PCP proteins, such as Vangl2, appear to mediate polarity by localizing asymmetrically at cell junctions and transmitting asymmetry from cell to cell. However, it remains unclear how the localization of PCP proteins translates into a coordinated pattern of planar polarity across the developing epithelium. In the chicken's basilar papilla (BP), differentiation of stereociliary bundles is concomitant with a rough uniform bundle orientation. Initially, hair cells face to the abneural organ edge with their kinocilia or the tallest row of stereovilli displaying a large variance in orientation angles. Later on, during PCP refinement, hair cells undergo a phase of reorientation which leads to a complex, yet highly organized, PCP pattern in the mature avian auditory epithelium.

During early attainment of hair cell orientation, Vangl2 protein is present at supporting cell-supporting cell junctions orthogonal to the polarity axis. In contrast, adjacent to the prosensory epithelium, cells of the abneural limbus, such as border cells, express Vangl2 in a perpendicular axis. During the course of development, there is a striking shift in the asymmetric localization of Vangl2, associated with hair cells that reorient toward the apex (distal end of the organ).

38 Gata3 Is Essential for Cochlear Neurosensory Development

Jeremy Duncan¹, Bernd Fritzsch¹

¹University of Iowa

The zinc finger protein Gata3 is expressed in most sensory epithelia of the developing otocyst as early as embryonic day 8.5 and mutations of Gata3 cause hearing loss in humans. Gata3 null mice remain cystic at embryonic day 11.5 (E11.5). We show that older null mutant mice (E16.5) have a variable inner ear phenotype ranging from an empty cyst with an endolymphatic duct to an inner ear that develops a cochlear duct without neurosensory epithelia, and a saccule with hair cells and innervation. We generated two conditional Gata3 knockout lines (CKO) using floxed Gata3 and Foxg1-cre and Pax2-cre. Pax2-cre CKO mice have a short cochlea with deformed hair cell patches and misaligned innervation and distorted vestibular sensory patches. Foxg1-cre CKO mice show a complete loss of cochlear sensory formation, closer matching the null phenotype. Foxg1-cre CKO mice show formation of a saccule, utricle, and severely disrupted anterior canal cristae, and loss of the posterior canal. In conclusion, Gata3 plays a crucial role in inner ear development in particular those sensory organs that show high level of early expression. In addition, histological development associated with these sensory organs is proportionally disrupted, and restriction of cells types to appropriate domains is perturbed.

39 Fate Commitment of Neuronal Precursors, But Not Hair Cell Precursors, Can Be Altered Through Misexpression of BHLH Genes

Israt Jahan¹, Ning Pan¹, Jennifer Kersigo¹, Ken A. Morris², Kirk Beisel³, Bernd Fritzsch¹ ¹University of Iowa, ²University of Illinois, ³Creighton University

Abstract:

Neurosensory development of inner ear obtains through mosaic cross-regulatory interactions of several bHLH

genes crucial for specific cellular identity. The bHLH gene Neurog1 is essential for the specification of all inner ear neurons, Neurod1 for differentiation and maintenance of most cochlear and vestibular neurons and Atoh1 is essential for hair cell differentiation. While the development of the particular cell type in the absence of a given bHLH gene is disrupted, transformation of one cell type into another one has also been proposed (Matei et al., 2005; Ma et al., 2000) and recently demonstrated (Jahan et al., 2010). Loss of *Neurog1* leads to reduction of hair cells, but also differentiation of nonsensory cells as hair cells in the greater epithelial ridge and in the ductus reuniens (Matei et al., 2005; Ma et al., 2000). To further test this transformation ability we constructed a knockin (KI) mouse where Atoh1 was replaced by Neurog1. Surprisingly, while *Neurog1* is expressed in hair cells in heterozygous mice, it cannot differentiate hair cells in the homozygous mutants. In addition, Neurod1 is upregulated by Neurog1 in these undifferentiated patchy hair cells; whereas it is not present in Atoh1 null mice. This contrasts with the retina where Neurod1 can maintain developing ganglion cell differentiation if misexpressed under the Atoh7 promoter (Mao et al., 2008). We further tested this inability in mice with one allele of floxed *Atoh1* removed by *Tg* (*Atoh1cre*) allowing only the Neurog1-KI expression in undifferentiated hair cells. These mice express Neurog1 and Neurod1 without any significance on differentiation of hair cells. In contrast to neuronal precursors, which can differentiate as hair cells if Neurod1 is replaced by Atoh1 (Jahan et al., 2010), hair cells are at the time of *Atoh1* upregulation incapable to switch their phenotype upon misexpression of two neuronal bHLH genes, Neurog1 and Neurod1.

40 Rps6 Expression During the Development of Mice Inner Ear

Na Lu^{1,2}, Yong Tang¹, Zheng-Yi Chen¹ ¹*Massachusetts Eye and Ear Infirmary,* ²*Department of Otolaryngology, Eye & ENT Hospital, Fudan University* The protein kinase mammalian target of rapamycin (mTOR) has recently emerged as a central regulator of progression of the cell cycle and cell growth. Previous studies have shown that mTOR pathway is involved in the regeneration of adult ganglion cell axon, liver cell proliferation, and the regulation of cell size. The ribosomal protein S6 kinase (S6K) is downstream effector of mTOR pathway and ribosomal protein S6 (Rps6) is a S6K substrate. As part to study of mTOR pathway in mammalian inner ear, we investigated the expression pattern of Rps6 in the developing mouse inner ear.

Rps6 was prominently detected in the stato-acoustic ganglion region and the medial portion of the otocyst at E10.5. Rps6 is localized to the whole length hair cell kinocilia at E18.5, and is restricted to the top of kinocilia at P1. Within outer hair cell soma Rps6 is asymmetrically localized to proximal region that is adjacent to supporting cells, reminiscent of localization of Vangl2 . At P6, Rps6 is localized to the whole length of stereocilia as well as to the Pillar cells of basal and middle turns, which gradually extends to the apex. In adult, Rps6 is further restricted to the shorter stereocilia of both inner and outer hair cells.

Also in adult, Rps6 is strongly expressed in Pillar cells and is weakly expressed in the limbus, spiral ganglion neurons(SGN) and stria vascularis region.

The dynamic expression pattern of Rps6 in developing mouse inner ear indicates that Rps6 may play a role in hair cell development including stereocilia formation and planer cell polarity (PCP). As Rps6 is a downstream effector of pTen, which negatively regulates inner ear cell growth, the expression analysis provides a basis on which a link between the growth of inner ear and the development of hair cells can be studied.

41 Conditional Deletion of Mycn Derails Cochlear and Vestibular Development and Results in Altered Behavior and Abnormal Three Dimensional Ear Organization

Benjamin Kopecky¹, Bernd Fritzsch¹

¹University of Iowa

Conditional Deletion of *Mycn* Derails Cochlear and Vestibular Development and Results in Altered Behavior and Abnormal Three Dimensional Ear Organization.

Myelocytomatosis oncogene, neuroblastomas derived, or Mycn, is one of three highly conserved Myc protooncogenes (*Myc*, *Mycl1*) that regulate the cell cycle (Singh and Dalton, 2009. Cell stem cell, vol. 2, p 141) and are implicated in tumor formation (Modak and Cheung, 2010. Cancer treatment reviews, vol. 4, p 307 and Bell et al, 2010. *Cancer letters*, vol. 2, p 144). We have used both Tg(Pax2-Cre) and Foxg1^{Kicre} to generate *Mycn* conditional knockout mutants (CKOs) in the inner ear and other tissue. Both Mycn CKO mouse lines have smaller ears with a truncated cochlea and an abnormal apical tip. In addition, these ears have confluent gravistatic endorgans [utricle and saccule] which are also in continuity with the base of the cochlea. The morphogenesis of the vestibular semicircular canals is also disrupted. Mycn CKOs show neuronal pathfinding defects with cochlear fibers innervating not only the organ of Corti, but also the The posterior canal crista is typically unsaccule. innervated in Foxg1^{Kicre} CKO or receives a reduced to no innervation in Tg(Pax2-Cre) CKO mice. While the Foxg1^{Kicre} CKO is postnatally lethal, Tg(Pax2-Cre) CKO survive for over 200 days. These mice show reduced vestibular function using a Noldus Catwalk ® system. Thin-sheet imaging laser microscopy, TSLIM (Santi et al., Biotechniques, vol. 4, p 287), provides non-2009. destructive optical sectioning and three dimension reconstruction showing a massive reduction in the cochlea and spiral ganglia volumes as well as abnormal structure in the Tg(Pax2-Cre) CKO at postnatal day 35. We see that over time, vestibular functioning does not improve and that our Mycn CKOs perform worse on average with respect to gait regularity and mean paw pressure than controls. This behavioral data is consistent with the morphological and connectional abnormalities noted using TSLIM and other imaging techniques.

Supported by NIDCD R01 DC005590

42 Testing the Responsiveness of Chicken Statoacoustic Ganglion Neurons to Morphogens in Vitro

Kristen Fantetti¹, **Donna Fekete¹**

¹Department of Biological Sciences, Purdue University Mechanosensory hair cells of the chicken inner ear are innervated by the peripheral processes of statoacoustic ganglion (SAG) neurons. Several families of morphogens are expressed within and surrounding the chick inner ear during SAG axon outgrowth and pathfinding. We hypothesize that some morphogens may function to guide axons as they are navigating towards their peripheral sensory targets. To test this hypothesis, three-dimensional collagen cultures were used to grow E4 chick SAG explants in the presence of BMPs, FGFs, Shh, Wnts or Wnt inhibitors (sFRPs). To test for concentrationdependent effects, purified proteins were added to culture medium at a range of concentrations that are known to be bioactive on chick tissue. Vehicle solutions were added to control cultures. Explants were cultured in serum-free conditions supplemented with growth factors for 24-40h, immunostained with ß-tubulin and imaged with a confocal microscope. To determine effects on neurite outgrowth, average neurite length and density were quantified using NIH ImageJ software. Results show that BMP4, BMP7 and FGF8 can each promote SAG neurite outgrowth, suggesting these molecules may function as attractants during development. A concentration-dependent effect was found for Shh, where low concentrations of Shh promote neurite outgrowth and high concentrations inhibit outgrowth. In contrast, SAG neurons appear unresponsive to Wnts or Wnt inhibitors, suggesting that these are not used as guidance cues on E4-E6. Wht bioactivity was confirmed using E6 chick spinal cord explants under comparable culture conditions. Current studies are aimed at testing remaining candidates and determining whether effects on neurite outgrowth involve axon guidance or neuron survival.

This work is supported by NIDCD.

43 Tbx5 and Tbx15 Regulate CamK2B2 Levels for Proper Development in the Zebrafish Lateral Line

Heather Whitehurst¹, Viviana Gallardo Mendieta¹, **Shawn Burgess**¹

¹National Human Genome Research Institute/NIH

The posterior lateral line (pLL) of the zebrafish is a mechanosensory organ that enables fish to detect movement in the aqueous environment. Due to its location on the surface of the fish body, the pLL is highly useful for the study of tissue patterning and differentiation of hair cells during development and hair cell regeneration following damage. From approximately 24 - 48 hpf, a mass of cells called the primordium migrates along the horizontal myoseptum, depositing masses of 15 - 20 cells, called protoneuromasts at regular intervals. These protoneuromasts mature to form neuromasts, which contain hair cells that detect movement around the fish. At 4 days post fertilization, the lateral line is composed of

7-9 neuromasts. T-box transcription factors are widely recognized for their roles in development and tissue patterning. Recent evidence suggests that two members of this family, tbx5 and tbx15, have a role in pLL development and hair cell regeneration. We used morpholinos against each of these genes to show that defects in the lateral line are apparent following knockdown of tbx5 and tbx15. Along with defects in the number and spacing of neuromasts, we documented alterations in the size, shape and tissue patterning of the Additional morpholino studies migrating primordium. demonstrate rescue of the tbx5 phenotype when tbx15 is also knocked down, suggesting that the two transcription factors work in a feedback loop on the same pathway. Similar pLL defects are noted following knockdown of CamKII-ß2, a known downstream target of Tbx5, suggesting a mechanism of action. Rescue of the tbx5 phenotype is accomplished via ectopic expression of human CamKII-∂C while the tbx15 phenotype is worsened in the presence of ectopic CamKII-∂C. Furthermore, in situ hybridization has verified expression of these genes in the developing pLL and has indicated that expression of known markers of tissue patterning in the migrating primordium are affected in predictable ways. Based on this and other evidence, we conclude that tbx5 and tbx15 are involved in tissue patterning in the migrating primordium are essential components of hair cell differentiation.

44 Allometry of the Middle Ear in *Trachemys Scripta Elegans*

Katie Willis¹, Kimberlee Potter², Jakob Christensen-Dalsgaard³, Catherine Carr¹

¹University of Maryland, ²Armed Forces Institute of Pathology, ³University of Southern Denmark

One notable characteristic of many chelonian species is a large middle ear cavity. An early hypothesis for the function of this cavity was that it resonated at ecologically important frequencies, enhancing sound perception. Wever (1978), however, calculated the best resonance frequency for the cavity in air to be 6kHz, above the upper limit (1200 Hz) of the turtle's audiogram (Patterson, 1966). Auditory brainstem responses and laser vibrometry in lightly anesthetized turtles, however, revealed a best sensitivity to underwater sound pressures of 300-500 Hz (Christensen-Dalsgaard et al., 2010). The ear was about 10dB less sensitive to underwater sound pressures than in air, which in terms of sound intensity shows that thresholds in water are lower than in air, indicating a specialization for underwater hearing. We hypothesize that the large middle ear cavity is adapted for hearing underwater and that its best resonance frequency underwater will reflect the animal's auditory needs. We used MRI to obtain accurate shape and volume information about the cavity. Animals from 4 to 8 inches in length were imaged. Image stacks were reconstructed in 3-D and analyzed using NeuroLucida by tracing the borders of each cavity and using the volume calculator. The middle ear cavity has an approximately elliptical form, scaling with head size, which indicates a small decrease in resonance frequency with

increasing head size. Preliminary calculations show best resonance frequencies for the cavity underwater to be about 750-1000 Hz, well within the species' hearing range. The lateral boundary of the cavity is a cartilaginous disk (the extracolumella), covered by skin. The extracolumella is connected to the columella. Given these structures, motion of the air in the middle ear cavity could drive the tympanic disk underwater. This would allow the cartilaginous disk to be vibrated from both the outside (in air) and the inside (in water).

45 High-Quality 3-D Surface Models of the Gerbil Middle Ear Morphology: State-Of-The-Art Micro-CT of Bone, Complemented by Optical Sectioning of Soft Tissue

Jan Buytaert¹, Wasil Salih¹, Pieter Vanderniepen², Manuel Dierick², Joris Dirckx¹

¹University of Antwerp, ²Ghent University

Correct Finite Element Modeling (FEM) of the Middle Ear (ME) is needed to improve our understanding of this complex mechanical system. In order to have realistic results of these simulations, correct morphological data are still needed as input for the FEM calculations.

Up till now, most FEM models of the ME use rudimentary shapes for the ossicles and hardly incorporate any (measured) soft tissue structures. It has been shown, however, that these tissue structures greatly influence the ME behavior.

By merging Three-Dimensional (3-D) data from state-ofthe-art micro-Computed Tomography (μ CT) recordings on gerbil with data from Orthogonal-Plane Fluorescence Optical-Sectioning microscopy (OPFOS) on the same specimen, we achieve complete and high-quality surface models. The μ CT setup yields accurate data of the 3-D shape of the surrounding bone and ossicles, while OPFOS delivers high-resolution 3-D shapes of the soft tissue structures like muscles, tendon, ligaments, nerve and artery of the ME. We will show and discuss some properties of the measured data and models.

The effective resolution, quality and completeness of the 3-D gerbil surface model are unprecedented. We make these data and models freely available on our website for academic and research purposes. In addition, also highresolution μ CT models of the bony structures of rat and rabbit can be found there.

46 Experimental and Modelling Study of Gerbil Tympanic-Membrane Vibrations

Nima Maftoon¹, Shruti Nambiar^{1,2}, Robert Funnell¹, Willem Decraemer³, Sam Daniel¹

¹*McGill University*, ²*University of Waterloo*, ³*University of Antwerp*

The vibration pattern of the tympanic membrane has an important effect on the overall behaviour of the middle ear, and is an important factor when validating any quantitative model that tries to represent middle-ear mechanics. In order to measure the vibrations of the gerbil tympanic membrane, the animal is anaesthetized, then the cartilaginous ear canal and the soft tissues covering the bulla are removed and the tympanic membrane is exposed by drilling the bony canal. We place at least five microbeads over the tympanic membrane and at least one on the manubrium, and excite the ear by an acoustical frequency sweep from 200 Hz to 10 kHz. Laser Doppler vibrometry is used to measure the motion of the microbeads.

The experimental work is complemented by quantitative modelling of the middle ear using the finite-element method. The geometry of the finite-element model is based on reconstruction of the middle ear using a microCT dataset, supplemented by histological images. Linear dynamic finite-element analysis is done and the results of the simulations are compared with the experimental measurements in the frequency domain. The sensitivity of the model to various parameters is explored.

47 Efficiency of Chinchilla Middle Ears

Michael Ravicz¹, **David Chhan^{1,2}**, John Rosowski^{1,2} ¹Eaton-Peabody Laboratory, MEEI, ²Speech&Hearing Bioscience & Technology, HST, MIT

For hearing to occur, sufficient sound power must be transferred from the external environment to the cochlea to excite the sensory cells that produce the hearing sensation. The amount of sound power transferred to the cochlea for a given external sound pressure depends on power collected by the external and middle ear and the efficiency of sound transmission throughout the sound conduction path through the middle ear and into the cochlea. Middle-ear efficiency (MEE) can be defined as the ratio of the power delivered to the cochlea and the power entering the middle ear. Previous estimates of MEE are complicated by the fact that they were calculated from a combination of data sets gathered in different laboratories in different animals. We present MEE calculated from measurements of sound power flow in each of 7 individual chinchillas over the frequency range 0.1–18 kHz. The calculations depend on measurements of the middle-ear input admittance Yt, the middle-ear pressure gain Gmep, and the cochlear input impedance Zc. Yt. Gmep. and Zc were similar to measurements reported in the literature. The computed MEE varies with frequency and from ear to ear. The efficiency tends to be largest at frequencies between 0.1 and 2 kHz, where it varies between 0.1 and 1 with a median value of 0.3 across animals and frequency. At frequencies above 2 kHz the efficiency generally decreases as frequency increased, though in 5 ears a second peak in efficiency occurs near 10 kHz. The new computations have several features in common with previous estimates, including the low-frequency region of high efficiency and the secondary peak near 10 kHz as well as the magnitude of the efficiency. The contribution of a frequency dependence in middle-ear efficiency to the frequency dependence of audiometric thresholds will be discussed. [Supported by NIDCD]

48 Interaural Canal Effects in the Chicken with Closed Sound Systems in Vivo Christine Koeppl^{1,2}

¹Carl von Ossietzky University Oldenburg, ²University of Sydney

Avian middle ears are not enclosed in bony bullae but are instead open to multiple skull spaces, collectively termed the interaural canal. This physical interaural connection forms a pressure-gradient receiving system which potentially creates a directional sensitivity of eardrum motion and may enhance binaural level and timing cues. However, the extent of these effects is likely to differ between species and is sensitive to experimental conditions.

The aim of the present experiments was to assess the extent of interaural-canal effects in anaesthetized chickens, aged P21 and older, under the experimental conditions commonly used for invasive neurophysiology. Closed, individually calibrated sound systems were used to deliver monaural and binaural tone-burst stimuli. Surgical openings in the skull provided middle-ear ventilation. Cochlear microphonic potentials (CM) were recorded simultaneously from both ears with wire electrodes near the round windows. Recordings were repeated after injection of liquid petroleum jelly to block the interaural canal.

With monaural stimulation, a comparison of ipsi- and contralateral CM amplitudes indicated the most pronounced interaural transmission at frequencies between 1.5 and 2.5 kHz. Blocking the interaural canal significantly reduced this cross-talk. Phase differences between ispi- and contralateral CM suggested a pronounced decline in interaural transmission delay with increasing frequency. Large time delays of more than 1 ms were observed at 100 and 333 Hz. We also presented binaural stimuli with varying interaural time differences (ITD). Under these conditions, both CM clearly modulated in amplitude with ITD. Blocking of the interaural canal abolished this modulation.

These measurements demonstrated clear interaural canal effects in chickens with nearly mature head sizes. Interaural transmission occurred with minimal attenuation at frequencies around 2 kHz.

Supported by the Australian Research Council (DP0984692)

49 Elastic Characterization of the Gerbil Pars Flaccida Using in Situ Inflation Experiments

Jef Aernouts¹, Joris Dirckx¹

¹University of Antwerp

Finite element modelling is a powerful method for the investigation of middle ear mechanics. In current finite element models, the pars flaccida is assumed to be a linear homogeneous isotropic elastic material. This is an approximation, since in general biological tissue behaves highly non-linear. Furthermore, the pars flaccida has never been elastically characterized. In current models, a modulus is assigned which ranges from one-twentieth up till half the value of the modulus of the pars tensa.

This paper presents an elastic characterization of the gerbil pars flaccida. The gerbil is one of the common animal models in middle ear mechanics research. Its pars flaccida has a nearly flat circular shape. Over about three quadrants of its border it is supported by bone. Over the other quadrant it is connected to the pars tensa by a clearly definable fold.

Characterization was carried out by applying a uniform pressure on the membrane and measuring the resulting full-field deformation with moiré profilometry. Next, the data was used in an inverse finite element analysis in which the optimal elasticity parameters were found.

Results showed that the currently used linear stiffness guesses might be at least one order of magnitude wrong. Moreover, we found that a linear elastic material is not appropriate to describe pars flaccida's behaviour for high pressures. In order to describe the observed stagnation of membrane displacement at high pressures, a Veronda-Westmann material was used. Finally, it was found that incorporating an in situ strain in the models was necessary for a good description of membrane displacements at small to moderate pressures.

50 Dynamic Tympanic Membrane Elasticity Measured with an Indentation Setup

Jef Aernouts¹, Joris Dirckx¹

¹University of Antwerp

In hearing science, finite element modelling is used commonly to study the mechanical behaviour of the middle ear. In order to quantify static elasticity parameters of the tympanic membrane, we recently introduced a point indentation approach. In this method a quasi-static tissue indentation is applied and the resulting force and membrane deformation are measured and optimized in an inverse finite element analysis.

Previous studies on tympanic membrane elasticity mostly used quasi-static loading conditions, while the ear's main function is in the acoustic frequency range. It is known that biological tissues are sensitive to strain rate. Therefore, in this study tympanic membrane behaviour was studied under dynamic indentation loadings. Experiments were performed on gerbil tympanic membranes, one of the common models in middle ear mechanics research.

In the dynamic setup the needle was driven by a shaker. The needle was positioned so that it was locally perpendicular to the membrane surface to avoid slippage at the point of contact. The motion of the indenter was controlled with a feedback unit and a vibrometer. The tympanic membrane sample was placed in a holder that was attached to a load cell.

On the basis of a moiré shape measurement, a finite element mesh of the initial tympanic membrane geometry was made. Subsequently the elasticity parameters in a finite element model of the experiment were optimized to fit experimental force indentation data.

The setup allowed us to measure both under quasi-static conditions and up to the acoustic regime at low frequencies till 150 Hz. In this way, the influence of strain rate at tympanic membrane elasticity was investigated.

51 Motion of the Manubrium of the Human Tympanic Membrane Measured by Stroboscopic Holography

Jeffrey Cheng¹, Mohamad Hamadeh¹, Michael Ravicz¹, Ellery Harrington², Cosme Furlong^{1,2}, Saumil Merchant^{1,3}, John Rosowski^{1,3}

¹Massachusetts Eye and Ear Infirmary, Harvard Medical School, ²Worcester Polytechnic Institute, ³Harvard-MIT Division of Health Sciences & Technology

Rotation and bending motions of the manubrium of malleus within the tympanic membrane (TM) have been observed in cat [Funnell et al. JASA 1992; 91:2082-90] and gerbil [de La Rochefoucauld et al. Hear. Res. 2010; 263:9-15], but haven't been systematically studied in the human TM. In the past, we have used opto-electronic stroboscopic holographic interferometry to quantify the displacement of about 300000 points on the human TM surface to sound stimuli with frequencies from 200 to 20000 Hz. These high spatial-density measurements allow us to define the motion of the TM along the entire lateral surface of the manubrium, from superior to the lateral process (LPM) down to the umbo, with high spatial resolution of about 10 µm. In this study, we use tonal sound from the ear canal side to drive the TM while measuring the displacement amplitude and phase along the manubrium. Preliminary results suggest the motions of the manubrium of the human TM produced by ear canal acoustic stimuli are frequency dependent. A simple rotation-like motion of the manubrium with an axis superior to the LPM dominates at low frequency, while the motion of the manubrium becomes more complicated at frequencies above a few kHz, with a combination of rotation, translation and bending-like motions observed. We will examine at what degree the simple ossicular lever with a fixed axis-of-rotation can be supported by the data. We will also use Laser-Doppler vibrometry (LDV) to measure the motion of the medial surface of the manubrium to determine how tightly coupled the human TM surface is to the boney manubrium. Finally, we will investigate whether wave travel along the manubrium can account for a significant portion of the middle ear delay, as has been shown in gerbil (de La Rochefoucauld et al. 2010).

[Work supported by F32 & R01 from NIDCD and a donation from L. Mittal.]

52 The Effects of the Asymmetric Shape of the Tympanic Membrane on the Asymmetry of Ossicular Displacements for Positive and Negative Static Pressures

Willem F. Decraemer¹, Nima Maftoon², Joris J.J. Dirckx¹, W. Robert J. Funnell²

¹University of Antwerp, ²McGill University

The inward and outward displacements of the middle ear ossicles (umbo, lenticular process of the incus, stapes head and footplate) have been found to be significantly asymmetric for positive and negative pressures across various species (human: Hüttenbrink, Kobrak; human, cat, gerbil: Dirckx). In most cases the umbo displacement, for example, was about twice as large for negative as for positive pressures in the ear canal. In a paper on tympanic membrane (TM) displacement for static over- and underpressures at different stages of dissection of the middle ear in gerbil temporal bones (Dirckx and Decraemer, Hear. Res. 157, 2001,) it was shown that the asymmetry was unchanged when the cochlea, stapedial ligament, stapes and tensor tympani were removed consecutively. The malleus-incus (M-I) complex is attached to the TM at the manubrium and it is elastically suspended in the middle-ear cavity. The anterior mallear process makes close contact with the cavity wall and the incudal short process is connected to the cavity wall in a tightly enclosing niche, the incudal fossa, by means of a thick ligament. None of these connections seem to be prone to strong asymmetry in their elastic behavior so the asymmetry in the TM-M-I system presumably originates elsewhere. The TM itself has a strong inward and outward asymmetry in its shape, which forms an inward directed cone with outward bulging surfaces of its pars tensa. Using a non-linear finite-element model study of middle ears with dislocated stapes for human, cat and gerbil, we explore the effects of the peculiar shape and curvature of the TM on the asymmetry of the middle ear response (volume displacement of the TM, displacement of the umbo and of the lenticular process) when large positive and negative static pressures are applied.

Keywords: gerbil, tympanic membrane, asymmetry, static pressure, deformation, non-linear finite-element modeling

53 Test of "Biological Gear" in the Human Middle Ear Through FE Analysis

Hongxue Cai¹, Ryan Jackson², Charles Steele¹, Sunil Puria^{1,3}

¹Department of Mechanical Engineering, Stanford University, ²Department of Bioengineering Engineering, Stanford University, ³Department of Otolaryngology-HNS, Stanford University

A mammal's ability to hear high-frequency sound is due to unique structures found in their hearing organs, such as radial and circumferential collagen fibers in the eardrum, and three distinct middle-ear (ME) ossicles. In larger mammals such as human, the ME features a cylindrical malleus cross section, differing eardrum areas on each side of the malleus handle, and a mobile saddle-shaped malleus-incus joint (MIJ). These three features favor the existence of a "twisting" motion of the malleus-incus complex in addition to the classical hinge-like motion. We argue that this twisting motion is necessary for efficient high-frequency sound transmission in larger mammals, due to higher moments of inertia (MOI) for hinge-like motion in these species. To test this hypothesis, the motion modes of human middle-ear structures were investigated using finite-element (FE) analysis. Our current FE model, including the ear canal, eardrum, ossicles (malleus, incus, and stapes), suspensory soft attachments, and ME joints, was based entirely on a 3D reconstruction of micro-CT images. The MIJ and incus-stapes joints were modeled as mobile and fluid-filled by assigning complexvalued Young's moduli. Frequency responses of acousticsstructure interactions were calculated using COMSOL Multiphysics solvers. Our results indicate that at low frequencies hinge-like motion is dominant, as expected, and that the orthotropy of the eardrum boosts the ME gain due to increased peak displacement. However, at high frequencies we observe multi-resonance vibration modes at the eardrum and a bevel-gear-like motion at the MIJ, and the orthotropy of the eardrum makes the rotation axis of the malleus more coincident with its long axis. This supports the hypothesis that a twisting motion of the malleus and incus is required in larger mammals at high frequencies in order to compensate for higher MOI due to larger ossicular masses. [Work supported in part by grant No. R01 DC05960 and ARRA supplement from the NIDCD of NIH]

54 Influence of Ear Canal Morphology on Measures of Reflectance and Transmission

Richard D Rabbitt^{1,2}, Natalie Souza³, Ronald Miles⁴, Jonathan H. Siegel^{3,5}

¹Dept. of Bioengineering, University of Utah, ²Marine Biological Laboratory, ³Roxelyn and Richard Pepper Dept. of Comm. Sci. and Disord, Northwestern Univ., ⁴Dept. of Mechanical Eng., SUNY Binghamton, ⁵Hugh Knowles Center

The use of a Thévenin-equivalent calibrated probe sealed in the ear canal is becoming more common and enabling direct wideband measurement of the input impedance Z to the ear. In addition to the direct information Z provides about middle ear function, Z is also important because it has the potential to eliminate challenges caused by variations in probe insertion depth, standing waves, and ear canal resonances. Using Z, 1D acoustic theory is commonly applied to separate the forward pressure wave (FP) traveling toward the tympanic membrane from the reverse pressure wave (RP) traveling toward the concha. The ratio of the two waves is the reflection coefficient (R=RP/FP) and the subtraction is the transmitted pressure (TP, corrected to reference area A) delivered to the cochlea. Based on conservation of energy, R should be the same independent of the location in the ear canal where the measurement is made. 3D acoustic theory supports this expectation, but also indicates that computing R from Z and 1D theory will introduce an artifact due to the non-uniform morphology of the canal. To test this predicted sensitivity to morphology, we measured R and TP at different locations in non-uniform physical models and in human ear canals. Results show position sensitivity when R is estimated from Z in non-uniform canals, but show constant values along the length in the same ears when estimated using a method that accounts for the morphology. [Supported by NIH R01DC004928 (Rabbitt), and R01 DC008420 and Northwestern Univ. (Siegel and Souza)]

55 Dynamic and Quasi-Static Mechanical Properties of Human Ear Tissues

Rong Z. Gan¹, Xiangming Zhang¹, Don Nakmali¹ ¹School of Aerospace and Mechanical Engineering and Bioengineering Center, University of Oklahoma

The mechanical properties of soft tissues in the ear change in various middle ear diseases and affect the transmission of sound and sense of hearing. However, the mechanical properties of ear tissues are largely unknown due to the extremely small size, irregular shape, and limitation of measurement tools. This paper reports our studies on measuring ear tissue mechanical properties in the recent years with a focus on dynamic properties of the tissue over auditory frequencies. Using the material testing system (MTS) and digital imaging correlation (DIC) method, we measured the quasi-static properties of the human tympanic membrane, stapedial tendon, tensor tympani tendon, anterior malleolar ligament, and the most recently, the stapedial annular ligament and incus-stapes joint. The nonlinear stress-strain relationship and stressrelaxation function were characterized for each tissue. To investigate dynamic properties of the tissue over frequency domains, three measurement techniques: the split Hopkinson tension bar, acoustic driving with laser Doppler vibrometry, and dynamic mechanical analyzer (DMA) with frequency-temperature trade-off method, are developed in our lab and used for measuring ear tissues including the tympanic membrane, stapedial annular ligament, and round window membrane. The standard linear model was employed to describe the constitutive behavior of the tissue. The relaxation modulus in time domain and complex modulus in frequency domain were determined. The mechanical properties of middle ear tissues obtained through a series of studies provide important data for modeling the human ear and advancing our knowledge in biomechanical behavior of the ear. (Supported by NIH R01DC006632)

56 Interactive Computer Model of the Eardrum for Training in Myringotomy

Andrew K. Ho¹, Hussain A. Alsaffar^{1,2}, Philip C. Doyle¹, Sumit K. Agrawal^{1,2}, **Hanif M. Ladak**¹ ¹The University of Western Ontario, ²London Health

Sciences Centre

Myringotomy is a common surgical procedure in which an incision is made in the eardrum, primarily to treat ear infections. It is the first ear operation that Otolaryngology surgical residents learn and numerous mistakes are made during training. A virtual-reality myringotomy simulator is being developed to provide an alternative training approach to operating on patients. The current simulator indicates incisions with a line on a flat, static digital image of an eardrum. Experienced surgeons have indicated that it is important to model the 3-dimensional shape, deformation and cutting of the eardrum for proper training. A virtual eardrum that represents the true shape of a human eardrum and supports interactive cutting has been created. The eardrum model uses mass-spring simulation to predict deformations. In the mass-spring (MS) method, the surface to be modeled is represented by a mesh of

elements in which nodes of each element are connected by springs, rather than by a surface as in the finite-element (FE) method. The MS model's deformation characteristics compare well to an FE model of the same eardrum. Three algorithms for cutting of the MS model were implemented. The "element-removal" algorithm is the simplest and involves deleting elements of the MS model that are contacted by the virtual blade. In the "Delaunay" algorithm, elements of the MS mesh are split and reconfigured so that the mesh satisfies the Delaunav mesh-quality criterion. A novel "direction-prediction" algorithm was also developed to overcome the initial delay in starting a cut that is experienced with the Delaunay algorithm. The realism of each of these algorithms was assessed and compared by 8 staff Otolaryngologists and 4 senior residents using a questionnaire. The Delaunay algorithm was perceived to be the most realistic. Initial delays in starting the Delaunay cutting algorithm can be overcome by combining it with our novel direction-prediction algorithm.

57 Effect of Middle-Ear Pathology on Non-Invasive Measures of Middle-Ear Status in a Temporal Bone Preparation

Gabrielle R. Merchant^{1,2}, Mohamad A. Hamade^{1,3}, Lorice Mahfoud^{1,3}, Christopher Halpin^{1,4}, Hideko H. Nakajima^{1,3}, Saumil N. Merchant^{1,3}, John J. Rosowski^{1,3}

¹Eaton-Peabody Laboratory, Massachusetts Eye and Ear Infirmary, ²Speech and Hearing Bioscience and Technology, Harvard-MIT Division of Health Sciences and Technology, ³Department of Otology and Laryngology, Harvard Medical Schoo, ⁴Department of Audiology, Massachusetts Eye and Ear Infirmary

Currently, the diagnosis of various middle-ear pathologies prior to operative exploration is limited in patients with an intact tympanic membrane and an aerated middle ear. Although widely available, single-frequency tympanometry cannot differentiate most middle-ear pathologies This project aims to explore two multiaccurately. frequency measures of middle-ear mobility, which may aid in pre-operative differential diagnoses of middle-ear disorders. Prior work has found that the first measurement, determination of umbo velocity (UV) by laser-Doppler vibrometry, is effective in differentiating between a variety of conductive disorders; however this measurement is generally not available for clinical use. Energy Reflectance (ER) is a simpler measurement that can be made relatively easily with a device that was recently approved by the FDA, but it has not vet been established if this technique can differentiate between various conductive pathologies. Using a temporal bone preparation, we investigate the effect of middle-ear pathology on these diagnostic techniques. Measurements have been made in five preparations, each of which has been manipulated to mimic pathologies including stapes fixation, malleus fixation, and ossicular discontinuity. Our data will be compared to UV and ER measurements that have been made in normal subjects and patients with various conductive pathologies including ossicular fixations, ossicular discontinuities. and semicircular-canal

dehiscence (see Hamade et al, this meeting). This work was funded by NIDCD/NIH.

58 Energy Reflectance and Laser Doppler Vibrometry: Non-Invasive Tools to Diagnose Middle-Ear Pathologies

Mohamad Hamade^{1,2}, Gabrielle Merchant^{1,3}, Lorice Mahfoud^{1,2}, Christopher Halpin^{2,4}, Hideko Nakajima^{1,2}, Saumil Merchant^{1,2}, John Rosowski^{1,2}

¹Eaton-Peabody Laboratory, Massachusetts Eye and Ear Infirmary, ²Department of Otology and Laryngology, Harvard Medical School,³MIT-Harvard Division of Health Sciences and Technology: SHBT, ⁴Department of Audiology, Massachusetts Eye and Ear Infirmary

Other than standard single-frequency tympanometery, the measurement of middle-ear mobility to aid in the diagnosis of middle-ear disease is not common. Here we compare two multi-frequency techniques that are in use for this purpose. Laser-Doppler Vibrometry, to measure umbo velocity, is a research tool that has been demonstrated to be effective in separating out various conductive disorders, but is as yet unavailable for use in the general clinic. Energy Reflectance is an acoustic measurement that is easy to perform and that is FDA approved for general clinical use. We use measurements in the large clinical population at the Massachusetts Eye and Ear Infirmary to compare the efficacy of these techniques in the diagnosis of various conductive disorders. After determining normal standards from a large population of normal ears, we have begun making measurements in patients with hearing loss. In each ear, we measure umbo velocity using a customized Polytec HLV and energy reflectance using Mimosa Acoustics HearID systems. So far, we have tested 113 ears from 60 patients with pathologies that include ossicular fixations, ossicular discontinuities and others. We will present preliminary comparisons of the efficacy of the two techniques in the identification of hearing pathology.

59 Mapping Vibrations of Tympanic Membrane in Ears with OME and AOM

Chenkai Dai^{1,2}, Xiying Guan³, Don Nakmali³, Rong Z. Gan³

¹Bioengineering Center and School of Aerospace and Mechanical Engineering, University of Oklahoma, ²School of Medicine, Johns Hopkins University, ³Bioengineering Center and School of Aerospace & Mechanical Engineering, University of Oklahoma

Mapping vibration change patterns of tympanic membrane (TM) is a potential approach to solve one of major challenges for otologists: to discriminate ear infection (e.g., acute otitis media, AOM) and inflammation (otitis media with effusion, OME). We hypothesize that mechanical changes among four quadrants of the TMs induced by TM tissue change and middle ear fluid, which vary in AOM and OME, are different. We further hypothesize that the change of TM motion in four quadrants due to spread infection in AOM ears are more equivalent than that in OME ears, which are mainly affected on inferior part of the TM by mass loading of the middle ear fluid. To test these hypotheses, we create AOM and OME models by

inoculating the left ear of guinea pig with Streptococcus pneumoniae (ATCC 6303) and lipopolysaccharide into the middle ear, respectively, and measured the ΤM movements in response to sound (0.2 - 20 kHz) at different quadrants of the tympanic membrane using a laser vibrometer. The results show that the attenuations of TM vibration on four quadrants were slightly different in AOM ears while the significant differences were observed in ears with OME. Different phase changes of TM movement were also found between AOM and OME ears. These results suggest that the change of TM vibration in response to sound between the AOM and OME may be mapped by the multipoint mechanical measurements with laser vibrometer. (Work supported by OCAST HR09-033 and NIH R01DC006632)

60 3D Finite Element Modeling Analysis on Surgical Implantation and Function Characterization for Implantable Hearing Devices

Xiangming Zhang¹, **Rong Z. Gan¹** ¹University of Oklahoma

A 3D finite element (FE) model of the human ear consisting of the external ear canal, middle ear, and cochlea was constructed from histological sections of a human temporal bone. The spiral cochlea connected to the footplate at the oval window and to the middle ear cavity at the round window, had two and half turns. The space inside the cochlea was divided by the basilar membrane and Reissner's membrane into three chambers: the scala tympani, scala media and scala vestibule, and filled with viscous perilymphatic fluid. The material properties of the middle ear soft tissues, such as the tympanic membrane, ligaments, joints, and round widow membrane, were obtained from the material tests completed in our lab (details can be found in another ARO paper reported by Gan et al.). After validation of the FE model with experimental measurements in human temporal bones, the model was used for investigating the relations between surgical implantation methods and functions of the middle ear implants and cochlear implants for restoration of hearing. The studies include: 1) efficiency of forward mechanical driving with different actuators attached to the ossicles; 2) efficiency of reverse mechanical driving with actuators placed on the round window membrane; 3) combined electro-acoustic stimulation of cochlear implants for conservation of residual hearing level. The FE modeling results include the middle ear transfer function induced by active implantable devices and cochlear function in terms of basilar membrane vibrations. These data are useful for optimizing the design of implantable hearing devices in correlation with surgical procedures. (Supported by NIH R01DC006632)

61 Conductive Hearing Loss Induced by Experimental Middle Ear Effusion in a Chinchilla Model Reveals Impaired TM-Coupled Ossicular Chain Movement

Keely Chevallier^{1,2}, Jennifer Thornton^{1,3}, Kanthaiah Koka¹, James Eric Lupo⁴, Kristin Uhler⁴, Daniel Tollin^{1,3} ¹Dept of Physiology and Biophysics, University of Colorado Denver, School of Medicine,²University of Colorado, Denver, School of Medicine, MD Training Program, ³Neuroscience Training Program, University of Colorado Denver School of Medicine, ⁴Dept of Otolaryngology, University of Colorado Denver, School of Medicine Otitis media with effusion (OME) causes a conductive hearing loss (CHL) of up to 30 dB, but the exact cause of this hearing loss remains unknown. Possible causes include: altered compliance of the tympanic membrane (TM), inefficient movement of the ossicles, decreased compliance of the oval window-stapes footplate complex, or dyssynchronous input to the oval and round window due to conduction of sound energy through middle ear fluid. In this study, tympanometry, laser Doppler vibrometry, and cochlear microphonics (CM) were measured to study the contribution of changes in TM motion and umbo velocity (Huv) to CHL caused by middle ear fluid in the chinchilla. Huv and CM as a result of sinusoidal tone pip stimuli (125 Hz-14 kHz) were measured simultaneously before and after filling the middle ear with different volumes (0.5 - 2.0 ml) of silicone oil (viscocity, 350 cSt). As a function of increasing stimulus level, the mean slopes of the CM amplitudes (μ V/dB) and Huv (mm/s/dB) were ~1 and consistent across all conditions. Concurrent increases in CM thresholds and decreases in Huv were noted after the middle ear was filled with 1 mL of fluid. Across animals, completely filling the middle ear with fluid caused a 20-40 dB increase in CM thresholds and 15-30 dB attenuation in Huv, with a significant correlation (0.98) between the increase in CM thresholds and the decrease in Huv. Clinic-standard 226-Hz tympanograms were insensitive to fluid-associated changes in CM thresholds until the entire middle ear cavity had been filled (~ 1.5 ml) in contrast to higher frequency tympanograms which were more In general, tympanometric findings lagged sensitive. behind evidence of CHL based on CM thresholds. The attenuations (20-40 dB) observed in the current study are similar to the CHL (~30 dB) due to OME in humans. The changes in Huv, CM thresholds, and tympanograms due to experimentally-induced OME suggest CHL arises secondary to impairment of TM and TM-coupled umbo motion.

62 Effect of Unilateral Conductive Hearing Loss on the Amplitudes and Phases of the Cochlear Microphonic During Bone Conduction: An Experimental Investigation of the Classic Weber Test

Blake J. Hyde¹, J. Eric Lupo², Kanthaiah Koka³, Daniel J. Tollin³

¹University of Colorado Denver, School of Medicine, ²Department of Otolaryngology, University of Colorado Denver, School of Medicine, Aurora CO, USA, ³Dept. Physiology and Biophysics, University of Colorado Denver, School of Medicine

Various theories exist as to the physiologic basis of perceived sound lateralization to a unilateral conductive hearing loss (CHL) during the Weber Test. Different theoretical mechanisms surrounding how low frequency bone conduction affects both interaural timing differences (ITD) and interaural level differences (ILD) have been To date, studies have examined either implicated. amplitude and/or phase changes by measuring the cochlear microphonic (CM) responses predominately with occlusion of the external ear canal (the occlusion effect). Furthermore, previous work has proposed that the degree of perceptual lateralization should be proportional to the dearee of CHL. To further explore the reasons for lateralization of bone conducted sound in unilateral CHL, varying degrees of experimentally-induced CHL in the Chinchilla lanigera were employed to study both amplitude and phase recordings of the CM before and after various types of CHL were induced. Acoustic and bone conducted stimuli were delivered across a range of frequencies (0.25-8 kHz, pure tones) and amplitudes. CM thresholds to acoustic stimulation were attenuated in 7 ears by 10-60 dB as a function of the experimentally-induced CHL interventions as compared to baseline acoustic stimulation. However, there were no significant differences in bone conducted CM thresholds between baseline and CHL conditions for any of the test frequencies. Although varying degrees of CHL were confirmed acoustically (i.e., attenuation), the degree of CHL did not produce consistent effects across animals in CM levels or phase in response to bone conducted stimulation. A variety of explanations will be discussed regarding why the physiologic bases for the Weber Test were not found in our experimental paradigm.

63 A Mouse Model for Reversible Conductive Hearing Loss During Early Postnatal Development

John H. Thompson¹, Jonathon P. Whitton^{1,2}, Sara B. Anastas¹, Daniel B. Polley^{1,3}

¹Eaton-Peabody Laboratory, Mass Eye & Ear Infirmary, ²Harvard-MIT Division of Health Sciences and Technology, ³Harvard Medical School

Otitis media (OM) is the most commonly diagnosed childhood illness in the US. While the conductive hearing loss (CHL) associated with OM typically resolves in early childhood, the adverse effects of developmentally degraded hearing on auditory perception can persist for

A recent study characterized neural many years. correlates of these persistent auditory deficits in a rat model where the auditory meatus was ligated for an extended time period and then reopened prior to neurophysiological recordings (Popescu and Polley, 2010). Although effective for creating stable CHL, ligation removal was an acute procedure, which prevented us from characterizing the stability of reorganization over a period of time following the reinstatement of normal hearing. The present studies describe the development of a mouse model for short-term non-invasive developmental CHL. Unilateral CHL was induced in CBA/CAJ mouse pups (P14-21) using one of three methods: 1) filling the tympanic cavity with high viscosity silicone oil, 2) filling the tympanic cavity and meatus with Fibrin Sealant and 3) blocking the meatus with an earplug. Levels of peripheral hearing loss were tracked daily with auditory brainstem response (ABR) and distortion product otoacoustic emissions (DPOAE) in manipulated and healthy ears. All methods induced short-term CHL that was more complete at high frequencies (> 11 kHz) than low. DPOAE amplitudes decreased by an average of 84/85% and then recovered to 59/83% of normal over a period of 7 days following silicone oil or Fibrin Sealant injections, respectively. By contrast, DPOAE amplitudes returned to 99% of normal within 2 days following earplug removal. Ongoing studies are examining changes in ABR amplitude and threshold for each CHL method. Future studies will vary the age of CHL and neurophysiological recordings to further explore the potential contribution of maladaptive plasticity to the perceptual sequelae brain of developmental CHL.

64 Middle-Ear and Cochlear Responses in Aging Animals: A Neural, Mechanical and Morphological Study

Diana Turcanu¹, Ernst Dalhoff¹, **Anthony W. Gummer¹** ¹University Tuebingen

Hearing loss with advancing age in guinea pigs has been attributed in many studies to age-related inner-ear pathology. Nevertheless, two studies have shown that middle-aged and old guinea pigs suffer from conductive hearing loss. Using a laser Doppler vibrometer to measure the vibrations of the umbo and the stapes, together with evaluation of neural threshold using compound action potential (CAP) threshold tuning curves and imaging of the temporal bone using high-resolution X-rav microtomography (micro-CT), we investigated the possibility of middle- and inner-pathologies in aging animals. Vibration measurements were performed on the umbo and the stapes of young (3-5 months) and aging (1-3 years) guinea pigs. Vibration measurements were made of the frequency responses of the umbo and stapes. followed by vibration distortion product otoacoustic emissions (DPOAEs). Hearing loss, found in 14 of the 18 aging animals, was accompanied by reduced vibration amplitudes (6-42 dB). The mechanical losses were more pronounced below 4 kHz. The slopes of the DPOAE inputoutput (I/O) functions proved to be less steep by a factor of about 4-6 than in the control animals, indicating middleear pathology. There was concomitant loss of CAP thresholds, such that the neural losses could be attributed to middle-ear pathology. Three animals showed normal neural and middle-ear vibration responses and one animal signs of inner-ear pathology. Micro-CT of the temporal bone showed fixation of the malleus-incus complex (especially malleus head) to the walls of the bulla; fixation of the stapes was seen only in extreme cases, whereas stapes footplate was not affected in any stage. These findings indicate fixation of the malleus-incus complex in 78% of the aged guinea pigs in our breeding colony. Therefore, aging guinea pigs might not be suitable as a model for studying age-related inner-ear changes, but rather for studying fixation of the malleus-incus body to the walls of the middle-ear.

65 Sensitivity of Non-Mammalian Prestins on Membrane Thickness

Chisako Izumi¹, Jonathan Bird¹, Kuni Iwasa¹ ¹*NIDCD*

Prestin is important for mammalian hearing by generating force in outer hair cells by changing the membrane area in response to receptor potential. Previously we changed the thickness of plasma membrane by perfusing with gammacyclodextrin, which are loaded with phosphatidylcholines with various hydrocarbon chain lengths, and showed that mammalian prestin is sensitive to membrane thickness. A reduction in membrane thickness led to a positive shift in the operating point of the membrane potential at which charge transfer associated with motile response takes place. The shift observed was very large and up to 150 mV. An increase in membrane thickness had the opposite effect. On average shifts were about 6 mV for 1% change in thickness. This result was interpreted as an indication that conformational change of prestin, namely the conformation with larger membrane area has thinner hydrophobic area that faces lipid bilayer. In the present study, we examined whether or not non-mammalian prestins are also sensitive to membrane thickness. We found that the membrane thickness dependence of platypus prestin was quantitatively similar to that of mammalian prestin. However, chicken prestin did not show systematic membrane thickness dependence. These results demonstrate that chicken prestin does not undergo conformational changes that are similar to those in mammalian or platypus prestin. These findings are therefore consistent with the presence of mechanoelectric coupling in platypus prestin and the absence of such coupling in chicken prestin.

66 In Vivo Prestin Labelling in a Knockin Mouse

Tetsuji Yamashita¹, Jie Fang¹, Anders Fridberger², Jian Zuo¹

¹St.Jude Children's Research Hospital, ²Karolinska University Hospital

Prestin is essential for outer hair cell (OHC) electromotility and cochlear mechanical amplification that contributes to remarkable hearing sensitivity in mammals. Although prestin function can be explained by its voltage-dependent conformational change within OHC lateral membrane, it remains to be investigated how prestin creates the OHC electromotility.

In this study, we created prestin-mvYFP (monomer venus YFP) knockin mice where mvYFP is fused with prestin at the C-terminus. The knockin mice were viable and displayed no detectable behavioural abnormalities. Hearing sensitivities in $prestin^{mvYFP/+}$ mice were indistinguishable from wild type controls between 4 and 22 kHz at 1 month, suggesting that prestin-mvYFP is functional in the low-to-middle frequency range. In 20 day old prestin^{mvYFP/+} and 21 day old prestin^{mvYFP/mvYFF} cochleae, bright mvYFP signals were observed only at lateral walls of all OHCs where prestin is specifically expressed. No YFP signals were observed at both top and bottom of the OHCs. YFP signals were brighter at basal turn than that at apical turn in 5 day old *prestin^{mvYFP/+}* and *prestin^{mvYFP/mvYFP}* cochleae. The YFP signals were distributed at apical pool of the OHCs. Therefore, the mvYFP distributions recapitulate those of prestin during development as well as at adult stages in cochleae. No YFP signals were observed in 20 day old prestin^{mvYFP/+} vestibular systems, sperms, and 21 day old prestin^{mvYFP/mvYFP} vestibular systems. Hence, prestinmvYFP knockin mice provide a powerful tool to analyze protein behaviour in live OHCs as well as biochemical properties of prestin in vivo.

This work is supported by the ALSAC and NIH grants DC006471, DC008800, and CA21765.

67 Creation of a Novel Pendrin Protein with Both Transporter and Motor Functions

Jie Tang¹, Xiaodong Tan¹, Jason Pecka¹, Kirk Beisel¹, David He¹

¹Creighton University

Pendrin (SLC26A4) is a membrane transporter capable of exchanging anions between the cytosol and extracellular fluid. Deleterious mutations in pendrin causes either DFNB4 with enlarge vestibular aqueduct or Pendred syndrome, an autosomal recessive disorder characterized by sensorineural hearing loss. Prestin (SLC26A5) is the membrane-bound motor protein of cochlear outer hair cells (OHCs). Pendrin and prestin both belong to a distinct anion transporter family called solute carrier protein 26A (SLC26A). While other SLC26A family members are transporters, prestin functions as a voltage-dependent molecular motor with the capability to perform rapid electromechanical and mechanoelectrical conversion on a microsecond time scale. We identified a segment of 11 residues in prestin that is critical for its unique motor function. To determine whether it was possible to create a novel pendrin protein with both transporter and motor functions, we substituted the corresponding residues in human pendrin with those from gerbil prestin. Two essential electrophysiological properties representing the prestin-like cellular motor were measured from chimeric pendrin-transfected HEK cells. Nonlinear capacitance (NLC), which reflects electromotility-related charge displacement in transfected cells, was measured using voltage-clamp technique. Voltage-evoked cell motion was

examined by a photodiode-based displacement measurement system. Transport function was determined by conventional radioisotope uptake technique. We show, for the first time, that domain swapping from gerbil prestin was able to convert pendrin into a voltage-dependent motor that exhibits gating current and somatic motility. These are hallmarks of the prestin motor. The gain of motor function is not to the detriment of its transport function. Thus, this novel chimeric protein is capable of both transporting anions and generating force and confirms the identification of an electromotility motif.

68 Motor Characteristics of Outer Hair Cells Derived from V499G/Y501H Prestin

Heterozygous Mice

Kazuaki Homma¹, Khurram Naik¹, Mary Ann Cheatham¹, Peter Dallos¹

¹Northwestern University

V499G/Y501H prestin (499-prestin) has very little motor activity under physiological conditions although it is properly inserted into the basolateral membrane of outer hair cells (OHCs), thereby providing normal stiffness and morphology to the cells. Hence, the mouse model expressing 499-prestin has served as an appropriate model for demonstrating the necessity of prestin motor activity for normal hearing in mammals (Dallos et al., 2008).

Interestingly, we found that young 499 heterozygous (499het) mice, which have wild-type prestin (wt-prestin) and 499-prestin genes, show normal compound action potential (CAP) thresholds and tuning functions although the expression of wt-prestin in 499het OHCs is ~50% of that derived from wild-type OHCs.

To understand the normal hearing of young 499het mice with significantly reduced expression of wt-prestin, we examined nonlinear capacitance (NLC) and electromoltility of isolated 499het OHCs, and compared the results to those of wt OHCs. We found that 499-prestin and wtprestin can form functional prestin heteromers, and that the mechanoelectric coupling efficiency of 499het OHCs is ~150% of that of wt OHCs. The greater mechanoelectrical coupling efficiency of 499het is associated with a statistically significant change in alpha. Although this parameter change in NLC provides greater electromotility, there is still a small deficit to overcome in order to explain the normal CAP thresholds/tuning of 499het mice. We argue that this discrepancy is overcome in vivo by efferent feedback regulation that keeps the amplifier gain at an optimal level, below the attainable maximum, under normal conditions. The possibility suggests that the amplifier in wt mice is not working at full efficiency in order to maintain stability and avoid oscillation. [Supported by NIH Grant DC00089 and the Hugh Knowles Center].

69 Homology Modeling of Prestin 2: The STAS Domain

Benjamin Currall¹, Kate Dempsey², Heather Smith¹, Hesham Ali², Richard Hallworth¹

¹Creighton University, ²University of Nebraska - Omaha Despite extensive study, it is still unclear how prestin performs its remarkable motor function. Understanding of prestin function would be greatly aided by high resolution structural models of the protein, but, so far, prestin structure remains unresolved. In part 2 of this 2 part poster, the sulphate transporter and anti-sigma factor antagonist (STAS) domain is examined. HHPred analysis of the STAS domain reveals that the STAS domain shares little homology with the rest of its ATP-Grasp clan members. Secondary structure analysis reveals a conserved $\beta 2$, $\alpha 1$, $\beta 3$, $\alpha 2$, $\beta 4$, $\alpha 3$ folding. Motif finding software and a novel Post Alignment Identity Matrix algorithm identifies conserved regions including $\beta 2$, $\beta 4$, and a DSSG motif. Homology modeling of the STAS domain against the Thermotoga maritima STAS domain solved structure (2KA5) reveals a tertiary structure similar to other ATP-Grasp family members. Mutations of the putative phosphorylation site in the DSSG motif, were analyzed by non-linear capacitance, to measure function, and Förster resonance energy transfer, to measure structure. The DSSG mutations caused significant change to both prestin function and structure. Based on the mutational analysis, structural models, and evolutionary relationships, we propose that the STAS domain serves as an 'NTP gate' that regulates prestin function.

Supported by N.S.F.-E.P.S.Co.R. EPS-0701892, N.C.R.R. (N.I.H.) P20 RR16469, C06 RR17417-01

70 Membrane Prestin Expression Correlates with Magnitude of Prestin-Associated Charge Movement

Michelle L. Seymour¹, Lavanya Rajagopalan^{2,3}, Matthew J. Volk², Haiying Liu¹, William E. Brownell², Fred A. Pereira^{1,2}

¹Huffington Center on Aging and Molecular and Cellular Biology, ²Bobby R. Alford Department of Otolaryngology -Head and Neck Surgery, Baylor College of Medicine, ³W.M. Keck Center for Interdisciplinary Bioscience Training, Houston

Prestin, a protein expressed in the lateral wall of cochlear outer hair cells (OHCs), is known to be both necessary and sufficient for OHC electromotility, generation of non-linear capacitance (NLC), and normal mammalian hearing. Since increasing membrane expression of prestin parallels the maturation of OHC electromotility, we investigated the conventional assumption that the level of prestin membrane expression directly correlates with prestinassociated electromotility and charge movement. Using an inducible prestin-expressing cell line, we show that the magnitude, but not the peak, of prestin-associated charge movement (charge density) does directly correlate with the amount of prestin in the plasma membrane. This correlation is evident in studies involving both time-course of induced prestin expression and inducer dose-response. Conversely, removal of the inducer results in a gradual,

concurrent decline in magnitude of prestin-associated charge movement and in membrane levels of prestin. In summary, we have demonstrated that prestin-associated charge movement directly correlates with the level of prestin expression in this inducible prestin-expressing cell line. This study also suggests that the maturation of NLC during OHC development involves two distinct aspects: the increase in the magnitude of NLC, which seems to directly reflect increases in membrane expression of prestin during development, and the shift of the peak of NLC, which does not appear to be affected by changing membrane levels of prestin expression.

This work was funded by DC00354 (NIDCD; to WEB and FAP), DC008134 and DC009622 (NIDCD; to FAP), and NIH/NIA 5T32 Training Grant AG00183 (MLS).

71 Prestin Affects Cholesterol Content of SF9-Cell Plasma Membrane

Chongwen Duan¹, Jessie Chen¹, Tareishap Dunlap¹, Peter Dallos¹, Jing Zheng¹

¹Northwestern University

Prestin is the motor protein of outer hair cells (OHCs) that drives OHCs' electromotility. In the prestin-KO mouse model, OHCs were shorter than normal, and progressive OHC death was observed. In order to eliminate potential deleterious effects due to the anatomical change, a new prestin-knockin mouse model (499-KI) was created. Mice (499-KI) carry a V409H/Y501H mutation in which prestin loses >90% of its motile function but retains its ability to target the plasma membrane. The 499-KI mice lack cochlear amplification just as the prestin-KO do but without changes in OHC length, stiffness or forward transduction (Dallos, et al., 2008). However, progressive OHC death was still found in the 499-KI mice. To restate: OHCs that lack prestin, as well as OHCs that lack fully functional prestin show significant cell death compared to their wt littermates or mice expressing altered but functional prestin. In order to understand the causes of OHC death in different prestin mouse models, three stable SF9 cell lines that can continually synthesize either GFP tagged WT-prestin, 499mut-prestin, or a blanket vector, were established. Because cholesterol contents in the plasma membrane can significantly affect OHC function and survival, cholesterol concentrations in these cell lines. as well as in non-transfected cells, were measured by both colorimetric assay and Filipin labeling. Western blot and GFP fluorescence density were used to measure prestin and other protein concentrations among different cell lines. Our results showed that these three cell lines have different cholesterol contents. WT-prestin-expressing cells have the lowest cholesterol concentration. We are further investigating the relationships among cell death, prestin structure and cholesterol (Work supported by NIH Grants DC00089 and DC010633).

72 Chloride Flux in Prestin-Expressing Cells

Sheng Zhong¹, Shumin Bian¹, Dhasakumar Navaratnam¹, Joseph Santos-Sacchi¹

¹Yale University School of Medicine

In prestin-expressing cells, intracellular Cl⁻ ([Cl⁻]_i) flux plays a preeminent role in promoting prestin activity, especially since the resulting V_h shift in prestin's state-probability function (measured as a nonlinear capacitance-NLC) along the V_m axis will effect a motile response. We are interested in uncovering mechanism(s) underlying [Cl]_i flux near prestin. Previous attempts to monitor chloride flux in transiently transfected cells under perforated patch clamp were hampered by poor signal (NLC) to noise issues. Using a stable prestin-expressing HEK cell line with high prestin expression levels we are able to overcome this problem. Under perforated patch clamp with local perfusion, changing extracellular CI⁻ concentration from 1 mM to 140 mM using prestin's NLC as a measure of intracellular Cl⁻ indicated a several mM increase in Cl⁻ concentration. Treatment with 1 mM DIDS (a Cl⁻ channel blocker) indicated that CIC channels do not underlie the CI⁻ influx. Such Cl influx was also confirmed by MQAE fluorescence spectroscopy. We are still trying to determine whether Cl⁻ entry into these cells is mediated by prestinrelated or a prestin-independent mechanism.

In order to overcome MQAE deficiencies, we fused prestin with genetically encoded YFP CI-sensor (*FEBS Lett.*, 2001, 499, 220; J. Neurosci. Meth., 2008, 170, 67), so as to non-invasively determine [CI]_i flux near prestin in prestin-expressing HEK cells by simultaneously monitoring of fluorescence signals and non-linear capacitance by whole-cell recording. In addition, we are performing ratiometric imaging with CFP/YFP indicators. Preliminary results indicate that these methods will help define local CI flux near prestin's intracellular binding site.

(Supported by NIDCD DC00273 to JSS and NIDCD DC 008130 to JSS and DN)

TRANE AND ADD TO A STATE OF THE TABLE TO A STATE OF THE TABLE TO A STATE OF T

Ben Harland¹, Wen-han Lee¹, William Brownell², Sean Sun¹, Alexander Spector¹

¹Johns Hopkins University, ²Baylor College of Medicine Prestin is a membrane protein critical to outer hair cell (OHC) motility and active hearing in mammals. Electromotility is driven by changes in the membrane and the actual mechanism of potential, such electromechanical coupling involves a system of electric charges associated with the protein and the membrane, as well as ions inside and outside of the cell. The local electric field inside and in the vicinity of prestin is of fundamental importance to the understanding of the protein function. We simulate this electric field by taking into account the available experimental and modeling information on the involved electric charges, including the electric charge transferred by prestin, internal protein charges, membrane charges associated with the phospholipid head groups, and electrolytes outside the membrane. The position of the charge transferred by prestin is computed by solving a Fokker-Planck equation (Sun et al., 2009). The prestin

internal charges are determined on the basis of available versions of the prestin secondary structure (Fakler and Dallos, 2002; Bai et al., 2009). The resulting electrostatic problem is reduced to the numerical solution of a Poisson-Boltzmann equation under axisymmetric conditions. We obtain two- dimensional distributions of the electric potential and electric field inside and in the vicinity of prestin. In particular, we find the forces that act on the transferred charge by taking into account not only the external electric field but also the local electrostatic environment included in our model. In the AC+DC case, we compute the amplitude and phase of the local electric characteristics as functions of frequency of the externally applied field. The developed approach can be used in studies of prestin structure, ions involved in prestinassociated charge transfer, and effects of the membrane composition. Supported by research grants R01 DC 000354 and DC 002775 from NIDCD.

74 Cholesterol Alters the OHC Electromotility Via Regulating the Rigidity of the Membrane-Cytoskeleton Complex

Seiji Kakehata¹, Takahiko Nagaki¹, Michio Murakoshi², Hiroshi Wada², Rei Kitani¹, Hideichi Shinkawa¹ ¹*Hirosaki University,* ²*Tohoku University*

Cholesterol is a necessary component of biological membranes and regulates their fluidity and rigidity. Our preliminary studies showed that outer hair cells (OHCs) treated with M β CD or cholesterol exhibited changes in stiffness, capacitance and motility. Those results suggest that reconstruction of the cytoskeleton may be induced by M β CD or cholesterol. We also reported that intracellular signaling pathways involving G proteins may modulate the changes in voltage-dependent capacitance caused by M β CD or cholesterol.

Membrane capacitance of isolated guinea pig OHCs were assessed using a two-sine voltage stimulus protocol superimposed onto a voltage ramp (200 ms duration) from -150 to +140 mV. One group of OHCs was treated with $100\mu M$ GTP γ S, the GTP analog, administrated into the cell via patch pipettes. Another group of OHCs was internally perfused with $600\mu M$ GDP β S.

The effects of $M\beta$ CD were attenuated when GTP γ S was administered into the OHCs. On the other hand, the effects of cholesterol were attenuated when GDP β S was administered in to the OHCs. These results demonstrated that internally perfused GTP γ S inhibited the M β CD effects and GDP β S inhibited the cholesterol effects, suggesting that G proteins may be involved in the cholesterol mediate pathway.

To clarify the detailed mechanism between cholesterol and the OHC cytoskeleton, Young's modulus and the amount of filamentous actin (F-actin) of OHCs were measured. To investigate the rigidity of the lateral wall after M β CD treatment, Young's modulus was measured with an atomic force microscopy (AFM). The average Young's modulus in 1 and 3 mM M β CD incubated OHCs was 2.13±0.72 mN/m (n=6) and 5.21±0.79 mN/m (n=5), respectively, indicating that M β CD loading increases stiffness in a concentration dependent manner. The amount of filamentous actin (F- actin) of OHCs with/without M β CD was investigated by confocal laser scanning microscopy. The amount of F-actin increased by M β CD. These results suggest that M β CD structurally modifies OHCs so that they become stiffer due to an increase in the amount of F-actin.

Our results indicate that cholesterol alters the OHC electromotility via regulating the rigidity of the membranecytoskeleton complex, suggesting that not only modification of prestin but also of the surrounding lipid in the membrane affects cochlear amplification and hearing acuity.

75 Reduced Membrane Cholesterol Enhances Cochlear Electromechanics

William Brownell¹, Stefan Jacob², Pierre Hakizimana², Mats Ulfendahl², Anders Fridberger²

¹Baylor College of Medicine, ²Karolinska Institutet

Outer hair cell electromotility contributes to the electromechanical response of the cochlear partition. Prestin is a part of the membrane-based motor underlying outer hair cell electromotility and its function is altered by changing membrane cholesterol concentration. The mechanical response of the guinea pig cochlear partition to acoustic and/or electrical stimulation was measured in an excised temporal bone preparation. Measurements were made before and after depletion of membrane cholesterol with methyl-β-cyclodextrin (M_βCD) using laser interferometry and optical flow confocal microscopy. The electromechanical response in untreated preparations was asymmetric with greater displacements in response to positive currents. Perilymphatic perfusion with MBCD enhanced the electromechanical response and its asvmmetry. Sodium salicylate reversibly blocked the enhanced electromechanical response in cholesterol depleted preparations. Cochlear partition tuning and cochlear microphonics were similar before and after depletion. Cellular integrity was assessed with confocal imaging and in several preparations remained unchanged after several hours of exposure to M_βCD. Filipin labeling of the cochlea revealed the continued presence of membrane cholesterol in supporting cells. The enhanced electromechanical response reflects an increase in outer hair cell electromotility and may reveal features about membrane cholesterol distribution and trafficking in the outer hair cell.

Research supported by Swedish Research Council, the Wallenberg Foundation and grants NIH/NIDCD R01 DC000354 & DC002775.

The Three-Dimensional Structural Model of Mammalian Presin (SLC26A5) and the Identification of an Eleven Amino Acid Electromotility Motor Motif

Kirk Beisel¹, Sándor Lovas¹, Xiaodong Tan¹, Oseremen Okoruwa¹, Jason Pecka¹, Jie Tang¹, David He¹ ¹Creighton University

Prestin (SLC26A5) is the motor protein of mammalian cochlear outer hair cells with unique capability to perform direct, rapid, reciprocal electromechanical conversion.

Several models of the membrane topology are proposed but are insufficient to provide a cohesive account of all the site-mutagenesis, deletion and chimeric experimental results. Furthermore, no experimental crystallography data for any SLC26A protein exist. Thus, we used the pGenTHREADER and YASARA homology modeling techniques to predict the membrane topology and subsequently the three-dimensional (3D) structure of prestin. In order to analyze the sulfate transporter (SulpTP) domain, the sequences of prestin orthologs and paralogs were N- and C-terminally truncated to predict the 3D fold of the SulpTP region, which encompasses the hydrophobic membrane spanning domains. Using nine transporter proteins as templates YASARA predicted that the 3D fold of rat prestin SulpTP was similar to that of the glutamate/aspartate transporter, GltPh. Further refinement of the SulpTP structure using Molecular Dynamics simulation showed similar conformational characteristics to that of GLTPh in both movement and potential speed. Using the combined approaches of comparative genomic, evolution, structural diversification and the predicted SulpTP structure, an 11 amino acid sequence of mammalian prestin was identified as the electromotility motor motif (EMM). Chimeras of chicken and zebrafish SLC26A5 containing the gerbil EMM demonstrated a gain of motor function with the acquisition of nonlinear capacitance (NLC) and membrane motion in transfected HEK 293 cells. Transporter function in the chimeric chicken and zebrafish prestin proteins was retained. These combined approaches suggest that the transporter and electromotility properties are conferred by different portions of prestin's SulpTP domain and provide new insights into the structural architecture of prestin that is similar with that of GltPh.

77 Effect of Membrane Mechanics on Prestin-Associated Charge Transfer

Alexander Spector¹, Natalie Nilsen¹, Sean Sun¹, William Brownell²

¹Johns Hopkins University, ²Baylor College of Medicine Prestin is a crucial part of the somatic motor driving cochlear outer hair cells (OHCs). Other cells transfected with prestin acquire active properties similar to those in the native cell. While the mechanism of prestin has vet to be fully understood, the electric charge transfer is its critical component. Here we extend our model of electric charge transfer by prestin (Sun et al., 2009) to investigate the effect of the mechanics of the surrounding membrane. We simulate various changes in the membrane mechanics via the corresponding changes in the free energy of the membrane-prestin system. We consider native OHCs and cells transfected with prestin. We analyze the effects of changes in membrane tension and membrane elastic moduli. In the case of OHC, we simulate changes in the longitudinal and/or circumferential stiffness of the cell composite membrane. In the case of cells transfected with prestin, we vary the membrane areal modulus. For cells of both types, we simulate changes in membrane tension by changing cell turgor pressure. In our model, the prestinassociated charge can be at any position inside the

membrane characterized by a probability density. We show the effects of membrane mechanics on this probability density as well as the total probability of the charge being transferred. We also study the effects of the membrane mechanics in the high-frequency case characterized by the amplitudes of the charge-associated probabilities. Previously, several experimental studies (Kakehata and Santos-Sacchi, 1995; Adachi et al., 2000; Adachi and Iwasa, 1997) analyzed the effect of membrane mechanics on the electric charge and nonlinear capacitance. We compare our total probability of the charge being transferred under purely DC-field conditions with the experimental charge and show good qualitative and quantitative agreement with the experiment. Our results can help further elucidate the structure and function of prestin. Supported by DC 002775 from NIDCD.

[78] Homology Modeling of Prestin 1: The SulP Domain

Benjamin B. Currall¹, Kate Dempsey², Heather Smith¹, Hesham Ali², Richard Hallworth¹

¹Creighton University, ²University of Nebraska Omaha Despite extensive study, it is still unclear how prestin performs its remarkable motor function. Understanding of prestin function would be greatly aided by high resolution structural models of the protein, but, so far, prestin structure remains unresolved. In part 1 of this 2 part poster, the transmembrane SulP domain is examined. HHPred analysis reveals homology between the SulP domain and three other domains: HCO3, Xanthine Uracil Permease, and BenE. According to hydrophobicity analysis, all four domains share similar transmembrane topologies. Further, motif finding software and a novel Post Alignment Identity Matrix algorithm identifies conserved regions within the first four putative transmembrane helices as well as putative transmembrane helices 7-11. Template based homology modeling of prestin and the structurally similar HCO3 channel suggests that transmembrane helices 1-3 and transmembrane helices 8 and 9 form two pore regions. While empirical verification of these pore regions is invaluable, this study represents an approach to higher resolution models of prestin structure.

Supported by N.S.F.-E.P.S.Co.R. EPS-0701892, N.C.R.R. (N.I.H.) P20 RR16469, C06 RR17417-01

79 Membrane Cholesterol Strongly Influences Hop Diffusion of Prestin Ramsy Kamar¹, Robert Raphael¹

¹Rice Universitv

Prestin is the membrane motor protein that drives outer hair cell (OHC) electromotility via electromechanical coupling of membrane potential to whole cell length changes. Various groups have demonstrated the importance of the interaction of prestin with the membrane environment. Biochemical evidence and optical microscopy strongly suggest that prestin localizes in cholesterol rich microdomains, and electrophysiology shows prestin associated charge movement depends on membrane cholesterol concentration. We have previously measured prestin diffusion using fluorescence recovery

after photobleaching (FRAP). However FRAP is an ensemble measurement making it difficult to discriminate between free and confined diffusion resulting from interactions with the cytoskeleton or confinement in membrane compartments. We have thus measured diffusion of prestin molecules in a model system using single particle tracking and total internal reflection microscopy. Utilizing a combination of single molecule fluorescence microscopy and site-directed labeling with a highly photostable fluorophore, we have robustly determined that prestin diffuses in and hops between confinement zones on the order of 1 μ m in average size. We observe that depletion of membrane cholesterol increases average confinement size and decreases confinement strength. Statistical analysis of squared displacements reveals that depletion of cholesterol removes domains of intermediate size between 142 and 500 nm. From measurements of the initial increase of the mean squared deviation with time, the microscopic diffusion constant was determined to be 0.05 μ m²/s, and was unchanged by cholesterol depletion. Our results suggest that membrane cholesterol affects prestin function by changing prestin crowding in confinement zones, consistent with the hypothesis that the microscale organization of prestin in the membrane influences prestin function.

80 Continuous Detection of Development of Newly Synthesized Motor Protein Prestin

Shumin Bian¹, Dahsakumar Navaratnam¹, **Joseph Santos-Sacchi¹**

¹Yale School of Medicine

Prestin is the motor protein important for mammalian cochlea amplification, and its development and maturation have been linked to the onset of hearing. Using a YFPtagged tetracycline-inducible expression cell line, we have exploited the charge-transfer properties of prestin to observe continuous development of newly synthesized prestin inserted into the plasma membrane. Continuous whole-cell patch clamp was used to monitor the real-time development of non-linear capacitance, which measures prestin charge transfer across the cell membrane; simultaneous live cell fluorescence imaging was used to monitor total prestin expression. Low temperature block enabled us to monitor the synchronous release of newly synthesized prestin to the membrane from the trans-Golgi network. Our system provides a way to study events affecting prestin development in the very early stages of motor maturation.

(Supported by NIDCD DC00273 to JSS and NIDCD DC 008130 to JSS and DN)

81 Chloride and OHC Electromotility: Another Hurdle for Prestin to Overcome? Lei Song¹, Joseph Santos-Sacchi¹

¹Department of Surgery, Yale University School of Medicine. New Haven, CT 06510

Mammalian outer hair cell (OHC) electro-motility results from voltage-dependent conformational changes of the membrane protein prestin, with the cell's nonlinear capacitance (NLC) being considered a surrogate measure of electromotility. A number of physiological factors shift prestin's voltage dependence, including changes in intracellular CI and membrane holding potential (pre-pulse effect), each presumably affecting electromotility and NLC equivalently.

Last year we studied the consequences of combined CI and pre-pulse manipulations on electromotility with simultaneous measurements of NLC and video imaging. We found, as expected from our previous work, that OHCs patched with 140 mM intracellular Cl show robust depolarizing shifts of NLC upon negative pre-pulse, with electromotility displaying a similar shift. We now find that lower, more physiological levels of intracellular chloride (1 and10 mM), induce an uncoupling of mechanical responses from NLC. That is, voltage dependence of motility is shifted in the depolarizing direction compared to that of NLC. The uncoupling shows hysteresis, being greater with depolarizing voltage polarity. We have found disparities as large as 50 mV. Interestingly, we find that diamide can reduce the disparity, suggesting that chloride modulates a cytoskeletal coupling between prestin's conformational state and whole cell mechanics. Finally, the uncoupling we find imposes an additional challenge for the voltage-sensitive protein prestin to drive the cochlear partition during acoustic stimulation, since the whole cell mechanical response is variably uncoupled from voltage depending on phase of receptor potential. (Supported by NIH/NIDCD DC 000273 to JSS)

82 Mechanical and Electrical Response of the Organ of Corti to Outer Hair Cell Motility: A Computational Study

Jong-Hoon Nam¹, Robert Fettiplace²

¹University of Rochester, ²University of Wisconsin-Madison The organ of Corti (OC) is a specialized epithelium in the mammalian cochlea that houses the sensory hair cells. It is believed that the OC functions to optimize the force transmission from the outer hair cell (OHC) to the basilar membrane and inner hair cell. Recent studies suggest that the OC can no longer be considered as a rigid body and has a complex mode of deformation (i.e. Karvitaki and Mountain, 2007). Many previous studies reduced OC mechanics to rigid bars and elastic springs hinged at their ends. Recently we suggested a different approach (Nam and Fettiplace, 2010), a fully deformable 3-D finite element analysis of the OC that does not compromise its mechanical details. We have further extended the previous study to include dynamic analyses, hair bundle's mechanotransduction and the OHC electrical circuit. Geometric information was taken from a gerbil cochlea at 2 and 10 Cochlear partitions of several mm from the stapes. hundred micrometers long were simulated. The model includes all structurally significant components: OHCs, pillar cells, Deiters cells, reticular lamina. Channel kinetics (Nam and Fettiplace, 2008) were combined with a simplified hair bundle mechanics. The OHC electrical representation incorporated the transduction channel conductance, nonlinear capacitance of cell membrane and piezoelectric properties (Dong, Ospeck and Iwasa, 2002).

We simulated: (1) phase relations between the mechanical stimulus, hair bundle mechano-transduction current and OHC depolarization; (2) OC deformation due to spontaneous oscillations of OHC hair bundle and (3) OC deformation due to electrical stimulations. The results revealed several qualitative differences in OC deforming pattern between passive and active conditions.

83 A Synthetic Prestin Reveals Protein Domains and Molecular Operation of Outer Hair Cell Piezoelectricity

Dominik Oliver¹, Thorsten J. Schaechinger², Dmitry Gorbunov¹, Christian R. Halaszovich¹, Sebastian Kugler³, Bernd Fakler²

¹*Philipps-University Marburg,* ²*University of Freiburg,* ³*University of Goettingen Medical School*

Prestin, a transporter-like protein of the SLC26A family. acts as a piezoelectric element that mediates the fast electromotility of mammalian outer hair cells required for active cochlear amplification and auditory acuity. Nonmammalian orthologs of prestin are bona-fide electrogenic anion transporters devoid of piezoelectric activity. Here, we generated synthetic prestin (SynPres), a chimera from mammalian and non-mammalian prestin that exhibits both, piezoelectric properties and electrogenic anion transport activity. SynPres delineates two distinct domains in the transmembrane core of the protein that are necessary and sufficient for electromotility and the associated non-linear charge movement (NLC). Functional analysis of SynPres showed that the amplitude of NLC and hence electromotility are determined by the transport of monovalent anions. Interdependence of NLC and anion transport is well described by an alternating access mechanism for antiport of mono- versus divalent anions, in which occupancy of an anion-bound state determines the availability of electromotile active prestin molecules. Thus, prestin-mediated electromotility is a dual-step process: transport of anions by an alternate access cycle, followed anion-dependent transition generating bv an electromotility. The findings define structural and functional determinants of prestin's piezoelectric activity and indicate that electromotility evolved from an ancestral transport mechanism.

84 Tectorial Membrane Traveling Waves Underlie Abnormal Hearing in Tectb Mutant Mice

Roozbeh Ghaffari^{1,2}, Alexander J. Aranyosi¹, Guy P. Richardson³, Dennis. M. Freeman^{1,2} ¹Massachusetts Institute of Technology, ²Harvard-MIT Division of Health Sciences Technology, ³University of Sussex

Remarkable sensitivity and exquisite frequency selectivity are hallmarks of mammalian hearing, but their underlying mechanisms remain unclear. Cochlear insults and hearing disorders that decrease sensitivity also tend to broaden tuning, suggesting that these properties are inextricably linked. However, a recently developed mouse model of genetically altered hearing (*Tectb^{-/-}*) shows decreased

sensitivity and sharper frequency selectivity. Here we show that the Tectb mutation reduces the spatial extent and propagation velocity of tectorial membrane (TM) traveling waves. These changes in wave properties provide information about the underlying material properties of the TM. We compute the shear storage modulus (G') of the TM from the propagation velocity of waves and show that the *Tectb* mutation reduces G' of *Tectb*^{-/-} TMs with respect</sup>to wild type TMs. Best fit estimates (mean \pm s.d.) of G' in basal Tectb^{-/-} TMs (G' = 18 ± 1 kPa; n = 3 TM preparations) were smaller than those of wild type TMs (G'= 42 ± 10 kPa; n = 7 TM preparations). Across apical TMs, the material properties of Tectb^{-/-} samples (G' = 1 \pm 0.1 kPa; n = 3 TM preparations) were also reduced with respect to those of wild types ($G' = 14 \pm 4$ kPa; n = 4 TM preparations), but by a larger factor. Taken together, the differences in material and traveling wave properties of the TM are likely to account for all of the hearing abnormalities associated with the mutation. By reducing the spatial extent of TM waves, the Tectb mutation decreases spread of excitation and thereby increases frequency selectivity. Furthermore, the decrease in Tectb TM wave velocity reduces the number of hair cells that effectively couple energy to the basilar membrane, which thereby reduces sensitivity. These results highlight a new mechanism that is complementary to those in conventional theories, in which increased gain tends to sharpen tuning. Such a complementary mechanism may be essential for attaining high sensitivity without suffering poor temporal resolution that would result if frequency selectivity were increased excessively.

85 Interferometric Measurements of the Visco-Elastic Properties of Mutant Tectorial Membranes

Gareth Jones¹, Ian Russell¹, Andrei Lukashkin¹ ¹School of Life Science, University of Sussex

The tectorial membrane (TM) is visco-elastic and supports propagation of longitudinal travelling waves. This study investigates these travelling waves in mice with mutations to TM specific proteins and consequent changes to TM structure. The propagation velocity of the travelling waves was measured using a laser interferometer focused on the marginal edge of TM driven radially at acoustic frequencies (1-20kHz). The sheer storage modulus G' (ratio representing energy elastically stored and viscously lost) and shear viscosity n (ratio between pressure exerted and velocity) of TM sections taken from the basal region were calculated and compared between three groups of mutants (exon18 +/-, tecb -/- and OTOA -/-) lacking key TM proteins; α-tectorin, β-tectorin, otoancorin, respectively, and wild types. The striated sheet matrix, a core component of the TMs structure is severely disrupted in exon18 +/- mice and missing from tectb -/- mice. Otoancorin is an attachment protein and OTOA -/- mice are reported to have normal TM morphology but no attachment to the spiral limbus. The G' and η values calculated for the wild type mice are similar to estimates derived using other methods (G'=~25.5kPA, n=~0.40Pa S for β -tectorin wild type littermates and G'=~26.7,

η=~0.48Pa·S for s129 mice). TMs of the exon18 +/- and tecb -/- mutants are much more elastic and have reduced longitudinal coupling required for effective travelling wave propagation. TMs of OTOA -/- mutants still exhibit visco-elasticity, but with characteristics different to the wild type mice (G'=~11.6 η=~0.19Pa·S), indicating that the otoancorin protein may also affect TM structure. These data provide more evidence that the TM's visco-elastic properties and longitudinal coupling along it are important for cochlear signal processing. Supported by MRC and BBSRC.

86 Dynamic Response of the Otoconial Membrane of the Turtle Utricle

Myles Dunlap¹, Corrie Spoon¹, Wally Grant¹ ¹*Virginia Tech*

Introduction: The utricle of the red-eared turtle was subjected to forced sinusoidal oscillations across various frequencies (10-125Hz) and amplitudes (5-15µm) to determine utricle dynamic characteristics.

Experiment: After removing the utricle, the overlying membrane was trimmed to expose the otoconial crystals without disturbing the otoconial membrane (OM). The utricle was then fixed to a large glass cover slip with 3 single strands of dental floss, while positioning the ampullae on 2 chips of 0.5mm thick glass. This made the OM parallel to the glass slide and the utricle act as a rigidly attached mass, while not impairing the natural OM displacement. A piezoelectric-actuated platform was fitted into the stage of the microscope and created controlled vibrations along the medial-lateral direction of the utricle. The OM surface crystal's displacement was measured through the microscope with high speed video (1500fps & resolution = 144nm/pixel). The membranous shelf that overlies the lateral macula of the utricle was filmed under identical amplitude and frequency inputs to ensure the specimen wasn't slipping on the glass slide. A custom Matlab program was written to determine OM and shelf displacements using 2-D cross correlation. All images were passed through a Wiener filter and histogram equalization. A series sinusoidal fit was applied to determine the maximum displacement of the OM and membranous shelf relative to the piezoelectric actuator, thus determining amplitude ratios. Signal processing was used to determine phase lag of the OM.

Results: Fitting a single degree of freedom spring-dashpot model to measured values (n=9) of amplitude ratios and optimizing by a sum of the least squares determined the utricle's natural frequency of 383±78Hz (mean±SD) with a mean damping ratio of 1.18. Column filament shear modulus was measured at 10.26±4.12Pa. (Supported by: NIH NIDCD R01 DC 005063)

87 Investigation of a Second Traveling Wave Through Modeling of the Tectorial Membrane and the Organ of Corti

Jessica S. Lamb¹, Richard S. Chadwick¹ ¹*NIDCD, Section on Auditory Mechanics* The simplest model of Organ of Corti (OC) motion describes the basilar membrane (BM) as supporting a traveling wave that peaks at a particular spatial location according to input frequency. Experiments have previously suggested the existence of a second cochlear frequency map often attributed to resonance of the tectorial membrane (TM) (Allen and Fahey 1993; Gummer, Hemmert et al. 1996, Zwislocki 1986). By calculating the traveling wave with a model in which motions of the TM and BM are regarded as different degrees of freedom we find a system in which both masses carry two waves each. This produces a different tuning curve for the TM than for the BM. We show traveling waves on both the BM and TM, and evaluate their shapes, compositions, and phases. We also discuss how the TM stiffness and coupling stiffness influence the characteristics of the waves and tuning curves.

This work is supported by the NIDCD intramural program.

88 Cochlear Tuning: A Dual Resonance

David Mountain¹

¹Boston University

The cochlea amplifier is a process that increases the sensitivity and frequency selectivity of the local mechanical motion in the organ of Corti which is transduced by the inner hair cells. The available experimental evidence suggests that a pure-tone stimulus produces a traveling wave that propagates passively down the cochlea to a relatively small (~0.5 mm) amplification region. This amplification region is located around and just basal to the best place for the stimulus frequency. The outer hair cells (OHC) appear to be the active elements in this process but the known properties of the OHCs cannot explain why amplification takes place over such a small region. Both the OHC mechanical-to-electrical transduction process and the electrical-to-mechanical (somatic motility) show no evidence of tuning. It therefore seems likely that where the amplification starts and where it ends are determined by the passive mechanical properties of the cochlea.

In order to quantify the properties of cochlear responses in a way that may help shed light on why the spatial extent of amplification is limited, I have developed a dual resonance model for cochlear tuning and have used the model to fit cochlear impulse responses (revcor functions) derived from a large population of cat auditory nerve fibers (Carney and Yin 1988, J. Neurophys. 60:1653). The results indicate that the relative difference between the two resonant frequencies changes with cochlear location in a manner consistent with the width of neural tuning curves. The decay constants associated with the two resonances differ between apical and more basal regions. In the apex, the lower-frequency resonance has the longer time constant while for cochlear locations basal to the 1 kHz place, the higher-frequency resonance has the longer time constant. These differences in time constants lead to an upward frequency glide for high CF fibers and a downward glide for low CF fibers. Supported by grant DC 000029 from NIDCD

89 A Nonlinear Transmission Line Model of the Cochlea with Feed-Forward and Delay

Robert Szalai¹, Bastian Epp², Alan R. Champneys¹, Martin Homer¹

¹University of Bristol, ²Carl von Ossietzky University of Oldenburg

In this poster we compare and contrast the effects of spatial feed-forward and temporal delay on a fluid-structure transmission-line model of the mammalian cochlea, via the inclusion of different forms of nonlinearity. The stark conclusion is that the spatial feed-forward and fluid coupling terms are the most important effects for enhancing compression and thus capturing experimental data on basilar membrane vibration. In fact, only a relatively weak compressive nonlinearity is required in the micromechanical model of the organ of Corti. This is contrary to recent reports in the literature, which suggest that quite precise local adaptive nonlinearities are required in the organ of Corti to produce realistic tuning characteristics.

We also show that there is no direct equivalence between the time-delay and the feed-forward mechanism, although qualitatively similar results can be achived by both, albeit in very different regions of parameter space. With the inclusion of nonlinearity, though, our detailed investigation of the models shows that the feed-forward mechanism is highly robust to parameter variation and gualitatively fits experimental data. On the other hand, the model with timedelay can easily become unstable and exhibit unexpected dynamical phenomena. Moreover, our analysis indicates that the compressive nonlinearity is greatly enhanced by longitudinal coupling through fluid and the feed-forward coupling mechanisms. This suggests that local micromechanical models need only be slightly compressive to achieve the strong overall compression of 0.1dB/dB for frequencies slightly above the characteristic frequency.

90 How Is Power Transported, Dissipated and Distributed in Gerbil Cochlea?

Duk Joong Kim¹, David Mountain¹, Allyn Hubbard¹ ¹Boston University

A Sandwich model of the cochlea (Hubbard et al 2003) that reproduces measured basilar membrane (BM) responses (Ren 2001) was used to calculate power along the length of the cochlea. In the model, the outer hair cells (OHC) are represented by two types of forces, active (prestin) and passive (cell wall and cytoskeleton). The model was stimulated with a 44 dB pure tone at the ear canal and the acoustical power generation/dissipation in the cochlea was studied. Power generation due to OHCs started about 0.65 mm prior to the peak of the traveling wave on the basilar membrane and continued about 0.25 mm past the peak along the length of the cochlea. The maximum power generated by the active OHC forces, accumulated down the length of the cochlea was twenty times the power input into the stapes, thereby demonstrating cochlear power amplification. The passive OHC load, the BM, the reticular lamina and the organ of Corti showed power dissipation, with the BM consuming the most power. The power from the input at the stapes is largely dissipated approaching the region of OHC power generation and this is the reason that the maximum motion in the active case occurs further down the length of the cochlea than in the passive case. In the passive case, input power is transported with little loss down the scalae, but is simply dissipated before reaching the region where the cochlear amplifier would normally have generated power.

This work is supported by NIH grant DC 000029.

91 Consequences of Cochlear

Preprocessing on Perception: Finestructure Effects in Modulation Perception in the Light of a Cochlea Model

Bastian Epp¹, Manfred Mauermann², Jesko L. Verhey¹ ¹AG Neuroakustik, Institut für Physik, Carl von Ossietzky Universität Oldenburg, Germany, ²Medizinische Physik, Institut für Physik, Carl von Ossietzky Universität

A quasi periodic variation of the threshold in quiet is often found in normal hearing listeners when their audiogram is measured with a high frequency resolution. This variation, commonly referred to as threshold finestructure, was hypothesized to be a consequence of nonlinear and active processing at the level of the cochlea. Several studies have shown that the finestructure also seems to influence perception at supra-threshold levels such as, e.g., modulation detection thresholds. The data from Heise et al. [2009, J. Acoust. Soc. Am. (126), 2490-2500] are compared with model predictions of a nonlinear and active transmission line model of the cochlea which has been shown to simulate various aspects of psychoacoustical and physiological data with a single parameter set [Epp et al., J. Acoust. Soc. Am., accepted]. Among others, the model is able to account for threshold finestructure with spontaneous otoacoustic emissions in finestructure minima and a compressive regime in the input-output function. Applied to a modulation detection paradigm, the differences found in cochleograms for sinusoidally amplitude modulated tones with low carrier levels are in agreement with psychoacoustical data on level- and frequency dependent modulation detection thresholds. This indicates that the influence of finestructure on modulation detection thresholds is largely due to the behavior of the active nonlinear cochlea. Heise et al. suggested either spectral filtering, beating effects, or sychronization with cochlear resonances as three different mechanisms to account for the observed effects. They suggested sychronized interaction of cochlear resonances with the carrier of a sinusoidally amplitude modulated tone as the dominant mechanism for most of the observed effects. The hypotheses of Heise et al. to account for finestructure effects in modulation perception are discussed in the light of the internal representation of the model.

92 On Similarities and Differences Between Hopf-Bifurcation and Van Der Pol Oscillator Models of the Mammalian Cochlea Hendrikus Duifhuis¹

¹University of Groningen

The idea to model spontaneous oto-acoustic emissions by van der Pol oscillators arose around 1980 at the 5th ISH symposium, where it was presented as a comment by P.I.M. Johannesma. We were one of the groups picking up the idea, and we started to analyze the properties of such oscillators in a model cochlea. At the time there was no doubt that the normal cochlea was nonlinear. The most direct proofs came from basilar membrane measurements of tuning, and from many different sources of data on responses to 2f₁-f₂. Based on the analysis of J.L. Hall it was clear that the predominant nonlinearity had to be found in a non-linear damping term, that was growing with level, and primarily of even order shape so that it would generate odd order intermodulation products more strongly than even order ones. This nicely fits the van der Pol oscillator properties of the damping, with the primary difference that around zero velocity, the oscillator becomes active and emits power rather than dissipating it.

The solution of the van der Pol equation in the context of a cochlea model with the RK4 method, involves splitting each single second order into two first order differential equations. One of these shows an extremely strong similarity to the Hopf-bifurcation equation, originally proposed by Choe, Magnaso and Hudspeth as a model for chicken's ears. They suggest that the properties occur universally in hair cells (hair-bundle stiffness properties, transduction channels), and this has been followed up and promoted by others (e.g. Stoop & Kern, 2003) as a proper model for the mammalian cochlea. The theoretical discussion leads to an almost identical Hopf-bifurcation as arises from the van der Pol oscillator, but the underlying biophysical parameters appear to be different. Moreover, ignoring the vestibular fluid motion brings us back to a Helmholtz cochlea.

93 The Combined Effect of Roughness and Active Processes on Traveling Waves in the Cochlea

Yizeng Li¹, Karl Grosh¹

¹University of Michigan, Ann Arbor

Fluctuations in the cochlear microstructures, such as missing hair cells or stereocilia, will lead to small variations in the material properties along the cochlea. These fluctuations are typically called roughness because they represent a deviation from a smooth variation of the properties. Roughness is hypothesized to contribute to the fine structures in the recorded otoacoustic emissions (OAEs) (Talmadge et al., JASA, 108, 2911). OAE fine structures arise from scattering from inhomogeneities as well as from nonlinear force generation and linear reflection (Talmadge et al., JASA, 105, 275). In this work a cochlear model that couples the mechanical, electrical, and acoustical fields (Ramamoorthy et al. JASA, 121, 2758, Meaud and Grosh JASA, 127, 1411) is used to study

the interplay between roughness of specific cochlear structures (outer hair cell hair bundles) and active processes in the cochlea. The response under internal force excitations (such as those that would generate OAEs) as well as to external acoustic stimuli is simulated. The model predictions show that roughness gives rise to fine structures in the frequency response of the basilar membrane gain to stapes excitation as well as the emitted spectrum due to internal forcing. The spatial phase accumulation due to roughness can give rise to standingwave-like behavior. Furthermore, we show that roughness affects the stability of the cochlear response and that a nominally stable smooth system may become unstable in the presence of roughness. (We would like to acknowledge funding from the NIH, grant NIH-NIDCD R01-04084.)

94 Response to a Single Tone Using a Computational Model of the Mammalian Cochlea: Compressive Nonlinearity, Harmonic Distortion and DC Shift

Julien Meaud¹, Karl Grosh¹ ¹University of Michigan

The stationary nonlinear response of the mammalian cochlea to a single tone is simulated using a nonlinear computational model in the frequency domain. The model is based on a three dimensional representation of the fluid and structure and includes the electrical domain and feedback from outer hair cell somatic motility. A physiologically relevant nonlinearity is introduced in the mechanotransduction channel. The model predicts amplification at low intensity of stimulation and a nonlinear compressive response despite the RC filtering by the OHC basolateral impedance. The model predictions are compared to the results from a previously developed linearized model and to experimental data. The generation and propagation of harmonic distortion is analyzed and compared to measurements. Relationships between DC shift and harmonic distortion are discussed. The results support the theory that somatic motility is the cochlear amplifier and that the nonlinearity of the cochlea is due to the transduction channels.

Funded by NIH grant NIH-NIDCD R01-04084.

95 Further Study of Inverted Direction of Wave Propagation (IDWP) in the Cochlea Egbert de Boer¹, Alfred L. Nuttall^{2,3}

¹Academic Medical Centre, Room D2-226, University of Amsterdam, ²Oregon Health & Science University, ³Kresge Hearing Research Institute, University of Michigan

Inverse-solution procedures are used to find parameters of cochlear models that are designed to simulate data from measurements. A modified inverse solution has been used to analyze the properties of a "hidden" wave in the cochlea, namely, a wave evoked by nonlinear effects. Basilar membrane (BM) velocity data were obtained on the Distortion Product (DP) with frequency 2f1-f2, where f1 and f2 are the frequencies of two primary tones (f2>f1). The data were converted from the frequency to the location domain and interpreted as indicating a DP wave.

Over the main part of the length of the BM that wave is a *forward*-traveling wave. This finding confirms the result obtained by other investigators, in different types of experiments; however, it does not agree with current theory. Therefore, further study is called for.

We have used a three-dimensional model. Although the DP wave is not driven by the stapes a "modified stapes velocity" has to be inserted in order to keep the fluid volume constant. Resynthesis of the DP wave including this modified stapes velocity produces a predominantly forward traveling DP wave. This expedient apparently solves the enigma of "Inverted Direction of Wave Propagation" (IDWP) for DP waves. In this case it is the physics of the fluid that requires a definite operation to preserve fluid volume. It is stressed that such an action is only necessary in cases where new frequency components are generated, such as in nonlinearity. For a linear phenomenon as coherent reflection it is not necessary, because in the process of reflection and scattering the fluid volume is preserved and classical theory will be sufficient. Supported by NIDCD DC 00141.

96 Stimulus-Frequency Otoacoustic Emissions Originate Predominantly in the Peak Region of the Traveling Wave

Jeffery Lichtenhan^{1,2}, John Guinan^{1,2}, Christopher Shera^{1,2}

¹Eaton-Peabody Laboratory of Auditory Physiology, ²Harvard Medical School

A low-frequency bias tone modulates the gain of the cochlear amplifier by bending outer-hair-cell (OHC) stereocilia. We used bias tones in cats to understand where along the cochlea stimulus-frequency otoacoustic emissions (SFOAEs) are generated and to understand the mechanisms involved in producing bias-tone effects. We quantified biasing effects using both the modulation of SFOAEs from continuous tones and the suppression of compound action potentials (CAPs) from tone pips presented at different bias-tone phases. Results from probe frequencies in the range 2.8-27 kHz indicate that the bias-tone level required to produce a constant modulation of SFOAE or CAP probes increased by ~6 dB per octave of the probe and that the bias phase for maximum CAP suppression remained constant. Furthermore, there was a strong correlation between the bias levels needed for criterion CAP suppression and for maximal SFOAE modulation, as assayed by the level of first-order SFOAE sidebands. Since CAPs from moderate level tone-pips arise from the peak region of the traveling wave (i.e., near the tone-pip's best place), we conclude that most of the SFOAE is generated in the same region as the CAP. If a significant portion of the SFOAE evoked by a lowfrequency probe came from the basal, high-frequency region of the cochlea, as hypothesized by others, then the low-level bias tone needed to produce criterion SFOAE modulation would not be intense enough to bias these basal-turn sources and we would not then have obtained good quantitative agreement between SFOAE biasing and CAP biasing. The ~6 dB/octave increase in bias level as probe frequency increased is consistent with both (1) the

bias tone producing less motion in the base because of increased basilar-membrane (BM) stiffness and (2) the coupling of this BM motion to the bending of OHC stereocilia being relatively constant across the frequency region tested.

Supported by NIDCD grants F32 DC010112, RO1 DC00235, R01 DC03687, and P30 DC05029

97 Temporal Aspects of DPOAE Suppression

Joyce Rodriguez¹, Stephen Neely¹

¹Boys Town National Research Hospital

Temporal features of suppression have potential implications for (1) modeling of cochlear mechanics, (2) determining the masking effects of background noise, and (3) the peripheral encoding of speech stimuli for the development of signal processing in hearing aids. The purpose of this study was to examine the time course of mechanical suppression using a novel method to measure suppression of distortion product otoacoustic emissions (DPOAEs) in which the suppressor was a tone burst. In this way DPOAE temporal suppression was measured in 7 normal-hearing humans. Data were collected with $f_2 = 4.0$ kHz and $f_1 = 3.333$ kHz ($f_2/f_1 = 1.2$) for a fixed L_2-L_1 combination: 50 and 65 dB SPL, respectively. For the f_2 , L_2 combination, suppression was measured for 3 suppressors (f_3 = 3.834, 4.166 & 4.282 kHz) and at 3 levels (55, 60, & 65 dB SPL). To quantify suppression in dB, changes in DPOAE level due to the suppressor were converted to decrements (L_d) . Decrement slopes were similar to previously reported values for DPOAE suppression. The onset-delay latencies for suppression showed a level and frequency effect for $f_3 = 3.834$ kHz at 55 dB SPL. At 60 dB SPL, the onset-delay latencies of the 3 suppressors were nearly the same, whereas at 65 dB SPL, f_3 = 4.282 kHz showed the fastest onset delay and f_3 = 3.834 kHz, the slowest onset delay. In general onsetdelay latencies were \leq 5 ms. The main finding was that suppression does not persist beyond suppressor termination by more than 2 ms. The low-side suppressor $(f_3 = 3.834 \text{ kHz})$ showed no evidence of persistence. The high-side suppressors ($f_3 = 4.166$ and 4.282 kHz) showed persistence ≤ 2 ms, except at 55 dB SPL for S1. These persistence estimates suggest little or no temporal integration associated with suppression, but are in agreement with auditory nerve fiber studies (e.g., Arthur et al., 1971) that suggest suppression results from instantaneous compression of the waveform. [Work supported by the NIH R01 DC8318 and P30 DC4662].

98 Variability in Estimates of Cochlear-Response Growth Based on DPOAE Measurements

Stephen T. Neely¹, Michael P. Gorga¹, Judy Kopun¹, Hongyang Tan¹

¹Boys Town National Research Hospital

In several previous studies, estimates of cochlearresponse growth that have been based on distortionproduct otoacoustic emission (DPOAE) measurements, such as input/output (I/O) slope and suppression growth

rate, have shown expected trends when applied to means across groups of subjects, but failed to show similar trends when applied to data from individual subjects. DPOAEs are the nonlinear byproduct when two tones $(f_1 \& f_2)$ are presented to the ear. The purpose of the present study was to determine whether averaging across DPOAEs from five closely spaced f₂ frequencies could provide a means obtain more reliable cochlear-response growth to estimates in individual ears. Such averaging is expected to reduce contributions to the DPOAE from the reflection source at the $2f_1$ - f_2 place in the cochlea. Reliability was assessed by evaluating correlations between sets of regression parameters that were fit separately to DPOAE I/O and suppression-decrement data from 9 subjects. Four parameters (L_i, L_o, S₁, S₂) were fit to I/O functions and two parameters (L₃-slope, L₂-slope) were fit to decrements (amount of suppression). Because the compressive growth of basilar-membrane vibration is common to both sets of measurements, some correlation between these two sets of parameters was expected. Prior to averaging across f_2 , the only significant correlation (p<0.05) was between L_0 & L_3 -slope. After averaging across f_2 , the only additional significant correlation was L_o & L₂-slope. In neither case were I/O slopes significantly correlated with decrement slopes. Although 9 subjects may be too few for a definite answer, the marginal improvements in correlations that were observed after averaging across f₂ suggest this may not be an effective method of eliminating whatever is causing within-subject comparisons to be less reliable than comparisons of means across groups of subjects. [Work supported by the NIH R01 DC8318, R01 DC2251, and P30 DC4662].

99 Evaluation of Cochlear Compression Using the Generator Component of Distortion Product Otoacoustic Emissions (DPOAE)

Maryam Naghibolhosseini¹, Simon Henin¹, Glenis Long¹ ¹Graduate Center, City University of New York

Our ability to process a wide dynamic range is a result of more amplification of low level sounds and less amplification of high level sounds (cochlear compression). Damage to the cochlea amplifier leads to a reduction of this compression resulting in reduced dynamic range. Input/Output (I/O) functions of distortion product otoacoustic emissions (DPOAE) can potentially provide a tool for evaluating cochlear compression. However DPOAE fine structure (pseudo-periodic fluctuations in DPOAE amplitude and phase due to interactions of two components from different sources in the cochlea) introduces unwanted variability in estimates of DPOAE I/O functions. Separating the two components reduces this variability (Mauermann and Kollmeier, JASA, 116 2199-2212, 2004). The two components were separated using logarithmic sweeping primary tones (Long et al, JASA 124, 1613-1626, 2008). The slopes of the I/O functions of the extracted generator component was estimated by dividing the I/O function into three linear regions. The estimated slope from mid-level stimuli provides an indication of compression. We found highly significant correlation between the estimated I/O slope and behavioral thresholds from subjects with a range of thresholds. Moreover, in individual subjects, changes in threshold across frequency were highly correlated with the estimated slopes, consistent with expectations that increasing hearing loss leads to increased reduction of compression. (This work was supported in part by the Tinnitus Research Initiative and the Graduate Center of the City University of New York).

100 The Effect of Sweep Rate on Estimates of Distortion Product Otoacoustic Emission (DPOAE) Fine Structure and Properties of Separated DPOAE Components Obtained with Continuously Sweeping Primaries

Simon Henin¹, Glenis Long², Carrick Talmadge³ ¹Graduate Center, City University of New York, ²Graduate Center, Clty University of New York, ³National Center for Physical Acoustics, University of Mississippi

Continuously sweeping primaries provide an efficient tool for measuring DPOAE amplitude and phase over a wide range of frequencies (Long et al, JASA 124, 1613-1626, 2008). Different analyses of data collected in this way permits one to either extract the total DPOAE providing information about the DPOAE fine structure generated by the interaction of the two major DPOAE components, or to separate the two components and evaluate the two components separately. When using sweeps of 2s/octave of less there is little difference between the pattern of DPOAE maxima and minima obtained with up and down sweeps. When the sweep rate is increased in an attempt to collect more data in a short period of time (from e.g., 2-s per octave to 0.25-s per octave), frequency shifts of the DPOAE fine structure are seen, which result from the phase-distortion associated with the dispersive nature of cochlear wave propagation. The frequency maxima obtained with upsweeps are higher than the frequency of maxima obtained with constant frequency primaries and the maxima obtained with down-sweeps are lower. These frequency shifts can be modeled using the known frequency-swept signal and the measured group delay of the observed signal with frequency, and thus eliminated from the data if one wants to estimate the pattern of fine structure that would be obtained using constant frequency primaries permitting the use of faster sweep rates to collect data. Reconstruction of the continuous-tone DPOAE paradigm using the fast-swept and comparisons to data collection using the continuous-tone DPOAE paradigm will be presented. (This work was supported in part by the Graduate Center of the City University of New York and the Navy).

101 Level Dependence of DPOAE Phase Is Attributed to Component Mixing

Carolina Abdala^{1,2}, Radha Kalluri^{1,2}, Sumitrajit Dhar³, Abigail Rogers³, Shannon Luckovich¹

¹House Ear Institute, Div of Communication & Auditory Neuroscience, ²University of Southern California, Neuroscience Graduate Program, ³Northwestern University, Roxelyn & Richard Pepper Dept of Communication Sciences & Disorders

Distortion product otoacoustic emissions (DPOAEs) measured in the ear canal represent the vector sum of components produced at two different regions along the basilar membrane by two distinct cochlear mechanisms. Stimulus parameters impact the degree of interference between these components and shifts in their relative contribution to the ear canal DPOAE. In this study the 2f1f2 DPOAE was measured using a high-resolution swepttone protocol at four stimulus levels: 65-55, 55-45; 50-40 and 45-35 dB SPL with fixed f2/f1 = 1.2. The effect of primary tone level on DPOAE fine structure and phase was evaluated in 22 young adult subjects across a three-octave range (500-4000 Hz). DPOAE fine structure became more prevalent and spacing became narrower and deeper with decreasing stimulus levels. Ear-canal DPOAE phase vs. frequency functions, as well as functions from both DPOAE sources (nonlinear distortion generated around f2 and the putative reflection source at 2f1-f2), were fit with loess trend lines. Ear canal DPOAE phase vs. frequency functions manifest an increasingly steep phase gradient with decreasing level. However, when functions from each component were fit separately, distortion source phase showed no level dependence; reflection source phase showed a modest level dependence. This modest level effect cannot explain the significantly steepened phase gradient observed in the ear canal DPOAE signal. Rather, mixing between components and shifts in their relative contribution, account for most of the level dependence of ear canal DPOAE phase. Measures of component magnitude support this conclusion, confirming that the relative contribution from the reflection source increased with decreasing stimulus level. The implications of this finding for DPOAE-based studies of cochlear development in human newborns will be considered.

102 Group Delays of Electrical Distortion Products Recorded at the Round Window

Wenxuan He¹, Edward Porsov¹, David Kemp², Alfred Nuttall¹, Tianying Ren¹

¹Oregon Health & Science University, ²University College London

The cochlear microphonic potential (CM) recorded from the round window has been used to study the propagation mechanisms of sounds inside the cochlea. Since the CM results from many electrical generators distributed along the spiral cochlear partition and the excitation pattern of the partition varies with stimulus frequency and level, the remotely recorded CM may not reflect the delays of cochlear traveling waves. This hypothesis was tested in the current study by measuring the magnitude and phase of two tone-induced electrical distortion product (DP) and single tone-induced CM at the round window in sensitive gerbil cochleae. The phase of the CM was referred to the stapes vibration. Motion of the partition was also recorded at the cochlear base near the round window. The data show that, for either the DP or single tone, the CM phase decreases with frequency at frequencies below 2 kHz indicating a significant delay. The phase decrease rate becomes smaller with frequency at frequencies above 2 kHz for both single tone and DP. For single tones at high frequencies or at high stimulus levels, the CM phase is independent of frequency, indicating no significant delay. In contrast, the cochlear partition vibration at the DP or stimulus frequency shows a progressive phase lag with frequency. The local application of tetrodotoxin decreased the magnitude and group delay of DP and single-tone CMs below 2 kHz. These results indicate that, at frequencies below 2 kHz, the round window CM is contaminated by the auditory neurophonic potential, and, at high frequencies, it provides no temporal information on wave propagation inside the cochlea.

Supported by NIH-NIDCD.

103 Intermodulation DPOAEs in Mice Below and Above the Eliciting Primaries

Mary Ann Cheatham¹, Khurram Naik¹, Jonathan Siegel¹, Peter Dallos¹

¹Northwestern University

We sought to learn if distortion product otoacoustic emissions (DPOAE) elicited by relatively low-frequency primaries in mice are dominated by the source region where the primaries (f1, f2) overlap or by the more apical DP place. We also evaluated threshold shift in prestin mouse models for intermodulation-distortion components below f1 and above f2.

Using a custom, low-distortion emission probe, isoresponse DPOAEs for 2f1-f2 were obtained from DPgrams collected at a series of levels for equal-level primaries in wildtype (WT) mice. A DPOAE threshold was then obtained by noting the level required to produce a 0 dB response for each primary pair. When plotted at f1, the low-frequency cutoff/slope of the DPOAE iso-response (threshold) curve approximated the cutoff of the CAP threshold curve recorded with closed bulla. When plotted at the DP frequency, the emission cutoff occurred at a lower frequency than that for the CAP. Although all other DPOAE measures were collected with f2/f1=1.2, the DPgrams used to obtain the iso-response functions were recorded using f2/f1=1.3 in order to expand the separation between curves plotted as a function of f2, f1 or 2f1-f2. The observation in WT mice, that the DPOAE appears to be dominated by the source region, is consistent with data from humans and with results in mice for f2 less than ~20 kHz reported by Banakis et al. (2008) who used a suppression paradigm to separate DP components from the source and place regions. By comparing prestin knockout (KO) and 499 knockin (KI) with WT measurements, we observed amplitude reductions for 2f1f2, as previously reported in mice lacking prestin (Liberman et al., 2004). However, for 2f2-f1 whose frequency is greater than f2, WT, KO and KI magnitudes were comparable. These results are useful not only for characterizing animals lacking motor function but they may also have implications for DPOAE generation. (Work supported by NIDCD DC00089).

104 DPOAE Generation Source Analysis in Adult Japanese Quail (Coturnix Coturnix Japonica)

Katharine Belzner¹, Lincoln Gray², Sumitrajit Dhar³, Brenda Ryals²

¹Massachusetts Eye and Ear Infirmary, ²James Madison University, ³Northwestern University

The most commonly understood source of nonlinearity contributing to the generation of distortion product otoacoustic emissions (DPOAE) comes from somatic motility of mammalian outer hair cells (OHC) (Brownell et al. 1985). Further evidence supports additional nonlinear contributions associated with the stereocilia bundles atop sensory hair cells (Fettiplace, 1985). Comparative studies in species with and without somatic motility offer an opportunity for better understanding the role of these and other physiological mechanisms underlying nonlinearity in the inner ear and generation of the DPOAE. Hair cells of the avian basilar papilla do not exhibit somatic motility (He et al, 2003) thereby eliminating it as a possible DPOAE generation source. In the present study, DPOAE fine structure was assessed in 22 adult Japanese quail across a F2 range of 500-6,000Hz. Using inverse Fouriér transformation, phase and amplitude estimates of both the nonlinear and reflective DPOAE sources were quantified for 50, 60, and 70 dB SPL input levels (L1=L2). Similar to mammals (Bergevin et al, 2008), DPOAE phase patterns in Japanese quail proved to be unaffected by intensity, with a nonlinear source that is frequency-independent and a reflection source that is frequency-dependent. At the highest input level, the amplitude of the nonlinear source dominated the reflection source. As input level decreased, the nonlinear amplitude dominance over the reflection source amplitude decreased to a nearly equal contribution. Our results confirm at least two distinct generation sources of the DPOAE in birds (Bergevin et al, 2008). Further. they imply that without somatic motility as the nonlinear generation source in quail, a common generator such as stereocilia resonance may play a fundamental role in DPOAE generation in both avian and mammalian species. Supported by NIDCD R01DC001372 & NIH P30 DC04664.

105 Test-Retest Reliability of DPOAEs in the Common Marmoset (*Callithrix Jacchus*)

Michelle Valero¹, Rama Ratnam¹

¹University of Texas at San Antonio

The purpose of this study was to determine the test-retest reliability of distortion-product otoacoustic emissions (DPOAEs) in ketamine-anesthetized common marmosets (*Callithrix jacchus*). DPOAE gain functions were measured at 16 f₂-frequencies between 3 - 24 kHz with L₁ = 38 - 74 dB SPL. Test-retest reliability was assessed at the following time intervals: 1) Interleaved, in which 2 gain functions were obtained at each frequency before advancing to the next f₂-frequency, 2) Immediate, wherein

one gain function was collected at each of the 16 frequencies and then the procedure was immediately repeated without removing/replacing the probe tip, 3) Short-term, in which the retest followed a 10-min period with the probe removed, and 4) Long-term, wherein the retest procedure was conducted after 2 - 16 weeks following the initial test. The standard error of measurement (SEM) was calculated for each time-interval. The combined SEM (across all frequencies) decreased with increasing primary-tone level ($L_1 = 50 - 74 \text{ dB SPL}$) at each time-interval (1 - 4). Measurements were most reliable in the interleaved test condition (1), regardless of primary-tone level and frequency. At frequencies above 12-kHz, reliability was greatest when the probe tip was not removed between test and retest (1, 2). For lower frequencies, there was a larger effect of time under anesthesia on test-retest reliability with test conditions 1 and 4 showing greatest reliability. These results have implications for DPOAE measurements in cases where repeated measures are required, as when assessing the effects of contralateral stimulation, aging, or ototoxic insults.

106 Third-Order Distortion Product Otoacoustic Emissions Evoked by Multitone Stimuli

Sebastiaan W.F. Meenderink¹, Marcel van der Heijden¹ ¹Erasmus MC

With a few exceptions, studies of distortion product otoacoustic emissions (DPOAEs) have used two-tone stimuli to evoke third-order DPOAEs. From a mathematical point of view, however, third-order DPOAEs arise from the interaction of three frequency components. When denoting the stimulus frequencies as f, g and h, they result in DPOAEs at frequencies $\pm f \pm g \pm h$. Since *f*, *g*, and *h* need not be all different, these third-order terms include DPOAEs at 2f-g (for which f = h). Thus, third-order DPOAEs evoked by tone pairs are a limited subset of the more general case of interacting triplets of tones. It occurred to us that there is no need to restrict the study of DPOAEs to two-tone interactions only. In fact, including DPOAEs from threetone interactions allows for a more extensive analysis of the emissions in terms of the underlying cochlear mechanics.

When using multitone (N>2) stimuli, the number of thirdorder DPOAEs grows as the third power of the number of stimulus components N. It can easily happen that multiple DPOAE-components coincide. Such coincidences limit the analysis, because the characteristics of the DPOAE may not only depend on its own frequency, but also on the exact frequencies of the primaries. We carefully designed the stimuli such that all third-order interactions resulted in a unique frequency, which ensures that each DPOAE component can be uniquely identified in terms of the three primaries that evoked it.

Here we present ear canal sound pressure recordings from the Mongolian gerbil in response to multitone (N=3...12) stimuli. Each stimulus thus contains multiple primary triplets, and gives rise to several hundreds of simultaneous DPOAEs. We describe several properties of these DPOAEs in terms of the combinatorics of the primaries, and explore their dependence on the four frequencies involved: three primary frequencies and one DPOAE frequency.

Supported by NWO-VENI grant 863.08.003 to SWFM.

107 Nonlinear Version of SFOAE Does Not Show Overshoot to Noise Composed of Multiple Random-Phase Tone

Tatsuhiko Harada¹

¹International @University of Health and Welfare Atmi Hospital

Introduction: A nonlinear version of stimulus frequency otoacoustic emission (nSFOAE) is a novel method presented by Walsh for measuring temporal change of stimulus frequency otoacoustic emission (SFOAE). Walsh et.al. reported that SFOAE shows overshoot phenomenon to simultaneously stimulated band noise. On the other hand, former studies showed that SFOAE are suppressed to additional tones. To confirm whether SFOAE overshoot surely occurs and to find out the difference in the effect of tone and noise to SFOAE, nSFOAE measurement with simultaneously stimulated noise which is composed of multiple random-phase tone is planned.

Methods: ER-10C (Etymotic Research) and Rp2.1(Tucker Davis) were used for sound generation and recording. PC (Versa Pro, NEC) and custom software written with LabVIEW (National Instruments) were used for stimulus signal generation and processing of recorded sounds. Stimuli are composed of 3 patterns, (1)Probe tone (4000Hz 60dBSPL)+noise from receiver 1 (2)The same probe tone from receiver 2 (3)Simultaneous stimulation from receiver 1 and receiver 2. (1)+(2)-(3) of the recorded sounds was calculated, and was band pass filtered, the pass band was 3800-4200Hz. Then, 20 ms-long 1ms-step moving rectangular window was applied, and root mean squares of windowed waveforms were calculated. The noise was composed of multiple tones with random phase in three bandwidth (100-3800Hz, 4200-6000Hz, 100-6000Hz except for 3800-4200Hz, each tones are 12Hz interval, 25dBSPL). Noise started 100ms after the beginning of 4000Hz tone.

Results: At present, two normal hearing volunteers, ages were 21, were measured. The RMS level was decreased soon after the onset of noise in 0.5-2dB. Wide band noise (100-6000Hz) induced largest decrement. No overshoot was seen in all of the conditions.

Conclusion: The nSFOAE method is useful for detecting temporal change of SFOAE, but existence of SFOAE overshoot to additional noise needs further verifications.

108 ATP Uncouples Gap Junctions Between Supporting Cells in the Cochlea

Yan Zhu¹, Hongbo Zhao¹

¹Dept. of Surgery – Otolaryngology, University of Kentucky Medical Center

Supporting cells in the cochlea are well-coupled by gap junctions. Gap junctions in the inner ear play an important role in hearing. Connexin mutation can induce a high incidence of hearing loss. Our previous study shows that gap junctional hemichannels can release ATP in the cochlea (Zhao, et al., 2005). ATP-mediated purinergic signaling plays an important role in the cochlear development and the regulation of hearing. ATP is also required for K+-sinking in the cochlear supporting cells (Zhu and Zhao, 2010). Here, we report that the gap junction between supporting cells can be uncoupled by ATP. Application of micro-molar ATP reduced input capacitance of the coupled cochlear supporting cells to the single cell level in the patch clamp recording. The input currant was also reduced and the membrane potential was shifted to the hyperpolarization direction. Under the same circumstance, no change in the input capacitance was observed in the single cell recording. This uncoupling effect is reversible and repeatable. ATP evoked an inward current in both the single cell and the coupling cells. Blocking of ATP-activated purinergic (P2x) receptor activity by PPADA (50 uM) could eliminate the inward current and uncoupling. However, blocking of Ca++ channel activity could not abolish the ATP-evoked uncoupling. These data indicate that ATP can mediate intercellular communication in the inner ear. ATP may activate P2x receptors permeable to (inflowing) Ca++ to increase intracellular Ca++ concentration uncoupling gap junctions. This ATPmediated uncoupling effect on gap junctions between the cochlear supporting cells may play an important role in the control on the ionic and metabolite movement in the organ of Corti and hearing sensitivity, given changes in gap junctional coupling between the cochlear supporting cells can mediate outer hair cell electromotility (Yu and Zhao. 2008, 2009).

Supported by DC05989

109 Restoration of Hearing in Cx30^{null} Mice by Transgenic Over Expression of Kcnj10 to Establish the Endocochlear Potential

Shoeb Ahmad¹, Wenxue Tang¹, Chang Qing¹, Yunfeng Wang¹, Binfei Zhou¹, Xi Lin¹

¹Emory University School of Medicine.

Genetic studies have indicated that gap junctions (GJs) play vital roles in the cochlear homeostasis and hearing sensitivity. However, molecular mechanisms underlying the pathogenesis of deafness due to null mutations in either Cx26 or Cx30 remain unknown. In Cx30^{null} mice, endocochlear potential (EP) was never established and degeneration of organ of Corti was observed after the onset of hearing (Teubner et al., 2003). Kcni10 is expressed in the membrane of the intermediate cells where the EP was first established and our previous studies found that its protein expression was significantly reduced in the $Cx30^{null}$ mice. In this project, we tested whether over-expressing Kcnj10 in Cx30^{null} mice is sufficient to restore the EP and normal hearing. BAC^{Kcnj10}mice were generated by expressing extra copies of Kcnj10 gene from a bacterial artificial chromosome (BAC; clone: RP23-78O24) introduced into mouse Presence of BAC in mouse genome was genome. confirmed by PCR and Southern blot analyses from tail snip's DNA. BAC^{Kcnj10}founder mice were bred with *Gjb6*^{-/-} mice to obtain BAC^{Kcnj10};Gjb6^{-/-} mice in the second generation. Genotype of BACKcnj10;Gjb6-/- mice for the presence of BAC and absence of the Gjb6 gene was further confirmed by PCR and Southern blot analyses. Measurements of the auditory brainstem responses (ABRs) of BAC^{Kcnj10};Gjb6^{-/-} mice showed that hearing thresholds across a frequency range of 4-32 kHz were comparable to the wild type mice in about half (n=41) of the transgenic mice. In addition, EP values (75±7 mV) in these mice also restored to near WT levels (83±9 mV). Preliminary results based on western and guantitative PCR suggest that the restoration of hearing in a subset of BAC^{Kcnj10};Cx30^{-/-} mice is dependent on the expression levels of Kcnj10 protein. Hearing is rescued only in those mice that showed at least 3 fold increase in Kcnj10 protein The BAC clone: RP23-78O24 contained the levels. sequence of three other genes (Kcnj9, Pigm and Igsf8) and partial sequence of Atp1a2. To rule out the effect of these genes, the above BAC clone was modified in which Kcnj10 sequence was replaced with neomycin resistance gene. Breeding of these control mice in the Gjb6^{-/-} background is underway. In summary, our results suggest that the loss of EP was solely responsible for causing hearing impairment in the Cx30^{null} mice. Hair cells in the cochlea of Cx30^{null} mice are fully functional before they are degenerated. A time window of opportunity may therefore be exploited for therapeutic interventions of deafness caused by Cx30^{null} mutation, with a focus on the means to regenerate the EP.

110 Pannexins Have Distinguished Expression and Function from Connexins in the Cochlea

Xiao-Hui Wang¹, Liang Zong¹, Yan Zhu¹, Chun Liang¹, Hong-Bo Zhao¹

¹Dept. of Surgery - Otolaryngology, University of Kentucky Medical Center

Pannexin is a new found gap junction gene family in vertebrates. Our previous study (Wang et al., 2009) demonstrated that pannexins have distinct expression in the mammalian cochlea. All three pannexin isoforms have been found to be expressed in the cochlea. To further explore the pannexin function in the cochlea, we investigated pannexin cellular expression and the relationship between pannexin expression and connexin expression in the cochlea. Double immunofluorescent staining for Panx1 and Cx26 or Cx30, which are two predominant connexin isoforms expressed in the cochlea, was used. Other than Cx26 and Cx30 expression, double immunofluorescent staining shows that there is no overlap of labeling for Panx1 and Cx26 or Cx30 in the cochlea. In the single cell preparation, Panx1 and Cx26 or Cx30 also show distinct subcellular locations and do not co-located in the same gap junctional plague. Different from connexin expression, pannexin has an abundant expression in the cytoplasm. These data indicate that the pannexin may play divergent, rather than redundant, functions in the cochlea. Pannexin deficiency may also be able to induce hearing loss.

Supported by DC05989

111 Selective Deletion of Cx26 Expression in Deiters and Pillar Supporting Cells Reduces Active Cochlear Mechanics

Yan Zhu¹, Liang Zong¹, Chun Liang¹, Hilary Hughes¹, Hong-Bo Zhao¹

¹Dept. of Surgery – Otolaryngology, University of Kentucky Medical School

Gap junction channels between the cochlear supporting cells play a crucial role in coordinating exchange of molecules and ions but also in a wide spectrum of cellular activities. Our previous study (Yu and Zhao, 2009) revealed that gap junctional coupling between Deiters supporting cells can modulate outer hair cell (OHC) electromotility. To further explore its effect on active cochlear mechanics in vivo, we created Cx26 conditional knockout mice that targeting-ablate Cx26 in the Deiters and pillar supporting cells using an inducible Cre mouse line, Prox1-CreERT2. Auditory brainstem response (ABR) and distortion product otoacoustic emission (DPOAE) were measured to assess active cochlear mechanics and hearing function. The littermates of wide type (WT) mice were used as controls in the recording. We found that the DPOAE intensities in the Cx26 conditional knockout mice were significantly reduced in comparison with those measured in the WT control group. However, the ABR thresholds had no significant difference between these two groups. In consistent with our in vitro recording (Yu and Zhao, 2009), these in vivo recordings show that deficiency of gap junctional coupling between Deiters and pillar cells can reduce active cochlear mechanics. These data also indicate that DPOAE is more sensitive than ABR for assessing OHC function and hearing. Supported by DC05989

Supported by DC05989

112 GluT10 Expression Pattern in the Hair Cells Suggest a New Transcellular Glucose Pathway in the Cochlea

Wenxue Tang¹, Yunfeng Wang¹, Shoeb Ahmad¹, Qing Chang¹, Binfei Zhou¹, Yuhua Li², Xi Lin¹

¹Departments of Otolaryngology, Emory University School of Medicine, ²National Engeering Center for Biochip at Shanghai

Two families of glucose transporters have been described: the energy-dependent Na+-sugar co-transporters and the facilitative glucose transporters (GluT). The SLC2A gene family encodes 13 members of GluT isoforms that share a common structure and all have been cloned. It is known that glucose is the main cellular energy source in the cochlea. Expressions GluT1 and GluT5 in the cochlea have been reported. It has been proposed that GluT1 combined with cochlear gap junctions (GJs) constitute the major route for transferring glucose from blood vessels to supporting cells and fibrocytes in the cochlea. However, the expression and function of GluT isoforms and their relations with GJs in the cochlea are far from clear. The aim of this study was to identify the expression pattern of novel GluTs in the inner ear.

The CodeLink Mouse Whole Genome Bioarray was used to investigate the gene expression profile of the mouse

cochlea. Nine probes representing 9 transcripts of SLC2A family were identified by the microarray. Analysis showed the strongest expressions of Slc2a1 (coding for GluT1) and SIc2a10 (coding for GluT10) mRNA in the mouse cochlea. Semi-quantitative RT-PCR was performed to examine the expressions of GluT1 and GluT10 mRNAs. Positive detection of GAPDH validated a 100% success rate in the RT-PCR reactions and negative controls excluded genomic DNA contamination. Results indicated that both GluT1 and GluT10 mRNAs were expressed at significant levels in the normal cochlear cells. Protein expression of GluT10 was further examined by using an anti-GluT10 ployclonal antibody for Western blotting. GluT10 protein band in the cochlea was detected and the band location consistent with liver positive control. was а Immunostaining showed GluT10 immunoreactivity in both inner and outer hair cells, with the most intense labeling in the cuticular plate. A weaker staining pattern was observed in the spiral ganglion neurons as well. Our results and observations from previous studies suggest that the alucose supply of hair cells is maintained by a network of gap junctions and multiple types of GluTs.

113 Flotillin-1 (Reggie-2) Immunolocalization in the Human Inner Ear

Audrey Calzada¹, Ivan Lopez¹, Gail Ishiyama², Akira Ishiyama¹

¹University of California-Los Angeles Division of Head and Neck Surgery, Los Angeles, California, ²University of California-Los Angeles Department of Neurology

Flotillin-1 (also called Reggie-2) is a lipid raft microdomainassociated protein that recruits signaling proteins to lipid This protein has been detected in regenerating rafts. retinal ganglion cells and has been shown to be crucial for the assembly of signaling complexes regulating cytoskeletal remodeling. Flotillin-1 immunoreactivity (IR) has not been previously described in the human inner ear. We determined the expression of flotillin-1 in the human inner ear by immunocytochemistry. Formalin fixed auditory and vestibular endorgans were microdissected from normal temporal bones obtained at autopsy. Cryostat sections were obtained and immunostained with affinity purified antibodies against flotillin-1. The immunoreaction was visualized using fluorescent microscopy. Flotillin-1-IR was found in type I and type II spiral ganglia neurons (SGN), with strong flotillin-1-IR in type II SGN. Neurofilament-IR was found to colocalize with flotillin-1 in the SGN. In the cristae ampullaris and the macula of the utricle, flotillin-1-IR was found in nerve fibers coursing through the stroma and terminal endings within the vestibular sensory epithelia. Neurofilament-IR also colocalized with flotillin-1 in the nerve fibers and terminals of the vestibular epithelia. Strong flotillin-1-IR in type II SGN suggests a protective role for this protein given the role of type II SGN in the inner ear. Importantly, we show here that flotillin-1-IR can be used as a marker for spiral ganglia neurons and terminals in the human temporal bone for future studies of human inner ear sensory epithelia.

114 Expression of a Local Hypothalamic-Pituitary-Adrenal Equivalent Signaling System in the Mouse Cochlea and the Roles of CRFR1 in Hair Cell Innervation and Adult Function

Christine Graham¹, **Douglas Vetter¹**

¹Tufts Univ. Sch. Med.

Cells of the inner ear face constant metabolic and structural based stress. Exposure to intense sound or various drugs destroys cochlea hair cells, which in mammals do not regenerate. Thus, an endogenous stress response system may exist within the cochlea to protect it from everyday stressors. We recently described the existence of Corticotropin-Releasing Factor (CRF) in the mouse cochlea. The CRFR1 receptor is considered the primary and canonical target of CRF signaling, and systemically it plays an essential role in coordinating the body-wide stress response via activation of the hypothalamic-pituitary-adrenal (HPA) axis. Here we describe an essential role for CRFR1 in auditory system development and function, and offer the first description of a molecularly complete HPA-equivalent signaling system expressed by cells within the cochlea. To reveal the role of CRFR1 activation in the cochlea, we have used mice carrying a null ablation of the CRFR1 gene. CRFR1 null mice exhibited elevated auditory thresholds at all frequencies tested, indicating reduced sensitivity. I/O growth curves combined with DPOAE and ABR threshold analysis suggest that the threshold elevation arises as a complex, multifaceted mechanism that includes both neural and hair cell/EP elements. Furthermore, our results suggest that CRFR1 may regulate auditory sensitivity via effects on glutamate-glutamine cycling between hair cells and support cells, as well as having developmental effects on inner hair cell morphology and afferent synapse distribution. Given the role of HPA signaling in maintaining local homeostasis in other tissues, the presence of a cochlear HPA signaling system suggests important roles for CRFR1 activity not only in auditory processing, but also in auditory protection and cochlear development. These data highlight the complex pleiotropic mechanisms modulated by CRFR1 signaling in the cochlea.

115 Rescue of Channel Function in DFNA2 Mutants by KCNQ Channel Openers

Michael G. Leitner¹, Christian R. Halaszovich¹, Daniela N. Schreiber¹, Dominik Oliver¹

¹Institute for Physiology and Pathophysiology, Philipps-University Marburg

Mutations in the voltage-gated potassium channel KCNQ4 (Kv7.4) lead to a progressive form of hereditary hearing loss, DFNA2, that accounts for up to 5% of all autosomal dominant non-syndromic hearing disorders. These mutations lead to loss of channel function, by disrupting either ion permeation, channel gating, or membrane targeting. KCNQ4 provides the dominant K⁺ conductance of outer hair cells (OHCs) and loss of this conductance causes degeneration of OHCs that leads to profound deafness in most affected individuals.

Epileptogenic mutants of the related channel isoform KCNQ2 can be functionally rescued by KCNQ-specific channel openers. We reasoned that similar rescue of KCNQ4 function in DFNA2 may protect from hair cell loss and therefore investigated the action of channel activators on disease-causing loss-of-function mutations of KCNQ4.

KCNQ4 wildtype channels and mutants described as causative for DFNA2 were expressed in CHO cells and analyzed by whole-cell patch clamp. Application of retigabine and zinc pyrithione increased current amplitudes and shifted the voltages of activation to hyperpolarized voltages for wild type channels. Channels carrying mutations in the pore region produced no detectable current either in the absence and presence of all channel openers tested. In contrast, currents from KCNQ4 with a DFNA2 mutation in transmembrane domain 6 (G321S) were partially rescued by combined application of retigabine and zinc-pyrithione. Similarly, these openers fully rescued KCNQ4 currents from inhibition resulting from PI(4,5)P₂ sequestration by aminoglycoside antibiotics.

Our data suggest that KCNQ agonists may be able to reverse loss of KCNQ function in some DFNA2 patients. Pharmacological stabilization of the KCNQ4 conductance. may protect OHCs from degeneration.

This work was supported by the Deutsche Forschungsgemeinschaft [SFB 593, TP A12] and by a research grant of the University Medical Center Giessen and Marburg, UKGM [42/2010 MR] to D.O.

116 Olivocochlear Effects on OHCs Are Reduced in Mice Lacking BK Channels

Stéphane F. Maison^{1,2}, Hajime Usubuchi^{1,2}, Andrea L. Meredith³, Sonja J. Pyott⁴, M. Charles Liberman^{1,2} ¹Harvard Medical School, ²Massachusetts Eye & Ear Infirmary, ³University of Maryland School of Medicine, ⁴University of North Carolina Wilmington

Medial olivocochlear (MOC) effects on OHCs require $\alpha 9/\alpha 10$ nAChRs mediating an ACh-induced Ca²⁺ influx and subsequent activation of a Ca²⁺-dependent K⁺ channel. *In vitro* studies suggest that the K⁺ channel is the apaminsensitive SK2 channel, and targeted deletion of SK2 eliminates MOC-mediated suppression of cochlear responses *in vivo*. However, *in vivo* pharmacology has shown that classic MOC suppression is resistant to apamin, and recent *in vitro* work suggests that iberiotoxin-sensitive BK channels mediate cholinergic effects on OHCs outside of the apical turn.

To study *in vivo* contributions of BK channels to OC function, we measured cochlear function in mice lacking the BK α subunit (Kcnma1^{-/-}). Cochlear sensitivity in mutants was characterized by measuring 1) ABR amplitude vs. level functions at 7 log-spaced frequencies from 5.6 to 45.2 kHz, 2) DPOAE amplitude vs. level functions evoked by primaries with f₂ at the same 7 frequencies, and 3) the magnitude of DPOAE suppression evoked by electric stimulation of the OC bundle. Groups of mice homozygous for the deletion were compared with wildtype littermates.

Cochlear threshold sensitivity was unchanged by $BK\alpha$ deletion, and DPOAE amplitude vs. level functions were

normal. However, suprathreshold neural responses in BK α -null mice showed a frequency-independent amplitude reduction for wave 1 to roughly 30% of wildtype levels. This decreased neural response is consistent with the reduction in sound-evoked discharge rates in auditory nerve fibers in BK knockout mice, thought to reflect the normal role of neural BK channels in reducing after-hyperpolarization and thus refractory period.

The magnitude of MOC suppression evoked by electric stimulation of the OC bundle was reduced by half (in dB) at all test frequencies (11 to 45 kHz). Thus, BK channels contribute significantly to cholinergic effects on OHCs throughout much of the cochlear spiral *in vivo*.

Research supported by a grant from the NIDCD: R01 DC0188

117 Myogenic and Ca²⁺ Spark Mediated Mechanisms of Vascular Diameter Control Differ Between Genders and Between the Spiral Modiolar Artery and Radiating Arterioles

Katrin Reimann¹, Gayathri Krishnamoorthy¹, Withrow Gil Wier², Philine Wangemann¹

¹Kansas State University, ²University of Maryland Blood flow regulation is critical for hearing due to the exquisite sensitivity of the cochlea to ischemia and oxidative stress. Similar to the brain, the cochlea can autoregulate flow within normal limits despite variations of systemic blood pressure. The site of autoregulation along the vascular tree, myogenic control of vascular diameter and the role of Ca^{2+} sparks remained undetermined. In this study, spiral modiolar arteries (SMA) and radiating arterioles (RA) from male and female gerbils were isolated and pressurized using concentric pipette systems. Inner diameter (ID) and Ca²⁺ sparks, visualized by fluo4, were recorded by confocal laser scanning microscopy. Percent myogenic tone was calculated as (ID_{passive} - ID_{active}) x 100/ ID_{passive}, with ID_{passive} detected in Ca²⁺-free solutions and ID_{active} detected in the presence of 1 mM Ca²⁺ and 10 μ M At 60 cmH₂O, which is close to estimated L-NNA. pressure in vivo, ID_{passive} was gender-independent; SMA: 78.3±2.6 µm (n=13) and RA: 51.2±1.7 µm (n=8). Myogenic tone was different in male SMA (~15% at ≥30 cmH_2O) compared to female SMA (~5% at $\geq 60 cmH_2O$) whereas myogenic tone in RA was gender-independent (~15% at ≥60 cmH₂O). Ca²⁺ sparks at 60 cmH₂O in female SMA and RA were similar in frequency (0.89±0.07 Hz, n=17 vs 0.91±0.09 Hz, n=37), and in sensitivity to 10 µM ryanodine. Increases in pressure increased spark frequency at individual sites in SMA but not in RA. Recruitment of additional spark sites was observed in RA. In conclusion, myogenic and Ca²⁺ spark mediated mechanisms of vascular diameter control differed between genders and different segments of the cochlear vasculature.

Supported by NIH-R01-DC04280 and NIH-P20-RR017686.

118 2-Aminoethoxydiphenyl Borate (2-APB) Inhibits Voltage-Gated K⁺-Channels (K_V) in Smooth Muscle Cells and Gap Junction Channels in Guinea-Pig Cochlear Arteries Ke-Tao Ma^{1,2}, Yugin Yang¹, Alfred Nuttall¹, Zhi-Gen

Ke-Tao Ma⁺⁺, Yuqin Yang⁺, Alfred Nuttall⁺, **Zhi-Gen** Jiang¹

¹Oregon Hearing Reserach Center, Oregon Health & Science University, ²Department of Physiology, Shihezi University Medical College

There is a pressing need for highly selective potent blockers and activators in biomedical research as well as clinical use. 2-Aminoethoxydiphenyl borate (2-APB) was reported to inhibit gap junction channels composed of connexin26 and/or connexins32 and used as a blocker of electro-coupling-mediated EDHF and secondary relaxation in rabbit iliac artery. However, its potency in blocking vascular junctional channels and its side actions on nonjunctional channels remain undetermined. Using whole-cell voltage-clamp and intracellular current clamp techniques, we studied these actions on vascular smooth muscle cells (VSMC) in situ of the acutely isolated arteriolar segments and in dispersed VSMCs and endothelial cells (EC) from the cochlear spiral modiolar artery (SMA). We demonstrated that 1) 2-APB and its analog DPBA both reversibly suppressed the input conductance (Ginput), or increased the input resistance, in a concentrationdependent manner, with an IC_{50} of 8.0 and 4.4 μ M, respectively. A complete electrical isolation of the recorded VSMC was achieved at 100 µM. A similar gap junction blockade was observed in tubules of endothelial cells. 2) 2-APB and DPBA (\geq 10 µM) reversibly depolarized the cells with larger amplitudes than that by 18β-glycyrrhetinic acid (18BGA). 3) On dispersed VSMCs, 2-APB and DPBA (100 μ M) had no significant effect on G_{input} or I/V relation in a range between -140 and -40 mV but inhibited the delayed rectifying potassium current (K_{DR}). 4) The inhibition of K_{DR} was concentration-dependent with a similar IC_{50} of ~120 μM for both 2-APB and DPBA compared to ~50 μM for 18βGA. 5) The inhibition of K_{DR} was always more pronounced at potentials ≤20 mV than at 40 mV and was more pronounced for the fast than the slow component in step-activated current, similar to that by 4-AP but not that by TEA. 4-AP (10 mM) nullified this action of 2-APB. 6) The junctional and non-junctional actions were not affected by IP₃ receptor antagonist xestospongin C. We conclude that 2-APB and DPBA are about half as potent as 188GA in blocking the arteriolar gap junctions and K_{DR} channels in VSMCs. The K_{DR} inhibition of 2-APB is mainly on voltagegated, not Ca²⁺-activated, K⁺-channels. Supported by NIH NIDCD DC 004716 (ZGJ)

119 Functional Expression of P2X(4) Receptor in Capillary Endothelial Cells of the Cochlear Spiral Ligament and Its Role in Regulating the Capillary Diameter

Tao Wu¹, Xiaorui Shi¹, Min Dai¹, Alfred Nuttall¹ ¹Oregon Health & Science University The cochlear lateral wall generates the endocochlear potential (EP), which creates a driving force for the hair cell

transduction current and is essential for normal hearing. Blood flow at the cochlear lateral wall is critically important for maintaining the EP. The vulnerability of EP to hypoxia suggests that the blood flow in the cochlear lateral wall is dynamically and precisely regulated to meet the changing metabolic needs of the cochlear lateral wall. It has been reported that ATP, an important extracellular signaling molecule, plays an essential role in regulating cochlear blood flow. However, the cellular mechanism underlying the ATP-induced regional blood flow changes has not been investigated. In the current study, we demonstrate that 1) P2X(4) receptor is expressed in endothelial cells (ECs) of spiral ligament (SL) capillaries. 2) ATP elicits a characteristic current through P2X(4) on ECs in a dose dependent manner (EC₅₀=0.16 mM). The ATP current has a reversal potential around 0 mV, is inhibited by LaCl₃, PPADS and extracellular acidosis, and is less sensitive to αβmeATP and BzATP. 3) ATP elicits a transient increase of intracellular Ca2+ in ECs. 4) In accordance with the above in vitro findings, perilymphatic ATP (1 mM) caused dilation in SL capillaries in vivo by 11.5 %. L-NAME. a nonselective inhibitor of nitric oxide synthase, significantly blocked the dilation. These findings support our hypothesis that extracellular ATP regulates cochlear lateral blood flow through P2X(4) activation in ECs. A subsequent increase of [Ca²⁺] in ECs leads to a release of NO from ECs. NO and its downstream signals may lead to a relaxation of the contractile apparatus in ECs and pericytes. Supported by DC005983, DC000141 (ALN), DC008888 (XS). DC008888S1 (XS) and DC010844 (XS).

120 Bassoon and the Synaptic Ribbon Organize Ca2+ Channels and Vesicles to Form a Large Number of Release Sites and Promote Replenishment

Thomas Frank^{1,2}, **Mark A. Rutherford**¹, Nicola Strenzke^{3,4}, Andreas Neef², Tina Pangršic¹, Darina Khimich¹, Anna Fetjova⁵, Eckart Gundelfinger⁵, M. Charles Liberman⁴, Benjamin Harke⁶, Zhizi Jing³, Keith E. Bryan⁷, Amy Lee⁷, Alexander Egner⁶, Dietmar Riedel⁸, Tobias Moser^{1,2} ¹Inner Ear Lab, University of Göttingen Medical Center, ²Bernstein Center for Computational Neuroscience, ³Auditory Systems Physiology Group, University of Göttingen Medical Center, ⁴Eaton Peabody Laboratory, Massachusetts Eye and Ear Infirmary, ⁵Dept. of Neurochemistry and Molecular Biol., Leibniz Inst. for Neurobiol., ⁶Dept. of Nanobiophotonics, Max Planck Institute for Biophysical Chemistry, ⁷Department of Molecular Physiology and Biophysics, University of Iowa, Iowa City, ⁸Lab. of Electron Microscopy, Max Planck Inst. for Biophysical Chemistry

At the presynaptic active zone, Ca2+ influx triggers fusion of synaptic vesicles. It is not well understood how Ca2+ channel clustering and synaptic vesicle docking are organized. Here we studied structure and function of hair cell ribbon synapses following genetic disruption of the presynaptic scaffold protein Bassoon. Mutant synapses most lacking the ribbon - showed a reduction in membrane-proximal vesicles, with ribbonless synapses affected more than ribbon occupied synapses. Ca2+ channels were also fewer at mutant synapses and appeared in abnormally shaped clusters. Ribbon absence reduced Ca2+-channel numbers at mutant and wildtype synapses. Despite reduced release rates, coupling of the remaining Ca2+-channels to exocytosis was normal in mutants. In vitro and in vivo recordings revealed impaired vesicle replenishment, and mechanistic modeling of the in vivo data independently supported morphological and functional in-vitro findings. We conclude that Bassoon and the ribbon (1) create a large number of release sites by organizing Ca2+ channels and vesicles, and (2) promote vesicle replenishment.

121 Evidence for Purinergic Cochlear Connective Tissue to Epithelial Cell Signaling Joe Adams¹

¹*Massachusetts Eye & Ear Infirmary*

The function of cochlear sensory cells requires the presence of unlimited K+ ions in endolymph that are recycled after passing through hair cells. Type II fibrocytes are generally accepted as the cells that take up the bulk of K+ ions for recycling from perilymph to the stria vascularis. Supporting the high metabolic load of this function is a high density of mitochondria within type II fibrocytes. It is common for cells with high ATP consumption to release ATP or other purines when they are active. The released purines act as autocrine and/or paracrine signals. This appears to the case for type II fibrocytes. Purinergic signaling between type II fibrocytes and adjacent root cells is evidenced by the presence of immunostaining of root cells for the purinergic receptors P2X2, P2X7, P2Y14, and the adenosine receptor A1. The presence of the adenosine receptor appears to be coupled to root cell immunostaining ecto-5'-nucleotidase/CD73, which produces for extracellular adenosine. The functional significance of extracellular adenosine and a receptor for it is suggested by the presence of staining in the root cell plasma membrane for the K+ channel Kir6.2, which is known to be highly sensitive to purinergic activation. This signaling pathway may serve as a feedback system to regulate K+ efflux from root cells by ATP release from type II fibrocytes. The presence and responsivity of P2X2, P2X7, and P2Y14 in root cells suggest that these receptors may also control ion flux from root cells and/or signaling among epithelial cells via connexins and/or annexins in response to release of purines by type II fibrocytes. Noise exposures induce increased staining for P2X2, P2X7 and P2Y14 in root cells. These findings indicate the presence of a feedback system from the spiral ligament to the sensory epithelium in response to effects of sound-induced increased ion flux, which suggests the presence of a dynamic interaction between cochlear epithelial and connective tissue cells.

122 Metabotropic Glutamate Receptor Expression in the Mouse Cochlea

Marcello Peppi^{1,2}, Albena Kantardzhieva^{1,2}, Melissa Landa^{1,2}, William F. Sewell^{1,2}

¹Harvard Medical School, ²Massachusetts Eye and Ear Infirmary

Although ionotropic glutamate receptors mediate afferent transmission in the cochlea, metabotropic receptors are also known to be present in the auditory nerve. There is little systematic analysis of their presence or distribution. Metabotropic glutamate receptors are a family of eight subtypes (mGluR1-8). We investigated their expression and distribution in the cochlea using quantitative RT-PCR and confocal microscopy. Most mGluR subunits were detected by RT-PCR. Levels in the cochlea were generally much lower than those in the brain. Highest levels of mRNA in the cochlea were detected for mgluR 4, 7, and 8, the former showing high variability among animals (n=7). Lowest levels were detected for mGluR 2 and 5. We were unable to detect significant mRNA for mGluR6 in either the cochlea or the brain. We performed immunohistochemical analysis for mGluR 4, 7 and 8. Two of them- mGluR 7 and 8 were expressed in spiral ganglion cells and in afferent terminals, while mGluR4 was present in afferent terminals. Our previous immunochemical analysis of mGluR1 and mGluR5 receptors (Manning et al, ARO 2006) also localized metabotropic receptors to spiral ganglion cells and afferent terminals. This data support the idea that metabotropic subunits might play a role in sound transmission in cochlea.

123 Kainate Receptors in Cochlear Afferent Transmission

Marcello Peppi¹, Melissa Landa², William F. Sewell¹ ¹*Harvard Medical School,* ²*Massachusetts Eye and Ear Infirmary*

Synaptic transmission between the cochlear hair cell and its afferent fiber is mediated by glutamate receptors. Although all three types of ionotropic glutamate receptors (AMPA, kainate, and NMDA) appear to be present in afferent neurons, information on the presence, distribution and role of kainate receptors in the cochlea is sparse. GluK receptor subunits (GluK1, 2, 4, and 5) are seen in spiral ganglion cell bodies by in situ hybridization (Niedzilski and Wenthold, 1995), but it is not known whether the receptors, once generated, are distributed at the hair cell afferent synapse or on the presynaptic terminals in the cochlear nucleus. We have approached the examination of GluK receptors in the mouse cochlea with gRT-PCR, confocal microscopy, and pharmacology. All kainate receptor subunits GluK (1-5) were observed in gRT-PCR in the cochlea with GluK5 most highly expressed. Immunolabel for both ampa (GluR2) and kainate (GluK1-5) subunits were found together in intense puncta (synaptic plaques) at the base of IHCs. Interestingly, even at the same inner hair cell, different terminals showed different ratios of ampa receptor to kainate receptor immunoreactivity. And even within the same synaptic plaque, ampa (GluR2) and kainate receptor immunoreactivity sometimes showed differential clustering.

To determine whether kainate receptors functioned in afferent transmission, we infused UBP296, an antagonist for the GluK1 (GluR5) kainate receptor subunit, into the scala tympani. At 300 micromolar, UBP296 increased ABR thresholds but did not alter DPOAEs, implicating kainate receptor function in afferent transmission of auditory responses.

124 Estrogen Receptors in the Auditory System in Different Hormonal Conditions

Konstantina Charitidi¹, Inna Meltser¹, Barbara Canlon¹ ¹*Karolinska Institutet*

How do fluctuations of estrogen levels affect hearing? Previous experimental and clinical work suggests that sex hormones interact with the auditory system and estrogen receptors (ERs) have been mapped in the cochlea as well as in the central auditory system. Estrogens' actions are mainly mediated by estrogen receptors alpha and beta (ER α and ER β). We examine the expression levels of these two proteins in different regions of the auditory system in different hormonal states. Both the peripheral (cochlea) and central auditory system (cochlear nucleus and inferior colliculus) are examined. Two different experimental models were studied in order to determine the effects on estrogen receptor expression in the auditory system. The first model included ovariectomized females that were supplemented with either estradiol or vehicle. The second model was to determine how estrogen receptor expression varies during the different phases of the estrous cycle (proestrous, estrous, metestrous and diestrous) in intact mice. Methods that are used include western blot for the protein levels and gRT-PCR for the transcription levels. These results provide information that will promote our understanding of estrogens' actions in the auditory system, and how these effects change with hormonal status.

¹Supported from the Swedish Medical Research Council, Karolinska Institutet, Funds of Karolinska Institute, Tysta Skolan.

Keywords: estrogens, cochlea, hearing, inner ear, estrogen receptors

125 Structural and Immunocyotchemical Studies of the Extracellular Matrix and Fibrocytes in the Spiral Ligament of CD/1 Mice

Shanthini Mahendrasingam¹, **David Furness¹** ¹*Keele University*

Fibrocytes in the spiral ligament (SL) function in cochlear homeostasis, helping to recycle potassium and maintain the endocochlear potential. Fibrocyte degeneration contributes to presbyacusic or noise induced hearing loss, and as these cells are located relatively superficially in the cochlear lateral wall, they may be amenable to replacement by cell transplantation therapy. Successful replacement of cells will, however, rely on a number of local factors such as surviving extracellular matrix (ecm). We have investigated the SL by scanning and transmission electron microscopy in young and aged animals and by immunogold labelling for collagens II and V to better understand its complex architecture. Five main types of fibrocyte were distinguished by location and morphology, similar to previous descriptions. Type I fibrocytes are elongated with few surface folds. Type II fibrocytes are commonly rounded, with many fine folds interdigitating with those of adjacent cells. Type III are small and elongated with a complex honeycomb of fine peripheral processes. Type V, like type II cells, have many fine surface processes with thicker ones extending into scala vestibuli. The ecm is organised into branched dense fibres composed of fine 20 nm fibrils passing through a looser network of 20 nm and smaller fibrils. The dense fibres and network are found between the processes and cell bodies of all except type IV fibrocytes which lie in hollows enclosed by a thick mat. The loose network extends with type V processes into the scala vestibuli. The dense fibres and the network both label for collagen II, particularly 20 nm fibrils; collagen V mostly labels the finer network fibrils. In older animals, the ecm structure is retained even when fibrocytes are lost. These data suggest that a framework of ecm exists, in which fibrocytes are interwoven, that persists throughout life. It thus represents a natural scaffold into which fibrocytes may be transplanted to repair the SL.

126 Missing Mitochondrial Mpv17 Gene Function Induces Tissue Specific Cell Death Pathway in the Degenerating Inner Ear Angela-Maria Meyer-zum-Gottesberge¹, Thomas Massing¹, Stefan Hansen¹

¹Dept. of ORL, University of Duesseldorf Discoverers of Mpv17 in early 1990s mistakenly concluded that the protein produced by the gene was located in the peroxisome, an organelle involved in metabolism of ROS. However, recent studies established its actual location inside the inner membrane of mitochondria (Trott and Morano, 2004). The loss of function in Mpv17-/- mice leads to early sensorineural deafness associated with severe inner ear degeneration and late onset of kidney failure (Meyer zum Gottesberge et al., 1996). In humans, Mpv17 mutations are responsible for a severe mitochondrial depletion syndrome, mainly affecting the liver and the nervous system (Spinazzola et al., 2006). Our study demonstrates (i) that an inactivation of the mitochondrial Mpv17 gene induced tissue specific mitochondrial morphological alterations of the inner ear and (ii) that the onset of the degeneration of cochlear neuroepithelia is related to the onset of the auditory function and appears to be first restricted to the outer hair cells (OHC) that subsequently undergo fast degeneration. At the age of 18 days, the OHC lateral membrane degenerated and we observed an extensive vacuolization of the cytoplasm followed by lyses of the OHCs. Such degenerative processes have been seen for the first time in relation to the auditory dysfunction. The structural degeneration pattern of the OHC appears to be similar to the described paraptotic processes (alternative form of programmed cell death) discussed as a cause of cytoplasmatic neurodegeneration (Sperandio et al. 2000). In contrast, the neural crest origin melanocytes-like intermediate cells, located in the stria vascularis, undergo apoptosis, which was documented ultrastructurally and with TUNEL assay from the age of 18 days, whereas the delayed degeneration of mitochondria-rich marginal cell is associated with activation of caspase-9. It is obvious that a lack of the Mpv17 protein function in the mitochondria initiates tissue specific cell death pathways readily resulting in the pathology

seen during the degeneration.

127 Abnormal Cochlear Potentials Recorded by Transtympanic Electrocochleography from Patients with Auditory Neuropathy Due to Mutations in the Otoferlin or OPA1 Gene

Rosamaria Santarelli¹, Arnold Starr², Ignacio del Castillo³, Taosheng Huang², Edoardo Arslan¹

¹University of Padua, ²University of California, ³Hospital Ramón y Cajal

Auditory neuropathy (AN) is a disorder characterized by disruption of auditory nerve activity resulting from lesions involving the auditory nerve, inner hair cells (IHCs) and/or the synapses. Affected subjects show impairment of speech perception beyond that expected for the hearing loss, abnormality of auditory brainstem potentials and preserved outer hair cell activities (otoacoustic emissions microphonic, and/or cochlear CM). Abnormal neurotransmitter release from IHCs has been proposed as the mechanism underlying AN in patients with mutations in the OTOF gene (pre-synaptic AN), while disruption of auditory nerve function may underlie the disorder with OPA1 mutations (post-synaptic AN).

Transtympanic electrocochleography was recorded from 4 children with OTOF mutation and 2 adults with mutation in the OPA1 gene. Cochlear potentials to clicks were compared to recordings obtained from 16 normally hearing children. Electrically-evoked compound action potentials (CAPs) were also obtained following cochlear implantation. Cochlear neural potentials were of negative polarity with reduced amplitude and prolonged duration compared to controls. The prolonged potentials were recorded as low as 50-90 dB below behavioral thresholds in subjects with OTOF mutation whereas in patients with OPA1 mutation they were correlated with behavioral threshold. Auditory CAPs were superimposed on the prolonged responses in 3 subjects with OTOF mutations at high stimulus intensity while they were absent in OPA1 disorder. Electricallyevoked CAPs were only recorded from children with OTOF mutations.

In subjects with OTOF mutations the low-threshold prolonged potentials are consistent with abnormal neurotransmitter release resulting in reduced dendritic activation and impairment of spike initiation whereas the lack of CAPs in OPA1 is consistent with abnormal function of distal portions of auditory nerve fibers.

128 Tmprss3, a Transmembrane Serine Protease Deficient in Human DFNB8/10 Deafness, Is Critical for Cochlear Hair Cell Survival at the Onset of Hearing

Lydie Fasquelle^{1,2}, Hamish Scott³, Marc Lenoir^{1,4}, Jing Wang^{1,4}, Guy Rebillard^{1,4}, Sophie Gaboyard^{1,4}, Anne-Laure Mausset-Bonnefont^{1,4}, Elizabeth Neidhart², Christian Chabbert^{1,4}, Jean-Luc Puel^{1,4}, Benjamin Delprat^{1,4} ¹Inserm U583 - Institut des Neurosciences de Montpellier -France, ²Department of Genetic Medicine and Development, University of Geneva Medical School -Switzerland, ³Division of Molecular Medicine, The Walter and Eliza Hall Institute of Medical Research - Australia, ⁴Université Montpellier 1 - France

Mutations in the type II transmembrane serine protease 3 (TMPRSS3) gene cause non-syndromic autosomal recessive deafness DFNB8/10. This deafness is characterized by congenital or childhood onset bilateral profound hearing loss.TMPRSS3 is a transmembrane protein containing three extracellular domains. The LDLRA domain binds calcium and lipoprotein, the SRCR domain is involved in protein-protein interaction and the serine protease domain is the catalytic one.

In order to explore the role of TMPRSS3 in cochlear physiology, we have generated an ENU-induced mutant mouse in which the tyrosine 260 was changed into a STOP codon (Y260X), thus deleting the major part of the serine protease domain. Auditory brainstem responses revealed that wild type and heterozygous mice have normal hearing thresholds out to 5 months of age, whereas Tmprss3Y260X homozygous mice are completely deaf. Histological investigations revealed that both type of cochlear hair cell develop normally until hearing onset (postnatal day 12) and then began to degenerate in the basal turn, reaching complete degeneration in entire cochlea within 2 days. This is the first model showing a so drastic and rapid degeneration of both types of cochlear hair cells at the onset of hearing.

Given that auditory and vestibular deficits often co-exist, we evaluated the balancing abilities of Tmprss3Y360X homozygous mice by using rotating rod and vestibularspecific behavioural tests. We have shown that adult Tmprss3Y260X homozygous mice effectively displayed mild vestibular syndrome that correlated histologically with a slow degeneration of only saccular hair cells.

Our results show that TMPRSS3 acts as a permissive factor for cochlear hair cells survival at the onset of hearing and is required for saccular hair cell survival. This mouse model will allow us to decipher the molecular mechanisms underlying DFNB8/10 deafness and cochlea function.

129 Cellular and Molecular Mechanisms of Autosomal Dominant Form of Progressive Hearing Loss, DFNA2

Hyo Jeong Kim¹, Ping Lv¹, Choong-Ryoul Sihn¹, Ebenezer Yamoah¹

¹Dept. of Anesthesiology and Pain Medicine, Schoole of Medicine, University of California Davis

Despite advances in identifying deafness genes. determination of the underlying cellular and functional mechanisms for auditory diseases remains a challenge. Mutations of the human K+ channel hKv7.4 lead to postlingual progressive hearing loss (DFNA2), which is universal, affecting world-wide population with diverse racial background. Here, we have generated the spectrum of point mutations in the hKv7.4 that have been identified as diseased mutants. We report that expression of 5 point mutations in the pore-region, namely, L274H, W276S, L281S, G285C, and G296S, as well as the C-terminal mutant G321S in heterologous expression system vielded non-functional channels, owing to ER retention of the mutant channels. We mimicked the dominant diseased conditions by co-expressing the wildtype and mutant channels. Compared to expression of wildtype channel alone, the blend of wildtype and mutant channel subunits resulted in reduced currents. Moreover, the combinatorial ratios of wildtype:mutant and the ensuing current magnitude could not be explained by the predictions of a tetrameric channel and a dominant negative effect of the mutant subunits. The results can be explained by the dependence of cell-surface expression of the mutant on the wildtype subunit. A transmembrane mutation F182L, which has been identified in a pre-lingual progressive hearing loss patient in Taiwan, yielded cell-surface and functional features expression that were indistinguishable from the wildtype's, suggesting this mutation may represent redundant polymorphism. Collectively, these findings provide a unified cellular mechanisms for DFNA2 and set the stage for additional investigation on the unknown etiology of deafness associated with hKv7.4 mutants.

130 Antibody Microarray Analysis of the Coch^{G88E/G88E} Mouse Model for DFNA9

Donald Coling¹, Nahid G. Roberston², Samson Jamesdaniel¹, Anne B.S. Giersch^{3,4}, Cynthia C. Morton^{4,5}, Richard Salvi¹

¹Center for Hearing and Deafness, University at Buffalo, the State University of New York, ²Department of Obstetrics, Gynecology and Reproductive Biology, Brigham and Women's Hospital, ³Department of Pathology, Brigham and Women's Hospital, ⁴Harvard Medical School, ⁵Depts. of Obstetrics, Gynecol. and Reproductive Biol. and of Pathology, Brigham and Women's Hospital

Cochlin, encoded by *COCH*, is a highly abundant protein in murine, bovine, and human inner ears. Mutations in *COCH* have been reported worldwide to cause the lateonset hearing and vestibular disorder, DFNA9. DFNA9 is characterized by loss of fibrocytes and by the presence of eosinophilic material in cochlin-staining temporal bone

specimens, most notably in the spiral ligament and limbus. To gain insights into the pathobiological molecular mechanisms of DFNA9, proteomic profiles of a DFNA9 mouse model, *Coch*^{G88E/G88E} (backcrossed 12X into CBA/CaJ) and wild-type CBA/CaJ mice were assessed at 8-10 months of age, prior to the onset of detectable hearing loss which occurs at 20 months in this mouse model. Whole cochlear protein samples were prepared for each assay from 11-13 *Coch^{G88E/G88E}* and CBA/CaJ mice. Proteins were labeled with cyanine dyes and assayed for binding to an antibody microarray, detecting over 700 signaling proteins (Sigma XP-725). Four independent biological replicates were analyzed with the Significance Analysis of Microarrays software package. Significant differential expression (false discovery rate = 33%) was detected for three proteins: Grk2 (1.8X \uparrow), parkin (1.1X \uparrow), and Gfi1 (0.8X ψ). Grk2 has been reported to desensitize growth factor and G-protein coupled receptors, parkin is an E3-ubiguitin ligase associated with neurodegeneration in familial parkinsonism, and Gfi1 is a nuclear zinc finger protein that functions as a transcriptional repressor to control histone modifications. Differentially expressed proteins (51 proteins with largest fold changes) were significantly enriched for the focal adhesion signaling pathway ($p < 10^{-08}$) including the transcription factor c-Jun and several proteins whose genes contain predicted binding sites for JUN. Expression profiling on oligonucleotide microarrays is in progress for correlation and extension of this proteomic analysis. Results from expression studies provide a framework for development of testable hypotheses by which the G88E cochlin missense mutation causes sensorineural hearing loss and vestibular disease.

131 Different Pathogenetic Mechanisms of Double Heterozygous Mutation of Cx26 and Cx30 Induced Hearing Loss

Liang Zong¹, Yan Zhu¹, Chun Liang¹, Guang-Di Chen², Hong-Bo Zhao¹

¹Dept. of Surgery-Otolaryngology, University of Kentucky Medical School, Lexington, ²Center for Hearing & Deafness

Connexin26 (Cx26, GJB2) and Cx30 (GJB6) are predominant isoforms co-expressed in the cochlea. Mutations of either Cx26 or Cx30 can cause hearing loss. The heterozygous mutations of a large deletion in Cx30 combined with Cx26 point mutation (Cx26 mutation/Cx30 deletion) can also induce hearing loss and are the second most frequent cause of recessive deafness. However, the mechanism underlying this digenic inheritance of deafness remains largely undetermined. To investigate the pathological mechanism underlying this double heterozygous Cx26/Cx30 mutation induced hearing loss. we generated double heterozygous Cx26 and Cx30 alleles (Cx26^{+/-}/Cx30^{+/-}) mice. Auditory brainstem response (ABR) showed a moderate hearing loss in the tested frequency range from 4 to 40 kHz. Distortion product otoacoustic emission (DPOAE) was also measured. Double heterozygous Cx26^{+/-}/Cx30^{+/-} mutation mice had a significant reduction in the DPOAE amplitudes. Histological

examination shows that the cochlea appeared normal morphology under the light microscopy. Different from Cx26^{-/-} or Cx30^{-/-} KO mice, no significant hair cell loss was detected. Our data suggest that digenic inheritance of hearing loss caused by heterozygous Cx26/Cx30 mutations has different pathological changes in the cochlea in comparison with monogenic Cx26 or Cx30 mutations, which have apparent cochlear development disorder and hair cell loss. Our finding provides important and also very useful information for guiding application of therapeutic inventions. These heterozygous Cx26/Cx30 mutation individuals may be good candidates for cochlear implant, due to they retain most hair cells. Supported by NIH DC05989

132 Generation and Analysis of Mouse Models of Human Cx26 Related Deafness

Melanie Schütz¹, Joachim Degen¹, Anna Gehrt², **Nicola Strenzke²**, Tanja Auth¹, Felicitas Bosen¹, Melanie Jokwitz¹, Inken Körber¹, Nikolai Dicke¹, Tobias Moser², Klaus Willecke¹

¹University of Bonn, ²University Medicine Göttingen Functional gap junction channels are essential for cochlear function. Deficiencies in the genes coding for Connexin (Cx) 26 and Cx30 in the cochlea lead to hearing impairment in mice and me. Here, we generated two mouse models of Cx26 related human deafness. In the first line we knocked-in the human Cx26S17F mutation into the Gjb2 locus to model the human Keratitis-Ichthyosis-Deafness syndrome. While homozygous expression of Cx26S17F was embryonically lethal, heterozygous mice showed skin hyperplasia, wounded tails, annular tail restrictions and a pantonal increase in ABR thresholds by approximately 35dB. These mice thus resembled the human Keratitis-Ichthyosis-Deafness syndrome. ABR threshold increases correlated inversely with the endocochlear potential which was decreased by 20-40%. This suggests that reduced intercellular coupling by heteromeric channels composed of Cx26S17F and Cx30 contributes to the hearing impairment in heterozygous mice. The second mouse line expressed Cx32 (Gjb1) instead of Cx26 (Gjb2) in otogelin-expressing cells. ABR thresholds in mice carrying one Gjb1 allele under the control of the Gjb2 promotor and one or none Gjb2 allele were improved over those in mice lacking one or both copies of the Gjb2 gene, respectively. This suggests that Cx32 can functionally replace Cx26 in the cochlea.

133 Mouse Model Study for Cx26 Mutation Induced Late-Onset Hearing Loss

Hong-Bo Zhao¹, Liang Zong¹, Yan Zhu¹, Guang-Di Chen², Chun Liang¹

¹Dept. of Surgery - Otolaryngology, University of Kentucky Medical Center, Leington,²Center for Hearing & Deafness Mutations in connexin 26 (Cx26, GJB2) are the most common cause of nonsyndromic hearing loss. Deafness due to GJB2 mutations is not always prelingual. A large group of these patients (~30%) demonstrate a progressive, late-onset hearing loss, starting from high frequencies. These individuals are good candidates for applying therapeutic interventions because their hearing loss is a relatively slow process. Most importantly, due to their normal hearing in early stage of life, these individuals possess a big potential for applying protective interventions from deafness. However, little is known about the deafness mechanism underlying this late-onset hearing loss. In this study, we intend to develop a mouse model to investigate its deafness mechanism. By use of a novel tamoxifen (TAM)-inducible Cre-loxP recombination system. we selectively deleted Cx26 expression in the cochlea after birth. We found that the conditional KO mice had normal hearing after mature, then demonstrated a progressive hearing loss in auditory brainstem response (ABR) measurements. The hearing loss was severe at high frequency range and progressively extended to the lower frequency range. Different from deletion of Cx26 before/at the birth, the cochlea had no visible disorder in the development and appeared a normal morphology under the light microscopy. Hair cell loss is visible but not severe. Most hair cells retained integrity and appeared a normal shape. Our results suggest that Cx26 may not only play an essential role in the cochlear development but also achieve crucial functions in maintaining normal hearing in the adult cochlea. The data also suggest that Cx26 mutation induced late-onset hearing loss may have different pathologic changes in the cochlea from its congenital hearing loss. This is important for applying therapeutic and protective interventions.

Supported by NIH DC05989

134 Evidence for Mixed Sensorineural/ Conductive Hearing Loss and Resistance to Noise Exposure in a Mouse Model of CHARGE Syndrome

Elizabeth A. Hurd¹, Meredith E. Adams², Wanda S. Layman¹, Lisa A. Beyer¹, David F Dolan¹, Yehoash Raphael¹, Donna M. Martin¹

¹The University of Michigan, ²The University of Minnesota Heterozygous mutations in chromodomain-DNA-bindingprotein 7 (CHD7) cause CHARGE syndrome, a multiple anomaly condition which includes vestibular dysfunction and hearing loss (HL). Chd7^{Gt/+} mice have semicircular canal dysgenesis, abnormal inner ear neurogenesis, and mild HL, and are an excellent model of CHARGE syndrome. Detailed characterization of hearing ability and underlying cochlear pathology in Chd7 mutant mice has not been reported. In this study, we examined inner ear electrophysiology and expression of Chd7 in adult mouse cochleae. ABR tests showed mildly elevated thresholds in Chd7^{Gt/+} mice compared to wild type littermates. No measurable distortion product otoacoustic emissions (DPOAE) were observed in Chd7^{Gt/+} mice. The severity of the DPOAE findings and relatively mild elevation in ABR thresholds at low frequency (4 kHz) in Chd7GU+ mice suggests mixed sensorineural and conductive HL. CHD7 in outer hair cells (OHCs) and in spiral ganglion neurons was identified by co-immunofluorescence with antibodies against prestin and neurofilament. Prestin and neurofilament labeling were preserved in adult Chd7Gt/+ cochleae, and hair cell ultrastructure in Chd7Gt/+ mice

appeared normal by scanning electron microscopy. To test for susceptibility to injury, we exposed 6 month-old littermate $Chd7^{Gt/+}$ and wild type mice to broadband noise (123 dBSPL, 4 hrs) and examined hair cell loss by phalloidin fluorescence. Wild type, noise-exposed mice had severe loss of OHCs and mild loss of inner hair cells throughout the cochlea, whereas $Chd7^{Gt/+}$ mice did not. Together, our data indicate that $Chd7^{Gt/+}$ mice have combined conductive and sensorineural HL, with apparent protection from noise exposure. Further detailed analysis of middle and inner ear function at several ages is needed to clarify the precise role(s) of CHD7 in hearing and to provide critical information for developing therapeutic approaches for CHARGE patients.

Supported by the Hirschfield Foundation, and NIH/NIDCD grants DC009410, DC010412, and DC05188.

135 Pathogenic Effects of a Novel Mutation (C.664_681del) in KCNQ4 Channels Associated with Auditory Pathology

Jeong-In Baek¹, Hong-Joon Park², Kyungjoon Park³, Su-Jin Choi¹, Kyu-Yup Lee⁴, Jee Hyun Yi³, Thomas B. Friedman⁵, Dennis Drayna⁵, Ki Soon Shin³, Un-Kyung Kim¹

¹Dept. of Biology, College of Natural Sciences, Kyungpook National University, ²Soree Ear Clinics, ³Dept. of Biology, Dept. of Life and Nanopharmaceutical Sciences,

Kyunghee University, ⁴Department of Otorhinolaryngology-Head and Neck Surgery, College of Medicine, Kyungpook National Uni, ⁵National Institute on Deafness and Other Communication Disorders

Hearing loss is a common communication disorder caused by various environmental and genetic factors. Hereditary hearing loss is very heterogeneous, and most of such cases involve sensorineural defects in the auditory pathway. There are currently 57 known autosomal dominant non-syndromic hearing loss (DFNA) loci, and the causative genes have been identified at 22 of these loci. In the present study, we performed a genome-wide linkage analysis in a Korean family segregating autosomal We observed linkage on dominant hearing loss. chromosome 1p34, and at this locus, we detected a novel mutation consisting of an 18 nucleotide deletion in exon 4 of the KCNQ4 gene, which encodes a voltage-gated potassium channel. We carried out a functional in vitro study to analyze the effects of this mutation (c.664 681del) along with two previously described KCNQ4 mutations, p.W276S and p.G285C. Although the c.664 681del mutation is located in the intercellular loop and the two previously described mutations. p.W276S and p.G285C. are located in the pore region, all mutants inhibit normal channel function by dominant negative effect. Our analysis indicates that the intercellular loop is as significant as the pore region as a potential site of pathogenic effects on KCNQ4 channel function.

Key words: hearing loss, KCNQ4, K+ channel, mutation, dominant-negative effect

136 Targeted Mutation of Mouse *Grxcr2* Results in Hearing Loss Without Overt Vestibular Defects

Matthew Avenarius^{1,2}, Lisa Beyer¹, Thomas Saunders^{1,3}, David Dolan¹, Yehoash Raphael¹, David Kohrman^{1,2} ¹University of Michigan Medical School, Dept. of Otolaryngology/Kresge Hearing Research Institute, ²University of Michigan Medical School, Dept. of Human Genetics, ³University of Michigan Medical School, Transgenic Animal Model Core

Mutations in Grxcr1 underlie profound deafness in mouse and humans. A related gene, Grxcr2, encodes a similar glutaredoxin-like cysteine-rich protein that, like GRXCR1, is expressed in sensory hair cells in the cochlea and in vestibular organs and is localized to stereocilia. We have generated a conditional mutant allele of Grxcr2 and begun to characterize its auditory and vestibular phenotypes. Mice carrying homozygous germline deletions of exon 1 exhibit significant hearing loss by 3 weeks of age across all measured frequencies. Unlike null mutants of Grxcr1, which exhibit profound deafness together with circling and head shaking behaviors, the targeted Grxcr2 mutants do not show overt vestibular defects. These results indicate that Grxcr2 is required for normal hearing but may be dispensable for vestibular function. We are currently evaluating in greater detail the time of onset and potential progression of hearing loss in the Grxcr2 mutants. Additional expression analysis and morphological characterization of these mutants will provide insight into the critical role of *Grxcr2* in the development of auditory function.

Supported by NIH grants R01-DC003049 and P30-DC05188.

137 Derivation of Conditionally Immortalized Clonal Cell Populations from Strial Explants Derived from the Immortomouse: Modulation of Gene Expression by High Glucose and Hypoxia

Zachary Sutton¹, Linda Cheung¹, Eric Jesteadt¹, Daniel Meehan¹, Michael Anne Gratton², Duane Delimont¹, Marisa Zallocchi¹, **Dominic Cosgrove³** ¹*BTNRH*, ²*Saint Louis University*, ³*Boys Town National*

'BTNRH, ²Saint Louis University, ³Boys Town National Research Hospital

In diseases such as Alport syndrome and diabetes, progressive hearing loss is associated with thickening of the capillary basement membranes of the stria vascularis (SCBM), which may result in strial dysfunction. The cell biology underlying these changes is unclear. largely due to the inaccessibility of workable quantities of strial tissue. To circumvent this limitation, we attempted to derive conditionally immortalized clonal populations of strial cells from strial explants microdissected from the "immortomouse". We consistently observed three distinct cell morphologies, and selected representative clones of each for further characterization. We screened the clones for expression of a number of markers aiming to differentiate the strial cell types from which they arose. One clone was identified as a strial marginal cell line on

the basis of its differential expression of Na/K ATPase β 1, PanX3, and both KCNE1 (Isk) and KCNQ1. Another clone was identified as of basal cell origin on the basis of its differential expression of PanX2, Kir4.1, and connexin B1. A third clone was identified as of intermediate cell origin on the basis of its differential expression of Kir 4.1 and the absence of connexin β 1, KCNQ1, and ISK296 expression. When cultured in media containing high glucose (4.5g/L) versus low glucose (1g/L), the marginal cells showed upregulation of mRNA for laminin $\alpha 2$ (5-fold) and $\beta 2$ (12-fold) chains as well as MMP-9 (3-fold), while intermediate or basal cell clones did not respond to glucose. All three cell lines express a myriad of laminins, type IV collagens, and matrix metalloproteinases. All cell lines responded to hypoxia by up-regulating hypoxia-related factors (VEGFs and HIFs). Specific responses in this regard were unique for each clone. Thus, we have developed cell lines representative for three major strial cell types and show that the marginal cells uniquely respond to high glucose by up regulating matrix and matrix metalloproteinase genes. All three cells appear sensitive to hypoxic stresses as might result from diseases where SCBM thickening is observed. These cell lines should provide a useful system for studying the mechanism of hearing loss where strial dysfunction is implicated.

Supported by R01 DC004844 (DC) and R01 DC006442 (MAG)

138 Mice Homozygous for the Common GJB2 P.V37I Variant Are More Vulnerable to Noise and Reveal an Altered MAP Kinases Expression After Noise Exposure

Ying-Chang Lu^{1,2}, Chen-Chi Wu^{1,3}, Wen-Sheng Shen¹, Chuan-Jen Hsu¹

¹Department of Otolaryngology, National Taiwan University Hospital, ²Institute of Biomedical Engineering, National Taiwan University, ³Department of Medical Genetics, National Taiwan University Hospital

GJB2 is the most common deafness-associated gene. Although more than 100 GJB2 sequence variants have been reported, the pathogenetic mechanisms of certain common variants remain unclear, such as p.V37I (c.109G>A). Patients homozygous for p.V37I demonstrate a broad-spectrum of phenotypes, ranging from normal hearing to moderate-to-severe sensorineural hearing impairment, implicating an interplay between the genetic and environmental factors. In the present study, we compared the audiological response to noise (120 dB, 4k Hz for 3 hours) between knock-in mice homozygous for p.V37I (i.e. Gjb2tm1Dontuh/tm1Dontuh mice) and wildtype Gjb2+/+ mice. The expression of Cx26 protein and MAP kinases (including ERK, JNK, and p38), which have been related to noise-induced hearing loss, were also investigated Western blotting using and immunofluorescence methods. Normal hearing Gib2tm1Dontuh/tm1Dontuh (n=10) mice revealed a transient shift of hearing threshold to 72.0 ± 5.9 dBSPL 30 mins after noise exposure, which was significantly higher as compared to 57.6 \pm 3.5 dBSPL in Gjb2+/+ (n=10) mice (p < 0.05). The expression of Cx26 was increased in both

Gjb2+/+ and Gjb2tm1Dontuh /tm1Dontuh mice. On the other hand, phosphorylated p38, JNK1/2, and ERK1/2 were up-regulated in Gjb2+/+ mice, whereas only pp38 was up-regulated in Gjb2tm1Dontuh/tm1Dontuh mice. To summarize, Gjb2tm1Dontuh/tm1Dontuh mice appeared more vulnerable to noise and revealed an altered MAP kinases expression after noise exposure, indicating that environmental noise might influence the audiological phenotype associated with the GJB2 p.V37I variant.

139 Hair Cell Specific Isl1 Transgenic Mice Are Protected from Age-Related (ARHL) and Noise-Induced Hearing Loss (NIHL)

Mingqian Huang^{1,2}, Albena Kantardzhieva^{1,2}, M. Charles Liberman^{1,2}, Zheng-Yi Chen^{1,2}

¹Massachusetts Eye & Ear Infirmary, ²Harvard Medical School

IsI1 is a LIM-homeodomain transcription factor (LIM-HD) that is critical in the development and differentiation of multiple tissues such as heart, pancreas, and nervous system. In the inner ear, IsI1 is expressed in the prosensory region of otocyst, remains in the early supporting cells and hair cells, but is downregulated postnatally.

To study the functional role of IsI1 in the inner ear, we created a transgenic mouse model in which the Pou4f3promoter-driven IsI1 is overexpressed in the hair cells. The expression of IsI1 transgene is hair cell specific and persists in adult hair cells. The inner ear of the transgenic mice is grossly normal.

ABR tests showed significantly lower threshold shifts across all frequencies in transgenic than in control mice starting at 6 months of age, whereas at 3 months the ABRs were indistinguishable between the two groups. From 6 to17 months, ABRs in transgenic mice were similar. In contrast, ABR thresholds increased continuously in control mice and by 17 months all control mice were completely deaf. As all mice were homozygous for the Cdh23^{Ahl} mutation, our results strongly support that Isl1 transgene rescues the progressive hearing loss caused by this mutation. In the aged Isl1 transgenic mice outer hair cells in middle and base regions are well preserved, whereas a severe loss of outer hair cells is observed in the aged control mice, indicating that Isl1 transgene attenuates ARHL by promoting hair cell survival during aging. There was a significant reduction of type II neurons in controls compared with transgenic mice, likely due to the loss of outer hair cells. Isl1 transgenic mice also exhibited significantly lower ABR threshold shifts than controls after noise exposure, indicating that Is1I transgene also attenuates NIHL. Our study revealed a novel role of IsI1 in the protection from both ARHL and NIHL with potential clinic implication. It further underlies a likely common mechanism between ARHL and NIHL in our model.

140 Hearing Loss and Incident Dementia

Frank Lin¹, E. Jeffrey Metter², Richard O'Brien¹, Susan Resnick², Alan Zonderman², Luigi Ferrucci² ¹*Johns Hopkins,* ²*National Institute on Aging* Background: Earlier studies have suggested that hearing loss may be a risk factor for dementia, but this hypothesis

has never been investigated prospectively. Methods: We performed audiometry in 639 participants (age 36 - 90 y) of the Baltimore Longitudinal Study of Aging who were dementia-free in 1990-1994 and prospectively followed them for incident dementia. Hearing loss was defined by a pure-tone average of hearing thresholds at 0.5, 1, 2, and 4 kHz in the better-hearing ear (normal <25 dB, mild loss 25-40 dB, moderate loss 41-70 dB, severe loss >70 dB). Diagnosis of incident dementia was made in a consensus diagnostic conference. Cox proportional hazard models were used to model time to incident dementia according to the severity of hearing loss. Results: 58 cases of incident all-cause dementia were diagnosed during follow-up (median 11.9 y). The risk of incident all-cause dementia increased linearly with the severity of baseline hearing loss (HR 1.27 per 10 db loss, 95% CI: 1.06 - 1.50). Compared to normal hearing, the hazard ratio for incident dementia was 1.89 for mild hearing loss (95% CI: 1.00 - 3.58), 3.00 for moderate hearing loss (95% CI: 1.43 - 6.30), and 4.94 for severe hearing loss (95% CI: 1.09 - 22.4).

Conclusions: Hearing loss which is prevalent in over 60% of adults >70 years is independently associated with allcause dementia. Whether hearing loss is a marker for early stage dementia or is actually a modifiable risk factor for dementia deserves further study.

141 Age-Related Changes and the Effect of Stimulation Pulse Rates on Cortical Processing in CI Listeners

Lendra Friesen^{1,2}, Takako Fujioka³, Joseph Chen^{1,2} ¹Sunnybrook Health Sciences Centre, ²University of Toronto, ³Rotman Research Institute

Background: Because more individuals with hearing loss are being treated with a cochlear implant (CI), it is important to understand how aging affects physiological mechanisms underlying CI listening. It has been clinically observed that when older CI users' performance is poor, they tend to prefer listening with slower CI stimulation pulse rates. We hypothesized that this preference may reflect aging-related loss of neural synchrony with higher rate stimulation, which may in turn affect speech understanding. Auditory evoked potentials reflect neural activity related to stimulus processing in the auditory cortex. In particular, the P1-N1-P2 complex (responses at 50-200ms after stimulus onset) is known to be sensitive to age-related changes in acoustic feature processing such as the temporal properties of the stimulus. Therefore, the aim of this study was to determine whether the physiological representation of stimulation pulse rate as indexed by the P1-N1-P2 complex changes with age in CI users

Methods: 10 elderly CI listeners (aged 70 to 85 years) and 10 younger CI users (aged 30 to 45 years) having the

Advanced Bionics HiRes 90k device were tested. Auditory evoked potentials was recorded from the subjects while they received electrical stimulation consisting of a repeated pulse train of 200 ms-second duration presented directly to a median electrode of the CI device. The pulse rate was varied using 5000, 3000, 1000, and 500 pulses per second (pps) in separate blocks. Amplitudes and latencies of the P1, N1, and P2 waves were examined for the different pulse rates and between the two age groups.

Results: While P1 amplitude and latency were increased in the elderly group compared to the younger group, little effect of the stimulus pulse rate was observed on P1. These age-related P1 effects are similar to those observed in normal hearing listeners. In contrast with P2, an amplitude decrease and latency increase were observed for higher pulse rates compared to lower stimulus pulse rate conditions in the elderly group, while these effects of stimulus pulse rates were only weakly present in the younger group.

Conclusions: The higher stimulation pulse rates in elderly CI listeners attenuated P2 components which are generated from non-primary auditory cortical areas. This may explain some CI listener's preference for lower pulse rate. Our results indicate that higher-order perceptual processing for speech sounds may be affected by neurophysiologic aging effects which also plays an important role in processing with stimulation pulse rate in CI listening.

142 Benefits of Musical Training for Speech-In-Noise Perception in Middle-Aged Adults Alexandra Parbery-Clark¹, Samira Anderson¹, Dana

Strait¹, Emily Hittner¹, Nina Kraus¹

¹Northwestern University

Much of our daily communication occurs in the presence of background noise, compromising our ability to hear. While understanding speech in noise is a challenge for everyone, it becomes increasingly difficult as we age. The amount of speech-in-noise perceptual decline that occurs with aging cannot be fully accounted for by peripheral hearing ability; decreased cognitive skills and central factors also contribute to the difficulty older adults experience in understanding speech in noise. Musical experience improves the perception and neural processing of speech in noise in young adult musicians(1,2). Here, we investigated the effects of musical training on speech-innoise perception in middle-aged adults by comparing the performance of musicians and nonmusicians between the ages of 45-65 years. Consistent with the findings in young adults, middle-aged adult musicians demonstrated better behavioural speech-in-noise performance and higher auditory working memory ability accompanied by an overall enhancement in the neural encoding of speech. Thus musical training may mitigate the impact of the agerelated cognitive and perceptual decline, specifically for the perception of speech in background noise.

1. Parbery-Clark, A., Skoe, E., Lam, C. & Kraus, N. (2009). Musician enhancement for speech in noise. Ear and Hearing 30(6):653 - 661 2. Parbery-Clark A., Skoe, E. & Kraus, N. (2009) Musical experience limits the degradative effects of background noise on the neural processing of sound. Journal of Neuroscience 29:14100 - 14107

143 Age-Related Changes in Auditory Processing of Modulation Waveforms Assessed at the Population Level

Aravindakshan Parthasarathy¹, Paul Cunningham², Edward Bartlett^{1,2}

¹Department of Biological Sciences, ²Weldon school of Biomedical Engineering, Purdue University

Declines in detection of amplitude and frequency modulation observed in elderly human listeners may be correlated with declines in speech perception with age. This study aims to further understand processing of modulation waveforms of sound stimuli in aging using noninvasive electrophysiological measurements in a rat model system, which can be complemented by data obtained from single unit recordings. Amplitude modulation following responses (AMFRs) were assessed using sinusoidally amplitude modulated (SAM) tones presented to aged (20-22 months old) and young (3-5 months old) Fischer-344 rats. Changes in the efficacy of representing modulation periodicity and characteristics like depth and shape, with age, were assessed by comparing SAM tones with decreasing modulation depth, as well as slowly rising ramped or rapidly rising damped envelopes. Temporal processing deficits and changes in auditory filter widths were studied using tones with sinusoidal frequency modulation (SFM). The overall shapes and cutoff frequencies of the AMFR temporal modulation transfer functions (tMTFs) were similar between young and aged animals for SAM stimuli in quiet at 100% modulation depth. There were no significant age related differences in the nature of growth or AMFR amplitudes with change in sound level. However, there was a significant decrease in modulation detection thresholds for SFM and SAM stimuli with age. The aged animals also showed reduced precision in discriminating ramped, sinusoidal, and damped envelope shapes when compared to the young. The results show that the representation of temporally modulated stimuli in aged listeners is similar to the young under quiet, ideal listening conditions using simple periodic stimuli. However, the aged animals have severe deficits in detecting and discriminating various envelope shapes and modulation waveforms of sound stimuli

144 Expression Pattern of Oxidative Stress-Related Genes in the Aging Fischer 344/NHsd Rat Cochlea

Chiemi Tanaka^{1,2}, Donald Coling¹, Senthilvelan Manohar¹, Guang-Di Chen¹, Bo Hua Hu¹, Richard Salvi¹, Donald Henderson¹

¹Center for Hearing and Deafness, SUNY at Buffalo, ²Oregon Hearing Research Center, Oregon Health and Science University

Oxidative stress is thought to be a major contributor to aging. However, the contributions of genes related to

oxidative stress and antioxidant defenses are not fully understood. The current study used a Fischer 344/NHsd (F344/NHsd) rat model of age-related hearing loss (ARHL) to investigate the effects of age on oxidative stress and antioxidant defense-related genes in young (2 months old), middle-aged (12 months old), and old (21 months old) rats in relation to auditory function and outer hair cell (OHC) survival. Age-related expression changes in 84 genes were investigated by quantitative real-time reverse transcription polymerase chain reaction (RT-gPCR) arrays (RT² Profiler[™] PCR Array, SABiosciences Corp.) in the tissue homogenates consisting of the cochlear sensory epithelium and lateral wall. Auditory function was assessed by auditory brainstem response (ABR) and distortion product otoacoustic emission (DPOAE) testing and cochleograms were used to assess OHC loss. F344/NHsd rats showed age-related elevations in ABR thresholds and decreases in DPOAE amplitudes across all test frequencies. Moderate to severe OHC losses were present throughout the cochlea of old rats except in the middle turn. The results from RT-gPCR array revealed a significant age-related downregulation in Stearoyl-Coenzyme A desaturase 1 and upregulation in 12 genes: 24-dehydrocholesterol reductase, aminoadipatesemialdehyde synthase, cytoglobin, dual oxidase 2, glutathione peroxidase 3, glutathione peroxidase 6, glutathione S-transferase, kappa 1, glutathione reductase, NAD(P)H dehydrogenease, quinone 1, solute carrier family 38, member 5, thioredoxin interacting protein, and vimentin. Further analysis using linear correlation and regression analyses between gene expression and ABR/DPOAE revealed measurements significant correlations with one or more test frequencies with all 13 genes. Interestingly, upregulation of the genes related to glutathione metabolism and thioredoxin regulation (glutathione peroxidase 6, glutathione S-transferase, kappa 1, thioredoxin interacting protein, glutathione reductase) was observed in the middle age, which suggests the presence of oxidative stress at as early as 12 months of age. Several genes (glutathione peroxidase, glutathione S-transferase, glutathione reductase, and NAD(P)H dehydrogenease, guinone 1) which presumably possess antioxidant response elements in their promoter regions showed significant age-related upregulation in RTqPCR indicating the presence of oxidative stress in the aging cochlea.

145 Mitochondrial Sirt3 Mediates Reduction of Oxidative Damage and Prevention of Age-Related Hearing Loss Under Caloric Restriction

Shinichi Someya¹, Wei Yu¹, William C. Hallows¹, Jinze Xu², James M. Vann¹, Christiaan Leeuwenburgh², Masaru Tanokura³, John M. Denu¹, Tomas A. Prolla¹ ¹University of Wisconsin-Madison, ²University of Florida, ³University of Tokyo

It is well established that reducing food consumption by 25-60% without malnutrition consistently extends both the mean and maximum lifespan of a variety of species. Caloric restriction (CR) also delays the progression of a

variety of age-associated diseases such as cancer, diabetes, cataract, and age-related hearing loss (AHL) and reduces neurodegeneration in animal models of Parkinson's disease as well as Alzheimer's disease. Yet, whether the anti-aging action of CR in mammals is a regulated process and requires specific regulatory proteins such as sirtuins still remains unclear. Sirtuins are NAD+dependent protein deacetylases that regulate lifespan in lower organisms, and have emerged as broad regulators of cellular fate and mammalian physiology. A previous report has shown that lifespan extension by CR in yeast requires Sir2, a member of the sirtuin family, linking sirtuins and CR-mediated retardation of aging. Here we report that CR reduces nuclear oxidative DNA damage in multiple tissues and prevents AHL in wild-type (WT) mice, but fails to mediate these phenotypes in mice lacking the mitochondrial deacetylase Sirt3, a member of the mammalian sirtuin family. In response to CR, Sirt3 directly deacetylates and activates isocitrate dehydrogenase 2 (Idh2). This in turn leads to increased NADPH levels and enhancement of the glutathione antioxidant defense system in mitochondria. Thus, these results suggest that enhancing mitochondrial antioxidant status is a major mechanism of aging retardation by CR in the auditory system.

146 An Antioxidant-Enriched Diet Does Not Prevent Age-Related Sensorineural Hearing Loss in CBA/J Mice

Su-Hua Sha^{1,2}, Ariane Kanicki², Karin Halsey², Kimberly Wearne², Jochen Schacht²

¹*The Medical University of South Carolina, Department of Pathology and Laboratory Medicine,* ²*The University of Michigan, Kresge Hearing Research Institute*

Oxidant stress has been linked to noise- and drug-induced hearing loss as well as age-related hearing loss. Antioxidant supplementation has been shown to attenuate the deterioration of auditory function and hair cell structure after noise, aminoglycoside antibiotics and cisplatin insults but it is still uncertain whether antioxidants can protect the aging auditory system.

We have previously reported preliminary results of a diet study which now has been concluded. Two groups of female CBA/J mice with matched ABR thresholds and body weights were placed on a regular or antioxidantenriched diet at 10 months of age and monitored until 24 months of age. In general, inner ear pathology as determined by auditory brainstem responses (ABR), hair cell loss and spiral ganglion cell deterioration was similar but delayed compared to male CBA/J mice as previously reported (Sha et al., 2008) Antioxidant supplementation (vitamins A, C and E plus L-carnitine and alpha lipoic acid) significantly increased the antioxidant capacity of inner ear tissues and did not affect general health or survival rates. By age 24 months, ABR threshold shifts had developed in animals in both groups with no correspondence to their diet. Mice were chosen randomly for surface preparations to count hair cells and sectioning to calculate spiral ganglion density. Data showed no difference in hair cell loss or spiral ganglion cell degeneration between the

antioxidant and control groups. We conclude that antioxidant dietary supplement can alter the antioxidant capacity in the inner ear, but does not ameliorate agerelated sensorineural presbycusis.

This study was supported by program project grant AG025164 from the National Institutes on Aging, National Institutes of Health.

147 Role of Insulin-Like Growth Factor I in Age-Related Hearing Loss

Lourdes Rodriguez-de la Rosa^{1,2}, Silvia Murillo-Cuesta^{1,2}, Raquel Martinez-Vega^{1,2}, Rafael Cediel^{2,3}, **Isabel Varela-Nieto^{1,2}**

¹Instituto de Investigaciones Biomedicas 'Alberto Sols', CSIC-UAM, ²CIBERER, U-761. ISCiii, ³Facultad de Veterinaria. UCM.

Insulin-like growth factor I (IGF-I) is a member of the family of insulin-related peptides with a prominent role during inner ear development. Human IGF-I deficiency is associated with syndromic sensorineural deafness, poor and mental retardation (ORPHA73272; growth OMIM608747). Similarly, laf1 null mice present profound deafness, with ABR and DPOAE responses profoundly altered, and aberrant inner ear morphology with loss of spiral ganglion neurons from the onset of hearing. Recent findings showed that IGF-I deficit causes the down regulation of ERK and AKT signalling pathways and the activation of p38 stress kinase in the cochlea of embryonic mice. In addition, RNA arrays experiments with $lgf1^{-/-}$ and Igf1^{+/+} in E18.5 mouse cochleae have evidenced transcription factors FoxM1 and MEF2A and D like novel cochlear targets for IGF-I¹

Aging is associated with a decrease in circulating IGF-I levels and this reduction has been related to cognitive and brain alterations, although there was no information regarding the relationship between presbycusis and IGF-I biodisponibility. A longitudinal comparative study with $lgf1^{+/+}$ and $lgf1^{-/-}$ mice from 2 to 12 months revealed that wild type mice developed an age-related hearing loss associated with decrease in serum IGF-I levels and progressive loss of spiral ganglion neurons². On the other hand, $lgf1^{-/-}$ null mice developed a prematurely aged stria vascularis, reminiscent of the diabetic strial phenotype, and progressive blindness with altered electroretinographic responses.

Our data indicate that IGF-I is required for the correct development and maintenance of hearing during ageing, supporting the idea that IGF-I-based therapies could contribute to prevent or ameliorate age-related hearing loss.

¹Sanchez-Calderon et al. PLoS One. 2010; ²Riquelme et al. Frontiers Neuroanatomy, 2010.

148 Can Intratympanic Dexamethasone Protect Against Cisplatin Ototoxicity in the Presence of Age-Related Hearing Loss? Kourosh Parham¹

¹University of Connecticut Health Center

We have previously demonstrated that intratympanic dexamethasone (ITD) has a protective effect against

cisplatin ototoxicity in the young mouse (Hill et al. Otology & Neurotology, 2008). As over 60% of new cancer patients are older than 65 years of age with a large proportion of these patients likely having existing agerelated hearing loss, an important question is whether a protective property of ITD can be demonstrated in the aged ear. It's been postulated that both the aging process and ototoxicity are mediated by reactive oxygen metabolites, therefore there may be little reserve for free radical scavengers through which dexamethasone can bestow its beneficial effects. We treated 24-month-old CBA/J mice with a single dose of cisplatin (14 mg/kg, IP) and 6 days of ITD (24 mg/ml) in one ear and IT saline (ITS) in the opposite ear. Auditory brainstem responses (ABR) were measured before and after treatment using 4 msec tone bursts between 20 and 90 dB SPL at 8, 16, 24 and 32 kHz. ABR thresholds were determined. At baseline, aged ears displayed mean ABR threshold elevations up to 35 dB compared to young mice. In ITS ears, cisplatin treatment produced 7-10 dB ABR threshold elevations. In ITD ears, steroid treatment produced little protection at 8 or 16 kHz producing mean ABR threshold elevations of 6.5 and 6.9 dB, respectively. However, good protection was demonstrated at 24 and 32 kHz with mean ABR threshold elevations of 1.6 dB. A two-way repeated measures ANOVA demonstrated a significant main effect of IT Drug (p = 0.015) and an interaction between IT Drug and Stimulus Frequency at p = 0.07. Follow up one-way ANOVAs showed no significant differences between saline and ITD ears at 8 and 16 kHz, but a significant difference at 32 kHz (p = 0.001). These results are the first to demonstrate a protective effect of a treatment against an ototoxic agent in the presence of age-related hearing loss. Supported by Career Development awards from the American Geriatric Society (Jahnigen) and Triological Society.

149 The Heat Shock Response and Age-Related Hearing Loss

Tzy-Wen Gong^{1,2}, Lynne Fullarton^{1,2}, Shu Chen^{1,3}, Andrzej Galecki^{1,3}, David Kohrman^{1,2}, David Dolan^{1,2}, Richard Altschuler^{1,2}, Margaret Lomax^{1,2}

¹University of Michigan, ²Kresge Hearing Research Institute, ³Institute of Gerontology

The heat shock response is an evolutionarily conserved pathway that protects organs and tissues from physiological and environmental stresses. Heat shock transcription factor 1 (HSF1) regulates the induction of heat shock proteins (HSP). Stress activates HSF1, which binds to specific elements in HSP genes, leading to rapid transcriptional induction of protective HSPs. We used quantitative RT-PCR to measure induction of HSP genes in the cochlea of young (11-13 weeks old) vs 21 month old mice following whole body heat shock. Hsp70.1 and Hsp70.3 showed an approximately 600- to 800-fold change in young mice, while the induction decreased to 200- to 250-fold in old mice (p<0.05). Using a genetic approach, we are assessing the effect of a decrease in HSP induction on age-related hearing loss (ARHL). For this longitudinal study, we developed Hsf1-/- knockout mouse models on two different genetic backgrounds, each carrying an ARHL-resistant allele of the Cdh23/Ahl gene. We measured ABR thresholds of both male and female wildtype and Hsf1-/- mice at 4 frequencies (4, 12, 24, and 48 kHz) and at 3 ages: 4, 12 and 18 months. Hsf1-/- mice exhibited small (~10 db SPL) but statistically significant increases in ABR thresholds relative to wildtype mice at all frequencies and ages and on both genetic backgrounds. Model 1 was on a mixed genetic background (BALB/c,129SvJ). Both wildtype and Hsf1-/- mice exhibited the typical age-related increase in ABR thresholds seen in other aging studies. Model 2 consisted of F1 hybrids between Model 1 and a CBA/CaJ congenic strain and exhibited reduced variability in ABR threshold values as they aged. We are therefore following a subset of the F1 hybrids to 24 months to assess the effect of the Hsf1-/mutation at later ages.

Supported by NIH grants P01 AG025164, P30 DCO5188, and the Margaret G. Bertsch Research Endowment

150 Slc26a7 Is a Candidate Gene for Age-Related Deafness

Kyunghee X Kim¹, Joel D. Sanneman¹, Hyoung-Mi Kim¹, Jie Xu², Daniel C. Marcus¹, Manoocher Soleimani², Philine Wangemann¹

¹Kansas State University, ²University of Cincinnati

Slc26a7 is a Cl⁻ transporter in the Slc26 family that includes pendrin (Slc26a4) and prestin (Slc26a5). SIc26a7 is expressed in the stomach, kidney and thyroid. Dependent on location it codes for an anion channel, detectable by current measurements, or for an electroneutral anion exchanger. The goal of the present study was to determine whether S/c26a7 is expressed in the cochlea and critical for cochlear function. Messenger RNA, protein and channel activity of Slc26a7 were evaluated by gene array, confocal immunocytochemistry and whole-cell patch clamp. The significance of Slc26a7 expression for cochlear function was evaluated by auditory brain stem recordings. Experiments were conducted in wild-type mice (*Slc26a7*^{+/+}, WT), heterozygotes (*Slc26a7*^{+/-}, HET) and mice lacking *Slc26a7* expression (*Slc26a7*^{+/-}, KO). High levels of *Slc26a7* mRNA were found in Reissner's membrane. Protein expression in the cochlea was limited to the basolateral membrane of Reissner's membrane epithelial cells (Rmec). The onset of expression in Rmec was at postnatal day 5 (P5). Rmec from WT mice contained slightly outward-rectifying currents that were carried by $NO_3^- > CI^- > I^- >> NMDG$ and blocked by NPPB. Currents carried by $NO_3^- > CI^-$ were not seen in KO mice. Hearing thresholds at P15 were higher in KO compared to HET or WT mice. Thresholds at age P22, P60, P100 and P170 were similar between KO, HET and WT mice. Cell numbers of Rmec at P15 and P60 were similar between KO and WT mice; however, at P170 numbers were reduced in KO mice and apical membrane surface areas were increased. In conclusion, the data demonstrate that Slc26a7 codes in Reissner's membrane for an anion channel expressed in the basolateral membrane of the epithelial cells. Lack of expression delays the onset of hearing and promotes premature loss

of epithelial cells. *Slc26a7* is therefore a candidate gene for human age-related deafness.

Supported by NIH-R01-DC01098, NIH-R01-DC00212, NIH-P60-RR017686.

151 A Genetically Heterogeneous Mouse Population Showing Late-Life Hearing Loss: Initial Characterization of ABR, Hair Cell Loss, and MRNA Patterns

Richard A. Miller^{1,2}, Amir A. Sadighi Akha¹, Richard Altschuler³, David T. Burke⁴, Shu Chen⁵, David Dolan³, Andrzej T. Galecki⁵, Jochen Schacht³

¹Department of Pathology, Geriatrics Center, University of Michigan, ²Ann Arbor VA Medical Center, University of Michigan, ³Kresge Hearing Research Institute, University of Michigan, ⁴Department of Human Genetics, University of Michigan, ⁵Institute of Gerontology, University of Michigan

Most stocks of laboratory mice show profound hearing loss within the first year of life, impairing their usefulness as models for presbycusis. We introduce here a genetically heterogeneous model for age-related hearing loss: UM-HET4 mice, produced as the offspring of a mating between two different F1 hybrid mouse stocks, each chosen because it lacks the Cdh23753A allele at the Ahl1 locus, which would lead to hearing loss in the first third of life. Each UM-HET4 mouse is genetically unique, and a full sib of all others, making the model suitable for analysis of genetic and background-sensitive environmental and pharmaceutical effects on late-life hearing loss.

Over 500 female UM-HET4 mice were evaluated for ABR threshold at 8, 18, and 22 months of age, followed by assessment of outer hair cell pathology and cochlear mRNA levels. Initial observations revealed: (a) On average, UM-HET4 mice show a significant increase in ABR thresholds between 8 and 18 months, and also between 18 and 22 months, at both 4 kHz and 48 kHz. (b) 25% of the mice show > 20 dB change at 4 kHz, and a small proportion show 40 dB or more increase in ABR threshold at 4 kHz or at 48 kHz or both. (c) Some of the aged mice have poor hearing at 4 kHz, but retain youthful levels at 48 kHz, and vice versa. (d) Loss of apical OHC is correlated with ABR responses at 4 kHz, and loss of basal OHC is correlated with ABR at 48 kHz. (e) Evaluation of mRNA levels for 95 selected genes showed 25 in which high mRNA levels were significantly associated with resistance to age effects on thresholds at 48 kHz, and six others in which high mRNA was associated with poor hearing at 4 kHz. (f) Gene expression patterns associated with high and low frequency ABR in aged, noise-exposed mice (2 hr at 110 dB SPL at 20 months of age) were quite different from association patterns seen in aged mice that had not been exposed to noise.

Supported by P01 AG025164 from the National Institute on Aging, NIH.

152 Genetic Polymorphisms That Modulate Late-Life Hearing and Outer Hair Cell Counts in a Segregating Mouse Population, UM-HET4 Pieberd A Miller¹ Disbard Altachular² David T. Burke³

Richard A. Miller¹, Richard Altschuler², David T. Burke³, Shu Chen⁴, David Dolan², Andrzej T. Galecki⁴, Jochen Schacht²

¹Department of Pathology, Geriatrics Center, University of Michigan, ²Kresge Hearing Research Institute, University of Michigan, ³Department of Human Genetics, University of Michigan, ⁴Institute of Gerontology, University of Michigan

We further characterize here a genetically heterogeneous model for age-related hearing loss: UM-HET4 mice, produced as the offspring of a mating between (MOLF/Ei x 129S1/SvImJ)F1 females and (C3H/HeJ x FVB/NJ)F1 males. Each UM-HET4 mouse is a full sib of all the others, and none carry the Cdh23753A allele at the AhI1 locus, which would lead to hearing loss in the first third of life and thus interfere with studies of late-life presbycusis.

UM-HET4 mice were given ABR tests at 8, 18, and 22 months of age, and then euthanized for analysis of outer hair cell loss. Each mouse was genotyped at 58 SNP loci that discriminate among maternal alleles, and 52 SNPs that distinguish among paternal alleles. Gene/Trait associations were evaluated by a permutation test that yields experimentwise significance criteria. Two loci, on chromosomes 3 and 13, had significant effects (p < 0.05) on ABR thresholds in 8-month old mice. At least five loci, on chromosomes 2, 3, 7, 10, and 15, had significant effects on ABR thresholds at 18 months of age. The chromosome 7 polymorphism had effects on thresholds at 4 and 24 kHz, and the others modulate hearing at 48 kHz. Half of the mice were exposed to noise (2 hr at 110 dB SPL) at 20 months of age, and in these mice loci on chromosomes 9 and 12 were predictors of ABR thresholds at 22 months of age. In the mice not exposed to noise, loci on chromosomes 10 and 11 were associated with ABR outcomes, at 48 KHz and 12 KHz respectively, in mice tested at 22 months of age. Loci on chromosomes 11, 12, 17, and 19 were associated with preservation of apical outer hair cells (OHC), and a locus on chromosome 10 was associated with basal OHC numbers at 22 months of age. The genetic architecture of hearing in UM-HET4 mice is complex, with different patterns of alleles detected depending on mouse age, frequency tested, and past history of noise trauma.

Supported by P01 AG025164 from the National Institute on Aging, NIH.

153 Age-Related Morphological and Cellular Change in Outer Hair Cells and Their Efferent Fibers

Ming Zhang^{1,2}

¹University of Alberta - Faculty of Rehabilitation Medicine, ²Glenrose Rehabilitation Hospital

Schuknecht provided evidence of hair cell and nerve loss in presbycusis (1964). Prior to showing electromotility (Brownell 1986) and efferent effect (Warren and Liberman 1989) he was discussing the afferent components. We studied the efferent components and provide our results here. We knew several findings: inner hair cell loss causes chronic loss in dendrites (Rask-Andersen, Liu, and Linthicum 2010); de-efferent increases thresholds (Zheng et al 2000) but decreases both cochlear microphonics and the nerve spontaneous rate (Liberman et al 1990, 2000; Zheng et al 1997, 2000); losing innervation causes muscle atrophy (Ghahremani et al 1996); and absence of efferent does not affect the development of prestins, Ach-induced responses, and outer hair cell (OHC) afferents (He et al 1997, 1999; Liberman 2000). However, during aging it is unclear how OHCs and efferents change and affect each other. We hypothesized that they undergo an equivalent degeneration and aggravate each other. In our study, when compared to young animals, OHCs from the elderly were fatter/shorter/less-electromotile or became so in culture faster; and OHC efferents were thinner and lessdense in all turns from base to apex. This result supports our hypothesis of parallel degeneration. For aggravation, OHC loss makes the retention of efferents meaningless, so in this scenario the efferents may diminish with no negative effects. Efferent loss deprives OHC from overstimulationprotection. On the other hand, we knew that OHC loss occurs in the base first but we did not observe this pattern in efferent loss. Therefore, we speculate that efferent loss may occur before OHC loss in the apex but after OHC loss in the base. The knowledge from this report may help reveal the mechanisms of a complicated aging process, which may help develop better clinical assessment and treatment strategies.

154 Morphological Correlates of Gravity Receptor Functional Aging

Jessica Pierce¹, Sarath Vijayakumar¹, Sherri M. Jones¹ ¹East Carolina University

Cdh23^{ahl} (Ahl) is a genetic mutation located on mouse chromosome 10 that affects Cadherin23, a protein critical for sensory transduction. Ahl predicts age-related hearing loss; however, it may not predict vestibular functional aging. We are currently assessing vestibular functional and structural aging, and hypothesized that morphological aging of vestibular structures correlate with gravity receptor function as measured by vestibular evoked potentials (VsEPs). To test this hypothesis, we quantified hair cells, synaptic ribbons, and post synaptic receptor sites in the utricle of CBA/CaJ mice (6, 12, and 22 months of age, n = 4 to 6 specimens per age), and correlated the structural data with functional VsEP data from previous studies. CBA/CaJ mice have no known genetic mutations affecting the inner ear and serve as an aging control model. Utricles were dissected and stained with CtBP2 (a marker for synaptic ribbons) and Shank1a (a protein located within the post-synaptic density). Specimens were then imaged with a Zeiss LSM 510 confocal microscope. The number of hair cells, synaptic ribbons, and Shank1a were quantified and averaged for four distinct areas (~2300 μ m²) across each epithelium. The number of hair cells was similar at 6 (73.44 \pm 6.41) and 12 months (77.32 ± 7.17), but declined significantly by 22 months (56.28 ± 8.57). The number of synaptic ribbons per hair cell declined significantly from 6 (5.23 \pm 0.88) to 12 months (3.73 \pm 0.76) and from 12 to 22 months (2.17 \pm 0.67). Shank1a also declined significantly between 6 (7.40 \pm 1.76) and 12 months (4.52 \pm 1.01), but not between 12 and 22 months (3.40 \pm 0.82). CtBP2 and Shank1a counts per hair cell were significantly correlated with VsEP thresholds in that the number of synaptic ribbons and Shank1a per hair cell declined as VsEP thresholds became significantly elevated with age. Results suggest that gravity receptor functional decline with age is associated with an age related decline in synaptic and neural elements. Research was supported by NIH R01 DC006443 and DC006443-04S1.

155 Neural Coherence of Multiple Brain Structures as a Physiological Signature of Tinnitus

Jinsheng Zhang^{1,2}, Xueguo Zhang¹, John Moran³ ¹Department of Otolaryngology, Wayne State University School of Medicine, ²Dept Communication Sciences & Disorders, Wayne State University College of Liberal Arts & Sciences, ³Department of Neurology, Henry Ford Health System

Investigations over the last decade have demonstrated hyperactivity, hyper-synchrony and plastic reorganization in the central auditory system as physiological signatures of tinnitus. These notions were mostly based on evidence gleaned from single- and multi-unit recordings in a single auditory brain structure. It is not clear how these physiological signatures of tinnitus interact between different brain centers and what type of information flow contributes to the development and maintenance of tinnitus. In addition, it is unclear how strategies such as auditory cortex electrical stimulation (ACES), used to suppress tinnitus in both humans and animals, interactively modulate these signatures. In our lab, we set out to identify new physiological signatures of tinnitus by way of developing multistructural recordings from the dorsal cochlear nucleus (DCN), inferior colliculus (IC) and auditory cortex (AC), the structures that have been implicated to be related to the etiology of tinnitus. In the current study, nine rats were implanted in the left DCN, right IC and right AC following behavioral testing of toneinduced tinnitus. Coherence as a measure of neural connectivity was computed for all recording channels/sites within and across the DCN, IC and AC before and after ACES for both tinnitus(+) and tinnitus(-) animals as well as controls. Our preliminary data demonstrated that, compared to tinnitus(-) and control animals, there was increased coherence in auditory structures especially the AC of tinnitus(+) animals. The increased coherence in the AC tended to be suppressed by ACES, which is in line with the reported information that ACES suppresses tinnitus percepts in human subjects and our data that ACES suppresses behavioral evidence of tinnitus in rats. While the increased coherence in the AC of tinnitus(+) animals were suppressed by ACES, there were complex changes in the coherence values recorded from the DCN and IC. The current study supports our previous notion that suppression of tinnitus may involve neuromodulation and

gating adjustment at several brain centers. Coherence across different brain centers may serve as a new physiological signature of tinnitus.

156 Whole-Brain FMRI Without Increased Scanner-Generated Acoustic Noise: Application to Tinnitus

Jennifer Melcher^{1,2}, Kawin Setsompop^{2,3}, Inge

Knudson^{1,2}, Robert Levine^{1,2}

¹Mass Eye & Ear Infirmary, ²Harvard Medical School, ³Mass General Hospital

Mitigation of scanner-generated acoustic noise is an obvious priority for fMRI studies of tinnitus. Recent structural MRI studies [1,2] suggesting a role for widely distributed non-auditory brain centers in tinnitus present another priority: imaging the entire brain. These priorities – mitigation of acoustic noise and whole-brain imaging - are at odds because noise mitigation is typically accomplished by imaging only a portion of the brain [3,4]. A recent study [5] is typical: 10 brain slices spanning a little over half of the brain were imaged in brief (< 1 s) clusters separated by long (8 s) quiet periods.

To enable whole-brain fMRI while limiting scanner acoustic noise, an fMRI sequence was developed that acquires multiple brain slices for every one acquired by conventional means. Importantly, this is done without any additional activation of the scanner gradients, the single greatest source of scanner acoustic noise. As in our example [5], images are still acquired in brief clusters separated by long quiet periods, but three at a time instead of singly. The simultaneously acquired slices are disentangled from one another by combining information from the 32 channels of the imaging head coil in an off-line analysis.

The sequence has been tested and used to image 14 tinnitus and 16 threshold-, age-, and sex-matched non-tinnitus subjects. fMRI was performed during sound stimulation to extend our previous results showing elevations in sound-evoked activity related to tinnitus and hyperacusis in auditory centers [5] and in the absence of sound stimulation to test for abnormal functional connectivity between brain centers related to tinnitus. Results will be presented.

[1] Mühlau et al. Cereb Cortex (2006) 16: 1283-8.

[2] Knudson et al. ARO 2011.

[3] Edmister et al., Human Brain Mapp (1999) 7: 89 - 97.

[4] Hall et al., Human Brain Mapp (1999) 7: 213 - 223.

[5] Gu et al., J Neurophysiol (in press).

NIH-NIDCD, Tinnitus Research Consortium

157 A Comparison of Brain Structure Between Closely Matched Tinnitus and Non-Tinnitus Subjects

Inge Knudson^{1,2}, Robert Levine^{1,2}, Jennifer Melcher^{1,2} ¹*Massachusetts Eye & Ear Infirmary,* ²*Harvard Medical School*

Recent reports suggest that the brains of people with tinnitus are structurally different from those without tinnitus [1,2]. To further investigate this, we obtained whole-brain,

T1-weighted MR images in 50 subjects (MPRAGE, 1 mm³resolution). 23 subjects had tinnitus (mean age 47±1.8 yrs SEM, 12 men, 20 right-handed); 27 did not (46±1.5 yrs, 16 men, 25 right-handed). All subjects had normal or near-normal thresholds. Mean threshold differed between tinnitus and non-tinnitus subjects by less than 3 dB at any frequency from 0.25 - 8 kHz. Each brain was parcellated automatically (Freesurfer [3,4]). The volume of gray matter in 75 cortical regions plus the volume of 7 subcortical structures was determined for each hemisphere and normalized to total hemispheric gray matter volume. After exclusion of outliers, normalized volume (NV) differed significantly between tinnitus and non-tinnitus subjects in one region: right, caudal anterior cingulate cortex (cACC; p = 0.02, Bonferroni corrected). NV was less in the tinnitus group. Neither anxiety nor depression had a significant effect on the NV of the cACC in two-way ANOVA, suggesting that reduced NV was related to tinnitus rather than either of these commonly co-occurring conditions. The present results combined with previous reports of functional cACC activation during selective attention lead us to postulate a role for cACC in the diminished concentration and intrusiveness of the tinnitus percept reported by tinnitus patients.

[1] Mühlau et al. Cereb Cortex (2006) 16: 1283-8.

[2] Schneider et al. NeuroImage (2009) 45: 927-39.

[3] Fischl et al. Neuron (2002) 33: 341-55.

[4] Destrieux et al. NeuroImage (2010) 53: 1-15. Supported by the Tinnitus Research Consortium

158 Structural Brain Changes in Tinnitus and Hearing Loss

Kristiana Boyen¹, Dave Langers¹, Emile de Kleine¹, Pim van Dijk¹

¹University Medical Center Groningen

Tinnitus can be described as the perception of sound in the absence of an acoustic stimulus. Tinnitus may have a mild but also a devastating impact on the patient's quality of life. The underlying pathophysiology of tinnitus is still poorly understood. Several (f)MRI and PET studies support that mechanisms in the central auditory system play a crucial role in tinnitus generation. In 2 recent studies (Mühlau at al., 2006 and Landgrebe et al., 2009), alterations in the volume or concentration of grey matter (GM) in tinnitus patients have been detected.

In the current study, structural MRI scans in 30 tinnitus subjects and 16 controls were performed. All participants had moderate sensorineural hearing loss. They all filled out the Hospital Anxiety and Depression Scales (HADS) and the Hyperacusis Questionnaire (HQ). Additionally, the tinnitus subjects filled out the Tinnitus Handicap Inventory (THI). Voxel-Based Morphometry was applied to determine differences in GM volume and concentrations between the 2 groups. In addition, GM volume and concentrations were correlated with the questionnaire scores.

GM volume increase in tinnitus patients as compared to controls was found in the right caudate nucleus, right and left fusiform gyrus, and left inferior temporal gyrus. Also increases in GM concentrations were found in the latter 3 areas. The volume in the right inferior temporal gyrus and left anterior cingulate cortex was decreased. No significant decreases in concentrations were found. GM volume and concentrations of the right fusiform gyrus were significantly correlated with the HADS scores. HQ scores were significantly correlated with GM concentrations of the left inferior temporal gyrus. No significant correlations between THI scores and GM volume or concentration of any anatomical region were found.

These results suggest that areas outside the classical auditory system are involved in generating tinnitus.

159 Neuromagnetic Indicators of Tinnitus Masking in Patients with and Without Hearing Loss

Peyman Adjamian¹, Magdalena Sereda¹, Deborah Hall^{2,3}, Matthew Brookes⁴, Johanna Zumer⁴, Alan Palmer¹ ¹*MRC Institute of Hearing Researc, ²National Biomedical Research Unit in Hearing, ³Division of Psychology, Nottingham Trent University, ⁴Sir Peter Mansfield Magnetic Resonance Centre; University of Nottingham*

A number of recent neuroimaging studies indicate abnormal brain activity in people with tinnitus (TI) (Adjamian et al. Hear Res. 2009; 253:15-31), suggesting a central mechanism for this condition. Llinas and colleagues (TINS. 2005; 28(6):325-333) have proposed a model of thalamocortical dysrhythmia in which TI is due to disrupted coherent activity between thalamus and cortex following deafferentation. This model predicts that the TI state is associated with abnormally high slow-wave (< 8 Hz) and high-frequency (gamma, >30 Hz) oscillatory activity and is modulated by masker noise. So far the supporting evidence is limited to a single case and, while expected changes in slow-wave activity were found during TI masking, no results were reported for the gamma band.

Using MEG, we have tested the model predictions more thoroughly on 19 people with TI, with and without hearing loss and 8 'normal hearing' controls. A 10 s broadband white noise masker was presented 80 times at 50 dB SPL followed by 10 s of silence. Patients were asked to indicate the loudness of their TI during silence and the masking sound. Focal auditory cortical activity in a range of frequency bands was identified using a beamformer technique. For the silent condition, delta band power was significantly greater in TI patients compared to controls, with no differences in other frequency bands. For those TI patients with hearing loss who could mask their TI (N=9), delta band (1-5 Hz) power was significantly greater in the TI state than in the masker condition. No significant differences were found in other frequency bands. No differences were found in those patients where TI was not masked (N=5) or those with normal hearing (N=5). Our results illustrate how MEG can be used to search for a central TI mechanism, agree with the previous single case, and they partly agree partly with the thalamocortical dysrhythmia model.

160 PET Imaging for Cortical Activity in Tinnitus Patients

Leontien Geven^{1,2}, Emile de Kleine^{1,2}, Antoon Willemsen³, Anne Paans³, Pim van Dijk^{1,2}

¹Department of Otorhinolaryngology, University Medical Center Groningen, the Netherlands, ²Faculty of Medical Sciences, School of Behavioral and Cognitive Neurosciences, Groningen, ³Department of Nuclear Medicine and Molecular Imaging, University Medical Center Groningen

Objective: Tinnitus is believed to be the result of plastic changes and reorganisation processes in the auditory pathway and brain structures, most likely caused by deprivation of input. With Positron Emission Tomography (PET) increases in neural activity can be demonstrated. In the published literature, asymmetrical metabolic activity between the left and right auditory cortex has been reported, irrespective of various tinnitus localizations. The objective of this study was to measure the difference in cortical activity in chronic bilateral tinnitus patients compared to age-matched healthy control subjects with the use of [¹⁸F]deoxyglucose (FDG)-PET scanning.

Methods: FDG-PET scanning was performed in 20 chronic tinnitus patients and 19 control subjects, all right-handed. The tinnitus was bilateral in all patients. Subjects were scanned for 20 minutes, after an uptake time of 30 minutes in a resting state. Auditory input was prevented by ear plugs and a sound-isolating headphone. PET images were analysed using the SPM5 and its Anatomy Toolbox.

Results: Activity was lower in tinnitus patients, compared with control subjects, in the most frontal part of the left temporal lobe (p < 0.05, FWE). No brain areas showed higher activity in the patient group. The mean activity in the left and right primary auditory cortex was more symmetrical in the patient group than in the control group: the average symmetry indices were respectively +0.000014 and +0.0165 (t-test, p < 0.05), where the index range from -1 to +1 corresponds to extreme left and right lateralization.

Conclusion: Our results showed no cortical hyperactivity in tinnitus patients with FDG-PET scanning. Instead, part of the left temporal lobe showed lower activity in tinnitus patients, compared to the control group. The mean activity in the left and right primary auditory cortex was more symmetrical in patients than in controls, which is in contrast with previous imaging studies.

161 Noise Trauma Suppresses Cell Proliferation and Neurogenesis in Rat Hippocampus and Impairs Memory

Richard Salvi¹, Suzanne Kraus¹, Sneha Hinduja¹, Dalian Ding¹, Haiyan Jiang¹, Edward Lobarinas¹, Wei Sun¹ ¹University at Buffalo

Acoustic trauma has long been known to damage the inner ear; however, its effects on the central nervous system are poorly understood. Previous reports have suggested that intense noise exposure may impair memory. Since the hippocampus plays an important role in memory and is a major site of neurogenesis in the adult brain, we evaluated the effects of intense noise on the hippocampus. Nine rats

were unilaterally exposed for 2 h to a 126 dB SPL narrow band noise centered at 12 kHz. Rats were also screened for noise-induced tinnitus, a potential stressor which may suppress neurogenesis. Five rats developed persistent tinnitus-like behavior while the remaining four rats showed no signs of tinnitus. Age-matched sham controls showed no signs of hearing loss or tinnitus. The inner ear and hippocampus were evaluated for sensory hair cell loss and neurogenesis 10 weeks post-exposure. All noise exposed rats showed severe hair cell loss in the noise-exposed ear. but no damage in the unexposed ear. Frontal sections from the hippocampus were immunolabeled for doublecortin to identify neuronal precursor cells, or Ki67 to label proliferating cells. Noise-exposed rats showed a significant reduction of DCX neural precursors and Ki67 dividing cells compared to controls. No difference was noted between rats with behavioral evidence of tinnitus versus non-tinnitus rats. Performance on the Barnes maze revealed memory impairments in the noise-exposed group compared to age-matched controls. These results show for the first time that noise-induced hearing loss suppresses cell proliferation and neurogenesis in the hippocampus which may contribute to memory impairment. Supported by NIH grants R01DC00909101; R01DC009219

162 Effects of Tonabersat (SB-220453), a Novel Gap Junction Blocker, on Noise Induced Tinnitus

Edward Lobarinas¹, Caroline Shillitoe¹, Courtney Campbell¹, Richard Salvi¹

¹University at Buffalo

Over the last decade, there has been renewed interest in identifying drugs to suppress long term tinnitus. Some forms of tinnitus are thought to arise from central auditory dysfunction in response to peripheral ear injury. One hypothesis is that aberrant synchronous neural activity in the central auditory system could lead to the perception of tinnitus. Gap junctions are believed to provide a means of synchronizing neural activity over broad regions of the cortex and gap junction blockers have been proposed as a potential therapy for aberrant neural synchrony. То determine the potential efficacy of gap junction blockers on noise induced tinnitus we evaluated the ability of Tonabersat (SB-220453), a novel gap junction blocker, to suppress transient and persistent tinnitus. We used Gap Prepulse Inhibition of the Acoustic Startle (GPIAS) to probe for behavioral evidence of tinnitus in noise-exposed rats. We hypothesized that noise induced tinnitus could result from widespread propagation of neural activity similar to that observed in cortical spreading depression (CSD). Tonabersat is believed to attenuate CSD by reducing gap junction intercellular transmission. In support of this model. Tonabersat has been shown to attenuate migraines associated with auras, a form of visual hallucination preceding some migraine attacks. In the present experiment, rats were unilaterally exposed for 1 h to a 126 dB SPL, narrowband noise centered at 16 kHz. A subset of rats showed behavioral evidence of transient tinnitus at 16-20 kHz. A Tonabersat dose-effect curve showed a dose-dependent partial reversal of tinnitus at 48 h post-exposure. Behavioral tests conducted 2 weeks post-exposure showed a more modest suppression of tinnitus-like behavior. These results suggest that Tonabersat may attenuate some forms of noise-induced tinnitus and that some forms of central tinnitus may have characteristics of CSD.

Supported by: Tinnitus Research Initiative

163 The Effects of Salicylate, a Tinnitus Inducer, on Sound-Evoked Activity in the Amygdala

Guang-Di Chen¹, Daniel Stolzberg¹, Brian Allman¹, Richard Salvi¹

¹SUNY at Buffalo

Nearly 9% of the aging population suffers from persistent tinnitus. In addition to plasticity in the classical auditory pathway, the limbic system, which is largely responsible for the emotional response to our environment, has also been implicated in tinnitus generation. For example, tinnitus patients demonstrate increased metabolic activity in the limbic region as measured by positron emission tomography (PET), and up-regulated immediate early gene expression was observed in the limbic system in animals treated with salicylate, a tinnitus inducer, suggestive of a tinnitus-related plasticity. The amygdala, in particular its lateral nucleus (LA), which receives inputs from and projects outputs to the classical auditory pathway, was our first target in the investigation of the involvement of the Using a limbic system in tinnitus generation. microelectrode, we recorded the local field potential (LFP) and multi- and single-unit activity in the LA of anesthetized rats before and after a systemic salicylate injection (300 mg/kg, i.p.) known to induce tinnitus. The sound-evoked LFP had a prominent negative peak at ~20 ms and a positive peak at ~32 ms. Interestingly, after salicylate treatment, the LFP was significantly enhanced by ~40%. The LA neurons discharged in response to acoustic stimuli with latencies of about 15-25 ms and with transient or sustained response patterns. The discharge rate was stimulation frequency- and intensity-dependent. Both monotonic and non-monotonic input/output functions were A salicylate-induced enhancement of LA observed. neuronal activity was observed; however, it appeared to be dependent upon stimulation parameters and neuronal response pattern. The preliminary data indicate that salicylate treatment causes significant alterations in amygdala information processing which may be related to the generation of tinnitus.

Supported by NIH grants (R01DC0090910; R01DC009219-01)

164 Effects of Systemic Salicylate Administration on Spontaneous and Sound-Evoked Activity Across Lamina of the Auditory Cortex of Rats

Daniel Stolzberg¹, Brian Allman¹, Richard Salvi¹ ¹Center for Hearing & Deafness, University at Buffalo, the State University of New York

Tinnitus is characterized by the persistent perception of an inescapable phantom sound (e.g. ringing, buzzing) in the absence of any source in the environment. One leading theory of tinnitus implicates aberrant spontaneous activity permitted by cortical disinhibition. In support of this hypothesis, magentoencephalographic recordings from humans with tinnitus revealed decreased energy over the auditory cortex (AC) in the alpha band (8-12 Hz) - a frequency band which positively correlates with inhibitory processes - compared with normal subjects. Similarly, field recordings from the surface of the AC in chronically implanted awake rats showed a significant decrease in alpha energy following a high dose of salicylate; a drug known to reliably induce temporary tinnitus in humans and other animals. In order to investigate how salicylateinduced tinnitus affects inhibitory regulation of cortical activity, extracellular neural activity was recorded simultaneously across the lamina of the AC in anesthetized rats before and following a single systemic salicylate injection (300 mg/kg IP). Following salicylate administration, a decrease in alpha energy was observed near the brain surface and deeper electrodes; however, the middle layers of the AC responded with an increase in alpha-band energy. Multi-unit activity increased selectively in the middle layers. Interestingly, salicylate strongly affected sound-driven responses across the AC lamina in a manner indicative of a cortical disinhibition. In addition. frequency receptive fields of AC neurons expanded and the best frequency of the receptive fields of most neurons shifted towards the behaviorally assessed tinnitus pitch (10-20 kHz). These physiological changes support the hypothesis that cortical disinhibition plays a significant role in the generation of salicylate-induced tinnitus and that tinnitus may emerge from an overrepresentation of cortical neurons tuned to the tinnitus pitch. Supported by NIH (R01DC0090910; R01DC009219; F31DC010931-01)

165 Tinnitus and the Dorsal Cochlear Nucleus: A Balancing Act – Clinical Evidence from Hearing Loss, Auditory Nerve Transection, and Benzodiazepines Robert Levine¹

¹Harvard

A fundamental unanswered question regarding tinnitus and hearing loss, is why, with any degree of hearing loss some people develop tinnitus and others do not. Even with total hearing loss, 80% of people develop tinnitus, but 20% do not. The current tinnitus dorsal cochlear nucleus (DCN) disinhibition hypothesis cannot account for this fact, since it predicts tinnitus whenever auditory nerve fiber spontaneous activity diminishes. However, the addition of (1) the concept of a neural threshold for tinnitus and (2) consideration of type I inputs to the DCN output as primarily excitatory, and type II inputs to the DCN as primarily inhibitory, leads to a modification of the DCN hypothesis. Whether any degree of hearing loss will result in tinnitus will depend upon the relative interplay in changes in the degree of excitation and inhibition caused by Type I and Type II nerve fiber dysfunction relative to the neural threshold for tinnitus.

These modifications of the DCN hypothesis can now account for (1) one in five people not developing tinnitus despite a total hearing loss and (2) cochlear nerve transection abolishing tinnitus for some people but not for others.

Because (1) inhibition from Type II nerve fibers is mediated by GABA and (2) benzodiazepines potentiate GABA, quieting of tinnitus by benzodiazepines may be from potentiation of Type II nerve fiber DCN inhibition.

166 Noise Exposure Stimulus Properties and Temporal Development of Tinnitus in Rats

Jeremy Turner^{1,2}, Deb Larsen¹

¹Southern Illinois University School of Medicine, ²Illinois College

Fischer Brown Norway (FBN) rats (n=137) were isoflurane anesthetized and unilaterally exposed to a 16 kHz, octave band noise at all combinations of three different intensities (110, 116, and 122 dB SPL) and three different durations (30, 60, and 120 min), while 30 rats served as shamexposed controls. Rats were behaviorally tested for gapinduced inhibition and prepulse inhibition of the startle reflex using 60 dB SPL, 1/3 octave backgrounds or prepulse stimuli centered at the following frequencies: 4, 5, 6, 8, 10, 12, 16, 20, 25, and 32 kHz. Behavioral testing was conducted before noise exposure to establish a baseline, then at days 1, 3, 7, 14, 21, 28, and monthly thereafter. The study aims were to determine whether manipulating noise exposure intensity and/or duration led to the emergence of tinnitus with a different chronological feature (sooner vs later) or spectral pattern (broad vs narrow). Preliminary analyses suggest that a wide variety of noise exposures, but especially the longer and more intense stimuli, led to acute tinnitus measured one day after noise exposure. Acute (1-dav) tinnitus was generally seen at frequencies above the trauma center (i.e., 20-32 kHz), but also appeared to include a broader frequency range of deficits for the longer, more intense stimuli. Intensity and duration appeared to produce acute tinnitus in a dose-dependent manner. For example, gap responses in a 32 kHz background were significantly worse than pretest for the 2hr duration exposure for all three intensities, 110, 116, and 122 dB. However, shorter durations of 1/2 and 1hr were only associated with significant acute tinnitus when using the loudest exposure intensity of 122 dB. Sham controls did not show significant changes from pretest to day 1. Longitudinal data are still being collected, but preliminary findings suggest that chronic tinnitus is characterized by more variability and more complex relationships between exposure variables. In many cases the greatest evidence for chronic tinnitus

was present for shorter duration or less intense exposures. For example, evidence of sustained, 10-kHz chronic tinnitus appears after 5 months for 110 dB SPL exposures of 1hr and 2hr durations. Additional analysis of individual animal responses are explored.

Study funded by a grant from the Tinnitus Research Consortium.

167 Gap Detection and Prepulse Inhibition in CBA/CaJ Mice Following Noise Exposure Ryan Longenecker¹, Alexander Galazyuk¹

¹NEOUCOM

The CBA/CaJ mouse strain is known to retain normalhearing over much of its life. Therefore, this strain is well suited to study temporal characteristics of tinnitus development followed by noise exposure, the most common cause of this widespread hearing disorder. To address this issue we tested 24 two-month-old CBA/CaJ mice. The experimental group (n=16) was anesthetized with ketamine and zylozine and exposed to unilateral noise (16 kHz octave band noise, 116 dB SPL) for one hour. The control group (n=8) of mice was simply anesthetized without the exposure. Gap detection and prepulse inhibition (PPI) were tested at 70 dB SPL (third octave bands centered at ten different frequencies) before and after sound exposure at different time points (1, 3-4, 7, 14, 21, 30 days, and monthly thereafter). Thresholds of auditory brainstem responses were measured before, immediately after, and also 6 months following exposure. We found that on the next day after the exposure the experimental group performed poorly in both gap detecting and PPI at all frequencies tested compared to the control group. Over the course of several days these changes were still present at the frequencies used for the exposure whereas partially recovered at other frequencies. Temporal aspects of these changes are discussed in the context of the development of tinnitus.

Supported by the Research Incentive Grant from NEOUCOM

168 Tinnitus and Cochlear Implants

Francka Kloostra¹, Rosemarie Arnold¹, Pim van Dijk¹ ¹University Medical Center Groningen

The first report on subjective tinnitus being suppressed by a cochlear implant was published by House in 1976. After that, several studies have confirmed these results. In this study we evaluated the effect of cochlear implantation on subjective tinnitus and determined which factors are critical to this effect.

We retrospectively studied these effects by sending 2 questionnaire booklets to 212 cochlear implant patients; one about the situation before implantation and one about the situation after implantation. We mostly used standardized questionnaires which contained questions concerning tinnitus handicap, tinnitus characteristics, hearing loss, personality, anxiety/depression and life events. 122 of the approached patients completed the full questionnaire booklets and 35 patients completed a short

version of the questionnaire booklets. Of the included patients 51.3% reported tinnitus before implantation. Of these patients with preoperative tinnitus, 51.3% reported a reduction or cessation of their tinnitus after implantation. However, 9.0 % of the patients with tinnitus reported a postoperative deterioration of their tinnitus and of the patients without preoperative tinnitus 14.9% reported the start of tinnitus after implantation. The self-reported change of tinnitus correlated with the pre- and postoperative scores on the THI (Tinnitus Handicap Inventory) en THQ (Tinnitus Handicap Questionnaire). A preliminary analysis shows that the most important predictors of a positive influence of a cochlear implant on tinnitus are: high preoperative scores on THI or THQ and one-sided tinnitus. Other factors that seem to be associated with tinnitus are: speech understanding scores, HADS scores (Hospital Anxiety and Depression Scale) and type D personality factors.

Summarized, cochlear implantation reduces tinnitus in an important part of the patients. Cochlear implantation seems to be a good option to treat tinnitus in a select group of patients, including those with one-sided tinnitus.

169 Acoustic Enhancement of Activity in the Auditory and Adjacent Cortices of Anesthetized Rats

Xueguo Zhang¹, Yupeng Zhang¹, Edward Pace¹, Jinsheng Zhang^{1,2}

¹Department of Otolayngology, Wayne State University School of Medicine, ²Dept Communication Sciences & Disorders, Wayne State University College of Liberal Arts & Sciences

Acoustic signals go through much more complex processes at the thalamic and cortical levels than at the brainstem level. In addition to inducing hearing, acoustic stimulation may exert other influences on cortical activity. The current study was designed to characterize nonhearing-related cortical activity following acoustic stimulation. Both spontaneous and acoustic stimulusdriven multiunit activities were recorded in the auditory and adjacent cortices using chronically implanted microwire electrode arrays in nine rats. Acoustic stimuli were tone bursts of 2-43 kHz and 50 ms duration randomly delivered at 5-80 dB SPL and broad-band noise (BBN) bursts of 50 ms duration delivered at 80 dB SPL, both at 2 pulses per second. Among the total 142 channels recorded, data of 300 ms post-stimulus (both tone and BBN) activities were measured and compared with spontaneous activity, respectively. The results demonstrated that, compared to spontaneous firing rate, the post-stimulation activity rate was significantly enhanced following stimulation with either BBN or tone bursts. The increases were inversely related to the spontaneous firing rate. In addition, tone bursts appeared to produce stronger excitatory effects on neural activity than BBN bursts. The excitatory effects of acoustic stimulation were similar at both the auditory and adjacent cortices. These preliminary results suggest that acoustic stimulation may have an arousal effect in deeply anesthetized animals possibly by enhancing cortical

activity. Such an arousal effect may not necessarily be related to hearing.

170 Electrophysiological Diversity of Layer V Pyramidal Neurons in the Primary Auditory Cortex and the Belt Area of the Rat

Kateryna Pysanenko¹, Oliver Profant^{1,2}, Josef Syka¹, Rostislav Turecek¹

¹Institute of Experimental Medicine ASCR, Prague, Czech Rep., ²ENT Department, 1st Medical faculty, Charles University, Faculty Hospital Motol, Prague, Czech Rep. Previously, during extracellular recording of sound-evoked auditory cortex (AC) activity, striking differences were observed between the spiking patterns of neurons from the primary AC (A1) and surrounding belt area. Most A1 neurons displayed short latency onset responses, suggesting a phasic character of the neurons, unlike the prevalent tonic neurons in the belt area. It has been hypothesized that incoming signals could be processed differently by neurons in these areas. In the current study we have investigated the intrinsic electrical properties of layer V pyramidal neurons by patch-clamp recording in acute rat AC slices. Three distinct cell types were recognized in both AC areas: two regular-spiking slowly adapting types, RS1 and RS2, and intrinsically bursting cells (IB). RS neurons prevailed among cells in both auditory areas, while the lower frequency spiking subtype RS1 dominated in the belt. In contrast, the A1 neuronal population showed equal contributions of RS1 and RS2 neurons. The spiking ability of neurons from both areas was significantly altered in the presence of inhibitors of Ca2+-activated K+ channels. Apamin and TRAM-34 but not iberiotoxin, both increased the frequency of the action potentials (APs) evoked by long depolarizing stimuli. Consistent with the larger contribution of the RS1 subtype in the belt area, belt neurons showed a significantly stronger sensitivity to the inhibitory effect of apamin. In addition, neurons from the A1 and belt area differed in the amplitude of the hyperpolarization-activated cation current (Ih), resulting in a lower input resistance and a shorter latency of action potential generation in the A1 neurons. Our data support the hypothesis that differences in spiking patterns obtained in vivo could be at least partially explained by differences in the intrinsic passive and active electrical properties of the A1 and belt neurons. Supported by grants AV0Z50390512, GACR 309/07/1336 and LC 554.

171 Receptive Field Properties of Layer 5 Neurons in Rat Auditory Cortex

Yujiao Sun¹, Guangying Wu¹, Li Zhang¹ ¹USC

Sensory cortex influences its targets through topographically organized descending afferents originating in layers 5 and 6. Layer 5 is of particular interest because its cells form part of the cortical projection to the thalamus and the entirety of the cortical projection to subthalamic nuclei. Previous slice studies have shown that layer 5 contains several anatomic and physiological pyramidal cell types and a variety of interneurons. Whether these layer 5 neurons exhibit cell-type specific processing of auditory information in the auditory cortex has largely remained illusive.

In the present study, we carried out in vivo cell-attached and whole-cell current-clamp recordings in the rat primary auditory cortex (V1). Four major types of neurons in layer 5 have been identified according to their electrophysiological and receptive field properties. Type 1 neurons exhibit a short burst of spikes in response to bestfrequency tones, consistent with the intrinsic bursting (IB) neurons classified in previous in vitro studies. Type 2 neurons exhibit typical regular spike (RS) shapes, and they fire individual spikes in response to tone stimulation. Type 3 neurons exhibit narrow spike waveforms, consistent with fast spike (FS) inhibitory neurons. Type 4 neurons do not exhibit spike responses to tones. Instead, their spontaneous firings are suppressed, resulting in a void Vshaped area in the frequency-intensity space. Currentclamp recording from such silent type (ST) neurons revealed hyperpolarizing responses in the central region of the subthreshold tonal receptive field (TRF).

Quantification of bandwidths of TRFs indicated that IB neurons exhibit significantly broader TRFs than RS neurons. Such RF difference may reflect different functional roles of IB and RS neurons, which have been implicated in driving the corticothalamocortical pathway and direct feedforward pathway from primary to secondary and contralateral cortices, respectively.

172 Physiological Differences Between Histologically Defined Subdivisions in the Mouse Auditory Thalamus

Lucy Anderson¹, Jennifer Linden^{1,2}

¹Ear Institute, University College London, ²Dept. Neurosci., Physiol. & Pharmacol., University College London

The auditory thalamic area includes the medial geniculate body (MGB) and the lateral part of the posterior thalamic nucleus (Pol). The MGB can be subdivided into a ventral subdivision, forming part of the lemniscal (primary) auditory pathway, and medial and dorsal subdivisions, traditionally considered (alongside the Pol) part of the nonlemniscal (secondary) pathway. However, physiological studies of the auditory thalamus have suggested that the Pol may be more appropriately characterised as part of the lemniscal pathway, while the medial MGB may be part of a third (polysensory) pathway, with characteristics of lemniscal and non-lemniscal areas. We document physiological properties of neurons in histologically identified areas of the MGB and Pol in the anaesthetised mouse, and present evidence in favour of a distinctive role for medial MGB in central auditory processing. In particular, medial MGB contains a greater proportion of neurons with short first-spike latencies and high response probabilities than either the ventral or dorsal MGB, despite having low spontaneous rates. Therefore, medial MGB neurons appear to fire more reliably in response to auditory input than neurons in even the lemniscal, ventral subdivision. Additionally, responses in the Pol are more similar to those in the ventral MGB than the dorsal MGB.

Supported by the Wellcome Trust, Deafness Research UK, and the Gatsby Charitable Foundation.

173 Response Properties of Neurons in Auditory Cortical Fields of Awake Mice (Mus Musculus)

Bettina Joachimsthaler¹, Michaela Glowina¹, Frank Miller¹, Anja L. Dorrn¹, Günter Ehret¹, **Simone Kurt¹** ¹University Ulm

Response properties of neurons in fields of the auditory cortex (AC) are well described for anesthetized house mice (Stiebler et al., 1997). As demonstrated for other species, effects of anesthesia may play a critical role in generating response properties which are effective in situations of sound communication. Here we present multiunit electrophysiological mapping data from auditory cortical fields of adult, awake, head-fixed mice (outbreed hybrids (Mus musculus) of feral mice and NMRI-mice). We characterize neuronal pure tone responses from the left auditory cortex (AC) and discriminate the fields within the AC as described by Stiebler et al. (1997), namely primary fields (primary auditory field, AI, and anterior auditory field, AAF), and higher-order fields (second auditory field, AII, and dorsoposterior field, DP).

Among our results are the following: (1) Most neurons in all fields had high spontaneous rates (about 10 - 40 spikes/s); (2) response latencies varied between about 8 - 20 ms with longest latencies in All; (3) sharpness of frequency tuning expressed as Q40 values varied between about 0.5 - 7 with sharply tuned neurons occurring mostly in All and DP; (4) especially neurons in the fields All and DP showed phasic-tonic or tonic responses whereas phasic responses were mainly present in primary fields. These response characteristics of neurons in the AC of the awake mouse contrast with what is known from many recordings in anesthetized mammals.

174 Specialization of Binaural Responses in Ventral Auditory Cortices

Nathan Higgins¹, Douglas Storace¹, Monty Escabi^{1,2}, Heather Read^{1,2}

¹Department of Psychology, University of Connecticut, ²Department of Biomedical Engineering, University of Connecticut

The dual stream hypothesis based on primate parabelt responses suggests a functional division of "what" and "where" functional streams corresponding to dorsalposterior and ventral-anterior cortices. Here we measured cortical spike rate responses to interaural level difference (ILD) across multiple cortical regions in the rat in order to determine functional organization of this localization cue within ventral regions. Intrinsic optical imaging maps were used to systematically divide the cortex into discreet regions including primary (A1), ventral (VAF) and suprarhinal (SRAF) auditory fields. Multi-unit responses were then recorded to generate spike rate versus ILD curves for a fixed range of ILD and average binaural level (ABL) conditions, and modeled using linear, Gaussian and peaked sigmoid functions. The best fit for each curve was then calculated using automated bootstrapped predictions and analysis of residuals. From this fit we calculated best ILD, and two measures of ILD tuning. Sites with low best ILD values had the narrowest tuning, and were predominantly found in VAF and caudal SRAF, whereas sites with higher best ILDs had broader tuning and were typically found in A1 and rostral SRAF. SRAF was found to have the highest percentage of responses with narrow midline ILD tuning shaped by nonlinear binaural facilitatory and inhibitory interactions. This study joins several others in calling for a modified functional rubric where position cue sensitivity is a critical and ubiquitous organizational feature across multiple cortices, similar in many respects to organization of the visual cortices. NICHD: HD2080

175 The Array Drive : Optimizing the Yield and Flexibility of Chronic, Multielectrode Array Recordings

Bernhard Englitz¹, Stephen David¹, Didier Depireux¹, Shihab Shamma¹

¹University of Maryland, College Park

Information processing in the brain is distributed across large populations of neurons. Multielectrode recordings are one approach to deciphering the population code, especially when studying functional interactions between large numbers of simultaneously recorded neurons in the awake animal. Multielectrode Arrays (MEAs) are a convenient way of bundling a large number of electrodes (>100) and are available from a number of companies. However, MEAs are usually implanted at a fixed depth, thus preventing the possibility of adapting electrode position during recordings to improve isolation or sample different layers. To address this shortcoming we have developed a mechanical microdrive that allows movement of the entire MEA in depth. The MEA is fixed to a movable shuttle, which is mechanically restricted to precise depth movements by multiple positioning screws. The connector of the MEA is suspended by a tether and positioned away from the microdrive in order avoid inducing electrode movement in the brain when connecting and disconnecting the headstages. While this approach sacrifices individual positioning of electrodes, the greater number of channels (>100) easily surpasses the yield of individual electrode microdrives. The simpler mechanics reduce the time spent positioning electrodes and thus avoids repeatedly sedating/anesthetizing the animal, often required for individually drivable electrodes They also reduce the size and weight of the microdrive (<2-3g), making it useful for smaller species. The system has been designed for easy recovery of the MEA after completion of recordings. Finally, the costs of the present system will be less than the currently available microdrives and still offer a greater number of channels than any existing movable array.

176 How Local Is an Auditory LFP?

Yoshinao Kajikawa¹, Charles Schroeder^{1,2}

¹Nathan Kline Institute, ²Columbia Univ.

Field potentials (FP) recorded within the brain index net transmembrane currents that attend the excitation and inhibition of a local neuronal ensemble, and thus are

commonly referred to as a glocal field potentials h or LFPs. Because of volume conduction, however, the common practice of using an extra-cranial reference for FP recordings means that they may also reflect current flow occurring in locations distant to the recording site. In contrast, the second spatial derivative of the FP (current source density or CSD) eliminates volume conduction and allows isolation local electrical events. In the primary auditory cortex (A1) of the macaque monkey, both neuronal firing and FPs are tuned to spectral frequency of sound. Not surprisingly, FPs typically have wider tuning bandwidth than neuronal firing. In the present study, we compared the sharpness of frequency tuning for suprathreshold pure tones across 3 common measures multiunit activity (MUA), CSD and FP measures. The tuning bandwidth of those signals ranged in the order of MUA < CSD < FP. In addition, FP did not attenuate at frequencies octaves away from the local best frequency, while MUA driving vanished at such frequencies. Wider tuning of CSD than MUA was consistent with reflection of subthreshold synaptic currents by CSD. The much broader tuning of FP confirms that an FP response at a given site cortex reflects both distant and local contributions. Given this outcome also, it may be best to limit the use of the term LFP to signals obtained from first or higher order derivative recordings that reduce or eliminate the influence of volume conduction.

177 Effects of Stimulus Repetition on the Auditory N1 Peak Revealed by Standardized Low-Resolution Brain Electromagnetic Tomography (SLORETA)

Fawen Zhang¹, Chelsea Benson¹, Aniruddha Deshpande¹, Mathew Smith¹, James Eliassen¹, Qianjie Fu² ¹*university of cincinnati*, ²*House Ear Institute*

The purpose of this study was to understand the neural substrates of the response adaptation (amplitude reduction following stimulus repetition) of the N1 peak in the late auditory evoked potential (LAEP). Participants included 14 young normal listeners. Stimuli were presented in trains of ten with an inter-stimulus interval of 0.7 s and an inter-train interval of 15 s. Source density analysis was conducted for the N1 evoked by the 1st, 2nd, and 10th stimulus in the train (S1, S2, and S10) with standardized Low Resolution Electromagnetic Tomography (sLORETA). Three timeframes were used for sLORETA analysis: 70-100 ms, 100-130 ms, and 130-160 ms. Differences of the responses between two stimulus pairs: S1 vs. S2 and S2 vs. S10, were delineated in terms of LAEP waveform and sLORETA results. The adaptation index (AI, AI = 1-S10/S1) for 5 regions of interest (ROIs) including one in the transverse temporal gyrus (TTG) and 4 in other regions, were compared to describe their adaptation features.

The LAEP amplitude was the largest for S1 and greatly reduced for S2. There was no significant difference between the S1 and S2 response waveforms. The sLORETA results showed that the S1 response recruited different cortical lobes. The activation for the S2 response was much less than for the S1 response. The S10

response mainly recruited the temporal lobe in 70-100 ms and 100-130 ms but the parietal and frontal lobes in 130-160 ms. The sLORETA difference between S1 and S2 responses showed activation in the parietal lobe in 70-100 ms, the frontal lobe and limbic lobe in 100-130 ms, and the frontal lobe in 130-160 ms. The sLORETA difference between S2 and S10 responses was not significant. The AI was significantly lower for the TTG than for other ROIs. The results indicate that the contributing brain regions of the N1 have different adaptation features. The parietofrontal neural network may serve to enable the brain to filter out irrelevant stimuli and be alert for novel stimuli.

178 Tonotopy in Human Primary Auditory Cortex: Hemispheric Asymmetries and Effect of Age

Huib Versnel^{1,2}, Rianne Verhoef¹, Ralf Boerboom^{1,2}, Bas Neggers^{1,2}, Nick Ramsey^{1,2}, Bert Van Zanten^{1,2} ¹University Medical Center Utrecht, ²Rudolf Magnus Institute of Neuroscience

Our interest is to examine changes in the frequency organization in human auditory cortex due to hearing loss and tinnitus. For that purpose the cortical activation in response to pure tones was quantified in both young and old normal-hearing controls using functional magnetic resonance imaging (fMRI).

Experiments were performed in 14 normal-hearing subjects (age: 20-60 years) in a 3T MRI scanner using echo planar imaging (voxel size: 2x2x2 mm). Stimuli, consisting of 6 short and 6 long randomly sequenced tone pips, were presented in between scans, which were acquired according to a sparse sampling paradigm. Three different frequencies were monaurally presented (typically 1, 3 and 8 kHz) to either ear. Subjects had to indicate whether the last pip in the tone-train stimulus was short or long (30 or 120 ms). Image analysis was performed with SPM8. Activation measures were volume, percent signal change and center of mass. Slope and R^2 of the regression of center of mass and log(frequency) were used to quantify tonotopy.

The tonotopy in the primary auditory cortex was more distinct in the right than in the left hemisphere as demonstrated by a significantly steeper slope and higher R^2 . Moreover, the activated volume was larger in the right cortex. In each hemisphere the centers of mass were in comparable cortical locations for contra- and ipsilateral stimulation. The volumes and signal changes were, as expected, significantly larger for contralateral stimulation. The tonotopy did not substantially vary with age, however, activated volume decreased significantly with age.

The higher tonotopic order in the right hemisphere quantified in this study confirms earlier, mostly qualitative, observations. This might be related to a right-hemispheric specialization for pitch processing. The activation and tonotopic measures used in this study can be applied to compare tinnitus patients with controls. Age is a factor to be taken into account in these comparisons.

179 Perceptual and Modeling Estimates of Frequency Selectivity Suggest That Acoustic Stimulation Reduces Cochlear Gain

Skyler Jennings¹, Elizabeth Strickland¹ ¹*Purdue University*

A fundamental guestion in auditory science relates to how the perceptual dynamic range is coded in the auditory system given that the dynamic range of individual neurons is about 20-40 dB. The medial olivocochlear reflex (MOCR) may be one mechanism contributing to the perceptual dynamic range. This reflex acts as an automatic gain control by adjusting the gain of the cochlear amplifier. The experiments proposed involve a multifaceted approach of perceptual and computational modeling techniques to study how a reduction in gain (hypothetically via the MOCR) influences detection in auditory masking tasks. In the perceptual studies, a standard masking condition is compared with a condition where a precursor precedes the masker. This precursor is assumed to reduce cochlear gain. The standard condition and the condition with a precursor are compared using various psychophysical techniques sensitive to cochlear frequency selectivity and gain. These techniques include psychophysical tuning curves, notched noise tuning characteristics and growth of masking functions. The computational modeling approach will involve combining two established models; one related to the auditory periphery and the other related to masking. Model predictions will be obtained for two hypotheses regarding the effect of the precursor on masking threshold. The additivity of masking hypothesis assumes that the masking effect of the precursor and masker add at the output of the cochlea. Implicit in this hypothesis is the notion that cochlear gain remains fixed over time. The gain reduction hypothesis assumes the precursor reduces the gain of the cochlea, resulting in an adapted cochlear input/output function. Preliminary data are presented for the psychophysical and modeling experiments. These data support the gain reduction hypothesis. [Research Supported by a Grant from NIH(NIDCD) R01 DC008327]

180 The Dependence of Medial Olivocochlear Feedback on Signal-To-Noise Ratio During Auditory Intensity Discrimination

Nikolas A. Francis^{1,2}, John J. Guinan, Jr.^{3,4} ¹Harvard-MIT Division of Health Sciences and Technology, ²Speech and Hearing Bioscience and Technology Program, ³Department of Otology and Laryngology, Harvard Medical School, ⁴Eaton-Peabody Lab, Massachusetts Eye and Ear Infirmary,

Medial olivocochlear (MOC) feedback is believed to facilitate intensity discrimination in noise by reducing cochlear amplifier gain, which increases cochlear sensitivity to changes in sound level. At low signal-to-noise ratios (SNRs), where energetic masking is greater, increases in MOC feedback might be more beneficial, and therefore more pronounced. We tested four human subjects in a monaural two-interval same-different masked intensity discrimination task. MOC feedback was monitored in the task ear during the task by changes in the magnitude of click-evoked otoacoustic emission (CEOAE) frequency content. CEOAEs were evoked by 50 dB SPL, 80 µs rectangular pulses presented at a rate of 25 Hz. Intensity discrimination was performed on ~1 kHz, 20 ms tone-pulses presented during a continuous, 50 dB SPL, spectrally flat (0.1 to 10 kHz) masking noise. We used six experimental conditions with SNRs of -99, -10, 0, 10, 20 and 30 dB for the mean tone-pulse level in a block of trials. Each trial contained a pair of a tone-pulses, with each tone-pulse level randomly selected from the block's mean level ± half the difference limen determined from a 4down/1-up adaptive procedure estimating the 84.1% correct detection threshold. Subjects indicated by button press if the pair were the same or different. MOC feedback was measured in each trial by comparing CEOAEs before and just after presenting tone-pulse pairs. Subjects were trained for at least two hours. Data were also recorded without the task for each condition. Results show that the task tended to increase MOC feedback as SNR decreased. MOC feedback was largest near the task frequency and decreased away from the task frequency. This frequency dependence was not observed without the task. The results provide the best evidence to date that cochlear physiology is adjusted by MOC feedback according to the SNR and frequency content of discriminated sounds.

Supported by NIH NIDCD RO1 DC005977, P30 DC005209 and T32 DC00038

181 Medial Olivocochlear Reflex Contributes to Protect Sound Localization in Noise

Guillaume Andeol¹, **Christophe Micheyl**², Annie Moulin³, Lionel Pellieux¹, Sophie Savel⁴, Anne Guillaume⁵ ¹Institut de Recherche Biomédicale des Armées, ²Auditory Perception and Cognition, Department of Psychology, University of Minnesota, ³Laboratoire Neurosciences Sensorielles, Comportement et Cognition, CNRS, ⁴Laboratoire de Mécanique et d'Acoustique, CNRS UPR, Equipe Perception Auditive, ⁵Laboratoire d'Accidentologie et de Biomécanique

The cochlea receives efferent feedback from the superior olivary complex via the olivocochlear bundle. One of the two branches of this efferent system projects to the outer hair cells. Although the function of this medial olivocochlear system (MOCS) is still not entirely clear, it has been suggested that, by suppressing peripheral neural responses to background, the MOCS contributes to facilitate hearing in noise. Based on previous findings showing deficits in sound-localization in noise in cats with a lesioned MOCS, and on other findings showing marked interindividual differences in noise-induced MOCS activity (the 'MOCS reflex'), we hypothesized that interindividual differences in sound-localization performance in noise might be partly related to differences in MOCS-reflex strength. To test this hypothesis, we measured soundlocalization performance in guiet and in various levels of background noise, as well as noise-induced suppression of evoked otoacoustic emissions (EOAEs), a non-invasive

measure of the MOCS reflex, in 18 normal-hearing listeners. In the localization experiment, listeners had to localize a signal "signal" (a 200-ms, 55 dB SPL noise burst bandpass filtered between 0.3 and 9 kHz) emitted by one of 8 loudspeakers surrounding them in all three dimensions. The signal was presented in quiet or in the presence of wideband diffuse noise at signal-to-noise ratios (SNRs) ranging from -7.5 to +5 in 2.5-dB steps. OAEs were evoked by clicks and suppressed by broadband noise in the contralateral ear. Results showed significant positive correlations between contralateral OAE suppression and differences in localization performance between the guiet and three noisiest conditions (SNRS of -7.5 to -2.5 dB), indicating that the MOCS reflex contributes to protect sound-localization ability against high levels of background noise.

182 Psychoacoustical Characterization of Medial Olivocochlear Reflex Effects on Human Cochlear Responses

Enzo Aguilar¹, Peter T. Johannesen¹, **Enrique A. Lopez-Poveda**¹

¹University of Salamanca

The effect of medial olivocochlear reflex activation (MOCR) on human cochlear processing was investigated in normal hearing listeners using psychoacoustical methods. It was assumed that the MOCR is activated by contralateral white noise (CWN) at 60 dB SPL. Temporal masking curves (TMCs) and psychophysical tuning curves (PTCs) were measured in forward masking at 0.5 and 4 kHz with and without CWN. PTCs were measured considering masker frequencies from 0.5fP to 1.3fP, with fP being the probe frequency. PTCs were measured for masker-probe time gaps of 2, 10, 30 and 50 ms. TMCs for on-frequency maskers were measured considering time gaps from 2 to 100 ms. Additional linear-reference TMCs were measured for a probe frequency of 4 kHz and a masker frequency of 1600 Hz. Cochlear input/output curves were inferred from the TMCs by plotting the levels of the linear reference TMC against the levels of the on-frequency maskers for paired time gaps. Results show that CWN has a stronger effect at 0.5 than at 4 kHz. PTCs measured with CWN show a decrease in the masker level at probe detection threshold and wider tuning. These effects increase with increasing masker-probe time gap. I/O curves with CWN tended to show reduced gain. Results are discussed in relation with other studies on the effect of activation of MOCR on cochlear function (Work funded by the Spanish MICINN ref. BFU2009-07909).

183 Isoresponse Versus Isoinput Estimates of Cochlear Filter Tuning

Almudena Eustaquio-Martin¹, **Enrique A. Lopez-Poveda**¹ ¹University of Salamanca

The tuning of a linear filter may be equally inferred from the filter's isoresponse (e.g., tuning curves) or isoinput (e.g., isolevel curves) characteristics. This paper provides a theoretical demonstration that for nonlinear filters with compressive response characteristics like those of the basilar membrane, isoresponse measures can suggest strikingly sharper tuning than isoinput measures. The practical significance of this phenomenon is demonstrated by inferring the 3-dB-down bandwidths (BW3dB) of human auditory filters at 500 and 4000 Hz from behavioral isoresponse and isoinput measures obtained with sinusoidal and notched noise forward maskers. Inferred cochlear responses were compressive for the two types of maskers. Consistent with expectations, low-level BW3dB estimates obtained from isoresponse conditions were considerably narrower than those obtained from isolevel conditions: 69 vs. 174 Hz, respectively, at 500 Hz, and 280 vs. 464 Hz, respectively, at 4000 Hz. Furthermore, isoresponse BW3dB decreased with increasing level while corresponding isolevel estimates remained approximately constant at 500 Hz or increased slightly at 4 kHz with increasing level. It is suggested that comparisons between isoresponse supra-threshold human tuning and threshold animal neural tuning should be made with caution. [Work supported by the Spanish MICINN(ref. BFU2009-07909) and the William Demant Oticon Foundation.

184 The Effect of a Precursor on Growth of Masking Functions and Recovery from Forward Masking

Kristina DeRoy¹, Elizabeth Strickland¹

¹Purdue University

Growth of masking (GOM) functions are a psychophysical technique used to estimate the cochlear input-output (I-O) function. Another technique used to estimate the cochlear I-O function is the temporal masking curve (TMC) method, which is based on recovery from forward masking. The TMC method depends on the assumptions that the internal masker decay is the same regardless of masker level and frequency, and that the I-O function is static with delay. Previous studies in this laboratory have shown that a long precursor decreases the gain of the GOM function. This should be reflected in the rate of recovery from forward masking. In the present study, GOM functions and recovery from forward masking were measured for four normal-hearing subjects in two conditions. In the no precursor condition, listeners detected a 4-kHz signal when preceded by a 20-ms, 2-kHz masker. In the precursor condition, a 100-ms, 4-kHz precursor was presented before the masker and signal. GOM functions were measured with no delay between the masker and signal. As expected, the gain of the estimated I-O function was reduced following a precursor. Recovery from forward masking was measured for several masker levels by delaying the signal from the masker (and precursor, if present). The rate of recovery from forward masking varied with masker level and the presence of the precursor. I-O functions were estimated by fitting a curve to the GOM functions for the precursor and no precursor conditions. Signal thresholds from the recovery from forward masking curves will be passed through the I-O functions to estimate the rate of internal masker decay for each condition. Rate of internal masker decay will be compared across masker levels for each condition. Implications for longer duration maskers and TMCs will be discussed.

[Research Supported by a Grant from NIH(NIDCD) R01 DC008327]

185 Cues in Across-Channel Asynchrony Detection and Discrimination

Magdalena Wojtczak¹, Andrew J. Oxenham¹

¹University of Minnesota

Detection and discrimination of asynchrony for two spectrally remote tones were measured in listeners with normal hearing. Previous studies of asynchrony detection have suggested that listeners perform the task based on the operation of broadly tuned coincidence detectors. However, the studies did not control for the possibility that listeners could detect changes in excitation within a single channel excited by both test tones. The cues involved in asynchrony discrimination have not been as well studied but multiple cues could be used, including the overall duration. In this study, asynchrony detection and discrimination were measured for pairs of tones spectrally separated by at least two octaves. A band of noise centered on the geometric mean of the frequencies of the tones was used to mask the region of overlapping excitation. To investigate the role of onsets and offsets, as well as the role of overall duration, two durations of the test tones were used, 40 and 500 ms, including 10-ms ramps. A condition using 500-ms duration with a very gradual, 250-ms offset ramp was added to investigate the effect of reduced offset cues. The data showed asymmetry in asynchrony detection, with better performance observed when the low-frequency tone in a pair was leading versus when it was lagging. For a given pair of tones, asynchrony was generally better than asvnchronv detection discrimination, suggesting different mechanisms involved in performing the tasks. Similar thresholds for asynchrony detection for 40- and 500-ms tones, and for 500-ms tones with 250-ms offset ramps indicated a dominant role of onsets in asynchrony detection. Similar thresholds for asynchrony discrimination observed with 10- and 250-ms offset ramps suggest that overall duration was not used to perform the task. Asymmetries in detection and discrimination will be discussed in the context of travelingwave delays along the basilar-membrane. [Supported by NIH grant R01 DC010374].

186 Time-Efficient Measures of Frequency Selectivity

Karolina Charziak¹, Pamela Souza¹, Jonathan Siegel¹ ¹Northwestern University

Psychophysical tuning curves (PTCs) can be used to assess frequency selectivity of the auditory system. Fast methods for determining PTCs are time efficient and have been shown to closely correspond to traditionally measured PTC (Sek et al, Int J Aud, 44:408-420, 2005). This makes fast PTCs of special interest when assessing frequency selectivity and may provide a significant contribution to data interpretation (e.g. studies evaluating deficits in speech recognition). In the fast-PTC paradigm, a band of noise with changing center frequency is presented while the subject adjusts the masker level required for threshold. In one approach center frequency of the noise masker changes continuously, while in the other approach noise bands with discrete center frequencies are used. Both methods have been used by several investigators, but no comparisons of the PTCs obtained with the two paradigms have been made.

We measured fast PTCs with the two types of maskers at multiple probe frequencies in normal-hearing subjects. The most appropriate method of modeling raw PTC data was investigated. The PTCs collected with the two types of maskers resulted in similar estimates of tuning. The data obtained with the discrete center frequency-noise masker were affected by training and were less repeatable. Amplitude modulating the probe tone in the discrete-noise condition stabilized subjects' performance to the level observed in the swept-noise condition without affecting the features of PTCs. The Q_{ERB} values derived from the fast-PTC data were in good agreement with published notched noise data.

The swept-noise masker method provided high-resolution and repeatable PTCs, thus showing promise for use in laboratory or clinical settings as a time-efficient measure of frequency selectivity.

Supported by NIDCD grant DC006014 and Northwestern University.

187 Acoustic Startle Responses in Noise-Exposed Mice Suggest a Link Between Primary Neural Degeneration and Hyperacusis

Ann E. Hickox^{1,2}, M. Charles Liberman^{2,3}

¹Harvard-MIT Health Sciences and Technology, Speech and Hearing Bioscience and Technology Program, ²Eaton-Peabody Laboratory, Massachusetts Eye and Ear Infirmary, ³Department of Otology and Laryngology, Harvard Medical School

Moderate noise exposure can destroy up to 50% of cochlear nerve fibers without causing hair cell damage or permanent threshold shifts (Kujawa & Liberman, J. Neurosci, 2009). To probe the effects of this primary neural degeneration on auditory processing in quiet and in background noise, we used prepulse inhibition (PPI) of the acoustic startle response (ASR). Suppression of the ASR by a preceding stimulus (the prepulse) can provide a measure of prepulse detectability.

CBA/CaJ mice were noise exposed (8-16 kHz, 100 dB SPL, 2 hr) at 16-17 weeks. Measurement of ABRs and DPOAEs at 2 weeks post-exposure confirmed the primary neural degeneration phenotype: after initial threshold shifts, DPOAEs recovered at f2 frequencies from 5.6-32 kHz, whereas ABR amplitudes recovered at low (11.3 kHz), but not high (32 kHz) frequencies, mirroring the basal turn neuronal loss. PPI as a function of prepulse level was measured in exposed, and in age- and sexmatched unexposed controls, for prepulses consisting of either tone bursts (11.3 or 32 kHz) or broadband noise bursts, and presented either in quiet or in continuous broadband noise (60 dB SPL). Startle amplitudes were also measured as a function of startle-stimulus level (50-105 dB SPL) for tone burst or broadband startle stimuli.

Surprisingly, noise-exposed mice showed lower PPI thresholds for most stimulus conditions, as well as greater maximum PPI for tone burst prepulses. Exposed animals also showed reduced startle thresholds and enhanced startle amplitudes at moderate SPLs, suggesting a form of hyperacusis. The enhanced startle effects may be elicited by cochlear primary neural degeneration, but could also arise from exposure-induced stress. If there are also post-exposure changes in signal detectability, they may be masked in the ASR assay by this putative enhancement of neural excitability.

Supported by NIDCD T32 DC00038 and NIDCD R01 DC00188.

188 Trauma-Induced Tinnitus in Gerbils Centers Around the Induction Frequency

Manuela Nowotny¹, Martina Remus¹, Manfred Kossl¹, Bernhard Gaese¹

¹Goethe University Frankfurt

The occurrence of tinnitus is often associated with inner ear pathologies, like acoustic trauma. Therefore, an acoustic trauma model of tinnitus in gerbils was established using a modulated acoustic startle response. The trauma was evoked by narrow-band noise at 10 kHz (± 0.25 oct, 105 dB SPL, 1h duration). The resulting hearing damage and recovery was documented measuring auditory brain stem responses (ABR) and distortion product otoacoustic emissions (DPOAE). Successful induction of tinnitus resulted in a reduction of the gap prepulse inhibition of acoustic startle (GPIAS).

ABR and DPOAE thresholds were back to normal three to five weeks after trauma. At that time, a reduction of GPIAS at higher frequencies (16 - 20 kHz, 75 dB SPL noise level) was the first indication for tinnitus. Seven weeks post trauma the tinnitus-affected frequency range shifted to the center-trauma frequency at 10 kHz. Testing for GPIAS reduction at lower SPLs (55 - 75 dB) indicated that the 10 kHz tinnitus sound sensation was already present five weeks after the trauma, however too quiet for detection at higher noise SPL.

Taken together, this study in gerbils found that trauma induced tinnitus did not develop in the border frequency area but rather at the center of the trauma. This is an indication against the theory of lateral inhibition as the physiological basis of tinnitus. The animal model presented here can be further used in the search for medical tinnitus prevention possibilities.

This project is supported by the Adolf Messer-award 2009.

189 Spectral and Temporal Masking Release in the Low- And Mid-Frequency Range for Normal-Hearing and Hearing-Impaired Listeners

Agnès Léger^{1,2}, Brian C.J. Moore³, Christian Lorenzi¹ ¹Université Paris Descartes, CNRS, ENS, France, ²Neurelec, France, ³Department of Experimental Psychology, University of Cambridge "Macking, release" (MR), the improvement of speed

"Masking release" (MR), the improvement of speech intelligibility in modulated compared with unmodulated

maskers, is typically smaller for hearing-impaired (HI) than for normal-hearing (NH) listeners, presumably because of a limited ability of the former to "glimpse" speech in the spectral and temporal dips of maskers. Previous studies indicate that spectral MR is limited by frequency selectivity, whereas temporal MR may be limited by temporal mechanisms partly based on neural phase locking. The goal of this research was to determine whether deficits in temporal MR can be demonstrated in the absence of deficits in frequency selectivity, and thus of deficits in spectral MR. A first study investigated spectral and temporal MR for stimuli restricted to low frequencies (<1.5 kHz). A second study used stimuli covering the midfrequency range (1-3 kHz), because NH listeners can use glimpsing information up to 3 kHz. In both studies, both NH and HI listeners were tested, and the latter had hearing within normal limits over the frequency range covered by the stimuli, but had hearing loss at higher frequencies.

Spectral and temporal MR were assessed for lowpassand bandpass-filtered speech and noise. Consonant identification was measured in quiet and in the presence of a speech-shaped noise at signal-to-noise ratios of -6, -3 and 0 dB. The noise masker was either unmodulated, amplitude modulated, or spectrally modulated.

For both frequency regions, performance and phoneticfeature reception were poorer for the HI than for the NH listeners in all conditions, indicating auditory deficits for frequencies where audiometric thresholds were "normal". Modest deficits were found for both spectral and temporal MR. No clear dissociation was found between spectral and temporal MR, consistent with the notion that common factors (e.g., frequency selectivity) constrain the ability to "glimpse" speech in the spectral and temporal dips of maskers.

Acknowledgements

Léger, Moore and Lorenzi were supported by a grant from the Royal Society. Léger was supported by a grant from ANRT-Neurelec. Moore was supported by the MRC (UK).

190 Interactions Between Target Uncertainty, Masker Uncertainty and Hearing Loss

Eric Thompson¹, Gerald Kidd, Jr.¹

¹Boston University

The detectability of target tones was measured under conditions in which the target frequency was fixed within a block of trials, or was randomly chosen from two alternatives for each trial within a block. The targets were presented in guiet, in notch-filtered Gaussian noise, or in a complex of eight tones selected randomly for each trial. Seven young-adult listeners participated in the experiment. Four listeners had a moderate, bilateral sensorineural hearing loss (HL group), and three had clinically normal hearing (NH group). In quiet and noise, there was no significant difference in the thresholds or in the slopes of the psychometric functions between the fixed target frequency conditions and the random target frequency conditions, for either group. With the multitone masker, both groups had higher thresholds when the target frequency was randomly selected than when the target frequency was fixed. This suggests an interaction between the uncertainty of the masker and the uncertainty of the target frequency. The NH group had much shallower slopes of the psychometric functions with the multitone masker than in quiet or in noise and had thresholds at negative target-to-masker ratios (TMR). The slopes of the psychometric functions for the HL group with the multitone masker were about as steep as the psychometric function in quiet or in noise. The HL group also generally required a positive TMR to detect the target with the multitone masker, which suggests that the HL listeners was unable to perceptually segregate the target from the multitone background and may have had to rely on overall loudness as a cue to solve the task.

191 Partially Masked (Diluted) ITDs in Older and Hearing-Impaired Listeners

Michael Akeroyd¹, Sharon Suller¹ ¹*MRC Institute of Hearing Research*

In a typical listening environment a direct sound is quickly followed by reflections and reverberation. The target sound is, in effect, partially masked by multiple copies of itself, which will "dilute" the interaural time differences (ITDs) of the target and so should affect performance. This experiment measured thresholds for changes in the ITD of a target sound as a function of the amount of dilution. Thirteen older listeners (mean age = 65; BE-4FA = 4 to 49 dB HL) and five younger listeners (mean age = 25; BE-4FA = -1 to 10 dB HL) participated. The stimulus was a 500-ms burst of speech-shaped noise given a positive or negative ITD, then mixed with an interaurally-uncorrelated (r = 0) 500-ms burst of speech-shaped noise at a target-tomasker ratio (TMR) of +3, 0, -3 or -6 dB (so giving interaural correlations of the mix of 0.67, 0.50, 0.34, or 0.20). The target and masker were gated together so that they were perceived as one. The combined stimulus was presented over headphones and the task was to decide if it was to the left or right of the center of the head. Thresholds were derived from a curve fitted to four-point psychometric functions, assuming that d' was proportional to the ITD of the target. The results showed that as the TMR was reduced -- i.e., the dilution increased -- the ITD threshold increased. This relationship was accurately described by a power function, where ITD threshold was proportional to interaural correlation (or TMR) raised to a power p; p is the rate of change of ITD with dilution. The mean value of p was -1.6 for the older listeners and -1.7 for the younger listeners. These values are similar to Kolarik & Culling's (2009) measurements (-1.6) from a similar experiment using normal-hearing listeners. Within the older group hearing level was found to have no effect on p. The results demonstrate that neither age nor hearing impairment affects the rate of change of ITD with dilution.

192 Lateralization of Narrowband Sounds By Young and Elderly Human Listeners

Paul Allen¹, Emily Clark¹, Marina Dobreva¹, William O'Neill¹, Gary Paige¹

¹Dept. of Neurobiology & Anatomy, U. of Rochester School of Medicine and Dentistry

Sound localization relies on central processing of interaural timing and level difference (ITD & ILD) cues for auditory space. Age-related changes in peripheral encoding of sound and central neural processing could impair sound localization. Dobreva (2010) reported specific impairment in the elderly of low-frequency, ITD-dependent sound localization under free-field conditions. While young and elderly had similar localization abilities for the lowest frequency narrow-band targets, elderly subjects exhibited increased localization errors for bands \geq 1.25kHz, but in the young this only occurred for frequency bands \geq 1.5kHz. Our goal here was to investigate the influence of age on lateralization of narrowband low-frequency sounds under headphones when ILD and ITD are independently manipulated.

Subjects were young (N=6, mean age 23 years) and elderly (N=7, mean age 77 years). ILD and ITD measurements were all made in the presence of a 20dB SL background masker (0.1-4.5kHz), for which there was a significant 13dB threshold difference between young and elderly. Target stimuli were presented binaurally at 30dB SL and were 150ms cosine-gated noise bands (0.5-0.75, 0.75-1, 1-1.25, 1.25-1.5kHz). Audibility thresholds to these sounds were different between age groups, but did not differ by band. Target stimuli were presented in 5Hz trains and subjects responded with a button press whether they heard the sound to the left or right. ILD and ITD thresholds were averages of 3 measurements made using twoalternative forced choice and Bayesian adaptive strategy following training sessions with fixed superthreshold cues.

On a single training session with ILD = 10dB, all subjects responded perfectly. ILD thresholds averaged 1.2dB and did not differ by age or band. On training sessions with ITD = 600μ s, no subjects made errors for the lowest frequency bands, but some never attained perfect performance for the highest band after many attempts. For those who could attain perfect performance, ITD thresholds increased significantly with both Age and Band during the follow-up Bayesian tracking task.

A more difficult 2IFC ITD threshold experiment comparing eccentric ITD with 0 ITD control yielded more errors in training, except for the 500-750Hz band for which all subjects were perfect on the first session. Those who proceeded to threshold measurements had higher thresholds than the 5Hz ITD threshold, and there was an amplification of the increase in threshold with aging and frequency band. These results demonstrate age- and frequency-dependent deterioration of auditory spatial processing, and suggest robust age-related degradation in the ability to utilize ITD cues for sound localization.

Acknowledgements: This study was supported by NIH grants R01-AG16319, P30-DC05409, and P30-EY01319.

193 Natural Head Orientation in Listeners with Audiometric Asymmetry

W. Owen Brimijoin¹, David McShefferty¹, Michael Akeroyd¹

¹MRC Institute of Hearing Research

Attempting to understand speech in a noisy background is one of the most common and one of the most difficult tasks for a listener; hearing impairment exacerbates this difficulty and can result in a listener avoiding social environments entirely. Head movements are a means by which a listener might increase the audibility of a signal in noise, but it is not known whether listeners use orientation to maximize their comprehension. To address this question, we tracked the head movements of 36 listeners with varving degrees of hearing loss and audiometric asymmetry engaged in a speech reception threshold task. We found that given a target sentence spatially-segregated from a masking background noise, listeners with better left ears tended to orient approximately 60 degrees to the right of the target, and listeners with better right ears oriented 60 degrees to the left of the target. The same overall pattern of orientation was found for five different target-masker separations $(\pm 180, -90, +90, -30, \text{ and } +30 \text{ degrees})$. When compared to manneguin measurements of signal level and signal-to-noise-ratio (SNR) for these stimulus configurations, these findings suggest that the listeners were attempting to maximize the level of the target sentence in their better ear, irrespective of the position of the background noise. Such behaviour is not ideal from the perspective of maximizing SNR, often resulting in poor speech intelligibility due to loud background sounds at the better ear. Optimizing SNR, however, would require the listener to take into account the position of both the target and the background noise, and in some cases would require the listener to face away from the target sound. The strategy of maximizing target level may therefore be a behavioural consequence of attempting to see the target.

194 Development of Cartilage Conduction Hearing Aid -Loudness Given by Cartilage Conduction Transducer

Ryota Shimokura¹, Yuya Takaki¹, Tadashi Nishimura¹, Hiroshi Hosoi¹

¹Nara Medical University

Our research group is developing new hearing aid using the ear cartilage conduction. This study has an origin that professor Hiroshi Hosoi (Nara Medical University) found out the transmission of sound when the transducer fit on the ear tragus in 2004. At the present day, we made the test model of the hearing aid and are examining the performance. The cartilage conduction hearing aid is composed of a main unit, transducer and fitting part. The ring-shaped fitting part attached to the cartilage piezoelectric transducer is put in the entrance of the external ear canal. It provides the vibration to the ear cartilage and the sound for the ear canal at the same time, so that the insertion gain of hearing aid may be high. The purpose of this study is to examine the perceived loudness when the cartilage conduction hearing aid is used. Before the loudness measurement, the vibration at the ear tragus and sound in the ear canal were examined wearing the cartilage conduction transducer. The vibration and sound were measured by a subminiature charge accelerometers (Type 4374, B&K) and a probe microphone (Type 4182, B&K), respectively. The signals were pure tones from 125 Hz to 16 kHz stepping a 1/12 octave. As results, the property of output vibration at the tragus had low-pass filtered shape with the cutoff frequency of 1 kHz.. And the property of the sound in the ear canal had bandpass filtered shape with the spectral peak around 2.5 kHz.

The perceived loudness was determined by a method of adjustment. Putting the cartilage conduction transducer or ear phone (EarTone 3A, E-A-R) in the left or right ear, subjects adjusted the sound pressure level of the air conduction signal from the right ear in order to match the loudness of the cartilage conduction signal from the left ear. The signals were pure tones from 250 Hz to 8 kHz stepping 1/3 octave. The loudness measurements were curried out in the two conditions that the ear canal of the left ear was opened and closed by a earplug. In the condition of ear canal closed, the earplug did not touch the cartilage conduction transducer. The results show that the loudness curve in the condition of ear canal opened met the property of sound in the ear canal. On the other hand, the loudness curve in the condition of ear canal closed met the property of vibration at the tragus.

195 Speech-Based Self Assessment of Hearing for Mobile Phones

Junil Sohn¹, Dongwook Kim¹, Hongsig Kim¹, Kyungwon Lee², Junghak Lee²

¹Samsung Advanced Institute of Technology, ²Hallym University of Graduate Studies

A lot of people have mobile phones and needs for better sound quality in mobile phones has increased especially in various noisy environments. The improved sound quality gives elderly people great benefit like the enhanced speech intelligibility. For enhancing speech intelligibility, self assessment of user's hearing loss is a very essential process, but it is difficult that the traditional test with high fidelity like using various pure tones is applied in mobile phones. Because users have to spend a long time to respond to stimuli with various frequencies and amplitudes repetition, mobile phone is not good system for the hearing test with high fidelity, and users do not have knowledge of audiology.

In this study, we proposed new self assessment of hearing loss that uses a few phonemes instead of pure tones. It seems to be reasonable that phonemes are used as test sounds, because they have more information than pure tones with respect to spectral energy distribution as well as formant.

We carried out three stages of experiments to show that the proposed self assessment of hearing loss is suitable for the screening test. In the first experiment, we used 56 adult ears. Phoneme-based hearing thresholds were obtained using PCs, audiometers and headphones in soundproof rooms. The average difference was less than 10dB when compared with the pure tone-based hearing thresholds. 65 ears were participated in the second experiment using mobile phones and earphones. The phoneme-based hearing thresholds showed that the average difference was 3.29dB and sensitivity, specificity, positive predictive value and negative predictive value were greater than 92% at the criterion level of 35 dB HL. The averages of test time for the first and second ears were 34 seconds and 27seconds, respectively. In the last stage of experiments, we compensated hearing loss of 5 ears based on the phoneme-based hearing thresholds and could know that speech recognition thresholds were improved a few dB.

196 Training Children with ADHD to Become Less Impulsive in a Central Masking Threshold Task

Lincoln Gray¹, Brooke Miller², Steven Evans³ ¹James Madison University, ²Randolph Ear, Nose & Throat Associates, ³Ohio University

Impulsivity and distractibility are important symptoms of attention-deficit/hyperactivity disorder (ADHD). In this study, impulsivity is operationally measured using falsealarm rates in a central-masking task, where there is always a distracting noise in one ear and sometimes a soft tone in the other ear. Participants indicated whether the tone was present and received immediate feedback. The intensity of the masked tone was adaptively varied to track threshold. Seven school-aged children with ADHD (ages 10-18) and four adult controls were trained on this task for 900 trials per day over four consecutive days (3600 total trials). Results reveal significant negative linear and positive guadratic trends in false alarm rates, indicating that impulsivity decreased and approached asymptote. Some generalization of training was noted to a different (informational masking) task with an even more distracting background. In conclusion, children with ADHD can be trained to become less impulsive in a non-sensory masking task.

197 Developing a Game for Auditory Training

Daniel E. Shub¹

¹NIHR National Biomedical Research Unit in Hearing, School of Psychology, University of Nottingham

Auditory training based interventions have been successfully used for treating hearing impairment. To maximize patient benefit, multiple hours of training over many months will likely be needed. In order to sustain patient interest over the required time course, usability factors (e.g., interaction, immersion, and engagement) must be paramount in the design of the intervention. Here, the design process is described. The initial design specification was for a causal "video" game to train digit identification. In order to facilitate development, the suitability of existing free and open source games was examined. Based on this examination, the design specification was revised to include training for any closedset speech identification task. Additionally, the design specification was modified to include control over both (1) the stimulus, target speech and potentially masker, waveforms and (2) the ordering in which the stimuli are presented. Notably, the design specification does not require the "response" of the player to be known. As an initial proof of concept, the game Frozen Bubble (http://www.frozen-bubble.org) was chosen as a starting platform. The original game has been actively developed since 2001 and therefore the design goal was to determine the minimal set of modifications required to transform the existing game into a game suitable for training closed-set speech identification. The game was modified so that key information was presented acoustically instead of visually. In accordance with the goal of minimal changes, what the players were allowed to do with the key information was left unmodified. This seemingly minor change to the presentation modality caused a number of additional knock-on effects even though the initial game was chosen based on its apparent suitability for being converted to an auditory training game. As will be discussed, these additional knock-on effects are likely general to the process of converting a conventional game into an auditory training game. [Supported by the NIHR]

198 Modeling Spectral-Ripple Discrimination by Cochlear Implant Users

Gary Jones¹, Ward Drennan¹, Jay Rubinstein¹

¹University of Washington

Cochlear implant (CI) users can achieve remarkable success in understanding speech, but there is great variability in outcomes that is only partially accounted for by age, diagnosis and duration of deafness. Poor understanding of the factors that contribute to individual performance is a critical limitation affecting CI development. A promising path to improved results is the use of psychophysical tests to predict which sound processing strategies offer the best potential outcomes. In particular, the spectral-ripple discrimination test offers a time-efficient, nonlinguistic measure that is correlated with perception of both speech and music by CI users. What makes this test time-efficient, and thus clinically relevant, is that it is a "one-point" measure: only the ripple density parameter is varied. However, there is controversy within the CI field about what this one-point test actually measures.

The current work examines the relationship between thresholds in the one-point spectral ripple test, in which stimuli are presented acoustically, and interaction indices measured under the controlled conditions afforded by a research processor. The resulting matrix of interaction indices, measured at all electrodes along the implant array and at multiple electrode separations, also forms a core component of a phenomenological model of spectral-ripple discrimination. Preliminary results are as follows: 1) within individual subjects there can be large variations in the interaction index at each electrode separation, 2) interaction indices generally decrease with increasing electrode separation, 3) ripple discrimination thresholds increase with decreasing mean interaction index at electrode separations of 1 to 5 electrodes, and 4) trends in ripple thresholds predicted by the model are consistent with trends in the psychophysical data.

[Research supported by NIH-NIDCD Grants F32 DC011431 and R01 DC007525, the Advanced Bionics Corporation and NIH-NIDCD Grants P30 DC04661 and L30 DC008490.]

199 Maximizing the Spectral and Temporal Benefits of Fidelity120 and HiResolution Strategies for Cochlear Implants

Jong Ho Won¹, Kaibao Nie¹, Ward Drennan¹, Elyse Jameyson¹, Jay Rubinstein¹

¹VM Bloedel Hearing Research Center

Drennan et al. (2010) showed that Fidelity120 processing strategy provides better spectral sensitivity but with relatively poor temporal resolution, while HiResolution processing strategy can deliver more detailed temporal information for Advanced Bionics cochlear implant users. The goal of this study was to explore a new sound processing strategy intended to maximize the spectral benefit of Fidelity120 and the temporal benefit of HiResolution to improve both aspects of hearing. Using acoustic simulations of Fidelity120 and HiResolution strategies, two different dual-processing strategies were created by combining Fidelity120 in the low frequency channels and HiResolution in the high frequency channels (FH), or vice versa (HF). To evaluate the performance of the combined processing strategies, four measures were conducted in eight normal-hearing listeners: spectral-ripple discrimination, Schroeder-phase discrimination, temporal modulation detection, and speech perception in noise. Compared to Fidelity120, the dual-FH processing provided an improvement in performance for Schroeder-phase discrimination at 200-Hz and temporal modulation detection at 200-Hz with the cost of a slightly decreased performance for spectral-ripple discrimination relative to Fidelity120. Spectral-ripple discrimination was better with the FH processing than with HiResolution. No benefit was observed for speech perception in noise. Optimum combination of Fidelity120 and HiResolution should be explored in an effort to improve speech perception.

[Supported by NIDCD R01-DC007525, P30-DC04661, L30-DC008490, and F31-DC009755 and an educational fellowship from Advanced Bionics Corporation.]

200 Pitch Contour Identification with Combined Place and Temporal Pitch Cues

Xin Luo¹, David Landsberger², Monica Padilla² ¹*Purdue University,* ²*House Ear Institute*

Current cochlear implants (CIs) can be used to encode pitch with either place or temporal cues. Multidimensional scaling analysis on dissimilarity ratings of combined place and rate stimuli, as well as discrimination of such stimuli, have suggested that place and temporal pitch might be perceived in independent dimensions. This study investigated the integration of place and temporal pitch cues in a pitch contour identification (PCI) task. Adult CI users were tested on an apical and a medial electrode pair at the most comfortable level. Falling and rising pitch contours were first created by continuously steering current between adjacent electrodes or by changing amplitude modulation (AM) frequency over time. The percentages of rising-contour responses with various amounts of current steering or AM frequency change were recorded. The resulting psychometric functions resembled a sigmoid function, suggesting that both current steering and temporal AM were suitable for encoding pitch contours. The amounts of current steering that resulted in 76% correct PCI were found and added to stimuli with various amounts of AM frequency change. Similarly, the amounts of AM frequency change that corresponded to d' of 1 were found and added to stimuli with various amounts of current steering. It was found that the slope of psychometric function was significantly steeper (i.e., PCI was significantly better) with consistent place and temporal pitch cues than with inconsistent cues. Psychometric functions with consistent or inconsistent pitch cues departed from each other mostly when the combined place and temporal pitch cues were similarly discriminable in isolation. These results suggest that CI users are able to integrate place and temporal pitch cues in the PCI task, in which they are asked to make a single-dimensional pitch judgment. Current steering and temporal AM should be optimally combined to better transmit dynamic pitch information to CI users.

201 Voice Gender Discrimination Provides a Measure of More Than Pitch-Related Perception in Cochlear Implant Users

Tianhao Li¹, Qian-Jie Fu¹ ¹House Ear Institute

Normal-hearing (NH) listeners can almost perfectly recognize voice gender of natural speech and can use both temporal cues and spectral cues in voice gender discrimination (VGD). However, due to limited spectral and temporal resolution provided by cochlear implants (CI), VGD performance of CI users is largely affected by the inter-gender fundamental frequency and may be more susceptible to available spectral and temporal cues in the speech stimuli. Therefore, VGD performance of CI users tested with different talker sets and speech stimuli with different spectral/temporal cues may be useful for assessing individual CI users' performance, not only in pitch-related perception, but also in spectral and temporal processing. Furthermore, previous studies have shown the correlations between speech perception in quiet and spectral/temporal processing, and between speech perception in noise and pitch perception in CI users. If VGD can be a good indicator of CI users' pitch-related perception, spectral and temporal processing ability, VGD may also correlate with speech perception for CI users. In the present study, VGD by eight CI users was measured using several different stimulus sets, and was compared with phoneme recognition in quiet and noise backgrounds. The results showed that 1) VGD and speech recognition performance varied among individual CI users, 2) mean VGD performance differed for different stimulus sets, and 3) individual VGD performance was significantly correlated with speech recognition performance under certain conditions. Overall, the results suggest that VGD

measured with selected stimulus sets might be useful for quantifying pitch-related perception, spectral and temporal processing, and speech recognition by individual CI users.

202 An Evaluation of a Sound Processing Strategy for Cochlear Implants Inspired by Wavelet-Based Analysis

Bomjun J Kwon¹, Trevor Perry¹, Cassie Wilhelm¹ ¹Ohio State University

In typical cochlear implant (CI) systems used in clinical applications, electrical stimulation is delivered to neural populations by modulated pulse trains at a fixed stimulation rate. While both amplitude envelope and fine structure of the waveform must be available for speech understanding, the latter is largely inaccessible in CI. While stimulation at a higher pulse rate may increase the accessibility of fine structure, clinical trials of CI fitting at high stimulation rates, to date, have not demonstrated a clear benefit. The following factors may have attributed to the previous results. First, for FFT-based algorithms including ACE processing in some Nucleus systems, the temporal window for spectral analysis is typically unchanged; therefore, temporal resolution in high stimulation rates is in fact not as good as often presumed. Second, for filterbank-based algorithms in other systems, spectral resolution may have been compromised at the expense of better temporal resolution, and overly high stimulation rates on low-frequency channels may have compromised modulation sensitivity (Galvin & Fu, Hear Res. 2009).

Thus, in the present study, a new strategy was developed and implemented in the Nucleus system using higher stimulation rates and shorter temporal windows for spectral analysis of high frequency bands and vice versa for low frequency bands, with a rationale similar to that of a wavelet-based strategy (Gopalakrishna et al., IEEE Trans Biomed Eng, 2010). A range of stimulation rates were used, from about 2000 pulses-per-sec (pps) for mid-to-high frequencies to 125 pps for the lowest frequency. Results of word recognition measured in 6 subjects to date in an acute laboratory setting show a modest but clear improvement in 4 subjects, as compared to their everyday map. It appears that different priorities for temporal and spectral resolution in high and low frequencies may improve CI speech-processing strategies [study supported by NIH/NIDCD R03DC009061].

203 Single- And Multi-Channel Modulation Detection by Cochlear Implant Users

John Galvin¹, Qian-jie Fu^{1,2}

¹*House Ear Institute,* ²*University of Southern California* Previous studies (Galvin and Fu, 2005, 2009; Pfingst et al., 2007) have shown that for a fixed loudness level, cochlear implant (CI) users' single-channel modulation detection thresholds (MDTs) are poorer with high carrier stimulation rates. Recently, McKay and Henshall (2010) suggested that MDTs may depend on the absolute reference current level (rather than perceptual level), and that differences in MDTs across carrier rates observed in previous studies could be explained by McKay et al.'s (2003) loudness summation model. In that model, loudness is not sensitive to the distribution of pulses within the cochlea (i.e., within or across channels). If so, for a fixed number of pulses (and by extension, a fixed loudness), MDTs should be similar for single- and multi-channel MDTs. In this study, single- and 4-channel MDTs (10 Hz modulation frequency) were measured in six CI users. For single-channel stimuli, the stimulation rate was 500 or 2000 pulses per second (pps); for 4-channel stimuli, the stimulation rate was 500 pps/electrode. Within the 4-channel stimulus, all channels were equally loud. For a fixed loudness, single-channel MDTs were lower with the 500 pps rate than with 2000 pps rate: MDTs were similar between the single-channel 2000 pps and the 4-channel stimuli. For a fixed amplitude, MDTs were similar for the 4-channel stimuli and the 500 pps and 2000 pps single-channel stimuli, despite difference in loudness among the stimuli. Individual subjects' 4-channel MDTs were differently affected by the modulation sensitivity of the component channels, sometimes corresponding to the best channel, to the worst channel, and or to the average MDT across channels. The results suggest that adding pulses (whether within or across channels) increased loudness but not modulation sensitivity, in agreement with McKay and Henshall's (2010) prediction. However, CI users' multi-channel modulation detection may be influenced by the modulation sensitivity on individual channels.

204 Cochlear-Implant Gap Detection in Auditory Cortex of Awake Guinea Pigs Alana Kirby^{1,2}, John Middlebrooks¹

¹University of California at Irvine, ²University of Michigan The accurate transmission of temporal features of sound is necessary for cochlear implant listeners to understand speech. Gap detection thresholds reflect basic temporal sensitivity for both cochlear-implant listeners and normal hearing listeners. We measured detection thresholds and within-channel gap-detection thresholds in the primary auditory cortices of awake, passively-listening guinea pigs. We made extracellular recordings of multi-unit responses while varying electric pulse-rate (254 and 4069 pps) and pre-gap duration (196.6 and 23.6 ms) of electric pulse-train stimuli presented through a scala-tympani banded electrode array (Cochlear Americas).

Responses comprised combinations of multiple response types, including onset, offset, and tonic responses. The strength of each response component varied with stimulus level, duration, and pulse rate. Offset and tonic responses were driven better by long stimulus durations and lower pulse rates, consistent with observations of adaptation to high-rate pulse trains in auditory nerve fibers (Zhang et al., JARO 2007). Supra-threshold gap durations elicited onset responses to the start of the post-gap pulse train or offset responses were often elicited by shorter gaps than were onset responses. Gap detection thresholds derived from onset responses decreased monotonically with increasing stimulus current level while gap-detection thresholds derived from offset responses did not always display this behavior, suggesting a population code. Gap detection thresholds were shorter for longer pre-gap durations.

The current results show trends similar to those observed in anesthetized animals, but several key details are different, in part because offset and tonic responses were not observed under anesthesia. These results may be used to guide the design of cochlear implant processing strategies.

Support provided by NIH-NIDCD R01 DC04312

205 Threshold for Double Pulses with Different Amplitude Relations in Cochlear Implants

Sonja Karg¹, Christina Lackner¹, **Werner Hemmert¹** ¹Technische Universität München, IMETUM, Bio-Inspired Information Processing

In actual cochlear implant coding strategies pulsatile stimulation is applied by interleaved sampling. In order to code as much temporal information as possible, latest CI strategies aim to increase stimulation rates to encode more temporal information. High rate and interleaved sampling result in an even higher rate over all channels.

In human subjects we showed that temporal interaction due to sub-threshold stimulation lasts up to an inter-pulse interval (IPI) of 640 μ s. Now we studied the effect of amplitude relation in a double pulse (pre-, and probe pulse) with pre-pulse cathodic, probe pulse anodic leading phase at threshold. Therefore the amplitude relation was varied between 0 (only probe pulse) and 5 (5 times higher pre-pulse amplitude) at two IPI values: 20 and 80 μ s. We tested 5 subjects (7 ears) age 52 ± 21 (mean ± std) who had at least 3 years experience with MED-EL PulsarCI100 implants. We stimulated directly via the research interface RIB II.

The measurements revealed that the effect of threshold reduction was less for small pre-pulse stimuli than for large ones in relation to their absolute amplitude. The addition of the double pulse amplitudes was not linear. At IPI 20µs we found a maximal threshold reduction of $44\% \pm 2\%$, at IPI 80µs 39% $\pm 2\%$. The total charge at threshold for the double pulse was always higher than for a single biphasic pulse. Symmetric double pulses required the highest charge: 1.43 ± 0.06 times at IPI 20µs and 1.62 ± 0.05 times at IPI 80µs compared with a single biphasic pulse. Our experiments elucidate nonlinearities involved in the electrical excitation of the auditory nerve. In the future, our measurements will allow us to better predict nonlinear

206 Effect of Ossicular Chain Disarticulation on Round Window Stimulation with an Active Middle Ear Implant: A Temporal Bone and Animal Study

Kanthaiah Koka¹, Stephane Tringali^{2,3}, Arnaud Deveze^{4,5}, Herman A. Jenkins⁶, Daniel J. Tollin^{1,6}

¹Dept of Physiology and Biophysics, University of Colorado Denver, Aurora, CO, USA, ²Neurscien Sensorielles, Comportement, Cognition, Université de Lyon, Université Claude Bernard,Lyon, ³Dept of Otology and Otoneurosurg, Hospices Civils de Lyon, CentreHospitalier Lyon Sud, Pierre-Bénite, ⁴5Department of Otolaryngology, University Hospital Nord, Assistance Publique Hôpitaux de Marseille, ⁵Laborato Otologie, Neurotologie et Microendoscopie, University La Méditerranée, Marseille, France, ⁶Dept of Otolaryngology, University of Colorado Denver, Aurora, CO, USA

Mechanical stimulation of the round window (RW) membrane with active middle ear implants (AMEIs) has shown some functional benefit in clinical reports in patients with mixed hearing loss. In some of these cases, the ossicular chain was disrupted and the AMEI directly fitted onto the RW membrane. The aim of this study is to access the effect on AMEI performance of ossicular chain disarticulation during RW stimulation in both cadaveric temporal bones and in a chinchilla model.

Mechanical (stapes velocity) responses to sinusoidal stimuli were measured by laser Doppler vibrometry in five temporal bones (TB) with AMEI stimulation (Otologics MET, Boulder CO USA) of the RW before and after disarticulation of the ossicular chain. We also studied AMEI application on the RW in four chinchillas by simultaneously measuring both cochlear microphonic (CM) waveforms and stapes velocities. In the TB studies. RW membrane stimulation with the AMEI evoked an equivalent ear canal sound pressure level (LEmax in units of dB SPL) across frequency (0.25-8 kHz) of ~100 dB (95% confidence interval, ±3dB) for intact ossicles and a significantly higher (p < 0.0001) 105 dB (±3 dB) after disarticulation. There were no significant (p = 0.48)differences in the measured impedance and inductance of the AMEI between the intact and disarticulated conditions indicating that the mechanical loading of the AMEI on the RW was the same in both cases. In the animal studies, RW stimulation evoked a LEmax of ~70 dB (±5 dB) and a significantly higher (p = 0.002) 79 dB (±4 dB) with and without an intact ossicular chain, respectively. In general, AMEI stimulation of the RW produced significantly higher (~5-8 dB) LEmax after disarticulation of the ossicular chain in both the models tested. Support: Otologics LLC Education Grant (DJT and HAJ)

207 Active Middle Ear Implant Stimulation of the Round Window: Physiologic Assessment of Factors Influencing Implant Coupling to the Round Window Membrane

J. Eric Lupo¹, Kanthaiah Koka², Blake J. Hyde³, Herman A. Jenkins¹, Daniel J. Tollin^{1,2}

¹Department of Otolaryngology, University of Colorado Denver, ²Department of Physiology and Biophysics, University of Colorado Denver, ³School of Medicine, University of Colorado Denver

Active middle ear implant (AMEI) stimulation of the round window (RW) is a nascent technique to deliver vibrational energy to the cochlea in cases where ossicular delivery through the oval window is not possible (i.e., chronic ear disease, advanced otosclerosis, etc). Clinically, AMEIs have been implanted on the RW in human subjects with successful outcomes; however, the outcomes have been variable. Potential sources of outcome variability include

aspects of temporal interaction.

both patient-dependent variables (etiology of hearing loss, anatomy etc.) and AMEI loading-dependent variables. Here we explored three RW loading variables and the effects of varying these parameters on the physiologic responses to RW stimulation generated by an AMEI (Otologics Gen 2 MET, Boulder, CO USA). The three RW loading parameters under investigation included: 1) static loading force applied to the RW; 2) angle of approach to the RW; 3) interposed connective tissue (i.e., fascia). Cochlear microphonic (CM) and stapes velocity (H_{FV}) were measured in an animal model (Chinchilla, n=6 ears) in response to acoustic and AMEI generated tone pip stimuli (0.25-8kHz) across a range of intensities (-20-80 dB SPL and 0.01-1000 mV). The three loading parameters were studied in succession holding the other parameters constant. Measured variability in application of the AMEI to the RW itself was in the range of 2.5 dB and 5.0 dB for H_{FV} and CM thresholds, respectively. Neither loading pressure applied to the RW (51-574 dynes) nor the angle of approach (±30° with respect to coronal plane) produced significant effects on CM or H_{FV} thresholds. However, a significant improvement in CM and H_{EV} thresholds was observed for interposed connective tissue regardless of connective tissue type. Results support the surgical practice of interposed fascia between AMEI and RW and negate loading pressure and loading angle as important intraoperative considerations. [Support: AAO-HNSF CORE Resident Research Grant, Otologics Education Grant]

208 Improved Nitinol Shape-Memory Prosthesis for CO2 Laser Stapedotomy Glenn Knox¹

¹University of Florida

Various iterations of the Nitinol shape-memory prosthesis for stapedotomy have been sucessfully used around the world for the past ten years. However, concerns have persisted regarding nickel allergy as it relates to nitinol implants, which are made of a nickel-titanium alloy. In addition, it is theorized that thermal injury to the incus can occur during heating of the prosthesis, leading to delayed incus necrosis. Thus, an improved shape-memory stapes prosthesis has been developed. The shaft of the prosthesis is gold plated. This extends up to the crook area where there is placed an Au laser target. The remainder of the prosthesis is coated in polytef or other plastic insulator. The polytef and Au coating prevents allergic reactions to nickel, and the polytef's insulating properties prevents thermal injury to the incus. In vitro testing with prototypes in human temporal bones is described.

209 Hearing Results from Cochlear Implantation on Common Cavity Malformed Cochleae: Long Term Follow-Up Results

Hyun Woo Lim¹, Joong Ho Ahn¹, Woo Seok Kang¹, Jong Woo Chung¹, Kwang-Sun Lee¹

¹Asan Medical Center, University of Ulsan College of Medicine

Objective: To analyze hearing improvement from cochlear implantation performed on common cavity malformed cochleae.

Study design: Retrospective chart review Setting: Tertiary referral center

Patients and Methods: Total 11 patients (5 male and 6 female) were enrolled in this study. The mean age of the patients was 4.5 ± 2.8 years when they received cochlear implantation. During the insertion of electrodes, we used C-arm fluoroscopy to avoid intrameatal placement. We evaluated hearing improvement every 6 months and mean follow-up period is 49.6 \pm 11.4 months (from 36 to 60 months).

Results: During the operation, there were only 4 patients with fully inserted electrodes. There were cerebro-spinal fluid gushed out on 2 patients during the cochleostomy and there was no serious postoperative complications in all patients. From follow-up hearing evaluation results, the ability of hearing increased along with the age (the final average MAIS score was 90.3 ± 18 , CAP score was 4.9 ± 1.6 , and SIR score was 3.1 ± 0.9). One patient had to receive re-cochlear implantation due to mis-location in IAC due to migration and poor hearing outcome.

Conclusion: Cochlear implantation in common cavity malformed ear is a safe and therapeutic method for hearing restoration. It is important to control CSF gush-out during the cochleostomy and to prevent from over-insertion of the electrodes beyond cochlear cavity.

210 Insertion Speed of Cochlear Implant Electrode Arrays: Correlation with Electrode Type and Surgeon's Experience

Georgios Kontorinis¹, Timo Stoever^{1,2}, Thomas Lenarz¹, Gerrit Paasche¹

¹Hanover Medical School, ²Johann Wolfgang Goethe-University, Frankfurt am Main

Objectives: Although several studies have examined factors influencing the insertion forces, the impact of the electrode insertion speed still remains unknown. Our objective was to evaluate the effect of the insertion speed on the insertion forces and any clinical significance.

Methods: Cochlear implant electrode insertion speed was measured through videos of 116 human implantations, involving different surgeons and electrode types. The average insertion speed was calculated through the insertion length and time needed for the complete advance of the every time examined electrode. The results of previously performed human electrode insertion force measurements while applying different insertion speeds were correlated with the collected data.

Results: The previously performed force measurements had shown that progressive increase in insertion speed

from 10 mm/min to 200 mm/min resulted in a significant, proportional increase in the average insertion forces from 0.09 N to 0.185 N. The average insertion speed used in the theaters during human cochlear implantations was 96.5 mm/min. The lowest insertion speed (<60 mm/min) was documented when hearing preserving electrode arrays were implanted. In general, the insertion speed was dependent on the electrode type and the surgeons' experience. In particular, surgeons with less experience performed faster insertions. As the surgeons obtained more experience they improved their technique, using lower speeds, whereas later on, they applied intermediate but still slow electrode insertions.

Conclusions: As high insertion speeds cause significant increases in the insertion forces, low and stable speeds during the insertion are recommended. Insertion speed close to the average value used in the theaters should be applied in experimental models to approximate human implantation conditions.

211 Estimation of the Optimum Insertion Depth for the HiFocus 1J Electrode Array Based on High Resolution CT Images

Olga Stakhovskaya¹, Larry Lustig¹, Patricia Leake¹ ¹University of CA San Francisco, Department of Otolaryngology

Estimation of the optimum insertion depth of the electrode array prior to surgery can be an important tool in modern cochlear implantation. The depth of insertion may vary substantially in different individuals due to differences in cochlear size. Measurements of anatomical dimensions of the cochlea obtained from computed tomography (CT) images can provide detailed information about the insertion depth required for the electrode to cover a specific frequency range. Control over the desired insertion depth is also an important factor in preservation of residual hearing. Avoiding undesirable over-insertions can also reduce the extent of trauma caused during implantation.

Human temporal bones were harvested within 24 hours post-mortem and fixed with formalin. "Pre-operative" micro CT images were obtained using an isotropic nominal resolution of 18 μ m. Measurements of the basal turn diameters and outer/inner wall length were made directly on the CT images. The insertion depth required to reach 360° of rotation was estimated based on these measerements and specimens were implanted with HiFocus 1j array.

Measurements of cochlear dimensions obtained in CT images allowed prediction of the insertion depth to the desired point in two out of three specimens analyzed to date with an accuracy of 1 mm of the array length. The most accurate predictions were based on the direct measurements of the distances from the round window to a given point along the outer wall of the cochlea after adjustment for electrode thickness using a "wrapping factor" determined in other radiological studies by Dr. Charles Finley at the University of NC (personal communication). During implantation of the third specimen, resistance was noted prior to achieving the desired insertion depth. The anatomical dimensions of this cochlea are being examined to define additional specific metrics in the CT images, which could have predicted the difficulties encountered during implantation.

Research supported by Deafness Research Foundation, NIH-NIDCD Contract #HHS-N-263-2007-00054-C and the Epstein Endowment Fund. Electrode arrays were provided by Advinced Bionics.

212 Development of Hydrodynamic Injection Method for Cochlear Implantation in Gerbil

Vanessa Cervantes¹, Dominic Pisano², Elizabeth Olson¹ ¹Columbia University, ²Tufts University

Current cochlear implantation research is focused on the preservation of residual hearing through reducing surgically-induced trauma and inflammation, as well as promoting cell growth. We are developing a new surgical technique for cochlear implantation in gerbils (Meriones unguiculatus) that uses a hydrodynamic fluid-assisted injection method to deliver a silicone implant to the scala tympani (ST). The goals of this technique are to (1) achieve deep electrode insertions, (2) induce no trauma to intracochlear structures, and (3) preserve residual hearing. This technique could provide an alternate surgical technique for human cochlear implantation, and also be a useful animal model for implant-mediated drug delivery. METHODS: Silicone implants were injected into cochleae by loading them into a syringe filled with ~1% hyaluronic acid (HA) and injecting both the implant and HA into the ST via the round window. A scala vestibuli cochleostomy was made to serve as an exit port for the displaced perilymph and injected HA. Trauma was determined by histological examination, and hearing status in in-vivo implantations was determined through compound action potential measurements. RESULTS: In postmortem studies, implantations of up to 2 full turns were achieved with no apparent trauma to intracochlear structures. In the small number of in-vivo studies performed to date, 1.5-turn insertions were achieved. In the in-vivo studies hearing (as evaluated with compound action poetential) could be preserved through several steps of the procedure. However, the full procedure caused severe hearing loss and we are working to understand and improve this outcome.

213 Across-Site Patterns of Modulation Detection: Relation to Speech Recognition

Soha Garadat¹, Teresa Zwolan¹, Bryan Pfingst¹ ¹Kresge Hearing Research Institute, Department of Otolaryngology, University of Michigan

Electrical stimulation by multichannel cochlear implants (CIs) is tonotopically distributed based on a defined map where spectral and temporal information is allocated to specific stimulation sites. However, it has been shown that CI users do not effectively use all of the available sites and that their performance is widely variable across stimulation sites. It is hypothesized that variables including channel interaction and differences in neural survival might contribute to the variability in temporal acuity reported across sites of stimulation. The current study aimed to

identify differences in patterns of electrically-elicited perceptions across sites of stimulation using measures of temporal modulation detection threshold (MDT) and to determine their importance for speech recognition.

MDTs were surveyed across all available stimulation sites. Subjects were asked to discriminate a modulated signal from unmodulated signals in guiet and in the presence of an interleaved unmodulated masker presented on an adjacent stimulation site. Stimuli were 500 msec trains of symmetric-biphasic pulses presented at a rate of 900 pps using a monopolar electrode configuration (MP1+2). Pulse phase duration was sinusoidally modulated at 10 Hz around mean of 50 usec. Subjects' modulation sensitivity typically decreased when the masker was present. Based on the masked MDTs, two 10-channel processor MAPs contrasting in modulation sensitivity were constructed such that MAP 1 consisted of sites with the best masked MDTs and MAP 2 consisted of sites with the worst masked MDTs. Subjects' speech recognition was compared for the two MAPs. Initial results indicated that sentence recognition was better for the majority of the subjects tested when using MAP 1 while scores on consonants and vowels were less consistent. Findings suggest a possible relation between temporal modulation and speech recognition with multichannel cochlear implants. Further possible relationships will be evaluated.

Supported by NIH-NIDCD grants R01 DC010786 and F32 DC010318-01.

214 Comparative Electrical Stimulation of the Dorsal and Ventral Cochlear Nucleus in Rats

Javan Nation¹, Xuego Zhang¹, Christie Cheng¹, Jinsheng Zhang^{1,2}

¹Department of Otolaryngology, Wayne State University School of Medicine, ²Department of Communication Sciences & Disorders, Wayne State University College of Liberal Arts

Auditory brainstem implants (ABIs) are used to restore hearing by electrical stimulation of the cochlear nucleus (CN). Although speech perception has been achieved with ABIs, the clinical results vary widely across patients. The contributing factors include the physiological condition of the CN following surgical removal of an acoustic neuroma and structures stimulated. Although it has been reported that stimulation of the ventral cochlear nucleus (VCN) or the dorsal cochlear nucleus (DCN) induces hearing, it is unclear how DCN-stimulation-induced hearing compares to VCN stimulation-induced hearing. To answer this question, we chronically implanted microwire electrode arrays in the CN of 5 rats, with 8 channels in the DCN and 8 channels in the VCN. Behavioral evidence of hearing was tested by measuring electrical prepulse inhibition (ePPI) of acoustic startle responses (Zhang and Zhang, 2010). The DCN and VCN were stimulated with all-channel stimulation (25-75uA) in a bipolar mode and single-channel stimulation in a monopolar mode (100-200uA). The results demonstrated that bipolar electrical stimulation of all channels in both the DCN and VCN produced robust ePPI, resulting in electrical hearing. Single-channel electrical stimulation of either the DCN or the VCN in a monopolar mode produced similar behavioral results, compared to allchannel stimulation. In addition more monopolar channels in the DCN than the VCN produced behavioral evidence of hearing. The preliminary results indicate that the DCN stimulation seems to yield hearing that may be comparable to that derived from VCN stimulation. However, it remains to be determined as to how DCN stimulation-induced hearing differs from VCN stimulation-induced hearing. Obtaining such information is important to develop a new generation of ABIs.

215 Influence of Intracochlear Electrical Stimulation on the Neuronal Calcium Related Activity in Central Auditory Structures

Sebastian Jansen¹, Moritz Groeschel^{1,2}, Susanne Mueller³, Patrick Boyle⁴, Arne Ernst², Dietmar Basta^{1,2} ¹*Humboldt University of Berlin,* ²*Dept. of ENT at Unfallkrankenhaus Berlin,* ³*Charité University Medicine Berlin,* ⁴*Advanced Bionics Clinical Research*

Little is known about binaural interactions induced by simultaneous acoustic and electric stimulation of the auditory system in patients with unilateral deafness. The present study therefore aims at investigating the calcium related neuronal activity upon unilateral chronic intracochlear electrical stimulation within the ascending auditory pathway in an animal model.

Normally hearing guinea pigs were single-side deafened by the implantation of a standard HiRes 90k® cochlear implant with a HiFocus1j electrode array. The first 4 electrode contacts were used to stimulate the cochlear nerve fibers within the first turn of the cochlea. Six weeks after surgery, the speech processor (Auria®) was programmed based on tNRI-values and mounted on the back of the animals. The animals of the experimental group were stimulated for 90 days with a stimulation frequency of 275 Hz. Both experimental and control group (implanted but not stimulated) experienced a similar daily acoustic environment (16 hours per day).

After the stimulation, the calcium-dependent activity was observed by manganese-enhanced MRI (MEMRI) to monitor changes in activation of neural tissue. The calcium-dependent neural activity was measured by 7T-MRI scanning 24 hours after injection of a manganese chloride solution. The signal strengths in several auditory structures (DCN, VCN, SOC, IC, MGB and AC) were measured in both groups.

The data of the present study shows that electrical intracochlear stimulation leads to a lower calciumdependent activity in the auditory brain areas of stimulated animals compared to the controls. The higher calciumdependent activity in the control group seems to be a pathological effect of the deprivation which could be prevented or reduced by the electrical stimulation of auditory nerve fibers.

216 Neurotrophic Effects Elicited by Exogenous Brain-Derived Neurotrophic Factor (BDNF) Are Maintained After Several Months of Electrical Stimulation in Cats Deafened as Neonates

Patricia Leake¹, Gary Hradek¹, Alexander Hetherington¹, Olga Stakhovskaya¹, Ben Bonham¹

¹Dept. Otolaryngology-HNS; University of California San Francisco

Postnatal development and survival of cochlear spiral ganglion (SG) neurons likely depend upon both neurotrophic support and neural activity. Our earlier studies in neonatally deafened cats showed that electrical stimulation (ES) only partially prevents SG degeneration after early deafness, and neurotrophic agents may further enhance neural survival. Recently, we studied intracochlear BDNF infusion in this animal model of congenital deafness. Kittens were deafened at birth (neomycin, 60 mg/kg SID, 16-21d) and implanted at ~30 days of age with scala tympani electrodes containing a drug-delivery cannula connected to a mini-osmotic pump. BDNF (94 μ g/ml; 0.25 μ l/hr) or artificial perilymph was infused for 10 weeks.

After BDNF treatment, SG cell somata were slightly larger than normal and ~30% larger than cells in the contralateral cochleae (p<0.001). BDNF also elicited a 25% increase in SG density over the contralateral side, indicating a significant neurotrophic effect (P<0.001) in these developing animals. Further experiments examined whether improved SG survival was maintained when BDNF treatment was terminated and followed by 6-7 months of ES. Results suggested that both significantly improved SG survival and larger cell size were largely maintained after several months of ES, although cell density and area were reduced modestly (14% and 9%, respectively) from values measured immediately after BDNF treatment.

Other findings after combined BDNF and ES included higher density of the myelinated radial nerve fibers in the osseous spiral lamina, sprouting of these fibers into the scala tympani, reduction in EABR thresholds relative to initial thresholds for chronically stimulated channels (but not for the inactivate control channel), and maintenance of the fundamental tonotopic organization of the inferior colliculus (IC). Final EABR thresholds were well-correlated with minimum IC neural thresholds. Interestingly, IC thresholds were correlated with 2-dB activation widths in control subjects, but not in BDNF-treated animals.

Research supported by NIH-NIDCD Contract #HHS-N-263-2007-00054-C. BDNF donated by Amgen Inc, Thousand Oaks, CA.

217 Lysosomal Storage Disease and the Auditory System: A Comparative Examination of Human and Mouse Hearing in Niemann-Pick Disease, Type C (NPC)

Kelly King¹, Chris Zalewski¹, Nicole Yanjanin², Forbes Porter², Carmen Brewer¹

¹National Institute on Deafness and Other Communication Disorders, ²National Institute of Child Health and Human Development

Niemann-Pick disease, type C (NPC) is a rare (1:120,000-150,000) autosomal recessive lysosomal lipidosis resulting in progressive and fatal neurological deterioration. With a central nervous system phenotype similar to Alzheimer's disease, NPC results from biallelic mutations in either NPC1 (18q11) or NPC2 (14q24.3) and there is much about the pathogenesis and natural history of this complex, heterogeneous disorder that is unknown.

Limited literature suggests the auditory system is affected via defects in intracellular transportation of cholesterol in NPC. Auditory pathology has likely been underreported given the difficulty obtaining behavioral data in this neurologically compromised population and the inability of many affected patients to self-report hearing loss. We present auditory data from 55 patients with NPC seen at the NIH between 8/14/2006 and 8/25/2010. Data confirm a prevalent high frequency hearing loss that appears to be progressive, and auditory brainstem response (ABR) abnormalities suggest a profile of auditory neuropathy/dyssynchrony. Large amplitude and prolonged activity, interpreted as cochlear microphonic, was commonly present during the ABR. Data from late-onset cases suggest hearing loss is a premonitory symptom in this disease subcategory.

Disease manifestations in the BALB/c-npc1nih mouse model for NPC are clinically, biochemically, and morphologically comparable with affected humans. Brainstem histopathology localized to the auditory pathway has been documented, but hearing has not been evaluated. We present ABR and otoacoustic emission data detailing a high frequency hearing loss in mutant mice present at postnatal day 20. Similar auditory phenotypes between affected humans and mutant mice should aid in determining site of lesion. Early onset hearing loss in mutant mice may have implications for understanding the role of NPC pathogenesis on the developing auditory system and may serve as a marker for future treatment trials.

218 Development of an Animal Model to Test an Active Noise Cancellation System for Infant Incubators

Zohra Tridane¹, Xun Yu¹, Glenn Nordehn², **Janet Fitzakerley²**

¹University of Minnesota Duluth, ²University of Minnesota Medical School

Medical and technological advancements, including the use of incubators and the development of neonatal intensive care units (NICUs), have significantly improved the survival of premature infants. However, high levels of

noise in the NICU results in numerous adverse health effects, including hearing loss. Since the mammalian auditory system is most vulnerable to noise immediately after the onset of function. development of a device that protects against noise-induced hearing in the NICU loss could significantly improve quality of life, both while neonates are in the NICU, and long term.

The goal of our research is to develop a version of an existing active noise cancellation (ANC) system that can be used to reduce sound levels in NICU incubators. The basic principle of the ANC system is to cancel the unwanted primary noise through the introduction of a destructive anti-noise sound. Experimental results showed a reduction of greater than 15 dB in the primary noise. Ultimately, this transparent actuator could be built into the side of an infant incubator, providing noise protection without adding equipment to the already crowded NICU environment.

It was hypothesized that a frequency translation based on the cochlear frequency/place relationship could be used to convert incubator noise into an appropriate stimulus for ANC testing mice. Neonatal mice were exposed to untranslated incubator noise (IN) or frequency-shifted incubator noise (FSIN) during the critical period, and hearing sensitivity measured following the noise exposure. IN had no effect on acoustic thresholds, but FSIN caused a moderately severe (60-70 dB) high frequency hearing loss in all mice tested. The FSIN stimulus represents an accurate model of neonatal noise-induced hearing loss. Future experiments will use this model to test the ability of the ANC system to protect against hearing loss.

219 Xylene-Induced Auditory Dysfunction Adrian Fuente¹

¹University of Chile

The aim of the research was to determine a possible association between xylene exposure and peripheral and central auditory dysfunction. Thirty xylene-exposed laboratory workers (study group) and 30 gender-and agematched non-exposed subjects (control group) were recruited. Noise dosimetry was conducted during a whole work shift (8 hours) on each subject. Only those subjects exposed to noise levels below 85 dBA TWA were selected. All subjects presented with type A results for tympanometry and no conductive hearing loss. Xylene airborne concentration and methyl hippuric acid (a metabolite of xylene) concentration per gram of creatinine in urine were obtained for each xylene-exposed subject. The test battery comprised of pure-tone audiometry (250-8000 Hz), Transient Evoked Otoacoustic Emissions (TEOAEs), Distortion Product Otoacoustic Emissions (DPOAEs), Auditory Tests of Temporal Resolution (ATTR, Lister & Roberts, 2005), Dichotic Digit test (DD, Fuente & McPherson, 2006), Hearing-in-Noise test (HINT, Nilsson et al., 1994), and Auditory Brainstem Response (ABR). Results showed significant differences in hearing thresholds between groups in the mid and high frequency range (with an adjusted p value according to Bonferroni correction). No significant differences between groups for TEOAEs, DPOAEs, ATTR, and ABR results were found (with Bonferroni correction). Xylene-exposed subjects obtained poorer results for DD and HINT tests. Xyleneexposed subjects exhibited an abnormal left ear disadvantage for the DD test. Findings of the present research provide some evidence on the possible association between xylene exposure and auditory dysfunction, mainly characterized by poorer hearing thresholds, reduced speech discrimination in both quiet and noise, and deficient dichotic listening performance. A possible dysfunction of the upper auditory pathways may be involved as evidenced by DD test results. Further research using auditory cognitive evoked potentials should be conducted.

220 Auditory Evoked Cortical Potentials Do Not Reliably Reflect Hearing Aid Gain

Kelly Tremblay¹, Curtis Billings² ¹University of Washington, ²NCRAR

There is interest in using P1, N1, and P2 peak responses to evaluate experience-related plasticity associated with amplification; however, little is known about hearing aid signal processing on the auditory evoked response. The purpose of this study was to determine the effect of (1) overall hearing aid gain, and (2) signal-to-noise ratio (SNR) on the latency and amplitude of P1, N1, and P2 waves of the cortical auditory evoked potential (CAEP). Evoked potentials and in-the-canal acoustic measures were recorded in nine young normal-hearing adults who were tested in unaided and aided conditions. In the aided condition, a 40 dB signal was delivered to a hearing aid that was programmed to provide four different levels of gain (0, 10, 20, and 30dB). Unaided stimulus levels were matched to aided condition outputs (i.e., 40, 50, 60, and 70 dB) for comparison purposes. When signal levels are defined in terms of output level, corresponding latency and amplitude values of the aided CAEPs did not reliably reflect the stimulus level produced by the hearing aid. Longer latencies and smaller amplitudes for the aided condition indicate that hearing aid signal processing leads to less efficient neural encoding. More specifically, we demonstrate that different noise sources are amplified by the hearing aid, resulting in aided SNRs being smaller than unaided SNRs when absolute signal level is equivalent. These results reinforce the notion that hearing aids modify the signal (e.g., SNR) which in turn impacts the CAEP. For this reason, interpreting CAEP results obtained from people who wear hearing aids should be done with caution.

221 Detecting Recruitment Phenomenon Using Auditory Steady-State Response

Toshinori Kubota¹, Tsukasa Ito¹, Tomoo Watanabe¹, Masaru Aoyagi¹

¹Yamagata University Faculty of Medicine

Detecting a recruitment phenomenon in hearing-impaired patients is very important when adjusting the gain of a hearing aid. A frequency-specific examination for detecting a recruitment phenomenon in infants has not been established. Therefore, the gain of hearing aids cannot be accurately adjusted in hearing-impaired infants. To solve this problem, we attempted to detect the recruitment phenomenon using auditory steady-state response (ASSR), which is an objective measurement that has high frequency specificity.

We examined 2 groups of subjects: 14 normal subjects (mean age, 23.4 years) with thresholds \leq 20 dB HL at a frequency of 1000 Hz, and 11 subjects (mean age, 56.4 years) with unilateral hearing impairment in whom the recruitment phenomenon was detected by the alternate binaural loudness balance test. Their average threshold in worse ear was 47.7 dB HL at 1000 Hz. We used sinusoidally amplitude-modulated tones as stimuli. The carrier frequency was 1000 Hz, and modulation frequencies were 40 Hz in waking subjects and 80 Hz in sleeping subjects. The stimuli were presented in intensity of 70 dB nHL and decreased in intensity by 5 dB steps until 10 dB nHL. One sweep had 512 points (analog-digital conversion rate, 1024 Hz), and 200 sweeps were collected at each intensity. The averaged sweeps were analyzed using fast Fourier transform. We used a Mann-Whitney U test to statistically compare the amplitude of response in the 2 groups.

The correlation between the stimulus intensity and amplitude of response was statistically significant in both the groups. The amplitude of response increased with the stimulus intensity and was statistically higher in the hearing-impaired subjects than in normal subjects at 15, 20, 25, and 35 dB SL in the waking subjects (p < 0.05) and at 20, 25, 30, and 35 dB SL in the sleeping subjects (p < 0.01).

We think that the higher amplitude increase rate in the hearing-impaired subjects than in normal subjects reflects a recruitment phenomenon.

222 Auditory and Cognitive Performance of 6-11 Year Old Children with Mild Hearing Loss

David Moore¹, Oliver Zobay¹, Melanie Ferguson² ¹MRC Institute of Hearing Research, ²National Biomedical Research Unit in Hearing

Mild hearing loss (MHL; 20-40 dB HL) is prevalent, affecting 17% of the adult (18-80 v.o.) and 2.5% of the young adult (18-30 y.o.) UK population in 1986. However, there are limited data on the consequences of MHL for hearing, communication and cognition due to the low attendance rate of affected individuals at audiology and research services, and a lack of population data. As part of a larger survey of hearing in 1621 children aged 6-11 years (Moore et al., Pediatrics, 126, 2010), we identified 152 mainstream school children with hearing loss (HL > 25dB) in at least one ear at 1 or 4 kHz (7 moderate, 1 severe, 9 unilateral). We examined 5 individual and 2 derived measures of temporal and frequency resolution and discrimination, a (VCV) nonsense speech-in-noise measure, and standardised cognitive measures: fluid reasoning (NVIQ), working memory (digit recall), language (nonword repetition) and literacy (word/nonword reading). Severity of hearing loss was age and SES independent. The highest correlations with severity of hearing loss were found for VCV thresholds (r = .35; p<0.001), nonword repetition (r = .36; p<0.001) and nonsense word reading (r = -.26; p = .002). MHL was thus most closely related to nonword coding. Other measures of auditory threshold and cognition correlated significantly (p<.05) but modestly with MHL. Some measures did not correlate, including discrimination, simultaneous frequency masking, frequency resolution, NVIQ, a parental assessment of communication (CCC-2, p = .08), and auditory threshold variability, a measure of attention. As the criteria for MHL became more stringent (# ears, frequencies affected), the proportion with poor (lowest 10%) VCV/cognition increased from 10/10% (normal hearing) to 37/47% (all 4 measures >25 dB HL). The results suggest audibility is the major deficit in MHL, but that other cognitive and auditory processing deficits follow. However, many individuals with MHL perform normally.

223 Intratympanic Free Radical Scavenger (Edaravone) as Rescue Therapy in Sudden Sensorineural Hearing Loss

Kazuma Sugahara¹, Makoto Hashimoto¹, Takefumi Mikuriya¹, Hiroaki Shimogori¹, Hiroshi Yamashita¹

¹Yamaguchi University Graduate School of Medicine The administaration of steroids are the most common choice and considered the best treatment option for the teraphy in sudden sensorineural hearing loss. However, in many case, the improvement of hearing are not sufficient. Edaravone is a free radical scavenger that is clinically used in Japan. This study was designed to describe the results of intratympanic edaravone in sudden sensorineural hearing loss after failure of prednisolone therapy.

Seven patients with idiopathic sudden sensorineural hearing loss were treated with intratympanic edaravone after failing in the treatment with systemic steroids. Pretreatment and post-treatment audiometric evaluations including pure tone average (PTA) were analyzed. Seven patients who were treated with 2 courses of systemic steroids were used as control.

The hearing threshold of 3 frequencies (125, 250 and 500 Hz) at the end of treatment was lower in the patients treated with intratympanic edaravone than in the patients treated with 2 courses of systemic steroids.

The results suggest that the intratympanic edaravone can be the candidate of the rescue therapy in patients suffered from sudden sensorineural hearing loss.

224 Computer-Based Auditory Training to Improve Speech Recognition in Noise by Children with Hearing Impairment

Jessica Sullivan¹, Linda Thibodeau², Peter Assmann³ ¹University of Washington, ²Univ. of Texas at Dallas, ³UT Dallas

While the improved hearing-assistive technology has made a considerable impact on the access to auditory input and language development, children with hearing loss still have great difficulty with speech recognition in noise. The purpose of this study is to assess how short-term training (7 hours) in interrupted and continuous noise can benefit speech recognition for children with hearing impairment. The experimental groups participated in computer-based auditory training that adapted based on performance in either interrupted or continuous noise. The control group participated in computer-based analytical thinking and memory task. All participants were administered the speech recognition test in interrupted and continuous noise: pre-training, post-training and 3-months post training. Participants in the auditory training in interrupted noise group demonstrated significant improvements. These data suggest that auditory training in interrupted noise may lead to improvements in speech recognition in noise abilities of children with hearing impairment.

225 An Objective Test to Detect Tinnitus in Human: Preliminary Study

Myung-Whan Suh¹, Kun Woo Kim¹, II-Yong Park², Seung-Ha Oh^{3,4}

¹Department of Otorhinolaryngology, Dankook University, ²Department of Medical and Biological Engineering, Dankook University, ³Department of Otorhinolaryngology, Seoul National University, ⁴Sensory Organ Research Institute, Seoul National University Medical Research Center

Objective. Recently, a new method to confirm tinnitus in animals has been reported. If tinnitus can be measured in animals, the same paradigm may be adopted to humans to develop an objective tinnitus test. The objective of this study was to prove a difference in N1 amplitudes when stimulated by the prepulse gap paradigm, between tinnitus patients and normal subjects. Materials and Methods. Five tinnitus patients and 8 normal subjects were recruited. Two hundred stimuli composed of a background noise and a pulse noise was presented to the subjects. In 100 stimuli there was a short gap in the background noise just before the pulse noise and in the other 100 stimuli there was no gap. The cortical response of N1 was measured with a conventional ERP system. The Gap condition / No gap condition amplitude ratio was analyzed as the primary outcome measure. Results. In the tinntius patient group, the Gap/No gap ratio was 95.6;3/419.9 while it was 79.2;³/₄14.7 in the normal control group. The Gap/No gap ratio was significantly smaller in the normal control when compared with the tinnitus patient group (p=0.037). Conclusion. As in animals, it seems that the prepulse gap paradigm is also applicable to human tinnitus subjects. By refining the stimulus and objective measurements, we may be able to develop an objective test which can detect tinnitus in humans.

226 Occurrence and Persistence of Tinnitus After Acute Acoustic Trauma by Gunshot

Yong-Won Lee¹, Yong-Ho Park¹

¹Chungnam National University

Background and Objects: Acute acoustic trauma(AAT) by gunshot can be the cause of hearing loss and tinnitus. Tinnitus after AAT frequently disappears with time. But the prognosis of this injury is very difficult to predict. This study tried to identify the factors influencing on tinnitus to occur and persist after AAT. Subjects and Method: A group of 268 military subjects who get the gunshot training with K-2 rifle once after conscripted was asked to answer the questions: age, otologic history, number of firing, usage of earplugs, presence of tinnitus after gunshot and its characteristics, relapsed time after firing, tinnitus severity index(TSI) questionnaire. Physical examination and pure tone audiometry were conducted to the subjects with existing tinnitus on the questionnaire. Results: 95 patients(36.4%) experienced tinnitus immediate after gunshot among 261 subjects. It is obvious that wearing earplugs could prevent immediate tinnitus after AAT. There was statistical significance between tinnitus with earplug and without it(p=0.000). At the time of questionnaire, 27(10.3%) were complaining of tinnitus. Among age, number of firing, wearing earplugs, severity of tinnitus and relapsed time after firing, only severity of tinnitus has the significant effect with the persistence of tinnitus(p=0.046). Conclusion : Wearing earplugs can prevent tinnitus immediately after AAT, but does not seem to be the factor decreasing the prevalence of tinnitus. It was a only factor for severity of tinnitus to be related with existing tinnitus.

227 Debilitating Tinnitus Triggered by a Single Noise Exposure Incidence VIshakha Rawool¹

¹West Virginia University

In most cases exposure to a single instance of loud sound is not considered serious as hearing commonly recovers although occasionally a permanent hearing loss can occur. This poster will discuss two patients who reported the perception of a highly debilitating tinnitus triggered by single instances of noise exposure. The first patient was a 69 year old man reporting a sudden onset of a bilateral, high pitched and highly debilitating ringing following exposure to noise from the closing of a car-trunk with a loud bang by someone else while the patient was standing next to it. An audiometric evaluation revealed a bilateral mild to severe sloping hearing loss. Following complete tinnitus evaluation, extensive counseling and information related to tinnitus was provided and hearing aids were recommended. The patient had made an appointment to try hearing aids after seeking advice from several experts. However, he died suddenly and the exact cause has not been revealed. The second case is a 52 year old woman who reported sudden onset of a click-like, loud tinnitus only in the right ear following a toilet flush. The tinnitus was described as very hard to ignore, interfered with speech perception including her own speech, and gave her the feeling of "a bug with fluttering wings being stuck in the outer ear or near the eardrum". Videootosopy revealed normal eardrum and canal and no foreign bodies. Audiometric, acoustic immittance and otoacoustic emission results were within normal limits. The patient was advised to seek a complete otolaryngological evaluation. She was informed about tinnitus retraining and cognitive behavior therapy and was also informed about other strategies including relaxation techniques and sound therapy. A follow-up call to the patient revealed that her tinnitus had disappeared following relaxation exercises. Detailed information about the patients and possible underlying

mechanisms for tinnitus in each case will be discussed in the poster.

228 Intervention for Restricted Dynamic Range and Reduced Sound Tolerance: Clinical Trial Using Modified Tinnitus Retraining Therapy

Craig Formby¹, Monica Hawley², LaGuinn Sherlock³, Susan Gold⁴

¹University of Alabam, ²Boston, MA, ³University of Maryland

Hyperacusis is the intolerance to sound levels that normally are judged acceptable to others. The presence of hyperacusis (diagnosed or undiagnosed) can be an important reason that some persons reject their hearing Tinnitus Retraining Therapy (TRT), originally aids. proposed for the treatment of persons with debilitating tinnitus, offers the significant secondary benefit of increased Loudness Discomfort Levels (LDLs) in many persons. TRT involves both counseling and the daily exposure to soft sound from bilateral noise generator devices (NGs). We implemented a randomized, doubleblind, placebo-controlled clinical trial to assess the efficacy of TRT as an intervention for reduced sound tolerance in hearing-aid eligible persons with hyperacusis and/or restricted dynamic ranges. Subjects were assigned to one of four treatment groups: 1) full treatment, both counseling and NGs, 2) counseling with placebo NGs, 3) NGs without counseling, and 4) placebo NGs without counseling. They were evaluated at least monthly, typically for five months or more, on a variety of audiometric tests, including LDLs, the Contour Test for Loudness for tones and speech, word recognition measured at each session's comfortable and loud levels, and on electrophysiological measures. Results show that subjects are more likely to increase LDLs when using NGs along with counseling (full treatment), although some subjects improved when given only partial treatment. Supported by NIH R01 DC04678.

229 Frequency Discrimination Training: Evidence of Benefit for Tinnitus in a Randomised Controlled Trial

Derek Hoare¹, Victoria Kowalkowski¹, Paula Stacey², Deborah Hall^{1,2}

¹National Biomedical Research Unit in Hearing, ²Nottingham Trent University

That auditory training provides a potentially efficacious therapy for tinnitus draws on observations that link tinnitus and hearing loss with altered activity at different levels of the auditory system, and that auditory perceptual training produces neural plasticity of the tonotopic representation. We present a randomised controlled, double-blind, trial of frequency discrimination training involving 42 participants who have chronic subjective tinnitus. Participants were randomly assigned to train (1) at a frequency within their region of normal hearing, (2) at a hearing loss frequency, or (3) using a missing fundamental harmonic complex tone composed of higher harmonics in their region of hearing loss. Participants did 20 training sessions of 30 minutes over a 4 week period, and were assessed before and after training, and at a 1 month follow-up. Outcome measures were the Tinnitus Handicap Questionnaire (THQ), a Visual Analogue Scale (VAS) of tinnitus loudness, and psychoacoustic measures of tinnitus frequency spectrum and loudness. The most improved group had trained at a frequency in the region of normal hearing, suggesting that tonotopic reorganisation of the hearing loss region is not the mechanism of benefit for auditory training in this instance. Benefit was observed to be partially maintained one month after training.

230 Alternate Current Electrical Stimulation on Round Window for Tinnitus Suppression

Won Sun Yang¹, In Seok Moon², Jae Young Choi¹ ¹Department of Otorhinolaryngology, Yonsei University College of Medicine, ²Department of Otorhinolaryngology, Chung-Ang University College of Medicine

Objectives : Electrical stimulation is one of various methods of treatment for patients with irresistible tinnitus. The purpose of this study is to find out the clinical effect of alternate current electrical stimulation on round window for tinnitus suppression.

Subjects and Methods : Twenty-seven patients who have suffered from disabling tinnitus with unilateral moderatesevere hearing loss(>56dB) were enrolled for this study. Electrical stimulation on round window was performed with alternative current giving changes of sound level and frequency (1.0-4.6mA, 500-6000Hz). Short-term effect on subjective tinnitus was assessed during the stimulation and long-term effect was estimated at the time of onemonth visit after the stimulation.

Results : During the stimulation, two patients reported complete suppression of their tinnitus and eleven patients reported attenuation of tinnitus. Fourteen patients said it was unchanged. One patient complained of dizziness at the time of stimulation, and the other patient said the character of tinnitus was changed after the stimulation. Residual suppression or attenuation of tinnitus was achieved in 2 patients.

Conclusion : Alternate current electrical stimulation on round window is to be considered a worthwhile attempt for tinnitus treatment, and could help select candidates for an implantable electrical simulator which may provide longterm beneficial effect on tinnitus.

Key words : Tinnitus, Unilateral hearing loss, Alternate current Electrical stimulation, Round window

231 Incidence of Bacterial Biofilms on Explanted Cochlear Implants

Karen Pawlowski^{1,2}, Elena Koulich¹, Pamela Kruger¹, Brandon Isaacson¹, Peter Roland^{1,2}

¹University of Texas Southwestern Medical Center at Dallas, ²University of Texas at Dallas

Biofilms are microbial colonies that occur throughout nature as a means to survive harsh living conditions. Biofilms occur on the surfaces of implanted devices and are often associated with recurrent infections. Biofilms are present on cochlear implants (CIs) explanted after recurrent infection, as well as devices where no infection was detected. The exact nature of the relationship between presence of a biofilm and the recurrent infection remains unclear. A better understanding of this relationship can lead to better treatments, reducing the necessity for device removal.

In order to determine the incidence of biofilm formation on CIs at our facilities, we have analyzed all CI devices which were removed due to recurrent infection or due to device failure. Twenty six devices were removed at 2 tertiary care facilities over a 4 year period, between September 2007 and September 2010. They were photographed, swabbed for detection of bacterial DNA, and, when possible, biologic surface material was removed prior to returning the device to the manufacturer. Imaging by confocal microscope and scanning electron microscope was performed on the biologic material harvested from the devices to determine biofilm presence. Devices studied were from three major CI manufacturers. Age of individuals from which the implant was explanted ranged from 2 to 80 years. Time between device implantation and removal due to recurrent infection ranged from weeks to 10 years. PCR was performed for bacteria known to cause infections in the temporal bone (S. aureus, S. pneumoniae, S. epidermidis, H.influenzae, P. aeruginosa, M. catarrhallis). Several (7/26 devices) had signs of infection and biofilms were found on all but one of those devices. Biofilms were also present on several electrodes. Bacteria were detected on implants with and without the presence of biofilms. Results and implications for the role of biofilms in recurrent infection of CIs will be further detailed.

232 Biofilm Formation on Platinum/Iridium Electrodes Subjected to Low-Level Electrical Current

Elena Koulich¹, Karen Pawlowski²

¹University of Texas Medical Center at Dallas, ²University of Texas Southwestern Medical Center at Dallas

The pathogenesis of device-related infections is widely recognized to be related to the presence of bacteria in biofilms. In the biofilm state, microorganisms are tightly bound to the surface of the device and are highly resistant to conventional antimicrobial treatments and host defense mechanisms, thereby posing a public health problem. As most biomaterials are negatively charged, electrostatic forces between bacteria and surfaces are, as a rule, repulsive. These repulsive forces can be, potentially, enhanced by the application of electrical current to reduce the probability of biofilm formation and induce the surface detachment of an existing biofilm. The aim of the present study was to determine the effect of exposure to lowintensity, clinically relevant electrical direct current (DC) on platinum/iridium electrodes on the development of S.aureus biofilm and its viability.We find that adhesion of bacteria is affected by DC current. S.aureus adheres more readily to charged vs. uncharged platinum/iridium electrodes, with positively charged electrodes being the most populated. The ultrastructure of the biofilm is currentdependent with positive charge inducing a more extensive production of extracellular polymers. While a +50µA current creates the largest biofilms, most bacteria are dead after 4h of DC current exposure. Since as little as 100nA of DC current can affect the behavior of *S. aureus* at the surface of an electrode, the presence of charge buildup on the surface of that electrode can induce biofilm formation on indwelling devices such as cochlear implants. Additional data on other relevant bacterial strains, effect of current density on biofilm and comparision of DC and AC electrical stimulations will be combined with these results and reported in this presentation.

233 Assessment of Pneumolabyrinth After Middle Ear Trauma: Our Experience and Meta-Analysis

Hiroshi Hidaka¹, Makiko Miyazaki¹, Tetsuaki Kawase¹, Toshimitsu Kobayashi¹

¹Tohoku University Hospital

Pneumolabyrinth is a condition in which air is present in the vestibule and/or cochlea. The presence of air inside the inner ear is clear proof of a pathological connection between the inner ear and the middle ear cavities. We previously reported the effects of perilymphatic air perfusion on cochlear potentials in guinea pigs. Reversible sensorineural hearing loss occurred following air intrusion into the scala tympani, whereas profound and irreversible hearing loss was observed following air intrusion into the scala vestibuli. Clinically, pneumolabyrinth is often related to perilymphatic fistula, with sensorineural hearing loss and dizziness. However, there is no agreed management protocol for this condition due to the extremely limited number of cases.

We report herein 3 cases of pneumolabyrinth caused by penetrating trauma by a chopstick or ear pick. The first case showed pneumolabyrinth and pneumocochlea on high-resolution СТ imaging. With regard to pneumocochlea, the air bubble extended into both the scala vestibuli and the scala tympani. Audiometry showed deafness. Conservative management, including injection of steroid and antibiotics, bed rest, and avoidance of pressure and straining, failed to cure the patient. Exploratory tympanotomy revealed an incudostapedial dislocation and luxation of the stapes. Surgical treatment included sealing of the oval window and closing a perforation of the tympanic membrane. Postoperatively, the patient's vertigo subsided, but his hearing loss remained. The other two cases showed pneumolabyrinth only into the vestibule on CT findings, and both cases recovered their hearing and vestibular symptoms with conservative management.

To date, only 40 cases of pneumolabyrinth have been described in the medical literature. Review of these cases revealed that hearing status after medication was improved in more than 50% of cases in which the pneumolabyrinth was limited to the vestibule. In contrast, the recovery rate was no greater than 20% in cases in which the pneumolabyrinth extended to the cochlea. Both the time course of clinical observation and assessment of pneumolabyrinth extension into the inner ear are mandatory for the management of perilymphatic fistula.

234 In-Vitro Validation of Percutaneous Cochlear Implantation

Theodore McRackan¹, Ramya Balachandra¹, Jack Noble², Daniel Schurzig¹, Gregoire Blachon³, Jason Mitchell³, Benoit Dawant², J. Michael Fitzpatrick², Robert Labadie¹

¹Department of Otolaryngology--Head and Neck Surgery, Vanderbilt University Medical Center, ²Electrical Engineering and Computer Science, Vanderbilt University, Nashville, Tennessee, USA, ³Mechanical Engineering, Vanderbilt University, Nashville, Tennessee, USA

While the rate of individuals receiving cochlear implantation has increased dramatically in the past twenty years, there have been very few advances in surgical technique. The present study serves to describe a novel method of image guided surgery termed percutaneous cochlear implantation (PCI). This technique accesses the cochlea from the lateral cranium through the facial recess using a single pass of a surgical drill. The involved steps include: acquisition of preoperative CT scan, preoperative intraoperative fiducial trajectory planning, marker placement. acquisition of the intraoperative CT. intraoperative planning, design and fabrication of customized microstereotactic frame, attachment of frame and drilling, insertion of CI electrode array. Here, we performed the procedure on three cadaveric temporal bones and radiologically and histologically confirmed electrode placement. All samples had successful intracochlear insertion. Two of the samples were inserted in the scala tympani and one was inserted entirely in the scala vestibuli. This is the first description of PCI done in completion in a cadervic temporal bone. These results show PCI to be a viable technology that we hope to use invivo in the near future.

235 Force Threshold Gauge in Ear Surgery Francis Crieghton¹, N Wendell Todd¹

¹Emory

Knowing the amount of force exerted on tissues and prosthesis is implicit in ear surgery. Too much force may cause unnecessary tissue damage (e.g., harmful contact to membranous structures during insertion of a cochlear implant electrode); a tight prosthesis may dislocate the stapes into the vestibule. Minimal force may prolong the surgical procedure, and contribute to a disappointing postoperative result.

Surgeons learn "enough force" by observing mentors operate, and by trial and error. Thus, surgeons learn "enough force" analogous to a shade tree mechanic learning how much to tighten a nut: observing a mentor, but mostly trial and error. Though the official engineering stance is to quantitate force, heretofore there has been no method for a surgeon to determine the amount of force being exerted.

We demonstrate a clinically useable readily observable novel "force threshold gauge" that enables its user to apply a force while ensuring that a predetermined maximal force threshold is not exceeded. With a graduated series of such gauges, the amount of force exerted can be approximated. The force threshold gauge is an elastically deformable material, which theoretically obeys the mechanical properties governing the buckling of rods under compressive forces. Data support the prediction with Euler's formula, of the maximum force our device can apply in the direction of its longitudinal axis.

A clinically useable force threshold gauge may enable more scientific surgery, and a satisfying post-operative result. The gauge may enable a more scientific description of a "somewhat frozen" ossicle, and of normal laxness.

236 A Novel Tool to Navigate to the Round Window: A Cadaveric Pilot Study

Mark Praetorius¹, Sara Doll¹, Philipp van de Weyer¹, Ioana Herisanu¹, Peter K. Plinkert¹, Stefan Rohde¹ ¹University of Heidelberg

INTRODUCTION. Disorders affecting the inner ear as hearing loss, tinnitus and vertigo are affecting an estimated 13 million people in Germany alone. Curent remedies are technical. For acute interventions, local delivery of drugs as corticosteroids is under current investigation. The application uses the round window membrane as entry to the inner ears' fluid spaces. The present pilot study aimed at facilitating the application with a navigational tool to quide a 23 g needle in the outer ear canal. METHODS. Five adult heads were fitted with a plastic tube with lid and reversibly fixed in the conchal cave with dental rubber. The heads were scanned with computational tomography and the angle and the distance to the round window niche was calculated. RESULTS. 10 ears were investigated. Only in 7 ears, an unobstructed access to the Round window could be achieved, the three others had bony exostosis which blocked a straight access. The mean angles were in the coronary plane right 86 degrees, in the transversal plane 91.5 degrees, The mean distance was 4,76 cm. On the left, these figures were 84,5 dgrees, 99 degrees and 4,68 cm, respectively. CONCLUSIONS. We could show the feasibility to use a low budget navigational tool to calculate the trajectory of a needle through the tympanic membrane to the round window niche. This might benefit future local application

237 Hearing Improvement on ACEMg in a Child with Connexin 26 Hearing Loss

Glenn Green¹, Colleen Le Prell², Josef Miller¹ ¹University of Michigan, ²University of Florida

Mutations in the gene encoding Connexin 26 usually result in hearing loss ranging from mild to profound. This hearing loss is typically stable, but may be relentlessly progressive. The reason for progression is unknown, but is assumed to involve common pathways for otologic insults causing hearing loss. Antioxidants have been associated with attenuation of hearing loss from a variety of insults chemotherapeutics, and including noise, hypoxia aminoglycosides. One particular dosing regimen within US Institute of Medicine ranges consists of a vitamin A precursor, vitamins C & E, and magnesium (ACEMg); this regimen is nontoxic and has constituents available over It was therefore of interest to see if the counter. supplementation with ACEMg would have an effect on

progressive hearing loss associated with Connexin 26 mutations.

SB is an 11-year-old boy with Connexin 26 hearing loss who has the mutations 35delG/167delT in GJB2. Over 7 years, his pure tone average (at 500, 1000 and 2000 Hz) dropped an average of 2.17 dB/year. He was placed on a high dose daily oral regimen of beta-carotene, L-ascorbic acid, vitamin E and magnesium. Subsequent to beginning this daily supplement paradigm, audiometric evaluations have not only demonstrated no further decreases but have shown an actual improvement in hearing of 1.7 dB/year over nearly two years. These changes are statistically significant (p<0.05).

While the etiology of progression in Connexin 26 is unknown, and inferences drawn from a single case presentation are necessarily limited, examination of antioxidants in a larger therapeutic trial appears worthwhile.

238 AudGenDB: a Public, Internet-Based, Audiologic/ Otologic/ Genetic Database for Pediatric Hearing Research

John Germiller^{1,2}, Roger Marsh³, Samuel Cohn¹, Megan Reinders¹, Michael Italia⁴, Jeffrey Pennington⁴, Byron Ruth⁴, Peter White^{4,5}, Joy Peterson³, Ian Krantz^{5,6}, E. Bryan Crenshaw^{1,3}

¹Division of Pediatric Otolaryngology, The Children's Hospital of Philadelphia, ²Dept. of Otorhinolaryngology, University of Pennsylvania, ³Center for Childhood Communication, The Children's Hospital of Philadelphia, ⁴Center for Biomedical Informatics, The Children's Hospital of Philadelphia, ⁵Dept. of Pediatrics, University of Pennsylvania, ⁶Division of Human Genetics, The Children's Hospital of Philadelphia

Objective: Major advances in pediatric hearing research often require data from multiple specialties and large cohorts of patients. We have developed an integrated biomedical computing infrastructure, AudGenDB, that incorporates audiologic, otologic, and genetic data, to serve as a resource for researchers internationally. AudGenDB will soon be publicly accessible to qualified hearing researchers via the Internet. We present the current content and capabilities of this resource.

Methods: A team of audiologists, otolaryngologists, geneticists, and medical informaticists has been developing a large-scale relational database and robust web-based user interface. Monthly extraction of data from the electronic medical record ensures that the data resource contains the latest clinical information.

Results: AudGenDB currently contains 57,280 audiograms, 55,997 tympanograms, 16,784 ABR datasets, 15,059 radiology reports, and 22,604 surgical procedures from 37,273 patients. A highly intuitive user interface enables exploration of resource data in advance of queries, and permits queries on demographics, hearing loss severity, type, configuration, and laterality, radiology interpretations, genetic data (e.g., GJB2 mutational analysis), and existence of SNP array data. Users can view original temporal bone CT / MRI images from almost 5,000 complete studies, and take detailed measurements. Ultimately, AudGenDB will provide access to highresolution genomic data and contact information to direct users to the original DNA samples. Public release of AudGenDB is expected by early 2011.

Conclusions: AudGenDB represents the first large-scale database resource for pediatric hearing research. Using an intuitive web-based interface, both beginner and advanced users can access abundant audiologic, otologic, radiologic, and genetic datasets. By design, this resource is self-renewing and will continue to grow as we establish interfaces with additional pediatric centers.

239 Newborn Genetic Screening for Hearing Impairment: A Preliminary Study at a Tertiary Center

Chen-Chi Wu^{1,2}, Chia-Cheng Hung², Shin-Yu Lin², Wu-Shiun Hsieh³, Po-Nien Tsao³, Chien-Nan Lee⁴, Yi-Ning Su², Chuan-Jen Hsu¹

¹Department of Otolaryngology, National Taiwan University Hospital, ²Department of Medical Genetics, National Taiwan University Hospital, ³Department of Pediatrics, National Taiwan University Hospital, ⁴Department of Obstetrics and Gynecology, National Taiwan University Hospital

To investigate whether genetic screening for common deafness-associated mutations could assist in identifying infants with slight/mild, progressive, or late-onset hearing impairment who are usually missed in conventional universal newborn hearing screening (UNHS), 1017 consecutive newborns in a tertiary hospital were subjected to both newborn hearing screening (NHS) using a two-step distortion-product otoacoustic emissions (DPOAE) screening and newborn genetic screening (NGS) for deafness. The NGS targeted 4 deafness-associated mutations commonly found in the Taiwanese population, including p.V37I (c.109G>A) and c.235delC of the GJB2 gene, c.919-2A>G of the SLC26A4 gene, and mitochondrial m.1555A>G of the 12SrRNA gene. The results of the NGS were then correlated to the results of the NHS. Of the 1017 newborns, 16 (1.6%) had unilateral DPOAE screening failure, and 22 (2.2%) had bilateral DPOAE screening failure. A total of 199 (19.6%) babies were found to have at least 1 mutated allele on the NGS for deafness, 11 (1.1%) of whom were homozygous for GJB2 p.V37I, 6 (0.6%) compound heterozygous for GJB2 p.V37I and c.235delC, and 1 (0.1%) homoplasmic for m.1555A>G, who may potentially have hearing loss. Among them, 3 babies, 5 babies, and 1 baby, respectively, passed the NHS at birth. Comprehensive audiological assessments in the 9 babies at 3 m identified 1 with slight hearing loss and 2 with mild hearing loss. NGS for common deafness-associated mutations may identify infants with slight/mild or potentially progressive hearing impairment, thus compensating for the inherent limitations of the conventional UNHS.

240 Otoacoustic Emission Test in Large Scale Newborn Hearing Screening and the Effect of Kaliopenia and Hypocalcemia

chun liang^{1,2}, QI HONG¹, Tao-Tao Jiang¹, Yan Gao¹, Xiao-Xing Luo¹, Xiao-Fang Yao¹, Yan Jin¹, Xiu-Hui Zhuo¹, Guang-Jin Lu¹, Hong-Bo Zhao²

¹Maternal and Children Health Care Hospital of Baoan, Shenzhen, ²University of Kentucky Medical center

More than 80% of permanent hearing loss in children are congenital. Newborn hearing screening (NHS) can early detect hearing loss to provide early therapeutic interventions. Otoacoustic emission test reflects the activation of active cochlear mechanics and can sensitively detect cochlear hair cell function. In this study, we examined the neonate and infant hearing function by measuring transient evoked otoacoustic emission (TEOAE). A total 6,626 babies (13,252 ears) were tested, of which 5,311 babies were health (a normal group) and 915 babies had complications (a high-risk group). In the normal group, 9,582 ears were passed in the first screening test and 1,040 ears were rejected; the passing percentage is 90.20%. In the high-risk group, 1,103 ears were passed and 177 ears were rejected; the passing percentage is 83.83%. In the high-risk baby group, there are 550 premature infants, 26 babies with kaliopenia, and 27 babies with hypocalcemia. Their passing percentages are 78.36%, 48.08%, and 61.11%, respectively. Our data show that the passing percentages in the high-risk baby group and premature infants have a significant reduce. Kaliopenia and hypocalcemia can also reduce otoacoustic emission, suggesting that they may affect the ionic environment in the cochlea to influence hair cell activity including outer hair cell electromotility.

Supported by Shenzhen Science Foundation No. 200703016.

241 A Cell Culture Model of Facial Palsy

Maggie Kuhn¹, Vladimir Camarena¹, James Gardner¹, Rosalia Perez-Castro², Mariko Kobayashi¹, Angus Wilson¹, Ian Mohr¹, Moses Chao^{1,2}, Pamela Roehm¹, Pamela Roehm³

¹NYU School of Medicine, ²Skirball Institute of Biomolecular Medicine, ³New York University School of Medicine

A variety of circumstantial evidence has suggested that herpes simplex virus type 1 (HSV1) reactivation is the etiologic mechanism underlying both Bell's palsy and delayed facial palsy (DFP) after trauma. To demonstrate ability of geniculate ganglion neurons (GGNs) to reactivate following latent HSV1 infection, cultures of GGNs were latently infected with HSV1 expressing green fluorescent protein. Four days later cultures were treated with trichostatin A (TSA), a known chemical reactivator of HSV1. Cultures were monitored daily by fluorescent microscopy for GFP positivity. To model intraoperative surgical trauma, superior cervical ganglion (SCG) neuron cultures were latently infected with HSV1. Six days later, injuries modeling surgical trauma were performed. Severed, heated or oxygen-starved neurons were monitored for GFP expression. GGN cultures displayed a reactivation rate of 65% after treatment with TSA (baseline 9%), demonstrating that latent infection and reactivation of HSV1 can occur in these neurons. SCG cultures reactivated at a rate of 44% after application of TSA (baseline 2.5%). Following axon cleavage, HSV1 reactivation rates did not increase, although cultures were reactivation competent. No HSV1 reactivation occurred after exposure of SCG to elevated temperature. Hypoxia yielded increased HSV1 reactivation (75%). In conclusion, we have shown that cultured GGNs can be latently infected with HSV1 and that have shown that hypoxia, but not axonal cleavage or heat shock, induced HSV1 reactivation in our system. We propose that maintenance of latent HSV1 infection may be dependent on mTORC1 signaling, which can be disrupted by hypoxia. Future studies will explore relevance of this pathway to HSV1 reactivation in facial palsy, and explore the use of small molecule inhibitors as preventative treatments for DFP.

242 Proof of Concept: Effective and Expedient Deployment of a Community-Based Research Network for Collecting Grant Pilot Data in Tinnitus and Dizziness

Kristine Schulz^{1,2}, David Witsell², Debara Tucci² ¹American Academy of Otolaryngology - Head and Neck Surgery Foundation, ²Duke University Medical Center Background/Significance:

CHEER – Creating Healthcare Excellence through Education and Research (www.cheerresearch.org) – is a community-based research network currently funded by an NIDCD R21/33 grant [DC-07-002]. An academic center serves as the overall coordinating center, in partnership with a professional society that provides support for project leadership and member relationships. The mission of the network is to become the national resource for practicebased clinical research in hearing and communicative sciences. The focus of CHEER is research education -- to standardize Coordinator education across academic and community sites, so sites are 'at the ready' to participate, patients are protected and safe, and the integrity of gathered data is assured and maintained.

Objective: To deploy a descriptive, epidemiologic study on two conditions – tinnitus and dizziness – for the purpose of: proof-of-concept of capability of a community-based research network; and, as pilot data for subsequent grant submissions. The two conditions were identified by grant PIs and associated expert panels were assembled based on this original selection.

Results:

Proof-of-Concept achieved and data used as basis for additional grant submissions.

•Over 1,000 patients enrolled (presenting with Tinnitus, Dizziness or both Tinnitus and Dizziness) in 6 months across 15 sites (and still enrolling) or 68% of the network. Conclusions and Lessons Learned:

•Use of a Community-Based Research Network is a highly successful way to collect data and deploy projects of multiple purposes – i.e. descriptive epidemiologic baseline data as well as more complex research grants and studies.

•Engaging coordinators in the thought leadership of a community-based research network is a crucial component of the success and viability of the network. In our model, the Coordinator Advisory Board (CAB) serves in that role, with coordinators representing perspectives of all site types. When the network was polled, 74% indicated that the coordinator was the most important person in terms of staying committed and engaged in the network.

•The biggest challenges for the network remain to be financial incentives for site participation and time and resource commitment, as most community sites do not have a dedicated research coordinator.

243 Efferent Innervation of Vestibular End Organs in Turtle, Bird and Mouse

Paivi Jordan¹, Joseph Holt¹

¹University of Rochester

Vertebrate vestibular end organs receive a dense efferent innervation that begins as a small collection of neurons within the brainstem and ends as thousands of terminals within the sensory neuroepithelium. In amniotes, these efferent neurons terminate on three distinct targets: type II hair cells, bouton afferents innervating type II hair cells, and the outer face of calyx afferents. Ultimately, the response of vestibular afferents to efferent stimulation is derived from the combined activation of different efferent receptors at each of these distinct targets. Understanding how efferent synapses operate also requires an understanding of their innervation patterns and structural organization. However, vestibular efferent markers have not been well characterized in turtle, the animal model currently utilized in our lab. Consequently, the goals of the current study were as follows: (1) To establish vestibular efferent neuronal markers in the vestibular periphery of the turtle, (2) To visualize how these efferent synapses are organized, and (3) To compare labeling patterns of these markers in turtle to those seen in avian and mammalian vestibular tissue. Fluorescent immunohistochemistry with antibodies against choline acetyltransferase (ChAT), synapsin I, SV2, and syntaxin was utilized to label efferent fibers and terminals in the vestibular end organs of the redeared turtle (Trachemys scripta elegans), zebra finch (Taeniopygia guttata), and mouse (Mus musculus). Vestibular hair cells and afferents were counterstained for myosin VIIa and calretinin, respectively. In all species, ChAT clearly labeled a population of thin fibers, morphologically-distinct from larger-diameter afferent fibers. ChAT-positive efferent fibers terminated on type II hair cells as well as both classes of afferent fibers, and colocalized with the synaptic markers synapsin I, SV2, and syntaxin. Implications of the observed efferent innervation patterns are discussed. (Supported by NIH DC008981)

244 Efferent-Mediated Inhibition and Excitation of Turtle Crista Afferents Are Driven by Pharmacologically-Distinct Nicotinic ACh Receptors Joseph Holt¹

¹University of Rochester

In the vestibular end organs of amniotes, cholinergic efferent neurons can provide synaptic input to three distinct cellular targets: type II hair cells, their bouton afferents, and afferent calyces. Ultimately, the response of a vestibular afferent to efferent stimulation is derived from the combined activation of different efferent receptors at each of these available targets. Under such regime, the effects of one efferent input may outweigh another and, as such, shape the final response. In the turtle posterior semicircular canal, all three efferent targets are present and the resultant efferent actions on afferent discharge include a rapid inhibition of bouton afferents and a rapid excitation of calyx/dimorphic (CD) afferents. Efferentmediated inhibition invariably involves the activation of alpha9/alpha10-containing nicotinic ACh receptors $(\alpha 9/10 \text{nAChRs})$ on type II hair cells. Calcium influx through α 9/10nAChRs activates SK potassium channels, subsequently hyperpolarizing hair cells and decreasing transmitter release. In contrast, efferent-mediated excitation of CD units is generated by activating nAChRs located on calyceal terminals that directly depolarize the afferent. Several pharmacological agents, with putative selectivitv towards $\alpha 4\beta 2$ -containing nAChRs ($\alpha 4\beta 2^*nAChRs$), block the efferent-mediated excitation in CD afferents with little to no effect on a9/10nAChRmediated inhibition of type II hair cells. Similar nAChRs on bouton afferents are also activated during efferent stimulation, but the subsequent excitation is typically masked by hair cell inhibition, and can be best seen after selectively blocking a9/10nAChRs. Conversely, selective blockade of a4b2*nAChRs allows a convenient way to distinguish calyx from dimorphic afferents by revealing the α 9/10nAChR-mediated inhibition of type II hair cells synapsing on dimorphs. These results may be directly applicable to efferent responses of mammalian vestibular afferents. (Supported by NIH DC008981)

245 Otolin Is a Secreted Multimeric Glycoprotein That Is Present in All Extracellular Matrices of the Mammalian Inner Ear and Binds the Otoconial Proteins Cerebellin and Otoconin-90

Michael Deans^{1,2}, Jonathan Peterson^{1,3}, G. William Wong^{1,3}

¹Johns Hopkins School of Medicine, ²Dept. of Otolaryngology, ³Dept. of Physiology

The otoconial membrane is a dense extracellular matrix containing bio-mineralized otoconia that provides the mechanical stimulus necessary for vestibular hair cells to respond to linear accelerations and gravity. cDNAs encoding components of the otoconia and otoconial membrane have been identified and mutations in these genes result in abnormal otoconia formation and balance

deficits. Here we describe the cloning and characterization of mammalian Otolin, a secreted glycoprotein of ~70 kDa that is a constituent of the otoconial membrane. Otolin has a C-terminal globular domain homologous to the immune complement C1q. Using FPLC gel filtration we find that like other C1g family members, Otolin assembles into high molecular weight complexes greater than 600 kDa. Furthermore immunoprecipitation of recombinant proteins expressed in vitro shows that Otolin forms complexes with Cerebellin and Otoconin-90, two protein constituents of otoconia crystals. Together these results argue that Otolin complexes may anchor the otoconia to the otoconial membrane. Consistent with this immunohistochemical analyses reveal Otolin protein in the otoconial matrix. Protein is also visualized in support cells of the maculae and canal cristae indicating that these cells are the source of Otolin synthesis and secretion. Remarkably Otolin is also detected in support cells and non-sensory cells of the cochlea as well as in the tectorial membrane. Thus in the mouse Otolin contributes to all of the extracellular matrices of the inner ear. We further demonstrate by RT-PCR analyses that otolin mRNA is restricted to the ear and that otolin expression initiates at early stages of embryogenesis. Otoconia detachment and entrapment in the semicircular canals can result in benign paroxysmal positional vertigo (BPPV). Our characterization of the biochemical properties and distribution of Otolin are consistent with possible roles for altered Otolin function in the molecular etiology of BPPV.

246 Na+K+ ATPase Is the Major Potassium Provider During the Development of the Endolymph in Cultured Mouse Utricle

Sylvain Bartolami¹, Sophie Gaboyard-Niay², Jacques Barhanin³, Christian Chabbert²

¹Université montpellier II, ²Inserm U583, ³Université de Nice

Vestibular function depends on homeostatic regulations of the endolymph because maintaining high potassium concentration ([K+]) is essential for hair cell excitation. Such maintenance requires a global balance between K+ secretions and absorptions but little is known about the processes that govern the development of the endolymphatic compartment. In order to shed light on such developmental mechanisms, we took advantage of a unique vestibular organotypic model, the mouse utricular cyst that regenerates a genuine endolymphatic compartment from immature utricle (postnatal day 2). Endolymphatic [K+] and transepithelial potential occurrences were measured during cyste formation. Experimentally driven alterations in both features were electrophysiologically determined in order to examine the involved molecular processes. K+ accumulates in cysts during the first 4 days after the epithelial wall closure and steady [K+] is obtained by the 5th day. Ouabaine and bumetanide treatments, as well as KCNE1 gene deletion affect [K+]. Bumetanide reduces partially and transiently the [K+], while ouabaine and KCNE1 deletion almost abolish [K+]. Conversely, inhibition of K+ efflux, carried out by hair cells, leads to an enhanced [K+] whatever the blocker used (FM1.43, amikacin, gentamicin and gadolinium). This global analysis, weighting the involvement of the various regulators of endolymphatic homeostasis at the organ level, points to the Na+ K+ ATPase pump as a key endolymphatic K+ provider and confirms that expression of KCNE1 channel is necessary to K+ secretion; while the bumetanide target, the NKCC1 co-transporter, has little importance in K+ influx during the formation of the endolymphatic compartment.

247 Excitotoxicity and Repair at the Vestibular Peripheral Synapses Back to Development

Sophie Gaboyard-Niay^{1,2}, Aurore Brugeaud², Cécile Travo¹, Audrey Broussy², Aurélie Saleur², Christian Chabbert^{1,2}

¹INSERM U583, ²Sensorion-Pharmaceuticals

In the inner ear, the consequences of excitotoxicity have been well studied for the cochlea but are far less described for the vestibule. Following vestibular lesion, it has long been thought that central vestibular compensation was the only mechanism for functional recovery. We recently demonstrated that a repair process could also occur at the peripheral vestibular synapses following a mild excitotoxic damage of afferents. In this study, we induced a more severe injury by unilateral trans-tympanic injection of kainic acid in rats. The excitotoxic lesion results in a transient impairment of the vestibular behavior that correlates with histology of afferents in cristae and maculae. Following steps occurred throughout 48hrs, from excitotoxic injury to synaptic repair. First, two hours after the lesion, behavioral deficit was maximal, with afferent terminals extensively damaged displaying large swellings in both cristae and macculae. However, no loss of hair or supporting cell was quantified. A second step of swelling resorbtion and fiber retraction occurred during the following hours. Eventually, repair of the synaptic terminals was observed. Twenty four hours after the injury, the vestibular deficit was reduced by 30%. no more swelling was observed but only 25% of type I hair cells appeared correctly innervated in utricles. In fact, after retraction of calyces, a competition between efferent and afferent nerve endings occurred to re-innervate type I hair cells and, finally repaired the injured vestibular sensory epithelium. Noteworthy, this repair process mimics the developmental set up of vestibular fibers observed during synaptogenesis. In conclusion, vestibular terminal afferents undergo excitotoxicity and have capacities of self repair using a developmental-like process. Our next goal is to pharmacologically protect the extend of excitotoxicity by limitation of synaptic damages and/or enhancement of the repair process to potentially treat the injured vestibular endorgans.

ARO Abstracts

248 Modeling Fluid Flow Stimulation of Vestibular Hair Cells Using Computational Fluid Dynamics

Joseph Welker¹, Wally Grant¹

¹VA Tech

Vestibular hair cell bundle stimulation by endolymph flow is studied using computational fluid dynamics. Bundles have previously been modeled as simple geometries such as half-ellipsoids and hinged planes. Only recently has a realistic hearing bundle been analyze with endolymph flow loading (Baumgart et al., USNC TAM, 2010).

An average Type-II hair cell bundle found in the striolar region of a turtle utricle was modeled for this study. It contains 56 stereocilia (SC) arranged in 17 rows and 7 columns (heights = $1.4-5 \mu m$) and a single kinocilium (height = $10.15 \mu m$). All were rigid with no interconnecting The model was created, meshed, and solved in links. ANSYS Workbench. Shear flow stimulation with a maximum velocity of 10 µm/ms was applied in the excitatory direction. The flow patterns and resulting forces on the SC and kinocilium are the results of interest.

Results show that there is virtually no fluid flow through the bundle. Fluid flows around the bundle and up the front as if there were a solid plane connecting the tops of the SC. Forces on the SC result from fluid flow pressure and viscous shear stress. Total forces acting on the peripheral SC are substantially higher than on the inner SC. There is a substantial twisting moment on the peripheral SC from shear stress. The greatest load is on the tallest SC in the outer-most columns. Also, there is a substantial suction effect on the tallest row of SC nearest the kinocilium. These negative pressure loading patterns appear to be the primary cause of deflection in the tallest row of SC. These results suggest that the rear row of SC is sucked in the direction of the flow; this excitatory deflection then propagates throughout the bundle. The fluid pressure and shear loading on the peripheral SC cause deflection and twisting of these SC. This may cause peripheral ion channels to open prior to the opening of channels on the interior SC.

(Supported by: NIH NIDCD R01 DC 005063)

249 Oncomodulin Expression Defines a **Toplogically Distinct Subpopulation of Hair Cells in the Murine Utricle**

Dwayne Simmons¹, David Sultemeier², Gurbir Behniwal¹, Larry Hoffman²

¹UCLA, ²Geffen School of Medicine at UCLA

The expression of oncomodulin (Ocm: aka parvalbumin b) was recently reported in hair cells of various inner ear sensory epithelia. Through the present investigation we further explored its expression in mouse utricular hair cells, testing the hypothesis that it defines a subpopulation distinct from other phenotypic markers of the utricular striola (e.g. calretinin in afferent calyces). This was achieved in mature (21 - 35 days of age) utricles from C57BL/6N mice. Immunohistochemistry was performed on freshly fixed (4% paraformaldehyde) specimens using antibodies to Ocm (Swant), calretinin (Chemicon), and

neurofilament (NF-2, NeuroMab). We also used fluorophore-conjugated phalloidin to label hair cell stereocilia for definition of hair cell morphologic polarization and to assist in navigating the utricular topography. Type I and II hair cells were distinguished by the presence of calyces labeled with anti-neurofilament. Similar to previous reports regarding the distribution of calretinin-labeled calyces in the mouse striola, Ocmpositive hair cells form a distinctive crescent-shaped band medial to the line of hair cell polarity reversal (LPR). Anti-Ocm labeling exhibited a diffuse intracellular distribution throughout the hair cell cytoplasm. Consistent with recent reports of striolar hair cell morphologic polarization, most Ocm-labeled hair cells were found medial to the LPR and exhibited similar stereocilia polarization. In specimens double-labeled with anti-Ocm and anti-neurofilament we found that virtually all Ocm-positive hair cells were associated with an afferent calyx, indicating that Ocm expression was predominantly limited to type I hair cells. Because of their topographically restricted location, Ocmpositive hair cells were largely associated with a calretininpositive afferent calvx. However, this association was not exclusive, as we found many Ocm-positive hair cells were associated with calyces that were calretinin-negative. This indicates that Ocm expression was not exclusively dependent upon factors that also delineate the type I_c class of hair cells (i.e. those associated with calretininpositive calyces). In summary, these data support the conclusion that Ocm-expressing hair cells reflect a distinct subpopulation within the mouse utricular striola.

250 Distribution of the Na,K-ATPase α Subunits in the Rat Vestibule

Olga Pylaeva¹, Will J. McLean², Elisabeth Glowatzki³, Ruth Anne Eatock², Sonja Pyott¹ ¹UNC Wilmington, ²Harvard Medical School, ³Johns

Hopkins University

The Na,K-ATPase (NKA) is essential for excitable cells that maintain hyperpolarized membrane potentials and sodium and potassium concentration gradients. The distribution of the NKA in the inner ear has been studied most extensively in structures that maintain the spiral ligament; however, previous work also identified the NKA alpha 3 subunit in afferent and efferent terminals and also the NKA alpha 1 subunit in GLAST-expressing supporting cells of the cochlea. These findings motivated comparable examination of NKA alpha subunits in the vestibular periphery. Therefore, we performed a variety of double labeling experiments with antibodies against three of the alpha isoforms of the NKA (NKA alpha 1-3) and markers identifying particular subsets of neurons or cells in whole mount preparations of vestibular tissue (cristae and utricle) from rat. We observed immunoreactivity against the NKA alpha 3 subunit, but not the NKA alpha 1 or 2 subunits, in calvces surrounding type I hair cells. No NKA alpha immunoreactivity was observed in bouton terminals contacting type II hair cells. These findings suggest unique mechanisms to regulate neuronal excitability and regulate glutamate transport between the cochlea and vestibule.

251 Hair Cell Transduction in the Turtle Utricle

Michaela Meyer¹, Ruth Anne Eatock^{1,2} ¹Department of Otolaryngology,Harvard Medical School, Eaton Peabody laboratory, MEEI, ²Department of Neurobiology, Harvard Medical School

The utricular macula of the turtle (*Trachemus scripta elegans*) is a valuable model system to investigate transduction mechanisms in hair cells of an adult vertebrate otolith organ. Advantages are the prominent zonal organization and a large database on the morphology of hair cells and accessory structures (e.g., Xue and Peterson 2006).

We recorded transduction currents from type I and type II hair cells in different zones of an excised, semi-intact preparation of the turtle utricular macula. Hair bundles were deflected with a stiff probe driven with sinusoidal (2 to 100 Hz) and step waveforms. Current-displacement relations were generated from the 100 Hz or step responses. Adaptation was measured by fitting half-maximal step responses with single- or double-exponential functions.

Here we compare data pooled from type I (zone 3) and type II hair cells (zones 2 and 3) of the striola with data from the type II hair cells with smaller bundles of zone 4 (medial extrastriola). Striolar hair cells had larger peak transduction currents: 212±13 pA, SE (17 cells) vs. 140±18 pA (7); narrower peak operating ranges: 701±60 nm (15) vs. 1890±254 nm (7); and much faster and more extensive Striolar cell adaptation was fit by two adaptation. exponentials with mean T values of 3.2±0.4 ms and 46.4±8 ms (15) and an extent of 76±2.1% (15) at the end of 400 ms. Four medial extrastriolar cells showed no adaptation in 400 ms. Three cells adapted slightly and monoexponential fits to the time course yielded a mean T of 22±14.45 ms and a smaller extent of adaptation: 34±8%. These results are consistent with vertebrate afferent data showing that striolar afferents have greater high-pass filtering and phase leads than extrastriolar afferents. Supported by DC05063

252 An Apamin-Sensitive K(Ca) Current Contributes to the AHP in Vestibular Calyx Terminals

Frances Meredith¹, Gang Li¹, Katie Rennie¹ ¹University of Colorado Denver

Sensory hair cells in the vestibular periphery are innervated by afferent fibers that vary in their firing properties. Calyx fibers terminate as cup-shaped endings on type I hair cells and have irregularly spaced action potentials with variable interspike intervals. Bouton fibers contact type II hair cells, fire regularly and have uniform interspike intervals. Studies have shown that synaptic morphology is not the sole determiner of discharge regularity, suggesting important roles for intrinsic membrane properties. Ionic currents may influence discharge patterns by shaping after-hyperpolarization potentials (AHPs) which set interspike intervals and recovery of post-spike excitability. In other neurons, K channels, including calcium-activated K channels, moderate AHP size and duration. Large conductance calcium-activated K (BK) channels mediate fast AHPs whereas small conductance calcium-activated K (SK) channels contribute to slow AHPs. We have used whole cell patch clamp on isolated calyx terminals still attached to type I vestibular hair cells to investigate ionic conductances that could influence firing patterns. Apamin, a selective blocker of SK channels, was tested on calyx terminals isolated from gerbil semicircular canals during the first postnatal month. Lowering extracellular Ca or applying apamin (20-500 nM) blocked slowly activating outward currents in voltage clamp. Amlodipine (10 uM) also reduced outward currents. Calyx K channel expression increased markedly during the first postnatal month and outward currents were on average much larger at P27 compared with P1. Immature action potentials were present at P1, but the AHP only became prominent after the first postnatal week. After the first two postnatal weeks, apamin reduced the action potential AHP in whole cell current clamp. The presence of SK channels in calvx terminals could contribute to development of the AHP. which may in turn influence discharge regularity. Supported by NIDCD DC008297 (KJR).

253 Afferent Terminal Arbor Structure in Turtle Utricle

Janice Huwe¹, Barbara Williams¹, Michael Rowe¹,

Ellengene Peterson¹ ¹Ohio University

To understand utricular organization, we examined afferent terminal arbors labeled by BDA injections into CN8 or immunostained for calcium binding proteins (CBPs) calretinin (CR) and calbindin (CB), visualized by peroxidase reaction, and quantified in Neurolucida.

Previously we identified 4 macular zones. Lateral (LES, zone 1) and medial (MES, zone 4) extrastriolae contain type II hair cells. In the striola, zone 2 is a band of type II hair cells; zone 3 is a band of type I hair cells and some type IIs. We found distinctive afferent terminal arbors in each zone. We also identified a new macular division medial to the calyx band, the juxtastriola, based on arbor structure and CBP reactivity.

LES arbors are the largest in the macula (median 3800 μ m², n=8), richly branched, with many widely spaced boutons. In the striola, the calyx band contains calyceal and dimorphic afferents (zone 3; n=57 arbors). It is flanked laterally (zone 2) and medially (juxtastriola) by large (2612 μ m², n=16; 2011 μ m², n=29) elongated bouton arbors. Some of these have claw-like structures and are CR⁺ and/or CB⁺. In one utricle immunostained for CR, we found 76 calyceal, 24 dimorphic, and 8 bouton CR⁺ afferents, all in the striola. MES afferents outside the juxtastriola (n=28) have the smallest diameter axons and arbors (588 μ m²) and are sparsely branched with few, large boutons.

These data extend our earlier findings, based on hair bundle structure, mechanics, and coupling to the otoconial membrane (OM), that the striola and juxtastriola comprise multiple, distinctive bands, and that properties of the LES and MES differ significantly. MES hair cells are tightly coupled to the massive OM and tend to adapt slowly (Meyer and Eatock ARO 2011). This and the small terminal arbors of their postsynaptic afferents suggest that the MES may provide a high resolution map of head tilt direction.

Support by NIH RO1DC05063

254 Age-Related Vestibular Dysfunction in Inbred Mouse Strains: Influence of the *Ahl* Locus

Sarath Vijayakumar¹, Sherri Jones¹

¹East Carolina University

The Ahl locus mapped to chromosome 10 has been identified as a major contributor to age-related hearing loss and has also been identified as a variant of the cadherin 23 (Cdh23) gene. While this mutation may lead to profound hearing impairment in aged mouse strains. Mock et al. (2009) showed that it does not predict functional aging of the gravity receptor organs. For example, C57BL/6J mice maintain normal vestibular function despite losing hearing beyond 10 months of age. The purpose of the present study was to examine a potential role for Ahl in vestibular aging by characterizing gravity receptor function in the B6.CAST-*Cdh23*^{Ah/+}/Kjn (B6.CAST) strain that carries the normal functioning Cdh23 allele. We assessed gravity receptor function by measuring linear vestibular evoked potentials (VsEPs) in 45 mice aged 2 to 20 months. Auditory function was also assessed with auditory brainstem response (ABRs) testing. VsEP parameters and ABR thresholds were compared to age-matched data from C57BL/6J mice previously studied in our lab. Synaptic architecture of the utricular hair cells was examined by immunolabeling the synaptic bodies (anti-CtBP2) and postsynaptic AMPA receptors (GluR2/3). Consistent with published studies, ABR thresholds revealed minimal agerelated hearing loss in the congenic animals. VsEP thresholds ranged from -4.5 to -13.5 dB re: 1.0g/ms and at +6 dB re: 1.0 g/ms, P1 peak latencies ranged from 1.25 to 1.63 ms while P1-N1 amplitudes ranged from 0.40 to 1.42 µV. Linear regression slopes for VsEP thresholds were -0.07 dB per month for the congenic mice compared to 0.12 dB per month for the C57BL/6J strain. Indeed, vestibular function aging in both of these strains is significantly less than CBA/CaJ (model with no known genetic mutations affecting the inner ear). Preliminary histological findings do not indicate structural differences in the synaptic morphology. These data out to 20 months suggest no significant effect of age on VsEP threshold or P1-N1 amplitudes for the B6.CAST. Furthermore, they suggest that the Ahl locus does not play a significant role in gravity receptor aging and the maintenance of function for both C57BL/6J and B6.CAST is likely due to other genetic modifiers that remain to be determined. Research supported by NIDCD R01DC006443 and DC006443-04S1.

255 Sensory Learning During Spaceflight: Alterations in Synapse Density Following Exposure to Microgravity

David Sultemeier¹, Patricia Quinones¹, Felix Schweizer¹, Larry Hoffman¹

¹Geffen School of Medicine at UCLA

Exposure to the microgravity conditions associated with spaceflight results in alleviation of the load normally placed upon the utricular epithelium by the otoconial membrane under conditions of the Earth's gravitational field. Previous ultrastructural studies reported, based upon serial reconstructions of entire hair cells, an upregulation in synapse density in utricular hair cells during spaceflight; however, it was not tested whether this could be generalized to hair cells distributed across the utricular topography. We have addressed this issue using contemporary techniques of double-label immunohistochemistry and volumetric image analysis to enable a broader sampling than previously conducted. Here we report our initial findings from hair cells of the medial extrastriola. Utricles were obtained from C57BL/6J mice that were aboard a 15-day mission of the space shuttle Discovery in April 2010. Specimens were harvested 3 - 5 hours after landing, and temporal bones were removed within 5 min of euthanasia. They were immersion-fixed for 2 hrs in 4% paraformaldehyde. Following microdissection, immunohistochemistry was performed on intact specimens to label synaptic ribbons (anti-CtBP2) and the postsynaptic complex (anti-Shank1A). Secondary antibodies were utilized, along with fluorophore-conjugated phalloidin, to enable 3-channel confocal imaging (LSM5 Exciter). Ground control specimens were identically processed. A double-blind strategy was employed for synapse quantification in 6 regions of medial extrastriola, each measuring 900µm², in flight and control utricles (n=4 each). Only objects exhibiting colocalization of CtBP2 and Shank1A were identified as a synapse. Synapse densities were found to decrease in flight animals compared to Earth controls in hair cells of the medial extrastriola. Additional internal (consisting of flight and control horizontal cristae) and laboratory controls are currently being analyzed to further test the veracity of our finding. These data corroborate previous investigations demonstrating the capability of utricular hair cells for adaptive responses to alterations in the ambient gravity, though this sensory learning may be heterogeneous in hair cells from different regions of utricular topography.

256 Injection of Virus Vector Targeting Vestibule in Mice

Hiroko Okada¹, Takashi lizuka¹, Kazusaku Kamiya¹, Hiromi Kasagi¹, Ayako Inoshita¹, Katsuhisa Ikeda¹ ¹Department of Otorhinolaryngology, Juntendo University School of Medicine

It is known that a lot of children with a congenital deafness have a disorder in vestibular function. We examined the gene transfer to the inner ear using glass tube. In the mouse, three main routes of gene delivery are possible, namely scala media approaches (via a cochleostomy),

semicircular canal approaches (via a canalostomy) and round window membrane approaches. In this study, adenovirus (AdV) carrying the green fluorescent protein (GFP) gene were injected in mouse inner ear through the round window and a canalostomy for the purpose of the gene transfer to vestibule. To evaluate the influence of the operation on auditory function and balance function, ABR and the balance test were assessed pre- and postoperatively. Thereafter, transgene expression was observed in the mouse cochlear and vestibular organ. In injection of AdV through the round window, GFP-positive cells were present at the perilymphatic spaces and ampulla. In canalostomy approach, GFP-positive cells were present at perilymphatic space in most samples, and at endolymphatic space in several samples. The signs of vestibular dysfunction were not observed. ABR thresholds did not show any significant changes between before and after the operation of cochleostomy. In this study, gene delivery for vestibular hair cells and supporting cells succeeded in all methods, but injection of adenovirus vector (AdV) via round window resulted in mild hearing loss. On the other hand, injection of adeno-associated virus vector (AAV) via semicircular canal did not result in any hearing loss. In addition, gene expression in vestibular fibrocytes were not obtained at AdV transfection, though it obtained at AAV transfection. It is suggested that the method using adeno-associated virus via semicircular canal is safety and useful for the purpose of gene transfer to vestibule. To optimize gene delivery, we intend to assess efficiency of each method. The method of this noninvasive transfection into vestibular cells may have a potential to repair balance disorders in human.

257 NIDCD Workshops: Training/Career Development Workshop and Early Stage/New Investigator Workshop

Janet Cyr¹, Nancy Freeman¹, Christopher Moore¹, Shiguang Yang¹

¹NIH/National Institute on Deafness and Other

Communication Disorders

NIDCD will offer two concurrent mini-workshops targeted to specific audiences. One workshop is targeted to individuals interested in Training and Career Development. The second workshop is targeted to Early Stage and New Investigators.

The Training and Career Development Workshop will include an overview of research training and career development opportunities appropriate for graduate students, postdoctoral fellows and new clinician investigators. The discussion will include the submission and review of individual NRSA fellowship awards (F30, F31 & F32), as well as the mentored career development awards (K08, K23 & K99/R00) and the NIH Loan Repayment Program. Recent changes in the peer review process will also be presented. Drs. Janet Cyr and Christopher Moore will lead the presentation.

The Early Stage/New Investigator Workshop will provide practical information on how grant applications are processed within NIH/NIDCD including Institute and study section assignments, Advisory Council activities, pay lines and the roles of program and review staff. With a goal of providing information to early stage investigators to facilitate their successful transition from trainee to independent investigator, specific information will be presented regarding funding opportunities for early stage investigators (ESIs), including the NIH Research Program Grant (R01) and the NIDCD Small Grant Award (R03), and recent changes in peer review. Drs. Nancy Freeman and Shiguang Yang will lead the presentation.

258 Dissemination of Resources Derived from NIDCD Grants

Roger Miller¹, John Doucet², Christopher Platt¹ ¹National Institutes of Health, ²Food and Drug Administration

How can novel hardware and software developed during grant supported projects be distributed across the biomedical research community? NIDCD program staff will describe how the various research grant, contract, and Core Center grant mechanisms have been used to develop and distribute special purpose hardware and software products across the research community. A brief overview of the proprietary and legal issues involved with technology transfer, such as intellectual property, open source licensing, patents, and the roles of investigators and institutions will be presented. Specific grant mechanisms designed to support activities leading to commercialization, such as the Small Business Innovation Research (SBIR) and Small Business Technology Transfer (STTR) programs will discussed. Finally, a brief overview of the regulatory process required for the approval of devices for use with human subjects will be presented. Substantial time will be available for guestions and open discussion to explore the issues faced by researchers seeking to share and ultimately commercialize resources developed with NIH support.

259 Bilateral Loss of Vestibular Sensation -An Unmet Need: An Introduction to the Symposium on Prosthetic Stimulation of the Vestibular System

Charles C. Della Santina¹, Howard J. Hoffman² ¹Dept. of Otolaryngology - Head & Neck Surgery, Johns Hopkins School of Medicine, ²Epidemiology & Statistics Program, National Institute on Deafness and Other Communication Disorders

Bilateral profound loss of vestibular sensation is disabling. Affected individuals suffer illusory drift of visual fields during head movement, chronic disequilibrium and postural instability caused by failure of vestibulo-ocular and vestibulo-spinal reflexes. Data from the Balance and Dizziness Supplement to the 2008 United States National Health Interview Survey conducted by the U.S. National Center for Health Statistics (NCHS) has revealed that 81/100K U.S. adults suffer a constellation of symptoms consistent with chronic, severe or profound bilateral loss of vestibular sensation (i.e., all of the following: dizzy in the past year, visual blurring during head movement despite little/no problem reading a newspaper [while still], unsteadiness, symptom duration >1 yr, and severity of problem "big" or "very big"). This extrapolates to ~500,000 adults in the U.S. & Europe, or ~3 million worldwide. Those reporting this symptom often stopped driving due to their symptoms and incurred a 24-fold increase in fall risk (95% Cl: 6.1-93.7) in comparison to the nationwide average. There is no adequate treatment for individuals disabled by bilateral vestibular loss despite optimal medical and rehabilitative intervention.

An implantable prosthesis that accurately emulates normal sensory transduction of head rotation could significantly improve quality of life for these individuals. Progress toward such a device has accelerated over the past decade. Speakers in this symposium will provide comprehensive introduction and update on prosthetic vestibular stimulation, including patient perspectives; the neurophysiologic basis of current prosthesis development efforts; comparison of different stimulation and encoding strategies; adaptive responses to chronic single- and multichannel stimulation; results of initial feasibility studies in humans; and updates on other recent developments in this exciting and rapidly evolving area of research. Support for NHIS: NCHS/CDC and NIDCD/NIH.

260 Losing Balance: A Patient's Perspective Richard Gannon¹

Losing vestibular sensation in both ears causes chronic unsteadiness, blurry vision, difficulty driving and increased risk of falling. I will talk about my experiences with this problem and what I hope a vestibular prosthesis can do to help me.

261 The Genesis of the Angular Vestibulo-Ocular Reflex (aVOR) Bernard Cohen¹

¹Mount Sinai School of Medicine

The last 50 years have seen an explosion of information about the structure and function of the angular vestibuloocular reflex (aVOR). Present in the same form for hundreds of million years, there is probably no sensorymotor system that is faster, more accurate, better understood, or that is more distressing when it is crippled by disease or injury. The authors, who were intimately involved in the early studies on the aVOR, will review the development of the field, with particular emphasis on the relevance of this work for generation of vestibular prostheses.

262 Responses Evoked by a Vestibular Implant Providing Chronic Stimulation. Part 1: VOR Responses Evoked by Chronic Stimulation

Daniel Merfeld¹, Rick Lewis¹, Wangsong Gong², Csilla Haburcakova², Keyvan Nicoucar¹

¹Harvard Medical School, ²Mass. Eye and Ear

Many of our studies have focused VOR responses evoked by chronic electrical stimulation provided via a vestibular implant. This talk will present a review of findings to-date as well as some of our latest research results. A brief list of findings follow: 1) Pulsatile electrical stimulation of neurons always provides excitatory stimuli; we have shown that animals accommodate to the inherent afferent response increase caused by any vestibular prosthesis. 2) We have also shown that - despite this accommodation a compensatory VOR remains and that this VOR adapts appropriately. 3) We have shown that the VOR evoked by bilateral stimulation sums in a nearly linear manner. 4) We have shown that pulsatile stimulation evokes a highfrequency eye oscillation at the frequency at which pulsatile stimulation is applied; this eye response, which could cause visual blurring, habituates substantially in about 15 minutes. In general, these studies show that the VOR adapts appropriately when pulsatile stimulation is provided chronically.

Funded by NIH/NIDCD R01 DC03066, R01 DC008167, and European Commission 225929.

263 Responses Evoked by a Vestibular Implant Providing Chronic Stimulation: II. Responses Evoked in Rhesus Monkevs

Richard Lewis¹, Csilla Haburcakova¹, Wangsong Gong¹, Daniel Lee¹, Daniel Merfeld¹

¹Harvard Medical School

We are studying the effectiveness of a semicircular canal prosthesis to improve postural control, perception of spatial orientation, and the VOR in rhesus monkeys with bilateral Balance is examined by vestibular hypofunction. measuring spontaneous sway of the body during quiet stance and postural responses evoked by head turns and rotation of the support surface; perception is measured with a task derived from the subjective visual vertical (SVV) test during static and dynamic rotation in the roll plane; and the angular VOR is measured during rotation about the roll, pitch, and yaw axes. After the normal responses are characterized, bilateral vestibular loss is induced with intratympanic gentamicin, and then multisite stimulating electrodes are chronically implanted into the ampullae of the six canals. The postural, perceptual, and VOR responses are then characterized in the ablated state, and then bilateral, chronic electrical stimulation is applied to the ampullary nerves using a prosthesis that senses angular head velocity in three-dimensions and uses this information to modulate the rate of current pulses provided by the implanted electrodes. We are currently characterizing two normal monkeys with these paradigms, and vestibular ablation and electrode implantation are planned for the near future. In one prior rhesus monkey tested with this approach, we found that a one-dimensional (posterior canal) prosthesis improved balance during head turns, perceived head orientation during roll tilts, and the VOR in the plane of the instrumented canal. We therefore predict that the more complete information provided by a three-dimensional prosthesis that modulates activity in bilaterally-paired canals will exceed the benefits provided by the one-dimensional, unilateral approach used in our preliminary studies.

Funded by NIH/NIDCD grants R01 DC006909 and R01 DC008362 to RF Lewis

264 Restoring the Sixth Sense in 3D: An Update on the Johns Hopkins Multichannel Vestibular Prosthesis Project

Charles Della Santina^{1,2}, Gene Y. Fridman¹, Chenkai Dai¹, Natan S. Davidovics², Bryce Chiang^{1,2}, Mehdi Rahman², Diana Mitchell³, Kathleen E. Cullen³, Zaven Kalayjian⁴, Andreas Andreou⁴, Americo A. Migliaccio⁵, Russell Hayden², Thuy-Anh Melvin¹, TjenSin Lie⁴, JungHo Ahn¹, Daniel Sun¹, Noble Jones¹, Nicholas Valentin² ¹Dept. of Otolaryngology - Head & Neck Surgery, ²Dept. of Biomedical Engineering, Johns Hopkins School of Medicine, ³Dept. of Physiology, McGill University, ⁴Dept. of Electrical Engineering & Computer Engineering, Johns Hopkins University, ⁵Neuroscience Research Australia A neuroelectronic prosthesis that emulates normal

transduction of head movement into vestibular nerve activity could improve the lives of individuals disabled by bilateral loss of vestibular sensation. Simultaneously achieving sufficient stimulation selectivity and intensity to accurately encode the full range of natural 3-dimensional (3D) head movements is a key challenge. We have developed electronics, electrode arrays, optimized stimulus encoding protocols and surgical techniques for a multichannel vestibular prosthesis (MVP) intended to restore 3D sensation of head rotation. In rodents and rhesus monkeys rendered bilaterally vestibular-deficient by gentamicin, the MVP partly restores the 3D vestibuloocular reflex (VOR) for head rotations about any axis, and VOR alignment improves adaptively with chronic use. Auditory brainstem responses and otoacoustic emissions demonstrate intact hearing during MVP stimulation. Our current efforts focus on refinement of electrode designs; optimization of stimulus protocols; reduction of device size and power consumption; characterization of peripheral and central effects of acute and chronic prosthetic stimulation; and creation of support tools for programming MVPs in a clinic setting.

Supported by NIDCD R01DC9255, K08DC6216, R01DC2390, F31DC10099, F32DC9917, T32DC23, T32EB3383

265 Restoring the Sixth Sense in 3D: Central Responses to Prosthetic Stimulation

Kathleen Cullen¹, Diana Mitchell¹, Charley Della Santina², Soroush Sadeghi^{1,2}

¹McGill University, ²Johns Hopkins University School of Medicine

We have previously shown that, immediately following unilateral vestibular loss, both the VOR gain and head rotation sensitivity of Type I PVP neurons on the intact side decreases dramatically (~50% of normal) but then recovers to near normal values within a few weeks (Sadeghi et al. 2010). In contrast, we have found that following bilateral loss neurons remain unresponsive to head motion even when produced by voluntary head motion. In the present study, we examined how a neuroelectronic prosthesis that emulates normal transduction of head movement into vestibular nerve activity drives the activity of central vestibular nuclei neurons to contribute to the recovery of the VOR follow bilateral vestibular loss. Single neurons were first characterized during standard eye and head movement paradigms, and then responses to biphasic current pulses delivered by vestibular prosthetic stimulation were characterized as a function of pulse amplitude. We found that once recruited, VOR interneurons and eye motion could be driven by single pulses at latencies consistent with the fixed delays of the direct VOR pathway.

Sadeghi SG, Minor LB, Cullen KE (2010) Neural correlates of motor learning in the vestibulo-ocular reflex: dynamic regulation of multimodal integration in the macaque vestibular system. J Neurosci 30:10158-68.

Supported by NIDCD R01DC2390 & R01DC9255 and by the Canadian Institutes of Health Research

266 Clinical, Scientific and Regulatory Roadmap for a Human Vestibular Implant

Jay Rubinstein¹, James Phillips¹, Kaibao Nie¹, Leo Ling¹, Steven Bierer¹, Elyse Jameson¹, Trey Oxford¹

¹University of Washington

Our team has obtained regulatory approval to proceed with the first therapeutic implantation of a vestibular neurostimulator. The first target condition for our device is refractory Meniere's Disease. This condition was chosen because its treatment with an implant is potentially superior than existing treatments, is potentially less complex than for other vestibular disorders, and represents a simpler regulatory path to clinical experience with these devices. The experience obtained with these human subjects will be combined with basic knowledge obtained in a number of laboratories around the world to develop the means to possibly treat a broad variety of vestibular disorders. For example, we have studies ongoing to determine if the device can improve VOR gain in an animal model of unilateral vestibular loss. Such studies, combined with safety data obtained in our human Meniere's trial would provide the basis for regulatory approval of human implantation in cases of chronically uncompensated unilateral vestibular loss. In addition, linkage of implanted Meniere's subjects to existing accelerometers will provide data necessary to seek approval for treating bilateral disease. These are exciting opportunities to potentially offer treatment for a variety of vestibular disorders for which there is currently little effective therapy.

(Supported by NIDCD, The Wallace H Coulter Translational Research Partnership and Cochlear, Ltd)

267 Use of Single Unit Recording to Understand the Neural Mechanism of a Vestibular Implant

James Phillips¹, Leo Ling¹, Steven Bierer¹, Albert Fuchs¹, Chris Kaneko¹, Trey Oxford¹, Kaibao Nie¹, Amy Nowack¹, Jay Rubinstein¹

¹University of Washington

Electrical stimulation of canal afferents with biphasic pulses delivered with a chronic vestibular implant produces consistent and robust slow phase eye velocities. These velocities increase with increasing stimulation current or frequency. Modulation of either of these parameters in real

time produces a predictable modulation of eve velocity across a significant range of modulation frequencies. Increasing sinusoidal AM or FM modulation frequency produces increases in peak slow phase velocity. This modulation interacts with the naturally elicited vestibuloocular reflex (VOR) to produce a summation of eye velocity. However, the dynamics of these processes are not the same. To understand the neural mechanism underlying these behavioral observations, we implanted rhesus monkeys with vestibular prostheses and recorded from vestibular nucleus neurons (VNs) during natural rotation, smooth pursuit, saccades, fixation, and electrical stimulation. VNs often displayed a time-locked discharge following electrical stimulation over a broad range of stimulation frequencies. Some neurons responded to electrical stimulation from multiple canals, but neurons typically responded at the lowest thresholds to stimulation of the canal aligned with their natural rotational sensitivity. Modulation of stimulation current did not change the discharge frequency of VNs. Summation of electrical and rotational responses did occur in individual neurons, but only at low stimulation frequencies. Changes in eye movement behavior were not fully explained by the discharge of VNs under the same conditions. These data suggest significant integration of electrically elicited vestibular signals downstream of neurons in the vestibular nucleus.

268 Vestibular Implants: First Experiments in Humans

Jean-Philippe Guyot¹, Izabel Kos¹, Alain Sigrist¹, Conrad Wall², Marco Pelizzone¹

¹ENT Department, University Hospital, Faculty of Medicine, University of Geneva, ²Jenks Vestibular Diagnostic Laboratory, MEEI, Harvard Medical School Progresses towards the development of a vestibular implant are being made by several investigators. Before such a prosthesis could be used in humans, some fundamental questions must be addressed. One is where to place the electrodes that should selectively stimulate the structures of the vestibular system. In 3 deaf patients, we demonstrated (with the collaboration of Conrad Wall) that it is possible to place one electrode in the vicinity of the posterior ampullary nerve. Biphasic pulse trains elicited vertical nystagmus whose slow component velocity could be smoothly modulated by varying pulse amplitude and pulse repetition rate. Subsequently, in 3 patients suffering from a disabling Menière's disease, we demonstrated that it is possible to place one electrode in the vicinity of the lateral ampullary nerve to elicit horizontal eye movements without stimulating the facial nerve. In both experiments, surgery was performed under local anesthesia, via the external auditory canal prior to a cochlear implantation or a transcanal labyrinthectomy. The second question we addressed is whether a human subject could adapt to continuous electrical stimulation of the vestibular system. and if it is possible to elicit eye movements via modulation of the stimulation, to mimic the angular vestibuloocular reflex. One bilaterally deaf patient with a bilateral vestibular loss received a custom modified Med-El© cochlear implant in which one electrode was implanted in the vicinity of the posterior ampullary nerve which was activated with biphasic pulse trains of 400 µs phase duration delivered at a repetition rate of 200 ppc. Eye movements were recorded using 2D binocular video oculography. Successive "on-off" cycles of continuous electrical stimulation resulted in progressively shorter duration of nystagmus responses. Once the adapted state was reached using constant stimulation, amplitude or frequency modulations of the stimulus produced smooth horizontal eye movements. Based on this patient only, results suggest however that human can adapt to electrical stimulation of the vestibular system without too much discomfort, and once in the adapted state, modulations of the electrical stimulation elicit smooth eye movements. Therefore, some prerequisites for the feasibility of a vestibular implant for human use are fulfilled.

269 Photoactivation of the Vestibular Crista Ampullaris

Suhrud Rajguru¹, Gregory Dittami², Claus-Peter Richter^{1,3}, Stephen Highstein⁴, Richard Rabbitt^{2,4} ¹Northwestern University, Chicago, IL, ²University of Utah, ³Hugh Knowles Center, Northwestern University, ⁴Marine Biological Laboratory

Results from the oyster toadfish, O. tau, showed that the semicircular canal crista ampullaris is exquisitely sensitive to infrared radiation (IR) applied in vivo. IR pulse trains (1862nm, ~200 µs/pulse, 1-100 pulses/sec.) delivered to the sensory epithelium by a 200 µm optical fiber coupled to a diode laser evoked changes in phasic and tonic discharge rates of post-synaptic afferent neurons. Phasic afferent responses to pulsed IR occurred with a latency of <8ms while tonic responses developed with a time constant of ~7ms-10sec following the onset or cessation of the radiation. Afferents responded to direct irradiation of the sensory epithelium but did not respond to thermal stimuli generating equivalent temperature increases of the whole organ. Some afferent neurons fired an action potential in response to each IR pulse delivered to the sensory epithelium, at phase-locked rates up to 96 pulses per second. The latency between IR pulses and afferent nerve action potentials was ~7.6ms, much greater than synaptic delay and spike generation. The long latency suggests that there is a signaling delay interposed between the IR pulse and the action potential. To examine potential origins of the IR-evoked responses, neonatal rat ventricular cardiomyocytes (myocytes) were loaded with Fluo-4 AM and excited by pulsed IR. IR stimuli evoked robust intracellular [Ca2+] transients in myocytes followed by ryanodine-sensitive [Ca2+] spikes. Pharmacological results from the myocytes and cochlea implicate a combination mitochondria mNCX, MCU and thermally gated TRPV ion channels as the most likely source of IRevoked calcium transients. While the biophysical mechanism(s) underlying the sensitivity of mitochondria or TRPV to IR remain unknown, IR modulation of intracellular [Ca2+] in hair cells can lead to the modulation of synaptic transmission and resulting afferent nerve discharge as observed.

Supported by NIH R01DC006685, R01DC004928 (Rabbitt, RD) and R41DC008515 (Richter, CP)

270 Role of the Na/K ATPase in Development and Function of Drosophila Johnston's Organ Dan Eberl¹

¹Universitv of Iowa

The Na/K ATPase is an integral membrane protein important for establishing and maintaining Na and K gradients across plasma membranes and across epithelia. It can function as an ion pump, as a signal transducer to the nucleus, or as a cell adhesion component. In Drosophila, the alpha subunit and the nrv3-gene-encoded beta subunit, are required for hearing. The alpha subunit is highly upregulated and essential in the scolopale cells of Johnston's organ, while nrv3 may be restricted to the sensory neurons. I will summarize fly hearing, and discuss how these two subunits contribute to auditory system development and function.

271 Stem Cells and Smell Cells: The Developmental Pathways Underlying Olfaction Randall Reed¹

¹Johns Hopkins University

Mammalian sensory systems are faced with two major challenges - they must detect information about the outside world with exquisite sensitivity and specificity while at the same time protecting themselves from the hostile environment that provides the sensory stimulation. In olfaction, the sensory neurons are directly exposed to the toxins, pathogens and environmental hazards that we breathe every day. The olfactory system has the capacity to regenerate new neurons throughout adult life from at least two distinct populations of progenitors. This regeneration is highly regulated during normal life and in disease states including acute trauma and inflammation. We are currently elucidating the origins and regulation of tissue-specific stem cells responsible for initial establishment and continually regeneration of olfactory neurons throughout adult life and repopulation of the tissue after environmental assault.

272 Molecular Regulation of Taste Bud Development and Regeneration Linda Barlow¹

¹University of Colorado School of Medicine

Taste buds are multicellular sensory organs, which possess both neural and epithelial characteristics. Like neurons, taste receptor cells transduce external stimuli into electrochemical signals, which are conveyed to the brain by synapses on gustatory nerve fibers. However, taste buds closely resemble epithelial cells, in that they develop directly from oral and lingual epithelia rather than from neurogenic ectoderm during embryogenesis; and taste cells are continually renewed from proliferative basal keratinocytes throughout adult life. To date, both the Wnt/ß-catenin and Shh pathways have been shown to regulate embryonic development of taste buds. Now, we have begun to explore how these pathways regulate adult taste cell renewal, and if altering Wnt or Shh signaling in adult mice also influences taste-mediated behavior.

273 Intrinsic and Extrinsic Factor Regulation of Mammalian Photoreceptor Development Nadean Brown¹, Amy N. Riesenberg¹

¹*Cincinnati Childrens Hospital Research Foundation* This talk presents an overview of multiple inputs regulating rod and cone photoreceptor development. A hierarchy of transcription factors controls this process: including Otx2 and Crx, which demarcate bipotential photoreceptor precursor cells; and Nrl and Nr2e3, which promote rod fates. Our lab and several others have demonstrated that in the mouse retina Notch signaling cell autonomously suppresses photoreceptor development, particularly that of cones. Interestingly, this block occurs upstream of Otx2, Crx, Nrl and Nr2e3 activation. However, it remains unclear whether Notch signaling suppresses cell cycle exit, or the transcriptional activation of early photoreceptor pathway genes.

274 Hair Cell Development: The Yin and Yang of Atoh1 Regulation Matthew Kelley¹

¹Laboratory of Cochlear Development, NIDCD/NIH

Hair cells act as the primary transducers of mechanosensation in the auditory and vestibular systems of all vertebrates, as well as in the lateral line neuromasts in fish and amphibians. The identification of the basic Helix-Loop-Helix transcription factor Atoh1 as a molecule that is both necessary and sufficient for the formation of hair cells represented a significant milestone in our understanding of how hair cells are formed. More recently, in an effort to understand how the number and position of hair cells within the inner ear are determined, research from a number of laboratories has examined the signaling pathways and specific molecules that regulate the expression of Atoh1. Interestingly, to date, the results of these efforts have identified more factors that apparently act to inhibit Atoh1 expression and/or activity (Sox2, Ids, Ngn1, NeuroD1, Fgfr3, and Notch signaling), than act to promote Atoh1 activity (Wnt/beta-cat, Fgf20). The results of these studies are leading to the elucidation of a signaling web involving both upstream and downstream components as well as reciprocal signaling interactions that synergize to precisely regulate Atoh1 expression/activity and therefore hair cell formation. In this talk I will summarize these data and discuss outstanding issues that should be addressed in future research projects.

275 Getting to the Root of Stereocilia Development

Inna A. Belyantseva¹, Thomas B. Friedman¹ ¹NIDCD/NIH

Bundles of unidirectionally oriented actin filaments support many chemo- and mechano-sensory cellular processes including microvilli, Drosophila bristles, and inner ear hair cell stereocilia. Although derived from microvilli, stereocilia have a more elaborate shape and structure. They are longer and larger in diameter, have a different set of Factin cross-linking proteins, a well-developed taper region, and prominent rootlets. Fundamental questions pertaining to the development of stereocilia have not yet been answered. What mechanisms regulate the mature stereocilia length and width and how are stereocilia rootlets formed? What proteins are crucial to shape and maintain the stereocilia taper? Recent data on twinfilin, GRXCR1, TRIOBP and taperin have shed light on some of these questions.

276 Regeneration of Hair Cells in Mature Animals

Jennifer Stone¹

¹University of Washington

Regeneration of hair cells requires production of new cells and acquisition of proper fates to re-establish epithelial patterning. This process is not simply a recapitulation of development; however, signaling pathways critical for embryogenesis are indeed re-activated once damage occurs. I will discuss properties of hair cell progenitors in mature birds and molecular processes that direct new hair cell formation using mitotic and non-mitotic mechanisms. I will address signals that control differentiation and maintenance of regenerated hair cells, with comparisons to development in birds and mammals. Finally, I will examine strategies for forming new hair cells in mature mammals after damage.

277 Temporal Integration Within the Thalamus Due to Electrical Stimulation of the Inferior Colliculus

Roger Calixto¹, Minoo Lenarz^{1,2}, Anke Neuheiser¹, Thomas Lenarz¹, Hubert Lim^{1,3}

¹Hannover Medical University, ²Universitätsklinik Regensburg, ³University of Minnesota

Two clicks, when presented in short temporal succession (~5ms window), are perceived as one event with a lower threshold (1). Consequently, somewhere along the auditory pathways sequential information is being integrated. Here we present data demonstrating that at least part of this integration is performed within the thalamus.

Experiments were performed in seven ketamineanesthetized guinea pigs. We electrically stimulated different regions of the central nucleus of the inferior colliculus (ICC) with an auditory midbrain implant (ring electrodes along a silastic carrier of 0.4 mm diameter; Cochlear Ltd.) while recording neural activity from the primary auditory cortex (A1). Stimuli consisted of 2 biphasic. 200µs/ph. cathodic-leading pulses with amplitudes up to 54dB (re.1µA). Interstimulus delays (ISDs) varied between 0.5-100ms. Cortical local field potentials (LFPs) were averaged and the LFP areas were calculated. We particularly analyzed the responses on A1 sites with a similar best frequency to the stimulated ICC sites (0.15±0.11 octave differences).

We observed that stimulation of all ICC sites elicited a marked increase in A1 LFP area with for ISDs less than 6ms when compared to the area for ISDs between 6-10ms. This enhancement of activity increased continuously as ISD decreased to 2ms at which the LFP area decreased with shorter ISDs. This decrease in LFP area appears to be due to the refractory period of the activated neurons. When we stimulated 2 separate locations within a similar ICC frequency lamina with one pulse on each site instead of 2 pulses on the same site, we did not observe this refractory effect. Instead, the LFP areas continued to increase with shorter ISDs.

In conclusion, temporal integration is observed for input activity into A1 induced by electrical stimulation of output projections from the ICC, thus appears to occur within the auditory thalamus. Since greater enhancement was achieved through multi-site stimulation, the thalamus may rely on integrating inputs across neurons along the isofrequency dimension of the ICC.

1) Viemeister NF, Wakefield GH. Temporal integration and multiple looks. J Acoust Soc Am. 1991 Aug;90(2 Pt 1):858-65.

This research was supported by the SFB 599 and Cochlear Ltd.

278 Top-Down Modulation of Stimulus-

Specific Adaptation in the Auditory Thalamus Flora Antunes¹, Manuel Malmierca¹

¹Auditory Neurophysiology Unit. Institute of Neuroscience of Castilla y León. Salamanca, Spain

The adaptation of neuronal responses to a repeated stimulus (Stimulus-specific adaptation, SSA), provides a mechanism for emphasizing rare and potentially interesting sensory events. SSA has been demonstrated to occur from the midbrain up to the auditory cortex in the auditory pathway (e.g., Ulanovsky et al., 2004; Malmierca et al., 2009). For similar stimulation conditions, using an oddball paradigm, we have demonstrated that the medial geniculate body (MGB) of the thalamus exhibit SSA levels (Antunes et al., 2010) as high as those found in the inferior colliculus and primary auditory cortex (AC). This adaptation is very strong in the non-lemniscal MGB, i.e., in the dorsal and medial subdivisions, with the medial subdivision exhibiting the strongest SSA levels. The MGB receives massive descending projections from the AC, raising the hypothesis that this strong SSA is inherited by the MGB through the corticothalamic pathway.

Here, we recorded from single neurons throughout the MGB of the anaesthetised rat, before, during and after reversibly inactivating the auditory cortex using a cooling loop (Lomber et al., 1999), while presenting the oddball paradigm. Our results show that the responses (i.e., firing rate, frequency response area, and first spike latency reliability) of the high SSA neurons change during AC inactivation. However, their degree of SSA remains mostly unaffected. These data suggest that the AC does not pass on this property to the non-lemniscal MGB, but rather, it regulates SSA in a delicate gain control manner.

Financial support was provided by the Spanish MEC (BFU2009-07286), EU (EUI2009-04083) and JCYL-UE

(GR221) to MSM; FMA held a fellowship from the Spanish MEC (BES-2007-15642).

279 Multiple, Simultaneous Recordings in Two Auditory Cortical Areas in the Awake, **Behaving Primate**

Elliot Smith¹, Bradley Greger¹

¹University of Utah

Much of the neurophysiology in the awake, behaving primate has utilized acute single electrode recordings. In order to gather simultaneous information about response properties of populations of auditory neurons, we recently implanted two microelectrode arrays in a rhesus macaque trained on two-alternative forced-choice detection and delayed match-to-sample discrimination tasks. One array was implanted several millimeters within the lateral fissure and the second was implanted on the superior temporal gyrus, in the rostral parabelt area of auditory cortex. We've recorded isolated units and local field potential in response to pure tone and band-passed noise stimuli on both arrays simultaneously during task performance. We examined responses of multiple units in different locations to the same stimulus at the same time. Peri-stimulus time histograms and spectrotemporal receptive fields were generated for multiple units over many trials of the same stimulus between tasks. The majority of these units have narrow frequency response contours and short latencies, suggesting that the lateral fissure array is indeed implanted in core auditory cortex. Future work will emphasize observation of population encoding and decoding of auditory stimuli in the awake, behaving primate. This will include examining the differences in spatiotemporal patterns of activity across the electrode arrays in response to the same stimulus, between tasks. We will also examine the representation of auditory information in parabelt cortex as well as any transformation of information that may occur between the two cortices in a putative rostral auditory processing stream.

280 Sensitivity and Validity of the ACC for **Speech-Modeled Frequency Transitions** Barbara Cone¹, Daniel Duran¹

¹Universitv of Arizona

The Acoustic Change Complex (ACC) is a cortical auditory evoked potential (CAEP) obtained in response to an acoustic change in an otherwise steady-state stimulus. The ACC may be used as an estimate of the neural capacity for stimulus discrimination. ACCs have been obtained in response to changes in frequency, amplitude, vowel formant and consonant manner, as well as to the amplitude modulation present in consonant-vowel or vowel-consonant transitions. The purpose of this experiment was to determine the validity and sensitivity of the ACC in response to stimuli modeled on second formant (F2) vowel-to-consonant transitions. Validity was defined as the ACC being present only for the stimuli that had a frequency change and not for the steady-state control stimulus. Sensitivity was defined as the likelihood that ACC was present for perceptible frequency changes. Thirteen adult listeners were tested using ascending and

descending stimulus sets, in which frequency transitions from 825-1000 Hz, with a 25-150 Hz step size, were embedded. The stimuli were modeled after the F2 changes for the consonant-to-vowel portion of /ugu/ as measured by Perceptual performance indicated Öhman (1965). discrimination thresholds of 17-20 Hz, while ACCs were present for frequency-steps of 50 Hz or greater. Using a conservative statistical criterion for judging the presence of ACC, the sensitivity of ACC with respect to perceptual performance was > 80% and validity was 100%, with no false positives for the no-change control condition. The amplitude of the ACC varied systematically with the frequency-step size with a slope of 0.01 µV/Hz. ACC latency was stable over the range of frequency steps tested. The ACC appears to be a valid and sensitive electrophysiologic index of acoustic feature discrimination in adults and might prove useful to estimate speech feature discrimination ability in infants.

281 Mapping Tonotopy in Human Auditory **Cortex Using Minimally Salient Tone Stimuli**

Dave Langers¹, Pim van Dijk¹ ¹UMCG - University Medical Center Groningen

Tonotopy is a primary organizational principle in the entire auditory processing pathway. However, in spite of numerous neuroimaging studies, the layout of tonotopic gradients in human auditory cortex is still debated. In this functional magnetic resonance imaging (fMRI) study, we identified tonotopic maps using minimally salient (i.e. soft and unattended) auditory stimulation to avoid widespread activation.

20 subjects with normal hearing (<20 dB HL at 250-8000 Hz) were presented with 100-ms tones at a frequency of 1/4, 1/2, 1, 2, 4, or 8 kHz, a level of 25 or 45 dB HL, and a rate of 5 Hz. At the same time, subjects performed a task that involved the emotional assessment of displayed pictures (negative/neutral/positive); this task was chosen to be highly engaging, but completely unrelated to the sound stimuli. A sparse fMRI sequence (TA 2 s; TR 10 s; 1.5×1.5×1.5 mm³ resolution) was used to record evoked responses in the temporal lobe.

Activation to all twelve conditions (6 frequencies \times 2 levels) was extracted with a standard fMRI regression model. Activation to low-frequency stimuli peaked in lateral Heschl's Gyrus (HG); with increasing frequency, activation progressively shifted to bordering regions in the anterior and posterior flank of medial HG.

In addition, we performed principal component analysis on the responses of all activated voxels, identifying a component that reflected differential activation to low or high frequency stimuli in a pattern consistent with the aforementioned gradients.

Our results suggest the existence of at least two abutting tonotopic gradients more or less perpendicular to HG. This diverges from previous literature that suggests gradients along the axis of HG, but closely agrees with other recent findings (e.g. Humphries et al., Neuroimage 2010).

The present study shows that reliable tonotopic maps can be obtained with fMRI using minimally salient sound presentations.

282 Adaptation to Global Temporal Statistical Structure of Sounds in the Mammalian Auditory Cortex Maria Geffen¹

¹University of Pennsylvania School of Medicine

By the efficient coding hypothesis, sensory systems have evolved specialized neural mechanisms to efficiently encode information about the environment. The temporal structure of environmental sounds within a particular spectral channel scales with its center frequency. Recent studies showed that in the primary auditory cortex (A1), neuronal encoding of sounds is highly context-dependent (Azari and Zador, 2010).

We recorded neuronal responses in A1 to a novel stimulus, in which the global temporal structure was controlled relative to the frequency of the specific spectral band. We examined the changes in encoding of the local spectro-temporal information, in the context of varying global temporal structure of the sound. Reliable spectrotemporal receptive fields could be mapped for 20% of recorded neurons. 33% of these neurons (group 1) responding to sounds exhibited adaptation in their receptive field structure, which mimicked the global temporal structure of the stimulus. No changes were detected in the receptive field of 26% of these neurons (group 2). 16% of the neurons exhibited a temporal reversal effect (group 3): the receptive field of these neurons contained a secondary, temporally delayed receptive field, which accelerated as the temporal structure of the stimulus slowed down.

A two-pathway linear-non-linear model was fitted to the neuronal responses, using the spectro-temporal envelope of the stimulus as the basis for one pathway, and the chirponset matrix as the basis for the second pathway. The responses of neurons in group 2 were best fitted by the second pathway, and thus may be described as chirp detectors. The responses of the rest of the neurons could be modeled as a linear combination of the two pathways, whose relative weight was adjusted based on the global structure of the stimulus.

Thus, the two-pathway model based on the envelope and the chirp-onset structure of the stimulus accounts for the global temporal of the context-dependent effects.

283 Exploring the Relationship Between Principles of Temporal Coherence and Coding Strategies in the Auditory System Michael Carlin¹, Mounya Elhilali¹

¹The Johns Hopkins University

Analysis of modulation profiles of natural sounds such as speech suggests that slow temporal modulations are a signature feature of such sounds and likely underlie important aspects of robust sound perception. To what extent this notion of slow temporal coherence is reflected in the coding principles of auditory cortex and how it reconciles with known sparse properties of cortical ensembles remains unclear. In this study, we explore (1) how the principle of temporal coherence captures the statistics of natural acoustic signals over time and (2) how coherence influences the characteristics of a computational model of auditory cortical spectro-temporal receptive fields (STRFs). By constraining the ensemble output to be coherent in time, the resulting learned receptive fields shed light on connections between coherence and sparseness in auditory sensory representations. Moreover, the approach provides a new framework for understanding coding strategies in the auditory system.

284 Neural Selectivity for Vocalizations in Auditory Scenes Transforms Between the Primary and Secondary Auditory Forebrain David M. Schneider¹, Sarah M. N. Woolley¹

¹Columbia University

Vocalizations often occur in noisy and distracting environments. Psychophysical experiments and everyday experience suggest that the brain may suppress background sounds and/or selectively amplify target sounds. However, the neural mechanisms by which these processes are accomplished remain unclear. Here, we investigated how the neural encoding of vocalizations changed with varying levels of background sound by recording from neurons along the auditory pathway of awake zebra finches. We recorded from single neurons in the auditory midbrain (MLd), primary forebrain (Field L) and secondary forebrain (NCM) during free-field presentation of individual zebra finch songs, a zebra finch chorus and auditory scenes composed of individual songs and the chorus. Auditory scenes were presented with varying signal-to-noise ratios (SNRs) by systematically varying the song intensity between +/- 15dB while keeping the chorus intensity constant.

MLd and Field L neurons responded strongly to song, chorus and auditory scenes. For these neurons, average firing rates to song decreased linearly with sound level, and firing rates to scenes were largely SNR invariant. Conversely, NCM neurons fired more strongly to song than to chorus or scenes. In NCM, firing rates to song decreased non-linearly and firing rates to scenes were highly dependent on SNR.

SNR had a strong impact on the spike train structure of Field L and MLd neurons. At high SNRs, neural responses to scenes closely resembled responses to song. As the SNR decreased, neural responses to the scene linearly transformed to more closely reflect responses to the chorus. In NCM, neural responses to high SNR scenes resembled neural responses to song, but as the SNR decreased, neurons abruptly ceased firing. These data show that the neural representation of auditory scenes is markedly transformed between Field L and NCM, where neurons may extract signal from noise during the processing of individual vocalizations in background sounds.

285 Specialization of Auditory Cortices for Sound Localization Cues

Heather Read¹, Nathan Higgins¹, Douglas Storace¹ ¹University of Connecticut

Dual stream models highlight a functional division for processing "where" and "what" a sound is, based on differences in parabelt cortex in primates. Here we ask if core and belt cortices in rat might have a similar functional duality. High-resolution optical imaging was employed to delineate the borders between three core, and four putative belt auditory regions in the rat temporal cortex. This allowed us to compare responses across regions in the same animal. Multi-unit spike rate responses to noise with varying interaural level difference (ILD) cues were probed as a measure of neural sensitivity to sound position in the horizontal dimension. Responses were compared across primary (A1) and ventral (VAF) auditory fields and caudal and rostral halves of the putative belt region, suprarhinal (SRAF) auditory field. A continuous range of tuning to ILD cue was observed across all cortical regions. The highest degree of horizontal position cue tuning was observed in VAF and caudal SRAF. Conversely, the lowest was observed in A1 and rostral SRAF. SRAF was further specialized as it had the highest number of sites exhibiting spike rate facilitation for midline position cues with binaural versus monaural sound presentation. These data suggest that caudal and rostral cortices are specialized to respond to sounds near and far from the body midline, respectively. These distinctions of core and putative belt cortex in the rat could be the antecedent of the "what" and "where" functional divisions of parabelt cortices observed in primates.

286 fMRI and Multi-Voxel Pattern Analysis of Direction of Spatial Auditory Attention in Human Auditory Cortex

Lingqiang Kong¹, Jascha D. Swisher², David C. Somers¹, Barbara Shinn-Cunningham¹

¹Boston University, ²Vanderbilt University

Single-unit recordings of auditory activity in anesthetized animals reveal broad spatial tuning in cortical responses to sound. However, spatial sensitivity in cortex is both enhanced in awake animals engaged in a spatial (vs. a non-spatial) task (Lee, Macpherson, and Middlebrooks, 2009) and more pronounced when competing streams are present than when a single source is presented from various directions (Middlebrooks, ARO, 2010). These results suggest that spatially based attention modulates cortical responses to sound, even if spatial effects are relatively weak in the absence of competition for attention. Here, listeners were asked to perform a simple one-back memory task in one of two competing streams (one from the left, one from the right). By forcing listeners to direct spatial attention to one of two simultaneous, competing streams, we hoped to enhance spatial auditory sensitivity in cortical responses observed through functional MRI. To this end, we contrasted the BOLD response in an "attend" condition, in which subjects attended to an auditory stream based on its direction, to responses in a "passive" condition, in which subjects were told to passively listen to

both streams. Traditional univariate analysis based on a general linear model showed a significant, bilateral increase in auditory cortex activation when subjects attended to a particular direction compared to passive listening. However, this analysis did not reveal any significant difference between attend-left and attend-right conditions. In contrast, a multi-voxel pattern analysis method applied to activation patterns in auditory cortex was able to predict the attended direction with an accuracy significantly better than chance. These results provide further evidence that human auditory cortex is modulated by spatially directed attention, even when effects are not evident in large-scale changes in BOLD amplitude. [Supported in part by CELEST, an NSF Science of Learning Center (NSF SBE-0354378)]

287 Activations of Human Auditory Cortex During Spatial Discrimination and Memory Tasks

Teemu Rinne^{1,2}, Sonja Koistinen¹, Patrik Wikman¹ ¹Institute of Behavioural Sciences, University of Helsinki, Finland, ²Advanced Magnetic Imaging Centre, Helsinki University of Technology, Finland

Our previous study (Rinne et al, J Neurosci, 2009) compared activations of the human auditory cortex (AC) during pitch discrimination and memory tasks. The results showed distinct functional differences between anterior and posterior AC during the two non-spatial tasks. In the present study, we compared AC activations during spatial discrimination and memory tasks in an otherwise similar experiment.

During spatial (n-back) memory blocks (duration 15 s), subjects were required to attend to sounds (duration 200 ms, mean rate 0.9 s) consisting of two successive 90 ms noise bursts (0 or 15° location difference between the parts). The sounds were presented either 75-120° to the left, 75–120° to the right, or $\pm 15^{\circ}$ of midline. Subjects' task was to indicate when a sound belonged to the same spatial category (left, right, or middle) as the one presented 1-3 trials before (depending on the difficulty level). In spatial discrimination blocks, the sounds were otherwise similar as during the memory blocks but the first and last half of each sound were separated by 0, 30, 45 or 60° (depending on the difficulty level). Subjects were required to indicate when the two halves of a sound were presented from the same location. During visual attention blocks, subjects detected slight luminance changes in visual taskinstruction symbols. Before the experiment, subjects (N=16) were carefully trained to perform the demanding tasks.

Initial fMRI data analysis showed bilateral AC activations to task-irrelevant sounds presented during the visual task. These activations were strongly dependent on whether subjects performed spatial memory or discrimination tasks and there was a distinct difference between the anterior and posterior AC activation patterns during these tasks. In particular, spatial discrimination was associated with increased activations in the anterior AC while spatial memory was associated with increased activations in the posterior AC. Together our previous and present results indicate that discrimination and memory tasks activate anterior and posterior AC areas differently and that this anterior-posterior division is present both when these tasks are performed on spatially invariant (pitch discrimination vs. memory) or spatially varying (spatial discrimination vs. memory) sounds.

288 Binaural Responses of Primary Auditory Cortex and Posterior Auditory Field in Congenitally Deaf Cats

Peter Hubka¹, Jochen Tillein², Andrej Kral¹ ¹Medical University Hanover, ²MedEl Company

Congenital deprivation of auditory inputs was shown to cause substantial deficits in the ability of the primary auditory cortex to process and represent incoming information. Despite these deficits, peripheral stimulation of auditory nerve is still able to reach and activate cortical structures in the field A1. Further spread of the activation to nonprimary auditory fields has, however, not yet been investigated. Present study is aimed on the functional analysis of responses in the primary auditory cortex and the posterior auditory field (PAF) evoked by binaural electrical stimulation using cochlear implants. Local field potentials from four congenitally deaf cats (CDC) and three hearing controls were recorded simultaneously in AI and PAF by means of two 16-channel microelectrode arrays (Neuronexus probes). All animals were electrically stimulated; binaural responses were evoked by pulse trains (500Hz, 3 pulses) at intensities of 0-10 dB above response thresholds. In CDC, the cortical activation in PAF was repeatedly found in latency range corresponding to the activation pattern in hearing controls (peak latencies in the range of 20-30 ms) indicating propagating activation from the primary cortical fields. Amplitudes of the evoked responses were significantly smaller in PAF of CDCs. Significant differences were found also in distribution of their latencies. These results demonstrate that PAF can be activated by cochlear implants stimulation in deaf cats. However, substantial decrease in LFP amplitudes together with changed latency distribution in PAF indicate reduction bottom-up propagation of activity of and/or its desynchronisation in deaf animals.

289 Neurodegeneration After Repeated Noise Trauma Within the Central Auditory Pathway

Moritz Gröschel^{1,2}, Anne Stehr¹, Romy Götze², Sebastian Jansen², Arne Ernst¹, Dietmar Basta^{1,2}

¹Dept. of ENT, Unfallkrankenhaus Berlin, Germany, ²Dept. of Biology, Humboldt-University of Berlin

Noise exposure leads beside cochlear hair cell loss to profound long term changes within the central auditory pathway. A modified spontaneous activity, neurodegeneration and changes in neurotransmitter action were reported for several auditory structures. Recent studies have shown that a single noise trauma is followed by a dramatic reduction of cell densities in several structures involved in central auditory processing. This effect occurs within the first days after acoustic overstimulation and is accompanied by a significant hearing loss. By now, it remains unclear to what extend the affected structures are influenced in case of a recurrence of traumatic impact. The present study should thus clarify the effect of a second noise exposure on hearing thresholds and cell densities within the ascending auditory pathway. Therefore, normal hearing mice were noiseexposed (3h, 115 dB SPL, white band noise 5-20 kHz) under anaesthesia. One group was kept in their home cages, whereas the remaining animals received a second noise trauma one week later under similar conditions. Fourteen days after the first treatment, hearing thresholds were determined in both experimental groups by measurements of the frequency specific auditory brainstem response. In addition, cell densities were determined in auditory brain areas using histological staining techniques to identify a modified cytoarchitecture. The results demonstrate that auditory thresholds are only slightly increased after a second noise exposure. In contrast, anatomical data show a significant cell loss in these animals compared to the single noise exposure group. This holds true for most investigated structures, whereby changes occur to a lesser extend in relation to the first noise trauma.

290 Neural Deficits in Auditory Temporal Processing in Auditory Thalamus of Ectopic BXSB/MpJ Mice

Lucy Anderson¹, G. Bjorn Christianson¹, Jennifer Linden^{1,2}

¹Ear Institute, University College London, ²Dept. Neurosci., Physiol. & Pharmacol., University College London

How does the mammalian auditory system perform the complex temporal processing required for the perception of sound? The answer to this question may become clearer if we can understand how malfunctions of the auditory system cause auditory temporal processing deficits. In humans, auditory processing deficits such as difficulty perceiving rapidly changing sounds are often associated with developmental disorders, such as dyslexia. Inbred mice of the BXSB/MpJ strain are one of the best animal models of auditory temporal processing disorder. Approximately half the animals within a BXSB/MpJ litter develop malformations in their prefrontal and parietal cortices whereby nests of neurones (ectopias) form in layer I. These ectopias are similar to those observed in some humans with developmental disorders.

Previous behavioural work has shown that despite having normal hearing sensitivity, ectopic male BXSB/MpJ mice have auditory temporal processing deficits, such as difficulty perceiving rapid changes in sounds. In other animal models of auditory temporal processing disorder, neocortical micro-abnormalities like ectopias have been associated with anatomical abnormalities in the auditory thalamus. Here, we report evidence for physiological abnormalities in the auditory thalamus of ectopic male BXSB/MpJ mice. We recorded from single neurons and multi-neuron clusters throughout the auditory thalamus of male BXSB/MpJ mice and found neural deficits in auditory temporal processing in ectopic animals. In particular, neurons recorded from ectopic males had significantly attenuated responses to brief gaps in noise and lower limits of synchronised following to rapid trains of clicks, compared to non-ectopic animals. Other aspects of thalamic processing, such as first-spike latency distributions and response thresholds, were normal. Thus, ectopic male BXSB/MpJ mice appear to have a specific neural deficit in auditory temporal processing, which is evident at the level of the thalamus.

Supported by the Wellcome Trust.

291 Reduced Auditory Lateral Suppression in Schizophrenia

Joel Snyder¹, Erin Ramage¹, David Weintraub¹, Griffin Sutton¹, Erik Ringdahl¹, Aaron Boren¹, Nick Thaler¹, Daniel Allen¹

¹University of Nevada

Auditory processing deficits such as impaired frequency discrimination and reduced suppression of auditory brain responses have been documented in individuals with schizophrenia (SZ). These auditory processing deficits may contribute to abnormal social interactions by interfering with the accurate perception of vocal affect during conversation. Lateral suppression of non-stimulated neurons by stimulated neurons, which has not been previously assessed in SZ, likely plays an important role in precise encoding of sounds during frequency-based auditory tasks. Therefore, the purpose of this study is to determine whether lateral suppression of activity in auditory cortex is impaired in SZ patients. SZ patients and control participants watched a silent movie with subtitles while listening to trials composed of a 0.5 s control stimulus (CS), a 4 s comb-filtered masking noise (CFN), and a 0.5 s test stimulus (TS). The CS and TS were identical on each trial and had energy corresponding to the high energy (recurrent suppression) or low energy (lateral suppression) portions of the CFN. Event-related potentials were recorded during stimulus presentation, and suppression was measured as the change in amplitude between the CS and TS. Mean amplitude of the auditory P2 component (160-230 ms) showed no group differences for recurrent suppression, but SZ patients showed reduced lateral suppression for this component. This reduced lateral suppression in SZ patients may lead to overlap of neuronal populations representing different auditory stimuli. Such imprecise neural representations may contribute to the difficulties SZ patients have in discriminating simple auditory stimuli in laboratory tasks and more complex stimuli such as vocal affect in everyday life.

Supported by a President's Research Award from the University of Nevada, Las Vegas and NIH grant R21MH079987.

292 Multi-Electrode Configurations to Focus and Steer Electrical Current with Cochlear Implants

Julie Bierer¹

¹University of Washington

A major limiting factor of cochlear implant performance in complex listening environments is spectral resolution. I will discuss two techniques intended to improve the transmission of spectral information by using multiple current sources to manipulate spatial activation along the cochlea. First, current focusing (e.g., partial tripolar, phased array) can lead to potentially less channel interaction but is limited by higher current requirements and sensitivity to the electrode-neuron interface. Second, current steering can create intermediate pitch percepts but may not translate to a greater number of independent spectral channels. Potential approaches for patientspecific implementation of these techniques will be discussed.

293 Combining Acoustic and Electric Stimulation

Christopher Brown¹

¹Arizona State University

Many deaf or severely hearing-impaired individuals can understand speech in quiet environments using a cochlear implant. However, their speech understanding typically declines significantly in even small amounts of background noise. For individuals who retain some low frequency hearing, combining electric and acoustic stimulation (EAS) can significantly improve speech understanding, particularly in background noise. We have characterized the cues responsible for this EAS benefit, and are working to use this information to extend the benefits of EAS to those implant users who do not possess enough residual hearing to show a benefit typically, and to enhance this benefit for those who do.

294 Binaural Sensitivity in Bilateral Cochlear Implant Users Ruth Litovsky¹

¹University of Wisconsin

Despite the success of cochlear implants, many listeners have a gap in performance relative to normal hearing people. Bilateral cochlear implants have been provided to thousands of patients world‐wide in order to improve functional abilities such as sound localization and speech recognition in noise. However, clinical processors are fitted independently in the two ears, thus binaural cues are not provided to listeners with fidelity. This talk will present recent findings using research processors are discussed in the context of auditory development and plasticity, in children and adults who have undergone varying degrees of auditory deprivation prior to implantation

295 Understanding and Improving Pitch Perception by Cochlear Implant Users

Robert Carlyon¹, Olivier Macherey¹, John Deeks¹ ¹MRC Cognition & Brain Sciences Unit

Although many cochlear implant (CI) users understand speech well in quiet, pitch perception is usually poor. As a result, CI users have trouble in "picking out" one voice from a mixture, and their enjoyment of music is greatly diminished. This talk will discuss the limitations inherent in the two ways CI users extract the pitch of a sound, and describe ways in which these limitations can be partially overcome. Variations in temporal pitch can be produced by varying the periodicity of an electric pulse train. Temporal pitch suffers from an upper limit, typically 300 Hz, above which it does not increase. This limit is not specific to pitch perception and, in bilaterally implanted users, can be observed in tasks where subjects judge the location of a sound. The limit is impervious to many stimulus manipulations, including those designed to reduce the deterministic nature of the auditory nerve response. It can, however, be raised slightly by selectively stimulating the apex of the cochlea, probably as a result of better neural survival in that region. Pitch changes produced by varying the place of excitation within the cochlea are limited by current spread and, in "bipolar" stimulation, by a bimodal pattern of neural excitation. These limitations can be alleviated by focussed stimulation methods and/or by the use of asymmetric pulse shapes.

296 Protective and Plastic Effects of Neurotrophins and Chronic Intracochlear Electrical Stimulation

James Fallon^{1,2}, Robert Shepherd^{1,2} ¹Bionic Ear Institute, ²Department of Otolaryngology,

University of Melbourne

Sensorineural hearing loss initiates a cascade of anatomical and functional changes within the auditory system. The secondary loss of spiral ganglion neurones (SGNs), the target cells of cochlear implants, is the most critical peripheral change: and there are a range atrophic changes within the central auditory pathway. However, equally important are the functional changes, particularly the degradation in spatial (spectral) and temporal processing, that occur within the central auditory pathway. Numerous studies over the past decade have demonstrated that the intracochlear application of exogenous neurotrophins and chronic electrical stimulation (NT+ES) can prevent the ongoing degeneration of SGNs. Chronic behaviourally relevant ES has also been shown to reverse some of the deafness induced changes in central auditory processing. However, clinically relevant neurotrophin delivery methods are not currently available; nor are the effects of chronic NT+ES treatment on the processing within the central auditory pathway clear. We have therefore developed a long-term, clinically relevant neurotrophin delivery method, that when combined with ES from a cochlear implant results in significant SGN survival. We have also assessed the functional consequences of chronic NT+ES delivery on processing within the central auditory pathway, and found that NT+ES treatment has no

adverse affects on spatial processing. The timely clinical application of chronic neurotrophin treatment and cochlear implantation should result in improved performance for cochlear implant patients by preventing (or reducing) much of the secondary degenerative changes within the auditory system and reversing some of the changes that may have already occurred as a result of long-term deafness.

This work was funded by NIDCD (HHS-N-263-2007-00053-C) and The Garnett Passe and Rodney Williams Memorial Foundation. The Bionic Ear Institute acknowledges the support it receives from the Victorian Government through its Operational Infrastructure Support Program.

297 Active Middle Ear Implantable Hearing Aids

Daniel J. Tollin^{1,2}, Kanthaiah Koka¹, Herman A. Jenkins² ¹Department of Physiology and Biophysics, University of Colorado Medical School, ²Department of Otolaryngology, University of Colorado Medical School,

Active middle ear implantable hearing aids (AMEIs) are designed to bypass the normal route of sound transmission to the inner ear via the tympanic membrane and ossicular chain and instead transmit vibrations directly to the ossicles via a mechanical stimulator. AMEIs are proving effective in treating moderate to severe sensorineural hearing loss as well as mixed and conductive loss. Empirical research exploring methods to optimize the performance of AMEIs remains necessary. Here we review our efforts using both human cadaveric temporal bone preparations and animal models to improve the performance of AMEIs by optimizing the coupling the transducer to various parts of the ossicular chain or the round window of the cochlea. Support: Otologics LLC education grant

298 Psychophysics of Electric Stimulation of the Human Cochlea, Brainstem, and Midbrain Robert V. Shannon¹

¹House Ear Institute

Quantitative psychophysical measures will be compared across patients with electric stimulation of the cochlea (cochlear implants: CI), cochlear nucleus (auditory brainstem implants: ABI), and inferior colliculus (auditory midbrain implant: AMI). Threshold as a function of stimulation pulse rate is different for CI and ABI. Threshold functions for ABI and AMI are similar. These differences may reflect processing differences or differences in the biophysical properties of the stimulated neurons. Equal loudness contours are guite different between CI and ABI and similar for ABI and AMI. CI dynamic range increases as the pulse rate increases, while ABI and AMI dynamic range is largest at low rates and decreases at higher rates. The pattern of results for ABI and AMI implies an integration time constant of longer than 50ms. Temporal processing capabilities were assessed in all three implant locations with gap detection, forward masking, and modulation detection. Similar patterns of results were observed cross devices. In general, modulation and gap detection are mildly correlated with speech recognition

performance and so are better in CI than in ABI and AMI. However, for equivalent levels of speech recognition there was no clear difference in these measures between CI and ABI. Overall these results show that many simple psychophysical capabilities are not limited by peripheral processing because they are similar between normal hearing and prosthetic hearing that bypasses peripheral mechanisms.

299 Inhibitory Scale Defines Two Complementary Mechanisms for Sound Duration Coding

Mu Zhou¹, Baohua Liu¹, Guangying Wu¹, Huizhong Tao¹, Li Zhang¹

¹USC

The coding of sound duration by neurons in the central auditory system can be achieved in two different ways: the neuron can respond continuously during the presentation of the sound stimulus (sustained response); or it can respond transiently to the onset and offset of the sound stimulus (phasic response). In the dorsal cochlear nucleus (DCN), using loose-patch cell-attached recordings, we found that principal neurons exhibited either sustained or phasic spike responses to tones of various durations. In vivo whole-cell current-clamp recordings revealed that for "sustained-type" neurons, tone stimuli evoked sustained depolarization during the course of the stimulus, while sustained hyperpolarization was generated in "phasic-type" neurons with depolarization or spiking appeared only around the onset and offset of the stimulus. With wholecell voltage-clamp recordings, we further dissected the excitatory and inhibitory synaptic inputs underlying the two types of tone-evoked responses. Both the "sustained-type" and "phasic-type" neurons exhibited long lasting excitatory and inhibitory synaptic currents during the course of the tone stimulation. The sustained depolarization/spiking responses are determined by the synaptic integration between strong excitatory and relatively weaker inhibitory inputs, while sustained hyperpolarization can be attributed to relatively stronger inhibition. Thus, the balance between excitation and inhibition largely determine how the neurons respond to long-duration tone stimuli.

300 In Vivo Whole-Cell and Juxtacellular Recordings in the Auditory Brainstem

J. Gerard G. Borst¹, Tom T.H. Crins¹, Marcel van der Heijden¹, Thomas Kuenzel¹, Christopher Kushmerick², Jeannette A.M. Lorteije^{1,3}, Silviu I. Rusu¹

¹*Erasmus MC, University Medical Center Rotterdam,* ²*Instituto de Ciências Biológicas, Universidade Federal de Minas Gerais,* ³*Netherlands Institute for Neuroscience* Extracellular recordings tell when cells spike, but not what makes them spike. The in vivo whole-cell recording technique can reveal information about the synaptic inputs and voltage-dependent ion channels that control the initiation of action potentials in auditory neurons. By gaining direct access to the cytoplasm, both the membrane potential and the composition of the cytoplasm can be manipulated. Three disadvantages of the in vivo whole-cell technique are that it is often difficult to get recordings, that the normal cellular function can be distorted, and that the typically high series resistance in combination with the pipette and cell capacitance constitutes a low-pass filter. Juxtacellular recordings can provide an alternative to whole-cell recordings. Because of the unexpectedly large size of extracellular potentials obtained when pushing a patch pipette into a cell, subthreshold changes in the membrane potentials can be picked up. By making simultaneous juxtacellular and whole-cell recordings from principal neurons in the medial nucleus of the trapezoid body (MNTB), we showed that the juxtacellular recordings can be used to estimate both synaptic conductance and postsynaptic excitability. In vivo whole-cell recordings and juxtacellular recordings of principal neurons of the MNTB have both shown a lack of evidence for the presence of short-term synaptic depression at the adult mouse calvx of Held synapse. More recently, we have used the in vivo juxtacellular technique to study the developmental regulation of short-term synaptic plasticity at the calvx of Held synapse, to quantify tuning and timing of synaptic inhibition of spherical bushy cells, and to study the binaural inputs to neurons in the medial superior olive. Both the in vivo juxtacellular and the whole-cell technique can thus be used to investigate the cellular mechanisms of sound localization.

301 When Excitation Should Be Inhibition: In Vivo Whole Cell Recordings Reveal Novel Features of Neurons That Code Interaural Intensity Disparities in the Inferior Colliculus George Pollak¹, Na Li¹

¹The University of Texas at Austin

Many cells in the inferior colliculus (IC) are excited by contralateral and inhibited by ipsilateral stimulation and are thought to be important for sound localization. These excitatory-inhibitory (EI) cells comprise a diverse group, even though they exhibit a common binaural response property. Previous extracellular studies showed the diversity results from different circuits that generate the same EI property among the IC population, where some inherit the property from a lower nucleus, e.g., LSO, some are formed de novo in the IC whereas others inherit EI features that are modified by inhibitory circuits. Here we evaluated the differential circuitry by recording inputs (PSPs, postsynaptic potentials) and outputs (spikes) with in vivo whole cell recordings from the IC of awake Mexican free tailed bats. From the whole-cell recordings, we also derived synaptic conductance waveforms evoked by monaural and binaural signals. We show that a minority of El cells either inherited their binaural property from a lower binaural nucleus or the EI property was created in the IC via inhibitory projections from the ipsilateral ear, features consistent with those observed in extracellular studies. However, in most EI cells ipsilateral signals evoked subthreshold EPSPs that behaved paradoxically in that EPSP amplitudes increased with intensity, even though binaural signals with the same ipsilateral intensities generated progressively greater spike suppressions. Moreover, conductances showed that the cells were receiving a far more complex set of projections than were

ARO Abstracts

apparent from either extracellular recordings or the pattern of PSPs evoked by monaural and binaural stimuli. We propose circuitry that can account for the responses we observed and suggest that the ipsilaterally evoked EPSPs, together with other features of the circuit, could influence the responsiveness of IC cells to dynamic signals with interaural intensity disparities that change over time, such as moving sound sources or multiple sounds that occur in complex acoustic environments. Supported by NIH grant DC7856.

302 Development of Synaptic Receptive Fields in Rodent Primary Auditory Cortex Robert Froemke¹

¹New York University School of Medicine, Skirball Institute, Dept Otolarnygology, Physiol/Neurosci

Early in life, neural circuits are highly susceptible to outside influences. The organization of the primary auditory cortex (AI) in particular is driven by acoustic experience primarily during the critical period. This neonatal sensitivity to the structure of sensory inputs is believed to be essential for constructing stable representations of the auditory world and for the acquisition of language skills by children. Previous studies have shown that the critical period for rodent AI occurs during the second and third weeks of postnatal life. During this time, AI synaptic properties mature (Oswald and Reves 2008) and tonotopy can be influenced by passive exposure to structured auditory stimuli such as pure tones (de Villers-Sidani et al. 2007). However, it is unclear how background stimuli engage mechanisms for synaptic plasticity at the cellular and network levels to control AI organization and development. Here I will describe our experiments using in vivo wholecell recording to measure AI synaptic receptive fields in anesthetized young rats. We first asked how excitatory and inhibitory frequency tuning curves are organized from P12-30. While tone-evoked synaptic currents could be evoked at all ages, excitatory and inhibitory frequency tuning profiles were uncorrelated early in life (P12-16), indicating that excitation and inhibition are imbalanced at the onset of the critical period. By P21, however, excitatory and inhibitory inputs were highly correlated, similar to older animals. Repetitive tonal exposure during P12-21 increased excitation and inhibition together in a dynamic manner, enhancing excitatory-inhibitory balance. Thus consistent experience with reliable sensory stimulation refines intracortical inhibition precisely in proportion to excitation. Progressive remodeling of inhibitory receptive fields by sensory experience leads to balanced synaptic activity and limits further exposure-induced modifications, closing the AI critical period.

303 Non-Overlapping Sets of Synapses Drive On-Responses and Off-Responses in Auditory Cortex

Ben Scholl¹, Xiang Gao², **Michael Wehr²** ¹UT Austin, ²University of Oregon

Neurons in visual, somatosensory, and auditory cortex can respond to the termination as well as the onset of a sensory stimulus. In auditory cortex, these off-responses may underlie the ability of the auditory system to use sound offsets as cues for perceptual grouping. Offresponses have been widely proposed to arise from postinhibitory rebound, but this hypothesis has never been directly tested. We used in vivo whole-cell recordings to measure the synaptic inhibition evoked by sound onset. We find that inhibition is invariably transient, indicating that off-responses are not caused by post-inhibitory rebound in auditory cortical neurons. Instead, on- and off-responses appear to be driven by distinct sets of synapses, because they have distinct frequency tuning and different excitatoryinhibitory balance. Furthermore, an on-on sequence causes complete forward suppression, whereas an off-on sequence causes no suppression at all. We conclude that on- and off-responses are driven by largely nonoverlapping sets of synaptic inputs.

304 Cell Type-Specific Studies Using Fluorescent Activated Cell Sorting (FACS) in Neuro-Epithelia

Ronna Hertzano¹, Neil Segil²

¹University of Maryland, ²House Ear Institute

The sensory epithelia of the mammalian auditory and vestibular systems are complex organs that consist of multiple cell types. In the last 10 years tremendous progress has been made in understanding the cell and developmental biology of these organs thanks to the application of modern histological and molecular biology techniques. Fluorescence Activated Cell Sorting (FACS) has been used since the early 1970s to count, sort, and functionally characterize cell populations in a single cell suspension, primarily in the immune system. More recently, FACS purification has been developed to study selected cellular populations in solid organ systems such as the brain and retina. Despite the popularity of FACS as a method both in routine laboratory diagnostics and in research, and the availability of transgenic lines expressing fluorescent proteins in a cell-type restricted pattern in the inner ear/lateral line, a relatively small number of studies have been published using this method in our field. The goal of this workshop is to introduce the concepts and applications of FACS of cells from solid organs and extend the add FACS to the armamentarium of more researchers in the hearing field.

305 Exploring Ganglion Cell Development and Maturation Through Single Cell Profiling Jeffrey Trimarchi¹, Connie Cepko²

¹Iowa State University, ²Harvard Medical School

Previous attempts to uncover the gene networks responsible for the production of retinal ganglion cells relied on screening methods that sampled the entire retina. Since multiple types of retinal neurons are generated during overlapping intervals in development, whole tissue strategies obscure the genetic programs present in only a small number of cells. This is especially true for ganglion cells since they represent a very small proportion (~1%) of the total cells in both the developing and adult retina. To gain insight into the gene expression programs that produce retinal neurons, gene expression profiling was carried out on individual retinal cells that were isolated using several strategies, including the specific expression of fluorescent molecules. These experiments have allowed for the identification of gene networks correlated with early differentiation and diversification of ganglion cells and provided insights into the genes that define the different subsets of ganglion cells in the adult retina.

306 Cre-Mediated Expression of Fluorescent Proteins in Specific Cell-Types in the Mouse Cochlear Sensory Epithelium Jian Zuo¹

¹St. Jude Children's Research Hospital

The mammalian cochlear organ of Corti contains more than five cell types: inner and outer hair cells, Deiters', pillar, and inner phalangeal cells. Despite their morphological differences, little is known about their molecular makeup that distinguishes their diverse functionality. It had been difficult to collect large quantities of each cell type. Now Cre-mediated expression of fluorescent proteins (i.e., GFP) specifically in each cell type at different times in transgenic mice followed by FACS offers an unprecedented opportunity to accomplish this difficult task. It is now possible to determine differential expression profiles of each cell type during development or under pathological conditions. Here I will present our effort to express GFP in inner and outer hair cells, Deiters', pillar , inner phalangeal cells, and spiral ganglia in neonatal mouse cochleae. We used inducible Cre transgenic mice that also contain the GFP-reporter gene by injecting tamoxifen at birth to activate Cre. The reporter GFP is then permanently expressed in these cell types that have Cre activity. We then sorted these cells by FACS. Efforts are under way to collect large amounts of GFP-positive cells from these transgenic mice for expression profile analysis. This work is supported by NIH DC06471, DC05168, DC008800 and CA21765; Office of Naval Research: N000140911014; the American Lebanese Syrian Associated Charities (ALSAC) of St. Jude Children's Research Hospital; The Hartwell Individual Biomedical Research Award.

307 Cell Type-Specific Sorting in the Mouse Inner Ear Using Cell Surface Markers

Ronna Hertzano¹, Rani Elkon², Siaw-Lin Chan¹, Annie Morrison¹, David Eisenman¹, Scott Strome¹

¹University of Maryland, ²The Netherlands Cancer Institute The auditory and vestibular sensory epithelia are complex organs that consist of multiple cell types. Fluorescence Activated Cell Sorting (FACS) is commonly used to separate selected cellular populations for further studies. While mice expressing GFP under the control of cell typespecific promoters can be used to study selected inner ear cellular populations, one could also use naturally expressed cell surface proteins to sort cells by FACS. We describe and discuss a new protocol for cell type-specific sorting of inner ear cellular populations from newborn wildtype mice.

308 Assessing the Developmental Potentials of Cochlear Sensory Cells Patricia White¹

¹University of Rochester School of Medicine

If mammalian inner ear regeneration is possible, then supporting cells must retain capacities beyond what they express in vivo: to re-enter the cell cycle, and to differentiate into the lineally-related sensory hair cell. Classically, intrinsic plasticity is measured by isolating the cell type and manipulating its environment. Such experiments have the goal of identifying both the cell's repertoire and the signals to which it responds. Using FACS and the tools of neural stem cell biology, we have begun to elucidate the signals that may regulate cell cycle re-entry in supporting cells, a phenomenon never observed in a wild-type animal

309 Transcriptional Signature of Supporting Cells in the Zebrafish Lateral Line

Martine Behra¹, Viviana Gallardo², Shawn Burgess² ¹UPR School of Medicine, ²NHGRI

The lateral line is an excellent alternative organ model to study hearing pathology. Like inner ear's neuroepithelia, neuromasts (superficial sensory patches) are composed of hair cells and supporting cells. Whereas hair cells are extensively studied, the paucity of information on supporting cells is a real challenge. To remedy to this, we use a zebrafish transgenic line, expressing GFP exclusively in supporting cells, to establish their transcriptional signature. We FAC sort homogenates of transgenic larvae, enriching for GFP +cells, extract their RNA and hybridize it against reference RNA from whole larvae. Supporting cells' specific genes will show as "upregulated", profiling a transcriptional signature for this poorly characterized cell population.

310 Sorting of Otic Progenitors, Hair Cells, and Supporting Cells Using FACS and MACS Saku T. Sinkkonen¹, Meike Herget¹, Felix Gahlen¹, Taha Jan¹, Renjie Chai¹, Alan Cheng¹, Stefan Heller¹ ¹Stanford University

Using fluorescent proteins, fluorescent dye uptake, fluorescent metabolic products, and surface markers, we are able to isolate specific inner ear cells from chicken and mouse for cell culture experiments, proteomics analyses, and deep transcript sequencing. I will provide an overview of the different techniques, the difficulties that we experienced and the alternative technologies, such as magnetic cell separation. Using combinations of surface markers and reporter genes, we are currently able to simultaneously separate up-to five different cell populations from the postnatal organ of Corti - a powerful example how cell sorting techniques are enhancing inner ear research.

311 Enlargement of the Cochlea and Endolymphatic Sac Precedes Endolymphatic Acidification During Embryonic Development in a Mouse Model of *SLC26A4*-Related Deafness

Hyoung-Mi Kim¹, Philine Wangemann¹

¹Kansas State University

Mutations of SLC26A4 are one of the most prevalent forms of childhood deafness. Enlargement of endolymphatic spaces and acidification due to lack of HCO₃ secretion are key events in the etiology of deafness in mice lacking Slc26a4 expression. The goal of this study was to determine the onset of Slc26a4 expression, epithelial enlargement and luminal acidification during embryonic development. Expression of pendrin, the protein encoded by Slc26a4, and epithelial enlargement were determined by confocal microscopy. Fluid pH was measured with double barrel microelectrodes in isolated superfused inner ears from S/c26a4^{+/-} (HET) and S/c26a4^{-/-} (KO) mice. In the endolymphatic sac, the onset of pendrin expression was E (embryonic day) 11.5. At E14.5 epithelial cells were stretched by factor 1.8 in KO mice but no difference in endolymphatic pH was observed between KO and HET mice; pH 7.26 in HET and KO mice (n=4 each). At E17.5 endolymph was further enlarged and more acidic, pH 6.54 vs pH 6.82 (n=3 or 4), in KO compared to HET mice. In the cochlea, the onset of pendrin expression was E13.5. At E14.5 scala media was enlarged but no difference in endolymphatic pH was observed between KO and HET mice. The endolymphatic pH was 7.45 in HET and KO mice (n=2 or 3). At E17.5 scala media was further enlarged and more acidic, pH 7.13 (n=4) vs 7.44 (n=1) in KO compared to HET mice. Throughout, the superfusate and perilymph were pH 7.35. In conclusion, the data demonstrate that the onset of pendrin expression precedes endolymphatic enlargement and acidification consistent with a causal relationship and the presence of endolymphatic buffers. These findings are critical toward an understanding of the mechanisms that cause the enlargement that is the key event in the etiology of deafness in mice, and possibly humans, lacking expression of pendrin.

Supported by: CVM-SMILE, NIH-R01-DC01098, NIH-P60-RR017686.

312 Expression of DNA Methyltransferases *(Dnmt*s) in Developing Auditory Epithelium and Possible Role in Auditory Function

Hideki Mutai^{1,2}, Susumu Nakagawa², Kazunori Namba^{1,2}, Masato Fujii², Tatsuo Matsunaga^{1,2}

¹Lab of Hearing Disorders, ²National Institute of Sensory Organs, National Tokyo Medical Center

DNA methylation is a major epigenetic mechanism that mediates cell type specific gene expression/repression and chromosomal stability. Previously, we demonstrated the existence of epigenetic regulatory system in the developing rat auditory epithelium, through identification of a DNA highly methylated region (2009 Develop Neurobiol 69:913-930). Based on the hypothesis that DNA methylation is important for development and maintenance of hearing, we studied expression of DNA methyltransferases (*Dnmt*s) in mouse auditory epithelium and sought the changes of genomic methylation levels at the time of hearing loss.

Total RNA extracted from postnatal auditory epithelia from FVB/NJ, a mouse strain with normal hearing, at postnatal day 1 (P1), P14, and 12 weeks (12w) was subjected to quantitative RT-PCR to study transcriptional levels of *Dnmts. Dnmt3a* expression appeared to be relatively high at P1 and P14, and decreased at 12 weeks. In contrast, *Dnmt3b* expression remained stable at 12w. Immunohistochemical study demonstrated intense signal of Dnmt3a in the hair cells and supporting cells of the organ of Corti at P14 and its disappearance in the adult, while Dnmt3b signal was detectable in the adult auditory epithelium.

In the next experiment, changes of methylation levels in several genomic regions in the auditory epithelia of mouse strain DBA/2J, a model of age-related hearing loss, were measured by methylation sensitive restriction enzymemediated qPCR. DNA extracted from auditory epithelia at 4w and 12w were treated or untreated with *Hpall* enzyme and subjected to qPCR by using sets of PCR primers designed for amplifying GC-rich genomic regions that were predicted to be important for auditory function. Several regions showed changes in their methylation levels as well as the expression levels between 4w and 12w. We named them **d**ifferentially **m**ethylated regions in **a**ge-related **h**earing loss (*DMahl*s). Possible role of DNA methylation in auditory function will be discussed.

313 Formation of the Stria Vascularis Is Compromised in Lmx1a Mutant Mice

David Nichols¹, Kirk Beisel¹, Bernd Fritzsch²

¹Creighton University, ²University of Iowa

The stria vascularis is a composite epithelial-mesenchymal structure located in the abneural wall of the cochlear duct that is required to maintain the ionic composition of the endolymph. This structure fails to assemble in mice mutant for the LIM-homeodomain transcription factor Lmx1a (Lmx1a-dr) and they are likely to be congenitally In non-mutant (wildtype) animals periotic deaf. mesenchyme (POM) begins to aggregate beneath the prestrial epithelium in the abneural wall of the basal cochlear duct by embryonic day (E) 18.5. By postnatal day (P) 7 this cuboidal epithelium and the underlying mesenchyme have formed a maturing stria vascularis consisting of marginal, intermediate and basal layers in all but the extreme apex of the duct. The marginal layer is derived from the pre-strial epithelium, the intermediate layer from neural crest melanocytes and the basal layer from the POM. In Lmx1a mutants the pre-strial epithelium is present but melanocytes are absent and mesenchymal cells, though present, fail to form a basal layer. At these ages (E18.5-P7) wildtype ears would strongly express Lmx1a and Fgf receptor 2 (Fgfr2) in the outer spiral sulcus and the paired box transcription factor Pax2 in the prestrial epithelium. Using in situ hybridization we have found that Lmx1a mutants weakly express both Fgfr2 and Pax2 and that expression of both is diffusely spread across both the outer spiral sulcus and the pre-strial epithelium. No stria forms in mice mutant for either Fgfr2 or Pax2. Thus Lmx1a expression focuses and strengthens the expression of two genes in and adjacent to its expression domain both of which are required for successful formation of the stria vascularis.

314 Morphological Analysis of Converging Inputs on MNTB Neurons During the Period of Calyx Growth

Brian Hoffpauir¹, Tom Deerinck², Guy Perkins², Mark Ellisman², George Spirou¹

¹West Virginia University, ²National Center for Microscopy and Imaging Research

Principal neurons of the mouse medial nucleus of the trapezoid body (MNTB) are innervated by multiple inputs from the ventral cochlear nucleus at embryonic day 17, when the MNTB is first discernable as a distinct cell group. We have shown previously that these initial synaptic contacts are functional but remain small during a four day waiting period until postnatal day (P)2. A period of rapid terminal growth occurs over the next 48 hours until P4, when most MNTB neurons are innervated by one large calyx of Held terminal. In this study, we utilized serial section electron microscopy to characterize the converging inputs that innervate MNTB neurons at P3, a period of dynamic terminal growth. Complete reconstructions of 20 MNTB neurons revealed that MNTB cell bodies, with somatic surface areas ranging from $381 - 1455 \,\mu\text{m}^2$, were innervated by as many as 7 inputs (average = 4). Each neuron typically had 3 primary dendrites that were also innervated by several (>10) small synaptic contacts. We measured the somatic surface area that was directly apposed to each input as a metric for terminal size. Interestingly, axons that formed the largest of the converging inputs typically tracked along one of the primary dendrites and initially contacted the MNTB cell at or near the base of these dendrites. We found that the cells fell into three categories: 1) cells (n=10) with only small inputs that covered < 35 μ m², 2) cells (n=6) with one dominant input (83 – 360 μ m²) and other small (< 25 μ m²) inputs, and 3) cells (n=4) with two intermediate sized inputs $(35 - 140 \mu m^2)$ and other small inputs. These data fit well with our electrophysiological studies of converging inputs on MNTB neurons and suggest that competitive mechanisms may select the individual dominant input that will eventually form the mature calyx of Held terminal.

315 Adenomatous Polyposis Coli Protein (APC) Is Required for Normal Hearing

Tyler Hickman¹, Maria Gomez-Casati², Gabriel Corfas², Michele Jacob¹

¹*Tufts University, Sackler School of Biomedical Sciences, Department of Neuroscience,* ²*Children's Hospital and Departments of Neurology and Otolaryngology, Harvard Medical School*

While originally believed to function mostly as a tumor suppressor protein, adenomatous polyposis coli (APC) has recently been found to play a critical role in neuronal

development. APC functions to promote polarization, direct axon outgrowth and enhance synapse assembly and maturation. Moreover, studies in migrating fibroblasts show that APC interacts with fragile X mental retardation protein (FMRP) and is required for localizing selected mRNAs at sites of local translation. The critical role of APC in neurons is further supported by the association of mental retardation and autism with APC gene mutations in humans. APC's Despite importance for proper development, its role in the cochlea has yet to be defined. Our preliminary studies show that APC is concentrated at α 9/10-nAChR-containing efferent olivocochlear synapses of sensory hair cells. In addition to nicotinic synapses, APC is also enriched at glutamatergic synapses, suggesting a role at spiral ganglion neuron contacts with inner hair cells.. To define APC's role in the cochlea, we have characterized the auditory phenotype of our APC conditional knock-out mouse. We find abnormal auditory brainstem responses (ABRs) and distortion product otoacoustic emissions (DPOAEs) compared to control littermates. The molecular organization of auditory synapses is also altered in the APC cKO mouse. Our findings suggest that APC expression is necessary for cochlear development and normal hearing.

316 Phenotypic Analysis of Two Cochlear Hair Cell Specific Conditional Mouse Models for Thyroid Hormone Receptors α and β

Christoph Franz¹, Juliane Dettling¹, Lukas Ruettiger¹, Ulrike Zimmermann¹, Frederic Flamant², Jian Zuo³, Robert Feil⁴, Niels Brandt⁵, Jutta Engel⁵, Marlies Knipper¹ ¹Tuebingen Hearing Research Centre, Molecular Physiology of Hearing, ENT Clinic Tuebingen, ²National Centre for Research Sciences, Institute of Functional Genomics, University of Lyon, ³Department of Developmental Neurobiology, St. Jude Childrens Research Hospital, ⁴Interfaculty Institute for Biochemistry, University of Tuebingen, ⁵Department of Biophysics, Saarland University, Homburg/Saar

It is long known, that a lack of thyroid hormone (TH) can have a tremendous effect on embryonic development regarding not only overall body growth but also on the maturation of the brain and the hearing system.

Since more than 10 years, we focus our investigation on how TH can regulate the maturation of the cochlea from an immature pre-hearing organ into a hearing sensory organ via its receptors thyroid-hormone-receptor $\alpha 1$ (TR $\alpha 1$) and $\beta 1$ (TR $\beta 1$) that are present in the cochlea. We here present the phenotypic analysis of two conditional and tamoxifen inducible mouse models with perinatal knock-in mutation of TR $\alpha 1$ and deletion of TR $\beta 1$.

The aim of this study is to obtain a better understanding of the regulatory function of TH and its impact on maturation to bring it into common therapies in the clinic.

This work has been supported by the Minigraduiertenkolleg of the University of Tuebingen and the Deutsche Forschungsgemeinschaft DFG Kni:316-4-1.

317 LRIG2 Is Required for Normal Cochlear Function in Mice

Tony del Rio¹, Daniel Berman¹, M. Charles Liberman², Lisa V. Goodrich¹

¹Dept. Neurobiology, Harvard Medical School, ²Eaton-Peabody Laboratory, Massachusetts Eye and Ear Infirmary

The family of leucine-rich and immunoglobulin domain (Lrig) proteins consists of three poorly understood transmembrane proteins with homologous extracellular domains. All three family members are prominently expressed in the developing inner ear, with Lrig1 and Lrig3 largely overlapping in the otic epithelium and Lrig2 restricted to the cochlear-vestibular ganglion. While Lrig1 has been shown to negatively regulate several receptor tyrosine kinases, no molecular function has yet been assigned to either Lrig2 or 3.

To investigate a potential role for Lrig2 in the neurons of the inner ear, we utilized a gene trap line, RST656. Lrig2RST656/RST656 homozygous mice show dramatically reduced levels of Lrig2 with no obvious balance defects. However, ABRs of Lrig2 mutant mice showed a significant decrease in response amplitudes (measured at 8kHz and 16kHz). Since DPOAEs were normal in most affected animals, spiral ganglion neuron (SGN) function may be compromised. However, a subset of mutants also show significant DPOAE threshold elevations suggesting hair cell dysfunction, although morphological defects are not seen in mutant cochleas. Since SGNs appear to play a major role in the ABR phenotype, we have begun to investigate the cellular and molecular function of Lrig2 in neurons. In one approach, the subcellular distribution of an Lrig2-GFP fusion was analyzed in cultured neonatal SGNs. We found that Lrig2-GFP protein localizes to vesicles along the length of the neurites, suggesting a role for Lrig2 in intracellular trafficking. To gain additional insights into Lrig2 function, we have undertaken a search for novel binding partners. We have begun a yeast-two-hybrid screen of the Lrigs against the human ORFeome, and generated novel and specific rat monoclonal antibodies against Lrig2 and Lrig3. Preliminary yeast-two-hybrid results suggest that Lrig2 interacts with molecules involved in the regulation of trafficking. A molecular analysis of endogenous interacting proteins is underway.

318 MafB in Synaptogenesis of Auditory Neural Circuits

Wei-Ming Yu¹, Jessica Appler¹, Lisa Goodrich¹ ¹Department of Neurobiology, Harvard Medical School

Hearing impairment is the most common disabling sensory birth defect in humans, with at least half of the cases caused by genetic mutations. Understanding how auditory circuits assemble, especially the synaptogenesis of auditory neurons, may lead to the development of new therapies and broaden opportunities for patient treatment. We have identified the transcription factor MafB as a potential master regulator of synaptic development in auditory circuits based on its expression pattern, functions in other developing systems, and ability to control the expression of known synaptic molecules. To investigate the function of MafB during auditory circuit assembly, we generated a floxed allele of MafB and specifically disrupted MafB protein in spiral ganglion neurons. MafB conditional knock-outs (MafBCKO) are viable and exhibit no obvious behavioral abnormalities. Analysis of auditory function in MafBCKO mice by auditory brainstem responses shows that the mutants could still detect sound even at low intensities but the neural response was significantly delayed relative to controls. More detailed analyses of the MafBCKO mice and genome wide studies to identify MafB target genes will be performed to help us understand how MafB contributes to the formation of auditory circuits.

319 Spontaneous Oscillations in the Developing Gerbil Neocortex in Vivo Exhibit Interlaminar Synchrony

Martin Pendola¹, Adrian Rodriguez-Contreras¹, Vibhakar Kotak²

¹Department of Biology, City College of the City University of New York, ²Center for Neural Science, New York University

During early stages of development and prior to the onset of hearing, cells in the auditory system exhibit bursts of spontaneous electrical activity. Very little is known about the patterns of spontaneous activity in the primary auditory field in the neocortex. In brain slices of postnatal day (P) 3-5 gerbils, cortical activity occurs as spontaneous oscillations (SOs) and calcium waves that travel via the thalamorecipient auditory cortex (Kotak et al., 2007), consistent with cortical early network oscillations described in the rat neocortex after birth (Garashuck et al. 2000). Therefore, the objective here was to test whether SOs, a key salient feature of traveling cortical waves, exist in the neocortex of gerbil pups. Broadband extracellular (0.1-10 kHz) were obtained with multirecordings electrode silicon probes inserted at a maximum depth of 400-800 µm into the cortical lamina of P4 gerbil pups (chloral hydrate anesthesia, 50-75 mg/kg, n = 3 gerbils). Using the band pass filtered signal (1-5 kHz) we analyzed cortical multiunit activity recorded in 16 channels distributed across four different shanks. We found that SO's have durations of 4.3 ± 3.2 seconds and inter-event intervals of 18.8 ± 10.7 seconds (values are mean ± sd, n=303 SO's). Postmortem histological analysis showed that 2 of the recordings were located at rostral locations in the temporal cortex, while the third site was located at the caudal end, within the perirhinal cortex. A remarkable property of SO's was the high synchrony observed across recording sites. Together, these findings demonstrate the presence of SO's in the gerbil neocortex and provide the tools to characterize SOs specifically in the developing primary auditory cortex, to compare its relationship to patterns originating in the cochlea and to explore their developmental significance. (Supported by NIH grants G12-RR03060 and 1SC1HD068129-01 (AR-C), and DCD 006864 (DH Sanes and VCK).

320 The Development of Glycinergic and GABAergic Neurons in LSO and MNTB

Alison Hixon¹, Diana Lurie¹, Josh Lawrence¹ ¹The University of Montana

Acoustic processing in the lateral superior olive (LSO) requires high fidelity signaling of excitatory and inhibitory neurons. The LSO receives excitatory input from the ipsilateral cochlear nucleus and inhibitory input from multiple sources, including the medial nucleus of the trapezoid body (MNTB). We explored the development of inhibitory neuron subtypes in LSO and MNTB using transgenic mice in which YFP or GFP is driven by promoters for the calcium binding protein parvalbumin (PV) or the GABA synthesizing enzyme GAD65, respectively. We hypothesized that YFP and GFP would be differentially expressed in glycinergic (PV) or GABAergic (GAD65) cell types during development. Frozen sections (10 µm) were collected from the brains of each mouse strain and examined with confocal microscopy. Alternate sections were immunolabeled with antibodies to synaptophysin (SYP 1:500). Before P14, numerous GAD65-GFP+ neurons in LSO and MNTB with widely branching projections were observed. By P14, the number of GAD65-GFP cell bodies greatly decreased, and the fibers appeared refined. At P22, few GAD65+ cell bodies or fibers were observed in either LSO or MNTB. In contrast, YFP was expressed primarily in the calyces of MNTB and in the fibers of LSO at P4-P11. At P22, YFP expression was observed in a large number of PV+ cell bodies in LSO and MNTB. Consistent with glutamatergic innervation of glycinergic cells, SYP and PV were localized to MNTB calvces at all ages examined. SYP+ terminals were also observed on the few GAD65-GFP neurons in the adult LSO and MNTB. Our results provide evidence for an inverse relationship between the number of GABAergic and glycinergic neurons during development. This suggests differential roles of inhibitory circuits during development.

321 Developmental Changes in Short-Term Plasticity in the Rat Calyx of Held Synapse

Tom Crins¹, Silviu Rusu¹, Gerard Borst¹

¹Erasmus MC

Each principal neuron in the medial nucleus of the trapezoid body (MNTB) of the auditory brainstem is contacted by a single, giant, axosomatic terminal, called the calyx of Held. Because of its accessibility in slice preparations, this synapse has been instrumental as a model synapse to elucidate mechanisms of short-term plasticity (STP). We studied the developmental changes that allow it to function as a relay within the superior olivary complex in the adult animal. In vivo recordings from youngadult mice have shown that this synapse displays low release probability and that the average size of synaptic potentials does not depend on recent history (Lorteije et al, 2009). We used a ventral approach to make juxtacellular recordings from the calyx of Held synapse in Wistar rats ranging in age from 3 days postnatal (P3) to P30. Before the onset of hearing (at about P11) the cells fired in bursts of activity. In these recordings the size of the extracellularly

recorded EPSPs depended greatly on the interval between events. We observed evidence for the presence of both short-term depression, which recovered slowly (time constant in the seconds range) and short-term facilitation, which decayed more rapidly. During development, the amount of depression decreased, which might be due to a reduction of release probability. The amount of short-term facilitation also decreased, and the time course of its decay became much more rapid in older animals, which may be due to changes in presynaptic intracellular calcium clearance following an action potential. Similar developmental changes were observed in slice experiments. Our data thus show large developmental changes in the extent and time course of STP at the calyx of Held synapse. They suggest that a reduction in synaptic depression, and reduced and more rapidly decaying synaptic facilitation are important developmental changes in the transformation of this synapse into a reliable auditory relay synapse.

(1977 characters.)

322 The Calyx of Held Develops Adult-Like Dynamics and Reliability by Hearing Onset in the Mouse in Vivo

Mandy Sonntag¹, Bernhard Englitz^{2,3}, Marei Typlt¹, Rudolf Rübsamen¹

¹University of Leipzig, ²MPI MIS Leipzig, ³University of Maryland, College Park

Synaptic transmission at the calyx of Held is known for its high reliability and fast signal transmission. In the present study we investigated the development of these properties in vivo in P8-P28 mice focussing on developmental changes within spontaneous discharge patterns around hearing onset. We used extracellular recordings to measure single-unit activity in the medial nucleus of the trapezoid body which enable simultaneous acquisition of pre- and postsynaptic activity reflected by a complex voltage signal. To precisely quantify the timing and the relative size of the single components, we developed a fitting algorithm which (I) decomposes the complex waveform of individual transmission events into the presynaptic action potential (AP), the excitatory postsynaptic potential (EPSP) and the postsynaptic AP and (II) at the same time accounts for overlaps between components from one or consecutive transmission events. Before hearing onset, we found signal transmission to be unreliable and of high variability in transmission delay. Also, EPSP and postsynaptic AP amplitudes were depressed strongly as a function of preceding activity. Around hearing onset (P12-P14) signal transmission gained the properties found at the mature calvx of Held, i.e. reliable in transmission with a low variability in both the transmission delay and in the amplitude of the EPSP as well as postsynaptic AP. Though activity-dependent depression was still seen in APs, EPSP depression no longer seemed to play a prominent role. In summary, we found the calyx of Held to mature just in time for the onset of acoustically evoked signal processing.

323 Expression of Synaptotagmins 1 and 2 in the Immature Auditory Brainstem: Transiently Expressed Synaptotagmin 1 Co-Localizes with Vesicular Glutamate Transporter VGLUT3

Alan Cooper¹, Deda Gillespie¹

¹McMaster University

The lateral superior olive (LSO) compares converging excitatory and inhibitory inputs to compute interaural intensity differences. As this computation requires precise, tonotopic alignment of the two inputs, a major question concerns how the glutamatergic (VCN-LSO) and GABA/glycinergic (MNTB-LSO) inputs achieve registration during early life. Developmental refinement in the GABA/glycinergic MNTB-LSO pathway may require corelease of glutamate before hearing onset. Recent data from the lab suggest that release probabilities (P release) differ between VCN-LSO and MNTB-LSO synapses, and between GABA/glycine and glutamate release at the MNTB-LSO synapse, and that these P release mature quickly in the first postnatal week. We considered that differential expression of Ca++-sensing synaptotagmin (Syt) isoforms might underlie some of these developmental changes and varied release probabilities in the LSO.

We characterized Syt1 and Syt2 expression in auditory brainstem tissue from rats postnatal day 1-21 (P1-21). To determine synapse type, we used immunoreactivity for the vesicular glutamate transporters VGLUT1/2 and VGLUT3 and the vesicular inhibitory amino acid transporter VIAAT to identify classical glutamatergic terminals, glutamatereleasing immature inhibitory terminals, and inhibitory terminals. After P1, Syt2 was expressed throughout the superior olivary complex and colocalized with markers of both excitatory and immature inhibitory synapses. Svt1 expression peaked around P9, decreasing to levels below background shortly after hearing onset. Additionally, Syt1 expression was localized to the LSO and superior paraolivary nucleus, where it colocalized almost exclusively with markers for immature inhibitory terminals, VGLUT3 and VIAAT. We suggest that immature MNTB terminals within the LSO may contain two vesicle populations, an adult-form population in which VIAAT and Svt2 are co-expressed, and a transient second population in which VGLUT3 and Syt1 are co-expressed.

324 Pre- And Post-Synaptic Maturation in the Pathway from Ventral Cochlear Nucleus to Lateral Superior Olive: Prominent GluN2B-Mediated Transmission During Functional Refinement Preceding Hearing Onset Daniel Case¹, Xiwu Zhao¹, Deda Gillespie¹

¹McMaster University

Neurons of the lateral superior olive (LSO) integrate converging excitatory and inhibitory inputs to compute interaural intensity differences. As this computation requires that the excitatory inputs from the ventral cochlear nucleus (VCN) be tonotopically matched with the inhibitory inputs from the medial nucleus of the trapezoid body (MNTB), how the LSO brings converging inputs of opposite sign into precise tonotopic register during early postnatal life is a major question. Much is already known about refinement in the MTNB-LSO pathway; here we examined synaptic maturation in the immature VCN-LSO pathway.

Acute brainstem slices were obtained from rats aged postnatal day 1 to 12 (P1-12; hearing onset at P12) for whole-cell voltage-clamp recordings from LSO principal neurons in response to electrical stimulation of the ventral acoustic stria. Input-output curves and minimal stimulation experiments were performed in order to estimate input number and strength. Pharmacology was used to isolate different receptor currents (strychnine, 1µM; picrotoxin, 50µM; CNQX, 5µM; D-APV, 50µM; IEM 1460 µM, 100µM; ifenprodil 10µM).

As has been shown in the MNTB-LSO pathway, the number of VCN inputs decreased before hearing onset, while the strength of the remaining inputs increased. Both NMDAR- and AMPAR-mediated responses were present in the immature VCN-LSO pathway, as previously reported, but we found no evidence for mGluR responses or for GluR2-lacking AMPAR responses. NMDARmediated responses were highly sensitive to ifenprodil before P8, but ifenprodil-sensitivity decreased after P8 and nearly disappeared at P12. This evidence for developmental regulation of receptor subunits is suggestive of a role for GluN2B-containing NMDARs in the changes in synaptic strength. Finally, changes in pairedpulse ratios between P2 and P3 point to a stepwise maturation in neurotransmitter release at P3, an event that may correlate with the onset of a window for synaptic refinement.

325 Mutation Analysis of the MYO7A and CDH23 Genes in Japanese Patients with Usher Syndrome Type 1

Hiroshi Nakanishi¹, Masafumi Ohtsubo¹, Satoshi Iwasaki², Yoshihiro Hotta¹, Yoshinori Takizawa¹, Katsuhiro Hosono¹, Kunihiro Mizuta¹, Hiroyuki Mineta¹, Shinsei Minoshima¹

¹Hamamatsu University School of Medicine, ²Shinshu University School of Medicine

Objective: Usher syndrome (USH) is an autosomal recessive disorder characterized by retinitis pigmentosa (RP) and hearing loss (HL). USH type 1 (USH1) is the second common type and is frequently caused by mutations in MYO7A and CDH23, which account for 70-80% of USH1 cases. To date, several mutation analyses of the genes were performed in patients from various ethnic origins, including Caucasian, African and Asian. However, there have been no reports of mutation analysis for any responsible genes for USH1 in Japanese patients. The aim of this study is to analyze mutations in the MYO7A and CDH23 genes in Japanese patients with USH1. Methods: Five unrelated Japanese patients from various regions of Japan participated in the study and met the criteria of USH1. Mutation analysis of MYO7A and CDH23 was performed by direct sequencing technique using genomic DNA extracted from peripheral lymphocytes. Results: Mutation analysis of MYO7A and CDH23 in the five unrelated Japanese patients revealed five different

probable pathogenic mutations (three in MYO7A and two in CDH23) in four patients. Of these, two mutations were novel. One of them, p.Tyr1942SerfsX23 in CDH23, was a large deletion causing the loss of 3 exons. The mutation was found in homozygous state, which is probably accounted by consanguinity. This is the first large deletion to be found in CDH23. Conclusion: The incidence of the MYO7A and CDH23 mutations in the study population was 80%, which was consistent with previous findings. Therefore, mutation screening for these genes is expected to be highly sensitive for diagnosing USH1 among the Japanese. One novel mutation, p.Tyr1942SerfsX23 of CDH23, was a large deletion. The homozygosity resulting from consanguinity probably led to the relatively easy identification. It is possible that similar exonal deletions latently exist in a compound heterozygous state in some USH1 cases in which only one mutation has been found.

326 Spectrum and Frequencies of Mutations in GJB2 and GJB6 Among Argentinean Patients with Sensorineural Non-Syndromic Deafness

Viviana Dalamon¹, Maria Florencia Wernert¹, **Ana Belen Elgoyhen¹**

¹Institute for Research in Genetic Engineering and Molecular Biology

Genetically caused congenital deafness is a common trait affecting 1 in 2000 children. Most cases are non-syndromic and of autosomal recessive inheritance. To date, over 40 different genes have been identified as genetic cause of deafness worldwide. The aim of this study was to investigate and report the spectrum and frequency of mutations in GJB2, GJB6, OTOF and MT-RNR1, in deaf patients from Argentina. A total of 773 samples were analyzed; 439 from non-syndromic unrelated Argentinean deaf patients (99 familial and 340 sporadic cases) and 334 from relatives and siblings. Most of them were of prelingual onset (83%). At the time of the study 78 patients were already cochlear implanted.

Mutations in GJB2 and GJB6 genes were found in 156 patients, accounting for 36% of the sample. Overall 38 different sequence variations were identified. The mutation c.35delG accounted for 55/439 (13%) of the patients studied, resulting in 35% of the detected mutations, becoming the most frequent causing mutation in our population, in accordance with other reports worldwide. Only 2% of patients showed mutations in the GJB6 gene (seven del(GJB6-D13S1830) and three del(GJB6-D13S1854)). In addition, 35 sequence variations different from c.35delG, were identified in the GJB2 gene: T8M, L10P, G12V, S19T, V27I, M34T, V37I, E47X, 167delT, R75W, R75Q, c.233insG, W77R, I82M, F83L, V84L, L90P, c.269insT, V95M, c.312del14nt, G109V, c.333delAA, R127H, I128I, E129K, R143W, V153I, G160S, M163V, M163L, K168R, R184P, V190D, c.682 C>T (3'UTR), IVS1+1G>A. Four of them are reported for the first time (L10P, c.233insG, G109V and V190D). None of the samples showed mutations either in OTOF or in MT-RNR1.

The present study demonstrates that different mutations in the GJB2 and GJB6 genes are prevalent in our Argentinean population. These findings strengthen the importance of genetic screening in hearing-impaired patients for the contribution towards an adequate genetic counseling and treatment planning.

327 Ten Year Follow-Up Phenotypic Characterization of Hereditary Hearing Impairment Linked to DFNA41

Xue Zhong Liu¹, Hui Jun Yuan², Xiaomei Ouyang¹, Lilin Du¹, Xue Jun Zhou¹, Denise Yan¹, Don Yi Han² ¹Department of Otolaryngology, University of Miami, Miami, Florida, USA, ²Institute Of Otolaryngology, General Hospital of Chinese PLA

We mapped a novel locus for non-syndromic sensorineural deafness autosomal dominant type 41 (DFNA41) on the long arm of chromosome 12q24gter (Blanton SH et al., 2002). The DFNA41 family is a large five multigenerational Chinese family that is segregating for an autosomal dominant adult onset form of non-syndromic hearing loss. All affected subjects had bilateral sensorineural hearing loss with a significant gender difference in initial presentation. To confirm the gender difference in initial frequency involvement and to determine progression of hearing loss, we performed an audiological evaluation after ten years since our initial visit in 1997. We demonstrated that there are three types of audiograms identified in the DFNA41 family: a slope audiogram with high frequency loss was found in all affected male individuals with <40 years old, an ascending audiograms with low frequency loss in all female affected members with <40 years old, and a flat audiogram with whole frequency loss in both genders with >40 years old. In both genders, hearing loss progresses with increasing age until the 40's, with affected males showing low frequencies and affected females showing high frequencies. In addition, we screened 11 potential inner ear enriched genes for mutation but DNA sequencing of coding and exon-intron boundaries of the genes in affected subjects did not reveal any disease causing mutation in the DFNA41 family.

328 Effect on Hearing After Estrogen Substitution in Turner Mice

Åsa Bonnard¹, Rusana Simonoska¹, Annika E. Stenberg¹, Anette Fransson², Malou Hultcrantz¹

¹CLINTEC, ²KNV

Background: In Turner syndrome (loss of one Xchromosome) ear and hearing problems affecting both outer, middle and inner ear are common. These women often present with a rapid decrease in their hearing due to pre-aging of the ear (presbyacusis) at the age of 35. This is much earlier compared to the general population of women who have a similar decease in hearing but during menopause when the estrogen are low, around the age of 50-60. An animal model, the Turner mouse, lacking one Xchromosome, has been developed and shown to have similar ear and hearing problems as women with Turner syndrome. It's been shown in other studies, from our research group that the number of estrogen receptors (ER) a and ß, that mirrors the estrogen levels, in the inner ear of rats differ depending of maturation, development and pregnancy. Could it be possible to postpone the pre-aging deterioration and thereby preserve the hearing in Turner mice by estrogen substitution?

Aim: The effect on hearing after estrogen substitution of Turner mouse compared to a control group.

Methods: 10 Turner mice and 10 CBA mice was divided into two groups and injected with either estrogen (estradurin 0,15mg/ml, 0,01ml x weight of mice) or saline every three weeks for two months. ABR was measured in all specimens before and after substitution.

Results: From start the Turner mice had an all over worse hearing than the control group of CBA mice. After finishing injection and when comparing the two groups, the CBA mice still had a better hearing whether substituted or not, while the Turner mice seem to follow their original decline. Conclusion: The time point for injecting estrogen will be further discussed.

329 Abnormally Long & Thin Stereocilia in Tasmanian Devil Mutant Mice: Grxcr1 and Its Contribution to This Specific Phenotype

Beatriz Lorente¹, Selina Pearson¹, Karen P Steel¹ ¹Wellcome Trust Sanger Institute

Tasmanian devil (tde) mice exhibit defects in the organization of stereocilia bundles of sensory hair cells in the cochlea and have excessively long and thin stereocilia. The mutants also exhibit circling behavior, which indicates a defect in the vestibular system (Erven et al., 2002. Eur. J. Neurosci. 16:1433-41).

The origin of this mutation is the insertion of a transgene, which seems to be disrupting the expression of the *Grxcr1* gene, as has been recently published (Odeh et al., 2010. Am. J. Hum. Gen. 86:148-60). Our experiments indicate that *Grxcr1* exons and transcript sequences are not affected by the transgene insertion in *tde* mutants. Furthermore, 5'RACE PCR experiments show the presence of two different transcripts of the *Grxcr1* gene, expressed in homozygotes and in wildtype controls. However, quantitative analysis of *Grxcr1* transcripts reveals a significantly decreased level in *tde* mutants compared to heterozygotes.

It remains unknown how the mutation affecting the *Grxcr1* gene causes the specific phenotype shown in *tde* mutants. The abnormally thin and long stereocilia of *tde* mutant mice suggests a problem in the stereocilia growth and maturation processes. Espin and myosinVIIa are both proteins known to be involved in the normal organization of the stereocilia hair bundle (Prosser et al., 2008. Mol. Cell. Biol., 28: 1702-12; Zheng et al. 2000. Cell 102: 377-85). We have analyzed the immunoreactivity of these two proteins in *tde* mutants and in controls to determine if these proteins might be directly or indirectly interacting with *Grxcr1*.

Funded by the Wellcome Trust and EuroHear.

330 Cloning and Quantification of BK Channel Exons and C-Terminal Types in the Developing Mouse Cochlea

Yoshihisa Sakai¹, Margaret Harvey¹, Bernd Sokolowski¹ ¹University of South Florida

Variations in the BK channel are the result of diverse alternative splicing of the BK gene. We identified 27 BK variants from Embryonic Day (ED) 14 ear, and Postnatal Day (PD) 14, and 30 cochleae, classified by exons and VYR, ERL, and DEC C-terminus types. We found 11 variants: 1 VYR, 6 DEC, 2 ERL, and 2 N+C types from PD14 and 30, and 16 variants: 8 VYR, 5 ERL, and 3 N+C types from ED14. N+C types represent two predicted open reading frames (ORFs), N- and C-termini BK, generated potentially from one BK transcript. We performed RT-PCR for 3 unique exons, using total RNA from ED14, PD4, 14, 30, and 34 mice. While 3 predicted start codons, MAN, MSS, and MDA are predicted in exon 1, only MDA and MSS are found, with MDA showing the greatest expression. Amplification using exon 8 forward and exon 9alt reverse primers revealed 2 fragments. One contains exon 8-9alt and is detectable on PD14 and 30. The other contains exon 8-9-9alt and includes an N+C type variant with 2 different putative ORFs in exon 9alt that are upregulated on ED14 and decrease after birth. STREX and STREXalt variants are alternatively spliced between exons 18 and 20, and are upregulated on ED14. As hearing matures, STREX upregulates on PD4 and downregulates on PD14, whereas STREXalt upregulates on PD14. STREX upregulates again, surprisingly, on PD34. gRT-PCR was performed using ED14, PD4, 14, and 30 mice and apex, middle, and basal regions of the cochlea with VYR, DEC, and ERL specific primers. Previous studies suggest DEC has a low affinity for the cell surface. VYR and ERL upregulate on ED14, whereas DEC upregulates after birth. On PD30, DEC expression is greatest in all 3 regions, ERL is greatest in the base, relative to other regions, and VYR is constant over all regions. The results suggest that BK alternative splicing characterizes cochlear organization, sound signaling, channel localization, and hearing maturation.

Supported by NIDCD grant R01DC004295 to BS.

331 High-Throughput Auditory Brainstem Response Phenotyping Identified Hearing Impairment in Mice Deficient in Dual-Specificity Phosphatase 3 (Dusp3)

Neil Ingham¹, Selina Pearson¹, Karen Steel¹ ¹Wellcome Trust Sanger Institute

Recordings of auditory brainstem responses (ABR) of mice aged 14 weeks were made as part of a high-throughput phenotyping pipeline of mice carrying targeted mutations (WTSI Mouse Genetics Programme). Mice maintained on a high fat diet were anaesthetised with a Ketamine / Xylazine mixture for recording of ABRs. Mice carrying a targeted mutation of *Dusp3* (Dual-Specificity Phosphatase 3) produced variable elevated thresholds for ABRs recorded in response to clicks and tones ranging from 6-30kHz. Average thresholds for *Dusp3*^{-/-} mice (n=9) were elevated by 15-20dB relative to $Dusp3^{+/+}$ mice (n=9) and were beyond a 2 standard deviation wide baseline population of wildtype mice.

Initial observations were extended using ABR recordings in mice raised on a normal diet. At 14 weeks old, all wildtype mice had good thresholds (n=5), whereas a proportion of $Dusp3^{+/-}$ and $Dusp3^{-/-}$ mice showed significant threshold elevations; 27% of $Dusp3^{+/-}$ mice (n=15 total) and 50% of $Dusp3^{-/-}$ mice (n=6 total) showed severe hearing impairment. By 6 months old, thresholds had deteriorated in the 5 wildtype but were similar to the unaffected Dusp3^{+/-} & Dusp3^{-/-} mice. Click ABRs indicated that thresholds in the affected Dusp3^{+/-} & Dusp3^{-/-} mice had deteriorated further from 14 weeks to 6 months of age. The pattern of auditory phenotype seen in these mice may indicate that loss of Dusp3 causes a variable penetrance dominant effect on hearing. Dusp6 has a similar variable effect on hearing in mice (Li et al., 2007) and is thought to act as developmental feedback regulator of FGF-stimulated ERK signalling. Dusp6 is a MAPK phosphatase (MPK) type of dual-specificity phosphatase (DSP). In contrast, Dusp3 is an atypical DSP (Alonso et al., 2004) and loss of this gene may produce a hearing impairment phenotype via other protein tyrosine phosphatase-dependent mechanisms.We thank the WTSI Mouse Genetics Programme for generation of mutant mice and The Wellcome Trust & Medical Research Council for funding.

332 A Low-Cost Exon Capture Method Suitable for Large-Scale Screening of Genetic Mutations in Deafness Genes by the Massively-Parallel Sequencing Approach

Wenxue Tang¹, Dong Qian¹, Shoeb Ahmad¹, Douglas Mattox¹, N. Wendell Todd¹, Harrison Han¹, Huawei Li², **Xi** Lin¹

¹*Emory Univ School of Medicine,* ²*Eye & ENT hospital, Fudan Univ*

Targeted gene capture followed by resequencing with the next-generation sequencing (NGS) approach has been used feasibly to screen mutations in large numbers of disease-linked human genes in a single test. Major remaining barriers for large-scale uses of NGS technology to identify mutations in disease-causing genes, however, appear to be the high per-sample cost and the accuracy of genotype calls demanded by clinical applications. Per-run cost of NGS machines is rapidly coming down and molecular barcoding readily reduces per-sample cost even more. For widespread clinical applications the main cost component and a key factor determining the sequencing accuracy have been the enrichment of targeted disease genes. Here we tested and validated a low-cost cDNAprobe-based approach for capturing exons of genes known to cause deafness in humans. The size and complexity in exon structure of these genes are chosen to cover the range of currently-known deafness genes. Results showed that our approach achieved specificity. multiplexicity, uniformity and depth of coverage in exon captures suitable for accurate sequencing by the NGS method in order to consistently detect genetic mutations. Reliable genotype calls for both homozygous and heterozygous single-nucleotide substitution as well as small insertion/deletion mutations were achieved. The results were confirmed independently by conventional Sanger sequencing techniques.

We are currently validating our method to include allknown deafness genes and candidates for applications such as genetic hearing screening in newborns. The high coverage depth, accuracy in genotype calls, and cost benefits of the cDNA-probe-based exon capture approach may also facilitate widespread NGS applications in clinical practices beyond deafness gene screening.

333 Application of Proteomics and Immunohistochemical Techniques to Identify and Characterize DFNB59 in Human Temporal Archival Tissue

Fred H. Linthicum, Jr.^{1,2}, **Orlando Valerino**¹, Ana Cordero¹, Robert Gellibolian¹, Jose N. Fayad^{1,2} ¹House Ear Institute, ²House Ear Clinic

Known mutations in the DFNB59 gene have been linked to cause a particular type of non-syndromic autosomal recessive deafness with the associated protein responsible believed to be Pejvakin (PJVK). In this study, we used human temporal bone sections exhibiting the unique DFNB59 histopathology, micro-dissected the affected regions and extracted and identified proteins. The experiment was compared to normal controls. We describe some of the first otopatholocial findings of DFNB59 found in post-mortem human samples. Pejvakin protein was identified confirmed using LC/MS/MS and with bioinformatic mining to > 80% probability. The unique peptide sequence linking to the PJVK protein was undetected in the control bone. This data was substantiated through immunohistochemical detection on the same archival tissue by a comparative direct fast red protocol. It was used to rule out possible paralogs, in particular DFNA5, which could result in a false positive. The pathology of the diseased bone indicates the osseous spiral lamina is empty throughout the cochlea. The spiral ganglion count is 2,016 in the right ear and 3,276 in the left. Normal for the age is 22,871+/-5,988. The organ of Corti, including supporting cells were absent in all segments. In addition, there is no tectorial membrane in the DFNB59 section. The neurites between the inferior Scarpas ganglion and the saccule have atrophied, but the superior vestibular nerve appears normal. The complete function of the PJVK protein is still unknown, however it is grouped with the gasdermin family of proteins, which may indicate some function with cell apoptosis, or metabolic product of a secretory pathway.

Key words: DFNB59, Pejvakin, otopathology, proteomics, immunohistochemistry, bio-informatics.

334 Impact of Murine Chronic Middle Ear Inflammation on Ion Homeostasis Gene Expression

Carol MacArthur¹, Fran Hausman¹, J Beth Kempton¹, Dennis Trune¹

¹OHSU

Ion homeostasis genes are responsible for movement of ions and water in the various spaces in the inner ear and epithelium of the middle ear. To what extent ion homeostasis is a factor in the fluid accumulation seen in the middle ear with chronic otitis media (OM) is not well known. C3H/HeJ mice, aged 6 months, were screened for chronic OM. Uninfected mice were used as controls. Mice were euthanized, the bullae harvested, and total RNA isolated from the middle ear tissues. A total of 24 ion homeostasis genes were analyzed for expression with quantitative RT-PCR from the following gene families: Na⁺,K⁺-ATPase, tight junction claudins, K⁺transport channels, epithelial Na ⁺channels, gap junctions, and aquaporins. Genes in every category were shown to experience down-regulation (p<0.05) with the exception of the claudin family, which was upregulated. Decreased gene expression was statistically significant for the Na⁺, K⁺-ATPase genes, K⁺transport genes, gap junction genes and aquaporins. Inflammatory genes were also analyzed: MIP-2, IL-6, IL-1β, IL-10, TNF, IL-1α, VEGF, and Mapk8. All of these inflammatory genes were up-regulated more than two-fold, with expression of IL-6, TNF and KC statistically significant compared to controls. The upregulation of the inflammatory genes indicates that a chronic inflammatory condition was present in the middle ear of the mice. This inflammation, coupled with the observed down-regulation of the ion homeostasis genes, suggests chronic OM suppresses many of the ion homeostasis genes and causes the fluid accumulation seen with otitis media, both acute and chronic.

[Research supported by NIH-NIDCD R01 DC009455]

335 Effect of Furanone as a Quorum Sensing Inhibitor in Experimentally Induced Chronic Otitis Media Animal Model Sun-Gui Kim¹, Yong-Ho Park¹

¹Chungnam National University

Background and Objectives : Many microorganisms use special signaling system to monitor their population density and to exchange many information for their comfortable environment. This type of signaling system is termed quorum sensing(QS). It plays important roles in bacterial communication one another. Also it controls a variety of bacterial virulence and is involved in biofilm formation. Inhibition of QS may provide alternative treatment for chronic infectious diseases that have resistance to conventional antibiotics. In this study, We aimed to evaluate the effect of furanone as a QS inhibitor on biofilm in experimentally induced chronic otitis media animal model. Subjects and Methods : Chronic otitis media was induced in rats by transtympanic injection of p.aeruginosa and biofilm formation was identified by electron microscopy at 4weeks after injection. And biofilm formations were

evaluated in control, furanone, antibiotics, and furanone + antibiotics group. Results : The biofilm formations were significantly reduced in furanone and furanone + antibiotics group than others. But the infections were more severe and prolonged in furanone group than others. Conclusions

: These findings suggest that furanone might play a inhibitory role in biofilm formation in experimental chronic otitis media animal model. And the synergistic effect of furanone and antibiotics might be another tool for chronic infectious disease.

336 Epithelial Surface Liquid Volume in Human Middle Ear Epithelium Is Regulated by Chloride Secretion Via Protease Activated Receptor-2

Sang Cheol Kim¹, Sung Huhn Kim¹, Jae Young Choi¹ ¹Department of Otorhinolaryngology, Yonsei University College of Medicine

Protease activated receptor-2 (PAR-2) has been thought to have a key role in regulating airway secretion via controlling ion transport such as chloride and sodium through airway mucosal epithelium. However, the role of PAR-2 in middle ear epithelium has been barely reported. Therefore we conducted this study to investigate the presence of PAR-2 in human middle ear epithelial cells (HMEEC) and their role in chloride secretion and epithelial surface liquid volume regulation by using molecular, electrophysiological study, and 3D z-stack analysis of surface liquid height with confocal microscopy. In cultured HMEEC, mRNA transcripts for PAR-2 were identified on RT-PCR. Surface liquid height (30.3 ± 2.4 im) increased 20 minutes after PAR-2 (10 iM) treatment on the apical side $(35.5 \pm 1.6 \text{ im})$ and baolateral side $(36.3 \pm 4.6 \text{ im})$ in the 3D z-stack analysis by using confocal microscopy. PAR-2 mediated chloride current was noted and decreased after choride channel blocker niflumic acid (100 iM) application on the Ussing chamber experiment with cultured HMEEC. Human airway trypsin-like protease (HAT), PAR2 activator, was isolated from middle ear effusion in western blot and PAR-2 expression was observed more prominently at the basement membrane of human middle ear epithelium by immunohistochemistry. These results imply that serine protease such as HAT in the middle ear epithelial surface liquid might regulate epithelial surface liquid volume by controlling chloride secretion via PAR-2.

337 Up-Regulation of Macrophage Migration Inhibitory Factor Induced by Lipopolysaccharides in Experimental Otitis Media with Effusion in Mice

Kaori Hashimoto¹, Shin Kariya¹, Mitsuhiro Okano¹, Kazunori Nishizaki¹

¹Okayama University

Otitis media with effusion is one of most common diseases in children. Multiple factors affect the course of otitis media with effusion. Several cytokines and chemokines including interleukin-1beta (IL-1 β) and tumor necrosis factor-alpha (TNF- α) have been detected in middle ear effusions of

patients with otitis media with effusion. Macrophage migration inhibitory factor is one of pro-inflammatory cytokines, and has multiple functions both within and outside of the immune system. The concentration of macrophage migration inhibitory factor in middle ear effusions of adult patients with otitis media with effusion is positively correlated with that of lipopolysaccharides. The purpose of this in vivo study is to disclose whether lipopolysaccharides directly inoculated into the middle ear cavity induces macrophage migration inhibitory factor production, and to determine the role of macrophage migration inhibitory factor in otitis media with effusion. BALB/c mice (male, 6-10 weeks old) were divided into 2 groups and their middle ears injected with either lipopolysaccharides or phosphate buffered saline (PBS). Mice were sacrificed at 6 hrs, 12 hrs, or 1, 3, 7, or 14 days after injection. Concentrations of macrophage migration inhibitory factor, IL-1 β and TNF- α in middle ear effusions were measured with enzyme-linked immunosorbent assay. Concentrations of macrophage migration inhibitory factor in the lipopolysaccharides group at 1 day, and 3 days were significantly higher than the PBS control group. Concentrations of IL-1 β in the lipopolysaccharides group at 6 hrs, 12 hrs, 1 day, and 3 days were significantly higher than controls. Concentrations of TNF- α in the lipopolysaccharides group at 1 day, and 3 days were significantly higher than controls. Concentration of macrophage migration inhibitory factor in the lipopolysaccharides group was positively correlated with that of IL-1 β and TNF- α . We clearly show in this study that direct injection of lipopolysaccharides into the middle ear causes production of macrophage migration inhibitory factor in an experimental mouse model of otitis media with effusion. Down-regulation of macrophage migration inhibitory factor may become a new approach for the management of otitis media with effusion.

338 Innate Immune Gene Networks and the Resolution of Otitis Media

Allen F. Ryan^{1,2}, Anke Leichtle³, Jorg Ebmeyer⁴, Jasmine Lee⁵, Emily Zuckerman⁵, Chelsea Wong⁵, Stephen I. Wasserman⁶

¹ENT UCSD, ²San Diego VAMC, ³ENT University of Lubeck, ⁴ENT Bielefeld Academic Teaching Hospital, ⁵Biology UCSD, ⁶Allergy/Immunology UCSD

Initial defense of body surfaces is mediated in part by families of receptors that recognize infecting organisms and mobilize defenses without need for prior sensitization. While cognate immunity relies upon adaptive recognition of foreign molecules, innate immunity uses a large set of invariant receptors, each of which responds to different classes of molecules produced by pathogens but not the host. To assess innate immunity's role in otitis media (OM), we evaluated the expression of innate immune genes in the normal vs infected middle ear (ME). We also compared OM induced by nontypeable Haemophilus influenzae in wild-type mice with that observed in mice lacking various Toll-like receptors (TLRs), NOD-like receptors (NLRs) or adaptor molecules that link them to intracellular signaling cascades. Many innate immune genes were expressed during OM. Moreover, defects in any of the molecules evaluated resulted in deficits in ME bacterial clearance, as well as prolonged OM. This was often associated with defects in leukocyte behavior. The greatest effect was seen for adaptor molecules, which typically link the responses of a variety of receptors to signaling cascades that mobilize cytokines, chemokines and leukocytes. Thus mutation of the TLR adaptor MyD88 or the NLR adaptors RIP2 or ASC induced more intense and persistent OM than did lack of individual receptors. The results indicate that an intact innate immune system is required for the normal defense of the ME from infection, even by a single organism. This in turn suggests that the cellular responses elicited by different innate immune receptors are not completely overlapping, since the activation of many different receptor types is required to elicit a fully effective response. Innate immunity may thus be designed to produce tailored responses to different types of organisms, depending upon the combinations of receptors that are activated. [Supported by NIH/NIDCD grants DC000129 and DC006279 and the VA Research Service.]

339 Otitis Media in a New Mouse Model for CHARGE Syndrome with a Spontaneous Mutation in the Chd7 Gene

Cong Tian¹, Heping Yu¹, Fengchan Han¹, Peter Scacheri¹, Cindy Benedict-Alderfer¹, Bin Yang¹, **Qing Yin Zheng¹** ¹Case Western Reserve University

CHARGE syndrome is a genetic disease caused by heterozygous mutation in the Chd7 gene. Patients with CHARGE syndrome showed symptoms such as growth retardation and abnormalities in eye, heart, choana, reproductive organ, and ear/hearing. Among the diseases discovered in the ears of CHARGE syndrome patients, otitis media was seen in near 100% of the patients. Although mouse models for human CHARGE syndrome have been reported and several features were studied, otitis media and related hearing loss have not been reported and studied yet. Here, we report a mouse model with a spontaneous mutation in the Chd7 gene, showing chronic otitis media with effusion. Otitis media in the Chd7 mutant mice is characterized by early onset age, eustachian tube dysfunction, epithelial hyperplasia, tympanic membrane retraction, middle ear effusion, and hearing loss. This is the first report of otitis media in the Chd7-deficiency mice and will facilitate the study of Chd7 in auditory system function and development. Supported by NIH grants R01DC009246 to QYZ.

340 A Mutation of the Sh3pxd2b Gene Is Correlated with Severe Otitis Media

Bin Yang¹, Fengchan Han¹, Heping Yu¹, Cong Tian¹, Rami Azem¹, Qing Yin Zheng¹

¹Department of Otolaryngology,Case Western Reserve University

Craniofacial defects that occur through gene mutation during development can lead to an increased incidence of otitis media. These defects have been shown to increase vulnerability to eustachian tube dysfunction. We examined

the effects of a mutation in the sh3pxd2b gene on the progression of otitis media and hearing impairment at various developmental stages. We used a mouse model to mirror craniofacial dysmorphology and otitis media in humans. Our findings showed that all mutant mice that had the sh3pxd2b mutation went on to develop craniofacial dysmorphologies and subsequently otitis media, by as early as 11 days age. We found bacterias in the exudates from middle ears in the mutant mice, and Proteus mirabilis are the dominant species. Hearing was tested by auditory-evoked brainstem response (ABR) and all mice were found to have hearing impairments, with lower frequency hearing impairment being more pronounced. The expression of TNF- α , TLR-2, and IL-1, which correlate with inflammation in otitis media, were found to be upregulated examined by immunostaining and Semiquantitative RT-PCR in the mutant mice .

*Supported by NIH grants R01DC007392 and R01DC009246 to QYZ

341 Regulation of Epithelial Sodium Channel by Prostasin and It's Inhibitor in Human Middle Ear Epithelium

Ju hyun Jeon¹, Sung Huhn Kim¹, Jae Young Choi¹ ¹Department of Otorhinolaryngology, Yonsei University College of Medicine

Epithelial sodium channel (ENaC) is important role on regulation of airway surface liquid (ASL) in human middle ear epithelial cells (HMEEC) and prostasin and it's inhibitor regulate activity of ENaC. We assumed that their balance was related to pathophysiologic mechanism of otitis media with effusion (OME). We identified prostasin and it's inhibitor, hepatocyte growth factor activator inhibitor (HAI-1) in HMEEC by reverse transcription polymerase chain reaction (RT-PCR). When pro-inflammatory cytokine, IL-1beta was treated in HMEEC, prostasin was upregulated. On sample of middle ear effusion, prostasin and HAI-1 was detected by western blot. In the ussing chamber, When aprotinin, kunitz type inhibitor similar HAI-1, was treated in HMEEC, ENaC-dependent current decreased. When trypsin was treated in HMEEC, ENaC-dependent current increased. These finding suggest that unbalance of protasin and HAI-1 causes pathological condition in middle ear like otitis media with effusion.

342 Conductive Hearing Loss in Acute Otitis Media Model of Guinea Pig

Xiying Guan¹, Rong Z. Gan¹

¹School of Aerospace and Mechanical Engineering and Bioengineering Center, University of Oklahoma

Acute otitis media (AOM) is characterized by a rapid middle ear infection symptoms such as purulent middle ear effusion and bulged opaque tympanic membrane (TM). The purpose of this study is to investigate the factors that contribute to conductive hearing loss in AOM ears. The AOM model was created in guinea pigs by transbulla injection of Streptococcus pneumoniae serotype 3. Three days after inoculation, the model was evaluated by otoscopy and tympanometry examination. The vibration of the TM and the auditory brainstem response (ABR) were measured in diseased ears at three experimental stages: 1) intact middle ear cavity including effusion and pressure (AOM-1), 2) pressure released only (AOM-2), and 3) effusion drained (AOM-3). The TM vibration was recorded by a laser vibrometer when 80 dB SPL pure-tone sweep from 0.2 to 40 kHz was applied in ear canal. Tone-burst ABR threshold was assessed at 2, 4, 8, 16, and 32 kHz. The displacement amplitude of the TM (dTM) in AOM-1 ears was significantly lower than that in control ears, and increased when the middle ear pressure was released by a hole punctured in the bulla wall (AOM-2). As the purulent effusion was drained from the cavity (AOM-3), dTM showed considerable improvement compared with AOM-2 ears, however, was still lower than control ears, which indicates the changes in mechanical properties in AOM ears. The ABR threshold changes along the three stages in AOM ears generally agree with the results of laser measurement. We conclude that the middle ear pressure, purulent effusion, and mechanical property change are three main factors that lead to conductive hearing loss in AOM ears. (Supported by OCAST HR09-033 and NIH R01DC006632)

343 Tissue Remodeling in the Acute Otitis Media Mouse Model

Nathan Sautter¹, Katherine Delaney^{1,2}, Dennis Trune^{1,2} ¹Oregon Health Sciences University, ²Oregon Hearing Research Center

Chronic otitis media is associated with fibrosis, scarring and osteogenesis within the middle ear. The bone morphogenetic protein (BMP) and fibroblast growth factor (FGF) families of cytokines and the matrix metalloproteinase (MMP) family of proteinases are known to contribute to tissue remodeling in other diseases. Their role in otitis media, however, remains unknown.

Heat-killed Streptococcus pneumoniae or Haemophilus influenzae was injected into the middle ears of Balb/c mice and tissues harvested at 1, 3, 5 and 7 days following injection (n=8 each time point). Middle ears were processed using RT-PCR to assess gene expression of BMP2, 3, 4, 5, 6, 7, 8a, 8b, 9, 10, FGFr1 & 2, FGF1, 3, 4, 5, 6, 7, 8, 10 and MMP2, 3, 7, 8, 9, 12 and 14. Results were compared to untreated and PBS treated controls (n=8 each time point). Immunohistochemistry was performed for BMP3, FGF3, FGF7 and MMP8 (n=4).

Significant upregulation of BMP1, BMP7, FGF3, FGF7, MMP2, MMP3 and MMP12 was observed at several time points in both bacteria treatment groups (p < 0.05). MMP3 in particular was elevated 2-18 times baseline levels. Staining for FGF3 and FGF7 was moderately positive, localizing to cells within the middle ear mucosa and submucosal stroma.

Upregulation of several tissue remodeling cytokines and proteinases in the acute otitis media mouse model may play a significant role in subsequent middle ear tissue remodeling. Further understanding of these molecular processes may allow for the development of treatment modalities aimed at preventing middle ear tissue remodeling. Supported by NIH NIDCD R01 DC009455 and DC009455S1.

344 Transduction, Tuning, and Spike Timing in the Rat Saccular Macula

Jocelyn Songer^{1,2}, Ruth Anne Eatock^{1,2}

¹Massachusetts Eye and Ear Infirmary, ²Harvard Medical School

We are exploring cellular mechanisms of frequency selectivity and afferent spike timing in a semi-intact preparation of the rat saccular epithelium (P0-P8). We deflect hair bundles with a rigid probe and compare transduction currents, receptor potentials, postsynaptic responses and spike rates and regularity.

Transduction currents evoked by sinusoidal stimuli manifest transducer adaptation as high-pass filtering. In striolar type I hair cells, two corner frequencies are seen (3.9±0.6 Hz (SEM, n=12) and 45±4 Hz (7)), consistent with the two adaptation time constants seen in step responses of the mouse utricle (Vollrath & Eatock 2003). Receptor potentials show additional high-pass filtering below 10 Hz by K⁺ current activation and low-pass filtering above 20 Hz from membrane capacitance. In striolar type I cells, this bandpass filtering had a mean best frequency of 21±3 Hz (9), a broad quality factor (Q_{3dB}) of 0.36±0.03 (4), and corner frequencies of 4±1 Hz (4) and 76±10 Hz (9). In preliminary results, Q_{3dB} values for EPSCs, EPSPs and spike rates become progressively larger, indicating sharper tuning. Spike thresholds may sharpen spike rate tuning by eliminating EPSPs that are too small to trigger a spike.

Afferent spike timing varies with zone. Recent work has implicated low-voltage-activated (LV) K channels in making spike timing irregular (Kalluri et al. 2010). Ganglion cell bodies with LV channels fire an onset spike in response to a depolarizing current step ("transient" response) and generate irregular spike timing in response to trains of synthetic EPSPs with pseudo-random timing. Consistent with the work on the cell bodies, we find that striolar complex calyces produce transient responses to current steps and have LV channels (21/22) while extrastriolar simple calyces belonging to dimorphic afferents tend to lack LV channels and make sustained responses (13/17). *Supported by NSBRI through NASA NCC 9-58.*

345 The Resting Potential and Membrane Time Constant of Cochlear Outer Hair Cells

Maryline Beurg¹, **Robert Fettiplace**², Stuart Johnson³, Walter Marcotti³

¹INSERM U587, Université Victor Segalen Bordeaux 2, France, ²University of Wisconsin-Madison, ³University of Sheffield

Outer hair cells (OHCs) are thought to mediate sharp tuning and amplification in the mammalian cochlea. The most accepted mechanism for this OHC role is somatic force generation underpinned by voltage-dependent gating of the motor protein prestin (Zheng et al. 2000). However, a criticism of the mechanism is that at high frequencies the OHC receptor potential will be attenuated by reported membrane time constants (Mammano & Ashmore 1996). In order to address the problem, we have determined time constants in OHCs of isolated rodent cochleas at five locations with characteristic frequencies (CF) from 0.35 to14 kHz. When hair bundles were exposed to low (0.02 -0.04 mM) Ca²⁺ similar to endolymph, about half the mechanotransducer (MT) channels were open at rest producing a large inward current that, in animals around the onset of hearing, depolarized OHCs to about -30 mV and reduced their membrane time constant (T). Voltagedependent K⁺ conductances (in post natal day 18 animals) and MT conductances grew in parallel as a function of CF. The in vivo resting membrane potential of OHCs was estimated by inserting MT and K⁺conductance values, corrected to body temperature, in an equivalent electrical circuit that included a 90 mV endolymphatic potential. The calculations indicated for all CFs a mean resting potential of -34 mV thus fully activating the voltage-dependent K⁺ conductance and minimizing the membrane time constant, which decreased with CF; the corner frequency $(1/2\pi\tau)$ increased from 0.35 to 7 kHz for CFs of 0.35 - 14 kHz. The predicted OHC resting potential is similar to the halfactivation voltage for prestin (approximately -40 mV in rat; Mahendrasingam et al. 2010) and produces a corner frequency roughly matching CF. Such attributes ensure optimal activation of prestin by receptor potentials at CF and facilitate prestin's role as the cochlear amplifier. Work supported by NIDCD grant RO1 DC01362 to RF and grants from the Wellcome Trust and RNID to WM.

346 Bundle-Fluid Interaction in Mammalian Auditory Mechanotransduction

Sonya Smith^{1,2}, Richard Chadwick²

¹Howard University, ²NIDCD

During the process of mechanotransduction in the mammalian cochlea, the inner hair cell stereocilia bundle performs the role of transducer. Hydrodynamic stimuli deflect the hair bundle to open ion channels, resulting in cation influx and subsequent neurotransmitter release at the base of the cell $\frac{1.2}{2}$. Hypotheses for mechotransduction include fluid shear-driven motion between the tectorial membrane and the reticular lamina to deflect the bundle $\frac{3.4}{1.4}$. It is presumed that 'molecular gates' sense tension in tip-links that connect three stepped rows of stereocilia to open the ion channels $\frac{5}{2}$. However, the details of the flow of the endolymphatic fluid in the micron-sized gap surrounding the bundle and the sub-micron sized gaps between individual stereocilia rows are unknown. Here we show how each row of stereocilia and their associated tip links and gates move with corresponding oscillatory flow patterns that are determined from a multi-scale computational model with nanometer resolution. The model confirms the crucial role of the tectorial membrane in hearing, and explains how this membrane amplifies and synchronizes the timing of peak tension in the upper and lower tip links via an unexpected mechanism.

1. Corey, D.P. & Hudspeth, A. J. Ionic basis of the receptor potential in a vertebrate hair cell. Nature 281: 675-677, 1979.

2.Hudspeth, A.J. How the ear's works work. Nature 341:397-404, 1989.

3.Billone, M.C. & Raynor S. Transmission of radial shear forces to cochlear hair cells. J Acoust Soc Am 54:1143-1156, 1973.

 Freeman, D.M. & Weiss, T.F. Hydrodynamic forces on hair bundles at low frequencies. Hear Res 48:17-30, 1990.
Howard, J. & Hudspeth, A.J. Mechanical relaxation of the hair bundle mediates adaptation in mechanoelectric transduction by the bullfrog's saccular hair cell. Proc. Natl. Acad Sci 84, 3064-3068, 1987.

347 Phantom Tones and Suppressive Masking from Active Nonlinear Oscillation by the Hair-Cell Bundle

Jeremie Barral^{1,2}, Pascal Martin^{1,3} ¹Institut Curie, ²Université Denis Diderot, ³Université Pierre et Marie Curie

It is a well-known fact of human psychoacoustics that twotone stimulation at nearby frequencies f_1 and f_2 evokes additional tones in the auditory percept. The auditory nonlinearity that underlies these phantom tones is also associated with suppressive masking, the phenomenon by which the perceived loudness of a single tone diminishes if a second tone is present. These phenomena are thought to emerge from nonlinear mechanical interference of sound-evoked vibrations within the inner ear and to rely on the striking compressive nonlinearity that accommodates a vast dynamic range of sound intensities into a much narrower range of vibration amplitudes. It is noteworthy that nonlinear compression reveals itself only near a characteristic frequency of maximal responsiveness to sound. Mechano-electrical transduction by sensory hair cells is thought to provide nonlinear feedback on inner-ear mechanics. However, the mechanism that mediates frequency specificity of auditory nonlinearities remains a central question of auditory physiology.

Here, we evaluate in vitro the effects of active hair-bundle motility on distortion products and two-tone suppression by a single hair-cell bundle from the bullfrog's saccule. We show that spontaneous hair-bundle oscillations provide a characteristic frequency near which these nonlinear phenomena are enhanced. At resonance, a two-tone stimulus of only 1 pN is sufficient to elicit a cubic distortion product $2f_1$ - f_2 . Moreover, this product increases in proportion with the primaries so that their relative levels remain nearly constant. Finally, the distortion magnitude displays a steep dependence on the frequency separation f_2 - f_1 . With nonlinear amplification afforded by active hairbundle movements, the nonlinearities inherent to the mechano-electrical transduction process acquire properties that are found in hearing, suggesting that active nonlinear oscillators shape the sensation of sounds at the periphery of the vertebrate ear.

348 High-Speed Recording and Image Analysis of the Motile Responses of Outer Hair Cells Stimulated at Frequencies of 50 Hz to 4 KHz

Rei Kitani¹, Federico Kalinec¹ ¹*House Ear Institute.*

Detailed studies of outer hair cell (OHC) motility at acoustic frequencies have been hampered by limitation in the image recording systems. In this presentation we will describe the motile responses of isolated guinea pig OHCs stimulated with an external alternating electrical field at frequencies between 50 Hz to 4 kHz recorded and analyzed with a novel ultra-high speed imaging system. The imaging system consists of a video camera able to record up to 100,000 fps combined with a LED-based illumination device and image analysis software that simultaneously and automatically tracks several individual features in the cell's image frame-by-frame. OHCs were stimulated in continuous, burst, and sweeping modes for periods of up to 10 s, and changes in electromotile amplitude and in total cell length were analyzed off line. Cell responses were dependent on the frequency as well as the mode and intensity of the stimulation, with electromotile amplitudes ranging from 0.3% to 3.2% of the total cell length and total cell length usually decreasing in amounts varying from 0.1% to 4.3%. At any frequency electromotile responses followed cycle-by-cycle the electrical stimulus, but the amplitude of the movement increased during the first 1 to 3 s until reaching a plateau. Slow motile responses, in contrast, were undetected by about 800 ms after the beginning of the stimulation, but then developed continuously. When OHCs were stimulated with 50 Hz to 4 kHz square wave's sweeps, electromotile amplitude was near constant up to 200Hz, progressively decreased between 200 Hz and 2 kHz, and then remained constant until the end of the experiments at 4 kHz. Fast motility, but not slow motility, was affected by incubation of the cells with 10 mM salycilate; incubation with 3 mM gadolinium, in contrast, affected both fast and slow motile responses. These results provide new clues about the cellular and molecular mechanisms underlying the motile response of guinea pig OHCs.

Supported by NIH Grant DC010146.

349 Local Re-Assembly of

Mechanotransduction Apparatus at the Stereocilia Tips in Cochlear Inner Hair Cells Artur Indzhykulian¹, Ruben Stepanyan¹, Gregory

Frolenkov¹

¹University of Kentucky

Mechanosensory apparatus of the inner ear hair cells includes a yet unidentified mechanotransduction channel, an extracellular "tip link" conveying mechanical force to the channel, and the molecules responsible for Ca²⁺dependent decay (adaptation) of the mechanotransduction response. A predominant model postulates that this apparatus is assembled at the base of hair cell stereocilia and transported to the stereocilia tips by a myosin-based adaptation motor. We studied disruption and re-assembly of tip links and other stereocilia links in the inner hair cells

of young postnatal mice that lose almost all stereocilia links in Ca²⁺-free BAPTA-buffered medium. Using highresolution scanning electron microscopy, we found that the tip links re-appear at the tips and never at the bottom of stereocilia. Immunolabeling with the antibodies raised against the tip link component, protocadherin-15-CD3, did not show gross redistribution of this protein. It was still present at the tips of stereocilia before, immediately following BAPTA treatment, and after short time of recovery. Likewise, we did not observe any signs of redistribution of other isoforms of protocadherin-15 after BAPTA treatment. The recovery of the amplitude of mechanotransduction responses followed exactly the recovery of tip links, while normally fast adaptation reappeared long after the full set of stereocilia links and the mechanotransduction current maximal were reestablished. During the recovery, the slope of the peak current - displacement curve did not change indicating that the geometry factor of the nascent tip links is likely to be the same as that of fully recovered tip links. We concluded that the inner hair cell mechanotransduction apparatus is gradually re-assembled at the tips of stereocilia and is not transported there as a fully functional unit.

Supported by NIDCD/NIH (R01 DC008861 and ARRA supplement 3R01DC008861-01A2S1).

350 The Active Process in Coupled Hair Cells in the Frog Sacculus

Clark Elliott Strimbu¹, Lea Fredrickson-Hemsing¹, Dolores Bozovic¹

¹UCLA

Hair bundles of the frog sacculus do not exhibit spontaneous mechanical oscillations in vitro with the otolithic membrane left intact. However, we observe other signs of the active process under native loading conditions. In particular, hair bundles exhibit a biphasic response, similar to the twitch seen in individual cells, when the otolithic membrane is stimulated by a pulse train. When deflected in the excitatory direction by a sinusoidal pulse, hair bundles first follow the stimulus but show significant up to 10 nm – motion in the inhibitory direction and then return to their resting position with a time constant on the order of a millisecond.

We have measured the strength of the mechanical coupling between the hair bundles and the otolithic membrane. We find that the coupling is primarily elastic rather than viscous with an elastic strength that can be up to an order of magnitude times larger than the hair-bundle stiffness. We hypothesize that in addition to providing passive mechanical coupling between hair bundles, the elastic load of the otolithic membrane maintains the hair cells in a quiescent but active regime.

351 Steady State Deflections Reveal New **Bundle Dynamics**

Lea Fredrickson Hemsing¹, C. Elliott Strimbu¹, Dolores Bozovic¹

¹UCLA

In an *in-vitro* preparation of the bullfrog sacculus, hair cell bundles exhibit spontaneous oscillations when transepithelial ionic gradients are maintained and the bundles have been decoupled via the removal of the overlaying otolithic membrane. These oscillations have been described by a system of nonlinear differential equations whose solutions undergo a bifurcation from a quiescent to an oscillatory state. In our experiments, we find that applying a slow displacement to the bundle tip during spontaneous oscillation leads to a qualitative change in the oscillation profile, implying the crossing of a second bifurcation. We further observe that application of a small steady-state displacement in the direction of tallest stereocillia can enhance bundle sensitivity. We compare these results to bundle offset position under more natural conditions, where the bundles are still coupled to the otolithic membrane.

352 Mechanical Overstimulation of Hair **Bundles and Its Effect on Spontaneous** Oscillations

Albert Kao¹, C. Elliott Strimbu¹, Lea Fredrickson Hemsing¹, Dolores Bozovic¹ ¹UCLA

We investigate the effects of large mechanical stimulus on bullfrog (Rana catesbeiana) saccular hair cells in vitro. Spontaneous oscillations are believed to be a signature of the amplifying and tuning mechanism in auditory vestibular system in amphibians. Applying displacements in the micron range on hair cell bundles allows us to probe the responses to stimulus outside the physiological intensity range. We observed changes in the spontaneous oscillations at time scales far slower than the known adaptation mechanisms. Large recurring stimulus induces an offset in bundle position up to hundreds of nanometers, and suppresses spontaneous oscillations. Cells slowly return to their original position, resume oscillating again with increasing amplitude and recover to their pre-stimulus condition on the order of seconds.

353 Interactions of Mechanical and Electrical **Oscillations in Bullfrog Saccular Hair Cells**

Alexander Neiman¹, Lijuan Han^{1,2}, Andrey Shilnikov³ ¹Ohio University, ²Beijing Institute of Technology, ³Georgia State Universitv

Spontaneous active oscillations of hair bundles documented in saccular hair cells of lower vertebrates contribute to enhanced sensitivity and selectivity of these peripheral mechano sensors. Recent experimental studies have shown that the membrane potential of the same type of hair cells may also undergo spontaneous oscillations. Thus a single hair cell system embeds two nonlinear oscillators coupled bi-directionally. We use computational modeling to study how these two compartments, mechanical and electrical, interact to produce coherent self-sustained oscillations and how this interaction contributes to overall sensitivity and selectivity of the hair cell. Our model incorporates a mechanical active hair bundle oscillator coupled to a Hodgkin-Huxley type system describing basolateral ionic currents of bullfrog saccular hair cells. The mechanical compartment is stochastic, as it includes thermal noise from the Brownian motion of the

hair bundle and from stochastic cluttering of mechanoelectrical transduction channels. We found that basolateral ionic currents may significantly alter the dynamics of hair bundle motion. In particular, two oscillatory compartments may be brought to synchrony which results in significantly enhanced coherence of spontaneous bundle oscillations and consequently to enhanced selectivity and sensitivity to sinusoidal mechanical stimuli. This supports a hypothesis on the functional role of voltage oscillations to regularize hair bundle motion. On the other hand, the model also demonstrates chaotic voltage oscillations reflected in complex multi-mode traces of hair bundle motion, consistent with recent experimental study of Ramunno-Johnson et al [Hearing Res. 2010]. We show that these complex oscillations result in broad-band encoding of external mechanical stimuli.

354 Numerical Study of the Complex Temporal Pattern of Spontaneous Oscillation in Bullfrog Saccular Hair Cells

Yuttana Roongthumskul¹, Dolores Bozovic¹, Lea Fredrickson Hemsing¹, Albert Kao¹

¹UCLA

Spontaneous oscillations observed in hair cells from the bullfrog sacculus reveal complex temporal characteristics, not fully captured by a simple limit-cycle oscillation. Multiple frequencies are apparent in the innate movement, with prolonged quiescent interval interspersed with oscillatory behavior. These oscillation profiles change considerably upon mechanical loading or the application of a steady-state deflection to the bundles. An imposed mechanical load reduces the occurrence of quiescent intervals, leading to a more regular oscillation pattern. We use numerical modeling to reproduce these complex effects and elucidate their underlying mechanisms.

355 Fast Length Changes in Outer Hair Cell Stereocilia Bundle Are Modulated by Endocochlear Currents

Pierre Hakizimana¹, William E. Brownell², Stefan Jacob¹, Anders Fridberger¹

¹Karolinska Institutet, ²Baylor College of Medicine

Sound-induced mechanical vibrations of the hair cell stereocilia bundle generate receptor potentials that initiate sound perception. In the mammalian cochlea, the tips of the tallest outer hair cells (OHC) stereocilia are anchored firmly in the tectorial membrane while the inner hair cell (IHC) stereocilia appear to be freestanding. Each stereocilium is a membrane-covered structure with a core extensively cross-linked actin filaments. of The stereocilium bends at a neck-like thinning near its insertion into the hair cell's cuticular plate and more than three decades of study have shown that the bending of the bundle is important for mechanoelectrical signalling. Aside from its ability to bend at the neck, the stereocilium is usually considered as a stiff inelastic rod and there have been no studies on its axial mechanics. Indeed, the idea that axial length changes could take place during sound transduction and their possible importance, to our knowledge, have never been explored before.

Here we show that the length of the stereocilia bundle of mammalian OHC changes during sound transduction and that the magnitude of the length change is regulated by currents passing through the stereocilium. The greater the length changes, the smaller the bundle deflection. The magnitude of the length change is reduced with currents that mimic normal in vivo endocochlear currents. IHC bundles undergo smaller axial length changes and current induced modulation was not detected. These findings show that the apparent elastic properties of the OHC stereocilia bundle are altered by electrical current. Normal hearing appears to require a greater axial stiffness for the OHC bundle most likely to boost the deflection.

356 Reactive Components of the Cochlear Microphonic

Peter Scully¹, John Oghalai², William Brownell¹ ¹Baylor College of Medicine, ²Stanford University

Prestin-associated charge movement is routinely measured to assess prestin function in cochlear outer hair cells. Prestin makes a conspicuous contribution to the reactive, or imaginary (as opposed to the ohmic, or real) component of the complex, whole-cell impedance. The underlying mechanoelectrical coupling has been modeled as a piezoelectric. We analyze the cochlear microphonic to determine if prestin-associated charge movement makes a contribution to the magnitude and phase of acoustically evoked high frequency intracochlear currents. A recording electrode is inserted through the round window of 21-35 days old mice. The cochlear microphonic in response to acoustic stimulation is amplified and fed to a lock-in amplifier, which measures the in-phase and out-ofphase portions of the AC signal. After recording the control response, salicylate, a competitive inhibitor of prestin-associated currents, is added via diffusion through the round window. The average voltage response at 48 kHz frequency was 10.5 µV at 40 dB. After adding salicylate, this response decreased to $8.3 \,\mu$ V. In addition to the decrease in voltage magnitude, adding salicylate was associated with a shift in the phase angle of 0.12 radians. Tests were also performed at a frequency of 6kHz: salicylate decreased the voltage from 6.3 µV to 4.6 µV and shifted phase of by 0.08 radians. At both frequencies, the change in the out of phase component was greater than the in phase voltage component. Results will be compared with expectations from a piezoelectric circuit model.

Research supported by NIH/NIDCD R01 DC000354 & DC002775 and T32 DC007367.

357 Basilar Membrane Measurements from Prestin 499 Mice: Linking Vibration to Sensation, Frequency Shifting, and Obligatory Amplification by Prestin

Thomas Weddell¹, Marcia Mellado-Lagarde^{1,2}, Victoria Lukashkina¹, Andrei Lukashkin¹, Jian Zuo², **Ian Russell¹** ¹University of Sussex, ²St. Jude Children's Research Hospital

Basilar membrane measurements from prestin 499 mice: linking vibration to sensation, frequency shifting, and obligatory amplification by prestin.

Tom Weddell¹, Marcia Mellado-Lagarde^{1,2}, Victoria Lukashkina¹, Andrei Lukashkin¹, Jian Zuo² and Ian Russell¹.

¹ School of Life Sciences, University of Sussex, Falmer, Brighton, East Sussex, BN1 9QG, UK

² Department of Developmental Neurobiology, St. Jude Children's Research Hospital, Memphis, TN 38105;

Cochlear microphonic (CM) and compound action potentials (CAP) were measured from the round window, and basilar membrane (BM) displacements were measured from the cochleae of wild type and V499G/Y501H (499) knockin mice¹, 499 mice suffer progressive outer hair cell (OHC) loss, thus we limited our measurements to 16 -21 day-old mice. OHC lengths and axial stiffness of 499 and wild type mice are similar. OHCs of prestin knockout (KO) mice are shorter and ~70% less stiff¹. CM asymptotes in response to 10 kHz tones were similar in wild type and 499 mice. CAP thresholds in wild type and 499 mice were similar to those reported by Dallos et al. but more sensitive at high frequencies. BM frequency tuning curves recorded from the ~60 kHz region of wild type mice cochleae were similar to those recorded previously² with thresholds (0.2 nm criterion) \sim 30 dB SPL at the tuning curve tip (CF). Post mortem (PM), compression measured at CF disappeared and the tuning curve tips broadened, desensitized and moved to lower frequencies. BM tuning curves measured from 499 mice were similar to those recorded PM from wild type mice and did not change noticeably PM. Our findings for 499 homozygous mice resemble those for prestin KO mice in that BM tuning curves measured alive and PM were similar and that the CF shifted to lower frequencies compared with wild type mice. The CF of the tuning curves of prestin KO mice are, however, ~20 dB more sensitive than in 499 and PM wild type mice². Our measurements from 499 and prestin KO mice support the notion^{2,3} that prestin evolved to enhance mechanical coupling between BM vibration and IHC hair bundle shear. This process resulted in desensitization of BM motion and upward shift in CF, necessitating prestin-dependent amplification at the higher CF.

¹Dallos et al., Neuron. 2008;58,333–339. ²Mellado et al., Curr. Biol. 2008;18,200–202

³Santos-Sacchi, Curr. Biol. 2008;18,R304

Supported by Medical Research Council, 5R01DC006471, Wellcome trust

358 High Frequency Mechanical Stimulation and Motion Analysis of the Organ of Corti

Aleks Zosuls¹, Laura Rupprecht¹, David Mountain¹ ¹Boston University

Accurately identifying the paths for mechanical motion and fluid motion propagation in the organ of Corti (OC) and basilar membrane (BM) is essential in order to understand phenomena such as the cochlear amplifier and otoacoustic emissions. Here we present the results from a new highfrequency mechanical stimulation system that was designed to provide more precise local excitation and motion sensing of the OC/BM complex. It is based on mechanical tissue excitation via a small vibrating probe and sensing using stroboscopic video microscopy. The system is currently capable of measuring sub micrometer motion at frequencies from DC to 60 kHz.

Measurements were performed on excised Gerbil cochlea. The turn of interest was isolated from the rest of the cochlea and windows in scala tympani and scala vestibule were carefully opened to expose the OC and then mounted on an inverted microscope. The underside of the basilar membrane was mechanically stimulated in the direction normal to the membrane with a 10um diameter glass probe mounted to a piezoelectric stack. While the membrane was sinusoidally stimulated, images were acquired at 8 phases per cycle using a computercontrolled stroboscope to reconstruct the motion of the tissue at the stimulus frequency. Data was collected at multiple focal planes from the BM to the tectorial membrane in order to capture motion for a variety of cellular and extracellular structures. Regions of interest such as inner hair cell hair bundles and tunnel crossing fibers were selected and displacements quantified using a cross correlation technique.

Displacement magnitude and phase was measured as a function of distance from the probe and a function of stimulus frequency. Both magnitudes and phases decreased with distance from the probe in a manner that suggests that both direct longitudinal coupling and wave propagation were contributing to the responses. Supported by NIDCD grant DC 000029

359 Vibration Modes of the Mammalian Cochlear Partition, *in Vitro* Nigel Cooper¹, Robert Szalai²

¹Keele University, ²Bristol University

In order to increase our understanding of cochlear mechanics, we have studied the electrically and acoustically evoked vibration patterns of various *in vitro* cochlear preparations. Light microscopic access to the excised middle and/or apical turns of gerbil and rat cochleae was combined with laser interferometry to measure the transverse vibrations of the basilar and tectorial membranes (BM, TM), the reticular lamina (RL), and various locations within the organ of Corti.

We observed electrically evoked vibrations that were both complex and frequency-dependent. Our low frequency measurements confirmed previous reports that the TM (along with most of the RL) moves roughly ten times more that the BM, and that it moves in antiphase to the BM, during electrical stimulation¹. Under these conditions, the region of the BM near the feet of the outer pillar cells moved less than the BM's arcuate and pectinate zones (so the BM vibrated in two lobes, but both lobes were "in phase"). As the frequency of the electrical stimulus was increased, however, the BM vibrations in the region beneath the organ of Corti gradually accumulated an additional 0.5 cycles of phase-lag to become in phase with the RL vibrations (a situation which may allow the outer hair cells to amplify sound-evoked BM motion by positive feedback, *in vivo*). The high frequency, electrically-evoked BM vibrations were therefore more truly "bimodal" (i.e. biphasic), with only the most lateral aspects of the BM vibrating in antiphase to the RL.

In contrast, when stimulated acoustically, the BM, TM and RL all moved in phase with one another, and the BM had its maximal vibration amplitude near the feet of the outer pillar cells, as observed elsewhere *in vivo*^{2,3}.

Supported by the BBSRC and Deafness Research UK. References

 F. Mammano & J.F. Ashmore (1993) Nature 365, 839
N.P. Cooper & W.S. Rhode (1995) Hear. Res. 82, 225
N.P. Cooper (1999) In: Recent Dev. Auditory Mechanics, World Scientific, p109ff

360 Imaging Vibration of the Cochlear Partition from a Temporal Bone Preparation Niloy Choudhury¹, Yaguang Zeng¹, Anders Fridberger¹,

Fangyi Chen¹, Dingjun Zha¹, Steven Jacques¹, Alfred Nuttall¹, Ruikang Wang¹

¹Oregon Health & Science University

Measuring the sound stimulated vibration from various structures in the organ of corti is important in understanding how the small vibration was amplified and detected. In this study we examine the feasibility of using phase-sensitive Fourier domain optical coherence tomography (PSFD-OCT) to measure vibration inside the organ of Corti. PSFD-OCT is a low coherence interferrometry system where the interferrogram is detected as a function of wavelength. The phase of the Fourier transformation of the detected spectra contains path deference (between the sample arm and the reference arm) information of the interferometer. In PSFD-OCT this phase is measured as a function of time and thus any time dependent change in the path difference between the sample arm and the reference arm can be detected. In the experiment, we excised a guinea pig cochlea and made a surgical opening at the apical end to access the organ of Corti. By applying tone with different frequencies via the intact middle ear, we recorded the vibration inside the organ of Corti using the PSFDOCT system. Vibration amplitude and phase of different substructures were mapped on a cross-section view of the organ of Corti. Although the measurements were made at the apical turn of the cochlea, it will be possible to make vibration measurement from various turns of the cochlea. The noise floor of the system was 0.3 nm, calibrated using a piezo stack. Supported by NIDCD R01 DC 000141 (AN) and R01 DC 010399 (AN).

361 Phase of the Active Force Deduced from in Vivo Cochlear Responses to Acoustic Stimulation

Sripriya Ramamoorthy¹, Alfred Nuttall¹ ¹Oregon Health & Science University

The mammalian cochlea is extremely sensitive to low level sounds while less sensitive to loud sounds. Measurements have confirmed that the gain of basilar membrane (BM) velocity relative to the stapes for low level acoustic stimulation can be nearly 60 dB higher than for high level stimulation. It is now widely believed that the active force arising from outer hair cells in vivo, either via hair bundles or through the basolateral membrane motor, acts on the BM with appropriate timing to significantly amplify its motion. It has been hypothesized, and some models have shown, that in order to add energy and amplify the BM motion the active force would be in-phase with the BM velocity basal to the characteristic place. Such a phase relationship is yet to be confirmed by experiments. We deduce the phase of the active force from in vivo measurements available in the literature. The derived phase is discussed with reference to contemporary understanding.

362 The Physical and Physiological Basis for Traveling-Wave Dispersion in the Cochlea

Sripriya Ramamoorthy¹, Dingjun Zha¹, Alfred Nuttall¹ ¹Oregon Health & Science University

The wave propagation in the cochlea as evidenced by measurements of basilar-membrane velocity, as well as auditory-nerve responses to sound, demonstrates significant dispersion, in addition to tonotopic gain and active amplification. The biophysical basis for this dispersion remains elusive. In this work, a simple analytical model, along with experimental validation using physiological measurements from guinea-pigs, is presented to identify the origin of the traveling-wave dispersion in the cochlea. We show that the dispersion in the cochlear base as well as the apex is fundamentally due to the coupled fluid-structure interaction between the basilar membrane and the scala fluids. It is further influenced by the variation in physical and geometrical properties of the basilar membrane, the sensitivity or gain of the hearing organ, and the relative dominance of the compression mode about one-third octave beyond the best frequency.

363 Effect of Superior Semicircular Canal Dehiscence Size on Intracochlear Pressures of Scala Vestibuli and Scala Tympani

Hideko Nakajima^{1,2}, Saumil Merchant^{1,2}, John Rosowski^{1,2} ¹*Harvard Medical School,* ²*Massachusetts Eye and Ear Infirmary*

Simultaneous measurement of basal intracochlear pressures in scala vestibuli (SV) and scala tympani (ST) in human cadaveric temporal bones enables determination of the differential pressure across the cochlear partition, the stimulus that excites the partition, providing a close measure of what a live human would hear. We are using

intracochlear pressure measurements to study superior semicircular canal dehiscence (SCD), an additional opening in the bony wall of the inner ear which does not exist in normal ears. The dehiscence provides an alternative path through which the stimulus fluid displacement of the oval window motion can flow. SCD can result in conductive hearing loss, but the precise mechanism is presently not well understood. For example, it is unknown why some individuals with SCD have hearing loss while others do not. In this study, dehiscences of various sizes (0.5, 1, 2 mm long) are made in the superior canal while the differential pressure across the cochlear partition is measured. Preliminary results show that SCD decreases the pressure in both SV and ST for low frequencies (< 500 Hz), and the SCD effects can be reversed by patching the dehiscence with dental cement. The calculated differential pressure (input across the partition) also decreases due to SCD. These effects at low frequencies become more pronounced with increase in the size of the dehiscence. For frequencies above 500 Hz, the effects on SV and ST due to various SCD size are more complex and varied across individual ears. It appears that an SCD shunts fluid flow away from the cochlea, resulting in decreased pressure difference across the cochlear partition, leading to hearing loss. The larger dehiscences appear to result in greater hearing loss as measured by reduction in differential pressure.

364 Observing Cochlear Mechanics in the Basal Region of CBA/J Mice

Wei Dong¹, Polina Varavva¹, Elizabeth Olson¹

Historically, the mouse was not used for studies of cochlear mechanics because its cochlea is tiny with limited access to the basilar membrane (BM), and its frequency range is shifted up substantially relative to human. However, the use of genetically modified mice in auditory science has been accelerating, producing mouse models with, for example, modified stereocilia, tectorial membrane and gap junctions. These models offer opportunities to probe fundamental questions of cochlear mechanics and motivated our development of techniques to measure BM motion and intracochlear pressure in mice.

Using laser-Doppler vibrometer and micro-pressure sensor, cochlear mechanics was studied by measuring the BM velocity and scala tympani (ST) pressure in the cochlear base of the CBA/J mouse. A new version of our micro-pressure sensor uses a single mode optical fiber coupled to a super-luminescent diode. With this sensor, the outer diameter could be minimized to ~ 81 μ m, which could fit into the mouse ST through the round window opening. The BM velocity was measured in the same region through the transparent round window membrane. Our results in CBA/J mice showed that: (1) Compound action potential had thresholds of ~ 40 dB SPL at frequencies between 10 to 50 kHz, then increased to 70 dB SPL at 70 kHz; (2) The mouse cochlear anatomy varied substantially even within the same strain, for example, the size and tilting of the round window. This uncertain anatomy adversely affects the mechanical measurements.

(3) BM velocity and ST pressure in the very basal region were similar to those in other species, and active cochlear mechanics are difficult to measure even in normal animals.

365 Electrically Induced Outer Hair Cell Motion Measured in the *in Vivo* Organ of Corti by OCT

Dingjun Zha^{1,2}, Fangyi Chen¹, Alfred Nuttall¹ ¹Oregon Health & Science University, ²Xijing Hospital, Fourth Military Medical University

Electrically induced outer hair cell (OHC) motility, demonstrated extensively by a number of investigators in isolated OHC and in vitro and in vivo cochlear preparations, has been considered to be a key mechanism in the active process which brings about the excellent sensitivity and frequency selectivity of mammalian hearing. In this study, electrical-to-mechanical transduction in the quinea pig cochlea, evoked by sinusoidal electrical current injected into the ST and SV, was demonstrated in vivo by direct measurement of basilar membrane and reticular lamina motion. The optical (low) coherence tomography (OCT) method enabled both the imaging of the organ of Corti and the determination of tissue displacements at auditory frequencies. The key aspects of the electrically evoked motion were that the basilar membrane and the reticular lamina moved in antiphase and the motion of the reticular lamina was several times larger than the basilar membrane. Our measurements supply in vivo direct evidence that outer hair cell force can drive the "upper and lower" surfaces of the organ of Corti in antiphase. The electrically induced relatively larger magnitude is consistent with RL "gain" that occurs in sensitive cochleae with acoustic stimulation. The implication of the RL motion and complexity will be discussed. Supported by NIDCD R01 DC 000141 and R01 DC 0010399.

366 Viscoelastic Properties of Plasma Membrane Varies with Cholesterol Level

Nima Khatibzadeh¹, Sharad Gupta², Mohammad Sarshar², William E. Brownell³, Bahman Anvari² ¹Department of Mechanical Engineering, University of California, Riverside, ²Department of Bioengineering, University of California, Riverside, ³Bobby R. Alford Department of Otolaryngology-Head and Neck Surgery, Baylor College of Medicine

Membrane cholesterol content modulates the membrane charge movement and electromotility in outer hair cells [1]. We have examined the effects of membrane cholesterol on viscoelastic properties of the plasma membrane. Optical tweezers are used to form plasma membrane nanotubes (tethers) from human embryonic kidney cells. The cells were treated with 3 and 5 mM concentrations of water soluble cholesterol and methyl-beta-cyclodextrin for cholesterol enrichment and cholesterol depletion experiments, respectively.

Tether pulling experiments were performed with single and multi-speed protocols in order to obtain time-resolved tether force profiles. The tether formation force, tether equilibrium force and effective membrane viscosity of the plasma membrane are quantified and correlated to the changes in the membrane cholesterol level. Tether formation force increases as membrane cholesterol is decreased. Higher tether equilibrium force and membrane stiffness is also associated with cholesterol depleted cell membranes. Tether effective viscosities were determined using multi-speed pulls and show higher plasma membrane viscosities in cholesterol enriched cells.

Acknowledgments: This work was supported in part by grants from the National Institutes of Health (2R01-DC02775), and National Science Foundation (BES-0522862). Additional support was provided by the Bourns College of Engineering and the Bioengineering Center at University of California, Riverside.

1-Rajagopalan et al, Tuning of the outer hair cell motor by membrane cholesterol, Journal of biological chemistry, Vol. 282, NO. 50, pp. 36659–36670.

367 Click Responses from Auditory-Nerve Fibers from the Apical Half of the Cochlea Show Two Response Regions That Are Driven by Different Outer-Hair-Cell Active Mechanisms

Hui Nam^{1,2}, John Guinan^{3,4}

¹Harvard-MIT Division of Health Sciences & Technology, ²Speech and Hearing Bioscience and Technology Program, ³Eaton-Peabody Labs, Mass. Eye & Ear Infirmary, ⁴Dept. of Otology & Laryngology, Harvard Medical School

Apical cochlear mechanics is poorly understood and difficult to study. A window on the movement of inner hair cell (IHC) stereocilia in the cochlear apex is provided by responses of auditory nerve (AN) fibers. Click responses from apical AN fibers show 2 regions that are strongly inhibited by stimulation of medial olivocochlear (MOC) efferents: (1) the ringing response from low-level (LL) clicks which is thought to be enhanced by a "cochlear amplifier", and (2) the AN initial peak (ANIP) response from moderate-to-high level (~70-100 dB pSPL) rarefaction clicks. Since MOC fibers synapse on outer hair cells (OHCs), this MOC inhibition indicates that active processes in OHCs are heavily involved in producing click responses in both regions. Here we explore the role of OHC stereocilia position in the production of these 2 clickresponse regions by presenting rarefaction clicks at different phases of 50 Hz, 70-110 dB SPL bias tones. Preliminary results were obtained from 18 AN fibers in 8 anesthetized cats. Bias effects on the LL response followed the traditional pattern of twice-a-bias-tone-cycle suppression with more suppression at one phase than the other. This suppression is attributable to the bias tone moving the OHC stereocilia toward low-slope, saturation regions of the mechano-electric transduction function with the rest position being closer to one saturation region. A somewhat similar pattern was found for ANIP responses except that the phases of the largest suppressions were different in ANIP versus LL responses, often by nearly 180 degrees. The data are consistent with the LL and ANIP responses both being due to active processes in OHCs that are controlled by OHC stereocilia position. The different phases of the LL and ANIP suppressions indicate

that different mechanisms, and perhaps different vibration patterns in the organ of Corti, are involved in the production of LL and ANIP responses.

Supported by NIDCD grants RO1 DC00235, T32 DC00038 and P30 DC05029

368 Wideband Stimulus-Frequency Otoacoustic Emissions in Normal Hearing Subjects Lin Bian¹

¹Arizona State University

Our understanding of hearing and hearing loss has been advancing rapidly at cellular and molecular levels. However, there lacks a comprehensive tool that can assess hearing function at a compatible precision. Otoacoustic emissions (OAEs) are noninvasive tools for evaluating inner ear outer hair cell (OHC) functions. Due to the complexity of multiple sources associated with the twotone evoked distortion product OAEs that are clinically available, an alternative approach needs to be developed. Evoked by a single tone, stimulus-frequency otoacoustic emission (SFOAE) which arises from the traveling-wave peak area in the cochlea can potentially provide an accurate estimate of the OHC status in a restricted location. In this study, SFOAEs were measured from 1 to 5 kHz with 32-Hz spacing in human ears with clinically normal hearing. The probe tone levels were varied from 25 to 50 dB SPL and SFOAEs were extracted with a high-side suppressor tone. The SFOAE amplitudes as a function of frequency showed level-dependent variations. Fine structures with very narrow dips were more pronounced at lower signal levels. Superimposed on the fine structure were wider variations spanning from a fraction of to more than an octave. These variations often manifested as notches with depths of more than 15 dB, especially within 2 to 4 kHz range. The notches and other variations in SFOAE amplitude were better revealed at the probe levels of 40 to 45 dB SPL. The phase-frequency functions demonstrated a sloping change of about 20 cvcles over the 4 kHz frequency range with slightly shallower slopes at higher levels. It was also noted that the phase slope became flat or even increased within the observed notch region. The results suggest that the OHC function varies across a wide frequency range. There could be possible early degradation or even loss of OHCs although the hearing thresholds were still normal. Thus, SFOAE is a sensitive and high-precision diagnostic tool for cochlear disorders.

369 Stimulus-Frequency Otoacoustic Emissions in Human Newborns

Radha Kalluri^{1,2}, Carolina Abdala^{1,2}, Srikantha Mishra¹, Lucy Gharibian¹

¹House Ear Institute, ²University of Southern California Neuroscience Graduate Program

Otoacoustic emissions (OAEs) are difficult to measure in infants, especially at low stimulus intensities where the cochlea is expected to be functioning linearly. Thus, OAE measurements in newborns have been limited to distortion-prodport and click-evoked otocoustic

ARO Abstracts

emissions ((DPOAEs and CEOAEs) elicited by moderate to high stimulus intensities. Interpretation of DPOAEs and CEOAEs is complicated by many factors including mixing between emissions generated by different mechanisms. Here we present the first reported measurements of stimulus frequency otoacoustic emissions (SFOAEs) in 10 human newborns (<48 hours after birth). SFOAEs have shown to be a powerful tool for studying the mechanics of the adult cochlea, this study will enable comparable an examination of the developing human cochlea. SFOAEs were measured at probe levels ranging from 10 to 45 dB SPL over a 500 Hz frequency range between 1 and 2 kHz. At each frequency, the SFOAE was computed as the complex difference between the ear canal pressure when a probe tone was presented alone and in the presence of a second higher-level tone (60 dB SPL) at a 44 Hz below the probe frequency. SFOAE input/output transfer (or describing) functions were obtained as a function of stimulus frequency at various levels. Above 30 dB SPL, newborn SFOAE transfer functions were on average level dependent or nonlinear. Between 10 and 30 dB SPL, the average input/output transfer function was nearly level independent, suggesting that at these probe levels the mechanics of the infant cochlea are nearly linear. Models of SFOAE generation based on linear-systems theory relate the phase-gradient-group delay of SFOAEs to the sharpness of cochlear filters; sharper filters should have longer delays. To describe cochlear tuning in newborns, we will present preliminary data comparing SFOAE group delays of infants and adults.

370 Otoacoustic Emissions in Neonates Measured in Different Acquisition Protocol Modalities

Wiktor Jedrzejczak¹, Stavros Hatzopoulos², Lech Sliwa¹, Krzysztof Kochanek¹, Henryk Skarzynski¹

¹Institute of Physiology and Pathology of Hearing, ²Department of Audiology, University of Ferrara,

The purpose of the study was to investigate transiently evoked otoacoustic emissions (TEOAEs) recorded in neonates using non-linear and linear stimulation protocols. In the non-linear protocol modality, a series of four clicks was delivered to the cochlea, with three clicks at the same level and polarity and with the fourth click being three times greater in amplitude and inverted in polarity. In the linear protocol modality all stimuli were presented at the same level and polarity. TEOAEs were also measured with the QuickScreen protocol, which records signals in a shorter 12 ms window. For each subject an average of 260 responses, per protocol, was recorded for off-line matching pursuit (MP) analyses.

The MP method allowed the decomposition of the TEOAE signals into waveforms of defined frequency, latency, time span, and amplitude and also identified patterns of resonance modes, that were characteristic for the TEOAEs recorded in each individual ear.

The results indicate that TEOAE recording windows with reduced length (i.e. QuickScreen) can be used only in fast detection of an OAE presence. For more sophisticated

clinical analyses the standard 20 ms TEOAE recording window is more appropriate.

371 Stimulus-Frequency Otoacoustic Emissions as a Probe of Cochlear Tuning in the Common Marmoset

Christopher Bergevin¹, Joshua H. McDermott², Sabyasachi Roy³, Feipeng Li³, Christopher Shera⁴, Xiaoqin Wang³

¹Otolaryngology/Head & Neck Surgery, Columbia University, ²Center for Neuroscience, New York University, ³Department of Biomedical Engineering, Johns Hopkins University, ⁴Eaton-Peabody Laboratory, Harvard Medical School

Humans have the longest stimulus-frequency otoacoustic emission (SFOAE) delays of any species so far examined, including cat, guinea pig, chinchilla, chicken, and various species of lizards and frogs. The goal of this study was to help understand the origin of the long human SFOAE delays and whether they might be correlated with basilarmembrane (BM) length and/or sharpness of cochlear Because inter-species comparisons can be tuning. complicated by phylogenetic differences, we sought to minimize these confounds by measuring SFOAE delays in the marmoset (Callithrix jacchus), a New World primate with a relatively short BM (~14 mm) and good high frequency hearing. Using a frequency range of 0.4-13 kHz and 40 dB SPL level, we measured robust SFOAEs above 0.8 kHz in all 14 ears tested in 10 normal-hearing individuals of varying age and sex. Each ear exhibited a unique and reproducible set of magnitude peaks and valleys. Marmoset SFOAE delays decreased monotonically from about 3.3 ms to 0.7 ms over the range examined and were significantly shorter than those reported for either the rhesus monkey (BM length ~25 mm) or the human (~35 mm). Between 1-8 kHz, marmoset delays are longer than those reported for domestic cat (~26 mm), but are similar in both species for 10-13 kHz. These data suggest a correlation between SFOAE delay and BM length among primates, although the comparison with cat demonstrates that BM length cannot, by itself, explain delay differences across species. If SFOAE delays provide a reliable measure of cochlear tuning, as proposed, the data suggest that tuning is sharper in marmoset than in cats below 8 kHz, encompassing a frequency range relevant for the monkey's vocalizations. Further quantitative interpretation of SFOAE delays in marmoset requires knowledge of their cochlea's tonotopic map. [Work supported NIH grants R01 DC005808 and DC003687]

372 Using Otoacoustic Emissions to Explore Cochlear Tuning and Tonotopy in the Tiger Christopher Bergevin¹, Edward Walsh², JoAnn McGee², Christopher Shera³

¹Otolaryngology/Head & Neck Surgery, Columbia University, ²Boys Towns National Research Hospital, ³Eaton-Peabody Laboratory, Harvard Medical School Stimulus-frequency otoacoustic emissions (SFOAEs) have been shown to provide reliable correlates of cochlear tuning in a variety of mammalian and non-mammalian species, including the domestic cat (Felis catus). Here, we apply the same methodology to explore peripheral auditory function in the largest member of the cat family, the tiger (Panthera tigris). We measured SFOAEs in 9 unique ears of 5 anesthetized tigers. The tigers, housed at the Henry Doorly Zoo, were of both sexes and ranged in age from 3-10 yrs. Probe levels were fixed at 40 dB SPL in the ear canal and probe frequencies were swept over a fouroctave range (0.7-13 kHz). Measured SFOAE phases were corrected for acoustic propagation delays using estimates of the residual ear canal length (~7 cm). Our results indicate that overall SFOAE levels in the tiger are similar to those in the domestic cat. Tiger SFOAE phasegradient delays, however, are significantly longer than in the cat, by approximately a factor of two above 2 kHz and even more at lower frequencies. Based on the correlations between tuning and delay established in other species, our results imply that cochlear tuning in the tiger is significantly sharper than in the cat. Furthermore, if the excitation pattern produced by a low-level tone at corresponding cochlear locations has a similar width in these two members of the cat family, as argued for other more phylogenetically disparate mammalian species (Shera et al. JARO 2010), then our data imply that the space constant (mm/octave) of the cochlear tonotopic map is larger in the tiger than the cat by roughly the same factor of two that relates their SFOAE delays. A longer space constant in tiger is consistent both with ABR thresholds, which suggest a lower upper limit of hearing in the tiger, and with measurements of basilar-membrane (BM) length, which at roughly 36-39 mm in the tiger is about 1.5 times longer than the BM in the cat (~25 mm). [Work supported by NSF Grant #0823417 and NIH grant R01 DC003687]

373 Auditory Brainstem Responses and Otoacoustic Emissions in Lizards: Comparisons Across Species and Temperatures

Christian Brandt¹, Christopher Bergevin², David Velenovsky³, Kevin Bonine⁴, Jakob Christensen-Dalsgaard¹

¹Center for Sound Communication, Institute of Biology, University of Southern Denmark, ²Otolaryngology/Head & Neck Surgery, Columbia University, ³Speech, Language and Hearing Sciences, University of Arizona, ⁴Ecology & Evolutionary Biology, University of Arizona

Given the large morphological variation across species, the lizard ear provides a unique window into how sound is transformed from vibrations in air into neural signals (i.e., forward transduction). For example, properties such as the number of hair cells (ranging over 50-2000) and tectorial membrane (TM) morphology can vary significantly across species. Recent reports have used stimulus-frequency otoacoustic emissions (SFOAEs) to explore how various morphological features, in addition to temperature variations (lizards are ecothermic), affect certain functional aspects of the lizard ear such as frequency selectivity. However, a more direct connection between SFOAE generation mechanisms and actual forward transduction is desirable. To this end, we measured both auditory brainstem responses (ABRs) and SFOAEs in the same animal for several different species: Whiptail lizards (Aspidoscelis), Tegus (Tupinambis), & Alligator lizards (Elgaria). Furthermore, these measurements were made in both 'cold' (~25°C) and 'warm' (~30°C) conditions. In all species, ABR thresholds decreased by 5-20 dB at higher frequencies (>1 kHz) with increasing body temperature. The latency of the first ABR peak decreased with increasing body temperature. The latencies (in ms) for the cold/warm conditions were as follows: Aspidoscelis -1.89/0.99, Tupinambis - 2.2/1.6, and Elgaria 1.51/1.06. SFOAE characteristics were highly similar to ABRs. Robust SFOAE activity (evoked using a 20 dB SPL stimulus) occurred at frequencies matching the most sensitive regions of the ABR audiogram. Furthermore, SFOAE magnitudes shifted upwards in frequency with temperature in a fashion similar to ABRs. Overall, temperature effects appeared more pronounced in species with а continuous overlying tectorial membrane (Aspidoscelis, Tupinambis) than those without (Elgaria). As previously suggested by Manley, this disparity likely stems from differences in coupling strength across hair cells.

374 Correlation of SFOAE Amplitude and Medial Olivocochlear Inhibition with Hyperglycemia in People with Diabetes

Peter G. Jacobs^{1,2}, Eric A. Wan², Garnett McMillan¹, Daniel McDermott¹, David Kagen^{1,2}, Dawn Konrad-Martin^{1,2}

¹Portland VA Medical Center, ²Oregon Health & Sciences University

In this developmental study, we investigated the influence that hyperglycemia has on stimulus frequency otoacoustic emissions (SFOAE) and medial olivocochlear (MOC) inhibition of SFOAEs in subjects with diabetes mellitus. Prior work has shown that maintaining stable blood glucose levels is necessary for maintaining normal cochlear function. Specifically, there is evidence that hypoglycemia reduces the endocochlear potential (EP) and that disruption of this metabolic energy source impacts the outer hair cell (OHC)-mediated cochlear microphonics. In addition to metabolic influences, prior work has shown that ATP, a product of the breakdown of glucose, acts as a neurotransmitter in outer hair cells. Introduction of ATP into perilymph in the presence of calcium ions has been shown to influence the operating point of the cochlear amplifier, and was shown in vitro to impact OHC motility. The MOC is known to regulate calcium ions in OHCs, suggesting that the MOC may play a role in mediation of ATP neurotransmitter influences. We present results from an experiment in which 6 diabetic subjects (5 tested twice) underwent glucose tolerance testing (GTT) while SFOAEs and MOC inhibition was measured. The purpose of the GTT was to elevate the subjects' blood sugar over 4 hours through consumption of 80 g of sugar subjects fasted overnight. SFOAEs were elicited using a 55 dB SPL tone and a 75 dB SPL suppressor. MOC was elicited using broadband noise ipsilaterally, contralaterally, and bilaterally at levels below elicitation of the subjects' middle

ear muscle reflex. Results show that SFOAE amplitudes increased during hyperglycemia (p=0.049). Hyperglycemia was also found to increase MOC inhibition of SFOAEs for all subjects and elicitors; ipsilateral (p=0.001), contralateral (p=0.022), and bilateral (p=0.001). Prediction of hyperglycemia using MOC and SFOAE metrics using mixed effects ROC analysis demonstrated an AUC of 0.85. (Work supported by NIH 1R21DK079283-01A1)

375 Transient-Evoked Otoacoustic Emission Suppression Using Speech and Speech-Like Contralateral Suppressors

Tracy Fitzgerald¹, Monita Chatterjee¹, William Bologna¹, Christina Do¹, Marquitta Merkison¹

¹University of Maryland College Park

The medial olivocochlear (MOC) portion of the auditory system is thought to suppress the response of the inner ear to background noise, permitting the auditory system to more effectively respond to other transient signals, including speech sounds (e.g., Kawase et al., 1993). MOC function has been investigated non-invasively in humans by measuring otoacoustic emission (OAE) suppression. Evidence suggests enhanced responses in auditory cortex in response to spectro-temporally complex, natural, or ecologically relevant stimuli (e.g., Deprieux et al., 2001; Jenkins et al., 2010; Sadagopan and Wang, 2009). It appears reasonable to speculate that corticofugal pathways extending to the cochlea will have differential effects on OAE suppression with natural stimuli versus with steady noise; however, few studies in the area have used stimuli other than steady state noise suppressors. In the present study, the magnitude of transient-evoked OAE (TEOAE) suppression was measured in normal hearing adults (18-30 years, acoustic reflex thresholds < 65 dB SPL) using a continuum of contralateral stimuli ranging from broadband noise (BBN) to speech. The contralateral suppressors included steady-state BBN, amplitude modulated BBN, speech-spectrum-shaped noise, speechenvelope-modulated noise, 4-channel noise-band-vocoded speech, time-reversed speech, and speech. All stimuli were low-pass filtered at 6 kHz and presented at equal average rms (60 dB SPL). Preliminary results indicated markedly reduced suppression with speech-like and speech suppressors relative to steady-state noise suppressors in adults. These results have important implications for the role of efferent suppression in everyday listening environments.

376 Maturation of the Medial Olivocochlear (MOC) Reflex in Humans: 12 Years Later

Carolina Abdala^{1,2}, Srikanta Mishra¹, Silvia Batezati¹, Jacque Wiley¹

¹House Ear Institute, ²University of Southern California, Neuroscience Graduate Program

In this preliminary report, 23 term-born infants, 26 adolescents and 20 adults served as subjects to study maturation of the medial olivocochlear (MOC) reflex. Preliminary data from a small group of prematurely born neonates will also be presented. A study of the MOC

reflex in human neonates was conducted over a decade ago in our lab, using a more limited protocol that did not control factors now understood to be important for OAEbased metrics of medial efferent system function. The current study records the 2f1-f2 DPOAE with a fine resolution, swept-tone program across a three-octave range (8 sec/oct). Contralateral acoustic stimulation (CAS) was presented at 4 levels (55 - 70 dB SPL) in non-infants and 60 and 65 dB SPL in newborns. The MOC reflex was quantified as follows to control for unwanted component mixing between DPOAE sources that might contaminate measures of the reflex: 1) the difference between no-CAS and +CAS conditions (dB, normalized fraction of unsuppressed DPOAE and magnitude of the vector difference) was calculated at DPOAE fine structure peak frequencies only where components are presumably summing in-phase and 2) the effects of CAS on distortionand reflection-source components were independently calculated after IFFT-derived component separation. Additionally, a metric of the middle ear muscle reflex is currently being developed to assess its contribution to measures of the MOC reflex. Preliminary results show that term-born neonates manifest MOC reflex strength equivalent to adult and teen values (~1.5 dB overall), trending toward more robust when measured as a vector difference (normalized to unsuppressed pressure) or as a component-specific metric. Like adults, newborns show a significantly stronger effect of CAS on the DPOAE reflection-source compared to the distortion source. Although there are too few prematurely born neonates at present to make general statements about the magnitude of the MOC reflex in this group, one preliminary observation is noteworthy: although the confound of component interference has been accounted for, contralateral broadband noise evokes significantly more episodes of DPOAE level enhancement in premature newborns than any other age group.

377 MOC-Induced Changes in Stimulus Frequency Otoacoustic Emissions

Wei Zhao¹, James Dewey¹, Jungmee Lee¹, Sumitrajit Dhar¹

¹Department of Communication Sciences and Disorders, Northwestern University

Mammalian stimulus frequency otoacoustic emissions (SFOAEs) are low-level sounds evoked by tonal probes and recorded in the ear canal (Kemp and Chum 1980). Linear coherent reflection and nonlinear distortion mechanisms have been proposed to underlie SFOAE generation (Zweig and Shera 1995; Talmadge et al. 2000). Peaks and valleys in SFOAE amplitude as a function of probe frequency, commonly referred as the SFOAE fine structure, may arise from both mechanisms as well as their interactions (Goodman et al. 2003).

SFOAEs along with all other types of OAEs can be modulated by acoustical activation of the medial olivocochlear (MOC) efferents. Activation of the MOC pathway by contralateral noise shifts distortion product otoacoustic emission (DPOAE) fine structure (Sun 2008; Abdala et al. 2009; Deeter et al. 2009) and spontaneous otoacoustic emissions (SOAEs) (Mott et al. 1989; Harrison and Burns 1993) towards higher frequencies. The effect of contralateral noise on SFOAE fine structure however, has never been documented. Characterizing the MOC modulation of SFOAE fine structure would enhance our knowledge of SFOAE generation and MOC function.

SFOAEs were recorded using the compression method with and without activating the MOC efferents by a 60-dB SPL contralateral broadband noise. Middle-ear muscle contraction was ruled out by the group delay method (Guinan et al. 2003). SFOAE fine structure in the presence and absence of contralateral noise will be quantified and compared. Short- and long-latency SFOAE components were obtained by inverse FFT and the MOC effects on each component will be reported.

378 Separating Olivocochlear and Acoustic Reflex Actions on Otoacoustic Emissions in the Time Domain

Kendra Marks¹, Jonathan Siegel^{1,2}

¹*Roxelyn and Richard Pepper Dept. of Comm. Sci. & Disord.; Northwestern University,* ²*Hugh Knowles Center* Separating effects of olivocochlear bundle (OCB) efferent activation by acoustic stimuli delivered to the contralateral ear from effects due to activation of the middle ear muscles (MEM) has been difficult because the two mechanisms are co-activated over a fairly wide range of contralateral stimulus levels and have a similar time course (Guinan, et al., JARO, 4:521-540, (2003)). The effects OCB and MEM on stimulus frequency otoacoustic emissions (SFOAE) can be distinguished by measuring the group delay of the vector change induced by contralateral stimulation (Guinan, et al., (2003)), but this is a relatively time-consuming procedure.

We found that a simple technique to detect purely OCBmediated changes in otoacoustic emissions evoked by transient stimuli (TEOAEs) in humans. Effects of stimulating the contralateral ear with broadband noise were measured in 13 normal hearing subjects. Linear averages of the response to 2 ms gated tone pips were collected first without, then with stimulation of the contralateral ear. The subtracted time averages revealed the changes induced by contralateral stimulation. The full amplitude of the TEOAE was measured separately using a scale-subtract protocol described previously (Placek and Siegel, ARO, 2007). Purely OCB-mediated effects were clearly differentiated from MEM only or combined MEM/OCB action by a change in the time interval following the stimulus, but with no detectable change during the stimulus interval. This procedure is thus a very sensitive null detector of MEM activation.

Despite considerable intersubject variability in thresholds for both OCB and MEM effects, we were able to reliably detect OCB suppression of TEOAE at levels below our sensitive measure of the middle ear reflex in most subjects. Results of this study show that a linear TEOAE averaging paradigm can be used to rapidly and accurately differentiate OCB and MEM suppression.

Supported by NIDCD grant R01 DC008420 and Northwestern University.

379 Paget's Disease of the Temporal Bone: A Histopathological Study

Panagiotis Dimitriadis¹, Doris-Éva Bamiou¹, Athanasios Bibas²

¹UCL Ear Institute, ²University of Athens

Background: Paget's disease of bone (PDB) is a fairly common condition affecting almost 3% of people over 40 years of age. Its main characteristic pathophysiologic abnormality is unbalanced remodelling of bones that leads to major disabilities long-term. Aims: The purpose of this study is to describe the histopathological findings of temporal bones (TB) with PDB, as assessed by means of light microscopy. Where possible an attempt was made to correlate the histopathology findings of the study with the reported audiovestibular functional state of patients with PDB. Methods: This is an archival human temporal bone study of 8 subjects diagnosed with PDB from the temporal bone collection of the UCL Ear Institute, UK. Telepathology facilitated the examination of the TB. The following structures were studied: middle ear cavity, ossicles, otic capsule, Organ of Corti, Reissner's membrane, Stria vascularis, spiral ligament, vestibule, saccule utricle, semicircular canals, internal auditory canal, oval and round window, vestibular and cochlear aqueducts, and Cotugno's canal. Results: A fractured stapes footplate was observed in 1 temporal bone. Extensive bone remodelling and obstruction of Cotugno's canal were observed in 78% of Several abnormalities TBs. (such as fixation, hypertrophy, atrophy) were also observed in middle and inner ear structures including middle ear ossicles otic capsule, internal auditory meatus, spiral ligament and the stria vascularis. Discussion: This study is the first to report a fractured stapes footplate as a causative lesion of conductive HL (CHL) in PDB. The inconsistent presence of several abnormalities supports Shuknecht's theory, who postulated that CHL in PDB results from changes in quality, mass, density and form of the TB.In our study, extensive bone remodelling around Cotugno canal was a frequent finding, not reported before in the literature. We hypothesize that occlusion of Cotugno's canal results in venous congestion in the cochlea, which in turn may lead to SNHL. This is consistent with experimental evidence in animals. An intracochlear vestibular schwannoma was observed in 1 bone.Conclusion: We propose that SNHL of patients with PDB of TB may, in some cases, be attributed to occlusion of Cotugno's canal, thus, obstructing the venous drainage of the cochlea, with subsequent damage to the stria vascularis and Organ of Corti. CHL may result from fracture of the stapes footplate, a finding not previously reported.

380 Otosclerosis as a Primary, Bony, Invasive Neoplasm of the Otic Capsule Leslie Michaels¹, Sava Soucek²

¹University College London, ²Imperial College London In order better to interpret the histological appearances of otosclerosis we reviewed the development of the otic capsule. This differs from other bones in producing very large numbers of bony, especially Volkmann's, canals (VC), as well as lamellar bone (LB). The external periosteal layer, except for the region overlying the fissula ante fenestram, undergoes marked hypertrophy during fetal life and is renewed by periosteal osteoblasts throughout life.

In 65 autopsy temporal bones with otosclerosis there were 63 with a large plaque of the disease posteriorly in the cochlear otic capsule. All showed a continous base in the periosteum adjacent to the tensor tympani /processus cochleariformis complex. A similar plague was found anteriorly in 42 of the 65 bones with a base along the canal of the internal carotid artery. Both plaques (and indeed all otosclerotic tissue studied) were composed of a sharply defined replica of external layer otic capsule tissue, with VC and LB. Both plaques probably arise from periosteal osteoblasts. The otosclerotic tissue spreads towards the cochlea, the plaques showing differing levels of their cochlear side edges, and all showing there a darklystaining invasive front of poorly differentiated otosclerotic tissue. Earlier formed tissue of each plague has undergone differentiation, so that the periosteal region of the plaques displays highly differentiated LB and VC, while between that region and the invasive front there is moderate differentiation, often with otospongiotic differentiation of VC. The posterior plaque invades stapes footplate, and often cochlea, saccule and vestibule, extensively, producing symptoms of conductive and sensorineural hearing loss and also imbalance and vertigo. Clinical features may arise perhaps in that order, depending on the exact pathway of invasion.

It is suggested that otosclerosis is a primary, invasive bony neoplasm derived from osteoblasts of the external periosteal layer of the otic capsule.

381 Temporal Bone Histopathology in Neurofibromatosis Type 2

Sungil Nam¹, Saumil N. Merchant¹

¹Department of Otology and Laryngology, Harvard Medical School, Massachusetts Eye and Ear Infirmary

Neurofibromatosis 2 (NF2) is an autosomal dominant disorder characterized by bilateral cochleo-vestibular schwannomas. We studied 5 cases (9 ears) with NF2 in the temporal bone collection at the Massachusetts Eye & Ear Infirmary. All 9 temporal bones were prepared in the standard manner for light microscopy. All 5 individuals developed bilateral progressive sensorineural hearing loss with poor speech discrimination and eventually became profoundly deaf in both ears. Histopathology showed extensive intra- and extra-labyrinthine schwannomas in all cases (multicentricity), consisting predominantly of Antonitype A pattern. In general, the schwannomas were aggressive, often eroding bone and invading parts of the inner ear. Except in one case, the sensory and neural structures within the cochlea were severely degenerated. Our data showed that cochleo-vestibular schwannomas in NF2 are biologically more aggressive that those seen in sporadic cases. Furthermore, the tumors in NF2 exhibit features that make it particularly challenging to successfully preserve hearing in these patients.

382 Hemorrhage in Endolymphatic Sac; a Cause of Hearing Deterioration in Patients with Enlarged Vestibular Aqueduct

Minbum Kim¹, Sung Huhn Kim¹, Jinna Kim², Jae Young Choi¹

¹Department of Otorhinolaryngology-Head & Neck Surgery, Yonsei University College of Medicine, ²Department of Radiology, Yonsei University College of Medicine

We analyzed magnetic resonance images and endolymph in the endolymphatic sac of patients with enlarged vestibular aqueduct (EVA), in order to demonstrate that hemorrhage in endolymphatic sac is a cause of sudden hearing deterioration. A total of 25 EVA patients (50 ears) who had more than 70dB hearing loss were included. Medical records were reviewed including the history of sudden hearing loss. Temporal magnetic resonance (MR) scans were performed on a 3-tesla MR system. Fluidattenuated inversion recovery (FLAIR) image was undertaken in 8 ears. In two patients, endolymphatic sac fluid was aspirated during cochlear implantation. On T2weighted MR images, enlarged endolymphatic sac was observed in all 50 ears, and hyposignal compartment in endolymphatic sac (CES) was shown in 17 ears. Interestingly, CES was observed more frequently in the "sudden hearing loss" group (12/14) than the "stable hearing" group (5/36) (Fisher's exact test, p<0.01). Moreover, CES revealed higher signal than cerebrospinal fluid in all the 8 ears of the "sudden hearing loss" group on FLAIR images, which suggests that CES are filled with high protein fluid or hemorrhage. In contrast, no significant difference in mean hearing thresholds was shown between the patients with CES and the others (Mann-Whitney test, p>0.05). Probability of detecting a CES in profound hearing loss group (11/29) is not significantly different, compared to severe hearing loss group (4/11) (Fisher's exact test, p>0.05). By analyzing aspirated fluid from the endolymphatic sac, we demonstrated that CES consists of blood components. In summary, patients who experienced sudden hearing drop had CES more frequently, and hemorrhage in endolymphatic sac was confirmed in ears with CES by MR scans and fluid analysis. Our study strongly supports the theory that hemorrhage in endolymphatic sac and reflux of hyperosmolar contents into cochlea is a possible pathophysiology of sudden hearing deterioration of patients with EVA.

383 Comparing the Cochlear Spiral Modiolar Artery in Type-1 and Type-2 Diabetes Mellitus: A Human Temporal Bone Study

Shin Kariya¹, Sebahattin Cureoglu², Hisaki Fukushima³, Norimasa Morita³, Muzeyyen Baylan², Kazunori Nishizaki¹, Michael Paparella⁴

¹Okayama University, ²University of Minnesota, ³Kawasaki Medical School, ⁴Paparella Ear Head & Neck Institute This study examined whether pathological findings were present in cochlear vessels for patients with diabetes mellitus. Twenty-six temporal bones from 13 patients with type 1 diabetes mellitus and 40 temporal bones from 20

patients with type 2 diabetes mellitus were examined. Type 2 diabetic temporal bones were divided into 2 groups according to diabetic management (22 temporal bones with insulin therapy, and 18 with oral hypoglycemic drugs). Age-matched normal control temporal bones were also selected. The vessel wall thickness in the cochlear spiral modiolar artery was measured under a light microscope, and the vessel wall ratio (vessel wall thickness / outer diameter of the vessel ~100) was calculated. The vessel wall thickness and vessel wall ratio in type 1 diabetes mellitus were significantly greater than in normal controls. Type 2 diabetic patients with insulin therapy showed significantly greater vessel wall thickness and vessel wall ratios than controls. In type 2 diabetes mellitus, the vessel wall thickness and vessel wall ratio were greater in patients treated with insulin therapy than in those treated with oral hypoglycemic agents. Type 2 diabetic patients with insulin therapy showed an increased vessel wall thickness and vessel wall ratio compared to patients with type 1 diabetes mellitus. In conclusion, the cochlea in patients with diabetes mellitus shows circulatory disturbance compared to age-matched normal controls.

384 Selective Inner Hair Cell Loss in Premature Infants

Monica Amatuzzi¹, M. Charles Liberman², Clarinda Northrop²

¹Universidade de Sao Paolo, ²Massachusetts Eye and Ear Infirmary

Infants from the neonatal intensive care unit (NICU) are at high risk for sensorineural hearing loss. Many risk factors have been suggested including birth weight, respiratory distress, hyperbilirubinemia and ototoxic drugs; however, little is known about the underlying cochlear histopathology. In a prior study of 15 temporal bones from NICU patients, selective inner hair cell loss was seen in three cases (Amatuzzi et al [2001] Arch Otolaryngol HNS 127:629). The finding was surprising since selective inner hair cell loss is an uncommon pathology in both the human (Slack et al (1986) Clin Otolaryngol All Sci 11: 443) and animal literature (Liberman et al., [2006] JARO 7:211). The finding was also intriguing, because all three cases were preterm babies.

To better understand the frequency of selective inner hair cell loss in infants, and its relation to gestational age, we studied 100 temporal bones, collected from the NICU at the Hospital de Ninos in San Jose, Costa Rica between 1977 and 1993. The sample included 27 cases (54 ears) from pre-term babies (30 to 34 wks gestation) and 23 cases (46 ears) from full-term babies. The two samples were matched with respect to age at death. Selective inner hair cell loss was found in 9 ears, 8 of which were from 4 pre-term babies (with bilateral presentation) and only one of which was from a (unilateral) full-term case. Loss of spiral ganglion neurons was not detectable in any case.

Loss of inner hair cells will result in an "auditory neuropathy" phenotype, i.e. absent ABRs with maintenance of otoacoustic emissions, if the rest of the cochlear duct is functioning normally. A recent hearing screen of NICU patients (Xoinis et al [2007] J Perinatol 27:718) reports an increased incidence of "auditory neuropathy" in pre-term babies. The present study suggests that the underlying pathology may be loss of inner hair cells rather than neuronal damage.

Research Supported by grants from the Temporal Bone Foundation and from the NIDCD (R01 DC0188 to MCL)

385 Cochlear Ion Homeostasis Mechanisms Are Suppressed in Autoimmune Inner Ear Disease and Restored by Glucocorticoid Treatment

Dennis Trune¹, Fran Hausman¹, Beth Kempton¹ ¹Oregon Health & Science University

It is generally assumed that autoimmune inner ear disease (AIED) is caused by cochlear inflammation and glucocorticoids restore hearing by immunosuppression. However, little attention has been given to the susceptibility of cochlear ion and water transport pathways in AIED and steroid control over their recovery. Therefore, MRL/lpr autoimmune disease mice were evaluated to determine how systemic disease and glucocorticoid treatment affect the ion homeostasis mechanisms in the ear. Mice were tested for hearing at either 2 months of age (prior to disease, N=8) or 6 months of age (after hearing loss onset, N=7). Additional 6 month old mice (N=8) were given oral prednisolone for two weeks. Inner ears from all were collected for qRT-PCR of 24 genes responsible for endolymph homeostasis, including channels for transport of sodium, potassium, chloride, and water, as well as tight junctions and gap junctions. Mice developed hearing loss at 6 months and 22 of the 24 cochlear ion and water transport genes were significantly Inflammatory cytokine genes were downregulated. actually suppressed in the ear, not elevated. Steroid treatment significantly increased expression of several homeostasis genes, including the potassium channel Kcne1, the epithelial sodium channel, several gap junction proteins (Gja1, Gjb2, Gjb6), and aquaporin 3, all of which are involved in K^{\dagger} transport and endolymph production. Steroid treatment had no significant effect on inflammatory gene expression in the cochlea. It was concluded that circulating autoantibodies and immune complexes may cause hearing loss by disrupting the blood labyrinth barrier and genes required for endolymph homeostasis. Steroid treatment appeared to improve hearing by restoring these homeostatic genes without impacting inflammation. This provides new insight into one potential mechanism of AIED and how glucocorticoid therapies may help to restore hearing. [Supported by NIH-NIDCD R01 DC05593]

386 Hearing Function and Cochlear Morphology in Diabetes Mellitus Model Mice Takeshi Fujita¹, Daisuke Yamashita¹, Sayaka

Katsunuma¹, Shingo Hasegawa¹, Ken-ichi Nibu¹ ¹Kobe University Graduate School of Medicine Objectives

There are two major types of diabetes: Type1 diabetes mellitus (T1DM) and Type2 diabetes mellitus (T2DM). The aim of the present investigation was to induce these two

types of diabetes in C57BL/6 mice and then evaluate hearing dysfunction and morphological change in cochleae.

Methods

Forty-eight C57B6 mice (male, 8 weeks) with a normal Preyer's reflex were used in this study. The subjects were randomly divided into three experimental groups: Control group (n=15), T1DM group (n=15), and T2DM group (n=15). T1DM was induced by intraperitoneally injection of streptozotocin (100mg/kg of body weight) on two consecutive days. T2DM was induced with a high fat diet (HFD32, CLEA Japan). Control groups were injected normal saline and fed standard chow and water ad libitum. Blood glucose, body weight and hearing function by auditory brainstem response (ABR) were measured at each time point; baseline (pre-treatment), 1, 3 and 6months. After measuring final ABR, cochleae were removed and used for histological assessment. Results

The average body weights of T1DM group decreased significantly as compared with Control group, while T2DM group exhibited significant weight increase. The mean blood glucose level was significantly higher in both T1DM group and T2DM group, as compared with Control group. At the time point of both one and three months after induction of diabetes, compared to Control group, hearing threshold shifts were significantly increased in T1DM group at 4 kHz, while T2DM group has showed threshold elevation only at the time point of one month. On the histological findings, there was no apparent difference to whole cochlea including hair cells in all groups at the time point of one month. As for T1DM group, at three months, a tendency to increase of cell death in spiral ganglion and degeneration of stria vascularis was seen. We will show the assessment of hearing function and morphological changes at the time point of six months in addition.

387 Parkin Deficiency Causes Progressive Hearing Loss in Mice Through Outer Hair Cell Loss

Norio Yamamoto¹, Kiyomi Hamaguchi¹, Takayuki Nakagawa¹, Juichi Ito¹

¹Department of Otolaryngology, Head and Neck Surgery, Kyoto University Graduate School of Medicine

Parkinson's disease (PD) is the second most common neurodegenerative disorder and is characterized by muscle rigidity, tremor and a slowing of physical movement. Although most PD cases are sporadic, 5-10% of them are hereditary. Recently, some specific genetic mutations causing PD have been identified from familial PD cases. One of these genes includes Park2 (Parkin) whose loss-of-function mutation causes autosomal recessive juvenile parkinsonism in human. Parkin protein is an E3 ubiquitin-protein ligase suggesting that this protein is involved in quality control of other proteins. In Drosophila, parkin null mutants show decreased adult lifespan, apoptotic muscle degeneration and male infertility, but no apparent in vivo neuronal phenotypes have been observed in Parkin deficient mice. Last year in this meeting, we presented that Parkin knockout (KO) mice showed progressive hearing loss detected by auditory brain stem response (ABR). Since progressive hearing loss is mostly caused by sensorineurial hearing loss, we performed hisotological and functional analyses on cochlear organs including organs of corti, stria vascularis and spiral ganglion cells in Parkin KO mice. We identified that the cause of progressive hearing loss in Parkin KO mice were loss of outer hair cells from several results we got in this study such as negative distortion product of otoacousitic emission (DPOAE), decreased numbers of outer hair cells, normal endocochlear potentials and normal looking of spiral ganglion cells and stria vascularis.

We assumed that outer hair cell loss was caused by mitochondrial disorders because maintenance of hair cells are highly dependent on mitochondria and Parkin is recently reported to be involved in the quality control of mitochondria as well as proteins.

388 CTL2/SLC44A2 Isoform Expression in Human Inner Ear Tissue Samples, EBV Transformed Lymphocytes and Cultured Epithelial Cells

Thankam S. Nair¹, Pavan K. Kommareddi¹, Maria M. Galano¹, Stevan A. Telian², H. Alexander Arts², Hussam K. El-Kashlan², Thomas E. Carey¹

¹KHRI, University of Michigan, ²University of Michigan Hospital

CTL2/SLC44A2 is a target of antibody-induced hearing loss and transfusion-related acute lung injury (TRALI). CTL2 has two full-length isoforms that differ in the first 10-12 amino acids resulting in proteins of 704 or 706 amino acids. Human isoform 1 (iso1) uses exon 1a encoding 10 amino acids; isoform 2 (iso2) uses exon1b encoding 12 amino acids. Mice and guinea pigs have tissue-specific differences in CTL2 isoform expression. In the developing murine inner ear both isoforms are expressed but at different levels during maturation. The purpose of the present study was to examine CTL2 isoform expression patterns in human inner ear samples, human lymphocytes immortalized by EBV, and squamous cell carcinoma lines. Reverse transcription-PCR primers were designed to individually amplify iso1 and iso2. Only iso1 was expressed in EBV transformed lymphocytes which were derived from 19 Meniere's patients. Similarly, in vestibular epithelial tissue from 76 patients underaoina translabyrinthine surgical procedures only iso1 was found including: 54 with acoustic neuromas, 21 with intractable Meniere's disease, and 1 with persistent vertigo. CTL2 is also expressed in oral mucosa therefore we also analyzed cDNA from a panel of 4 pairs of primary and recurrent or metastatic human squamous carcinoma cell lines. Unlike inner ear and lymphoblasts, all four sets of squamous cell lines, all expressed both iso1 and iso2, and three of the four exhibited had higher iso2 expression. Normal proliferating cultured human keratinocytes also expressed both isoforms. In contrast to mice, humans only express iso1 in inner ear. Similarly lymphoblasts express only iso1 but squamous cells express both isoforms. These findings

are consistent with tissue specific differences in CTL2 isoform selection and suggest that CTL2 may have different functions in different tissues depending on the isoform expression profile which is likely driven by promoter usage.

NIH NIDCD DC03686, P30 DC05188

389 Force-Controlled Cochlear Implant Insertion in Human Cochlea by a Mechatronic Device

Yann Nguyen^{1,2}, Mathieu Miroir^{1,2}, Guillaume Kazmitcheff^{1,2}, Evelyne Ferrary^{3,4}, Olivier Sterkers^{3,4}, Alexis Bozorg Grayeli^{3,4}

¹UMR-S 867 Inserm, Paris, France, ²UMR-S 867 Université Paris 7, Paris, France, ³UMR-S 867 Inserm / Paris 7, Paris, France, ⁴AP-HP, Hospital Beaujon, ENT departement, Clichy, France

Background: Damages to inner ear structures are potentially related array insertion forces during cochlear implantation. The aim of the study was to evaluate force profiles during array insertion in human cochlea specimens and evaluate a force controlled robot-based array inserter.

Material and methods: Eight fresh frozen human temporal microdissected for array bones were insertion experiments. In each temporal bone, the scala vestibuli of the basal turn was opened in order to expose the basilar membrane and follow the array progression on 360°. A J1 electrode array (Advanced Bionics Inc., Valencia, CA) was employed. A mechatronic insertor was designed, combining a linear electromagnetic actuator and a micromanipulator. A one-axis force sensor (range: 0-0.4N, precision 1%) was placed between the insertor and the base of the array and a six-axis force sensor was fixed onto the temporal bone. Video microscopy acquisition was performed to follow array insertion.

Results: Force profiles varied between specimens (maximum peak 0.1N - 0.8N) and were correlated with length of insertion. Coupling the force sensor and the actuator, a force controlled insertion could be performed with an automatic stop and pull back of the array insertion once a force threshold had been reached.

Conclusion: Using a simple sensor included in the insertor, we were able to measure forces during cochlear implantation. This tool can be potentially used intraoperatively to provide real-time information to the surgeon during the procedure.

This work was supported by Advanced Bionics Inc., Valencia, CA.

390 Mechano-Electrical Transduction After Intense Mechanical Stimulation

Ruben Stepanyan¹, Artur Indzhykulian¹, Gregory Frolenkov¹

¹Department of Physiology, University of Kentucky

Acoustic overstimulation is able to produce permanent damage to the hair bundles of cochlear sensory cells leading to the shift of hearing thresholds and permanent hearing loss. The level of damage observed can range from the loss of stereocilia links to stereocilia floppiness, disarray and fusion or even complete loss of stereocilia, all of which should clearly impair mechano-electrical transduction (MET). However, it has never been thoroughly studied whether acoustic overstimulation induces changes of the MET machinery before any obvious damage to the hair bundle.

We have used fluid-jet (and piezo-driven rigid probe) stimulation to induce large bundle deflections and then high-resolution scanning electron microscopy to assess the level of resulting damage in the cochlear inner hair cells of young postnatal mice. We found that intense deflections of stereocilia result in a considerable reduction of the maximum MET currents. Surprisingly, only very few changes in the stereociliary bundle ultrastructure accompanied this substantial reduction of the MET current. Most if not all of the tip links remained intact and only some instances of the fusion of the tips of shorter stereocilia into the side of the taller ones were noticed. These preliminary results show that the MET machinery may exhibit extremely high sensitivity to overstimulationinduced damage. Further studies are necessary to determine if these changes in MET are due to the development of sustained abnormal forces within a damaged hair bundle or the damage to the MET apparatus itself.

Supported by NIDCD/NIH (R01 DC008861)

391 The Role of Oxidative Stress and Antioxidants in Zebrafish Lateral Line Hair Cell Damage

Hoseok Choi^{1,2}, Edwin Rubel¹, David Raible^{1,3}, Henry Ou^{1,4}

¹Virginia Merrill Bloedel Hearing Research Center, Dept. Oto-HNS, University of Washington, ²Department of Otolaryngology, Inha University School of Medicine, Incheon, South Korea, ³Department of Biological Structure, University of Washington, ⁴Seattle Children's Hospital There is strong evidence that reactive oxygen species (ROS) and reactive nitrogen species (RNS) play a role in cisplatin and aminoglycoside-induced hair cell death in a number of animal models. However, the role of ROS and RNS in hair cell death in the zebrafish lateral line has not been extensively studied. Due to the ease of live imaging and large quantitative experiments in the zebrafish, we sought to explore the role of oxidative stress in the zebrafish lateral line. Using the ROS indicator dye CM-H2DCFDA (Invitrogen) we studied production of ROS in response to ototoxic drugs. There was a rapid increase in CM-H2DCFDA signal within 10 to 20 minutes of neomycin and gentamicin exposure. We examined the effect of antioxidants on this signal and found that pretreatment with the antioxidants N-acetylcysteine (NAC) and glutathione (GSH), but not D-methionine (D-Met), decreased the CM-H2DCFDA signal in neomycin-treated hair cells. We then examined the role of reactive nitrogen species with immunohistochemistry using anti-nitrotyrosine antibody and found that the nitrotyrosine signal increased in hair cells after 20 minutes of neomycin treatment. This increase (and subsequent hair cell death) was blocked by glutathione but not D-methionine.

These qualitative ROS and RNS findings correlated well quantitative dose response curves with which demonstrated that both GSH and NAC protected effectively against neomycin, gentamicin, and cisplatin. However, the GSH and NAC doses required for protection were between 500 μ M and 1000 μ M, far exceeding the 10 to 100 µM dose range that is typically required with other protective drugs in the zebrafish lateral line. In addition, even at high doses D-methionine did not protect against any of these ototoxicants. These results shed light on the role of oxidative stress in hair cell death in the zebrafish lateral line, and potentially provide reasons for the limitations of antioxidant therapy.

392 Presynaptic Ribbons Within Inner Hair Cells Persist After Loss of Postsynaptic Terminals Due to Excitotoxic Trauma in Vitro

Qiong Wang¹, Swapnil Mehta^{1,2}, Dylan Todd¹, Arianna Lark¹, Steven Green¹

¹Departments of Biology and Otolaryngology, University of Iowa ²Department of Neuroscience, Amherst College We use a neonatal rat organotypic cochlea explant culture, which preserves synaptic interactions between spiral ganglion neurons (SGNs) and hair cells. A brief application of glutamate agonists (NMDA and kainate, "NK treatment") causes rapid degeneration of SGN synaptic terminals on inner hair cells (IHCs), mimicking in vivo excitotoxicity and, possibly, postsynaptic consequences of noise trauma. Here we ask whether loss of postsynaptic terminals necessarily results in loss of presynaptic ribbons (PSRs). PSRs were visualized as CtBP2-immunoreactive puncta and postsynaptic densities (PSDs) were visualized as PSD95-immunoreactive puncta. SGN peripheral axons were visualized by NF200 immunoreactivity. At the midpoint of control non-NK-treated explants, we counted 20.1±2.7 PSRs/IHC and 19.6±4.9 PSDs/IHC. PSDs and PSRs colocalized, showing that synapses are maintained intact in vitro. As we have previously shown, 99% afferent terminals degenerated immediately after NK, most PSDs disappear within 4 h post-NK but there is some regeneration of PSDs up to 72 h post-NK although PSDs remain much sparser than in control non-NK-treated explants (1.5±1.7 PSDs/IHC). Nevertheless, throughout the entire period post-NK, the number of PSRs did not change significantly, in spite of the absence or near absence of PSDs. Remaining PSDs on IHCs colocalized with PSRs suggesting that they are structurally intact synapses. However, we did observe a change in the spatial distribution of PSRs within the IHCs post-NK. In IHCs in control explants, nearly all PSRs are located at the level of or basal to the cell nucleus (20.0±2.9 of 21.0±2.7 PSRs/IHC), a location we term "typical." Only 1.0±0.7 PSRs/IHC are located apical to the cell nucleus, a location we term "apical." While there was no significant change in the number of "typical" or "apical" PSRs up to 18 h after NK treatment, at 72 h post-NK, the number of "apical" PSRs/IHC increased significantly to 5.6±2.5. "Apical" PSRs did not colocalize with PSDs. These results support a conclusion that PSRs can be maintained for at least several days in the absence of postsynaptic terminals but can become mislocalized within the IHC as a consequence. Rapid loss of PSRs in IHCs after noise trauma may be a consequence of a direct effect of noise on the IHC rather than a consequence of loss of SGN synaptic terminals.

Funded by a grant from NIH R01 DC02961 (SHG)

393 Neurotrophic Factor Expression in the Rat Organ of Corti (OC), Cochlear Nucleus (CN), and Spiral Ganglion After Deafening Erin M. Bailey¹, Jonathan C. Kopelovich², Steven H.

Green^{1,2}

¹University of Iowa Department of Biology, ²University of Iowa Department of Otolaryngology

Hair cells and OC supporting cells (OCSCs) release neurotrophic factors (NTFs) that can support spiral ganglion neuron (SGN) survival. Following loss of hair cells, SGNs degenerate and gradually die but many SGNs can survive for months or years. We conjecture that during this period there is an alternative source of NTF and here assess NTF expression in tissues in contact with SGN somata or peripheral or central axons: OC, cochlear nucleus (CN), and spiral ganglion (SGNs and glia). Rats were deafened by daily systemic kanamycin injections P8-P16. Deafness was verified by ABR. NTF expression in the OC and CN was compared by gPCR at five time points post-deafening and in age-matched control hearing littermates: P16, immediately after deafening; P23, when degeneration is first evident in the spiral ganglion; P32, when SGN density is first significantly lower in deafened than in control hearing rats; P60, when ~50% of the SGNs have died and P88-P90, when ~90% of the SGNs have died (Alam et al., 2007). We focused on NTFs previously implicated in SGN survival. Microarray-based gene profiling shows that TrkB and TrkC (but not TrkA), GFRalpha1 & 2 (but not 3 & 4), N-CAM (but not Ret) and the CNTF receptor are expressed in the spiral ganglion and their level of expression does not change significantly post-deafening at P32. NT-3, but not BDNF, is expressed in the postnatal OC. NT-3 expression falls by >90% immediately after hair cell death suggesting that hair cells are either the only significant source or that they are necessary for NT-3 synthesis by OCSCs. GDNF expression in the OC declines with age and also is reduced significantly after hair cell loss. Nrtn is expressed in the OC at all postnatal ages assessed and its expression does not decline significantly post-deafening. Because a potential receptor system (GFRalpha2 & N-CAM) exists in the spiral ganglion. Nrtn is a candidate for a NTF that can maintain SGN survival after hair cell loss. Both NT-3 and BDNF are expressed in the CN, although at relatively low levels, and is maintained after deafening. Supported by NIH grant DC002961

394 TRPA1-Mediated Damage Sensing in the Inner Ear

A. Catalina Vélez-Ortega¹, Ruben Stepanyan¹, Artur Indzhykulian¹, Gregory I. Frolenkov¹

¹Department of Physiology, University of Kentucky

Supporting cells in the inner ear are extremely sensitive to extracellular ATP, a signaling molecule that is thought to be released into the cochlear fluids during acoustic overstimulation. Stimulation of P2Y receptors induces the generation of IP₃ and subsequent release of Ca²⁺ from intracellular stores, and this response propagates to neighboring cells by diffusion of IP₃ through gap junctions and further release of ATP through hemichannels. In addition, these Ca²⁺ waves in the supporting cells are accompanied by the changes in cell shape as observed with bright field imaging.

ATP is not the only signaling molecule released during cochlear insults. For instance, oxidative stress induces lipid peroxidation leading to the generation of several byproducts, such as 4-hydroxynonenal (4-HNE), which could activate the transient receptor potential ankyrin 1 (TRPA1) cation channel, a channel that is involved in sensing cold, mechanical and chemical noxious stimuli by nociceptive neurons. TRPA1 is highly expressed in the sensory epithelium of the inner ear. Therefore, we have utilized 4-HNE to study the response of supporting cells to yet another 'damage' signal.

Application of 4-HNE to the cultured explants of the auditory sensory epithelium of young postnatal mice produced robust Ca²⁺ responses in the Hensen cells, Deiters' cells and other supporting cells, but very small responses in the hair cells. Remarkably, the supporting cells of Kolliker's organ exhibited changes in cell shape following 4-HNE application. Theses shape changes were coincident with the Ca²⁺ waves both in duration and in the area, similar to the responses to extracellular ATP stimulation. 4-HNE failed to induce Ca²⁺ responses in any cells of the auditory sensory epithelium in TrpA1 knock-out mice. We concluded that the same supporting cells can sense damage through different pathways but may still use a similar (if not the same) mechanism to propagate the signal.

Supported by NIDCD/NIH (R01 DC009434)

395 Modulation of Salicylate-Induced Tinnitus by the NMDA Antagonist Memantine

Massimo Ralli^{1,2}, Edward Lobarinas¹, Guang-Di Chen¹, Anna Rita Fetoni², Diana Troiani³, Gaetano Paludetti², Richard Salvi¹

¹Center for Hearing and Deafness - State University of New York at Buffalo, ²Institute of Otolaryngology, Università Cattolica del Sacro Cuore, ³Institute of Human Physiology, Università Cattolica del Sacro Cuore Short-term tinnitus has been consistently reported

following administration of high doses of salicylate. Previous studies have suggested that cochlear NMDA ion channels play a key role in the induction of salicylateinduced tinnitus. The aim of this study was to determine whether systemic treatment with memantine, a NMDA channel blocker, would prevent the onset of tinnitus assessed by gap prepulse inhibition of acoustic startle (GPIAS). Twenty-eight rats were divided into 3 groups and were treated daily for four consecutive days with salicylate alone (300 mg/kg/d, i.p., n-8), memantine alone (5 mg/kg/d, i.p., n=6) or the combination of salicylate plus memantine (n=14). All rats were tested for tinnitus using GPIAS; hearing function was measured with DPOAE and the ABR. Rats treated with memantine alone showed no evidence of tinnitus. Rats treated with salicylate alone showed tinnitus-like behavior starting 2 h after treatment and lasting for the entire 4 day treatment. However, when rats were treated with salicylate plus memantine tinnituslike behavior was attenuated, particularly on the first day of treatment, suggesting that systemic memantine may suppress salicylate-induced tinnitus. Memantine alone had no effect on DPOAE amplitude whereas salicylate alone caused a progressive decrease in DPOAE over the 4 d treatment. Interestingly, treatment with salicylate plus memantine resulted in a decline in DPOAE amplitude comparable to salicylate alone. These results suggest that memantine did not block the effect of salicylate on OHC function, but must suppress tinnitus-like behavior at NMDA receptors located at the inner hair cell-afferent synapse, as previously suggested by Puel and colleagues, or at more centrally locations in the nervous system. Finally, none of the treatments caused any permanent changes in ABR thresholds, DPOAE or GPIAS. Supported in part by NIH (R01DC0090910; R01DC009219-01)

396 Hearing Impaired Animals with and Without Tinnitus Unravel a Tinnitus Specific Trait

Marlies Knipper¹, Wibke Singer¹, Annalisa Zuccotti¹, Masahiro Matsumoto², Lukas Rüttiger¹

¹University of Tuebingen THRC Molecular Physiology of Hearing, ²Department of Otolaryngology Head and Neck Surgery Kyoto University

Tinnitus is a prevalent audiologic complaint characterized by auditory perception without an external physical source. About 10% of the American and European population are subjected to chronic, persistent tinnitus that dramatically affects quality of life. Tinnitus, due to a broad variety of possible etiologies and pathogeneses, is one of the most challenging clinical problems (Eggermont, 2007). Nevertheless, the molecular basis of tinnitus is still elusive. In most cases, tinnitus can be linked to a damage to the peripheral hearing system (Sindhusake et al., 2004), probably even in cases where an impairment cannot (yet) be assessed by standard clinical audiometry (Shiomi et al., 1997). Considering the likelihood of hearing impairment in subjects with tinnitus, why does hearing loss NOT automatically lead to tinnitus? One way to answer this question is to examine tinnitus specific features in a standardized animal model, comparing animals with and without tinnitus, both suffering from hearing loss after equal sound exposure. In the present study we compared equally acoustically exposed rats with similar hearing impairment, that were behaviorally selected (Rüttiger et al., 2003) in groups with and without tinnitus. In a comprehensive study, we were looking for tinnitus specific changes including the cochlea, the auditory pathway and the auditory cortex. Striking results did show up, that may suggest a novel tinnitus specific trait.

Supported by the Marie Curie Research Training Network CavNET MRTN-CT-2006-035367, and the Deutsche Forschungsgemeinschaft, grant DFG-Kni-316-4-1.

397 Na⁺/K⁺-ATPase α 1 Identified as an Abundant Protein in the Blood-Labyrinth Barrier That Plays an Essential Role in the Barrier Integrity

Yue Yang¹, **Min Dai**¹, Teresa Wilson¹, Irina Omelchenko¹, John Klimek¹, Phillip Wilmarth¹, Larry David¹, Alfred Nuttall¹, Peter Gillespie¹, Xiaorui Shi¹ ¹Oregon Health & Science University

Disruption of the blood-labyrinth-barrier is closely associated with a number of hearing disorders. Many proteins of the blood-brain-barrier and blood-retinal-barrier have been identified, leading to significant advances in understanding their tissue specific functions. In contrast, capillaries in the ear are small in volume and anatomically complex. This presents a challenge for protein analysis studies, which has resulted in limited knowledge of the molecular and functional components of the bloodlabyrinth-barrier. In this study, we developed a novel method for isolation of the stria vascularis capillaries from the mouse cochlea and provided the first database of protein components in the blood-labyrinth barrier as well as evidence that the interaction of Na⁺/K⁺-ATPase α 1 (ATP1A1) with Protein kinase C eta (PKCn) and occludin is one of the mechanisms of loud sound-induced vascular permeability increase. Using a mass-spectrometry, shotgun-proteomics approach combined with a novel "sandwich-dissociation" method, more than 600 proteins from isolated stria vascularis capillaries were identified. The ion transporter ATT α 1 was the most abundant protein in the blood-labyrinth barrier. Pharmacological inhibition of ATP1 α 1 activity resulted in hyperphosphorylation of tight junction proteins such as occludin which, in turn, increased the blood-labyrinth-barrier permeability. PKCn directly interacted with ATP1 α 1 and was an essential mediator of ATP1 α 1-initiated occludin phosphorylation. Moreover, this identified signaling pathway was involved in the breakdown of the blood-labyrinth-barrier resulting from loud sound The results presented here provide a novel trauma. method for capillary isolation from the inner ear and the first database on protein components in the bloodlabyrinth-barrier. Additionally, we found that ATP1 α 1 interaction with PKCn and occludin was involved in the integrity of the blood-labyrinth-barrier. Supported by NIDCD R01 DC 000141 (AN), R01 DC000105 (AN), P30 DC005983 (XS), and Oregon Opportunity funds to the OHSU Proteomics Shared Resources.

398 NT-3 Is a Highly Localized Signal in Maintenance and Regeneration of Inner Hair Cell (IHC) to Spiral Ganglion Neuron (SGN) Afferent Synapses in the Postnatal Organ of Corti

Qiong Wang¹, Catherine Kane¹, Steven Green¹ ¹Departments of Biology & Otolaryngology, University of Iowa

The neurotrophins NT-3 and BDNF are expressed in the developing organ of Corti and the cognate receptor protein-tyrosine kinases, TrkB and TrkC, are expressed in spiral ganglion neurons (SGNs). After birth in rodents, BDNF expression declines to an insignificant level, while NT-3 continues to be expressed, mainly in IHCs and immediately adjacent supporting cells (SCs), till adulthood. Using neonatal rodent organotypic cochlea explant cultures, we have previously shown that endogenous NT-3 in the postnatal organ of Corti has a distinctive role, not mimicked by BDNF, in promoting type 1 SGN axon growth and synapse regeneration on IHCs. Here we investigated the spatial constraints on NT-3 signaling by examining innervation and reinnervation of IHCs by SGNs in mice with "mosaic" organs of Corti in which NT-3 was randomly deleted from some but not all IHCs. We obtained such cochleae by generating Atoh1-CreER^{T2}; NT-3^{flox/flox}; Z/EG mice. Injection of tamoxifen (TX) at postnatal day 0 (P0) results in activation of Cre recombinase in a random set of hair cells (HCs), which in turn, both excises the "floxed" NT-3 gene and allows expression of GFP in the same cells from the Z/EG transgene. Six days after TX injection, 27% of the IHCs expressed eGFP. These were scattered apparently randomly among the non-eGFP-expressing IHCs. We compared innervation of NT-3-lacking/eGFPpositive IHCs with their eGFP-negative neighbors in an organotypic cochlear culture which preserves the synaptic interactions between SGNs and HCs. Innervation of NT-3lacking/eGFP-positive IHCs was deficient and degenerating afferent terminals could be observed below them. Fewer postsynaptic densities (PSDs) were observed on individual NT-3-lacking IHCs. A 30 min exposure to 0.5 mM kainic acid causes rapid degeneration of type 1 SGN synapses on IHCs followed by a partial regeneration over the ensuing 72 h. We found that, 72 h post-trauma, NT-3lacking IHCs were selectively bypassed by regrowing SGN axons, while adjacent NT-3-expressing IHCs were reinnervated and new PSDs could be observed in contact with them. This indicates that NT-3, although a diffusible molecule, acts as a remarkably short-range signal for synaptic maintenance. NT-3 from even immediately adjacent IHCs or SCs has little influence.

Funded by a grant from NIH R01 DC02961 (SHG)

399 Noise Induced Damage at the Top and Bottom of Hair Cells

Jian Wang^{1,2}, Hui Wang³, Shouhuan He¹, Shankai Yin³ ¹Dalhousie University, ²SouthEast University, ³The Sixth affiliated hospital, Jiao Tong University

It was reported recently that a noise exposure that caused no permanent hearing loss might damage the spiral

ganglion neurons (SGNs) permanently in mice. This is interesting because if occurs in human subjects, the noise induced damage could be subclinic. In the attempt to generalize this finding, we assess if such a permanent SGN damage may occur in guinea pigs. A broadband noise was used at 110 dB SPL for 2 hours to create cochlear lesion in guinea pigs. The hearing function was evaluated by auditory brainstem response (ABR) in farfield and compound action potential (CAP) and cochlear microphonics (CM) through round-window electrode. The damage to SGNs and their distal fibers were observed in cochlear cross-sections and quantified by counting the number of SGNs in Rosenthal Canal and the number of fibers through habenula perforata. The damage to the stereocilia at the top of hair cells was also observed quantitatively. One day after the noise exposure, the crossfrequency averaged threshold shift was 26.9±5.16 dB over 1-48 kHz. This was reduced to 7 ± 2.33 dB one month after the noise exposure and significant loss was seen only at 8 kHz (32.5±5.44 dB) and 4kHz (10±2.89 dB). A slight reduction of fiber number at habenula perforata was found one day after the noise. The reduction was not significant and remained unchanged one month after the noise. The density of SGNs in Rosenthal canal was also slightly but not significantly reduced as examined 1 day and 1 month after the noise. The change of SGNs and their distal fibers is corresponding to the CAP amplitude change. The result suggested that the damage to the SGNs/fibers, if there is, is not so servere as reported in mice. Our study also demonstrated that the damage to the stereocilia of hair cells could be largely recovered after the noise exposure. This is corresponding to the change of CM.

Key words: noise-induced hearing loss; spiral ganglion neuron; auditory nerve fibers; stereocilia; compound action potential; cochlear microphonics.

400 Noise-Induced Primary Neural Degeneration in Guinea Pig: Does Vulnerability Depend on Spontaneous Discharge Rate?

Harrison Lin^{1,2}, **Adam Furman^{2,3}**, Sharon Kujawa^{1,2}, M. Charles Liberman^{1,2}

¹Department of Otology and Laryngology, Harvard Medical School, ²Eaton-Peabody Laboratory, Massachusetts Eye and Ear Infirmary, ³Harvard-MIT Health Sciences and Technology, Speech and Hearing Bioscience and Technology Program

In mice, noise exposures that are reversible based on cochlear thresholds can lead to immediate and irreversible loss of cochlear nerve peripheral terminals, followed by slow death of spiral ganglion cells, without hair cell loss (Kujawa & Liberman 2009, J Neurosci 29: 14077).

To test the generality of noise-induced primary neural degeneration, to facilitate rescue studies via local neurotrophin delivery, and to simplify sampling of auditory nerve activity, we moved to a guinea pig model. We exposed young adults (300 - 400 g) to octave-band noise (4 - 8 kHz) at 106 dB SPL for 2 hrs and quantified threshold shifts acutely. From 10 to 24 days later, ABRs and DPOAEs were re-measured, and/or single-fiber

recordings were obtained from the auditory nerve, then cochleas were immunostained for pre-synaptic ribbons and post-synaptic terminals.

ABRs and DPOAEs show acute post-exposure threshold shift of 40-60 dB followed by complete threshold recovery 10 days later. DPOAE suprathreshold amplitudes return to normal, but suprathreshold recovery of ABR wave 1 amplitude is incomplete at high frequencies. Confocal analysis shows loss of ribbons and terminals despite no hair cell loss. Synaptic loss is detectable from 8 – 45 kHz and maximal (~50%) at 22 kHz. Single fiber recordings confirm threshold recovery but suggest that degeneration is confined to fibers with low- and medium spontaneous rates.

Finding primary noise-induced neural degeneration in guinea pig, as in mouse, suggests this putatively excitotoxic effect is also present in humans – sobering, given that damage risk criteria assume that threshold recovery indicates cochlear recovery. The finding that (high-threshold) fibers with low- and medium-SR are particularly vulnerable helps explain why thresholds return to normal, but suggests that noise-induced neural loss might cause problems with hearing in a noisy environment, given that low and medium-SR fibers are particularly resistant to noise masking.

Supported by research and training grants from the NIDCD (R01 DC0188 to MCL and R01 DC08577 to SGK and T32 DC0038 to ACF)

401 Noise-Induced Primary Neural Degeneration: Effects of Spectrum, Duration, Intensity and Survival

Sharon G. Kujawa^{1,2}, Steven Micucci¹, M. Charles Liberman^{1,2}

¹Massachusetts Eye and Ear Infirmary, ²Harvard Medical School

Noise exposure producing reversible threshold shift can cause immediate loss of cochlear nerve terminals and delayed loss of spiral ganglion cells. This neuropathy is reflected in ABR amplitude reductions, not threshold shifts; lack of hair cell damage is reflected in recovery of both DPOAE amplitudes and thresholds. As exposed ears age, further ABR decrements accrue without further changes in DPOAEs (Kujawa & Liberman 2006, 2009).

The present study has two aims: to determine 1) if postexposure age-related ABR reductions reflect ongoing loss of cochlear terminals and 2) whether noise-induced primary neural degeneration occurs for exposures of different spectra, intensity and duration.

Acute (24 hr), initial permanent (2 wk) and delayed (16-64 wk) effects of noise exposure were evaluated in CBA/CaJ mice exposed to octave-band noise (8-16 kHz or 4-8 kHz) at various time-intensity combinations. Threshold shifts were assessed by ABR and DPOAE (5.6 – 44.7 kHz). Synaptic ribbons and cochlear nerve terminals were quantified at three locations by confocal immunohistochemistry.

The 8-16 kHz exposures comprised an equal-energy series or held level (and cochlear place) constant while duration was varied. All exposures produced large acute

threshold shifts and basal-turn ribbon loss evident at 24 hr. Noise-exposed ears that recovered threshold sensitivity nevertheless suffered permanent and ongoing ABR amplitude declines between 2 and 16 wk, although DPOAE amplitudes recovered stably to control values. Ongoing synaptic analysis suggests progressive ribbon loss as well. For 4-8 kHz noise, ribbon loss was minimal and also confined largely to the base, even when exposure severity was increased (115 dB/6 hr) to produce large permanent threshold shift.

Results suggest 1) that primary noise-induced neurodegeneration is primarily a basal-turn phenomenon but 2) that basal-turn neural loss occurs without hair cell loss under a variety of noise exposure regimens.

Research supported by grants from the NIDCD: R01 DC008577 to SGK and R01 DC0188 to MCL

402 Increase of Aggregations After Noise Injury in Guinea Pig

Takefumi Mikuriya¹, Kazuma Sugahara¹, Yoshinobu Hirose¹, Eijyu Kanagawa¹, Syuhei Yoshida¹, Hiroaki Shimogori¹, Hiroshi Yamashita¹

¹Yamaguchi University Graduate School of Medicine Aggregations, made of damaged protein, misfolding protein and abnormal product cause the cytotoxic activity and cell death when they are formed. Neurodegenerative diseases example for Alzheimer fs disease and systemic amyloidoses, have been recognized to be associated with inappropriate deposition of protein aggregates. Although the mechanism of pathogenic aggregations is not fully understood, several reports targeting at aggregations are reported in animal researches. Especially, molecular chaperon, heat shock response plays a critical role in these reports.

Heat shock response is characterized by induction of heat shock proteins (HSPs) in response to stresses such as heat shock. HSPs act as molecular chaperones which stabilizes denatured proteins, facilitates their removal or repair, and some HSPs also inhibit apoptotic pathways. Previously, we demonstrated that HSPs expression was altered during aging and some aggregation with Hsp70 were increased in spiral ganglion cells. We considered that the correlation with aggregations and stresses with aging may be exist in inner ear as same as other neurodegenerative diseases. To demonstrate this hypothesis, we changed the stress condition to noise injury model. Here, we report that the result that aggregations in cochlear cell increased after noise injury as same as aging model. These results suggest that aggregations may be involved in the mechanism of inner ear damage and show a new strategy for diseases in inner ear.

403 Noise Induced Permanent Hearing Loss in CBA and C57 Mice: Comparison of Their Morphology and Hearing

Shi-Nae Park¹, Sang A. Back¹, Hong Lim Kim², Kyoung Ho Park¹, Omar Akil³, Laurence Lustig³, Sang Won Yeo¹ ¹Department of Otolaryngology-HNS, The Catholic University of Korea, ²Laboratory of Electron Microscopy,

The Catholic University of Korea, ³Department of

Otolaryngology-HNS, Univertiy of California San Francisco This study was performed to compare morphologic and audiologic changes after noise exposure in two different strains of mice (CBA and C57) and to get morphologically proven models for noise induced hearing loss (NIHL) at our experimental setting. Mice were exposed to 110dB SPL white band noise for 1 h at the age of 1 month. Hearing thresholds and outer hair cell functions have been evaluated by not only auditory brainstem response (ABR) recordings but also distortion product otoacoustic emission (DPOAE) immediately and 22 days after the noise exposure. Cochlear pathology has been observed and compared by light and electron microscopic study. Both mice strains showed hearing threshold shift with decreased outer hair cell function immediately and 22 days after the noise exposure. More severe ABR threshold shifts have been observed in C57 mice compared with CBA mice at click, 8, 16 and 32 kHz tone burst stimuli. Cochlear morphologic study demonstrated that predominant outer hair cell degeneration at the basal turn of cochlea in both mice strains but more severe in C57 mice. Scanning electron microscopic study also revealed more severe ultra-structural damage of outer hair cells at each turn of cochlea in C57 mice. Both mice strains showed consistent noise induced permanent hearing loss with different susceptibility. Further studies to investigate the mechanism of this different vulnerability to noise exposure between two mice strains are ongoing in our laboratory.

404 MicroRNA Expression in Rat Cochlear Sensory Epithelia: The Expression Pattern in Normal Cochleae and Alteration Following Exposure to an Intense Noise

Bo Hua Hu¹, Qunfeng Cai¹, Donald Coling¹ ³State University of New York at Buffalo

MicroRNAs (miRNAs) are a group of small non-coding RNA that regulate cellular function through the RNA interference pathway and post-transcriptional regulation of mRNA function. miRNAs have been implicated in normal development and pathogenesis of various species. To determine the expression pattern of miRNAs in normal cochlear sensory epithelia and the expression changes after acoustic trauma, we measured the expression levels of 375 highly characterized miRNA transcripts, as well as five reference small RNAs using TagMan Rodent MicroRNA Arrays (Applied Biosystems). Young Sprague Dawley rats were exposed to an intense noise at 120 dB (SPL) for 2 hours, which caused an average threshold shift of 80±11 dB (TTS, measured at 1.5 hours post-exposure). Total RNAs containing small RNAs were extracted from cochlear epithelia containing the sensory and the supporting cells. RT-qPCR screening showed that about one half of the examined miRNAs were expressed in the rat cochlear epithelia. Among these expressed miRNAs. 12 are designated as rat transcripts and 170 as mouse sequences. The highly expressed miRNAs include mmumiR-191, mmu-miR-204, mmu-miR-150, mmu-miR-24, mmu-miR-30c, mmu-miR-133a, mmu-miR-30b, mmu-miR-

574, mmu-miR-200c and mmu-miR-182. Following exposure to the intense noise, all highly-expressed miRNAs (Ct <30) remained unchanged (defined as the fold change less than 3). Alteration in the expression levels was observed only in those miRNAs that were expressed at a low level in the normal condition (Ct>30). However, these expression changes were not statistically significant due to the inconsistency of the changing directions. We speculate that this inconsistency may be related to the individual variation in the level of cochlear damage, a phenomenon commonly seen after acoustic trauma. (Supported by NIH R01 DC010154-01A2)

405 Activation of Small GTPases in Noise-Induced Hearing Loss Su-Hua Sha¹

¹The Medical University of South Carolina, Department of Pathology and Laboratory Medicine

The structural integrity of the cytoskeleton of the organ of Corti is required for accurate processing of acoustic information and the assembly and disassembly of actin is an important aspect of cochlear homeostasis. Small GTPases have been identified as key regulators of the actin cytoskeleton in all eukaryotic cells. As molecular switches, small GTPases act as major mediators in transmembrane signaling and in the control of intracellular pathways. The activation of Rac, for example, can activate NADPH oxidase leading to the formation of reactive oxygen species and thereby influence homeostatic pathways on a different level.

In the current study, we investigated Rho GTPase-linked signaling pathways and NADPH oxidase in CBA/J mice after exposure to broadband noise (2-20 kHz, 106 dB for 2 The exposure initially disturbed the actin hrs). arrangement of the stereocilia, resulting in a permanent threshold shift of about 50 dB (12 to 48 kHz) and causing hair cell loss. The hair cell loss started in the basal turn and spread apically with time after exposure. Apoptotic and necrotic hair cell death were detected in the basal region and both caspase-dependent and-independent hair cell death pathways were observed. Furthermore, noise trauma increased active Rac1, decreased active RhoA and promoted the formation of a Rac1-p67phox complex, a subunit of NADPH oxidases. These data suggest that noise trauma invokes small GTPase pathways that regulate the actin cytoskeleton and activate NADPH oxidase, leading to structural disruptions and increased ROS formation in the inner ear.

Supported by grant R01 DC009222 from the National Institute on Deafness and Other Communication Disorders, National Institutes of Health.

406 The Effects of Noise Exposure on TAK1 Expression in the Organ of Corti

Mark Parker^{1,2}, Kevin Jiang², Caitlin Simmons¹, Judith Kempfle², Kunio Mizutari², Albert Edge^{2,3} ¹*Emerson College,* ²*Massachusetts Eye & Ear Infirmary,*

³*Harvard Medical School* TGF-b activated kinase-1 (TAK1), a member of the MAPKKK family, mediates the activation of the NF- $\kappa\beta$ and

c-Jun N-terminal Kinase (JNK) signaling pathways and serves as the target of a number of pro-inflammatory cytokines. Neither the function nor expression pattern of TAK1 during the development of the cochlea has been defined. Here we examine the expression levels of TAK1 in E12.5, E16, P0, P4, P16, and adult cochleas via RT-PCR and immunohistochemistry and test the hypothesis that noise exposure affects the level of TAK1 expression in the adult cochlea. The results indicate that at E12.5, TAK1 is expressed ubiquitously within the otic vesicle and periotic mesenchyme. Co-labeling with Jag1 confirmed TAK1 expression in the early sensory epithelium. As the cochlea matures, TAK1 expression becomes more restricted to supporting cells. At E16, TAK1 is broadly expressed throughout the developing cochlear sensory epithelium and is co-localized with the hair cell markers myosin 7a, calbindin, and Atoh1. From P1 to P4, TAK1 expression is limited to cells of the stria vascularis, hair cells, supporting cells, and cells of the greater epithelial ridge. RT-PCR data indicates that TAK1 expression decreases during the course of development. By P16. TAK1 expression is limited only to Deiters cells, inner phalangeal cells, and inner border cells. TAK1 expression remains limited to these cells though P16 and into adulthood, with little to no expression present in any other cells types throughout the mature cochlea. To test the hypothesis that TAK1 is involved in the inflammatory response of murine cochlea, we measured the expression of TAK1 using immunohistochemistry at 1, 7, 14, and 28 days after a 2 hr exposure to an 8-16 kHz noise at 112 dB SPL. TAK1 expression increased in noise exposed cochleas compared to contralateral control ears that tympanectomies. received Further studies usina quantitative PCR will be used to verify these results.

407 Involvement of Retinoic Acid-Induced Peroxiredoxin 6 Expression in Recovery of Noise-Induced Temporary Hearing Threshold Shifts

Jhang Ho Pak¹, Bom Yi Chung¹, **Jong Woo Chung²** ¹Asan Institute for Life Science, Asan Medical Center, University of Ulsan, College of Medicine, ²Asan Medical Center, University of Ulsan, College of Medicine Oxidative stress in the cochlea is considered to play an important role in noise-induced hearing loss (NIHL). Several studies have provided evidence that all trans retinoic acid (ATRA) reduces hair cell loss and hearing deterioration in NIHL-induced animal models, yet the molecular details of its effect are poorly understood. In present study, we investigate the involvement of peroxiredoxin 6 (Prdx 6) in ATRA-mediated auditory threshold shift after temporary NIHL. Mice fed with ATRA before or after exposure to white noise resulted in faster recovery than untreated controls (fed with sesame oil only) within a week period. A significant increase in cochlear Prdx 6 protein expression from ATRA fed mice was evident, compared with those of controls. Treatment of a mouse organ of Corti-derived cell line (OC-k cells) with ATRA induced the expression of Prdx 6 mRNA and protein in a dose- and time-dependent manner, indicating

transcriptional and translational upregulation by ATRA. To further elucidate molecular mechanism of ATRA-induced Prdx 6 expression, we identified a putative retinoic acid receptor (RAR) binding site in a 668 bp of murine Prdx 6 promoter region, and analyzed the promoter activity in ATRA-treated OC-k cells, using a luciferase reporter assay. Prdx 6 promoter activities were elevated in full length (668 bp) reporter plasmid-transfected cells, whereas no significant change in the activity was observed in those of RAR binding site deleted mutant reporter. Moreover, expression of exogenous RAR resulted in dose-dependent increases in the promoter activity, implying that RAR functions as a transactivator of Prdx 6 gene expression. These findings suggest that ATRA-induced Prdx 6 expression may be associated with rapid recovery process from temporary NIHL.

408 Effect of Etanercept on the Expression of Noise-Induced Inflammatory Factors in the Mouse Cochlea

Teresa Wilson¹, Irina Omelchenko¹, Min Dai¹, Xiaorui Shi¹, Alfred Nuttall¹

¹Oregon Health & Science University

The generation of reactive oxygen species (ROS) is one of the underlying mechanisms of noise-induced damage to tissues in the inner ear. Acoustic trauma results in the secretion and expression of tumor necrosis factor (TNF)- α , a key proinflammatory cytokine, which leads to an increase in cellular ROS levels and activation of oxidative stressresponsive signaling pathways including the mitogenactivated protein kinase cascades and nuclear factorkappa B. To better understand the link between acoustic trauma and TNF- α mediated stress signaling in the cochlea, we treated CBA/CaJ mice with 25 mg/kg of the TNF- α antagonist, etanercept, at 48, 24, and 1 hour prior to a 2 hour exposure to 100 dB wideband noise, a level of noise exposure that results in a temporary hearing threshold shift. Auditory brainstem responses (ABR) were measured at 1 and 2 weeks post noise exposure with the finding that etanercept treatment did not prevent noiseinduced shifts in ABR threshold levels. Next, we examined whether etanercept treatment would affect the mRNA levels of inflammatory factors that are upregulated by acoustic overstimulation. Quantitative RT-PCR analysis was performed on total RNA extracted from cochlear lateral walls at 4 hours post noise exposure. Consistent with previous data from our laboratory, inducible nitric oxide synthase (iNOS) transcript levels were increased approximately 2.5 fold in the lateral wall of noise exposed Pretreatment with etanercept significantly animals. attenuated this increase. These preliminary data indicate that blocking TNF- α activity may reduce noise-induced inflammation in the inner ear. Supported by NIH NIDCD DC000105 (AN) and NIH NIDCD DC010844 (XS).

409 The Expression of Pigment Epithelium-Derived Growth Factor and Its Down-Regulation in Noise-Exposed Mouse Cochleae

Min Dai¹, Teresa Wilson¹, Xiaorui Shi^{1,2}

¹Oregon Health & Science University, ²Chinese Academy of Medical Sciences & Peking Union Medical College The blood-labyrinth barrier in the cochlear stria vascularis is critical for maintaining cochlear homeostasis, which is essential for normal hearing. While it is well recognized that vascular endothelial growth factor (VEGF) can increase vascular permeability, how vascular permeability is controlled by anti-permeable factors is not fully understood. Recently, expression of pigment epitheliumderived growth factor (PEGF), the most potent endogenous inhibitor of vasopermeability, has been demonstrated in the inner ear, including stria vascularis. But little is known about its cellular distribution or potential involvement in sound induced vascular permeability. In this study, with immunohistochemistry combined with confocal microscopy, we found that PEDF was robustly expressed in intermediate cells, but not in marginal cells and basal cells in the stria vascularis. The mRNA and protein levels of PEDF expression in the inner ear were similar to that of the retina as shown by the RT-PCR and immunoblotting techniques respectively. Moreover, broadband noise at 117dB/SPL caused a significant down-regulation of PEDF expression in the strial capillaries. We postulate that PEDF may be a key player for maintaining cochlear haemostasis in the inner ear and down-regulation of PEDF by noise stimulation may be part of the hyper-vasopermeability mechanism in response to noise. Supported by NIDCD R03 DC 008888 (XS) and R01 DC 010844 (XS).

410 Exposure to Intense Noise Alters the Expression Pattern of Adhesion- And Extracellular Matrix-Related Genes in Cochlear Sensory Epithelia

Qunfeng Cai¹, Donald Coling¹, Bo Hua Hu¹ ¹State University of New York at Buffalo

Exposure to acoustic stimuli elicits the vibration of the basilar membrane. Excessive sound exposure stretches the organ of Corti and compromises cell adhesion. We suspect that activation of adhesion signal transduction due to acoustic overstimulation contributes to the degenerative process of sensory cells. To understand the molecular links between the adhesion signaling and sensory cell degeneration, we profiled the expression pattern of multiple adhesion- and extracellular matrix-related genes in the cochlear sensory epithelia. Young Sprague Dawley rats were exposed to an intense noise at 120 dB SPL for 2 hrs. This level of noise exposure caused significant hearing loss with an average TTS of 65±24 dB and a PTS of 25±14 dB. At 2 hrs, 1 or 24 days post-exposure, the cochlear sensory epithelia were collected for assessment of the mRNA expression levels of 84 adhesion- and extracellular matrix-related genes using a RT-qPCR array technique. In the normal control cochleae, 76 out of 84 examined genes were expressed in the sensory epithelia.

Following the noise exposure, 15 genes were up-regulated and 23 genes were down-regulated at the early phases of cochlear pathogenesis (2 hrs and 1 day post-exposure). Among these genes, Mmp3, Mmp7, Sele, Sell, Timp1 exhibited the greatest fold increase, and Cntn1, Pecam1, and Mmp9 showed the greatest fold decrease. At 28 days post-exposure, the hearing level became stable. However, the expression levels of 28 genes that were altered at the early phases of cochlear pathogenesis remained different from those seen before the noise exposure. Importantly, transcription regulation was elevated or suppressed for 26 genes whose expression was not altered at the early phase of cochlear damage. We hypothesize that some or all of these genes are involved in the repair processes, or that these changes may be an indication of permanent molecular changes in response to scar formation. (Supported by NIH R01 DC010154-01A2)

411 Increased Prestin Expression in OHCs That Remain After Noise-Induced Hearing Loss

William Clifton¹, Ilene Chiu², Andrew Groves³, Fred Pereria^{2,4}, John Oghalai⁵

¹Baylor College of Medicine, ²Baylor College of Medicine-Otolaryngology, ³Baylor College of Medicine-

Neuroscience, ⁴Baylor College of Medicine- Huffington Center on Aging, ⁵Stanford University- Otolaryngology

Outer Hair Cell (OHC) prestin is necessary for electromotility. Previously, we found that OHC prestin expression was higher in transgenic mice with tectorial membrane malformations in which some OHCs were functionally neglected. Herein, we sought to determine the effects of noise trauma on prestin expression in residual OHCs. We exposed cohorts of four-week-old wild type mice to four hours of noise (8-20 kHz at 98 dB SPL). Compared to baseline, ABR and DPOAE thresholds over the frequency range of 12.6-46.7 kHz were elevated one day after the noise exposure (19.3 and 12.4 dB respectively, p<.001, n=44) and demonstrated partial recovery one week afterwards (7.3 and 8.6 dB respectively, p<.001). DPOAE growth curve slopes measured at f2=17.5 kHz demonstrated increases from 0.71 dB/dB to 1.00 dB/dB one day afterwards (p<.001, n=44) and partial recovery to 0.82 dB/dB one week after the exposure (p<.005). We assessed the cochlear epithelium by immunolabeling for prestin and imaging using two-photon microscopy. This demonstrated the expected pattern of OHCs loss at the basal end of the cochlea. We then quantified prestin within the OHC lateral wall and found a 1.78 fold increase in the fluorescence intensity from noise-damaged compared to control cochleae (p<.001, n=45 and 87 images respectively, from 9 cochleae). Next, we used single whole-cochlea preparations to measure prestin protein and mRNA expression. The values seven days after noise exposure were compared to normal controls. Myosin VIIa was used as the reference protein to estimate the amount of prestin per hair cell. Noise exposure produced a 1.68 fold increase in the prestin/myosin ratio (p<.05, n=15 noise/control pairs) and a 2.03 fold increase in the expression of prestin mRNA (p<.01, n=17 noise, 14 control). Together, these results demonstrate that while our noise exposure protocol produces OHC loss, there is an associated increase in prestin protein and mRNA in the remaining OHCs.

Supported by the HHMI Medical Fellows Program, NIH grants DC006671 and DC006185, and DOD CDMRP DM090212

412 Low Level Blast Overpressure Exposures Produce Hemorrhage in Perilymph: Support for a Sentinel Role of Auditory and Vestibular Findings

Carey Balaban¹, Ronald Jackson², Michael Hoffer², Ben Balough²

¹University of Pittsburgh, ²Naval Medical Center San Diego Confusion, headache, dizziness and hearing loss are common symptoms of mild traumatic brain injury after wave exposure. This study provides shock histopathological evidence of the inner ear effects of low intensity (5, 10-11 psi or 15-17 psi) blast overpressure (BOP) in female Sprague-Dawley rats. After survival times ranging from 2 hours to 42 days after BOP exposure, the rats were euthanized and perfused with paraformaldehyde fixative.. The skinned heads were decalcified, embedded in paraffin and sectioned serially at 6-8 microns in the horizontal plane. Sets of every fiftieth section were stained with hematoxylin and eosin for histopathologic analysis. Alternate sets of sections were stained immunohistochemically to visualize molecules that included vascular endothelial growth factor, fibrin, 18 alpha 1, interleukin 8 receptor B, procollagen angiopoietin 1 and manganese superoxide dismutase 2. The primary finding was the presence of red blood cell ghosts and hematoma in the scala tympani, particularly in proximity to the cochlear aqueduct. Lymphocytes and macrophages were found occasionally within these aggregates. Their location suggests an origin from the cochleovestibular vein, near its junction with the inferior petrosal sinus. A light protein exudate was commonly present within the perilymph of both scalae tympani and vestibuli. These features were seen at all survival times, suggesting а link to persistent or worsening audiovestibular symptoms. Further, because the perilymph is confluent with the cerebrospinal spinal fluid, these pathologic findings are a form of subarachnoid hematoma. Hence, they can contribute to headache as well as audiovestibular symptoms. These studies motivate clinical examination of the value of balance and auditory testing as sentinels for the presence of mild traumatic brain injury after blast wave exposure.

413 Does the Infrasound from Wind Turbines Affect the Inner Ear? Alec N. Salt¹

¹Washington University School of Medicine

There is controversy whether prolonged exposure to the sounds generated by wind turbines adversely affects human health. The unweighted spectrum of wind turbine noise slowly rises with decreasing frequency, with greatest

output in the 1-2 Hz range. As human hearing is insensitive to infrasound (needing over 120 dB SPL to detect 2 Hz) it is claimed that infrasound generated by wind turbines is below threshold and therefore cannot affect people. The inner hair cells (IHC) of the cochlea, through which hearing is mediated, are velocity-sensitive and insensitive to low frequency sounds. The outer hair cells (OHC), in contrast, are displacement-sensitive and respond to infrasonic frequencies at levels up to 40 dB below those that are heard. A review found the G-weighted noise levels generated by wind turbines with upwind rotors to be approximately 70 dB G. This is substantially below the threshold for hearing infrasound which is 95 dB G but is above the calculated level for OHC stimulation of 60 dB G. This suggests that most wind turbines will be producing an unheard stimulation of OHC. Whether this is conveyed to the brain by type II afferent fibers or influences other aspects of sound perception is not known. Listeners find the so-called amplitude modulation of higher frequency sounds (described as blade "swish" or "thump") highly annoving. This could represent either a modulation of audible sounds (as detected by a sound level meter) or a biological modulation caused by variation of OHC gain as operating point is biased by the infrasound. Cochlear responses to infrasound also depend on audible input, with suppressing audible tones cochlear microphonic responses to infrasound in animals. These findings demonstrate that the response of the inner ear to infrasound is complex and needs to be understood in more detail before it can be concluded that the ear cannot be affected by wind turbine noise.

This work was supported by research grant RO1 DC01368 from NIDCD/NIH.

414 Auditory Brainstem Responses Predict Auditory Nerve Single-Unit Thresholds and Frequency Selectivity Following Noise Induced Hearing Loss in Chinchillas

Kenneth S. Henry¹, Sushrut Kale², Ryan E. Scheidt³, Michael G. Heinz^{1,2}

¹Department of Speech Language, and Hearing Sciences, Purdue University, ²Weldon School of Biomedical Engineering, Purdue University, ³School of Electrical and

Computer Engineering, Purdue University Non-invasive Auditory Brainstem Responses (ABRs) are commonly used to assess cochlear damage in both clinical and research environments. In the current study, we evaluated the relationship between ABR measurements and more direct measurements of cochlear physiology. We recorded ABRs and auditory nerve (AN) single-unit responses in seven chinchillas with noise induced hearing loss. ABRs were recorded for 1-8 kHz tone burst stimuli both before and several weeks after four hours of exposure to a 115 dB SPL, 50 Hz band of noise with a center frequency of 2 kHz. ABR thresholds, wave I amplitude, and wave I latency were compared to measurements of AN threshold and frequency selectivity from single-unit tuning curves. As expected, noise exposure generally resulted in an increase in ABR thresholds and decrease in wave I amplitude at equal SPL.

Wave I amplitude at equal sensation level (SL), however, was similar before and after noise exposure. In addition, noise exposure resulted in decreases in ABR wave I latency at equal SL and, to a lesser extent, equal SPL. The shifts in ABR measurements were significantly related to shifts in AN thresholds and frequency selectivity in the same animal at the same frequency. Larger shifts in ABR thresholds and ABR wave I amplitude at equal SPL were associated with greater AN threshold elevation. Larger shifts in ABR wave I latency at equal SL, on the other hand, were associated with greater losses in AN frequency selectivity. This result is consistent with linear systems theory, which predicts shorter time delays for broader peripheral frequency tuning. Taken together with other studies, our results affirm that ABR thresholds and wave I amplitude provide useful estimates of cochlear sensitivity. Furthermore, wave I latency differences at equal SL may prove useful for detecting and characterizing loss of peripheral frequency selectivity. This research was supported by NIH Grant# R01-DC009838.

415 The Effects of Cigarette Smoking on Hearing Recovery of Mice from Noise-Induced Temporary Hearing Threshold Shifts

Joong Ho Ahn¹, Jong Woo Chung¹, Jin Kyung Suh¹, Harry Kim¹, Hyun Suk Joo², Seung Hyo Choi³ ¹Asan Medical Center, University of Ulsan, College of Medicine, ²University of Ulsan, College of Medicine, ³Jeju National University, School of Medicine

Objective: To evaluate the effects of cigarette smoking on hearing recovery after noise exposure.

Materials and Methods: BALB/c mice with normal Preyer's reflex were divided into 4 groups (Control, Smoking, Noise and Smoking-with-noise). For cigarette smoking, mice were exposed passive smoking for 2 weeks (5 times of 4 cigarette smoking per day) before noise exposure. Mice were exposed continuously to 110 dB SPL white noise for 3 hours once. We assessed hearing via auditory brainstem response (ABR) with tone burst stimulation and distortion product otoacoustic emissions (DPOAE) at before noise exposure and at 1st, 3rd, 5th, 7th, 14th, 21th, and 28th day after noise exposure.

Results: There were no shift of hearing thresholds in both control and smoking only group. Hearing threshold increased abruptly in both of noise only and smoking with noise group after noise exposure. In noise only group, increased hearing threshold promptly returned to pre-noise exposure level after 2 weeks. However, in smoking with noise group, we observed initial significantly higher hearing loss which continued and did not return to previous level until 4 weeks after noise exposure. Conclusion: From this study, we can conclude that cigarette smoking may potentiate the harmful effect of noise on hearing and disturb the recovery mechanism in cochlea.

416 Glucocorticoid Receptor Pathways in Cochlear Explants

Inna Meltser¹, Barbara Canlon¹

¹Karolinska Institutet

Dept. of Physiology and Pharmacology, Karolinska Institutet

The vulnerability of the auditory system to acoustic injury can be modulated by glucocorticoids and glucocorticoid receptors (GR) (Tahera et al, 2006). The role of GR in spiral ganglion neurons (SGN) was found to be critical for the recovery of the auditory function after acoustic trauma. It is established that glucocorticoids can trigger protection or degeneration in different types of neurons depending on the dose and duration of the exposure. It is also known that downstream pathways and the regulation of sensitivity to glucocorticoids, as well as the final targets for GRs are tissue-specific. Here we study the GR pathway in SGN using mouse cochlear explants as an in vitro model. The GR agonist dexamethasone was used alone or in combination with an ototoxic neurotransmitter glutamate. The activation of several proteins (MAPK, TrkB, TrkC) involved in GR-mediated signaling in the cochlea was evaluated. The dynamics of GR activation in SGN in response to different durations and concentrations of dexamethasone was determined. The GR antagonist RU486 was used in the control experiment in combination with dexamethasone in order to confirm the specificity of the GR-mediated effects. The effect of the combined treatment of dexamethasone and glutamate on the activation of GR-mediated pathways, GR activation and glutamate-induced apoptotic processes in SGN was determined. These findings are important for defining the effects of steroid treatment on the auditory system and understanding the mechanisms responsible for stress effects on hearing.

Supported by Tysta Skolan and Karolinska Institute

417 The Development of the Innervation of the Ear with Altered Patterns of Neurotrophin Expression

Tian Yang¹, Bernd Fritzsch¹

¹University of Iowa

The spatial expression changes of *Bdnf* and *Ntf*3 (formerly Nt3) guide the targeted growth of cochlear innervation and support survival of properly grown fibers (Fritzsch et al. 2004. Prog Brain Res. 146: 265-78). The loss of either neurotrophin causes loss of subpopulations of the spiral and vestibular neurons: Ntf3 null mutants lose all spiral neurons in the basal turn resulting in an innervation of the base from neurons in the middle turn (Coppola et al. 2001. Development. 128(21): 4315-27) whereas loss of Bdnf diminishes the radial fiber density in the apex (Bianchi et al. 1996. Development 122(6): 1965-73). By studying the innervation of spiral sensory neurons in single or double mutants of Bdnf and Ntf3, we found haploinsufficiency of Bdnf on an Ntf3 null background expands the loss of spiral neurons, which suggests the two neurotrohpins are additive. Loss of either Ntf3 or Bdnf results in reduced radial fiber growth to the third row of outer hair cells. Combining Ntf3 null with Bdnf haploinsufficiency or vice versa reduces the growth to outer hair cells even further, implying a concentration effect. Replacing *Ntf3* expression with *Bdnf* (*Ntf3*^{kiBdnf/kiBdnf}), rescues not only the *Ntf3* null phenotype of basal spiral neuron loss but also results in rerouting of vestibular fibers to the cochlea (Tessarollo et al. 2004, J Neurosci. 24(10):2575-84) and a more profound fiber outgrowth to the third row of outer hair cells. We would like to propose that the amount of available neurotrophins will determine the radial fiber growth to the outer hair cells.

418 NMDA Receptors at the Inner Hair Cell – Spiral Ganglion Neuron Synapse in the Developing Auditory System

YingXin Zhang¹, Masayoshi Mishina², Dwight Bergles¹ ¹Johns Hopkins University, ²University of Tokyo

Synapses between inner hair cells (IHCs) and spiral ganglion neurons (SGNs) in the mammalian cochlea perform the crucial role of transforming IHC activity into action potentials in auditory nerve fibers (ANFs). At these ribbon synapses, glutamate is released in response to IHC depolarization, resulting in activation of ionotropic glutamate receptors in the postsynaptic membranes of ANFs. Although AMPA receptors provide sufficient current to elicit action potentials in ANFs, the involvement of NMDA receptors (NMDARs) in excitation is uncertain, despite anatomical evidence that NMDARs are expressed by SGNs. To determine if NMDARs are present at these synapses, we applied NMDA or D-aspartate to afferent terminals while recording from postsynaptic SGNs in cochleae isolated from postnatal prehearing rats. Both agonists induced robust firing of SGNs that was blocked by NMDAR antagonists, indicating that functional NMDARs are present in ANFs at this early stage of development. To determine if NMDARs contribute to excitation of ANFs in response to release of glutamate at synapses, we depolarized IHCs with local application of high K⁺ and monitored SGN activity using cell-attached patch recording. The majority of SGNs exhibited IHC-induced activity that was only blocked by co-administration of both AMPA and NMDA receptor antagonists, indicating that glutamate released from IHCs activates NMDARs in ANFs. NMDARs in central neurons are important for survival and morphogenesis, and enable activity-dependent changes in synaptic strength. To determine whether NMDARs contribute to the proper development of IHC-afferent synapses and maturation of SGNs, we deleted the obligatory NMDAR subunit NR1 from SGNs by crossing NR1 floxed mice with Pax2-Cre mice. Despite the absence of NMDARs, functional synapses were formed and SGNs exhibited spontaneous activity, indicating that NMDARs are not required for synapse formation or SGN survival at this age. Supported by DC008860 and DC009464.

419 Netrin-1 Mediated Axon Guidance in Mouse Embryonic Stem Cells Overexpressing Neurogenin-1

Gerhard Hill, III¹, Erin K. Purcell¹, J. Matthew Velkey², K. Sue O'Shea², Richard A. Altschuler¹, **R. Keith Duncan¹** ¹Kresge Hearing Research Institute, University of Michigan, ²Cell and Developmental Biology, University of Michigan

The overexpression of Neurogenin-1 (Neurog1) in mouse embryonic stem cells (mESCs) induces a functional neuronal phenotype with a glutamatergic neurochemical profile (Reyes et al., J Neurosci, 2008; Tong et al., AJP-Cell Physiol, 2010). Understanding the inherent properties of these mESC-derived neurons is critical in order to devise effective therapeutic strategies for treating sensory nerve loss. A major barrier to stem cell therapy in neurodegenerative disease is the challenge of guiding integration with host tissue. We sought to identify major axonal guidance cues present in the Neurog1-induced Microarray analysis indicated that Neurog1 neurons. upregulated several receptors for the diffusible axon guidance molecule Netrin-1, including DCC and NEO1. These data were confirmed by quantitative PCR, showing a 2-fold increase in NEO1 and a 36-fold increase in DCC in Neurog1-induced compared with control mESCs. Immunohistochemistry indicated that DCC was primarily expressed on TUJ1-positive cells, while NEO1 was expressed on TUJ1-positive and TUJ1-negative cells. Differential expression profiles could indicate different roles for Netrin-1 in these cell populations. As further support, we found that DCC was highly expressed in the soma and growth-cones of induced neurons, whereas NEO1 was primarily localized to the soma. Recombinant Netrin-1 bound to induced neurons, indicating that these receptors were expressed on the cell surface and suggesting that Netrin-1 may act as a guidance cue. Induced mESCs were co-cultured with aggregates of HEK293 cells stably transfected with Netrin-1. Axonal outgrowth was directed preferentially toward the Netrin-1 secreting aggregates, whereas outgrowth was unaffected by aggregates of control HEK293 cells. Our results indicate that DCC and NEO1 are downstream products of Neurog1 and may guide the integration of Neurog1-induced mESCs with target cells secreting Netrin-1. Supported by NIH T32 DC005356 and NIH P30 DC05188.

420 Lithium Alters Growth-Cone-Mediated Neurite Outgrowth from Adult Spiral Ganglion Neurons

Samit Shah¹, Albert Feng¹, Richard Kollmar² ¹University of Illinois at Urbana-Champaign, ²SUNY Downstate Medical Center

Neuronal growth cones play a vital role in regulating the rate and direction of neurite extension during development. However, molecular signaling cues that can stimulate and guide regeneration after injury in adult animals are not well understood. The Wnt signaling family is involved in growth-cone morphogenesis and axon pathfinding during development. To follow up on our recent finding that a

subset of the Frizzled receptors are expressed in adult spiral ganglion neurons, we investigated the effect of pharmacological modulators of the three Wnt signaling pathways on neurite outgrowth. We found that lithium chloride, an inhibitor of glycogen synthase kinase-3ß (GSK-3ß) and an activator of canonical Wnt signaling, produced alterations in growth cone morphology. Specifically, at a concentration of 2.5 mM and above, lithium chloride increased the area, width, and turning behavior of growth cones, whereas lower concentrations increased the circularity of growth cones. At the same time, primary neurites were significantly longer at 7.5 mM, but stunted at 12.5 mM lithium chloride. These changes were not accompanied by an accumulation of ß-catenin in the nucleus. Our results suggest that inhibition of GSK-3ß in adult spiral ganglion neurons directly affects cytoskeletal dynamics in the growth cone. We conclude that GSK-3ß may be a key target for modulating growth-cone-mediated neurite outgrowth and guidance from spiral ganglion neurons after injury to the adult cochlea.

421 High Content Analysis of Neurite Lengths in Cultures of Dissociated Spiral Ganglia

Donna S. Whitlon^{1,2}, Mary Grover¹, Michaela Lie¹ ¹Department of Otolaryngology, Feinberg School of Medicine, Northwestern University, ²Hugh Knowles Center, Northwestern University

Complicating the assessment of drugs, genes and factors that regulate neurite growth and regeneration in the cochlea, is the near impossibility of systematically testing thousands of different conditions in vivo. Prescreening of factors before in vivo testing is logical, but even in vitro, the analyses are time-consuming and must be limited. To provide increased screening efficiency on spiral ganglion neurons, we explored the use of High Content Analysis (HCA) for automated imaging and measurements of neurite lengths. Using our typical dissociated cultures of postnatal mouse spiral ganglia cultured with BMP4 or LIF, we tested the effect of the Rho kinase inhibitor H-1152 on neurite length. Neurons in fixed cultures were immunofluorescently labeled (anti-ßIII tubulin). Nuclear yellow visualized nuclei. Images were either manually acquired and measured with the software Metavue; or automatically acquired and measured with the Cellomics ArrayScan VTi and software. By hand, the longest neurite per neuron was measured. By HCA, total neurite length/neuron was calculated. The ArrayScan acquired sixteen 10X, non-overlapping fields per well, which were processed by the Neuronal Profiling Bio-application of the Cellomics software. Both hand measurements and HCA were similar. The rank order (longest to shortest) of population neurite lengths for each culture condition was: LIF+H-1152>LIF>BMP4+H-1152>BMP4. Hand photography and measurements of 917 neurites (4 conditions, three replicate experiments) took weeks; HCA of the neurites from 937 neurons took hours. Twelve cochleas can provide enough material for 144 cultures in a 384 well plate. These data demonstrate the efficiency and feasibility of using primary cultures of dissociated spiral

ganglia together with high content analysis for prescreening neurite growth promoting genes and drugs. (Supported by the Georgia Birtman Fund, Hugh Knowles Center, and Department of Otolaryngology, Northwestern University).

422 Osteoprotegerin Signaling During Postnatal Development of the Murine Cochlea: Implications for Survival and Differentiation of Spiral Ganglion Neurons

Shyan-Yuan Kao¹, Argryo Bizaki¹, Arthur G. Kristiansen¹, Michael J McKenna^{1,2}, Konstantina M. Stankovic^{1,2} ¹Massachusetts Eye and Ear Infirmary, ²Harvard Medical School

Osteoprotegerin (OPG), a member of the tumor necrosis factor ligand and receptor superfamily, is expressed in perilymph and cochlear soft tissues at exceptionally high levels. We have shown that mice lacking OPG have mixed conductive and sensorineural hearing loss. The conductive hearing loss is attributed to the pathologic remodeling and resorption of the middle ear ossicles. To gain insight into the mechanisms of sensorineural hearing loss, we have studied developmental expression of key members of the OPG signaling pathway in the postnatal murine cochlea using in situ hybridization, real-time quantitative RT-PCR, and immunoblot. In bone, OPG is known to act as a soluble neutralizing antagonist for receptor activator of nuclear factor kappa b ligand (RANKL), preventing it from binding to RANK on osteoblasts, thus inhibiting maturation and function of osteoclasts. In tumor cells, OPG has been show to bind TNF-related apoptosis-inducing ligand (TRAIL), preventing it from interacting with death receptor 5 (DR5) thus inhibiting apoptosis. We show that OPG, RANK, RANKL, TRAIL and DR5 are expressed in the cochlea in a developmentally controlled manner. Our results suggest that OPG regulates survival and differentiation of spiral ganglion neurons.

423 BDNF Alone Is Not Sufficient to Enlarge the Soma Area of Spiral Ganglion Neurons in Vitro

Felicia L. Smith¹, Robin L. Davis¹

¹Rutgers University

The action potential is transmitted through the cell body of bipolar spiral ganglion neurons and as a consequence soma size can impose limits on firing frequency and timing. Although this feature has been shown to vary with cochlear location, the factors involved in its regulation are not yet known. The focus of our study is to examine whether the same factors that regulate the electrophysiological firing patterns and synaptic protein levels can also regulate spiral ganglion somata size.

One of these factors, brain derived neurotrophic factor (BDNF), has been shown to not only profoundly affect the electrophysiological signature of spiral ganglion neurons (Adamson et al., *J. Neurosci.* 2002), but when infused into damaged cochleae increases their soma area (Leake et al., *Hear Res.* 2008; McGuinness et al., *Otol. Neurotol.*

2005). In order to determine whether BDNF has a direct or indirect effect on this parameter, we examined the soma area of spiral ganglion neurons in vitro. BDNF at a range of concentrations (1, 5, 10, 50 and 100 ng/ml) significantly enhanced neuronal survival yet had little or no effect on neuronal soma area. The soma area of apical neurons did not change after the application of BDNF at any concentration tested. Only basal neurons supplemented with 10 ng/ml of BDNF (326 \pm 17 μ m², n=3) compared to base control (268 ± 3 μ m², n=3; p<0.05) enhanced soma area, yet all other concentrations tested had no effect. Based upon our experiments evaluating spiral ganglion neurons isolated from their synaptic targets, we hypothesize that BDNF effects on soma area are indirect. Whether this is mediated through another cell type or co-factor remains to be requires a determined. Nevertheless, these observations indicate that BDNF affects spiral ganglion morphology differentially from the

424 The Transcriptional Response of Spiral Ganglion Neurons to Deafferentation Is Partially Ameliorated by Acute Electrical Stimulation

direct effect that it has on electrophysiological phenotype.

Supported by NIH NIDCD R01 DC-01856.

Jonathan Kopelovich¹, Erin Bailey², Alain Cagaanan², Stephen Butcher², Paul Abbas^{1,3}, John Manak², Steven Green^{1,2}

¹University of Iowa Department of Otolaryngology Head and Neck Surgery, ²University of Iowa Department of Biology, ³University of Iowa Department of Speech Pathology and Audiology

Hair cells are the primary but not sole source of trophic support to spiral ganglion neurons (SGNs) of the cochlea. In the absence of hair cells, SGNs have a tendency to apoptosis that may be mitigated by membrane depolarization and/or neurotrophins. A number of molecular and genetic mechanisms whereby membrane depolarization prevents apoptosis have been studied in our lab. The objective of the current study is to contextualize activity of neurotrophic and apoptotic pathways in the transcriptomes of SGNs of hearing and recently deafened rats and to investigate how activation of these pathways is altered by acute patterened electrical stimulation (ES) comparable to that provided by a cochlear implant (CI).

The rat model is ideal for this investigation because its genome has been sequenced, rat SGN apoptosis has been studied extensively in our lab, and it is anatomically suitable for studies of ES.

Gene expression microarrays were generated from spiral ganglia of P32 rats. Briefly, perinatally deafened rats were unilaterally implanted at P32 for 8 hours of acute ES (monopolar, biphasic, 100 Hz, amplitude 2x threshold). Microdissected spiral ganglia were split into apex and base. Contralateral cochleae were used as unstimulated operative controls. Age and litter-matched deafened and hearing controls were also assayed using expression arrays. RT-qPCR, western blot and in situ hybridization were used to follow up on genes of interest.

141

45 out of 544 genes that had significant (>2 fold) modulation after deafferentation were also reversed by electrical stimulation. Direct neurotrophin and apoptotic precursors were not significantly changed. Interestingly, deafferentation induced a decrease in transcription of calcium signaling mediators that was then reversed with ES.

425 Age-Related Changes in Myelin Basic Protein Expression and Glial Cell Numbers in the Human Auditory Nerve

Hainan Lang¹, Juhong Zhu¹, Quy Tran¹, Judy Dubno¹, Richard Schmiedt¹, John Mills¹, Bradley Schulte¹ ¹Medical University of SC

Glial cells are non-neural cells that provide support and nutrition, participate in signal transmission, and form myelin in the nervous system. The myelin sheath enclosing the auditory nerve axon has a unique multilamellar structure. The integrity of this compacted multilamellar structure plays an important role in determining the speed of transmission of action potentials. Myelin basic protein (MBP) is one of the most abundant proteins in the nervous system and is used as a key marker for myelin. The aims of the present study are: 1) to identify the pattern of MBP expression in the human auditory nerve and 2) to assess the effects of age on myelin and/or the number of glial cells in the inner ear. We examined 13 temporal bones from 10 subjects including 4 subjects aged 38-46 (two female and two male; middle-aged group) and 6 subjects aged 63-91 (two female and four male; older group). The temporal bones were removed and fixed by perilymphatic perfusion less than 6 hours after death. Each bone was decalcified, embedded in Paraplast X-TRA@ medium, and sectioned serially in the horizontal plane at a thickness of 6 µm. Every 10th or 20th section was stained with hematoxylin and eosin. Selected sections were immunoassayed with anti-MBP, antineurofilament 200 (NF200, neuronal marker), anti-class III β -Tubulin (TuJ1, neuronal marker), and anti-synaptophysin (unmyelinated fiber marker). Intense immunostaining of MBP was present throughout the auditory nerve including its peripheral component within the osseous spiral lamina and Rosenthal's canal and its central component within the modulus and internal auditory canal. MBP+ auditory fibers were present in both the middle-aged and older groups; however, marked losses and/or thinning of MBP+ fibers occurred in certain segments of the auditory nerve in the older ears. A marked decrease of NF200+ or TuJ1+ neuronal cells was also seen in older ears. Importantly, loss of glial cells occurred in the auditory nerve of 4 of 6 The glial phenotype was identified by older ears. morphological characteristics and glial cell markers. In the middle-aged group, MBP expression was absent around the perikarya of most spiral ganglion neurons, but was expressed around the cell bodies of about 7-10% of spiral ganglion neurons in the middle and basal turns. In the older group, no MBP expression was seen associated with the perikarya of the spiral ganglion neurons in any turn. The present study provides the first evidence that declines in MBP expression and reduced glial cell number occur in

the auditory nerve of older humans. Supported by NIH DC00422 (H.L., R.A.S., J.H.M. and J.R.D.); NIH DC00713 (B.A.S.)

426 Contribution of Merlin Inactivation by Phosphorylation to Spiral Ganglion Schwann Cell Responses to Deafening

Ju Hyoung Lee^{1,2}, Iram Ahmad¹, Isaac Sheffield¹, J. Jason Clark¹, Marlan Hansen¹

¹University of Iowa, ²Gachon University of Medicine and Science

Following deafening by hair cell loss and associated neural degeneration, spiral ganglion Schwann cells (SCs) dedifferentiate, proliferate, and provide support for possible axonal regrowth. The molecular mechanisms that initiate the response of SCs to loss of axonal contact are unclear. Merlin is the protein product of the neurofibromatosis 2 (NF2) tumor suppressor gene that mediates cell-cell contact information to regulate SC proliferation and survival. Merlin function is regulated by its conformation, adopting an inactive, growth permissive state following serine 518 (S518) phosphorylation. To explore the role of merlin in spiral ganglion SCs responses following deafening, we immunostained frozen sections from P32 rats deafened by kanamycin injection (P8-16) with an antiphospho S518 merlin (p-merlin) antibody. Deafening led to increased p-merlin immunolabeling in SCs of the osseous spiral lamina that have lost axonal contact, correlated with their re-entry into cell cycle, raising the possibility that merlin inactivation by phosphorylation facilitates SC proliferation following neural degeneration. To address the contribution of merlin inactivation to SC proliferation and eventual apoptosis following denervation, we performed sciatic nerve axotomies in P0Schdel(39-121) mice which express a mutant merlin isoform in SCs. P0Schdel(39-121) mice demonstrated a four-fold reduction in SC apoptosis following sciatic nerve sectioning compared with wild-type mice. We are now correlating the effects of merlin mutation on SC proliferation following denervation with kinase signaling. Taken together, these results raise the possibility that merlin inactivation by phosphorylation contributes to spiral ganglion SC responses to deafening, facilitating SC proliferation and survival.

427 Mouse Models for Auditory Nerve Regeneration in the Cochlea

Hideto Fukui¹, Seiji B. Shibata¹, Lisa A. Beyer¹, Yehoash Raphael¹

¹*KHRI, Dept. of Otolaryngology, University of Michigan* Recent technology has allowed inducing regeneration of auditory nerve fibers into deaf ears, as shown in the guinea pig model. Such regeneration is important for enhancing the function of the cochlear implant and for augmenting future therapies such as hair cell regeneration and stem cell transplantation. To benefit from the powerful molecular tools available for mice, it is necessary to create a mouse model for auditory nerve regeneration. As a first step, it is essential to have a model where inner hair cells and auditory nerve fibers are absent. This can be done either by inducing their degeneration, or by using a

ARO Abstracts

mutation in which these cells either fail to develop or die early in life. We have explored these possibilities using neomycin-induced pathology and Brn-3.1 mutants. In the neomycin model, CD1 mice were infused with 1µl of 10% neomycin into the scala media endolymph via cochleostomy and examined at 1 or 2 weeks after the insult. Ears of Brn-3.1 mutant mice were examined at ages 3 or 6 months postnatal age. For both models, whole-mounts of auditory tissue were stained for F-actin, Myosin VIIa and neurofilament. We determined that the neomycin eliminates all hair cells and alters supporting cell morphology. Also, no nerve fibers were present in the auditory epithelium. Ears of Brn-3.1 mutant mice at 3 and 6 months of age also were found to have no hair cells. At the 3 months time point, patches of supporting cells resembled a sheet of polymorphic flat cells similar to the flat epithelium described in guinea pigs. Most nerve fibers were absent. More complete degeneration of non-sensory epithelial cells was seen at 6 months. These results show that both neomycin and Brn-3.1 models are useful for studies of different degenerative changes in the auditory epithelium, and for testing methods of regenerating nerve fibers in the deaf ear.

428 Development of Stem Cell Therapy to Replace Lost Spiral Ganglion Neurons

Jianxin Bao¹, **Aizhen Yang**¹, Zhaoyu Lin¹, Yongmin Wang¹ ¹Washington University

Spiral ganglion neurons (SGNs) play an important role in carrying auditory signals from inner ear to brainstem. In mammals, SGN loss is one of the major causes underlying permanent hearing loss, and this neuronal loss is irreversible. Stem cell therapy is one of possible clinical methods to treat permanent hearing loss due to SGN loss. Although previous work shows that SGN-like neurons can be derived from several types of stem cells and they can survive in vivo, there still are two major roadblocks before their possible clinical applications: (1) whether transplanted neurons can send their axons and make functional connections with neurons inside of brainstem; and (2) how transplanted neurons can avoid possible host immunorejection. Recent work shows that the issue of immunorejection can be avoided by using patient specific induced pluripotent stem (iPS) cells. To address the first issue, we have established mouse-strain specific iPS cell lines from YFP-SGNs transgenic mice under C57BL/6J genetic background. These iPS cells were induced neural stem cells. The neural stem cells were then injected into the spiral ganglion nerve of C57BL/6J mice. Our result showed that the transplanted cells were YFP positive, and could survive in vivo for at least over two months. Most importantly, their axons were observed in brainstem one month after transplant. Thus our work suggests that it is feasible to derive and transplant SGN-like neurons from iPS cells, and these neurons can send their axons to the brainstem. Futher functional studies will determine whether these neurons can carry auditory information from inner ear to brainstem.

429 Single Neuron Recordings from Unanesthetized Mouse Dorsal Cochlear Nucleus

Wei-Li Ma¹, Stephan Brenowitz¹ ¹NIH

The goal of this study was to characterize the range of basic sound-evoked responses in single neurons of the unanesthetized mouse DCN. To accomplish this, we developed a decerebrate preparation similar to that used in cat and gerbil. We recorded response maps, rate-level functions in response to best frequency (BF) tones and broadband noise (BBN), and peri-stimulus time histogram (PSTH) data. Neurons producing complex spikes were distinguished as cartwheel cells and other neurons were classified according to the response map scheme. The most commonly observed response map was type III. In classical type III responses, described in cat both and gerbil, neurons exhibit similar saturating firing rates in response to BBN and BF tones. However, in mouse some neurons had noise responses that either exceeded the saturation level of the BF-tone response or showed a much weaker response. Similar to results in gerbil, we rarely observed type II responses, which have been attributed to tuberculoventral neurons. Consistent with this observation, there was less evidence for inhibitory regions in the response maps of putative DCN principal neurons. These findings contrast with observations in cat DCN. Our data are put into context with what is already known about DCN and future directions are discussed.

430 Type IV Neurons in Dorsal Cochlear Nucleus of Anesthetized Rats

Yang Li¹, Tessa-Jonne Ropp¹, Eric Young¹ ¹Johns Hopkins University

The dorsal cochlear nucleus (DCN) is part of the first primary nucleus in the central auditory pathway. The principle neurons in DCN fire in a non-linear fashion, which is attributed to the inhibitory interaction within the DCN circuit. This, along with its specific intermediate position in both auditory and non-auditory pathways, makes DCN an important structure in normal and abnormal processing of sound localization, attention modulation, tinnitus, etc.

DCN responses to sound are classified according to the distribution of excitatory or inhibitory responses in the frequency x intensity space. Principle neurons give type III and type IV responses, which differ in the strength of inhibition at best frequency (BF). These two types of neurons are believed to be morphologically identical with different response properties because of different strengths of inhibitory input. Previously type IV neurons have been reported to be uncommon in rodents (gerbil, chinchilla and guinea pig), although ~33% of the neurons in decerebrate cat DCN are type IV. Because of the importance of rodent preparations in current auditory research, it is important to clarify these apparent differences.

Here we report that robust type IV neurons with properties similar to those in cat are observed in the rat DCN under light ketamine anesthesia. Extracellular single-neuron activity is collected with tungsten microelectrodes. We study tuning with tone response mapping and rate-level functions. We also test the neurons' non-linearity with the random shape spectral (RSS) stimulus developed in our previous studies. Our data shows both type III and type IV activity exist in this preparation. Type IV neurons exhibit significant inhibitory activity at high sound level as well as non-linearity. As an ongoing study, we are collecting data from both normal animals and those with hearing impairment. We will compare the spontaneous activity and cross-neuron synchrony of firing between normal and pathological subjects.

Supported by NIDCD grant RC1DC10594.

431 Unipolar Brush Cells Express DCX in Dorsal Cochlear Nucleus, Paraflocculus and Flocculus of Adult Rat

Senthilvelan Manohar¹, Sarah Hayes¹, Nicholas Paolone¹, Richard J. Salvi¹, Joan S. Baizer¹ ¹University at Buffalo

Adult neurogenesis is now a well-established phenomenon for granule cells of the dentate gyrus of the hippocampus and the subventricular zone (SVZ), the source of new cells that migrate to the olfactory bulb. However, some preliminary studies suggest that limited neurogenesis may also occur in the brainstem and cerebellum. To investigate this possibility, we used immunoreactivity for doublecortin (DCX) to identify immature neurons. We discovered many DCX-labeled cells in the granule cell layers of three circumscribed regions, the dorsal cochlear nucleus (DCN) and adjacent regions of the cerebellum in the flocculus (FL) and a small region of the ventral paraflocculus (PFL). DCX-labeled cells had the morphological appearance of unipolar brush cells (UBCs) with an oval cell body and a single dendrite ending in a "brush". Double-label immunofluorescence showed colocalization of DCX with calretinin (CR) or with epidermal growth factor substrate 8 (Eps8), two well-known markers for unipolar brush cells. There was no colocalization of DCX with GFAP ruling out the possibility that the DCX-labeled cells were glia. These data suggest the possibility of adult unipolar brush cells proliferation in the DCN, PFL and FL. These DCX-positive neurons may participate in neuroplastic processes (e.g., localization, tinnitus) in the auditory or vestibular system (e.g., vestibular compensation). Supported by NIH grants (R01DC0090910; R01DC009219-01)

432 Cholinergic Modulation of Neurons and Synapses in the Dorsal Cochlear Nucleus

Philip Tipton¹, Stephan Brenowitz¹

¹National Institute on Deafness and Other Communication Disorders

Descending cholinergic projections from the superior olivary complex (SOC) to the cochlea have important and well-characterized roles in protecting the cochlea from noise exposure and enhancing signal detection in noisy environments. However, the role of cholinergic input to the dorsal cochlear nucleus (DCN) is not yet understood. We have begun to investigate the responses of specific types of neurons in the mouse DCN to agonists and antagonists of both muscarinic and nicotinic acetylcholine receptors (mAchRs and nAchRs, respectively). Cholinergic input to the cochlear nucleus originates in two brain regions. Medial olivocochlear (MOC) neurons project to the cochlea send axon collaterals that terminate and also predominantly in the granule cell domain of the cochlear nucleus. An additional population of neurons in the ventral nucleus of the trapezoid body (VNTB) projects directly to Previous anatomical the cochlear nucleus. and electrophysiological studies have shown that both mAchRs and nAchRs are present in the DCN and enhance spontaneous firing in DCN neurons. Our data indicate strong excitatory effects of Gailo-coupled mAchRs, on DCN granule cells, generating high levels of spontaneous excitatory postsynaptic currents in their postsynaptic cartwheel cell and fusiform cell targets. Cartwheel cells also exhibit excitatory responses to both mAchR and nAchR activation. Current experiments are addressing the cholinergic responses of fusiform cells, as well as attempting to define the cellular mechanisms activated by mAchR and nAchR activation both preand postsynaptically. Our findings demonstrate diverse effects of acetylcholine in the DCN. By determining the neurons targeted by acetylcholine in the DCN and the cellular mechanisms engaged by activation of their cholinergic receptors, our studies will contribute to understanding the role of descending cholinergic efferents in auditory function.

433 Spontaneous Firing of Cartwheel Cells in the Dorsal Cochlear Nucleus Evokes Endocannabinoid Release and Retrograde Suppression of Parallel Fiber Synapses

Miloslav Sedlacek¹, Stephan Brenowitz¹

¹National Institute on Deafness and Other Communication Disorders

Endocannabinoids act as retrograde messengers that are released from postsynaptic neurons and regulate synaptic strength over short and long time scales. Neuronal depolarization can evoke global endocannabinoid release throughout a neuron's dendritic arbor by a mechanism that relies on elevation of postsynaptic calcium. Here, we activity-dependent short-term investigated plasticity mediated by endocannabinoids at the synapse formed between parallel fibers and cartwheel cells (CWCs) in the dorsal cochlear nucleus (DCN) of the mouse. Depolarization evokes release of endocannabinoids from voltage clamped CWCs, causing suppression of PF inputs that lasts tens of seconds. However, dendritic calcium levels accompanying these voltage steps exceeded 5 microM and may not be reached under physiological conditions. Therefore, we examined dendritic calcium signals in CWCs and the resulting suppression of PF synapses that occur during more realistic firing patterns, using patch clamp recordings from mouse brain slices and two-photon calcium imaging. CWCs are spontaneously active neurons that fire both simple and complex spikes. During spike trains, dendritic calcium reached a concentration plateau in the low micromolar range. These spike trains suppressed PF inputs by 50-90% and this suppression required the activation of CB1 receptors.

Thus, prolonged but modest elevation of dendritic calcium in CWCs evokes endocannabinoid release that regulates the strength of PF synapses. These findings indicate that endocannabinoid signaling may occur under physiological conditions and thereby influence the output of the DCN.

434 Zinc Receptor-Mediated Modulation of Glutamate Release Via Endocannabinoid Signaling

Tamara Perez-Rosello¹, Natan Arotsker², Michal Hershfinkel², Elias Aizenman^{2,3}, Thanos Tzounopoulos^{1,3} ¹Department of Otolaryngology, University of Pittsburgh, ²Department of Morphology, Ben Gurion University, ³Department of Neurobiology, University of Pittsburgh School of Medicine

Anatomical studies have revealed that glutamatergic terminals of parallel fibers (PF) projecting to fusiform cells (FC) in the dorsal cochlear nucleus (DCN) contain high levels of vesicular zinc. Yet, the role of synaptically released zinc in the DCN has not been explored. We found that exogenous $Zn^{2^{+}}$ (50-200 $\mu M)$ depressed basal eEPSCs amplitudes (29 \pm 1.4%; n=7; p<0.05) in FCs. Zn²⁺ induced a reduction in release probability from PF terminals since the $1/CV^2$ decreased to $45 \pm 1\%$ of control eEPSCs (n=6; p<0.05). As endocannabinoids (ECs) induce similar effects at PF to FC synapses, we tested whether Zn²⁺ influenced this signaling system. Incubation of slices with AM251 (1 µM), an antagonist of cannabinoid receptors (CB1Rs), completely prevented the Zn^{2^+} -mediated decrease of EPSCs. A Zn^{2^+} -sensing receptor (ZnR/GPR39) has recently been described, and shown to be present in vesicular zinc-rich regions of the hippocampus. We observed strong immunofluorescent labeling of GPR39 in the DCN, primarily as punctuate staining at the periphery of FCs. ZnR/GPR39 is a $G_{\alpha/11}$ receptor coupled to phospholipase C (PLC) activity, which could be responsible for EC production. Indeed, both YM-254890 (1µM), a specific $G_{\alpha q}$ protein inhibitor, and U73122 (5 μ M) a PLC inhibitor, effectively blocked the Zn²⁺mediated effects on eEPSCs in FCs. In hippocampal CA1 pyramidal cells we also noted that exogenous Zn²⁺ could inhibit eIPSCs (28 \pm 1 %, n=6; p<0.05) in response to stimulation from CB1R-positive terminals but not from CB1R-negative terminals. We thus propose that Zn²⁺ activation of ZnR/GPR39 can activate widespread EC signaling, thereby affecting synaptic transmission in the brain. This work was supported by NHI-NIDCD Grant RO1 DC-007905 to T. Tzounopoulos.

435 Early Development and Mature Organization and Function of the Cochlear Nucleus Is Modulated by Pax6 Expression Kathleen Yee¹

¹Tufts University School of Medicine

Developmental gene expression studies provide insights into factors that regulate the organization and function of the cochlear nucleus (CN). We have previously reported that the paired homeodomain transcription factor, Pax6, is expressed in the developing cochlear nucleus. Pax6 is detectable in the ventral subdomain at embryonic day 16.5 and in the molecular/granule cell layer and portions of the dorsal CN as early as postnatal day (P)0.

Examination of P0 Pax6 -/- mice revealed that the cellular organization of the CN is perturbed and the expression domain of Math5 (ATOH7), a molecular marker for the ventral cochlear nucleus (VCN) [Saul et al., 2008], is reduced in volume compared to wild type. We have identified erbB4 as another marker expressed in specific CN subdomains. ErbB4 is expressed in the molecular/granule cell layer and in cells positioned around and within the VCN core. In P0 Pax6 -/- mice, expression levels of erbB4 mRNA are comparable to wild type littermates, but only scattered cells are evident at the periphery of the VCN core and few, if any, erbB4-positive cells are distributed within the core region.

Since Pax6 -/- mice are not viable after birth, we have examined Pax6 loss-of-function in heterozygous adult mice. Small to mid-size cell bodies positioned in the lamina below the molecular layer are well delineated by immunolocalization of glutamic acid decarboxylase (GAD)65 and GAD67 in wild type mice. In contrast, Pax6 heterozygous mice lack prominently labeled GAD65 and GAD67-positive cell bodies and show increased broad diffuse terminal labeling in the CN. Physiologically, the auditory brainstem response amplitudes of wave 2 are increased at high frequencies in Pax6 +/- compared to Pax6 +/+ mice. Together, these data support a role for Pax6 in the early formation of the CN and in the mature animal. Altered distributions of GAD may contribute to decreased inhibition resulting in increased auditory brainstem responses.

436 Reciprocal Connectivity Between the Central Nucleus of the Inferior Colliculus and the Dorsal Cochlear Nucleus of the CBA/CaJ Mouse

Michael A. Muniak¹, **Vikas N. Kodali¹**, Makoto Tanigawa¹, Catherine J. Connelly¹, Kristyna Hnizda¹, Nadia F. McMillan¹, Tan Pongstaporn², David K. Ryugo^{1,2} ¹Johns Hopkins University, ²Garvan Institute of Medical Research

Recent observations suggest that descending projections in the brain outnumber ascending ones (Winer and LaRue, 1987; Jones, 2000), but few reports have been published that describe the synaptic organization of these projections. Descending pathways are an essential element of sensory systems, and may facilitate the realtime modification of neural responses to external stimuli at any stage from periphery to cortex. In the auditory system, the cochlear nucleus (CN) is key because it initiates all ascending pathways, including a direct contralateral projection to the inferior colliculus (IC). Studies of descending projections in rat and guinea pig suggest that colliculo-cochlear nucleus projections originating in the central nucleus of the IC (CNIC) terminate bilaterally and topographically in the dorsal CN (DCN, Caicedo and Herbert, 1993; Malmierca et al., 1996). We have confirmed this projection in the CBA/CaJ mouse by using multiunit recordings and dye injections in the CNIC. The

frequency of the IC injection site matches the frequency location in the DCN as determined by a 3-D frequency atlas created for the mouse CN (Muniak et al., 2011). Moreover, by applying anterograde (dextran amines) and retrograde (beta subunit of cholera toxin) tracer injections in CNIC, we were able to demonstrate that anterogradely labeled descending projections form bouton contacts in close proximity to retrogradely labeled cells in the contralateral DCN. This relationship suggests that the descending pathway from CNIC terminates on the same DCN neurons from which the ascending projections originate. If such synaptic connectivity is verified using electron microscopy, it would provide a direct pathway for modulating ascending auditory information, and could be involved in "egocentric feedback" enhancing signal discrimination and/or underlying selective attention. Supported by NIH/NIDCD grant DC004395 and a LSRA

437 Long Term Effects of Somatosensory Inputs on Neuronal Discharges in the Dorsal Cochlear Nucleus of Normal and Noise-Exposed Guinea Pigs

from New South Wales, AU.

Susanne Dehmel¹, Shashwati Pradhan¹, Malav Parikh¹, Kevin Anderson¹, Susan Shore^{1,2}

¹Kresge Hearing Research Institute, Department of Otolaryngology, University of Michigan, ²Department of Molecular and Integrative Physiology, University of Michigan

In addition to auditory inputs, the dorsal cochlear nucleus (DCN) receives somatosensory inputs from the head, face, neck, upper body and limbs, which are transmitted via the parallel fiber system to synapse on fusiform and cartwheel cells (Itoh et al., Brain Res, 1987; Zhou and Shore, J Neurosci Res, 2004; Haenggeli et al., J Comp Neurol, 2005). Long term synaptic plasticity of parallel fiber synapses has been shown to influence the discharges of DCN fusiform and cartwheel cells in vitro (Tzounopoulos et. al, Nature Neurosci, 2004). We previoulsy showed that damage to the auditory input pathway leads to modifications of somatosensory inputs and their effects in the DCN (Shore et al., Eur J Neurosci, 2008; Zeng et al., J Neurosci, 2009). Here we studied the duration of the somatosensory modulation of acoustically evoked discharges in DCN neurons in vivo in normal- and animals over-exposed with a narrow band noise. The noise exposure resulted in a temporary threshold shift in ABRs and extracellulary recorded neuronal thresholds but a persistent increase in spontaneous and sound-evoked firing rates and increased steepness of rate-level functions. As shown previously for normal animals, paired stimulation of somatosensory and auditory pathways lead to suppression or enhancement of acoustically-evoked discharges with dominating suppression that progressively increased for up to an hour after the bimodal stimulation (Shore, Eur J Neurosci, 2005; Pradhan et al., ARO abstract. 2010). Noise exposure resulted in а strengthening of the long-term suppressing and enhancing effects and an enlargement of the subpopulation of units showing enhancing effects of the somatosensory inputs. It is hypothesized that damage to the auditory nerve triggers compensatory changes in the somatosensory inputs and that long-lasting changes in synaptic plasticity might be one underlying mechanism for tinnitus generation.

Supported by NHI RO1 DC004825, NHI P30 05188, and the Tinnitus Research Consortium.

438 Somatosensory-Induced Changes in Neural Synchrony in Dorsal Cochlear Nucleus

Seth Koehler^{1,2}, Susan Shore^{1,3}

¹Dept. of Otolaryngology, University of Michigan,

²Biomedical Engineering, University of Michigan, ³Dept. of Molecular and Integrative Physiology

The dorsal cochlear nucleus (DCN) is the first site in the brain where tinnitus is generated, as suggested by the increased spontaneous rates that correlate with tinnitus. Neural synchrony, another correlate of tinnitus identified in auditory cortex (Seki and Eggermont 2003), has recently been shown to increase in DCN following an acoustic trauma known to induce tinnitus (O'Donohue 2010). Since somatic manipulations can modulate tinnitus. а multisensory mechanism must be involved in its process. The DCN is known to be a site of multisensory integration, receiving somatosensory input from the trigeminal system. Stimulation of spinal trigeminal nucleus (Sp5) can modulate both the rate and spike timing of responses to sound and thus may also induce changes in neural synchrony. Repeated somatosensory stimulation can suppress subsequent spontaneous activity for short time periods, up to 10 minutes (Zhang and Guan 2008)while pairing of Sp5 and sound stimulation can alter the firing rate of the subsequent neural response for much longer times, up to 50 minutes (Pradhan 2010). In this study, we evaluated the long-term influence of paired auditory and Sp5 stimulation on neural synchrony in DCN. Multichannel recordings of spontaneous and continuous soundevoked spike activity were recorded before and after paired Sp5 and auditory stimuli. Synchrony between pairs of neurons was measured with cross-correlations and synchrony between groups of three to five neurons was measured using a frequent episode mining algorithm (Diekman, Sastry et al. 2009). Preliminary results suggest that synchrony within a subset of neurons is significantly altered after paired Sp5 and auditory stimulation, suggesting a putative role in the modulation of tinnitus. Supported by NIH RO1 DC004825, NIH P30 05188, T32 DC00011 (SDK), and the Tinnitus Research Consortium.

439 Physiological Activation of Muscarinic AChRs Controls Associative Synaptic Plasticity Via Modulation of Endocannabinoid Signaling

Yanjun Zhao¹, Thanos Tzounopoulos^{1,2}

¹Department of Otolaryngology, University of Pittsburgh, ²Department of Neurobiology, University of Pittsburgh School of Medicine

Cholinergic and endocannabinoid signaling represent two major neuromodulatory pathways in the brain. However,

ARO Abstracts

the mechanistic interaction of these neuromodulators in shaping long-term synaptic plasticity has not been addressed. The dorsal cochlear nucleus (DCN) is a good site to study this interaction as it receives robust cholinergic input and its circuit exhibits endocannabinoidmediated long-term synaptic plasticity. Previous studies have shown that DCN fusiform cells (FC) exhibit Hebbian spike-timing dependent plasticity (STDP) (Tzounopoulos at al., 2004, 2007). In this study, we reveal anti-Hebbian LTD in FCs, when muscarinic acetylcholine receptors (mAChRs) were either synaptically or pharmalogically activated. MAChR-mediated LTD was converted to LTP when applying CB1 receptor antagonist AM251, indicating that conversion of Hebbian LTP to anti-Hebbian LTD requires the activation of endocannabinoid signaling. Anti-Hebbian LTD was blocked by intracellular application of GDPbS (G protein blocker). LTD was also blocked when slices were incubated with U73122, an inhibitor of phospholipase C (PLC). Therefore, these data indicate that mAChR-mediated enhancement of endocannabionid release mediates the conversion of Hebbian LTP to anti-Hebbian LTD. In addition, anti-Hebbian LTD was also blocked by the NMDA receptor antagonist APV, APV has been also shown to block Hebbian-LTP (Tzounopoulos et al., 2007), suggesting that activation of NMDA receptors is required for both LTP and LTD. Together, our findings suggest that the interaction between the cholinergic and endocannabinoid signaling may provide a general mechanism for dynamic, context-dependent modulation of associative synaptic plasticity in the brain. This work was supported by NIH-NIDCD Grant R01 DC-007905 to T. Tzounopoulos.

440 Distribution of Inhibitory Axosomatic Synapses in the Inferior Colliculus

Jennifer Chikar¹, Megan Miller¹, Douglas Oliver¹ ¹University of Connecticut Health Center

Axosomatic synapses may influence firing patterns by their proximity to the action potential initiation site of the neuron. Thus, determining the distribution and interaction of excitatory and inhibitory synapses on the cell body is important for a complete understanding of signal In the inferior colliculus (IC), we have processing. previously found that large GABAergic neurons within the IC receive a high density of excitatory axosomatic Here we describe the distribution of the synapses. inhibitory axosomatic synapses in the IC of the rat. We used immunohistochemistry against the glycine reuptake transporter 2 (GLYT2), which is selectively located in the presynaptic terminals of glycinergic synapses, and glutamic acid decarboxylase 67 (GAD67) which labels GABAergic presynaptic terminals as well as cell bodies. We found little anatomical evidence of co-localization of GLYT2 and GAD67 terminals within the IC. We found that GAD67 axosomatic terminals are more prevalent than GLYT2 axosomatic terminals. The density of GLYT2 and GAD67 axosomatic terminals varies with both cell type and cell size. Large GABAergic neurons (perimeter >60µm) have a low density of GLYT2 terminals. Large glutamatergic neurons, in contrast, show a high density of

GLYT2 terminals. This density is higher than that seen in either GABAergic or glutamatergic small neurons. The distribution of GAD67 axosomatic terminals may follow these same trends. These data suggest that the distribution of glycine and GABA synapses on the cell body may play different roles for different cell types in the IC. In particular, large glutamatergic neurons may be heavily regulated by glycinergic axosomatic inputs.

441 GABAergic Projections in the Auditory Tectothalamic System in the Guinea Pig

Jeffrey Mellott¹, Susan Motts¹, Brett Schofield¹ ¹Northeastern Ohio Univ. Coll. Med.

GABAergic cells form a substantial part of the projection from the inferior colliculus (IC) to the medial geniculate body (MG) in cats and rats. We combined retrograde tracing with immunohistochemistry to determine the extent to which GABAergic cells contribute to this pathway in guinea pigs. We injected Fast Blue, FluoroGold or red fluorescent microspheres into the MG to label tectothalamic cells. Injections were large and involved all MG subdivisions. We then stained the IC with anti-glutamic acid decarboxylase (GAD) to identify GABAergic cells. We quantified tracer- and immuno-labeled cells in the IC ipsilateral and contralateral to the MG injection. Preliminary analysis is based on >27,000 tracer-labeled cells.

In the ipsilateral IC, GAD-immunoreactive (GAD+) cells made up, on average, 12% of the tracer-labeled cells in the central nucleus; 18% of tracer-labeled cells in the dorsal cortex and 17% of the tracer-labeled cells in the external cortex. These percentages are lower than those reported for cat (20-30%) or rat (20-50%), but still represent a substantial number of cells.

An IC projection to the contralateral MG is described in numerous species but is often considered minor. We counted cells in both ICs in two experiments and found 5.226 contralaterally projecting cells and 23,201 ipsilaterally projecting cells. Thus, the contralateral projection is about 18% of the size of the ipsilateral projection. A GABAergic component of the contralateral projection has been described only in cats. In our experiments, the contralateral projection contained a significant number of GAD+ cells, comprising, on average, ~12% of the tracer-labeled cells in each IC subdivision. We conclude that GABAergic cells in the IC of guinea pigs contribute substantially to both ipsilateral and contralateral projections to the auditory thalamus. Supported by NIH DC04391.

442 Descending Projections from the Auditory Cortex Contact GABAergic Cells in the Ipsilateral Inferior Colliculus That Could Cause Inhibition in Both Inferior Colliculi Kyle Nakamoto¹, Brett Schofield¹

¹Northeastern Ohio Univ. Coll. Med.

Unilateral stimulation of the auditory cortex (AC) elicits inhibition bilaterally in the central nucleus of the inferior colliculi (ICc). The cortico-collicular pathway is excitatory and sends projections predominantly to the ipsilateral IC. It has been assumed that AC axons contact GABAergic IC cells in the IC dorsal cortex or external cortex that then project to the central nucleus on each side. However, many questions remain about the locations and projections of the GABAergic cells; in fact, cortical contacts onto GABAergic cells have not been identified anatomically in any IC subdivision.

We injected an anterograde tracer into the left AC to label cortico-collicular axons and a retrograde tracer into the right IC to label commissural projections to the right IC in guinea pigs. We labeled GABAergic cells with immunohistochemistry for glutamic acid decarboxylase (GAD). We then examined the left IC for apparent contacts between cortical boutons and GAD positive (GAD+) cells. Contacts on GAD+ cell bodies and dendrites were found in all subdivisions of the IC, but were less common in the ICc. In all subdivisions, some of the cortically-contacted GAD+ cells were labeled by the retrograde tracer, identifying them as commissural cells.

We conclude that AC axons contact GABAergic cells in all subdivisions of the ipsilateral IC. Local axons of these cells could provide for cortically-driven inhibition throughout the ipsilateral IC. In addition, some of the cortically-contacted, GAD+ cells project to the contralateral IC. These cells could provide for cortically driven inhibition throughout the contralateral IC. Overall, the massive projection from the AC to the ipsilateral IC could elicit inhibition bilaterally via local and commissural IC connections. Supported by NIH DC04391 and DC010958.

443 The Role of the Interplay of Excitation and Inhibition in the Temporal Precision and Adaptation to Different Stimulus Contexts in the Inferior Colliculus

Nadja Schinkel-Bielefeld¹, Mai El-Zonkoly¹, Nicholas Lesica², Benedikt Grothe³, Daniel Butts¹ ¹NeuroTheory Lab, Department of Biology, University of Maryland, ²Ear Institute, University College London, ³Division of Neurobiology, Department Biology II, Ludwig-

Maximilians-Universität München Neuronal processing in the auditory system has been shown to change in different stimulus contexts. For example, the linear receptive field of inferior colliculus (IC) neurons in the gerbil can change in the context of background noise. Such adaptation can be shown to be advantageous to stimulus processing, but how the neuron computes these changes is hard to infer from the linear receptive field alone.

Here, we use a General Nonlinear Modeling (GNM) approach to describe the receptive fields of IC neurons in the context of temporally modulated narrow band stimuli that reproduce the temporal characteristics of vocalizations. For a characterization of separate excitatory and inhibitory inputs, typically intracellular recordings are necessary. However, the GNM employs efficient maximum likelihood estimation techniques applied to extracellular data, and can separate the influences of excitatory and inhibitory receptive fields.

The GNM generally finds excitation and inhibition of similar tuning, but a delay between excitation and inhibition. It

performs significantly better than linear models, based on cross-validated vocalization stimuli with and especially without ambient noise. Furthermore, the GNM suggests an underlying source for the "adaptive" changes observed in the context of linear models in the presence of background noise. We see that such changes do not arise from different temporal tuning of excitation and inhibition as suggested by the linear receptive field, but rather changes in their relative strength. Because the temporal processing of excitation and inhibition is temporally offset, changing their relative response has effects on the overall temporal processing of the neuron, reflected in the change in the time kernels of linear models.

Thus, considering the interplay of excitation and inhibition provides a more accurate description of the computation underlying IC neuron responses, and provides insight into their adaptation in different stimulus contexts.

444 Differential Roles of GABAergic and Glycinergic Input on FM Selectivity in the Inferior Colliculus of the Pallid Bat

Anthony Williams¹, Zoltan Fuzessery¹

¹University of Wyoming

Multiple mechanisms have been shown to shape FM selectivity within the pallid bat IC. Here we focus on the mechanisms associated with sideband inhibition. The relative arrival time of inhibition as compared to excitation can be used to predict FM responses as measured using a two-tone inhibition paradigm. An early-arriving, lowfrequency inhibition (LFI) prevents responses to upward sweeps, and thus shapes direction selectivity. A latearriving, high-frequency inhibition (HFI) suppresses slow FM sweeps and thus shapes rate selectivity for downward sweeps. Iontophoretic application of gabazine (GBZ) to block GABA receptors or strychnine (STRYCH) to block glycine receptors was used to assess the effects of removal of inhibition on each form of FM selectivity. GBZ and STRYCH had a similar effect on FM direction selectivity, reducing selectivity in 65-75% of neurons tested. FM rate selectivity was more resistant to receptor blockade, with less that 25% of neurons affected. In addition, only STRYCH could eliminate FM rate selectivity while GBZ alone was ineffective. The effect of drug application on elimination of FM selectivity was directly correlated with a loss of the respective inhibitory sideband that shapes that form of selectivity. The elimination of LFI correlated to a loss of FM direction selectivity while elimination of HFI correlated to a loss of FM rate selectivity. In neurons where LFI remained intact, FM direction selectivity was also unaffected. Similarly, in neurons where HFI remained intact, FM rate selectivity was unaffected. Results indicate 1) while most FM direction selectivity is created within the IC, most rate selectivity may be inherited from lower levels of the auditory system, 2) a loss of LFI corresponds to a loss of FM direction selectivity and is created through either GABAergic or glycinergic input, and 3) a loss of HFI corresponds to a loss of FM rate selectivity and is created mainly through glycinergic input.

[445] Inhibition Shapes Neuronal Selectivity to Vocalizations in the Inferior Colliculus of the Awake Mouse

Zachary Mayko¹, Patrick Roberts², Christine Portfors¹ ¹Washington State University, ²Oregon Health & Science University

Neurons inferior colliculus the (IC) display in species-specific heterogeneous responses to vocalizations. When presented with a broad range of individual vocalizations, some neurons show highly selective responses to a few vocalizations whereas other neurons respond to the majority of vocalizations (low selectivity). One potential mechanism to explain the heterogeneous responses of IC neurons to vocalizations is inhibition. It is well known that inhibition is important in shaping how IC neurons respond to various sound features and there is evidence in bats that inhibition is important in creating selectivity to vocalizations. In this study, we examined the role inhibition plays in shaping selectivity to vocalizations in the IC of awake CBA/CaJ mice. We compared single cell responses in the IC to pure tones and a variety of different ultrasonic mouse vocalizations before and after iontophoretic application of bicuculline and strychnine. Blocking inhibition in the IC broadened neuronal excitatory frequency tuning curves, decreased thresholds and increased spike rates to pure tone stimuli. In addition, blocking inhibition increased the number of vocalizations that evoked a response from a neuron (decreased selectivity). This decreased selectivity created less heterogeneity in the population of IC neurons that responded to vocalizations. These results show that inhibition is important for shaping responses to behaviorally relevant sounds, and also for creating the diversity of responses to vocalizations seen in the IC.

446 The Effect of Acoustic Stimulation During the Sensitive Period of Development on the Response Properties of Inferior Colliculus Neurons in the Rat

Zbynek Bures^{1,2}, Jolana Grecova¹, Tetyana Chumak¹, Jiri Popelar¹, Josef Syka¹

¹Institute of Experimental Medicine, Academy of Sciences of the Czech Republic. ²College of Polytechnics Jihlava It was shown previously that the exposure of adult rats to an acoustically enriched environment (EE) improves the response parameters of cortical neurons. The auditory system of rats, however, undergoes extensive refinement during early ontogeny; furthermore, cortical and subcortical structures may be influenced differently by an EE. For this reason, we explored the effect of an EE during early postnatal development on the response properties of inferior colliculus (IC) neurons. In the period from14 to 28 postnatal days, the rats were exposed 12h a day to complex acoustic stimulation consisting of a broad-band rippled noise (average level 55dB SPL) with six embedded signals (at 60dB SPL), three of which triggered a reward release. At the age of 3 months, the response properties of the IC neurons of the enriched rats were recorded and compared with those obtained from age-matched controls

raised under standard conditions. As the frequencies of the embedded signals ranged from 3 to 8 kHz, the neurons were divided according to their characteristic frequency (CF) into two CF bands: 2-8 kHz and above 8 kHz. Most of the significant differences occurred in the 2-8 kHz CF range: compared with the controls, the enriched rats had lower thresholds, sharper frequency tuning, and lower spontaneous activity. Furthermore, the enriched rats had a markedly higher proportion of neurons with a strictly monotonic rate-intensity function. Interestingly, those neurons that did reach saturation had a narrower dynamic range and lower maximum response magnitudes in the enriched animals. The results indicate that an EE during the sensitive period of postnatal development significantly influences the maturation of the auditory system. The alterations are consistent with the hypothesis that an EE sharpens frequency discrimination and influences intensity coding; these changes are retained to adulthood. Supported by AV0Z50390512, GACR 309/07/1336, GACR 309/08/H079, LC 554.

447 Graded and Modular Expression Patterns of EphAs and Ephrin-Bs in the Developing Central Nucleus and External Cortex of the Inferior Colliculus

Mark Gabriele¹, Sarah Kavianpour¹, Kelly Chamberlain¹, Devon Cowan¹, Matthew Wallace¹, Melissa Reitano¹, Rachel Kokal¹, Donald Brubaker¹

¹James Madison University

The central nucleus (CNIC) and external cortex of the inferior colliculus (ECIC) receive a wide array of ascending and descending connections necessary for processing complex auditory and multisensory tasks. Such convergence demands highly organized circuits. The CNIC is tonotopically arranged with afferents that establish layered patterns, while projections targeting ECIC laminae exhibit a more modular or compartmentalized organization. Previously, we have shown that spatially precise inputs to the CNIC and ECIC are established prior to the onset of hearing in a variety of species. The present study confirms early projection specificity in the mouse IC, and implicates certain members of the Eph-ephrin signaling family in organization. guiding its initial Tract-tracing, immunohistochemistry, and X-Gal staining of lacZ mutants reveal EphA4, ephrin-B2, and ephrin-B3 expression patterns that correlate with the developing tonotopic, layered, and modular arrangements of the CNIC and ECIC. Expression patterns are graded across the tonotopic axis of the CNIC, with label most concentrated in ventromedial, high-frequency regions. Quantitative measures indicate clear gradients at birth that persist throughout the first postnatal week, consistent with the timing and shaping of tonotopically arranged axonal layers. Observed gradients significantly flatten at later developmental stages and are seemingly down-regulated by the onset of experience. Interestingly, Eph-ephrin expression in the ECIC is not graded, but rather exhibits a periodic distribution of modules or compartments throughout the rostrocaudal extent of the nucleus. Ongoing experiments in control and Eph-ephrin mutant mice should

provide insights into the specific role these proteins play in instructing the observed early topography and projection specificity in the developing IC.

448 Does the Auditory Cortex Mature More Rapidly Than the Inferior Colliculus?

Zoltan Fuzessery¹, Terese Zumsteg¹, Anthony Williams¹ ¹Univ Wyoming

Neurons of the inferior colliculus (IC) and auditory cortex (AC) of the pallid bat share similar expressions of selectivity for the downward FM sweep of its biosonar pulse, similar underlying mechanisms, and similar percentages of neurons that exhibit selectivity. Examining the development of selectivity at the levels of both IC and AC produced some unexpected results. Development of selectivity for FM sweep direction was similar. At both levels, the percentage of neurons selective for the downward sweep direction was about half that seen in adults from 2-7 weeks of age. However, the development of sweep rate selectivity differs. From 2-7 weeks of age in the AC, the percentage of rate-selective neurons, and the rates they prefer is already very similar to the adult condition. In contrast, at 2 weeks of age in the IC, a significantly higher percentage of neurons are rate selective than in adults, but the majority of neurons respond to much higher sweep rates than adults, suggesting an immature condition. From 2 to 4 weeks, the percentage of rate-selective neurons drops dramatically to about half that seen in adults. At 5 weeks of age, the percentage of rate-selective neurons increases, and is similar in both the IC and AC. It thus appears that sweep rate selectivity matures 3 weeks earlier in the AC than the IC. One explanation is that the AC may respond to experience earlier, and maintain its rate selectivity. It is also possible that corticofugal, top-down instruction may facilitate the delayed IC development, as has been inferred from studies of human auditory development. Retrograde tracing was used to determine whether the corticofugal pathway is in fact present early in development. This pathway is present at 4 weeks of age, and adult-like in terms of the number of labeled neurons in the AC. Whether this circuitry is mature and capable of instruction is not clear.

449 Cooling Induced Neural Inactivation of the Inferior Colliculus Demonstrates Commissurally Mediated Modulation of Responses in the Contralateral Inferior Colliculus

Llwyd Orton¹, Paul Poon^{1,2}, Adrian Rees¹ ¹Newcastle University, UK, ²National Cheng Kung University, Taiwan

The inferior colliculi (IC), the principal auditory nuclei in the mammalian midbrain, are interconnected via the commissure of the inferior colliculus (CoIC). Whilst numerous studies have identified the anatomical nature of the CoIC, little is known about its functional role in auditory processing.

To investigate the physiological contribution of the CoIC, acute experiments were performed on young adult guinea pigs anaesthetised with urethane and Hypnorm. The cerebral cortex over the IC on one side was aspirated and a cryoloop (Lomber et al, (1999) J. Neurosci Methods 86:179) was placed in contact with the lateral surface of the exposed IC. Cooling the cryoloop allowed neural activity within the IC to be suppressed reversibly. Sound stimuli were presented to the animal through a closed acoustic system. Single neurons, local field potentials (LFPs) and evoked potentials (EPs) were recorded before, during and after cooling.

Responses of single units in the cooled IC during the first 10 degrees of cooling showed either an increase or decrease in firing. All responses were suppressed by cooling below 20°C. Single units from the opposite (uncooled) IC were similarly modulated in a two phase manner during the cooling cycle.

With monaural stimulation of the ear contralateral to the cryoloop, LFPs and EPs in the cooled IC were suppressed as a function of temperature. With stimulation of the ear contralateral to the un-cooled IC, cooling first potentiated the responses in the un-cooled IC, before suppressing them. Lesioning the CoIC markedly reduced these suppressive effects in the IC contralateral to cooling.

These results are consistent with our hypothesis that the representation of sound in each IC is formed from the converging outputs of brainstem nuclei and the contralateral IC. Thus, information ascending through each brachium of the IC is a representation of the bilateral activity in the auditory brainstem and midbrain.

450 Neural Responses Across the Isofrequency Laminae of the Inferior Colliculus to Species-Specific Vocalizations in Guinea Pigs

Thilo Rode¹, Tanja Hartmann¹, Roger Calixto¹, Minoo Lenarz¹, Andrej Kral¹, Thomas Lenarz¹, Hubert H. Lim² ¹Experimental Otology, ENT Clinics, Hannover Medical University, ²Biomedical Engineering, University of Minnesota

Anatomical and functional studies have shown that neurons located in different locations along an isofrequency lamina of the inferior colliculus central nucleus (ICC) receive differential projections from distinct brainstem nuclei and exhibit some systematic spatial organization of coding properties (e.g. latencies, modulation sensitivity, tuning curves, thresholds). However, it remains unknown if neural response properties systematically vary across an ICC lamina in response to complex stimuli such as species-specific vocalizations. Information on differences in response properties to complex auditory stimuli would provide insight into improved stimulation strategies for ICC-based auditory prostheses.

Data were obtained from 6 ketamine-anesthetized adult normal-hearing guinea pigs. Eight different vocalizations (30-70 dB SPL, 10 dB steps) were presented through calibrated loudspeakers and the corresponding multi-unit activity was recorded across the ICC. Multi-site electrode arrays (NeuroNexus Technologies) were placed into the ICC to record from 6-10 different locations in each animal. In total 185 multi-unit clusters were compared across animals. We confirmed the location of each site based on frequency response maps and histological reconstructions (arrays were stained with a red dye, Di-I). These reconstructions allow us to pool data across animals. Post-stimulus time histograms (PSTHs) were compared to the envelope in the frequency response area of the given multi-unit cluster.

We observed response patterns that were generally similar across different locations along an ICC lamina. Although there were slight differences in the latencies and peaks of the PSTHs across neurons, most responses appeared to follow the envelope pattern of the stimulus. These data support the hypothesis that most neurons along an ICC lamina follow the general envelope pattern of a stimulus yet specific information about the stimulus is coded within the interval spike timing between those neurons.

Supported by BMBF Bernstein Focus Neurotechnology Göttingen and Cochlear Ltd.

451 Serotonin Selectively Shapes Vocalization Responses in Mice

Laura Hurley¹, Patrick Roberts², Christine Portfors³ ¹Indiana University, ²Oregon Health & Science University, ³Washington State University

The neuromodulator serotonin has complex effects on the response properties of auditory neurons. Serotonin alters spike rate and timing in different ways even for responses to simple stimuli like tone burst and FM sweeps. This makes it difficult to predict the effects of serotonin on responses to spectrotemporally rich stimuli such as species-specific vocalizations. In the current study we directly measured the effects of serotonin on the responses of IC neurons in female CBA/CaJ mice to recorded vocalizations. Single neurons were recorded extracellularly in anesthetized mice, and serotonin was iontophoretically applied through 'piggyback' multibarreled pipettes. Natural and synthesized vocalizations recorded from male and female mice in identified behavioral contexts were used as stimuli. Serotonin influenced both the rate and timing of spikes in response to the vocalizations. The response rate usually decreased in the presence of serotonin, but could also increase. In rare cases, serotonin had opposite effects on the responses rates of single neurons to different calls. Serotonin could also alter both the latency and variation in latency (jitter) of spikes, but the effects of serotonin on spike timing were not always correlated with its effects on spike rate. We conclude that serotonin selectively shapes both the rate and timing of responses to species-specific vocalizations in mice, and that its effects are partly dependent on the structure of the vocalization.

452 Cisplatin Suppresses Hippocampal Neurogenesis and the Antioxidant D-Methionine Blocks the Effects of Cisplatin

Sneha Hinduja¹, Kari Suzanne Kraus¹, Senthilvelan Manohar¹, Laura Lewicki¹, Harmann Singh¹, Richard Salvi¹ ¹Center for Hearing and Deafness, University at Buffalo The hippocampus, which has connections with the auditory pathway, plays an important role in memory, mood and spatial navigation. Interestingly, the hippocampus contains a stem cell niche; approximately 9000 new cells are born in the rat hippocampus each day and roughly half of these differentiate into neurons. The anticancer drug, cisplatin, has been used for decades to study ototoxicity and cell death in the inner ear. In recent studies we and others have found that cisplatin can have a profound effect on cell proliferation and neurogenesis in the hippocampus. Rats treated with a high dose of cisplatin, which caused only mild hearing loss and cochlear pathology, had an 80% decrease in hippocampal neurogenesis as reflected in doublecortin (DCX) immunolabeling. Hippocampal neurogenesis was still suppressed by 50% 21 days post-Previous studies have shown that the treatment. antioxidant D-methionine protects against cisplatin-induced sensory hair cell degeneration, nephrotoxicity, weight loss and hearing loss in rats. To determine if D-methionine could block the cisplatin-induced suppression of neurogenesis in the hippocampus, rats were treated with cisplatin alone, D-methionine alone, cisplatin plus Dmethionine, or received no treatment. Cisplatin, which has traditionally been thought to primarily damage the cochlea, had a profound effect on cell proliferation and neurogenesis in the hippocampus and could lead to memorv impairments. When D-methionine was administered with cisplatin, it completely prevented cisplatin-induced body weight loss and restored hippocampal neurogenesis to normal levels. Surprisingly, when D-methionine was administered alone, the level of neurogenesis increased by nearly 50% compared to normal levels. In summary, the antioxidant D-methionine may serve as a potential treatment to counteract the negative effects of cisplatin on hippocampal neurogenesis. Supported by NIH (R01DC00909101; R01DC009219)

453 D-Methionine Protects Against Cisplatin-Induced Neurotoxicity in Auditory Cortex Networks in Vitro

Kamakshi Gopal¹, Calvin Wu¹, Bibesh Shrestha¹, Ernest Moore¹, Guenter Gross¹

¹University of North Texas

Cisplatin (cis-diamminedichloroplatinum(II) (CDDP)) is a platinum-based chemotherapeutic drug that is used for the treatment of cancer. Patients undergoing cisplatin treatment often suffer from chemo brain, which is characterized by symptoms such as cognitive impairment and memory lapse, along with hearing loss, tinnitus and seizure. D-Methionine (D-Met) has been shown to prevent cisplatin-induced ototoxicity in animals without antitumor interference. In this study, we have used an in vitro model of auditory cortex networks (ACNs) to investigate cisplatin neurotoxicity and the protective effects of D- Met. Dissociated neurons from auditory cortices of mouse embryos were grown on microelectrode arrays with 64 transparent indium-tin oxide electrodes that enabled continuous recording of neuronal activity. Cisplatin was applied on spontaneously active ACNs (N=30), at from 0.05 to concentrations ranging 1.0 mM. Concentrations of 0.05 to 0.25 mM increased spiking activity by 50%. At 0.5 mM and higher, cisplatin induced irreversible loss of neuronal activity and neuronal cell death within two hours. Application of 1.0 mM D-Met one hour prior to cisplatin exposure prevented excitation of neuronal activity for cisplatin concentrations of 0.05 to 0.25 mM, caused sustained excitation for cisplatin concentration of 0.5 mM without neuronal death, and did not provide protection for cisplatin concentrations of 0.75 and 1.0 mM. Concurrent application of D-Met and cisplatin was less protective than consecutive application of D-Met and cisplatin. We conclude that pretreatment of ACNs with 1.0 mM D-Met one hour prior to the application of cisplatin provides effective protection against cisplatin-induced neurotoxicity up to a concentration of 0.75 mM.

454 Cross-Modal and Compensatory Plasticity in Adult Deafened Cats: A Longitudinal PET Study

Min-Hyun Park¹, Hyo-Jeong Lee², Jin Su Kim³, Jae Sung Lee⁴, Dong Soo Lee⁴, Jeong Hun Jang⁵, Seung Ha Oh^{5,6} ¹Boramae Medical Center, Seoul metropolitan government-Seoul National University, ²Department of Otolaryngology, Hallym University College of Medicine, ³Molecular Imaging Research Center, Korea Institute of Radiological and Medical Science, ⁴Department of Nuclear Medicine, college of medicine, Seoul National University, ⁵Department of Otorhinolaryngology, College of medicine, Seoul National University, ⁶Research Center for Sensory Organs, Medical Research Center, Seoul National University

Although much is known of the cerebral neural plasticity that occurs after deafness, it is not clear how much time is required for its development, or what other cortical changes may consequently take place. This study provides a longitudinal assessment of cerebral cortical neural plasticity, as manifested by adult deafened cats. A total of five male cats were subjected to whole-cortex analysis of glucose metabolic activity via 2-deoxy-2[18F] fluoro-Dglucose (FDG) micro-positron emission tomography (PET). The imaging was performed at a baseline state of normal hearing, and then at 4-, 9-, 24-, and 33-month intervals after induction of deafness. We compared the glucose metabolism between normal hearing state and each deafened state using voxel-based statistical analysis (P<0.005). Significant changes were observed in the primary auditory (A1) and primary visual (V1) cortices. A bilateral metabolic decrease was observed in A1 areas and in temporal auditory fields, the extent of which was significantly enlarged at Month 9. Then it was declined at Month 24. And finally it was disappeared by Month 33. Auditory cortical plasticity, subsequent to deafness, was thus demonstrated. Furthermore, a significant metabolic upsurge occurred in bilateral occipital areas at 33-month intervals. This increase, involving occipital and thalamic areas of V1 bilaterally, suggests compensatory hyperactivity of visual cortex after deafness.

455 GABA_A Agonist Rescues Cortical Inhibitory Synaptic Function Following Developmental Hearing Loss

Vibhakar Kotak¹, Anne Takesian¹, Dan Sanes¹ ¹NYU

An elementary theory in developmental neurobiology is that early experience regulates synapse maturation. Further, many disorders of the CNS are closely associated with reduced inhibitory synaptic transmission. For example, early hearing loss disrupts the maturation of GABAergic transmission in auditory cortex (Kotak et al. 2005; 2008; Sarro et al. 2008; Takesian et al. 2010). Therefore, one goal is to determine whether inhibitory deficits can be reversed following hearing loss. We test the prediction that augmentation of GABAergic signaling immediately after hearing loss can rescue the ensuing at inhibitory synapses. Following conductive deficits hearing loss (CHL) at P10 (i.e. 2 days prior to hearing onset), gerbil pups were treated with a GABAA receptor subunit specific agonist (zolpidem, 10mg/kg) for 7 days. A thalamocortical brain slice was obtained at P19-22 and intracortically-evoked spontaneous and minimum amplitude inhibitory synaptic currents (sIPSCs, min-evoked IPSCs) were recorded in whole-cell voltage-clamp from thalamorecipient L2/3 pyramidal neurons in the presence of ionotropic glutamate receptor blockers. sIPSCs in CHL neurons were significantly smaller than age-matched sIPSC amplitude. controls. (Mean pA±SEM: Control=28.4±2.4, n=10 vs. CHL=20±2.8, n=7, p=0.04). In contrast, sIPSC amplitudes in zolpidem-treated CHL animals resembled control sIPSCs indicating restoration. (Control=28.4±2.4, n=10 vs. zolpidem-treated CHL: 31.7±3.9, P=0.48). Further, the min-evoked IPSCs in CHL neurons were significantly smaller than controls while the min-eovked IPSC amplitudes in zolpidem-treated CHL animals resembled control IPSCs. (Mean min-evoked IPSC amplitude, pA±SEM: Control=13.9±2, n=11 vs. CHL=6.7±0.7 pA, n=8, P=0.005. Min-evoked IPSC amplitude: Control=13.9±2 pA, n=11 vs. zolpidem-treated CHL:10.5±0.8, n=4, P=0.5). Together, these results show that it is feasible to pharmacologically restore inhibitory synapse function following developmental hearing loss.

456 Noise Exposure Induced Hyperacusis Behavior

Wei Sun¹, Brian L. Allman¹, Aditi Jayaram¹, Brittany Gibson¹

¹University at Buffalo

Hyperacusis, a marked intolerance to normal environmental sound, can significantly affect people's quality of life. Unfortunately, there is no cure for hyperacusis partly because the neural mechanism underlying the disorder is not well understood. Previous animal studies suggest that the peripheral lesion caused

by noise exposure or ototoxic drugs not only damages the cochlea, but also alters central auditory processing. Importantly, these central changes may affect sound loudness perception and reduce sound tolerance. То study hyperacusis behavior and changes in central auditory system function caused by noise exposure, we compared the acoustic startle reflex and responses of the inferior colliculus (IC) and the auditory cortex (AC) in rats before and after noise exposure. A bilateral narrow band noise centered at 12 kHz (120 dB SPL for one hour) was used to induce high frequency hearing loss. Noise exposure caused a significant increase of the startle reflex amplitude at the super-threshold levels (80 – 100 dB SPL) at 16 kHz one hour after the exposure, suggestive of increased loudness perception- a sign of hyperacusis. This elevated startle amplitude gradually recovered to the baseline level three days post-exposure. The IC and AC responses monitored chronically implanted using electrodes were affected differently: noise exposure induced a significant decrease in the IC response, yet resulted in a transient increase in the AC field potential and firing rates. Our results suggest that enhanced AC responsiveness may be related to the manifestation of hyperacusis behavior induced by noise exposure.

Supported by The Royal National Institute for Deaf People (RNID) and American Federation for Aging Research (AFAR)

457 Tracking Neuronal Changes in the Auditory System Following Noise-Induced Hearing Loss

Carl Parsons¹, Cherylea Browne¹, Spencer Chen¹, John Morley¹

¹University of Western Sydney

Noise-induced hearing loss results in significant changes throughout the auditory system. Significant changes in the distribution of characteristic frequencies are observed in the inferior colliculus (IC), medial geniculate nucleus (MG) and primary auditory cortex (A1), but only in A1 and MG are these changes thought to be due to plastic reorganisation. A growing body of evidence suggests that hearing loss and its accompanying neuronal changes are also involved in tinnitus. Thus, understanding the development of neuronal changes following noise-induced hearing loss may aid us in understanding the neural basis of tinnitus. We examined neuronal changes at three different levels of the auditory pathway and at different time-periods up to 7 months following exposure to a damaging, narrow band noise. Male Long Evans rats aged 3-4 months (n = 21) were unilaterally exposed to a 115 dB SPL 16 kHz 1/10th octave bandpass noise for 1-hour. We simultaneously recorded from dorsal cochlear nucleus (DCN), IC and A1 using 32 or 64 channel electrodes in different groups of rats up to 7 months following noise exposure. Six unexposed rats served as controls. Hearing was assessed before and at different time-points following the noise trauma using auditory brainstem response (ABR) audiograms. Tone pips (1-44 kHz, 50 ms duration, 0-80 dB SPL, 1 Hz presentation rate) were used to obtain frequency tuning curves. At 30 days following noise exposure the majority of multi-unit clusters recorded in A1 had two peaks in their frequency tuning curves (9-12 kHz and 30-35 kHz), which bordered the spectral range of the noise-trauma stimulus. Similar changes were also evident through to 6-7 months after noise trauma. Less pronounced tonotopic changes were observed in the IC. The only reliable effect shown in the DCN was an absence of neuronal activity in response to 16 kHz stimulation.

458 Tracking the Expression of GABAA Receptor Subunit á1, Glutamic-Acid Decarboxylase-67, N-Methyl-D-Aspartate Receptor Subunit 2A in Rat Auditory Pathway Following Noise-Induced Hearing Loss

Cherylea Browne¹, John Morley¹, Carl Parsons¹ ¹The University of Western Sydney

Excessive exposure to loud noise or a mechanical insult results in damage to the cochlea, which can lead to a range of neuronal changes in key nuclei in the auditory pathway. Neuronal changes that have been observed include plasticity of tonotopic organisation, changes in the pattern of spontaneous activity and in the balance of excitatory and inhibitory transmitter systems. Moreover, a cochlear hearing loss is strongly associated with tinnitus in humans. This suggests that one or more of these neuronal changes may be involved in generating tinnitus, although the mechanisms and site remain unknown. In an attempt to determine which area(s) may be involved in the generation of tinnitus, we are investigating neuronal changes at a number of levels of the auditory pathway (auditory cortex (AC), inferior colliculus (IC) and dorsal cochlear nucleus (DCN)), primarily focusing on the balance of excitatory and inhibitory transmitter systems. In this study we examined the time-course of changes in the expression of the GABAA receptor subunit á1 (GABAARá1), Glutamic-Acid Decarboxylase-67 (GAD-67), N-Methyl-D-Aspartate receptor subunit 2A (NMDAR2A) in AC, IC and DCN up to 32 days following exposure to a 16 kHz bandpass (1/10th octave noise (115 dB SPL)). Male Long Evans rats (n = 15) were unilaterally exposed to the damaging noise for 1-hour. At 0, 4, 8, 16 or 32 days following the noise exposure, rats were euthanased, the brain was removed and processed for western blot analysis to identify GABAARa1, GAD-67 and NMDAR2A expression, which were subsequently quantified in the AC, IC and DCN. Following unilateral sound exposure we saw an immediate increase of NMDAR2A in the contralateral and ipsilateral AC. We also observed a significant decrease in GAD-67 in the ipsilateral and contralateral DCN over the 32 days following exposure. These changes may reflect an attempt to balance excitatory and inhibitory transmission, which is known to increase following noiseinduced hearing loss.

459 Stress Hormone Levels and Hippocampal Neurogenesis Following Acoustic Trauma

Sarah Hayes¹, Senthilvelan Manohar¹, Brian Allman¹, Richard Salvi¹

¹Center for Hearing and Deafness. University at Buffalo High intensity noise exposure has long been known to damage the inner ear; however, our recent study demonstrated that a single unilateral noise exposure (2h, 126dB, 12kHz) resulted in decreased hippocampal neurogenesis measured 10 weeks post noise exposure. Given the known ability of stress hormones to reduce hippocampal neurogenesis, we hypothesized that the reduction in hippocampal neurogenesis following unilateral noise exposure might be mediated by a sustained elevation in stress hormone levels. To test this hypothesis we monitored blood plasma levels of the stress hormone corticosterone in rats following acoustic trauma. Rats were divided into 4 groups: (1) unilateral or (2) bilateral noise exposure (2h, 126dB, 12kHz) under isoflurane anesthesia, (3) bilateral noise exposure (2h, 110 dB, 12kHz) unanaesthetized, or (4) 2h isoflurane anesthesia control. Blood samples were collected before, 45 minutes after and 1-6 weeks post exposure and plasma corticosterone levels were measured using an enzyme immunoassay kit. DPOAEs, a measure of OHC function, were suppressed 24 hours post noise exposure. Noise exposure caused a short term increase in corticosterone levels: however. corticosterone levels did not remain elevated in the weeks following noise exposure. Thus the reduced neurogenesis, as previously observed, is not likely to be mediated by a sustained elevation in corticosterone levels following noise Further investigation into the effects of trauma. manipulating corticosterone levels during and following noise exposure will help clarify this point. Unexpectedly, we observed that 2 hours of isoflurane anesthesia dramatically (>10 fold) increased corticosterone levels measured 45 minutes post exposure. This increase in corticosterone was much greater than the effects of noise exposure alone; this may underlie the protective effects of isoflurane against noise trauma previously reported. Supported in part by NIH grants R01DC0090910 & R01DC009219-01.

460 Auditory Cortex Neuronal Death and Hippocampal Neurogenesis Following Blast-Induced Traumatic Brain Injury

Brian Allman^{1,2}, Senthilvelan Manohar^{1,2}, Laura Lewicki^{1,2}, Dalian Ding^{1,2}, Edward Lobarinas^{1,2}, A. Jensen Newman^{1,3}, Joseph Mollendorf^{1,3}, Richard Salvi^{1,2}

¹State University of New York at Buffalo, ²Dept.

Communicative Disorders & Sciences, ³Dept. Mechanical & Aerospace Engineering

In addition to damaging the inner ear, blast wave exposure can induce traumatic brain injury (TBI). Previous reports have identified the hippocampus, one of two regions in the adult brain where neurogenesis occurs, as particularly vulnerable to TBI; however, little is known about how blast exposure affects hippocampal neurogenesis or auditory structures. We exposed adult rats to repeated blast waves (6 blasts; ~190 dB pSPL) and assessed the extent of damage in the cochlea, central auditory system and hippocampus at various times after exposure. At 7-days post-blast, we observed considerable structural and functional damage in the cochlea; the majority of hair cells were missing, and there was a significant reduction in the distortion product otoacoustic emissions (DPOAE) compared to baseline measures. Intravenous injection of FLIVO, a cell permeant probe which fluoresces in the presence of active caspases, was used to visualize apoptosis in the inferior colliculus and auditory cortex (AC) after blast exposure. The AC showed extensive cell death 7-days post-blast, perhaps due to its vulnerability to contusion injury on the temporal cortex. Coimmunolabeling with either neuronal nuclei (NeuN) or glial fibrillary acidic protein (GFAP) confirmed that neurons, not glia, were undergoing blast-induced apoptosis. The effect of blast exposure on hippocampal neurogenesis differed over time; at 7-days post-blast, doublecortin (DCX) immunolabeling revealed an increase in neurogenesis. whereas there was suppression of neurogenesis 42-days post-blast. This early up-regulation of neurogenesis is consistent with previous findings following other models of TBI. Given the critical role of the hippocampus in learning and memory, we speculate that suppression of neurogenesis in the weeks following blast exposure may contribute to the cognitive deficits common in military personnel exposed to blast trauma.

Supported by NIH grants (R01DC0090910; R01DC009219-01)

461 A Two-Variable Reduction of the Rothman-Manis Model for Phasic Firing

Xiangying Meng^{1,2}, John Rinzel^{1,3} ¹Center for Neural Science, New York University, ²Dynamics and Control, Beihang University, ³Courant Institute of Mathematical Sciences, New York University Many neurons in the auditory brain stem fire phasically. They fire only one or a few spikes at the onset of an adequate depolarizing current (lapp) step in contrast to tonic neurons that can fire repetitively for constant or slow lapp. Phasic neurons show strong sensitivity to the rate of depolarization, having a threshold for the speed of a depolarizing lapp ramp (McGinley & Oertel, 2006). Rothman and Manis in 2003 developed a conductancebased model (we call it RM03) for cochlear nucleus neurons; it is widely used for MSO (and other) neurons. It contains a sodium current (I_{Na}), a low threshold potassium current (I_{KLT}), a high threshold potassium current (I_{KHT}) and a leak current (I_{leak}). In RM03, I_{KLT} is responsible for the phasic behavior; its conductance activates rapidly (1-2 ms), and inactivates slowly (200 ms) but not totally.

We have developed a 2-variable reduction of the 9variable RM03 model. Our reduced model contains I_{Na} , I_{KLT} and I_{leak} . We were able to combine, into a single variable, the inactivation gating variable, h, of I_{Na} and the activation gating variable, w, of I_{KLT} because they have similar time scales and h and w satisfy a near-linear relationship when their trajectory during spiking is plotted in the w-h plane. Also, we freeze slow gating variables in RM03. Our reduced model retains phasic properties of the full RM03 model: it fires only an onset spike for an lapp-step, sensitivity to the slope of an lapp-ramp, precise phase locking, and a U-shaped frequency vs mean lapp relation for a noisy lapp. Our reduced model permits a phase-plane analysis and thereby prediction and insight into the phasic firing properties. Another potential mechanism for phasic behavior, as found in some MSO neurons, is low-voltage inactivation of I_{Na} . We compare these two mechanisms using phase plane analysis.

Supported by NIH/NIDCD-008543.

462 Slow GABAergic Transmission Mediated by Asynchronous GABA Release and Spillover in Nucleus Laminaris Neurons

Zheng-Quan Tang¹, Yong Lu¹

¹Northeastern Ohio Universities Colleges of Medicine and Pharmacy

Nucleus laminaris (NL) neurons receive a feedback GABAergic input from the ipsilateral superior olivary nucleus (SON). Using whole-cell recordings in slice preparations obtained from late chicken embryos, we investigated the temporal characteristics of this input in response to different stimulation frequencies and the underlying mechanisms. Voltage clamp recordings showed that the temporal profile of evoked inhibitory postsynaptic currents (IPSCs) in NL neurons depended on the stimulation frequency in a coding frequency-specific manner. The decay time course of IPSCs in lowcharacteristic frequency (CF) neurons was significantly distinguishable from that in middle-/high-CF neurons. When the SON-NL pathway was activated by electrical shocks at a low stimulation frequency (1 Hz, single pulse), IPSCs of low-CF neurons decayed significantly faster than those of middle-/high-CF neurons. However, when the pathway was activated at high stimulation frequencies approximating in vivo SON firing rates (e.g. 100 Hz, 20 pulses), a sustained IPSC with an unusually slow decay developed in both low- and middle-/high-CF neurons. Presynaptic asynchronous GABA release, as well as GABA spillover and subsequent activation of extrasynaptic GABAA receptors, contributed to this slow IPSC decay, and diminished the decay time difference of IPSCs seen between the low- and middle-/high-CF neurons under low stimulation frequencies. Current clamp recordings showed that synaptically released GABA triggered by high frequency stimulations depolarized the membrane for a period exceeding the stimulation duration, accelerated the time course of excitatory postsynaptic potentials, and improved coincidence detection in NL neurons. Supported by NIH Grant DC008984 to YL.

463 Directionality of Gecko Auditory Nerve Fibers with Free Field Stimulation

Jakob Christensen-Dalsgaard¹, Catherine E. Carr² ¹University of Southern Denmark, ²University of Maryland Lizard ears are the ultimate pressure-gradient receiver ears. The extreme directionality is created by strong acoustical coupling of the eardrums, with almost perfect transmission from the contralateral ear (Christensen-Dalsgaard and Manley, J Exp Biol 208:1209-1217, 2005). Single-unit recordings with closed-field experiments in the Tokay gecko show equal sensitivity to ipsi- and contralateral stimulation, as well as dependence on interaural time and level differences, also indicative of strong interaural transmission (Christensen-Dalsgaard, Tang and Carr, submitted).

To exploit the consequences for directional processing in lizards we have investigated the responses to directional sound in auditory nerve fibers in the Tokay gecko. We exposed the auditory nerve dorsally and recorded responses of single units to free-field sound from speakers radially distributed around the gecko. The fibers are strongly directional both at low (2-400 Hz) and high frequencies (1-2 kHz) with an ovoidal directivity that resembles the eardrum directivity. Geckos are highly vocal, and the nerve fiber directionality to components of the call is very pronounced.

Since the auditory nerve fibers show strong directionality, effectively every neuron in the lizard auditory pathway is directional, and the processing of sound direction in the lizard CNS is likely very different from animals with uncoupled ears. The ovoidal directionality will produce a very strongly lateralized response by simple binaural comparison (EI-type neurons), which may be sufficient to orient the gecko to sound.

464 Azimuthal Tuning of Inferior Colliculus Neurons in the Unanesthetized Rabbit as a Function of Stimulus Level and Binaurality

Duck O. Kim¹, Brian Bishop¹, Shigeyuki Kuwada¹ ¹University of Connecticut Health Center

The virtual auditory space (VAS) method is an efficient way to study a neuron's sensitivity to sound source location. We measured head related transfer functions (HRTFs) in individual rabbits in an anechoic chamber and generated VAS stimuli by filtering noise with the rabbits' own HRTFs. These VAS stimuli were delivered through earphones coupled to custom-fitted ear molds. Neural recordings were made with tungsten-in-glass microelectrodes and lowered into the inferior colliculus of a restrained, unanesthetized rabbit. We determined the neuron's best frequency (BF) and used this information to choose one of three band limited noises. We tested the neuron's azimuthal sensitivity by presenting VAS stimuli representing different azimuths separated by 15 degree steps in random order. For each neuron, we determined its neural threshold and then delivered the stimuli at 10 - 50dB (re:threshold) in 10 dB steps. We also presented the VAS stimuli binaurally and monaurally.

Most neurons were spatially tuned to an azimuth on the contralateral side (re: recording site) between $0 - 90^{\circ}$. The azimuth tuning tended to broaden with stimulus level although the degree of broadening differed among neurons. Near threshold, azimuthal tuning was remarkably similar regardless of whether the VAS stimuli were presented binaurally or only to the contralateral ear. At high sound levels, the azimuth tuning became broader for contralateral stimulation compared to binaural stimulation.

465 The Encoding of the Acoustical Cues to Sound Location by Neurons in the Inferior Colliculus as a Function of Source Distance Using Virtual Space Stimulation

Heath Jones¹, Kanthaiah Koka¹, Jennifer Thornton¹, Daniel Tollin¹

¹University of Colorado School of Medicine

Although the auditory system has the capacity to determine sound location in 3-dimensions - azimuth, elevation and distance - most neurophysiological studies have examined only the neural encoding of the localization cues themselves [i.e., interaural time and level (ILD) differences and spectral shape cues] or have used freefield or virtual space (VS) techniques to measure neural spatial receptive fields (SRFs) for sources at a fixed distance. However, it is known that some of the cues to location are greatly affected by source distance; for example, low-frequency ILDs increase substantially as the source-to-observer distance decreases. Thus, for a given source location the ILD cue to location is not invariant with distance. Here we tested the hypothesis that lowfrequency sensitive neurons in the central nucleus of the inferior colliculus (ICC) of the chinchilla can encode the distance-dependence of ILDs. Data are based on 110 ILD-sensitive ICC neurons. Although most of these neurons had high (>3 kHz) characteristic frequencies, there were many low-frequency neurons that were also ILD sensitive. Across the population of ICC neurons, the ILD sensitivities were found to be sufficient to cover the range of acoustical ILDs physically experienced by chinchillas, except for low frequencies (< 3 kHz) where neural sensitivity to ILDs (~±20 dB) exceeded the range of acoustical ILDs (±3-4 dB) measured under typical laboratory conditions (i.e., 1 m distance). Here we show that the SRFs in azimuth resulting from presentations of VS stimuli (generated from directional transfer function measurements) were shifted in azimuth as a function of source distance. These shifts were correlated with the distance-dependent changes in the ILD spectra. In general the results show that ILD-sensitive ICC neurons can encode source azimuth over a range of physiologically-plausible source distances, but that the neural representation of azimuth is not invariant with distance. Supported by NIDCD R01-DC6865.

466 Efficient Coding of Naturalistic Sounds in the Superior Olivary Complex

Michiel Remme¹, Jason Mikiel-Hunter², Roberta Donato², John Rinzel¹, David McAlpine²

¹New York University, ²University College London

Neurons in the medial superior olive (MSO) and lateral superior olive (LSO) code for sound source location along the azimuth by extracting interaural time differences (ITD) from the fine structure or envelope of sound stimuli. MSO and LSO neurons are among the most metabolically active cells in the central nervous system. The efficient coding hypothesis states that sensory systems are optimized to process natural signals, maximizing the information conveyed to the brain while minimizing the required

energy. Given that combined behaviorally relevant and background noise stimuli typically display a decreasing signal to noise ratio with increasing frequency, the theory predicts that frequency tuning of MSO and LSO cells should change from bandpass to lowpass with increasing best frequency along their tonotopic axes.

We tested this prediction by determining the impedance profiles of cells along the tonotopic axis of the guinea pig MSO and into the LSO, using ZAP current injection. In agreement with the efficient coding theory we found that low best frequency cells show bandpass filters, which makes them suited to act as coincidence detectors; while high best frequency cells show lowpass filtering, making them function as integrators to extract the stimulus envelope. Combining experiments with computational modeling we identified the biophysical mechanisms that shape the impedance profile, with a central role attributable to the K-LVA current. We used guinea pig vocalizations to generate synaptic input to LSO and MSO cell models and compared the ITD sensitivity of the neural filters with a set of mismatched filters. Finally, our results suggest that a review of cochlear implant coding strategies may be necessary to improve speech recognition.

467 Spatiotemporal Receptive Fields in the Owl's Map of Auditory Space

Yunyan Wang¹, Sharad Shanbhag², Jose Luis Peña¹ ¹Albert Einstein College of Medicine, ²North Eastern Ohio Universities Colleges of Medicine

Receptive field (RF) analysis using brief stimuli from randomized locations in space, also called white-noise analysis, has shown to be a powerful technique in studying temporal properties of RFs in the visual system. In previous applications of white-noise analysis to the auditory system, auditory space was studied in cortical regions using virtual-space stimuli. We studied auditory spatiotemporal RFs in the external nucleus of the inferior colliculus (ICx) of the barn owl (Tyto alba). RFs were measured in real-space using a hemispherical speaker array with 10-degree resolution in azimuth and elevation. Our paradigm more closely mirrors the use of white-noise analysis in visual systems because like the retina, and auditory cortex, a well-characterized unlike the topographical representation of auditory space exists in ICx. We observed that neurons exhibit sharper RFs when randomized, overlapping, noise bursts are played, a difference that is likely due to lateral inhibition from areas surrounding the center of the RF. First-order white noise analysis showed delayed inhibitory modulation during the response to noise bursts from the center of the RF. Neural response were most effectively inhibited when sound bursts from the surround were played 10-20ms preceding sound played from the center of the RF. In addition, inhibitory modulation showed a consistent asymmetry, being stronger from the ipsilateral side relative to the recording site. This finding may represent the basis of topographically represented movement-direction selectivity. Second-order analysis and sound-motion tests support this observation. White-noise analysis in ICx thus offers a unique window into spatial and temporal dynamics

of auditory RF as well as local circuitry for representing space and motion in the auditory system.

468 Directionally Sensitive Auditory Brainstem Responses in the American Alligator (*Alligator Mississippiensis*)

Hilary Bierman^{1,2}, Catherine Carr², Christian Brandt³, Bruce Young⁴, Jakob Christensen-Dalsgaard³

¹Center for Evolutionary Biology of Hearing, ²Department of Biology, University of Maryland College Park, ³Center for Sound Communication, Institute of Biology, University of Southern Denmark, ⁴Department of Physical Therapy, University of Massachusetts Lowell

Initially, acoustical cues for localization are processed by filtering of sound waves by the head, generating a range of interaural time and level differences. Unlike frequency, which is mapped along the sensory epithelium, the location of a sound is primarily determined through computation of binaural information. In mammals and birds these computations primarily occur at the level of brainstem nuclei. Using directional masking of auditory brainstem responses (ABRs), we show that the brainstem of a crocodilian, Alligator mississippiensis, is strongly directional at 1000Hz. Masked ABRs (mABRs), or the response to a short broad-band stimulus minus the response to the same stimulus in the presence of a pure tone masker (Christensen-Dalsgaard et al., Biol Lett 2010), were elicited in awake restrained animals, using a stimulus emitted from a speaker placed lateral to the animal's head and a second speaker emitting a masker tone at eight different radial positions around the animal. Depending on the animal, the mABR varied by as much as 5 - 20 dB with position. Masking was greatest when the speakers were positioned on opposite sides of the animal's head. Observed directional sensitivity to 1000Hz tones cannot be accounted by head shadowing because the tone wavelength is much larger than the head diameter of the juvenile animals studied. Further, this effect was observed during the initial part of the mABR, suggesting directional sensitivity at the level of the auditory nerve. CT scans demonstrated that alligators have a complex of cranial sinuses linking the two tympani, similar to the interaural canal system in birds. In some lizards, interaural coupling generates highly directional pressure-difference receiver ears (Christensen-Dalsgaard et al., JARO 2008), and we hypothesize that alligator ears may also be acoustically coupled.

469 A New Approach for Predicting Binaural Detection Thresholds for Sounds in Quiet from the Monaural Thresholds

Heinrich Neubauer¹, **Peter Heil¹**

¹Leibniz Institute for Neurobiology

The question whether the absolute threshold, measured with simultaneous input to the ears, is lower than the same threshold obtained monaurally, has been studied for a long time. A frequently cited review by Ira Hirsch entitled "Binaural summation – a centuary of investigation" was published more than 60 years ago (Psychol. Bull. 45, 193-

206, 1948). But still, the magnitude of the effect and the underlying mechanism (e.g. binaural energy summation, probability summation or neuronal summation at threshold) are not fully understood. If both ears had identical monaural thresholds and if there were a perfect summation of energy at some level in the auditory system, the binaural threshold, specified in dB SPL, ought to be lower by about 3 dB. A summation effect of that magnitude was found in a number of studies, but values significantly different from 3 dB have also been reported. Here, we present a new approach for predicting binaural absolute thresholds for sounds in quiet from their two directly comparable monaural counterparts, based on our model for monaural absolute thresholds. This monaural model consists of leaky integration of the stimulus amplitude, event formation, and temporal summation (LIEFTS; e.g. Neubauer and Heil, Brain Res. 1220: 208-223, 2008). The new approach allows the prediction of binaural thresholds even if the monaural thresholds are not identical and individual differences in sensitivity between the two ears are not equated. Our predictions are evaluated with a large number of measurements of monaural and binaural absolute thresholds (> 120 sessions with 6 threshold measurements for each of the 3 conditions) for tones of different envelopes from more than 30 human subjects. Based on the excellent agreement of these data with our predictions we draw specific conclusions regarding underlying mechanisms of binaural summation. Supported by the Deutsche Forschungsgemeinschaft

470 Prediction of Monaural and Binaural Level Discrimination in Presence of Distracting Stimuli on Basis of the Stochastic Properties of Brain Stem Neural Coincidence Detector Cells

Tal Klap¹, Miriam Furst¹ ¹*Tel Aviv Universitv*

Binaural level discrimination of simple tones has been investigated by a variety of psychoacoustical experiments over the years. Findings of these experiments have shown that monaural level discrimination tasks are influenced by an existence of distracting stimuli either when it exists at the same ear or at the contra lateral ear. These findings suggest that stimuli level estimation is a binaural process for both binaural and monaural tasks.

The common modeling approach for level discrimination is to distinguish between monaural and binaural peception. In particular, monaural level discrimination is attributed to cochlea and the auditory nerve models, while binaural level discrimination models include an additional interaural processing by brain stem neural cells models.

We suggest modeling both monaural and binaural level discrimination by the same mechanism. We assume that all level estimation tasks are performed at the brainstem level and the dominant mechanism is an excitatoryinhibitory (EI) coincidence neural cells that receives inputs from both ears.

The model includes a complete cochlear model with integrated outer hair cells, inner hair cells model, and a half rectifier as a synapse model. As result, the auditory

nerve instantaneous rate is derived. El cells receive inputs from both auditory nerves.

Let assume that the auditory pathway behaves as an optimal estimator, and then it is possible to predict the psychoacoustical JND results by deriving the Cramer Rao lower bound (CRLB) of the El cell output. We have recently showed that El cells behave as non-homogeneous Poisson process (NHHP) if their inputs also behave as NHHP, and thus CRLB can be derived analytically.

In using this approach, we have successfully predicted a number of level discrimination experimental results including monaural thresholds as a function of frequency, and BMLD with different binaural setups.

471 WITHDRAWN

472 Perceptual Weights for Loudness Judgments of 6-Tone Complexes

Walt Jesteadt¹, Daniel Valente¹, Suyash Joshi¹ ¹Boys Town National Research Hospital

In a series of studies, 6 subjects with normal hearing (NH) and 3 with sensorineural hearing loss (SNHL) judged the overall loudness of 6-tone complexes comprised of octave frequencies from 0.25 to 8 kHz. In two tasks, tones were equated in level in dB SPL or in sensation level (SL) and a range of SPL or SL values was tested. Both tasks used two-interval forced-choice trials, with level "jitter" introduced by selecting the level of each tone from a normal distribution with specified mean level and standard deviation of 5 dB. Subjects were instructed to indicate which complex was louder. In the "loudness" task there was no difference in mean level across the two intervals. In the "sample discrimination" task, the two complexes differed by an average of 5 dB. For both tasks, perceptual weights were derived by correlating the differences in level between matched-frequency tones in the complexes and the loudness decision on each trial. Weights derived from the loudness task (no mean level difference) were highly correlated with weights derived from the sample discrimination task (5-dB difference). For SPL conditions, both NH and SNHL subjects placed less weight on the lowest frequency and greater weight on higher frequencies with increasing intensity of the complexes, with larger effects for NH subjects. This effect was not observed in conditions where levels were equated in SL. Weights derived from a single-interval categorical loudness scaling task, where subjects judged the overall loudness of 6-tone complexes, were highly correlated with those from the other tasks. Simulation of these experiments using a model of loudness perception [Moore and Glasberg, J. Hear Res. 188 (70-88)] yielded weights for these stimuli that were highly correlated with specific loudness, but the observed weights did not agree with predicted weights. This suggests that model assumptions regarding specific loudness are not correct. [Supported by R01 DC006648 and T32DC000013]

473 Non-Simultaneous Across-Frequency Interaction in Loudness

Jesko Verhey¹, Wiebke Heeren¹, Jan Rennies² ¹AG Neuroakustik, Institut für Physik, Carl von Ossietzky Universität Oldenburg, ²Fraunhofer IDMT Projektgruppe Hör-, Sprach- und Audiotechnologie

The level of a broadband signal is usually lower than that of an equally loud narrowband signal. This effect, referred to as spectral loudness summation, is commonly measured for broadband signals where all spectral components are presented simultaneously. The present study investigates to what extent spectral loudness summation also occurs for a non-simultaneous presentation of the frequency components. Spectral loudness summation is measured in normal-hearing listeners with an adaptive alternative-forced-choice procedure with interleaved tracks for sequences of short pure tone pips with varying frequencies (randomly chosen from a set of five frequencies). For each track, a different combination of starting level and repetition rate was used. The comparison stimulus consists of tone pips with the same frequency for all tone pips of the sequence and the same repetition rate and overall duration as the test signal. The results show that, in general, the level of the sequence of tone pips with varying frequencies is lower than that of the equally loud reference sequence with the same frequency for each tone pip, indicating spectral loudness summation even for a non-simultaneous presentation of the frequency components. The magnitude of spectral loudness summation decreases as the inter-pulse interval increases. A residual spectral loudness summation is found for inter-pulse intervals of more than a hundred milliseconds. The data are discussed in the light of the previously shown duration-dependence of spectral loudness summation for noise bursts and a persistence of specific loudness after the offset of each tone pip in the critical band centered at the tone-pip frequency.

474 Behavioral Evidence for Temporal Processing of Pitch in the Common Marmoset (Callithrix Jacchus) Michael Osmanski¹. Xiaogin Wang¹

¹Johns Hopkins University School of Medicine

Pitch is a fundamental perceptual dimension of many biologically relevant sounds, but precisely how the auditory system encodes pitch is not entirely understood. Recent human imaging studies and neurophysiological work in common marmosets have revealed a possible pitch processing center located in low-frequency regions of primate auditory cortex. A complete picture of pitch processing mechanisms requires psychophysical studies to link pitch perception behaviors to neurophysiological data. However, no studies have evaluated pitch processing capacities in common marmosets. In the present study, we have trained common marmosets on an operant conditioning task to measure their pitch discrimination ability using missing fundamental harmonic complex tones. Stimuli were constructed in such a way that the (missing) fundamental frequency (F0) and the envelope repetition rate, corresponding to spectral and temporal pitch,

respectively, could be varied independently. Results indicate that marmosets use both spectral and temporal processing mechanisms to extract pitch information from harmonic complex tones. This ability appears to be F0-dependent, qualitatively similar to that shown for humans, with marmosets relying more strongly on spectral cues at high F0's and temporal cues at low F0's. [Supported by NIH Grant R01-DC03180 (X.W.)].

475 Perception of the Pitch of the Missing Fundamental at 4 Months

Bonnie K. Lau¹, Lynne A. Werner¹

¹University of Washington

The perception of pitch information is critical in many complex auditory tasks including sound source segregation as well as speech and music perception. Infants as young as 7 months demonstrate adultlike abilities to perceive the pitch of the missing fundamental. Although electrophysiological responses to missing fundamental pitch changes have been reported to emerge between 3 and 4 months, there have been no published studies investigating whether infants younger than 7 months demonstrate complex pitch perception. In this study, an observer-based psychophysical procedure was used to assess complex pitch discrimination in 4 month olds. All stimulus tones were harmonic complexes based on a fundamental frequency of 160 Hz or 200 Hz combined in random phase and presented at 70 dB for 650 ms with a 50 ms rise/fall. For the first task, a complex with one of the two fundamentals is presented repeatedly. On signal trials, a complex with the other fundamental is played four times. Infants learned to respond when they heard this pitch change. On no-signal trials, the sound stayed the same. Infants able to perform this pitch discrimination task moved onto the next phase and were presented with a randomized sequence of complexes containing the fundamental and 6 randomly chosen consecutive harmonics. Infants learned to ignore spectral changes and responded only when the fundamental frequency changed. Infants able to perform this pitch categorization task were required to repeat the task with the fundamental frequency missing from all complexes. The criterion to pass each task was 4 of 5 consecutive nosignal and 4 of 5 consecutive signal trials correct. About 80% of 4 month olds were able to complete the missing fundamental categorization task suggesting adultlike perception of the missing fundamental at this age.

476 Complex Pitch Processing by School-Aged Children

Danielle Zion¹, Jaclyn Schurman¹, Mickael Deroche¹, Monita Chatterjee¹

¹Cochlear Implants & Psychophysics Lab, Dept. of Hearing & Speech Sciences, University of Maryland

The long-term goal of this project is to quantify schoolaged, normally-hearing (NH) children's processing of complex pitch, and to compare their performance with that of their cochlear-implanted peers, who only have access to temporal envelope cues for pitch. As a first step, we are conducting two experiments with NH children aged 6 – 16 years. The goal of Experiment 1 is to measure psychometric functions for an F0-discrimination task in a 3interval forced-choice paradigm. The stimuli are broadband harmonic complexes (cutoff frequency of 20,000 Hz) with a reference F0 of 100 Hz. Each partial in the complex is in sine-phase, producing a maximally peaky summed waveform with a very salient pitch. Stimuli are roved to eliminate loudness cues. Preliminary results suggest a developmental trend, with higher thresholds and shallower slopes in younger children. In Experiment 2, children's ability to discriminate the amplitude modulation (AM) rates of broadband sinusoidally AM noise is measured using an identical paradigm and a reference AM rate of 100 Hz. Preliminary results indicate that, as for adults, this task is far more difficult for the children than the F0 discrimination task: the pitch information conveyed by the envelope modulation alone (i.e. purely temporal) is much weaker than that conveyed by both spectral and temporal cues. No developmental trends have been observed so far in Experiment 2. In further analyses, possible effects of cognitive factors (e.g. conservativeness and inattention) will be modeled using the Ratcliff diffusion model. Preliminary analysis of response time (RT) and accuracy data obtained in these experiments indicates shorter RTs for correct responses than for incorrect responses, suggesting that the participants were not sacrificing accuracy for speed. [Work supported by NIDCD R01 004786-S1]

477 The Effect of Ambiguity on Pitch Discrimination of Simple and Complex Tones Pablo Karpenkopf¹, Miriam Furst¹

¹Tel Aviv University

Pitch discrimination of simple tones have been studied since the middle of the19th century with the classical research of Weber. Since then numerous studies have been elaborated including measurements and models. In most models, the main assumption is that the brain estimates the simple tone's pitch while considering only its frequency. A well known result for simple tone discrimination was obtained by Siebert (1968) and Heinz et al. (2001), where the pitch Just Noticeable Difference (JND) was derived by Cramer-Rao lower bound estimation on basis of the statistical properties of the auditory nerve fibers. In general, the derived pitch JND as a function of frequency reminded the experimental results, but the actual values were lower in orders of magnitude than the experimental results.

We suggest a different approach in estimating the pitch discrimination of simple tones. We assume that the brain uses a similar procedure to estimate the pitch of simple tones as well as complex tones. Models that explain phenomena of pitch of complex tones in particular missing fundamental and pitch ambiguity, usually consider in addition to the pitch's true frequency also its subharmonics.

We have derived the pitch JND in the brainstem level where excitatory-excitatory (EE) neurons exist. The pitch JND derivation is based on Barankin lower bound estimation, while considering the true frequency and also its sub-harmonics.

The derivations predicted the experimental results of both pitch discrimination of simple and complex tones. We thus suggest that for every input stimulus, the pitch estimation is performed by EE neurons in the brainstem in similar manners.

478 Tone and Formant Frequency Discrimination in Rabbits

Douglas C. Fitzpatrick¹, Nene Ugoeke¹, Charles C. Finley¹, Baishakhi Choudhury¹, Christine DeMason¹, Faisal I. Ahmad¹

¹University of North Carolina at Chapel Hill

A primary characteristic of an animal's hearing is the ability to discriminate frequency. In humans, for moderate and high intensities up to 2 kHz the frequency limen for tones is only a few Hz. Discrimination of a change in a formant frequency (e.g., the F2) within a vowel is more difficult, with about a 1.5% frequency limen or ~30 Hz at 2 kHz. In cats, the pattern of tone and formant discrimination is reversed, with a frequency limen to 1700 Hz tones of ~100 Hz, while the F2 formant discrimination for the same frequency is ~25 Hz, i.e., nearly the same as humans (Heinz et al, JASA 100:1052-1058,1996). For this study we tested the comparable discrimination in rabbits. Rabbits are being increasingly used as a physiological preparation for central auditory physiology, so knowledge of their frequency discrimination is of intrinsic interest. The results can also be used to determine if the pattern of discrimination between tone and formant frequencies is similar to that of humans or cats.

Four rabbits were trained with a two-alternative choice procedure using positive (food reward) reinforcement (Gai et al., JARO 4:522-538, 2007). In a sound-attenuated chamber, rabbits faced a row of three nose-poke holes with infrared detectors. A nose poke into the central hole initiated delivery of a free-field sound. For a standard frequency tone or F2 frequency in a synthesized vowel a nose poke in the left hole resulted in a food reward (a hit) while for a test tone or F2 higher than the standard a nosepoke in the right hole was rewarded (a correct rejection). Animals were first trained to detect the endpoints of the sounds until they reliably reached >80% correct responses. They were then tested with adaptive changes in the test frequencies using a 1 up/1 down procedure. Thresholds for a track were determined as the mean of the last eight of fourteen reversals. The tone and formant frequencies used as a standard were 1500 Hz, the duration was 500 ms, rise/fall time was 50 msec, and the intensity was 80 dB SPL.

Tone frequency discrimination was comparable to that in cats (~100 Hz). Similar to the pattern in humans, the F2 resolution was lower than tones, by a factor of 2-5 across the rabbits. These results indicate that the frequency resolution for tone and F2 frequencies in rabbits is lower than in humans, but that the pattern between them is similar.

Supported by NIDCD R21-DC009475 and T32-DC005360

479 Spectral-Shape Discrimination at High Frequencies

Christophe Micheyl¹, Huanping Dai², Andrew J. Oxenham¹

¹University of Minnesota, ²University of Arizona

The ability to detect or discriminate changes in the spectral shape of sounds ("profile analysis") plays an important role in numerous aspects of auditory perception. Although there have been many studies of profile analysis, relatively few of these have used stimuli at high frequencies (above 4-5 kHz), or have measured profile analysis for a variety of spectral shapes in the same listeners. Here we report the results of a series of discrimination experiments involving level changes to one or more components in inharmonic complex tones, bandpass filtered into either a "low" (1 to 1.6 or 2.4 kHz) or a "high" (8 to 12 or 17 kHz) spectral region. The complexes were produced by summing sinusoidal frequency components spaced 1 or 1.8 equivalent-rectangular auditory-filter bandwidths (ERBs) apart, ensuring that there were always four components within the stimulus passband. By varying the component levels, different spectral shapes were produced, including equal-amplitude components, one component raised relative to the others, and multiple components raised in various configurations. Overall level was either randomized across stimulus presentations or fixed, and thresholdequalizing noise was either present or absent. The results consistently higher thresholds showed for the discrimination of spectral shapes differing in the level of a single component than for the discrimination of spectral shapes differing in more than one component. In addition, thresholds were usually higher for the higher spectral region than for the lower spectral region, with the effect of frequency depending on the task. The data were compared against predictions of ideal and sub-optimal observer models with and without cross-channel correlations. The results provide new constraints on models of spectral profile analysis, and further insight into the cues and strategies used by human listeners to discriminate spectral shapes at low and high frequencies. [Supported by NIH grant R01 DC 05216.]

480 Behavioral and Modeling Studies of Amplitude-Modulation Detection Using Reproducible Modulation Maskers

Laurel H. Carney¹, Kristina S. Abrams¹, David R. Axe¹ ¹University of Rochester

Studies of detection in the presence of maskers have extended our understanding of coding and processing of sounds, especially in complex environments. Here, the use of reproducible maskers has been applied to a behavioral study of masked amplitude-modulation (AM) detection. Performance in a task with reproducible maskers provides a challenging test for models of masked detection. Many models are able to explain average performance, but not the detailed differences in performance from masker to masker. In behavioral experiments with Dutch-belted rabbits, hit and false-alarm rates were measured for a set reproducible, "frozen," modulation masker of or waveforms. Maskers were 32-Hz bandwidth noises

centered at the AM target of 64 Hz. The carrier was a 5 kHz tone, and stimuli were presented at 65 dB SPL. Performance varied significantly across masker waveforms. Performance for each masker waveform was characterized by a hit rate (the proportion of trials with sinusoidal AM targets that were correctly identified) and a false-alarm rate (the proportion of trials without AM targets that were incorrectly responded to as having targets.) Approximately 50% of the variance in the hit rates across masker waveforms could be explained by differences in the energy of the envelope, which is influenced differently from masker to masker by the addition of the target. The variance in false-alarm rates across different waveforms was also significant, but this variance was not explained by differences in energy across maskers. Responses of a multi-channel computational model for responses of inferior colliculus neurons were significantly correlated to both hit and false-alarm rates for the set of reproducible maskers. Related psychophysical experiments are underway in human listeners, as well as physiological studies of AM-tuned neurons in the inferior colliculus of awake rabbit using identical modulation masker waveforms. Supported by NIH-NIDCD-R01-001641.

481 Perception of Time-Compressed Modulation Patterns

David Ives^{1,2}, Christian Lorenzi^{1,2}

¹Universite Paris Descartes, ²Ecole Sormale Superieure The ability to recognize time-compressed amplitudemodulated (AM) and frequency-modulated (FM) patterns was measured in young normal-hearing listeners. An XAB discrimination procedure similar to that developed by Ardoint et al. (2008) was used. The basic stimuli to be discriminated were generated by modulating 1-kHz pure tones by either a two-component AM modulator, or a twocomponent FM modulator using modulation rates below 5 Hz and random starting AM and FM phases. The recognition tasks were performed in guiet for increasing time-compression factors applied to these complex modulators. Preliminary data indicate that normal-hearing listeners are relatively poor at recognizing both timecompressed AM and FM patterns, although the ability to resist time compression may be slight better for FM patterns. The results will be discussed in light of previous psychoacoustical (Ardoint et al., 2008) and speech perception data (Fu et al., 2001).

References

Ardoint, M., Lorenzi, C., Pressnitzer, D., & Gorea, A. (2008). Perceptual constancy in the temporal envelope domain. J Acoust Soc Am, 123, 1591-1601.

Fu, Q.-J., Galvin, J. J. & Wang, X. 2001. Recognition of time-distorted sentences by normal-hearing and cochlear-implant listeners. J Acoust Soc Am, 109, 379-384.

Acknowledgments

This work was supported by Starkey Laboratories, Inc.

482 Signal Detection and Criterion Setting in Ferret Psychoacoustics

Ana Alves-Pinto¹, Joseph Sollini¹, Chris Sumner¹ ¹*MRC Institute of Hearing Research*

Behavioural responses in psychoacoustical experiments can reflect not only the limitations of the sensory system but also the influence of non-sensory factors in the decision process. Understanding the factors that contribute to behavioural responses, especially in animals, may be important in correlating perception and neural responses. Here, a computational model based on signal detection theory, and trial-by-trial data analysis, was used to explore potential factors contributing to ferret behavioural responses in a tone-in-noise detection task.

A single-interval 2AFC procedure was used to measure ferret performance in the detection of a 10-kHz tone in a continuous background noise. Ferret's tended towards low false alarm rates, but the decision criterion depended on the range of stimulus levels presented within the session. We further manipulated the decision criterion by varying rewards, and obtained an ROC consistent with standard signal-detection theory. A simple model, which assumed a stationary internal noise component, and an across behavioural session variability in decision criterion, provided a reasonable explanation of the ferrets' behaviour. Inattention, modelled as a tendency to guess on a proportion of trials, did not seem to contribute substantially to the model fits. Rather, the model implied considerable variability in decision criterion.

Further analysis showed that decision criterion was in-fact varying on a trial-by-trial basis. For example, signalling the presence of a tone was more likely to occur after a correct rejection than after a hit. Furthermore, this trial-to-trial dependency occurred mostly at tone levels close to threshold and was minimal at clearly audible levels. An additional factor was introduced to the model to account for the trial to trial dependence observed. Thus ferrets' performance was consistent with signal-detection theory, with the outcome of recent trials being an important factor in determining their decision criterion.

483 Channelrhodopsin-2 Mediated Optical Stimulation of the Cochlea

Victor Hernandez¹, Hoch Gerhard¹, Nicola Strenzke¹, Zhizi Jing¹, Hideki Takago¹, Gerhard Vogt², Garnham Carolyne², Bamberg Ernst³, George Augustine⁴ ¹InnerEarLab, Department of Otolaryngology. University of Goettingen, ²MED-EL Deutschland GmbH, ³MPI for Biophysics, Frankfurt, ⁴Duke University

Electrical auditory prostheses are among the most advanced neuroprostheses. Providing auditory input to the auditory pathway, cochlear implants, the most commonly used prostheses, enable open speech comprehension in the majority of the implanted deaf subjects. Still, sound encoding driven by the current cochlear implants is limited. For example, cochlear implants make limited use of the tonotopically ordered projections to the brain employing only 12-22 separate channels in order to avoid electrode cross-talk. While the auditory performance of successful cochlear implant users highlights the incredible capabilities

of the CNS to extract information from the limited sensory input, it remains an important task to improve the frequency resolution of cochlear implants. Here, we explored the use of channelrhodopsin-2 (ChR2) expression in spiral ganglion neurons for optical stimulation of the auditory pathway. Coupling blue light (emitted by LED or laser) into a cochleaostomy of transgenic mice expressing ChR2 (Arenkiel et al., 2007) in the first auditory neurons caused large compound potentials in scalp recordings. These potentials were present also after acute deafening but were blocked when action potential generation was inhibited by application of tetrodotoxin and lidocaine. The dependence of response amplitude on stimulus duration, rate and light power was systematically explored. Neural responses to sound could be masked by optical stimulation. Single auditory neuron responses to optical stimulation of the cochlea are currently being studied in the cochlear nucleus and the inferior colliculus. In summary, ChR2-mediated optical stimulation of cochlea seems feasible.

484 Channelrhodopsin-2 Gene Transfection of Central Auditory Neurons: Toward an Optical Prosthesis

Leah Acker^{1,2}, Bernice Huang³, Ken Hancock³, William Hauswirth⁴, Ed Boyden^{5,6}, M. Christian Brown^{3,7}, Daniel Lee^{3,7}

¹*Harvard/MIT Division of Health Sciences and Technology,* ²*MIT Media Lab / Eaton Peabody Laboratory, Massachusetts Eye and Ear Infirmary,* ³*Eaton Peabody Laboratory, Massachusetts Eye and Ear Infirmary,* ⁴*Department of Ophthalmology, University of Florida,* ⁵*MIT Media Lab,* ⁶*MIT Biological Engineering / Brain and Cognitive Science,* ⁷*Department of Otology and Laryngology, Harvard Medical School*

The performance achieved by auditory brainstem implants is limited. A new prosthesis based on optical stimulation might offer more selectivity than those based on electrical stimulation due to a sharper focus of activation. Channelrhodopsin-2 (ChR2) is a light sensitive protein that can be expressed by mammalian neurons of the brain when delivered by an adeno-associated viral (AAV) vector. Visible light (473 nm) has been shown to depolarize photosensitized hippocampal neurons (Boyden et al. (2005) Nat Neurosci. 8:1263-68). We are applying a similar approach to neurons of the auditory brainstem. In short-term guinea pig and rat experiments, we deliver ChR2 to the cochlear nucleus (CN) using a craniotomy approach and single injection of AAV2 that includes a GFP-linked ChR2 gene and modified CBA promoter. Following a two to three week survival, we evaluated ChR2-GFP expression using both light and fluorescent immunohistochemistry. Labeling in successful cases was seen in all three CN subdivisions (AVCN, PVCN, and DCN). Labeling was also seen outside the CN - near the injection site - but not elsewhere in the brainstem. Although a variety of cell types within the CN were found to express ChR2-GFP, multipolar cells were the most commonly observed. In DCN, fusiform and cartwheel cells were labeled, consistent with the pattern seen by Shimano et al. (2009, ARO abstr. #1162). ChR2GFP expression was also seen in octopus cells of the PVCN as well as bushy cells of the PVCN and AVCN. The broad pattern of expression observed in our experiments may provide the foundation for future development of an optical auditory brainstem implant, but physiological data are needed to determine whether the pattern of excitation is more focused for optical vs. electrical stimulation. Supported by the Helene and Grant Wilson Auditory Brainstem Implant Program at MEEI, the NDSEG Fellowship program, NIH Grant DCD 01089, NSF, and the McGovern Institute and Media Lab at MIT.

485 Optical Stimulation of Cochlear Neurons: Role of TRPV Channels

Jennifer Decker¹, **Suhrud Rajguru**¹, Alan Robinson¹, Claus-Peter Richter^{1,2}

¹Northwestern University, ²Hugh Knowles Center, Northwestern University

A potential mechanism of optical stimulation of neurons with pulsed infrared radiation (IR) is via local, transient changes in temperature, which can affect thermally-gated ion channels. In neural tissues, several temperature-gated transient receptor potential vanilloid (TRPV) ion channels have been identified. TRPV channels are known to be of functional significance in both, the rat and the guinea pig cochlea. To study the potential role of TRPV channels in the mechanism of IR driven neural response, optical stimulation of the guinea pig cochlea was performed in the presence of the TRPV channel antagonists (capsazepine, ruthenium red and lanthanum chloride). Cochlear stimulation was achieved with a diode laser (Capella, LHM Aculight) at a wavelength of 1862 nm pulse duration of 100 us, and 10 Hz repetition rate. The radiation was delivered via a 200 µm fiber, which was placed through a basal turn cochleostomy. The channel antagonists were diluted in artificial perilymph solution at various concentrations so that dose-response curves could be determined. Perfusion was performed via a second basal turn cochleostomy at 3 µL/min and the perfusate allowed to drain from an apical cochleostomy. Cochlear function was measured by recording compound action potential (CAP) curves in control condition, after perfusion of artificial perilymph and after perfusion with the drugs. Guinea pig cochleae exposed to the TRPV antagonists showed a marked reduction in CAP amplitudes. The effect was reversible in many cases by wash with perilymph. The results demonstrate that TRPV channels in the cochlea play a significant role in the sensitivity of neurons to IR. In addition, given the ability to focus the radiation, pulsed IR could potentially be applied to provide new insights into the temperature-based mechanism of TRPV channel activation.

[This work has been supported by the NIH1R41DC008515-02 and by LMA]

[486] Temporal Properties of Inferior Colliculus Neurons from Cochlear Infrared Neural Stimulation

Agnella Matic¹, Suhrud Rajguru¹, Whitney Zirkle¹, Andrew Fishman¹, Claus-Peter Richter¹

¹Northwestern University

One of the key questions in stimulating cochlear spiral agnalion neurons with infrared neural stimulation (INS) is whether the temporal structure of speech can be precisely encoded with an optical stimulus. In the present study, we characterize the patterns of neuronal activity to irradiation of the cochlea with infrared pulses. A multichannel electrode placed in the central nucleus of the inferior colliculus (ICC) recorded neural activity in response to INS of spiral ganglion neurons, both in normal hearing and deafened guinea pigs. At 50 recording sites, the peristimulus histograms showed a single maximum with a latency of ~5.4 ms after the presentation of stimulus. Increasing the stimulus intensity elicited multiple maxima and reduced the latency of the first maximum to ~5.1 ms. A second maximum was typically observed at 7.7 ms, whereas the third maximum appeared in about one-guarter of the neuron clusters with a latency of 9.4 ms. Changing the stimulus pulse duration did not affect the response pattern. To measure the entrainment of the ICC neurons, the pulse repetition rate was varied from 10 to 300 pps. ICC neurons had an entrainment value of ~1 at repetition rates of up to 200 pps. At higher repetition rates, INSevoked spatial tuning curves became narrower and had higher thresholds at the best frequency. The results are in concert with data from traditional cochlear implant stimulation. The data suggest that cochlear INS could provide stimulation with the appropriate temporal resolution to encode speech in future optical cochlear implants.

Supported with federal funds from the NIDCD, NIH, Dept of Health and Human Services, Contract No. HHSN260-2006-00006-C / NIH No. N01-DC-6-0006.

487 Channel Separation During Infrared Neural Stimulation

Claus-Peter Richter¹, Laura Moreno¹, Agnella Matic¹, Suhrud Rajguru¹

¹Northwestern University

It has been shown that infrared neural stimulation produces more selective response profiles than electrical stimulation does. However, it is not clear whether the increased selectivity results in a larger number of channels that can be stimulated at the same time. With the present experiments, we estimate the number of channels that can be used in the cochlea for INS, based on the results obtained in the guinea pig cochlea.

Spread of excitation was mapped with a 16-channel NeuroNexus thin film electrode inserted into central nucleus of the guinea pig inferior colliculus. From the neural response, spatial tuning curves (STCs) were constructed and the widths of the tuning curves were measured. Histological reconstructions were made to correlate the spatial tuning curves with the actual stimulation sites along the cochlea. Temperature measurements using thermochromic ink were made in hemicochleae preparations to determine the heat load, which might occur for pulse repetition rates above 100 Hz and with radiation energies at threshold and ten times above threshold.

STC widths were measured for pure tones and for optical stimulation. INS is about four times more selective than monopolar electrical stimulation as INS stimulates only the structures that are in the beam path of the radiation. The heat load at threshold and at 400 Hz pulse repetition is nearly twice the diameter of the optical source - for the 200 μ m optical fiber it was about 300-400 μ m.

Supported with federal funds from the NIDCD, NIH, Dept of Health and Human Services, Contract No. HHSN260-2006-00006-C / NIH No. N01-DC-6-0006.

488 Infrared Radiation of Cochlear Spiral Ganglia: Optical Beam Size and Spread of Excitation in the Inferior Colliculus

Suhrud Rajguru¹, Agnella Matic¹, Brian Goico¹, Andrew Fishman^{1,2}, Claus-Peter Richter^{1,2}

¹Northwestern University, ²Hugh Knowles Center, Northwestern University

Infrared radiation (IR) to stimulate neurons has received considerable attention recently and the feasibility of cochlear implants based on IR irradiation of the spiral ganglion is being explored. A practical optical cochlear implant will need a balance between the optical beam size and the spread of excitation within the spiral ganglia. Individual optical fibers or the radiation beam need to be small enough to obtain a spatially restricted stimulation of the spiral ganglion. On the other hand, the optical beam size must provide stimulation to a relevant population of neurons to encode necessary information. In the present study, we determined the correlation between beam size and the width of the spatial tuning curves that were constructed from the responses in central nucleus of inferior colliculus (ICC) to straight-tip and angle-polished optical fibers. We recorded responses with a 16-channel NeuroNexus electrode, which was inserted into the ICC, perpendicular to the iso-frequency laminae. The spread of activity in the ICC from peripheral stimulation with different optical fiber sizes was monitored. Four fiber sizes, viz. 50, 100, 200 and 400 µm dia., were used to optically stimulate the spiral ganglion neurons of the normal hearing guinea pigs before and after deafening with a intracochlear injection of neomycin. Spatial tuning curves of ICC responses were recorded by varying optical radiation energy. Results show that the tuning curves corresponding to the activity of ICC were spatially restricted for smaller diameter fibers and fibers with angle-polished surfaces. Though a larger dynamic range was possible with the 200 and 400 µm fiber. The activation patterns recorded from ICC correlated with data from histology. The results are important for the design of a future cochlear implant device based on optical stimulation. [Supported by federal funds from the NIDCD, NIH, Dept of Health and Human Services, Contract No. HHSN260-2006-00006-C / NIH No. N01-DC-6-0006.]

489 Optical Stimulation of the Auditory Nerve: Effects of Pulse Shape

Renee Banakis¹, Agnella Izzo-Matic¹, Suhrud Rajguru¹,

Claus-Peter Richter¹

¹Northwestern University

It has been demonstrated by several groups that neurons can be stimulated with infrared radiation or IR (Richter et al., 2010). Previous studies revealed that pulse durations as long as 200 µs with repetition rates up to 200 Hz can continually stimulate spiral ganglion cells over 10 hours and evoke cochlear compound action potentials (CAPs) (Rajguru et al., 2010). Furthermore, for the deafened cochlea, shorter pulse lengths appear to be more efficient in evoking compound action potentials (Richter et al., The latter conclusion was made from graphs 2008). showing the peak-to-peak amplitude of the CAP versus the radiation exposure; however, if the same CAP amplitudes are plotted versus the radiation power, shorter pulse lengths no longer appear more efficient (Izzo, 2007). Considered together, these data suggest that the transient of the optical pulse and not the total energy is the important factor in determining the response. In the present study, the auditory nerves of acutely deafened gerbils were stimulated with IR, which was delivered to the spiral ganglion cells by an optical fiber placed in front of the round window. Optical stimuli consisted of four different pulse shapes (triangular, square, ramp up and ramp down) presented at varying pulse durations, radiant exposures, and fine temporal structures. Compound action potentials were recorded via a round window electrode for increasing radiant energy/radiant power. Results show that the peak power is the important variable for stimulating auditory neurons. It has also been demonstrated that variations in rise time (110-910 µs) do not affect optical thresholds, suggesting that more efficient stimulation may be obtained by using pulses with longer rise times.

This work has been supported by the NIH1R41DC008515-02 and by Lockheed Martin Aculight.

490 Optical and Electrical Co-Stimulation in the Cochlea

Michael J. Jung¹, Suhrud Rajguru¹, Claus-Peter Richter^{1,2} ¹Dept. of Otolaryngology, Northwestern University, ²Dept. of Biomedical Engineering, Northwestern University

Previous studies with the sciatic nerve have demonstrated that the simultaneous presentation of a sub-threshold electric current pulse and an infrared laser pulse can reduce the threshold for infrared neural stimulation (INS). The application of such co-stimulation in the cochlea may reduce the heat and energy necessary to stimulate the tissue with each optical pulse and prevent damage to the heat sensitive tissue.

To test the effect of co-stimulation, experiments were conducted in guinea pigs. The cochlea was exposed surgically and two cochleostomies were made, one for the optical fiber and the second for a silver ball electrode. A craniotomy was made to insert a 16-channel electrode into the inferior colliculus to record neural responses evoked from the peripheral stimulation in the cochlea. For selected channels, the field potentials were used to quantify the responses. During the experiments, the amplitude of the optical and the electrical stimuli were varied systematically; the range of the radiant energy was between 0 and 80 μ J, the current amplitude was between 0 and 500 μ A. Optical pulses were 100 μ s and electrical pulses were biphasic pulses 250 μ s per phase. Stimuli were presented at a rate of 4 Hz. The time between the optical and the electrical stimuli, and the order at which the two stimuli were presented, were also changed systematically.

Preliminary results suggest that the stimuli are synergistic if presented at the same time and antagonistic if presented with an inter-stimulus delay. Moreover the effect appears to be highly non-linear.

[Supported with federal funds from the NIDCD, NIH, Dept of Health and Human Services, Contract No. HHSN260-2006-00006-C / NIH No. N01-DC-6-0006]

491 Histological Evaluation of the Cochlea Following Chronic Infrared Neural Stimulation

Alan Robinson¹, Margaret Hwang¹, Suhrud Rajguru¹, Agnella Matic¹, Claus-Peter Richter^{1,2}

¹Northwestern University Chicago, ²Hugh Knowles Center, Northwesten University

Infrared neural stimulation (INS) has been explored as an alternative for neural interfaces, and one potential application is in cochlear implants. We have demonstrated that INS is possible in the cochlea, that the spatial tuning curves (STCs) constructed from neural activities in the inferior colliculus during INS are narrower in comparison to electrical stimulation, and that 10 hour continual stimulation at 200 Hz in the cat did not change optically evoked compound action potential amplitudes or result in tissue damage. To evaluate long-term safety of INS in the cochlea, cats were chronically implanted and stimulated six hours per day for up to six weeks. Cochlear function was tested periodically during the stimulation period and cochleae were examined histologically for thermal damage and tissue growth. Eight weeks following implantation, the cats were euthanized and the cochleae were fixed with 4% paraformaldehyde in Ringer's lactated solution. After fixation, cochleae were decalcified for ~1 month before they were paraffin embedded. Cochleae were sectioned at 10 µm and were subsequently stained with hematoxylin. Digital images of the sections were captured and cochleae were reconstructed using the Amira software. Α semiautomatic segmentation procedure was used for area and subsequent volume rendering. Histology revealed no gross abnormality of spiral ganglion cells. There was tissue growth which was mainly confined to the middle ear and to a small area close to the optical fiber.

[This work has been supported by the NIH1R41DC008515-02 and by Lockheed Martin Aculight.]

492 Linguistic Development in Children with Bilateral Cochlear Implants

Christi Hess¹, Shelly Godar¹, Cynthia Zettler², Sara Misurelli¹, Susan Ellis-Weismer¹, Ruth Litovsky¹ ¹University of Wisconsin- Madison, ²Nemours Growing evidence suggests that children who are deaf and

use cochlear implants (CIs) can develop spoken language. Age of implantation and length of experience with the CI may play an important role in a predicting a child's linguistic development. In recent years, the increasing number of children with bilateral CIs presents new variables such as length of bilateral listening experience and time between the two CIs that may also play a significant role in the development of hearing, speech, and language abilities. Children with bilateral CIs (n=43; ages 4-9) who are being followed longitudinally were tested on measures, the Test of standardized Language Development (TOLD) and the Leiter International Performance Scale-Revised (Leiter-R), to evaluate their expressive/receptive language and IQ/memory. Measures on these variables are compared with measures of spatial hearing abilities, and with published results of a cohort of children who underwent unilateral implantation prior to age 5 years (Niparko et al., JAMA. 303:1498-506, 2010). Preliminary results show that, while large intersubject variability exists, speech and language development improves as a function of both hearing age and bilateral experience. Age of implantation effects were observed for both speech and language scores as well as IQ scores.

493 Dynamic Binaural Detection in Bilateral Cochlear-Implant Users: Implications for Processing Schemes

Matthew Goupell¹, Ruth Litovsky¹, Seymanur Celik¹ ¹University of Wisconsin - Madison

A majority of binaural research in bilateral cochlear-implant (CI) users has employed constant-amplitude or regularly time-varying stimuli. The purpose of this work is to explore binaurally dynamic stimuli, namely detection of changes in interaural correlation and detection of out-of-phase sine tones embedded in in-phase noise (NoS π). These tasks were tested using bilaterally pitch-matched pairs of electrodes in eight bilateral CI listeners. The inherent envelope modulation rate and pulse rate of electrical stimulation were varied. CI listeners were on average worse at detecting changes in interaural correlation than normal-hearing (NH) listeners tested with vocoder simulations, although performance in the best CI listeners was similar to the average NH data. Some CI listeners showed effects of envelope modulation rate and stimulation rate, although inter-individual variability obscured overall significant effects. In comparison, NH listeners showed no effect of envelope modulation rate and stimulation rate. An analysis of the electrical stimuli properties suggests factors related to stimulus processing (e.g., electrical dynamic range, loudness growth curves, and compression) affected performance more than sensitivity to static interaural time differences. These data will be discussed in terms of challenges and

considerations for bilateral and multi-electrode processing strategies that are designed for speech understanding.

494 Do Bilateral Cochlear Implant Patients Have Binaurally Coherent Representations? Justin Aronoff¹, Qian-Jie Fu¹

¹House Ear Institute

In normal hearing (NH), there is a "binaural coherence" that binds the internal representations of sound from each ear. Interaural timing differences (ITDs) are interpreted in relation to this binaural coherence. However, with bilateral cochlear implants (CIs), this binaural coherence may be disrupted due to differences in the internal representations from each ear (e.g., spectral cues, timing cues), which may partly explain why bilateral CI listeners have difficulty using interaural timing differences (ITDs). We devised two ITDbased experiments to investigate binaural coherence in CI users: 1) bilateral detection of a tone in noise and 2) lateralization of an amplitude-modulated broadband noise. In both experiments, we manipulated the relationship between the representations from each ear by varying the interaural correlation of the noise. If binaural coherence is intact, reducing the interaural correlation should reduce performance. If binaural coherence is disrupted, reducing the interaural correlation should have no effect on performance. CI subjects were tested while using their clinical processors and settings. NH subjects were tested while listening to 8-channel CI simulations. In both tasks, NH performance improved with increased interaural In contrast, CI users demonstrated no correlation. sensitivity to changes in interaural correlation for either task. This suggests that binaural coherence may indeed be disrupted in bilateral CI users. The results further suggest that clinical fitting of bilateral CIs should aim to restore binaural coherence (e.g., spectrally matched patterns from each ear).

495 Effect of Target-Interferer Similarity on Spatial Release from Masking in Children with Bilateral Cochlear Implants and with Normal Hearing

Sara Misurelli^{1,2}, Shelly Godar^{1,2}, Ruth Litovsky^{1,2}

¹University of Wisconsin-Madison, ²Waisman Center Speech intelligibility improves when target speech and interferers are spatially separated, compared to when they are co-located, an effect known as spatial release from masking (SRM). SRM was studied in children with bilateral cochlear implants (BiCls), hearing-ages (HA) 4.0-6.5 and 6.5-9.0 years, and in children with normal hearing, matched for HA. SRM was measured for male-voice target stimuli in the presence of interferers that comprised of male talkers, and compared with previous results using female talker interferers, to evaluate effects of informational masking. In addition, effects of spatial cues were investigated by having the interferers positioned in azimuth either symmetrically (+/-90°) or asymmetrically (+90°). On average, normal hearing groups exhibited greater amounts of SRM with the male than female interferers, especially in the asymmetrical condition which allowed users to take advantage of both binaural and monaural (better ear) cues. In contrast, the two BiCl groups showed very small SRM with both male and female interferers. This may be due to the fact that cochlear implant processors do not preserve fine structure, interaural difference and pitch cues, which are relevant for source segregation in complex listening situations.

Work funded by NIH-NIDCD (Grant No. 5R01DC008365 to Ruth Litovsky)

496 Psychophysical Measures of Sensitivity to Interaural Time Difference Encoded in the Envelope and the Fine Structure with Bilateral Cochlear Implants

Victor A. Noel¹, Donald K. Eddington^{1,2} ¹Cochlear Implant Research Laboratory, Massachusetts Eye and Ear Infirmary, ²Department of Otology and Laryngology, Harvard Medical School

Today's commercial bilateral speech processors discard the signal's fine-structure and instead use unsynchronized pulse carriers. This results in an incorrect fine-structure interaural-time-difference (ITD). There is debate as to whether this lack of synchronization is important, because bilateral implantees have poor sensitivity to ITD at the high pulse rates commonly used. Recent neuron recordings in the inferior colliculus of a bilaterally implanted cat model demonstrated good ITD sensitivity to a 1000 pps pulse train if the pulses were amplitude modulated by a 40 Hz sine wave, suggesting that modulation could restore sensitivity to high rate pulses.

Motivated by the animal physiology findings, we tested the hypothesis that modulation could restore ITD sensitivity to high rate pulses in human bilateral cochlear implant users. Psychophysical ITD thresholds were measured while presenting modulated pulses for three conditions: ITD encoded in the carrier alone, in the envelope alone, and in the whole waveform. Our results showed no sensitivity to ITD in the 1000 pps carrier, even with modulation.

In a separate but related experiment, we investigated the sensitivity to ITD encoded only by the envelope while varying the envelope frequency. We found that sensitivity was best at modulation frequencies near 100 Hz, with thresholds almost as good as for 100 pps unmodulated pulse trains. However, if the modulation frequency was outside of the narrow optimal range of 50 to 100 Hz, sensitivity degraded very rapidly.

This work was supported by NIH grant R01-DC005775

497 Binaural Interference in Bilateral Cochlear Implant Listeners

Virginia Best^{1,2}, Bernhard Laback³, Piotr Majdak³ ¹Boston University, ²University of Sydney, ³Austrian Academy of Sciences

This work was aimed at determining whether binaural interference occurs in electric hearing, and if so, whether it occurs as a consequence of perceptual grouping (central explanation) or if it is related to the spread of excitation in the cochlea (peripheral explanation). Six bilateral cochlear implant users completed a series of experiments in which they judged the lateral position of a target pulse train, lateralized via interaural time or level differences, in the presence of an interfering diotic pulse train. The target and interferer were presented at widely separated electrode pairs (one basal and one apical). The results were broadly similar to those reported for acoustic hearing. All listeners but one showed significant binaural interference in at least one of the stimulus conditions. In all cases of interference, a robust recovery was observed when the interferer was embedded in an ongoing stream of identical pulse trains, suggesting that the interference was centrally mediated. Overall, the results provide an objective demonstration of both simultaneous and sequential grouping mechanisms in binaural electric hearing.

498 Dichotic Stimulation with Cochlear Implants: Maximizing the Two-Ear Advantage Ning Zhou¹, Li Xu²

¹*Kresge Hearing Research Institute University of Michigan,* ²*Ohio University*

The present study explored the potential benefit of dichotic stimulation for increasing spectral resolution in bilateral implantation. The novel dichotic speech processing strategy took advantage of the doubled number of functioning electrodes in bilateral implants so that incoming signals could be analyzed in twice the number of frequency channels. By assigning the left implant with the odd-numbered channels and the right implant with the even-numbered channels, the strategy stimulated the two implants dichotically with exclusive and complementary spectral information. The bandwidth per channel was half that in a single monaural implant or a bilateral implant that uses diotic stimulation. It was examined whether the increased spectral resolution via dichotic stimulation improved music perception, tone-language perception, and English speech perception in noise. Dichotic advantage was first evaluated in an acoustic simulation of bilateral implants using normal-hearing listeners. Music tests included a familiar melody test and a musical-interval discrimination test. Both tests used music stimuli without rhythmic cues. Mandarin tone perception was measured when the temporal envelope cue was band restricted to 160 Hz and 4 Hz, respectively. Frequency-place mismatches were examined in both music and tone perception tests but showed minimal effects. English speech recognition was measured in two types of noise: a competing female talker and a speech-shaped steadystate noise. Results of the simulation data showed a dichotic advantage for music perception, tone perception based on a place code (i.e., temporal cue restricted to 4 Hz), and speech perception in noise, particularly with the competing female talker. Five bilaterally implanted subjects were also tested with dichotic stimulation in a music interval discrimination test, a frequency discrimination test, and a speech reception threshold test. . Dichotic stimulation did not seem to have a significant effect on music perception; however, it significantly improved frequency discrimination and speech reception thresholds in cochlear implant subjects. Results of the study have

direct clinical implications for optimizing the mapping strategy in bilateral implant patients.

Work supported by NIH NIDCD Grants F31-DC009919 and R15-DC 009504.

499 Bimodal Benefit in Listeners Who Use a Hearing Aid (HA) and a Cochlear Implant (CI) in Opposite Ears

Mario Svirsky¹, Arlene Neuman¹, Susan Waltzman¹ ¹New York University

New audiometric criteria for cochlear implantation have yielded a quickly expanding group of patients who have some residual hearing and may benefit from use of a HA in the contralateral ear. Thus, it is important to examine the "bimodal benefit" a listener may develop after cochlear implantation: the difference between scores obtained in the bimodal condition and in the best unilateral condition.

The present study retrospectively examined speech perception in 32 bimodal CI users. Subjects were postlingually deaf adults who were tested with a hearing aid in the unimplanted ear before and after implantation (mean time post-implant=2.6 years), using the CNC word test. Subjects whose unaided thresholds in the unimplanted ear changed by 10 dB or more between the pre- and the post-implant session were excluded from this analysis. Bimodal benefit post-implantation was examined, as well as pre-to-post implant differences in speech perception under three conditions: binaurally, in the implanted ear, and in the unimplanted ear.

Bimodal benefit averaged 4.8% and ranged from +30% to -14% (negative numbers indicate bimodal interference rather than benefit). Binaural speech perception was significantly better post- than pre-implant for 25 of the subjects (NS difference for the other 7). Speech perception was significantly improved post-implant in the CI ear for all subjects except one, who showed no change, and there was a significant correlation between pre-implant and post-implant scores. Lastly, post implant speech scores in the unimplanted ear decreased significantly for eleven subjects and increased significantly for two subjects.

Taken together, these results support the practice of providing CIs to patients with residual hearing. Further studies are needed to determine why some individuals suffer from bimodal interference and why some unimplanted ears experience decreases in speech perception that cannot be explained by changes in hearing sensitivity.

500 Telephone Speech Perception by Electric and Acoustic Stimulation and Cochlear Implants

Yi Hu^{1,2}, Christina Runge-Samuelson², David Friedland², Philipos Loizou³

¹University of Wisconsin--Milwaukee, ²Medical College of Wisconsin, ³University of Texas--Dallas

Several studies have demonstrated the importance of lowfrequency information in combined electric and acoustic stimulation (EAS). The present study assesses the impact of introducing low or high frequency information in telephone speech perceived by bimodal users, who wear cochlear implant (CI) in one ear and hearing aid in the contra-lateral ear. In the proposed experiments, bimodal users were presented under quiet and noisy listening conditions with wide-band speech, bandpass-filtered (300-3400 Hz) telephone speech, high-pass filtered (f>300 Hz) speech and low-pass filtered (f<3400 Hz) speech. The filters are implemented according to the modified Intermediate Reference System (IRS) filters used in ITU-T P862. These experiments are designed to answer the following two questions: 1) Does use of hearing aid (HA) benefit perception of telephone speech by EAS listeners in quiet and noisy listening conditions? 2) Does telephone speech perception improve when access to low or high frequency information is provided? In guiet environments, results indicate that bimodal listening achieves the largest benefit when telephone speech was augmented with high (f>3400 Hz) rather than low-frequency information. For both cochlear implant alone and bimodal configurations, introducing low frequency information to telephone speech provided no significant improvement in intelligibility. These outcomes suggest that in quiet environments, in order to improve telephone speech recognition for both bimodal and CI users, techniques need to be developed to extend the signal bandwidth in the high frequencies. In noisy listening conditions, results indicate that for bimodal configurations, introducing low frequency information to telephone speech provided significant improvement in intelligibility.

501 Contributions of Processed Low-Frequency Acoustic Hearing to Single- And Concurrent-Vowel Recognition in Electro-Acoustic Hearing

Hsin-I Yang¹, Ling-Xuan Kong¹, Fan-Gang Zeng² ¹Department of Biomedical Engineering, University of California, Irvine, ²Department of Otolaryngology - Head and Neck Surgery, University of California, Irvine Both fundamental frequency and formants at low frequencies have been shown to contribute to concurrentvowel recognition in normal hearing subjects listening to cochlear implant (CI) simulations. To enhance the contribution of formants to electro-acoustic hearing, the first two formants were acoustically delivered to the residual low-frequency region through frequency lowering. Short-term training was conducted to help accommodation to the frequency-lowered vowels in a single- and concurrent-vowel recognition task. Five vowels were digitally synthesized to have the same duration and level. Eight normal hearing subjects and 4 CI subjects were trained and tested on 5 days under 7 listening conditions: (1) Unprocessed, (2) low-pass below 500 Hz, (3) frequency-lowering from 500-3000 Hz to 500-1000 Hz, (4) CI (5-channel CI simulation in normal controls and the clinically fitted processor in actual patients). (5-7) CI plus frequency-lowering, unprocessed. low-pass. and respectively. With 5-day training, asymptotic performance was achieved for single-vowel recognition. Training and testing continued for at least 3 days using 20 concurrentvowel pairs with 3 fundamental frequency combinations under the same listening conditions. The short-term training significantly improved learning and generalization of single- and concurrent-vowel recognition in normal and some CI subjects. In both recognition tasks, frequencylowering produced better performance than the low-pass condition, but did not produce additional electro-acoustic benefit to what was already achieved with the low-pass sound. The results suggested that the additional formant information provided by frequency-lowering overlaps with CI information, and that future improvement in combined acoustic and electric hearing needs to focus on efficient encoding of low-frequency fine structure.

502 Neuronal Masking Between Binaural-Bimodal Acoustic and Electric Cochlear Stimulation in Gerbil Inferior Colliculus and Lateral Lemniscus

Maike Vollmer¹, Tristan Bremer¹

¹Comprehensive Hearing Center, University Hospital Wuerzburg

There is increasing evidence that cochlear implant stimulation combined with contralateral acoustic hearing (binaural-bimodal stimulation, BBS) provides binaural benefits for subjects with unilateral deafness, including speech understanding in noise and directional hearing.

The goal of the present study was to examine neuronal interactions to BBS in the inferior colliculus (IC) and the dorsal nucleus of the lateral lemniscus (DNLL) of the Mongolian gerbil (Meriones unguiculatus). Normal hearing animals were unilaterally implanted with scala tympani electrodes, and an earphone was sealed to the contralateral auditory meatus for acoustic stimulation. Unmodulated electric pulse trains and acoustic tones at the neuron's characteristic frequency (CF) were presented using either a simultaneous- or a forward-masking paradigm. Extracellular single neuron responses were recorded ipsilateral to the acoustically stimulated cochlea using tungsten microelectrodes. Acoustic and electric stimuli served as both maskers and probes and were systematically varied in intensities.

Preliminary results show a small or no effect of the electric masker on the response rate and threshold to the acoustic probe. This finding was largely independent of the level of the electric masker. In contrast, electric probe responses were strongly suppressed by the presence of acoustic stimulation and exhibited marked increases in threshold as the level of the acoustic masker increased. This effect was particularly pronounced when the acoustic stimulus frequency (i.e., the neuron's CF) differed from the CF corresponding to the intracochlear location of the stimulating electrodes.

The results suggest that BBS leads to complex interactions of responses in the auditory brainstem and midbrain that are only partially dependent on the relative intensity of the given stimulus modes. The magnitude of masking between electric and acoustic responses appears opposite to that observed in unilateral combined electric and acoustic stimulation (EAS). Differences in the responses between IC and DNLL will be described in detail. Clinical significance of bimodal masking effects will be discussed. Supported by IZKF N-100 and MedEl.

503 Effect of Target Location on Dynamic Visual Acuity During Passive Horizontal Rotation

Meghan Appelbaum^{1,2}, Yiri De Dios^{2,3}, Walter Kulecz^{2,3}, Brian Peters^{2,3}, **Scott Wood**^{2,4} ¹USRP, ²NASA JSC, ³Wyle, ⁴USRA

The vestibulo-ocular reflex (VOR) generates eye rotation to compensate for potential retinal slip in the specific plane of head movement. Dynamic visual acuity (DVA) has been utilized as a functional measure of the VOR. The purpose of this study was to examine changes in accuracy and reaction time when performing a DVA task with targets offset from the plane of rotation, e.g. offset vertically during horizontal rotation. Visual acuity was measured in 12 healthy subjects as they moved a hand-held joystick to indicate the orientation of a computer-generated Landolt C "as quickly and accurately as possible." Acuity thresholds were established with optotypes presented centrally on a wall-mounted LCD screen at 1.3 m distance, first without motion (static condition) and then while oscillating at 0.8 Hz (DVA, peak velocity 60 deg/s). The effect of target location was then measured during horizontal rotation with the optotypes randomly presented in one of nine different locations on the screen (offset up to 10 deg). The optotype size (logMar 0, 0.2 or 0.4, corresponding to Snellen range 20/20 to 20/50) and presentation duration (150, 300 and 450 ms) were counter-balanced across five trials, each utilizing horizontal rotation at 0.8 Hz. Dynamic acuity was reduced relative to static acuity in 7 of 12 subjects by one step size. During the random target trials, both accuracy and reaction time improved proportional to optotype size. Accuracy and reaction time also improved between 150 ms and 300 ms presentation durations. The main finding was that both accuracy and reaction time varied as a function of target location, with greater performance decrements when acquiring vertical targets. We conclude that dynamic visual acuity varies with target location, with acuity optimized for targets in the plane of motion. Both reaction time and accuracy are functionally relevant DVA parameters of VOR function.

Acknowledgement: This work supported by the National Space Biomedical Research Institute through NASA NCC 9-58 (SA 02001).

504 Behavioral and Kinematic Measures of Balance in Normals and Patients with Vestibular Disorders

Helen Cohen¹, Ajitkumar P. Mulavara², Brian T. Peters³, Jacob J. Bloomberg⁴, Christopher Miller³, Haleh Sangi-Haghpeykar¹

¹Baylor College of Medicine, ²Universities Space Research Association, ³Wyle Laboratories, ⁴NASA/ Johnson Space Center

The literature describes many inexpensive tests of balance however their value in differentiating normals from

patients, and as potential screening tests of vestibular disorders and post-spaceflight balance decrements, is not clear. The goal of this study is to develop a valid and reliable screening battery that will: a) indicate the presence or absence of a vestibular impairment, b) take no more than 15 minutes, and c) be performed and interpreted with minimal equipment by staff without significant technical expertise in the vestibular system.

Patients with unilateral weakness, chronic post-operative acoustic neuroma resection and benign paroxysmal position vertigo were compared to normals on a battery of tests: a) tandem walking with eyes open and closed, b) walking with and without vaw head rotations, c) the Clinical Test of Sensory Interaction on Balance (CSIB) with head still, head yaw rotations and head pitch rotations and d) the shortened version of the Functional Mobility test, which is an obstacle avoidance test. Time was determined with a stopwatch. Kinematic measures were obtained from inertial motion sensors attached to the head and torso.

A subset of both behavioral and kinematic measures showed areater sensitivity to patients with vestibular impairments. These data support the evidence that some balance tests are more sensitive to vestibular disorders and therefore will be useful as screening measures. The final, reduced test battery will be selected from among these subtests.

Supported by NIH grant RO1-DC009031 and by the National Space Biomedical Research Institute through NASA NCC 9-58. We thank the staff of the Center for Balance Disorders for their invaluable technical assistance.

505 Value of Tilt Suppression Test in **Assessing the Otolithic Function**

Michel Toupet¹, Christian Van Nechel², Sylvie Heuschen², Daniele Bernardeschi³, Alexis Bozorg Grayeli³

¹Centre d'Exploration Otoneurologique, Paris France, ²Service de revalidation Neurologique, CHU de Brugmann,

Brusselles, Belgium, ³APHP, Beaujon Hospital, Otolaryngology dept., and Inserm, UMRS-867, Université

Paris 7, France Objective: The tilt suppression test (TST) is based on the modulation of the horizontal vestibulo ocular reflex by the otolithic detection of a forward head tilt (Hain T el al., 1988). The aim of this study was to investigate other otolithic stimulations (backward, lateral tilts, and vertical jump), to evaluate the value of this test for otolithic function, and to study the relation between the direction of mispercieved linear accelearations in patients with otolithic syndrome and the results of TST.

Materials and methods: 103 patients with dizziness and illusion of linear displacement were included in this prospective study. The population was composed of 61 females and 42 males with a mean age of 50 years (range : 21-88). The analysis of otolithic symptoms allowed the definition of a misperceived vector of displacement. A rotatory test (alternating 10 clockwise and 10 anticlockwise rotations, each with 360° in 6 s) combined to TST was carried out. Post-rotatory nystagmus was recorded, and 5 secondes after the stop, the effect of a

head tilt (forward, backward and lateral) or a vertical jump on the nystagmus was noted.

Results: Initial workup distinguished 66 otolithic syndromes, 19 central etiologies, 8 cases of dizziness exclusively related to stress, 5 bilateral caloric paresis, and 5 miscellaneous peripheral vertigos. TST led to the inhibition of the mean slow phase velocity of the post rotatory nystagmus in all tested head positions and by the vertical jump. This inhibition was more important after the forward head tilt. The inhibition was more important in otolithic syndrome cases than in patients with central dizziness. The direction of mispercieved displacement did not appear to be related to the direction of tilt with the most important inhibition during the TST.

Conclusions: Other stimulations than head flexion can inhibit the post rotatory nystagmus. TST can assess the otolithic function in addition to the cerebellar nodulus participation.

506 Role of Otolith Inputs in Cerebral Blood Flow & Blood Pressure Regulation

Jorge Serrador^{1,2}, Michael Falvo¹, Melissa Blatt¹, Brian Deegan³, Jessica Jasien¹, Scott Wood^{4,5}

¹NJ VA Health Care System, ²Harvard Medical School, ³National University of Ireland Galway, ⁴NASA,

⁵Universities Space Research Association

Assumption of the upright posture places the brain above the heart, causing a reduction in cerebral perfusion pressure due to hydrostatic pressure changes related to gravity. Since vestibular organs, specifically the otoliths, provide immediate feedback on position relative to gravity, vestibular inputs may assist in adaptation to the upright posture. The goal of this study was to examine the effect of direct vestibular stimulation using off vertical axis rotation (OVAR) on cerebral blood flow (CBF). During one session subjects were placed in a chair that was tilted 20° offvertical and accelerated at 25°/s2 to a constant velocity. Rotation occurred at three frequencies (0.03125, 0.125 and 0.5 Hz) and subjects heads were placed either forward, or turned 40° left or 40° right during each frequency. The purpose of changing head position relative to the body was to determine if changing otolith orientation relative to gravity would also shift the cerebral blood flow response, even though effects of centripetal acceleration on the body weren't changed. During testing, CBF (transcranial Doppler), blood pressure (Finapres), and end tidal CO2 (Puritan Bennet) were measured continuously. All rotations were done in the dark. Subjects demonstrated sinusoidal patterns of both cerebral blood flow (±2.6% at 0.5; ±8.8% at 0.125; ±8.7% at 0.03125 Hz) and blood pressure (±7.9 mmHg at 0.5; ±5.9 mmHg at 0.125; ±5.1 mmHg at 0.03125 Hz) that were related to the frequency of rotation. Turning subjects heads resulted in a phase shift in the associated CBF signal (42±29° at 0.5 Hz; 6±31° at 0.125 Hz; 52±20° at 0.03125 Hz). In contrast, oscillations in blood pressure were unaffected by head position. These data indicate that changing otolith position 40 degrees by head rotation resulted in a similar phase shift in CBF. The attenuated shift at 0.125 Hz may have been associated with the nauseogenic nature of the middle

frequency disrupting normal vestibular inputs into CBF control. Since trunk position remained unchanged, these data suggest that oscillations in CBF associated with OVAR are primarily due to otolith stimulation. Supported by NIH NIDCD and NASA.

507 Post Surgical Outcomes in Superior Canal Dehiscence (SCD) Syndrome: Recovery of Functional AVOR and Balance

Kristen Janky¹, M. Geraldine Zuniga¹, John Carey¹, Michael Schubert¹

¹Johns Hopkins University

Purpose/Hypothesis: The purpose of this study is to characterize the impairment and recovery of functional aVOR and balance outcomes following surgical repair of superior canal dehiscence (SCD) syndrome.

Number of Subjects: Normal controls (n = 21) and SCD patients (n = 35). Measures in patients were made Pre (n = 18), Post (<1 week, n = 16), and Chronic (>6 weeks, n = 22). Repeat testing was also done during the Post (n = 6) and chronic (n = 14) periods.

Materials/Methods: All subjects completed dynamic visual acuity (DVA) during active yaw, then passive (impulse) semicircular canal plane rotation (Yaw, RALP, LARP); Dynamic Gait Index (DGI); Clinical Test of Sensory Integration on Balance (CTSIB); Five Times Sit to Stand Test (FTSST); and Subjective Visual Vertical (SVV).

Results: Prior to SCD repair, we found no difference in active or passive DVA between patients with SCD and normal subjects. Additionally, each balance test was normal. However, Post SCD repair (mean 4.8 days), we observed significantly abnormal DVA for head rotation in active and passive yaw (right and left), and affected superior canal (SC) planes. At the Chronic measure (mean 196 days), DVA was still abnormal for passive rotations in the plugged SC plane for the majority of patients, as expected. Although DGI recovered by the Chronic time period, both CTSIB and FTSST were still abnormal beyond 6 weeks.

Conclusions: DVA for active head rotations in yaw to either side is initially abnormal but recovers contralesionally by 6 weeks. DVA remains abnormal to passive head rotation in affected SC planes beyond 6 weeks. Dynamic balance deficits after SCD repair suggest a need for longer-term rehabilitation therapy.

508 Dependence of Eye Movement Responses on Baseline Stimulation Rate During Prosthetic Electrical Stimulation of the Vestibular Nerve

Natan Davidovics¹, Gene Fridman², Charles Della Santina^{1,2}

¹Johns Hopkins University Department of Biomedical Engineering, ²Johns Hopkins University Department of Otolaryngology – Head & Neck Surgery

An implantable prosthesis that stimulates vestibular nerve branches to restore sensation of head rotation and visionstabilizing reflexes could benefit individuals disabled by bilateral loss of vestibular sensation. Our group has developed a vestibular prosthesis that partly restores normal function in animals by delivering pulse frequency modulated biphasic current pulses via electrodes implanted in semicircular canals. For unilateral prosthetic stimulation, adapting an animal to a non-zero baseline stimulation rate (BSR) allows encoding of both excitatory and inhibitory head rotations by modulating the pulse rate above and below the baseline. We investigated the effects of varying BSR on the vestibulo-ocular reflex (VOR) eye movements, hypothesizing that increasing BSR would expand the inhibitory dynamic range at the expense of excitatory dynamic range. We measured angular eye velocity during steps of stimulation pulse rate (range: 60-480 pulses per second) above and below different BSRs (range: 0-240 pulses per second). Greater BSRs resulted in smaller responses for excitatory steps (up-modulations) and larger responses for inhibitory steps (downmodulations). The former effect was more prominent than the latter, so that greater BSRs resulted in a significantly reduced overall dynamic range. These findings can be used towards selecting an optimal BSR that would maximize inhibitory VOR eye responses while maintaining sufficient dynamic range for both directions.

509 Adaptation of 3D Angular Vestibulo-Ocular Reflex to Chronic Stimulation Via a Multichannel Vestibular Prosthesis in Primates

Chenkai Dai¹, Gene Fridman¹, Natan Davidovics¹, Bryce Chiang¹, Mehdi Rahman¹, Charley Della Santina¹ ¹Johns Hopkins University

Bilateral loss of vestibular sensation can be disabling. We have shown that a multichannel vestibular prosthesis (MVP) can partly restore sensation of head rotation as evidenced by improvements in the 3-dimensional angular vestibulo-ocular reflex (3D aVOR). However, a key challenge is to minimize misalignment between the axes of eye and head rotation, which is apparently caused by current spread beyond each electrode's targeted nerve branch. We recently reported that rodents wearing a MVP markedly improve 3D aVOR alignment during the first week after MVP activation, probably through the same central nervous system adaptive mechanisms that mediate cross-axis adaptation in normal animals. We hypothesized that rhesus monkeys would exhibit similar improvements over time.

We created bilateral vestibular deficiency in two rhesus monkeys via intratympanic gentamicin. A MVP was mounted in a head chamber, and eye movements in response to whole body rotation were measured repeatedly over 1 week of head-motion-modulated prosthetic electrical stimulation. 3D aVOR responses to head rotations about each semicircular canal axis were measured on days 1, 3 and 7 of chronic stimulation. The aVOR gain before the prosthesis was turned on was negligible (0.05-0.1). On stimulation day 1, the aVOR gain was 0.5-0.8, but the axis of observed eye movements aligned poorly with head rotation (misalignment 30-40°). Substantial improvement of axis misalignment (down to 10-20°) was observed after 7 days of motion modulated prosthetic stimulation under normal diurnal lighting. VOR asymmetry gradually and slightly improved over time. Hearing was preserved (within 2-14 dB of pre-op) during chronic stimulation.

These findings demonstrate that the central nervous system rapidly adapts to multichannel prosthetic stimulation to markedly improve 3D aVOR alignment during the first week after MVP activation in nonhuman primates. Similar effects are likely to be seen in humans. Support: NIDCD R01DC9255

510 Restoration of 3D Vestibular Sensation Via a Multichannel Vestibular Prosthesis in Rhesus Monkeys

Chenkai Dai¹, Gene Fridman¹, Natan Davidovics¹, Bryce Chiang¹, Charles Della Santina¹

¹Johns Hopkins University

We describe the in vivo application of a head mounted, semi-implantable multichannel vestibular prosthesis (MVP) in rhesus monkeys. By sensing three dimensional head rotation using gyroscopes and electrically stimulating corresponding branches of the vestibular nerve with biphasic current pulses rate modulated by head angular velocity, a MVP should partially restore vestibular sensation to individuals disabled by loss of vestibular hair cell function. Previous experiments in vestibular-deficient chinchillas have shown that the MVP developed in our lab significantly restores 3D angular vestibulo-ocular reflex (aVOR) performance. Assuming that effects of current spread depend on distance between nerve branches, we hypothesized that the MVP would achieve similar or better performance when applied in rhesus monkeys.

Electrodes were implanted in four monkeys treated with intratympanic gentamicin to bilaterally ablate vestibular sensation. Eye movements mediated by the aVOR were recorded during sinusoidal head rotation in darkness at 0.2-5 Hz (peak 50jã/s) about each semicircular canal axis. During constant 100 pulse/s stimulation (not modulated by head motion), aVOR responses to head rotation exhibited profoundly low gain (<0.1) and large misalignment between ideal and observed eye movements. Motion-modulated prosthetic stimuli elicited a 3D aVOR with gain 0.4-0.7 and axis misalignment 30-40jã. Excitation-inhibition asymmetry of aVOR responses evident during monaural stimulation was significantly reduced during simultaneous binaural stimulation.

Acute responses to MVP stimulation in rhesus macaque monkeys were similar to those observed in chinchillas, despite a ~10-15% difference in inter-ampullary nerve separation. These observations suggest that in humans, an MVP will likely restore vestibular sensation to a similar degree. Computational and/or adaptive mechanisms to reduce misalignment will be important to achieve a wellaligned 3D aVOR.

Support by NIDCD R01DC9255

511 Encoding Contralateral Head Rotation in a Vestibular Prosthesis Using Anodic DC Stimulation to Selectively Inhibit Vestibular Nerve

Gene Fridman¹, Natan Davidovics¹, Chenkai Dai¹, Charles Della Santina¹

¹Johns Hopkins University

Previous work on the development of a vestibular prosthesis has demonstrated that pulse-rate modulated electrical stimuli delivered to the vestibular nerve are substantially more effective at encoding head rotation toward the implanted labyrinth than encoding rotation in the opposite direction. In an ear of a subject with typical bilateral vestibular dysfunction, the vestibular nerve still maintains a nearly normal spontaneous firing rate, but the motion transduction mechanism is damaged. The presentation of electrical pulses by the prosthesis increases the firing rate to emulate head rotation toward the implanted side, but it is not able to effectively inhibit the spontaneous activity to evoke the sensation of contralateral head rotation.

Stimulating the vestibular nerve with anodic direct current (aDC) was previously shown to nonselectively reduce spontaneous firing of vestibular afferents as evidenced by single unit recordings. In experiments with chinchillas rendered bilaterally vestibular deficient and implanted with intra-labyrinthine electrodes, we compared angular vestibular ocular reflex (aVOR) responses to two types of stimulation. In the first, we modulated prosthesis output with 2.5s steps from 60 pulses/second (pps) baseline stimulation rate to 0 pps. In the second we delivered 2.5s duration steps of 20-150 μ A aDC stimulation to the same electrodes.

Both stimulation paradigms evoked angular vestibular ocular reflex (aVOR) eye movements consistent with inhibition of the branch of vestibular nerve nearest to each of the implanted electrodes. The maximum inhibitory aVOR eye velocity responses evoked with aDC stimulation were 5 to 10 times higher than the corresponding motion elicited by pulse-rate modulation. The result suggests that incorporation of aDC stimulation in a stimulus protocol may help a multichannel vestibular prosthesis achieve more symmetric but directionally selective encoding of head movement.

Support: NIDCD R01DC9255, R01DC2390

512 Vestibular Evoked Myogenic Potentials to Estimate Saccular and Utricular Involvement According to the Stage of Ménière's Disease

M.Geraldine Zuniga¹, Kristen Janky¹, Michael Schubert¹, John Carey¹

¹Johns Hopkins University

Purpose: To assess saccular and utricular involvement in the stages of Ménière's disease (MD) by means of vestibular evoked myogenic potentials (VEMP).

Subjects: Healthy subjects (n=43, mean age 39 yr), and patients with unilateral definite MD (n=22, mean age 53 yr)

as defined by the American Academy of Otolaryngology– Head and Neck Surgery (AAOHNS) guidelines.

Methods: MD ears were staged based on AAOHNS guidelines using the closest audiogram to VEMP testing (mean 7 mos): stage 1 (n=7), stage 2 (n=2), stage 3 (n=8), and stage 4 (n=5).

Cervical and ocular VEMPs were evoked by air-conducted sound (ACS: clicks and tone bursts) and midline (Fz) bone-conducted vibration (BCV: reflex hammer and Mini-Shaker). Peak-to-peak amplitudes and asymmetry ratios (AR) were measured for all VEMPs.

Results: In all affected MD ears regardless of stage, means (±SE) of corrected amplitudes of click-evoked cVEMPs (0.47±0.09microvolts) and oVEMPs (0.97±0.24 microvolts) were significantly reduced compared to normal ears (cVEMPs: 1.96±0.13 microvolts; oVEMPs: 6.7±0.65 microvolts). Contralateral ears in MD also had reduced responses to clicks; thus, ARs were not increased for all stages of MD. Tone-evoked c- and oVEMPs did not show a clear involvement in stages 1-2. For Fz BCV, c- and oVEMP amplitudes from MD ears declined with increasing stage of MD.

Conclusion: Results from click-evoked VEMPs are consistent with saccular involvement in early stages of MD. Results from Fz BCV suggest utricular involvement occurs in later stages. Results also suggest saccular involvement in the asymptomatic contralateral ear in all stages as suggested by Lin et al, 2006.

Supported by NIH/NIDCD R01 DC005040

513 Intratympanic Steroids in the Treatment of Menieres Disease

Edward Cho¹, Judith White¹

¹Cleveland Clinic

Background: To evaluate the efficacy of intratympanic steroids for the treatment of vertigo in unilateral Meniere's disease.

Methods: This was a retrospective review of 46 patients treated with intratympanic steroid therapy from 2004-2008 at a tertiary care hospital. These patients had refractory vertigo despite maximal medical therapy for unilateral Meniere's disease. Other variables that might affect treatment were also studied such as demographics, Meniere's characteristics, and type of steroid injected.

Results: Acceptable vertigo control was achieved in 41/46 patients. Vertigo control required only one injection in 26 patients, 2 injections in 9 patients, 3 injections in 7 patients, and more than 3 injections in 4 patients. All 5 failures occurred within 18 months of the first injection. Only 1 of the failures required surgery for treatment of their vertigo while the other 4 were managed with intratympanic gentamicin. None of the other variables had a statistically significant influence on the outcome of intratympanic steroid therapy. However, some of the variables did trend towards significance. One was the length of time patients had had Meniere's prior to first being seen. For patients who had had Meniere's for ≥ 4 years, 93% were successfully treated with intratympanic steroids vs. 58% for less than 4 years (p=0.12). Another factor that trended towards significance was sex, with females tending to fail more frequently than males (p=0.10). Finally, all 8 patients who had a history of BPPV did not fail treatment with intratympanic steroids.

Conclusions: Intratympanic steroid therapy is an effective treatment for medically refractory vertigo in patient's with unilateral Meniere's disease. Many patients had satisfactory control of vertigo with just one injection.

514 Abnormal Vestibulo-Ocular Reflex in Autism

Tana Bleser¹, Keith White¹

¹University of Florida

Objectives: To develop methods for studying vestibuloocular reflexes (VOR) in children with autism spectrum disorders (ASD) for replicating and extending previous findings of abnormal VOR in ASD.

Background: Oculomotor and postural control deficits are commonly noted in children with ASD, yet the neurological underpinnings of these deficits are poorly understood. Typical and atypical VORs have been well studied and provide an excellent resource for studying neural mechanisms of visual-vestibular deficits in ASD.

Methods: Our lab developed a pediatric rotary chair (P-ROC) for testing VOR in children with ASD. Three children with ASD and three age-matched normal controls 6-12 years old participated in velocity step tests. Videonystagmography (VNG) recordings were taken during and after rotation for 8 trials. ASD diagnoses were confirmed by the Autism Diagnostic Observation Schedule (Lord et al., 2000).

Results: Although our sample is small and our sampling rate low (30 fps), our results are robust and replicated those of Ritvo et al. (1969). The ASD group compared to controls showed (a) significantly decreased duration of post-rotary nystagmus in the light (ASD = 6.3 sec and controls = 14.4 sec, p<0.001) and (b) no difference in the duration of post-rotary nystagmus in the dark (ASD = 31.6 sec and control group = 30.2 sec, p=0.091). Unlike Ritvo et al. (1969), we used VNG rather than ENG, which enabled us to identify additional aberrations in the quality of VOR in ASD which were not previously reported. We are currently analyzing these data and expect significant differences between the two groups.

Implications: VORs can be objectively measured early in development, thus, if certain deficits are specific to ASDs, such deficits may help identify risk early. VORs can also be used as treatment outcome measures or used for patient-treatment matching in ASD. Future studies will aim to thoroughly characterize abnormalities and elucidate the underlying neural mechanisms.

515 Interference Between Postural Control and Spatial Vs. Non-Spatial Auditory Reaction Time Tasks in Older Adults

Joseph Furman¹, Susan Fuhrman¹, J. Richard Jennings¹, Mark Redfern¹

¹University of Pittsburgh

The purpose of this study was to extend previous research regarding the relationship between postural control and cognitive task performance in older adults by comparing the effects of spatial vs. non-spatial auditory reaction time (RT) tasks. Subjects were healthy young (Y; n=18; 9F; 23.8+/-2.6yrs), young-old (Y-O; n=15; 9F; 68.7+/-3.2), and old-old (O-O; n=12; 8F; 78.7+/-2.6) adults. Subject testing used a dual-task paradigm wherein subjects performed two separate auditory reaction time (RT) tasks under four different postural conditions. Tasks were a non-spatial frequency discrimination task (FCRT) and a spatial lateralization task (LCRT); postural conditions included two floor conditions (fixed, sway-referenced) and two vision conditions (eyes open, eyes closed). Measures included RT and postural sway.

Results confirmed prior research indicating that RT difference from baseline (task cost) was significantly greater with eyes closed and on a sway-referenced floor. Our results extended prior research by indicating that there was a significant task x vision x group interaction (p=0.026). We probed this interaction. For the FCRT task, there was a significant (p=0.001) task cost in both older groups with eyes closed but no significant task cost with eves open for any group. For the LCRT task, there was a significant task cost for all groups with eyes closed (Y: p<0.001; Y-O: p =0.022; O-O: p=0.023) and a significant task cost for the older groups (Y-O: p=0.002; O-O: p=0.048) with eyes open. Sway results indicated that the type of RT task was not a significant factor for postural control. Performing either task reduced sway on a fixed floor and increased sway on a sway-referenced floor for Y-O subjects.

This study suggests that interference between cognitive tasks and postural control is greater for older subjects, particularly for spatial tasks.

This study was supported by NIH Grants AG 10009, AG 014116, AG 024827 and DC 05205.

516 A Walking Test Using Acceleration Sensor and Holter as a New Vertigo Examination

Ji Hye Bae¹, Mi Joo Kim¹, Eun Lee¹, Gyu Han¹, Soo-Chan Kim²

¹Gachon University, ²Graduate School of Bio & Information Technology, Hankyong National University

Objective:

Out of all the outpatients complaining dizziness, less than half of them showed positive diagnoses according to nystagmus and position change. As such patients increase, developing a device that monitors vestibular function in long term is urgently needed for accurate diagnose. This study focuses on developing diagnostic and monitoring device that is inexpensive and portable, and has high test sensitivity and singularity. The intention of the device is to perform objective, fast, and manageable test that patients can record by themselves. In addition, various sensors would be added to operate the device in remote clinic condition.

Methodology: Three or four 3-axis acceleration sensor (Freescale) was fixed to head-waste-tale and connected it to central control device that control and display the movement acceleration of each part for 24 hours. A switch was attached to the central control device that patient can

judge dizziness subjectively and record the event. Electrocardiography was also installed to measure and record vestibular autonomic reflex change for 24 hours as the acceleration change of body parts is recorded. Behavioral protocol was to repeat Romberg test and 40m rectilinear walking for three times. Subjects were selected from normal control group and from the patients who showed acute vestibular neuritis and vestibular disorders for 0 to 30 days. Attained raw data went through frequency analysis by self-produced program and only the highest frequencies were used to compile statistics.

Result: Romberg test using 3-axis acceleration sensor showed equal result as preexisting and expensive dynamic posture change. In case of normal walking test, it showed regular pattern with 3 peaks and also showed unique but regular pattern in frequency analysis. However, in case of acute vestibular disorder, previously explained pattern was not observed or first frequency had variations. This result was statistically significant.

Conclusion: Romberg test using three acceleration sensors reflects body sway in accordance with the disorders. Patients display abnormal walking pattern and further analysis of the pattern and frequency from cumulative data.

517 The Relationship Between Head Rotation Velocities and Body Balance Control in Healthy Young/senior Adults and Patients with Vestibular Hypofunction

Chung-Lan Kao^{1,2}, Yu-Pai Lin³, Shun-Hwa Wei³ ¹Taipei Veterans General Hospital, ²School of Medicine, National Yang-Ming University, ³Department of Physical Therapy and Assistive Technology, National Yang-Ming University

Background: In patients with vestibular deficits, high velocities of head movements would frequently induce dizziness, oscillopsia and imbalance. Degeneration of vision, poor proprioception, and decreased muscle contractions all lead to reduced balance ability in the seniors. Fall injuries caused by dizziness are among the major problems threatening the health of seniors and thus it is important to investigate human body balance control in varying speed of head movements. Purposes: (1) develop a computerized evaluation system for assessing Bodyequilibrium reactions induced by head rotation velocities (2) compare the results between healthy young/senior adults and patients with vestibular hypofunction. Methods: 15 healthy young adults, 11 community senior adults, and 12 patients with vestibular hypofunction were recruited. Postural sway was measured by a force plate during upright stance with eyes opened while oscillating their heads horizontally at the velocities of 90, 120, 150, 180, 210 degrees/second. Results: The sway angles in both senior adults and patients with vestibular hypofunction were significantly larger than those in healthy young adults at all velocities (p < 0.01). The difference was most pronounced at 180 deg/sec of head rotation between and senior healthy voung adults (80.6%). Discussion/Conclusion: Postural stability was compromised at faster speed of head movements in both

healthy and vestibular-deficit groups. Patients with vestibular hypofunction and elderly persons appear to have more difficulty in maintaining body equilibrium at higher head rotation velocities than young adults.

518 The Clinical Characteristics of Sudden Sensorineural Hearing Loss Concurrent with BPPV

Jeong-Seok Choi¹, Kyu-Sung Kim¹, Chang-Duk Han¹ ¹Inha University School of Medicine

Dizziness which coincides with sudden sensorineural hearing loss(SSNHL) presents 20 to 60% of occurrence, and symptoms subside depends on the severity of vestibulopathy. Authors tried to demonstrate the pattern of disease through discriminating patients of SSNHL with BPPV from all patients who experienced synchronized occurrence of SSNHL with vertigo. Within 90 patients who admitted for SSNHL from Jan. 2007 to Jun. of 2010, we sorted out a group of patients who were diagnosed with BPPV based on positioning test. We investigated their general characteristics, direction of diseases, types of BPPV, vestibular function test and audiometric outcomes. The total of 17 patients was included. (composed of 8 men and 9 women) The mean age was 49.5 years, and mean PTA outcome was 80.5dB (considering nonresponse as 110dB). Patients presenting canalithiasis of horizontal canal were twelve, and posterior canal canalithiasis was four patients. Ipsilateral comorbidity was found in 11 patients, and contralateral comorbidity was found in 6 patients. In terms of onset of dizziness, the onset was same as that of SSNHL in 9 patients, and the other 4 patients presented within 7 days after onset of SSNHL. Among the patients experiencing acute dizziness with SSNHL, concurrence of SSNHL and BPPV occurred at rate of 18.8%, the patients with canalithiasis of horizontal canal were more than the patients with posterior According canal canalithiasis. to epidemiologic investigation, BPPV patients with SSNHL are made of posterior canal type in 61.3%, lateral canal type in 32%. There was no specific pattern in sexualities, ages, and the onset of dizziness. Moreover, most of the patients had symptoms in the same side, and the onset of dizziness occurred at the same time with SSNHL. Authors want to help understanding the disease of SSNHL concurrent with BPPV, and to find a breakthrough in treatment of SSNHL concurrent with BPPV by scrutinizing clinical aspects.

519 Vestibular and Ocular Motor Function Following Blast Injury

Kristal N. Mills¹, Stephanie Cole², Andrew Stuart¹, Timothy A. Jones¹, Sherri M. Jones¹

¹*East Carolina University*, ²*Camp Lejeune Naval Hospital* The war on terror has produced over 30,000 wounded troops with approximately 68% of injuries attributed to blasts (Dept. of Defense, 2010; Chandler, 2006). Dizziness and imbalance are common complaints among blast injured (BI) military personnel. The purpose of the study was to characterize vestibular and oculomotor function in military personnel less than one year post blast (N = 33) and greater than one year post blast (N = 60). Overall, 33 of the 93 participants exhibited normal findings on all test results (less than one year, N = 10 and greater than one year, N = 23). Ocular motor abnormalities (OMA) were the most common finding with 51 of 93 participants demonstrating at least one abnormal finding. Saccadic latency was the most commonly observed OMA with mean latencies of 178 ms for those classified as normal and 345 ms for those with OMA. Less than 1 year post-blast, 7 out of 33 (21%) exhibited findings consistent with a unilateral weakness (UW). One participant in this group had findings consistent with a bilateral weakness (BW). Greater than 1 year post blast group, 4 participants (6%) showed a UW and 11 (18%) had findings suggestive for a BW. All participants were able to visually suppress the vestibular ocular reflex (VOR) and the vast majority (95%) could also visually enhance VOR gain. Vestibular evoked myogenic potentials were normal in 42 of the 47 participants tested suggesting that saccular function is not significantly affected by blast exposure. The Dizziness Handicap Inventory and the Activities-specific Balance Confidence scales were poor indicators of peripheral vestibular status. Participants' reported symptoms and case histories did not predict test outcomes. Overall, the findings suggest that peripheral vestibulopathy is not prevalent following BI at least during the time frame tested here (4 months to 5 years post blast); however, ocular motor abnormalities are common in the BI population.

520 The Use of the Balance Accelerometry Measure in Persons with and Without Concussion

Gabriel Furman¹, Chia-Cheng Lin¹, Jennica Roche¹, Gregory Marchetti², **Susan Whitney¹**

¹University of Pittsburgh, ²Duquesne University

Introduction: It has often been reported that post mild concussion, with or without loss of consciousness, persons suffer from altered postural control. The purpose of this study was to determine if the NIH Balance Accelerometry Measure (BAM) was able to detect differences in postural sway compared to an age matched control group.

Methods: Twenty-nine post concussion (mean age: 21 ±8 years, mean duration since concussion 34 ± 62 weeks) and 34 control subjects (mean age: 26 ± 6 years) agreed to participate in the study. All subjects were tested with the standard BAM protocol that included the following six standing balance conditions: feet together, eyes open (EO) and /closed (EC), feet together on foam, EO and /EC, and tandem Romberg, EO and /EC. Each condition, pelvic accelerations are recorded using a dual-axis accelerometer wirelessly transmitted via Bluetooth. The accelerometer system was affixed to a gait belt using Velcro around the subject's pelvis.

Data Analysis: Sway was quantified using normalized path length (mG/sec) of the accelerations in the anterioposterior direction that was calculated over 40 seconds, after the first 5 seconds of each condition was discarded. Using the normalized path length measure, a repeated measures analysis was used to test for within subject (sensory condition), between subject (concussion versus healthy) and interaction effects; this analysis included only subjects completing all six conditions.

Results: Twenty-two (76%) persons post-concussion and 30 (88%) healthy control subjects completed 45-second stance trials. Comparison of normalized path length of acceleration demonstrated a significant within-subject effect with all conditions showing greater sway when compared with EO condition (p < 0.01, Bonferroni adjustment for multiple comparisons). The EC/foam condition showed the greatest sway of all conditions (p < 0.01) followed by tandem stance with EC (p < 0.01 except when compared with eyes open/foam). There was a significant between-subjects effect, where subjects post concussion showing greater overall mean sway than healthy controls (p < 0.04). The group x sensory condition interaction effect was not significant.

Conclusion: Across all sensory conditions, subjects showed the greatest anterior-posterior sway with EC on foam. Greater sway was demonstrated by subjects' postconcussion compared with healthy controls, suggesting that the BAM may be sensitive in identifying increased postural sway in persons post-concussion.

This study is funded in part with Federal funds from the Blueprint for Neuroscience Research, National Institutes of Health under Contract No. HHS-N-260-2006-00007-C.

521 Age-Related Hearing Loss: Introduction and Overview

Robert Frisina¹ ¹University S. Florida

Due to significant increases in our aged population worldwide, presbycusis - age-related hearing loss (ARHL) - is a phenomenon that deserves increasing attention, in terms of both basic and clinical research. Recent progress has been made concerning biological mechanisms of presbycusis using animal models, which may underlie complex sound and speech processing problems. Advances have also been made in our understanding of the genetics of ARHL with several loci identified in the aging cochlea and central auditory system of mice. New information has been accumulated about changes in peripheral processing, including oto-acoustic emissions and the efferent feedback system, with age, as well as about anatomical and neurochemical age-related changes in the central auditory system, including declines in inhibitory neurotransmitters. Age-linked rates of decline of speech recognition depend on many factors, including gender and temporal coding capabilities. The symposium intends to integrate these different areas of research on the aging auditory system, and point out translational directions.

Supported by NIH-NIA P01 AG09524-16.

522 Gene/Environment Interactions in **Presbycusis Derived from Animal Models** Kevin K. Ohlemiller^{1,2}

¹Washington University Med. School, ²Dept. Otolaryngology

Examination of human audiograms and temporal bones has revealed only broad patterns concerning the cochlear

changes that underlie age-related hearing loss (ARHL). Animal models have made it possible to evaluate interdependency for survival among different cochlear cell types, and to identify environmental conditions and genes that promote loss of critical cells. For all three recognized forms of peripherally-based ARHL (sensory, neural, strial) it is increasingly clear that some apparent cases involve injury, yet the propensity toward injury is genetically influenced. Accordingly, the types of genes implicated in animal work prominently include those encoding regulatory and protective factors. Similar-acting genes have also found support in human genetic studies.

523 Age-Related Peripheral Hearing Loss: Anatomical and Physiological Changes Richard Schmiedt¹

¹Medical University of South Carolina

Results from animal models describe threshold shifts that occur under controlled losses of sensory cells and decreases in the endocochlear potential (EP). Sensory hair cell losses in the base are common with both ototoxic drug and noise exposures. The resulting threshold profiles are typically normal at lower frequencies with an abrupt transition to a loss that plateaus between about 50-70 dB at higher frequencies. Conversely, a lowered EP yields threshold profiles that have a mild, constant loss at lower frequencies with a gradually increasing loss at higher frequencies. Both sensory and metabolic presbyacusis can largely be understood in terms of outer hair cell gain and its relationship to the EP.

[Work supported by NIH/NIDCD]

524 Age-Related Peripheral Hearing Loss: Human Audiometric Phenotypes Judy R. Dubno¹

¹Medical University of South Carolina

Anatomic and physiologic changes observed in animal models with controlled pathologies can be used to predict underlying mechanisms of age-related hearing loss in older humans, including sensory and metabolic The metabolic presbyacusis hypothesis phenotypes. largely explains the most common audiometric profile of a mild, flat hearing loss at lower older humans: frequencies coupled with a gradually sloping hearing loss at higher frequencies. In addition to examinations of audiogram profiles, supporting evidence of presbyacusis phenotypes in older humans can be derived from demographic information (age, gender), environmental exposures (noise and ototoxic drug histories), and suprathreshold auditory function beyond the audiogram. [Work supported by NIH/NIDCD]

525 Age-Related Maladaptive Inhibitory Changes and Temporal Uncertainty in Central Auditory Structures Donald Caspary¹

¹Southern Illinois University School of Medicine Presbycusis or age-related hearing loss results in deficits in speech comprehension, especially in a complex

acoustic environment. Inability to clearly process speech is a contributing factor leading to a tendency of elderly individuals to withdraw from active participation in society. inhibitory Circuits utilizing the amino acid neurotransmitters, glycine and GABA, are critically involved in improving the precision of the temporal coding of complex acoustic signals at multiple levels of the Aged rats display behavioral and auditory neuraxis. single-unit temporal processing deficits at several central loci consistent with an age-related net decrease in preand postsynaptic inhibitory function. Age-related presynaptic changes in the cochlear nucleus include reduced glycine levels, while in the auditory midbrain and cortex, GABA synthesis and release are altered. Perhaps in response to an age-related decrease in presynaptic production and release of inhibitory neurotransmitters, there are age-related postsynaptic subunit changes in the makeup of glycine and GABA_A receptors. These receptor pharmacological and changes alter physiological responses consistent with a net down-regulation of functional inhibition. Central auditory unit responses to modulated signals are less precise, while spontaneous and driven rates are paradoxically higher from cochlear nucleus to cortex in aged brains. This loss of inhibitory function in circuits coding complex sounds results in reduced damping/increased jitter potentially, in part, responsible for the loss of speech understanding observed in elderly humans. Understanding age-related changes in the makeup and function of the inhibitory amino acid receptors could eventually lead to the development of selective pharmacotherapy for a subset of presbycusic individuals.

Supported by NIH DC000151 and NIH DC008532.

526 Sensitivity to Temporal Intervals in Auditory Sequences by Aging Humans Peter Fitzgibbons¹

¹Gallaudet University

Psychoacoustic discrimination studies conducted with older human listeners provide evidence of diminished sensitivity to the temporal properties of sound stimuli. Much of the evidence comes from measures of duration discrimination, conducted either with simple tone bursts presented in isolation or embedded as single components within multi-tone sequences. The results reveal diminished sensitivity to changes in stimulus duration among older listeners, with the magnitude of the age-related discrimination deficit being greater for signals within sequences. Other related evidence reveals that older listeners have difficulty discriminating changes in the time interval separating successive onsets of brief tonal signals. This difficulty can be pronounced for short onset-to-onset tone intervals, but is reduced considerably if an interval is repeated within the context of longer isochronous tone sequences. In many cases, the degree of improvement in discrimination performance observed for repetitive stimulus intervals is greatest among older listeners. Cumulative evidence from several studies also reveals that the presence of age-related hearing loss does not have an important influence on temporal discrimination for clearly

audible stimuli. These results and possible sources of diminished temporal sensitivity among older listeners are topics of discussion.

527 Multi-Disciplinary Investigations of Peripheral Vs. Central Presbycusis in Rodent Animal Models

Josef Syka¹

¹Institute of Experimental Medicine, Academy of Sciences of the Czech Republic

For better understanding of the mechanisms underlying human presbycusis, experimentation with appropriate animal models is necessary. We characterize here two different rat strains: the Fischer 344 (F344) strain, which serves as a model of fast and profound presbycusis, and the Long Evans (LE) strain, in which the deterioration of hearing progresses relatively slowly. Hearing thresholds begin to increase in the F344 strain during the first year of life; toward the end of the second year the thresholds are very high. In contrast, age-related threshold shifts in the LE strain are smaller, even at the end of the second year. Similar differences between the strains are present in the rate of deterioration of distortion product otoacoustic emissions with age. The age-related changes in inner ear function are accompanied by impaired acoustical signal processing within the central auditory system, based on impaired GABA inhibition and other defects, for example age changes in the presence of calcium binding proteins. Sound-evoked behavioral reactions are also impaired in old F344 rats to a greater extent than in the LE strain. Due to the accumulated experimental data on such age-related changes, the F344 and LE rat strains serve as useful models for studying the neural mechanisms of presbycusis.

528 Speech Processing and Aging: Examples of Decline and Preservation Sandra Gordon-Salant¹

¹University of Maryland

Older people may appear to have exceptional difficulty understanding speech in everyday situations, but are their problems unique to aging? This is a fundamental guestion of research concerned with aging and audition. Convergent findings from numerous studies indicate that most of the speech understanding problems of older listeners in guiet and noisy environments can be explained by reduced signal audibility and abnormal frequency selectivity associated with peripheral, age-related hearing loss. However, there are age-related alterations in central timing mechanisms that are thought to impact perception of speech in which temporal information is stressed or altered, including speech spoken at fast or variable rates, or speech spoken with an accent. Decline in cognitive abilities with aging can also impact an older person's ability to perceive distorted speech signals. This presentation will review recent investigations that demonstrate the relative import of these peripheral and central/cognitive mechanisms on speech perception performance of older listeners. Promising techniques to preserve or restore lost function in speech perception abilities of older listeners also will be considered.

529 Developmental Plasticity - Where We've Been, and Where We're Going: A Personalized and Biased View Edwin Rubel¹

¹University of Washington

It probably started with Aristotle, but I like to trace the modern era back to Levi Montalcini and Hamburger on one side and Riesen, Hubel and Weisel on the other. I will trace what I feel are the important milestones that define the phenomenology we want to understand at the cellular and molecular levels. I'll then try to conceptually break down the issues by considering cellular interactions of the component processes regulated by presynaptic events, synaptic events and target cell stability and plasticity.

530 Wiring the Cochlea for the Perception of Sound

Lisa Goodrich¹, Jessica Appler¹, Noah Druckenbrod¹,

Cindy Lu¹, Wei-Ming Yu¹

¹Harvard Medical School

Sound is detected in the cochlea and perceived in the brain. The first intermediaries in this process are the spiral ganglion neurons, which collect information from the hair cells and then rapidly transmit appropriate signals to target neurons in the cochlear nucleus complex. To capture the frequency, intensity, and timing of each stimulus, spiral ganglion neurons rely on tonotopically ordered connections, differences in spontaneous firing rates, and synapses that are specialized for fast and accurate transmission. We have been investigating how spiral ganglion neurons acquire these unique properties during development. We have catalogued the progression of auditory circuit assembly in the mouse from E12 to the onset of hearing both at the cellular level and at the molecular level. Through these studies, we identified sets of genes that are expressed specifically in auditory neurons as they extend their processes towards the organ of Corti (E12/13), select pre- and post-synaptic targets (E16-P0), elaborate synapses (P0-P6), and acquire mature firing properties (P0-P15). To begin to define how auditory-specific genes contribute to spiral ganglion neuron development and differentiation, we are focusing on two transcription factors, Gata3 and Mafb. We find that Gata3 plays an ongoing role throughout auditory circuit assembly, acting initially to direct the auditory fate decision while simultaneously holding neurons in an undifferentiated state. Subsequently, the neurons begin to differentiate and express Mafb, which we propose promotes SGN maturation, including the development of appropriate synapses and firing properties. Our findings indicate that Gata3 is a master regulator that acts upstream of Mafb to coordinate auditory circuit assembly. Current studies are aimed at understanding how a single transcription factor influences multiple aspects of spiral ganglion neuron development and differentiation.

531 The Cochlear Nucleus Is a Trophic Center in Auditory System Development Stephen Maricich¹

¹Case Western Reserve University

The mammalian cochlear nucleus (CN) originates from anterior regions of the rhombencephalic neuroepithelium. Many of these neurons are specified by the basic helixloop-helix transcription factor Atoh1. We used two Credriver lines (Egr2-Cre and Hoxb1-Cre) to generate conditional knockouts (CKOs) of Atoh1 in hindbrain regions that give rise to the anteroventral and posteroventral CN, respectively. These Atoh1-CKO animals show distinct patterns of primary neuronal loss in the CN and secondary neuronal loss in the spiral ganglion and other regions of the central auditory system. These findings reveal the importance of the CN for support of peripheral and central auditory neurons

532 Cues That Determine Crossed Projections to MNTB Karina Cramer¹

¹University of California

Projections from VCN to contralateral MNTB are essential for the computation of interaural intensity differences used in sound localization. During development, VCN axons grow past ipsilateral MNTB without terminating, and proceed to the contralateral side before forming the terminal calyx of Held. Axon guidance molecules likely play a role in ensuring that VCN axons terminate on contralateral, but not ipsilateral MNTB. We examined projection patterns in several lines of mice with various types of mutations in genes encoding Eph receptor tyrosine kinases and their ephrin ligands. We found that EphB2 null mutations and ephrin-B2 mutations both resulted in a significant number of calyceal projections from VCN to ipsilateral MNTB, along with the normal contralateral projection. Our observations, together with analysis of Eph protein expression patterns, suggest that EphB2 mediates reverse signaling necessary for prevention of ipsilateral projections. EphB reverse signaling occurs in MNTB neurons in response to signals from VCN axons. These studies, together with studies of unilateral deafferentation, suggest a mechanism by which VCN axon terminals actively inhibit the formation of ipsilateral VCN-MNTB projections.

533 Synchronous Maturation of Postsynaptic Neurons and Presynaptic Organization

George Spirou¹, Brian Hoffpauir¹, Glen Marrs¹

¹Center for Neuroscience, West Virginia University Functional maturation of neurons has been linked in several brain regions to formation of synaptic connections in emerging neural circuits. We studied the temporal relationship between functional maturation and synaptic organization in the medial nucleus of the trapezoid body (MNTB), a primary cell group of the superior olivary complex (SOC). MNTB neurons, at maturity, are innervated by a single large terminal, called the calyx of Held. Assembly of this neural circuit begins when axons of ventral cochlear nucleus (VCN) neurons reach the region of the SOC, by embryonic day 14 (E14), and await arrival of migrating MNTB cells at E17. Synaptic connections form at E17 and are immediately functional. At E17, stimulation of auditory-nerve fibers can activate neurons of the contralateral MNTB, indicating that activity in the auditory periphery can be transmitted to the MNTB. Four days of synaptic activity precedes a rapid shift, between P2-4, in synaptic organization of the MNTB from multi-innervation of individual cells by small inputs to mono-innervation of most cells by large calyceal inputs. Minimal stimulation techniques and large-volume serial section EM confirm up to 7 converging inputs at P3, with the most rapid terminal growth occurring between P3-4. This transformation is synchronous with changes in electrophysiological properties of MNTB cells, including a sudden increase in action potential threshold, growth of cell bodies, and alterations in gene expression. We propose that the decrease in excitability provides a mechanism to select a single input for calvx formation in a process that likely generalizes to other neural systems.

534 Maturation of Superior Olive Physiology Deda Gillespie¹

¹McMaster University

To ensure that computation of interaural level differences is performed using stimuli from a single sound source, principal neurons of the lateral superior olive (LSO) require glutamatergic input from the anteroventral cochlear nucleus (AVCN) and glycinergic input from the medial nucleus of the trapezoid body (MNTB) that is tonotopically matched. How this precision is established during early postnatal life is particularly interesting in the LSO because the inputs are of opposite sign. In rats, functional refinement in the MNTB-LSO pathway is known to occur before hearing onset at postnatal day 12 (P12), and similar activity-dependent refinement has been presumed to take place in the AVCN-LSO pathway.

Recording in whole-cell voltage clamp in acute slices of rat auditory brainstem, we have examined the maturation of pre-and post-synaptic properties of the AVCN-LSO and MNTB-LSO pathways. We find that the average number of AVCN inputs to a single LSO neuron decreases before hearing onset and that the average response amplitude to stimulation of single AVCN fibers increases. Functional refinement in the two pathways thus appears to proceed with roughly the same timecourse. In both pathways, the GluN2B NMDA receptor subunit is a prominent contributor to the NMDAR response during the first postnatal week. At about P8, which may be the close of a sensitive period for refinement in the MNTB-LSO pathway, functional GluN2B expression rapidly decreases. Furthermore, a stepwise maturation of presynaptic release properties at about P3 is accompanied by increased expression of the presynaptic Ca⁺⁺ sensor Synaptotagmin 2.

We suggest that regulation of Synaptotagmin and NMDAR subunits may play a central role in developmental refinement of the LSO.

535 Photonics of the Auditory and Vestibular System

Claus-Peter Richter¹, Agnella Matic¹, Suhrud Rajguru¹ ¹Northwestern University

Stimulation of neurons with visible light was attempted as early as 1891. Subsequent experiments by Arvanitaki and Chalazonitis demonstrated that inhibition and excitation could be triggered in nerve cells by irradiation with different wavelengths of light, ranging from the visible to the nearinfrared. However, it is difficult to view these results as a logical progression towards the present methods of neural stimulation, infrared neural stimulation (INS) and optogenetics. Most notably, the optical parameters and techniques used in early experiments differ significantly from those used more recently.

For INS, a pulsed infrared laser has been used to stimulate the nerves. INS is defined as the direct induction of an evoked potential in response to a transient, targeted deposition of optical energy. One advantage of using pulsed infrared radiation for neural stimulation is its spatial resolution. Only neural tissue that is directly in the optical path will be stimulated. For INS radiation wavelength, irradiation time, energy, as well as the optical properties of the irradiated tissue determine the laser–tissue interaction. Careful selection of optical parameters is crucial for INS.

Photostimulation or "optigenetics" is another highly promising technique for photochemical neural activation in mammalian neurons, which requires expression of channelrhodopsins in the cell membrane of the target neuron(s). Channelrhodopsins are naturally occurring, rapidly gated, light sensitive algal proteins. Most often, neurons are transfected with channelrhodopsin-2, after which the cells can be depolarized upon irradiation with 500 nm (blue) light pulses. The research field is rapidly expanding and other chromophores have been identified. The expression of halorhodopsin, for example, can be used to inactivate neurons when they were irradiated with yellow (577 nm) light.

536 Laser-Tissue Interaction Primer and Overview of Infrared Neural Stimulation E. Ducco Jansen¹

¹Vanderbilt University

The existing research will be reviewed on infrared neural stimulation (INS), a means of artificially stimulating neurons that has been proposed as an alternative to electrical stimulation. INS is defined as the direct induction of an evoked potential in response to a transient targeted deposition of optical energy. The foremost advantage of using optical radiation for neural stimulation is its spatial resolution. Exogenously applied or transgenically synthesized fluorophores are not used to achieve stimulation. In addition, a brief overview of bio-optics will be presented, including optical properties of tissues, and types of interaction mechanisms between lasers and tissue.

537 Controlling Brain Circuits with Light Edward Boyden¹ ¹*MIT*

Over the last several years we have adapted from nature a number of light-activated ion channels and pumps (or opsins) for use in neurons, genetically targeting these optogenetic reagents to specific cells embedded in the brain and nervous system, and thus making these cells activatable and silenceable by light. In this talk I will discuss these different molecular reagents (e.g., ChR2, Halo/NpHR, Arch, Mac), as well as novel reagents with improved and new functions that we are developing. These reagents are in wide use in basic neuroscience, for the study of the nervous system, where they are used to tease apart the causal contribution of cell types to behaviors and pathologies. I will also present a variety of devices that can deliver light into the brain, supporting a diverse set of optical neural prosthetics, appropriate for delivering information into the brain for therapeutic purposes. Finally, I will present some of our results using opsins for prototype therapeutic purposes, including work that we are pursuing in safety testing in non-human By opening up a new kinds of prosthetic primates. platform, we anticipate benefits in our ability to understand and treat intractable neural disorders.

538 Infrared Neural Stimulation of the Cochlea

Agnella Matic¹

¹Northwestern University

An attractive feature of infrared neural stimulation (INS) versus the use of electric current is the possible simultaneous but non-overlapping stimulation of many discrete sites along the cochlea. Activation of small neuron populations would overcome some of the issues of contemporary cochlear prostheses. INS may afford the possibility to independently stimulate small populations of neurons, increasing the number of perceptual channels, which are required for music perception and speech recognition in noise. At present, INS of the auditory nerve has been studied in the gerbil, mouse, guinea pig and cat using multiple lasers. Threshold radiant exposures varied with pulse duration, with smaller threshold values for shorter pulse durations. In acutely and chronically deaf gerbils, thresholds for optically evoked compound action potentials (CAPs) were not significantly elevated when stimulating with short pulse durations. Experiments in pigmented guinea pigs were used to determine whether optical stimulation of the cochlea was as selective as stimulation with acoustic tone pips. The optical radiation was delivered in the basal cochlear turn and the spread of activation of cochlear optical stimulation was estimated from neural responses in the central nucleus of the inferior colliculus (ICC). The results indicated that the spread of activation due to optical stimuli is comparable to that produced with acoustic tones. Experiments also demonstrated that the optical path in the cochlea varies according to the orientation of the optical fiber and that best frequencies of stimulation depend on the orientation of the optical fiber. Longterm acute stimulation was

achieved for up to 10 hours in the gerbil and the cat at 200 Hz stimulation rate, with stable CAP amplitudes for the duration of the stimulation. Chronic implantation experiments are underway, examining electrophysiological changes over the length of the stimulation and post-experiment histology.

539 Infrared Neural Stimulation of the Cochlear Nucleus

Daniel Lee^{1,2}, Ken Hancock^{1,2}, Sudeep Mukerji^{1,2}, Rohit Verma^{1,2}, M. Christian Brown^{1,2}

¹Massachusetts Eye and Ear Infirmary, ²Harvard Medical School

Performance of auditory brainstem implants based on electrical stimulation may be limited by current spread and consequent excitation of broad regions of the cochlear nucleus. Focused infrared neural stimulation (INS) using a low power diode laser has been shown to activate the auditory periphery (Izzo et al. (2006) Lasers Surg Med 38: 745-53; Richter et al. (2008), Hear Res 242: 42-51). Using a similar approach, we demonstrate that INS can activate the auditory brainstem. In acute experiments, an optical fiber was used to deliver pulsed radiant energy to the surface of the rat cochlear nucleus (CN). An opticallyevoked auditory brainstem response (oABR) was recorded and consisted of multiple waveform peaks over several milliseconds. The oABR had some similarities to the acoustically evoked ABR and electrically evoked ABR but its amplitude was smaller and latency was longer. Control experiments demonstrated that blocking the optical path and euthanasia eliminated the oABR. No thermal tissue damage was found on histological examination when stimulating with brief pulse durations at radiant exposures exceeding threshold. Our work suggests that midwavelength infrared lasers are capable of acutely stimulating either the neurons or axons of passage within the cochlear nucleus without tissue damage. These findings may provide the basis for novel auditory brainstem implant designs based on optical stimulation. Supported by the Helene and Grant Wilson Auditory Brainstem Implant Program at MEEI.

540 Pulsed Infrared Stimulation of the Vestibular Semicircular Canal Sensory Epithelium

Richard D Rabbitt^{1,2}, Suhrud M. Rajguru³, Gregory M. Dittami⁴, Claus-Peter Richter^{3,5}, Stephen M. Highstein² ¹Dept. Bioengineering, Univ. Utah, ²Marine Biological Laboratory, ³Dept. of Otolaryngology, Northwestern Univ., Chicago, IL, ⁴Dept. of Bioengineering, Univ. Utah, ⁵Hugh Knowles Center, Dept. of Comm. Sci. and Disorders, Northwestern Univ.

Semicircular canal afferent neurons respond dramatically to pulsed infrared radiation (IR, 1862nm) applied to the sensory epithelium *in vivo*. Some afferent neurons fire an action potential for each IR pulse delivered to sensory hair cells, with a repeatable latency (7-10ms) leading to phase locking of action potentials up to frequencies of ~100 spk/s. Other units do not phase lock to each IR pulse but respond with large changes in discharge rate, in some cases doubling the resting discharge while in other cases completely silencing the unit. The presentation will review vestibular afferent responses to IR stimulation of the hair cell sensory epithelium and present new data examining the origins of these remarkable IR responses. [Supported by NIH R01DC006685, R01DC004928 (Rabbitt) and R41DC008515 (Richter)]

541 Optogenetic Stimulation of the Cochlea

Tobias Moser^{1,2}, Victor Hernandez^{1,2}, Gerhard Hoch^{1,2}, Nicola Strenzke^{1,2}, Zhizi Jing¹, Hideki Takago^{1,2}, Ernst Bamberg³, George Augustine⁴

¹University of Goettingen School of Medicine, ²Bernstein Focus for Neurotechnology Goettingen, ³MPI for Biophysics Frankfurt, ⁴Duke University

Channelrhodopsin-2 (ChR2) expression in spiral ganglion neurons of transgenic mice was used for optical stimulation of the auditory pathway. Blue light emitted by micro-LED or laser was coupled into the cochlea via a cochleostomy. Light evoked large auditory neuronal population responses in ChR2-expressing mice. These potentials were present also after acute deafening but were blocked when action potential generation was inhibited by application of tetrodotoxin or lidocaine. The dependence of the response amplitude on stimulus duration, rate and light power was systematically explored. Neural responses to sound could be masked by optical stimulation. Single auditory neuron responses to optical stimulation of the cochlea are currently being studied in the cochlear nucleus and the inferior colliculus. In summary, ChR2-mediated optical stimulation of the cochlea seems feasible.

542 Stress Confined Laser Pulses Activate the Peripheral Auditory System

Gentiana I. Wenzel¹, Lenarz Thomas¹ ¹Medical University Hannover

Visible light is a source of energy known to activate the visual system through absorption by photoreceptors in the eye. When the so-called stress-confinement condition is fulfilled, laser light can induce an acoustic signal through an optoacoustic effect. We sought to assess, if visible light with parameters that induce an optoacoustic effect (i.e., 532 nm, 10 ns pulses) could be used to stimulate the peripheral hearing organ. Optically-induced ABRs (OABRs) were elicited with single laser pulses applied to the tympanic membrane, on bony structures within the middle ear, as well as towards the round window membrane and into the scala tympani. The OABRs increased with laser energy and varied in magnitude depending on the location of stimulation. It was also possible to elicit localized neural activation within the inferior colliculus cochlear nucleus (ICC), which appeared to be dependant on the stimulation location. Our findings demonstrate that visible light can activate the peripheral auditory system. We propose that this novel, non-contact laser stimulation method, may be used to improve implantable and non-implantable hearing aids as well as for research purposes.

543 Imaging the Inner Ear: A Tribute to Joseph Hawkins

Jochen Schacht¹, Yehoash Raphael¹

¹University of Michigan

"Imaging" of anatomical structures is as old an endeavor as anatomy itself. While we will marvel at the sophisticated techniques presented in this symposium we should also reflect on the science and the art of our predecessors. From the end of the 17th century, when useful microscopes became available, and well into the 20th century hand drawings and engravings were the only means for information and scholarly dissemination. Splendid examples from those days, such as Corti's observations and Retzius' plates, provide insights that we still must appreciate today. Photography obviated the need for tedious manual renditions but remained a rather simple tool of documentation until the arrival of analytical and digital imaging a few decades ago. Joseph Hawkins, in a career spanning over 60 years, expertly exploited what was then state of the art "imaging" to detail the cytoarchitecture and vascular patterns of the cochlea. Continuing in the tradition of one of his teachers, the great Swedish otolaryngologist Hans Engström, Joe Hawkins (together with his long-time collaborator Lars-Göran Johnsson) also perfected the use of microdissections and surface preparations to give us some of the finest renditions of human inner ear pathology. By demonstrating the amazing advances in imaging technology in Otolaryngology, for both research and clinical purposes, this symposium honors the pioneers in inner ear anatomy who laid the foundations for our progress.

544 Advances in Thin-Sheet Laser Imaging Microscopy (TSLIM) and 3D Reconstruction of Mouse and Zebrafish Inner Ear Structures

Peter Santi¹, Shane Johnson¹, Peter Schacht¹, Heather Schmitz¹

¹University of Minnesota

We developed an optimized version of a light-sheet microscope called a thin-sheet laser imaging microscope (TSLIM). It nondestructively, optical sections whole mouse and zebrafish inner ear at subcellular resolution. Its advantage over two-photon and confocal microscopy is that it sections much deeper within tissues and minimized photobleaching and phototoxicity as only a thin portion of the tissue is exposed to the light at any one time. It is an optical microtome/microscope that can image live, transparent organisms such as the zebrafish embrvo and large opaque tissues that have been made transparent by fixation, decalcification, dehydration and clearing. It is compatible with immunohistochemical labeling and transfected cells labeled with fluorochromes that can be excited with either blue and green laser illumination. Construction of TSLIM will be described and we will show examples of its ability to characterize different inner ear structures and produce reliable morphometric data. TSLIM includes a high speed line-scan camera to reduce stack collection time and photobleaching while increasing specimen area and pixel density. Since the z-stack of optical sections produced by TSLIM are well aligned, they can be used to produce 3D reconstructions of inner ear structures that allow for novel visualization of cochlear cytoarchitecture and pathology.

545 New Probes and Techniques for Imaging **Excitation-Secretion Coupling in Living Cells** Daliang Li¹, Shiuhwei Chen¹, Jie Liu¹, **Wen-hong Li¹**

¹University of Texas Southwestern Medical Ctr at Dallas To examine regulated secretory activity in fully intact cells with high spatial and temporal resolution, we have developed a new class of fluorescent sensors for imaging exocytosis. These probes can be applied to cells in tissues or physiological preparations where normal cell-cell interactions are maintained. Combined with imaging modalities of high three dimensional selectivity and sensors for reporting intracellular signaling, these probes and techniques offer unprecedented opportunities for investigating the regulation and mechanism of excitationsecretion coupling in living cells.

546 Imaging the Functional Mammalian Inner Ear with Fluorescence Microendoscopy Mark Schnitzer¹

¹Stanford / HHMI

Progress in the field of hearing research and in clinical otolaryngology has been hindered by the lack of means to directly image the sensory cells of the living inner ear. We have developed a minimally invasive method, termed fluorescence microendoscopy (FME), for imaging live hair cells and spiral ganglion neurites within the intact guinea pig cochlea. FME may be a promising tool for addressing many current challenges in mammalian auditory research and in clinical otolaryngology, since it might provide hearing researchers the first technique capable of directly visualizing the functional microanatomy of the inner ear. Further technological developments may enable future therapeutic strategies tailored to the specific pathology and microanatomy of individual patients, and allow longitudinal processes such as development, degeneration, and regeneration to be observed with cellular-level resolution.

547 Imaging of Cochlear Implants

Timothy Hullar¹, Richard Chole¹

¹Washington University

Successful cochlear implantation depends on the time of onset of deafness, duration of deafness, and optimal programming of the device. Less well appreciated is the importance of proper placement of the implant within the cochlea. This variable has been difficult to explore because of a lack of adequate methods for determining the location of the implant following surgery.

Typical methods for evaluating implant position, such as computed tomography (CT), are limited by artifact caused by metal in the device. We have pursued ex vivo and in vivo techniques for improving our ability to image the implant and the surrounding cochlea in light of this consideration. Ex vivo techniques have included using micro CT scans, light microscopy, fluorescence microscopy, and subtractive offline processing of pre- and postimplantation medical CT scans on cadaveric human specimens. In vivo studies have allowed us to determine CT scan parameters optimized to reduce noise, increase resolution, and minimize radiation exposure.

These efforts to image the cochlea in multiple complementary ways have shown that we can determine the intracochlear location of an implant with confidence. Advances in imaging of cochlear implants such as will help improve surgical implantation techniques and electrode array designs, allowing for better patient outcomes.

548 Functional Neuroimaging of Musical Improvisation

Charles Limb^{1,2}

¹Johns Hopkins University School of Medicine, ²Peabody Conservatory of Music

Creativity, defined as the generation of novelty, is poorly understood, particularly when considered in an artistic context. Here I discuss studies of central mechanisms that give rise to the spontaneous production of novel musical material. To investigate the neural substrates that underlie spontaneous musical performance. we examined improvisation in professional jazz pianists using functional MRI. We sought to identify the neural substrates that give rise to spontaneous musical creativity, defined as the immediate, on-line improvisation of novel melodic, harmonic, and rhythmic musical elements within a relevant musical context. We found that improvisation (compared to production of over-learned musical sequences) was consistently characterized by a dissociated pattern of activity in the prefrontal cortex: extensive deactivation of dorsolateral prefrontal and lateral orbital regions with focal activation of the medial prefrontal (frontal polar) cortex. Such a pattern may reflect the difference between neural processes required for spontaneous creative behaviors such as improvisation, and processes that typically mediate self-monitoring and conscious volitional control of ongoing performance.

549 Genetic Evidence Supports a Role for Protocadherin 15 and Cadherin 23 in the Tip-Link Complex and Mechanotransduction

Kumar Alagramam¹, Richard Goodyear², Ruishuang Geng¹, David Furness³, Alexander van Aken², Walter Marcotti^{2,4}, Cornelis Kros², Guy Richardson²

¹Case Western Reserve University, ²University of Sussex, ³Keele University, ⁴University of Sheffield

Morphological, immunocytochemical and/or biochemical studies have shown that protocadherin 15 (Pcdh15) and cadherin 23 (Cdh23) proteins are associated with the tip links of hair bundles. To evaluate tip links in mice carrying mutations in Pcdh15 (Ames waltzer, av) or Cdh23 (waltzer, v) we examined three spontaneous mouse mutants. The av3J and v2J mice each carry a point mutation that is predicted to result in loss-of-function of Pcdh15 or Cdh23 respectively, and the av6J mice have an in-frame deletion predicted to remove most of the 9th cadherin ectodomain from Pcdh15. In early postnatal animals, severe disruption in bundle morphology is observed throughout the cochlea of av3J/av3J and v2J/v2J mice; in contrast, mild to

moderate disruption of the bundle is predominantly evident in the mid-apical turn of av6J/av6J mice. In av3J/av3J mice, early postnatal hair cells are unaffected by gentamicin exposure, transduction currents are severely reduced, and the uptake of [3H]-gentamicin and FM1-43 is abolished. In contrast, hair cells from av6J/av6J mice load with FM1-43 and [3H]-gentamicin, transduce, and are sensitive to aminoglycosides. Transduction currents can be recorded from hair cells of all three mutants but are reduced in amplitude or only detected at positive holding potentials. Scanning electron microscopy of cochlear hair cells reveals apparent tip links of normal morphology in av6J/av6J mice but not in v2J/v2J mice. Analysis of mature vestibular hair bundles, which are less severely affected than those in the cochlea, reveals an absence of tip links in the av3J/av3J and v2J/v2J mice and a reduction in the av6J/av6J mouse. The results presented here shows genetic evidence consistent with Pcdh15 and Cdh23 being part of the tip-link complex and being necessary for normal mechanotransduction.

550 Stereociliary Defects in Espin-Null Mice: Does Espin's Cooperative Over-Twisting of Actin Filaments Hold the Key?

Homin Shin¹, Gabriella Sekerkova², Kirstin Purdy Drew³, Gerard Wong⁴, Gregory Grason¹, **James Bartles²** ¹Univ. of Massachusetts-Amherst, ²Northwestern Univ. Feinberg Sch. of Medicine, ³Claremont McKenna College, ⁴Univ. of California-Los Angeles

At the core of stereocilia is a parallel actin bundle (PAB) scaffold that contains espins and other actin-bundling proteins. Scanning electron microscopic analysis of congenic jerker mice with a CBA/CaJ genetic background revealed dramatic defects in stereocilium morphogenesis and stability in jerker homozygotes, which lack espin proteins owing to a mutation in the espin gene. Stereocilia failed to increase in diameter and showed little differential elongation. Then, most experienced degeneration involving shrinkage and collapse. Given that stereocilia contain multiple actin-bundling proteins (fimbrins/plastins, espins, TRIOBPs, fascin-2), it is remarkable that other actin-bundling proteins cannot compensate for the lack espins. What unique property does an espin convey? One possibility reflects a newly discovered activity of the espins: the ability to cooperatively over-twist actin filaments in PABs. Small-angle x-ray scattering analysis of isolated PABs revealed that actin-bundling proteins overtwist actin filaments ~1 degree from the native -2.167 monomers/turn to

-2.154 monomers/turn, maximizing the number of aligned monomers between neighboring filaments in the PAB. Espins differ from other actin-bundling proteins, e.g., fascin, in that they over-twist actin filaments at low stoichiometry (espin-actin ratio, 1:50), suggesting an unusual degree of conformational rigidity. Thus, although espins can increase PAB diameter and length directly, their cooperative over-twisting could also pre-align prospective binding sites on neighboring filaments that will later become occupied by other actin-bundling proteins. Similarly, espin-containing PABs may make better substrates for myosin motors and actin cappers. We propose that espins act a critical early-intermediate step in stereocilium morphogenesis to make an optimal PAB substrate on which the proteins involved in stereocilium size regulation and stability operate. (NSF DMR08-04363, GW; NIH DC004314, JB).

551 Fascin 2b Is a Component of Stereocilia That Lengthens Actin-Based Protrusions

Shih-Wei Chou¹, Phil Sang Hwang¹, Gustavo Gomez¹, Carol Fernando¹, Megan West¹, Lana Pollock¹, Jennifer Lin-Jones², Beth Burnside², **Brian McDermott, Jr.**¹ ¹Case Western Reserve University, ²University of California

Stereocilia are modified microvilli, distinguished by their extreme length, height gradation, and rigidity-qualities necessary for hearing and balance. To identify proteins that organize the stereociliary cytoskeletal matrix, we scrutinized the hair-cell transcriptome of zebrafish. One promising candidate encodes fascin 2b, a filamentous actin-bundling protein found in retinal photoreceptors. Immunolabeling of zebrafish hair cells and the use of transgenic zebrafish that expressed fascin 2b fused to green fluorescent protein demonstrated that fascin 2b localized to stereocilia specifically. When filamentous actin and recombinant fusion protein containing fascin 2b were combined in vitro to determine their dissociation constant, a high binding affinity ($K_d \approx 0.37 \ \mu$ M) was observed. Electron microscopy showed that fascin 2b-actin filament complexes formed tightly packed, parallel actin bundles in *vitro*. We demonstrated that expression of either fascin 2b or espin, another actin-bundling protein, in COS-7 cells induced formation of long filopodia. Coexpression showed synergism through the formation of extra-long protrusions. Using phosphomutant fascin 2b proteins, which mimicked either a phosphorylated or an unphosphorylated state, in COS-7 cells and in transgenic hair cells, we showed that both formation of long filopodia and localization of fascin 2b to stereocilia were dependent on residue serine 38. Overexpression of wild-type fascin 2b in hair cells was correlated with increased stereociliary length relative to controls. These findings indicate that fascin 2b plays a key role in shaping stereocilia.

This research is supported by National Institute of Health Grant DC009437 and was funded by a Basil O'Connor Starter Scholar Research Award from the March of Dimes.

552 Expression and Vesicular Localization of Mouse TRPML3 in Stria Vascularis, Hair Cells, Vomeronasal and Olfactory Receptor Neurons But Not in Taste Receptors, Retinal and Somatosensory Neurons

Andrew Castiglioni¹, **Natalie Remis**¹, Emma Flores¹, Jaime García-Añoveros¹

¹Northwestern University

TRPML3 is a member of the mucolipin branch of the Transient Receptor Potential cation channel family. A dominant missense mutation in Trpml3 (also known as Mcoln3) causes deafness and vestibular impairment characterized by stereocilia disorganization, hair cell loss and endocochlear potential reduction. Both marginal cells of the stria vascularis and hair cells express Trpml3 mRNA. Here we use in situ hybridization, quantitative RTqPCR (reverse transcription-quantitative polymerase chain reaction) and immunohistochemistry with several antisera raised against TRPML3 to determine the expression and subcellular distribution of TRPML3 in the inner ear as well as in other sensory organs. We also use Trpml3 knockout tissues to distinguish TRPML3-specific from non-specific immunoreactivities. We find that TRPML3 localizes to LAMP1-containing vesicles (late endosomes and lysosomes) of hair cells and strial marginal cells, but not to stereociliary ankle links or pillar cells, which nonspecifically react with two antisera raised against TRPML3. Upon cochlear maturation TRPML3 protein redistributes to perinuclear vesicles of strial marginal cells and augments in inner hair cells versus outer hair cells. Although TRPML3 has been proposed as a salt taste receptor present in taste buds, we do not detect significant levels of TRPML3 in taste receptor cells, in the similar chemosensory solitary cells or in retinal and somatosensory neurons. However we find that vomeronasal and olfactory sensory receptor cells do express TRPML3 mRNA and protein, which localizes to vesicles in their somas and dendrites as well as at apical dendritic knobs, but not at sensory microvilly.

Financial Support: The Hugh Knowles Foundation (to JGA), T32 NRSA NS041234 (to AJC and ENF), F31 NRSA DC010529 (to NNR).

553 HCN Channels Are Necessary for Normal Vestibular Hair Cell Function

Geoffrey C. Horwitz¹, Jessica R. Risner-Janiczek¹, Sherri M. Jones², Jeffrey R. Holt¹

¹University of Virginia, ²East Carolina University

The hyperpolarization-activated current I_h is carried by homomeric and heteromeric assemblies of four protein subunits from the HCN gene family. While I_h has been identified in vestibular hair cells of the inner ear, its molecular identity and functional contribution have not been elucidated.

The expression of HCN mRNA in the vestibular system was examined using a quantitative RT-PCR screen for each subunit at postnatal (P) day 8, revealing HCN1 as the most highly expressed subunit. Expression ratios in the utricle for HCN1-4 were 509:150:1:31 respectively. Immunohistochemistry supported this result, revealing HCN1 in most utricle hair cells.

Vestibular I_h was characterized in mice ranging from P0 to P25. We found I_h was present in type I and type II hair cells, with a maximum conductance of 4.2 ± 1.8 nS (n=22) and 4.5 ± 2.6 nS (n = 49), respectively. I_h was blocked using ZD7288 or Cilobradine, reducing the conductance to 0.4 ± 0.2 nS (n = 5) or 0.5 ± 0.2 nS (n = 7), respectively. We verified contributions of HCN channels using a dominant negative mutation in HCN2, which reduced the conductance to 1.5 ± 0.3 nS (n = 12). In order to determine which subunits carried I_h , we examined mice deficient in HCN1, 2, or both. We found no evidence of I_h in HCN1^{-/-}

mice (n = 40) or HCN1/2^{-/-} mice (n = 8), however I_h from HCN2^{-/-} appeared similar to wild type cells (4.2 ± 1 nS, n = 8).

To elucidate the functional contribution of I_h , we injected 50 pA of hyperpolarizing current and measured the sag and rebound potentials. We found that activation of I_h evoked a 5-10 mV sag depolarization and a subsequent 15-20 mV rebound upon return to rest. Both the sag and rebound were absent after blocking I_h . Interestingly, HCN1-deficient mice showed VsEP and rotarod deficits. Similar deficits were present in mice with HCN1 deletion restricted to the inner ear using a Cre-Lox strategy. We therefore conclude that HCN1 is required for vestibular hair cell function and normal balance.

554 Efficacy of Synaptic Inputs to Type II Cochlear Afferents

Catherine Weisz¹, Rodrigo Martinez-Monedero², Elisabeth Glowatzki^{1,2}, Paul Fuchs^{1,2}

¹Johns Hopkins University School of Medicine Department of Neuroscience, ²Johns Hopkins University School of Medicine Department of Otolaryngology-Head and Neck Surgery

Type II spiral ganglion neurons receive synaptic inputs from multiple cochlear outer hair cells (OHC). Intracellular recordings from the dendrites of type II afferents under OHCs show that postsynaptic potentials average 4 mV in amplitude, requiring spatial and temporal summation to reach action potential threshold. Therefore, it is necessary to determine the number and location of inputs onto individual type II afferents, as well as the synaptic strength of individual inputs to determine the stimulus strength necessary for action potential initiation. Dendritic electrophysiological recordings were performed in postnatal day 5-9 rats. Individual OHCs were stimulated to release neurotransmitter using 10 ms 'puff' application of high KCl solution while recording excitatory postsynaptic currents (EPSCs) in the post-synaptic type II dendrite. Using this method in three experiments, we found that 12 of 67 OHCs tested were presynaptic, producing EPSCs within 30 ms of the puff. 'Response probability' varied, ranging up to 0.46, with an average of 0.22. EPSCs could be measured after stimulating OHCs as far as 178 microns from the recording site, yielding partial maps of type II afferent receptive fields. EPSCs in type II dendrites averaged 28.3 ± 8.3 pA. Physiological mapping will be combined with immunolabeling to more completely describe the numbers and locations of synapses on individual type II afferents. We are studying the expression of presynaptic ribbons (CTBP2) and postsynaptic markers in the OHC area in tissue in which a neuronal tracer included in the electrode solution filled the type II dendrite during electrophysiological recordings. This will determine the number of synaptic contacts on an individual type II afferent and the proportion of synapses that contain a presynaptic ribbon. Supported by NIDCD grants R01 DC000276 and R01 DC006476, F31DC010948, T32 DC000023 and a grant from the Blaustein Pain Foundation of Johns Hopkins.

555 Pinball Wizard, a Deafness and Blindness Gene in Zebrafish, Encodes a Novel Transmembrane Protein Essential for Hair Cell Transduction and Synaptic Transmission

Shuh-Yow Lin¹, Melissa Vollrath², David Corey³ ¹UC San Diego, ²McGill University, ³Harvard Medical School

Although the general principles of synaptic transmission are largely understood, the essential molecular components underlying sensory specializations such as the ribbon synapses in sensory receptors that mediate graded transmitter release are only beginning to be identified. In a large-scale insertional mutagenesis screen in zebrafish designed to identify mutants with sensory defects, we found one line, pinball wizard (pwi), with a deafness and blindness phenotype. The pwi gene encodes a novel transmembrane protein with a coiled-coil region. Using antibodies against pinball we show punctate staining at basolateral surfaces and intracellular organelles of hair cells. The staining is largely colocalized with the synaptic ribbon marker Rab3. Electrophysiologically, the mutant inner ear hair cells have reduced mechanotransduction as revealed by microphonic potential measurement. Furthermore, by utilizing the Ca2+ intensity sensor GCaMP3 and expressing it in the statoacoustic ganglion, we found that the sound evoked Ca2+ signals in the acoustic sensitive neuron is significantly reduced and the transmission is not reliable in mutant fish. Finally mutant hair cells fail to correctly transport Otoferlin, which is required for vesicle exocytosis and replenishment, to the basolateral synaptic area. Similarly vesicle associated motor Myosin VI is mis-targeted as well. In contrast the subcellular distribution of non-vesicle binding motor Myosin VIIa, which is enriched in hair cell bundles and soma, is not affected. Since Pinball is not expressed in hair cell bundles, mis-targeting of Myosin VI or other components of the transduction apparatus likely causes the reduction in mechanotransduciton. Taken together, our results demonstrate that pinball wizard is critical for conveying sensory information in vertebrate auditory hair cell by regulating trafficking of vesicle proteins essential for ribbon synapse function and stereocilia transduction.

556 A Large-Scale Ensemble Analysis of Proteins in Affinity-Purified Synaptic Ribbon Cores

Albena Kantardzhieva^{1,2}, Marcello Peppi^{1,2}, William Sewell^{1,2}

¹Massachusetts Eye and Ear Infirmary, ²Harvard Medical School

The synaptic ribbon, which is found in hair cells, photoreceptors, and retinal bipolar cells, is an enigmatic, protein-rich structure thought to generate transient response capability in a synapse otherwise optimized for graded responses. Recent investigations into the structure and role of the synaptic ribbon have led to widespread scientific and clinical interest in understanding its detailed

function, but at present the knowledge of its molecular composition is rather limited.

We have performed a large-scale, affinity purification of the ribbons from 1000 mouse retinas, followed by a multidimensional, mass spec-based proteomics analysis. For affinity purification, we used antibodies to the B domain of CtBP to collect ribbons and IgG as a control for nonspecific binding. This resulted in much better discrimination of noise vs. signal in our data, setting it apart from previous attempts for biochemical characterization of the ribbon, and allowing stochiometric comparison of the major components. We observed most of the major proteins previously described to be part of the ribbon core. Interestingly, our quantification data suggest that there is as much Cast and ELKS (ERC1 and 2) protein in the ribbon as CtBP, and each of these groups contributes only about 10% of the total molar ratio of proteins arguing against previous estimates of CtBP content. Another unexpected finding is the presence of a multitude of kinases and phosphatases in the ribbon, collectively amounting to more protein than CtBP, and suggesting tightly regulated control of the function and dynamics of the other proteins present in the complex. Tubulin was present in relatively high molar amounts too. Our data also suggests that the presence of some enzymes from the glycolytic pathway may be specific to the ribbon itself. We speculate that their final products serve as substrates for CtBP possibly influencing its conformation and function.

557 Click Chemistry and Mass Spectrometry to Measure Protein Turnover in Oxidatively Stressed Hair Cells

Josh Katz¹, Peter Gillespie², Jung-Bum Shin¹

¹University of Virginia, ²Oregon Health Science University Although the mammalian inner ear has largely lost the capacity to renew sensory hair cells, hair cell function can be restored after damage. Restorative processes likely depend on degradation and de-novo synthesis of damaged proteins. Our lab is therefore interested in studying the role of protein turnover in various cochlear pathologies, both in the context of hair cell repair and in hair cell death.

We are examining whether the repair of damaged hair cells is accompanied by a change in protein synthesis activity. To this end, we expose explant cultures of chicken and mouse auditory and vestibular organs to oxidative stress and determine the protein synthesis activity in affected hair cells. Utilizing a detectable methionine analogue called azidohomoalanine (AHA), newly synthesized proteins can be detected and visualized in situ using the Click reaction, which attaches a fluorophore to the reactive azido group of AHA. Using this method, we have found that basal protein synthesis activity differs in vestibular and auditory hair cells, and preliminary results indicate that oxidative stress significantly influences protein synthesis rates. In the future, using mass spectrometry analysis of hair cells that have been metabolically labeled with isotopically heavy amino acids, we will measure the protein synthesis rate of individual proteins in response to oxidative stress. In summary, we are using a combination

of imaging and mass spectrometry analysis to study the relationship between hair cell damage and protein turnover in hair cells.

558 In Vivo Imaging of Functional Mammalian Hair Cells with Fluorescence Microendoscopy

Shelley Batts¹, Eunice Cheung^{1,2}, Ashkan Monfared^{1,3}, Nikolas Blevins¹, Gerald Popelka¹, Mark Schnitzer^{1,4} ¹Stanford University, ²St. Lawrence University, ³George Washington University, ⁴HHMI

Hearing loss is a pervasive health problem that often results from the death of the sensory cells of the cochlea, the auditory hair cells. Hair cells are susceptible to damage from environmental and chemical toxins, and do not regenerate in mammals. Non-destructive cellular level imaging of the functional inner ear has been prohibitive due to the cochlea's extreme fragility and inaccessible location. We have developed a minimally invasive method for imaging living hair cells and spiral ganglion neurites within the intact mammalian cochlea, called fluorescence microendoscopy (FME). We show FME is a promising tool for addressing many current challenges in auditory research, and demonstrate through auditory brainstem measurements that FME can inspect functional ears that are engaged in hearing. Histological analyses performed to date indicate that FME does not prompt apoptosis or expression of early markers of cellular damage in auditory hair cells. Thus, cochlear microendoscopy is poised to provide hearing researchers the first tool capable of directly visualizing the functional microanatomy of the inner ear, which might enable future therapeutic strategies tailored to the specific pathology and microanatomy of individual patients.

Support: NIH Individual Postdoctoral National NRSA Award (1F32DC011232-01), HHMI, Coulter Foundation, Beckman Foundation, Stanford Medical Free Electron Laser Program, NOHR

559 Manipulation of Inner Ear Hair Cells Via Magnetic Nanoparticles

David Rowland¹, Damien Ramunno-Johnson¹, Dolores Bozovic¹, Jae-Hyun Lee², Jinwoo Cheon²

¹University of California at Los Angeles, ²Yonsei University Hair cells constitute the primary system responsible for nonlinear amplification and frequency selectivity. Once their overlying membrane is removed, hair cells of the amphibian sacculus show spontaneous oscillations. To explore the dynamics of oscillation without an imposed external load, we combined fast camera recording techniques with a physical manipulation system that minimally alters the natural oscillation of a hair bundle. Here we present a technique for the attachment of magnetic nanoparticles to hair cell stereocilia and their subsequent mechanical actuation by a moving permanent magnet. We used this technique to impose static displacements on freely oscillating bundles. Our data indicate that steady-state offsets affect both the frequency and the accompanying amplitude of the oscillations. Further deflection in the negative direction changed the temporal profile of the oscillation with prolonged myosin motor climbing.

560 Cotransfection of PAX2 and Math1 Promotes Cochlear Supporting Cell to Proliferate and Differentiate to Hair Cells After Neomycin Insult

Yan Chen¹, Huawei Li¹

¹EENT Hospital of Shanghai Medical College of Fudan University

Hair cell damage/loss is a major cause of sensorineural hearing loss. Since mammalian cochlear hair cells cannot be replaced spontaneously, hearing loss would be permanent once these cells are injured. Overexpression of Math1 has been demonstrated to induce support cell to transdifferentiate into ectopic hair cells. However, the survival supporting cells of organ of Corti are limited after hair cell loss. The ideal strategy for hair cell regeneration is to promote surviving cell proliferation followed by induction of hair cell differentiation. Our previous study suggested that Pax2 expression is essential to progenitor cell proliferation in developing inner ear. In this study, cultured neonatal mouse organs of Corti were treated with neomycin for 24h to eliminate hair cells, followed by incubation with recombined adenovirus (Ad.EGFP, Ad.PAX2-IRES-EGFP. Ad.Math1-IRES-EGFP and Ad.PAX2-IRES-Math1). BrdU, a mitotic tracer, was used to label proliferating cell. Double immunofluorescence of SOX2 and EGFP confirmed the efficiency of gene delivery to cochlear support cells. Our results showed that PAX2 significantly overexpression of promoted proliferation of supporting cells located beneath preexisting hair cells, as indicated by SOX2 and BrdU double immunofluorescence. In Ad.PAX2-IRES-Math1 incubation group, more new hair cells were observed in damaged region at two weeks after neomycin insult, compared with Ad.PAX2-IRES-EGFP treated cochleae. Most new hair cells were labeled by BrdU, suggesting that newborn cells underwent cell proliferation. Moreover, newborn hair cells were PAX2 immunopositive, suggesting that these cells originated from transfected cells. Putting together, these data demonstrated that cotransfection of PAX2 and Math1 promoted support cells to proliferate and differentiate to new hair cells.

561 Functional Properties of Newly Trans-Differentiated Hair Cells Induced by Math1

Juanmei Yang^{1,2}, Ebenezer Yamoah¹, Fanglu Chi², Zhao Han²

¹Dept. of Anesthesiology and Pain Medicine, Program in Communication Science, University of Californ, ²Eye & ENT Hospital of Fudan University, Department of Otolaryngology-Head and Neck Surgery

Math1, a mouse homolog of the drosophila Atonal, is a basic helix-loop-helix transcription factor required for hair cell development. It is reported that math1 over expression induces ectopic hair-cell-like cells both *in vitro* and *in vivo*. Moreover, it is unclear whether the math-induced ectopic hair cells share the functional phenotype of normal hair

cells. Here, ad5-*EGFP-math1* was used to over express math1 in the cochlea of neonatal rats in vitro. Ad5-*EGFPmath1* infected cells at the lesser epithelial ridges (LER) and greater epithelial ridges (GER) under went morphological changes, converting from flat shape into cup-like or oblong shape, and assuming hair-cell-like morphology 36 hrs after infection.

Patch clamp technique was used to determine the electrophysiological properties of the newly differentiated hair cells. Sodium current appeared ~36-hrs after infection, and continued up to day 15. Moreover, L-type calcium current appeared ~60 hrs after infection. Potassium currents undergo gradual alterations, changing in kinetics and magnitude. It is worth noting that the HCN-type current appeared at the earlier time points (5 to 10 days), and gradually disappeared at later time points (15 to 20 days). FMI-43, a dye that permeates open mechanotransducer channels of normal hair cells, also could permeate the newly differentiated hair cells. We will demonstrate that newly differentiated hair cells at the LER and GER induced by Math1 undergo not only morphological but also functional changes that are reminiscent of the developing and regenerating hair cell.

Key words: ad5-*EGFP-math1*, LER and GER, Transdifferentiation, hair cells

562 Biophysical Properties and Molecular Identity of Voltage-Gated Sodium Channels in Rat Cochlear Inner Hair Cells

Tobias Eckrich¹, Stuart L Johnson¹, Wibke Singer², Marlies Knipper², Stephanie Kuhn¹, Walter Marcotti¹ ¹University of Sheffield, UK, ²University of Tübingen Before the onset of hearing mammalian inner hair cells (IHCs) transiently generate spontaneous calcium action potentials (APs; Marcotti et al 2003 J Physiol 548: 383-400). This spontaneous activity is thought to control important developmental processes such as the refinement of synaptic connections or the guidance of intrinsic IHC development regarding ion channels and synaptic proteins (Kros et al 1998 Nature 394: 281-284). The frequency of IHC APs is influenced by various membrane currents, including a transiently expressed TTX sensitive sodium current (Marcotti et al. 2003 J Physiol 552.3, 743-761). In the present study, we used single-cell patch clamp recording and immunolabelling to characterise the biophysical properties of the sodium current, its role in AP activity and the channel isoforms potentially involved in underlying the sodium current expressed in rat cochlear IHCs.

Using current-clamp recordings, we found that APs in rat IHCs occurred spontaneously until postnatal day 7 (P7). Furthermore, APs could be triggered up to P11 in the majority of IHCs by injecting small depolarising currents. The biophysical properties of the sodium current were characterized using voltage-clamp recordings. Before the onset of hearing, a rapidly activating and inactivating sodium current was found to be present in all IHCs investigated. The sodium current showed high temperature dependence and both the size and kinetics change with development/IHC position along the cochlea. The

expression of sodium channel subunits in both apical and basal IHCs was investigated using immunolabelling. We found that the different characteristics of the spontaneous AP activity between IHCs positioned in the apical and the basal regions of the cochlea could be explained, at least in part, by a differential expression of sodium channels. *Supported by The Royal Society, Wellcome Trust, RNID. T.E. is an MRC funded PhD student.*

563 Patterning of Spontaneous Action Potentials in Immature Inner Hair Cells Varies with Cochlear Location and Is Dependent on Acetylcholine

Stuart L. Johnson¹, Tobias Eckrich¹, Valeria Zampini^{1,2}, Stephanie Kuhn¹, Christoph Franz³, Kishani Ranatunga⁴, Sergio Masetto², Marlies Knipper³, Corné J. Kros⁴, Walter Marcotti¹

¹University of Sheffield, ²University of Pavia, ³University of Tübingen, ⁴University of Sussex

Patterned spontaneous action potential (AP) activity occurs during critical periods of mammalian sensory system development and is hypothesized to drive the refinement of synaptic connections before the onset of sensory-induced activity (Katz, Shatz 1996 Science 274: 1133-8). Position dependent patterning of AP activity has been observed prior to the onset of hearing in chick auditory brainstem neurones (Lippe 1995 Brain Res 703: 205-13). It is likely that such activity is driven by AP firing in cochlear inner hair cells (IHCs) (Kros et al 1998 Nature 394: 281-4). It remains uncertain whether IHC AP activity is intrinsically generated or initiated by waves of ATP released from nearby supporting cells (Tritsch et al 2007 Nature 450: 50-5).

AP activity was investigated in IHCs of altricious rodents maintained at 35-37°C in perilymph-like extracellular solution using whole-cell current clamp and cell-attached voltage clamp recordings. We show that during the first postnatal week, AP activity is intrinsically generated by IHCs and its frequency and pattern differ as a function of position along the cochlea, with apical IHCs exhibiting bursting as opposed to more sustained firing in basal cells. The difference in pattern is likely to be determined by the efferent neurotransmitter ACh, which by fine-tuning the IHC's resting membrane potential (Vm) is crucial for the bursting pattern present in apical IHCs. Endogenous extracellular ATP also contributes to maintaining the required Vm of both apical and basal IHCs via the activation of SK2 channels.

We hypothesize that the difference in IHC firing pattern along the cochlea during the first postnatal week guides the functional differentiation of IHCs along the tonotopic axis (Johnson et al 2008 J Neurosci 28: 7670-8) and refines tonotopic maps along the auditory pathway before the onset of sensory experience (Kandler et al 2009 Nat Neurosci 12: 711-7).

Supported by the Wellcome Trust, RNID, Deafness Research UK, The Royal Society and the MRC

564 The Role of Kir2 Channel Expression in Mouse Utricle Hair Cell Signaling

Michaela E. Levin¹, Laura Digilio¹, Jeffrey R. Holt¹

The potassium inward rectifier current (I_{K1}) has been previously identified in mechanosensory hair cells of the mouse utricle. We were interested to identify its molecular composition and its function in hair cells. Based on previous work we focused on the potassium selective inward rectifier 2 gene family, Kir2.

Using quantitative RT-PCR we show expression of all four Kir2 family genes in the mouse utricle at developmental stages from P0 to adulthood with Kir2.1 being the most highly expressed. To confirm expression of Kir2.1 subunits in hair cells we used phalloidin-Alexa543 and an antibody specific to Kir2.1. Antibody specificity was validated in utricles harvested from mice that lacked Kir2.1. To examine the molecular composition of I_{K1} we recorded voltage-dependent currents from type II hair cells in response to 50-msec steps from -124 to -24 in 10 mV increments. Wild type cells had rapidly activating inward currents with reversal potentials close to the potassium equilibrium potential. The whole cell conductance was 3.3±1.3 nS (n=31). Utricle cells from mice that lacked Kir2.1 had no potassium-selective inward currents (n=78) at any of the stages examined.

To identify the functional contribution of I_{K1} to hair cell signaling we recorded membrane potentials in currentclamp mode. Hair cells from mice that lacked Kir2.1 had significantly (p<0.0001) more depolarized resting potentials (-53±4 mV; n=22) than wild type cells (-60±5 mV; n=22). In response to -40 pA steps cells that lacked Kir2.1 had slower (τ =43±23 msec; n=16) and larger amplitude responses (-131±21 mV; n=16) than those of wild type cells (τ =12±6 msec; -88±8 mV; n=16).

The evidence shows that Kir2.1 is required for I_{K1} in type II utricle hair cells. As such, Kir2.1 contributes to more hyperpolarized resting potentials and affects the amplitude and speed of the receptor potential in response to small input currents that could arise from small bundle deflections or efferent neurotransmission.

565 Lipid Raft Organization of BK-Type Potassium Channels in Chick Hair Cells

Erin Purcell¹, Liqian Liu¹, Paul Thomas¹, R. Keith Duncan¹ ¹University of Michigan

The large-conductance BK-type potassium channels underlie the electrical tuning of hair cells and open in a voltage- and calcium-dependent manner. As a calciumactivated channel, BK requires close proximity (estimated to be within tens of nanometers) to voltage-gated calcium channels (VGCCs). We hypothesized that 'lipid rafts' compartmentalize BK and VGCCs into spatially restricted signaling complexes in the hair cell membrane. Lipid rafts are classically defined as sphingolipid- and cholesterolenriched microdomains which are resistant to disruption with non-ionic detergents. We present several lines of evidence supporting the localization of BK and VGCCs in lipid rafts in hair cells: (1) immunocytochemistry demonstrates expression of a prototypic lipid raft marker (cholera toxin B) in punctae at the hair cell base; (2) immunoblotting following sucrose-gradient ultracentrifugation reveals BK removal from lipid raft (buoyant, detergent-resistant) fractions after cholesterol depletion with methyl-beta-cyclodextrin (MbCD); and (3) whole-cell voltage-clamp data shows a ~50% reduction in peak steady-state calcium-sensitive outward current in chick hair cells following MbCD treatment (Control=700.1 +/- 62.2 pA, MbCD=361.7 +/- 80 pA, p<0.05, n=15 cells, ANOVA). There was a slight increase (~30%) in peak inward calcium current following cholesterol depletion, ruling out loss of calcium channels and/or function as a cause of reduced calcium-dependent outward current (Control=-58 +/- 9.7 pA, MbCD=-77.6 +/- 9.5 pA, p<0.05, n=32, ANOVA). The loss of outward current could be compensated by overwhelming the internal cell solution with saturating concentrations of calcium (>20 uM). Our results support the hypothesis that VGCCs and BK channels are compartmentalized in the hair cell membrane in lipid rafts. Lipid rafts may be a key mechanism for modulating ion channel function in hair cells, with potential significance for hearing loss in dyslipidemic patients.

566 The Calcium Dependence of AChRs in Avian (*Gallus*) Hair Cells

Gi Jung Im^{1,2}, Marcela Lipovsek³, Eleonora Katz³, Ana Belen Elgoyhen³, Paul Albert Fuchs¹

¹Johns Hopkins Medical Institutes, ²Korea University College of Medicine, ³INGEBI

Efferent cholinergic inhibition of mammalian and avian auditory hair cells is thought to be mediated by heteromeric $\alpha 9\alpha 10$ acetvlcholine receptors (AChRs). Gating of the AChR leads to activation of calciumdependent potassium channels to hyperpolarize the hair cell. Heterologous expression in Xenopus oocytes has shown that mammalian (rat) $\alpha 9\alpha 10$ AChRs have a substantial permeability to calcium ($pCa/pK \sim 9$) similar to that of the native AChR (pCa/pK ~8, Gomez-Casati et al.,2005 J. Physiol. 566:103). In contrast, avian (chicken) $\alpha 9\alpha 10$ in oocytes is significantly less Ca²⁺-permeable (pCa/pK <3), and here we provide a comparison with properties of the native chicken hair cell AChR. Wholecell, giga-ohm seal intracellular recordings were made on 'short' (abneural) hair cells approximately at the midpoint of the 4 mm long basilar papilla (chicken auditory organ) from late-stage embryos (E17-20) using intracellular cesium/BAPTA (10 mM) and extracellular apamin (300 nM) to minimize the SK current. Puff application of ACh (1 mM, 200 ms) elicited inward currents at negative membrane potentials that reversed near 0 mV. The reversal potential was determined using 'ramp' voltage commands from -100 to +40 mV, 200 ms duration, designed to coincide with the steady maximal response to ACh. In most cells a standard voltage-step protocol also was used. These measurements (n = 5) were carried out in 1, 3, and 10 mM calcium saline. The ACh-evoked current was largest in 3 mM calcium, and displayed sharp outward rectification. Outward rectification was more pronounced in higher calcium concentrations and could be reduced by conditioning depolarization – both observations

supporting a 'calcium permeation and block' effect. There was no significant effect of calcium on reversal potential for these concentrations. Thus, like cloned avian $\alpha 9\alpha 10$, the native chicken hair cell AChR appears to have a relatively low permeability to calcium.

Supported by NIDCD R01DC001508, the National Research Foundation of Korea Grant funded by the Korean Government MEST, Basic Research Promotion Fund (NRF-2010-013-E00015) and a Howard Hughes International Scholar Grant.

567 Localizing SK2 Channels and α 9/10-NAChRs at Olivocochlear Postsynaptic Sites

Elizabeth K Storer¹, R. Keith Duncan², Michele H Jacob¹ ¹*Tufts University School of Medicine*, ²*Kresge Hearing Research Institute, University of Michigan*

Cochlear hair cell function is modulated by cholinergic innervation from efferent olivocochlear fibers originating in the brainstem. At olivocochlear postsynaptic sites in hair cells. q9/10 nicotinic acetvlcholine receptors (nAChRs) colocalize with and are functionally coupled to small conductance Ca²⁺-sensitive SK2 potassium channels. Activation of this synapse by acetylcholine results in hair cell hyperpolarization. These inhibitory responses are critical for normal regulation of sound sensitivity and frequency selectivity. However, the mechanisms underlying olivocochlear synapse assembly are poorly Our work is identifying the molecular understood. mechanisms that direct the co-localization and functional coupling of a9/10-nAChRs and SK2 channels at postsynaptic sites in avian hair cells. We are defining the role of SK2 alternative splicing in SK2 channel protein interactions and assembly of the synapse. We show that an SK2 splice variant, previously identified in posthatch chicks, is also present at embryonic stages and exhibits in abundance throughout development. changes Importantly, we find that SK2 variants differ in their interactions with protein binding partners. These differences may influence the targeting and/or retention of the SK2 splice variants and α 9/10-nAChRs at the synapse. Based on these studies, we propose that SK2 alternative splicing regulates the assembly and function of olivocochlear synapses by altering protein interactions of SK2 channels.

This work is supported by NIH NIDCD grants 5F31DC010114 (to EKS) and R01DC008802 (to MHJ).

568 The Effects of β -1 and β -4 Subunits on Single Channel Kinetics of Chick Slo Channel Jun-Ping Bai¹, Dhasakumar Navaratnam¹

¹Yale University Dept. of Neurology

Electrical tuning is a mechanism of frequency selectivity in the auditory epithelium of non-mammalian species, including chick and turtle. Hair cells in those animals are arranged in a tonotopic manner and have a continuously changing frequency of membrane potential oscillation along the tonotopic axis. The variation of kinetic properties in the BK channel plays an important role in changing intrinsic oscillation frequency in hair cells along the tonotopic axis. Beta subunits of the BK channels have been shown to affect the kinetic properties of the BK channel in hair cells and other systems. Here we use an oocyte expression system and the inside-out patch clamp technique to determine subunit effects on the kinetics of chicken Slo single channel activities.

We found that the beta-4 subunit increases channel burst duration, an effect similar to the beta-1 subunit, albeit not as pronounced. The increase in burst duration is achieved by a combination of increased open times and number of openings within a burst. In addition to its effects on burst duration, both beta subunits also increase interburst duration at each given P_o . We determined a high correlation between burst duration of single channels and relaxation times after a voltage step. Similarly, mean open times of single channels correlated with macroscopic relaxation times. The beta-1 and beta-4 effects prolonging burst duration in single channel recordings, and activation and deactivation times in macroscopic currents suggest the beta subunits slow the transition from open to close states and vice versa.

In our macroscopic currents recordings, we determined that the beta-4 subunit caused the channel to dramatically increase opening in response to physiological increases in Ca^{2+} concentrations (5-50 μ M) at a hair cells operating membrane voltage (-60 to -40 mV). In contrast, cSlo alone shows minimal opening at these voltages. The action of beta-1 subunits results in a channel that is near maximally open at these voltages even with resting concentrations of Ca^{2+} (5 μ M). These data bring us closer to a molecular understanding of how electrical tuning is modulated. Supported by NIH grant R01 DC 007894

569 The Role of β-1 and β-4 Subunits in Surface Expression of Chick Slo Channel Jun-Ping Bai¹, Alexei Surguchev², Dhasakumar

Navaratnam¹

¹Yale University Dept. of Neurology, ²Yale University Dept. of Otolaryngology

BK channels encoded by the Slo gene are the principal determinant of electrical resonance in hair cells of the nonmammalian inner ear. These channels show variable kinetic properties in hair cells along the tonotopic axis. Earlier studies suggested that the association of cSlo channels with other interacting proteins, including beta-1 and beta-4 subunits, might bring about variation of cSlo previous channel kinetics tonotopically. Our immunofluorescence staining data implied that the expression of cSlo gradually increases from the low to high frequency fractions of chicken papilla. In contrast, cSlo transcript levels show the inverse pattern with high levels of expression at the low frequency end of the papilla. Since chicken beta 1 and beta 4 subunit transcripts also show higher expression level in the low frequency end, we sought to ascertain if beta subunits modulate the surface expression of cSlo. Macroscopic current recordings from injected oocytes showed the distribution of currents from cSlo shifts to a lower range with co-expression of either beta-1 or beta-4 subunits. Using fluorescence-activated cell sorting (FACS) analysis, we noted a significant decrease in surface expression of Slo when co-expressed with either of the two beta subunits, leaving the total amount of intracellular Slo unchanged. To examine if the decrease in Slo surface expression is physiologically important, chick cochlea were kept in culture with siRNA to beta-1 and separately beta-4 subunits. As measured by fluorescent antibody labeling, siRNA to beta-1 and beta-4 resulted in a significant increase in surface expression of Slo. Taken together, our data indicated that beta-1 and beta-4 subunits play a significant physiological role in surface expression of Slo in chick hair cell.

Supported by NIH grant R01 DC 007894

570 The Acetylcholine Receptor Current in Neonatal Mouse Inner Hair Cells

Michael G. Evans¹, Helen J. Kennedy²

¹*Keele University,* ²*Bristol University*

We have investigated responses to acetylcholine (ACh) in mouse inner hair cells (IHCs) at 6-10 days after birth. During this period IHCs receive efferent cholinergic innervation. The apical turn of the cochlea was isolated and the basal surfaces of the IHCs were exposed by mechanically stripping away the outer rim of the organ of Corti, following removal of the tectorial membrane. Wholecell recordings were made in artificial perilymph and ACh (0.1 mM) was applied from a puffer pipette positioned nearby. The I-V relation for the ACh-sensitive current showed inward and outward rectification with a reversal potential at 0 mV (Cs⁺-based internal filling solution with 10 mM BAPTA). The current activated over about 0.5s. The mean current, measured at +60 mV, -60 mV and -100 mV was +0.53 nA. -0.32 nA and -0.99 nA respectively (n=7). The current was cationic since in low (30 mM) external Na⁺ (replaced by n-methyl-glucamine) the reversal potential was -19 mV and currents were much smaller, especially at negative voltages. Preliminary data is suggestive of a block of the AChR by external divalent cations since the largest responses were observed in solutions lacking calcium or magnesium. The I-V data was fitted with a single energy barrier model, which assumes a single blocking site within the channel pore (Kros et al., 1992, Proc Roy Soc), usually assumed to be occupied by divalent cations. The fit indicated that the blocking site was about 0.4 of the way through the channel from the outside. In comparison with data from adult outer hair cells the main difference is that ACh application in IHCs produces larger and more slowly activating cationic currents, although it is unclear whether this reflects differences in the respective AChRs. The large size of the AChR current in neonatal IHCs is ideal for future investigation of channel activation and ion permeation.

571 Volume Regulation in Frog Auditory Hair Cells: Additional Evidence for Water Permeable Channels

Nasser Farahbakhsh¹, Peyman Farhangi Oskuei¹, Dwayne Simmons¹, Peter Narins¹ ¹UCLA

When amphibian papillar hair cells (APHCs) of the leopard frog, *Rana pipiens pipiens*, are osmotically challenged,

they exhibit a characteristically asymmetric (rectifying) response: Small decreases (5%, or less) in the extracellular solution's osmolarity do not significantly affect the cells' volume (iso-volumetric response); larger decreases produce a relatively slow volume increase in APHCs, while exposure to a hyperosmotic medium leads to rapid shrinking of these cells. Furthermore, the rate of volume change appears to be a function of the rate of extracellular osmotic change.

In addition to the slow and perfusion-rate-dependent volume increase, APHCs also exhibit a delayed (classical) regulatory volume decrease (RVD) when exposed to hypo-osmotic solutions: for a 50% reduction in osmolarity, the time-to-peak-volume is 383 ± 51 s and 1285 ± 153 s for the flow rates of 1.6 and 0.23 ml/min, respectively. During the remainder of a 30-min-long exposure, APHC volume falls to $78.6 \pm 2.7\%$ and $93.1 \pm 2.1\%$ of the peak, for the two flow rates, respectively.

Upon return to the iso-osmotic solution, the APHC volume undershoots to $74.6 \pm 2.3\%$ and $88.6 \pm 3.1\%$ of the initial volume, respectively. The regulatory volume increase (RVI), however brings the cell volume to $87.1 \pm 3.9\%$ and $97.7 \pm 3.1\%$ of its initial volume in 30 min. The two flow rates used in these experiments are equivalent to 52.3 and 7.5 mOsm/min osmolarity change, respectively.

Our earlier work suggests that the volume changes of APHCs induced by osmotic challenge require the presence of one or more aquaporin channels, but no specific water channel has been identified in vertebrate hair cells. Immunocytochemistry was used to identify a member of the aquaporin family of water channels. Aquaporin-4 (AQP4) was identified in isolated APHCs as well as in whole tissue of the amphibian papilla. In isolated APHCs, AQP4 was identified in basal and apical aspects and shows uniform immunoreactivity.

These results suggest that at much lower (physiological) rates of osmolarity change, APHCs might be able to maintain their shape and thus preserve their level of vitally important mechanical, electrical and chemical activities. The significance of transmembrane solute transport and water channel expression in amphibian auditory hair cells will be discussed.

572 The CNGA3 Channel Subunit Binds to the Intracellular C1q Domain of EMILIN1

Dakshnamurthy Selvakumar¹, Marian Drescher¹, Khalid Khan², Dennis Drescher¹

¹Wayne State University, ²Kuwait University

Olfactory forms of CNG (cyclic nucleotide-gated) ion channels are expressed by hair cells in the cochlea (Drescher et al., Mol. Brain Res. 98: 1-14, 2002), and the CNG channel has been considered as a candidate for the hair cell mechanotransduction channel. Previously, we described full-length sequence for three variants of the cone/olfactory type cGMP-gated CNGA3 that are expressed in a teleost saccular hair cell preparation. A custom antibody raised against a peptide antigen present in the amino terminus of teleost hair-cell CNGA3, specific to cone/olfactory type CNGA3 and not found in chemosensory cell CNGA3, localized CNGA3 to the hair cell stereocilia in the trout saccule. We demonstrated that the carboxy terminus of this CNGA3 variant binds to the intracellular C1g domain of EMILIN1 by yeast two-hybrid protocols (Selvakumar et al., Assoc. Res. Otolaryngol. Abstr. 33: 28, 2010). EMILIN1 is an extracellular matrix protein, a member of the elastic fiber system which interacts with B1-integrin. Confirmation of the binding between CNGA3 and EMILIN1 with trout saccular hair cell proteins has now been obtained with pull-down assays and surface plasmon resonance. Further, both CNGA3 and EMILIN1 are expressed in rat organ of Corti. Protein binding between CNGA3 and EMILIN1 also occurs with rat organ of Corti proteins, demonstrated with three proteinprotein binding protocols. CNGA3 immunoreactivity has been localized with confocal microscopy to stereocilia of outer hair cells in mouse organ of Corti, also a site of EMILIN1 localization. Phosphodiesterase 6c, which the degradation of cGMP catalvzes in cone photoreceptors, decreasing cGMP gating of CNGA3 in photoreceptor sensory transduction, has been identified in the saccular hair cell preparation and immunolocalized to cochlear hair cell stereocilia (Dowdall et al., Assoc. Res. Otolaryngol. Abstr. 33: 201-202, 2010), where it could potentially also regulate CNGA3 channel conductance. [NIH DC004076, DC000156]

573 The Distribution of the Plasma Membrane Calcium Pump in Rat Cochlear Hair Cells

Qingguo Chen¹, **Robert Fettiplace¹**, David Furness², Carole Hackney³, Jaqueline Tickle²

¹University of Wisconsin-Madison, ²Keele University, ³University of Sheffield

Calcium plays a prominent role in the performance of outer enters hair cells (OHCs). lt through the mechanotransducer (MT) channels during stimulation and its intracellular concentration controls MT channel adaptation and modulates OHC electromotile behavior. Calcium is extruded via a plasma membrane (PMCA) pump which exists in four isoforms. We examined the distribution of PMCA isoforms at different cochlear locations during development of the rat cochlea. Immunolabeling was performed with a polyclonal antibody specific for the PMCA2 isoform, thought to be concentrated in the hair bundle (Dumont et al 2001), and a monoclonal antibody against all four isoforms. Confocal immunofluorescence demonstrated prominent labeling against PMCA2 in the OHC hair bundles with little in the OHC soma or in inner hair cells (IHC). During development, label first appeared at the base of the cochlea around post-natal day 0 (P0) followed by the middle and then the apex by P3. The timing difference between base and apex closely matches maturation of the MT channels in rat OHCs (Waguespack et al 2007). After P8, there was little change in the OHC bundle labeling. The monoclonal antibody gave some labeling of the OHC soma early in development but this was not visible after the onset of hearing. IHC bundles and soma also labeled with the monoclonal indicating presence of other isoforms. High resolution immunogold labeling in P26 rats showed PMCA2 was distributed along the lengths of all three rows of OHC stereocilia at similar densities and also occurred in the apical plasma membrane. This observation contrasts with the distribution of the MT channel, which is thought to be restricted to stereociliary rows two and three (Beurg et al 2009). Gold particle counts revealed no large difference in PMCA density between apical and basal OHC bundles despite there being a several fold larger MT current in basal OHCs. QC supported by the China Scholarship Council and JT by a grant from the RNID.

574 HCN Channels in Cochlear Hair Cells

Neeliyath Ramakrishnan¹, Marian Drescher¹, Khalid Khan², James Hatfield³, Dennis Drescher¹

¹Wayne State University, ²Kuwait University, ³John D. Dingell VA Medical Center

Z-stack confocal microscopy with 3-D reconstruction indicates expression of HCN1 protein in hair cell stereocilia of the mouse cochlea, for multiple sources of primary antibody, consistent with evidence that HCN1 specifically binds the stereociliary tip-link protein protocadherin 15 CD3 (Ramakrishnan et al., J. Biol. Chem. 284: 3227-3238, 2009). HCN2 protein was also immunolocalized to cochlear hair cell stereocilia with confocal microscopy. HCN1 and HCN2 co-localized to afferent nerve fibers innervating inner hair cells and HCN1 localized to afferents innervating outer hair cells. Both HCN1 and HCN2 have been localized to hair cell stereocilia and their rootlets in the rat organ of Corti with pre-embedding immunogold electron-microscopy protocols.

HCN isoform message has been quantitated relative to the housekeeping gene, GAPDH, in wild type mouse organ of Corti. The relative abundance, by QT-PCR, for HCN1:HCN2:HCN3:HCN4 was consistent with a unique spectrum for auditory sensory epithelium compared to whole cochlea. The organ of Corti represents only ~ 1% of the cells of the cochlea, and therefore its mRNA expression pattern may not be reflected in whole-cochlear mRNA patterns if there are other cell sources of the HCN isoforms, such as those that exist in spiral ganglion and lateral wall. We have obtained evidence that an HCN1 knockout is not a complete knockout, with HCN1 mRNA encompassing the in-frame deletion not degraded but still expressed in the organ of Corti of the knockout, consistent with our results for HCN1 mRNA and protein expression in brain of the knockout (Ramakrishnan et al., Assoc. Res. Otolaryngol. Abstr. 33: 23, 2010). Quantitatively, there are higher levels of mutant HCN1 in organ of Corti of the knockout than in wild type HCN1 controls. The HCN1 amino terminus is still expressed in the knockout, available to bind the carboxy terminus of protocadherin 15 CD3, and theoretically, to participate in HCN channel formation. [NIH DC004076, DC000156]

575 Lack of Otoferlin Alters the Trafficking of FM1-43-Labelled Vesicles in the Adult Mouse Cochlea

Jonathan Ashmore^{1,2}, Jacques Boutet de Monvel², Sylvie Nouaille², Christine Petit², Saaid Safieddine²

¹University College London, ²Institut Pasteur

The styryl dye FM1-43 has been used as a marker of hair cells in many epithelial systems because it permeates cationic channels present in the apical membrane and diffuses through the cytoplasm. It is also taken up by endocytosis at specific apical sites on the hair cell and then undergoes trafficking down to the cell base. In mouse cochlear hair cells, the dye labels the lumen of the vesicular compartment, and can be detected at punctuate locations, some of which are likely to correspond to synaptic release sites. We have explored the FM1-43 trafficking in inner hair cells (IHCs) of the in situ adult mouse cochlea (postnatal day P25-35) in the isolated temporal bone imaged by 2-photon laser scanning microscopy using 840 nm excitation. Hair cells from the cochlear 10-15 kHz region were exposed to 3 µM FM1-43 applied in normal perilymph onto the surface of the organ of Corti with no washout. The build up of fluorescence was observed for 600s at different cellular depths. In wild-type IHCs, FM1-43 fluorescence increased to a steady state with half-time dependent on cellular position. Modelled as a continuum process, fluorescence build up was consistent with dve diffusion from the cell apex. In otoferlin-deficient cochleas, IHCs were 20% shorter, but a similar diffusion constant described the fluorescence kinetics. However the local build up of fluorescence near putative ribbon release sites showed different dynamics, with slower formation of 'hotspots' compared to wild type. Such proposed ribbon release sites also showed a slowed recovery after localized photobleaching (FRAP). These findings are compatible with otoferlin playing a role in the vesicular trafficking in IHCs in addition to its proposed function as the calcium sensor for synaptic exocytosis. Supported by a Chaire Blaise Pascal (JFA). College de France (JBM) and EuroHear.

576 The Role of Nitric Oxide in Retrograde Facilitation of Efferent Cholinergic Synapses on Cochlear Hair Cells

Jee Hyun Kong^{1,2}, Paul Albert Fuchs¹

¹Center for Hearing and Balance, Otolaryngology-HNS, Johns Hopkins University School of Medicine, ²Otology, Stanford University

²Otolaryngology, Stanford University Prior to hearing onset, inner hair cells (IHCs) of the

mammalian cochlea are inhibited by efferent synaptic currents (IPSCs) resulting from the sequential activation of $\alpha 9/\alpha 10$ -containing receptors and small conductance, calcium-activated (SK) potassium channels. These transient efferent contacts on IHCs are known to facilitate markedly (Goutman *et al.*, 2005, *J. Physiol.* 566:49). We found that efferent synapses are further strengthened by a process of retrograde signaling from the postsynaptic hair cell. Raising hair cell calcium by release from cytoplasmic stores or by voltage-gated influx led to a gradual increase in the quantum content of the presynaptic efferent terminal. This retrograde facilitation was not altered by glutamate receptor antagonists and did not require glutamate release from the hair cell. To identify the retrograde signal, we applied a nitric oxide (NO) scavenger, carboxy-PTIO in the bath while the membrane-impermeant ryanodine receptor agonist cyclic ADP ribose (cADPR) was applied through the whole-cell patch pipette on IHCs in excised apical turns of cochleas from young (P7-9) rats, cADPR (100 µM) increased the amplitude and duration of the calciumdependent SK component of spontaneous and electricallyevoked IPSCs, as expected for enhanced cytoplasmic calcium. In addition, cADPR increased the probability of evoked transmitter release during electrical stimulation protocols. The NO scavenger carboxy-PTIO blocked this effect of cADPR on release probability. During cADPR treatment and exposure to 1mM carboxy-PTIO, the efferent quantum content was ~0.5 at 1 Hz (n=6). With removal of carboxy-PTIO, quantum content rose to ~1.5. Carboxy-PTIO was equally effective at preventing retrograde facilitation produced by voltage-gated calcium influx into the IHC. These observations suggest that a rise in hair cell calcium stimulates synthesis of NO which diffuses freely to enhance efferent transmitter release. Supported by NIDCD R01 DC001508 and P30 DC005211.

577 The Ultrastructure of Synaptic Cisterns at Efferent Synapses on Mouse Outer Hair Cells

Paul Albert Fuchs¹, Mohamed Lehar¹, Hakim Hiel¹ ¹Center for Hearing and Balance, Otolaryngology-HNS, Johns Hopkins University School of Medicine

The inhibitory synapse on vertebrate hair cells is formed by cholinergic neurons that project from the brainstem. Outer hair cells (OHCs) of the mammalian cochlea have 2 or 3 efferent terminals that contact the basal pole of the cell. A near-membrane postsynaptic cistern is co-extensive with the efferent contacts. To better predict potential functions for this cistern, we have quantified its dimensions in OHCs of mice in which acetylcholine receptors and SK channels have been eliminated or altered: α 9 knockouts that lose cholinergic sensitivity, a9L9'T knock-ins with enhanced cholinergic inhibition, and SK2 knockouts in which cholinergic function and the majority of synaptic contacts In middle turn wildtype OHCs the efferent are lost. synaptic contact area extends 2-3 microns along the synaptic pole and the postsynaptic cistern is perfectly coextensive, forming a 'pancake' 2x3 microns in appositional area. Throughout that entire area the cisternal membrane lies a mere 12-14 nm from the hair cell's plasma membrane, with impressively little variance throughout. This inter-membrane gap was identical in all OHCs. The second feature we studied was the cisternal volume. In order to compare this between different synapses we divided the volume (computed from serial reconstructions) by the synaptic appositional area, yielding a term for 'lumenal width'. This ranged between 15 and 20 nm for all wildtypes and the α 9 knockouts. Lumenal width was significantly greater in the α 9L9'T knockins, averaging 29 ± 6 nm (SD). This increased lumenal width was due in part

to a greater tendency for 'stacked' cisterns in α 9L9'T knockin OHCs. Synaptic cisterns in SK2 knockout OHCs could be found with or without associated efferent terminals. The lumenal width of surviving cisterns in SK2 knockouts (basal turn) was narrowed, 15 ± 1.6 nm compared to wildtype (basal turn) 20 ± 2 nm (SD). Supported by NIDCD R01 DC001508 and P30 DC005211

578 Onset of Cholinergic Efferent Synaptic Transmission at the Rat Inner Hair Cell

Isabelle Roux¹, Michael McIntosh², Paul Fuchs¹, Elisabeth Glowatzki¹

¹Department of Otolaryngology, Head and Neck Surgery, Johns Hopkins School of Medicine, ²Department of Biology, Department of Psychiatry, University of Utah

In the developing cochlea, the inner hair cells (IHCs) receive a transient efferent innervation originating in the medial portion of the superior olivary complex. This input is inhibitory; it is mediated by $\alpha 9/\alpha 10$ nicotinic acetylcholine receptors (nAChRs) and subsequent activation of calcium-dependent SK potassium channels (Glowatzki and Fuchs, 2000).

To study the ontogenesis of the cholinergic efferent input to IHCs, we used whole-cell voltage-clamp recordings from IHCs in acutely excised apical turns of the rat cochlea from embryonic day 21 (E21) to postnatal day 3 (P3). Responses to 1 mM acetylcholine (ACh) were not detected at E21 (n = 5), but were present in 98% of IHCs recorded from P0 on (n = 102). ACh-activated currents increased with age (with on average 285 pA at P3) and could be completely blocked by 10 µM strychnine or tubocurarine, or partially blocked by 300 nM α-conotoxin RgIA, suggesting that they were mediated by $\alpha 9$ and/or $\alpha 9/\alpha 10$ nAChRs at these early ages. Interestingly, we found that at P0 the ACh response was not coupled to SK channels, as the current voltage relation of the ACh response reversed around 0 mV. Coupling to SK (resulting in an ACh-induced outward current at -30 mV) was detected earliest at P1 in 48% of IHCs and by P3 in 100% of IHCs. To test for the onset of efferent synaptic activity, we raised the external potassium concentration to 80 mM to depolarize efferent endings. Similar to the onset of SK, synaptic currents were first detected at P1 in 40% of IHCs and by P3 in 100% of IHCs. Additionally, at P2, we first saw clustering of nAChRs in the IHC plasma membrane using Alexa 488-abungarotoxin as a probe.

In summary, as in the muscle, nAChRs are present in the IHC plasma membrane before functional efferent synapses are formed. In a second step, ACh receptor clustering, coupling to SK channels and inhibitory synaptic currents appear.

Supported by EMBO ALTF 952-2006 and NOHR Foundation Research Award 2010 to IR, NIDCD R01DC000276 to PF and NIDCD R01DC006476 to EG.

579 Synaptotagmins 1 and 2, Unlike Otoferlin, Are Not Essential Ca2+ Sensors for Synaptic Exocytosis in Mature Cochlear Inner Hair Cells

Maryline Beurg¹, Nicolas Michalski², Saaid Safieddine³, Yohan Bouleau¹, Ralf Schneggenburger², Edwin R. Chapman⁴, Christine Petit³, Didier Dulon¹ ¹Inserm, University of Bordeaux, ²Ecole Polytechnique Fédérale de Lausanne, ³Institut Pasteur, Inserm,

⁴University of Wisconsin

To clarify the respective roles of otoferlin and synaptotagmins (Syts) as putative Ca2+ sensors at the IHC ribbon synapse, we studied their expression and analyzed Ca2+-dependent exocytosis in IHCs from Otof-/and several Syt-/- mutant mice. We showed that Ca2+evoked exocytosis in mouse IHCs switches during cochlear maturation from an otoferlin-independent to an otoferlin-dependent mechanism at postnatal day 4. During exocytotic this early immature period, several synaptotagmins (Syts), including Syt1, Syt2 and Syt7, were detected in IHCs. The IHC exocytotic properties were, however, unchanged in newborn mutant mice lacking Syt1, Syt2 or Syt7. We only found a defect in Ready Releasable Pool recovery in Syt1-/- mice which was apparent as a strongly reduced response to repetitive stimulations. In post-hearing Syt2-/- and Syt7-/- mutant mice, IHC synaptic exocytosis was unaffected. The transient expression of Syt1 and Syt2, which were no longer detected in IHCs after the onset of hearing, indicates that these two most common Ca2+-sensors in CNS synapses are not involved in mature IHCs. Our findings reinforce the idea that otoferlin is a key Ca2+ sensor for exocytosis at the mature IHC ribbon synapse.

580 Synaptic Mechanisms of Phase-Locking at a Mature Hair Cell Ribbon Synapse

Geng-Lin Li¹, Henrique von Gersdorff¹

¹Vollum Institute, Oregon Health & Science University In response to pure tones auditory nerve fibers tend to fire spikes only at a certain time point (phase) of sinusoidal cycles of stimulation. This phenomenon of phase-locking has also been observed in vivo in many other auditory neurons in brainstem and cortex, but its synaptic mechanisms are poorly understood at the hair cell ribbon synapse level where it first originates. We took advantage of paired patch-clamp recording on hair cell-afferent fiber pairs in a semi-intact preparation of adult bullfrog amphibian papilla to reconstitute the phenomena of phaselocking (Keen and Hudspeth, 2006; Li et al., 2009), Hair cells from our preparation have a resonant frequency of about 400 Hz when injected by a constant current pulse. By stimulating hair cells with sinusoidal voltage commands (400 Hz sine wave with a amplitude that varied from 5 to 20 mV peak-to-peak amplitude), we were able to reestablish the phenomena of phase-locking under in vitro conditions. Consistent with in vivo observations from the frog eight nerve, phase-locking of spikes in afferent fibers improved significantly with stronger stimulations (vector strength = 0.44 for 10 mV, 0.54 for 20 mV), but the

preferred phase did not change significantly $(80.3 \pm 25.0^{\circ})$ for 10 mV, 74.9 ± 26.4° for 20 mV; Student's t test, p>0.05). With the same sine wave stimulation protocol, we also recorded EPSCs in afferent fibers with paired recordings under voltage-clamp. Most stimulation cycles failed to evoke EPSCs, and the success rate of EPSC was determined to be 14.7% for 5 mV stimulations. For stronger stimulations of 10 mV, the success rate was increased significantly to 151% from the 5 mV level and it was further increased by 248% of 5 mV level for stimulations at 20 mV (p<0.001). Remarkably, the averaged EPSC amplitude remained unchanged for sine wave stimulations of different amplitudes. Our results suggest that the timing and rate of action potentials in the afferent fiber nerve can independently encode information about the frequency and intensity of sound waves.

581 Kinetics and Ca²⁺ Sensitivity of Reloading of Release-Ready Vesicles Increase With Maturation Of Developing Chick Hair Cell Ribbon Synapses

Snezana Levic¹, Maryline Beurg¹, Yohan Bouleau¹, **Didier Dulon**¹

¹INSERM and University of Bordeaux

To sustain synaptic vesicle release during continuous stimulation, auditory hair cells must have a very efficient reloading process of synaptic vesicles at the ribbon active zone. The molecular mechanisms underlying this fast replenishment of synaptic vesicles remain largely unknown. While we know that the kinetics and Ca²⁺ sensitivity of vesicle release increase with developmental maturation of the hair cell ribbon synapses, we don't know how the reloading of synaptic vesicles change during maturation. To address this issue, we characterized the kinetics of exocytosis and vesicular replenishment in developing chick auditory hair cells. Experiments were done using the intact chick basilar papilla from E10 to P2 (two days post-hatch) by monitoring changes in membrane capacitance during various voltage stimulations. We found that exocytosis in immature hair cells (E10-E12) as compared to matured hair cells (E18-P2) displayed a smaller RRP (281 ± 62 vs 1221± 164 vesicles), slower kinetics (τ =89 ms vs 39 ms) and a poor Ca²⁺ efficiency (0.6 ± 0.1 fF/pC vs 6.4 ± 1.0 fF/pC). The average number of ribbons per hair cells largely increased with development from 2.1 \pm 1.6 at E12 to 9.3 \pm 2.2 at P2. When varying the inter-pulse interval of a 100 ms paired-pulse depolarization protocol, kinetics of RRP recovery largely increased with maturation (τ =6 s vs 0.7 s). Remarkably, increasing intracellular EGTA from 0.5 to 2 mM largely increased paired-pulse depression in matured HCs but not in immature hair cells. This suggested that the vesicular refilling process, while becoming more efficient, turn out to Ča²⁺ sensitive with maturation. be Interestingly, immunoreactivity of otoferlin largely increased with development in chick hair cells to reach maximum level at E18-P2. Our data show that auditory hair cells undergo effective remodeling of their synaptic machinery during development to simultaneously promote fast release and efficient Ca²⁺ sensitive vesicle replenishment.

582 Developmental Changes in Synaptic Transmission Properties at the Transient Efferent-Inner Hair Cell Synapse in the Mouse Cochlea

Javier Zorrilla de San Martin¹, Jimena Ballestero¹, Paul Fuchs², Ana Belén Elgoyhen¹, Eleonora Katz^{1,3} ¹INGEBI (CONICET), ²Center for Hearing and Balance,

Dept. Otolaryngol-Head and Neck Surgery, Johns Hopkins Univ, ³Dept. Physiology, Molecular and Cellular Biology, FCEN, University of Buenos Aires

From birth until the onset of hearing (postnatal day (P) 12), IHCs are transiently innervated by cholinergic medial olivocochlear (MOC) fibers. At this synapse, transmitter release is supported by both N- and P/Q-type voltagegated calcium channels (VGCCs) (Zorrilla de San Martín et al., J. Neurosci 2010). The fast formation and retraction of the MOC-IHC synapse suggest there may also be associated changes in synaptic transmission throughout this period. Short term plasticity (STP) is a dynamic process that depends on the balance between facilitation and depression of synaptic responses caused by preceding activity. Our goal is to determine whether there are changes in STP at the MOC-IHC synapse during development and, if so, to understand the mechanisms underlying them. Synaptic activity was recorded in voltageclamped IHCs from excised apical turns of the mouse cochlea at two developmental stages (P5-7 and P9-11) during electrical stimulation of the MOC fibers. Ten-pulse trains at 10, 20, 40 and 100 Hz applied to P5-7 MOC-IHC synapses led to 1.8±0.3; 1.7±0.2; 1.8±0.3 and 2±0.4-fold increase in synaptic efficacy, respectively, estimated as the ratio between the mean amplitude of the fifth and the first evoked synaptic current (S5/S1); n=7-10. The same protocols applied to P9-11 synapses led to a progressive decrease of the S5/S1 value (0.8±0.1; 0.7±0.1; 0.6±0.1; 0.4±0.1 for the 10, 20, 40 and 100 Hz trains, respectively; n=12-18). Depression upon high frequency stimulation at P9-11 was reversed to facilitation when reducing guantal output either by decreasing [Ca2+]o or by blocking P/Qtype VGCCs with ω -Agatoxin IVA (200 nM). Our results show there is a developmental switch from facilitation to depression upon high frequency stimulation consistent with the increment in the probability of release. We are now studying whether these changes in synaptic transmission can be accounted for by differences in the coupling between calcium influx and transmitter release.

Supported by grants from University of Buenos Aires(EK), ANPCYT (ABE, EK), NIDCD R01DC001508 (PAF, ABE) and HHMI (ABE)

583 Paired-Pulse Depression and Facilitation in Adult Auditory Hair Cell Synapses

Soyoun Cho¹, Geng-Lin Li¹, Henrique von Gersdorff¹ ¹*The Vollum Institute, Oregon Health & Science University* We studied short-term plasticity of adult bullfrog (Rana catesbeiana) auditory hair cell synapses using a pair of stimuli. We measured exocytosis by recording EPSCs from postsynaptic afferent fibers, and presynaptic membrane

ARO Abstracts

capacitance from hair cells. We found that the hair cell synapses can show paired-pulse depression and facilitation depending on the holding potentials of hair cells, the durations of pulse and/or inter-pulse intervals. When we depolarized hair cells from -50 mV to -20 mV for 20 ms with various interstimulus intervals (20ms, 50 ms, 100 ms and 200 ms), only paired-pulse depression was observed. When hair cells were depolarized from -80 mV to -20 mV for 20 ms, both paired-pulse facilitation with limited range of inter-pulse intervals and depression with other intervals were observed. The differential results from distinct holding potentials of presynaptic hair cells suggest that the paired-pulse depression dominates over an underlying masked facilitation at the hair cell synapses under more physiological conditions. We studied the role of calcium by changing internal calcium buffer conditions or by altering external calcium concentrations. According to our data, paired-pulse depression and facilitation mainly stemmed from presynaptic mechanisms. Although we observed very limited facilitation, the calcium dependent mechanism of this short-term plasticity is similar to that of conventional synapses. There were multiple kinetic components of transmitter release from hair cells and depression seemed to result from depletion of synaptic vesicles, not because of desensitization or saturation of postsynaptic AMPA receptors. Vesicle replenishment is believed to allow rapid recovery from depression. In hair cells, this replenishment may be mainly from vesicles recruited from different pools rather than from immediately recycled vesicles.

584 Expression of Snapin in the Rat Organ of Corti

Neeliyath Ramakrishnan¹, Marian Drescher¹, Dennis Drescher¹

¹Wayne State University

Snapin is a small protein of approximately 15 kDa that regulates vesicle release from afferent nerve endings by interacting with SNAP-25 and other SNARE proteins, such as syntaxin, synaptotagmin 1, and VAMP (Ilardi et al., Nat. Neurosci. 2: 119-124, 1999). More recently, it has been shown that such interaction is essential for synchronized vesicle release from neurons (Pan et al., Neuron 61: 412-424, 2009). Hair cells also show synchronous vesicle release in response to depolarization following elevated calcium in the region of the ribbon synapse. Little is known about the molecular constituents contributing to synchronized release in hair cells. In rat organ-of-Corti preparations, we detected the expression of Snapin by PCR amplification with specific primers. Using GST fusion proteins of the full-length Snapin in pull-down assays, we detected its interaction with syntaxin 1A in rat brain lysates. Further, we detected Snapin pull-down interaction with otoferlin when bacterially-expressed otoferlin regions were mixed with GST-Snapin and detected by an antibody against the otoferlin fusion tag. We also detected interaction of Snapin with otoferlin C2 domains via surface plasmon resonance assays using immobilized otoferlin protein and purified GST-Snapin protein. These studies

are designed to explore the nature of interaction of Snapin with the hair cell SNARE complex. [NIH DC000156, DRF]

585 Calcium Regulation of Vesicle Trafficking at Hair Cell Ribbon Synapses

Michael Schnee¹, Jee-Hyun Kong¹, Manuel Castellano-Munoz¹, Joseph Santos-Sacchi², **Anthony Ricci¹** ¹Stanford University, ²Yale University

The input output function at the hair cell afferent fiber synapse is linear so that sound intensity is encoded by increased firing rate. Capacitance measurements, used to monitor vesicle fusion, however reveal multiple pools of saturable vesicles and most recently a novel superlinear component of fusion where capacitance changes exceed that predicted by the calcium influx. This superlinear component was identified in both turtle and mammalian cochlea. Initial release rates varied directly with calcium entry; however the superlinear rate was invariant, larger Ca influxes resulting in earlier onset times for a superlinear response. Perforated patch experiments also had linear and superlinear responses similar to those observed in whole cell. Higher Ca buffering slowed release rates, delaying the onset of both linear and superlinear release components. The size of the capacitance changes as well as the effects of Ca buffers suggests that vesicle recruitment to the synapse is required for superlinear release and that this trafficking is Ca dependent. Normalizing data to frequency location by counting synapse numbers indicates that initial components of release were the same between high and low frequency but that the onset of the superlinear component was faster in low frequency cells. Swept field confocal Ca imaging (Fluo 4ff) during capacitance measurements produced two Synapses were identified surprising results. bv incorporating a fluorescent peptide that localizes at the ribbon into the recording pipette. First, the Ca signal near to the synapse rose rapidly to a plateau and then increased to a peak value followed by a decline in fluorescence all while Ca infux was constant. Measurements away from the synapse revealed a slow increase in Ca followed by a rapid rise to a peak that also declined during a constant influx. The rate of rise and the peak value were both greater away from the synapse suggesting the involvement of Ca release from stores. (Work supported by NIDCD DC009913 to AJR and

DC00273 to JSS.)

586 A Novel Explanation for the Seemingly Linear Ca2+-Dependence of Exocytosis in Hair Cells

Peter Heil¹, Heinrich Neubauer¹

¹Leibniz Institute for Neurobiology

Fast release of neurotransmitter by receptor cells and neurons via fusion of transmitter-containing vesicles with the cell membrane (exocytosis) is a calcium (Ca2+) dependent process. In most preparations, including hair cells from immature and various mutant animals, exocytosis grows in a highly supra-linear (3rd to 4th power) fashion with the Ca2+-entry into the cell. These relationships match well with findings that the ubiquitous Ca2+-sensors involved in fast exocytosis (synaptotagmins I and II) bind 3 (or more) Ca2+-ions in a highly cooperative fashion. In contrast, several recent studies of mature auditory and vestibular hair cells, and of visual and olfactory receptor cells, have observed nearly linear relationships between exocytosis and Ca2+-entry. These relationships have therefore been suggested to be mediated by different Ca2+-sensors with low Ca2+cooperativity, although there is evidence to the contrary, at least for mammalian inner hair cells. Others have proposed a nanodomain control of release according to which the vesicle with its Ca2+-sensors is in such close proximity to a Ca2+-channel that it senses the gating of this single channel only, and Ca2+-influx through this single channel is sufficient to trigger the vesicle's fusion. The evidence for such control in hair cells is not unequivocal.

Here, we propose that the nearly linear dependencies emerge as an epiphenomenon of measuring the sum of several supra-linear, but saturating, dependencies with different sensitivities at individual active zones of the same cell. We show that published experimental data can be accurately accounted for by this superposition model, without the need to assume altered Ca2+-cooperativity or nanodomain control of release. There is a large body of evidence for our model. Thus, it provides an attractive and parsimonious reconciliation of the seemingly discrepant experimental findings in different preparations.

Supported by the Deutsche Forschungsgemeinschaft

587 Atoh1 Promotes Mitotic and Non-Mitotic Forms of Auditory Hair Cell Regeneration in Post-Hatch Chickens

Rebecca Lewis¹, Clifford Hume¹, Jennifer Stone¹ ¹University of Washington

In birds, non-sensory supporting cells divide and regenerate auditory hair cells after injury through two distinct processes: mitosis and direct transdifferentiation. The transcription factor Atoh1 is necessary and sufficient for developmental hair cell specification, but its role in hair cell regeneration is poorly understood. To address this, three plasmids were electroporated into supporting cells in cultured auditory epithelia of post-hatch chickens: pJ2Xn-GFP (gift from Jane Johnson)(reports endogenous atoh1 transcriptional activity), pM1-GFP (forces expression of mouse atoh1), and two control plasmids, pMES-GFP and Cultures were examined 7 days after pShuttle-GFP. electroporation to determine if transfected cells differentiated hair cell-like features (mvosinVI immunoreactivity) or entered the cell cycle (took up BrdU). Two days after electroporation with pJ2Xn-GFP or pM1-GFP. GFP levels correlated well with Atoh1 protein levels. indicating that the plasmids behaved as an atoh1 reporter and an atoh1 misexpression vector, respectively. After 7 days, in epithelia transfected with pJ2Xn-GFP, 66% of GFP-positive cells developed myosinVI immunoreactivity, signifying that atoh1 transcriptional activity is only a moderate predictor of hair cell differentiation. Following pM1-GFP-driven overexpression of mouse atoh1, 67% of GFP-positive cells developed myosinVI immunoreactivity, compared to 25% of cells transfected with control plasmid. Further, after pM1-GFP-driven overexpression of mouse atoh1, a higher proportion of supporting cells incorporated BrdU (14%) than in epithelia electroporated with control plasmid (1%). These findings demonstrate that, although atoh1 transcriptional activity does not dictate differentiation along the hair cell pathway, high atoh1 expression appears to significantly increase a supporting cell's likelihood of undergoing one form of regeneration – mitotic or non-mitotic.

588 Time-Course of Growth Hormone Effects in Zebrafish (Danio Rerio) Auditory Hair Cell Regeneration

Huifang Sun¹, Yajie Wang¹, Michael E. Smith¹

¹Department of Biology, Western Kentucky University Our previous microarray analysis, validated via RT-PCR, showed that growth hormone (GH) was significantly durina zebrafish auditorv hair upregulated cell regeneration. In addition, intraperitoneal injection of carp GH promotes cell proliferation in the zebrafish inner ear. We propose that GH plays an important role in auditory hair cell regeneration. To test this hypothesis, we utilized the well-characterized zebrafish model, of which a time line of acoustic trauma-induced auditory hair cell death and regeneration has been established. We induced auditory hair cell damage by exposing zebrafish to a 150 Hz pure tone at 179 dB for 36 hours. Immediately afterwards, the fish were injected intraperitoneally with carp GH and placed in a recovery tank. At 1, 2 and 3 days following acoustic trauma, saccular hair cell densities, quantified by counting phalloidin-labeled stereocilia bundles at specified locations, were recorded to examine the effects of GH on hair cell regeneration. In addition, cell proliferation and apoptosis were measured by BrdU- and TUNEL-labeling, respectively, to identify possible cellular mechanisms associated with auditory hair cell regeneration in zebrafish. The GH-treated group showed significantly greater numbers of saccular hair cell bundles compared to buffertreated fish at all three time points. Similarly, cell proliferation was greater in the saccules, lagenae, and utricles of GH-treated fish on days 1 and 2 post-trauma, but only in the utricles at day 3. GH treatment also suppressed trauma-induced apoptosis in saccules, lagenae, and utricles at 1 day post-trauma, and in lagenae at 2 days post-trauma. Our results suggests that exogenous growth hormone promotes post-trauma auditory hair cell regeneration through stimulating proliferation and suppressing apoptosis. Future research will examine the pathways involved in GH-promoted auditory hair cell regeneration.

Supported by NIH P20-RR16481.

589 Identification of Neuromast Supporting Cell Subtypes with Differential Potentials in Hair Cell Regeneration

Sang Goo Lee^{1,2}, Mingqian Huang^{1,2}, Nikolaus Obholzer², Marco Petrillo^{1,2}, Sean Megason², **Zheng-Yi Chen**^{1,2} ¹*Mass Eye & Ear Infirmary,* ²*Harvard Medical School* In zebrafish lateral line neuromasts, hair cells are regenerated through proliferation and transdifferentiation of supporting cells after hair cell loss. Despite the evidence that there are heterogeneous supporting cell populations, the molecular markers for the subtypes of supporting cells or their specific function remain to be determined.

We have shown that FGF signaling is required for neuromast hair cell regeneration. Systematic screening of FGF components identified Fafr1 expression in the supporting cells along the dorsal-ventral axis within a neuromast, whereas the supporting cells along the posterior-anterior axis are devoid of FGF expression. Thus, neuromast supporting cells can be divided into Fgfr1(+) and Fgf(-) subtypes. Distribution of Fgfr1 suggests that it may mark hair cell precursors that directly give rise to new hair cells; whereas Fgf(-) supporting cells may serve as more primitive progenitor cells. To study their specific roles, we performed laser ablation to ablate Fgfr1(+) or Fgf(-) supporting cells. Hair cell regeneration was significantly suppressed after ablation of hair cells and Fgfr1(+) supporting cells, comparing to hair cell ablation alone. In contrast, hair cells were fully regenerated after ablation of hair cells and Fqf(-) supporting cells. Furthermore, ablation of Fgf(-) supporting cells severely reduced the number of cells re-entering cell cycle; whereas ablation Fgfr1(+) supporting cells had minimum effect on the number of dividing cells. Our study thus identified Fgfr1 as a marker for hair cell precursors with limited proliferation potential; whereas Fgf(-) supporting cells have a greater proliferation capacity and contribute indirectly to hair cell regeneration, consistent with their role as progenitor cells involved in the replacement of hair cell precursors. Fgf signaling is therefore likely required for the maintenance of hair cell precursors. The study has implications in exploring the FGF pathway for mammalian hair cell regeneration.

590 Identification of Modulators of Hair Cell Regeneration in the Zebrafish Lateral Line

Parhum Namdaran^{1,2}, Kelly Owens^{1,2}, Jennifer Stone^{1,2}, Edwin Rubel^{1,2}, David Raible^{1,3}

¹Virginia Merrill Bloedel Hearing Research Center, ²Department of Otolaryngology-HNS, ³Department of Biological Structure

The external location of the zebrafish lateral line makes it a powerful model for studying mechanosensory hair cell regeneration. We developed a screening platform to search for FDA-approved drugs and biologically active compounds that modulate hair cell regenerative pathways in zebrafish. This preparation allowed us to efficiently screen 1,680 compounds by observing hair cell numbers 48 hours after neomycin exposure. We confirmed 6 inhibitors and 2 enhancers of regeneration. The two

enhancers, dexamethasone and prednisolone, glucocorticoids. Both potentiated hair cell numbers during regeneration and induced hair cell addition in the absence of neomycin. BrdU analysis confirmed that the extra hair cells arose from mitotic activity. Surprisingly, studies of zebrafish caudal fin regeneration (Mathew et al. 2007, J Biol Chem 282:35202-10) revealed that glucocorticoids suppress regeneration via the glucocorticoid receptor pathway. We also observed that dexamethasone and prednisolone inhibit caudal fin regeneration, indicating that hair cell regeneration occurs by a distinct process. Two of the six inhibitors identified, flubendazole and topotecan, both significantly suppress hair cell regeneration by preventing the proliferation of neuromast support cells. Flubendazole was found to halt support cell division in Mphase, possibly by interfering with microtubule activity. Preliminary data suggests a similar increase of mitotic figures in chick basilar papilla treated with flubendazole. Topotecan killed both hair cells and proliferating hair cell precursors. Our observation that hair cells do not regenerate when support cell proliferation is impeded suggests that cell division is the primary route for hair cell regeneration in zebrafish. Studies are underway to determine the mechanisms by which the remaining 4 inhibitors act. Our screen has allowed us to identify, with high sensitivity, compounds that influence hair cell regeneration from large drug libraries.

591 Cochlear Stem Progenitor Cell Characterization in Nestin-GFP and GFAP-GFP Mice

Etienne Savary¹, Ibtihel Smati¹, Vincent Capelle¹, Emilie Grande¹, Jean-philippe Hugnot¹, Alain Uziel^{1,2}, Azel Zine¹ ¹Institute for Neurosciences of Montpellier, ²Service d'ORL, CHU Gui de Chauliac

Loss of hair cells in the mammalian cochlea leads to permanent sensori-neural hearing loss. Hair cells degenerate and their places are taken by phalangeal scars formed by non-sensory supporting cells. Current data indicate that early postnatal postmitotic supporting cells can proliferate and differentiate into hair cell-like cells in vitro.

In this study, we used GFAP and nestin promoter-GFP transgenic mice in combination with other stem cell markers to characterize supporting cell subtypes in the postnatal day-3 and adult organs of Corti with potential stem/progenitor cell phenotype.

In P3 organ of Corti, we show GFAP-GFP signal in all the supporting cell subtypes while the nestin-GFP was restricted to the supporting cells in the inner hair cell area. At this stage, GFAP and selected stem/progenitor markers (Jagged1, Sox2, and Abcg2) displayed overlapping expression pattern in the supporting cell population.

In contrast, GFAP and Abcg2 proteins were expressed in the inner sulcus limbal cells (i.e. interdental cells) outside the mature organ of Corti's area. By using qPCR, we found a significant decrease in transcripts for Jagged1, Sox2 and nestin in adult as compared to P3 cochleae.

We also used GFAP transgenic mice to isolate GFAP cells by fluorescence-activated cell sorting (FACS) from the

ARO Abstracts

postnatal cochleae. We further characterize their ability to form spheres and their stem/progenitor cell potential.

The GFAP-GFP reporter system would be useful for identification, isolation and characterization of inner ear stem/progenitor cells.

592 Cisplatin Damages Resident Stem Cells of the Mammalian Inner Ear

Eric Slattery¹, Kazuo Oshima², Stefan Heller², Mark Warchol¹

¹Washington University School of Medicine, ²Stanford University School of Medicine

Cisplatin is a widely used chemotherapeutic agent that can cause permanent hearing loss. Notably, cisplatin treatment can also diminish the regenerative ability of the nonmammalian inner ear. The avian cochlea and vestibular organs can quickly regenerate after aminoglycoside ototoxicity, but those organs cannot regenerate after cisplatin injury (Slattery and Warchol, J Neurosci 30: 3473, 2010). Otic regeneration in mammals is very limited, but the mammalian vestibular organs do possess a small population of sphere-forming pluripotent stem cells (Li et al., Nature Med 9: 1293, 2003). The present study examined the effects of cisplatin treatment on resident stem cells in the mammalian ear. Organotypic cultures of utricles and spiral ganglia were prepared from neonatal (P3) mice and treated for 24 hr with cisplatin. We then attempted to derive stem cells from these specimens, following previously described methods (e.g., Li et al., 2003). Treatment with cisplatin (5-20 µM) resulted in a dose-dependent reduction in sphere derivation from both utricular epithelia and spiral ganglia. In contrast, we observed no reduction in sphere formation from utricles that were pretreated with 2 mM neomycin. Proliferation of cells within spheres from neomycin-treated utricles was confirmed by BrdU uptake, while treatment with cisplatin caused a dramatic reduction in BrdU labeling. Also in a separate series of experiments, we examined the effects of cisplatin on supporting cells of the chick utricle and cochlea (which serve as progenitors to regenerated hair cells). Although supporting cells survived after the initial wave of hair cell death, their numbers were also reduced at seven days after cisplatin treatment. Together, these data indicate that cisplatin is toxic to stem cells of the inner ear.

593 Stem Cell Potential of the Organ of Corti Is Related to Sox2 Epigenetic Status

Jörg Waldhaus¹, Jelka Cimerman², Henning Gohlke³, **Marcus Müller**¹, Hubert Löwenheim¹

¹Hearing Research Center, University of Tübingen Medical Center, ²Institute of Pharmacy, Pharmacology and Toxicology, University of Innsbruck, Austria, ³Sequenom GmbH

A latent regenerative potential of the mammalian inner ear is suggested by the ability of the isolated postnatal auditory epithelium to form spheres. These sphere forming cells are deemed as multipotent stem cells or progenitor cells due to the fact that they self-renew and differentiate into different cell types of the otic lineage. The intent of our study was to discover if otosphere formation is due to an activation of a dormant stem cell population or if it depends on a reprogramming like response of postmitotic supporting cells into proliferating primordial like cells. Using gRT-PCR we found that the transcription factor Sox2 to be differentially expressed during OC development. This pattern served as a reporter to evaluate a potential dedifferentiation occurring in the otosphere assay. Sox2 is proposed to control the oppositional phenomena of selfrenewal and differentiation in otic progenitors. Epigenetic (methylation) status was determined using Sequenom's MassARRAY platform. We found that (1) sequence specific reprogramming/demethylation of the otic Sox2 enhancer element NOP2 correlated with dedifferentiation of postmitotic supporting cells into proliferating otic progenitor/stem cells, and (2) the sequence specific methylation of enhancers NOP1/2 correlated with a cellular phenotype devoid of self-renewing potential. Applying a differentiation protocol or the growth factor EGF to otic stem cells independently triggered the sequence specific methylation of enhancers NOP1/2 correlating with a cellular phenotype devoid of self-renewing potential. Therefore, the regenerative potential of the organ of Corti depends on reprogramming of Sox2 epigenetic status. We speculate that our observations validate the continued exploration treatment strategies aimed of at reprogramming and rejuvenating differentiated cochlear cells.

Supported by the BMBF

594 Proliferation and Differentiation Capacity of Different Cell Populations of Postnatal Mammalian Organ of Corti

Saku T. Sinkkonen¹, Taha A. Jan¹, Renjie Chai¹, Roman D. Laske¹, Kazuo Oshima¹, Alan G. Cheng¹, Stefan Heller¹ ¹Stanford University School of Medicine

The mammalian organ of Corti lacks in vivo regenerative potential. Neonatal mammalian cells, however, when isolated from the organ of Corti, transiently display proliferative potential and ability to differentiate into hair cell-like cells. To determine the proliferation and differentiation capacity of different cell populations of neonatal mouse organ of Corti we have utilized specific cell surface markers in combination with multi-parameter fluorescence-activated cell sorting. For the purified cell populations, we conducted two different assays to determine their proliferative capacity: clonal sphere formation and clonal adherent colony formation. We show that different supporting cell populations display distinct proliferative potentials in both assav conditions. Using an adherent cell differentiation assay, we demonstrate that hair cell-formation is a distinct feature of defined supporting cell subpopulations. The ability to isolate specific organ of Corti cell populations without the use of transgenic reporters has the potential to substantially expedite molecular and cellular investigations of specific cochlear cell types. Ultimately, we plan to further characterize defined cochlear cell populations to identify targets for potential therapeutic approaches toward hair cell regeneration.

595 FGF9 and FGF20 Influence Cell Cycle Entry and Spatial Patterning During Vestibular Regeneration

Courtney Voelker¹, Mark Warchol¹ ¹Washington University School of Medicine

The fibroblast growth factor (FGF) signaling pathway serves diverse roles in the development of the inner ear and in tissue regeneration, but the possible involvement of FGF's in avian hair cell regeneration has not been extensively explored. Expression profiling data suggest that the mature chick utricle expresses FGF16 and FGF20, which are both members of the FGF9 family of ligands. In addition, the distribution of these FGF's is spatially patterned. Expression of FGF20 is enhanced in the striola, while FGF16 is enhanced in the extrastriolar region (Alvarado et al., Dev Dyn 238: 3093, 2009). We have used small molecule inhibitors and treatment with FGF9 family molecules to investigate the function of FGF signaling during regeneration in the avian utricle. Initial experiments examined ongoing proliferation in normal (uninjured) utricles. Utricles were explanted from posthatch chicks and cultured for 48 hr with either the FGFR inhibitor SU5402 (30 μ M) or with FGF20 (1 μ g/ml). Neither treatment affected ongoing cell proliferation. We then focused on the influence of FGF's on hair cell regeneration after ototoxic injury. Cultured utricles were treated for 24 hr with 1 mM streptomycin and then allowed to recover for 2 or 7 days. Treatment with the FGFR inhibitors SU5402 (30 µM) or PD173074 (100 nM) had no effect on regenerative proliferation. In contrast, treatment with FGF20 (1µg/ml) reduced the number of S-phase cells (sampled at 48 hr after streptomycin), to about 30% of This finding suggests that exogenous control levels. FGF20 either reduces regenerative proliferation or alters the kinetics of cell cycle entry. Finally, treatment for seven days with either FGF9 or FGF20 (1 µg/ml) resulted in decreased hair cell recovery in the striola, but not in the extrastriolar region. This finding suggests that FGF9family ligands may be involved in spatial patterning during hair cell regeneration.

(Supported by NIDCD grants R01DC006283 and P30DC04665)

596 Evidence for Hair Cell Regeneration Via Direct Transdifferentiation in the Adult Mouse Vestibular System Using a Pou4f3-Diphtheria Toxin Receptor Lesion Model

Justin Golub¹, Ling Tong¹, Tot Bui Nguyen¹, Richard Palmiter¹, Edwin Rubel¹, Jennifer Stone¹ ¹University of Washington

We present a new method to ablate utricular hair cells using genetically engineered mice expressing the diphtheria toxin receptor (DTR) downstream of the Pou4f3 promoter (Pou4f3DTR/+). Injection of diphtheria toxin (DT) into adult Pou4f3DTR/+ mice reduced hair cell numbers to 5% of control (Pou4f3+/+ sibling) mice, by 14 days post-DT. In contrast, DT injection did not cause hair cell loss in control mice. Pou4f3DTR/+ mice that survived 40 days after DT treatment showed a 2.5 fold increase in the hair cell numbers compared to the 14-day survival point; this was equivalent to 14% of control hair cell numbers. This trend continued at 60 days post-DT, with an observed 3.8 fold increase in hair cell numbers compared to 14 days post-DT, equivalent to 20% of control hair cell numbers. Phalloidin labeling of hair cells revealed numerous immature-appearing stereociliary bundles at 40 and 60 days post-DT, concentrated in the striola. These immature bundles were not evident at 14 or 28 days post-DT. At 60 days, we also observed a 19% reduction in supporting cell numbers, suggesting that hair cell regeneration may have occurred via direct conversion of hair cells into supporting cells. This interpretation was supported by the absence of BrdU uptake into supporting cell or hair cell nuclei of Pou4f3DTR/+ mice between 14 and 60 days post-DT. These data suggest that hair cell regeneration via direct transdifferentiation naturally occurs in adult mouse utricles following near-complete targeted ablation of hair cells.

597 Generation of Inner Ear Sensory Cells from Human Bone Marrow-Derived Mesenchymal Stem Cells

Beatriz Duran Alonso¹, Ana Feijoo Redondo¹, Magnolia Conde de Felipe¹, Azucena Fontecha Santos¹, Victor Vendrell Laguna¹, Thomas Schimmang¹

¹Instituto de Biologia y Genetica Molecular

Worldwide, 500 million people are estimated to be affected by some form of hearing loss, making hearing impairment the most common sensory disorder in humans. In the majority of the cases, the cause is directly or indirectly linked to degeneration and death of hair cells of the cochlea in the inner ear, and their associated neurons. The former perform the essential conversion of mechanical stimuli to neural signals and their loss may result from aging, excessive exposure to loud stimuli, bacterial and viral infections, or ototoxic drugs. In mammals, unlike in birds and lower vertebrates, loss of hair cells is irreversible because regeneration does not take place. Similarly, there is no clinically significant regeneration of auditory neurons, in contrast to what is seen with peripheral motor neurons and some other sensory neurons.

Different avenues have been explored in order to tackle the problem of hearing loss, such as gene therapy, delivery of neurotrophic factors, and, recently, the differentiation of stem cells into sensory cell types that can be used for future transplantation cell therapy approaches. Embryonic stem cells, as well as mesenchymal stem cells (MSCs), mostly of murine origin, have been shown to differentiate into inner ear sensory cells. The aim of our work is to differentiate human MSC into either hair cell-like or auditory neuron-like cell types. Application of published methods to our cultures did not yield the expected results. Instead, we had to modify the culture conditions in order to obtain a significant increase in the expression of various gene combinations that characterize either hair cells (e.g. Atoh-1, considered a master gene in the hair cell lineage, Myosin VIIA and Calretinin) or auditory neurons (e.g. Sox-2, Calretinin and Ngn1), as shown by QRT-PCR and immunocytochemistry analyses. Injection of hMSC-derived

sensory cells into developing chick otocysts to test their integration into the inner ear in vivo is currently underway.

598 Directed Differentiation of Human Pluripotent Stem Cells Toward an Otic Progenitor Cell Fate

Parul Trivedi¹, Cynthia Chow², Daniel Brunner¹, Erin McMillan³, SuChun Zhang¹, **Samuel P. Gubbels^{1,4}** ¹Waisman Center, ²Department of Communicative Disorders, ³Department of Dermatology, ⁴Department of Surgery - Otolaryngology Division, University of Wisconsin - Madison

Pluripotent stem cells, by definition, can be used to generate any type of differentiated cell in the body. Due to this quality, stem cells can be used for the purposes of developmental modeling, drug discovery and possibly as novel cell-based treatments for some diseases. Previous studies have demonstrated the potential of mouse embryonic and induced pluripotent stem cells to differentiate into otic progenitor cells and functional inner ear hair cells. While the ability of human embryonic and induced pluripotent stem cells to generate differentiated cell types from other sensory placodes, such as the retina, has been well characterized, the capacity for pluripotent stem cells of human origin to form otic placode derivatives has not been clearly delineated. We have developed a method to direct human embryonic and induced pluripotent stem cells to an otic progenitor cell fate. Human pluripotent stem cells, through the stepwise addition of growth factors and signaling molecules, can be used to generate a population of cells with a gene and protein expression profile consistent with otic progenitor cells. The sequence of expression of many otic progenitor cell markers among the differentiating stem cells was found to be consistent with that seen during development of the mammalian inner ear. Ongoing studies based on these findings aim to optimize the method of directing the differentiation of human pluripotent stem cell types towards an inner ear fate in order to generate a robust population of otic progenitor and mature hair cells that could be used for future translational purposes.

599 Directed Integration of Neural Stem Cells Into Organ of Corti with Electric Fields

Dongguang Wei¹, Lin Cao¹, Min Zhao¹, Ebenezer Yamoah¹

¹UC Davis

Extensive studies have been performed on implanting stem cells to replace damaged cochlear hair cells and spiral ganglion neurons. However, the integration of the stem cells into damaged Organs of Corti and the honing of their implantation remain challenging. Successful directed migration of grafted stem cells and their integration into damaged Organs of Corti can significantly enhance stem cell therapy. Basilar membrane movement, followed by SGNs rewiring, could activate grafted cells situated at the Organ of Corti to achieve functional restoration. However, random integration, as opposed to directed integration, may compromise cochlear function. In this study, we demonstrated that applying physiological range electric fields (EFs) produces an effective guiding signal. This guiding signal would override repellent forces and break down the tight junctions, thus allowing neural stem cells (NSCs) to migrate toward the Organ of Corti and eventually integrate within it. In addition, we discussed the signaling mechanisms underlying EF-directed migration and integration of adult NSCs. Understanding the control signals of directed cell migration and integration will help develop novel therapeutic approaches. This in turn will allow for a translation of stem cell therapy from bench side to bedside.

600 Insulin-Like Growth Factor1 (IGF-1) Protects Cochlea Hair Cells Against Aminoglycoside Via Both the Phosphatidylinositol 3-Kinase (PI3K)/Akt Pathway and the Mitogen-Activated Protein Kinase Kinase (MEK)/extracellular Signal-Regulated Kinase (ERK) Pathway

Yushi Hayashi¹, Norio Yamamoto¹, Takayuki Nakagawa¹, Juichi Ito¹

¹Kyoto University

It is thought that IGF-1 is an important factor for inner ear development, and we have found and reported that local treatment of IGF-1 protects cochlea hair cells against damage induced by sound exposure and ischemia. We have started clinical trial of IGF-1 local treatment for sudden hearing loss patients and finished I-IIa phase. Hearing improvement was found in 40% of patients, but the mechanism was not evident. In ARO midwinter meeting of last year, we reported establishment of IGF-1 treatment model using ex vivo of mouse cochlea sensory epithelium. This time, we have focused on the PI3K/Akt and the MEK/ ERK pathway which are thought to be concerned with cell proliferative and anti-apoptotic action and investigated whether these molecules work as downstream of IGF-1 signaling cascade or not using ex vivo model of IGF-1 treatment. We used quantitative reverse transcriptase-PCR (qRT-PCR) to estimate in gene level and inhibitor assay to estimate in protein level. The gene expression level of Akt and ERK1/2 was upregulated after IGF-1 treatment in qRT-PCR. Next, we cultured sensory epithelia with inhibitor of PI3K/Akt. LY294002 and inhibitor of MEK/ERK, PD98059. Cell number which stereocilia remained was significantly reduced after LY294002 or PD98059 treatment. This finding indicated that PI3K/Akt and MEK/ERK are activated also in protein level. In conclusion, PI3K/Akt and MEK/ERK are upregulated in both gene level and protein level by IGF-1, and cell proliferative and anti-apoptotic action of these molecules are thought to be important in cochlea hair cell protection. This works was supported in part by a Grant-in-Aid for Scientific Research from the Ministry of Education, Culture, Sports, Science and Technology of Japan and by Grant-in-Aid for Research Sensorv on and а Communicative Disorders from the Ministry of Health, Labour and Welfare of Japan.

601 Effect of Hair Cell MicroRNAs on Gene **Expression Profiles of Cultured Mouse Otic** Precursor Cells

Timothy Hallman¹, Garrett Soukup¹ ¹Creighton University

Hair cell loss caused by environmental and genetic factors is exacerbated by the inability of mammalian auditory hair cells to spontaneously regenerate. Recent studies demonstrate that mechanosensitive hair cells can be derived from embryonic or induced pluripotent stem cells, and that Atoh1 can induce ectopic hair cells in the embryonic mouse inner ear. These studies suggest important guidance strategies for regenerating hair cells that might be used in non-immunogenic therapies, but the efficacy of other factors in effecting hair cell fate remains to be elucidated. We have previously shown the conservation and specific expression of microRNA-183 family members amongst vertebrate hair cells, and that microRNAs are necessary for the differentiation and maintenance of hair cell in the mouse inner ear. We are currently investigating the ability of hair cell microRNAs in conjunction with Atoh1 to influence gene expression profiles in presumptive prosensory precursor cells derived from the embryonic mouse otocyst. Microarray analyses of cells transfected with plasmids expressing Atoh1 and/or hair cell microRNAs exhibit mild changes in gene expression consistent with the function of microRNAs. Nevertheless, preliminary results indicate that hair cell microRNAs can specifically affect the downregulation of certain genes associated with alternative cell fate while supporting upregulation of other genes associated with hair cell fate. The data implicate developmentally relevant target genes for hair cell microRNAs and suggest that microRNAs might be useful factors in guidance strategies for hair cell regeneration.

(Support: NIH-NIDCD R01DC009025 and Nebraska State LB606.)

602 A Method to Derive a Cochlear Transducer Function from Cochlear Microphonic Using Low-Frequency Bias Tone Chul-Hee Choi¹, Lin Bian², Mark E. Chertoff³

¹The Catholic University of Daegu, ²Arizona State University, ³University of Kansas Medical Center

A cochlear transducer function was derived from the summating potential using a low-frequency bias tone. However, another method can used to derive the cochlear transducer function from the cochlear microphonic (CM) using the same low frequency modulation method. Before real experiment, mathematical exploration and computer simulation suggested that the CM magnitude is essentially proportional to the first derivative of the cochlear transducer function.

Electrical responses to two high frequency tones (6 and 12 kHz) ranging from 70 to 90 dB SPL in 10 dB step and a low frequency bias tone of 25 Hz with a high level (130 dB SPL) were simultaneously recorded at an active electrode placed on the round window at gerbils. After the use of a band-pass filter removing the low frequency CM responses, the CM modulated envelopes were obtained and analyzed.

Experimental results presented that the CM modulation envelope as a function of the bias levels has a shape which is similar to the cochlear transducer function. Furthermore, comparing the cochlear transducer function derived from the CM to those obtained from the SP previously described by Choi et.at.(2004), the parameters of the Boltzmann functions fitted to the CM responses were significantly different from thoses of the SP responses.

Another method to derive a cochlear transducer function from CM using a low-frequency bias tone was significantly different from that constructed from SP. The most significant difference between the cochlear transducer functions obtained from CM and SP was the dynamic range and symmetricity. The cochlear transducer function derived from the CM was greater than those from SP. The cochlear transducer function from the CM was more symmetric than those from the SP. These features in the cochlear transducer function from the CM may reflect the origin of outer hair cells (OHCs) while those from SP indicate the origin of inner hair cells (IHCs). Therefore, the major difference between the cochlear transducer functions obtained from the CM and the SP may result from different contribution of IHCs and OHCs.

603 Ossicular Chain and Round Window Immobilization; No Effect on BC Threshold; **BC Activation Via Fluid Channels**

Ronen Perez¹, Cahtia Adelman², Haim Sohmer³ ¹Department of Otolaryngology-Head and Neck Surgery, Shaare Zedek Medical Center, ²Speech and Hearing Center, Hadassah University Hospital, ³Department of Physiology, Hebrew University, Hadassah Medical School Classical (traditional) theories of auditory stimulation, whether by air (AC) or bone (BC) conducted stimulation, are thought to begin with sound induced relative motion between the cochlear shell and the stapes footplate, producing a passive mechanical traveling wave along the basilar membrane. In previous research we have shown that immobilizing the round window does not affect auditory nerve-brainstem evoked response (ABR) thresholds to AC and BC stimuli, suggesting the existence of an alternative theory. The present study was designed to further assess this possibility. The study was conducted on five Psammomys obesus (highest auditory sensitivity between 0.5 to 5.0 kHz) that initially underwent ablation of their left ears. Following baseline recording of ABR thresholds to AC and BC broadband click stimulation to the right ear, glue was applied to the middle ear immobilizing the ossicles and the round window. This was followed by repeat measurement of ABR threshold to AC and BC stimuli. The mean ± SD baseline ABR thresholds for AC and BC were 52±4.5 and 87±5.8 dB respectively. After application of glue to the middle ear and round window membrane, mean AC threshold was elevated by 49 dB and BC threshold was unchanged (mean air and bone ABR threshold 101±14.8, 89±4.2 dB respectively). Subsequently the bone vibrator was applied to a saline filled pocket created between the skull and the soft tissue around it in three animals, and ABR thresholds were 85, 100 and 90 dB. ABR bone conduction measurements were repeated with the bone vibrator in air, in order to control for possible activation by AC from the vibrator. The results of this study show: 1) bone conduction thresholds remained unchanged following immobilization of the middle ear; 2) stimuli from the bone vibrator were transferred to the inner ear through a fluid medium, without bulk fluid displacement and without a passive traveling wave.

604 Mechanisms of the Cochlear Stimulation Through the Round Window

Andrei Lukashkin¹, Thomas Weddell¹, Ian Russell¹ ¹School of Life Sciences, University of Sussex

The round window membrane (RW) functions as a pressure relief valve in conventional hearing allowing structures of the middle ear to move. Investigations in recent years have shown that middle ear implants can be used to stimulate the cochlea via the RW. Isolated clinical uses of this technique have been applied but more thorough theoretical and empirical studies are required to make the outcome of this technique more predictable. Using guinea pigs as test subjects we have investigated physiological effects of RW stimulation using a simulation of active middle ear prosthesis (AMEP), a cylindrical neodymium iron boron disk magnet placed upon the RW which can be stimulated by an electromagnetic coil positioned in close proximity to the magnet.

Compound action potentials of the auditory nerve (CAP) and mechanical responses of the RW and ossicles to sinusoidal stimuli were measured by electrode and laser interferometry in guinea pigs in response to acoustic stimulation and to AMEP stimulation (movement of the magnet placed on the RW).

The cochlear neural threshold did not change after placement of the magnet on the RW (up to 3 hours after the placement). The coil voltage - magnet displacement relationship is linear and frequency dependent. Magnet displacement threshold curves demonstrate extremely high sensitivity of the cochlea to the RW stimulation in the sub nm range. At neural threshold levels and above when the cochlea is driven with an AMEP, ossicular movement was only observed at low frequencies <5 kHz and high stimulation amplitudes. Due to the relatively high impedance of the ossicles as seen from the cochlea and the fact that the magnet did not entirely cover the RW. part of the RW, which was not covered by the magnet, could function as a pressure shunt during the RW stimulation. We propose that the basilar membrane is directly driven via near-field particle displacement generated in the vicinity of the RW by vibrations of the magnet. Supported by the MRC

605 Preventative Effect of Various Fluids Filled in the Epitympanic Bulla on Deterioration of Cochlear Function During Labyrinthectomy

Ryoukichi Ikeda¹, **Kazuhiro Nakaya¹**, Takeshi Oshima¹, Tetsuaki Kawase¹, Toshimitsu Kobayashi¹ ¹Tohoku University

Vestibulotomy causes significant decrease in the endocochlear potential (EP). The effect of artificial perilymph and endolymph administration during vestibulotomy on hearing preservation was evaluated in Hartley guinea pigs divided into groups: the epitympanic bulla was filled with distilled water, the epitympanic bulla was filled with artificial endolymph, the epitympanic bulla was filled with artificial perilymph, and the epitympanic bulla was not filled with any solution (control group). The EP and [K+] were monitored using double-barreled ionselective microelectrodes in the second turn of cochlea. EP was not significantly different among the distilled water, artificial perilymph and endolymph groups, although all groups showed better preservation of EP compared to the control group. The [K+] of the artificial endolymph group was significantly higher than that of the distilled water group or the artificial perilymph group. Preventing leakage of endolymph during vestibular destruction may be important in the acute phase.

606 In Anesthetized Mice, Contralateral-Noise Suppression of DPOAEs Persists After Elimination of Olivocochlear and Middle Ear Reflexes

Stéphane F. Maison^{1,2}, Hajime Usubuchi^{1,2}, Douglas E. Vetter³, A. Bélen Elgoyhen⁴, Steven A. Thomas⁵, M. Charles Liberman^{1,2}

¹Harvard Medical School, ²Massachusetts Eye & Ear Infirmary, ³Tufts University School of Medicine, ⁴CONICET, ⁵University of Pennsylvania

Suppression of ipsilateral DPOAEs by contralateral noise is used to assay olivocochlear (OC) reflex strength. However, depending on species and anesthesia, contributions of other reflexes can cloud interpretation. Here, we assess the contributions of OC and middle-ear muscle (MEM) reflexes to contralateral-noise suppression in CBA/CaJ mice anesthetized with ketamine/xylazine or urethane/xylazine.

Ipsilateral DPOAEs were evoked by low-level primaries $(f_2=16 \text{ kHz}; \text{SPLs set to evoke a DPOAE 10 dB > noise floor})$. After measuring baseline DPOAEs, broadband contralateral noise was presented continuously for ~8 min, at SPLs ranging from 40 to 130 dB SPL. Contralateral-noise threshold for DPOAE suppression was ~75 dB SPL. At contralateral-noise levels near cross-talk threshold (~105 dB SPL), DPOAE suppression was as great as 6-8 dB, and mean suppression was 1.2 dB. Contra-noise suppression disappeared upon contralateral cochlear destruction.

Lack of MEM contribution to contralateral-noise suppression was suggested by: 1) lack of noise-correlated changes in ear-canal SPL of an ipsilateral 500-Hz tone interleaved among DPOAE measures, 2) persistence of suppression after cutting the facial nerve, and 3) enhancement of suppressive effects after paralysis with curare.

Lack of MOC contributions to contra-noise suppression was demonstrated by persistence of the effect: 1) following strychnine (10 mg/kg, i.m.) that abolished all shock-evoked OC suppression, 2) in α 9- or α 10 nAChR-knockout mice where shock-evoked OC suppression is abolished, and 3) after cutting the OC bundle. Furthermore, suppression was normal in an α 9 knockin line where shock-evoked OC suppression is hugely enhanced.

Thus, it appears that neither MEM nor MOC reflexes are involved in contralateral-noise effects on DPOAEs in ketamine/xylazine or urethane/xylazine anesthetized mice. Further investigations will focus on possible involvement of the autonomic innervation of the inner ear in this effect.

Research supported by a grant from the NIDCD: R01 DC0188

607 Power Gain Measured in the Sensitive Living Cochlea

Tianying Ren¹, Wenxuan He¹, Peter Gillespie¹ ¹Oregon Health & Science University

The extraordinary sensitivity of the mammalian ear is commonly attributed to the cochlear amplifier, a cellular process thought to locally boost vibration of the cochlear partition response to soft sounds, yet cochlear power gain has not been measured directly. Using a scanning laser interferometer, we determined the volume-displacement and volume-velocity of the cochlear partition vibration by measuring its transverse vibration along and across the partition. In response to soft sounds, the transverse displacement at the peak-response location was >1,000 times greater than the displacement of the stapes, while the volume-displacement of an area centered at the peakresponse location was ~10-fold greater than that of the stapes. Using the volume-velocity and cochlear-fluid impedance, we determined that power at the peakresponse location of the cochlear partition is >100-fold greater than that at the stapes. These results confirm experimentally that the cochlea locally amplifies soft sounds, offering insight into the mechanism responsible for the cochlear sensitivity.

Supported by NIH-NIDCD.

608 The Anatomical Basis of Frequency Tuning in Geckos and Pygopods

Geoffrey Manley^{1,2}, Christine Koeppl¹, Johanna Kraus³ ¹Carl von Ossietzky University, ²Technische Universitaet Muenchen, Germany, ³University of Vienna

Among lizards, the lizard family Gekkonidae, which includes the legless group known as Pygopodidae, have the most complex papillae. The papillar area processing frequencies above 1 kHz consists of two separated but parallel groups of hair cells, both of which contain hair cells oriented neurally and others oriented abneurally. In a previous model of the papilla of the well-studied species *Gekko gecko*, anatomical details, including hair-cell bundle height, stereovillar numbers and tectorial masses

suggested that the response frequencies of the two groups might differ by almost an octave (Authier S, Manley, GA, 1995, Hear. Res. 82: 1-13). A physiological frequency map of the papilla showed, however, a uniform map spread along the papillar axis.

A recent study of the hearing capabilities of a sub-group of the pygopod geckos indicated that they, for lizards, hear very high frequencies indeed, up to ~14 kHz (Manley, G.A., Kraus, J.E.M., 2010, J. Exp. Biol. 213, 1876-1885). Evoked responses to frequencies above 8 kHz (that were not present in Gekko gecko) formed a secondary sensitivity peak, suggesting that they may be processed in a different way. To begin to understand function in these papillae, we have studied the heights of bundles in the two high-frequency areas of pygopods. The bundles were, on average, much shorter than those of Gekko gecko. Interestingly, although these bundle heights differ between the two hair-cell areas in Gekko gecko, they were indistinguishable in three papillae, one each of the pygopod species Lialis burtonis, Delma pax and Delma *haroldi*. Thus differences in bundle height cannot form part of an explanation of hearing patterns of pygopods.

609 Scanning and Transmission Electron Microscopy Imaging of Odontocete Cochlea

Maria Morell¹, Marc Lenoir², Jean-Luc Puel², Thierry Jauniaux³, Willy Dabin⁴, Marisa Ferreira⁵, Iranzu Maestre⁶, Eduard Degollada⁷, Chantal Cazevieille⁸, José-Manuel Fortuño⁹, Michel André¹

¹Laboratori d'Aplicacions Bioacústiques. Universitat Politècnica de Catalunya, ²Institut des Neurosciences de Montpellier, ³Université de Liège, ⁴Centre de Recherche sur les Mammifères Marins. Université de la Rochelle, ⁵Sociedade Portuguesa de Vida Selvagem/CBMA, ⁶AMBAR. Sociedad para el Estudio y la Conservación de la Fauna Marina, ⁷Asociación EDMAKTUB para el estudio y divulgación del medio acuático, ⁶Centre Régional d'Imagerie Cellulaire (CRIC), ⁹Institute of Marine Sciences (CSIC)

The morphological study of the Odontocete organ of Corti as well as possible alterations associated to sound exposure represent a key conservation issue to assess the effects of acoustic pollution on marine ecosystems. In addition, since odontocetes produce species-specific various acoustic signals at frequency ranges. morphological differences in the cochlea may be expected among species. Through the collaboration with stranding networks and rehabilitation centres from several European countries that followed an ear extraction and fixation protocol (defined at the Necropsy Workshop 2009 in Liège, Belgium), 117 ears from 13 species of Odontocetes that stranded in the Mediterranean Sea, North Atlantic and North Sea were processed. Due to technical and experimental constraints, all the cochlea were chemically fixed post-mortem, at least 6 hours after death. Here, we present scanning and transmission electron microscopy images of several cochlea structures: e.g. inner (IHC) and outer hair cell (OHC) stereociliary bundles, supporting cells, spiral ganglion neurons and OHC stereocilia imprints in the undersurface of the tectorial membrane of common

dolphin (Delphinus delphis), harbour porpoise (Phocoena phocoena), striped dolphin (Stenella coeruleoalba) and bottlenose whale (Hyperoodon ampullatus). By contrast with the rapid decomposition process of the sensory epithelium after death, spiral ganglion neurons and tectorial membrane appeared to be more resistant to postmortem autolysis. Interestingly, the tectorial membrane structure still remains in acceptable condition for analysis when the cochlea was fixed more than 20h post-mortem. The analysis of the stereocilia imprints on the tectorial membrane is allowing gaining insights in odontocete hair cell stereocilia organization and detecting possible ultrastructural alterations.

610 Imaging of the Intact Mouse Cochlea by Spectral Domain Optical Coherence Tomography

Simon Gao¹, Anping Xia², Tao Yuan³, Patrick Raphael², Ryan Shelton⁴, Brian Applegate⁴, John Oghalai² ¹*Rice University*, ²*Stanford University*, ³*Baylor College of Medicine*, ⁴*Texas A&M University*

Current medical imaging modalities, such as MRI and CT, do not provide high enough resolution to detect minor changes in the cochlea. We sought to develop the technique of optical coherence tomography (OCT) to image the cochlea noninvasively and within its native environment. We used spectral domain OCT with 950 nm as the center wavelength and a bandwidth of ~100 nm to image freshly excised normal mouse cochlea at different developmental ages. The OCT system has an axial resolution of 4 µm (in air) and a lateral resolution estimated at ~10 µm. When we imaged normal adult mouse cochleae through the round window membrane, Reissner's membrane, the basilar membrane, the tectorial membrane, the spiral ligament, the spiral limbus, and the modiolus could be clearly identified. When we imaged intact adult cochleae, we were able to image through ~130 µm of bone and tissue to see up to a depth of ~600 µm, and all of the previously identified structures were still visible. Imaging of early postnatal mice during the timeline of cochlear development permitted visualization of many of the expected structural differences from adult cochleae. Therefore, we conclude that spectral domain OCT is an effective technique for noninvasive imaging of the murine cochlea.

Supported by DOD CDMRP DM090212 and the John S. Dunn Foundation Collaborative Research Award.

611 Monitoring of Cochlear Tissue Viability by Measurement of Light Scattering Change

Takeshi Matsunobu¹, Satoko Kawauchi², Akihiro Kurita¹, Daisuke Kamide¹, Takaomi Kurioka¹, Katsuki Niwa¹, Shunichi Sato³, Makoto Kikuchi², Akihiro Shiotani¹ ¹Department of Otolaryngology, National Defense Medical College, Japan, ²Department of Medical Engineering, National Defense Medical College, ³Division of Biomedical Information Sciences, National Defense Medical College Research Institute

Monitoring of tissue viability, especially in the brain, is becoming increasingly important in transplantation and regenerative medicine, as well as in neurosurgery and emergency medicine. Measurement of intrinsic optical signals (IOSs) is an attractive technique for monitoring tissue viability in brains since it enables noninvasive, realtime monitoring of morphological characteristics as well as physiological and biochemical characteristics of tissue. We previously showed that light scattering signals reflecting cellular morphological characteristicswere closely related to the IOSs associated with the redox states of cytochrome c oxidase in the mitochondrial respiratory chain. In otological field, acute sensorineural hearing loss, such as sudden deafness, acoustic trauma, is sometimes resistant against treatment after the critical period. Therefore it is very important to know the viability of the inner ear tissue which indicates the therapeutic critical period. According to the brain measurement, viability of inner ear tissue should be related not only to energy metabolism but also to morphological characteristics of cells in the cochlear tissue.

In the present study, we examined the light scattering of the lateral wall of the guinea pig cochlea. A guinea pig was anesthetized, the retroauricular incision was made and the right bulla was opend. Light scattering signals were measured through the lateral bony wall of the cochlea. After the measurement of the room air condition, the 100% N2 gas was introduced. 200-300 seconds after introducing 100% N2, the big response of the light scattering signal was observed. This response was quite similar to that of brain. These findings suggest that light scattering signal can be used as an indicator of loss of tissue viability in the cochlea.

612 Specific Localization of Five Phosphatidylcholine Species in the Cochlea by Using Mass Microscopy

Yoshinori Takizawa¹, Kunihiro Mizuta¹, Takahiro Hayasaka¹, Hiroshi Nakanishi¹, Jun Okamura¹, Hiroyuki Mineta¹, Mitsutoshi Setou¹

¹Hamamatsu University School of Medicine

Phosphatidylcholine (PC), a phospholipid, is a basic structural component of cell membranes. PC species exhibit various binding patterns with fatty acids; however, the distributions of PC species have not been studied in the cochlea. In recent years, imaging mass spectrometry has been used as a biomolecular visualization technique in medical and biological sciences. We recently developed a "mass microscope" consisting of a mass spectrometry imager with high spatial resolution equipped with an atmospheric pressure matrix-assisted laser desorption/ionization and guadrupole ion trap time-of-flight analyzer. In this study, we applied the mass microscope to analyze cochlear tissue sections. The imager allowed visualization of the localization of PC species in each region of the cochlea. The structures of the PC species were determined using tandem mass spectrometry. PC(16:0/18:1) was highly localized in the organ of Corti and the stria vascularis. PC(16:0/18:2) was observed mainly in the spiral ligament. PC(16:0/16:1) was found primarily in the organ of Corti. These distributional

differences may be associated with the cellular architecture of these cochlear regions.

613 Differential Distribution of Innate Antioxidant Enzymes in Cochlear Turns

Hae Kyung Lee¹, Jong Bin Lee², Seung Won Kim¹, Jiyoung Min¹, Seong Jun Choi², Chunjie Tian¹, Younju Kim¹, Yun-Hoon Choung¹

¹Ajou University School of Medicine, ²College of Medicine, Konyang University

Purposes : Noise- or drug- induced hearing loss or presbycusis typically shows hearing loss at high frequencies. The differential distribution of innate antioxidant enzymes has been suggested as a cause for base-to-apical gradient of hair cell susceptibility to ototoxic stimuli. The purpose of the study is to evaluate the correlation of differential vulnerability along cochlear turns and hair cell rows in gentamicin (GM)-induced hair cell damage with distribution of innate antioxidant enzymes (glutathione, superoxide dismutase) in organ of Cortis.

Materials and Methods : Sprague-Dawley rat (250g, 12 weeks) were classified into two groups, the control group and GM group (GM 160mg/kg, Intraperitoneal injection for 10 days). After cryo-fixation of cochleas, immunostaining for expression of glutathione (GSH), superoxide dismutase 1, 2 (SOD1, SOD2) was performed. The cochleas were co-labeled with Phalloidin (hair cell markers) and DAPI (nucleus detection). The intensity of antioxidant expression was quantitatively evaluated along cochlear turns and hair cell rows using image J program

Results : The expression of GSH was higher in inner hair cells (IHCs) and inner pillar cells (IPCs) compared to in outer hair cells (OHCs) but was not significant different along cochlear turns (basal/middle/apical). For SOD1, the intensity was higher in IHCs than OHCs and in basal turns than middle and apical turns. While SOD2 was highly detected in Deiter cells but not in IHCs and OHCs. The expression pattern of antioxidant enzymes in cochleas treated with GM was similar to that in control rats.

Conclusions : The distribution of innate antioxidant enzymes seems to be not directly related with the differential vulnerability across cochlear turns in GMinduced hair cell damage. However, the relatively higher resistance of IHCs to GM may depend on the higher content of GSH and SOD1 in IHCs, and adjacent inner pillar cells.

614 Glial Cell Distribution in the Mouse Inner Ear

Stefan Hansen¹, Pia Erfkemper², Stefan Dazert², Joerg Schipper¹

¹University of Duesseldorf, ²University of Bochum

Only little is known about the function and effects of the non-neuronal cells like glial cells that are found in close contact and nearby spiral ganglion neurons and their neurites.

In order to study the effects of neurite-accompanying and co-cultivated cells on spiral ganglion neurites, we have used immunohistochemistry, as well as scanning electronic microscopy and spiral ganglion cell cultures of C57BL/J6 mice. We examined the temporal and spatial distribution of glial cell markers on sections of the mouse cochlea during the hearing development.

Our findings suggest an important role of glial cells in spiral ganglion outgrowth. The results indicate that differentially distributed glial cells in the spiral ganglion tissue culture could control the projection of spiral ganglion neurites, as it was described in cultured retinal ganglion cells and neurons of the central and peripheral nervous system before.

Further investigations should also focus on factordependent effects on these cells, moreover this culture model provide a basis on cochlear implant research and improvement of neurite-electrode contact as well as regeneration of spiral ganglion neurites.

615 Altered Radial and Longitudinal Patterns of Noise-Induced Outer Hair Cell Loss in the TectaC1509G/+ Mouse

Anping Xia¹, Christopher Liu², Sunil Puria¹, Charles Steele¹, Simon Gao³, Yuan Tao², John Oghalai¹ ¹Stanford University, ²Baylor College of Medicine, ³Rice University

University Tecta $^{\rm C1509G/+}$ mice have a point mutation in alpha-tectorin, a tectorial membrane (TM) protein. They have a shortened TM that only contacts the first row of OHCs. As well, Tecta^{C1509G/+} mice have increased expression of outer hair cell (OHC) prestin. Because humans with this mutation have progressive hearing loss, we sought to determine how these changes impact OHC survival in our mouse model. DPOAE thresholds in a guiet environment did not change to six months of age. However, noise exposure produced acute threshold shifts that fully recovered in Tecta^{+/+} mice but only partially recovered in Tecta^{C1509G/+} mice. While Tecta^{+/+} mice lost OHCs primarily at the base and within all three rows, Tecta^{C1509G/+} mice lost OHCs in a more apical region of the cochlea and nearly completely within the first row. Both wild type and mutantconditions were simulated in a computational model for the mid-turn of a gerbil cochlea. The calculated sheer force between the TM and the tall cilia, normalized by the pressure and multiplied by the basilar membrane width, was calculated to be 0.27, 0.07, and 0.06 for OHC rows 1, 2, and 3 respectively for the wild type. However, it was 0.4 for just the one row of the mutant condition. The stress distribution levels were 18, 16, and 13 kPa, for OHC rows 1, 2 and 3 respectively in the wild type for a 1 Pa input pressure at the basilar membrane. However, it was 24 kPa for the mutant condition. We then measured OHC electromotility in situ and found increased reticular lamina motion in Tecta^{C1509G/+} mice. This was associated with an increased risk of OHC death measured by vital dye staining. Together, these findings demonstrate that Tecta $^{\rm C1509G/+}$ mice have a higher risk of OHC loss after noise exposure and that this occurs in an atypical pattern. Both the mechanics of how the malformed TM stimulates the OHCs and the increased membrane permeability associated with increased OHC electromotility contribute to this higher risk profile.

Supported by NIH grants DC006671, DC07910, and the HHMI Medical Fellows Program.

616 Otoancorin Knockout Mice Reveal Inertia Is the Force for Hearing

Thomas D. Weddell¹, Kevin P. Legan¹, Victoria A. Lukashkina¹, Richard J. Goodyear¹, Lindsey Welstead¹, Christine Petit², Ian J. Russell¹, Andrei N. Lukashkin¹, Guy P. Richardson¹

¹University of Sussex, ²Institut Pasteur

The human auditory system responds to sound pressure levels ranging over six orders of magnitude with a sensitivity that enables us to perceive subatomic vibrations of the ear drum. These properties, and the acute temporal and frequency resolution of the auditory system, depend on non-linear power amplification through the activity of the outer hair cells. We demonstrate that in Otoa EGFP/EGFP mice, in which the inner-ear-specific protein otoancorin is absent, excitation of the outer hair cells and cochlear amplification is almost normal. This finding is remarkable because the tectorial membrane, although remaining functionally attached to the outer hair cell bundles, is completely detached from the spiral limbus. Therefore, as in ancestral vertebrate auditory organs, where inertia provides the excitatory force to the hair cells, it is the inertia of the tectorial membrane that must be important for exciting the outer hair cells, setting the sensitivity of their transducer conductance, and determining the precise timing of cochlear amplification.

Supported by the Medical Research Council and Wellcome Trust,

617 KCNQ1 Protein Is Mislocalized in the COL4a3 "Alport" Mouse

Sina Samie¹, Joseph Rutledge¹, Jacinta Robenstine¹, Michael Anne Gratton¹

¹Saint Louis University

The stria vascularis is responsible for the high potassium content of the cochlear endolymph as well as the +85mV endocochlear potential (EP) critical for auditory transduction. The driving force for secretion of potassium into the endolymph and EP generation is the Na,K-ATPase activity of strial marginal cells (MC) in conjunction with a cadre of potassium ion channels. The voltage-gated ion channel, KCNQ1, located on the apical MC surface is known to be involved in some hearing losses. In Alport syndrome, progressive hearing loss is associated with strial dysfunction following thickening of the strial capillary basement membranes. Prior work in our lab has shown that mice modeling the autosomal recessive form of Alport syndrome have a lower EP and decreased Na,K-ATPase activity.

To further examine how cochlear homeostasis is altered in Alport syndrome, KCNQ1 expression was characterized in the stria of adult Alport and wild-type (WT) mice. Light microscopic examination of immunoreactivity revealed that reactivity for KCNQ1 in the Alport and WT cochlea was very specific to the apical surface of the MC. However at high magnification, immunoreactivity in the Alport mouse appeared to include the cytosol near the apical surface. Immunoelectron microscopy was used to determine the sites of KCNQ1 protein in greater detail. Svstematic counts were made of KCNQ1-conjugated gold particles in the profile of the strial MCs in both the apical and basal While the number of particles along the turns. plasmalemma was the same in the Alport and WT mice, the particle number in the MC cytosol of the Alport mice exceeded that of the WT mouse. This suggests that KCNQ1 protein in the Alport mouse has mislocalized to a cytosolic site where it cannot function as an membrane channel in the Alport mouse It is possible that normal production but reduced turnover of the protein in the apical cell membrane of the MC is the cause of the cytosolic KCNQ1 protein in the Alport mouse.

618 MMP-13 Deficiency Causes Mineralization Defects in Cochlear Capsule Bone Matrix and Hearing Loss

Betty Tsai¹, Omar Akil², Mary Beth Humphrey^{2,3}, Tamara Alliston², Lawrence Lustig²

¹Vanderbilt University, ²University of California, ³University of Oklahoma Health Science Center

Patients with bony dysplasias exhibit various degrees of sensorineural hearing loss (SNHL); however, the mechanism behind this has been elusive. We recently showed that disruption of the highly mineralized cochlear bone matrix is responsible for SNHL in one bone syndrome, cleidocranial dysplasia. Because the mineralization and material properties of cochlear bone matrix are essential for normal hearing, we sought to investigate the mechanisms that define these unique features and how their disruption contributes to hearing loss. We hypothesized that matrix metalloproteinase 13 (MMP13), a protease that cleaves collagen and is essential for endochondral ossification and bone remodeling, is required for normal cochlear bone matrix quality and hearing.

Using immunohistochemistry, we found that MMP13 protein is expressed specifically in the wild-type mouse cochlear capsule in the endochondral layer that is responsible for the primary cochlear ossification. Microcomputed tomography reveals that MMP13 is required for normal cochlear mineralization since MMP13-/- cochlear bone has heterogeneous mineral deposition relative to wild-type bone. To determine if defective bone mineralization was associated with hearing loss, we measured the auditory brainstem response (ABR) and distortion product otoacoustic emissions (DPOAE) of MMP13-/- mice. MMP13-/- mice exhibit a significant high frequency hearing loss compared to their wild-type littermates. While average DPOAEs were not significantly different, MMP13-/- mice had very heterogeneous DPOAE responses, corresponding to the heterogeneous bone matrix mineralization. Although additional study is needed to identify mechanisms of hearing loss in MMP13-/- mice, histology shows no gross differences between the organ of Therefore, current studies aim to Corti or ossicles. determine if the relationship between the abnormal bone quality and hearing loss that we observe in MMP13-/- mice is a causal one.

619 The Effect of Zinc-Deficient Diet on the Hearing in CBA Mice

Woo Seok Kang¹, Hyun Woo Lim¹, Jin Kyung Suh¹, Harry Kim¹, Jong Woo Chung¹

¹Asan Medical Center, University of Ulsan College of Medicine

Objective : To evaluate the effect of zinc-deficient diet on the hearing in CBA mice and to verify whether this hearing change is reversible by supplementation of zinc afterwards.

Materials and Methods : We used nine four-week-old CBA mice with normal hearing and Preyer's reflex. Mice were divided into two groups, zinc-deficient diet group (n=6) and control group (n=3). Zinc-deficient diet group was fed with zinc-deficient diet (0.5-1 mg zinc/kg diet), and the control group with normal diet (50mg zinc/kg diet; Teklad, Madison, WI). Eight weeks later, we subdivided the zinc-deficient diet group into two groups and three mice maintained the zinc-deficient diet (Group A) and the remaining three fed with the normal diet (Group B). We assessed hearing via auditory brainstem response (ABR) with tone burst stimulation in 4, 8, 16, and 32 kHz and distortion product otoacoustic emissions (DPOAE) in 4, 5.6, 8, 11.3, and 16 kHz every 5 to 7 days for 3 months.

Result : The control group did not present ABR threshold change over all frequencies, showing about 30 dB SPL of ABR threshold. The ABR threshold of zinc-deficient diet group started to increase after 4 weeks of the zincdeficient diet and reached the plateau around the 7th week. As the measured frequency became higher, the ABR threshold difference between zinc-deficient diet group and control group became greater. The ABR threshold difference on the 43rd day was 12.5, 17.5, 30, and 27.5 dB SPL in 4, 8, 16, and 32 kHz respectively. Then zinc supplementation for 2 weeks restored the ABR threshold to normal in group B. However, the ABR threshold of group A did not recover to normal over all frequencies. The DPOAE threshold of zinc-deficient diet group and control group increased by 20 to 30 dB SPL in 4 and 5.6 kHz frequency at 29th day and the increased threshold did not recover to normal afterwards. However, there was no shift of DPOAE threshold in group A, group B, and control group in 8, 11.3, and 16 kHz.

Conclusion : From this study, we can conclude that zincdeficient diet may influence hearing in CBA mice and show greater effect in higher frequency. And zinc supplementation afterwards can restore hearing to normal.

620 State of Arousal Dramatically Affects the Noise-Evoked Suppression of DPOAEs in Mice

Anna R. Chambers^{1,2}, Kenneth E. Hancock¹, Jeremiah Cohen³, Stéphane F. Maison^{1,2}, M. Charles Liberman^{1,2}, Daniel B. Polley^{1,2}

¹Eaton-Peabody Laboratory, Mass Eye & Ear Infirmary, ²Harvard Medical School, ³Center for Brain Science, Harvard University

Genetic tools make the mouse a powerful model to study modulation of cochlear function by descending control systems. Suppression of the distortion product otoacoustic emission (DPOAE) by contralateral acoustic stimulation provides a robust assay of descending modulation that is readily implemented in the mouse. However, tests of contralateral suppression (CS) in animals are typically performed under anesthesia, a condition that is likely to reduce the level of suppression imposed by descending pathways. Here, we describe an approach to measure CS in the awake mouse. Headposted awake mice were restrained between two closed acoustic systems, with an artifact-rejection system in place to minimize contamination from self-generated sounds and movements. DPOAE amplitude vs. level functions (20-80 dB SPL primaries) were measured at six log-spaced f2 frequencies (5.6 - 32 kHz). To measure CS, an f2 frequency was selected, and primary levels were set to evoke a small DPOAE (~15 dB above the noise floor). Following measurement of baseline DPOAEs, contralateral white noise was added (75 - 80 dB SPL) for an additional 480 sec. CS measurements in awake mice were compared to those observed under different anesthetics: ketamine/xylazine, pentobarbital/chlorprothixene. urethane/xvlazine. and isoflurane. Multiple measurements were made in each animal over the course of several days, and many animals were tested in both anesthetized and awake conditions. Whereas DPOAE amplitudes were relatively constant between awake and anesthetized mice, CS of the DPOAE was 5-fold greater in the awake state. For example, compared with ketamine/xylazine (N=7), maximum awake CS increased from 1.3 dB (± .48) to 6.4 dB (± 2.42). Ongoing experiments with knockout mice lacking the $\alpha 9$ acetylcholine receptor will test whether these robust sound-evoked effects in awake mice are olivocochlear in origin. Research supported by grants from the NIDCD (R01 0188 to MCL, R03 009488 to DP and P30 DC5029).

621 Ethacrynic Acid-Induced Cochlear Lesions in Vitro

Hong Liu^{1,2}, Dalian Ding¹, Xuewen Wu^{1,2}, Haiyan Jiang¹, Richard Salvi¹

¹Center for hearing and deafness, University at Buffalo, ²Dept. Otolaryngology-Head and Neck Surgery, The Third Xiang Ya Hospital, Central South University

Ethacrynic acid (EA) is a potent loop inhibiting diuretic that inhibition the sodium-potassium-chloride acts bv cotransporter. When EA is administered at high doses in vivo it can induce temporary hearing loss by abolishing blood flow in the vessels in the stria vascularis. EAinduced strial pathology disrupts the blood-labyrinth barrier thereby enhancing the ototoxicity of gentamicin and cisplatin. However, the ototoxic effects of EA in vitro are not fully understood. To evaluate the ototoxicity of EA in vitro, we treated cochlear organotypic culture system of postnatal rat with EA for 24 h with doses ranging from 50 µM to 1000 µM. Concentrations of EA exceeding 500 M resulted in dislocation of cochlear hair cells due to the degenerations supporting cells. Auditory nerve fibers and spiral ganglion neurons also degenerated with EA doses exceeded 500 M. Surprisingly, the epithelium of stria vascularis was remarkably intact even with the highest dose of EA. Thus, the ototoxic effects of EA on organ of Corti supporting cells and spiral ganglion neurons of postnatal cochlear cultures is remarkably different from the systemic ototoxic effect of EA on the stria vascularis of adult animals.

622 Ototoxicity of Lead in Rat Cochlear Organotypic Cultures

Xuewen Wu^{1,2}, Dalian Ding^{1,2}, Hong Liu^{1,2}, Richard Salvi¹ ¹Center for Hearing & Deafness, University at Bufflao, ²Dept. Otolaryngology Head and Neck Surgery, the Third Xiangya Hospital, Central South University

Lead is a major environmental toxicant throughout the world. Lead can induce severe neurotoxicity including irreversible hearing impairment. Many in vivo studies have shown that lead can damage the auditory neuron system, but previous reports suggest that lead has little or no effect on cochlear sensory hair cells. To gain insights on its ototoxic effects, lead acetate was applied to postnatal day 3-4 rat cochlear organotypic cultures for 24 or 72 h with doses ranging from 0.1 to 2 mM. After 24 or 72 h treatment with various doses of lead acetate, 100% of cochlear hair cells were intact. However, the peripheral auditory nerve fibers projecting to the hair cell and the spiral ganglion neurons were damaged or destroyed when the concentration of lead acetate reached the highest dose, 2mM. These results suggest that spiral ganglion neurons and auditory nerve fibers are the major targets of lead in the cochlea. Considering that neuron damages only appeared at the highest dose after 72 h treatment, 2mM of lead acetate might be just above the j°deathj± threshold in vitro. The morphological features of leadinduced spiral ganglion neurons degeneration was associated in some cases with cell shrinkage or in others with cell swelling which suggests that spiral ganglion neuron degeneration may occur either by apoptosis or necrosis. Further studies are underway to further the characterize lead-induced cell death in the inner ear.

623 Bumetanide Enhances Aminoglycoside Uptake in MDCK Cells by Hyperpolarizing Cells Via Activation of Cl⁻-Channels

Tian Wang^{1,2}, Yuqin Yang¹, Qi Wang¹, Peter Steyger¹, **Zhi-Gen Jiang**¹

¹Oregon Hearing Reserach Center, Oregon Health & Science University, ²Institute of Otology, Central South University

A loop diuretic such as bumetanide synergistically enhances the ototoxicity of aminoglycosides (AG). The mechanisms underlying this ototoxic synergy remain poorly understood. MDCK cells share many membrane properties with cochlear marginal cells and have been used to study AG-permissive channel mechanisms. Using gramicidin-perforated patch-clamp techniques and fluorescent gentamicin (GTTR) imaging analysis, we found that (1) the non-selective cation channel (NSC) blocker La³⁺ (5 mM) reduced input conductance in all cells tested with a net current reversal potential of \sim -10 mV, and La³⁺ suppressed GTTR uptake. 2) Uptake of GTTR by MDCK cells was enhanced by bumetanide and furosemide in a concentration-dependent manner; this enhancement was suppressed by La3+, the Cl-channel blocker Nphenylanthranilic acid (PAA, 10- 100 µM) (Di Stefano et al., 1985; Lang et al., 1990) or extracellular low Cl⁻ (40, 75 mM), but not by potassium channel blockers TEA, 4-AP or glipizide. 3) Bumetanide (10 µM) hyperpolarized MDCK cells by 10.5 mV from a mean of -32.1 (p<0.01). 4) Bumetanide increased the slope conductance of the whole-cell I/V curve (from ~0.2 to ~1.5 nS at -60 mV). Bumetanide-induced net current I/V curve reversed its polarity between -60 to -90 mV. 5) The membrane action of bumetanide was suppressed by low Cl⁻ and PAA but not by flufenamic acid, niflumic acid, 4-AP, TEA, glipizide, La³⁺ or Gd³. We conclude that our data support NSC mediation of AG-uptake, that bumetanide enhances La³⁺-sensitive AG-uptake in MDCK cells, and that this enhancement is likely due to bumetanide-induced hyperpolarization that increases the electrical driving force for cationic AG influx. In addition, our data suggest that bumetanide causes cellular hyperpolarization via activation of a PAA-sensitive Cl channel, and that the Cl equilibrium is a major contributor to the membrane potential of MDCK cells. Funded by NIDCD R01 04716 (ZGJ), R01 04555 (PSS) and P30 05983.

624 p53 Is Not Required for Cisplatin-Induced Hair Cell Death in Organ Cultures of Adult Mouse Utricle

Tiffany Baker¹, Shimon Francis¹, Inga Kramarenko¹, Carlene Brandon¹, Fu-Shing Lee¹, Lisa Cunningham¹ *Medical University of South Carolina*

Cisplatin is an effective chemotherapeutic drug used to treat a variety of cancers in both adults and children. However, a proportion of patients who receive cisplatin develop significant permanent hearing loss. The ototoxic side effects of cisplatin result in part from damage to sensory hair cells; however, the molecular mechanisms underlying cisplatin-induced hair cell death are poorly understood. DNA damage, reactive oxygen species, and inflammation have been implicated as mediators of cisplatin-induced hair cell death. p53 is a well-known tumor suppressor and transcription factor that induces apoptosis in response to DNA damage. The p53-mediated DNA damage response is a major mechanism by which cisplatin kills cancer cells. p53 is activated in cisplatin-treated neonatal rat cochlea and utricle in vitro, and chemical inhibition of p53 suppresses cisplatin-induced hair cell death in these cultures. In order to further examine the role of p53 in cisplatin-induced hair cell death, we exposed utricles from adult $p53^{-7}$ mice and their wild-type littermates to various cisplatin concentrations. p53^{-/-} utricles were not protected against cisplatin-induced hair cell death. Immunochemistry data indicate that cisplatin-induced p53 stabilization occurs primarily in stromal cells and not in hair cells or supporting cells. These data suggest that the p53mediated DNA damage response may not be a major mediator of cisplatin-induced hair cell death. In addition to binding DNA, cisplatin has also been shown to induce oxidative stress and elicit an inflammatory response in the inner ear. HSP32 (a.k.a. heme oxygenase-1) is a stressinduced protein that inhibits both oxidative stress and

inflammation in multiple systems. We have shown that the HSP32 inducer cobalt protoporphyrin IX inhibits cisplatininduced hair cell death *in vitro*. We are currently examining the mechanisms by which HSP32 inhibits cisplatin-induced hair cell death. *Supported by NIDCD 5R01DC07613 and F30DC010522*.

625 Ototoxicity and Neurotoxicity of Nedaplatin in Cochlear Organotypic Cultures

Dalian Ding¹, Xuewen Wu^{1,2}, Hong Liu^{1,2}, Haiyan Jiang¹, Richard Salvi¹

¹Center for Hearing & Deafness, University at Buffalo, ²Dept. Otolaryngology of the Third Xiang Ya Hospital, Central South University

Nedaplatin is the third platinum compound which has entered widespread clinical use for cancer chemotherapy. Nedaplatin appears to be less nephrotoxicity, neurotoxicity and gastrointestinal-toxic than cisplatin. However, there is very little information on the ototoxicity associated with nedaplatin, even though nedaplatin appears on the list of ototoxic drugs. To evaluate the ototoxic and neurotoxic effects of nedaplatin in the cochlea, cochlear organotypic cultures were treated with nedaplatin at doses ranging from 10 µM to 1000 µM for 24 or 48 hours. After 24 h treatment with nedaplatin treatment, most cochlear hair cells were present. However, the peripheral auditory nerve fiber terminals and synapses projecting out towards the hair cell were disrupted or missing when the concentration of nedaplatin exceeded 50 µM. After 48 h treatment, spiral ganglion neuron degeneration was only observed with nedaplatin concentrations of 500 µM or more. Interestingly, 10 µM of nedaplatin initially destroyed the inner hair but did not affect outer hair cells. However, when the concentration of nedaplatin reached 50-100 µM, the outer hair cells were also destroyed. Unexpectedly, the degree of outer hair cell degeneration was reduced when the concentration of nedaplatin exceeded 500 µM. This intrinsic resistance of outer hair cells to high levels of nedaplatin is very similar to our previous studies in which hair cells were found to be resistant to very high concentrations of cisplatin due to reduced uptake of labeled cisplatin into hair cells. Unlike outer hair cells, the nerve fiber and spiral ganglion neurons were destroyed in a dose-dependent manner and were not resistant to high doses of nedaplatin.

626 Assessing the Synergistic Ototoxicity of Anti-Cancer Drug Combinations Using the Zebrafish Lateral Line

Yoshinobu Hirose^{1,2}, Edwin Rubel¹, David Raible^{1,3}, Julian Simon⁴, Henry Ou^{1,5}

¹Virginia Merrill Bloedel Hearing Research Center, Dept. Oto-HNS, University of Washington, ²Department of Otolaryngology, Graduate School of Medicine, Yamaguchi University, ³Department of Biological Structure, University of Washington, ⁴Fred Hutchinson Cancer Research Center, ⁵Seattle Children's Hospital

Many anti-cancer drugs are known to have ototoxic effects. We previously screened a library of anti-cancer drugs (National Cancer Institute Approved Oncologics Library) for ototoxic effects using the zebrafish lateral line. Our screen successfully identified many known ototoxins (e.g. cisplatin, oxaliplatin, vincristine, vinblastine) as well as potentially novel ototoxins.

Since anti-cancer drugs are typically used in combination, we evaluated multiple common combination drug regimens involving the anti-cancer drugs identified by our ototoxicity screen. Five dpf zebrafish (Danio rerio) larvae were exposed to anti-cancer drugs individually and in combination for 6 hours. Immunohistochemistry using anti-parvalbumin antibody was then performed to quantify hair cell loss for dose response curves.

The results demonstrated that while some combinations were simply additive, other anti-cancer drug combinations (e.g. cisplatin+vincristine, cisplatin+vinblastine) demonstrated synergistic or potentiated ototoxicity. These combination effects suggest that when determining the risk for ototoxicity with anti-cancer drugs, a patient's entire drug regimen should be assessed rather than considering drugs in isolation.

627 Modulation of Cisplatin Serum Kinetics by N-Acetylcysteine, and Cochlear Expression of the Copper Transporter -ATP7A - By Cisplatin

Thomas Dickey¹, Qi Wang¹, Martina Ralle¹, Amanda Phillips¹, Martha Sibrian-Vazquez², Robert Strongin², Peter Steyger¹

¹Oregon Health and Science University, ²Portland State University

Animal studies and clinical trials have shown that thiosulfates such as N-acetylcysteine (NAC) can protect against platinum-induced toxicities. The mechanism of this protection or cisplatin entry into cells has not been fully elucidated.

We have previously shown that intravascular injections of Texas Red-tagged cisplatin (DDP-TR) revealed preferential cytoplasmic uptake within 1 hour in marginal cell and intra-strial tissues of the stria vascularis compared to fibrocytes in the lateral wall. In the present study, Long-Evans rats were given DDP-TR 2mg/kg IV 15 minutes after NAC 400mg/kg IV. The animals were sacrificed 1, 3 and 24 hours after treatment. NAC was shown to reduce serum platinum levels and modulate uptake into the cochlea. Kidney proximal tubule cells showed increased DDP-TR uptake after NAC treatment.

ATP7A is a vital copper transporter and a candidate cisplatin transporter. For ATP7A immunofluorescence and confocal microscopy, rat stria vasculari and choroid plexi were fixed, excised and immunolabeled. In untreated rats, ATP7A immunoexpression is present in the perinuclear cytoplasm of marginal cells and intermediate cells. Three hours after DDP-TR injection, marginal cell ATP7A expression had re-distributed to include the apical membrane. Twenty-four hours after DDP-TR injection, ATP7A immunoexpression is greatly up-regulated in both marginal cells and choroid plexi. This is suggestive of increased ATP7A-mediated vesiculation and efflux trafficking. Thus, strial expression of ATP7A is up-regulated following treatment with DDP-TR.

By determining which cells in the cochlea take up cisplatin, and which candidate cisplatin transporters are expressed and appropriately located to traffic cisplatin across the BLB into specific cell types during chemotherapy, we can begin to develop new strategies to prevent cochlear uptake of cisplatin and subsequent cisplatin-induced ototoxicity. Funded by NIDCD R21 10231 and P30 05983.

628 Kidney Epithelial Cells Exhibit Functional Channels with Characteristics of Gentamicin Uptake-Related TRPV4 Channel

Yuqin Yang¹, Tian Wang^{1,2}, Takatoshi Karasawa¹, Qi Wang¹, Peter Steyger¹, Zhi-Gen Jiang¹

¹Oregon Hearing Reserach Center, Oregon Health & Science University, ²Institute of Otology, Central South University

Aminoglycosides (AGs) are polyvalent cations and lipidinsoluble. We hypothesize that AG transmembrane trafficking occurs via permeation of large conductance, non-selective cation (NSC) channels such as TRPV4. Kidney epithelial cells, like cochlear cells, express TRPV4 channels at high levels (Karasawa et al., 2008; Liedtke et al., 2000; Plant et al., 2007). We have shown that Texas Red-tagged gentamicin (GTTR) enters cultured kidney cells (MDCK and KPT2) independently of endocytosis and the uptake is enhanced by low $[Ca^{2+}]_0$ and by exogenous expression of TRPV4 in KPT2 cells (KPT2-TRPV4 cells) (Karasawa et al., 2008; Myrdal et al., 2005a; Myrdal et al., 2005b), suggesting an important role for this channel in transmembrane trafficking of gentamicin. However, functional existence and characterization of TRPV4 channels in these cells remain to be investigated. In this study, using whole-cell and patch-clamp recording techniques, we identified a channel in MDCK and KPT2-TRPV4 cells that showed characteristics of TRPV4 (Nilius et al., 2004; Plant et al., 2007).

We found: (1) In physiological pipette and bath solutions, cell-attached and outside-out patches from MDCK and KPT2-TRPV4 cells frequently displayed unitary current activity with a reversal potential near zero mV and a singlechannel conductance of ~100 pS for outward current and 30 - 60 pS for inward current. The unitary activity (P_0) was enhanced by low extracellular Ca²⁺ and suppressed by Gd³⁺, La³⁺ and Ruthenium Red. (2) Hypotonic media (225 mOsmol), 100 μ M ATP and 1 μ M 4 α -phorbol 12,13didecanoate (4aPDD), a selective TRPV4 activator, stimulated this unitary activity. (4) The spontaneous or 4aPDD-elicited unitary current was not sensitive to chloride channel blocker niflumic acid, flufenamic acid (FFA) or N-phenylanthranilic acid. (3) In whole-cell recordings, 4aPDD caused a net current with an I/V curve reversing its polarity near zero mV. (5) Control cells with vector (KPT2-pBabe) showed verv emptv rare spontaneous NSC unitary currents. 4aPDD (2 µM) failed to elicit the unitary activity or whole-cell I/V change in the KPT2-pBabe cells. We conclude that MDCK and KPT2-TRPV4 cells express functional TRPV4 channels; our data further substantiates the role of TRPV4 as a route for cellular gentamicin uptake and/or clearance.

Funded by NIDCD R01 04716 (ZGJ), R01 04555 (PSS), F32 DC008465, R03 DC009501 (T.K.) and P30 05983

629 Oxaliplatin Induced Lesions of the Vestibular Sensory Epithelium in Organotypic Culture

Xuewen Wu^{1,2}, Dalian Ding^{1,2}, Hong Liu^{1,2}, Richard Salvi¹ ¹Center for Hearing & Deafness, University at Bufflao, ²Dept. Otolaryngology Head and Neck Surgery, the Third Xiangya Hospital, Central South University

Oxaliplatin is a platinum based anti-tumor drug widely used in the treatment of colorectal cancer. It is generally considered less nephrotoxicity than cisplatin, but treatment is often associated neuropathies and sometime ototoxicity. In our previous studies with cochlear organotypic cultures, we discovered that oxaliplatin damaged the hair cells and spiral ganglion neurons in the cochlea. However, the toxic effects of oxaliplatin on the vestibular system are not well To evaluate the vestibulotoxic effects of understood. oxaliplatin, we prepared organotypic cultures of the vestibular end-organs from postnatal day 3 rats. Vestibular organotypic cultures were treated for 24 h with doses of oxaliplatin ranging from 10 µM to 5000 µM. Specimens were double stained with phalloidin which preferentially labels filamentous actin in hair-cell stereocilia, and TOPRO3 which intensely labels nuclei. Oxaliplatin toxicity was quantified by assessing the density of vestibular hair cells in macula of the utricle. Mean vestibular hair cell density in the normal utricle was 85.4/0.01mm2. Treatment with 10µM oxaliplatin reduced the hair cell density to 63.8/0.01mm2. 50 µM oxaliplatin caused hair cell density reduction to 51.4/0.01mm2. Hair cell density decreased to 35.8/0.01mm2 with 100 µM, 27.4/0.01mm2 with 500 µM and 25.8/0.01mm2 after 1000 µM. Finally, nearly all utricular hair cells were destroyed in 5000 µM. These results indicate that oxaliplatin causes a dose-dependent decrease in vestibular hair cell survival. Vestibular hair cell nuclei labeled with TOPRO3 were condensed or fragmented after oxaliplatin treatment indicating that hair cell death was occurring largely by apoptosis rather than necrosis. Additional studies are underway to better characterize the apoptotic signaling pathways.

630 Cochlear Uptake of Fluorescent Gentamicin in LPS-Induced Sepsis Model

Jawon Koo^{1,2}, Hongzhe Li³, Peter Steyger³

¹Seoul National University College of Medicine, ²Seoul National University Bundang Hospital, ³Oregon Health and Science University

Systemic injection of vasoactive peptides like serotonin and histamine can reduce cochlear uptake of fluorescent gentamicin (GTTR), likely due to permeability changes in the blood-labyrinth barrier (BLB). To test the hypothesis that bacterial sepsis can modulate BLB permeability, and increase cochlear uptake of aminoglycosides, we used a lipopolysaccharide (LPS) induced sepsis model and compared the serum levels of vasoactive peptides and the cochlear distribution of GTTR with controls. LPS (0.1, 1, 2.5, 10 mg/kg) or saline was injected via mouse tail vein, and after 24 hours 2 mg/kg of GTTR was injected intraperitoneally. Mice were fixed 1 and 3 hours later, and vibrotomed kidney sections or wholemounts of apical or basal cochlear coils were examined using confocal microscopy to quantify the cellular intensity of GTTR. Venous blood was collected to obtain serum gentamicin, histamine and serotonin levels.

Serum GTTR levels were significantly elevated in 2.5 mg/kg and 10 mg/kg of LPS-treated groups compared to controls, while 0.1 mg/kg and 1 mg/kg groups had similar serum levels as controls. GTTR fluorescence in renal proximal tubules decreased with increasing LPS concentrations and 10 mg/kg statistically significant (p<0.05). GTTR fluorescence at all LPS concentrations (0.1, 1, 2.5 and 10 mg/kg) was significantly elevated in most strial tissues. Serum serotonin levels were significantly decreased in every LPS group, but attenuation of serum histamine levels was significant only in the 10 mg/kg LPS group.

Increased cochlear uptake of GTTR in 2.5 mg/kg and 10 mg/kg LPS groups is likely due to increased serum levels and poor renal excretion of GTTR. However, lower concentrations of LPS also increased cochlear uptake of GTTR without elevated serum GTTR levels or renal damage. We conclude that systemic bacterial infection can potentiate gentamicin ototoxicity via attenuation of serum serotonin levels that may increase BLB permeability.

631 Distribution of Fluorescent Cisplatin and Candidate Transporters in Murine Cochleae

Matthew Miller¹, Qi Wang¹, Martha Sibrian-Vazquez², Robert Strongin², Peter Steyger¹

¹Oregon Health and Science University, ²Portland State University

Cisplatin is essential to treat a wide variety of malignancies, including squamous cell carcinoma of the head and neck. Cisplatin therapy is often limited due to irreversible, high-frequency sensorineural hearing loss. Candidate transporters for cisplatin trafficking include the copper transporters, Ctr1, ATP7A and ATP7B, yet their distribution and the trafficking of cisplatin into the murine cochlea are not well described.

Mice received a single intraperitoneal injection of 4 mg/kg of cisplatin tagged with Texas Red (DDP-TR), and were cardiac-perfused with fixative 1, 3, 6, and 24 hours later. Cochleae, choroid plexus, liver, and kidneys were isolated using a dissecting microscope. All tissues were also immunolabeled with anti-Ctr1, anti-C77 (intracellular C-terminus of ATP7A) or anti-ATP7B and examined using confocal microscopy.

DDP-TR was preferentially localized in the stria vascularis and hair cells in a time-dependent manner, with peak uptake at 3-6 hours and decreased labeling at 24 hours (clearance). DDP-TR was also taken up and retained by choroid plexi and kidney proximal tubules over 24 hours. Ctr1 was intensely localized to the marginal cell layer; ATP7A within the intermediate cell layer and hair cell stereocilia, while ATP7B was present in tight junctions of lumenal cells lining the scala media. DDP-TR treatment down-regulated Ctr1 immunoexpression in the stria vascularis.

The localization of candidate cisplatin transporters and distribution/time-course of DDP-TR uptake is suggestive of a trans-strial trafficking route from strial capillaries to hair cells via endolymph for cisplatin. The presence of these transporters in the stria vascularis may allow inhibition of trafficking into the cochlea at the blood-labyrinth barrier (rather than at the hair cells), potentially decreasing ototoxicity, while maintaining the anti-neoplastic effects at the tumor level.

632 Proteins Bind Aminoglycosides Through a Basic Peptide Motif

Pavan K Kommareddi^{1,2}, Jochen Schacht^{1,2} ¹Kresge Hearing Research Institute, ²University of Michigan

Despite their ototoxicity, aminoglycosides remain indispensable for the treatment of gram-negative infections and tuberculosis and for prophylaxis in cystic fibrosis. A novel indication is the application of "designer aminoglycosides" for the attenuation of genetic diseases. Some mechanisms of ototoxicity have been elucidated, notably oxidative stress, and exploited for pharmacological protection. Other aspects remain unclear including issues of uptake and intracellular localization. By their positive charge, the drugs have a strong affinity to anionic sites on lipids or nucleotides. Little is known about proteins as targets of the drugs.

We previously identified 14 aminoglycoside-binding proteins involved in ribosomal biogenesis, mitochondrial respiration and transcription. These proteins have a motif of predominantly basic amino acids that is responsible for their interactions with nucleic acids and that acts as nucleolar targeting signal (NLS). To test the hypothesis that this motif is a binding site for aminoglycosides, we investigated human immunodeficiency virus 1 (HIV1) Tat protein which is well characterized and has a similar NLS. After establishing binding between aminoglycosides and Tat we made several deletion constructs of HIV 1 Tat in expression vectors to identify the peptide(s) involved in the interaction with aminoglycosides. We identified two essential peptides: a cysteine-rich peptide (CRP) and NLS. Further experiments suggested that CRP was not a direct binding site but promoted the dimerization of Tat protein. The potential binding mechanism was further tested in inhibition assays with free peptides which confirmed that HIV 1 Tat protein must exist as a dimer in order to combine with aminoglycosides via its NLS. The consequences of this novel mechanism of aminoglcysoide-protein interaction will be discussed.

Supported by R01 DC003885 from The National Institute of Deafness and Communication Disorders, NIH.

633 CLIMP-63 Is a Gentamicin-Binding Protein That Is Involved in Drug-Induced Cytotoxicity

Takatoshi Karasawa¹, Qi Wang¹, Larry David¹, Peter Steyger¹

¹Oregon Health & Science University

Inner ear sensory hair cells and kidney proximal tubule cells are the two cell types that retain aminoglycosides and are prone to aminoglycoside-induced cytotoxicity. Although there are a number of cell death mechanisms that are induced by aminoglycosides, we have little understanding of how these drugs induce cytotoxicity. We hypothesize that aminoglycosides bind specific proteins in kidney proximal tubule cells and hair cells to trigger cell death mechanisms.

To understand how aminoglycosides, including gentamicin, induce cytotoxicity in the kidney proximal tubule and the inner ear, we identified gentamicin-binding proteins (GBPs) from mouse kidney cells by pulling down GBPs with gentamicin-agarose conjugates and mass spectrometric analysis. Among several GBPs specific to kidney proximal tubule cells, cytoskeleton-linking membrane protein of 63 kDa (CLIMP-63) was the only protein localized in the endoplasmic reticulum (ER), and was co-localized with gentamicin-Texas Red (GTTR) conjugate after cells were treated with GTTR for 1 hour. In Western blots, kidnev proximal tubule cells and cochlear HEI-OC1 cells, but not kidney distal tubule cells, exhibited a dithiothreitol (DTT)resistant dimer band of CLIMP-63. Gentamicin treatment increased the presence of DTT-resistant CLIMP-63 dimers in both kidney proximal (KPT11) and distal (KDT3) tubule cells. CLIMP-63 siRNA transfection enhanced cellular resistance to gentamicin-induced toxicity, which involves apoptosis, in KPT11 cells. Since both KPT11 and HEI-OC1 cells are from drug-susceptible tissues and express the dimer forms of CLIMP-63, the dimerization is likely an early step in aminoglycoside-induced cytotoxicity. Gentamicin also enhanced the binding between CLIMP-63 and 14-3-3 proteins, and we also identified that 14-3-3 proteins are involved in gentamicin-induced cytotoxicity, likely by binding to CLIMP-63.

Supported by NIH NIDCD grant R03 DC009501 (T.K.), R01 DC04555 (P.S.S.), and P30 grants DC05983, EY10572, and CA069533

634 Gene Delivery to the Auditory and Vestibular Inner Ear Via Systemic Injection of AAV9 in Mice

Mark A. Crumling¹, Kevin D. Foust², Yehoash Raphael¹, Brian K. Kaspar²

¹Kresge Hearing Research Institute, Department of Otolaryngology, University of Michigan, ²Department of Gene Therapy, The Research Institute at Nationwide Children's Hospital

Introducing gene delivery vectors to the inner ear, usually accomplished via cochleostomy, canalostomy, or round window penetration, often causes damage to the delicate workings of the auditory and vestibular end organs. This is counterproductive if the ultimate goal is, for example, protection of existing hearing from loss due to deafnesscausing alleles. Therefore, it would be beneficial to develop non-damaging methods for putting exogenous genes into the inner ear. Recent studies have found that systemically administered adeno-associated virus 9 (AAV9) vectors can traverse the blood-brain barrier, transducing cells in the brain and spinal cord. The inner ear is protected by a similar barrier, so we explored whether systemic AAV9 vectors can also overcome this impediment to transduce cells within the auditory and vestibular end organs. To test this, auditory and vestibular epithelia were examined from FVB-strain mice injected systemically with an AAV9 vector carrying a GFP reporter gene. Each animal received 5 x 10¹¹ viral particles injected via the temporal vein on postnatal day 1. The animals were perfused with paraformaldehyde on postnatal day 20. Inner ear tissues from the mice were prepared for epifluorescence microscopy and examined for GFP fluorescence. GFP expression in the cochlea was found in the lateral wall, spiral limbus, inner sulcus, Deiters' cells, pillar cells, outer hair cells, and inner hair cells. In the ampulae and utricle, GFP-positive cells were found in both sensory and non-sensory epithelia. By providing transduction of both supporting cells and hair cells, systemically delivered AAV9 vectors could be of use for clinical inner ear gene therapy and for basic science research on the physiology of the inner ear.

635 Advanced Gene Transfer Into the Inner Ear by the Use of Laser-Induced Stress Wave(LISW)

Takaomi Kurioka¹, Takeshi Matsunobu¹, Akihiro Kurita¹, Daisuke Kamide¹, Yasushi Satoh², Sho Kanzaki³, Takahiro Ando⁴, Takuya Akiyama⁴, Shunichi Sato⁴, Akihiro Shiotani¹ ¹Department of Otolaryngology, National Defense Medical College, Japan, ²Department of Anesthesiology, National Defense Medical College, ³Department of Otolaryngology, Keio University, ⁴Department of Biomedical Information Science, National Defense Medical College

Gene transfer into the inner ear is an attractive technology for clinical application.

It offers the hope of treating sensorineural hearing loss and preventing hearing disorders.

Recently nonviral physical methods have received much attention because present methodology using viral vectors has problems associated with safety and limited targeting characteristics.

Laser-mediated gene transfection is widely utilized as a new physical method for targeted gene therapy in terms of its high spatial controllability of laser energy.

It is known that efficient gene expression was obtained in brain, skin, and muscle using Laser-Induced Stress Wave(LISW).

LISW are generated by irradiating a laser-absorbing material with 532-nm Q-switched Nd:YAG laser pulses.

In this study, we assessed transgene expression using LISW with enhanced green fluorescent protein(EGFP) as a reporter gene in the cochleae of guinea pigs.

Plasmid DNA encoding EGFP was injected intra scala tympani and LISW were applied.

Two weeks after laser irradiation, the expression of EGFP in the cochlea was observed and evaluated by fluorescence images of a confocal laser scanning microscope.

With irradiating LISW , gene expression was observed in specifically supporting cells and hair cells, although , not observed without LISW (control)

Auditory brainstem response assessment was carried out to assess adverse reactions before irradiation, immediately after irradiation, and after 3 days.

As for threshold of hearing, no apparent loss was observed with LISW.

In summary, by the use of LISW, EGFP was selectively expressed in the inner ear , and its expressions were confined to specific sites , the areas of supporting cell and hair cell exposed to the LISW. No major side effects were observed.

We confirmed gene transfection by use of LISW is an effective method for targeted gene transfer.

636 Restoration of Hearing in VGLUT3 Knockout Mice Using Virally-Mediated Gene Therapy

Omar Akil¹, Rebecca Seal², Robert Edwards¹, **Lawrence** Lustig¹

¹University of California San Francisco, ²University of Pittsburgh

While a number of studies have described the utility of gene therapy for hearing restoration, translating this into the clinical setting has been elusive. Mouse models of inherited deafness are the most logical starting point for these endeavors, though again limited success has been achieved in this arena as well.

Prior studies have shown that mice lacking the glutamate transporter VGLUT3 (VGLUT3 KO) are born deaf due to the absence of glutamate release from the inner hair cells. In the present study, we attempted to correct this genetic defect through virally-mediated gene therapy. In vivo microiniection of adeno-associated virus with a VGLUT3 insert (AAV-VGLUT3) into the endolymph of P10-12 VGLUT3 KO mice via a cochleostomy or direct injection through the round window membrane was performed. ABR testing demonstrated restoration of hearing 12 days of following gene delivery to thresholds similar to that seen in wild-type mice. RT-PCR demonstrated expression of VGLUT3 mRNA in the wild-type and KO-rescued cochlea tissue but not in the KO mice. Immunofluorescence with a VGLUT3 antibody demonstrates VGLUT3 expression in inner hair cells (IHCs), though interestingly, expression in no other cell types despite wide-spread cellular viral uptake in the KO-rescued mice throughout the cochlea. Lastly, long-term follow-up of the rescued KO mice showed preservation of hearing thresholds through 3 months with AAV-VGLUT3 delivery via the round-window, and at least through 6 months via a cochleostomy.

These results demonstrate functional hearing recovery in a genetic model of human deafness due to loss of VGLUT3 function, and support the concept that early restoration of a specific genetic defect can result in restoration of hearing.

Whether these results can be applied to other forms of genetic deafness remain to be determined.

637 Gene Therapy for the Preservation and Regeneration of Spiral Ganglion Neurons After Deafness

Patrick Atkinson^{1,2}, Andrew Wise^{1,2}, Tian Tu^{1,2}, Brianna Flynn¹, Bryony Nayagam², Cliff Hume³, Rachael Richardson^{1,2}

¹*The Bionic Ear Institute,* ²*The University Of Melbourne,* ³*University of Washington*

The administration of exogenous neurotrophins to the deafened cochlea via mini-osmotic pumps can promote spiral ganglion neuron (SGN) survival and fibre regrowth. However, an additional consequence of pump-based neurotrophin delivery is that the peripheral fibres regrow in a disorganised manner. Furthermore, the survival promoting effects of neurotrophins is lost following the cessation of delivery indicating that long-term neurotrophin treatment is required for sustained benefits.

During normal cochlea development localised sources of neurotrophins help the growing peripheral fibres find their target hair cells. Using this concept we aim to provide localised sources of neurotrophins in the aminoglycosidedeafened cochlea that will not only promote long-term SGN survival but will also provide directional cues to guide fibre regrowth. To achieve this goal we have administered a viral vector into the scala media compartment of the cochlea in order to initiate neurotrophin production by the transfected cells. Our initial studies have shown an increase in SGN survival and directed regrowth after three weeks of treatment with the neurotrophin vector compared to a control vector. Although these results are promising the longer-term effectiveness of this treatment remains to be established. Therefore, in our current study we are examining the effectiveness of neurotrophin gene therapy after long-term deafness as well as the long term effects of gene therapy on SGNs. Results obtained thus far have shown that neurotrophin gene therapy is unable to promote SGN survival after 4 or more weeks of deafness in the guinea pig. This suggests that there is a level of structure required within the organ of Corti needed for neurotrophin gene therapy to be effective.

Supported by Garnett Passe and Rodney Williams Memorial Foundation, Royal National Institute for Deaf People, NIDCD, The Bionic Ear Institute and The University of Melbourne.

638 OTO-104, a Sustained Release Formulation of Dexamethasone, Offers Effective Protection Against Hearing Loss

Anne Harrop¹, Xiaobo Wang^T, Rayne Fernandez¹, Luis Dellamary¹, Qiang Ye¹, Jay Lichter¹, Carl LeBel¹, **Fabrice Piu**¹

Otonomy Inc

Hypothesis / Background: In the US alone, it is estimated that about 30 million individuals suffer from hearing loss. Causes of the debilitating condition are many, including noise induced hearing loss (NIHL) and exposure to

ototoxicants (such as chemotherapy drugs, e.g. cisplatin). At the cellular level, mechanisms involving inflammation and hair cell death are responsible for permanent hearing loss. The corticosteroid dexamethasone is a potent antiinflammatory with demonstrated activity in otic disorders.

Methods: OTO-104, a poloxamer-based hydrogel containing dexamethasone, is a clinical stage formulation currently being developed for the treatment of Meniere's disease. Poloxamers, a class of glycol polymers, exhibit mucoadhesive and thermoreversible properties and behave as sustained release drug delivery vehicles. OTO-104 was administered to guinea pigs intratympanically and its activity in models of acoustic trauma and cisplatin-induced hearing loss evaluated.

Results: Following a single intratympanic injection of OTO-104, significant and prolonged exposure to dexamethasone in the inner ear was observed ranging from several days to a few months. In the NIHL setting, OTO-104 provided effective protection against acoustic trauma when administered prior and after noise exposure. Furthermore, the extent of the protective effects were dependent upon the OTO-104 dose administered. Data from the cisplatin-induced hearing loss model will also be presented.

Conclusions: OTO-104 appears to provide a well-tolerated and controllable delivery system to achieve effective protection against hearing loss in a variety of conditions

639 Clinical Efficacy and Safety of Topical IGF1 Application Using Gelatin Hydrogels for Sudden Sensorineural Hearing Loss

Takayuki Nakagawa¹, Tatsunori Sakamoto¹, Harukazu Hiraumi¹, Yayoi Kikkawa², Norio Yamamoto¹, Yasuhiko Tabata¹, Satoru Teramukai¹, Shiro Tanaka¹, Ken-ichi Inui¹, Juichi Ito¹

¹Kyoto University, ²University of Tokyo

Previously, we reported the efficacy of topical IGF1 application using gelatin hydrogels for noise- or ischemiainduced hearing loss in animal models. Recently, we have demonstrated the expression of IGF1 receptors in inner ear hair cells and the activation of cell survival pathways by IGF1. Such basic findings indicate the potential of topical IGF1 treatment for the treatment of sudden sensorineural hearing loss (SSHL) in clinical settings. We then tested the safety and efficacy of topical IGF-1 application using gelatin hydrogels as a treatment for SSHL. Patients with SSHL that showed no recovery to systemic glucocorticoid administration were recruited. We applied gelatin hydrogels, impregnated with recombinant human IGF1, into the middle ear. The primary outcome measure was the proportion of patients showing hearing improvement 12 weeks after the test treatment. The secondary outcome measures were the proportion of patients showing improvement at 24 weeks and the incidence of adverse events. The null hypothesis was that 33% of patients would show hearing improvement, as was reported for a historical control after hyperbaric oxygen therapy. In total, 25 patients received the test treatment at a median of 23 days (range, 15-32) after the onset of SSHL, between 2007 and 2009. At 12 weeks after the test

treatment, 48% (95% CI, 28–69%; P = 0.086) of patients showed hearing improvement, and the proportion increased to 56% (95% CI, $35\neg$ -76%; P = 0.015) at 24 weeks. No serious adverse events were observed. Topical IGF1 application using gelatin hydrogels is well tolerated and may be efficacious for hearing recovery in patients with SSHL that is resistant to systemic glucocorticoids.

640 Intratympanic Delivery of Cidofovir Through Novel Technologies

Alisa Reece¹, Jonette Ward¹, Kevin Li², Daniel Choo^{1,2} ¹Cincinnati Childrens Hospital Medical Center, ²University of Cincinnati

Sensory neural hearing loss (SNHL) occurs in 5 to 10% of children with asymptomatic congenital Cytomegalovirus (CMV). It has been identified as a primary cause of bilateral and unilateral hearing loss in children. Although positive hearing outcomes result from systemic antiviral treatments, the side effects are severe. Intratympanic (IT) therapies have proven to be a novel route in drug delivery while avoiding the systemic side effects. Therefore, the lab is exploring a unique application of IT drug delivery using temperature sensitive gels.

IT injection is an effective clinical treatment for inner ear disorders. Although, obtaining an effective, continuous dose is difficult. The goal is to achieve enhanced control and sustained delivery of antivirals into the middle ear via thermo-sensitive PLGA-PEG-PLGA gels. is а biodegradable and biocompatible block copolymer that has a sol-to-gel transition with temperature change. By incorporating cidofovir (CDV) into the copolymer, in vitro data show the effective life of CDV is extended. Using the quinea pig model, early in vivo safety studies days 1 to 14 indicate that the gel alone does not cause any audiologic or morphologic damage to the inner ear. MRI reveals fluid distribution through the middle and inner ear validating that the gel and/or drug localizes at and penetrates the round window. Pharmacokinetic data (PK) corroborates the MRI position that CDV is located in the cochlea. PK results show enhanced and sustained drug delivery to the cochlea when delivered IT. Histological, audiological, and PK data are being examined further for potential inner ear toxicities. The lab is also pursuing other gel formulations to further enhance drug delivery.

641 Detection of Drugs in Cochlear Fluids Following Round Window Membrane Application in the Rat

Hao Xiong¹, Lukas Ruettiger¹, Marlies Knipper¹ ¹*Tuebingen hearing Research Center, University of Tuebingen*

The treatment of sudden hearing loss and tinnitus by local delivery of drugs to the cochlear round window (RW) has become a preferential method. By local application, drugs can be delivered in much higher concentrations than systemically and side effects or damage in other organs can be minimized. Through the last decade substantial evidence has accumulated about the pharmacokinetic in cochlear fluids and predictive models have been introduced that describe the drug allocation in cochlear

fluids based on morphometrical and pharmacological studies (Salt & Plontke 2009, Hahn et al. 2006, Plontke et al. 2004). Here, we present data for the intrusion of distinct peptides and drug compounds into the cochlear fluids of the rat after local application to the RW using a gel foam carrier. Cochlear fluids were taken by micropipettes in vivo and ex vivo, blotted to a nylon membrane and the drugs detected by antibody staining. Immunoblot results will be correlated to functional hearing tests and related to the presumptive drug concentration in the respective compartments in the cochlea.

642 Magnetic Nanoparticle Driving for Drug Delivery Through a Cochlear Implant

Yann Nguyen^{1,2}, Mathieu Miroir^{1,2}, Guillaume Kazmitcheff^{1,2}, Evelyne Ferrary^{3,4}, Olivier Sterkers^{3,4}, Alexis Bozorg Grayeli^{3,4}

¹UMR-S 867 Inserm, Paris, France, ²UMR-S 867 Université Paris 7, Paris, France, ³UMR-S 867 Inserm / Paris 7, Paris, France, ⁴AP-HP, Hospital Beaujon, ENT departement, Clichy, France

Introduction: Several studies have identified potential therapeutic agents capable of preventing inner ear damage or regenerating cochlear sensory cells. The ideal delivery system should be sterile, refillable and able to deliver the drug for months or even years. The system should include an easy on/off mechanism, a programming possibility, low energy consumption and be able to target different cochlear turns. It should not interfere with cochlear physiology in term of inner ear liquids osmotic or ionic composition, flow rate, pressure, and temperature. An electromagnetic pump coupled to super paramagnetic nanoparticles (MNP) can potentially fulfill all these criteria. The aim of this study was to investigate the displacement of these vehicles by a local magnetic field.

Material and methods: Catheters (Ø: 1mm) were filled with 200 nm coated MNP (0.8mg/ml, Ademtech, Pessac, France) in saline serum. In order to drive the particles, solenoids (Ø: 1mm; length: 2mm) were placed around the catheter (30 turns of 0.05 mm diameter copper wire). The influence of current intensity (50, 100, 150 mA), length of separation between 2 solenoids (5, 10, 15 mm), and gravity (0, 30, and 60° of catheter tilt) on MNP kinetics was studied. MNP kinetics was measured by sequential digital pictures (1/30 minutes), and analysis of the yellow pixel intensity and surface in the catheter (Image J software, NIH).

Results: MNP could be driven by a magnetic field generated by a current as low as 50 mA(\approx 3mT). Nanoparticles could be driven using sequential solenoid activation at 150 mA during 24 hours. Solenoid activation could partially counterbalance the effect of gravity up to 60° tilt and reduce passive diffusion.

Conclusion: MNP can be easily controlled with solenoids and a current level compatible with current cochlear implant design. Multiples solenoids included in the electrode array can potentially provide a precise drug delivery by these particles in different cochlear regions. This work was supported by MED-EL, Innsbruck, Austria.

643 Dexamethasone Eluted from Silicone Electrodes Provides Long-Term Protection of Pure-Tone Evoked Hearing Thresholds Against Electrode Insertion Trauma-Induced Losses in Guinea Pigs

Thomas Van De Water¹, Jorge Bohorquez², Jiao He¹, Simon Angeli¹, Christine Dinh³, Adrien Eshraghi¹, Roland Hessler⁴, Soeren Schilp⁴, Carolyn Garnham⁴, Claude Jolly⁴, Fred Telischi¹, Thomas Balkany¹

¹Cochlear Implant Research Program, University of Miami Ear Institute, ²Dept. Biomedical Engineering, University of Miami, ³Residency Training Program, Department of Otolaryngology, Miller School of Medicine, ⁴MED-EL Hearing Implants

Background: Dexamethasone base (DXMb) protects auditory hair cells (HCs) and hearing from trauma/inflammation-induced losses. A recent study demonstrates that micronized DXMb can be reliably released from silicone cochlear implant blanks.

Material and Methods: In Vitro- organ of Corti (OC) explants tested the efficacy of polymer-eluted DXMb to prevent tumor necrosis factor (TNF)-alpha induced HC apoptosis and to initiate changes in gene expression. Real time RT-PCR determined the expression levels of 3 apoptosis-related genes and 1 pro-inflammatory gene. In Vivo- Experimental animals were adult pigmented guinea pigs (GP); hearing thresholds were obtained by recording cochlear action potentials (CAPs) via an implant electrode and auditory evoked brain stem responses (ABRs) via a dura contacting screw electrode in response to 0.5, 1, 4, 16 kHz pure tone stimuli. Thresholds were determined by a deconvolution program developed by JB. GP electrodes were of 2 types: 1) silicone only; and 2) silicone containing 10% DXMb and were inserted purposefully with additional moderate trauma to a depth of 5 mm into the scala tympani via a basal turn cochleostomy.

Results: In Vitro- Polymer-eluted DXMb is as effective as the natural form of DXMb in both protecting HCs and initiating changes in gene expression in TNF-alpha challenged OC explants. In Vivo- Cochleae implanted with silicone electrodes experienced approximately a 38 dB SPL increase in thresholds for all 4 frequencies at 30 d post-electrode insertion trauma (EIT), in contrast the threshold increase at 30 d post-EIT in the silicone/DXMb electrode ears was only approximately 2 dB SPL higher than pre-EIT levels. Initial threshold losses were similar in both groups following insertion of the 2 different electrode types, i.e. 40 vs. 41 dB SPL.

Conclusion: There was a highly significant level of protection of hearing thresholds against EIT-induced losses in the cochleae receiving the DXMb-eluting electrodes.

644 Round Window Niche Delivery of AM-111 Via Hylumed to Prevent Hearing Loss Post Electrode Insertion Trauma in a Guinea Pig Model of Cochlear Implantation

Adrien Eshraghi¹, Chhavi Gupta¹, Jorge E Bohorquez¹, Maria Victoria Talamo¹, Thomas Van De Water¹, Carolyn Granham², Thomas Meyer³, Claude Jolly², Roland Hessler², Fred Telischi¹, Thomas J. Balkany¹

¹University of Miami Miller School of Medicine, ²MEDEL Corporation, ³Auris Medical

Electrode insertion during Background: cochlear implantation causes both acute and delayed hearing loss. AM-111 is an inhibitor of JNK activation of c-Jun, and in our previous work in a guinea pig model of electrode insertion trauma induced hearing loss; it has effectively acted as an otoprotective drug. In our previous study this drug was delivered via a mini-osmotic pump for 8 days in those trauma-protection experiments. Recent reports have demonstrated that hyaluronic-acid (HA)-based hydrogels are efficient, stable and a sustainable vehicle for the local delivery of dexamethasone into the scala tympani of the cochlea. The objective of the present study is to test the concentration and method of AM-111delivery via a HAhydrogel as an otoprotective drug prior to cochlear implantation.

Methods:

5 μ l of AM-111 (100 μ M) in a sterile Hylumed gel or a sterile Hylumed gel alone was placed directly into the round window niche half an hour before the initiation of electrode insertion into the scala tympani. Control groups were the non treated contra-lateral ears without electrode insertion and Hylumed gel alone treated ears with electrode insertion.

Hearing function was tested by differences in frequencyspecific compound action potential (CAP) thresholds and pure-tone evoked auditory brainstem responses (ABRs) between AM-111 treated and non treated implanted cochlea. CAPs and ABRs were recorded one day before surgery and day 1,3,6,14,30 and 90 after surgery.

Results: There was no significant increase in the hearing thresholds of either the contra lateral control ears or in the ears of the AM-111 treated trauma animals was observed. However there was a progressive increase in both CAP and ABR thresholds after electrode insertion trauma in untreated and in Hylumed only treated cochlea following electrode insertion-. Local treatment of the cochlea with AM-111 prevented the progressive increase in CAP and ABR thresholds that occurs following electrode insertion trauma.

Conclusion: Round window niche delivery of AM-111 via Hydrogel 30 minutes before cochleostomy and cochlear implantation is a promising pre-trauma therapy to prevent electrode insertion trauma induced hearing loss.

645 Modification of the Cochlear Implant for Drug Delivery: A Preliminary Study on PLLA as a Potential Carrier's Coating

Piera Ceschi¹, Henning Rohm², Katrin Sternberg², Verena Scheper¹, Klaus-Peter Schmitz², Manfred Kietzmann³, Thomas Lenarz¹, Timo Stöver^{1,4}, Gerrit Paasche¹ ¹Hannover Medical School, ²Rostock University, ³University of Veterinary Medicine Hannover, ⁴KGU, Frankfurt/M

Cochlear implantation is the standard surgical procedure in the treatment of human sensorineural hearing loss. The benefit of this procedure is usually remarkable. Nevertheless, the following tissue reaction, which causes an increase in the impedance of the stimulation contacts of the cochlear implant, can prejudice its use.

For this reason we investigate the incorporation of antiinflammatory drugs in a biodegradable polymeric coating, which should permit the gradual release of these drugs in the cochlea. Polymeric coatings have been used to improve the performance of coronary stents, but little is known about their effects in the more closed environment of the inner ear.

In the first part of our study we determined the survival rates of fibroblasts and spiral ganglion cells (SGC) on poly(L-lactide) (PLLA) as potential drug carrier in comparison to silicone. Subsequently, in order to investigate the effects of the degradation of PLLA in the scala tympani, a prototype consisting of a silicone carrier covered by PLLA was developed and implanted bilaterally in guinea pigs for 1, 2, 3, and 6 months. After sacrifice results were compared to the effects of uncoated silicone carriers. Cochleae were embedded in epoxy with the samples in situ, stained, and grinded and documented for evaluation of surviving SGC.

In vitro data demonstrated that fibroblasts and SGC grow on the PLLA surfaces as on silicone. The in vivo study showed that only after two months the survival rate of SGC in the PLLA-treated group is reduced in comparison to the respective controls whereas SGC density compared to not implanted cochleae is only reduced in PLLA groups but not in control groups. These reductions in SGC survival are limited to the basal and first middle turn of the cochlea.

Supported by German Research Foundation SFB/TR37 TP C4.

646 Consecutive Treatment with BDNF and Electrical Stimulation Has a Protective Effect on Spiral Ganglion Cells

Verena Scheper¹, Thomas Lenarz¹, Timo Stöver², Gerrit Paasche¹

¹Medical University Hannover, Hannover, Germany, ²Johann Wolfgang Goethe-University Frankfurt a.M.

Objective: The cochlear implant (CI) directly stimulates the spiral ganglion cells (SGC). Therefore the density and health of SGC are factors influencing the success of a CI. Several studies indicate that SGC degeneration can be reduced by brain-derived neurotrophic factor (BDNF) or electrical stimulation (ES). In clinic, chronic drug treatment of SGC could start directly after CI implantation whereas

ES via the implant begins after first fitting. The present study was conducted to determine the effects of consecutive BDNF and ES treatment on SGC density and electrical responsiveness.

Methods: Guinea pigs were systemically deafened and three weeks later an electrode-drug delivery device (Cochlear Ltd) was implanted unilaterally. Five experimental groups were set up: two groups received intracochlear infusion of artificial perilymph (AP/-) or BDNF (BDNF/-); two groups were treated with AP respectively BDNF in addition to chronic ES (AP/ES; BDNF/ES); one group received BDNF until day 34, when the reservoir was disconnected and ES started (BDNF \rightarrow ES). Electrically evoked auditory brainstem responses (EABR) were recorded on experimental day 21 and subsequently every week. After one month treatment the tissue was harvested, processed for histology and the SGC density was determined.

Results: BDNF/ES as well as BDNF \rightarrow ES caused a significant increase in mean SGC density compared to the contralateral untreated ear. The mean SGC densities of the treated cochleae of the BDNF/-, BDNF/ES and BDNF \rightarrow ES groups were significantly increased compared to the mean SGC density of the AP/- treated cochleae. The evoked responses of the AP/ES and BDNF \rightarrow ES group decreased significantly.

Conclusion: Consecutive treatment with BDNF and ES was as successful as the simultaneous combined treatment in terms of protection of SGC from degeneration and increase in electrical responsiveness and might therefore also be considered for clinical application.

Acknowledgement: The authors thank Cochlear Ltd. for providing the cochlear implant electrodes.

647 Effectiveness of HPN-07 in Combination with N-Acetylcysteine in the Treatment of Acute Acoustic Trauma in Rats

Jianzhong Lu^{1,2}, Xiaoping Du^{1,2}, Wei Li¹, Charles Stewart², Kejian Chen³, Robert Floyd², Richard Kopke^{1,2} ¹Hough Ear Institute, ²Oklahoma Medical Research Foundation, ³Naval Medical Center at San Diego

Acute acoustic trauma results in oxidative stress that has been recently identified as the pivotal pathway of cochlear damage. This study was aimed to analyze the time course of the pathogenic mechanisms of noise-induced cochlear damage and the therapeutic efficacy of a combination of two antioxidant drugs, namely HPN-07 and Nacetylcysteine (NAC), in reducing noise ototoxicity. Acoustic trauma was caused by 115 dB SPL one-octave band noise centered at 14 kHz for 1 hr. Rats were assigned to two groups, one (the medication group) treated with the drug combination, initially 1h after noise exposure and twice daily for the next 2 days, and one (the control group) with saline using the same schedule. The hearing ability was evaluated using auditory brainstem responses (ABRs) and distortion product otoacoustic emissions (DPOAEs) in the frequency range of 2-16 kHz. The ABR threshold shifts and DPOAE level shifts were compared between the two groups at 8 hrs, 24 hrs, and 7 and 21 days after noise exposure. Morphological changes were assessed by hair cell counts. The ABR threshold measured 8 hrs after acoustic trauma was elevated in the control group to an average of 65 dB across all test frequencies. Within the first 7 days, following acoustic trauma, there was a partial recovery of acoustic thresholds of about 15 dB to reach a final threshold elevation of about 50 dB; there was no further significant recovery from 7 to The medication group showed a similar 21 davs. temporary threshold shift but a clear improvement in the recovery of ABR thresholds, with a permanent threshold shift decrease of about 20 dB; this improvement was also clearly seen with a significant reduction in both DPOAE level shift and hair cell loss. These findings suggest that the HPN-07/NAC combination can protect the cochlea against acute acoustic trauma.

Supported by the Office of Naval Research (grant N00014-09-1-0999)

648 Electrophysiological Study of Treatment of Acute Noise Injury Induced Hearing Loss with HPN-07

Ning Hu^{1,2}, Richard Kopke^{1,2}, Don Nakmali¹, Xiaoping Du^{1,2}, Chul-Hee Choi¹, Robert Floyd²

Du^{1,2}, Chul-Hee Choi¹, Robert Floyd² ¹Hough Ear Institute, ²Oklahoma Medical Research Foundation

HPN-07 is a derivative of 4-hydroxy phenyl N-terbutyInitrone (4-OHPBN) that has been used as a new nitrone-based free radical trap and an inhibitor of inducible nitric oxide synthase to treat hearing loss induced by acute noise injury (AAT). Compared to regular 4-OHPBN, the advantage of HPN-07 is safety. In the current study, we used a chinchilla model of noise-induced hearing loss by exposing animals for six hours to 4 kHz octave band noise at 105 dB SPL. HPN-07 was dissolved in saline and intraperitoneally administrated to animals for three days starting four hours after AAT. Auditory brainstem response (ABR) and distortion product otoacoustic emission (DPOAE) in chinchilla were measured on the third, tenth and twenty-first days after AAT for both noise exposed untreated and HPN-07 treated animals. Compound action potential (CAP) and endocochlear potential (EP) were measured in some of animals. It was found that ABR threshold shifts at stimulus frequencies from 2 to 8 kHz (tone-bursts) and click stimuli were significantly lower for the HPN-07 treated group than for the untreated group. The degree of ABR threshold recovery from day 3 to day 21 was greater for the HPN-07 treated group than that for the untreated group. DP amplitudes at 60 dB stimulus level were slightly greater for the HPN-07 treated group on day 10 and day 21 after AAT. For both groups, reduced EPs were recorded on the day 3, and tended to recover to the normal range after 10 days. CAP threshold showed a trend similar to ABR. These electrophysiological findings support the effectiveness of HPN-07 treatment of hearing loss resulting from AAT. A six month long-term study and histological and immunohistochemical examination to determine hair cell loss, cell injury, cell death, and inflammation in the organ of Corti, stria vascularis, spiral ganglions are underway. (Work supported by Office of Naval Research Grant #N00014-09-1-0998)

649 Hydrogen in Drinking Water Attenuates Noise-Induced Hearing Loss in Guinea Pigs

Ying Lin^{1,2}, Akinori Kashio², Takashi Sakamoto², Keigo Suzukawa², Akinobu Kakigi², **Tatsuya Yamasoba²** ¹Department of Otolaryngology, Xijing Hospital, ²Department of Otolaryngology, University of Tokyo Molecular hydrogen acts as a therapeutic and preventive antioxidant by selectively reducing the hydroxyl radical, the most cytotoxic of the reactive oxygen species. It has been shown that inhaled hydrogen gas can prevent or reduce pathological or biochemical changes in animal models of cerebral infarction, neonatal hypoxia ischemia, hepatic injury, intestinal ischemia injury, myocardial ischemiareperfusion injury, and cisplatin-induced nephrotoxicity. In the present study, we tested the hypothesis that acoustic damage in guinea pigs could be attenuated by the consumption of molecular hydrogen. Guinea pigs received normal water or hydrogen-rich water for 14 days before they were exposed to 115 dB SPL 4-kHz octave band noise for 3 hours. Animals in each group underwent measurements for auditory brainstem response (ABR) or distortion-product otoacoustic emissions (DPOAEs) before the treatment (baseline) and immediately, 1, 3, 7, and 14 days after noise exposure. The ABR thresholds at 2 and 4 kHz were significantly better on post-noise day 1, 3, and 14 in hydrogen-treated animals when compared to the normal water-treated controls. Compared to the controls, the hydrogen-treated animals showed greater amplitude of DPOAE input/output growth functions during the recovery process, with statistical significance detected on post-noise days 3 and 7. These findings suggest that hydrogen can facilitate the recovery of hair cell function and attenuate noise-induced temporary hearing loss.

650 Neuroprotective Effects of SA4503 Against Noise-Induced Hearing Loss

Daisuke Yamashita¹, Tatsuo Matsunaga², Takeshi Fujita¹, Shingo Hasegawa¹, Ken-ichi Nibu¹

¹Kobe University, ²National Tokyo Medical Center

It is thought that sigma receptor distributed over the brain widely is associated with various physiologies, particularly higher brain function. On the other hand, there are still many questions in the function in molecular level. However in late years, many investigators have reported that sigma receptor has functions for control of cell death and nervous regeneration/differentiation as endoplasmic reticulum chaperone. SA4503, which is ligand acting on a sigma receptor selectively with a new small molecule compound, is expected by neuroprotection effects which affect the nervous plasticity, regeneration and maturity for various kinds of neurodegenerative disease. Therefore we examined the neuroprotective effects of SA4503 for inner ear protection against noise-induced hearing loss.

C3H/He mice (male, 6-8 weeks of age, 20-25 g) with a normal Preyer's reflex were used in this study. At first, as pilot study, we examined the expression of sigma receptor in the mature mouse inner ear. By the Western Blot method, the expression of sigma receptor was found in the inner ear. Also, the localization in the cochlea had the distribution widely in organ of Corti, lateral wall, spiral

limbus, spiral ganglion by immunostaining. Next mice received treatment with SA4503-enhanced water (3, 30 mg/kg) or untreated water (control) beginning 10 days prior to noise exposure and continuing through this study. All subjects were exposed to 4 kHz octave-band noise at 120 dB SPL for 2 h, which present permanent threshold shift (PTS) model. Auditory thresholds were assessed by sound-evoked auditory brainstem response at 4, 8, and 16 kHz, prior to and 10 days following noise exposure. Hair cell damage was analyzed by quantitative histology. SA4503 significantly reduced threshold deficits and hair cell death. These results suggest SA4503 reduces noise-induced hearing loss and cochlear damage, suggesting functional and morphological protection.

651 Effect of Substance P on the Recovery from the Acoustic Trauma

Eiju Kanagawa¹, Kazuma Sugahara¹, Hideki Toyota¹, Takefumi Mikuriya¹, Kenji Takeno¹, Hiroaki Shimogori¹, Hiroshi Yamashita¹

¹Yamaguchi University Graduate School of Medicine Substance P is a polypeptide composed of 11 amino acids, and it is known as a perception neurotransmitter. We have already reported changing VOR gain by the administration of substance P to the inner ear. In the experiment, the nystagmus after the vestibular disorder was suppressed. In the present study, we administered substance P to the inner ear after the acoustic trauma, and examined the hearing function and the hair cell loss.

Hartley male guinea pigs (350 - 400 g) with normal tympanic membranes and normal preyer reflexes were used in this study. After the post-auricular incision, mastoid bulla was opened with the drill. Gelatine sponge which include substance P(10-3 M, 10-2 M) was placed on round window membrane. The mastoid bulla was closed with the dental cement. Gelatine sponge without substansc P was used as a control. The ABR threshold was measured immediately after this operation to confirm that the hearing function did not change. The animals were exposed to the intense band noise (130 dBSPL as the PTS model and 110dBSPL as TTS model). The ABR threshold was measured 24 hours later, three days seven days and fourteen days after the intense noise exposure. At the end of experiments, the temporal bone was removed to evaluate the loss of the outer hair cells.

After the intense sound exposure (130 dBSPL), the threshold shifts continued for seven days in both substance P group and the control group, and there is no significant difference in the ABR threshold and the outer hair cells loss rate. On the other hand, the animals exposed to the intense sound exposure showed the improvement of the ABR threshold fourteen days after the operation. The ABR thresholds recovered faster in substance P group than in control group.

We have reported the effect of substance Pin the vestibular functional restoration. However, the effect of substance P in cochlea is unclear. The previous reports assumed that substance P has amplified the cochlea nerve compound action potential and that substance P protected the spiral ganglion. In the present study, we show the

effect of substance P in the temporal threshold shift after the intense noise exposure. The result suggests that the polypeptide promotes the recovery of the cochlear function after noise trauma.

652 Protective Effect of Estradiol in Acoustic Injury of the Mouse

Isao Uemaetomari¹, Keiji Tabuchi¹, Mariko Nakamagoe¹, Bungo Nishimura¹, Kentaro Hayashi¹, Syuhou Tananka¹, Tomofumi Hoshino¹, Akira Hara¹

¹University of Tsukuba

Estradiol reportedly exhibit to have a protective effect on the cochlea against gentamicin ototoxicity. The purpose of the present study was to examine the protective effect of estradiol on the cochlea in acoustic injury. Female ddY mice of 8 weeks of age were used in this study. Animals were subjected to a 4 kHz pure tone of 128 dB SPL for 4 hours through an open field system inside a soundexposure box. Auditory brainstem response (ABR) was examined before, one and two weeks after acoustic overexposure. After final ABR measurements at two weeks after acoustic overexposure, whole mounts of organ of Corti were stained for the nucleus with propidium iodide, and missing hair cells (missing of staining with propidium iodide) were counted every 0.33 mm segments. Estradiol significantly improved the ABR threshold shifts and decreased hair cell loss two weeks after acoustic overexposure when it was administrated before acoustic overexposure. The present findings suggest that estradiol has protective effects against acoustic injury of the cochlea.

653 A Possible PLZF Link in Dexamethasone-Mediated Protection from Acoustic Trauma

Marcello Peppi¹, Sharon G. Kujawa^{1,2}, William F. Sewell¹ ¹Harvard Medical School, ²Massachusetts Eye and Ear Infirmary

We previously identified a corticosteroid-responsive transcription factor, PLZF (Proleukemia Zinc Finger protein), which is essential to mediate cochlear protection from acoustic trauma. Mutant mice deficient in PLZF can not induce such protection. To determine whether PLZF might also mediate the protective effects of administered corticosteroids we characterized the effects of dexamethasone on PLZF mRNA production and on protection from acoustic trauma in CBA mice. Dexamethasone (i.p.) up-regulated PLZF mRNA in cochlea and brain, with peak levels observed 6-8h after injection. Dexamethasone also protected the cochlea from noise damage, with optimal doses between 0.5 and 1.5 mg/Kg. However, higher and lower doses were not effective. Dexamethasone induced protection whether it was administered before or after the noise. Optimal protection was observed when dexamethasone was given 24h after the noise exposure. The mineralcorticoid, aldosterone. had less protective activity than dexamethasone. Both, aldosterone and dexamethasone had greater protective effects on the ABR than the DP. We were unable to demonstrate protective effects with dexamethasone in B6 mice (the strain in which the PLZF mutation is carried). Thus a more stringent test of whether PLZF is involved in corticosteroid induced hearing protection awaits backcrossing the PLZF mutation into CBA mice.

The work was supported by grants from the National Institutes of Deafness and other Communication Disorders (DC 767 to WFS and DC 8577 to SGK).

654 Development of a Combination Therapy for Noise-Induced Hearing Loss

Michelle Hungerford¹, Debin Lei¹, Zhaoyu Lin¹, Jianxin Bao¹

¹Washington University

Noise is the most common occupational and environmental hazard. Noise-induced hearing loss (NIHL) is the second most common form of sensorineural hearing deficit, after age-related hearing loss (presbycusis). Although promising approaches have been identified for reducing NIHL, currently there are no effective medications to prevent NIHL. Development of an efficacious treatment has been hampered by the complex array of cellular and molecular pathways involved in NIHL. We have turned this difficulty into an advantage by asking whether NIHL can be effectively prevented by a combination therapy targeting multiple signaling pathways. We have recently found that antiepileptic drugs blocking T-type calcium channels have both prophylactic and therapeutic effects for NIHL. NIHL can also be prevented by an up-regulation of glucocorticoid signaling pathways. Based on these finding, we have tested a combination therapy for NIHL that includes ethosuximide and from zonisamide anticonvulsants dexamethasone and and methylprednisolone from synthetic GC drugs in one mouse NIHL condition [white noise, 110 dB sound pressure level (SPL) for 30 minutes], which has dramatic changes for permanent threshold shifts (PTS). We have first determined the dose-effect for amelioration of PTS by administering each drug two hours before the noise exposure. The median effective dose (ED50) against NIHL for three drugs was determined. We have subsequently tested the synergistic effect for possible two-drug combinations between these two drug families, and have indentified one combination with the strongest synergy against NIHL based on the combination index (CI) method. Thus, our study has clearly showed the feasibility to develop pharmacological intervention in multiple pathways, and discover effective drug combination with a synergistic effect to prevent permanent NIHL.

655 Dietary Nutrients Attenuate Cell Death Events in the Inner Ear After Noise Insult

Colleen Le Prell¹, Dustin Lang¹, Debbie Joseph¹, Nader Kalantar¹

¹University of Florida

Noise-induced hearing loss is caused by damage to the sensory cells in the inner ear. Much of the damage to the sensory cells is induced by metabolic stress and related free radical production. Noise induced free radical production also triggers chemical cascades that result in caspase-dependent apoptosis. Caspase expression following noise has been observed in hair cells and spiral ganglion cells, as well as the stria vascularis, spiral ligament, and lateral wall. Here, we present immunocytochemical evidence for 3-nitrotyrosine (3NT) production and caspase-8 expression in the inner ear after noise exposure and describe decreased expression of both molecules in animals treated with beta-carotene, vitamins C and E, and magnesium beginning 1 day prior to noise insult.

Guinea pigs were exposed to 115 dB SPL octave band noise (centered at 4 kHz) for 4 hours and euthanized 2 hours, 7 days, or 35 days subsequent to noise insult. Experimental animals received a single dose of betacarotene, vitamins C and E, and magnesium 1 day prior to noise insult and on the day of the noise exposure. Subjects in the 7-day and 35-day survival groups also received treatments once/day for 7 days post-noise. Control animals received saline and oral vegetable oil vehicle in the absence of nutrient additives. The primary antibody was omitted in additional negative control tissues. The data from noise-exposed control animals confirm other reports that free radicals are produced in the inner ear after noise insult and that caspase-8 activation contributes to noise-induced cell death. The data from treated animals showed that dietary nutrients can specifically reduce both early oxidative stress events and caspase-8 expression in the inner ear. These data provide a further understanding of the mechanisms underlying the efficacy of antioxidants to protect tissues of the inner ear from noise-induced pathology.

Supported by University of Florida Office of Graduate Research Opportunity Award to CL.

656 cGMP-CGKI Signaling and PDE5 Inhibition Preserves Cochlear Hair Cells and Hearing Function After Noise Trauma

Mirko Jaumann¹, Juliane Dettling¹, Martin Gubelt¹, Ulrike Zimmermann¹, Andrea Gerling², Susanne Feil², Stephan Wolpert¹, Niels Brandt³, Stephanie Kuhn¹, Jutta Engel³, Iris Köpschall¹, Karin Rohbock¹, Joachim Hütter⁴, Peter Sandner⁴, Robert Feil², Marlies Knipper¹, **Lukas Rüttiger¹** ¹University of Tübingen, Hearing Research Centre, ²University of Tübingen, Interfakultäres Institut für Biochemie, ³Saarland University, Department of Biophysics, Medical Faculty, ⁴Bayer Schering Pharma AG, Global Drug Discovery

Noise-induced hearing loss (NIHL) is a global health hazard with considerable patho-physiological and social consequences. So far, there is no effective treatment for NIHL and age-related hearing loss (presbycusis). A promising starting point was the discovery of the NOcGMP signaling pathway in the inner ear. This pathway has been described to facilitate protecting, but also damaging, processes in response to traumatic events. In previous reports we could show that the auditory function and the cochlear phenotype of mice with a genetic deletion of the cGMP-dependent protein kinase type I (cGKI) was significantly disturbed following acoustic overstimulation, pointing to an otoprotective role of cGMP-cGKI mediated metabolic processes. In the cochlea, cGMP is hydrolyzed by phosphodiesterase 5 (PDE5). PDE5 was found to be expressed in hair cells in a similar subcellular distribution as cGKI, which suggests PDE5 inhibitors as a pharmacological tool for increasing cGMP levels in the cell. We studied the otoprotective and therapeutic potential of cGMP-cGKI signaling treatment with a PDE5 inhibitor and found almost complete protection from NIHL, OHC damage, and IHC synapse damage, even when administered after trauma induction. However, PDE5 inhibitors failed to rescue hearing function after noise exposure in cGKI-deficient mice, pointing out that cGKI is the main target of the NO-cGMP protecting signaling pathway.

The specific expression of $cGKI_{\alpha}$ and $cGKI_{\beta}$ isoforms in cochlear tissues will be presented and discussed in the context of OHC loss and deterioration of IHC synaptic structure. Our results identify an otoprotective cGMP-cGKI signaling pathway in hair cells and indicate a high potential for PDE5 inhibitors in the protection and therapy of NIHL.

Supported by DFG Ru419, DFG Kni316/3-2, DFG Ru571/4-1, SFB 430-B3, Fortune 816-0-0, European Commission, Marie Curie Research Training Network CavNET MRTN-CT-2006-035367, TRI, Hahn Stiftung (Index AG) and Bayer-AG

657 Prostaglandin E Receptor EP4 Is Involved in the Maintenance of Hearing by Protecting Outer Hair Cells in Mammals

Kiyomi Hamaguchi¹, Takayuki Nakagawa¹, Norio Yamamoto¹, Juichi Ito¹

¹*Graduate School of Medicine, Kyoto University* Prostaglandin E (PGE) has been used for treatment of sudden sensorineural hearing loss; however, mechanisms for the effect of PGE have not been fully elucidated. The physiological effects of PGE are mediated through four types of receptors, EP1, EP2, EP3 and EP4. To elucidate the mechanisms of the PGE effect against sensorineural hearing loss, we decided to determine the function of EP4 among four PGE receptors because EP4 has various effects including anti-apoptotic effect compared with other receptors. So far, we have reported that EP4 was expressed in mouse cochlea and EP4 agonist had otoprotective effect against noise exposure (NE) in guinea pigs suggesting that EP4 is involved in hearing maintenance in mammals.

In this study, to confirm the effect of EP4 agonist against NE in other mammals than guinea pigs, it was applied into mouse cochleae through round window membrane before NE. Next, to elucidate the function of EP4 receptor by inhibiting its function, EP4 antagonist was applied into mouse cochleae through round window membrane before mild NE. In both studies, auditory brainstem responses (ABRs) and morphology of cochleae were evaluated.

The result demonstrated that local EP4 agonist treatment significantly attenuated ABRs thresholds shifts. Histological analysis revealed that local EP4 agonist treatment significantly suppressed the loss of outer hair cells. In the second study, we found that the mice applied EP4 antagonists were more susceptible to the NE both functionally and histologically.

These findings demonstrate that EP4 is involved in the maintenance of hearing by protecting outer hair cells. In addition, its agonist can be useful for protecting hearing from noise trauma in clinical situation because it is effective in two different mammals, mice and guinea pigs.

658 Overview of the NIOSH Basic Science Strategic Goal in Hearing Loss Prevention Rickie Davis¹

¹NIOSH

The National Institute for Occupational Safety and Health (NIOSH) has organized its research efforts into ten industry sectors. Cross-sector programs are common to many industries. The Hearing Loss Prevention (HLP) Program is a cross-sector program.

The Hearing Loss Prevention Program has five strategic research goals. The first four are: surveillance, noise control, hearing protectors and hearing conservation programs. The fifth strategic goal is: Preventing occupational hearing loss through studies of risk factors. Five subgoals have been identified—impulse noise, individual susceptibility, ototoxicity, long term effects of hearing loss and otoprotectants.

Impulse noise has been shown to be more damaging to the ear than equal energy continuous noise. NIOSH is currently supporting research to develop metrics for describing impulses and developing hardware to collect impulsive noises.

Individual susceptibility has to do with genetic vulnerability to noise. NIOSH is currently conducting a field study of workers looking at nine genetic alleles.

Some chemicals in the work environment interact with noise to produce greater hearing loss. NIOSH has partnered with the Nordic Expert Group to document most known ototoxicants. *www.nordicexpertgroup.org*

Animal work has demonstrated that early-life exposures lead to greater hearing loss later in life than a later-life exposure. NIOSH currently has no project associated with this subgoal.

Some chemicals and compounds have been shown in animals to protect the ear from noise. NIOSH currently is interested in the human trials but does not have an active project.

The vision of SG 5 is by better understanding the basic mechanisms of hearing loss to reduce the number of OSHA recordable annual hearing losses from 30,000+ in 2004 to less than 22,000 in 2016.

659 Functional Role of Hyperpolarization-Activated Cyclic Nucleotide-Gated Channels in Mouse Spiral Ganglion Neurons

Ye-Hyun Kim¹, Geoffrey C. Horwitz¹, Jeffrey R. Holt¹ ¹University of Virginia

The hyperpolarization-activated current, I_h , is carried by members of the HCN channel family. I_h contributes to resting potential and firing properties in cells of various organs, including the auditory system. Recent work (Yi et al., 2010) has shown that HCN1, 2, and 4 are present in

rat spiral ganglion neurons (SGNs), however, the expression pattern and function of HCN subunits in murine SGNs are not fully understood. To this end, we used the whole-cell, tight-seal technique to record I_h from SGN cell bodies acutely excised from wild type (WT), HCN1, 2, and 1/2 double knockout (KO) mice at postnatal day 1-3.

Voltage-clamp recordings revealed slowly activating inward currents in response to 4-second hyperpolarizing voltage steps from -64 to -144mV, in all four groups. Relative to WT controls (2.1 \pm 0.8 nS, n=28), G_h was significantly reduced in HCN1 KOs (1.6 \pm 0.6 nS, n=27, p<0.01), HCN2 KOs (1.5 \pm 0.6 nS, n=17, p<0.02), and HCN1/2 KOs (0.9 \pm 0.4 nS, n=6, p<0.002). I_h activation kinetics, taken from τ_{fast} of double exponential fits to currents evoked at -144 mV, were much slower in both HCN1 (423 \pm 134 msec, n=27) and HCN1/2 (531 \pm 81 msec, n=6) KOs compared to WT (161 \pm 48 msec, n=28) and HCN2 (135 \pm 60 msec, n=17) KOs.

In current-clamp, resting potential was significantly (p<0.001) more hyperpolarized in HCN1 KOs (-88±6 mV, n=21) than in WT (-79±7 mV, n=25), but no differences were found among other groups. In response to 10 pA hyperpolarizing current injections, HCN1 KOs (-29±9 mV, n=21) showed a significant (p<0.0001) difference in depolarizing sag amplitude compared to WT (-15±8 mV, n=25) and HCN2 (-16±9 mV, n=16) KOs.

Blockage of residual I_h in HCN1 and HCN1/2 KOs by the HCN antagonist ZD7288 indicated the contribution of another HCN subunit, possibly HCN4. Taken together our data indicate that HCN1, and perhaps HCN4, contribute to the membrane properties of SGNs and may play a role in temporal aspects of signal transmission between the cochlea and the brain.

660 Evaluation of Voltage-Gated Ca²⁺ Channel α-Subunits in Murine Spiral Ganglion Neuron Firing Patterns

Wei Chun Chen¹, Qing Liu¹, Hui Zhong Xue¹, Shail Patel², Robin Davis¹

¹*Rutgers University,* ²*University of Medicine and Dentistry of New Jersey*

Spiral ganglion neurons (SGN) possess diverse firing properties that are systematically organized along the cochlear contour. Furthermore, voltage-gated K^+ channels, presynaptic, and postsynaptic proteins are also tonotopically organized. Here, we focus on voltage-gated Ca²⁺ channels (VGCC) to further understand the fundamental properties of these primary afferents.

Perfusion experiments were carried out to determine whether VGCC modify SGN activity *in vitro*. When 50-100 μ M CdCl₂ was applied, action potential (AP) duration and latency were systematically decreased from apex to base (duration: apex, Δ [before and after perfusion] = 0.37 ± 0.03 ms, *n* = 3, *p* < 0.01; middle, Δ = 0.28 ± 0.04 ms, *n* = 6, *p* < 0.01; base, Δ = 0.25 ± 0.03 ms, *n* = 5, *p* < 0.01; latency: apex, Δ = 3.53 ± 1.01 ms, *p* = 0.07; middle, Δ = 6.72 ± 1.34 ms, *p* < 0.01; base, Δ = 5.24 ± 1.84 ms, *p* < 0.05). A similar tonotopic trend was also observed in response to 10 mM tetraethylammonium application (Duration: apex, $\Delta = 19.7 \pm 12.9$ ms, n = 6, p = 0.19; middle, $\Delta = 6.48 \pm 2.20$ ms, n = 4, p = 0.10; base, $\Delta = 3.03 \pm 0.64$ ms, n = 4, p < 0.05). These results indicate that VGCC contribute to AP duration and latency in SGN, and that their effects are tonotopically-regulated.

Immunocytochemistry was used to identify specific VGCC. We found that Ca_v1.3, Ca_v2.2, and Ca_v3.3 subunits were localized primarily in neurons, Ca_v2.1, Ca_v2.3, and Ca_v3.1 subunits in neurons and glia, and Ca_v1.2 subunit in satellite cells. Analysis of neuron-specific VGCC showed that Ca_v1.3 and Ca_v3.3 subunits were higher in base (antibody luminance = 552 ± 69 ; n = 4; p < 0.05; 464 ± 73 ; n = 5; p < 0.05, respectively) than apex (396 ± 36 ; 298 ± 15). In comparison, Ca_v2.2 subunit was uniformly distributed between apex and base (205 ± 38 , 216 ± 42 , respectively; n = 3; p = 0.30). Future experiments will focus on how the distribution and regulation of specific VGCC contribute to SGN firing patterns. Supported by NIH RO1 DC01856.

661 Identification of the Voltage-Gated Ion Channels That Regulate a Non-Monotonic Distribution of Intrinsic Excitability in Murine Spiral Ganglion Neurons

Qing Liu¹, **Edmund Lee**¹, Robin Davis¹ ¹*Rutgers University*

Inner hair cells send discrete auditory signals to 20-25 auditory nerve fibers, each forming one synapse on a single receptor. Although these fibers convey identical frequency information, they display diverse thresholds and spontanteous rates. This is important because it extends the coding range of the neuronal population by shifting their rate level functions. Moreover, nerve fibers in the midcochlear display specialized sensitivity (Taberner and Liberman, 2005), which overlaps with animals' best frequency range.

Our previous characterization of the intrinistic excitability of spiral ganglion neurons shows heterogeneous voltage thresholds in each region, which, interestingly, are also most sensitive in the mid-cochlea (Liu and Davis, 2007). We further measured resting potential to examine whether it coordinates with threshold regulation to augment firing sensitivity in the middle neurons. Our data did demonstrate an elevated resting potential from this area (-68.09±0.42, n=38, -65.53±0.57, n=35, -65.49±0.65 mV, n=32 from base to apex; the same order applies hereinafter). To elucidate the determinants of the specialized intrinsic excitability, α-DTX was applied to block the shaker-related potassium channels. It non-monotonically altered both neuronal threshold (A=-25.73±2.04, n=11; -14.19±1.28, n=8; -14.86±2.23 mV, n=7) and resting potential $(\Delta = +9.95 \pm 0.70, n=4; +7.84 \pm 0.89, n=8; +7.21 \pm 0.31 \text{ mV},$ n=8). Additionally, blockade of I_h with CsCl revealed another regulatory component of the resting potential (Δ =-3.32±0.55, n=10; -2.74±0.70, n=8; -3.94±0.83 mV, n=5). In summary, our investigation of spiral ganglion neuron intrinsic excitability based on resting potential and voltage threshold measurements suggests that in addition to middle ear mechanics (Rosowski, 1991) and synaptic

mechanisms (Merchan-Perez and Liberman, 1996; Meyer

et al., 2009), the neurons themselves have the potential to contribute to auditory nerve *in vivo* responses. Supported by NIH NIDCD R01 DC-01856

662 Calretinin and Calbindin Distributions Specify Subpopulations of Neurons Within the Murine Spiral Ganglion

Wenke Liu¹, Robin. L. Davis

¹Rutgers University

Accurate auditory signaling requires a rich repertoire of neural responses. Spiral ganglion neurons display tonotopically graded firing patterns and nonmonotononically distributed excitability features (Adamson et al *J. Comp. Neurol.* 2002, Liu and Davis, *J. Neurophysiol.* 2007). To further characterize the complex signaling capacity of these neurons we have begun to evaluate the distribution of calcium binding proteins, which are widely used markers for subgroups of neurons in the nervous system.

Acute cochlear whole mounts co-labeled with anticalretinin and anti-calbindin antibodies showed a complementary pattern in spiral ganglion neurons. The pattern was retained in vitro in cultured isolated spiral ganglion neurons. Measurements revealed that neurons with high calretinin staining luminance (normalized value>0.5) were low for normalized calbindin luminance (mean 0.109) and neurons with high calbindin luminance (normalized value>0.5) possessed low level of calretinin luminance (mean 0.210), indicating that calretinin and calbindin marked distinct subpopulations of spiral ganglion neurons. Putative type II neurons in isolated cultures with high peripherin staining luminance were consistently low in calretinin staining luminance; the frequency histogram was best fit by a single Gaussian (mean 0.057±0.019, n=7). On the other hand, the range of normalized calbindin staining luminance in putative type II neurons spanned low (0.013±0.035) to high (0.757±0.063) levels (n=6).

Calbindin and calretinin are calcium buffers proposed to be regulated differently in the cochlear nucleus in response to peripheral hearing loss (Idrizbegovic et al. *Hear. Res.* 2003). The complementary pattern observed in the spiral ganglion suggests that they may specify different neural responses even under normal conditions. Investigation into the difference between the two subpopulations may also help clarify the physiological properties of type II neurons. Supported by NIH NIDCD R01 DC-01856.

663 Intrinsic Electrical Properties of Spiral Ganglion Neurons in Long-Term Cultures

Pavel Mistrik¹, Dan Jagger¹, David McAlpine¹

¹UCL Ear Institute

Spiral Ganglion Neurons (SGNs) of the cochlea form a critical functional interface between mechano-electrical transduction in the inner ear and neural processing by the central nervous system. It is not clear at the moment if SGNs exhibit any particular intrinsic electrical tuning that enhances their firing in a specific frequency range. Such feature would be compatible with the resonance properties of neurons at higher auditory centres, such as those in the brainstem (Mikiel-Hunter et al., ARO 2010). We

ARO Abstracts

investigated the complement of ion channels in long-term cultured spiral ganglion neurons from P4-P5 rat cochleae using the whole-cell patch clamp-techniques. Such an experimental approach permits proper clamping of isolated neurons and, also, the potential to tune electrical properties of their membrane by the over-expression of appropriate ion channels using DNA transfection techniques. Despite some variability between neurons, several conductances important for the firing of action potentials were revealed under such culturing conditions in the voltage-clamp analysis, including fast sodium current I_{Na} , outwardly-rectifying potassium currents I_{K} and the hyperpolarization-activated cation current In. The voltagedependence of activation as well as the kinetics of such currents were typical of those reported for adult, mature SGNs. The neuronal identity of such cultured cells was confirmed by immuno-labelling with an anti-neurofilament antibody NF200. The presence of I_h and outwardly rectifying potassium currents opens a possibility that the SGN impedance could exhibit a resonance with respect to the frequency of the stimulus, as such conductances could interfere with the low-pass filtering typical for passive membranes. We have investigated such scenario in the current-clamp mode using 'ZAP' input at subthreshold voltage levels. The co-involvement of I_h or outward I_K currents was tested using specific blockers (ZD7288 and dendrotoxin, respectively).

664 Time Course of Dynamic Range Adaptation in the Auditory Nerve

Bo Wen^{1,2}, Grace I. Wang^{1,3}, Isabel Dean⁴, Bertrand Delgutte^{1,2}

¹Eaton-Peabody Laboratory, Massachusetts Eye and Ear Infirmary, ²Dept. of Otology and Laryngology, Harvard Medical School, ³Dept. of EECS, Massachusetts Institute of Technology, ⁴Ear Institute, University College London Auditory nerve (AN) fibers show both classic firing rate adaptation and dynamic range adaptation to the mean sound level in a dynamic stimulus (Wen et al., J. Neurosci. 29:44). We investigated the time course of dynamic range adaptation by recording from AN fibers in anesthetized cats in response to stimuli in which the mean sound level switches between two values every 5 s. During each 5-s half-cycle, the stimulus level was randomly drawn every 50 ms from a broad distribution containing a 12-dB wide highprobability region (HPR) in which levels occurred with 80% probability. We found that in response to these "switching-HPR" stimuli, the adaptation of AN average firing rate, influenced by both forms of adaptation, occurs over just a few hundreds of msec. However, limited recording time made it difficult to isolate the time course of dynamic range adaptation from that of firing rate adaptation in these experiments.

To better characterize the time course of dynamic range adaptation, we developed a phenomenological "dual adaptation" model that accounts for the adaptation behaviors observed in the AN. The model comprises two linear adaptation modules connected in cascade with a saturating nonlinearity defining the shape of rate-level functions sandwiched in between. The first adaptation module operates on sound levels to produce dynamic range adaptation, while the second adaptation module operates on firing rates to produce firing rate adaptation.

Using a maximum likelihood approach and assuming Poisson discharges, the model could adequately fit the time course of AN fiber firing rates in response to switching-HPR stimuli with only 6 free parameters. After fitting model parameters to the data, we computed model responses to a switching-HPR stimulus containing a large number of switching cycles in order to characterize the evolution of the dynamic range after each switch onset with fine time resolution. The time constants of dynamic range adaptation estimated from model responses ranged from 200 to 600 ms and were comparable to those of firing rate adaptation measured from the same stimuli. These findings suggest that the adaptive processing in the auditory periphery in response to changes in sound level distribution occurs very rapidly.

Supported by NIH grants RO3 DC011156, RO1 DC002258, and P30 DC005209.

665 Assessment of Phase-Locking Using Population Responses at the Auditory Nerve and Round Window

Eric Verschooten¹, Luis Robles², Philip Joris¹ ¹Lab. of Auditory Neurophysiology, Leuven, Belgium, ²Program of Physiology and Biophysics, Universidad de Chile

Neural phase locking or stimulus synchronization is a fundamental property of the peripheral auditory system. In single auditory nerve fibers, phase locking declines with frequency and becomes undetectable at an upper frequency limit which differs between species. The upper frequency limit in humans is unknown, and widely differing values are assumed in the interpretation of psychophysical results. Our aim is to develop a stimulus and recording characterize paradigm to phase-locking electrophysiologically with population responses which may be recordable in humans. We placed ball electrodes on the round window (RW), in the nape of the neck, and on the auditory nerve (AN) in anesthetized chinchillas and cats. The ground electrodes were connected at the contralateral mastoid. The stimuli consist of a tone and a forward masked tone, which alternated in polarity in sequential presentations. To disambiguate contributions of receptor and neural origin, we compare the sum and difference of responses to alternate polarities. Response components that are asymmetric (i.e. that are not cancelled by summing responses to alternate polarity) and that are maskable are considered to be of neural origin. Asymmetric components were found in the responses from both RW and AN, and were completely maskable and therefore of neural origin. Symmetric components were also found at both locations: they were completely maskable at the AN but only partially at the RW, depending on frequency. For both locations, adaptable, asymmetric components decreased with tone frequency and merged with the background noise at 2kHz. Adaptable symmetric components behaved similarly but were still above noise level at 3kHz (AN) and 5kHz (RW). We conclude that a phase-locked component can be measured with population responses with an upper limit similar to that measured in single nerve fibers. Supported by grants from FWO and BOF (Flanders, Belgium) and a BOF visiting professorship; grant CONICYT 1080227 to LR.

666 Synchronization to Pure and Amplitude-Modulated Tones in the Auditory Nerve of Macaque Monkey

Pascal Michelet¹, Myles Mc Laughlin¹, Marcel van der Heijden¹, Philip Joris¹

¹Laboratory of Auditory Neurophysiology

In recent years macaque monkeys have gained popularity as models of human auditory processing. However, knowledge of the physiology of peripheral auditory structures in the monkey is limited and predates current concepts. We studied the auditory nerve (AN) of two macaque species and characterized their ability to synchronize to the fine-structure and envelope of tonal stimuli.

We recorded responses from 255 single fibers in 16 pentobarbital-anesthetized macaques (11 m. fascicularis and 5 m. mulatta). The AN was exposed through a fossa posterior craniotomy and partial cerebellectomy. Glass micropipettes filled with 3M NaCl were advanced into the AN with a hydraulic microdrive. Stimuli were presented over closed speakers calibrated at the entrance of the ear canal. For every fiber encountered we recorded a frequency tuning curve to determine its characteristic frequency (CF). A rate-intensity curve to tone pips at CF was then obtained, as well as responses to sinusoidally amplitude modulated (SAM) stimuli and non-harmonic tonal complexes ('zwuis').

Compared to the cat, the distribution of spontaneous rate (SR) was more continuous. Synchronization to finestructure was similar in terms of maximal vector strength magnitude (Rmax) and upper frequency limit. However, Rmax values in high SR fibers were systematically higher than in low SR fibers. A form of peak-splitting was observed which was restricted to the first response cycles, over a large range of SPLs, and which was unlike the peak-splitting and phase shifts encountered at high SPL in the cat. Cutoff frequencies of modulation transfer functions tended to be lower than in the cat.

We conclude that the overall distribution of phase-locking to fine-structure is similar to that in the cat when quantified with vector strength, but that differences are apparent at a finer level of analysis.

Supported by grants from FWO (G.0633.07) and BOF (OT/09/50) (Flanders, Belgium) and an IWT fellowship to PM (SB-81346).

667 The Effect of Noise Bandwidth on Auditory Receptive Field Estimation

Haoxin Sun¹, Edgar Walker¹, Dennis Barbour¹ ¹Washington University

Accurate identification of a neuron's receptive field (RF) is critical in characterizing and modeling the processes used by the auditory system to encode sounds. Classically, neuronal RFs in the auditory system have been measured using pure tone stimuli, but pure tones of any frequency or intensity have typically been poor stimuli for neurons of the lateral belt in auditory cortex. These neurons will often respond robustly, however, to bandpass noise stimuli of particular bandwidths centered at the estimated characteristic frequencies (CFs) of the neurons. Consequently, these neurons have been characterized as having a frequency-dependent nonlinearity preferring certain stimulus bandwidths over others, a phenomenon referred to as bandwidth tuning. In this study, we evaluated the effects of using bandpass noise to characterize neuronal properties such as CF. We constructed computational models that simulate both simple linear auditory neurons and sounds with the same properties as those used in previous neurophysiology experiments. We then demonstrated that the usage of bandpass noise stimuli having as their center frequencies inaccurately estimated neuronal CFs can result in a systematic bias that leads to the bandwidth tuning phenomenon. This effect is greatest when stimuli are applied to auditory neurons with asymmetric receptive fields. These results raise the possibility that bias in neuronal parameter estimation using bandpass noise may be able to partially explain the occurrence of bandwidth tuning in certain neurons. The use of bandpass noise in characterization of auditory neurons therefore should be performed with diligence to avoid such bias.

Supported by NIH grant R01-DC009215.

668 Predicted Effects of Reverberation on Pitch and Spectral Coding in the Auditory Nerve

Ananthakrishna Chintanpalli¹, Michael G. Heinz¹ ¹*Purdue University*

The neural basis for robust speech perception exhibited by normal-hearing listeners in reverberation is still unknown, even for simple speech sounds. The present study used computational modeling to compare the relative effects of reverberation on acoustic and neural representations of the pitch and spectra of harmonic tone complexes (HTCs) and synthetic vowels.

Reverberant conditions were simulated by convolving the original stimuli with reverberant impulse responses. Pooled auto-correlation functions were computed using a computational auditory-nerve model. A template contrast technique was then used to estimate pitch and its salience. Rate-place and temporal-place metrics were used to evaluate vowel spectral coding.

For HTCs, pitch was estimated correctly from neural responses for drv and reverberant conditions. Reverberation degraded pitch salience relative to dry, but much less in the neural representation than the acoustic. Furthermore, neural pitch salience decreased less with increasing degrees of reverberation than acoustic pitch salience. Similar findings were observed for vowel stimuli, although variation was observed across vowels depending on the proximity of the first two formants. Preliminary results suggest that formant coding based on temporalplace representations average-localized (e.g.,

synchronized rate) is more robust in reverberation than rate-place. The present results provide a useful baseline for future work with concurrent HTCs and vowels that will explore neural effects of reverberation related to source segregation.

Comparisons between acoustic and neural analyses suggest that the cochlea may be the first stage in the auditory system that partially compensates for the acoustic degradation caused by reverberation. These results may provide useful physiological insight towards the development of new signal-processing strategies to improve hearing aids and cochlear implants in real-world listening environments.

Supported by NIH, R01DC009838.

669 Auditory-Nerve Responses Predict Pitch Attributes Related to Musical Consonance and Dissonance for Normal and Impaired Hearing

Gavin M. Bidelman¹, Michael G. Heinz^{1,2} ¹Department of Speech, Language, & Hearing Sciences, Purdue University, ²Weldon School of Biomedical Engineering, Purdue University

Behavioral studies reveal that human listeners prefer consonant over dissonant musical intervals and that the perceived contrast between these classes is reduced with cochlear hearing loss. Population-level activity of normal and impaired model auditory-nerve (AN) fibers were examined to determine (1) if peripheral auditory neurons exhibit correlates of consonance and dissonance and (2) if the reduced perceptual difference between consonance and dissonance observed for hearing impaired listeners can be explained by impaired AN responses. Neural pitch salience was computed from responses to musical intervals and chords using a computational model of the AN. Among the chromatic pitch combinations of music, consonant intervals yielded more robust salience magnitudes than dissonant intervals and correctly predicted the ordering of hierarchical pitch and chordal sonorities described by Western music theory. Cochlear hearing impairment compressed pitch salience estimates reducing the contrast between neural representations of consonant and dissonant intervals and chords. The reduced contrast in neural responses following cochlear hearing loss may explain the inability of impaired listeners to distinguish musical qualia as clearly as normal hearing listeners. Results ultimately show that basic pitch relationships governing music are already present in initial stages of neural processing at the level of AN.

670 Temporal Coding of Harmonic and Inharmonic Tone Complexes in Auditory Nerve Fibers Following Noise-Induced Hearing Loss

Sushrut Kale¹, Michael G. Heinz² ¹Weldon School of Biomedical Engineering, Purdue

University, ²Department of Speech, Language, and Hearing Sciences, Purdue University

Discrimination thresholds for harmonic and inharmonic tone complexes are often higher for hearing impaired (HI) listeners than for normal hearing listeners. Recent perceptual studies have suggested that increased thresholds for HI listeners may indicate a reduced ability to use temporal fine structure (TFS) cues, a deficit that has been hypothesized to be associated with degraded phase locking or loss of frequency selectivity. The present study quantified TFS cues in chinchilla auditory nerve (AN) fiber responses to harmonic and inharmonic tone complexes following noise-induced hearing loss.

Single unit responses were measured for two stimulus sets, both of which used a harmonic tone complex as a reference (REF). The first stimulus set included test tone complexes (TEST) that were generated by changing the fundamental frequency (i.e., harmonic tones that differed from REF in both TFS and envelope). The second set used a TEST stimulus generated by shifting the frequency of all components equally (i.e., inharmonic complex tones that differed from REF in TFS only). From each fiber, data were collected for complex tones with harmonic ranks that ranged from partially resolved to unresolved. All stimuli were presented in background noise. TFS cues for discriminating TEST and REF stimuli were evaluated in terms of decreases in the neural cross-correlation coefficient for TFS computed from shuffled cross correlograms.

For both F0 and frequency shifted stimuli, strong TFS cues were available for both partially resolved and unresolved conditions. No differences were observed in neural TFS cues between normal-hearing and HI responses. These results suggest alternative factors may explain the perceptual TFS deficit with sensorineural hearing loss (SNHL). The salience of envelope and rate-place cues as well as the influence of degraded frequency selectivity and loss of tonotopicity following SNHL are currently being explored.

Supported by NIH grant R01DC009838.

671 Abnormal Loudness Adaptation in Pre-But Not Post-Synaptic Auditory Neuropathy Dwight Wynne¹, Shrutee Bhatt², Arnold Starr², Fan-Gang Zena³

¹Department of Biomedical Engineering, University of California, ²Department of Neurology, University of California ³Department of Otolaryngology–Head and Neck Surgery, University of California

Auditory neuropathy (AN) encompasses disorders affecting the inner hair cells, auditory nerve, or both. Recent advances have allowed classification of many ANs into pre- and post-synaptic disorders based on evidence of

genetic mutations affecting the ribbon synapse (e.g., OTOF) and auditory and other cranial or peripheral nerves (e.g., OPA1). Here we measured AN subjects' loudness adaptation, a task that has traditionally been used to differentiate cochlear and retrocochlear hearing loss. We predicted that pre-synaptic AN subjects would have normal loudness adaptation, whereas post-synaptic AN subjects would have severe adaptation. We presented three-minute tones at low and high frequencies to 2 pre-synaptic, 5 post-synaptic, and 2 AN subjects with unknown site of lesion. As controls, we also tested subjects with cochlear loss or acoustic neuroma. Contrary to our prediction, presynaptic subjects showed significant loudness adaptation at both low and high frequencies, similar to the acoustic neuroma control; whereas post-synaptic and undefined subjects showed no adaptation at low frequencies, similar to normal hearing and cochlear loss controls, and variable high frequencies. adaptation at То understand physiological mechanisms underlying these paradoxical findings, we recorded auditory brainstem responses to a 20-click train with 11-ms inter-click interval and 500-ms inter-train interval. Wave V in normal hearing subjects showed no adaptation in amplitude but prolonged latency from the 1st click to the 5th click. Pre-synaptic subjects showed slight amplitude adaptation resulting in a loss of Wave V by the 20th click, and delayed but normal-latency adaptation. On the other hand, like the acoustic neuroma control, most post-synaptic subjects showed no identifiable Wave V to the click train. These physiological data suggest that the observed loudness adaptation difference between pre- and post-synaptic disorders cannot be simply explained by peripheral mechanisms.

672 Tinnitus Without Hearing Loss: Computational Model and Physiological Evidence for Obscured Cochlear Damage Roland Schaette¹, David McAlpine¹

¹UCL Ear Institute

An outstanding issue in current knowledge about tinnitus is whether or not those individuals who report tinnitus, but have a normal audiogram, do have some form of cochlear damage. Normal hearing thresholds do not necessarily indicate the absence of cochlear damage: in mice, mild acoustic trauma that causes only a temporary shift in hearing thresholds leads to a permanent deafferentation of about half of the auditory-nerve (AN) fibres in the highfrequency range (Kujawa and Liberman, J Neurosci 2009). Using a computational model, we first determined whether such cochlear damage could also lead to tinnitus. Deafferentation of AN fibres decreases the overall activity of the AN and also reduces the mean activity of central auditory neurons. When these neurons attempt to stabilize their activity by activating homeostatic plasticity, their response gain is increased. For the patterns of deafferentation reported by Kujawa and Liberman (2009), our model then displays spontaneous hyperactivity, a putative neural correlate of tinnitus.

In order to test the model's prediction of a link between obscured cochlear damage and tinnitus, we measured auditory brainstem responses (ABRs) in 14 female tinnitus (mean age 35.4 ± 2.6 years) and 15 female control subjects (mean age 34.2 ± 2.3 years). All subjects had normal hearing thresholds. We measured ABRs using 50µs clicks at 90 and 100 dB SPL, and observed that the mean amplitudes of ABR wave I in the tinnitus group were significantly smaller than in the control group (90dB: 0.087 ± 0.009 µV vs. 0.119 ± 0.012 µV; 100dB: 0.151 ± 0.016 µV vs. 0.197 ± 0.019 µV; p = 0.01, 2-way ANOVA), indicating a reduced number of responsive AN fibres at high intensities. The amplitudes of ABR wave V did not differ significantly, suggesting that, by the level of the midbrain, homeostatic mechanisms have adjusted neural gain in response to the reduced input. Thus, tinnitus with and without hearing threshold shift might both be linked to cochlear damage.

673 High Amplitude Electrical Current Damages Spiral Ganglion Peripheral Processes

Jonathan Kopelovich¹, LinJing Xu¹, Barbara Robinson¹, Bruce Gantz¹, Marlan Hansen²

¹University of Iowa Department of Otolaryngology Head and Neck Surgery, ²university of Iowa Department of Otolaryngology Head and Neck Surgery

A subset of patients with residual low frequency hearing who receive Hybrid cochlear implants (CI) lose hearing after activation of the CI, including some who required high current levels at activation. Here we used both in vitro and in vivo approaches to investigate potential toxicity of electrical stimulation (ES) to the structures of the hearing cochlea. Cochlear explant cultures including the organ of Corti and spiral ganglion were subjected to either high voltage patterned ES or depolarizing media (80 mmol K+, 80K). Cultures were immunostained with anti-MyoVIIa and neurofilament antibodies and labeled with terminal deoxynucleotidyl transferase dUTP nick end labeling (TUNEL). Hair cells in cochlear explant cultures exposed to high voltages or depolarizing media for 3 or 24 hours, respectively, were no different in number, morphology or TUNEL staining from controls. Peripheral neurites, however, appeared abnormal with blebbing, fragmentation and involution of the peripheral processes in high voltage ES and 80K. ES reduced the number of peripheral neurites by nearly 50%. For in vivo stimulation, P32 hearing rats were subjected to suprathreshold acute ES for 2 hours. Current amplitude was increased at 20 min intervals to the point at which acoustic hearing threshold was increased or to 5mA maximum. Surface preparations, cross-sectional histology and electron microscopy were used to assess damage to different cell types within the cochlea. Similar to our in vitro findings, high current ES had no gross effect on hair cells on surface preparations of hearing cochleae. Peripheral neural processes were also grossly normal on peri-modiolar cross-section. TEM analysis is in progress. High voltage ES appears to be detrimental to peripheral spiral ganglion processes but not hair cells in vitro. Further investigation is warranted to elucidate possible mechanisms whereby neurite damage occurs.

674 Effects of Unilateral Cochlear Implantation on Auditory Nerve Synapses and Globular Bushy Cells in Congenitally Deaf White Cats

Jahn N. O'Neil¹, Charles J. Limb¹, Kate C. Flores¹, Adam Rosenblatt¹, David K. Ryugo^{1,2}

¹Department of Otolaryngology-Head and Neck Surgery, Johns Hopkins University, Baltimore, MD 21205, ²Program in Neuroscience, Garvan Institute of Medical Research Congenital deafness represents an extreme form of

Congenital deafness represents an extreme form of auditory deprivation and results in abnormalities of synaptic structures in auditory nerve endings of the deaf white cat. Abnormalities at the endbulb of Held include reduced branching, hypertrophy of postsynaptic densities and reduction in postsynaptic spherical bushy cell size. Previous work in our lab has shown that unilateral cochlear implantation restores the endbulb synapse on the stimulated side of cats implanted at 3 months of age. Modified-endbulb globular bushy cell synapses of deaf cats, unlike the endbulb of Held, demonstrate no reduction in branching complexity although they do exhibit hypertrophy of postsynaptic densities. We sought to determine whether auditory stimulation of congenitally deaf cats by cochlear implantation would restore modifiedendbulb globular bushy cell synapses to their normal state, as seen with endbulbs of Held. Three-month-old congenitally deaf cats were electrically stimulated with a unilateral cochlear implant for a period of 10-19 weeks using human speech processors. Implanted cats were trained to respond only to a specific acoustic stimulus, confirming the presence of functional hearing. Surprisingly, modified-endbulb synapses showed restoration on the unstimulated contralateral side of the 3month implanted cats, with normalization of postsynaptic density size, shape and distribution. Synapses of the electrically stimulated ipsilateral auditory nerve, however, showed no recovery. The differential effects of deafness and restoration of electrical activity on the synapses of spherical and globular bushy cells emphasize the variability of biological behavior even within the cochlear nucleus. The results demonstrate that auditory stimulation with a cochlear implant does not restore all ipsilateral auditory pathways and raises intriguing questions about the specific mechanisms by which cochlear implants restore hearing.

Supported by: NIH/NIDCD DC000232, DC005211, EY01765, The Emma Liepmann Endowment Fund, and Advanced Bionics Corporation. Dr. Limb is a consultant for Advanced Bionics and receives support for unrelated work.

675 Binaural Comparison of Spiral Ganglion Cell Counts in Profound Deafness:

Implications for Cochlear Implantation

Mohammad Seyyedi¹, Donald K. Eddington¹, Joseph B. Nadol¹

¹*Massachusetts Eye and Ear Infirmary*

The counts of spiral ganglion cells (SGC) in normal and hearing-impaired ears with different etiologies have been reported. One question that has not been directly studied is the difference in the number of SGCs between the left and right ears of an individual deafened by the same etiology when the hearing sensitivity is similar. This is of interest because a small difference would imply that one ear could be used as a control ear in evaluating the impact on SGC survival of a medical intervention in the other ear.

Forty two temporal bones from 21 individuals with bilaterally-symmetric profound hearing impairment were studied. Both ears in each individual were deafened by the same etiology. Rosenthal's canal was reconstructed in two-dimensions and segmental and total SGCs were counted. Correlation analysis and t-test were done to compare segmental and total counts of left and right ears. Statistical power calculations were done to illustrate how the results can be used to estimate the effect size that can be reliably identified as a function of sample size.

Left segmental and total counts were very highly correlated with those in the right ears. Coefficients of determination (R2) for segments 1 to 4 and total count were respectively 0.645, 0.905, 0.928, and 0.905 and 0.979. The hypothesis that mean segmental and total counts of right and left are the same was not rejected by t-test as all p values in all paired groups were greater than 0.05.

Given that the difference in the number of SGCs between ears is not statistically significant, one ear can be used as a matched control for the other ear in hearing impaired seubjects. Required sample size for a specific effect size can be computed in studies which assess the impact of a variable on SGC count in one ear.

676 Developing a Diagnostic Test of Auditory Nerve Survival: Influence of Cochlear Outer Hair Cell Pathology

Brian Earl¹, Mark Chertoff¹, Ashlee Martz¹, Megan Ash¹ ¹University of Kansas Medical Center

Advanced diagnostic techniques that can pinpoint the cochlear location of hair cell loss and neural degeneration will be crucial for future implementation of regenerative therapies for individuals with sensorineural hearing loss. Our recent research in developing these techniques has focused on quantifying auditory nerve density in normal-hearing animals by tracking the amplitude of compound action potentials (CAPs) while varying the high-pass cutoff frequency of simultaneous masking noise. In the clinic, however, hearing-impaired patients will likely present with both hair cell loss and neural degeneration. The objective of this study was to determine if outer hair cell (OHC) pathology alters neural density functions and confounds the estimate of neural survival.

Mongolian gerbils with gentamicin-induced OHC pathology (n=10) were compared to normal-hearing gerbils (n=9). CAPs were evoked with broadband chirps at 60 and 90 dB SPL. The masking noise (white noise) was high-passed in 1/3 octave intervals between 0.4 and 50 kHz, spanning nearly the entire length of the gerbil cochlea. Dependent measures were bandwidth (i.e., spread of neural firing) and peak location (i.e., peak of neural firing) of the neural density functions.

Results for chirps at 60 dB SPL indicated that the bandwidth of the neural density functions did not differ

across groups, but the peak location of the gentamicinexposed group was closer to the apex than the peak location of the normal-hearing group. For chirps at 90 dB SPL, neither the bandwidth nor the peak location of the neural density functions differed across groups. These data indicate that OHC damage does alter the distribution of neural firing for moderate-level stimuli but not for highlevel stimuli, suggesting that high-level neural density functions may provide a location-specific diagnosis of auditory nerve survival in impaired ears.

Supported by The Royal National Institute for Deaf People, United Kingdom

677 Octopus Cells: The Temporally Most **Precise Neurons in the Brain?**

Philip X. Joris¹, Philip H. Smith²

¹University of Leuven, ²University of Wisconsin

Work in vivo and in silico has highlighted the remarkable specializations of octopus cells of the cochlear nucleus (CN), but in vivo data are limited. We are interested in temporal response features to stimulus transients, which unfortunately trigger large fields so that clean responses from single neurons are often hard to obtain in the CN. A point of interest are also the responses to amplitude modulated (AM) stimuli: octopus cells may be the only CN cell type with a bandpass rate modulation transfer function (MTF) and an almost flat temporal MTF, suggesting they may constitute a modulation filterbank.

We recorded from axons of octopus cells and other cell types as they exit the cochlear nucleus, via the dorsal and intermediate acoustic stria, in barbiturate-anesthetized cats. Cells were classified by their response pattern to short tone bursts, and a small number of fibers was intraaxonally labeled with neurobiotin.

Octopus cells, identified morphologically or by their pure onset responses to tones, could be driven at very high rates by click trains. Exquisitely timed spikes entrained to the click trains: skipping of cycles occurred at frequencies > 500 Hz. This behavior occurred over most of the suprathreshold range, with little dynamic range interposed between threshold and full entrainment. The temporal precision could be sustained over the stimulus duration: vector strengths were near maximal and standard deviations of spike timing were routinely < 100 µs. In response to AM stimuli, rate tuning to modulation frequency was present and the responses were tightly phase-locked to stimulus envelope, but response rates were low and the range of best modulation frequencies was limited.

We conclude that octopus cells can sustain high rate responses with a temporal precision that is unequalled by other auditory or nonauditory neurons, particularly to stimuli with sharp transients.

Supported by grants from FWO (G.0633.07) and BOF (OT/09/50) (Flanders, Belgium).

678 Dendritic Delay in Octopus Cells of the Mammalian Cochlear Nucleus: A

Computational Investigation Martin Spencer^{1,2}, Ian Bruce^{1,3}, David Grayden^{1,4}, Hamish Meffin^{1,2}, Anthony Burkitt^{1,4}

¹University of Melbourne, ²National ICT Australia,

³McMaster University, ⁴Bionic Ear Institute

Octopus cells are neurons in the auditory brainstem of mammals that respond most strongly to the onset of broadband sounds. They receive many (>60) connections from auditory nerve fibers with a range of characteristic frequencies.

Our investigation used a compartmental Hodgkin-Huxley model to investigate the hypothesis that the octopus cell's dendritic delay provides compensation for the frequencydependent traveling wave delay introduced by the cochlea. This hypothesis has been suggested by previous experimental investigations.

Most model parameters were adjusted to match previously published experimental data, however the sodium channel conductance strength and position was adjusted to optimize the behavior of the cell.

The dendritic propagation time of the post-synaptic potential was quantified in a model that simulated in vitro conditions. A realistic periphery and auditory nerve model was then used to create a model that simulated in vivo conditions and test the effects of the dendritic delay on the octopus cell's response to sound. The model was first tested with the anatomically correct configuration; low characteristic frequency auditory nerve fibers making synaptic connections proximally, and high characteristic frequency auditory nerve fibers making connections distally. The sound frequency range used as input was chosen so that the dendritic delay matched the traveling wave delay. This mode of innervation was then varied to test the validity of these initial assumptions.

Evidence was obtained relating to the necessary number of synapses, the frequency span of the octopus cell's input, the role of active channels in the dendrite, and the influence of the location of sodium channels.

The in vivo octopus cell model behaved most realistically when auditory nerve fiber synapses were connected so that the dendritic delay was compensating for the traveling wave delay. This result strongly supports the hypothesis.

679 Intrinsic Firing Properties and Their **Role in Integration and Temporal Envelope Coding by Cochlear Nucleus Angularis** Neurons

Katrina MacLeod¹, Arslaan Arshed¹, Lauren Kreeger¹ ¹University of Maryland

In the avian auditory brain stem, cochlear nucleus magnocellularis (NM) initiates the timing pathway for computing interaural time differences while nucleus angularis (NA) encodes intensity information for the detection of interaural level difference. NA, like the mammalian ventral cochlear nucleus, contains neurons with a diversity of intrinsic properties, but how these properties contribute to sound coding is still poorly

understood. The intrinsic properties of tonically-firing neurons in the cochlear nucleus help encode intensity by promoting integration across multiple inputs and, by regularizing firing, reduce phase-locking to fine temporal structure of the inputs. It has been unclear, however, how the intrinsic properties might affect slower temporal modulation of their inputs due to envelope modulation of the sound stimulus. We investigated the firing responses of different cell types in the NA to noisy current injections during patch clamp recordings in brain stem slices. The current injections had DC (average current step level) and (filtered white noise) components that could be AC modulated independently. Responses were analyzed by plotting firing rate versus DC current level (FI curves) and by shuffled autocorrelation functions to determine temporal reliability. Tonically-firing neurons had FI curves that were insensitive to the AC fluctuations (with the exception of a threshold effect), but encoded the DC level. Single spiking neurons of NA, with similar intrinsic properties to NM and NL, were very sensitive to the AC fluctuations.firing repeatedly to noisy current injections. which allowed them to encode the DC level of noisy, but not flat, inputs. All NA neurons followed the temporal pattern of the noisy AC component of the stimulus. This suggests that the spike generation mechanism does not preclude temporal envelope coding but that tonic neurons can encode both DC levels and slow temporal fluctuations of their inputs.

680 A Simulation of Chopper Neurons in the Cochlear Nucleus with Wideband Input from Onset Neurons

Andreas Bahmer¹, Gerald Langner²

¹Goethe University Frankfurt, ²Technical University Darmstadt

The unique temporal and spectral properties of chopper neurons in the cochlear nucleus cannot be fully explained by current popular models. A new model of sustained chopper neurons was therefore suggested based on the assumption that chopper neurons receive input both from onset neurons and the auditory nerve (Bahmer and Langner in Biol Cybern 95:4, 2006). As a result of the interaction of broadband input from onset neurons and narrowband input from the auditory nerve, the chopper neurons in our model are characterized by a remarkable combination of sharp frequency tuning to pure tones and faithful periodicity coding. Our simulations show that the width of the spectral integration of the onset neuron is crucial for both the precision of periodicity coding and their resolution of single components of sinusoidally amplitudemodulated sine waves. One may hypothesize, therefore, that it would be an advantage if the hearing system were able to adapt the spectral integration of onset neurons to varying stimulus conditions.

681 Conversion of Phasic to Tonic Firing in the T Stellate Cell Pathway

Xiao-Jie Cao¹, Samantha Wright¹, **Donata Oertel**¹ ¹University of Wisconsin

The population of T stellate cells (choppers) in the ventral cochlear nucleus (VCN) feeds information about the spectrum of sounds (Blackburn and Sachs, 1990; May et al., 1998) to the dorsal cochlear nucleus (Oertel et al., 1990), to medial olivocochlear efferent neurons in the ventral nucleus of the trapezoid body (Smith et al., 1993), to the lateral superior olive and/or lateral olivocochlear efferent neurons (Doucet and Ryugo, 2003), to the ventral nucleus of the lateral lemniscus (Smith et al., 1993), and to the inferior colliculus. In contrast with other principal cells of the VCN which encode transients with temporal precision, T stellate cells convert the phasic input from auditory nerve fibers to more tonic firing (chopping) through cellular and circuit-level mechanisms. 1) T Stellate cells fire tonically when depolarized; 2) T Stellate cell have relatively large excitatory currents through slow NMDA glutamate receptors; 3) AMPA receptors that underly evoked excitation contain GluR2 subunits that slow their kinetics; 4) synaptic depression is lower in excitatory inputs of T stellate cells than of other principal cells of the VCN (Chanda and Xu-Friedman, 2010); 5) feed forward excitation among T stellate cells prolongs excitation (Ferragamo et al., 1998); 6) transient excitation from auditory nerve fibers is coactivated with transient inhibition from D stellate cells (onset-choppers) (Paolini et al., 2005). The mechanisms that promote tonic firing smear the timing of excitatory postsynaptic potentials and account for the chopping firing pattern whose structure does not reflect the fine structure of sounds. Also in contrast with other principal cells of the VCN, T stellate cells are sensitive to small steady currents evoked by neuromodulatory neurotransmitters. serotonin. norepinephrine and acetylcholine (Oertel and Fujino, 2001). This work was supported by a grant from the NIH DC00176.

682 Physiological Classification of Single-Unit Activity in Ventral Cochlear Nucleus of the Mouse

Matthew Roos¹, Bradford May¹

¹The Johns Hopkins University

Techniques for genetic manipulations in mice make this animal an appealing model for auditory researchers. Application of transgenic mouse models to central auditory function requires a system for relating physiological response patterns to the discrete neural populations that inhabit the major processing centers of the brain. With this goal in mind, we introduce a physiologically based classification system for single-unit activity in the ventral cochlear nucleus (VCN). To allow comparisons with existing functional descriptions, our system is based on the temporal properties of responses to short tone bursts, which are visualized in the form of peri-stimulus time histograms (PSTHs: Blackburn and Sachs, 1989). Classification criteria include the overall shape of the PSTH, the coefficient of variation for interspike intervals, adaptation patterns of interspike intervals (ISI), and initial

spike latencies. A histogram of the coefficient of variation early in the stimulus response (CV-E) is used to distinguish irregular primarylike units and regular chopper units. Primarylike units are further classified as primarylike with notch (PN) or ordinary primarylike (Pri) units based on the statistical separability of their first and second spike latencies. Chopper units are assigned a transiently adapting classification (ChT) based on an abrupt increase in ISI at stimulus onset. The remaining chopper units are classified as sustained (ChS) or slowly adapting (ChA) depending on less abrupt changes in ISI and the coefficient of variation late in the stimulus response (CV-L). These metrics correspond well with the general properties of physiological classification that have been derived for other mammalian species. This presentation will summarize the statistical analyses that objectively define each classification and will provide additional physiological descriptions for the resulting response classes.

(This research was supported by NIDCD grant 1F31DC010095-01A1)

683 Synaptic Transmission at the AVCN Endbulb of Held in Mice Deficient for Bassoon Protein

Chongyu Ren¹, yong wang¹

¹University of Utah

Normal hearing relies on faithful synaptic transmission at the ribbon synapse between the inner hair cell (IHC) and auditory nerve dendritic afferent terminals. Bassoon is an important scaffolding protein involved in anchoring synaptic vesicles to the ribbons in the IHC. Mice with a mutated Bassoon (Bsn) have a severe loss of IHC afferent terminals (~80%) and elevated hearing thresholds without a concomitant loss of spiral ganglion cells and functional deficit of the outer hair cell. Moreover, temporal coding (onset coding) in the auditory nerve is disrupted in Bsn mutant mice (Buran et al., 2010). However, deficient Bassoon has very mild effects on central synaptic transmission in general (Altrock et al., 2003). We hypothesized that deficit in the auditory nerve activity may affect synaptic transmission at the endbulb of Held between the auditory nerve fiber and the bushy neuron in the AVCN. Using a slice preparation, we investigated synaptic transmission at the endbulb in Bsn mutant as well as in wildtype control mice. By and large, intrinsic bushy neuron membrane properties are unaffected in Bsn mutant mice. AMPA receptor mediated mEPSCs recorded from bushy neurons appear not to be affected; however, there were fewer mEPSC events in Bsn mice. ANF convergence ratio on busy cells appears to have reduced to 1:1. Postsynaptic firing precision and reliability was reduced in Bsn mutants. Thus, abnormal activities in the auditory nerve may affect synaptic transmission at the endbulb. Bsn mutant mice may be a good animal model to study a human condition called auditory neuropathy.

684 Target-Specific Roles of Glycinergic Inhibition to the Principal Cells of the Ventral Cochlear Nucleus

Ruili Xie¹, Paul Manis¹

¹University of North Carolina at Chapel Hill

Bushy and T-stellate cells of the ventral cochlear nucleus are innervated not only by the excitatory inputs from the auditory nerve, but also by glycinergic inhibitory inputs from various sources. While the excitatory inputs have been well studied, the function of the inhibitory inputs is less clear. We studied the kinetics and synaptic dynamics of the glycinergic inhibitory postsynaptic currents (IPSCs) in bushy and T stellate cells using whole-cell recordings from mouse cochlear nucleus brain slices. We found that the decay time constants of glycinergic IPSCs in bushy cells were eight times slower than those in T stellate cells. The slow IPSC time course seems counter to the notion that bushy cells process temporal information on a faster time scale than T stellate cells. We next tested the role of glycinergic inhibition by assessing the spike jitter to repetitive auditory nerve stimulation, without and with The IPSPs onto bushy cells summate to strychnine. generate a tonic inhibition, which decreases the temporal spike jitter. In contrast, the fast inhibition onto T stellate cells did not summate improved spike timing on a millisecond time scale by suppressing late spikes. The results indicate that the kinetics of glycinergic IPSCs are target-dependent. Inhibition to the bushy cells tonically modulates the membrane potential, improving spike timing by adjusting the engagement of postsynaptic ion channels. The fast inhibition in stellate cells is suitable for enhancing the temporal contrast of spike trains for more slowly timevarying stimuli, such as amplitude modulated sounds. Supported by NIDCD grant R01DC004551 (P.B.M) and a

DRF Research Grant (R.X.).

685 Synaptic Activity-Induced Ca²⁺ Signaling in Avian Cochlear Nucleus Magnocellularis Neurons

Liecheng Wang^{1,2}, Zheng-Quan Tang¹, **Yong Lu¹** ¹Northeastern Ohio Universities Colleges of Medicine and Pharmacy, ²Anhui Medical University

Neurons of the avian cochlear nucleus magnocellularis (NM) receive glutamatergic inputs from the spiral ganglion cells via the auditory nerve, and feedback GABAergic inputs primarily from the superior olivary nucleus. Previous studies have shown that application of exogenous glutamate or GABA increases the intracellular Ca2+ concentration ([Ca2+]i) in NM neurons. However, it is unknown whether synaptically released glutamate or GABA results in [Ca²⁺]i rises in these neurons, and if so, which receptors for each neurotransmitter mediate the responses. Here, using ratiometric Ca²⁺ imaging in chicken brain slices, we found that electrical stimulation applied to the glutamatergic and GABAergic afferent fibers innervating NM elicited transient [Ca2+]i rises in NM neurons, and the amplitude of the [Ca²⁺]i rises increased with increasing frequency or duration of the electrical stimulation. The [Ca²⁺]i rises were largely blocked by antagonists for ionotropic glutamate but not ionotropic GABA receptors, suggesting that synaptically released glutamate but not GABA induced the Ca²⁺ signaling. In support of this observation, electrical stimulation applied to only the GABAergic pathway caused no noticeable [Ca²⁺]i rises in NM neurons. However, activation of GABAA receptors with exogenous agonists inhibited synaptic activity-induced [Ca²⁺]i rises in NM neurons, suggesting a role of GABAA receptors in regulation of Ca²⁺ homeostasis in the avian cochlear nucleus neurons.

Supported by NIH Grant DC008984 to YL.

686 Convergence of Inhibitory and Excitatory Inputs Causes a Dynamic Shift of Coding Paradigm in Gerbil Spherical Bushy Cells

Thomas Kuenzel¹, J. Gerard G. Borst¹, Marcel van der Heijden¹

¹Erasmus MC

Spherical bushy cells (SBC) are contacted by giant synaptic endings of the auditory nerve, the Endbulbs of Held (EoH). Numerous studies in brain slice preparations have shown that the EoH synapse has a high release probability, causing synaptic events to be suprathreshold by a large margin. Strong short-term depression was observed in vitro, which can cause transmissions to fail during trains of stimulation. Surprisingly, no indication of synaptic depression has been found in vivo. Instead, in vivo failures appear to be related to inhibition. However, the contribution and relative importance of other causes for failures are still unclear.

Here we report on juxtacellular recordings from 39 SBC from the AVCN of anesthetized, adult gerbils. By analyzing the waveforms of individual events we estimated the strength of synaptic events as well as the threshold eEPSP: the strength of a synaptic event necessary to trigger an AP.

We found two main intrinsic causes for failures: first, in vivo the EoH has a smaller release probability and operates much closer to threshold, as suggested by the presence of frequent failures owing to subthreshold events and the absence of short-term depression. Second, the refractory period of the postsynaptic membrane caused a strong interval-dependence of the threshold eEPSP.

During sound stimulation we observed an additional, noninterval dependent increase of the threshold eEPSP, which we attribute to inhibitory inputs onto the SBC. Inhibition showed similar tuning but higher thresholds than excitation. The output rate of SBC was strongly reduced when inhibition was strong. Remaining AP were however triggered by larger synaptic events, which showed better phase-locking to the stimulus than smaller events. Thus, with increasing sound intensity, the inhibitory inputs cause the SBC to become less sensitive and trade the rate-code of stimulus level for an accurate temporal coding of stimulus fine structure.

687 Modeling of Entrainment and Synchronization in Globular Bushy Cells Using Depressing and Non-Depressing Synapses

Marek Rudnicki^{1,2}, Werner Hemmert^{1,2} ¹Technische Universität München, ²Bernstein Center for Computational Neuroscience

Cochlear Nucleus (CN) is the first station in the central nervous system where processing of auditory signals takes place. It consists of several neuron types that receive direct inputs from auditory nerve fibers (ANFs) and show various firing properties.

The goal of this study is to develop a model of Globular Bushy Cells (GBC) that are one of the principle cell types in CN. They fire action potentials with high temporal precision and with good entrainment for low-frequency pure tone stimuli. We examine how those firing properties are influenced by introducing depression into synapses that has been reported in many in-vitro studies (e.g. Yang and Xu-Friedman 2009). We compare results with a model without synaptic depression as observed in-vivo (Borst 2010).

Our model of GBCs is a point neuron with Hodgkin-Huxley type ion channels (HPAC, Kht, Klt) described previously by Rothman and Manis (2003). It receives several excitatory inputs from an inner ear model simulating responses of ANFs. ANF activity drives endbulb of Held synapses located directly on the GBC soma. Short-term depression is modeled phenomenologically using an extended exponential recovery model from Tsodyks and Markram (1997).

Simulations show that for both synaptic models synchronization improved (SI > 0.9) at low stimulation frequencies compared to synchronization of ANFs. However, high entrainment levels where achieved only by the model without synaptic depression. This model was also able to reproduce experimental results obtained from pure tone stimulations: PSTH, ISIH and receptive field maps.

We conclude that the model of GBC with converging ANF excitatory inputs captures basic properties of those cells. Additionally, the results suggest that depression in-vivo is much lower than in-vitro. In the future, the model will allow us to study the response of GBCs to complex natural stimuli like speech.

Supported by the BMBF within the Bernstein Center for Computational Neuroscience, Munich (01GQ0441 and 01GQ1004B).

688 Activity Dependent Changes in Action Potential Transmission at Giant Synapses of Held in Vivo

Marei Typlt^{1,2}, Bernhard Englitz^{3,4}, Mandy Sonntag¹, Rudolf Rübsamen¹

¹University of Leipzig, ²University of Western Ontario, ³MPI MIS Leipzig, ⁴University of Maryland

Signal transmission at the synapses of Held is known to underlie strong short-term plasticity. In the present study we investigate activity dependent changes at the endbulb and calyx of Held in vivo of adult animals. The size of these synapse enables the simultaneous examination of the presynaptic activity, the excitatory postsynaptic potential (EPSP) and the postsynaptic action potential (AP) within a single extracellular recording. The precision and the reliability of the synapse and the underlying dynamics are analyzed by quantifying the amplitudes of these components in single transmission events and their temporal relations. To precisely measure the components a fitting procedure is utilized that decomposes individual transmission events into their sub-components to account for overlaps between components from one or consecutive events.

While we find signal transmission at the endbulb of Held to be highly variable and unreliable, signal transmission at the calvx is consistent and reliable. Most of the variation in signal transmission seen at the endbulb can be attributed to short-term depression. With shorter inter-event-intervals (<3ms) the EPSP amplitude decreases up to 60% and the probability of AP failures increases. The AP amplitude is affected by the preceding inter-event-intervals as well which is probably due to sodium channel inactivation. However, the activation of different inputs contributes to the overall variation. Specific activation of inhibitory inputs decreases the EPSP amplitude up to 46%. The AP amplitude decreases up to 52%. Interestingly, at the same time the amplitude of the prepotential increases during inhibitory stimulation which can indicate an enhancement of presynaptic activity by inhibitory neurotransmitters.

For the differences in the variability of signal transmission between the endbulb and the calyx synapses differences in their size, the number of converging inputs, and membrane properties can account.

689 Mapping Local Circuitry in the Ventral Cochlear Nucleus with Photostimulation Luke Campagnola¹, Paul Manis¹

¹University of North Carolina at Chapel Hill

The ventral cochlear nucleus (VCN) integrates information from the auditory nerve, encoding specific sound features before relaying to downstream nuclei. Although much is known about the output of the VCN, its function is still not fully understood. Recently, numerous studies have demonstrated the importance of local circuitry in shaping the output properties of VCN neurons. Three different local inputs to the VCN are hypothesized to exist: inhibition from tuberculoventral cells in the dorsal cochlear nucleus (DNC), inhibition from D-stellate cells in the VCN, and excitation from T-stellate cells in the VCN. All three input types are closely associated with auditory nerve fibers, making them difficult to interrogate by electrical stimulation. Thus, little is known about the strength, kinetics, and convergence of these inputs. We have used laser photostimulation to focally activate neurons in cochlear nucleus slices, generating detailed maps of synaptic inputs to bushy and stellate cells in the VCN. Slices were taken coronally at an angle which preserves the connection between anteroventral cochlear nucleus (AVCN) and DCN. Results: 1) Nearly all bushy and stellate cells in the AVCN receive strong inhibitory input from a

single, focal location in the deep DCN. These results agree with previous reports of inputs from tuberculoventral cells in the DCN. 2) Most cells also receive local inhibitory inputs from the region immediately adjacent (within about 150 μ m), presumably from D-stellate cells. The strength and number of D-stellate inputs varies widely between cells. 3) In all cells, local excitatory inputs are either absent or too weak to measure. This indicates that local connections from T-stellate neurons are likely to be rare, have low release probability, or are not present in this plane of section. Supported by NIDCD R01DC004551 (PBM) and F31DC10320 (LC).

690 Effects of Group I MGIuR Activation in the Anteroventral Cochlear Nucleus Soham Chanda¹, Matthew Xu-Friedman¹

¹University at Buffalo

Group I metabotropic glutamate receptor (mGluR) activation can affect neuronal activity through a number of different mechanisms. We studied the consequences of mGluR activation in bushy cells in the anteroventral cochlear nucleus. We found that mGluR activation using dihydroxyphenylglycine (DHPG) caused bushy cells (BCs) to depolarize. This was accompanied by a rise in intracellular calcium. These effects appear to be mediated by calcium influx through L-type calcium channels. L-type calcium channel activation also further activated TRP channels. DHPG had no effect on neurotransmitter release from presynaptic auditory nerve (AN) fibers. BC depolarization significantly enhanced the firing probability of BCs in response to AN stimulation and reduced the latency and jitter of spike timing.

691 Effects of Group Specific MGluR Antagonists on GABAergic Transmission in Neurons of the Chicken Nucleus Magnocellularis

Emilie Hoang Dinh¹, Yong Lu¹

¹Northeastern Ohio Universities Colleges of Medicine and Pharmacy

Nucleus magnocellularis (NM) neurons, the second order neurons of the chicken auditory pathway, faithfully encode the temporal dimension of auditory signals, a critical step in interaural time difference processing and thus in sound localization. While reliable and temporally precise glutamatergic transmission at the auditory nerve-NM neuron synapse is achieved through endbulbs of Held, GABAergic inputs to NM neurons play a crucial role in enhancing phase-locking accuracy of NM neurons. Our previous studies showed that the GABAergic inputs are dynamically modulated by both GABAb receptors and metabotropic glutamate receptors (mGluRs). To determine which mGluRs endogenously modulate the GABAergic transmission, we studied the effects of group-specific mGluR antagonists on evoked inhibitory postsynaptic currents (IPSCs) of NM neurons, using whole-cell voltage clamp in brainstem slices obtained from late chicken embryos. Concurrent activation of both the glutamatergic and the GABAergic pathways was elicited by electrical train stimulations (3.3 Hz, 5 pulses) applied to the area lateral to the NM. IPSCs were isolated after blocking ionotropic glutamate receptors. We found that application of LY341495 (10 or 100 nM), a specific antagonist for group II mGluRs, tended to increase the amplitude of IPSCs, as did CPPG (50 nM), a specific antagonist for group III mGluRs. On the other hand, blockade of group I mGluRs (50 μ M LY367385 and 1 μ M MPEP for mGluR1 and mGluR5, respectively) produced varying effects in different cells. These results suggest an ongoing modulation of GABA activity in NM neurons, by at least groups II and III mGluRs. The strength of the modulation is proposed to be correlated with the activation level of the glutamatergic pathway.

Supported by NIH Grant DC008984 to YL.

692 Glycinergic Inhibition Is Modified in Spherical Bushy Cells of Deaf Mutant Mice

Jeremy Sullivan^{1,2}, Alexander Borecki¹, Bettina Zens¹, Tan Pongstaporn¹, David Ryugo¹, Sharon Oleskevich^{1,2} ¹*Garvan Institute of Medical Research,* ²*University of New South Wales*

In the cochlear nucleus, spherical bushy cells (SBCs) and globular bushy cells (GBCs) initiate neural pathways that encode interaural time and level differences, respectively. SBCs and GBCs receive significant excitation from the auditory nerve but also inhibition from unknown sources. For this study we investigated whether this inhibition is modified by congenital deafness. We used Shaker-2 mutant mice with a point mutation of the MYO15A gene that leads to abnormal hair cell stereocilia and deafness. Whole cell recording was performed on visualised neurons in brainstem slices of 15-21 day old mice. Bicuculline, D-AP5, CNQX and TTX were added to help isolate glycinergic miniature inhibitory postsynaptic currents (mIPSCs) that were subsequently blocked by strychnine. In normal hearing, heterozygous Shaker-2 mice, glycinergic miniature inhibitory postsynaptic currents (mIPSCs) were similar between SBCs (n=5) and GBCs (n=3). In contrast, glycinergic mIPSCs in deaf, homozygous Shaker-2 mice were significantly slower in SBCs than in GBCs. SBCs showed increases in rise time $(0.96 \pm 0.07 \text{ vs } 0.65 \pm 0.09; \text{ p} < 0.05)$, half width (3.9 ± 0.16) vs 2.32 ± 0.38; p<0.01) and decay kinetics (8.67 ± 0.70 vs 4.30 ± 0.32 ; p<0.01). When comparing between the two types of bushy cells in normal and deaf mice, only SBCs showed differences in synaptic time course. These preliminary findings suggest that glycinergic inhibition of SBCs is susceptible to deafness-induced modulation of synaptic transmission. Changes in the time course of bushy cell mIPSCs is consistent with previous implications that a lack of auditory nerve activity caused by deafness may initiate a cascade of events that ultimately produce a delay in the developmental shift of the glycine receptor subunit. Ongoing electron microscopic analyses of SBC and GBC inputs in Shaker-2 may provide clues that help explain these results.

Support: Australian Deafness Research Foundation and a LSRA from New South Wales, Aus.

693 Activity-Dependent Regulation of PMCA2 and Its Role in Dendritic Plasticity

Yuan Wang¹, Edwin W. Rubel¹ ¹University of Washington

It is well known that calcium signaling plays a role in synaptic regulation of neuronal structure. We are exploring the role of plasma membrane calcium ATPase type 2 (PMCA2), a high-affinity calcium efflux protein, in dendritic plasticity of nucleus laminaris (NL) neurons. Dendrites of NL neurons segregate into dorsal and ventral domains, receiving excitatory input from the ipsilateral and contralateral respectively, via ears. nucleus magnocellularis (NM). Unilateral cochlea removal silences excitatory input to NM leading to rapid reduction of PMCA2 immunoreactivity and structural changes of NL dendrites in, and only in, activity-deprived domains.

In the current study we used a whole brainstem preparation, which anatomically preserves all excitatory and the major inhibitory connections to NL neurons, to clarify the role of PMCA2 in activity-regulated dendritic plasticity. This preparation eliminates VIIIth nerve activity, thereby eliminating presynaptic action potentials to both NL domains. Without further manipulation, after 2 hours in vitro, the intensity of PMCA2 immunoreactivity was significantly higher in the dorsal than in the ventral domain, suggesting differential mechanisms regulate PMCA2 expression in each domain. Direct transection of NM axons to the ventral NL dendrites led to localized reduction of PMCA2 immunoreactivity in this domain. This reduction was preserved in calcium-free conditions and may be due to alterations in calcium-independent miniature EPSP activity. Restoring presynaptic action potentials by superthreshold electrical stimulation increased the intensity of PMCA2 immunoreactivity in activated domain. This effect was blocked by bath application of ionotropic glutamate receptors blockers (BNQX+APV), indicating that glutamate transmission regulates PMCA2 expression or localization. Determining the specific receptors involved in glutamatedependent PMCA2 regulation is under current investigation.

694 Functional Role of Developing NMDA-Rs in Binaural Auditory Neurons

Jason Sanchez¹, Armin Seidl¹, Edwin Rubel¹, Andres Barria¹

¹University of Washington

During development, NMDA-type glutamate receptors (NMDA-Rs) are thought to be involved in fine-tuning synaptic and intrinsic neuronal properties. Previously, we characterized the development of NMDA-Rs in nucleus laminaris (NL), an auditory brainstem structure responsible for binaural processing. We found that NMDA-R subunit composition changes from embryonic day (E) 11 to E19 accelerating the kinetics of NMDA-R mediated currents. Here we asked if the changing subunit composition influences action potential (AP) generation in developing NL neurons. In current-clamp, we recorded distinct AP firing patterns to afferent stimulation. Low-frequency stimulation always resulted in the generation plateau (DP)

was observed at E11, but not at E19. The DP at E11 was blocked by application of APV, an NMDA-R antagonist. Using high-frequency stimulation, E11 neurons always fired two initial APs followed by a DP. In contrast, E19 neurons fired almost exclusively a single AP and had little or no DP. Few E19 neurons presented with more than one AP, which was always followed by a DP. To confirm that the DP was due to NMDA-R activation, we performed voltage-clamp recordings and found a 3-fold increase in summated NMDA-R currents at E11 compared to E19, presumably due to slower kinetics and subunit content. Next, we addressed whether summating NMDA-R current caused suppressed AP activity. Blocking NMDA-Rs at E11 resulted in an increase in AP firing and a reduction in the DP, suggesting that the prolonged NMDA-R mediated depolarization inactivates sodium channels and prevents repetitive AP generation. At E19, this phenomenon occurred in the subset of neurons that had more than one AP and a DP. Otherwise, blocking NMDA-Rs had no effect on AP generation. The differential effects of NMDA-Rs on AP generation in NL may provide a mechanism to compensate for developing potassium currents.

695 In Vivo Juxtacellular Recordings of the Gerbil Medial Superior Olive

Marcel van der Heijden¹, Jeannette Lorteije^{1,2}, J. Gerard G. Borst¹

¹Erasmus MC, ²The Netherlands Institute for Neuroscience Neurons in the medial superior olive (MSO) receive excitatory information from both ipsi- and contralateral spherical bushy cells of the cochlear nucleus. Cells in the MSO are sensitive to the arrival times of tones at both ears, suggesting that they function as coincidence detectors. However, direct measurements of their synaptic inputs during auditory stimulation have not yet been reported. To investigate how cells in the MSO process interaural time differences we therefore made juxtacellular recordings from anesthetized gerbils. In the absence of auditory stimulation, all recorded cells showed small, positive-going events, which had a duration that matched those of EPSPs in slice recordings. Despite the high frequency of these events (>400 events/s) the spontaneous firing frequency of MSO neurons was typically low (<10 sp/s). During tone stimulation, the amplitude of these events increased and the largest events could trigger spikes, which showed excellent phase locking at low frequencies (vector strength typically >0.8). The correlation between the event size and spike initiation suggests that these events represent extracellularly recorded EPSPs. Remarkably, the response to lowfrequency (<300-Hz) tones presented to either ear often consisted of a stereotyped sequence of inputs with preferred delays. During stimulation with binaural beats, neurons were sensitive to phase disparities between the inputs from both ears. The resulting binaural input pattern generally matched the prediction from sequential monaural stimulation to both ears well. Our data thus show that in vivo juxtacellular recordings can be used to study the inputs from both ears to MSO neurons.

696 Influence of Serotonergic Inputs on the Principal Neurons of the Medial Superior Olive

Sukant Khurana¹, Aaditya Nagaraj¹, **Nace Golding¹** ¹Section of Neurobiology, Institute for Neuroscience, University of Texas at Austin

Serotonergic inputs are known to provide information about stimulus context and behavioral state to many auditory nuclei, including those in the superior olive, but the mechanism and functional impact of these influences are not well understood. We examined the role of serotonin in principal neurons in the medial superior olive (MSO), which compute binaural cues for sound localization. To address this guestion we made whole-cell patch recordings from MSO principal neurons in horizontal brainstem slices from Mongolian gerbils (>P17; 24 or 35°C). While single synaptic stimuli gave rise to synaptic potentials that were eliminated by blockade of AMPA, NMDA, and glycine receptors, trains of synaptic stimuli (50-500 Hz, 1-2 s duration) either medial or lateral to the cell body layer induced a small and long lasting depolarization (up to 3mV; half-amplitude duration 1-3s). The slow in rise and decay is suggestive of a paracrine nature of the release. The amplitude of depolarizing responses was frequency dependent, and reached saturation at 250 Hz. Surprisingly, synaptic responses were blocked by greater than 70% by specific antagonists of ionotropic 5-HT3 receptors (MDL72222, granisetron, ondansetron, tropisetron), while the remaining component was blocked by mecamylamine, an antagonist of nicotinic acetylcholine receptors. Using voltage-clamp recordings from MSO neurons, focal pressure application of both serotonin and specific 5-HT3 agonists, both in the presence and absence of metabotropic serotonergic blockers, we found that 5-HT3 receptors were expressed postsynaptically both on the soma and dendrites. Functionally, despite the excitatory nature of 5-HT3 receptors, their synaptic activation during trains of stimuli reduced the input resistance and membrane time constant of MSO neurons by 20 to 50%. These results are consistent with a strong activation of low voltage-activated potassium channels by the slow, long duration depolarization. The decrease in input resistance and membrane time constant of MSO is likely to narrow its ability to detect coincidence of binaural inputs. Hence our findings indicate that apart from the known attentional modulation of responses in higher auditory centers such as the inferior colliculus, serotonin likely modulates auditory responses at the brainstem level too. We also find that this effect on the temporal resolution is not exclusive to MSO neurons but also present to different degrees in the other time coding auditory brainstem neurons.

697 Distribution and Developmental Changes of Urocortin Expression in Neurons of the Lateral Superior Olive and Lateral Cochlear Efferents of the Gerbil

Alexander Kaiser¹, Olga Alexandrova¹, Benedikt Grothe¹ ¹Ludwig-Maximilians-Universitaet Muenchen

There exist two populations of olivocochlear neurons that are associated with the lateral superior olive (LSO), the shell and the intrinsic lateral olivocochlear (LOC) neurons. The LOC neurons project to the inner hair cell region of the cochlea and use acetylcholine as a main transmitter plus a variety of cotransmitters as GABA, CGRP, dynorphins, enkephalins and others. Recently, along with the discovery and characterization of the stress-related family of urocortins (Ucn), neurons containing Ucn were described for many nuclei throughout the brain, including just one auditory nucleus, the LSO (Bittencourt et al. 1999). Ucn-IR fibers have been described within the olivocochlear bundle and the cochlea, thus, suggesting that at least a part of the LOC neurons use Ucn as a cotransmitter. Using retrograde labeling of olivocochlear neurons in combination with double-labeling for Ucn-immunoreactivity, we have shown that a subpopulation of intrinsic, but not shell, LOC neurons uses Ucn as a cotransmitter and projects to the afferent dendrites that innervate the inner hair cells. Using multi-labeling for anti-Ucn and other antibodies, we investigated the distribution of Ucn-IR neurons in the LSO and the Ucn-IR terminals in the cochlea during postnatal development of the gerbil from postnatal day 9 (P9) to P70 covering pre-hearing, hearing onset, maturation and adulthood. Our analysis of the different stages showed a transient change of Ucn expression from P9 to adult in both the LSO and the cochlea. Whereas Ucn-IR was restricted to the regions representing high and middle frequencies in P9 and adult gerbils, in post-hearing onset animals the expression of Ucn was present throughout the LSO and the cochlea. These findings suggest a specific transient upregulation of the stress-related and neuropeptide urocortin in lateral olivocochlear neurons after hearing onset that is related to corresponding tonotopic gradient in the LSO and the cochlea.

698 Bidirectional Glutamate Spillover Allows NMDA Receptor-Mediated Crosstalk Between Immature Excitatory and Inhibitory Pathways in the Auditory Brainstem

Javier Alamilla¹, Deda Gillespie¹

¹McMaster Universitv

The lateral superior olive (LSO) of the auditory brainstem computes interaural intensity by comparing glutamatergic input from the ipsilateral ventral cochlear nucleus (VCN), with frequency-matched inhibitory glycinergic input from the ipsilateral medial nucleus of the trapezoid body (MNTB). Synapses under the VCN-LSO pathway utilize both AMPA and NMDA receptors (NMDARs). Before hearing onset in rats, MNTB-LSO synapses also release glutamate presynaptically and express NMDA receptors (NMDARs) postsynaptically. We asked whether it might be possible for spillover of glutamate from one pathway to activate NMDARs at synapses of the opposite pathway, a situation that could allow for developmental "crosstalk."

We used whole cell voltage clamp in acute brainstem slices from postnatal day 1-12 (P1-12 rat pups. LSO principal cells that received glutamatergic input from both the VCN and the MNTB were patched, and the NMDAR component was then pharmacologically isolated. Baseline NMDAR-mediated responses to stimulation of the MNTB and in the VCN pathway were collected, and the usedependent NMDAR blocker MK-801 was applied (10 µM). After a period for MK-801 wash on, one of two protocols was used to test for spillover. Either one pathway was stimulated until fully decremented and then the second pathway was stimulated, or the two pathways were alternately stimulated. The amplitude of the first responses in both pathways after MK-801 application were then compared to baseline amplitudes. Under both designs, the first response was reduced more in the second pathway stimulated than in the first pathway. Additionally, the exponential decay in response amplitude was shortened with interspersed stimulation of the opposing pathway. These data suggest that spillover of glutamate from excitatory to inhibitory synapses, and vice versa, can activate functional postsynaptic NMDARs. If so, excitatory and inhibitory synapses might be able to directly signal each other before hearing onset.

699 A Dopaminergic Pathway from the Lateral Lemniscus to the Inferior Colliculus

Renee K. Afram¹, Takashi Shimano², Bozena Fyk-Kolodziej¹, Avril Genene Holt¹

¹Wayne State University, School of Medicine, ²Kansai Medical University

We have previously identified dopaminergic somata and terminals in the inferior colliculus (IC) and lateral lemniscus (LL) of the central auditory system (Tong et al., 2005). This led us to postulate that a dopaminergic pathway may exist from the LL to the IC.

In the present study we focused on examining a pathway projecting from the LL to the IC. After injection of Fluorogold, a retrograde tract tracer, into the central nucleus of the IC (ICc) of adult Sprague Dawley rats (n = 6) the dorsal (DNLL), intermediate (INLL) and ventral (VNLL) nuclei of the LL were analyzed for the presence of Fluorogold labeled cell bodies. In each region of the LL Fluorogold labeling was identified with the VNLL showing the most robust labeling.

In order to assess whether this pathway was dopaminergic we performed immunocytochemistry for tyrosine hydroxylase (TH), a key enzyme in the production of dopamine. We found that 30.4% of TH labeled cell bodies in the DNLL, 30.6% of TH labeled cell bodies in the INLL, and 24.7% of TH labeled cell bodies in the VNLL were also labeled for Fluorogold suggesting that dopaminergic cell bodies projecting to the ICc were found throughout the LL. In addition, immunocytochemistry for DBH and PNMT, key enzymes in the production of other catecholamines (noradrenaline and adrenaline respectively), were performed to further investigate whether TH labeled neurons in the LL produce dopamine. Labeling for DBH was scarce to nonexistent while no labeling for PNMT was observed. In the future we plan to use HPLC to compare dopamine levels in the LL before and after sound conditioning.

700 Cellular Properties and Synaptic Transmission of Large Synapses in the Ventral Nucleus of the Lateral Leminsucs of Mongolian Gerbils

Felix Felmy¹, Elisabeth Meyer^{1,2}, Benedikt Grothe^{1,3} ¹Ludwig-Maximilians-University, ²Friedrich Miescher Institute, ³Bernstein Center for Computational Neuroscience Munich

In the auditory brainstem large calyceal synaptic terminals are present. The auditory nerve fibre gives rise to the endbulb of Held in the cochlear nucleus (CN), the bushy cells to the calyx of Held in the medial nucleus of the trapezoid body (MNTB) and the octopus cells to large terminals in the ventral nucleus of the lateral lemniscus (VNLL). Synaptic transmission has been well studied at the synapses in the CN and the MNTB, but presynaptically, only the calyx of Held has been investigated. The features of synaptic transmission of large terminals in the VNLL are largely unknown, and thus no physiological comparison of auditory presynaptic terminals is available so far.

To compare the calyx of Held and terminals in the VNLL we used pre- and postsynaptic whole-cell current- and voltage-clamp recordings and ratiometric fura Ca²⁺- measurements from visually identified terminals of brain slices of Mongolian gerbils of postnatal day 9-11 at 34°C.

We find that both terminals have resting membrane potentials of -68 mV that the input resistance is lower and the membrane time constant faster in terminals in the VNLL. Action potential (AP) half width is not different, but its size was ~20 mV smaller in terminals in the VNLL. The resting Ca2+ concentration and the endogenous calcium binding ratio are slightly larger in the VNLL. The VNLL synapse generates AMPA and NMDA currents (3.1 nA and 2.3 nA respectively) of about half the amplitude of clayx of Held synapses. Both AMPA and NMDA currents are faster in their kinetic profile in VNLL. Despite the large synaptic currents a single terminal in the VNLL is not able to trigger a postsynaptic AP. A transient potassium channel present in the postsynaptic VNLL somata appears responsible for suppressing the AP generation by a single terminal in the VNLL. In contrast to the calvx of Held information transfer in the VNLL is based on coincidence detection or temporal summation instead of a reliably one-to-one transmission.

701 Binaural Lemniscal Recordings in the Chinchilla (*Chinchilla Laniger*)

Peter Bremen¹, Philip X. Joris¹

¹Laboratory of Auditory Neurophysiology

In humans the major cue for localizing low frequency (<1.5 kHz) sounds is the interaural time difference (ITD). In mammals the first stage of binaural convergence is the medial superior olive (MSO), which is thought to perform a coincidence analysis on the inputs of both ears. Currently only a limited number of studies report data from extracellularly recorded MSO neurons. However, more

high-guality data is needed in order to understand the mechanisms creating neuronal ITD sensitivity. Extracellular single-neuron recordings in MSO are difficult to obtain because (1) MSO action potentials are small and (2) a large mass potential locked to the stimulus frequency hampers spike isolation. To circumvent these difficulties we recorded from MSO axons in the lateral lemniscus (LL) of the chinchilla. A species with pronounced low frequency sensitivity and large bulla. We developed two surgical approaches for reaching the LL: (1) caudal and (2) transbulla. The transbulla approach gives direct access to the LL but opening of the bulla generates (1) asymmetries in the sound delivery between the two ears and (2) acoustical crosstalk. To evaluate these effects we recorded cochlear microphonics on the round window to binaural and monaural stimulation. Interaural attenuation was >60 dB over the frequency range of .1 to 1.2 kHz. In both caudal and transbulla approaches we employed high impedance (Z>60 M Ω) micropipettes to bias the recordings towards axons. Recordings of ITD-sensitive neurons were obtained of both axonal and somatic origin. We verified the axonal nature of the recordings both physiologically (monopolar spike shape) and histologically (visualization of electrode track with fluorescent dye). The main difficulty was mechanical instability. We conclude that axonal MSO recordings are feasible and are a promising avenue towards a further characterization of this nucleus. [Supported by grants from FWO (G.0714.09), BOF (OT/09/50) (Flanders, Belgium), BOF fellowship to PB]

702 Characterization of Synaptic Input-Output Functions in Neurons of the Dorsal Nucleus of the Lateral Lemniscus in Juvenile Mongolian Gerbils

Christian P. Porres¹, Elisabeth M. M. Meyer^{1,2}, Benedikt Grothe^{1,3}, Felix Felmy¹

¹Ludwig-Maximilians-University Munich, ²Friedrich Miescher Institute for Biomedical Research, ³Bernstein Center for Computational Neuroscience Munich

In the ascending auditory pathways the dorsal nucleus of the lateral lemniscus (DNLL) receives excitatory inputs from the superior olivary complex (SOC) and provides GABAergic inhibition to both inferior colliculi and the contralateral DNLL. The spike timing of DNLL neurons *in vivo* reflects substantially that of its excitatory inputs. Therefore DNLL neurons must be capable of temporally precise high frequency firing. Focusing on the synaptic integration of excitatory inputs in DNLL neurons we investigated their biophysical properties and synaptic input-output functions (IO-Fs).

Whole-cell patch-clamp recordings in voltage- and currentclamp mode from visually identified DNLL neurons were obtained from acute brainstem slices of Mongolian gerbils of postnatal day 14-17. Pharmacologically isolated excitatory postsynaptic currents (EPSCs) and potentials (EPSPs) were evoked by stimulating afferent fibers with a glass electrode and recorded at ~35 °C bath temperature.

Input resistance, membrane time constants and resting potential appeared to be highly variable between DNLL neurons. Nevertheless, in all neurons sustained firing and monotonic IO-Fs could be evoked by current injections. Estimated from minimal stimulation and quantal analysis 4-5 fibers releasing in total ~100-125 vesicles were required to generate a single postsynaptic action potential (AP). A strong single presynaptic fiber shock, however, was capable of triggering multiple postsynaptic APs. These synaptic IO-Fs were strongly dependent on NMDA receptor mediated currents which also enhanced spatial and temporal EPSP summation. Other depolarizing currents such as mediated by Ca²⁺ channels, did not affect EPSP summation. Thus, NMDA receptor mediated currents strongly modulate the IO-Fs of DNLL neurons and amplify postsynaptic activity.

703 Amplitude Modulation of Acoustic Tones and Electrical Pulse Trains Increases Cochleotopic Spread of Sustained Activation (Response Width) in the Central Nucleus of the Inferior Colliculus (IC)

Matthew Schoenecker¹, Olga Stakhovskaya¹, Alexander Hetherington¹, Steve Rebscher¹, **Ben Bonham¹**, Russell Snyder¹, Patricia Leake¹

¹Epstein Laboratory, UCSF

Previously we reported that the widths of IC responses evoked by unmodulated acoustic tones and monopolar electrical pulse trains are similar. We now extend those results by comparing response widths for tones and pulse trains that are sinusoidally amplitude modulated (SAM) to investigate neural correlates of psychophysical interactions known to occur across large differences in carrier frequency.

Cats and guinea pigs (GPs) were stimulated using 60dB SPL acoustic tones (AC) or electrical pulse trains 2-6dB re. threshold (ES). Stimulating signals were 100, 20, or 0% modulated at 50 or 125Hz. Evoked activity was recorded along the tonotopic axis of the IC using 32-channel probes at sites that had sustained responses to unmodulated tones/pulse trains. The response width was determined based upon spike rate or phase-locking of evoked activity.

Based on measured response rate, mean response widths were broader for 100%-50 Hz SAM stimulation than for unmodulated stimuli (AC & ES); the greatest difference between modulated and unmodulated response widths was seen in chronically-deafened cats. Mean response widths were greater for 100%-125Hz modulation than for unmodulated stimuli in chronically-deafened cats (ES) and in guinea pigs (AC & ES). When mod depth was reduced from 100% to 20%, response width expansion with 50Hz SAM was less, and there was no expansion for 125Hz SAM (ES in chronically-deafened cats). Measures of phase-locking showed that neurons with characteristic frequencies or locations that were substantially different from the center of cochlear stimulation could be strongly phase-locked to the modulating waveform. Phase-locking in chronically-deafened cats was stronger, yet more variable, than in normal cats (ES) or GPs (AC & ES).

Response width differences for modulated and unmodulated stimuli, and comparisons between chronically-deafened and normal animals, may inform theories of auditory coding and future cochlear implant design.

NIDCD 1F31DC00890 & HHS-N-263-2007-00054-C; Hearing Research, Inc; Epstein Fund

704 fMRI Reveals an Orthogonal Representation of Frequency and Modulation Rate in the Inferior Colliculus

Simon Baumann¹, Timothy Griffiths¹, Li Sun¹, Christopher Petkov¹, Alexander Thiele¹, **Adrian Rees¹**

¹Newcastle University

Speech and other ethologically important sounds are characterised by their frequency content and by the temporal fluctuations that shape the sound's envelope. It is well established that sound frequency is mapped tonotopically in the inferior colliculus along the dorsal to ventral axis in a stack of frequency-band laminae. On the basis of electrophysiological evidence it has been proposed that modulation rate is represented across the surface of these laminae (Schreiner and Langner, 1988, J Neurophysiol 60, 1823). This finding has not been corroborated with an ascertainment free method and here we address this question in the inferior colliculus of an awake primate (*Macaca mulatta*) using fMRI.

We measured the blood oxygenation level dependent (BOLD) signal in the IC at high spatial resolution (1 mm x 1 mm in-plane) in three animals in multiple sessions with two types of stimuli. To identify the tonotopic gradient we presented narrow bands of noise modulated at 10Hz containing spectral frequencies ranging between 0.5-16 The existence of an analogous temporal kHz. (periodotopic) gradient was tested using broad band noise stimuli amplitude modulated at rates ranging between 0.5-512 Hz. Stimuli were presented at ~75 dB SPL using modified electrostatic headphones. Data were recorded in a 4.7 T MRI scanner (Bruker Biospec 47/60 VAS) using a sparse sampling paradigm to avoid interference from the scanner noise. The contrast between stimulus and silence in the BOLD response was analysed using SPM 5.

The data demonstrate that spectral frequency is mapped along the dorso-lateral to ventro-medial axis of the IC with amplitude modulation rate represented orthogonally to this frequency gradient, consistent with the previous electrophysiological findings. This systematic representation of frequency and modulation rate in the inferior colliculus highlights their fundamental importance as key sound dimensions processed within specific neural channels.

Supported by the Wellcome Trust.

705 Envelope Coding Differs Along the Pathway from Lateral Superior Olive to Inferior Colliculus in Decerebrate Cats Nathaniel Greene¹, Kevin Davis¹

¹University of Rochester

Neurons in the central nucleus of the inferior colliculus (ICC) of decerebrate cats show three major response patterns when tones of different frequencies and sound pressure levels are presented to the contralateral ear. The

frequency response maps of type I units are uniquely defined by a narrow V-shaped excitatory area at best frequency (BF) and flanking inhibition at higher and lower frequencies. Units that produce type I maps typically have high BFs (>3 kHz), receive ipsilateral inhibition and show binaural excitatory/inhibitory interactions. Given this constellation of properties, it has been hypothesized that the contralateral lateral superior olive (LSO) provides the dominant excitatory input to type I units. Our previous direct, quantitative comparisons of the response properties of LSO and ICC units support this interpretation, but suggest that additional inputs transform LSO influences in the ICC.

Amplitude modulations (AM) are important features in speech and other behaviorally relevant sounds, and prior work has suggested a role for the LSO pathway in the processing of AM information. Here, we compare the responses of LSO and ICC type I units to monaural, amplitude-modulated sinusoidally BF tones. The responses of single units were described in terms of synchronization and discharge rate as a function of modulation frequency. In response to fully modulated stimuli, both LSO and ICC units synchronize strongly to tones with low modulation frequencies. In contrast, the rate-modulation functions of LSO units are weakly peaked or low-pass in nature, whereas ICC type I units may show significantly sharper peaks at a particular modulation frequency. These data suggest a sequential enhancement to a rate-based code for envelope frequency along the LSO to ICC pathway. Supported by NIDCD grants R01 DC 05161, T32 DC 009974 and P30 DC 005409.

706 Neural Coding of Amplitude Envelope in Reverberation: Dynamic Aspects

Michael Slama^{1,2}, Bertrand Delgutte^{1,2}

¹Harvard-MIT Division of Health Sciences and Technology, ²Eaton-Peabody Laboratory, Massachusetts Eye and Ear Infirmary

Speech reception depends critically on temporal modulations in the amplitude envelope of the speech Reverberation encountered in signal. everyday environments substantially can attenuate these modulations. To assess the effect of reverberation on the neural coding of amplitude envelope, we recorded from single units in the inferior colliculus of awake rabbit using sinusoidally amplitude modulated broadband noise stimuli presented in simulated anechoic and reverberant environments.

We compared the time course of the neural responses to the time course of the modulations in the stimulus. In some neurons, phase locking to each modulation cycle of a reverberant stimulus sharply degraded during the first 100 ms before stabilizing, paralleling the evolution of modulation depth in the stimulus as reverberant energy builds up. However, in other neurons, phase locking was stable or even slowly increased over time, despite the decrease in stimulus modulation depth. We measured separately in the same neurons the nonlinear transformation from stimulus modulation depth to neural phase locking to the modulation, and used this static inputoutput function to predict the time course of neural phase locking from the time course of modulation depth in the reverberant stimulus. In most neurons, phase locking in reverberation was stronger than predicted from the inputoutput function, even in later portions of the stimulus, suggesting that the neural encoding of modulation cannot be represented by a static input-output function, but depends dynamically on preceding stimulation history.

Overall, our results point to an important role of dynamic neural processes for robust stimulus coding in reverberation.

Supported by NIH grants RO1 DC002258, P30 DC005209, and T32 DC00038.

707 Effect of Binaurally-Coherent Jitter on Neural ITD Coding with Bilateral Cochlear Implants

Kenneth E. Hancock^{1,2}, Yoojin Chung¹, Samantha Blasbalg³, H. Steven Colburn³, Bertrand Delgutte^{1,2} ¹Massachusetts Eye & Ear Infirmary, ²Harvard Medical School, ³Boston University

Poor sensitivity to interaural time difference (ITD) constrains the ability of human bilateral cochlear implant users to listen in everyday noisy acoustic environments. ITD sensitivity to periodic pulse trains degrades sharply with increasing stimulus pulse rate, but can be restored at high pulse rates by jittering the interpulse intervals in a binaurally coherent manner (Laback et al., PNAS 105:814).

We investigated the neural basis of the jitter effect by recording from single inferior colliculus (IC) neurons in three groups of bilaterally-implanted, anesthetized cats. Two groups were deafened with ototoxic drugs, either 1 week (acutely-deafened, ADC) or 6 months (long-term deafened, LTD) before experimentation. The third group comprised congenitally deaf white cats (DWC). Neural responses to trains of biphasic pulses were measured as a function of pulse rate, jitter, and ITD.

An effect of jitter on neural responses was most prominent for pulse rates above 300/sec. High-rate periodic trains evoked only an onset response in most IC neurons, but introducing jitter increased ongoing firing rates in 55% of neurons in ADC/LTD, compared to 29% in DWC. Neurons that had sustained responses to jittered high-rate pulse trains showed ITD tuning comparable to that produced by low-rate periodic pulse trains. Thus, jitter appears to improve neural ITD sensitivity by restoring sustained firing in many IC neurons.

Action potentials tended to occur at sparse preferred times across repeated presentations of a high-rate jittered pulse train. A combination of reverse correlation analysis and computational modeling suggests that spiking tends to occur at times when several stimulus pulses occur in rapid succession, allowing the membrane potential to exceed its adapted threshold. The integrative nature of this mechanism may limit the precision with which fine structure ITD can be encoded with jittered pulse trains. Supported by NIH Grants R01 DC005775 and P30 DC005209.

708 Binaural Mechanism of El/f Neurons Revealed with In-Vivo Whole Cell Recordings

Na Li¹, Joshua Gittelman¹, George Pollak¹

¹University of Texas at Austin

Cells that receive excitation from one ear and inhibition from the other (El cells) process interaural intensity disparities, the cues all animals use for localizing high frequencies. El cells in the inferior colliculus (IC) fired to contralateral stimulation, while progressively introducing an ipsilateral stimulation suppressed the spike-count evoked by contralateral stimulation. The facilitated EI (EI/f) cell is a variation of EI cells in that facilitated spike-counts, higher than those evoked by the contralateral signal, were generated at low ipsilateral intensities. IID of 0dB. Thus El/f cells respond best to the sound coming from straight ahead. To evaluate the mechanism underlying El/f cells, we made whole cell patch-clamp recordings in 11 EI/f cells in the IC of Mexican free-tailed bats. Both spikes and postsynaptic potentials (PSPs) evoked by contralateral, ipsilateral and binaural signal were recorded. Moreover, excitatory and inhibitory synaptic conductances were derived from each response record. Two mechanisms were underlying the facilitation in EI/f cells. First is that the excitation evoked by ipsilateral signal sums with the contralaterally evoked excitation to produce a larger excitation. This larger excitation generates a larger EPSP than that evoked by a contralateral signal alone. Second is that a reduction of inhibition was evoked by contralateral signal while introducing an ipsilateral signal. The contralateral signal evoked both excitation and inhibition. Thus a smaller inhibition allows excitation generate a larger EPSP and more spikes. By monitoring both inputs and outputs of a cell, we were able to study the mechanism underlying the El/f cells. Supported by NIH Grant DC007856.

709 Effect of Corticosteroids on the Development of Tinnitus Following Noise Trauma

Didier Depireux¹, Roger Lee¹

¹University of Maryland

Tinnitus is the perception of sounds when no external source is present. While it is not a single disease, but a symptom of an underlying condition, a common cause of tinnitus is inner ear damage, due to trauma, medication and other factors. We have recently developed a rat model of tinnitus, with which we behaviorally measure evidence of tinnitus while recording from the midbrain of the rat before, just after and several weeks after noise-trauma. We can then compare both the behavior as well as the changes in neural responses in the Inferior Colliculus before and after the trauma and possible tinnitus has been established.

For humans, there is a largely empirical and not always consistent body of literature on the effect of various drugs provided before or just after noise trauma, and their effect on preventing or attenuating the subsequent development of hearing loss and tinnitus. One of these drugs are the corticosteroids, normally given post-trauma to mitigate the effect of the trauma (Eisenman and Arts 2000). In this work, we gave Dexamethasone at various times (right away to several days) and with different regimens (pulse or taper) to rats following noise-trauma. We report on the effect of dexamethasone on preventing tinnitus and on its effect on the coding of sounds in the midbrain following trauma.

710 A Rat Model of Noise-Induced Tinnitus

Davina Gassner¹, Vedran Dupanovic¹, Jennifer Thompson¹, Hinrich Staecker¹, Thomas Imig¹, Dianne Durham¹

¹University of Kansas Medical Center

The rat has been widely studied as a model of ototoxin induced tinnitus and a variety of behavioral and physiologic approaches are available to document tinnitus in this animal model. Noise trauma induced tinnitus is a common disorder in a variety of industrial and military settings that to date has not been studied in rats. Adult rats were unilaterally exposed to a 16kHz pure tone sound at either 114 dB for 1 hr, 114 dB for 2 hrs, 118 dB for 1 hr or 123 dB for 1 hr. Hearing loss was measured at regular intervals post noise exposure by DPOAE and ABR. The presence of tinnitus was assessed by gap detection. Outcomes are correlated to cytocochleograms and histology. We found that a subset of animals failed to startle to the gap detection test, even prior to noise exposure, and that regular repeat testing resulted in habituation of the startle response. Sound exposures of 114 dB for 2 hrs or 118 dB for 1 hr generated a reliable hearing loss and evidence of tinnitus as measured by gap detection in most animals. Sound exposures of 123 dB for 1 hr resulted in severe hearing loss and no startle response. Sound exposures of 114 dB for 1 hr resulted in less hearing loss.

Supported by a grant from the Department of Defense (PR081241)

711 Modulation of Evoked Brain Responses by the Combination of Stimulus Exposure and Task Performance in Auditory Perceptual Learning

Gardiner von Trapp¹, David Poeppel¹, Beverly A. Wright² ¹New York University, ²Northwestern University

How auditory perceptual learning is achieved is a fundamental question for hearing research. In order to drive learning on many perceptual tasks, stimulus exposure alone is not sufficient; the task to be learned (e.g. frequency discrimination) must be performed. Implicit in this finding is the presupposition that continuous task performance is the most effective way to achieve learning. Recent striking behavioral evidence demonstrates that a combination of task performance and additional stimulus exposure can enhance learning in different types of auditory perceptual tasks (e.g., Wright et al. 2010, J. Neuroscience). Here we ask how the dynamics of evoked brain responses are affected during a single session combining periods of task performance and additional exposure. Sixteen native English speakers were scanned using MEG during a speech discrimination experiment (n=8 per condition group). Stimuli were three CV syllables varying along a /mba/-/ba/-/pa/ voice-onset-time (VOT)

continuum, with a pre-voiced /mba/ as a non-native stimulus. One group received a block of task performance (identification) followed by a block of additional exposure, the other group the reverse order. Forty auditory channels were analyzed. Beyond well-characterized M100 effects, we report that, during task performance, the response amplitude between 300-500 ms after stimulus onset, well beyond the P2m, was markedly enhanced by preceding stimulus exposure. This result is contrary to the expectation of adaptation or fatigue. The response to additional stimulation following a period of task performance was not similarly enhanced. Thus, the magnitude of the late response may serve as a noninvasive neurophysiological index for how prepared the observer is for perceptual learning.[Support NIH R01DC05660 to DP and NIH R01DC004453 to BAW.]

712 Monkey Auditory Cortex Responses in Active and Passive Listening

Roohollah Massoudi¹, Marc van Wanrooij¹, Huib Versnel², Sigrid van Wetter¹, John van Opstal¹ ¹Radboud Uni. Nijmegen, Donders Ins. for Brain, Cognition and Behaviour, Dep. Biophysics, Nethelands, ²Uni. Medical Center Utrecht, Rudolf Magnus Ins. of Neuroscience, Dep. Otorhinolaryngology

To investigate how the auditory system analyzes and perceives acoustic scenes, we recorded from single neurons in the auditory cortex (AC) of trained macaque monkeys. An important question is whether AC cells exclusively encode acoustic features, or whether they are also involved in high-level processing related to task, perception and reward, and, if so what happens with respect to analysis of acoustic features in auditory cortex.

First, to assess the acoustic processing, we measured the spectrotemporal receptive fields (STRFs) of AC cells, which describe the dynamics of a cell's spectral sensitivity to complex dynamic stimuli. The STRF was determined by using broadband dynamic rippled stimuli (0.25-19 kHz), with a variety of ripple velocities (8-40 Hz) and ripple densities (-2.0 to +2.0 cycles/octave).

Furthermore, to assess the influence of task, the ripple sounds were presented in two different paradigms: in the passive paradigm the monkey listens to the sounds, yet is not involved in a behaviorally relevant task. In the active paradigm the monkey initiates the trial by pressing a bar, and is required to detect a change in the sound (after a random delay) to receive a reward.

If an AC cell is only involved in acoustic feature extraction, neural activity for passive and active conditions are expected to be the same. However, our data (over 400 cells, two monkeys) show that the firing patterns to identical sounds for active and passive listening conditions differ markedly for the far majority of neurons. Interestingly, a comparison of the STRFs from the two paradigms indicates that they are virtually identical. This shows that AC cells preserve their precise tuning to acoustic spectrotemporal features, while at the same time they are modulated by other, non-acoustic factors relevant for the task. We conclude that auditory cortex, besides accurately processing acoustic features, is simultaneously involved in other aspects of auditory perceptio

713 Local Field Potential and Spike Representations of Periodicity in the Auditory Cortex of Freely Moving Ferrets

Kerry Walker¹, Jennifer Bizley¹, Fernando Nodal¹, Andrew King¹, Jan Schnupp¹

¹University of Oxford

Electrophysiological recordings of auditory cortex activity were made in freely moving ferrets while they performed a two-alternative forced choice pitch discrimination task. On each trial of the task, ferrets were presented with two artificial vowel sounds, and were required to indicate, by spout choice, whether the second sound was higher or lower in pitch than the first (Walker et al., 2009, JASA 126:1321-35). Microelectrode arrays were implanted bilaterally prior to testing, allowing us to make simultaneous recordings from up to 16 independent tungsten electrodes in each hemisphere. Electrodes were advanced through the cortical depth over the course of a year. Voltage traces were recorded at a high resolution during the behavioural task and during periods of passive exposure to the same sounds. Local Field Potentials (LFP) and spike data were then extracted from these signals offline. We have previously shown, using receiver operating characteristic analysis, that LFP power discriminated high and low pitch targets during the task, but often provided even better discrimination of the animals' behavioural choice (Bizley et al., ARO 2010). Here, we show that LFPs recorded in passively listening animals were informative about the periodicity of vowels, but differed considerably in their amplitude, shape and tuning from those recorded when the same animals were actively performing the task. The spiking responses of single neurons and small clusters of neurons show broad periodicity tuning, and these were also compared across active and passive conditions. These data indicate that neural representations of periodicity in auditory cortex are strongly modulated by behavioural context, and are encoded within LFPs as well as spike rate responses at the single neuron level.

714 Different Weighting of Acoustic Attributes in Discrimination of Natural Sounds by Guinea Pigs

Hisayuki Ojima¹, Yasuhiro Kumei¹, Shigemi Katsuyama¹, Masato Taira¹

¹Tokyo Medical and Dental University

To examine what acoustic attributes small animals depend on to distinguish sounds, we trained guinea pigs, a wellknown vocal animal species, in a classical conditioning paradigm.

Through a systematic training with food as the unconditioned stimulus, animals could associate it with a natural sound (target) and reported the association by conducting a set of distinct actions such as swinging head and circling near a food outlet of training arena. Some animals stood up and watched out from the training arena, too. Once animal learned this association, a stimulus set including the target and 7 non-target sounds was presented in the second stage training. They quickly distinguished the target sound from non-targets with the behavioral set of actions associated only with the target. These actions were initiated immediately after the sound onset but prior to the food delivery, indicating that they were conditioned to the target sound but not to sounds generated during food delivery. Animals did not show such actions to non-target sounds, usually keeping still or just approaching to the food outlet without head-swinging or circling actions.

Thereafter, to identify what acoustic attributes were used for animals to distinguish the target from the non-targets, the target sound was modified in such a way that it was low-pass filtered, high-pass filtered, time-reversed, or elongated by increasing the intervals between component segments of the target sound. These modifications were effective in restraining animals from initiating the actions, with the time-reverse version of the target sound most effective and the variation of inter-segment intervals least effective. Low-passed sounds were more effective than high-passed sounds.

The results suggest that animals depend on several acoustic attributes to identify natural sounds and that these factors are not equally evaluated by animals but may be processed with different weights for the recognition of sounds. Supported by KAKENHI (C) no.22500368 to H.O.

715 Modulation of Auditory Cortical Response Properties by Orbitofrontal Cortex

Daniel Winkowski^{1,2}, Sharba Bandyopadhyay^{1,2}, Shihab Shamma^{1,2}, Patrick Kanold^{1,2}

¹University of Maryland, ²Institute for Systems Research Attention and behavioral demand based changes in auditory cortical response properties are likely to be the consequence of top-down signals originating in higher order cortical areas. Using standard anatomical tract tracing methods, we identified a region (orbitofrontal cortex, OFC) in the mouse prefrontal cortex (PFC) that projects directly to the primary auditory cortex (A1) and characterized the projection patterns within A1. Using electrical microstimulation in the OFC and simultaneously monitoring neural activity in A1 we show that these connections are indeed functional. Using in vivo twophoton calcium imaging, we show that pairing electrical microstimulation of OFC with presentation of a fixed frequency sound, on average, rapidly changes auditory cortical neurons' tuning properties to show enhancement near the paired frequency and suppression to other sound frequencies based on tuning measurements before and after the pairing episode. However, within the population, response changes resulting from the OFC-sound pairing episode at the single cell level were diverse. We investigated the diversity of changes in individual cells with principal component analysis, to show distinct components of response changes related to the pairing frequency, underlying the diversity of changes observed. We hypothesize that such distinct components may result from

the engagement of different direct and indirect pathways by OFC activation or may reflect changes across different cell types in ACX. Such mechanisms may underlie topdown modulation (like attention) of auditory cortical responses by providing different coding strategies to maximize information about a particular sound of interest in a noisy "cocktail party"-like environment.

716 Modulation of the Inhibitory Synaptic Transmission in the Auditory Cortex by Serotonin

Bin Luo¹, Hai-Tao Wang¹, Lin Chen¹

¹Central Auditory Processing Laboratory, University of Science and Technology of China

Serotonin is an important neural modulator in the central nervous systems and its functional role has intensively been studied. In the auditory cortex, however, little is known about how serotonin modulates the neural activity. In the present study, we examined the effects of serotonin on the inhibitory synaptic transmission through recordings from pyramidal neurons in layer II/III of the auditory cortex with whole-cell patch-clamp technique and brain slice preparation. Serotonin (40 µM) had a significant and transient enhancing effect on the spontaneous inhibitory postsynaptic current (sIPSC), as demonstrated by an increase in both amplitude and frequency of sIPSCs following perfusion of serotonin. In contrast, serotonin significantly depressed the evoked inhibitory postsynaptic current (eIPSC) and increased paired pulsed ratio (PPR), suggesting that serotonin reduced the neurotransmitter release. Our findings indicate that serotonin has bidirectional modulatory effects on the central auditory system to accommodate different functional states. This work was supported by the National Natural Science Foundation of China (Grants 30970977 and 30730041), the National Basic Research Program of China (Grants 2007CB512306 and 2011CB504506) and the CAS Knowledge Innovation Project (Grant KSCX1-YW-R-36).

717 Frequency-Specific Remodeling of Auditory Thalamocortical Synaptic Transmission

Carol Peiyi Wang¹, Xiuping Liu^{1,2}, Jun Yan¹

¹University of Calgary, ²Hebei University Health Sciences Centre

Auditory cortex demonstrates frequency-specific receptive field (RF) plasticity following auditory learning and experience. Because of direct thalamocortical projections into the cortex, it has been speculated that modulations of thalamocortical synaptic transmission underlies cortical plasticity. To date, the neural basis for frequency specific cortical plasticity remains poorly understood. The present study investigated in vivo long-term remodeling of thalamocortical synapses in mice. Tungsten electrode was placed in the thalamocortical recipient layers of the primary auditory cortex for local field potential (LFP) recording. High-frequency tetanic electrical stimulation was applied to the ventral division of the medial geniculate body (MGBv) of the thalamus to induce long-lasting changes in the

cortical local field potentials. Unlike previous reports, we demonstrated that cortical LFP could be either enhanced or reduced following tetanic stimulation of the MGBv. The incidence of reduction in LFP appeared to be much higher than that of enhancement. Further analysis indicated that the enhancement or reduction of cortical LFPs depended on the frequency tunings of the stimulated thalamic neurons in relation to that of the recorded cortical neurons. Cortical LFP was enhanced when cortical and thalamic best frequencies (BFs) were similar. On the contrary, cortical LFP was reduced when thalamic BF was different from cortical BF. The greater the BF difference, the smaller the reduction of cortical LFP. Interestingly, the changes in cortical LFPs appeared to be correlated to modifications in the receptive field of cortical neurons following tetanic stimulation of the MGBv. Our data suggest that modulations in thalamocortical synaptic transmission could be a vital neural substrate for frequency-specific plasticity of the auditory cortex.

This work is supported by the Canadian Institute of Health Research (MOP82773), the Natural Sciences and Engineering Research Council of Canada (Discovery Grant), the Alberta Innovates – Health Solutions and the Excellent Going Abroad Experts Training Program of Hebei Province of PR China.

718 Tonotopic Map Plasticity in Mature Auditory Cortex Following Passive Exposure to Behaviorally-Irrelevant Sounds

Martin Pienkowski¹, Raymundo Munguia¹, Jos J. Eggermont¹

¹University of Calgary

Prolonged passive exposure of adult cats to random, bandlimited tone pip ensembles at moderate intensities (~70 dB SPL) has been shown to suppress neural activity in auditory cortex to sounds in the exposure frequency range, and enhance activity outside that range, reminiscent of the reorganization that follows restricted hearing loss. When the exposure bandwidth is decreased from ~2 to <1 octave, the suppression extends beyond the exposure frequency range in Al but to a lesser extent in All, consistent with a bottom-up mechanism for the plasticity (Pienkowski and Eggermont, Hear Res 268 [2010] 151-162). Reversal of the suppression proceeds for months after the cessation of exposure, a finding with potentially troubling implications for people who work/live in moderately noisy environments.

Here we add two new chapters to this story. The first is a demonstration of similar plasticity upon exposure to bandlimited white noise. Though the noise and tone ensemble have the same long-term power spectrum, they sound very different as the tone ensemble is less spectrally dense and its modulation spectrum shows dominantly frequencies below 30 Hz. One interesting difference is that the band of maximum response suppression in both AI and AII appears shifted to lower frequencies following noise compared to tone exposure; i.e., for a 4-20 kHz exposure, the maximum suppression occurs over ~4-20 kHz for tones but over ~2-14 kHz for noise. The different suppression frequency ranges also

seem inconsistent with a frequency-specific top-down habituation process.

We also determined the time course of the progression of response suppression in AI and AII following the onset of exposure. Neural responses to sound were found to be maximally suppressed in the exposure frequency range by some time between 2 and 7 days post exposure onset. For narrowband exposure, suppression beyond the exposure frequency range progressed more slowly, reaching a maximum after 14 to 28 days of exposure. Reorganization of the frequency representation in AI, i.e., the reactivation of suppressed neurons by frequencies above and below the exposure band, develops yet more slowly, after months of exposure.

719 Sound Evoked Responses in Neonatal Subplate Neurons in Auditory Cortex

Jessica Wess¹, Didier Depireux¹, Patrick O Kanold¹ ¹Dept. of Biology, Institute for Systems Research, University of Maryland

Subplate neurons (SPns) are among the earliest generated neurons in the cerebral cortex. They receive thalamic axons and project into the developing cortex, particularly to thalamorecipient layer 4. Thalamic axons remain in the subplate for a "waiting period" before growing into layer 4. Thus SPns potentially relay early spontaneous and later, sensory evoked activity into developing layer 4. SPns are also required for the formation and functional refinement of thalamocortical connections (Kanold & Luhmann 2010) but it is unknown how SPns play this role. In particular, it is unknown if SPns respond to sensory stimuli. To reveal the role of SPns in development, we investigate the functional responses of SPns in vivo. We record from SPns and neurons in the overlying cortical plate in the developing auditory cortex (ACX) by extracellular single unit recording in anesthetized ferrets between postnatal day (P) 22 and 34. We found that putative SPns exhibited sound driven responses as early as P23. At these same developmental ages neurons in upper cortical layers exhibited less sensory driven activity, consistent with SPns relaying sensory information to layer 4. Our data show that the ACX receives auditory information earlier than previously thought. In particular, SPns respond to sound early in neonatal life and thereby might sculpt the development of auditory responses in layer 4 and beyond.

720 Distribution of Parvalbumin-, Calbindin-And Calretinin-Immunoreactivity During Postnatal Development in the Medial Geniculate Body of the Mustached Bat Julia Heyd¹, Marianne Vater¹

¹Institute for Biochemistry and Biology, University of Potsdam

Mustached bats are able to hear shortly after birth but echolocation behavior and specialized hearing capabilities gradually develop during the 1st postnatal month. This study investigates the anatomical maturation of the medial geniculate body (MGB) in juveniles in comparison to adult

bats with doubleimmunofluorescence techniques using antibodies against parvalbumin (PV), calbindin (CB) and calretinin (CR). These calcium binding proteins (CaBPs) are known to be differentially expressed in different subdivisions of the MGB.

In adults, CB- and CR-immunoreactivity was abundant in all main divisions of the MGB. CB-immunostaining was most intense in the dorsal division (MGBd); and virtually absent in the suprageniculate nucleus (SG). PVimmunoreactivity was heaviest in the SG and absent in the superficial dorsal nucleus of MGBd. PV-immunoreactive (ir) somata and neuropil occured in the rostral pole nucleus (RP), medial division (MGBm), dorsal nucleus and ventral division (MGBv). In these areas the population of PV-ir neurons overlaps with CR- and CB-ir neurons.

In the 1st postnatal week (pw), the MGBd already contained strongly CB-ir somata and neuropil but strongly CB-ir somata where rarely observed in RP, MGBm and MGBv. Their abundance increased with age but did not match the adult in pw4.

Strongly CR-ir somata and neuropil were abundant in MGBd, RP, MGBm and MGBv in the 1st pw. This pattern did not change significantly in the following weeks.

Virtually no PV-ir somata were present in the 1st pw in the MGB but the neuropil in SG and medial part of MGBv was strongly labeled. In the 2nd and 3rd pw, PV-ir neurons were confined to SG. Only in the 4th pw, additional PV-ir neurons started to emerge in MGBv.

An adult-like CaBP-distribution pattern was not achieved in the 4th pw and no double-labeling of PV-ir somata with CB or CR was present. Hence, the differential expression of CaBPs during development might indicate a successive maturation of functional aspects within the MGB.

721 Event-Related Potential Correlates of Change Deafness

Melissa Gregg¹, Joel Snyder¹

¹University of Nevada

Change deafness is the remarkably frequent inability of listeners to detect changes occurring in their auditory environment. Demonstrations of change deafness imply that our experience of the world is not as detailed as our subjective impressions would suggest. In this project, we measured event-related potentials (ERPs) to scenes consisting of naturalistic auditory objects to delineate the neural processes underlying change deafness. On each trial. listeners heard a group of four simultaneous sounds for 1 sec, followed by 350 msec of noise, and then either the same four sounds as in the first scene (no-change trial) or three of the same sounds plus a new sound (change trial). Listeners completed a change detection task by making a same/different judgment for the two groups of sounds. The behavioral data indicated substantial change deafness: There were substantially more errors on change trials (35%) than on no-change trials (3%). In change trials, ERP activity during the P1 period (90 - 130 msec) was more positive in the pre-change scene on trials in which the change was not detected. This finding suggests that change deafness is preceded by less efficient neural activity, which could result in poorer scene representations

with more overlap among the objects within the scene. ERPs to the post-change scene revealed a reduced late positivity (450 - 650 msec) for non-detected change trials, which may reflect lack of memory updating or attentional preparation during change deafness. Overall, the results provide novel information regarding the stages of processing critical for successful change detection and the cause of change detection failures in natural auditory scenes.

722 Change Deafness for the Omission of One Stream in a Multi-Tone Scene

Christian Starzynski¹, Alexander Gutschalk¹

¹Department of Neurology, University of Heidelberg

We are able to detect extremely small changes in quite, but may often fail to note supra-threshold changes of the auditory scene when multiple sound sources interact. One approach to study this phenomenon is the "change deafness" paradigm. Previous studies [e.g. Eramudugolla et al., 2005] presented multiple natural sounds, which could be identified as distinct auditory objects, and repeated the same scene with one object omitted. Listeners were able to report all omissions up to about 4 objects, but missed more and more omissions when the set size was further increased.

Here we adopted this paradigm, but used pure-tone streams instead of natural objects. To this end, pure tones with a duration of 75 ms were repeated with a randomized inter-stimulus interval of 100 - 300 ms to form coherent auditory streams. Tones were arranged in 12 discrete frequencies between 250 Hz and 5000 Hz, in equal logarithmical steps. Each stream was presented monauraly, with adjacent frequencies played to opposite ears.

In the psychoacoustic experiment, scenes with a set size of n=3, 4, 6, 8, 10, or 12 streams were played for 5 s. After an interrupting noise burst of 0.5 s, the sequence was repeated identically (20%) or with one stream omitted (80%). After each trial, listeners indicated, whether the number of streams in the first and second presentation was identical or not. Results showed that the hit rate decreased as set size was increased. The average hit rate was ~90% for n=3, decreased to ~60% at n=6, and decreased further to ~30% at n=10-12.

In the MEG experiment, participants listened passively to a set of similar stimuli, presented in blocks of 10 s. The amplitude of the P1m in auditory cortex decreased with increasing set size, similar to the behavioral response.

723 Cortical Neural Coding of Speech in Simple and Complex Auditory Scenes Nai Ding¹, Jonathan Z. Simon¹

¹University of Maryland

We study the neural coding of speech in auditory cortex by recording Magnetoencephalographic (MEG) responses of human subjects listening to a spoken narrative. For monaural stimuli, the bilateral MEG responses precisely track the slow temporal modulations and broad spectral modulations of the speech. The functional properties of this neural response can be characterized by a spectrotemporal response function (STRF). When a speech masker is dichotically presented together with the narrative (speech target), auditory cortical response tracks separate features from both the speech target and masker. Nevertheless, the neural representation of the speech target is substantially stronger than that of speech masker. The neural representation of speech is dominated by low frequencies (1-8 Hz) and is lateralized to the right hemisphere. These results demonstrate a precise and robust coding of spectro-temporal modulations in speech and also demonstrate that spatially separated speech streams are segregated in human auditory cortex.

724 Stimulus Density Dependence in the Mouse Auditory Thalamus

Ross S Williamson^{1,2}, Lucy A Anderson³, G Bjorn Christianson³, Maneesh Sahani¹, Jennifer F Linden^{3,4} ¹Gatsby Computational Neuroscience Unit, UCL, ²CoMPLEX, UCL, ³Ear Institute, UCL, ⁴Dept. Neurosci., Physiol. & Pharmacol., UCL

How does the auditory system achieve its remarkable capacity to operate in acoustic conditions ranging from almost perfect quiet to dense, complex sound environments? To address this question, we recorded extracellularly from the auditory thalamus of anaesthetised mice during presentations of spectrotemporally rich dynamic random chord (DRC) stimuli with varying spectral density (number of tone pips per octave). We quantified how the DRC-driven responses were modulated over time by decomposing the total response power (variance over time) into stimulus-dependent "signal power" and stimulus independent "noise power" (Sahani & Linden, 2003). We found that the signal power decreased as stimulus density increased, while noise power remained relatively constant. This finding indicates that a sparse stimulus is capable of eliciting greater modulation of the neural response than a dense, more complex stimulus.

We then fit the data using both linear spectrotemporal receptive field (STRF) models, and multilinear context models (Ahrens et al., 2009) capable of capturing nonlinear local interactions related to forward suppression and combination sensitivity. As the stimulus density increased, the predictive power of the linear STRF models decreased, suggesting that the neural response becomes more nonlinear as the stimulus becomes denser and more complex. The predictive power of the multilinear context models was dramatically higher than that of the linear STRF models at all stimulus densities (70-90% for the multilinear context models, 40-60% for linear STRF models), and did not change significantly as stimulus density increased. Our results show that auditory thalamic processing involves significant nonlinear local interactions in sparse as well as dense acoustic environments.

Supported by EPSRC, Gatsby Charitable Foundation, Wellcome Trust, and BBSRC.

725 Tonotopic Representation in Auditory Cortex Becomes Level-Invariant with Increasing Spectrotemporal Sound Density Martin Pienkowski¹, Jos J. Eggermont¹

Viartin Plenkowski⁺, Jos J. Eg

¹University of Calgary

In an influential paper, Phillips et al. (Exp Brain Res 102 [1994] 210-226) demonstrated a considerable mismatch between isofrequency contours drawn in cat primary auditory cortex (AI) based on unit characteristic frequencies (CFs), and AI regions activated by pure tones at suprathreshold SPLs (the higher the SPL, the bigger the mismatch). This follows primarily from the fact that most AI frequency-tuning curves units' (FTCs) broaden considerably at higher SPLs, not unlike those of auditory nerve fibers. Phillips et al. reasonably concluded that, "The representation of any tonal stimulus lies not in the isofrequency line corresponding to the test frequency, but in the spatial distribution of activity evoked by the signal. That distribution may bear little relation to the isofrequency line." (p. 223).

In contrast to FTCs derived from individual tone pip presentations at low repetition rates, AI spectrotemporal receptive fields (STRFs), derived from more dense stimulus ensembles, typically feature much sharper tuning, mostly a consequence of the nonlinear response property termed "forward suppression". Using random chord train stimulation with a mean pip presentation rate of 20 /s and a modulation spectrum resembling those of animal vocalizations and speech, Valentine and Eggermont (Hear Res 196 [2004] 119-133) found that a large majority of STRFs in cat AI had frequency bandwidths that were invariant over a wide range of SPLs.

Here we show that the mismatch between CF-based isofrequency contours and activity patterns evoked at higher SPLs is relatively small under more natural stimulation. This is true for both spikes and local field potentials evoked in anesthetized cat AI. This implies a more robust place code for sound frequency (and frequency-specific computation) in AI than has generally been supposed.

726 Neural Correlates of Auditory Scene Analysis Based on Inharmonicity in Monkey Primary Auditory Cortex

Mitchell Steinschneider¹, Yonatan Fishman¹ ¹Albert Einstein College of Medicine

Segregation of concurrent sounds in complex acoustic environments is a fundamental feature of auditory scene analysis. A powerful cue used by the auditory system to segregate concurrent sounds, is inharmonicity. This can be demonstrated when a component of a harmonic complex tone is perceived as a separate tone "popping out" from the complex as a whole when it is sufficiently mistuned from its harmonic value. The neural bases of perceptual "pop out" of mistuned harmonics are unclear. We recorded multiunit activity from primary auditory cortex (A1) of behaving monkeys elicited by harmonic complex tones that were either "in tune" or that contained a mistuned third harmonic set at the best frequency of the neural populations. Responses to mistuned sounds were enhanced relative to responses to "in-tune" sounds, thus correlating with the enhanced perceptual salience of the component. Consistent mistuned with human psychophysics of "pop out," response enhancements increased with the degree of mistuning, were maximal for neural populations tuned to the frequency of the mistuned component, and were not observed under comparable stimulus conditions that do not elicit perceptual "pop out." Mistuning was also associated with changes in neuronal temporal response patterns phase locked to "beats" in the stimuli. Intracortical auditory evoked potentials paralleled noninvasive neurophysiological correlates of perceptual "pop out" in humans, further augmenting the translational relevance of the results. Findings suggest two complementary neural mechanisms for "pop out," based on the detection of local differences in activation level or coherence of temporal response patterns across A1. Supported by DC00657.

727 Rate-Place and Temporal Representations of the F0s of Concurrent Harmonic Complex Tones in Monkey Primary Auditory Cortex

Yonatan Fishman¹, Christophe Micheyl², Mitchell Steinschneider¹

¹Albert Einstein College of Medicine, ²University of Minnesota

Many natural sounds, e.g., animal vocalizations and human speech, display harmonic structure, containing frequency components at integer multiples of a common fundamental frequency (F0). When two harmonic complex tones (HCTs), such as vowels or musical sounds, occur simultaneously, the auditory system must disentangle the resulting acoustic mixture to recover the properties (pitch, timbre, loudness) of each constituent source. A difference in F0 between two concurrent HCTs, such as two voices, serves as a powerful cue for their segregation. While abundant spectral (rate-place) and temporal (phaselocking) information relating to the F0s of concurrent HCTs is present at the level of the auditory nerve (e.g., Larsen et al., 2008), it remains unclear how well the F0s of concurrent HCTs are represented at the cortical level. we evaluated rate-place and Here, temporal representations of the F0s of concurrent HCTs in primary auditory cortex (A1) of awake macaques using a stimulus design employed in auditory-nerve studies (Larsen et al., 2008). We examined multiunit responses to single and double concurrent HCTs, each containing 12 equalamplitude harmonics (60 dB SPL/component), and with an F0 difference of 4 semitones, which is sufficient for their perceptual segregation. Using the principle of scaling invariance, F0 was varied in small increments (1/8 harmonic number), such that harmonics of the HCTs either fell on the peak or on the sides of the neuronal pure-tone tuning functions. Resultant rate-versus-harmonic number functions displayed a periodic pattern reflecting lower, resolved harmonics of the HCTs. From this pattern, the F0s of the two HCTs could be recovered using harmonic templates. F0s below 350 Hz were also represented in

temporal discharges phase-locked to the periodicities of the HCTs. Findings suggest that spectral and temporal information sufficient for segregating concurrent HCTs based on a difference in F0 is available at the level of A1.

728 The Role of Interactions Between Excitatory and Inhibitory Receptive Field Components in Encoding Harmonic Structures in Auditory Cortex of Awake Marmosets

Lei Feng¹, Xiaoqin Wang¹

¹Johns Hopkins University

Many natural and man-made sounds, such as animal vocalizations, human speech and music, contain harmonic structures. Although the peripheral auditory system searegates sounds into narrow frequency channels, harmonically related frequency components of a complex sound need be grouped together by the central auditory system to form a single percept. Previous studies with single tone and two-tone stimuli showed that some neurons in auditory cortex have excitatory and inhibitory inputs from frequencies that are harmonically related to the characteristic frequency (CF) of a neuron. However, it remains unclear how such neurons extract the harmonic structure of a complex sound and whether their properties reflect an orderly organization in auditory cortex. In the present study, we systematically examined how harmonic structures were processed by single neurons in auditory cortex of awake marmoset (Callithrix Jacchus) using harmonic tone complexes of different fundamental frequencies and random harmonic tone stacks (RHS) that contained harmonic components with randomized amplitudes. From the responses to these stimuli, we calculated linear spectral weights to determine the extent of excitatory and inhibitory inputs at each harmonic frequency and estimated the harmonic structure that a neuron preferentially responded to. We found that a subpopulation of neurons in the primary auditory cortex selectively responded to harmonic tone stacks of certain fundamental frequencies. The RHS response also showed that harmonic excitatory and inhibitory inputs to such neurons were organized along the frequency axis in such a way that they could extract particular harmonic spectral structures by a rate code. Our findings suggest that the interaction between harmonically related excitatory and inhibitory receptive field components of single neurons in auditory cortex helps extract harmonic spectral structures of complex sounds.

729 Nonlinear Temporal Processing of Natural Sounds in Auditory Cortex

Stephen David¹, Nima Mesgarani², Shihab Shamma¹ ¹University of Maryland, ²University of California

A major goal of sensory neuroscience is to understand how the brain represents and extracts information from complex natural stimuli. General predictive models that map the functional relationship between arbitrary complex stimuli and neural responses provide one approach to this problem. However, this approach has been limited by problems of dimensionality. Models that make few assumptions about mechanism tend to require a large number of parameters. Low-dimensional models that explicitly model important mechanisms in fewer parameters should, in theory, perform well, but knowing a priori which mechanisms are important is not possible. Here we describe an iterative approach that uses complex nonlinear models focused in a limited stimulus domain to identify key mechanisms that can subsequently be tested in a more general model framework.

Previous studies of primary auditory cortex (A1) have suggested that a major limitation of current models is their ability to predict the nonlinear temporal dynamics of neural responses. In recent experiments, we have collected data from A1 using a reduced-dimensionality stimulus composed of band-pass noise modulated by a natural sound envelope. This stimulus permits fitting models that span only a single spectral dimension, leaving more power to model complex temporal integration. The resulting fits suggest that both feedforward synaptic depression and interactions between co-tuned excitatory and inhibitory inputs play a role in neural response dynamics. The same nonlinear mechanisms may also explain robust A1 responses to speech embedded in a noisy background. Ongoing work is implementing these mechanisms explicitly in more general spectro-temporal models.

730 Spatial and Non-Spatial Sound Processing in the Primary Auditory Cortex of Awake Marmoset

Yi Zhou¹, Xiaoqin Wang¹

¹Laboratory of Auditory Neurophysiology, Dept. of

Biomedical Engineering, Johns Hopkins University

A realistic listening environment often consists of multiple sounds with distinct spectro-temporal features from variable spatial locations. However, it remains unclear how the auditory system delineates spatial and non-spatial features in a multisource acoustic environment. In this study we examined (1) structural details of spatial receptive field (SRF) in the primary auditory cortex (A1) of awake marmoset and (2) frequency selectivity of A1 neurons across space using a two-speaker method. Our results showed an extended inhibitory region in SRFs, and similar frequency selectivity at center and surround locations of SRFs. These findings indicate that the spatial selectivity of A1 neurons is constrained by inhibitory mechanisms under conditions with multiple sounds.

Considering that directional filtering of head and pinna introduces considerable irregularity in sound spectrum at the eardrums, we proposed that location-invariant frequency selectivity observed in A1 resulted from an internal spectrum-equalization mechanism for extracting the non-spatial features of sound. To test this hypothesis, we compared SRFs of a neuron in response to pure-tone and broadband noise stimuli. A greater mismatch occurred when pure-tone frequencies were within the spectral notch region of marmoset HRTFs relative to those outside, suggesting involvement of spectral-notch sensitive neurons in the spectrum equalization process. Overall, this study showed that A1 neurons are capable of simultaneously encoding spatial and non-spatial attributes of sounds. The effect of spectral content on spatial tuning provides evidence that the neural mechanisms sustaining the spatial and non-spatial aspects of sound analyses are inseparable in the primary auditory cortex. [Supported by NIH grant DC03180 (X.W.).]

731 Neural Correlates of the Lombard Effect in the Primate Auditory Cortex

Steven Eliades¹, Xiaoqin Wang¹ ¹Johns Hopkins University

Speaking is a sensory-motor process involving selfmonitoring of vocal feedback to correct perceived differences between intended and produced vocalizations in order to ensure accurate vocal production. The Lombard effect is an important auditory-vocal behavior in which subjects increase vocal intensity in responses to noise masking during speaking. This behavior requires mechanisms for continuously monitoring auditory feedback during vocal production. Such mechanisms are poorly understood. We examined the activities of neurons in the auditory cortex of marmoset monkeys (Callithrix jacchus) during vocal production in the presence of masking noise that gave rise to the Lombard effect. The disruption of auditory feedback by masking noise altered the response properties of neurons in the auditory cortex. Both vocalization-induced suppression and excitation were reduced as a result. These changes in neural activity were not predicable from the sensory responses of auditory cortex neurons. When the marmosets increased their vocal intensity as a result of the Lombard effect, there were further changes in neural activity in auditory cortex that compensated the effects of the masking noise. These observations suggest that the auditory cortex participates in self-monitoring of auditor feedback and plays a role in feedback-mediated vocal control behaviors like the Lombard effect.

732 Bilateral Cholinergic Lesions in the Nucleus Basalis Impair Sound Localization and Learning-Induced Plasticity

Nicholas D. Leach¹, **Victoria M Bajo Lorenzana¹**, Patricia M. Cordery¹, Fernando R. Nodal¹, Andrew J. King¹ ¹University of Oxford

Cortical cholinergic modulation has been implicated in a number of functions, including experience-dependent cortical plasticity and the processing of sensory stimuli under challenging circumstances. This study investigated the role of acetylcholine in auditory perception (sound localization in azimuth) and plasticity (adaptation to unilateral an earplug). Adult ferrets were trained on an approach-to-target localization task using spectrallyrandomized broadband noise bursts (0.5-30 kHz) of differing duration (40-2000 ms). Their ability to adapt to the altered spatial cues produced by occluding one ear was also tested.

Cholinergic impairments were induced with bilateral injections of the neurotoxin ME20.4-SAP into the nucleus basalis (NB), resulting in substantial loss of both p75^{NTR}-and choline acetyltransferase-positive cells in the nucleus

itself and of acetylcholinesterase-positive fibres in auditory cortex. Compared to control ferrets, animals with confirmed lesions were significantly impaired in their ability to localize broadband sounds, particularly at shorter stimulus durations, making fewer correct responses over all stimulus locations, which were accompanied by larger mean unsigned errors and a greater incidence of frontback errors. No changes in the accuracy of sound-evoked head-orienting movements were apparent, however, suggesting that the cholinergic lesioned animals suffer from a perceptual rather than a sensorimotor deficit. These animals were also less able to adapt to perturbed spatial cues introduced by occluding one ear. After training they exhibited less complete recovery of localization performance than control animals, adaptation taking place at a substantially slower rate.

We conclude that cholinergic efferents arising in the NB exert a substantial effect on sensory processing, particularly for shorter duration stimuli, and modulate the ability of adult ferrets to relearn to localize sound in the presence of altered binaural cues.

733 Experimentally-Induced Unilateral Conductive Hearing Loss Substantially Alters the Interaural Level and Time Difference Cues to Sound Location

Jennifer Thornton¹, Keely Chevallier², Kanthaiah Koka³, Eric Lupo⁴, Daniel Tollin^{3,4}

¹Neuroscience Training Program, University of Colorado Denver, ²University of Colorado Denver School of Medicine, ³Dept. of Physiology and Biophysics, University of Colorado Denver, ⁴Dept. of Otolaryngology, University of Colorado Denver

Otitis media with effusion (OME) is a pathologic condition of the middle ear that leads to a mild conductive hearing loss (CHL) as a result of fluid filling the middle ear space. Recurring OME in children during the first few years of life has been shown to be associated with poor detection of sounds in a noisy environment, which is hypothesized to result due to altered cues to sound localization. To explore this hypothesis, the middle ear space of adult chinchillas (n=7) was filled with different viscosities of silicone oil to simulate varying degrees of OME. Cochlear microphonic (CM) recordings were measured to determine the effects that silicone oil in the middle ear had on binaural sound localization cues. Previous studies have used similar methods to determine what effects OME has on interaural level difference (ILD) cues, but little work has been done to understand how OME affects interaural time difference (ITD) cues. In this study, CM amplitudes and phases were measured in response to sinusoidal tone pip stimuli (0.125-12 kHz) delivered from 25 different locations in azimuth both before and after filling the middle ear with different volumes (0.5-2.0 mL) and viscosities (50 cSt-60,000 cSt) of silicone oil. Across animals, significant attenuations of sound (i.e., CM amplitude reductions) were observed at all viscosities relative to baseline measurements. Significant attenuation of sound (20-40 dB) was seen when the middle ear space was filled with at least 1.0 mL of 350 cST (or above) viscous silicone oil. As expected, the ILD cues to

location were shifted by ~ 40 dB. In addition, the ITD cues were shifted by ~600 μ s across all locations in azimuth for low frequency stimuli (<4 kHz). Both the ILDs and ITDs were consistently shifted in the direction of the ear that did not have fluid in the middle ear space. The data demonstrate that in an experimental model of OME, both the ILD and the ITD cues to sound location can be substantially altered. Support: NIDCD F31 DC011198-01

734 Adaptive Plasticity of Sound Localization in Cats

Amy Hong¹, Janet Ruhland¹, Tom Yin¹

¹University of Wisconsin

Azimuthal sound localization relies on interaural disparities in time of arrival and level of sound at the ear. Vertical localization, however, relies on spectral cues from the direction-dependent filtering properties of the head and pinnae, or head-related transfer function (HRTF). Perturbation of spectral cues by pinna occlusion in humans and ferrets dramatically diminishes localization performance. Here, we studied whether cats are able to adapt to new spectral cues. We constructed bilateral custom ear molds for the cats, altering their HRTFs. The cats localized noise targets along the horizontal and vertical plane with head unrestrained gaze shifts. The accuracy of localization performance is summarized by the slope of the linear regression relating the localization responses of the cats to corresponding target positions. Both the horizontal and vertical components of saccadic gaze shift responses with the head unrestrained were guite accurate before application of the ear molds. Localization accuracy had appreciably declined once the ear molds were inserted during testing, especially for the vertical components of both the horizontal and vertical targets. Approximately two weeks after introducing the new spectral cues, we added bimodal (light plus noise) trialtypes to provide visual feedback. Within a week, localization accuracy of the auditory only trials had significantly improved for the vertical component of horizontal targets with only slight improvement in accuracy for the vertical component of vertical targets. Longer latencies exhibited after ear mold application indicate a greater difficulty in localizing sounds in elevation. Results show that cats appear to be capable of adapting to new spectral cues.

Supported by NIH grant DC07177.

735 Learning to Localize Band-Limited Sounds in Vertical Planes

Piotr Majdak¹, Thomas Walder¹, Bernhard Laback¹ ¹Austrian Academy of Sciences

Sound localization in the vertical planes, including the ability to distinguish front from back, relies on spectral cues described by so called head-related transfer functions (HRTFs). It is assumed that the presence of spectral cues above 8 kHz is important for accurate vertical-plane sound localization. Studies on the effect of bandwidth have been performed acutely and potential adaptation effects were not considered. Given that humans' auditory system is usually exposed to broadband sounds, it is not clear if it

may also adapt to other bandwidths. Previous studies have shown that the auditory system is able to re-learn sound localization based on modified spectral cues. Hence, it is unclear if the effect of the stimulus bandwidth is based on the limited availability of spectral cues or due to long-term adaptation to broadband sounds.

In this study, normal-hearing listeners were trained on sound localization using 8-kHz-band-limited noise filtered with subjects' individual HRTFs. Audio-visual training covering the full 3-D space was performed two hours per day over three weeks. The performance was tested in a pre-test, daily during the training, and in a post-test. HRTFs with strongly-modified spectral cues were included as a control condition.

For broadband stimuli, localization performance (front-back confusion rate and localization blur) was similar to that from previous studies. In the pre-test, the performance relative to the broadband condition was significantly degraded for the band-limited condition and even more for the control condition. Over the course of the training, the performance for the band-limited condition significantly improved, ending up approximately at the performance found for broadband stimuli in the post-test.

These results show that humans are able to learn accurate sound localization with 8-kHz-band-limited stimuli. This may have implications for hearing-impaired listeners using hearing aids with restricted bandwidth.

736 Early Cochlear Implantation Promotes Faster Sound Localization Development

Filip Asp^{1,2}, Gunnar Eskilsson², Erik Berninger^{1,3} ¹Department of Clinical Science, Intervention and Technology, Karolinska Institutet, ²Department of Cochlear Implants, Karolinska University Hospital, ³Department of Audiology, Karolinska University Hospital

This study was initiated to understand which factors that contribute to sound localization performance in children fitted with bilateral cochlear implants (BiCls). Sixty-six subjects (62 sequentially implanted) with a median age of 5.6 years (2.8 years - 17.3 years), were tested in a 5loudspeaker sound localization task spanning the frontal horizontal plane from -90 to 90 degrees azimuth. Forty-five subjects were tested once, while 21 subjects were tested at several occasions. The effects of BiCl experience, interimplant interval and ages at implantation of the first and second implant on sound localization performance were evaluated. BiCI experience was the most important factor for sound localization performance and the subjects who received the second implant before 4 years of age revealed twice as fast sound localization development than those who received the second implant after 4 years of age. This means that the subjects who had listened longer with BiCIs localized better than those with shorter listening time, and that an early implantation of the second ear promoted a more rapid improvement of sound localization. Both findings were confirmed for the entire study group as well as intra-individually. In addition, the subjects who received their first implant before 2 years of age showed significantly better sound localization performance than the subjects who were implanted with the first implant after 2

years of age. The results have both clinical and methodological implications, i.e. early implantation may be important in order to develop sound localization and children with longer experience of BiCls are likely to perform better in a sound localization task.

737 An Unsupervised Learning Approach to **'What and Where' in the Auditory System Nicol Harper**^{1,2}, Bruno Olshausen¹

¹Redwood Center for Theoretical Neuroscience, University of California, ²Department of Physiology, Anatomy, and Genetics, University of Oxford

Determining 'what and where' for a sound is key to an animal's survival, and central to the function of the auditory system. Sounds reach our ears after being convolved by the head related impulse response (HRIR). The HRIR depends on the direction of the sound, and is caused by the acoustic properties of the outer ear and head. A useful calculation for the brain would be to disentangle this convolution, allowing the animal to locate the sound position and identify the source. In many cases it is likely that the brain must do this: 1) for natural sounds 2) without an explicit training signal 3) without hard-wired knowledge of the exact HRIRs and sources and 4) using both ears but capable with one ear. We present a model that, with these restrictions, aims to disentangle this convolution and represent the sound in a form useful for localization and identification.

The idea behind the model is efficient sparse representation - representing the sound with few of the representational variables being non-zero. The input to each 'ear' in the model is a smoothed log spectrogram of the convolution of an HRIR and a natural sound - this takes advantage of the log power-spectrum of a convolution being a sum. The input log spectrogram is separated into the HRIR log power-spectrum and the source log spectrogram by fitting a generative model to the input, subject to a sparseness penalty on the model's latent variables. The model is the sum of an HRIR model, a source model, and Gaussian noise. The HRIR model is the latent variable-weighted sum of basis functions that differ at the two ears. The latent variables are the same over all time-segments of the spectrogram as the HRIR changes slowly with time. The source model is also the sum of latent variable-weighted basis functions, but the same at both ears. Here the latent variables differ over time-segments because the source can change quickly over time. Through inferring many different HRIR log power-spectra and source log spectrograms, the model learns basis functions that allow for efficient representation. For both monaural and binaural inputs, the model is able to recover to some approximation the HRIR log power-spectra and source log spectrograms. The latent variables for the HRIR model show spatially selective tuning curves. Tests of the model, and neurally plausible implementations will be discussed.

738 Adaptation of Sound Localization in the Direction of Eye Movement Is Linearly Related to Ocular Eccentricity

Kathryn Cooper¹, William O'Neill^{2,3}, Gary Paige^{2,3} ¹Neuroscience Program, College of Arts, Sciences and Engineering, University of Rochester, ²Dept. of Neurobiology & Anatomy, Center for Navigation & Communication Sciences, ³University of Rochester School of Medicine and Dentistry

Spatial information is encoded by very different mechanisms in the auditory and visual systems, yet the two modalities are integrated to give a unified sense of space. Visual space is mapped on the retina in eyecentered spherical coordinates, while auditory space is computed centrally and mapped in head-centered coordinates. Since the eyes move relative to the head and thereby misalign the two sets of coordinates, the brain must account for eye position to maintain space constancy.

In previous studies, we showed that prolonged eccentric eye position shifts the perception of auditory space in the same direction as ocular deflection (Qi et al., J Neurophysiol 103: 1020-35, 2010). This shift occurs in both azimuth and elevation, develops exponentially over several minutes, approaches 40% of ocular deflection, and extends to all spectral localization channels.

It is well established that eye position is linearly related to the activity of oculomotor neurons and extraocular muscles. The previous studies were all conducted at a single 20° ocular deflection angle. Here we determined whether the shift in auditory perception also grows linearly with increasing ocular eccentricity. Subjects localized auditory targets while fixating at azimuths of $\pm 10^{\circ}$, $\pm 20^{\circ}$, and $\pm 30^{\circ}$. The results showed that the average shift in auditory spatial perception across subjects was indeed linear with respect to eye position (R^2 = 0.9846), with shift magnitude approaching 35% of ocular deflection.

Current experiments are testing whether auditory space shifts in the absence of any visual fixation reference. Subjects localize the same set of targets as in the paradigm above, and maintain fixation after the fixation target is extinguished. Results so far show that auditory space also shifts in the direction of eye position in the absence of visual input, further supporting a purely oculomotor origin for this phenomenon.

Supported by NIH grants RO1-AG16319 and P30-DC05409 (Ctr. Nav. & Comm. Sciences)

739 The Vestibulo-Auricular Reflex (VAR) in Gaze Shifts to Proximal, Contralateral, and Vertical Targets

Janet Ruhland¹, Amy Hong¹, Tom Yin¹ ¹University of Wisconsin-Madison

We have previously described a compensatory counterrotation of the ear on the head that stabilizes the direction of the ear in space while cats localize peripheral (>15 deg) horizontal sounds and lights ipsilateral to that ear during rapid head-free gaze shifts (active VAR), and also during passive head movements made while the cat is rotated on a platform (passive VAR) (Tollin et al., 2009). The VAR has characteristics similar to the well-studied vestibuloocular reflex (VOR). Currently we investigate the active VAR during saccades to vertical, contralateral and more central (<15 deg) auditory targets. Cats were trained using operant conditioning to indicate apparent target locations via a gaze shift. Implanted search coils in the eyes, on the head, and behind the pinnae were used to monitor eye, head and ear position with the magnetic search coil technique. As previously shown, as the cats actively located ipsilateral targets in the frontal hemifield, the active VAR occurred about 80% of the time; i.e. the ipsilateral pinna exhibited short-latency, goal-directed movements towards the location of the target, which was followed shortly by a gaze shift (combined head and eye movement) during which the pinna maintained a fixed position in space by counter-rotating on the head with a velocity equal and opposite to the head movement. The incidence and gain of the VAR was highest for peripheral (>15 deg) ipsilateral targets and decreased for more central (<15 deg) ipsilateral targets, for vertical targets and for contralateral targets. In addition there was more variability between and within cats for the occurrence of the VAR in saccades to proximal and vertical targets. Supported by NIH grant DC07177

740 Cortisol Levels and Verbalization in High-Functioning Autism

Erikson G Neilans¹, Martin A Volker¹, Susan K Putnam², Marcus L Thomeer², Jennifer A Toomey³, Jonathan D Rodgers¹, Christopher Lopata²

¹SUNY University at Buffalo, ²Institute for Autism Research, Canisius College, ³Summit Educational Resources

Autism Spectrum Disorders are characterized by three domains of pathology which include 1) restricted repetitive and stereotyped patterns of behavior, interests and activities, 2) impairments in communication, and 3) impairment in social interaction. This study focused on the possible factors that may influence impaired social interactions. Studies have shown that individuals with ASDs secrete higher levels of cortisol during the day when compared to typical peers. It has been hypothesized that davtime school attendance and being subjected to a highly social environment may be contributing factors to the hyper-release of this stress-response hormone. There have also been numerous studies that have found a relationship between higher cortisol levels and decreased vocalizations in bulls, guinea pigs and a special population of human children with retardation. The current study examined the relationship between cortisol levels and frequency of verbalizations in a sample of children with high-functioning autism spectrum disorders (n=17). These children participated in two gaming sessions, each of which involved 20 minutes of playing UNO followed by a salivary cortisol collection. The videotaped game sessions were transcribed and the frequency of spoken words was then matched with the salivary cortisol measures. The results indicated a significant decrease in the frequency of verbalizations when cortisol levels were high and an increase in the rate of verbalizations when cortisol levels were low.

741 Sizing Up the Competition: Quantifying the Influence of the Mental Lexicon on Spoken Word Recognition

Julia Feld¹, Dennis Barbour¹, Mitchell Sommers¹

¹Washington University Given the enormity of the mental lexicon [minimum estimates suggest at least 40,000 words in the average adult lexicon (Aitchison, 2003)], discriminating between the appropriate lexical item and all other items in memory is a large and complex task. Remarkably, most humans are able to complete this task in an almost instantaneous and effortless fashion. A wealth of research has sought to describe the process by which information from the speech signal activates words in memory, how a specific word is selected from among the activated words, and how the Activationproperties of words influence recognition. Competition models of spoken word recognition [Neighborhood Activation Model (Luce & Pisoni, 1998); TRACE (McClelland & Elman, 1986)] propose that acoustic-phonetic input from a stimulus word activates a set of perceptually similar lexical candidates in memory, and that these lexical candidates compete for recognition. This lexical competition has been quantified using both continuous measures (e.g., assessing the perceptual similarity of two words using the probability that their segments will be confused) and categorically (e.g., establishing a cutoff of similarity, such as a single phoneme substitution) (Luce & Pisoni, 1998). The current research evaluated methods for quantifying lexical competition using metrics that are well-established in the literature as well as a novel statistical method for calculating lexical competition, based on the Phi-square statistic. The Phi-square statistic proved an effective measure for assessing lexical competition and explained significant variance in spoken word identification beyond that accounted for by traditional metrics. Because these values include the influence of many words in the lexicon (rather than only perceptually very similar words), it suggests that even perceptually dissimilar words may receive some activation, and therefore provide competition, during spoken word recognition.

TAD The Interaction of Envelope and Temporal Fine Structure Cues in Speech Perception

Rasha Ibrahim¹, Ian Bruce¹

¹McMaster University

The role of temporal fine structure (TFS) in speech perception has been the subject of much recent investigation and debate. Lorenzi et al. (PNAS 2006) utilized a vocoder scheme aimed at flattening the envelope in each frequency band, producing "TFS speech". They reported that normal-hearing listeners could learn over several sessions to understand TFS speech quite well, while perception by hearing-impaired listeners remained poor. However, speech envelope cues could be partly reconstructed by passing TFS speech through the narrowband filters of the normal cochlea, bringing into question the interpretation of these results.

Smith et al. (Nature 2002) created an alternative form of processing that uses a pair of vocoders to produce "auditory chimaeras" having the TFS of one signal and the envelope of another. This has the potential to at least partially mask any envelope reconstructed by cochlear filtering of the TFS signal. However, because of the different experimental paradigms utilized, it is not possible to directly compare the results of the two studies.

In our study, we compared perception of TFS-only speech with that of speech-noise chimaeras in a group of 5 normal hearing subjects. NU-6 words were processed to generate five types of chimaeras: i) speech envelope + white Gaussian noise (WGN) TFS; ii) speech envelope + matched-noise (MN) TFS; iii) speech TFS + WGN envelope; iv) speech TFS + MN envelope; and v) TFS-only speech. For each chimaera type, we utilized 50 words for 7 different cases of the number of vocoder filters used, giving a total of 1750 words tested. An ANOVA on phoneme recognition scores shows large significant effects of chimaera type and number of filters (p << 0.001 in both cases). Perception of the speech TFS + MN envelope chimaeras was worse than that of TFS-only speech, consistent with the hypothesis that reconstructed envelope cues contribute substantially to the perception of "TFS speech".

[Supported by NSERC DG 261736.]

743 Level- And F0-Based Segregation in a Three-Talker Sequential Listening Task

Nandini lyer¹, Douglas S. Brungart², Brian D. Simpson¹ ¹Air Force Research Laboratory, ²Walter Reed Army Medical Center

The impacts of pitch and level differences on sequential stream segregation were examined in a task that interleaved a five-word target speech signal on a word by word basis with two five-word masking phrases. For both the pitch and level difference cues, performance was best when the masking voices were set to the same parameter value and they were maximally separated from the target. However, pitch and level had very different effects on sequential stream segregation in cases where the target fell in between the two maskers. When the pitch of the target voice was systematically varied between the F0 values of a lower-pitched masker and a higher-pitched masker, performance was best when the target F0 was in between the two masker F0s. However, when the level of the target voice was systematically varied between the level of a quieter masker or a louder masker, performance was worst when the target was between the two voices and best when the target level matched the level of one of the two maskers. These results show that it is not possible to predict the sequential segregation of voices simply from the perceptual salience of the differences between the competing speech streams.

T44 The Effect of Manipulating Masker Intelligibility on the Shape of the Psychometric Function for Masked Speech Alexandra Woodfield^{1,2}, Michael Akeroyd¹

¹MRC Institute of Hearing Research (Scottish Section), ²University of Strathclyde

Speech-in-noise difficulties are common for many older listeners. While increasing the level of the target speech in comparison to the background noise usually helps to improve target speech intelligibility, the rate of this improvement is dependent on the type of background noise. Speech backgrounds often result in shallower rates of improvement -- i.e. shallower psychometric functions -than noise backgrounds. This experiment examines whether this effect is due to speech backgrounds containing intelligible words which may become confused with those of the target speech. This was tested using vocoded speech maskers whose intelligibility could be smoothly varied from completely intelligible to completely unintelligible.

17 older listeners (mean age = 69) and 7 younger listeners (mean age = 27) took part in the study. Target sentences were presented in the presence of a masker at a range of target-to-masker ratios. Maskers were 12-channel noise vocoded sentences, which were either intelligible or unintelligible. In the intelligible maskers all 12 channels came from one sentence, but in the unintelligible maskers channels 1-2 came from one sentence, channels 2-3 from a second sentence, and so on. Listeners were asked to identify key words from the target sentences, from which data 7-point psychometric functions were measured and their slopes calculated.

The results showed that slopes were shallower in the intelligible masker (4.7%/dB) than in the unintelligible masker (5.7%/dB) for older listeners. No such difference was seen for the younger listeners, however. Control conditions with maskers of natural speech and static noise gave slopes of 4.1%/dB & 12.9%/dB (older) or 4.8%/dB & 11.3%/dB (younger). No overall effect of age was found. Given the smallness of the difference in slopes between the intelligible and unintelligible maskers, the results demonstrated that masker intelligibility alone is unlikely to account for the shallow slopes seen for speech maskers.

T45 The Personnel Speech Recognition at Various Release Times on Automatic Gain Control

Semi Hwang¹, Yuyong Jeon¹, Heonjin Park², Kyusung Kim³, Sangmin Lee^{1,4}

¹Department of Electronic Engineering, Inha University, ²Department of Statistics, Inha University, ³Department of Otolaryngology-Head & Neck Surgery,Inha University School of Medicine, ⁴Institute for Information and Electronics Research, Inha University

Most people with cochlear hearing loss experience loudness recruitment due to a reduced dynamic range. The major role of automatic gain control(AGC) is to decrease the range of sound levels in the environment to better match the dynamic range of a hearing impaired person. AGC consists of main 4 factors: compression threshold, compression ratio, attack and release time. Many studies for the time factor, especially release time, have evaluated the word recognition score(WRS) or preference at just only 3 or 4 different release times and just with hearing impaired listeners. In this study, we try to compare two groups of people, the normal hearing and hearing impaired. And we assume that each person has their own optimum release time for the highest intelligibility. To consider more details, we subdivide into 7 release time, which are 0, 12, 64, 128, 512, 2094, and 4096ms. Twelve normal hearing twelve hearing impaired listeners and are participated. The word sets consist of 7 lists of one syllable words in quiet and 21 lists of sentences with 12, 6 and 0dB SNR, each of which has the same equal loudness, respectively. As a result, each group has differences in WRS as release time and SNR condition are changed. From the individual point of view, each person has the best speech score of intelligibility at a specific release time. And that score could be changed by each noisy condition. This feature can be seen with 90 percent of the people in the second trial. In conclusion, each group has significant differences and each person has an optimum release time for the best speech recognition in each SNR condition. If the hearing aids are set by the optimum release time in each person, it is more helpful for communication through speech. [This work was supported by the grant from the Korea Health 21 R&D Project, Ministry of Health & Welfare, Korea (A091039) and this study was supported by a grant of the technology R&D project, SMBA, Republic of Korea (S1057576).]

746 Is There a Relationship Between Olivocochlear Efferent Feedback and Hearing-In-Noise Ability?

Jordan Schramm¹, Anne Luebke²

¹University of Nebraska Medical Center, ²University of Rochester Medical Center

Approximately 17% of American adults report difficulty hearing in a noisy environment. The medial olivocochlear (MOC) efferent system, which provides efferent neural feedback from the midbrain to the inner ear, has been hypothesized to improve hearing in background noise. Collet and his colleagues tested this hypothesis by measuring MOC efferent feedback non-invasively using otoacoustic emission suppression, and revealed a relationship between MOC efferent feedback strength and the ability to detect (1) multi-tone complexes in noise (Micheyl et al. 1995); (2) pure tones in noise (Micheyl & Collet, 1996); and (3) intensity discrimination in noise (Micheyl et al. 1997). Kumar & Vanaja (2004) also revealed in children a relationship between speech perception in noise and MOC efferent strength. Contradictory results were recently obtained by Zenner et al., who found that speech-in-noise intelligibility did not correlate with MOC efferent strength (Wagner et al. 2008). One difficulty in comparing these studies is that Collet's group used transient-emmitted otoacoustic emissions (TEOAEs), while Zenner's group used distortion product otoacoustic emissions (DPOAEs). Furthermore, all previous studies only measured the contralateral suppression effects of MOC efferents rather than their binaural effects. We embarked on this study to settle this controversy. We enrolled adults (n=56) ages 18 to 30, and all subjects were tested for their pure tone thresholds, speech-in-noise ability, and MOC efferent feedback Speech-in-noise intelligibility was measured strenaths. using the Hearing-in-Noise Test (HINT). MOC efferent feedback was evaluated by measuring changes in amplitude induced by a binaural broadband suppressor for both TEOAEs and DPOAEs. Our results indicate that a left ear advantage in MOC efferent feedback strength did correlate with enhanced speech detection in noise ability. Supported by grants from NIH [R01 DC003086, P30 DC005409, and KL2 RR024136]

747 Spectral Cues for Mismatch Detection in Voice Pitch Auditory Feedback

Roozbeh Behroozmand¹, Oleg Korzyukov¹, Charles Larson¹

¹Northwestern University

It has been hypothesized that the motor system issues a copy of motor commands, referred to as efference copy, to predict sensory feedback arising from self-generated movement. By means of comparing the predicted and actual sensory feedback, the system can detect and correct for motor errors. Studies have provided evidence for such a feedback-based mechanism for voice control by showing that pitch shifts in voice auditory feedback elicit compensatory vocal responses that change voice fundamental frequency (F0) in the opposite direction to the pitch perturbation. However, during pitch shifts, not only the voice F0 but all of its harmonics (H1, H2, H3, etc.) are shifted. In the present study, we investigated which of these spectral components may contribute to pitch shift detection. Event related potentials (ERPs) were recorded in response to mid-utterance pitch shifts (200 cents magnitude, 200 ms duration) during sustained vocalization of the vowel sound /a/. Voice feedback complexity was manipulated by modifying auditory feedback with a pure tone at the F0 frequency, complex tones including F0+H1, F0+H1+H2, F0+H1+H2+H3 frequency components or subjects own voice. Results showed that the P2 responses (~200 ms after pitch shift) had smaller amplitudes for the simple (pure tone at F0) compared with complex (F0 with harmonics or voice) feedback. No difference was observed in P2 responses to pitch-shifted feedback including F0+H1, F0+H1+H2 or F0+H1+H2+H3 components. However, P2 responses were larger for pitch shifts of the subject's own voice than for the simple (F0) and complex (F0 with harmonics) feedback. These findings suggest that F0 may not be the only and best spectral cue for pitch shift detection in voice auditory feedback. In fact, the audiovocal system may benefit from information embedded in the harmonic components that give the voice feedback its complex structure. The system's performance is further improved for voice feedback which has it natural texture.

TAB The Neural System Supporting the Enhancement by Attention of the Processing of Degraded Speech

Conor Wild¹, Afiqah Yusuf^{1,2}, Daryl Wilson¹, Jonathan Peelle³, Matthew Davis³, Ingrid Johnsrude^{1,4}

¹Queen's University, ²McGill University, ³MRC Cognition and Brain Sciences Unit, ⁴Linköping University

Most real-world communication involves conversing in the presence of competing stimuli, and hearing speech when attention is elsewhere. We used fMRI to examine the degree to which unattended speech is processed, and whether such processing depends on the clarity of the speech. On every trial, subjects attended to one of three simultaneously presented stimuli: a sentence, an auditory distracter, or a visual distracter. Speech stimuli consisted of English sentences presented at one of four intelligibility levels: clear speech, six-band noise-vocoded speech (NVS; highly intelligible), compressed six-band NVS (marginally intelligible), and spectrally rotated NVS (always unintelligible). The Attention and Intelligibility factors were crossed to yield 12 conditions. We used a sparse-imaging procedure, with whole-brain EPI volumes acquired every 9 seconds and stimuli presented in the silent intervals between 2-second scans, with 21 volunteers (age 19-27 years). Following the scanning session, we tested recognition of the presented sentences from all conditions using an old/new discrimination task. The behavioral data indicate that whereas clear speech can be processed even when it is not attended, the processing of moderately intelligible speech is enhanced by attention, allowing it to be better remembered later. When attention was directed towards speech, activity in regions of bilateral superior temporal cortex correlated positively with the intelligibility of spoken sentences and activity in left inferior frontal cortex was elevated for degraded, compared to clear, speech, replicating previous studies. An interaction between Attention x Intelligibility was observed in left temporal and inferior frontal cortex: activity elicited by degraded speech was enhanced in the presence of attention. In contrast, activity in speech-sensitive regions around primary auditory cortex did not depend on attention. We conclude that activity in peri-auditory areas reflects automatic processing that can nonetheless be enhanced by attention, whereas the processing of degraded speech by inferior frontal regions, which are at a higher level in the anatomical (and functional) hierarchy, is less automatic and requires attention.

749 A New Channel-Selection Criterion for Better Speech Recognition in Reverberation by Cochlear Implant Users

Kostas Kokkinakis¹, Oldooz Hazrati¹, Philipos C. Loizou¹ ¹University of Texas at Dallas

The maximum channel-selection criterion used in the ACE strategy (Cochlear Ltd) works well in quiet environments, however, it is quite vulnerable to the effects of reverberation, particularly during unvoiced segments (e.g., stops) of utterances. This is because the ACE strategy mistakenly selects the channels containing reverberant energy since those channels have the highest energy. In this study, we propose a new speech coding strategy for reverberation suppression using a new channel-selection criterion based on the signal-to-reverberant ratio (SRR) of individual frequency channels. The SRR index reflects the ratio of the energies of the signal originating from the early reflections and the signal originating from the late reflections. In the proposed strategy, channels with SRR greater than a preset threshold are selected, while channels with SRR values smaller than the threshold are eliminated. For reverberant voiced segments (e.g., formants), the proposed strategy operates similar to the ACE strategy. However, for unvoiced sounds (e.g., fricatives, stops and stop closures) the proposed strategy only selects channels which remain unaffected by reverberation. Results indicate that the proposed speech coding strategy, employing the SRR-based channelselection criterion, can yield substantial gains in intelligibility when compared to the cochlear implant patients' daily strategy.

(Supported by NIH/NIDCD Grants R03 DC 008882 and R01 DC 007527)

750 Modulation of Phonetic Cue-Weighting in Adverse Listening Conditions

Matthew Winn¹, Monita Chatterjee¹, William Idsardi¹ ¹University of Maryland College Park

Several experiments were conducted to explore the use of acoustic phonetic cues by individuals in various adverse listening conditions, including those which simulate hearing loss and cochlear implantation. This series of studies attempts to unpack the oversimplification of traditional analysis, where aptitude for features like manner, place and voicing is assessed without regard to the processes by which they are recovered. Given the natural redundancy of cues for any particular speech contrast, it was hypothesized that listeners may find and adopt alternative listening strategies when adverse conditions compromise the primary cues. Experiments focused on the contrastive cues for tense/lax vowels, as well as those for initial and final consonant voicing; all of these have been previously shown to be robust to spectral degradation, hearing loss and/or background noise. Results of experiments using noise-band vocoding (simulating cochlear implantation), low-pass filtering (simulating hearing loss) and background noise show that listeners in challenging conditions are able to shift attention to naturally covarying acoustic cues previously regarded as less salient. Specifically, weighting of primary cues decreased, and weighting of orthogonal secondary cues increased. In addition to behavioral results, preliminary MEG imaging results using a multi-feature mismatch design will also be presented. Speech recognition results obtained to date imply that correct recovery of phonetic information by an impaired individual may not arise as a result of the same perceptual processes used by one with normal hearing. This perspective calls into question some assumptions made about what phonetic cues remain "intact" in the presence of adverse conditions; it may instead be the case that they are genuinely compromised but recovered by alternative means.

751 Modeling Speech Intelligibility for Hearing-Impaired Listeners Based on Reduced Sensitivity to Spectrotemporal Modulation

Elena Grassi¹, Ken W. Grant¹, Joshua G.W. Bernstein¹ ¹Walter Reed Army Medical Center

A model that can accurately predict speech intelligibility for a given hearing-impaired (HI) listener would be an important tool for hearing-aid fitting or hearing-aid algorithm development. Existing speech intelligibility models do a poor job predicting individual differences in speech recognition performance. This may be due to the fact that the models fail to incorporate suprathreshold deficits that are not well predicted by the audiogram. Together with the audiogram, detection thresholds for spectrotemporal modulation (STM) are strong predictors of differences in speech intelligibility across HI individuals. In study, an existing computational model of this spectrotemporal processing was used in conjunction with a peripheral model that incorporates individual audiometric thresholds, frequency selectivity and STM sensitivity. Differences in STM sensitivity across HI listeners were represented by adjusting the strength of an across-channel lateral inhibition network following cochlear processing. This modification was based on the idea that HI listeners miaht have difficulty making the across-channel comparisons needed to detect changes in the stimulus spectrum. An alternative approach to modeling individual differences in STM sensitivity based on the idea that HI listeners might have a reduced ability to use temporal fine structure to detect frequency sweeps was also examined. This impairment was modeled by adjusting the relative strength of an autocorrelation-based estimate of the stimulus spectrum.

A set of 11 individualized auditory models was evaluated for its ability to account for the general effects of hearing loss on STM sensitivity (reduced performance at low modulation rates and high spectral densities) and on speech reception performance, as well as for its ability to differentiate among HI individuals in these measures. The model proved to be more accurate in capturing individual differences than the audiogram-based Speech Intelligibility Index.

752 Transmission Pathways of Vibratory Stimulation as Measured by DPOAE and ASSR

Tomoo Watanabe¹, Tsukasa Ito¹, Toshinori Kubota¹, Hiroyuki Chiba¹, Rudolf Probst², Masaru Aoyagi¹ ¹Yamagata University School of Medicine, ²Zurich University Hospital

Traditionally, two different pathways of sound transmission to the inner ear are distinguished, air conduction and bone conduction. It has been assumed that the primary pathway of bone conduction is osseous, with vibratory stimuli transmitted as transverse waves along the skull bones to the temporal bone and the petrous bone. It has been shown recently that another major pathway of the vibratory stimuli could be the skull contents, particularly the cerebrospinal fluid (CSF). However, the relative importance and contribution of the skull contents remain a matter of debate. To clarify the skull content contribution to vibratory bone stimuli transmission and to determine such stimuli features, we compared distortion-product otoacoustic emission (DPOAE) and auditory steady-state response (ASSR) using a bone vibrator placed at different head sites, including the eye. The highest DPOAE and the best ASSR threshold were with the vibrator either on the mastoid of the measured side or on the temple fs

gultrasound window h. ASSR thresholds with the bone vibrator on the eye resembled those of the forehead and were about 10 dB higher than at the best sites. Distortion product OAEs were clearly present when air-conducted stimuli were presented through an insert earphone and with the bone vibrator on the eye. These results indicate that vibratory sound can be transmitted through skull content to the inner ear. The ultrasound window of the temporal region might offer a reliable, sensitive, and easy to use position for placing the vibrator during clinical measurements.

753 The Influence of Sleep Stage on Auditory Steady-State Response

Tsukasa Ito¹, Toshinori Kubota¹, Tomoo Watanabe¹, Yasuhiro Abe¹, Hiroyuki Chiba¹, Masaru Aoyagi¹ ¹Yamagata University Faculty of Medicine

Auditory steady-state response, a frequency specific response, is used to evaluate hearing level objectively in sleeping young infants. To investigate the influence of sleep stage on auditory steady-state response (ASSR), we measured amplitude of ASSR evoked by amplitudemodulated tone and electroencephalography to determine sleep stage simultaneously. Five subjects with normal hearing were tested and included 2 men and 3 women with an age range between 24 and 28 years (mean age: 25.4 years). Amplitude of ASSR was measured using our original system composed of electrical amplifier (SANEI), A/D converter (National Instruments), and analysis software Lab VIEW 8.6 (National Instruments). Sinusoidally amplitude-modulated tone with intensity of 50 dB nHL at carrier frequency of 1000 Hz and modulation frequencies of 40 Hz was applied to sleeping subjects via headphones. A sampling frequency was 1024 Hz and the frequency resolution was set at 2 Hz. One sweep was 500 ms and 200 sweeps were collected and analyzed using Fast Fourier transform. The amplitude of response was compared to the background noise level comprised of the amplitudes in adjacent regions of the spectrum, the average amplitude of 4 frequencies above and 4 frequencies below the response frequency. Sleeping state was classified into 5 stages, wake: W, non-REM1: N1, non-REM2: N2, non-REM3: N3, and REM: R, using polysomnography (Sensor Medics). Noise level was low especially in stage N3 and R, whereas there was no significant difference in response signal among sleep stages. Consequently, signal noise ratio was high in both stage N3 and REM. Sleep stage should be taken into account when hearing level is estimated from ASSR.

754 Customized Sound Stimulation Improves Pure-Tone Hearing Thresholds Eunyee Kwak¹, Sangyeop Kwak²

¹*Earlogic Auditory Research Institute,* ²*Earlogic Korea* Sound conditioning (i.e., prior exposure to low-level sounds) has been known to protect hearing ability against damage by traumatic noise in a number of mammalian species, including humans. It has also been reported that acoustic stimuli can slow progressive sensorineural hearing loss. Thus, exposure to a moderately augmented acoustic environment could delay the loss of auditory function in mice. In addition to these protection and retardation effects, long-term sound conditioning could enhance cochlear sensitivity.

In this study, we investigated if sound stimulation could improve hearing ability. Sound stimuli consisted of frequency-modulated pure tones and amplitude-modulated narrow band noises. Customized sound stimuli were produced to stimulate one or two target frequency region(s) of the worse ear. Participants listened to the customized sound stimuli twice a day (40 minutes at each time) during 2-3 weeks of sound stimulation period at the lowest audible level. We compared the pure-tone hearing threshold changes after a control period (without sound stimulation) with the changes after the sound stimulation period. The results showed that sound stimulation could significantly improve pure-tone hearing thresholds.

755 Electrophysiological Assessment of Auditory Temporal Processing: A Preliminary Report

II Joon Moon¹, See Youn Kwon¹, Sung Min Lee¹, Won-Ho Chung¹, Yang-Sun Cho¹, Sung Hwa Hong¹

¹Department of Otorhinolaryngology, Sungkyunkwan University School of Medicine,Samsung Medical Center Objectives

The ability to make fine temporal discriminations of acoustic signals plays an important role in speech discrimination and localization of sound. To measure the ability of the patients' temporal process, a method of observing the patients' response to the gap detection test has been used so far. The P1-N1-P2 complex is typically produced at the onset of a stimulus and is also produced when there is a change in the ongoing sound. The complex produced as a result of the change is termed,

ARO Abstracts

"acoustic change complex (ACC)". The objective of this study was to evaluate the auditory temporal processing in a group of normal hearing subjects using electrophysiological (ACC) and behavioral methods. Methods

Both behavioral and electrophysiological responses were recorded in 5 young adults (range, 26 to 37 years) with normal hearing. Broad-band white noise stimuli, 0.5 second duration embedded with several temporal gaps after 0.3 second, were applied to the subjects, and both behavioral detection thresholds and scalp recorded thresholds were obtained. The temporal gaps varied from 2 ms to 20 ms; latency and amplitudes of the ACC's were measured and analyzed. The ability to behavioral response to the stimuli was analyzed using 3AFC paradigm.

Results

P1, N1, and P2 of ACCs were easily identified for the temporal gaps inserted in continuous noise. There was a close association between gap detection thresholds measured behaviorally and electrophysiologically. In addition, the amplitudes of ACC's were significantly greater for long gap durations than for short ones.

Conclusions

The electrophysiological method provides useful objective measures for studying auditory cortical temporal processing in normal individuals. The electrophysiological procedures used in this study may be useful, when applied to evaluate patients who may not be able to produce reliable responses, such as children.

756 Comparison of Sound Sources for Ear Canal Measurements

Stephen T. Neely¹, Jonathan H. Siegel² ¹Boys Town National Research Hospital, ²Roxelyn and Richard Pepper Dept. of Communication Sciences and Disorders, Northwestern University

Calibration of sound levels in the ear canal is needed, for example, when measuring otoacoustic emissions. Measurement of sound levels in human ear canals may be unreliable at frequencies above 4 kHz due to reflected pressure from the eardrum. These reflections can be eliminated when the sound source is characterized as a Thévenin-equivalent source. This study compares Thévenin source parameters, source impedance and source pressure, for an ER-10C microphone (Etymõtic Research) with a modified tweeter design developed at Northwestern University. The separation of incident and reflected pressure works best when the sound source has (1) wide bandwidth, (2) low-distortion, and (3) low crosstalk between the sound source and the in situ microphone. The modified tweeter appears to extend the frequency range over which reflected pressure can be measured from 8 kHz (for the ER10C) to at least 16 kHz. The extended range of Thévenin source parameters for the modified tweeter should allow reliable measurements of sound level in human ear canals at frequencies above 8 kHz. [Work supported by the NIH (R01 DC8318 & R01 DC84208) and Northwestern University.]

757 Effect of Middle Ear Pressure on Wideband Middle-Ear Muscle Reflexes in Newborns

Lisa Hunter¹, David Brown¹, Maureen Sullivan-Mahoney², Patrick Feeney³, Douglas Keefe⁴

¹Cincinnati Childrens Hospital Medical Center, ²Good Samaritan Hospital, ³University of Washington, V. M. Bloedel Hearing Research Center, ⁴Boys Town National Research Hospital

Many newborns referred from otoacoustic emission (OAE) based hearing screening tests have outer or middle ear involvement. Wideband immittance tests, including the middle-ear muscle reflex (MEMR), may be useful to evaluate middle ear status for OAE screening referrals. As newborns evacuate amniotic fluid from the middle ear after birth, positive or negative middle ear pressure may develop and could affect MEMR thresholds. The effect of middle ear pressure on OAEs and MEMR is poorly understood in newborns. Both ears of 40 infants in wellbaby nurseries and 40 infants in neonatal intensive care units (NICUs) were screened using OAEs to determine pass or refer status. Tympanometric peak pressure (TPP) was measured using an absorbance tympanogram averaged between 0.8-2 kHz. Ipsilateral MEMRs activated by broadband noise were measured at ambient pressure and TPP to determine effects of pressure equilibration on MEMR threshold. Median TPP was slightly positive for the normal group and slightly negative for the NICU group. Median MEMR thresholds were lower for TPP compared to ambient tests. 'OAE refer' ears had a higher median TPP than 'OAE pass' ears. 'OAE pass' ears had lower MEMR thresholds. About 30% of ears had significant middle ear pressure, which may affect OAE pass rates and MEMR thresholds. Equilibration of TPP appears to improve MEMR thresholds and may offer an advantage for accurate measurements in newborns.

[Research supported by NIH grant DC010202.]

758 A Preliminary Study on Simultaneous Testing of Auditory Brainstem Responses and Transient-Evoked Otoacoustic Emissions

Xiao-Ming Sun¹, Carly Sturm¹

¹Wichita State University

Auditory brainstem responses (ABRs) and transientevoked otoacoustic emissions (TEOAEs) have been clinically utilized for decades in evaluating functional status of the sensory and neural components of the auditory system. To counteract their shortcomings in diagnosing or screening hearing loss, the two techniques have been included in certain test batteries, thus they complement each other. Few previous studies also proposed an alternative-simultaneous measurement of ABRs and TEOAEs, which should help reduce the testing time and cost. However, this new procedure has not been systematically investigated. The present study examined the simultaneous ABR/TEOAE procedure in 29 normalhearing adults and compared it with the conventional procedure-individual measurement of ABRs and

TEOAEs. For both procedures, clicks (75µs, rarefaction in polarity) were presented at 75 dB SPL through an insert earphone. Preliminary data analysis shows that the difference between the simultaneous and individual tests in TEOAE amplitude is, on average, within 1 dB for all five frequencies from 1 to 4 kHz. The difference in TEOAE signal-noise ratio is within 1 dB for three frequencies, but around 2 dB for 2 kHz and 3 kHz. The difference in TEOAE reproducibility is within 0.03. Similar outcomes were revealed as well for these TEOAE measures in terms of test-retest difference of the simultaneous procedure. It is also displayed that, for ABR tests, the difference between the simultaneous and individual procedures is 0.2 ms or less in latency for ABR waves I, III, and V, and is 1 ms or less in the interwave latencies. The difference between the two procedures in amplitude is within 0.03 µV for all three ABR waves and 0.05 µV for the wave V/III ratio. Results of the present study demonstrate similar outcomes of the simultaneous ABR/TEOAE procedure and the individual procedures. This indicates that the simultaneous ABR/TEOAE test warrants further investigations for potential clinical applications.

759 The History of Screening for Hearing Ability: Part 2 - Adult Robert Ruben¹

¹Albert Einstein College of Medcine

Adult hearing screening has historically has been used not to benefit patients but to protect a third party. The military uses screening to ensure personnel can function properly under military conditions. Industry screens to protect itself from potential suits by identifying any hearing loss and establishing levels of any loss before an employee is exposed to potential sound trauma. Occupational hearing loss has been recognized since 1700. The earliest systematic surveys of industrial hearing loss occurred in Germany - 1881 and Scotland - 1886. In Europe, at the end of the 19th Century, testing of industrial workers and military personnel was initiated using various qualitative and semi quantitative measurement technologies. Development of the Western Electric 100A audiometer in 1922 and subsequent technological establishment advances allowed for the of quantitative screening programs. One of the earliest examples of institutionalized awareness of personnel hearing loss was that of the United States Army Air Force in the 1920s. The United States submarine corps was also targeted as an area of concern regarding hearing. Both services adopted various forms of hearing screening prior to World War II. During WWII studies were undertaken to screen eustachian tube function as well. Although the technology was readily available for industrial hearing screening, little occurred before the last half of the 20th Century. The majority of reports concerning screening for industrial hearing loss occur in the 1960s, 1970s and 1980s. Occupational Safetv and early Health Administration (OSHA) regulations and the high cost of compensation for hearing loss have been driving engines for the adoption of pre-employment and employment hearing screening in industry in the United States.

Geriatric hearing screening is almost nonexistent since it falls outside military or industrial concerns, yet hearing impairment in the elderly has been well documented to result in decreased quality of life and to exacerbate dementia. Screening for hearing loss in the elderly fulfills all of "Cochran's postulates" for appropriate medical intervention. Routine hearing screening in the elderly needs to be instituted so as to reduce needless morbidity through effective intervention.

Text 760 Text Te

Pamela Roehm¹, Vladimir Camarena¹, James Gardner¹, Shruti Nayak¹, Angus Wilson¹, Ian Mohr¹, Moses Chao^{1,2} ¹NYU School of Medicine, ²Skirball Institute of Biomolecular Medicine

Herpes simplex type 1 (HSV1) is a nearly ubiquitous viral pathogen, with an 80-90% rate of seropositivity in the adult US population. Viral reactivation occurs in up to 30% of patients. Reactivation of latent virus in trigeminal ganglion neurons (TGNs) leads to common perioral cold sores. HSV1 reactivation has also been implicated in many head and neck syndromes, including vestibular neuritis, which is the syndrome of acute onset, prolonged peripheral vertigo. Previous studies have shown that neurotrophin (nerve growth factor/NGF) withdrawal in cervical ganglion neurons (which express TrkA, the NGF receptor) results in HSV1 reactivation. In contrast, in VGNs NGF and its high affinity receptor, TrkA, are not expressed; while in TGNs, all three Trk receptors (TrkA, B, and C) are expressed. We have studied the role of the neurotrophin brain-derived neurotrophic factor (BDNF) and its receptor, TrkB, in maintenance of quiescent HSV1 infections in dissociated VGN and TGN cell cultures. Our studies on these neurons demonstrate that generalized inhibition of Trk signaling leads to reactivation in both VGNs and TGNs, and specific inhibition of TrkB signaling in VGNs and TGNs leads to lytic HSV1 infection. We demonstrate that these effects are independent of the trophic effects of BDNF. These studies should improve understanding of HSV1 lifecycle regulation in these neurons and lead to novel treatment approaches for people with herpes simplex syndromes, including herpes labialis and early acute or recurrent vestibular neuritis.

761 The Contributions of Signal and Noise to Information Transmission Rates in Mammalian Vestibular Afferent Neurons

Dylan Hirsch-Shell^{1,2}, Michael Paulin³, Larry Hoffman² ¹Neuroscience Graduate IDP, UCLA, ²Division of Head & Neck Surgery, David Geffen School of Medicine at UCLA, ³Department of Zoology, University of Otago

Afferent neurons projecting from horizontal semicircular canal (HSC) cristae are a heterogeneous ensemble with diverse spontaneous and stimulus-evoked discharge characteristics. In general, afferents with high spontaneous discharge rates and low interspike interval (ISI) variability (i.e. regular afferents) show low sensitivities to rotation

stimuli, while those with low spontaneous rates and high ISI variability (irregular afferents) have higher sensitivities.

A recent study of macaque afferents found that regular afferents had very low magnitude noise spectra and high information transmission rates, while irregular afferents had higher magnitude noise spectra and lower information transmission rates. We recently found that these information transmission characteristics did not generalize to bullfrog HSC afferents; e.g. irregular afferents had sensitivities that were high enough to overcome the greater magnitude noise spectra, resulting in information transmission rates greater than in regular afferents.

We tested the hypothesis that at least some irregular afferents in another mammal, the chinchilla (*C. lanigera*), exhibit information transmission rates that are similar to those in bullfrogs (i.e. have information transmission rates that are at least as great as those exhibited by regular afferents).

Discharge characteristics of individual HSC afferents were recorded from barbiturate-anesthetized chinchillas. Spontaneous discharge and responses to sine and complex stimuli were recorded; complex stimuli were band-limited (primarily <4Hz) rotations with Gaussian velocity distributions (4°/s rms). Upper and lower bounds on information transmission rates (I_{UB} and I_{LB} , respectively) were determined from response-response and stimulus-response coherence measures, respectively.

We found that, similar to previous findings in mammals, I_{UB} and I_{LB} were relatively high in regular afferents—despite low signal magnitudes (i.e. sensitivity)—due to low perstimulus noise. However, some irregular afferents exhibited high signal magnitudes and high values of I_{UB} and I_{LB} despite high perstimulus noise. Other irregular afferents, identified as putative calyx-only, exhibited low signal magnitudes and high perstimulus noise, resulting in low information transmission rates.

762 Histamine H4 Receptor Antagonists as Potent Modulator of Mammal Vestibular Function

Gilles Desmadryl^{1,2}, Sophie Gaboyard^{1,2}, Aurore Brugeaud², **Christian Chabbert**^{1,2}

¹Inserm U583, ²Sensorion Pharmaceuticals

Histamine, exerting its effect through H1-H4 receptors (H1R-H4R), plays a significant role in regulating neuronal activity. Betahistine, the main histaminergic therapeutic drug prescribed for vestibular disorders is a H3R antagonist, which inhibits afferent discharges of lower vertebrate primary vestibular neurons. Recent cloning of H4R has lead to the identification the first non-imidazole selective H4R neutral antagonists.

Using western blot and immunolabelling, we demonstrated the expression of the H4R in mammal primary vestibular neurons, further confirmed by RT-PCR.

The effect of four different specific H4R antagonists on experimentally induced, severe vestibular deficits in rats were tested using a rating system evaluating 6 criteria: Bobbing, circling, retropulsion, as well as tail hanging, contact inhibition and air righting reflexes. Each compound significantly alleviated the induced vestibular deficits by 2030%. Neither betahistine nor thioperamide, tested as reference compounds, had significant effects.

In vitro electrophysiological recordings from cultured rat primary vestibular neurons revealed reversible inhibitory effects on evoked action potential firing by H4R antagonists.

The present study clearly demonstrates the potential of H4R in modulating vestibular function.

The mechanism underlying the observed behavioral effect is likely the decrease of the peripheral vestibular neurons excitability by H4R antagonists, demonstrated in vitro.

H4R antagonists are likely therapeutically applicable as a novel, highly efficient treatment of vertigo crisis caused by vestibular dysfunction.

763 Betahistine Produces a Biphasic Excitatory-Inhibitory Action on the Afferent Discharge of the Isolated Vestibule in Rodents

Enrique Soto¹, Aída Ortega¹, Adriana Báez¹, Rosario Vega¹

¹Universidad Autónoma de Puebla

the antihistaminics. betahistine Amona (BH). diphenhydramine combination (usually in with theophylline), meclizine, its derivate cyclizine, and promethazine have been the most commonly used drugs in the medical treatment of vertigo. Although BH is not approved for use in the management of vestibular syndromes in the United States, it is the drug most commonly used in the European countries, Canada and Latin America for the treatment of Ménière's disease. A prospective study in England demonstrates that, for the treatment of Ménière's disease, 92% of doctors prescribe BH.

Betahistine is an analog of histamine that has an antagonistic action on H_3 receptors. It also has a partial, weak agonist effect on H_1 and H_2 receptors. It is usually thought that pharmacological effect of histaminergic drugs takes place at the central nervous system. However, previous reports have shown that BH produces an inhibitory action on the afferent discharge of the semicircular canals of the amphibians. Evidence indicates that BH significantly reduces the response of the primary afferent neurons of the vestibular system to EAA agonists, thus significantly decreasing the synaptic input from hair cells

The aim of this work was to determine whether or not BH has a significant effect on the afferent electrical activity of the primary neurons in mammalian (rodent) vestibule. For this we developed an isolated vestibule preparation of the rat and mouse, where we have been able to register the electrical discharge of vestibular primary afferent neurons, and to study BH actions. BH was applied by bath perfusion. Recordings of the electrical discharge of the semicircular canal neurons were reliably obtained from the isolated inner ear of the mouse and rat. The actions of BH on the electrical discharge of vestibular afferents was tested in concentrations ranging from 1 to 0.001mM in rats (n = 41) and in mouse and (n = 34). Typically BH produced a biphasic excitatory-inhibitory concentration dependent

effect on the electrical discharge of the vestibular afferent neurons.

Our results indicate that BH (most probably acting through H1 and H3 type receptors) has a significant action on the afferent discharge of the isolated vestibular system, thus indicating that peripheral actions of BH on the mammalian vestibule may significantly contribute to its pharmacological action by modulating the afferent input to the central nervous system.

This work was partially supported by the National Council of Science and Technology of México (CONACyT) to E.S.; by (VIEP-BUAP)-CONACyT grants 20/SAL06-G and 20/SAL06-I to RV and ES; and grant from Solvay Pharma France (2008) to ES.

764 TRPV4 Channels as Primary Effectors of the Infra Red Laser Evoked Response in Sensory Neurons

Sandrine Albert¹, Jean Michel Bec², Fabrice Bardin^{2,3}, Karim Chekroud¹, Cécile Travo¹, Sophie Gaboyard Niay¹, Isabelle Marc^{2,4}, Michel Dumas², Christian Hamel¹, Agnes Muller^{1,5}, **Christian Chabbert**¹

¹U583 INSERM, ²Univ Montpellier 2, ³Univ Nimes, ⁴Ecole des Mines d'Ales, ⁵Univ Montpellier 1

Infra red laser irradiation has been demonstrated to be an appropriate solution to stimulate primary sensory neurons under conditions where the sensory receptor cells are impaired or lacking. Yet, clinical developments of such approaches have been impeded by the lack of information about the molecular mechanisms that support the laser induced neural responses. Here we directly address that question through pharmacological characterization of the neural response evoked by mid infra red (1870 mm) irradiation in retinal and vestibular ganglion cells isolated from rodents. Whole-cell patch-clamp recordings of the evoked neuronal responses reveal that both voltage-gated calcium (NiCd-sensitive) and sodium (TTX-sensitive) channels contribute to the laser evoked action potentials (LEAP). In addition selective blocks of the LEAP by micromolar concentrations of ruthenium red and RN1734 identify thermo sensitive TRPV4 channels as the primary effectors of the chain reaction triggered by mid IR laser irradiation.

765 Synaptic Events at the Calyx Ending of Vestibular Afferents in Rat Semicircular Canals

Soroush Sadeghi¹, Elisabeth Glowatzki¹

¹Department of Otolaryngology-Head and Neck Surgery, Johns Hopkins School of Medicine

Calyx endings of vestibular afferents receive their main input from type I vestibular hair cells. Previous studies (reviewed in Goldberg, 2000) have shown that afferents with calyx endings show irregular discharge patterns at rest and phasic responses to stimulation. To investigate the mechanisms mediating these properties, we studied the characteristics of synaptic activity in calyx endings. We used preparations of the horizontal and anterior cristae excised from 3-4 weeks old rats, in which hair cells, nerves, and Scarpa's ganglion were preserved. We performed whole call voltage clamp recordings from calyces, at holding potentials of -94 mV, at room temperature. We identified the calvces morphologically, as they surround type I hair cells typically showing a neck region. Physiologically, current voltage relations of calyx sodium recordings exhibited currents and hyperpolarization activated currents, both not present in hair cells. Resting membrane potentials were -61 ± 16 mV. EPSCs with different time courses were observed: 1) most recordings had fast EPSCs with durations < 10 ms; 2) some recordings showed slower EPSCs with durations of ~50 ms; 3) few recordings showed slow EPSCs with durations of 100-200 ms. Fast EPSCs were abolished by 10 µM NBQX, suggesting that they were mediated by AMPA receptors. EPSC amplitudes were 25 ± 10 pA (n = 635 EPSCs, 20 afferents). 10-90% rise times were 0.38 ± 0.07 ms and time constants of decay were 0.9 ± 0.2 ms, presenting a time course similar to those of EPSCs observed in immature auditory afferent fibers (Grant et al. 2010). When extracellular [K+] was raised from 5 to 40 mM to depolarize hair cells, both the rate of release and EPSC amplitude increased (45 ± 9 pA; n = 4179 EPSCs, 11 afferents, t-test, p < 0.0001). This change in EPSC amplitude does not occur in cochlear type I afferent fibers (Glowatzki and Fuchs 2002), suggesting differences in transmitter release mechanisms between vestibular and auditory hair cells.

This work was supported by the Vestibular Research Fund, Department of Otolaryngology Head and Neck Surgery at the Johns Hopkins School of Medicine and by NIDCD RO1DC006476 to EG.

766 Plasticity of Excitatory and Inhibitory Synaptic Transmission in Vestibular Nuclei Neurons During Early Vestibular Compensation

Mei Shao¹, June Hirsch¹, Kenna Peusner¹

¹George Washington Univ. Medical Center

The central vestibular system offers a good model to study brain plasticity after lesions. Behavioral recovery, known as vestibular compensation, occurs naturally after unilateral vestibular deafferentation. The principal cells of the chick tangential vestibular nucleus are all second-order vestibular reflex projection neurons which undergo major changes in spontaneous spike activity after unilateral vestibular ganglionectomy (UVG). Here, spontaneous and miniature excitatory (sEPSCs, mEPSCs) and inhibitory (sIPSCs, mIPSCs) postsynaptic currents were recorded from principal cells in brain slices using whole-cell voltageclamp approach from controls, operated chickens 1 day after UVG, and compensated and uncompensated chickens 3 days after UVG. EPSC frequency increased on the lesion side 1 day after UVG, and remained elevated 3 days after UVG in uncompensated chickens only. Also, IPSC frequency increased on the lesion side 3 days after UVG to a greater extent in compensated compared to uncompensated chickens. mIPSCs were primarily GABAergic in most recorded principal cells, but almost half the principal cells on the intact side of uncompensated

chickens had only glycinergic events. Also, 3 days after UVG, the decay time of mEPSCs in principal cells on the lesion side was slower and the decay time of mIPSCs was faster compared to principal cells on the intact side in compensated and uncompensated chickens. Changes in mIPSC kinetics were due to changes in GABAA-receptor mediated events. In summary, both excitatory and inhibitory events increased in frequency on the lesion side, with increased excitatory activity appearing first. In addition, changes in EPSC and IPSC kinetics were simultaneous and bilateral at 3 days after UVG in both compensated and uncompensated chickens. Altogether, vestibular compensation involves plasticity in both excitatory and inhibitory inputs. Knowledge of the phenotype of the changing inputs and their schedule for change provides the basis to determine which inputs to this identified class of vestibular nuclei neurons are responsible for the shift in synaptic activity occurring during early stages of vestibular compensation.

767 GABA and Glycine Immunolabeling in the Chicken Tangential Nucleus

Anastas Popratiloff¹, Kenna Peusner¹

¹George Washington Univ. Medical Center

In the vestibular nuclei, GABAergic and glycinergic neurons play important roles in signal processing for normal function, during development, and after peripheral vestibular lesions. The chicken tangential nucleus is a major avian vestibular nucleus, whose principal cells are projection neurons with axons sending signals to the oculomotor nuclei and/or cervical spinal cord. Antibodies against GABA, glycine and glutamate were applied to study immunolabeling in the tangential nucleus of 5-7 days old hatchling chickens using fluorescence detection and confocal imaging. All the principal cells and primary vestibular fibers were negative for GABA and glycine, but positive for glutamate. GABA is the predominant inhibitory neurotransmitter in the tangential nucleus, labeling most longitudinal fibers observed in transverse tissue sections and more than 50% of all synaptic terminals. A large fraction of GABAergic terminals were derived from the longitudinal fibers, with fewer horizontal GABAergic fibers detected. GABA synapses terminated mainly on dendrites in the tangential nucleus. In contrast, glycine labeling represented about one-third of all synaptic terminals, and originated from horizontally-coursing fibers. A distinct pool of alvcine-positive terminals was found consistently around the principal cell bodies. While no GABA or glycinepositive neuron cell bodies were found in the tangential nucleus, several pools of these immunolabeled neurons were observed routinely in neighboring vestibular nuclei, mainly in the descending vestibular and superior vestibular nuclei. GABA and glycine double-labeling experiments revealed little colocalization of these two neurotransmitters in synaptic terminals or fibers in the tangential nucleus. Our data support the concept of GABA and glycine playing critical roles as inhibitory neurotransmitters in the tangential nucleus. The two inhibitory neurotransmitters have distinct and separate origins and display contrasting

subcellular termination patterns, which underscore their discrete roles in vestibular signal processing.

768 Ischemic Change of Spontaneous Firing in Medial Vestibular Neurons

Masato Shino¹, Yukihiro Takayasu¹, Nobuhiko Furuya¹ ¹Department of Otolaryngology, Gunma University Vertebrobasilar insufficiency (VBI) is one of the most popular causes of vertigo in older people. The VBI is attributed to transient ischemia of brainstem and inner ear. Medial vestibular nucleus (MVN) is a brainstem nucleus and plays an important role for occurring vertigo. In this study, to evaluate the tolerance to transient ischemia for MVN, the electrophysiological change of spontaneous firing in MVN neurons were investigated with whole-cell patch clamp recording in rat brainstem slice preparations, when oxygen-glucose deprivation (OGD) stimulation was applied. Spontaneous firing was recorded under control solution and then OGD solution was perfused for five minutes, thereafter, control solution was re-delivered. In all neurons, disappearance of spontaneous discharge due to a transient hyperpolarization of membrane potential and gradual recovery of the discharge was observed. To verify the inhibitory inputs to MVN neurons, spontaneous inhibitory postsynaptic current (sIPSC) was recorded before and after OGD stimulation. The amplitude and frequency of sIPSC was different from neuron to neuron. Subsequently, to eliminate synaptic influences via neuronal network in remaining in slices on spontaneous 100 M picrotoxin, 10 M firing, strychnine, and 2 mM kynurenic acid were applied to both control and OGD solution. As a result, the disappearance of spontaneous firing and the reinitiation was also recorded in all MVN neurons. For further investigation, discharge properties of pre and post OGD stimulation were analyzed. Interspike intervals (namely, spike frequency) and the time to peak of the afterhyplarization (AHP) were sufficiently shortened after OGD stimulation. These results indicate that the disappearance of spontaneous firing due to transient hyperpolarization and recovery from silent state was occurred at the cellular level of MVN neurons.

769 Characterization of Cholinergic Vestibular and Olivocochlear Efferent Neurons in the Rodent Brainstem

Sara Leijon¹, Anders Fridberger¹, Yvonne Tallini², Michael Kotlikoff², Anna Magnusson¹

¹Karolinska Institutet, ²Cornell University

The neural code from the inner ear to the brain is dynamically controlled by central nervous efferent feedback to the audio-vestibular epithelium. Although such efference provides the basis for a cognitive control of our hearing and balance, we know surprisingly little about this feedback system. Here, we investigated the applicability of a transgenic mouse model, expressing a fluorescent protein under the choline-acetyltransferase (ChAT) promoter, for targeting the cholinergic audio-vestibular efferent neurons in the brainstem (Tallini et al., 2006 Physiol Gen. 27: 391-397). By using anatomical tract tracing in combination with immuonohistochemistry, it was

found that the mouse model is useful for targeting the vestibular efferents, which are fluorescent, but not the auditory efferents, which are not highlighted. This model enables, for the first time, physiological studies of the vestibular efferent neurons and their synaptic inputs. We next assessed the expression of the potassium channel family Kv4, known to generate transient potassium currents upon depolarization. Such potassium currents are found in auditory efferent neurons, but it is not known whether Kv4 subunits are expressed in these neurons. Moreover, it is not known if Kv4 is present and has a function in the vestibular efferent neurons. Double labelling with anti-ChAT and anti-Kv4.2 or Kv4.3 demonstrates that the Kv4.3 subunits are abundantly expressed in audiovestibular efferents, thus indicating that this subunit is a large contributor to the excitability and firing properties of the auditory efferent neurons, and most probably also for the vestibular efferent neurons.

770 Distribution of Gentamicin in the Efferent Vestibular Nucleus and Superior Olivary Complex After Intratympanic Administration

Yibo Zhang¹, **Chunfu Dai¹**, Peter Steyger² ¹Otology & Skull Base Surgery Department, Fudan University, Shanghai, China, ²Oregon Hearing Research Center, OHSU

Intratympanic administration of gentamicin is widely accepted as an effective and tolerable approach for patients with intractable vertigo. However, the mechanisms that eliminate or ameliorate vertigo are still insufficiently understood. Previous studies have demonstrated the localization of gentamicin and its pathological effects within the peripheral vestibular and cochlear sensory epithelia. Recently, we reported the temporal and spatial distribution of gentamicin after intratympanic administration. However, little is known about the distribution of gentamicin in the central auditory and vestibular systems.

In this study, we explored the distribution of gentamicin in the auditory and vestibular central system in the guinea pig brainstem after intratympanic administration, followed by immunofluorescent detection of gentamicin. Our results demonstrated gentamicin uptake and retention in the bilateral efferent vestibular nucleus (EVN), the bilateral superior olivery nucleus (SON) as well as the ispilateral cochlear nucleus 24 hour after injection, and retention as late as 30 days after intratympanic administration. No gentamicin was identified in the vestibular nuclei. We hypothesize retrograde transmission of gentamicin via efferent neurons is responsible for its distribution in the EVN, and diffusion via the cochlear duct to the ipsilateral cochlear nucleus. The absence of labeling in the vestibular nuclei was unexpected, and may be due to lack of vestibular afferent uptake and/or lack of retrograde transmission to vestibular nuclei.

Supported by Educational Ministry of China (No: NCET-06-0369); National Natural Science Foundation of China (No: 30772398) and NIDCD Dc 04555.

771 Property of Spontaneous EPSCs in Purkinje Cells in the Vestibule-Cerebellum and Their High Sensitivity to Oxygen-Glucose Deprivation

Yukihiro Takayasu¹, Masato Shino¹, Nobuhiko Furuya¹ ¹*Gunma University School of Medicine*

Cerebellar regions which have direct fiber connections to the vestibular nuclei or vestibular sensory organs are referred to as the vestibulo-cerebellum, which imposes the central vestibular system. However, the functional properties in neurons in the vestibule-cerebellum are less clear. In this study, we compared sEPSCs in Purkinje cells in the vermal lobules IX and X (also called uvula-nodulus) in the vestibule-cerebellum with those in vermal lobules IV. V and VI as control regions using whole-cell patch-clamp In the relationship between amplitude and recording. frequency of sEPSCs, sEPSCs in Purkinje cells in lobules IX and X tended to have larger amplitude and higher frequency than those in lobules IV, V and VI. The mean values of amplitude and frequency of sEPSCs at -60 mV were 35.0 \pm 2.4 pA and 17.7 \pm 2.2 Hz in lobules IX and X, 19.1 \pm 1.4 pA and 6.7 \pm 1.0 Hz in lobules IV, V, and VI respectively. These differences were statistically significant, suggesting that Purkinje cells in lobules IX and X receives strong and larger amount of excitatory inputs via parallel fiber synapses. Purkinje cell is one of the most vulnerable neurons to the ischemic insults in the brain, and excitotoxicity is well-known as a responsible factor. Next. we investigated the effects of oxygen-glucose deprivation on sEPSCs in Purkinje cells in lobules IX and X. sEPSCs in Purkinje cells in lobules IX and X shown marked enhancement of frequency during the short term treatment of oxygen-glucose deprivation. The mean values of frequency of sEPSCs increased 9.7 ± 3.7 fold in Purkinie cells in lobules IX and X during oxygen-glucose deprivation treatment, whereas corresponding value increased 1.7 \pm 0.2 fold in lobules IV, V, and VI. These results indicate that Purkinje cells in lobules IX and X are richer in the fundamental excitatory inputs than those in other vermal lobules, which results in high sensitivity to ischemic insults in vestibule-cerebellum.

772 Chemical Anatomy of Neurons in the Caudal Vestibular Nuclear Complex (VNCc) That Project to the Ventrolateral Medullary Regions Involved in Blood Pressure Control Gay R. Holstein^{1,2}, Victor L. Friedrich Jr. ^{1,3}, Giorgio P. Martinelli^{1,4}

¹*Mount Sinai School of Medicine,* ²*Depts. of Neurology, Neuroscience and Anatomy/Functional Morphology,* ³*Dept. Neuroscience,* ⁴*Dept. Neurology*

A substantial body of basic and clinical research supports the existence of a functional link between the vestibular system and blood pressure control mechanisms. It is currently thought that arterial baroreceptors participate in a regulatory feedback mechanism that determines and stabilizes sympathetic tone through the baroreflex while signals from the vestibular end organs drive a faster, feed forward mechanism that counteracts the effects of a change in posture. This latter circuit is often referred to as the vestibulo-sympathetic reflex. Primary vestibular afferents of this pathway terminate on cells in VNCc. These second order neurons, in turn, project to brainstem sites involved in the regulation of cardiovascular activity such as the rostral and caudal ventrolateral medullary regions (RVLM and CVLM, respectively). Cells in the RVLM are thought to integrate this vestibular input with baroreceptor and other sensory afferents, and send excitatory projections to preganglionic sympathetic neurons in the spinal cord. In addition, bulbospinal vasomotor RVLM cells receive direct monosynaptic GABAergic projections from the CVLM region, which tonically inhibit the RVLM neurons. Thus, CVLM cells can be viewed as sympathoinhibitory interneurons in the pathway regulating blood pressure. In the present study, retrograde tracer (Fluoro-Gold or cholera toxin B subunit) deposits were placed in either the RVLM or CVLM of rats 7 days prior to sacrifice and brain harvesting. Tissue sections through the medulla were stained for multiple (3label immunofluorescence visualization of the transported tracer together with markers for glutamate, GABA, IAA-RP, L-citrulline (to identify nitric oxideproducing cells), as well as c-fos-activity in activated VNCc neurons. The studies demonstrate the transmitter/modulator phenotypes of the vestibular cells with direct projections to the VLM in rats. Supported by NIH/NIDCD grant R01 DC008846.

773 Vestibular Stimulation at Low Frequencies Modulates Heart Rate and Blood Pressure and Generates a Vasovagal Response in the Anesthetized Rat

Bernard Cohen¹, Giorgio Martinelli¹, Dmitri Ogorodnikov¹, Gay Holstein¹, Sergei Yakushin¹

¹Mount Sinai School of Medicine

We determined how vestibular activation impacts blood pressure (BP) and heart rate (HR) in isofluraneanesthetized Long-Evans rats using sinusoidal oscillation of the rats in the pitch plane and sinusoidal galvanic vestibular stimulation (sGVS). Oscillations in pitch of $\pm 90^{\circ}$ were effective in a frequency range of 0.01-0.5 Hz. At 0.025 Hz modulations in HR were 0.06 beat*s⁻¹/G and in BP were 4.2 mm Hg/G. Significantly, the modulations of HR and BP were out-of-phase, indicating that the BP changes were due to alterations in peripheral resistance, and not to changes in HR.

Binaural sinusoidal GVS (2-4 mA) was done at similar frequencies via Ag/AgCl needle electrodes inserted over the mastoids. BP and HR were modulated at both the frequency of stimulation and at double the frequency. The double-frequencies were due to anodal activation of each labyrinth by the sinusoids. Additionally, there was a large drop in BP and HR at the onset of stimulation that slowly recovered over 1-6 min, suggesting a vasovagal response. The cycle-by-cycle, in-phase modulations of BP and HR were superimposed on the slow response. Effective frequencies of stimulation for producing the vasovagal and sinusoidal modulations in BP and HR were also slow, varying from 0.1-0.05 Hz. The slow modulations and large

drops in BP and HR were inconsistent across animals and habituated with repeated stimulation. The superimposed cycle-by-cycle in-phase drops in BP and HR were more consistent and could outlast the slow modulations.

These results demonstrate that the vestibular system can initiate at least three types of responses in the cardiovascular system: an out-of-phase modulation dependent on head position re gravity in which BP is altered through changes in peripheral resistance, and two in-phase modulations that alter BP through inhibitory control of the heart, one of which is similar to the vasovagal response in humans.

Support: DC008846 (GRH), DC004996 (SBY) and Core Center DC05204 (BC)

774 Vestibular Nucleus Changes in C57BL/6 After Exposed to 7 Tesla Ultra High Magnetic Field

Eun Lee¹, Mi Joo Kim¹, Ji Hye Bae¹, Gyu Han¹ ¹*Gachon University*

Objective:

Securing stability of ultra high magnetic field is necessary since 7 to 21 Tesla magnetic field is internationally used to develop high resolution MRI. Especially when subjects exposed to ultra high magnetic field complain of vertigo and amnesia, relation between vestibular system and ultra high magnetic field should be studied.

Methodology:

C57BL/6 mice are categorized into three groups according to age: 4 weeks to 8 weeks, 8 weeks to 24 weeks, and over 24 weeks old. Subjects were exposed to 7 Tesla magnetic field for an hour, then the brain tissue was fixed in 4% Paraformaldehyde to measure c-fos expression using immunohistochemical stain. Same procedure was done to other subjects after exposed to ultra high magnetic field for 2, 4, and 8 hours. Coronal section of brain tissue showing left and right vestibular nucleus is used to compare and compile statistics of c-fos over-expression which was measured and quantitated by self-produced program.

Result:

Control group and a group exposed to ultra high magnetic field for an hour did not express c-fos but the rest of the groups showed equal expression at left and right vestibular nucleus area. C-fos expression is found very selectively from medial or inferior vestibular nucleus unlike c-fos expression in subjects with unilateral labyrinthectomy. The c-fos in brain stem is actively expressed in order of medial vestibular nucleus, inferior vestibular nucleus, and vestibular compensation area in cerebellum. C-fos expression is also observed in facial nucleus, which indicates that strong magnetic field influences sensory nucleus rather than motor nucleus, notably along the sensory track related to human equilibrium. Depending on the age of the subjects, c-fos expression showed significant difference and even though the number of subjects was small, it is still significant result. Thus, the older the subjects were, the more magnetic field had influence on. Also, as exposure time to high magnetic field went longer, c-fos expression rate went higher. That magnetic field influences brain without discriminating right and left is also observed by comparing excitation signal from both sides of the brain.

Conclusion:

When a subject is continuously exposed to 7 Tesla ultra high magnetic field more than 2 hours, magnetic field triggers excitability to both left and right vestibular nucleus and excitability increases proportionally to age of the subject and exposure period.

T75 Ear and Brain: Cochlear Implant Lessons for Hearing Robert V. Shannon¹

¹House Ear Institute

Cochlear implants (CIs) and auditory brainstem implants (ABIs) have been successful beyond our wildest dreams. Auditory prostheses were originally thought to be a lipreading aid, with some sound awareness. The original approaches to prosthetic hearing failed to take into account the powerful pattern recognition capabilities of the brain. Today, most CI users and some ABI patients are capable of telephone conversation; some even enjoy However, the variability in patient outcomes music. continues to vex researchers, clinicians and device manufacturers. Given the same hearing technology and same etiology of deafness, implant recipients may perform very differently. These individual differences may reflect the relative health at different stages of auditory processing. Most likely, there are multiple processing subsystems in hearing, each with differing importance for auditory pattern recognition. The normal auditory system independently processes global envelope and spectrotemporal fine structure information, and the normal brain seamlessly merges these processing streams. While speech understanding in guiet is possible with coarse envelope information, fine-structure cues are critical for challenging listening tasks (e.g., musical perception, speech understanding in noise, etc.). In prosthetic hearing, these fine-structure cues are often unavailable, due to inability to transmit these cues and/or patients' inability to receive them. Optimization of auditory prostheses requires better understanding of the different processing modes and the differential effect of hearing pathologies on these systems. In this talk, I will review the progress with CI, ABI, and midbrain implant devices, discuss what we have learned about the brain's pattern processing power in hearing, and speculate on how these processing subsystems may impact the design of future prosthetic devices.

776 Opportunities and Challenges in Establishing Collaborative Relationships with Hearing Scientists in China Xiaoqin Wang¹

¹Johns Hopkins University

With a rapidly growing economy, a vast population and a large number of universities and research institutions, China provides a wide range of opportunities for scientific collaborations in both basic to translational research for hearing scientists from developed countries with strong auditory research establishment. A well-constructed collaborative relationship can be mutually beneficial to scientists on both sides and lead to productive research outcomes. In the past few yeas, we at Johns Hopkins University have established a venue with Tsinghua University, a leading Chinese university in Beijing, to jointly pursue research and education objectives. I will share with the audience of this symposium our experience in this exciting endeavor and lessons learnt in the process.

777 Cortical Neural Dynamics of Auditory Attention and Its Application in Neural Prosthesis

Bo Hong¹

¹Dept of Biomedical Engineering, Tsinghua University

The bottom-up and top-down attentional regulation plays an important role for auditory perception. To track the dynamics of cortical response in an auditory stimulus discrimination task, both scalp EEG recording on normal subject and intracranial EEG recording on epilepsy patients undergoing subdural electrode monitoring for surgical purpose are employed to map the attentional effects. Both low frequency event-related potential and high gamma oscillations were analyzed to obtain the property of early passive components and late active responses respectively. Moreover, these cortical neural dynamics was detected in an online fashion by machine learning algorithms to establish a prototype of auditory brain-computer interface, which is potentially useful for locked-in patients with vision impairment.(This work was partly supported by National Science Foundation of China Project 61071003 and 90820304)

778 Cochlear Implantation in Developing Nations

Shakeel Saeed¹

¹UCL Ear Institute

Cochlear implantation is arguably one of the greatest otological success stories of the 20th century: selected severely and profoundly congenitally deaf children implanted below the age of 2 years can be expected to develop age-appropriate speech and language and enjoy a mainstream education whilst many post-lingually deafened adult recipients exhibit effortless speech tracking. There remain however many challenges in this field including access to this technology at a national and global level. Cochlear implantation is a low-volume, high-cost healthcare intervention that relied in the developed nations at inception on charitable and research resources before state funding was established. In the developing world the challenges are even more acute both in terms of access and unmet need as well as financial resource allocation. This paper discusses these issues with reference to the author's experiences and difficulties in establishing a cochlear implant programme in one such country.

779 Acoustics of Different Languages: Implications for Cochlear Implant Design and Pooling of Data Across Countries Liat Kishon-Rabin¹

¹Communication Disorders Dept, Sackler Faculty of Medicine, Tel Aviv University

The efficacy of sensory devices for the hearing-impaired, such as cochlear implants (Cls), is known to be influenced by factors related to the individual (eg., age of onset of hearing loss, age at implantation) and factors related to the CI (e.g., type of speech processing). We propose that outcome performance with the CI is also influenced by the acoustics of the language and the interaction between the speech processing scheme of the CI device and its ability to transmit to the listener the relevant information. We also suggest that some of the inconsistencies in speech perception performance across languages can be explained by the fact that languages that share similar speech sounds may vary in their acoustics and in the cues for their perception. There is evidence showing that listeners from different countries may use different weighting of the temporal and spectral cues for the perception of the same phoneme. And, we cannot conclude without mentioning the existence of languages which use only prosodic (low frequency) information for the perception of some of these phonemes. These data have implications on (1) our ability to understand speech perception performance in CI within a given language, (2) the design of the speech processor of the CI, and (3) the ability to draw conclusions when CI data are pooled across languages.

780 Towards a Global Remote Temporal Bone Pathology Network Athanasios Bibas¹

¹UCL Ear Institute / University of Athens

Human temporal bones provide an important resource for the study of the pathology of deafness. Unfortunately, there are only a few remaining temporal bone laboratories worldwide with a sufficient number of specimens for further study. This has an impact not only on research collaboration but also on training of future researchers on temporal bone pathology. These difficulties may be partially overcome by using remote access microscopy through currently available server-client software, whereby specimens may be studied by researchers from any remote computer around the world. Thus, a virtual network of temporal bone laboratories may be constructed, where expertise may be shared for research and training.

781 Whole-Organ Stem Cell Transplantation of the Larynx

Paolo Macchiarini¹

¹University Hospital Careggi

The ramifications of stem cell research and therapy are enormous. Nevertheless, significant obstacles remain to their employment in every-day therapeutic or surgical interventions, not all of these obstacles related to the need for further scientific or clinical advances. Regulatory issues concerning the use of stem cells, for example, vary considerably across the globe, and often the appropriate surgeons, scientists and even patients are scattered across the globe, requiring that the necessary clinical and scientific expertise be brought onto a remote site that permits the use of potentially life-saving procedures on compassionate grounds. I will discuss the logistics, the science and the outcomes of our recent work in this field, harnessing an international team of clinicians and researchers to carry out pioneering life-saving procedures in country or region that permits their use in such circumstances. Our ongoing phase I clinical trial uses "dormant" stem cells that are either taken or recruited directly from the patient's body to repair untreatable tissues or organs, thus reducing considerably ethical or religious arguments to stem cell treatment that potentially hamper the uptake of stem-cell therapies.

782 Noise-Induced Hearing Loss in United Kingdom Conflict Veterans Rich Williams¹

¹Royal Navy

Noise is ubiquitous within the military environment. In some instances the exposure is controlled but for combatants it may be unpredictable and of high intensity. Research has demonstrated evidence of Woise Induced Hearing Loss (MHL) in 69% of a cohor of Royal-Marines recently returned from Afghabistan. Stringent audiometric monitoring of at tisk personnel is sponsored by The Ministry of Defence, yet reducing noise exposure remains troublesome. Hearing protection must balance its primary role without compromising situational awareness of the individual. Two questions remain: how well does a soldier need to hear and to what extent can further noise exposure be risked?

783 Neonatal Mouse Cochlear Cultures Demonstrate Phagocytosis of Hair Cell Debris by Resident Macrophages After Ototoxic Injury

Keiko Hirose¹, Song Zhe Li¹, Mark Warchol¹ ¹Washington University

Monocytes and macrophages play an important role as first responders in various paradigms of neuronal injury. In the mouse cochlea, resident macrophages are located in the lateral wall and the spiral ganglion and what role these professional phagocytes play in hair cell injury or repair is unknown. We have shown in prior studies that macrophages accumulate in the inner ear after acoustic trauma or during ototoxic injury. Here, we demonstrate using neonatal mouse organotypic cultures that cochlear macrophages participate in removal of cellular debris from hair cell apoptosis due to ototoxic injury. In this work, we utilized CX3CR1eGFP mice in which macrophages express green fluorescent protein to image and record the movement of cochlear macrophages in the organ of Corti after exposure to kanamycin. Time-lapse recordings using confocal microscopy and vital dyes to label apoptotic nuclei and hair cells reveal that macrophages move rapidly

and engulf apoptotic hair cell particles shortly after cell death. Because it is thought that both supporting cells and macrophages contribute to clearance of cellular debris, additional studies using liposomal clodronate, which selectively ablates phagocytes, were performed to evaluate the effect of macrophage depletion on hair cell clearance. We predicted that hair cell clearance would be delayed in the absence of resident macrophages. Interestingly, we have observed that macrophages are not necessary for hair cell clearance after kanamycin.

784 Nitroxidative Stress in Cisplatin Mediated Ototoxicity

Samson Jamesdaniel¹, Donald Coling¹, Sneha Hinduja¹, Dalian Ding¹, Richard Salvi¹

¹University at Buffalo

Cisplatin, a potent ototoxic agent, damages the inner ear through reactive oxygen species (ROS) and by the formation of DNA adducts. Cysteine nitrosylation and tyrosine nitration are important sequels of ROS induced signaling and, in some cases, damage. However, the role of these oxidative posttranslational modifications and the proteins that undergo modification in the inner ear are yet to be established. In this study, the correlation between cisplatin-mediated hearing loss and nitroxidative modification of cochlear proteins was evaluated in male Wistar rats, 3 days after treatment with an 8, 12 or 16 mg/kg dose of cisplatin. The distortion product amplitudes were consistent with expected dose and time dependent increases in hearing loss after cisplatin treatment. A 16 mg/kg dose of cisplatin induced a 10 – 15 dB decrease in DPOAE amplitude, at f2 frequency 8 kHz, 3 days posttreatment. Cisplatin induced a moderate loss of outer hair cells at the basal turn at lower doses (8 and 12 mg/kg) while a higher dose (16 mg/kg) induced a massive loss which was almost twice as great as that observed with 8 or 12 mg/kg. Immunoblots with a monoclonal antinitrotyrosine antibody and a polyclonal anti-Snitrosocysteine antibody indicated cisplatin induced posttranslational modification of cochlear proteins. Cisplatin-induced an increase in the nitrosylation of cysteine in whole tissue extracts while the increases in the nitration of tyrosine were more obvious in nuclear proteins. Consistent with the immunoblot results. immunoprecipitation with anti-nitrotyrosine also detected matching protein bands. The cisplatin-induced increase in nitrated proteins was detected in the spiral ganglion cells. spiral limbus, organ of Corti and stria vascularis, known targets of cisplatin ototoxicity. Collectively, these findings support the hypothesis that nitroxidative stress plays an important role in cisplatin mediated ototoxicity. (We acknowledge support from NIH: R03DC010225, SJ).

785 Non-Transcriptional P53 Activity Is Necessary for Aminoglycoside-Induced Hair Cell Death in the Zebrafish Lateral Line

Allison Coffin¹, David Raible¹, Edwin Rubel¹

¹University of Washington

The intracellular pathways necessary for hair cell death in response to different ototoxic challenges are incompletely

understood and may be specific for each type of damage. We use the larval zebrafish lateral line as a model system to study hair cell death and protection during ototoxic drug exposure. We previously reported that different ototoxic drugs appear to activate distinct and partially overlapping cell death pathways and that pharmacological inhibition of the pro-cell death protein Bax protects hair cells from neomycin but not gentamicin toxicity (Owens et al. 2009, Hearing Res 253:32; Coffin et al. 2010 ARO). We now report that inhibition of the tumor-suppressor protein p53 protects hair cells from damage due to either aminoglycoside. Since p53 can act directly on pro-cell death mitochondrial targets as well as indirectly by transactivating pro-cell death target genes, we have begun to selectively modify each of these pathways and examine the effects on lateral line hair cell death. Stabilization of cytoplasmic p53 with the indirect agonist nutlin-3a facilitates gentamicin-induced hair cell death, further evidence for the necessity of p53 signaling in this system. We then assayed hair cell death in a fish line carrying a mutation in the p53 DNA-binding domain that disrupts transcriptional activity. Mutant hair cells are not protected from aminoglycoside damage, suggesting a transcriptionindependent role for p53 in hair cell death. These data, in conjunction with previous studies of mitochondrial responses to aminoglycosides, lead to a working model in which p53 activates Bax in response to neomycin damage but unidentified downstream mitochondrial targets in response to gentamicin toxicity.

786 A Kanamycin Ototoxicity Animal Model in Pigmented Guinea Pigs

Kathleen Campbell¹, Morris Cooper¹, Nancy Khardori¹, Daniel Fox¹, Steven Verhulst¹, Kelen Seymour², Robert Meech¹

¹Southern Illinois University School of Medicine, ²Springfield Clinic

Kanamycin sulfate is an aminoglycoside rarely used in clinical settings because of its ototoxic and nephritic side effects. If the side effects could be alleviated, kanamycin would be a powerful treatment for bacterial infections that do not respond to other antibiotics. Organisms targeted by Staphylococcus kanamycin include aureus, Neisseria gonorrhoeae, Staphylococcus epidermis. Haemophilus influenza, Escherichia coli, Enterobacter spp, Salmonella spp, Klebsiella pneumonia, Shigella spp. Serratia spp, Providencia spp, and many strains of Proteus.

The purpose of this study was to develop a kanamycin ototoxicity animal model to study otoprotective drug treatments such as D-methionine.

Ten pigmented male guinea pigs received daily s.c. kanamycin injections for 23 days (250 mg/kg/day) and placebo. Auditory brainstem responses (ABR's) were recorded 2, 4, and 6 weeks after starting treatments. ABR stimuli comprised tone bursts centered at 4, 8, 14, and 20 kHz. Cochlear outer hair cell (OHC) counts were performed at the 4 cochlear regions corresponding to ABR frequencies.

This kanamycin model induced progressive ABR threshold shifts and OHC loss without mortality over a 6 week period. Average ABR threshold shifts at 6 weeks were 15.5 dB (13.42 SD), 19.5 dB (15.00 SD), 24 dB (19.23 SD), and 30 dB (16.66 SD) for stimuli centered at 4, 8, 14, and 20 kHz respectively. The average percentage of remaining OHCs by frequency region was 97.2 %(.05 SD), 89.70 %(0.15 SD), 81.52 %(0.30 SD), and 72.12 %(0.29 SD) for the cochlear frequency regions of 4, 8, 14, and 20 kHz respectively. This animal model induced ototoxicity without mortality and can be used for future otoprotection studies for kanamycin induced ototoxicity.

787 Is Acetaminophen/Hydrocodone Ototoxicity Mediated by Endoplasmic Reticulum Stress?

Gilda Kalinec¹, Pru Thein¹, Joshua Yorgason², William Luxford³, **Federico Kalinec¹**

¹House Ear Institute, ²University of Utah, ³House Clinic Pharmacological compounds containing acetaminophen (APAP for N-acetyl-para-aminophenol) and the opioid narcotic hydrocodone (HC), such as Vicodin®, Lortab®, Lorcet® or Norco®, were the top-selling pharmaceuticals in the U.S. in recent years. HC, like other opioids, is strongly addictive, and individuals using APAP/HC combinations frequently become abusers. In most cases, abusers develop tinnitus and a rapidly progressing, profound and irreversible bilateral sensorineural hearing loss after taking very high doses for as little as two months. We recently published results in mouse cochlear explants and HEI-OC1 auditory cells suggesting that APAP, rather than HC, is the primary otototoxic agent in these compounds (Yorgason et al, J Otolaryngol Head Neck Surg 142:814-9, 2010). Now, we are reporting studies using genomics, proteomics and molecular biology techniques aimed at elucidating whether APAP-induced apoptosis of HEI-OC1 cells is mediated by endoplasmic reticulum (ER) stress. Our preliminary results indicate that rebamipide, amiloride and vanadate, pharmacological agents that modulate ER stress-signaling pathways, decrease ROS production but not cell death induced by APAP and APAP/HC combinations. Gene microarray and quantitative proteomic (iTRAQ[™]) studies, on the other hand, identified APAP-induced changes in expression of genes and proteins associated with ER stress, but also in genes and proteins apparently unrelated to this response. A bioinformatic research project using the web-based Ingenuity Pathway Analysis (IPA) software has been initiated looking for identifying the molecular pathways activated by APAP and APAP/HC that trigger apoptosis of auditory cells and their potential association with ER stress responses.

788 Targeting Signal Transducer and Activator of Transcription 1 (STAT1)-Mediated Inflammation in the Treatment of Cisplatin Ototoxicity

Tejbeer Kaur¹, Debashree Mukherjea^{1,2}, Kelly Sheehan², Sarvesh Jajoo¹, Leonard Rybak^{1,2}, Vickram Ramkumar¹ ¹Southern Illinois University School of Medicine, Dept. of Pharmacology, ²Southern Illinois University School of Medicine, Dept. of Surgery

Ototoxicity and nephrotoxicity are common side effects of cisplatin, which is widely used in the treatment of various solid tumors. However, unlike nephrotoxicity which could be alleviated by diuresis and antioxidants, ototoxicity is more difficult to treat due to the inability to deliver protective agents at effective concentrations to the inner ear. A number of studies have implicated inflammation and inflammatory-related transcription factors in cisplatininduced ototoxicity. Of particular interest, a recent study implicates signal transducer and activator of transcription 1 (STAT1) in cisplatin-mediated killing of utricular hair cell cultures in vitro and in transient hearing loss produced by capsaicin, an activator of transient receptor potential vanilloid 1 (TRPV1) channel in the cochlea. In this study, we test the hypothesis that STAT1 contributes to cisplatininduced hearing loss. In UB/OC-1 cells, we show that cisplatin increased STAT1 Ser⁷²⁷ phosphorylation in a dose- and time-dependent manner. Increased STAT1 phosphorylation was dependent on reactive oxygen species (ROS) generated via the NADPH oxidase (NOX3) pathway. Cisplatin also increased STAT1 luciferase activity in UB/OC-1 cells transfected with a plasmid vector containing the STAT1 promoter linked to the firefly luciferase gene. Cisplatin also increased the expression of STAT1-responsive genes, such as inducible nitric oxide synthase (~1.5-fold), cyclooxygenase 2 (~2-fold) and tumor necrosis factor- α (TNF- α) (~1.5-fold). Knockdown of STAT1 by siRNA inhibited cisplatin induction of these inflammatory mediators. STAT1 siRNA also reduced cisplatin-induced apoptosis in UB/OC-1 cells, supporting the notion that STAT1 could mediate cisplatin apoptosis. Importantly, trans-tympanic administration of STAT1 siRNA to rats reduced cisplatin-mediated hearing loss and damage to OHCs. This protective action was also mimicked by trans-tympanic injections of etanercept, a clinically used TNF-a monoclonal antibody. These data support the conclusion that STAT1 couples ROS generation to cochlear inflammation and ototoxicity and suggest that STAT1 or its downstream inflammatory mediators represent novel targets for treating drug-induced hearing loss. (Supported by NIH grants R01DC02396 and R15CA135494 and funds from SIU SOM).

789 Identification of a Candidate Aminoglycoside Transporter in the Mammalian Cochlea

Peter Steyger¹, Qi Wang¹, Jawon Koo² ¹Oregon Health and Science University, ²Seoul National University College of Medicine

One approach to prevent aminoglycoside-induced ototoxicity is to inhibit cell death signaling pathways, promoting hair cell survival. An alternative approach is to block aminoglycoside (AG) entry into the cochlea, and prevent hair cell toxicity. AGs likely cross the bloodlabyrinth barrier by traversing the stria vascularis and enter endolymph. Loop diuretics inhibit the Na+K+Cl- cotransporter on the basolateral membrane of marginal cells, increasing the intra-strial concentration of Na+. This would increase the electrogenic activity of Na+-ligand symporters on the basolateral membrane of marginal cells. Loop diuretics greatly increase cochlear uptake of AGs. Na+symporters that traffic glycosides are Na+-glucose transporters (SGLTs) that are primarily expressed in the proximal tubules of kidneys. Can SGLT inhibitors block renal and cochlear uptake of AGs in vivo?

Control mice treated with fluorescently-tagged gentamicin (GTTR) or gentamicin (detected with anti-gentamicin antisera) have cytoplasmic fluorescence in proximal tubule cells, with intensely fluorescent puncta in the brush border region. Mice treated with a specific SGLT2 inhibitor prior to GTTR or gentamicin exposure had distinctly reduced fluorescence in proximal tubules compared to control mice. Immunofluorescence revealed that SGLTs are expressed in the stria vascularis, and SGLT2 in endothelial and marginal cells. Marginal cells and intra-strial tissues had greatly reduced GTTR fluorescence in mice pre-treated with the SGLT2 inhibitor compared to control mice. Control mice treated with kanamycin-Texas Red also have intense cytoplasmic fluorescence in proximal tubule cells, marginal cells, intra-strial tissues and hair cells compared to mice pre-treated with the SGLT2 inhibitor. Thus, SGLT2 inhibition reduces AG uptake in murine kidney and cochlear tissues. Inhibition of renal and strial SGLT activity may prevent AG-induced nephrotoxicity and ototoxicity. Funded by NIDCD R01 004555 and P30 05983.

790 Identifying the Intra-Cochlear Trafficking Route of Systemic Aminoglycosides to Hair Cells

Hongzhe Li¹, Qi Wang¹, **Peter Steyger¹**

¹Oregon Health and Science University

In the inner ear, cochlear sensory hair cells preferentially take systemically-administered qu and retain aminoglycoside antibiotics, a primary cause of druginduced deafness. The in vivo trafficking of aminoglycosides from the vasculature, across the bloodlabyrinth barrier and into hair cells is not well characterized. Two intra-cochlear trafficking routes have been proposed: 1) an endolymphatic route, in which aminoglycosides in the strial vasculature cross the stria vascularis into the endolymphatic scala media and enter hair cells via mechanoelectrical transduction channels on their stereociliary bundles, and 2) perilymphatic route, in which systemic aminoglycosides permeate into perilymph and enter hair cells across their basolateral membranes. We performed scala tympani perfusion experiments in guinea pigs to test these trafficking routes.

Three experimental groups were used: 1) systemic administration of fluorescently-tagged gentamicin (GTTR), 2) systemic GTTR and scala tympani wash with artificial perilymph, and 3) scala tympani infusion with serum levels of GTTR. Compound action potentials were obtained to ensure cochlear sensitivity during perfusion, prior to fixation, and hair cell fluorescence intensities obtained using confocal microscopy. Hair cells fluorescence intensities in conditions 1) and 2) were high and comparable after systemic administration, yet much reduced in condition 3). Similar observations occurred when GTTR was replaced by gentamicin detected by immunofluorescence. Collectively, the results suggest that aminoglycosides are primarily trafficked from the strial vasculature into endolymph and hair cells. This interpretation also implies the presence of aminoalvcoside transporters reside in the stria vascularis.

791 The Protective Effects of Estradiol Against Gentamicin Ototoxicity

Keiji Tabuchi¹, Mariko Nakamagoe¹, Isao Uemaedomari¹, Bungo Nishimura¹, Kentaro Hayashi¹, Tomofumi Hoshino¹, Masahiro Nakayama¹, Akira Hara¹

¹University of Tsukuba

Aminoglycosides including gentamicin are widely used antibiotics. The clinical usage of aminoglycosides has often been limited because of their ototoxic side effects. @Gentamicin is well known to damage hair cells of inner ear, inducing hearing loss and balance disturbance. Recent findings have demonstrated that gentamicin-induced hair cell death occurs, at least in part, through an apoptotic process. 17fÀ-Estradiol (E2) is the most potent estrogen, known to function as an antiapoptotic agent to prevent the death of various cell types. The purpose of the present study was to examine the effects of E2 on the apoptotic cell death of outer hair cells induced by gentamicin. Basal turn organ of Corti explants from p3 or p4 rats were maintained in tissue culture and exposed to 100 fÊM gentamicin for 48 hours. The effects of E2 on gentamicin-induced hair cell loss, JNK activation, and staining for terminal deoxynucleotidyl tranferase-mediated biotinylated UTP nick-end labeling (TUNEL) were examined. Effects of an E2 receptor antagonist, ICI 182,780, were also examined. E2 significantly decreased gentamicin-induced hair cell loss in a dose-dependent manner. JNK activation and TUNEL staining were observed in organ of Corti explants exposed to gentamicin, and staining levels were significantly decreased by E2 treatment. ICI 182,780 antagonized the protective effects of E2 against gentamicin ototoxicity. The results indicate that E2 decreases hair cell loss induced by gentamicin ototoxicity through binding estrogen receptors and the inhibition of JNK pathway.

792 PROTO1 Provides Robust Protection Against Kanamycin-Induced Hearing Loss in Rats

Edwin Rubel¹, Carol Robbins¹, Kelly Owens¹, David Raible¹, Julian Simon²

¹University of Washington, ²Fred Hutchinson Cancer Research Center

PROTO1 is a benzothiophene-carboxamide identified in a small molecule screen for modulators of aminoglycosideinduced hair cell death using the larval zebrafish lateral line (Owens et al., PLoS Genet, e1000020, 2008). PROTO1 protects lateral line hair cells across a wide range of neomycin concentrations, allows normal aminoglycoside uptake, and antibacterial action of aminoglycosides remain normal. To test efficacy in mammals, we examined PROTO1 protection of kanamycin-induced hearing loss in mature rats. Four groups of young adult rats were used: Kan-only rats (n=6) treated with kanamycin (500mg/kg/day, s.c.); Kan+PROTO1 rats treated with (n=6) PROTO1 (25mg/kg/day, i.p.) and kanamycin (500mg/kg/day, s.c.); and two control groups, normal controls (n=3) without any treatment and vehicle-only controls (n=3). Experimental animals were injected daily for two weeks (5 days on, 2 days off), and then untreated for two additional weeks. We determined ABR thresholds and input-output functions to pure tones at 2, 4, 8, 12, 16 and 32 kHz before treatments began, at two weeks (end of drug treatment), and at 4 weeks. Control groups showed no significant changes over time. Kan-only rats showed significant hearing loss at 16 and 32 kHz at 2 weeks (10dB, and 43dB, respectively) that spread to lower frequencies to include 8, 12, 16 and 32 kHz (13 dB, 23dB, 34dB and 47dB, respectively) at 4 weeks. When PROTO1 was given simultaneously with kanamycin, the hearing loss was eliminated at 16kHz and reduced to 16dB at 32kHz at two weeks. Protection was even more dramatic at the 4 week termination of the experiment. Hearing loss was limited to 32 kHz in Kan+PROTO1 rats (19dB compared to 47 dB in kan-only). There was no permanent hearing loss at lower frequencies. In summary, 1) PROTO1 represents a new class of compounds for protection against aminoglycosideinduced hearing loss, and 2) our high throughput larval zebrafish screen can reveal drugs effective for protecting mammalian hearing.

793 Urokinase-Type Plasminogen Activator Attenuates Hair Cell Damage Induced by Aminoglycoside

Akinori Kashio¹, Takashi Sakamoto¹, Akinobu Kakigi¹, Kenji Kondo¹, Tatsuya Yamasoba¹

¹1) Department of Otolaryngology University of Tokyo Apoptosis is involved in cochlear sensory hair cell injury caused by a variety of ototoxic insults such as expopsure to intense noise, aminoglycoside antibiotics and antineoplastic agent cisplatin. Applying drugs that will protect the cochlear cells from apoptosis will enable us to save patients from deafness. Urokinase-type plasminogen activator (uPA) and its receptor (uPAR) are recently shown to have an important role in cell proliferation/apoptosis, the control of extracellular matrix turnover, cell migration, and invasion. The effect of uPA/uPAR system is controversial. Some have shown that uPA-system has an anti-apoptotic effect, whereas other have suggested its pro-apoptotic effect. In the current study, we found that uPAR was diffusely expressed in the cochlea, more prominently in the organ of Corti and spiral ganglions. We also found that uPA attenuated degeneration of the hair cell induced by aminoglycoside in vitro. Cochlear organotypic cultures were prepared from postnatal day 7 rats and treated with medium with or without uPA (20nM or 2mM) for 1hr followed by kanamycin sulfate (KM) treatment with or without uPA for 12hr. Untreated cultures showed severe degeneration of the hair cells: compared to the control, approximately 75% of inner hair cell (IHCs) and 65% of outer hair cells (OHCs) were damaged. When treated with low dose uPA, the hair cell loss was reduced to be approximately 50% in the IHCs and 55% in the OHCs. High dose uPA treatment more significantly reduced the extent of the cell damage: only 20% of the IHCs and 10% of the OHCs were lost. These findings suggest that uPA/uPAR system plays an anti-apoptotic role in hair cell damage induced by aminoglycosides.

794 Transplatin Attenuates Cisplatin Ototoxicity by Inhibiting a TRPV1- And STAT1-Dependent Inflammatory Response

Debashree Mukherjea¹, Kelly Sheehan¹, Tejbeer Kaur², Sarvesh Jajoo², Leonard Rybak^{1,2}, Vickram Ramkumar² ¹Southern Illinois University, School of Medicine, Department of Surgery, ²Southern Illinois University, School of Medicine. Department of Pharmacology

It is believed that transient receptor potential (TRP) channels serve as entry ports for platinum-based chemotherapeutic agents (such as cisplatin) and aminoglycosides in the outer hair cells of the organ of Corti. Such a mechanism could explain the protective action of knockdown of TRPV1 channels against cisplatin ototoxicity. Previous studies from our laboratory have shown that transplatin, an inactive isomer of cisplatin, abrogates cisplatin ototoxicity in the rat. In this study, we show that the protective action of transplatin is dosedependent, with protection afforded by 1-5.5 mg/kg doses (i.p.). Moreover, transplatin also conferred otoprotection via the trans-tympanic route. Otoprotection was accompanied by reductions in the expression of cisplatininducible genes associated with ototoxicity, such as NOX3 NADPH oxidase, TRPV1 and kidney injury molecule 1 (KIM1). In addition. Transplatin reduced the activation of signal transducer and activator of transcription 1 (STAT1), transcription factor involved in mediating the inflammatory process. In addition, transplatin reduced the induction in inflammatory genes in the cochlea, such as TNF- α , iNOS, and COX2, and also the recruitment of CD14 cells (monocytes and macrophages) to the cochlea. Systemic administration of transplatin also protected the kidneys from cisplatin nephrotoxicity, as indicated by reduced serum blood urea nitrogen and creatinine levels. These data provide strong evidence that transplatin is effective

against cisplatin-induced hearing loss and nephrotoxicity. Thus, this drug could have tremendous translational potential in the treatment of these side-effects in cancer patients treated with platinum drugs. (Supported by NIH grants R01DC02396 to LPR, R15CA135494 to VR, 1F32DC009950 to DM and funds from SIU SOM).

795 Capsaicin Preconditions the Cochlea Against Cisplatin Ototoxicity

Vickram Ramkumar¹, Debashree Mukherjea², Kelly Sheehan², Tejbeer Kaur¹, Sarvesh Jajoo¹, Leonard Rybak^{1,2}

¹Southern Illinois University, School of Medicine, Department of Pharmacology, ²Southern Illinois University, School of Medicine, Department of Surgery

Previous studies from our laboratory suggest that cisplatin ototoxicity is linked, in part, to activation of transient receptor potential vanilloid 1 (TRPV1) channels in the cochlea. We have also demonstrated that direct activation of TRPV1 by capsaicin produced transient hearing loss (~25 dB shifts), assessed by auditory brainstem responses (ABRs) by 24 h, which recovered by 72 h. The hearing loss was not associated with damage or loss of outer hair cell (OHCs) but with increased expression of TRPV1, NOX3 NADPH oxidase and inflammatory mediators such as inducible nitric oxide synthase (iNOS), cyclooxygenase-2 (COX2) and tumor necrosis factor- α (TNF- α). The expression of these mediators recovered to pretreatment levels by 72 h. These studies suggest that capsaicin could be used as a preconditioning stimulus against hearing loss. In the current study, we determined whether capsaicin could precondition the cochlea to ototoxic drugs. Rats were administered a single dose of vehicle or capsaicin (50µl of 0.1µM) by the trans-tympanic route, followed by cisplatin (11mg/kg, i.p) 24 h later. Posttreatment ABRs were determined 72h following vehicle or cisplatin treatment and hearing loss was determined from pre-treatment ABR values. Cisplatin produced significant loss (~25 dB threshold shift), which was attenuated in rats pretreated with trans-tympanic capsaicin 24 h prior to cisplatin administration. The preservation of hearing was associated with no significant damage or loss of OHCs in rats pretreated with capsaicin prior to cisplatin administration, as compared to rats treated with vehicle plus cisplatin. This study provides evidence that TRPV1 preconditioning can aid in protecting the cochleae from cisplatin ototoxicity. To our knowledge, this is the first report which documents that activation of TRPV1 preconditions the cochlea from cisplatin ototoxicity. (Supported by NIH grants R01DC02396 to LPR, R15CA135494 to VR, 1F32DC009950 to DM and funds from SIU School of Medicine).

796 Why and How to Use M/EEG in Auditory Neuroscience Research Adrian KC Lee^{1,2}

¹Institute for Learning and Brain Sciences, University of Washington, ²Department of Speech & Hearing Sciences, University of Washington

Magneto- and Electro-encephalography (M/EEG) are neuroimaging techniques that have temporal resolution particularly suitable for auditory research. In this tutorial, I will briefly review the physics behind the neurophysiological responses recorded using these techniques. I will survey the different event-related field/potential measures used in the literature that address an array of questions relevant to speech and hearing neuroscience. I will also highlight the signal processing strategies that are commonly employed for artifact removal. I will then compare and contrast different source modeling techniques and the implicit assumptions in their approaches. Finally, I will present evidence on the benefits of combining both MEG and EEG measurements.

[Funding provided by NIDCD grant K99/R00 DC010196.]

797 Otoacoustic Emission Methodology: A Non-Invasive Probe to Inner Ear Function Christopher Bergevin¹

¹Columbia University

Otoacoustic emissions (OAEs) have become a useful tool for examining auditory function in both scientific and clinical contexts. As we learn more about the generation mechanisms in the inner ear that give rise to OAEs, novel applications are increasingly being explored/developed. This session will provide a functional overview of an OAE measurement system and is intended to be worthwhile to those who currently measure OAEs, as well as those either interested in doing such (but have little previous experience) or who just want a basic understanding of the methodology. Furthermore, the discussion will be general enough such that the methods discussed are applicable to both human (e.g., clinical) and animal ears. Several topics will provide focus: a brief overview on current thoughts about emission generation, methods for measuring spontaneous (SOAEs) and evoked emissions (e.g., CEOAEs, DPOAEs, SFOAEs), issues associated with noise and probe calibration, and strategies for incorporating emission phase into the analysis.

798 A1 and Beyond

Barbara Shinn-Cunningham¹

¹Boston University

Auditory and other sensory modalities share (and interact via) many of the same attentional and executive control circuits. These higher cortical areas (beyond A1) play a crucial role in processes critical for analyzing and understanding meaningful sounds in everyday settings, including attention, scene analysis, object formation, and working memory storage. This overview will highlight how the various talks making up this symposium explore these topics, providing insight into how auditory perception is affected by higher cortical mechanisms.

799 Effects of Context on Auditory Content in Active Processing Charles Schroeder¹

¹Columbia University

Active auditory processing depends on both attention and sensory context. In rhythmic processing (e.g., streaming), these influences are "effected" in ensembles of auditory cortical neurons by manipulation of their ongoing neuronal excitability fluctuations (oscillations). Attention enhances the effectiveness of auditory inputs in resetting and entraining oscillatory phase, thus aligning high excitability oscillatory phases with events in an attended stream, and amplifying the neural representation of these events. Attended non-auditory, "modulatory" inputs can also reset and entrain auditory cortical oscillations. When correlated with auditory "driving" inputs, their effects on responses to these inputs are facilitative; when not, their impact is often suppressive.

800 Control of Auditory and Visual Attention Shifts in the Human Brain Steven Yantis¹

¹Johns Hopkins University

Auditory and visual perception of natural scenes require deployments of selective attention that permit only behaviorally relevant sensory information to enter We have investigated the cortical awareness. mechanisms of voluntary attention in the human brain using fMRI and have identified domain-specific targets of attentional control signals in auditory and visual sensory cortex, respectively. We have also identified a domainindependent core network in prefrontal and posterior parietal cortex that is a source of control signals that initiate shifts of attention within and between these two modalities. Results from multivoxel pattern analysis reveal that this network expresses domain-specific patterns of activity that can predict the nature of the shift on a moment by moment basis. These findings contribute to a growing understanding of the brain mechanisms of attentional modulation of sensory input.

801 Neural Mechanisms of Auditory and Audiovisual Attention

Mikko Sams¹

¹University of Helsinki

A multitude of studies using different methods have shown that attention influences strength of the signals generated in the auditory cortex. However, our recent EEG study demonstrated that selective attention influences gain but also feature selectivity in the auditory cortex (Kauramäki, J. & al., PLoS ONE, 2007, 2(9): e909). Our new MEG data suggests that attention-related modification of feature selectivity is different in different auditory cortical areas (Kauramäki & al., unpublished data). Focusing attention to visual stimuli can also influence processing in the auditory cortex (Sams & al., Neurosci. Lett, 1991, 127, 141-145). We recently found that auditory-cortex 100 ms MEG responses (N100m) were equally suppressed in the lipreading and covert-speech-production tasks compared with the visual control and baseline tasks; the effects involved all frequencies and were most prominent in the left hemisphere (Kauramäki et al., J Neurosci., 2010, 30, 1314–1321). What we know about neural mechanisms of attention is based on well-controlled experimental setups requiring averaging of many signals. We are currently using new analysis methods to discover how attention works under more naturalistic conditions, such as watching a movie (Salmitaival et al, unpublished data).

802 Top-Down Contribution of Prefrontal Cortex to Auditory Processing Jonathan Fritz¹

¹University of Maryland

A guick review of studies of prefrontal cortex (PFC) reveals considerable evidence for its role in high-level executive functions including stimulus categorization, planning and decision-making, and working memory. The PFC is also known to play an influential role in controlling the flow of sensory inputs via top-down feedback to sensory cortical areas during behavior, reflecting attentional focus and task objectives and rules. Although many of these insights into prefrontal function have arisen from studies of visual processing, recently there has been renewed interest in exploring the contributions of PFC to auditory attention and processing. Our recordings from PFC (Fritz et al.(2010) Nature Neuroscience 13:1011-1019) in the behaving ferret have shown striking behavioral gating of acoustic inputs; rapid, flexible and highly selective encoding of functional classes of acoustic stimuli; post-behavioral persistence of attention-driven modulation; and feature-selective changes in inter-areal coherence between A1 and PFC. These findings mirror earlier results in A1, showing that attention triggered rapid, selective, persistent, task-related changes in spectrotemporal receptive fields. Moreover, stimulation of PFC, paired with pure tone presentation, elicits changes in receptive fields that are similar to those observed in attention-driven behavior. These results suggest that PFC and A1 dynamically establish a two-way functional connection during auditory behavior that controls the flow of salient sensory information and maintains a persistent trace of recent task-relevant auditory stimulus features. We speculate that that plasticity in the auditory network is driven not only by direct top-down projections from PFC to auditory cortex, but also by PFC pathways that recruit neuromodulators that are the engines of adaptive change in auditory processing.

803 Engaging the Oculomotor System Through Auditory Attention Adrian KC Lee^{1,2}

¹Department of Speech & Hearing Sciences, Univeristy of Washington, ²Institute for Learning and Brain Sciences, University of Washington

In vision, converging evidence identifies the oculomotor system as intimately involved in top-down spatial attentional control in addition to its well-known role in saccade production. In audition, microstimulation of the forebrain gaze control field in the barn owl sharpens the spatial selectivity of neurons in the deep layers of the midbrain optic tectum, and suppresses the responses of neurons with preferred sound receptive fields outside the stimulated gaze field location. In this talk, I will discuss the intimate link between the neural circuitry for saccadic control and the auditory attentional network as demonstrated in recent fMRI studies as well as in our own M/EEG data.

This work was supported by NIDCD grant K99/R00 DC010196.

804 Cortical Circuits for the Control of Attention

Maurizio Corbetta¹

¹Washington University School of Medicine

I will review evidence for 2 cortico-cortical systems involved in the control of attention to environmental stimuli: a dorsal attention network involved in stimulus-response selection and shifts of spatial attention, and a ventral attention network involved in stimulus-driven reorienting and network reset. These systems interact during normal perception and their disruption is responsible for some central disorders of attention.

805 Mutations in the PDZ Domain Containing Protein GIPC3 Cause Progressive Sensorineural Degeneration (AHL5 and JAMS1) in Mice and Recessive Hearing Impairment in Humans (DFMB95)

Nikoletta Charizopoulou¹, Andrea Lelli², Margit Schraders³, Kausik Ray¹, Ronald Admiraal³, Harold Neely¹, Joseph Latoche¹, John Northup¹, Hannie Kremer³, Jeffrey Holt², Konrad Noben-Trauth¹

¹NIDČD/NIH, ²University of Virginia, ³Radboud University Nijmegen Medical Centre

Progressive sensorineural hearing loss affects the quality of life and communication of millions of people but the underlying molecular mechanisms remain elusive. Recently, the age-related hearing loss 5 (ahl5) and juvenile audiogenic monogenic seizure 1 (jams1) loci were shown to underlie progressive hearing loss and audiogenic seizures in Black Swiss mice, respectively. Here, we identify ahl5 and jams1 as a 343G>A transition in Gipc3 changing the conserved Glv115 to Arg in its PDZ domain and causing a significant reduction in protein levels. Gipc3 localizes to inner ear sensory hair cells and spiral ganglia and we show that the mutation disrupts the structure of the stereocilia hair bundle affecting mechano-transduction currents and long-term survival of spiral neurons. We demonstrate an adverse effect of the Gipc3343A allele on wave I amplitudes of afferent neurons, which we correlate with susceptibility and resistance of audiogenic seizures. A Gipc3 transgene rescues both hearing loss and audiogenic seizures. Lastly, we identify a truncating mutation in human GIPC3 in a family segregating autosomal recessive hearing loss DFNB95. Our study reveals a novel and pivotal role of Gipc3 for the function of the stereocilia hair bundle and for synaptic transmission.

806 A Novel Mouse Model of Hearing Loss Associated with Enlargement of the Vestibular Aqueduct

Byung Yoon Choi^{1,2}, Kyu Yup Lee¹, Kelly Monahan¹, Yaqing Wen¹, Hyoung-Mi Kim³, Kiyoto Kurima¹, Elizabeth Wilson¹, Thom Saunders⁴, Ronald Petralia¹, Philine Wangemann³, Thomas Friedman¹, Andrew Griffith¹ ¹*NIDCD/NIH*, ²*Department of Otolaryngology, Seoul National University,* ³*Anatomy and Physiology Department, Kansas State University,* ⁴*Transgenic Animal Model Core, University of Michigan*

SLC26A4 mutations are a common cause of hearing loss associated with enlargement of the vestibular aqueduct (EVA). SLC26A4 encodes pendrin, an anion-base exchanger expressed in non-sensory epithelial cells in endolymph-containing spaces. There is already a $Slc26a4^{\Delta}$ (knockout) mouse but its much severe phenotype, comprising total deafness and global malformations of the inner ear, does not optimally model the less severe human phenotypes and cannot distinguish the roles of altered structural versus disrupted endolymphatic development homeostasis in the pathogenesis of hearing loss. To address this issue, a transgenic mouse line that expresses SIc26a4 upon tetracycline (doxycycline) exposure was generated and crossed onto the Slc26a4[∆] background. This system rescued the Slc26a4[∆] phenotype both functionally and morphologically by continuous doxycycline administration during embryonic development. Even though we detected a minimal leaky SIc26a4 expression in the absence of doxycycline, we observed a short half-life of Slc26a4 transcripts and rapid expression of Slc26a4 in response to doxycycline administration, allowing us to initiate or terminate pendrin expression at precise time point of development. Exposure to doxycycline from E16 or earlier led to normal inner ear morphology with normal hearing., while delayed exposure resulted in malformed inner ear and variable hearing loss. Termination of doxycycline exposure before P2 also resulted in malformed inner ear and variable hearing loss, demonstrating that E16.5 to P2 is a critical interval in which the inner ear requires pendrin for development of normal hearing and morphology. Presence of intermediate phenotypes, such as malformed inner ears with normal hearing implicate that disrupted endolymphatic homeostasis bv SLC26A4 mutations play a major role in the pathogenesis of hearing loss.

807 Deafness and Lateral Wall Defects in Spns2-Deficient Mice

Jing Chen¹, Neil Ingham¹, Selina Pearson¹, David Goulding¹, Karen Steel¹

¹Wellcome Trust Sanger Institute

Spns2 is thought to act as a sphingolipid transporter based upon a previous zebrafish mutant study. Little is known about its function in mammals. Spns2-deficient mice showed highly elevated auditory brainstem response (ABR) thresholds at 14 weeks in a high-throughput targeted mutagenesis programme (the Sanger Institute's Mouse Genetics Programme). Further ABR measurements showed hearing impairment in homozygous mutants started as early as 3 weeks of age. In 4-week old homozygous mutants, endocochlear potential was abnormally low and scanning electron microscopy revealed progressive degeneration of outer hair cells from around 4 weeks following normal earlier development. Disruption of tight junctions between marginal cells and tortuous and dilated capillaries in the stria vascularis were seen at 4 weeks old. Immunofluoresence of Spns2 displayed punctate labelling mainly around capillaries in the lateral wall. Together, these data suggest that defects in the lateral wall may play a key role in the deafness of Spns2-deficient mice, while hair cell degeneration is a secondary change.

Acknowledgements

Funded by The Wellcome Trust and EUMODIC.

808 Overexpression of the Tight Junction Protein *TJP2* Leads to Hearing Loss in Mice, Creating a New Mouse Model for DFNA51

Danielle R. Lenz¹, Shaked Shivatzki¹, Karen B. Avraham¹ ¹*Tel Aviv University*

Age-related hearing loss (ARHL) is a widespread phenomenon, yet the causative factors remain elusive. We recently discovered a tandem-inverted genomic duplication of the tight junction protein 2 (zona occludens 2), encoded by the TJP2 gene, leading to adult-onset progressive hearing loss in an Israeli kindred (Walsh et al. Am J Hum Genet 87:101-109, 2010). In lymphoblasts derived from human patients, TJP2 overexpression results in changes in GSK-3^β phosphorylation and apoptosis-related gene expression. We predict that these changes increase the susceptibility of inner ear cells to apoptosis and could account for the progressive hearing loss of carriers of the TJP2 duplication. A mouse model will allow us to test this hypothesis and aid in understanding the causes of ARHL, due to the progressive and late-onset nature of DFNA51. Towards this goal, we generated six transgenic mouse lines overexpressing the human TJP2 gene under the regulation of the ROSA promoter. The founder with the highest number of copies did not pass the transgene to any of his progeny, possibly due to the role of Tjp2 in the formation of the placenta, which in turn would result in embryonic lethality. A second founder, carrying 1-2 copies of the transgene, which is most similar to the human duplication of *TJP2*, presented with high frequency hearing loss at 5 months of age. Analysis of inner ear morphology demonstrated outer hair cell loss that progresses in a basal to apical gradient, in addition to spiral ganglion degeneration. As DFNA51 is characterized by high frequency adult-onset hearing loss, the Tjp2 transgenics appear to mimic the human phenotype, setting the stage for using this model to elucidate the mechanisms of this form of auditory dysfunction.

809 Reciprocal Rescue of Sensory Cilia Defects by Cep290 and MKKS Alleles

Helen May-Simera¹, Rivka Rachel², Norimoto Gotoh², Shobi Veleri², Byung Yoon Choi¹, Thomas Friedman¹, Matthew Kelley¹, Anand Swaroop² ¹*NIDCD, NIH*, ²*NEI, NIH*

Ciliopathies are developmental disorders that arise due to defects in cilia biogenesis and function, and affect various sensory systems including the auditory system. Involvement of multiple syndromic ciliopathy genes, whose protein products are thought to function as macromolecular complexes in both cilia and basal bodies, implicate dynamic regulation of ciliary protein interactions. Mutations in CEP290 (also known as NPHP6 or BBS14), have been found to cause several ciliary disorders [Leber congenital amaurosis (LCA), Senior-Loken syndrome, Joubert syndrome, nephronophthisis (NPHP), Meckel-Gruber syndrome (MKS) and Bardet-Biedl syndrome (BBS)]. Little is known about the function of CEP290, or how this protein interacts with other cilia-related proteins complexes. An initial finding of variants of MKKS (also known as BBS6) in LCA patients led to an exploration of epistatic interactions between CEP290 and MKKS. We found that the DSD domain of CEP290, which is deleted in a mouse model (Cep290^{rd16}) of LCA, directly interacts with MKKS, and that pathogenic variants of *MKKS* disrupt this interaction. Mice with either *Cep290^{rd16/rd16}* or *Mkks^{ko/ko}* genotypes exhibit structural and functional auditory, photoreceptor, and olfactory deficits. Unexpectedly, Cep290^{rd16/rd16};Mkks^{ko/ko} double mutants actually show a degree of functional and/or morphological rescue in all three sensory systems by comparison with either single mutant. Moreover, mice with triple allelic combinations of *Cep290^{rd16}* and/or Mkks^{ko} appear more fully rescued than *Cep290^{rd16/rd16}*; Mkks^{ko/ko} double mutants. Morphological analysis suggests that improved ciliogenesis forms the mechanistic basis for this functional rescue. Our data demonstrate reciprocal modifier effects between the CEP290 DSD domain and MKKS that provides insight into the regulation of cilia formation and function.

810 HearSpike: A Biological Pathways Resource for the Auditory System

Zippora Brownstein¹, Arnon Paz¹, Ran Elkon², Yosef Shiloh¹, Ron Shamir¹, Karen B. Avraham¹ ¹*Tel Aviv University,* ²*The Netherlands Cancer Institute*

¹*Tel Aviv University,* ²*The Netherlands Cancer Institute* Elucidating the auditory and vestibular regulatory and mechanistic pathways is a major challenge, which once met, will greatly enhance our understanding of hearing and balance. To cope with this challenge, we have developed HearSpike, a section of the SPIKE knowledge base. SPIKE (Signaling Pathway Integrated Knowledge Engine; http://www.cs.tau.ac.il/~spike/) is a database of highly curated biological signaling networks and an interactive software environment that graphically displays them as maps, allows dynamic layout and navigation through these maps, and enables the superposition of DNA microarray and other functional genomics data on them.

In HearSpike, auditory maps were constructed based on prior knowledge available in the SPIKE database, and each protein in these maps was confirmed to be expressed in the inner ear. On this initial backbone, interactions and regulations reported in the inner ear were added. Since this method reveals hundreds of proteins, small maps were constructed according to groups of proteins sharing the same function, pathway or expression. In constructing the auditory maps, we arbitrarily began with the myosin VIIA protein. Since this protein is involved in deafness and blindness, we constructed a "Hearing and Vision Proteins" network. This map includes genes implicated in cellular functions including development, cell survival, and apoptosis. The latter pathway led to the creation of another map, the "Apoptosis in the Ear" network, as cell death in the inner ear is a crucial mechanism leading to hearing impairment. To facilitate studies on smaller groups of interactions, selected segments of the comprehensive pathways were split into smaller maps, focusing on specific pathways or immediate interactions of proteins of interest. To date, four additional small maps have been constructed: "Myosin VIIA Interactions in the Ear," "Notch1 Signaling in the Ear," "Hearing-Related Six1 Interactions," and "Myosin IIIA-Interacting Proteins in the Hearing System" networks. The pathways underlying each map are regularly updated, and additional pathways will gradually be added. The maps are available on-line in a user-friendly web interface, as well as in an interactive stand-alone software tool, to allow researchers in the field to access and make use of the data.

811 Analysis of Transcriptional Profiles and Small Molecule Inhibitors in the Junbo and Jeff Mouse Mutants Identify VEGF Pathways as Critical for Chronic Otitis Media

Michael T. Cheeseman¹, Hayley E. Tyrer¹, Debbie Williams¹, Tertius A. Hough², Maria R. Romero¹, Helen Hilton¹, Sulzhan Bali¹, Andrew Parker¹, Lucie Vizor², Tom Purnell², Kate Vowell², Sara Wells², Mahmood F. Bhutta^{1,3}, Paul Potter¹, **Steve D. M. Brown¹**

¹MRC Mammalian Genetics Unit, MRC Harwell, ²Mary Lyon Centre, MRC Harwell, ³Nuffield Department of Surgical Sciences, University of Oxford

Otitis media with effusion (OME) is the commonest cause of hearing loss in children, yet the underlying genetic pathways and mechanisms involved are incompletely understood. Ventilation of the middle ear with tympanostomy tubes is the commonest surgical intervention in children and the best treatment for chronic OME but the mechanism by which they work remains uncertain. As hypoxia is a common feature of inflamed microenvironments, moderation of hypoxia may be a significant contributory mechanism. We have investigated the occurrence of hypoxia and hypoxia-inducible factor (HIF) mediated responses in Junbo and Jeff mouse mutant models which develop spontaneous chronic otitis media (Parkinson et al. 2006 PLoS Genetics; Hardisty et al. 2006 Hum. Mol. Genet.). We found that mutant mice labeled in vivo with Pimonidazole showed cellular hypoxia in middle ear mucosa and inflammatory cells in the middle ear lumen. There was upregulation of inflammatory gene networks in the middle ear WBC including cytokines such as II-1 and Tnfthat modulate HIF. Hif-1 aene expression was elevated in ear fluid WBC and there was upregulation of its target genes including Vegf and its receptor. We therefore investigated the effects of administration of VEGFR signaling inhibitors PTK787, SU-11248 and BAY 43-9006 to the mutant mice. We found that all the inhibitors reduced hearing loss significantly and modulated inflammatory changes in middle ear mucosa. The effectiveness of VEGFR signaling inhibitors in suppressing OM in our genetic models implicate HIF mediated VEGF as playing a pivotal role in otitis media pathogenesis via its actions in angiogenesis, vascular leakiness and inflammatory cell chemotaxis. Our analysis of the Junbo and Jeff mutants highlights the role of hypoxia and HIF mediated pathways and we conclude that targeting molecules in HIF-VEGF signaling pathways has therapeutic potential in the treatment of chronic otitis media.

812 Dearisch Mice Show Dominant, Low Penetrance Deafness Associated with Otitis Media

Jennifer Hilton¹, Neil Ingham¹, Selina Pearson¹, Jing Chen¹, Karen Steel¹

¹Wellcome Trust Sanger Institute

Otitis media is the most common disease diagnosed in children and if undertreated can lead to chronic otitis media with complications such as permanent hearing loss, meningitis and even death. The World Health Organisation recognises the health burden of otitis media as being equivalent to that of polio. It suggests that research emphasis should be placed on identifying the risk factors for otitis media. Mouse models of otitis media, such as the ENU-induced Jeff mutant have been used to identify genes like *Fbxo11* that have subsequently been shown to predispose to otitis media in humans.

The dearisch mouse mutant is also an ENU-induced mutant. It was identified as losing the Preyer reflex (ear flick in response to sound) by 5 months of age. Auditory Brainstem Responses however reveal that mice display raised thresholds from as early as three weeks of age. Pedigree analysis shows the threshold shift to be dominantly inherited with low penetrance. Middle ear dissections show mice with high ABR thresholds have white exudate and frequent incudomalleal fusion. Gross inner ear anatomy including round and oval window areas and the sensory hair cells all appear normal.

Due to the low penetrance of the phenotype, normal backcross mapping of the mutation has not been possible. Whole mouse exome sequencing is therefore being performed to identify the mutation.

813 Multiple Genes Affect Hearing in NIH Swiss Mice

James Keller¹, Konrad Noben-Trauth¹

The NIH Swiss line of mice exhibits substantial variation in hearing and is therefore a good model system for investigating the genetic architecture of hearing loss. By selectively breeding NIH Swiss mice based on hearing thresholds, we generated two new inbred lines that have markedly different hearing phenotypes. Mice of one line have early-onset severe hearing impairment at all frequencies (all frequency hearing loss, AFHL), while mice of the second line have normal hearing except at frequencies above about 32 kHz (high frequency hearing loss, HFHL). AFHL mice exhibit the abnormal hair bundle morphology typical in many types of severe sensori-neural hearing loss. The HFHL mice, which are of particular interest because their frequency specific hearing loss may have implications regarding tonotopic development, do not have any obvious morphological abnormality. The HFHL defect does, however, appear to be related to outer hair cell function since these mice have reduced DPOAE for frequencies above 30 kHz. The lack of obvious morphological phenotype and the subtle, frequencyspecific nature of the hearing loss in HFHL mice are reminiscent of hearing phenotypes observed in the aging Therefore, identifying the genes human population. responsible for hearing loss in the HFHL line may help elucidate the cause of a common but etiologically unclear form of human hearing loss. By backcrossing both lines to normal hearing mice, we were able to map each phenotype to a few loci with moderate to large effect. AFHL was found to be primarily the result of 2 loci of large effect on chromosome 10 that were subsequently identified as the previously discovered cdh23 and gipc3 mutations. HFHL was found to be the result of a number of loci of moderate effect, some of which were also present in the AFHL population.

814 A New Mouse Mutant of the Cdh23 Gene with Early-Onset Hearing Loss Facilitates Evaluation of Otoprotection Drugs

Fengchan Han¹, Heping Yu¹, Cong Tian¹, Hui E Chen¹, Cindy Benedict-Alderfer¹, Yuxi Zheng¹, Qiuju Wang², Xu Han¹, **Qing Yin Zheng¹**

¹Department of Otolaryngology-HNS, Case Western Reserve University, ²Department of Otolaryngology-HNS, Chinese PLA General Hospital

A novel mutation (erlong, *erl*) of the cadherin 23 (*Cdh23*) gene in a mouse model for DFNB12 was identified. The *Cdh23*^{erl/erl} mice were characterized by progressive hearing loss beginning from postnatal day 27 (P27). Genetic and sequencing analysis revealed a 208 T > C transition causing an amino-acid substitution (70S–P). Caspase expression was up-regulated in the mutant inner ears as early as P14. Hearing was preserved (up to 35-dB improvement) in pan-caspase inhibitor Z-VAD-FMK treated mutants in a time course observation (up to 12 weeks) compared with the untreated mutants (P < 0.05). Outer hair cell (OHC) loss in the cochleae of Z-VAD-FMK-treated

mutants was significantly reduced compared with those of untreated mice. Thus, the *erl* mutation can lead to hearing loss through apoptosis. This is the first genetic mouse model of hearing loss shown to respond to otoprotective drug therapy. The short interval from initial hearing loss to deafness (P27–P90) makes this model ideal for screening and validating otoprotective drugs.

*Supported by NIH grants R01DC007392 and R01DC009246 to QYZ

815 A Novel Deafness Gene Identified by Homozygosity Mapping in Pakistani Families

Zubair Ahmed^{1,2}, Rizwan Yousaf³, Byung Cheon Lee⁴, Shaheen Khan⁵, Sue Lee⁶, Tayyab Husnain⁵, Atteeq Ur Rehman⁶, Sarah Bonneux⁷, Vadim N Gladyshev⁴, Inna A Belyantseva⁶, Guy Van Camp⁷, Sheikh Riazuddin⁸, Thomas B. Friedman⁶, **Saima Riazuddin^{3,9}**

¹Division of Pediatric Ophthalmology, Cincinnati Children's Hospital Research Foundation, ²Department of Ophthalmology, College of Medicine, University of Cincinnati, ³Division of Pediatric Otolaryngology Head & Neck Surgery, Children Hospital Research Foundation, ⁴Division of Genetics, Brigham and Women's Hospital and Harvard Medical School, ⁵National Center of Excellence in Molecular Biology, University of the Punjab, ⁶Laboratory of Molecular Genetics, National Institute on Deafness and Other Communication Disorders, ⁷Department of Medical Genetics, University of Antwerp, ⁸Allama Iqbal Medical College-Jinnah Hospital Complex, ⁹Department of Otolaryngology, College of Medicine, University of Cincinnati

A locus for autosomal-recessive, nonsyndromic hearing loss segregating in three families was previously mapped to a 5.36 Mb interval on chromosome 12q14.2-q15, and designated DFNB74. Recently, we ascertained three additional consanguineous families segregating deafness linked to markers at this locus, and refined the critical interval to 2.31 Mb on chromosome 12g14.3. The proteincoding exons of the 18 genes in this interval were then sequenced. The affected individuals of the six apparently unrelated families were homozygous for the same transversion mutation in the DFNB74 gene. This mutation results in a substitution of glycine for cysteine, which cosegregated with deafness in the six DFNB74-linked families, but was absent in 262 ethnically matched normal hearing subjects. This cysteine residue is conserved in orthologs from yeast to humans. The mouse ortholog of the DFNB74 gene is expressed widely. In the inner ear is found in the sensory epithelium of the organ of Corti and vestibular end organs as well as in cells of the spiral ganglion and Reissner's membrane. In vitro, p.C89G abolished function of the encoded protein indicating that the mutation is a loss-of-function allele. Currently, we are constructing a mouse model to study inner ear function of the DFNB74 gene.

816 Connexin26 Plays Essential Roles in Many Aspects of Cochlear Development Before the Onset of Hearing

Qing Chang¹, Xi Lin¹

¹Emory University

Mutations in *GJB2* are responsible for approximately half of all cases of non-syndromic genetic deafness in humans. However, the underlying cellular mechanisms remain unclear. We have generated conditional *Gjb2* knockout mice (called cCx26KO mice), which displayed severe hereditary deafness. One of major findings in the cochlea of cCx26KO mice was that the tunnel of Corti was never opened (Wang et al, 2009), suggesting that the organ of Corti remains immature in the cCx26KO mice.

To further explore the effect of Gjb2 null on the normal development of the cochlea we compared multiple development milestones of the organ of Corti in cCx26KO mice and their littermate wile type (WT) controls. Development of ribbon synapses in hair cells was examined by immunostaining with antibodies against CtBP2 and GluR2/3. Postsynaptic GluR labeling overlapped with presynaptic CtBP2, suggesting formation of hair cell synapses in the cCx26KO mice. However, many synapses in the cCx26KO mice remained above the level of the hair cell nuclei, which is an immature feature of inner hair cells (IHCs). The number of ribbon synapses per IHCs was significantly reduced in the cCx26KO mice comparing to the WT at all developmental stages. Nerve innervation to hair cells was checked by retrograde filling fluorescent Dextron, or by immunolabeling with of antibodies against ß-tubulin and/or neurofilament. The afferent type I fibers under OHCs that normally retract around P6 were still present after P8 in the cCx26KO mice. Whole-cell potassium currents in the outer hair cells and supporting cells from the cCx26KO and WT mouse cochleae were compared. Results showed no significant differences in amplitude and voltage dependency of the currents. However, the spontaneous depolarizing activities in the supporting cells, which normally disappear in the WT cochleae after P6, remained strong in the cochlea of cCx26KO mice until at least P10. The spontaneous Ca²⁺ spikes and the spontaneous depolarizing activities were found to be most active and generated initially in the middle turn region, and spread to the basal and apical turns. Interestingly, we found that the earliest site of cell death was in the middle turn. These findings suggest that the abnormally-extended spontaneous Ca²⁺ spikes and depolarizing activities may be responsible for triggering cell death in the cochlea of cCx26KO mice.

817 Identifying the Roles of *Grxcr1* and *Grxcr2* in the Inner Ear by Structure-Function Analysis

Matthew Avenarius^{1,2}, Kristina Hunker¹, Yehoash Raphael¹, David Kohrman^{1,2}

¹University of Michigan Medical School, Dept. of Otolaryngology/Kresge Hearing Research Institute, ²University of Michigan Medical School, Dept. of Human Genetics

The mouse genome encodes two glutaredoxin-like cysteine-rich proteins, GRXCR1 and GRXCR2, each of which are expressed in the stereocilia of cochlear and vestibular hair cells of early postnatal and adult mice. Mutations in Grxcr1 underlie the profound deafness and vestibular dysfunction observed in the spontaneously arising mouse mutant pirouette. The stereocilia on sensory hair cells in pirouette mutants fail to increase in width during development, implicating a role for Grxcr1 in the proper establishment of stereocilia dimensions. Previous studies aimed at identifying functional properties of these proteins have demonstrated the conserved N-terminal domains of both proteins to be necessary and sufficient for proper localization to actin filament-rich (AFR) structures on the apical surface of epithelial cells. Furthermore, ectopic expression of these genes in explanted inner ear tissue demonstrates their ability to transform the dimensional properties of AFR structures on the apical surface of nonsensory cells. We are evaluating wild type and mutant versions of GRXCR1 and GRXCR2 to determine the relationships of protein-protein interactions to subcellular localization and effects on AFR structures in cultured cells and in tissue explants. These structurefunction studies will increase our understanding of the critical roles of these genes in the inner ear and of mechanisms that control stereocilia development.

Supported by NIH grants R01-DC003049 and P30-DC05188.

818 Sequential Expression of Fascin 1 and Fascin 2 in the Developing Hair Bundle Megan Lundeberg¹, Kate Saylor², Peter Gillespie¹

¹Oregon Health and Science University, ²National Institutes of Health

Inner-ear mechanotransduction occurs upon deflection of actin-based stereociliary bundles of hair cells. The distinct morphology of stereocilia is defined in part by actin crosslinking proteins. Using mass spectrometry, we identified several crosslinkers enriched in hair bundles, including fascins 1 and 2 (FSCN1 and FSCN2) and plastins 1, 2 and 3 (PLS1, PLS2 and PLS3). Using quantitative RT-PCR, we measured transcript levels of these proteins during embryonic development of the chicken basilar papilla (E7-E21). FSCN1 mRNA transcripts were abundant early in development, then decreased until E21. In contrast, FSCN2 and PLS1 transcripts increased from E7 to hatch. PLS2 increased early, peaking at E12, then gradually declined; PLS3 mRNA remained constant throughout development.

To characterize where and when these crosslinking proteins were expressed, we used immunohistochemistry

to determine protein localization and quantitative immunoblotting to measure protein concentration. We found by immunolocalization that both FSCN1 and FSCN2 are present in the hair bundle throughout basilar papilla development. FSCN1 localized specifically to the bundle between ages E14 and E21. Initially, FSCN2 was distributed between the bundle and soma, then between E12 and E14 concentrated in the bundle. Notably, the FSCN2 bundle-to-soma ratio was higher in apical than basal hair cells. By quantitative immunoblot, we found that FSCN1 expression in whole basilar papilla was high initially, then declined during development to 1/5 the concentration at E7 than E21. This pattern mirrored a 10fold increase in FSCN2 concentration over the same time window. Both trends matched the quantitative RT-PCR data. We hypothesize from our observation of sequential expression that FSCN1 plays a role in early stereocilia development, while FSCN2 is important for bundle maturation and maintenance.

819 Hair Bundle Length and Functional Maturation of Mammalian Auditory Hair Cells Are Regulated by Eps8

Valeria Zampini^{1,2}, Lukas Rüttiger³, Stuart L. Johnson¹, Christoph Franz³, David N. Furness⁴, Hao Xiong³, Carole M. Hackney¹, Matthew C. Holley¹, Nina Offenhauser⁵, Pier Paolo Di Fiore⁵, Marlies Knipper³, Sergio Masetto², **Walter Marcotti¹**

¹University of Sheffield, ²University of Pavia, ³University of Tübingen, ⁴Keele University ⁵IFOM

Mammalian cochlear hair cells are specialized for the dynamic coding of sound. The transduction of sound waves into electrical signals depends upon mechanosensitive hair bundles that project from the cell's apical surface. Each stereocilium within a hair bundle is composed of uniformly polarized and tightly packed actin filaments. Several stereociliary proteins have been shown to be associated with hair bundle development and function, and are known to cause deafness in mice and humans when mutated (Petit, Richardson 2009 NatNeurosciRev 12:703-10). The growth of the stereociliar actin core is dynamically regulated by elongation at the actin filament barbed ends in the stereociliary tip. However, the control of actin dynamics in stereocilia is still largely unknown.

We used a combination of single-cell electrophysiology, immunolabelling, electron microscopy and in vivo physiology to investigate the role of Eps8, a protein with actin binding, bundling and barbed-end-capping activities (Di Fiore, Scita 2002 IntJBiochemCellBiol 34:1178-83), in the cochlea. Using control and Eps8 knockout mice we show that this protein is a novel component of the hair cell hair bundle. Eps8 was localized predominantly at the tip of the tallest row of stereocilia and was essential for their normal growth and for maintaining the normal mechanosensitivity of the transducer apparatus. Moreover, we found that Eps8 knockout mice are profoundly deaf and that IHCs, but not OHCs, fail to develop the adult-like characteristics required to become functional sensory receptors. We propose that Eps8 directly regulates actin dynamics in hair cell stereocilia and also plays a crucial role in the physiological maturation of mammalian cochlear IHCs. Together, our results indicate that the multifunctional nature of Eps8 is critical for coordinating the maturation and functionality of mammalian auditory hair cells. Supported by: Wellcome Trust, RNID, Royal Society, Henry Smith Charity, CARIPLO Foundation

820 A Comparison of Methods for Virally-Mediated VGLUT3 Gene Delivery Into the Cochlea

Omar Akil¹, Rebecca Seal², Chuansong Wang³, Matthew During³, Robert Edwards⁴, Lawrence Lustig¹

¹UCSF Department of Otolaryngology-HNS San Francisco, ²Department of Physiology and Neurology, University of Pittsburgh, ³Depart. of Mol. Virology, Immunology and Medical Genetics, The Ohio State University, ⁴UCSF Department of Physiology and Neurology

While a number of studies have described the utility of gene therapy for hearing restoration, translating this into the clinical setting has been elusive while studies in mice have met with limited success as well.

One model for deafness that we have been studying has been the vesicular glutamate transporter VGLUT3 knockout mouse. Prior studies have shown that these mice are born deaf due to the absence of glutamate release from the inner hair cells. In the present study, we attempted to correct this genetic defect through virallymediated gene therapy using a VGLUT3 insert into an adeno-associated virus (AAV) vector. Three different methods were studied to assess the efficiency of transgene expression: 1) Direct injection of AAV-VGLUT3 into the scala tympani via the round window membrane (RWM); 2) Intra cochlear perfusion into the scala media through a separate cochleostomy; 3) Diffusion of virus across an intact RWM. The study demonstrated that simple diffusion of virus across the RWM did not lead to transgene expression within the cochlea nor was there a change in auditory thresholds in the knockout mice. In contrast, with either a cochleostomy or via direct injection through the RWM, hearing was restored 8 to 12 days following gene delivery to thresholds similar to those seen in wild-type mice. Immunofluorescence with a VGLUT3 antibody showed that delivery via RWM or cochleostomy led to VGLUT3 expression within inner hair cells in a dosedependent manner, with a larger viral delivery leading to a greater number of IHC's expressing VGLUT3. In the RWM-injection group, delivery in older mice (P21-P40) led to restoration of auditory thresholds in all animals for 14 days which was subsequently lost. In contrast, delivery of virus to younger mice (P10-12) caused restoration of auditory thresholds for up to 3months in the animals undergoing RMW-injection. In contrast, in animals undergoing viral delivery via a cochleostomy, only 17% of animals had hearing recovery, though the restoration of auditory thresholds in this group lasted up to 6 months. In both groups of animals, cochlear histology appeared normal except at the site of gene delivery

These results demonstrate functional hearing recovery in a genetic model of human deafness due to loss of VGLUT3 function, and support the concept that early restoration of a specific genetic defect performed via RWM or cochleostomie can result in restoration of hearing.

821 Dissection of Clarin-1 Function in Mouse Cochlea

Ruishuang Geng¹, Sami Melki¹, Suhael Momin¹, Daniel Chen¹, Sherri Jones², Kumar Alagramam¹ ¹Case Western Reserve University, ²East Carolina University

Mutation in the clarin-1 gene causes Usher syndrome IIIA, an autosomal recessive disorder with progressive hearing loss and vision loss. We previously demonstrated that clarin-transcript was expressed in hair cells and associated ganglion cells, and in loss of inner ear function in the homozygous knockout (Clrn1-/-) mice. Auditory Evoked Brainstem response (ABR) and vestibular evoked potential (VsEP) recordings showed significant loss of function accompanied by delayed peak latencies and reduced peak amplitudes. Scanning electron microscopy revealed defects in hair bundle morphology as early as postnatal day 2 (P2), and those defects were less severe than those observed in mice with mutation in orthologs of genes associated with Usher type 1 at P2. We hypothesize that mutation in Clrn1 affects hair cell function including the function of the ribbon synapse. To dissect Clrn1's role in hair cells the following experiments were done. Electrically evoked brainstem response (eEBR), a direct test of auditory nerve function, from P21 Clrn1-/- mice confirms delay in peak 1 latency previously observed in ABR and shows that latencies of peaks 2-4 are only secondarily affected (i.e. the interpeak latencies between peak II and III, and III and IV are comparable to control). These results suggest a delay in hair cell-to-afferent neuron communication. To determine whether the observed hair cell phenotype is the result of a defect in ribbon synapse development and/or mechanotransduction, we have initiated a series of experiments. These experiments are currently underway, and results will be presented at the meeting.

822 Expression and Localization of EHD Proteins in the Mouse Cochlea

Manju George¹, Sonia Sanchez², Laura Scheetz², Gowri Nayak³, Kevin Legan³, Guy Richardson³, Hamid Band¹ ¹Eppley Institute for Research in Cancer and Allied Diseases, UNMC, ²Creighton University School of Dentistry, ³University of Sussex

Eps 15 Homology Domain containing (EHD) proteins are members of the recently identified four member (EHD1-4) family of proteins that regulate endocytic recycling, the return of membrane and receptors back to the cell-surface following internalization. All members of the family are expressed in the mouse cochlea as demonstrated by Western blotting of cochlear lysates. Recently, EHD4 was reported as a novel interaction partner for CDH23, a component of the hair-cell tip-links and showed to coimmunoprecipitate and co-localize with overexpressed CDH23. Surprisingly, Ehd4 null mice did not exhibit hearing defects, but showed a compensatory upregulation of EHD1, a related family member. Interestingly, EHD3, another family member was identified as an interacting partner for Ptprg, which forms shaft connectors in hair-cell stereocilia. Co-immunoprecipitation experiments indicate that overexpressed EHD3 immunoprecipitates with Ptprg. Despite suspected roles for EHD proteins in the hair-cells, no information is available on the localization of EHD proteins in hair-cells. Therefore, we undertook a detailed characterization of EHD protein expression and localization in inner and outer hair cells of the organ of Corti using whole mount immunostaining as well as immunofluorescence on cochlear cross sections. Cochlea from single Ehd1, Ehd3 and Ehd4 knock-out mice that we generated were used as negative control for staining for EHD1, EHD3 and EHD4 respectively; while a no- antibody control was used for EHD2 staining. Our results demonstrate that all EHD proteins are expressed in haircells and localize to hair-cell stereocilia. Further studies are underway to examine developmental regulation of EHD protein expression in the mouse cochlea. Colocalization of EHD proteins with known markers of haircell stereocilia are also being carried out. Such studies will facilitate the analyses of cochlear phenotypes in mice with concurrent cochlear-specific deletion of EHD1, 3 and 4 that are being generated by breeding Ehd1 fl/fl; Ehd3 fl/fl; Ehd4 fl/fl mice with a tamoxifen inducible Atoh1 Cre line. We anticipate that these studies will pave the way for future studies to understand the role of this interesting family of endocytic recycling regulators in cochlear function.

823 Knockdown of MRNA Translation by Short Interfering RNA (SiRNA) as a Therapeutic Approach to Prevent Trauma/inflammation-Induced Hearing Loss

Christine Dinh^{1,2}, John Dinh¹, Ly Vu¹, Thomas Van De Water^{1,2}

¹University of Miami Ear Institute, ²University of Miami Miller School of Medicine

Background: Increased pro-apoptotic *Bax* gene expression has been associated with tumor necrosis factor alpha (TNF α)-induced auditory hair cell (AHC) death. Small interfering RNAs (siRNA) can block mRNA translation of a targeted gene and has potential to become a therapeutic approach for the treatment of trauma/inflammation-induced hearing loss (HL). This study will evaluate the effect of Bax siRNA on TNF α -damaged organ of Corti (OC) explants *in vitro*.

Methods: Whole OC explants were dissected from 3-dayold rats and placed in: (1) no treatment – control; (2) scrambled control siRNA; or (3) Bax siRNA. TNF α was added to all groups 24 hrs after onset of culture. After 4 days *in vitro*, the OC were stained with FITC-phalloidin and visualized under fluorescent microscopy; the number of viable AHCs was determined in all cochlear turns. Following RNA isolation and cDNA synthesis, *GAPDH* and *Bax* expression levels were determined using real-time PCR. Results: TNF α -exposed OC explants demonstrated a decrease in the number of viable AHCs (p<0.05) and an up regulation of *Bax* gene expression (p<0.05), when compared to untreated control explants. Treatment with *Bax* siRNA prior to and during TNF α exposure abrogated the effects of TNF α on the number of viable AHCs (p<0.05) and also blocked increases in the gene expression levels of *Bax*. AHC count results and *Bax* gene expression levels in OC explants treated with scrambled control siRNA + TNF α were not significantly different from TNF α -only cultures.

Conclusion: TNF α initiates cell death and up regulates proapoptotic *Bax* gene expression in AHCs *in vitro*. Treatment with *Bax* siRNA blocks TNF α -induced apoptosis in OC explants as demonstrated by an increase in the number of viable AHCs. *Bax* siRNA has the potential to become a therapy for trauma/inflammation-induced HL; however more studies need to be performed to further characterize its effects in the OC explants *in vitro* and determine its efficacy within an *in vivo* trauma model.

824 Hair Cell MicroRNA Depletion Affects Hair Cell Maintenance and Causes Progressive Hearing Loss

Marsha Pierce¹, Michael Weston¹, Heather Jensen-Smith¹, Edward Walsh², JoAnn McGee², Megan Korte², Bernd Fritzsch³, Sonia Rocha-Sanchez¹, **Garrett Soukup¹** ¹Creighton University, ²Boys Town National Research Hospital, ³University of Iowa

MicroRNAs (miRNAs) are small regulatory RNAs that posttranscriptionally repress target gene expression. The functional significance of small RNAs in development of the mouse inner ear is demonstrated using Dicer1 conditional knockout (CKO) to prevent mature miRNA production. We have previously shown that Pax2-Cre Dicer1 CKO in the otic placode results in severe defects in sensory epithelial morphohistogenesis, neurogenesis and innervation. Moreover, the extent of hair cell development correlates with residual expression of miR-183 family members (miR-183, miR-96, and miR-182), which are normally expressed in hair cells and sensory neurons and show basal-apical expression gradients in the mature cochlea. To further examine hair cell miRNA expression and function, we examined the effect of hair cell-specific Atoh1-Cre Dicer1 CKO. Hair cell-specific miRNA depletion is apparent by P18, at which point neither substantial hair cell loss or hearing deficits are observed. However, CKO mice exhibit significant basal outer hair cell loss, aberrant stereocilia, hearing loss and diminished DPOAE responses by P28. Microarray analysis of RNA isolated from P16 apical versus basal organ of Corti demonstrates that expression profiles are longitudinally more disparate in the absence of hair cell miRNAs. The data suggest that hair cell miRNAs function to subdue rather than establish longitudinal expression gradients in the organ of Corti, demonstrate that miRNAs are necessary for hair cell maintenance and survival, and indicate miRNA target genes that might be important in both the development and maintenance of hair cells.

(Support: NIH-NIDCD R01DC009025 and Nebraska State LB606.)

825 MiR-96 Regulates the Functional Maturation of Mammalian Cochlear Hair Cells

Stephanie Kuhn¹, Stuart L. Johnson¹, David N. Furness², Jing Chen³, Neil Ingham³, Jennifer Hilton³, Georg Steffes³, Morag Lewis³, Valeria Zampini^{1,4}, Carole M. Hackney¹, Sergio Masetto⁴, Matthew C. Holley¹, Karen P. Steel³, Walter Marcotti¹

¹University of Sheffield, ²Keele University, ³Wellcome Trust Sanger Institute, ⁴University of Pavia

MicroRNAs (miRNAs) are small non-coding RNAs able to regulate a broad range of protein-coding genes involved in many biological processes by decreasing the level of target mRNA in mammals (Guo et al 2010 Nature 466:835-40). MiR-96 is a sensory organ-specific miRNA (Xu et al 2007 J Biol Chem 282:25053-66) which is present during development in hair cells and auditory spiral ganglion neurons of the mouse cochlea (Sacheli et al 2009 Gene Exp Pattern 9:364-370). In humans, mutations in miR-96 cause non-syndromic progressive hearing loss (Mencía et al 2009 Nat Gen 41:609-13). The mouse mutant diminuendo has a single base change in the seed region of the *Mir96* gene leading to deafness and widespread changes in the expression of many genes (Lewis et al 2009 Nat Gen 41:614-18).

We investigated the effect of this mutant miR-96 on the functional maturation of hair cells using whole-cell patch clamp recordings in diminuendo mice. We found that in the absence of wildtype miR-96, the biophysical properties of hair cells do not develop leading to an embryonic/early postnatal-like expression and shape of voltage-gated potassium and calcium currents, spiking responses and calcium sensitivity of exocytosis. Moreover, maturation of the stereocilia bundle of hair cells and the remodelling of auditory nerve connections within the cochlea fail to occur in miR-96 mutants.

We conclude that miR-96 is a major coordinator of the physiological maturation of mammalian hair cells and thus regulates one of the most distinctive functional refinements of the mammalian auditory system.

Supported by the RNID, Wellcome Trust, Deafness Research UK and The Royal Society.

826 Increased Cochlear Inner Hair Cells in Transgenic MicroRNA-183 Family Misexpression Mice Implicate MicroRNA Mediation of Hair Cell and Supporting Cell Proliferation, Differentiation and Survival Michael Weston¹, Sonia Rocha-Sanchez¹, Marsha Pierce¹, Garrett Soukup¹

¹Creighton University

MicroRNAs (miRNAs) are negative post-transcriptional regulators of gene expression. Recent studies validate an evolutionary conserved role for the miRNA-183 family (miR-183, miR-182, miR-96) in mechanosensory cell fate identity and homeostasis in the vertebrate inner ear. We developed transgenic mice (Tg[GFAP-miR-183/miR-

96/miR182]) that misexpress the miR-183 family miRNAs in cell lineage related supporting cells in the organ of Corti (OC). This in vivo mammalian model is being used to uncover relevant morphologic and physiologic effects directly attributable to miRNA/target gene interactions of this miRNA family. We had previously characterized a progressive and complete loss of auditory hair cells (HCs) in this model, validating the potency and sensitivity of miR-183 misexpression in adjacent supporting cells, as predicted by the mutual exclusion hypothesis of miRNAtarget gene expression. At neonatal ages, prior to any evidence of hair cell loss, we have now quantified a significant increase in the number of inner hair cells (IHC) in the organ of Corti of Tg/Tg homozygotes. An 8-fold increase in IHC doublets in the apex, and an increase in the linear packing density of basal IHCs, together provide evidence in a mammalian system for influential effects of the miR-183 family previously demonstrated in zebrafish (Li et al. 2010). Additional cells were also observed in close apposition to IHCs, but most were negative for HC features (e.g. Mvo6 expression, stereocilia). The presence of extra cells, including IHCs, suggests that miR-183 family misexpression might prevent cell senescence in the maturing OC, consistent with correlations of miR-183 family misexpression in certain cancers. Conversely, miR-183 family misexpression might promote survival of cells from Kölliker's organ. These observations provide a clear proof of principle for studies to investigate miR-183 family microRNAs as molecular adjuvants for HC survival and regeneration in the mammalian cochlea. (Supported by NIH/NCRR P20RR018788)

827 Permeation of Phalloidin Into Live Hair Cells and Supporting Cells of the Inner Ear

Benjamin Thiede¹, Jeffrey Corwin¹

¹University of Virginia

We describe a method for labeling filamentous actin in live sensory hair cells and supporting cells. Some styryl dyes, such as DASPEI, FM1-43 and FM4-64 can be used to label live hair cells in vitro and in vivo. Evidence suggests that those dyes can permeate hair cells through mechanotransduction channels that are in the open state and through ligated P2X receptors. Microinjection of fluorophore-conjugated phalloidin, a toxin isolated from Amanita phalloides that binds with high affinity to F-actin, is useful in fluorescent speckle microscopy (FSM) for the visualization of actin dynamics in vitro. FSM is used for live imaging of single cells and because of the requirement for microinjection would not allow imaging of cells throughout live inner ear sensory epithelia. Phalloidin is not generally considered to be cell permeant, but it can enter hepatocytes via organic anion uptake transporters. It has been suggested to enter a limited number of other celltypes by pinocytosis.

To test the hypothesis that phalloidin might permeate living cells in the sensory epithelia of the inner ear we explanted whole mount utricles from embryonic to 7 day-old Rhode Island Red chickens and Swiss Webster mice into DMEM/F-12 medium, then incubated the living utricles in a solution containing 0.2-4U/mL fluorophore-conjugated

phalloidin for 10 to 30 minutes. When we visualized the live explants after washout in a control medium we observed strong flourescent labeling of filamentous actinrich structures in a subset of the hair cells and supporting cells in live utricle explants, which was maintained after Preliminary results from these aldehyde fixation. experiments suggest that labeling of cells persists in the utricle explant cultures for at least 2 days after the phalloidin incubation. Additional experiments suggest that the number of live hair cells that exhibit phalloidin labeling appears to be enhanced in cultures supplemented with 4mM CaCl₂ together with the conjugated phalloidin. These results indicate that fluorophore conjugated phalloidin can permeate live sensory hair cells and supporting cells in vestibular organ explant cultures and may provide a novel approach to study actin dynamics in the inner ear. Future investigations will be focused on identifying the mechanism by which phalloidin permeates in these cells.

(This work was supported by NIDCD grant RO1-DC000200 to JTC and the Pharmacology Training Program at the University of Virginia.)

828 The Striated Organelle in Vestibular Type II Hair Cells

Florin Vranceanu¹, Robstein Chidavaenzi¹, Steven Price¹, **Anna Lysakowski¹**

¹Univ. of Illinois at Chicago

We have previously described the striated organelle (SO) in type I hair cells, where it is particularly well developed. The SO is located in the subcuticular region of hair cells and consists of alternating thick and thin bands (Friedman et al., 1965; Ross and Bourne, 1983). In the type I hair cell, the striated organelle is shaped like an inverted openended cone that contacts the cell membrane along its entire circumference and is separated from the cuticular plate by a layer of large mitochondria. The SO is present in cochlear inner hair cells and all vestibular hair cells. In hair cells other than vestibular type I hair cells, our initial impression was that it was a much smaller structure and appeared to be free-floating. We have now studied its structure in type II hair cells in more detail with EM tomography and confocal microscopy and find that it is much more extensive (in height, breadth and radial depth) in type II hair cells than in type I hair cells. In a threedimensional tomographic reconstruction, we have not yet found a connection to the actin rootlets, as there was with the type I hair cell. The SO is, however, closely associated with mitochondria, although these are smaller in both volume and surface area than those in the subcuticular region of type I hair cells. EM immunogold experiments in both types of vestibular hair cells have demonstrated that antibodies to the actin-binding protein alpha fodrin (nonthe ervthroid spectrin) label SO. Confocal immunohistochemistry shows that the SO extends downward from the cuticular plate as two large sheets. Unlike the SO in type I hair cells, those in type II hair cells do not appear to be associated with a constriction in the neck of the hair cell, although the thick filaments do form cross-links and occasionally, thick filaments "morph" into thin filaments. We continue to study the structure and function of this intriguing organelle.

Supported by NIH DC-02521 and the 2008 Tallu Rosen Grant in Auditory Science (from the National Organization for Hearing Research Foundation).

829 Quantitative Proteomics Reveals Differences in Energy Metabolism Between Chicken Auditory and Vestibular Organs

Peter Gillespie¹, Kateri Spinelli¹, Jung-Bum Shin², John Klimek¹, Phillip Wilmarth¹, Dongseok Choi¹, Larry David¹ ¹Oregon Health & Science University, ²University of Virginia

Auditory and vestibular hair cells may differ in their use of calcium buffers, pumps, and energy pathways. We examined protein and mRNA expression in chicken basilar papilla and utricle sensory epithelia using liquidchromatography tandem mass spectrometry (LC-MS/MS) and Affymetrix genome arrays. To validate label-free LC-MS/MS guantitation, we demonstrated linearity of absolute expression and sample-to-sample ratioing using standard purified proteins spiked at different dilutions into a complex protein mixture (E. coli extract). Under the LC-MS/MS conditions we used, normalized molar intensities best reported protein expression. Because our basilar papilla preparation included the tectorial membrane, protein expression there was dominated by alpha- and betatectorins. We demonstrated in control experiments that high levels of a few proteins did not distort quantitation of the remaining proteins. which allowed us to computationally remove tectorin peptide identifications prior to quantitation of basilar papilla proteins. Comparing protein expression and genome array signals, we found that both protein expression levels and basilar papilla-toutricle ratios were strikingly uncorrelated with transcript expression levels. Glycolytic enzymes were a notable exception; in nearly all cases, enzymes involved in glycolysis were elevated 2- to 4-fold in basilar papilla as compared to utricle, a trend that was confirmed by genome arrav. Βv contrast. expression of oxidative phosphorylation enzymes like F1-ATPase subunits were reduced in basilar papilla. As previous reported, calbindin-28K was the most abundant basilar papilla protein; we determined that it accounted for 20% of protein on a molar basis. We suggest that in basilar papilla hair cells, high levels of calbindin can buffer calcium ions so thoroughly that the need for rapid calcium extrusion, and hence ATP production by oxidative phosphorylation, is reduced.

830 Locating Outer Hair Cell Damage Along the Cochlear Partition

Ashlee Martz¹, Brian Earl¹, Megan Ash¹, Mark Chertoff¹ ¹University of Kansas Medical Center

Recent advances in therapeutic techniques for curing hearing loss motivate the need for parallel advancement in diagnostic tools that can locate the anatomical sites of lesion responsible for hearing loss. The goal of this research is to develop a diagnostic tool that may be able to accurately locate damaged outer hair cells (OHCs) using the cochlear microphonic (CM), a physiologic signal that comes from the receptor currents of OHCs. Previous work has demonstrated that using a low frequency stimulus with high-pass masking can limit the CM response to populations of OHCs at specific locations along the cochlear partition. This method can identify the OHCs that are not functioning properly due to temporary noiseinduced hearing loss. The purpose of this study is to determine if the proposed method can accurately identify the location of damaged or missing OHCs in animals with permanent hearing loss.

Mongolian gerbils were assigned to either a control group or one of the following pure tone exposure groups: 12, 18, or 24 kHz. Each animal was exposed for two hours at approximately 115dB SPL, and was then allowed to recover for at least two weeks. CM recordings were obtained with a round window electrode in response to a 733 Hz tone-burst. The tone-burst was presented at 80 dB SPL in the presence of high-pass noise with 25 cutoff frequencies between 0.4 and 45 kHz.

CM amplitudes from each masker condition were normalized to the unmasked condition and plotted to create a cumulative distribution function (CDF). By differentiating the CDF, a probability density function (PDF) was obtained. These PDFs quantify the contributions of OHCs to the CM at particular locations along the cochlea. After damage, the PDFs shifted in a manner consistent with the frequency of induced damage. This suggests that the proposed technique can identify the location of permanently noise-damaged OHCs along the length of the cochlea.

Supported by: NIH R21/33

831 TBBPA Induced Apoptosis in Sensory Hair Cells

Channy Park^{1,2}, Hye-Min Ji¹, Ara Ryu¹, Jeong-Han Lee¹, Aihua Shen¹, Se Jin Kim¹, Sang-Heon Lee¹, Hong-Seob So¹, Raekil Park¹

¹Wonkwang University School of Medicine, ²Nambu University

Tetrabromobisphenol A (TBBPA) is widely used as a flame retardant and is suspected to be stable in the environment with possible widespread human exposures. The benchmark doses for effects on the brainstem auditory evoked potentials were similar to values for decreases in circulating thyroid hormones. In this study, TBBPA-induced hair cell death was observed in HEI-OC1 auditory cells and the neonatal (P2) rat organ of Corti explants. Treatment with TBBPA significantly decreased the viability of hair cells in organ of Corti explants and HEI-OC1 cells, which was accompanied with apparent apoptotic features, including fragmentation of nuclei, TUNEL positive cells and activation of caspase-3 protease. Treatment of HEI-OC1 cells with TBBPA resulted in an increase in intracellular reactive oxygen species (ROS). In addition, TBBPA induced expression of pro-inflammatory cytokines including TNF-alpha and IL-6. Taken together, these data suggested that the cytotoxic mechanism of TBBPA was ascribed to ROS generation and pro-inflammatory cytokine production in auditory cells.

This work was supported by the Korea Science & Engineering Foundation (KOSEF) through the Vestibulocochlear Research Center (VCRC) at Wonkwang University in 2010-2011.

832 Pretreatment with Flunarizine Protects the Sensory Hair Cells of Organ of Corti and Neuromast from Gentamicin Through Nrf2-Mediated Transcriptional Activation

Jeong-Han Lee¹, Channy Park¹, Hyung-Jin Kim¹, Wenxue Piao¹, Gi-Su Oh¹, Se-Jin Kim¹, Hong-Seob So¹, Raekil Park¹

¹Wonkwang University School of Medicine

Gentamicin (GM) is well known to cause the death of hair cells (HCs) in inner ear. Recently, we found that flunarizine, a T-type calcium channel blocker, protected the cisplatin-induced damages of auditory cell and HCs in organ of Corti. However, the effect of flunarizine on the GM-induced death of HCs is not elucidated. In this study, we demonstrated that GM induced hair cell death showing disruption of stereocilia, fragmentation of nuclei, disarray of the outer HC (OHC) and inner HC (IHC) row, and loss of FM1-43 staining in HCs from organ of Corti. Treatment with GM significantly also inhibited the gentamicin-induced HC death. Pretreatment with flunarizine did not attenuate GTTR uptake into OHCs and IHCs of organ of Corti explants. However, we observed that loss of OHCs and IHCs in tissue specimens of GTTR treated group whereas the loss of HCs in specimen of flunarizine plus GTTR group was markedly decreased. Pretreatment with flunarizine resulted in nuclear translocation of NF-E2related factor 2 (Nrf2), which was mediated by phosphatidvlinositol 3-kinase (PI3K)-Akt sianalina. Flunarizine also increased the expression of heme oxygenase-1 (HO-1) in cochlear explants. Furthermore, pharmacological inhibition of HO-1 abolished the flunarizine-mediated protection of hair cells by gentamicin. In zebrafish, GM induced a rapid loss of neuromasts. Flunarizine maekedly protected the neuromasts of zebrafish from GM. These results suggest that flunarizine activates the Nrf2-antioxidant response element (ARE) signaling pathway through PI3K-Atk signaling to increase the generation of HO-1, which prevents free radical stress on HCs from gentamicin in vitro and in vivo.

This work was supported by the Korea Science & Engineering Foundation (KOSEF) through the Vestibulocochlear Research Center (VCRC) at Wonkwang University in 2010-2011.

833 PDE-5 Inhibitors-Induced Damage of Sensory Hair Cells

Channy Park^{1,2}, Ara Ryu¹, Jeong-Han Lee¹, Tong-Ho Kang³, Hye-Min Ji¹, Hun Young Kim⁴, Se Jin Kim¹, Hong-Seob So¹, Raekil Park¹

¹Wonkwang University School of Medicine, ²Nambu University, ³Kyung Hee University, ⁴Gunsan Medical center A phosphodiesterase type 5 inhibitor (PDE5 inhibitor) is a drug used to block the degradation of PED5 on cyclic GMP in the smooth muscle cells lining the blood vessels supplying the corpus cavernosum of the penis. Recently, sudden hearing loss from PDE5 inhibitors was reported (The Laryngoscopy 2009, Laryngol Otol.. J 2009). However, the exact mechanism of hearing impairment by PDE5 inhibitor was not yet clearly revealed. In this study, we were designed to elucidate the signaling mechanisms of PDE5 inhibitors-induced cytotoxicity in auditory cells including HEI-OC1 auditory cells, VOT33 spiral ganglion cells, the rat cochlear explants of organ of Corti, spiral ganglion cells and neuromast of zebrafish. Treatment with PDE5 inhibitor significantly decreased the viability of HEI-OC1 cells and VOT33 cells, and hair cells inorgan of Corti explants. Also, immunofluorescence study showed that many of lateral line hair cells of zebrafish were markedly lost with exposure to PDE5 inhibitors. Furthemore we observed that treatment with PDE5 inhibitor significantly increased the generation of reactive oxygen species and NO in auditory cells. Taken together, these results suggested that cellular stress with free radicals generated by PDE5 inhibitor may result in reversible and/or irreversible damages in various components in auditory organ.

This work was supported by the Korea Science & Engineering Foundation (KOSEF) through the Vestibulocochlear Research Center (VCRC) at Wonkwang University in 2010-2011.

834 DMSO Enhances Cisplatin-Induced Hair Cell Death in Zebrafish (*Danio Rerio*)

Melissa Mueller¹, Julia Gleichman², Matthew Kramer¹, Douglas Cotanche³, **Jonathan Matsui^{1,4}**

¹Department of Molecular and Cellular Biology, Harvard University, ²Department of Biology, Pomona College, ³BioMedical Imaging Laboratory, Harvard School of Public Health, ⁴Department of Biology and Program in Neuroscience, Pomona College

Sensory inner ear hair cells die following treatment with aminoglycoside antibiotics (e.g. neomycin) or chemotherapeutic agents (e.g. cisplatin) causing permanent auditory deficits in humans. Previous studies using chickens and mice have shown that the ototoxic effects of these pharmaceutical agents are ameliorated by concurrent treatment with cell death inhibitors. Zebrafish (Danio rerio) are an emerging animal model used to study sensory hair cell death. We treated a transgenic line of zebrafish that expresses membrane-targeted green fluorescent protein under control of the Brn3c promoter/enhancer with cisplatin and counted the number of remaining hair cells to develop a dose-response curve. The Brn3c-transgenic zebrafish were then treated with cisplatin and two different cell death inhibitors that prevent aminoglycoside-induced hair cell death but have an unknown role in cisplatin-induced cell death. Instead of protecting hair cells from cisplatin-treatment, the inhibitors in conjunction with cisplatin caused more hair cells to die than cisplatin did alone. Investigating the solvent used to dissolve the cell death inhibitors, we found that cisplatin in the presence of the solvent dimethyl sulfoxide (DMSO) caused more death than cisplatin alone caused. DMSO alone did not kill hair cells. The specific properties of DMSO may enhance the ototoxic effects of cisplatin by potentially increasing the uptake of cisplatin into the tissues. Current studies are underway to see if other organic solvents enhance cisplatin-induced hair cell death.

835 Kanamycin Ototoxicity Is Associated with Differential Changes in Gene Expression That Mimic the Base to Apex Pattern of Auditory Hair Cell Sensitivity

John Dinh, B.S.¹, Ly Vu¹, Christine Dinh¹, Thomas Van De Water¹

¹University of Miami Miller School of Medicine

Background: Kanamycin (KM) is an aminoglycoside antibiotic that is known to cause apoptosis of basal and middle turn outer hair cells. The mechanism of action behind KM ototoxicity is multi-factorial and not completely understood, but has been attributed to inhibition of mitochondrial protein synthesis, activation of NMDA receptors, and formation of free radicals. Activation of *c*-*Jun*, a transcription factor that regulates a variety of apoptosis-associated genes, has also been associated with aminoglycoside ototoxicity. This study evaluates the effect of KM on expression levels of 1 housekeeping gene and 2 apoptosis-related genes.

Methods: Organ of Corti (OC) explants were dissected from 3-day-old rat pups and cultured in various concentrations of KM (i.e. 0-300 μ M). OC explants were stained with FITC-phalloidin after 96 hrs *in vitro* and viable inner, outer, and total hair cells were counted in all turns of the OC explants. For gene expression studies, the OC explants were divided into apical, middle, and basal turn segments after 48 hrs *in vitro*, real-time RT-PCR evaluated expression levels of *GAPDH* (housekeeping gene), *Bcl-2*, and *Bax* genes.

Results: KM ototoxicity was significantly greater in the middle and basal turns compared to the apical turns of the OC explants (p<0.05). In addition, KM ototoxicity was dose-dependent and >90% hair cell death was achieved at a 100 μ M concentration (p<0.05). Gene expression studies demonstrated up regulation of pro-apoptotic *Bax* gene expression levels and increases in the *Bax/Bcl-2* ratio at several different KM concentrations in the middle and basal turns of the cochlea compared to untreated, control explants (p<0.05). KM did not affect the expression levels of pro-survival gene *Bcl-2*.

Conclusion: KM-induced apoptosis of auditory hair cells may, in part, be the result of changes in gene expression that favor apoptosis in the more susceptible portion of the cochlea, i.e. middle and basal turns.

836 Ablation of Mouse Cochlea Hair Cells by Activating the Human Diphtheria Toxin Receptor (DTR) Gene Targeted to the Pou4f3 Locus

Ling Tong¹, Cliff Hume¹, Richard Palmiter², Edwin Rubel¹ ¹VM Bloedel Hearing Research Center, Dept. of Oto-HNS, University of Washington, ²Dept. of Biochemistry, University of Washington

Most congenital and acquired hearing loss is due to the loss of inner ear hair cells. To better understand and prevent transneuronal degenerative CNS changes that follow peripheral hearing loss we have created a mouse model in which all hair cells in cochlea can be conditionally eliminated at any age by expression and activation of a cell death activator, diphtheria toxin receptor (DTR), targeted to the *Pou4f3* locus. The human DTR was cloned into a homologous recombination vector containing 5.9 kb of the mouse Pou4f3 gene just before the initiation codon such that DTR represents the first open reading frame. After transfection into ES cells, appropriately recombined clones were identified and used to generate the *Pou4f3*^{DTR/+} mouse line.

Diphtheria toxin (DT) injections (50 ng/g body wt, i.m.) into mature (P28-35) *Pou4f3^{DTR/+}* mice results in complete loss of hair cells in all cochlear turns by 5 days, dramatic threshold elevation by 3 days, and elimination of ABR responses by 5 days. No recovery occurs and DT exposure has no effect on wild-type mice. At P5 much smaller concentrations of DT (5 ng/g) are required to achieve complete hair cell loss. At all ages support cells and axonal processes appear normal up to a week following DT exposure. We've also assessed this model on cochlear explants from 2-3 day old mouse pups treated in vitro with DT (25 ng/ml x 3 days), and found extensive, loss of hair cells with no immediate gualitative changes in supporting cells in cultures from mice with the $Pou4f3^{DTR/+}$ genotype. DT exposure in wild-type mice has no effect on cell survival. The $Pou4f3^{DTR/+}$ mouse is a new and exciting tool that can be used to assess how hearing loss of hair cell origin influences physiological, biochemical, anatomical and molecular properties of the developing and mature central auditory system. In addition, it will be of a great valuable for studying hair cell regeneration and cell-cell interactions in the cochlea and vestibular epithelium.

837 Age-Related Changes of the Regeneration Mode in the Mouse Peripheral Olfactory System Following Olfactotoxic Drug Methimazole-Induced Damage

Keigo Suzukawa¹, Kenji Kondo¹, Tatsuya Yamasoba¹ ¹*Tokyo Univ.*

We investigated age-related changes in the mode of regeneration in the mouse peripheral olfactory system after olfactotoxic drug-induced damage. Mice at postnatal ages of 10 days, 3 months, and 16 months were given an intraperitoneal injection of methimazole to produce damage in the olfactory neuroepithelium. The olfactory neuroepithelia were harvested and analyzed immunohistochemically at various post-lesion time points, from 1 day through to 94 days, to investigate neuroepithelial cell proliferation, the time course of differentiation, neuronal the reconstitution of neuroepithelium. The chronological pattern in the expression of Ki67, beta III tubulin, and olfactory marker protein, molecular markers for neuronal cell proliferation and differentiation, changed similarly among the different age groups. In contrast, the extent of neuroepithelial cell proliferation after injury decreased with age, and the final histological recovery of the olfactory neuroepithelium and the innervation of the olfactory bulb were significantly smaller in the 16-month-old group compared to the younger age groups. These results suggest that the agerelated decline in the capacity of olfactory neuroepithelium to reconstitute neuroepithelium is associated with its agerelated decrease in proliferative activity after the neuroepithelial injury rather than changes in the process of neuronal differentiation. This suggests that to promote the proliferation of basal cell would be important in the development of treatment strategy for damaged olfactory neuroepithelium associated with aging.

838 Effects of Ouabain Administration to the Round Window Membrane in the Guinea Pig Cameron Lind Budenz¹, Seiji Shibata¹, Yehoash

Raphael¹

¹University of Michigan, Department of Otolaryngology, Kresge Hearing Research Institute

Ouabain, a Na+/K+ ATPase pump inhibitor, has been shown to induce various inner ear cell and neuronal lesions depending on the method of toxin administration, thereby creating useful animal models for the study of auditory neuropathy and hearing loss. Prior studies in gerbils have demonstrated that this treatment leads to selective degeneration and loss of type I afferent spiral ganglion neuronal fibers, with preservation of the inner and outer hair cells. Through determination of the effects of ouabain in the guinea pig ear at various exposure levels, any selective toxicity for specific neuronal or cell populations of the inner ear can be exploited in future studies to help classify regenerated ear cells or neuronal fibers. The purpose of this study was to determine the effect of topical administration of ouabain to the round window membrane in the guinea pig ear. We initially applied ouabain using the same application protocol as that previously used in gerbils to selectively kill type I afferent neurons (20uL of 1mM ouabain applied topically to the round window membrane for 30 minutes), and, after one week of recovery, the guinea pig ear demonstrated the loss of all hair cells and neuronal peripheral fibers in the basal turns, with diminishing effects in the apical turns. Subsequently, decreasing ouabain concentrations and round window exposure times were utilized in a systematic fashion to determine the effects on the guinea pig cochlea. Ouabain's effects in the guinea pig ear varied from minimal toxicity to the peripheral neuronal fibers to complete loss of all hair cells and peripheral fibers, and this was in direct proportion to the ouabain concentration and exposure time

used. Ouabain can be used in guinea pigs to induce relatively selective loss of nerve fibers relative to hair cells. Supported by The A. Alfred Taubman Medical Research Institute, The Williams Professorship, and NIH/NIDCD grants DC010412, DC-007634, T32-DC005356, and P30 DC05188.

839 Conditional Deletion of Atoh1 with Either Atoh1-Cre or Pax2-Cre Provides Mouse Models for Testing Reconstitution of the Organ of Corti

Ning Pan¹, Israt Jahan¹, Jennifer Kersigo¹, Bernd Fritzsch¹ ¹University of Iowa

Atonal homolog1 (Atoh1) is a crucial bHLH transcription factor for inner ear hair cell differentiation. Misexpression of Atoh1 can generate extra hair cells (Zheng et al. 2000, Nat Neurosci 3:580; Gubbels et al. 2008, Nature 455:537; Izumikawa et al. 2005, Nat Med 11:271), signifying its essential role for hair cell formation in the ear. However some development of precursors has been reported in the absence of Atoh1 (Fritzsch et al. 2005, Dev Dyn 233:570), raising the possibility that Atoh1 may only be needed transiently to initiate hair cell differentiation. To directly test this possibility, we generated a conditional deletion of Atoh1 using Tg(Atoh1-Cre) (Matei et al. 2005, Dev Dyn 234:633), which shows a delayed expression of Cre relative to Atoh1 mRNA and protein, resulting in a limited and transient expression of Atoh1 in hair cell precursors. Despite early embryonic loss of Atoh1, hair cells displaying markers such as Myo7a and Pou4f3 develop in patches and survive for at least 38 days without Atoh1 signal. This demonstrates that a transient presence of Atoh1 can lead to formation and long term maintenance of hair cells, an important consideration for the reconstitution of hair cells. In addition, to test how long some prosensory domaindefining genes remain expressed in the undifferentiated hair cells in the absence of Atoh1, we generated another conditional Atoh1 deletion using Tg(Pax2-Cre) (Ohyama et al. 2004, Genesis 38:195), resulting in complete absence of hair cell differentiation in the cochlea. These mice show rapid loss of afferents prior to birth but no change after birth. The remaining afferents project primarily to precursor cells identified by Sox2 expression. By postnatal day 14 the developing organ of Corti has been transformed into a flat epithelium that continues to express markers such as *Bmp4*, *Fgf10* and *Gata3*. Further work will explore the use of these new mouse models to reconstitute a cochlea. Supported by an NIH grant R01 DC005590.

840 Selective Loss of Murine Cochlear Outer Hair Cells Following Conditional Deletion of Atoh1 by a Hoxb1Cre Driver Line: A New Model of Sensorineural Hearing Loss

Kurt Chonko¹, Bernd Fritzsch², Stephen Maricich¹ ¹Department of Pediatrics and Neuroscience, Case Western Reserve University, ²Department of Biology, University of Iowa

Atoh1 (Math1) is a basic helix-loop-helix transcription factor necessary and sufficient to produce hair cells in the

mammalian cochlea. Previous work from our laboratory demonstrated that conditional deletion (CKO) of Atoh1 using a Hoxb1Cre driver line resulted in abnormalities of distortion product otoacoustic emissions, a measure of cochlear function. We therefore sought to determine the expression pattern of Hoxb1 within the developing cochlea and to analyze cochlear morphology in Hoxb1Cre; Atoh1CKO mice. Lineage tracing in Hoxb1Cre; ROSA mouse cochleae revealed novel and unique mediolateral and apical-basal distributions of Hoxb1 expression during Hoxb1Cre Atoh1CKO mice embryonic development. exhibited several abnormalities of cochlear structure. First, these mice had several gaps in the inner/outer hair cell lines which were more numerous in the apical turn. Second, there was variable absence of the second and third rows of outer hair cells throughout the cochlea. This outer hair cell loss, though present at birth, appeared to progress as the mice aged. Finally, Hoxb1Cre Atoh1CKO mice lost spiral ganglion neurons after birth. Our preliminary data describe a new model of sensorineural hearing loss which may suggest novel functions of Atoh1in the maintenance of outer hair cells.

841 What Tuning Curves from Rbl2 Mutant Mice Reveal About the Influence of Supernumerary Sensory and Support Cells on the Mechanics of Inner-Ear Transduction Erin Hegner^{1,2}, JoAnn McGee¹, Sonia M. Rocha-

Sanchez³, Edward J. Walsh¹

¹Boy's Town National Research Hospital, ²University of Cincinnati, ³Creighton University School of Dentistry The retinoblastoma family of proteins, commonly referred to as pocket proteins, include the retinoblastoma protein (Rb), as well as the structurally and functionally similar retinoblastoma-like 1 (Rbl1) and 2 (Rbl2) proteins, frequently referred to as p107 and p130, respectively. Pocket proteins are thought to play a key role in the regulation of cell cycle dynamics involving hair cell (HC) and support cell (SC) proliferation and post-mitotic quiescence. In that light, both supernumerary HCs and SCs have been observed in the cochlea of pocket protein deficient mice. In *p130* knockout (KO) mice. supernumerary cell expression is limited to the apical half of the cochlea and both HC types conform to a more-orless normal cytoarchitectural distribution pattern, taking the form of one or two extra rows of both inner and outer HCs (see Rocha-Sanchez et al., 2011 ARO Abstract 1050). Aside from a small low frequency threshold elevation, ABR thresholds were normal in p130 KO mice, as were distortion product otoacoustic emissions (DPOAEs) (Rocha-Sanchez et al., 2010). The purpose of this investigation was to indirectly examine macromechanical transduction in the KO mouse by studying the properties of DPOAE suppression tuning curves (TCs) representing the apical half of the cochlea where supernumerary cells are observed and TCs from the anatomically normal basal half of the end organ. In KO animals, TC tip and tail thresholds, sharpness of tuning (Q10) and cochlear amplifier gain estimates were indistinguishable from control animals. Based on these observations, we conclude that certain aspects of inner ear macromechanics are normal in p130 mutant animals. Because p130 KO mice survive into adulthood, express a limited number of well organized inner ear hair and support cells and have relatively normal peripheral auditory function, these findings have significant implications in the context of sensory cell regeneration. Supported by NIDCD #5T35DC008757 & NCRR #2P20RR018788-06A1.

842 Mature Rbl2/p130-Deficient Mice Inner Ear Is Functional Despite the Presence of Additional Hair Cells and Supporting Cells

Sonia Rocha-Sanchez¹, Laura Scheetz¹, Melissa Contreras¹, Michael Weston¹, Megan Korte², Edward Walsh², Joann McGee²

¹Creighton University, ²Boys Town National Research Hospital

Unlike lower vertebrates, adult mammalian hair cells do not proliferate and hair cell death leads to irreversible neurosensory hearing loss and balance impairment. Recent advances have provided proof of principle for two sets of therapies: the use of the cyclin system or the retinoblastoma gene Rb1, to promote proliferation, and the effectiveness of Atoh1 to induce transdifferentiation of supporting cells into hair cells. Combined, these two approaches can mimic the ability of lower vertebrates to regenerate hair cells. However, beyond the proof of principle, attempts to regulate cell cycle through ablation of Rb1 are not likely to safely repopulate lost hair cells. Similar to Rb1, the two other members of retinoblastoma family of proteins (i.e., Rbl1/p107 and Rbl2/p130) are capable of inhibiting cell cycle progression and repressing transcription in many cell types. However, unlike other tissues, the biochemical and molecular pathways of these two retinoblastoma proteins in the inner ear is relatively unexplored. In this study, we identify p130 as an important regulator of mitotic quiescence of hair cell and supporting cells in the apical and upper middle turns of the cochlea. In the absence of p130 extra rows of inner hair cells, outer hair cells, and supporting cells are found in the more apical regions the organ of Corti. Interestingly, in spite of the presence of supernumerary sensory and supporting cells, p130 knockout mice exhibit normal peripheral auditory function.

843 Deletion of the Retinoblastoma Gene *Rbl2*/p130 Is Associated with Transcriptional Changes in the Expression of Mitotic-, Cell Growth-, and Differentiation Regulators in the Mouse Organ of Corti

Laura Scheetz¹, Michael Weston¹, Sonia Rocha-Sanchez¹ ¹Creighton University

Loss of neurosensory cells of the ear, caused by genetic and non-genetic factors, is becoming an increasing problem as people age, resulting in deafness and vestibular disorders. Unveiling useful mechanisms of cell cycle regulation may offer the possibility to generate new cells out of remaining ones, thus providing the cellular basis to induce new hair cell differentiation in the

mammalian ear. The retinoblastoma family of cell cycle regulators, composed of Rb1, Rbl1 (p107), and Rbl2 (p130), constitutes a central node controlling G1 to S phase transition in proliferating cells and cannot be bypassed without some cost to the cells. All three retinoblastoma genes have well-established roles as direct repressors of E2F transcription factors activity that, in turn, promotes the process whereby cell growth is arrested. Rb1 has been implicated as the major regulator of postmitotic guiescence in hair cells. Moreover, recent studies from our group have pointed to Rbl2/p130 as an important component of supporting cells guiescence maintenance in the adult organ of Corti. In order to assess the mechanism underlying p130 role in mitotic quiescence of supporting cells, a microarray analysis was performed on subdissected organ of Corti of adult p130 knockout mice. So far, our analyses suggest a minor role for p130 in DNA replication and cell cycle regulation in the organ of Corti. Nevertheless, p130 deletion in the organ of Corti affects a variety of genes largely involved in mitosis (i.e., Cdc20, Cdc2a, Ccna1), cell growth (i.e., Pdgf, Gas1, Gas2, p27^{Kip1}, Stat1, Tgf-3,E2f4), and differentiation (i.e., Zfp36, Id1, Id2). Results have been validated by RT-QPCR and immunohistochemistry, providing the base for a mechanistic understanding of p130 role in organ of Corti homeostasis, as well as its potential manipulation on hair cell regeneration through supporting cell proliferation.

844 Electroporation of Reprogramming Factors Into the Explant Culture of the Murine Organ of Corti

Koji Nishimura¹, Norio Yamamoto¹, Takayuki Nakagawa¹, Juichi Ito¹

¹Department of Otolaryngology, Head and Neck Surgery, Graduate School of Medicine, Kyoto University

Cochlear hair cells are damaged by various causes, including acoustic trauma, ototoxic drugs, and aging. It is well known that mammalian cochlear hair cells do not regenerate spontaneously, although most non-mammalian vertebrates are able to regenerate sensory hair cells after injury. However, the existence of tissue stem cells in the adult mammalian inner ear was recently confrimed by the finding that stem cells were still present in the vestibular organs of adult mice (Li, 2003). One possible way to regenerate lost cochlear hair cells is to dedifferentiate cochlear supporting cells into progenitors followed by redifferentiation into new hair cells. In this context, we previously reported that silencing p27 changes post-mitotic state of supporting cells into mitotic state in neonatal mouse cochleae (Ono, 2009). Induced pluripotent stem (iPS) cells is generated by dedifferentiating mature tissue cells using four critical factors, Oct3/4, Sox2, Klf4 and c-Myc. In this study, we aimed to induce sensory progenitor cells in the mammalian cochlea by defifferentiating mature epithelial cells. For this purpose, we examined the reprogramming potential of the plasmid containing complementary DNAs (cDNAs) of Oct3/4, Sox2, and Klf4 (Okita, 2008) in the explant culture of the murine organ of corti. The cochlear epithelia from P3 ICR mice cultured on sterile membranes in humidified atmosphere of 95% air

and 5% CO2 for 24 h were used for the electroporation experiments, for which we prepared three kinds of plasmid mixtures that included pEGF-N1 (Clontech, Palo Alto, CA), pCAG-OKS (gift from Okita K) and pEGFP-N1 and pCAG-OKS. A CUY21 electroporator (Nepa Gene, Chiba, Japan) was used to transfer the plasmid mixtures into the auditory epithelial cells from the explant cultures. Immunohistochemical analysis (Oct3/4, Sox2, Jagged1, Prox1, Nanog) was performed 48 h after electroporation.

845 Chemotactic Reinnervation of Hair Cells by Embryonic Stem Cell-Derived Neurons Yasheng Yuan¹, Fanglu Chi¹

¹EENT Hospital, Fudan University

Hearing loss can be caused by primary degeneration of spiral ganglion neurons or by secondary degeneration of these neurons after hair cell loss. Replacement of spiral ganglion neurons would therefore be one prioritized step in an attempt to restore sensory neuronal hearing loss. Recent studies have indicated that embryonic stem cells (ESCs) can be a source for the replacement of spiral ganglion neurons. However, the potential of ESC-derived neurons for functional synapse formation with auditory hair cells has not been elucidated. The present study therefore aimed to examine the abilility of ESC-derived neurons to form synaptic connections with hair cells in vitro.

As a source for implantation we used mouse ESC. Mouse ESC-derived neural progenitors were cocultured with explants of cochlea sensory epithelia obtained from postnatal day 3 mice under transwayfilter membrane. At day 3, the ESC derived neural progenetor cells began to show chemotactic differentiation and grew towards cochlea sensory epithelia. After 9-14 day culture, neurites of ESCderived neurons predominantly elongated towards hair cells. Immunohistochemical analyses revealed the fibers expression of GFP overlapped with PSD95(postsynaptic density) which is juxtaposed with CtBP2(presynaptic vesicle), indicating the new formation of synaptic connections. The present findings show that ESCderived neurons can make synaptic connections with both inner hairs and out hair cells and are ideal candidate for cell transplantation in inner ear to replace the lost spiral aanalion neurons.

846 Generation of New Synapses Between Mammalian Afferent Neurons and Hair Cells *in Vitro*

Mingjie Tong^{1,2}, Aurore Brugeaud¹, Albert Edge^{1,2} ¹Massachusetts Eye and Ear Infirmary, ²Harvard Medical School

Previous studies have shown that spiral ganglion neurons (SGNs) formed new synapses with deafferented hair cells in an organ of Corti explant. Examination of deafferented hair cells indicated that the pre-synaptic ribbons remained intact in the absence of afferent innervation throughout the period of culture. The regenerated synapses were detected by post-synaptic densities (PSD-95) in the SGNs. These PSD-95 positive puncta on the outer surface of the hair cells were aligned with the CtBP2 positive ribbons on

the inner surface of the hair cell membrane. The excitatory neurotransmitter glutamate has been implicated as a guidance molecule in the early stages of synaptogenesis in the CNS. To assess its possible role as a chemoattractant to guide the dendrites of SGNs in the organ of Corti explant, we performed re-innervation experiments using hair cells from glutamate vesicular transporter 3 (VGLUT3) mutant mice that do not release glutamate. After deafferentation, the organ of Corti from a VGLUT3 -/mouse was co-cultured with SGNs from a C57BL/6J mouse. Our hypothesis was that glutamate would be necessary for regeneration of the synapse. Surprisingly, after 6 days in vitro, new synapses were observed on hair cells of VGLUT3 -/- mice, identified by immunoreactivity of PSD-95 puncta on SGN fibers juxtaposed to the presynaptic ribbons of hair cells. The average number of newly regenerated synapses per hair cell was 2.8 +/- 0.4 in VGLUT3 -/- homozygotes, 4.0 +/- 0.2 in VGLUT3 heterozygotes and 4.2 +/- 0.5 in wild type mice. Differences were not significant (p>0.05, one-way Thus, our results suggest that the ANOVA). neurotransmitter glutamate is not required for synaptic regeneration in mammalian organ of Corti, and we propose that other axonal chemoattractants or chemorepellents are guiding the early stages of synaptogenesis.

Supported by NIDCD grants R01 DC007174 and P30 DC05209.

847 Ectopic Expression of Nex1 on Murine Embryonic Stem Cells Undergoing Neural Differentiation

David Miller¹, Karl Koehler¹, Takako Kondo¹, Eri Hashino¹ ¹Indiana University School of Medicine

Nex1 is a bHLH transcription factor that belongs to the During embryogenesis, Nex1 is NeuroD subfamily. expressed exclusively in glutamatergic neurons in the nervous system. We have found that Nex1 expression in the embryonic ear, detectable as early as E10.5, is confined to the spiral ganglion. Based on the specific expression pattern, we hypothesized that Nex1 is a molecular factor capable of promoting neuronal differentiation, maturation and/or survival. To test this hypothesis, we established an in vitro transgenic system, by which Nex1 is stably expressed in undifferentiated mouse embryonic stem cells (ESCs) that subsequently undergo neural differentiation. This system allowed us to analyze the effects of forced Nex1 expression on ESCs at various differentiation stages. A Nex1 transgenic cell line (pBud-cNex1-eGFP) and control cell line (pBud-eGFP) were either maintained as undifferentiated or subjected to neural differentiation. The progression of ESC differentiation was monitored with ESC markers as well as neural markers. At various time points before or after the start of neural induction, the cells were harvested and processed for qRT-PCR or immunocytochemistry. We found that expression levels of glutamatergic marker genes (GluR2, GluR4, Vglut2) as well as the glutamatergic selector gene TIx3 in Nex1-expressing ESC-derived cells were significantly higher than those in control cells at NI day 7. Additionally, expression levels of pan-neural (HuC, Syn, NSE, Tau) and GABAergic (Gad1, Pax2, Viaat) genes were significantly higher in Nex1-expressing cells than in the control. Results from immunohistochemitsry were consistent with the qRT-PCR results, demonstrating an increase in the number of cells expressing Synaptophysin and GluR4 in Nex1-expressing cells compared to control cells. These results suggest that Nex1 facilitates neural differentiation and maturation, but, unlike Tlx3, does not selectively promote the glutamatergic phenotype.

848 Brain Derived Neurotrophic Factor (BDNF) Affects the Electrophysiology of Neurogenin-Induced Neurons

Erin Purcell¹, Liqian Liu¹, Margaret Decker¹, Richard Altschuler¹, R. Keith Duncan¹

¹University of Michigan

Neurotrophic factors have been shown to affect the excitability of spiral ganglion neurons (SGNs). We sought to identify the electrophysiological effects of BDNF in neurons derived from stem cells differentiated via doxycycline (dox)-induced overexpression of Neurogenin-1 (Neurog1). These cells have a glutamatergic, 'spiral ganglion neuron-like' phenotype and may be useful in the repopulation of degenerated auditory nerves. Neurons were exposed to four days of either BDNF (10 ng/mL) or carrier control (diluted bovine serum albumin) following 3 days of dox induction. We observed a significant reduction in resting membrane potential (RMP) with BDNF exposure (Control, n=12: -38.8 +/- 2.0 mV; BDNF-treated, n=11: -49.4 +/- 2.3 mV, p<0.01, t-test). KCNQ-type potassium channels set the resting potential of inner hair cells. In addition, the low-to-high apex-to-base profile of BDNF mirrors the expression of KCNQ4 in SGNs in the cochlea. Based on these observations, we hypothesized that BDNF effects on RMP in our neurons resulted from an upregulation of KCNQ4. Preliminary data revealed a reversible 10 mV shift in the RMP toward more positive potentials when a BDNF-treated cell was exposed to the KCNQ4-blocker linopirdine (initial RMP=-50.7 mV. linopirdine-blocked RMP=-40.1 mV, washout RMP=-52.5 mV). BDNF exposure increased KCNQ4 gene expression by approximately 6-fold in comparison to controls (n=3 per condition). We are pursuing KCNQ4 immunocytochemistry and additional blocking experiments to further understand the effects of BDNF exposure on the expression of this ion channel. A connection between BDNF and KCNQ4 expression following Neurog1 induction has potential applicability in controlling the excitability of stem cell-derived neurons in an auditory nerve regeneration application. It also raises questions regarding a role for BDNF in the development and physiology of SGNs.

ARO Abstracts

849 Micropatterned Methacrylate Polymers Induce Schwann Cell and Spiral Ganglion Neurite Alignment

Joseph C. Clarke¹, Bradley Tuft², Jason Clark², John D. Clinger¹, Allan Guymon², Marlan Hansen¹ ¹University of Iowa Hospitals and Clinics. ²University of

Iowa

Significant advances in the functional outcomes achieved with cochlear implantation will likely require tissueengineering approaches to improve the neural prosthesis interface. One strategy is to direct spiral ganglion neuron (SGN) axon growth in a highly organized fashion to approximate or contact stimulating electrodes. Here we assessed the ability of micropatterns induced by photopolymerization in methacrylate (MA) polymer systems to direct cultured neonatal rat SGN neurite growth and alignment of SG Schwann cells (SGSCs). SGN survival and neurite length were comparable among various polymer compositions. Remarkably, there was no significant difference in SGN survival or neurite length between laminin and non-laminin coated MA polymer substrates, suggesting high biocompatibility with SG tissue. Micropatterning with photopolymerization generated microridges with a periodicity of 50 μ m and channel depths ranging from 1-9 µm. SGN neurites grew within the grooves of the micropattern. These topographies strongly induced alignment of dissociated SGN neurites and SGSCs to parallel the pattern. By contrast, fibroblast failed to align with the micropattern suggesting cell specific responses to topographical cues. The degree to which SG neurite growth aligned with micropatterns increased with the depth of the microgrooves. On polymers with shallow grooved patterns, laminin-coating was required to direct SG neurite growth. Deeper grooved micropatterns did not require laminin to direct SG neurite growth in dissociated cultures. SGN neurites extending from explants turned to parallel the pattern as they encountered the microchannels. The extent of turning was significantly correlated with the angle at which the neurite initially encountered the pattern. These results raise the possibility of using optimized micropatterns in MA polymers, induced by photopolymerization, as substrates to direct SGN outgrowth towards a stimulating electrode in a highly organized fashion.

850 Concentration-Dependent Effect of NGF on Cell Fate Determination of Neural Progenitor

Lei Zhang¹, Hui Jiang^{1,2}, Zhengqing Hu¹ ¹Wayne State University, ²Fudan University, Jinshan Hospital

Stem cell-based spiral ganglion neurons (SGNs) replacement therapy has been proposed to be a promising strategy to restore hearing via either replaces degenerated neurons or improves the efficacy of cochlear implants which rely on functional neurons. However, lack of suitable donor cells and low survival and differentiation rate of implanted cells are the major obstacles to successful implement of therapeutic transplantation. We

recently investigated the potential of mouse inner ear statoacoustic ganglion (SAG) derived neural progenitors (NPs) to differentiate toward glutamatergic, SGN-like cells and the influence of survival and differentiation when supplemented with nerve growth factor (NGF). We found that SAG-NPs could form neurosphere, proliferate, and differentiate into cells expressing neuronal proteins neurofilament and beta-III tubulin. NGF affected the cell fate of SAG-NP in a concentration-dependent manner in vitro. Low concentration NGF (2-5 ng/ml) promoted cell proliferation. Medium concentration NGF (20-40 ng/ml) stimulated SAG-NPs to differentiate into cells not only expressing general neuronal proteins neurofilament and beta-III tubulin (TUJ1), but also VGluT-1, a marker of SGNglutamatergic neurons. Moreover, like. medium concentration NGF may also stimulate neurite outgrowth from SAG-NP-derived neuronal protein expressing cells. High concentration NGF (100 ng/ml) could rescue cells from induced apoptosis. This finding raises the possibility to further induce these SAG-NPs to differentiate into SGNlike neurons in future study. In conclusion, given the capability of proliferation and differentiation into SGN-like cells with the supplement of NGF in vitro, SAG-NPs can serve as donor cell in stem cell-base SGN replacement therapy.

851 The Expression of P27Kip1 (A Protein Relevant for Hair Cell Regeneration) in Human Auditory and Vestibular Endorgans Microdissected from Temporal Bones Ivan Lopez¹, Gail Ishiyama¹, Rende Gu², Eric Lynch², Akira Ishiyama¹

¹UCLA School of Medicine, ²Sound Pharmaceuticals Using auditory and vestibular endorgan sections obtained from microdissected temporal bones we investigate the expression of a protein relevant to hair cell regeneration p27Kip1. This protein is a cyclin-dependent kinase inhibitor (also known as Cdkn1b), and functions as negative regulator of G1 progression (Inhibitor of cell cycle progression). The persistence of p27Kip1 expression in mature supporting cells may contribute to the maintenance of guiescence in this tissue and, possibly, to its inability to regenerate. p27Kip1 has been previously detected in supporting cells in the vestibule and cochlea in mice and rats, but not in the human inner ear. We performed immunohistochemistry for p27Kip1 using fixed frozen sections and paraffin sections of microdissected cristae macula utricle and saccule and cochlea obtained from normal human temporal bones and surgical specimens. We found that p27Kip1 is present in a population of cell nuclei located in the sensory epithelia of human the macula utricle and crista obtained at surgery and from autopsy specimens. In the organ of Corti a population of cell nuclei located in the supporting cells area was p27Kip1 immunoreactive. It has been postulated that the presence of p27Kip1 in supporting cells can be manipulated as a target for hair-cell regeneration, thus the detection of p27Kip1 in the human inner ear (from microdissected audio-vestibular endorgans) validate previous reports of its

expression in animal models, allowing translational studies in the field of hair cell regeneration. Supported by NIH/NIDCD grant 5U24 DC008635

852 Direct Entry of Gd-DTPA Into the Vestibule Following Intratympanic Application in Guinea Pigs

Elisha Thomas¹, Alec Salt², Hayden Eastwood¹, Stephen O'Leary¹

¹University of Melbourne, ²Washington University School of Medicine

While intratympanic (IT) administration of drugs has gained wide clinical acceptance, the distribution of drugs in the ear following IT administration is not well understood. Gadolinium (Gd) has been previously used as a marker in conjunction with Magnetic Resonance Imaging (MRI) to demonstrate qualitative distribution in inner ear fluids. In the present study we applied Gd to the round window quinea niche of 12 piqs in Seprapack (carboxlmethylcellulose-hyaluronic acid) pledgets, used to stabilize the fluid volume in the round window niche area. Gd distribution was monitored sequentially with time following application. Distribution in normal, unperforated ears was compared with ears that had undergone a cochleostomy in the basal turn of scala tympani and implanted with a silastic electrode. Results were quantified using image analysis software. In all animals, Gd was seen in scala tympani, scala vestibuli, and the vestibule. Although Gd levels in ST were higher than those in the vestibule in some ears, this was in a minority of cases. The majority of ears showed higher Gd levels in the vestibule than ST at both early and later time points. Quantitative computer simulations of the experiment, taking into account the larger volume of the vestibule compared to scala tympani, suggest a major proportion (up to 90%) of Gd entering the inner ear did not enter through the round window membrane, but entered the vestibule by another route, probably via the annular ligament of the stapes.

This work was supported by a scholarship from the University of Melbourne, research grant from the Royal Victorian Eye & Ear Hospital Australia, NHMRC 509206 and NIDCD/NIH DC01368 (AS).

853 Substances Enter Perilymph Near the Stapes as Well as Through the Round Window Membrane Following Intratympanic Applications in Guinea Pigs

Jared J. Hartsock¹, Elisha B. Thomas², P. Mason Bretan¹, Ruth M. Gill¹, Stephen J. O'Leary², Alec N. Salt¹ ¹Washington University School of Medicine, ²University of Melbourne

It is widely assumed that drugs enter perilymph predominantly through the round window membrane following intratympanic applications. As substances readily exchange between scala tympani (ST) and scala vestibuli (SV) across the spiral ligament, drug levels in SV and the vestibule were thought to follow an initial entry into ST. In the present study, we irrigated the round window (RW) niche area with the marker ion trimethylphenylammonium (TMPA), during which TMPA was monitored simultaneously in ST and SV in vivo with ion-selective microelectrodes sealed into the scalae. In other experiments, TMPA levels were determined in 10 perilymph samples taken sequentially from the lateral semi-circular canal after a 30 min application of 20 mM TMPA solution to the round window niche. This allowed TMPA levels throughout the perilymphatic space to be quantified. TMPA delivery was performed either to the entire RW niche or by protecting either the RW membrane or the stapes area with a two-part silicone adhesive. Results were interpreted with a new computer model of the inner ear that incorporates the fluid spaces of the vestibular system and allows entry via the RW membrane and the stapes independently. With irrigation of the entire RW niche, both in vivo measurements and sample data were consistent with substantial direct entry into the both the vestibule and ST of most animals. Entry into the vestibule remained after the RW niche was occluded with silicone. Simulation of the perilymph sample data showed the proportion of TMPA entering the inner ear in the area of the stapes averaged 34% (n=8) with individual animals varying from 13% to 62%, and with the balance entering through the RW membrane. Direct entry of drugs into the vestibule results in a greater volume of perilymph being loaded with drug and therefore more stable concentrations with time.

This work was supported by research grant RO1 DC01368 from NIDCD/NIH.

854 Evaluation of a Ten-Compartment Computer Model of the Inner Ear Fluid Spaces

Alec N. Salt¹, Jared J. Hartsock¹, P. Mason Bretan¹, Ruth M. Gill¹

¹Washington University School of Medicine

Prior computer simulations of drug movements in the cochlea utilize models based on the three scalae of the mammalian cochlea. In such models it is difficult to represent solute exchange between the fluids and tissuefilled compartments of the ear, such as the spiral ligament and spiral ganglion that they interact with. A computer program has been developed that simulates solute distribution throughout the fluid and tissue spaces of the combined cochlear and vestibular portions of the inner ear. The ability of the program to accurately represent the measured distribution characteristics of the marker ion trimethylphenylammonium (TMPA), which was applied and measured with a variety of protocols, was evaluated. TMPA was applied to the perilymphatic spaces by injections into either the basal turn of scala tympani (ST), the cochlear apex or the lateral semi-circular canal (SCC). TMPA concentration time courses were either measured in vivo with ion-selective microelectrodes, or in vitro in perilymph samples taken from the cochlear apex or lateral SCC using sequential sampling methods. Application protocols were designed to assess the exchange kinetics between scala vestibuli (SV) and ST through the spiral ligament or the kinetics of exchange between perilymph and tissue filled compartments during loading and sampling (washout) protocols. The goal was to establish kinetic parameters that allowed a variety of experimental procedures to be accurately simulated. As each compartment varies in cross-sectional area and length from base to apex in the cochlea, variation of fluid kinetics along the cochlea is complex. One goal has been to establish algorithms that appropriately account for base to apex communication differences. Improved understanding of the basic processes by which the fluid and tissue spaces interact will allow more meaningful calculations of drug distribution in the inner ear.

This work was supported by research grant RO1 DC01368 from NIDCD/NIH.

855 Long-Term Validation of a Reciprocating Micropump for Delivery of Microliter-Scale Volumes of Concentrated Drug to the Cochlea

Ernest Kim¹, Mark Mescher¹, Jason Fiering¹, Erin Pararas¹, Jeffrey Borenstein¹

¹The Charles Stark Draper Laboratory

Long-term Validation of a Reciprocating Micropump for Delivery of Microliter-scale Volumes of Concentrated Drug to the Cochlea

Ernest S. Kim, Mark J. Mescher, Jason Fiering, Erin E. Leary Pararas, Jeffrey T. Borenstein

We have conducted *in vitro* testing and validation of the long-term operation of a reciprocating micropump, a key component of an implantable, microelectromechanical system (MEMS)-based device for long-term precisioncontrolled intracochlear drug delivery currently in development. Initial testing of this reciprocating delivery system, reported previously, has been conducted using commercially available miniaturized pumps in a wearable configuration for short- and long-term intracochlear delivery to guinea pigs. Here we report on progress towards development of a micropump with size and power specifications suitable for full implantation for human clinical applications.

For our initial in vitro evaluation, we have tested the micropump on the bench continuously for over 3 weeks and have demonstrated consistent pumping properties over thousands of cycles by monitoring flow with a precision flow sensor (approximately 8 µL/min maximum flow rate and 1 µL maximum displaced volume). The micropump consists of a membrane-based displacement chamber, fluid channels and valves integrated on a substrate of machined and laminated polymer sheets. It is driven by an electromechanical actuator that is powered for several seconds during a three minute cycle. The reciprocating pump dispenses a fixed volume of concentrated drug through an implanted cannula into the cochlea, where the drug undergoes mixing with the perilymph, then slowly withdraws an equivalent volume. The system parameters are designed to provide safe. efficacious drug deliverv and appropriate an infuse/withdraw cycle to maximize the drug-perilymph mixing time and to enhance apical delivery. We have demonstrated tunable dispense volumes between 250 nL

and 1.5 μ L, maximum injection flow rates of 2 to 20 μ L/min, and maintained a clinically relevant delivery profile for several weeks.

The project described was supported by Award Number R01DC006848 from the National Institute on Deafness and Other Communication Disorders. The content is solely the responsibility of the authors and does not necessarily represent the official view of the National Institute on Deafness and other Communication Disorders or the National Institutes of Health.

856 Computational Reaction-Diffusion Model for Microfluidic Drug Delivery with Protein Interactions in the Guinea Pig Cochlea

Jeffrey Borenstein¹, Erin Pararas¹, William Sewell² ¹Draper Laboratory, ²Mass Eye and Ear Infirmary

We have developed a computational model describing drug transport and protein interactions in guinea pig perilymph in the scala tympani. The approach is based upon a reaction-diffusion model that incorporates drugprotein interaction as a simple binding event between mobile drug and a single type of immobile protein binding site, with rate constants for binding and dissociation. The analysis is structured as a set of coupled partial differential equations that are solved using a partial differential equation solver (MATLAB, MathWorks, Natick MA). These results are compared with experimental data obtained during acute drug infusion studies into the guinea pig cochlea using a microfluidic infusion system through a single cannula with a pulsatile delivery profile. These experimental data, reported previously, are based upon tonotopically generated compound action potentials (CAPs) at discrete locations along the length of the cochlea that signal the presence of administered DNQX, a hair cell neurotransmitter antagonist that attenuates the CAP. The time course of the effects of DNQX at different cochlear locations can be explained by modeling DNQX diffusion at its expected diffusion coefficient (based on its molecular weight) and incorporating protein binding and dissociation terms. The binding term serves to attenuate the penetration of the DNQX along the cochlear length while dissociation of the bound complexes provides free DNQX downstream of the infusion site, enhancing delivery.

857 Nanoparticle as Fluorescent Tag and Application to the Inner Ear for Imaging and Possible Use for Drug Delivery

IL-Woo Lee¹, Jaebeom Lee², Soo-Keun Kong³, Sung-Hwan Park³, Nam-Suk Myung¹, Eui-Kyung Goh³¹*Pusan National University Yangsan Hospital,* ²*Pusan National University, College of Nanoscience & Nanotechnology,* ³*Pusan National University Hospital*

Background: Quantum Dots(QDs) are non-toxic, organic fluorophore with high fluorescent yield and photo-stability. QDs' fluorescent yield and photo-stability are 20 and 100 times greater than organic molecules respectively. The aim of this study is to make QDs-Dexamethasone Nanocomplex(QDDN) and to know the possibility of application of QDs to the inner ear for staining and drug delivery. Methods: The newly synthesized QDDN was injected intratympanically into the bulla of Sprague-Dawley rats and the distribution of the QDDN in the cochlea was analyzed under the fluorescent microscope without any immunohistochemical staining.

Results: The QDDN was distributed throughout the entire cochlea in 1 hour and remained for 24 hours. The highest concentration of QDDN was noted at the spiral ganglion, spiral ligament, and organ of Corti especially in at the basal and middle turn of the cochlea. Distribution of the QDDN paralleled the locations of the glucocorticoid receptors.

Conclusions: QDDN can be used as a good fluroscent tag for the inner ear. QDDN could be a good vehicle for delivering steroids into the cochlea.

858 Biophysical Model Marginal Cell Ion Transport During Energetic Depletion

Marvin Thielk¹, Brian Chang², Robert Raphael³

¹Univ California Berkeley, ²Northwestern University, ³Rice University

The proper function of the cochlea requires active transport of potassium ions into the endolymph by the marginal cells of the stria vasculuaris, a very energyintensive process. However, the biophysics of marginal cell ion transport processes and the ability of the system to function under situations of energetic depletion are not fully understood. We have extended a previous mathematical model of marginal cell function by explicitly including the ATP sensitivity of the Na-K ATPase. The model can predict ATP concentrations at which the system begins to fail under normal operating conditions. Using the extended model, we investigated the sensitivity of the system to changes in important physiological variables. As previously observed, the system is particularly sensitive to changes in the potassium concentration in the intrastrial The system is also sensitive to the chloride space. concentration in the intrastrial space, with decreases in chloride increasing the transepithelial potassium current. We also found that over-activity of the apical potassium channel on marginal cells makes the system unstable when the intrastrial potassium concentration is high. Overall, the extended model provides a foundation for building larger and more complex systems models and investigating complex physiological and pathophysiological interactions between energetic status and marginal cell function that can potentially explain genetic predisposition to hearing loss during periods of oxidative stress.

859 Cytochemical Diversity of the Vestibular Membrane of the Saccule

Sungil Nam¹, Saumil N. Merchant¹, Joe C. Adams¹ ¹Harvard Medical School, Massachusetts Eye and Ear Infirmary

The vestibular membrane that borders the endolymphatic space of the saccule is morphologically specialized in humans by a conspicuous thickening in the anterior portion of the membrane. The functional significance of the thickening is not understood but the morphological specialization suggests that there is a functional specialization associated with the different morphological features. Immunostaining of the vestibular membrane in mouse supports the concept that it has functionally specialized divisions. The anterior portion of the membrane immunostains for aquaporin 1, which indicates that this portion of the membrane is specialized for water permeability and may play a role in control of endolymph volume. In contrast, the posterior portion of the membrane immunostains for the transient receptor potential channel TRPC3. This channel has been implicated in movement of calcium ions across apical membranes of kidney collecting duct cells and its localization within cells has been found to be sensitive to stimulation by vasopressin. These features suggest that its presence in the vestibular membrane may be associated with control of ion homeostasis in the saccule and that it may play a role in vasopressin-induced endolymphatic hydrops. In addition, the posterior portion of the vestibular membrane immunostains for connective tissue growth factor, a multifunctional protein that has been shown to regulate calcium signaling. Taken together these observations indicate that the vestibular membrane is complex and that it may play an active role in endolymph volume regulation, rather than acting as a passive barrier between the two distinct labyrinthine fluids.

860 Sodium Selectivity of Reissner's Membrane Epithelial Cells

Muneharu Yamazaki¹, Kyunghee X. Kim¹, Daniel C. Marcus¹

¹Kansas State University

Sodium absorption by Reissner's membrane is thought to contribute to the homeostasis of endolymph volume. It was shown (Kim et al., Amer. J. Physiol. 2009) that this sodium absorption is blocked by benzamil and amiloride. The most commonly-observed target of these drugs is the epithelial sodium channel (ENaC), comprised of the three subunits α - β - and γ -ENaC. However, other cation channels have also been observed to be sensitive in a similar concentration range. We determined the molecular and functional expression of candidate cation channels with gene array (GEO GSE6196), RT-PCR and whole-cell patch clamp recordings. Transcript expression analysis detected an absence of most acid-sensing ion channels (ASIC1a, ASIC2a, ASIC2b by RT-PCR) and cyclicnucleotide gated channels (CNGA1, CNGA2, CNGA4, CNGB3 by gene array). By contrast, α - β - and γ -ENaC were all previously reported as present in Reissner's membrane (gene array and RT-PCR; Kim et al. Am. J. Physiol., 2009). However, ENaC can occur with different ion selectivity depending on the stoichiometry of the The benzamil-sensitive cation currents and subunits. membrane conductance were found to be in the order $Li^+ >$ $Na^{+} >> K^{+}$, and there was no residual Na^{+} current after benzamil (NMDG⁺ substitution). These results are consistent with the benzamil-sensitive absorptive flux of Reissner's membrane mediated by highly Na⁺ -selective $\alpha\beta\gamma$ -ENaC. Reissner's membrane therefore absorbs only Na⁺ via the amiloride-sensitive pathway. This is in contrast to the outer sulcus and vestibular transitional cells that absorb Na⁺ but which also provide a parasensory K⁺ efflux

pathway (Lee et al., *J. Neurosci.*, 2001; Chiba & Marcus, *J. Membr. Biol.*, 2000). This high Na⁺ selectivity is similar to the epithelial cells of the semicircular canal duct (Wu et al., *ARO*, 2005). Supported by NIH grants R01-DC000212 and P20-RR017686.

861 A Novel Mechanism for the Regulation of HKv7.4 Channels by ANXA7 Protein - A Calcium-Dependent Process

Choongryoul Sihn¹, Hyo Jeong Kim¹, Ebenezer Yamoah¹ ¹UC Davis

Kv7.4 channels are expressed in hair cells and spiral ganglia neurons to generate IK,N. Mutations of the channel have been identified and have been associated with DFNA2, a progressive high-frequency hearing loss disease. Recent studies have shown that K+ current derived from Kv7.4 channels could be regulated by calmodulin binding to the C-terminus of the channel in response to increased intracellular Ca2+.

To identify additional cytoplasmic regulatory factors of Kv7.4 channels, we deployed the yeast two-hybrid assay with a full-length cytoplasmic C-terminal segment of Kv7.4 as a bait using mouse inner ear library. We have identified ANXA7 protein as a novel binding partner of Kv7.4 channels. ANXA7 is a membrane binding protein by the "core domain" that is able to bind with calcium ions. We demonstrate that interaction of Kv7.4 and ANXA7 occurs only in the presence of calcium. Moreover, in vitro, when cells were treated with Ca2+ ionophore to mediate increased intracellular Ca2+, ANXA7 associated with the plasma membrane and with Kv7.4 channels. The functional implications of ANXA7 association with Kv7.4 channels could not be tested in heterologous expression systems since e.g. CHO cells express endogenous ANX7A. We will demonstrate the functional significance of ANXA7 in Kv7.4 channel currents using RNAi strategies.

862 Impairment of Hearing and Cochlear Homeostasis in SIc4a11 KO Mice

Hannes Maier¹, Nicole Groeger², Henning Froehlich², Sawa Kostin², Thomas Braun², Thomas Boettger² ¹Medical University of Hannover, ²Max-Planck-Inst. Herzund Lungenforschung, Bad Nauheim

Introduction: Mutations in slc4a11 are found in the Harboyen syndrome, a congenital corneal endothelial dystrophy associated with progressive perceptive deafness. Here the role of the ion transporter slc4a11 in inner ear homeostasis and hearing is investigated in a targeted knockout mouse model.

Methods: Auditory-evoked brain stem responses (ABR) to clicks were recorded in anesthetized animals (16 mg/kg xylazine, 60 mg/kg S-ketamine). Click stimuli were delivered monaurally a rate of 21/s (400–2000 AVGs) while stimulus intensities were varied from 118 dB pe SPL to the threshold (5-dB steps). Measurements of endocochlear potential (EP) and potassium concentration ([K⁺]) were performed in anesthetized mice (14 mg/kg xylazine, 40 mg/kg S-ketamine). The bone over the 1st turn of the cochlea was opened below the stapedial artery and a single (EP) or double-barreled ([K⁺]) microelectrode was inserted. Potentials were recorded against an Ag/AgCl reference electrode and K-selective electrodes (K ionophore Fluka, 60398) were calibrated before and after each experiment.

Results: In the inner ear, antibody and LacZ staining marked type I, II, and IV fibrocytes underlying the stria vascularis. Up to 6 month of age gross morphological changes were not observed and the number of fibrocytes was constant (KO, 197.0 +- 6.4; WT, 188.0 +- 3.0 fibrocyte-nuclei/section, n = 6/7). Electron microscopy revealed stress-induced morphological changes of fibrocytes characterized by numerous intracellular vacuolations and extracellular edemas.

ABR hearing thresholds in KO mice were significantly reduced at 3w of age and remained constant in older mice. The endocochlear potential of KO compared to WT mice was strongly reduced (KO, 42.9 + 2.6 mV; WT, 111.3 + 2.9 mV; n = 8/7; p = 0.001). The potassium concentrations in the scala media was found normal in a smaller sample (KO, 135.7 + 2.3 mK; WT, 139.4 + 5.5 mM, n = 3/3, p = 0.56) suggesting that the hearing deficit is caused by the reduction in EP.

863 Manipulation of Dietary Sodium Alters Hearing in Natriuretic Peptide Receptor a (NPR-A) Knockout Mice

Janet Fitzakerley¹, Nina Holz¹, Aaron Clarke², George Trachte¹

¹University of Minnesota Medical School, ²Lake Superior College

Natriuretic peptides may have a role in the regulation of endolymph production, as suggested by the presence of their receptors in the stria vascularis. Preliminary data from loss- and gain-of-function models support the hypothesis that cyclic guanosine monophosphate (cGMP), produced by activation of natriuretic peptide receptor A (NPR-A), is part of a control system that regulates cochlear function. High salt diets have been shown to increase the plasma concentrations of atrial natriuretic peptide (ANP), which results in a dramatic increase in the movement of salt and water across epithelia. These experiments were designed to test the effects of manipulation of dietary sodium on hearing thresholds and on cochlear cGMP concentrations.

Animals were placed on either a sodium deficient diet (<0.01% sodium), a normal diet (0.49% sodium) or a high salt diet (8% sodium) on postnatal day 25 (P25). Thresholds were measured using auditory brainstem response (ABR) recordings before, during (P30) and after (P35) the dietary modification. Plasma osmolarity and renin concentrations were determined on P30 and P35 in order to determine the success of the diet treatments. Cochlear cGMP and plasma ANP concentrations were measured on P35.

Neither dietary manipulation had any effect on the hearing of CBA/J mice at any frequency, although cochlear cGMP and plasma ANP levels were increased in animals placed on the high salt diet. The effects of the diets on hearing was frequency dependent in the knockout mice, with larger effects at frequencies >8 kHz. The high salt diet protected knockout mice against the high frequency hearing loss that they experienced when on the low and normal Na diets. Cochlear cGMP and plasma ANP concentrations were increased in the wild-type and heterozygote NPR-A mice, but not in the homozygous mice. It can be inferred from these results that NPR-A may be involved in regulating the sensitivity of the cochlea to changes in dietary sodium.

864 Immunocytochemical Localization of the Translocase of the Outer Mitochondrial Membrane (Tom20) in the Human Cochlea

Ashley Balaker¹, Ivan Lopez¹, Gail Ishiyama¹, Akira Ishiyama¹

¹UCLA School of Medicine

Mitochondria are essential energy producing organelles in most eukaryotic cells. Aging and oxidative stress in pathological conditions like Meniere's disease, ototoxicity and otosclerosis likely affect mitochondrial function in the inner ear. The translocase of the outer membrane (Tom) is the universal entry gate for all proteins that are imported into mitochondria. In the present study we determined the localization of Tom20, the major mitochondrial import receptor, in 20 micron thick paraformaldehyde-fixed frozen sections from microdissected human cochlea obtained postmortem.

We used affinity purified rabbit polyclonal antibodies against Tom20 in addition to mouse monoclonal antibodies against the surface of intact human mitochondria and goat polyclonal antibodies to cytochrome-C to colocalize with Tom20. Tom20 had an almost ubiquitous distribution in the organ of Corti, allowing well delineated visualization of inner and outer hair cells. Tom20, cytochrome-C and mitochondrial antibodies colocalized in the neurons of the spiral ganglia, showing a punctated pattern in the cell cytoplasm. The neurons were identified with mouse monoclonal antibodies against pan-neurofilaments. This result suggests that Tom20 can be used as a marker for mitochondria and in combination with antibodies against cytochrome-C can indicate to some extent the functional status of these energy producing organelles. In addition, it shows that the use of microdissected endorgans and immunocytochemistry can be used for the detection and colocalization of various proteins that may not be feasible with other inner ear processing techniques or proteomics. Supported by NIH/NIDCD grant 5U24 DC008635

865 MUC1 Expression in Endolymphatic Sac Epithelial Cells

Sung Moon¹, Jeong-Im Woo¹, Mitsuyoshi Nagura², Kiweon Cha³, Paul Webster¹, Helge Rask-Andersen⁴, Johng Rhim⁵, David Lim^{1,6}

¹House Ear Institute, ²Hamamatsu University School of Medicine, ³Kyungpook National University, ⁴Uppsala University Hospital, ⁵Uniformed Services University of the Health Sciences, ⁶University of Southern California The endolymphatic sac (ES) is believed to be involved in homeostasis of inner ear endolymph. The disruption of inner ear homeostasis results in many inner ear disorders such as endolymphatic hydrops and Meniere's disease. A homogeneous substance found in the lumen of the vertebral ES appeared to contain glycoproteins and polysaccharides. Mucins are a family of heavily glycosylated proteins (glycoconjugate) produced by epithelial tissues in most metazoans and play a role in lubrication, chemical barriers and innate immunity against pathogen. In this study, we aimed to investigate the expression of mucin genes such as MUC1 in the ES and establish an in vitro model of human ES epithelial cells. RT-PCR analysis and immunolabeling showed the expression of Muc1 in the rat ES. We immortalized the human ES epithelial cells through infection with a retrovirus containing the E6/E7 genes of human papilloma virus type 16, which appeared to preserve the characteristics of normal ES epithelial cells such as cobblestone-like appearance, anchorage-dependency, and expression of ZO-1. Ultra-structural studies showed that our human ES epithelial cell line forms a junctional complex and has microvilli-rich and -poor subpopulations. Moreover, our human ES epithelial cell line appeared to preserve the expression of MUC1 and up-regulate MUC1 in response to the cocktails of growth factors. Altogether, our findings indicate that we successfully established the in vitro model of human ES epithelial cells, which will enable us to elucidate molecular mechanisms related to endolymph fluid homeostasis. As far as we know, we first demonstrated the expression of MUC1 in the ES, but the specific fuction of MUC1 in the ES remains to be further investigated. [Supported in part by 2010 DRF Hearing and Balance Science Research Grant]

866 Albumin-Like Protein Is the Major Protein of Luminal Fluid in Human Endolymphatic Sac

Sung Huhn Kim¹, Eun-Young Choi², Un-Kyoung Kim³, Won-Sang Lee¹, Jae Young Choi¹

¹Yonsei Üniversity, ²Yonsei Proteome Research Center, ³Kyungpook National University

The endolymphatic sac (ES) is a part of inner ear organs connected with cochleo-vestibular system through endolvmphatic duct. The main role of ES has been thought to regulate luminal fluid of inner ear by absorbing or secreting fluid. The luminal fluid of ES contains much higher protein concentration than any other compartment of inner ear. Such a high protein concentration is likely to contribute to the inner ear fluid volume regulation by creating an osmotic gradient between ES lumen and interstitial fluid. We identified protein profiles of ES luminal fluid in the patients (n = 11) with enlarged vestibular aqueduct (EVA) with proteomic analysis and tried to find the difference of protein profiles between the patients with recent hearing deterioration and the patients without hearing deterioration. Mean total protein concentration of the luminal fluid was 554.7 \pm 94.6mg/dl mg/dl. The total number of spots in the 2-DE image of the luminal fluid after MARC was 517, and 59 main spots among them were analyzed with MADI-TOF MS The protein profile of the luminal fluid was different from that of plasma. Proteins identified from 29 spots also exist in the MARC filtered human plasma, however, proteins identified from the other 26 spots did not exist in the MARC filtered human plasma. Most abundant protein in the luminal fluid was hypothetical

protein (gi|51476390) which was similar to human plasma albumin but it had five different amino acid sequences. The concentration of the hypothetical protein was higher in the patient without recent hearing deterioration than the concentration in the patients with recent hearing deterioration. If we consider that abnormal Euinner ear fluid volume increase would occur in the patients with EVA after recent hearing deterioration, it is tempting to speculate that the hypothetical protein is the main osmotic gradient regulator for inner ear fluid volume regulation in the pathological conditions such as endolymphatic hydrops.

867 Type-1 Allergy-Induced Endolymphatic Hydrops and the Suppressive Effect of Leukotrien and Histamin Antagonists

Naoya Egami¹, Akinobu Kakigi¹, Taizo Takeda², Setsuko Takeda², Rie Nishioka³, Tatsuya Yamasoba¹

¹University of Tokyo, ²Nishinomiya Municipal Center Hospital, ³Kochi University

Objective

TO investigate the allergic endolymphatic hydrops and inhibition effect of anti-allergic drugs.

Methods

Experiment 1: 46 guinea pigs were actively sensitized with dinitrophenylated-Ascaris (DNP-As) twice every month, and were provoked with an injection of DNP-BSA 1 week after the second sensitization. The alterations in the inner ear were investigated histologically at 1, 12, 24, and 36 hours following the provocation. Remaining 10 animals were the control group which received no sensitization but only distilled water.

Experiment 2: 29 guinea pigs (18 for leukoriene receptor antagonist (LRA) group, 11 for histamin H1-antagonist (H1A) group) were actively sensitized in the same manner. One week after the second sensitization, animals received oral administration of LRA (pranlukast hydrate 30mg/kg) or H1A (olopatadine hydrochloride 30mg/kg), and were provoked in the same manner 1 hour after then. The alterations in the inner ear were investigated histologically at 6, 12, 24, and 36 hours following the provocation.

Experiment 3: Expression of leukotriene receptors (CysLT1 and CysLT2) and histamine receptors (H1, H2, and H3) in the endolymphatic sac were investigated. Results

Experiment 1: EH was observed 12, 24, and 36 hours after the last sensitization. In the endolymphatic sac were observed the degranulation of mast cells.

Experiment 2: In the animal groups with LRA and H1A, EH was decreased, and the degranulation of mast cells was not observed in the endolymphatic sac.

Experiment 3, CysLT1 and histamine H1, H2, and H3 receptors were present in the endolymphatic sac. Conclusions

1) The sensitization with DNP-Ascaris produced type 1 allergic endolymphatic hydrops, and allergic emdolymphatic hydrops and the degranulation of mast cells in the endolymphatic sac were inhibited by LRA and H1A.

2) Cysteinyl leukotriene receptor CysLT1 and histamine H1, H3 receptors were present in the endolymphatic sac.

868 A 3-Dimensional Model of Frequency Representation in the Cochlear Nucleus of the CBA/J Mouse

Michael A. Muniak¹, Alejandro Rivas¹, Karen L. Montey¹, Bradford J. May¹, Howard W. Francis¹, David K. Ryugo^{1,2} ¹Johns Hopkins University, ²Garvan Institute of Medical Research

The relationship between structure and function is an invaluable context with which to explore biological mechanisms of normal and dysfunctional hearing. The systematic and topographic representation of frequency originates at the cochlea, and is retained throughout much of the central auditory system. Because the cochlear nucleus (CN) initiates all ascending auditory pathways, we have developed a 3-dimensional tonotopic model to explore possible frequency specializations at this early stage. Prior descriptions of tonotopy in the mouse CN include a 2-D cFos map (Ehret & Fischer, 1991), 3-D maps derived from reconstructions of injection sites (Muniak et al., ARO Abst., 2007), and multi-track electrophysiological sampling (Luo et al., 2009). Building upon our previous efforts, we have reconstructed in 3-D the trajectories of labeled auditory nerve (AN) fibers following multiunit recordings and dye injections in the anteroventral CN of the CBA/J mouse. We observe that each injection produces a continuous sheet of labeled ascending and descending branches of the CN, with a sharp turn when transitioning from ventral to dorsal subdivisions. Individual cases were combined using 3-D alignment procedures to provide a comprehensive view of the projection pattern of AN fibers in the CN with respect to frequency. AN fibers exhibit a systematic and tonotopic arrangement in each subdivision with a clear separation of isofrequency laminae. The combined dataset was used to derive a 3-D reference model of tonotopy throughout the entire volume of the CN. This model can serve as a tool for visualizing CN tonotopy (e.g., virtual arbitrary slices), and as a dataset upon which hypotheses concerning frequency and location in the CN can be tested.

Supported by NIH/NIDCD grants DC05909, DC05211, DC00232, DC04395, DC00143, DC00023 and a LSRA from New South Wales, AU.

869 Auditory Cortex Projects to Midbrain Cholinergic Neurons That Innervate the Cochlear Nucleus Brett Schofield¹

¹Northeastern Ohio Univ. Coll. Med.

The auditory cortex (AC) projects directly to midbrain cholinergic cells that innervate the inferior colliculus (IC) (Schofield and Motts, 2009, Br Res Bull 80:163-170). The cholinergic cells are located in the pedunculopontine and laterodorsal tegmental nuclei (PPT and LDT, respectively). These nuclei innervate the cochlear nucleus (CN), and could exert modulatory effects at the first stage of central auditory pathways. In the present study, we ask whether

AC axons contact midbrain cholinergic cells that project to the CN. We injected an anterograde tracer into left AC and a retrograde tracer into left CN. We stained cholinergic cells with anti-choline acetyltransferase (ChAT), a marker of cholinergic cells. We then examined the PPT and LDT for ChAT-immunostained, retrograde-labeled cells (i.e., cholinergic cells that project to the CN) that appeared to be contacted by labeled AC axons. We observed contacts on labeled cell bodies and dendrites in the left PPT and LDT and, less often, in the right PPT and LDT. The target cells included immunopositive and immunonegative cells. In some experiments, a third tracer was placed in the left inferior colliculus (IC) to label cells that project to the IC. We identified PPT and LDT cells that contained both retrograde tracers, indicating collateral projections to the CN and the IC. Some of these cells were ChAT immunopositive (i.e., cholinergic) and some also received contacts from labeled AC axons. The results suggest that AC axons, which are glutamatergic, could activate both cholinergic and non-cholinergic cells in the PPT and LDT that innervate the CN and, in some cases, both the CN and the IC. Such projections could allow higher cognitive functions to exert cholinergic influences over multiple levels (i.e., CN and midbrain) of the auditory pathways. These pathways may be related to functions such as arousal or sensory gating that have been attributed to the PPT and LDT nuclei. Supported by NIH DC04391.

870 Cross-Frequency Coincidence Detection in the Cochlear Nucleus

Grace Wang^{1,2}, Bertrand Delgutte^{1,3}

¹Eaton-Peabody Laboratory, Massachusetts Eye and Ear Infirmary, ²Department of Electrical Engineering and Computer Science, MIT, ³Research Laboratory of Electronics, MIT

Patterns of auditory nerve (AN) activity contain spatiotemporal phase cues to the pitch of harmonic complex tones that are more consistent with psychophysics than traditional rate-place or temporal cues (Cedolin and Delgutte J Neurosci 30:12712). These spatio-temporal cues might be extracted in the cochlear nucleus (CN) by a cross-frequency coincidence detection (CFCD) mechanism, where a CN neuron would fire preferentially when its AN inputs tuned to different frequencies discharge in synchrony.

We implemented a CFCD model receiving AN inputs from varying extents of the tonotopic axis. We used Huffman stimuli, which have flat magnitude spectra and a 2π phase transition, to manipulate the relative timing of spikes across neighboring AN fibers. Compared to AN responses, model CFCD neurons had larger late responses to Huffman stimuli with sharp phase transitions. In response to harmonic complex tones, model CFCD neurons receiving AN inputs from a wide range of characteristic frequencies (CF) responded preferentially when their CF fell halfway between two harmonics of the fundamental, even though AN fibers fire more when a resolved harmonic coincides with their CF.

We compared CFCD model predictions with responses of single CN neurons in anesthetized cats. To characterize a

CN neuron as a CFCD, we looked for (1) an increased late response to sharp transition Huffman stimuli and (2) an increased response to complex tones when the CF fell between two harmonics. While most CN neurons exhibited neither characteristic or exhibited one but not the other, several primary-like and primary-like-with-notch units had responses consistent with both descriptions. Overall, our results suggest that some CN neurons are capable of extracting the spatio-temporal cues in the patterns of AN activity.

Supported by an NDSEG fellowship, an NSF fellowship, and NIH grants RO1 DC002258 and P30 DC005209.

871 Ultrastructure of the CBA Mouse Anteroventral Cochlear Nucleus (AVCN) and Cochlear Nerve Root

Amanda Lauer¹, Catherine Connelly¹, Katanyu Pongstaporn², Mohamed Lehar¹, Charles Limb¹, David Ryugo^{1,2}

¹Johns Hopkins School of Medicine, ²Garvan Institute Cells of the mouse AVCN have historically been characterized and named according to cytologic criteria developed in cats. Detailed ultrastructural descriptions of AVCN cells in mice, however, have not been made. We used light and electron microscopy to characterize cell types and their inputs in CBA mice. At the light microscopic level, AVCN cell types shared many characteristics with cats, whereas cochlear root neurons resembled those of rats. The rostral AVCN contained bushy cells interspersed with multipolar cells. Bushy cells, small cells, and cochlear root neurons were identifiable in the nerve root. Many cells, however, could not be unambiguously identified because unique ultrastructural features were not discernable. Although bushy cells were contacted by numerous axosomatic inputs that covered a large proportion of the cell body, no clear dichotomy for spherical and globular bushy cells was evident on the basis of nuclear and perinuclear ultrastructural features. Virtually all bushy cells showed some stacked endoplasmic reticulum (ER) surrounding a pale round nucleus, but large perinuclear stacks of ER were seldom observed. Multipolar cells typically displayed invaginated, eccentrically located nuclei with prominent perinuclear stacks of ER, and were contacted by either many or few axosomatic endings, some of which were quite large. Cochlear root neurons were large, located in the nerve root, and varied in their morphology. Three types of synaptic terminals contacted AVCN and cochlear root cells: those with large round, small round, and pleomorphic or flat synaptic vesicles. Given the inescapable relationship between structure and function, it is important to identify cell types and the circuits they form. The difficulty in classifying cell types suggests that further anatomical investigation is required, the significance of which is emphasized by the emergent role of mice in auditory research. Support: DC005211, DC000232, LSRA from New South Wales, AU

872 Expression of Astrocytic Proteins in Cochlear Nucleus During Normal Hearing and Conductive Hearing Loss

Hongning Wang¹, Sandy Lu¹, Emily Cote², Maria Rubio¹ ¹University of Pittsburgh, ²University of Connecticut

Astrocytes, the most abundant type of glial cells, not only provide support and nutrition to neurons but regulate neuronal excitability by modulating synapse formation and function (Haydon, 2001; Volterra et al., 2005). In response to brain injury and neurological disorders astrocytes become reactive (Uckermann et al., 2004, Buffo et al., 2010), and are characterized by hypertrophy of their processes and up-regulation of glial fibrillary acidic protein (GFAP). In addition to GFAP, the expression levels of other glial proteins involved in glutamate and water homeostasis are altered, which consequently affects synaptic function. The role of astrocytes in auditory processing is unknown. Although, it was shown that blockade of auditory nerve activity led to reactive astrocytes in the chick nucleus magnocellularis (Rubel et al., 1994; 1992), suggesting that astrocytes may be involved in auditory function. Our current study aims to characterize morphologically and molecularly cochlear nucleus astrocytes in normal hearing and in response to monaural conductive hearing loss (earplugging). We used P30 Sprague Dawley rats with normal hearing and rats after 1-week unilateral earplugging. ABRs were recorded and the thresholds from plugged ears were found elevated by 25 dB. Immunohistochemistry or immunofluorescence procedures were performed for GFAP, aguaporin 4 (AQP4) that is essential for mediating water transport across astrocyte membranes, and glutamate transporter-1 (GLT1) and glutamine synthetase (GS) that are crucial for balancing glutamate levels in the synaptic cleft. Antibodies for all these proteins showed positive immunolabeling for cochlear nucleus astrocytes. Morphometric and densitometry analyses showed an increase in the thickness of astrocyte processes and in the expression levels of GFAP in the same and contralateral side to the earplugging. Our data suggest that astrocytes may play a key role during normal and abnormal auditory processing. Supported by NIDCD/NIH and Pennsylvania Lions Hearing **Research Foundation**

873 WITHDRAWN

874 Two Pore Domain Potassium Channel: Differential Expression and Neuronal Excitability in the Cochlear Nucleus

Bozena Fyk-Kolodziej¹, Mark D. Skopin², Scott C. Molitor², Avril Genene Holt¹

¹Wayne State University, School of Medicine, ²University of Toledo College of Engineering

Two pore domain potassium channels (K2PDs) are responsible for background leakage of K+ currents and therefore regulate the resting membrane potential and excitability of neurons. Our previous studies showed changes in K2PD subunit expression in both the CN (Holt et al., 2006) and IC (Cui et al., 2007) after bilateral cochlear ablation.

In the present work, quantitative real time PCR was used to demonstrate changes in K2PD gene expression of TASK subunits (TASK1, 3, and 5) 24 hours after sound exposure (10 kHz, 118dB, 4 hours) compared to normal hearing adult rats (n = 4). There were significant decreases in the expression of TASK5 in the DCN and VCN (59% and 86% respectively; $p \le 0.05$).

Immunocytochemistry was performed to identify the regional and cellular distribution of TASK subunits within the CN as well as double labeling immunofluorescence to determine potential subunit composition (homo- and/or hetero-dimers). Immunoreactivity for TASK1, 3 and 5 was seen almost exclusively in neuronal somata in the core of VCN as well as within the fusiform and deep core layers of the DCN. Labeling was less prominent in the granule cell domain of VCN and in the molecular layer of DCN. Many neurons co-expressing TASK1 and 3 as well as TASK1 and 5 subunits were observed.

In addition, computational models were used to examine how modulation of leak current may affect electrophysiological responses of CN neuronal populations (cartwheel, pyramidal/fusiform, spherical bushy cell with type II responses, stellate cells with type I-c and type I-t responses, and an octopus cells). Our results suggest that CN neurons with the least amount of voltage-gated channel activation near normal resting membrane potentials are most susceptible to changes in the leak currents: stellate cells \approx cartwheel cells > pyramidal cells >> bushy cells \approx octopus cells and that a change to leak channel reversal, has a larger impact on cellular excitability as compared to leak conductance magnitude.

875 Afferent Regulation of Auditory Brainstem Neurons: Rapid Changes in Phosphorylation of Elongation Factor 2 (EEF2)

Ethan McBride¹, Yuan Wang¹, Ed Rubel¹

¹University of Washington

Deprivation of excitatory input into the nucleus magnocellularis (NM) of the neonatal chicken auditory brainstem induces transneuronal cell death of approximately 30% of neurons. Previous studies demonstrated that 1-3 hours after deafferentation via cochlear removal or presynaptic blockade, NM shows a uniform decrease in protein synthesis, RNA synthesis, ribosome integrity, and ribosomal RNA. By 6-12 hours after cochlear removal, a subpopulation of NM neurons shows complete cessation of these biochemical processes. These cells die during the subsequent 2 days. The remaining neurons atrophy, but recover the majority of their synthetic activity. Intracellular events that cause changes in protein synthesis and ultimately determine the fate of NM neurons following cochlear removal remain unknown.

We are investigating the involvement of eukaryotic translation elongation factor 2 (eEF2) in deafferentation-induced cell death in NM. This molecule is required for the translation elongation step of protein synthesis.

293

Phosphorylation of eEF2 slows protein synthesis and is modulated by synaptic activity. In normally innervated NM, total eEF2 immunoreactivity is distributed uniformly throughout all neurons. Most NM neurons also exhibit dense immunoreactivity for phosphorylated eEF2 (peEF2). In some cases, clusters of NM neurons show noticeably less p-eEF2 immunoreactivity. Following unilateral cochlear removal, the intensity and distribution pattern of eEF2 remain unchanged within the first 6 hours in both the innervated and deafferented NM. We expected an increase in p-eEF2 immunoreactivity in the deafferented NM; however, we observed dramatic reductions in p-eEF2 immunoreactivity within 0.5-6 hours in a subpopulation of deafferented NM neurons. The correlation between changes in p-eEF2 and the fate of NM neurons is under current investigation by comparing peEF2 immunoreactivity with the amount of protein synthesis using autoradiography.

876 Accounting for the Size and Shape of Juxtacellular Recordings of Extracellular EPSPs and APs

Christopher Kushmerick¹, Silviu I. Rusu², J. Gerard G. Borst²

¹Instituto de Ciências Biológicas, Universidade Federal de Minas Gerais, ²Erasmus MC, University Medical Center Rotterdam

The juxtacellular recording configuration, in which a patch pipette electrode is advanced into neural tissue until large single unit action potentials are obtained, permits labeling, stimulation, and recording of single cells in vivo. Despite growing popularity of this technique, the underlying relationship between the membrane potential of the cell under study and the size and shape of the juxtacellular potential it generates is poorly understood. Here, we compared the potentials obtained by paired whole cell current clamp and juxtacellular recordings from mouse medial nucleus of the trapezoid body (MNTB) neurons in brainstem slices. We find that the shape of the juxtacellular potential can be well approximated as the scaled sum of the intracellular potential and its first derivative, suggesting it is generated by ionic and capacitive current through a patch of membrane close to the pipette tip. We show that especially in the case of a passive soma, these recordings can provide information about synaptic conductance and postsynaptic excitability. We find that extracellular potentials of >1 mV, as commonly observed during in vivo juxtacellular recordings, were only obtained when the patch pipette was pushed into the cell. Under these conditions, however, the size of the juxtacellular potential was much larger than that predicted based on the size of the pipette tip assuming a specific membrane capacitance of 1 μ F/cm². To account for this discrepancy, we present a model of the loose patch space formed by membrane surrounding the juxtacellular pipette and show that this membrane contributes directly to the coupling between intracellular potential and the juxtacellular recording, thus explaining the large amplitude of the latter.

877 Deafwaddler Mutants Reveal a Cell Size Gradient in the MNTB

Jessica A. Hill¹, Cornelia Kopp-Scheinpflug², Yuan Wang¹, Ian D. Forsythe², Edwin W. Rubel¹, Bruce L. Tempel¹

¹University of Washington, ²University of Leicester

The plasma membrane calcium ATPase 2 (PMCA2) pumps calcium from cytosol to extracellular space and is highly expressed in stereocilia of hair cells. Mutations have occurred in mice and humans that decrease PMCA2 expression and lead to hearing loss. The *dfw*^{2J} mutant is a null mutation causing deafness in homozygotes(-/-) and high frequency hearing loss in the heterozygotes(+/-) (McCullough and Tempel, 2004). While PMCA2 has been shown to be important in hair cells, little work has been done on the role of PMCA2 in the auditory brain stem. We used ICC to show that PMCA2 is highly expressed in medial nucleus of the trapezoid body (MNTB) neurons and localized to the membrane.

Because the hair cells of dfw^{2J} -/- mutants are abnormal and/or absent, we hypothesized there might be cell loss in the MNTB as well. To quantify morphological changes in the MNTB of dfw^{2J} mutants we used 40µm Nissl stained sections to measure the total MNTB volume, cell number, and cell size for +/+, +/-, and -/-. We found no significant difference in total MNTB volume or cell number between genotypes but there was a decrease in cell size between +/+ controls and dfw^{2J} -/-.

The MNTB is organized along a tonotopic axis with medial cells responding best to high frequencies and lateral cells responding best to low frequencies. To determine if this decrease in cell size was differentially regulated along the tonotopic axis we divided our cells into medial and lateral groups. In +/+ controls the medial cells were significantly smaller than the lateral cells suggesting the presence of a cell size gradient. This cell size gradient is decreased in dfw^{2J} +/- and absent in dfw^{2J} -/-, data which is corroborated by capacitance measurements. This cell size gradient in the +/+ MNTB suggests that cell size is based on the frequency to which a cell responds. The absence of a cell size gradient in dfw^{2J} -/- elicits questions as to what is required for the development and maintenance of this gradient.

878 Tonotopic Organization of the Superior Olivary Nucleus in Chicken (Gallus Gallus)

Kathryn Tabor¹, William Coleman², Edwin Rubel¹, R. Michael Burger²

¹University of Washington, ²Lehigh University

The long-term goal of this project is to explore how inhibition contributes to binaural auditory processing. In the chicken auditory brainstem the majority of inhibitory input arises from the superior olivary nucleus (SON). The SON receives excitatory input from the ipsilateral nucleus laminaris (NL) and nucleus angularis (NA) and GABAergic neurons in the SON project back to these two nuclei as well as to the ipsilateral nucleus magnocellularis (NM). In addition, the SON projects to the contralateral SON and midbrain. The tonotopic organization of NA, NM, and NL has been described in several species; however, the organization of the SON remains unknown. Understanding the organization of the SON is required in order to determine how inhibition shapes early auditory processing. Recently we found that (i) the SON-NL projection shows an unusually broad tonotopic arrangement and (ii) that the SON is composed of two cell groups, with distinct projection patterns, raising the possibility that the SON may show multiple or complex tonotopic maps.

Our current project uses *in vivo* physiology paired with post-hoc image reconstruction to analyze the tonotopic map of the SON. We recorded multi- and single-unit neuronal responses to pure tones presented to the ipsilateral ear. Maps of the characteristic frequency (CF; 0.2-4.5 kHz) at recording sites were reconstructed for each animal (n = 13; P6-P10). Initial results show a prominent tonotopic axis of neuronal responses dorsal-to-ventral across the SON: Low-CF units were recorded in the dorsal region of SON, while progressively higher CF neuronal responses were found at more ventral regions of SON. Our findings to date show at least one dimension of a tonotopic map, suggesting this GABAergic input from the SON can shape early auditory processing in a frequency-dependent manner.

879 Monaural Response Properties in the Avian Superior Olivary Nucleus Are Modulated by GABAergic and Glycinergic Inhibitory Inputs: An in Vivo Study

William L. Coleman¹, Sonia R. Weimann¹, R. Michael Burger¹

¹Lehigh University

The Superior Olivary Nucleus (SON) is the primary source of inhibitory input to the auditory nuclei involved in ITD processing in birds. While much is known about the role of inhibition from the SON at its targets, very little is known about how SON cells process auditory information or how inhibition influences its responses. Using in vivo recordings in chicks, we characterized monaural responses of single SON neurons to toneburst stimuli. We found that SON neurons have diverse response patterns during acoustic stimulation; 70% of the population had a sustained response, and 24% had an onset response. A small third category, (6%) were suppressed by acoustic stimulation. Most neurons responded monotonically with intensity increases, but 40% of both onset and sustained neurons showed rate depression at the highest intensities. SON neurons were broadly tuned, with an average Q10 value of 1.9. Of the units with sustained response, about half of low CF (<1kHz) neurons showed strong phase-locking capability, with vector strengths >0.5. This suggests that some SON neurons may provide phase-locked inhibition to their targets. The suppressed neurons typically had a high spontaneous rate that was reduced or eliminated during tone stimulation. The degree of this suppression was both frequency and intensity dependent. To test the role of inhibition in shaping SON response properties, we used multibarrel electrodes to locally iontophorese inhibitory receptor antagonists. Blockade of GABA-A receptors with bicuculline or glycine receptors with strychnine had similar effects on SON responses: both drugs increased spike

rates, and decreased the peak vector strength. Evidence of glycinergic signaling in the SON was a surprising and novel result. Thus, we confirmed the presence of the glycine receptor in the SON using immunohistochemistry. These studies reveal a mixture of cell types within the SON that are influenced by both GABAergic and glycinergic inhibitory inputs.

880 GABA and Glycinergic Synaptic Input to the Avian Superior Olivary Nucleus

Matthew Fischl¹, Stefan Oline¹, R. Michael Burger¹ ¹Lehigh University

The superior olivary nucleus (SON) is the main source of inhibitory input to nuclei in the avian auditory brainstem. These inputs to the nucleus angularis, nucleus magnocellularis and nucleus laminaris have been characterized and recent studies demonstrate glycinergic transmission in the nucleus angularis (Kuo et al., 2009). However, no data regarding synaptic inhibition within the SON itself has been published. Using in vitro whole-cell patch clamp techniques, both evoked and spontaneous inhibitory postsynaptic currents (IPSCs) were pharmacologically isolated and characterized. For evoked IPSCs, the vast majority of SON neurons contained both GABAergic and glycinergic components. GABAergic conductance accounted for approximately 50% of the peak amplitude and 65% of the area of the IPSC while the glycinergic component accounted for 50% of the peak amplitude and 35% of the area (n=13). Blockade of both GABAA and glycine receptors resulted in complete suppression of the evoked current in 10 of 13 cells. As expected, analysis of kinetic measures (halfwidth and τ decay) revealed a slower time course for the isolated GABAergic component, and a faster time course for the isolated alvcineraic component when compared to control. For spontaneous IPSCs, pharmacological manipulations indicate that SON neurons receive a variety of inhibitory inputs. Among these are purely GABAergic terminals as application of SR95531, a GABA_A antagonist, significantly reduced sIPSC frequency. Additionally, SON neurons receive terminals that release glycine or that co-release GABA and glycine, as was similarly reported in nucleus angularis (Kuo et al., 2009). While the origin or independence of each of these inputs remains unknown, these results taken together indicate that SON is composed of neurons that are inhibited by multiple modes of synaptic transmission. These data complement results using in vivo recording techniques by Coleman et al.

881 Planar Multipolar Cell Projections from Cochlear Nucleus to the Ventral Nucleus of the Trapezoid Body: Endings and Synapses Thane Benson¹, Keith Darrow^{1,2}, M. Christian Brown^{1,3}

¹Massachusetts Eye & Ear Infirmary, ²Worcester State University, ³Harvard Medical School

Planar cells are a subtype of cochlear nucleus multipolar cell. They project centrally to the ipsilateral lateral superior olive and to the contralateral ventral nucleus of the trapezoid body (VNTB; Doucet and Ryugo, 2003, J. Comp.

ARO Abstracts

Neurol. 461:452), where they contact medial olivocochlear neurons (Darrow et al., 2010 ARO Abstr. #756). We investigated their synapses in the VNTB by labeling planar multipolar cells with injections of biotinylated dextran amine (BDA, 10k MW) into the dorsal cochlear nucleus of mice. These injections labeled medium-sized multipolar neurons in the ventral cochlear nucleus that were identified as planar type by their size and shape. Axons presumed to be from planar multipolar cells were relatively thin (1-3 µm diam.) and projected via the ventral acoustic stria. giving off branches to the ipsilateral lateral superior olive and the contralateral VNTB. In the electron microscope, the axon in the contralateral stria and the initial portion of its branch were myelinated but the terminal region of the branch was unmyelinated. In the VNTB, labeled terminals were en passant and terminal boutons of small size (< 3 μ m diam., < 10 μ m² area). Some of the endings that appeared to contact a cell body in the light microscope were seen in the electron microscope to contact dendrites. Terminals contained round vesicles and could form asymmetric synapses onto dendrites and spines. These features suggest that planar multipolar neurons form excitatory synapses in the VNTB. Such synapses may cause medial olivocochlear and other VNTB neurons to respond to sound. Supported by: NIDCD RO1 DC01089.

882 Spectral and Temporal Effects on Masking in Mice with Enhanced or Deficient Medial Olivocochlear Feedback

Amanda Lauer¹, Ioan Lina², Judy Park², Jessica Stuyvenberg², Bradford May¹

¹Johns Hopkins School of Medicine, ²Johns Hopkins University

Activation of the medial olivocochlear system (MOCS) should enhance detection and discrimination of masked sounds since the response of the auditory nerve to a masking sound is reduced and the signal-to-noise ratio is increased with MOCS activation. Behavioral detection and discrimination studies of MOC anti-masking effects have produced conflicting results. We used auditory brainstem response measurements to investigate simultaneous and nonsimultaneous masking in MOCS-deficient or MOCSenhanced mice. In Experiment 1, masked thresholds and auditory filter shapes were measured using the notched noise method. Masked thresholds and auditory filters were abnormal in a subset of MOCS-deficient mice, but not in MOC-enhanced mice. In Experiment 2, we measured recovery from forward masking as a function of increasing masker-stimulus delays. MOCS-deficient mice showed variable response recovery with increasing masker-signal delays, with some animals showing very little recovery. MOCS-enhanced mice showed somewhat stronger recovery than normal, perhaps due to reduced auditory nerve adaptation. These results provide further evidence of the importance of MOCS activation for enhancing the neural representation of masked sounds. Supported by DC005211, DC009353, and an NOHR Research Grant.

883 Vesicular Zinc Neuroanatomic Localization in Developing Auditory Brainstem Neurons

Elisabet Garcia-Pino¹, Karl Kandler¹

¹University of Pittsburgh

Approximately 10% of total zinc in the mammalian brain is packaged into vesicles from where it is co-released with excitatory and inhibitory neurotransmitters. Zinc affects the function of a variety of ion channel receptors, including NMDA and GABAA receptors. The neuromodulatory role of zinc in the auditory system is poorly understood. In order to investigate a possible contribution of zinc in the maturation of developing auditory circuits, we explored the presence of vesicular zinc and zinc-related proteins in developing and mature mouse auditory brainstem. We used the autometallographic zinc–selenium method to label vesicular zinc and immunohistochemistry to detect the vesicular zinc transporter ZnT3 in mice aged from P2 to P30.

At all studied ages, we observed intense zinc-selenium precipitates in the form of punctate labeling in the molecular layer of the dorsal cochlear nucleus, as well as in small cell domains of the ventral cochlear nucleus, as previously described in adult rats (Rubio and Juiz, 1998, J Comp Neurol. 399:341). In mice up to two weeks of age but not in adults, a delicate but distinct zinc labeling was present surrounding cell bodies in the lateral superior olivary nucleus, the medial nucleus of trapezoid body, and the superior paraolivary nucleus. The labeling pattern of ZnT3 immunoreactivity mirrored that of the zinc-selenium labeling. In adult mice, the majority of ZnT3 immunoreactivity was located in the neuropil in the molecular layer of the dorsal cochlear nucleus. ZnT3 immunoreactivity was also apparent as punctate labeling around large cell bodies in the ventral cochlear nucleus. In prehearing mice, immunolabeling was present in the neuropil and around somata in the superior olivary complex. These findings suggest that synapses in the molecular layer of the dorsal cochlear nucleus are regulated by zinc-dependent signaling pathways. The transient presence of vesicular zinc in synaptic terminals in the superior olivary complex before hearing onset suggests that zinc signaling is involved in the developmental organization of SOC circuitry. Supported by NIDCD (004199)

884 Purinergic Signaling in Developing Auditory Brainstem Neurons

Sasa Jovanovic¹, Beatrice Dietz¹, Jana Nerlich¹, Rudolf Rübsamen¹, Ivan Milenkovic¹

¹University of Leipzig

Early in development of the auditory and visual system, endogenously generated spontaneous patterns of neuronal activity can provide an important instructive signal for the refinement of sensory maps before the actual function commences. In the auditory system, bursting activity before hearing onset (postnatal day 12) is primarily generated in the cochlea by ATP-mediated activation of the cochlear inner hair cells. Such bursting activity has been also observed in several nuclei along the ascending

auditory pathway, where it supports survival of target neurons, tonotopic refinement of afferent connections, and adjustment of synaptic strength. In the present study we conducted extracellular recordings in vivo and additionally combined whole cell recordings and Ca²⁺ measurements in acute brainstem slices from Mongolian gerbil to investigate development of purinergic signaling in neurons of the auditory brainstem circuit. Our results show that extracellular ATP evokes Ca2+-dependent bursting in neurons expressing purinergic P2 receptors. However, the expression of P2 receptors is developmentally and topographically regulated. The P2 receptor-mediated responses (membrane depolarization, inward current and intracellular Ca²⁺ signal) peak during the first postnatal week, but they are strongly down-regulated after hearing onset (>P12), consistent with its developmental role. Moreover, the expression of P2 receptors seems to be restricted to certain auditory brainstem nuclei and only to distinct neurons within the respective nuclei, suggesting that purinergic signaling might play a specific role in organization of developing neuronal circuits.

885 Olfactory Ensheathing Cells Promote Neurite Outgrowth from Co-Cultured Auditory Brain Stem Slice

Yu Jiao^{1,2}, Ekaterina Novozhilova¹, Alexandra Karlén³, Jonas Muhr³, Petri Olivius^{1,4}

¹Center for Hearing and Communication Research, Karolinska Institute, Sewden, ²ENT Department, Beijing TongRen Hospital, Capital Medical University, ³Ludwig Institute for Cancer Research Ltd, Karolinska Institutet, ⁴Department of Otorhinolaryngology, Head and Neck Surgery, Linköping University

Cell therapy aiming at the replacement of degenerated neurons is a very attractive approach. By using an established in vitro organotypic auditory brain stem (BS) slice culture we routinely screen candidate donor cells, with some of them being further functionally assessed in in vivo models of sensorineural hearing loss. Both in vitro and in vivo systems show that implanted cells face challenges of survival, targeted migration, differentiation and functional integration with the host tissue. Low success rates are possibly due to the lack of necessary neurotrophic factors, adhesion molecules and guiding cues. Olfactory ensheathing cells (OECs) have been shown to express a number of neurotrophic factors and to promote axonal growth through cell to cell interactions. In the present study we co-cultured OECs with organotypic BS slice in order to see if OECs can serve as a facilitator when screening candidate donor cells in a triple co-culture setup. Here we show that OECs when co-cultured with the organotypic auditory BS slice not only promote neurite outgrowth from the cochlear nucleus (CN) region of the BS slice but also serve as a support cells by having BS slice axons grow along their processes. These results suggest that OECs can possibly enhance survival and targeted migration of a candidate donor cells suitable for the cell therapy in triple co-culture or in a living animal.

Key words: OECs, auditory, brain stem slice, co-culture, neurite outgrowth

886 Role of Cav1.3 Calcium Channels for the Development of Topography in the Auditory Brainstem

Jan Hirtz¹, Katrin Janz¹, Désirée Griesemer¹, Eckhard Friauf¹

¹University of Kaiserslautern

The place principle of frequency analysis in the cochlea is preserved in a remarkably precise pattern along the auditory brainstem stations. The inhibitory projections from the medial nucleus of the trapezoid body (MNTB) to the lateral superior olive (LSO) process information from highto-low frequencies from medial-to-lateral. To assess the role of Cav1.3 in the activity-dependent development of this topographically organized circuit, we employed Cav1.3-/- mice (Platzer et al., 2000, Cell), in which the auditory brainstem nuclei are deprived from cochlea-driven activity. We found a reduction in volume throughout the auditory brainstem nuclei in Cav1.3-/- mice (see poster Friauf et al, this meeting). Also, the Cav1.3-/- LSO has lost its typical U-shape, in which the topography is realized.

In acute brain slices, focal photolysis of caged glutamate via a laser diode in the MNTB was combined with patchclamp recordings of LSO neurons to characterize frequency position maps of the MNTB-LSO projection. This method allows the determination of the MNTB area that converges to one single LSO neuron. We observed a nearly twofold broader medio-lateral width of this area in Cav1.3-/- mice at P10-12 (42±5 µm vs. 23±4 µm in wild type). No difference was observed in the dorso-ventral input width. These results suggest an impaired elimination of projections. The frequency position map was distorted in Cav1.3-/- mice, although the general order from medial-tolateral was still present. To assess whether stimulus conditions were unchanged in Cav1.3-/- mice, MNTB neurons were patch clamped. The maximal distance between the uncaging spot and the patched neuron at which APs could be evoked did not differ between genotypes (ca. 10 µm). Tracing of single MNTB axons is currently performed to gain further insight into the projection patterns. Together, our results indicate an important role of Cav1.3 for the development of topography in an inhibitory projection within the auditory brainstem.

887 Impaired Development of the Auditory Brainstem After Loss of Cav1.3 Calcium Channels

Eckhard Friauf¹, Michael Boesen¹, Nadine Braun¹, Florian Kramer¹, Britta Müller¹, Hans Gerd Nothwang^{1,2}, Jörg Striessnig³, Stefan Löhrke¹, Jan Hirtz¹

¹University of Kaiserslautern, ²University of Oldenburg, ³University of Innsbruck

Within the Cav1 family of voltage-gated calcium channels, Cav1.2 and Cav1.3 channels are the predominant subtypes in the central nervous system. Specific functions for each subtype were described in the adult brain, yet their role in the developing brain is still very poorly understood. Here we have addressed the issue of activitydependent development in the auditory brainstem of

Cav1.3 subunit-deficient (Cav1.3-/-) mice. Our study was prompted by the fact that Cav1.3-/- mice lack cochleadriven activity; thus their auditory centers are deprived from the peripheral input. We found a drastically reduced volume in all auditory brainstem centers (by 25-59%) which was manifest before hearing onset. The degree of volume decreases was disproportionately high compared to the whole Cav1.3-/- brainstem which shrunk by 24%. The lateral superior olive (LSO), a key nucleus in the medullary brainstem, was strikingly malformed in Cav1.3-/mice and had fewer neurons (ca. 500 or 1/3 less). The remaining LSO neurons displayed normal dendritic trees and received functional glutamatergic input, yet they fired action potentials predominantly with a multiple pattern on depolarization, in contrast to the single firing pattern prevalent in controls. The latter finding appears to be due to an observed reduction of low-threshold, dendrodotoxinsensitive potassium conductances. Our results imply that functional Cav1.3 channels are indispensable for brainstem development and particularly necessary in the auditory system. We propose that the unique LSO phenotype in Cav1.3-/- mice, which hitherto was not described in other hereditary deafness models, is caused by the synergistic contribution of two factors: on-site loss of Cav1.3 channels in the neurons plus lack of peripheral input.

888 Transient A-Type K Currents Contribute to the Electrical Properties of Superior Paraolivary Nucleus Neurons

Sara Leijon¹, Richard Felix², Anders Fridberger¹, Albert Berrebi², **Anna Magnusson**¹

¹Karolinska Institutet, ²WVU School of Medicine

Neurons in the superior paraolivary nucleus (SPON) respond to sinusoidally amplitude modulated tones with very high precision in vivo, making them suitable for detecting the temporal structure of human speech or animal communication cues. The cellular mechanisms that enable the SPON neurons to extract information about amplitude fluctuations in the acoustic signal remain unknown. Therefore, whole cell patch clamp recordings were obtained from physiologically and morphologically identified and reconstructed SPON neurons in brain slices from neonatal mice. When injected with sinusoidal frequency-modulated electrical currents (1-15Hz) in vitro, SPON neurons only fire action potentials at a specific frequency at threshold. The frequency selectivity becomes progressively less discriminate with stronger currents. This cellular tuning to frequency-modulated currents might result from voltage-dependent conductances that amplify or suppress the selectivity for particular frequencies. Voltage clamp recordings demonstrate the presence of an outward current that activates in the subthreshold voltage range and inactivates rapidly with a time constant of ~10 ms. This current is sensitive to the antagonist 4aminopyridine, which is consistent with the low voltageactivated transient outward potassium current (A), mediated by the Kv4 family of potassium channels. Immunohistochemistry verifies prominent expression of the Kv4.3 potassium channel subunit in the SPON, which mediates A-currents. In addition, results of double-labeling against Kv4.3 and the presynaptic marker SV2A indicate a postsynaptic expression of the channel subunit. We speculate that the A-current is one of the major voltagedependent currents that contributes to the specific firing characteristics and tuning of the SPON neurons to periodically fluctuating stimuli.

889 Mutations of the Genes That Encode the Kv11 Ion Channel Subunit, *Kcna1* in Mice, *KCNA1* in Humans, Affect Complex Auditory Processing in Both Species

James Ison¹, Conny Kopp-Scheinpflug², Gary Paige³, Claire Walker⁴, Rudolf Rübsamen⁵, Paul Allen³, Anita Karcz⁵, Daniel Schatz³, Bruce Tempel⁴

¹Univ. Rochester, ²Univ. Leicester, ³Univ. Rochester Medical Center, ⁴Univ. Washington, ⁵Univ. Leipzig Point mutations in the KCNA1 gene in humans result in Episodic Ataxia, Type 1 (EA1), with motor disorders of variable seriousness including seizures, myokemia, and stress related episodes of motor incoordination. In contrast, deletion of the mouse homolog, Kcna1, appears to affect both efferent and afferent processing: in vitro (Zhang et al. JNeurosci 1999; Brew et al. JPhysiol 2003; Kline et al. JNeurosci 2005) and in vivo (Kopp-Scheinpflug et al. JNeurosci 2003; Karcz et al. SFN 2007); and in sound localization studies in awake mice (Allen & Ison, in review). These data suggest that afferent function may also be affected in point-mutation EA1 patients and EA1 mouse models. We found that one EA1 mouse model (the heterozygote Kcna1 V408A/+ point mutation on a CBA background) was no different from +/+ mice on a rotorod test, but 8/11 mutants and 0/8 controls had motor incoordination or ataxia on a treadmill. ABR thresholds for tone pips were normal in mutants but suprathreshold amplitudes were elevated around Waves 3 and 4. Mutants also had higher spontaneous rates in single-cell in vivo recording in the MNTB, but unlike Kcna1 -/- mice, their behavioral acuity for sound location was normal. To date three EA1 patients with three different point mutations have been tested for sound localization using four band limited noise stimuli, from 250-500 Hz to 1500-1890 Hz. All appeared normal for the lowest frequency band, but for the higher bands two patients had errors in apparent location outside the expected range. This continuing research program may help to illuminate the neural bases of the diverse phenotypes found in EA1 patients and may provide novel targets for therapeutic intervention: but of special significance in this present context of ARO, these deficits in sound localization in humans provide evidence that in vitro and in vivo work with isolated cells and awake behaving mice does contribute to understanding the neural bases of human audition.

890 Changes in the Expression and Distribution of Potassium Channels at and Beyond Hearing Onset

Joel C Nicolau¹, Rafael Lujan¹, Jose M Juiz¹ ¹Institute for Research in Neurological Disabilities (IDINE), University of Castilla-La Mancha

Specific sets of potassium channels are involved in providing auditory neurons with their characteristic firing properties in response to sound. It seems relevant to understand how different populations of auditory neurons develop their own sets of potassium channels, and whether hearing onset involves changes in the expression of these ion channels. We have used RT-PCR arrays and immunocytochemistry to follow gene and protein expression sequence of voltage-dependent potassium channels in the IC before and after hearing onset in the rat. Three age points were examined: P9 (before hearing onset), P14 (right after hearing onset) and P30 (well beyond hearing onset).

A total of 84 ion channel-related genes were included in the RT-PCR microarrays. As far as voltage-dependent potassium channels are concerned, gene up-regulation predominated between P9 and 14 both in the CN and IC. After P14, up-regulation was much less significant, except for a few genes in the IC. Highly up-regulated potassium channels included Kv1.1 and Kv3.1 in both auditory nuclei. Other voltage-gated potassium channels, such as Kv1.3 and Kv4.2 were down-regulated. However, downregulation of analyzed genes was almost exclusive of the CN and it seemed to take place well beyond the hearing onset window. Immunocytochemistry showed that labeling for Kv1.1 and Kv1.3b (a spliced isoform of KV3.1)subunits in the anteroventral CN and IC was scarce at P9. At P14, however, labeling intensity had increased significantly in both auditory nuclei, with little changes in staining intensity between P14 and P30. Therefore, the time of hearing onset coincides with active up-regulation of potassium channel genes and corresponding proteins involved in preserving acoustic timing in auditory brainstem circuits. In the IC, up-regulation continues through P30, at least for some genes, which may account for progressive maturation of responses to sound well beyond hearing onset. On the other hand, progressive and extended downregulation of some potassium channel genes past hearing onset seems to be relevant in the CN.

891 Neural Correlates for the Detection of Tones in Reproducible Noise Maskers: A Physiological Study of the Inferior Colliculus in Awake Rabbit

Muhammad Zilany¹, Laurel Carney¹

¹University of Rochester

Understanding the mechanisms by which a subject detects a tone in background noise is a classical problem in auditory psychophysics and physiology. Reproducible noise maskers are particularly useful for these studies because performance of a listener varies across different noise waveforms. The use of reproducible noise maskers thus allows a detailed comparison of performance across listeners and helps test models for the detection of tones in specific noise maskers. To examine potential neural encoding strategies for the detection of tones in wideband noise maskers, tetrode recordings were made from the inferior colliculus of awake rabbits to a diotic (NOSO) stimulus paradigm for which rabbit behavioral results have been reported (Gai et al., JARO 8: 522-538, 2007). The stimuli consist of a set of reproducible wideband (100-3000 Hz) noise maskers presented either alone or with a 500-Hz tone. Neural detection thresholds were estimated based on average discharge rate and several other temporal metrics, such as synchrony to the tone frequency, temporal reliability across stimulus repetitions, and rapid fluctuations in the poststimulus time histograms (PSTH) of the responses. In addition, the hit and false-alarm rates for neural detection of tones in each of the reproducible noise maskers were estimated based on the above metrics. Signal-to-noise ratios in the stimuli were matched to both rabbit and human behavioral detection thresholds. Preliminary results suggest that the best neural detection thresholds, based on average discharge rate and the fluctuations in the PSTH, can explain the behavioral detection threshold observed in rabbit. Some neural responses also showed significant correlation with the corresponding rabbit behavioral hit and false-alarm rates. To date, neural responses in rabbit, tested with tone stimuli at the lower human thresholds, were not generally correlated to the corresponding human behavioral responses.

Supported by NIH-NIDCD R01-001641.

892 Distinct Integration and Encoding Time-Scales Lead to a Sparse Temporal Code for Elementary Spectro-Temporal Features

Chen Chen¹, Heather Read¹, Monty Escabi¹

¹University of Connecticut

Spectral and temporal sound cues are essential for sound recognition and discrimination, yet how the brain represents such cues is not known. We recorded neuronal responses in the auditory midbrain of cats to temporally dynamic and spectrally complex sounds and characterized the temporal structure of the resulting neural responses. The time-scale of the stimulus features that evoked neural responses as determined by the spectro-temporal receptive field (~10 msec integration time window) were roughly an order of magnitude larger than the time-scale of the neural output (~1.5 msec encoding time window, determined by the time scale of the shuffled autocorrelogram). The precisely timed neural responses typically occurred in isolation as confirmed by the interspike intervals which were more than an order of magnitude larger (~120 msec) than the average integration time. On average, the likelihood that multiple action potentials fall within a single integration time window was only 9 %, among which most were burst spikes. In particular, the spike-timing precision of the neural responses is positively correlated with the neuron's feature selectivity (r=0.5). Thus acoustic features were explicitly encoded by low probability but temporally precise unitary spikes, and neurons with higher selectivity tended to produce more precise responses. Finally, although the receptive fields of neurons were sometimes highly overlapped and shared similar acoustic preferences, the timing of spikes was in general asynchronous across the neural ensemble. Correlated activity was only observed for 6% of the neuron pairs and most of these were confined to pairs with similar best frequencies (90% within 1/3 octave). These results demonstrate that spectral and temporal sound features are represented by sparse ensemble code of temporally precise, feature specific, yet asynchronous spikes. (Supported by NIDCD R01DC006397).

893 Responses of Inferior Colliculus Neurons to Harmonic Complexes and Complexes with a Mistuned Component in Gerbils

Astrid Klinge¹, Georg Klump¹

¹Animal Physiology & Behavior Group, IBU, Carl-von-Ossietzky University

Harmonicity is an important simultaneous grouping cue binding the frequency components that are integer multiples of a fundamental frequency and separating them from frequency components that do not belong to the harmonic series. Previous psychophysical studies in humans and animal models showed that already small frequency shifts in a component of a harmonic complex (mistuning) can be detected by the auditory system. Especially some bird species (starlings, budgerigars, zebra finches), but also the gerbil are extremely sensitive to changes in the stimulus caused by mistuning a component of the complex. For example, we observed detection thresholds of as low as 0.008% Weber fraction for a 6400 Hz component of a 200 Hz complex in the gerbil (Klinge & Klump, 2010). How the auditory system processes such harmonic complexes and which stimulus characteristics result in the observed low mistuning detection thresholds in gerbils is still an open question.

For a comparison of the behavioral performance and the neuronal sensitivity, we recorded responses from neurons of the inferior colliculus of the anesthetized gerbil to harmonic complexes and complexes with a mistuned component. Random-phase or sine-phase complexes with a 200 Hz or 800 Hz fundamental and comprised of 12 harmonics were presented via headphones. For the mistuned complex the component closest to the neuron's best frequency was mistuned by 0.25%, 1%, 3%, 12% or by the behaviorally determined threshold value. The different stimuli were either presented in random order or in an oddball paradigm with the harmonic complex as the standard and the mistuned complex as the deviant. We analyzed both the rate response as represented by the spike counts over the course of the stimulus duration and the temporal response patterns as represented by interspike intervals in the response. The neuronal response patterns are discussed with respect to the gerbil's behavioral performance.

Supported by the DFG (SFB/TRR 31)

894 Local Field Potentials in the Dorsal Cortex of the Inferior Colliculus Evoked by Rarely Presented Tone Bursts

Chirag Patel¹, Carmela Redhead¹, Huiming Zhang¹ ¹University of Windsor

A sound deviant in pattern and location from a repetitively presented background acoustic stimulus can be perceived as a novel sound. Novel sounds are typically of behavioural significance. Neurons that are sensitive to novel sounds have been found in multiple auditory processing centres including the dorsal cortex of the inferior colliculus (ICd).

In this study, we conducted in vivo neurophysiolgoical recordings and pharmacological manipulations to find: (1) whether the neural sensitivity to novel sounds in the ICd could be revealed by local field potentials; and (2) whether the type A gamma-aminobutyric acid receptor (GABAA receptor) contributed to the neural sensitivity to novel sounds in the ICd. An oddball stimulus paradigm was used to assess the sensitivity of ensembles of neurons in the ICd to novel sounds. Our recordings revealed that a sound presented at a lower probability in an oddball paradigm evoked a response with larger amplitude, while the same sound presented at a higher probability evoked a response with smaller amplitude. This result indicates that an ensemble of ICd neurons displays stimulus-specific adaptation and sensitivity to novel sounds. Strong adaptation can be found when a large contrast exists between the two tone bursts in both frequency and probability of occurrence in an oddball paradigm. Moreover, a higher rate of tone burst presentation results in stronger adaptation. Application of the GABA_A receptor antagonist bicuculline increased the response to a sound both when it was presented at high or low probabilities. However, stimulus-specific adaptation in response to an oddball paradigm was not completely eliminated during drug application. Our results suggest that factors other than inhibition mediated by local GABAA receptors are involved in the generation of neural sensitivity to novel sounds in the ICd.

Research supported by NSERC of Canada

895 Stimulus-Specific Adaptation in the Inferior Colliculus: Effects of Frequency, Intensity and Firing Rate

Daniel Duque¹, Manuel S. Malmierca¹, David Perez-Gonzalez¹

¹Auditory Neurophysiology Unit. Institute of Neuroscience of Castilla y León. Salamanca

The ability to detect unexpected sounds from the environment is an important function of the auditory system, as they may require a rapid response. Recent studies using an oddball paradigm have found a decreased response to a repetitive stimulus (standard) but an increased response to rare and less frequent sounds (deviant) in individual neurons from the inferior colliculus (IC) upwards. This phenomenon, known as stimulusspecific adaptation (SSA; Ulanovsky et al., 2003), has been suggested to serve for change detection and as a single neuron correlate for mismatch negativity (MMN).

Currently, it is unknown how SSA varies within the receptive field of a single neuron, i.e. it is unclear whether SSA is a unique property of the neuron or a feature that is frequency and/or intensity dependent. Also it is not known if there is any relation between the firing rate of the neuron and SSA. In the present experiments we used the Common SSA Index (CSI; Ulanovsky et al., 2003) to quantify and compare the degree of SSA under different stimulation conditions. This descriptive statistic analyzes the neuronal adaptation to a pair of frequencies in an oddball paradigm. We calculated the CSI at different intensities and frequencies in each individual IC neuron, in order to map the neuronal CSI within the receptive field.

Our preliminary data show higher SSA at intensities near threshold and also at the best frequency and frequencies below it. Furthermore, neurons with higher firing rates show less SSA. These findings suggest a stronger adaptation to strange, discrete sounds from the acoustic scene and support the notion that SSA varies as a function of frequency and sound intensity.

cknowledgements: Financial support was provided by the Spanish MEC (BFU2009-07286), EU (EUI2009-04083) and JCYL-UE (GR221) to MSM. DD held a fellowship from "La Caixa" Foundation and from the Spanish MEC (BES-2010-035649).

896 Comparison of the Effects of Intense Sound Exposure on the Dorsal Cochlear Nucleus and Inferior Colliculus

Frank Licari¹, James Kaltenbach¹

¹Cleveland Clinic

Exposure to intense noise is a major cause of tinnitus and is a powerful inducer of hyperactivity in the central auditory system, which is considered a likely contributor to tinnitus. In the auditory brainstem, both the dorsal cochlear nucleus (DCN) and inferior colliculus (IC) develop hyperactivity after intense noise exposure. A key question that has not yet been examined is whether the IC hyperactivity induced by noise exposure is driven by hyperactivity in the DCN or is instead maintained independently by mechanisms intrinsic to the IC. We addressed this question by comparing the profiles of hyperactivity in the DCN and IC of the same animals. We reasoned that if hyperactivity in the IC is dependent on input from the DCN, then the profiles of hyperactivity in the IC and DCN should correspond. For example, activity in both structures should be elevated in similar tonotopic regions and reach a peak at corresponding tonotopic locations. Hamsters were divided into two groups, including animals exposed to intense sound (10 kHz tone, 4 hrs, 115-127 dB SPL), and a group consisting of unexposed (control) animals. Recordings conducted 1-2 weeks after exposure revealed several important differences between hyperactivity profiles in the IC and DCN of the same animal: First, the level of both normal activity in controls and elevated activity in exposed animals was found to be significantly lower in the IC than in the DCN of the same animal. Second, the location where hyperactivity peaked in the IC

sometimes differed greatly from the corresponding DCN. Third, IC hyperactivity was sometimes absent in frequency regions where hyperactivity was present in the DCN. Taken together, these differences may indicate that IC hyperactivity is to some extent independent of DCN hyperactivity. However, this inference should be taken as tentative until other explanations of these differences can be ruled out. (This work was supported by NIH grant R01 DC 009097).

897 Human Auditory Brainstem Responses to Musical Intervals Are Predicted by Phase Locked Neural Oscillation

Edward Large¹, Felix Almonte¹

¹Florida Atlantic University

The auditory nervous system is highly nonlinear. Some nonlinear responses arise through active processes in the cochlea, others in neural populations of the cochlear nucleus, inferior colliculus and higher auditory areas, in which neurons phase-lock to stimulus periodicities up to 1000 Hz. In humans, auditory brainstem recordings generated in the midbrain inferior colliculus (IC), reveal nonlinear population responses to combinations of pure tones, and to musical intervals composed of complex tones. Yet the biophysical origin of central auditory nonlinearities, their signal processing properties, and their relationship to auditory perception remain unknown. Here we show that a canonical model of phase-locked neural oscillation predicts the complex nonlinear population responses to musical intervals that have been observed in the human brainstem. The model provides insight into the nature of auditory population responses, and makes predictions about auditory signal processing and perception that are different from traditional delay-based models. We anticipate that the application of dynamical systems analysis will provide the starting point for sophisticated models of nonlinear auditory dynamics, and lead to a deeper understanding of functionally important auditory nonlinearities possibly arising in excitatoryinhibitory networks of the central auditory nervous system. This approach has the potential to link neural dynamics with the perception of pitch, music, and speech, and lead to dynamical models of auditory system development.

898 Assessment of Visual Modulation of Auditory Responses in Gerbil IC

Simon Jones¹, Georg Klump¹

¹Animal Physiology & Behavior Group, IBU, Carl-von-Ossietzky University

Multi-modal integration is an essential part of perception and has been demonstrated at higher, cortical levels. Given the powerful descending connections from auditory cortex to sub-cortical nuclei we investigated modulation of auditory responses by visual cues in the auditory mid-brain of awake gerbils, a mammalian animal model for auditory processing. 16-channel single-shank NeuroNexus multielectrode arrays were implanted in the Inferior Colliculus of gerbils under isoflurane anaesthesia. Stimulus driven recordings were made to guide implantation to the target nucleus. Post-recovery recordings were made chronically over multiple awake passive listening sessions. Stimuli included noise bursts, pure tones of varying frequency (300 - 18000 Hz) and level (10 - 80 dB SPL) and harmonic complexes (12 components f0 400/800 \text{ Hz}). The ambient incident light was varied and comparison made of the responses to identical acoustic stimuli under light and dark conditions.

899 Insulin-Like Growth Factor - 1 Peptide Can Protect Vestibular Hair Cells Against the Neomycin Ototoxicity

Shuhei Yoshida¹, Kazuma Sugahara¹, Eiju Kanagawa¹, Hideki Toyota¹, Hiroaki Shimogori¹, Hiroshi Yamashita¹ ¹Yamaguchi University Graduate School of Medicine

It was known that Insulin-like growth factor-1 (IGF-1) could protect mouse cochlear hair cells against aminoglycoside ototoxicity. We reported that substance P may act on vestibular endorgan as an excitatory factor via NK 1 receptors.

SSSR is the minimum peptide of IGF-1 which indicade multiplier effect with substance P to the epithelium extension. FGLM-NH2 is the minimum peptide of substance P which can bind to NK-1 receptor. The purpose of this study was to investigate the role of SSSR + FGLM-NH2 in mammalian vestibular hair cell death induced by aminoglycoside.

Cultured utricles of CBA/N mice were used. Cultured utricles were divided to five groups (contorol group, Neomycin group, Neomycin + SSSR group, Neomycin + FGLM-NH2 group, Neomycin + SSSR + FGLM-NH2 group).

Twenty-four hours after exposure to neomycin, the cultured tissues were fixed with 4% paraformaldehyde. To label hair sells, immunohistochemistry were performed using anti-calmodulin antibody. The rate of survival vestibular hair cells was evaluated with the fluorescence microscope.

The rate of survival vestibular hair cells in Neomycin + SSSR and Neomycin + SSSR + FGLM-NH2 group were significantly more than that of Neomycin group. These data indicated that SSSR and SSSR + FGLM-NH2 protects sensory hair cells against neomycin-induced death in mammalian vestibular epithelium. These results show that SSSR and SSSR + FGLM-NH2 can be used as the protective drug in the inner ear.

900 Nicotinamide Adenine Dinucleotide Protects Cochlea Against Ototoxic Effects of Oxaliplatin in Vitro

Haiyan Jiang¹, Dalian Ding¹, Yongqi Li¹, Richard Salvi¹ ¹Center for Hearing & Deafness, University at Buffalo

Oxaliplatin, an anticancer drug commonly used to treat colorectal cancer, has a number of serious side effects, most notably neuropathy and ototoxicity. In our previous in vitro studies with cochlear organotypic cultures, we found that oxaliplatin selectively damaged spiral ganglion nerve fibers at very low concentration, 1 μ M, consistent with its neurotoxic profile. Damage to hair cells and spiral ganglion neurons also occurred when the dose was 50

times higher. Previous studies have demonstrated that axonal degeneration involves biologically active processes which can be greatly attenuated by nicotinamide adenine dinucleotide (NAD). In earlier studies, we found that NAD protected auditory neurons and hair cells from mefloquine ototoxicity. To determine if NAD would protect spiral ganglion axons and the hair cells from oxaliplatin damage, we treated cochlear cultures with 10 µM or 50 µM of oxaliplatin alone or combined with 20 mM NAD. Treatment with 10 µM oxaliplatin alone for 48 hours resulted in the destruction of auditory nerve fibers, but spared cochlear hair cells. However, when cochlear cultures were treated with 10 µM oxaliplatin plus 20 mM NAD, most auditory nerve fibers were intact. Increasing the dose of oxaliplatin to 50 µM destroyed most of spiral ganglion neurons and also caused severe hair cell damage. However, when cochlear explants were treated with 50 µM oxaliplatin plus 20 mM NAD for 48 hours, neuronal degeneration was greatly reduced and hair cell survival was increased. These results indicate NAD provides significant protection against oxaliplatin-induced ototoxicity.

901 Quinoline Derivatives Protect Against Aminoglycoside-Induced Hair Cell Death in the Zebrafish Lateral Line

Sarah Keating¹, Edwin Rubel¹, David Raible^{1,2}, Julian Simon³, Henry Ou^{1,4}

¹Virginia Merrill Bloedel Hearing Research Center, Dept. Oto-HNS, University of Washington, ²Department of Biological Structure, University of Washington, ³Fred Hutchinson Cancer Research Center, ⁴Seattle Children's Hospital

The zebrafish lateral line is an effective model system for studying the effects of drugs and small molecules on hair cell survival. We previously screened a library of 1,040 FDA-approved drugs and bioactives (NINDS Custom Collection II) for drugs that protected against neomycininduced hair cell death (Ou et al., 2009). Of the multiple protective compounds identified, we chose to further investigate 9 compounds that share a quinoline ring component within their respective structures.

Dose response curves were completed for each compound to assess protection against 200 μ M neomycin. All 9 compounds elicited 75-100% hair cell survival at their optimal doses. Further dose response curves and screens were completed against cisplatin, gentamicin, and kanamycin. While all quinolines significantly protected against neomycin and gentamicin, there was no protection against cisplatin or kanamycin.

Since the quinoline-derivative quinine is known to be a potent blocker of aminoglycoside uptake into hair cells, we examined the effect of the quinoline derivatives on Texas red-conjugated gentamicin (GTTR) uptake into hair cells. Of the 9 compounds investigated, only 3 were found to greatly reduce uptake, suggesting the possibility of an intracellular mechanism of protection for some of the quinoline derivatives. These findings suggest that the quinoline ring structure may confer protection against aminoglycoside damage and further validates the zebrafish lateral line as an efficient model to identify novel protective drugs.

902 Protective Effects of Korean Red Ginseng on Vestibular Dysfunction and Hearing Loss of Rats Induced by Intratympanic-Gentamicin Injection

Chunjie Tian¹, Seung Won Kim¹, Jong Bin Lee², Jiyoung Min¹, Hae Kyung Lee¹, Younju Kim¹, Keehyun Park¹, Yun-Hoon Choung¹

¹Ajou University School of Medicine, ²College of Medicine, Konyang University

Background: We previously reported that Korea Red Ginseng (KRG) showed preventive effect on hearing loss in rates treated with systemic gentamicin (GM) injection. The purpose of the study was to investigate the protective effects of KRG against on vestibular dysfunction and haring loss of rats induced by intratympanic-injection (ITI) with GM.

Methods: Adult Sprague-Dawley rats (n=22) were classified into 2 groups, GM group and KRG+GM group. Left ears of GM group (n=12) were treated with ITI with GM (20ul of 500mg/ml conc.) every other day for 2 weeks and right ears were remained without any management. The KRG+GM group (n=10) was treated with both 2-week ITI of GM and daily oral feeding of KRG (500mg/kg) for 3 weeks, which started 7days earlier than GM. Rotarod treadmill, head tilt, tail hanging, and swimming tests for balance function and ABR test (16,32KHz) for hearing evaluation were performed at a day of pre-ITI, and post-1,8,15,22, and 30. respectively. Cochleas and utricles/saccules were harvested for morphological evaluation (SEM/Phalloidin staining).

Results: Head tilt test showed severe(>40°) head tilt in 4 rats and moderate(10-40°) head tilt in 3 rats in GM group but none in KRG+GM group. In GM group, 4 rats showed uncontrollable head rotation in tail hanging test and five revealed abnormal swimming behavior. In KRG+GM group, abnormal findings were rarely detected in tail hanging (no rats) or swimming tests (1 rat). In GM group, the hearing thresholds at 16 and 32kHz were 58.3±9.9dB and 57.1±8.7dB at post-1 day, and 45.8±9.5dB, 42.1±9.2dB at post-30 day. In KRG+GM group, the hearing thresholds at 16 and 32kHz were 51.0±10.8dB and 51.0±9.9dB at post-1 day, and 41.0±12.4dB, 37.5±13.0 dB at post-30 day. Although the hearing thresholds after treatments showed the tendency of better hearing at post-1 or 30 days in KRG+GM group than GM group, there was no significant difference between two groups. In morphologic study, SEM and phalloidin staining showed that hair cell damages in both cochleas and vestibules were significantly less in KRG+GM group than GM group (p<0.05).

Conclusion: KRG has strong protective effects against vestibular dysfunction but little effect on hearing loss when ototoxicity is induced by unilateral ITI of GM.

903 Unilateral Intra Perilymphatic Infusion of FGLM-Amide and SSSR Facilitates Vestibular Functional Recovery Against AMPA-Induced Vestibulotoxicity

Hideki Toyota¹, Hiroaki Shimogori¹, Syuhei Yoshida¹, Kazuma Sugahara¹, Hirotaka Hara¹, Hiroshi Yamashita¹ ¹Yamaguchi University Graduate School Of Medicine Substance P (SP) is an undecapeptide belonging to a class of neuropeptides, entitled tachykinins. In the inner ear, though many previous studies concerning localization of SP were reported in the nineteen- nineties, showing that SP exists abundantly in the vestibular endorgans, functional role of SP in the inner ear is still unknown. Recent studies from our laboratory have shown that SP may possess protective effects against AMPA-induced vestibulotoxicity. FGLM-amide is a tetrapeptide derived from the carboxyl terminus of SP and the combination of FGLM-amide and an insulin-like growth factor-1 (IGF-1)derived peptide (SSSR) stimulates rabbit corneal epithelial migration in vitro and rabbit corneal epithelial wound closure in vivo. The aim of the present study is to investigate the effect of FGLM-amide and SSSR, locally applied in guinea pig unilateral inner ear, on AMPAinduced vestibulotoxicity.

Hartley white guinea pigs with normal tympanic membranes and normal Preyer reflexes were used in this study. In each animal, a tiny hole was made adjacent to the round window in the right ear. A polyethylene catheter filled with 10 mM AMPA and connected to a syringe filled with the same agent was inserted into the hole. The syringe was set on a syringe pump and infusion was done at 0.6 ml/h for 5 min. Twelve hours after AMPA-infusion, 10 mM SP (SP group) and liquid containing FGLM-amide and SSSR (FGLM+SSSR group) were infused through this hole by osmotic pump. As a control, after AMPA-infusion, artificial perilymph was used in osmotic pump (control group). Spontaneous nystagmus was observed after AMPA-infusion. Rotation tests were performed before treatment and 3 days, 1 week and 2 weeks after treatment, and VOR gains were calculated.

All animals showed spontaneous nystagmus after AMPAinfusion. In FGLM+SSSR group, spontaneous nystagmus number decreased significantly. Moreover, FGLM+SSSR group showed a rapid recovery of VOR gains 3 days after treatment.

These results indicate the possibility that the combination of FGLM-amide and an SSSR may possess protective effects against AMPA-induced vestibulotoxicity.

904 Mechanisms of Celastrol-Mediation Protection Against Aminoglycoside Ototoxicity

Shimon Francis¹, Carlene Brandon¹, Inga Kramarenko¹, Fu-Shing Lee¹, Lisa Cunningham¹

¹Medical University of South Carolina

Aminoglycoside-induced hair cell death is associated with the induction of specific cell death signals, including mitochondrial dysfunction and JNK activation. Our previous work has shown that celastrol, a potent inducer of

inhibits protein (HSP) expression, heat shock aminoglycoside-induced hair cell death in vitro and hearing loss in vivo. Celastrol induces expression of HSPs -32 and -70. Here we have examined the mechanisms underlying celastrol's protective effect. Western blot analysis of JNK activation revealed that celastrol inhibits neomycin-induced JNK activation. In order to analyze mitochondrial function, we developed a technique for measuring oxygen consumption rates (OCR) in cultured utricles using a Seahorse Extracellular Flux Analyzer. Neomycin-treated utricles showed significantly reduced OCR, while celastrol inhibited the neomycin-induced reduction in OCR. These data suggest that celastrol preserves mitochondrial function in neomycin-treated hair cells. We previously showed that celastrol's protective effect is retained in utricles from Hsf-1-/-, the major HSP transcription factor (ANOVA F1,59 = 34.24, p < 0.001, n=57), suggesting that HSP expression is not required for celastrol's protective effect. However, mRNA analysis indicates that HSP32 expression is induced by celastrol in the absence of Hsf-1, possibly via the Nrf2 transcription factor. To determine if HSP32 is necessary for celastrol-mediated protection, we utilized the specific HSP32 inhibitor, ZnPPIX. ZnPPIX abolished the protective effect of celastrol (ANOVA, F1,29 = 26.35, p< .0001, n=30). CO is a product of HSP32 activity, so we analyzed its role in aminoglycoside-induced hair cell death using a CO donor, CORM2. CO protected hair cells against neomycin-induced hair cell death (ANOVA F1,25 = 79.29, p < 0.0001). These data indicate that HSP32 is a major mediator of the protective effect of celastrol and HSP32 product CO inhibits aminoglycosideinduced hair cell death.

This work is supported by NIH Grants: R01 DC07613 and F31 DC010559

905 Development of Novel Aminoglycoside Derivatives with Reduced Ototoxicity and Enhanced Suppression of Disease-Causing Premature Stop Mutations

Timor Baasov¹, Igor Nudelman¹, Marina Cherniavsky¹, Mariana Hainrichson¹, Fuquan Chen², **Jochen Schacht²** ¹Technion-Israel Institute of Technology, ²Kresge Hearing Research Institute, University of Michigan

Many human genetic diseases and numerous types of cancer are caused by single-point alterations in DNA creating stop codons in mRNA coding regions and leading premature termination of translation and to nonfunctional proteins. Such nonsense mutations represent about 12% of all mutations reported, including cystic fibrosis, Duchenne muscular dystrophy, Usher syndrome, and Hurler syndrome. An emerging therapy is to promote the selective translational readthrough of premature but not of normal stop codons, restoring the expression of a full-length protein. Gentamicin has successfully been used in this fashion in several disease models as well as in patients harboring mutations in CFTR or Dystrophin genes. However, severe toxic side effects and reduced suppression efficacy at subtoxic doses limit the use of gentamicin.

We describe here the systematic development of novel aminoglycoside derivatives exhibiting superior in-vitro readthrough efficiency in seven different DNA fragments derived from mutant genes representing Usher syndrome, cystic fibrosis, Duchenne muscular dystrophy, and Hurler syndrome. In addition to optimizing readthrough efficacy, the major concerns associated with a long-term therapy were also addressed. Ideally, the compounds should lack antibacterial activity so as not to cause emergence of resistant bacterial strains and be free of ototoxic side effects. The compounds presented here show much reduced inhibition of prokaryotic translation and essentially no antibacterial activity. Potential ototoxicity was initially evaluated as toxicity to hair cells in cochlear explants of the postnatal mouse and found to be significantly lower than that of gentamicin.

Supported by grant 2006/301 from the US-Israel Binational Science Foundation, grant 2010826 from the Horowitz Fund, and RO1 DC03685 and P30 05188 from the National Institute on Deafness and Communication Disorders, NIH.

906 Effects of Dorsal Cochlear Nucleus Ablation on Noise-Induced Hyperactivity in the Inferior Colliculus

James Kaltenbach¹, Frank Licari¹

¹Cleveland Clinic

Intense noise exposure causes hyperactivity to develop in the mammalian dorsal cochlear nucleus (DCN) and inferior colliculus (IC). It has not vet been established whether the IC hyperactivity is driven by hyperactivity in the DCN or instead is maintained independent of DCN input. We are investigating the extent to which IC hyperactivity is dependent on input from the contralateral DCN by comparing recordings of spontaneous activity in the IC of noise exposed and control hamsters before and after ablation of the contralateral DCN. One group of animals was binaurally exposed to intense sound (10 kHz, 115-127 dB SPL, 4 hrs) while the control group was not. Both groups were studied electrophysiologically 1-2 weeks later by first mapping spontaneous activity along the tonotopic axis of the IC to confirm induction of hyperactivity. Recorded of spontaneous activity were then recorded at a hyperactive IC locus over two 30-minute periods, one with DCNs intact, the other after ablation of the contralateral DCN. Thus far, we have studied the effects of ablations induced electrothermally and mechanically. Following recordings, the brains were fixed, and histological evaluations were performed to assess the extent of DCN ablation. Electrothermal ablation of the DCN resulted in major reductions of IC hyperactivity, with activity declining gradually to levels approximately 1/3 of the pre-ablation levels. Levels of post-ablation activity in exposed animals were similar to pre-ablation levels of activity in the IC of control animals, suggesting an almost complete loss of hyperactivity in exposed animals. The results from the mechanical ablation studies are still preliminary, but resemble those obtained by electrolytic ablation, except that the decline of activity is less dramatic. Additional studies are underway to test effects of chemical ablation of the DCN by surface applications of lidocaine. (This work was supported by NIH grant R01 DC 009097).

907 Cellular Mechanisms Underlying Dorsal Cochlear Nucleus Hyperexcitablity in Mice with Behavioral Evidence of Tinnitus

Shuang Li¹, Courtney Pedersen¹, Thanos Tzounopoulos¹ ¹University of Pittsburgh, Depts. of Otolaryngology and Neurobiology

Animal models of noise-induced tinnitus have shown increased spontaneous activity of Dorsal Cochlear Nucleus (DCN) fusiform cells (FCs). To identify the cellular mechanisms underlying this hyperactivity, we performed whole cell recordings on FCs from control mice and mice with behavioral evidence of tinnitus (tinnitus mice). To induce tinnitus, mice (P20~P22) were exposed to 116dB narrow bandpass noise centered at 16kHz for 45 minutes. We recorded several hours, two days and one week after noise-induction from control and from mice that were assayed for gap detection and prepulse inhibition. In tinnitus mice, the percentage of spontaneously firing FCs (r) and spontaneous firing rates (f) were significantly higher r_{week}=82%; = 61%, f_{control}= 8.3±1.7Hz, (r_{control} f_{hour} =17.3±3.3Hz, f_{day} = 20.6±2.3Hz, f_{week} =22.7±2.4Hz). Application of TTX (1µM) to stop spontaneous firing revealed that FCs from tinnitus mice showed more depolarized resting membrane potential (RMP) (RMP_{control} = -63.4 ± 1.5 mV, RMP_{hour} = -54.5 ± 2.3 mV, RMP_{dav} = -58.4±2.4mV, RMP_{week} =-55.2±2.4mV). Studies in our lab have revealed that differential expression of HCN channels and K_{ir} channels regulate RMP of FCs in control mice. Blocking K_{ir} channels with BaCl₂ (0.2mM) depolarized equally the RMP in control and tinnitus mice, while blocking HCN channels with ZD7288 (20µM) caused significantly less membrane potential change (ΔV) in tinnitus mice vs. control mice (ΔV_{ZD control}=-6.2±0.9mV, $\Delta V_{ZD \text{ hour}}$ =-2.0±1.1mV, $\Delta V_{ZD \text{ dav}}$ =-2.4±0.9mV, $\Delta V_{ZD \text{ week}}$ =-1.5±0.8mV). Applying ZD7288 and BaCl₂ together led to more depolarized RMP of FC in tinnitus mice vs. control mice $(RMP_{control} = -39.7 \pm 2.0 \text{mV}, RMP_{hour} = -29.3 \pm 2.0 \text{mV},$ RMP_{week}=-33.0±1.6mV), **RMP**_{dav} -26.1±2.4mV, = suggesting that HCN channels and additional conductances play important role in depolarizing FCs and trigger hyperactivity.

Support from American Tinnitus Association and Department of Defense (PR093405)

908 Mechanisms Underlying the Excitability Decrease in the Dorsal Cochlear Nucleus After Acoustic Over Exposure

Nadia Pilati¹, Matias Ison², Matt Barker³, Mike Mulheran⁴, Charles H. Large⁵, Ian D. Forsythe¹, Martine Hamann³ ¹MRC Toxicology Unit, University of Leicester, ²Department of Engineering, University of Leicester, ³Department of Cell Physiology and Pharmacology, University of Leicester, ⁴Medical & Social Care Education, University of Leicester, ⁵Neuroscience CEDD, GlaxoSmithKline

The mammalian dorsal cochlear nucleus (DCN) contributes to many aspects of auditory processing, and also integrates acoustic and non-acoustic information. The central importance of the DCN is highlighted by recent evidence of synaptic plasticity (Fujino and Oertel, 2003) and it is postulated that hyperactivity in the DCN could be a potential mechanism of central tinnitus following acoustic over exposure (AOE, Kaltenbach, 2007). The origins of these phenomena are unclear and may include both presynaptic and postsynaptic changes in transmitter release and/or neuronal excitability. We have been exploring the idea that hyperactivity is a compensatory phenomenon occurring weeks to months after AOE which results from an excitability decrease observed within a few days after AOE. Here we dissect the mechanisms underlying the decrease of excitability within the DCN 3-4 days after AOE.

Wistar rats (P17-P19) were exposed to a loud (110 dB SPL) single tone (15-kHz) for 4 hours (AOE protocol). Auditory brainstem response performed 3-4 days after AOE showed that the hearing thresholds were significantly elevated by about 20-30 dB SPL for frequencies above 15 kHz.

Whole-cell recordings from brainstem slices containing the DCN were performed 3-4 days after AOE and showed the presence of bursts in principal fusiform cells related to a down regulation of high voltage activated potassium currents. Postsynaptic potential amplitude and action potential firing frequency recorded in fusiform cells were significantly decreased after AOE and this was observed after stimulating the auditory or the multisensory inputs to those cells. Properties of spatial recruitment together with electron microscopy and modeling studies indicate that the decrease of excitability related to the auditory input stimulation is mainly linked to defect in the myelin surrounding the auditory nerve fibers within the cochlea whereas the decrease of excitability related to the multisensory input stimulation is related to a decrease of the granule cell membrane resistance.

In conclusion we showed that AOE triggers deafness at early stages and this is correlated with profound changes in the firing pattern and frequency of the DCN major output fusiform cells. Further studies are needed to understand whether these early changes could represent the initial network imbalance before the perception of tinnitus. References:

Fujino K, Oertel D. (2003).Proc Natl Acad Sci U S A.265-70.

Kaltenbach JA. (2007). Prog Brain Res. 89-106. Review.

909 Degeneration of Perisomatic Synapses of Cartwheel Cells in the Dorsal Cochlear Nucleus of Chinchilla Following Acute Acoustic Trauma and Effects of an Antioxidant Treatment

Xiaoping Du¹, Kejian Chen², Chul-Hee Choi¹, Weihua Cheng¹, Charles Stewart³, Ning Hu¹, Robert Floyd³, Richard Kopke¹

¹Hough Ear Institute, ²Spatial Orientation Center, Naval *Medical Center*, ³*Experimantal therapeutic Research* Program, Oklahoma Medical Research Foundation Our previous study demonstrated that noise exposure down-regulated synaptophysin expression in middle region of DCN and antioxidant treatment could restore expression to normal levels (2010 ARO abstract #239). However, the type of neurons affected by noise exposure has not been identified. In the present study, we have used cell type specific synapse activity markers, precerebellin, and neuron markers, PEP-19 and NeuN, as well as a transmission electron microscopic study (TEM) to examine synaptic degeneration in the DCN of chinchilla 10 days after a 105 dB SPL octave-band noise exposure. One group of chinchilla was treated with a combination of antioxidants (4-hydroxy phenyl N-tert-butylnitrone, Nacetyl-L-cysteine, Acetyl-L-carnitine) beginning 4 hours after noise exposure. Down-regulated precerebellin expressions were found only in the fusiform cell layer in the middle region of the DCN of noise exposure group. TEM showed enlarged vesicles and flattened synaptic membranes in perisomatic terminals of cartwheel cells in the middle region of the DCN, representing degeneration of nerve terminals. However, noise exposure used in the present study did not change the number of cartwheel cells (labeled by PEP-19) and the number of total neurons (labeled by NeuN) in the DCN. Antioxidant treatment significantly restored precerebellin expression in DCN and decreased degeneration of perisomatic synapses of Results of this study provide further cartwheel cells. evidence of acoustic trauma induced neural plasticity in the DCN. Results further suggest that early antioxidant treatment for acoustic trauma may not only rescue cochlear hair cells, but also has an impact on central auditory structures as well. (Supported by ONR grant # N00014-09-1-0998)

910 Up-Regulation of GAP-43 in the Rat Ventral Cochlear Nucleus May Protect Against Noise-Induced Persistent Tinnitus

Suzanne Kraus¹, Dalian Ding¹, Haiyan Jiang¹, Edward Lobarinas¹, Wei Sun¹, Richard Salvi¹

¹State University of New York at Buffalo

Some individuals exposed to intense noise develop persistent tinnitus whereas others do not. One factor which differentiates these two groups could be degree of neuroplasticity. Noise-induced hearing loss causes long lasting up-regulation of GAP-43 in the cochlear nucleus, a specific marker for synaptic plasticity. To examine the role of GAP-43 in tinnitus, we unilaterally exposed rats to narrow-band noise centered at 12 kHz at 126 dB SPL for 2

h and evaluated GAP-43 10 weeks later. This type of exposure allows rats to continue to hear through their unexposed ear. Experimental rats and age-matched controls were screened for tinnitus using gap prepulseinduced inhibition of the acoustic startle (GPIAS). Rats with tinnitus were unable to detect the gaps because tinnitus filled in the silent intervals. Before noise exposure all rats showed significant GPIAS (no tinnitus). At day 1-10 and week 8-10 after noise, 5 noise-exposed rats showed no GPIAS at one or more frequencies and were classified as having tinnitus; the other 4 rats continued to show GPIAS and were classified as not having tinnitus. All 9 noiseexposed rats had similar patterns of severe hair cell loss at mid to high frequencies. Eight rats showed strong upregulation of GAP-43 in the auditory nerve and medial ventral cochlear nucleus (VCN) of the exposed ear, but not in the dorsal cochlear nucleus (DCN). Rats without tinnitus showed significantly stronger up-regulation of GAP-43 in VCN than rats with tinnitus. The last experimental animal showed no GAP-43 in the auditory nerve, only weak upregulation in VCN, and no tinnitus despite hair cell loss with same degree and pattern as the other exposed rats. These results suggest that robust noise-induced upregulation of GAP-43 in VCN may suppress tinnitus. In contrast failure to sufficiently up-regulate GAP-43 in the VCN in response to traumatic noise exposure may predict susceptibility to noise induced tinnitus.

Supported by NIH R01DC00909101; 1R01DC009219-01

911 Acoustic Trauma Results in the Degeneration of Anteroventral Cochlear Nucleus Neurons

Tetsuji Sekiya¹, Agneta Viberg², Tatsunori Sakamoto¹, Takayuki Nakagawa¹, Juichi Ito¹, **Barbara Canlon²** ¹Department of Otolaryngology, Head and Neck Surgery, Kyoto University Graduate School of Medicine, ²Department of Physiology and Pharmacology, Karolinska Institutet

Acoustic trauma causes degeneration of the hair cells and spiral ganglia that will eventually cause alterations in the central nervous system. It is well established that acoustic trauma results in cochlear damage, but the secondary effects that occur in the central auditory system is not as well understood. Sprague-Dawley rats were exposed to an acoustic trauma giving rise to a severe permanent hearing loss. Prior to noise exposure and 9 weeks post trauma, auditory brainstem response thresholds and cochlear microphonics were obtained. The auditory brainstem response (ABR) and cochlear microphonics indicated that the auditory function was permanently reduced by the noise trauma. Using unbiased stereological methods the total number of neurons in the cochlear nucleus of the noise exposed animals (9 weeks post exposure) was compared to an unexposed group. The mean standard deviation for the DCN in the exposed brains was 9346 ±1873 neurons and for the unexposed DCN had 9298±1220. The exposed PVCN had 9795±5156 neurons while the unexposed PVCN had 14782±393. The AVCN from the exposed animals had 16242±5751 and in the unexposed animals there were 25217±6178 neurons. The AVCN demonstrated a statistically significant difference between the noise exposed and the unexposed groups ($p\leq0.021$, F= 6.897, df = 1, ANOVA) In conclusion, using quantifiable and highly reproducible experimental methods, we show how the auditory brainstem threshold responses are elevated and how the cochlear nucleus demonstrates region-specific loss of neurons affecting the AVCN but not the DCN and PVCN. These findings illustrate how peripheral insults influence central auditory structures and demonstrate the importance of understanding how peripheral auditory degeneration affects central auditory processes.

Acknowledgements. This work was supported by grants from the Swedish Research Council, Tysta Skolan, Karolinska Institutet, the Japan Health Foundation, Osaka Gas Group Welfare Foundation and ZENKYOREN.

912 Time Course of C-Fos Expression in the Central Auditory System After Noise Exposure and Antioxidant Treatment

Xiaoping Du¹, Jianzhong Lu¹, Kejian Chen², Weihua Cheng¹, wei Li¹, Robert Floyd³, Richard Kopke¹ ¹Hough Ear Institute, ²Spatial Orientation Center, Naval Medical Center, ³Experimantal therapeutic Research Program, Oklahoma Medical Research Foundation

Our previous study demonstrated that administration of antioxidant treatment after noise exposure not only rescues cochlear hair cells, but also impacts the central auditory structures (2010 ARO abstract #239). To further investigate the effects of antioxidant treatment on the central auditory system, time course of expression of an immediate-early gene c-fos was examined 8 hours to 21 days following noise exposure and antioxidant treatment. The animals in the noise group and the noise plus antioxidant treatment group were exposed to 115 dB SPL octave-band noise centered at 14 kHz for 1 hour. The antioxidant treatment (HPN07 plus NAC) was administrated 1 hour after the noise exposure and twice a day for the next 2 days. Rats receiving no noise exposure served as normal controls. Brainstems were harvested and processed for paraffin embedding and sectioning. Cfos immunohistochemical staining was conducted. A few c-fos positive cells were found in the VCN, but not in the DCN of the normal controls. In the DCN of the noise exposure group, numerous c-fos positive cells were found 8 hours after noise exposure. However, the number of positive cells significantly decreased at 24 hours and only few could be seen 7 days after noise exposure. In the VCN, numerous positive cells were found 24 hours and 7 davs after noise exposure. No positive staining was found in the DCN and the VCN 21 days after noise exposure. These results suggest a different time course of c-fos expression in the central auditory system: its expression appears early but returns to a normal level rapidly in the DCN, later but lasts longer in the VCN. Compared to the noise exposure group, a significant decreased number of positive cells was shown in the DCN and the VCN of the noise plus treatment group at every time point after noise exposure, suggesting the antioxidant inhibits c-fos

expression in the central auditory system. (Supported by ONR grant # N00014-09-1-0999)

913 Apoptotic Cell Loss in the Central Auditory Pathway After Noise Exposure

Annekatrin Coordes¹, Ulrike Erben², Anja Kühn², Katja Grollich², Moritz Gröschel³, Arne Ernst¹, Dietmar Basta¹ ¹Department of Otolaryngology at ukb Hospital of the University of Berlin, Charité Medical School, ²Department of Gastroenterology, Infectiology and Rheumatology, CBF, Charité, University of Berlin, ³Institute for Biology, AG Perinatal Adaptation, Humboldt-University of Berlin Introduction: Noise exposure leads, beside the well known cochlear damage, to dramatic physiological and anatomical changes within the central auditory pathway. Our group has already described a significant loss of neurons in different central auditory structures upon acoustic overstimulation. The aim of the present study was to investigate, if the declined neuronal cell density is caused by apoptotic mechanisms.

Methods: Mice were noise-exposed (3h, 5-20 kHz) at 115 dB SPL under anaesthesia and investigated immediately, 6 hours, 24 hours and 7 days after the exposure (n=15). Unexposed animals were used as controls (n=3). Apoptotic cells were detected by fluorescence microscopy after the TUNEL reaction. The TUNEL positive cells were determined in comparison to the cell density (diamidino-phenylindole (DAPI) positive cells) within the dorsal and ventral cochlear nucleus and the nucleus of the inferior colliculus.

Results: There was a significant increase of TUNEL positive cells in relation to a significant decrease of the cell density within all investigated auditory areas after acoustic overstimulation. Most TUNEL positive cells were detected after 6 and 24 hours.

Conclusion: Our results show that noise exposure induces apoptosis-related pathophysiological changes within the cytoarchitecture of the central auditory pathway. Further studies should focus on the specific cell types that are involved in this pathophysiological cascade. This could discover potential therapeutic targets and help to clarify the complex psychoacoustic phenomena of noise induced hearing loss.

914 Vesicular Glutamate Transporters Associated with Auditory and Non-Auditory Inputs to Cochlear Nucleus Are Redistibuted After Long-Term Unilateral Cochlear Damage Chunhua zeng¹, Ziheng Yang¹, Lauren Shreve¹, Susan

Chunhua zeng', Ziheng Yang', Lauren Shreve', Susan Shore¹

¹University of Michigan

Vesicular glutamate transporters, VGLUT1 and VGLUT2, are differently associated with auditory nerve and somatosensory inputs to the cochlear nucleus (CN) respectively: VGLUT1 is highly expressed in the magnocellular CN (VCNm), which receives auditory nerve inputs and VGLUT2 is predominantly expressed in the granular cell domain (GCD), which receives nonauditory inputs (Zhou, Nannapaneni et al. 2007). Based on our

previous findings in guinea pigs that 1 and 2 weeks after unilateral deafening, VGLUT1 was significantly decreased in the ipsilateral VCNm and VGLUT2 was significantly increased in the ipsilateral GCD after 2 weeks deafening (Zeng, Nannapaneni et al. 2009), we examined VGLUT1 and VGLUT2 changes 3- and and 6 weeks after unilateral deafening with kanamycin. At 3 weeks and 6 weeks after intracochlear injections of kanamycin, spiral ganglion densities in the ipsilateral cochlea were significantly decreased when compared with contralateral side. VGLUT1 in the ipsilateral VCNm was significantly decreased, whereas VGLUT2 in ipsilateral GCD and deep dorsal CN (DCN3) were significantly increased. The pathway-specific amplification of VGLUT2 expression in the CN suggests that, there are long-term compensatory responses to auditory de-afferentation, with a significant enhancement of the non-auditory influence on CN. (This work was supported by NIH R01DC004825 and P30 05188).

Zeng, C., N. Nannapaneni, et al. (2009). "Cochlear damage changes the distribution of vesicular glutamate transporters associated with auditory and nonauditory inputs to the cochlear nucleus." <u>J Neurosci</u> **29**(13): 4210-4217.

Zhou, J., N. Nannapaneni, et al. (2007). "Vessicular glutamate transporters 1 and 2 are differentially associated with auditory nerve and spinal trigeminal inputs to the cochlear nucleus." <u>J Comp Neurol</u> **500**(4): 777-787.

915 Experience Dependent Enhancement of Pitch Encoding in the Brainstem: Resolved Versus Unresolved Components

Christopher J. Smalt¹, Ananthanarayan Krishnan² ¹School of Electrical and Computer Engineering, Purdue University, ²Department of Speech Language Hearing Sciences, Purdue University

Neural encoding of pitch in the auditory brainstem has been shown to be influenced by long-term experience with language, implying that early sensory processing is subject to experience-dependent neural plasticity. However, to date, these effects have been observed only for speech/non-speech stimuli containing both place and temporal pitch cues (i.e., both resolved and unresolved components). Here, we examine whether this experiencedependent enhancement in pitch representation in native Mandarin speakers persists when listeners are provided only temporal pitch information. Brainstem frequency following responses (FFRs) were recorded from Chinese and English participants using alternating polarity in response to homologues of a Mandarin lexical tone containing either fully unresolved components, or both resolved and unresolved components. Noise masking was added with various SNRs to reduce the effect of 2f1 -f2 distortion products (DPs) that may contribute to the encoding of pitch. Pitch strength measurements were computed using autocorrelation algorithms for FFRs elicited by both sum and difference phase stimuli (which emphasize envelope and fine structure encoding. respectively). Cross-language comparisons of pitch strength revealed that the Chinese group, relative to the

English, exhibited more robust pitch representation in the stimulus containing both resolved and unresolved harmonics in the sum phase only. These findings demonstrate that temporal pitch cues alone (unresolved condition) are insufficient to produce language dependent enhancements to brainstem representation of linguistic pitch.

916 Human Frequency Following Responses: Correlates of the Pitch of Complex Stimuli with Inharmonic and Frequency-Shifted Components

Ananthanarayan Krishnan¹, Christopher Plack² ¹*Purdue University,* ²*University of Manchester*

Inharmonic complex tones produce competing pitches (pitch shift and or pitch ambiguity) rather than one definite pitch. In the present experiments, human frequency following responses (FFRs) were recorded to: 1. Amplitude modulated (AM) tones with fixed modulation frequency (Fm = 125 Hz) and different carrier frequencies (625 and 750 Hz harmonic; 687 and 733 Hz inharmonic) and 2. Two three-component complexes, one with the 2nd, 3rd, and 4th harmonic of a 244 F0 (harmonic) and the other with these components shifted downwards in frequency by 122 Hz (shifted). Autocorrelation and spectral analyses were performed on both the envelope-related phase locking and the fine-structure-related phase locking. Envelope FFRs showed ACF peaks that corresponded to the invariant envelope periodicity for both harmonic and inharmonic/shifted stimuli in both experiments. Consistent with this, the spectra showed peaks at the harmonic spacing, and at integer multiples of this value. In contrast, the fine structure FFRs showed ACF peaks corresponding to the F0 for the harmonic stimuli, and single or multiple ACF peaks for inharmonic/shifted stimuli. Although the spectral data for the fine-structure FFR showed peaks at the frequency components and at lower harmonics (presumably cubic difference distortion products) as expected, no clear peaks corresponding to the F0 were observed for the inharmonic/shifted stimuli. The FFR fine structure results are consistent with the auditory nerve response to AM tones (Cariani et al., 1996) and with the FFRs to inharmonic complex sounds (Greenberg et al., 1987). However, the FFR response appears to be a lowpass version of the auditory nerve response. The results suggest that information related to pitch shift and pitch ambiguity is contained at the midbrain level in the temporal distribution of neural activity phase-locked to the fine structure.

917 The Frequency Following Response (FFR) for Frequency-Shifted Complex Tones, Revisited

Hedwig Gockel¹, Christopher Plack², **Robert Carlyon¹** ¹*MRC-Cognition and Brain Sciences Unit,* ²*The University of Manchester*

When a constant frequency shift is imposed on all harmonics of a complex tone, pitch changes by an amount proportional to that shift. Here we investigated how pitch-

related information for frequency-shifted complex tones is represented in the FFR.

The FFR was measured for five subjects, using 100-ms, 75-dB-SPL complex tones containing harmonics 2-4 or 3-5 of a fundamental frequency (F0) of 244 Hz. Components were either at their nominal frequencies or were all shifted together by +/- 50% or 25% of the F0. Component starting phases were 0, 120 and 240 degrees for the low, middle and top component, respectively. Stimuli were presented in alternating polarity at a rate of 3.57 Hz. We used a "vertical" montage (+ Fz, - C7, ground=mid-forehead) for which the FFR is assumed to reflect phase-locked neural activity from rostral generators in the brainstem.

FFR waveforms for each polarity were averaged and then either added, to enhance temporal information related to stimulus envelope, or subtracted, to enhance temporal fine structure (TFS) information. FFTs for the added case showed clear peaks related to the stimulus envelope for all stimuli (peaks at/close to 244 Hz and integer multiples of 244 Hz). FFTs for the subtracted case showed clear peaks related to the TFS (peaks at/close to the frequencies of the components present in the stimuli). Autocorrelation functions (ACFs) showed a peak at the delay corresponding to the envelope repetition rate for the added case, but a peak at a delay shifted in the direction of expected pitch shifts for the subtracted case, at least for the 25% frequency-shifted stimuli. ACFs of the raw stimuli and of the output of an auditory-nerve model also showed the expected pitch shifts. Thus the neural responses measured by the FFR preserve temporal information important for pitch, but do not necessarily represent processing over and above that already present in the auditory periphery.

Acknowledgement

Supported by Wellcome Trust Grant 088263.

918 Brainstem Origins of the Differential Hemispheric Laterality for Linguistic and Nonlinguistic Pitch

Saradha Ananthakrishnan¹, Ananthanarayan Krishnan¹, Jackson Gandour¹, Gavin Bidelman¹, Christopher Smalt¹ ¹*Purdue University*

Linguistically relevant pitch has been shown to preferentially recruit left hemisphere, while non-linguistic pitch appears to exhibit a right hemisphere advantage. It is known that neural encoding of linguistic pitch in the brainstem can be modulated by language experience. The aim of this experiment is to evaluate if linguistic statusdependent ear asymmetries exist in pitch representation at the brainstem level. To this end, the brainstem frequency following responses (FFRs) elicited by monaural stimulation of the left- and right-ear were obtained from 15 native speakers of Mandarin using three speech stimuli (T2i, T2oe, and T2'oe) that varied across a continuum of linguistic relevance with respect to pitch and vowel quality. The continuum ranged from fully native (T2i) which had both native attributes, to an intermediate step (T2oe), which only had the pitch attribute, and to an extreme stimulus (T2'oe), which did not have either attribute. Asymmetry index derived from the magnitude of the F0 component in the FFR revealed a significant left ear advantage for the non-native stimulus (T2'oe) with no significant ear asymmetry for the linguistically relevant stimuli (T2i, T2oe). Also, for each ear and across stimuli, pitch representation was relatively more robust for stimuli with the native pitch contours. Finally, comparison of the pitch strength for T2oe and T2'oe revealed a significant reduction in the pitch strength for the right ear with no difference for the left ear suggesting increased contribution of the right ear as linguistic relevance of the stimulus increases. Collectively these results provide evidence in support of the notion that hemispheric advantage for pitch processing emerges early along the auditory pathway.

919 Enhanced Brainstem Pitch Encoding in Tone-Language Speakers Does Not Translate to Perceptual Benefits for Music

Gavin M. Bidelman¹, Ananthanarayan Krishnan¹, Jackson T. Gandour¹

¹Department of Speech, Language, & Hearing Sciences, Purdue University

Neural encoding of pitch in the auditory brainstem is known to be shaped by long-term experience with language or music, implying that early sensory processing is subject to experience-dependent neural plasticity. Recent findings show that domain-specific experience (e.g., speakers of a tone language or musical training) improves brainstem encoding of pitch stimuli outside a listener's domain of expertise, indicating that experiencedependent mechanisms provide cross-domain benefits to auditory processing. Whereas transfer effects from musical expertise to language processing are well-established, less is known about whether or not linguistic expertise transfers to music processing. The aim of this study was to compare frequency-following brainstem responses between nonmusicians, and native speakers of musicians. Mandarin Chinese, in response to tuned and detuned musical chords, and to determine whether or not improvements in subcortical processing translate to perceptual benefits. Results showed that both musicians and Chinese, relative to nonmusicians, had stronger brainstem representation for the defining characteristics of musical sequences regardless of chordal temperament. The neural data notwithstanding, two behavioral pitch discrimination tasks revealed that neither Chinese nor nonmusicians were able to discriminate subtle changes in musical pitch with the same accuracy as musicians. The discrepancy between neural and behavioral data suggests that even though tuning of subcortical pitch mechanisms may be enhanced regardless of the domain of a listener's pitch experience, perceptual benefits in pitch discrimination only emerge for stimuli which are behaviorally relevant to the listener. In the case of musicians, chordal temperament is a perceptually salient component of their auditory experience.

920 Automatic Auditory Brainstem Responses Detection System

Bartosz Trzaskowski¹, Wiktor Jedrzejczak¹, Krzysztof Kochanek¹, Edyta Pilka¹, Henryk Skarzynski¹ ¹Institute of Physiology and Pathology of Hearing

The aim of this research was to develop computer driven Auditory Brainstem Responses (ABR) detection system and to verify its appliance in clinical use.

Proposed algorithm relies on wave V identification in responses to click stimuli at levels from 10 to 100 dB nHL. It is based on predefined criteria concerning parameters and morphology of component structures of ABR. In order to objectively asses presence of response it involves statistical and signal analysis methodology. In the first step the presence of physiological response is objectively evaluated. Next, the position of wave V is determined. This is realized by peak selection by taking into consideration such properties of the signal as amplitude, latency, and morphology. Wave V identification process is supported by module evaluating quality of Latency-Intensity curve fitting. This module provides reliable criterion for wave verification preventing misidentifications.

System was tested on simulated data and on real click evoked ABRs. Obtained ABR thresholds and wave V latencies were compared to those marked by expert clinicians with years of experience in ABR. Differences between results from the system and experts were not significantly bigger than differences between experts themselves.

921 A Structural Equation Modeling Approach to Understanding Speech-In-Noise Perception in Older Adults

Samira Anderson¹, Alexandra Parbery-Clark¹, Emily Hittner¹, Nina Kraus¹

¹Northwestern University

Older adults frequently complain of difficulty hearing in background noise. The nature of speech perception in noise is complex, involving interactions between peripheral, central, and cognitive factors. Older adults have decreases in fundamental frequency representation and temporal resolution compared to younger adults, and these central deficits may contribute to speech-in-noise (SIN) difficulties. The brainstem response to speech stimuli is a particularly useful objective measure for evaluating central processing, as the transparency between stimulus and brainstem response waveforms allows for direct evaluation of brainstem encoding of frequency and timing components of the stimulus. We hypothesized that the frequency and timing aspects of the brainstem response account for a significant proportion of the variance in SIN perception in a structural equation model, and that measures of cognitive function are factors that contribute to the best fit of the model. Our subjects included 120 adults (ages 45 to 79), whose hearing levels ranged from normal hearing to mild to moderate sensorineural hearing loss. The test battery included the Hearing in Noise Test, the Woodcock-Johnson III Tests of Cognitive Abilities, and speech-evoked auditory brainstem responses. Using structural equation modeling, we found a significant relationship between brainstem measures (including pitch encoding and neural timing) and SIN perception, whereas the relationship between peripheral hearing measures and SIN perception was not significant. When measures of cognitive function (attention, memory, and cognitive efficiency) were added to the model, brainstem measures continued to uniquely predict variance in SIN perception ability. These findings demonstrate the importance of subcortical encoding for successful communication in challenging listening environments, and suggest that brainstem responses can be used as an objective measure of SIN perception.

922 Preliminary Study on Auditory Brainstem Responses in a Passive Oddball Paradigm

Lavinia Slabu^{1,2}, Sabine Grimm^{1,2}, Francisco Diaz Santaella^{1,2}, Carles Escera^{1,2}

¹Cognitive Neuroscience Research Group, Psychiatry and Clinical Psychobiology, Univ. of Barcelona, ²Institute for Brain, Cognition and Behavior (IR3C), University of Barcelona

The auditory evoked potential (AEP) objectively examines the auditory pathway from the brainstem to the cortex. AEP studies indicate that infrequent deviant sounds reliably elicit a negative potential approximately 100-300 ms after the stimulus onset called mismatch negativity (MMN) response, associated with change detection. Recent results from animal studies (Malmierca et al., 2009; Kraus et al., 1994) suggest that cognitive evoked potentials recorded from the human scalp might be preceded by even earlier novelty-related activity.

The goal of the current study is to investigate the effect of auditory deviance detection using an oddball paradigm for speech syllables from the frequency following response (FFR), an auditory brainstem (ABR) response (Russo et al., 2004).

ABR were recorded from 18 participants at Cz using right earlobe as reference. Five stimuli were generated with the Klatt speech synthesizer. The syllables were composed of five formants and differed in duration of the first and second formant transition (25, 40, 55, 70, 85 ms). The stimuli were perceived either as /ba/ or as a soft to a strong /wa/ (wa1, wa2, wa3, wa4). Three blocked conditions were presented: an oddball block with a deviant /wa/1 probability of p=0.2; a reverse oddball block with a deviant /ba/; and a control block in which the five stimuli were presented randomly, each with a probability of p=0.2. 8192-points Fourier analyses were applied for the ABR averages and the normalized mean spectral amplitude was calculated for 10 Hz wide bins surrounding the F0 (100 Hz) and the subsequent three harmonics, H2, H3, H4 (Chandrasekaran et al., 2009) within the 20-85 ms time period. The spectral amplitudes of the H2 (F2,34=5.312, p=0.017) and H4 (F2,34=6.172, p=0.010) for the /ba/ syllable were significant smaller for the deviant stimulus than for the responses elicited both to the standard and to the control stimuli. No significant effects were found for the /wa/1 syllable.

The results of the present study have revealed that auditory deviance detection can take place in human auditory brainstem, supporting the notion that novelty detection is a basic property of the functional organization of the auditory system that acts at different levels along the auditory pathway.

923 Central Contralateral Hearing Loss in Ipsilaterally Deafened Guinea Pigs

Jan Wagner¹, Moritz Gröschel², Sebastian Jansen², Dietmar Basta¹, Arneborg Ernst¹

¹UKB Hospital of the University of Berlin, ²Humboldt University Berlin Departement of Biology

The aim of the study was to evaluate the effect of unilateral deafening in normal hearing guinea pigs concerning peripheral contralateral central and hearing. Material/Methods: Guinea pigs unilaterally mechanically deafened and normal hearing animals of the same age were exposed to surrounding sounds (soundtrack of "Lord of the Rings") with levels of up to 65dB for 90 days. After this period ABR measurements were performed and the cochlea organs harvested for further exploration. Cochleogramms (whole mounts) of the basilar membranes were made and a hair cell count performed for the frequencies of 25kHz-0.4kHz. Hair cell loss of both groups and ABR measurements were evaluated. Results: After 90 days ABR measurements showed an almost complete hearing loss on the deafened side and a significant mean decrease of hearing threshold levels (4-20Hz) of 14dB SPL, SEM 2.9 (p=0.001, paired T-Test) on the contralateral side compared to the levels before deafening. Hair cell counts showed a mean loss of contralateral outer hair cells in the deafened animals of 1.3 (per 100µm), SEM 0.12 compared to the controls (mean loss of 1.6 (per 100µm), SEM 0.19). The difference was not statistically significant (u-Test p=0.542). Discussion: As no outer hair cell damage on the contralateral cochlea organs was detected, the increased contralateral ABR thresholds seem to be due to plastic changes in the lower central auditory pathway.

This seems to be a significant sign for interaural interaction in single sided deafness. Further analysis of cell density and activity in the nuclei of the lower auditory pathway and cell counts of the spiral ganglions could possibly confirm this hypothesis. In conclusion, our data shows that unilateral deafening in guinea pigs leads to a changed signal processing on the contralateral side even if the OHC structure is conserved.

924 Using Auditory Evoked Potentials to Examine Hearing Loss in Aquatic Animals: From Marine Mammals to Squid

T. Aran Mooney¹, Darlene R. Ketten^{1,2}, Paul E. Nachtigall³, C. Rogers Williams⁴, Keith Matassa⁵ ¹Woods Hole Oceanographic Institution, ²Department of Otology and Laryngology, Harvard Medical School, ³Hawaii Institute of Marine Biology, University of Hawaii, ⁴National Marine Life Center, ⁵Marine Animal Rehabilitation Center, University of New England Behavioral hearing tests for many animals are often complicated by the time and difficulty to condition responses. This is particularly true for aquatic animals which present a significant challenge to maintain in captive situations. Yet, increasing anthropogenic noise in marine environments necessitates the examination of noiseinduced and natural hearing loss in marine animals. Here we present the applications of auditory evoked potentials (AEPs) to non-invasively study hearing in cetaceans (dolphins and porpoises), pinnipeds (seals) and cephalopods (squid and cuttlefish), animals that are nontrivial to test by conventional methods. Animal subjects studied here were either sedated or trained, and tested with electrodes tailored to the anatomy of each species. Cephalopod AEP responses were only to low frequencies and doubled the tone-pip stimulus. Marine mammal AEPs consisted of several distinct waves to short duration stimuli and envelope following responses to amplitude modulated stimuli (similar to other mammals). Auditory impairments measured included experimentally induced losses from aminoglycosidic antibiotics in cephalopods, controlled noise exposures for temporary threshold shifts in dolphins, and pathologies such as otitis media and externa (pinnipeds). The results demonstrate that despite the diverse anatomy, AEPs can be used to study both basic hearing capabilities and assist diagnoses of hearing loss. These AEP applications in marine animals demonstrate that this methodology is feasible for measuring hearing, threshold shifts, and detection of auditory system disease in wild animals to address the effects of noise and other pollutants.

925 Blast and Acoustic Trauma Induced Tinnitus: Combined in Vivo MEMRI and Electrophysiological Studies

Xueguo Zhang¹, **Jessica Ouyang**¹, Pamela VandeVord², Jinsheng Zhang^{1,3}

¹Department of Otolaryngology and Head and Neck surgery, Wayne State University School of Medicine, ²Department of Biomedical Engineering, Wayne State University College of Engineering, ³Department of Communication Sciences & Disorders, Wayne State University College of Liberal Arts an

Available evidence supports the notion that tinnitus results from acoustic trauma- induced neural plasticity in auditory brain structures. However, it remains to be defined as to how acoustic trauma-induced plastic changes in the brain contribute to tinnitus. In this study, we investigated changes in auditory brain activity in rats that developed

tinnitus following blast and acoustic trauma, using in vivo manganese-enhanced magnetic resonance imaging (MEMRI) and multi-channel electrophysiology. Adult rats (n=52) were randomly divided into: control group (n=12), tone exposure group (n=20), and blast group(n=20). To induce tinnitus, both tone (10kHz, 120 dB SPL, 3 hours) and blast (14-18 psi) were used to expose the left ears of the rats. Behavioral testing of tinnitus was conducted using gap detection of startle reflex paradigm before and after blast and tone exposure, and between MEMRI imaging and electrophysiological recordings. ABRs were also measured to monitor hearing loss before and after tone or blast exposures. During MEMRI study, MnCl2 at 67mg/kg was injected introperitoneally as paramagnetic contrast agent. Intensity ratio of region-of-interest (ROI) over muscle was used as the parameter to compare accumulation of Mn2+. "MRIcro" was used to measure the intensity of ROI from 3D MRI images. Two months after MEMRI, animals underwent craniotomy for electrophysiological recordings from the auditory cortex. The animals that failed to uptake Mn2+ were excluded from the study. Preliminarily analyzed MEMRI data demonstrated that intensity ratio was the highest in control animals, followed by tone- and blast-exposed animals with tinnitus. This indicates tinnitus was associated with hearing loss. The electrophysiological data are underway. The study indicates that in vivo MEMRI is sensitive and reliable to investigate tinnitus-related activity in the brain.

926 Columnar and Tonotopic Organization of Core Fields in the Mouse Auditory Cortex

Wei Guo^{1,2}, Keith N. Darrow^{2,3}, Kenneth E. Hancock², Barbara Shinn-Cunningham¹, Daniel B. Polley^{2,4} ¹Dept. of Cognitive and Neural Systems, Boston University, ²Eaton-Peabody Laboratory, Mass Eye & Ear Infirmary, ³Worcester State University, ⁴Harvard Medical School

A tonotopic organization of preferred sound frequency has been documented in the primary auditory cortex (AI) of over twenty species. Traditionally, tonotopy has been reconstructed with microelectrode mapping of multiunit tonal frequency response areas (FRAs) in the middle Two recent studies have shown that cortical layers. mouse AI lacks the precise tonotopy commonly observed other species (Rothschild et al., 2010 and in Bandyopadhyay et al., 2010). This disparity could reflect either a species difference or a methodological difference. as both studies used single cell two-photon imaging of Ca2+ spikes from neurons in superficial cortical layers. Here, we directly explore the relative contributions of species and methodology differences by performing ultradense microelectrode mapping of FRAs from multiple layers in AI and the anterior auditory field (AAF) of the mouse. Consistent with reports from other species, we observed a precisely organized map of best frequency (BF) from the middle cortical layers of AI and AAF under both pentobarbital or ketamine anesthesia. Although the quality of pure-tone FRAs (e.g., threshold and bandwidth) varied considerably between layers and between anesthetic regimens, BFs and tonotopy in the superficial

and deep layers were comparable to that observed in the middle thalamorecipient layers. These data suggest that neighboring sites within a single cortical layer or along a vertical cortical column share highly similar BFs that are tonotopically organized across the caudal-to-rostral extent of mouse AI and AAF. Ongoing efforts to reconcile the disparity with Ca2+ imaging studies are focusing on the spatial precision of the measurement (single unit vs. multiunit) and/or a selection bias in cell type (measured indirectly by waveform shape). The combination of these recent findings in the mouse will reveal how cortical circuits are spatially organized to exhibit both local diversity and large-scale order.

927 Organizational Features in the Mouse Auditory Cortex

Sharba Bandyopadhyay¹, Shihab Shamma¹, Patrick Kanold¹

¹University of Maryland

Stimulus induced and noise correlations between neurons have a profound role in population coding of sensory information. However diversity in responses also allows for increase of coding capacity within populations of neurons. Response properties of cells in close vicinity in layer 2/3 of the mouse auditory cortex (ACX) measured by tone and noise evoked Ca responses using in vivo two-photon imaging show great degree of heterogeneity. With connectivity analysis based on simultaneous response measurements we find sparse connectivity among layer 2/3 neurons in the ACX. In spite of sparse connectivity we find similar response properties based on clustering of responses in a patchy manner over small spatial scales. Hence we investigate the spatial response diversity to uncover underlying organizational features in the ACX. Based on spatial response gradient analysis we show how frequency tuning properties of cells change spatially in different directions within ACX overlying broad tonotopy. We extend such analysis based on two different Ca2+ dyes, one (OGB-1 AM) that shows some subthreshold responses along with supra threshold responses, and one that shows primarily suprathreshold responses (Fluo-4 AM) to uncover patterns of synaptic input in layer 2/3 of ACX.

928 Functional Micro-Organization in Mouse Auditory Cortex

Paul Watkins¹, Patrick Kanold¹

¹Department of Biology, University of Maryland, College Park

Large-scale organization has been described in auditory cortex of many mammalian species usina electrophysiological techniques. In particular intrinsic imaging, single and multiunit recordings have shown that in mammalian A1 a tonotopic arrangement exists. In addition, patchy organization of other response properties is thought to exist at large spatial scales (greater than 500 microns). Recent work using in vivo 2-photon microscopy in mouse auditory cortex (Bandyopadhyay et al., 2010; Rothschild et al., 2010) has revealed that this large-scale organization breaks down at smaller scales (around 300

microns) and that instead nearby neurons show very heterogeneous frequency and level tuning properties. Here we investigate if there exists any organization of functional properties on small spatial scales. Using 2-photon microscopy in mouse auditory cortex we find that at smaller spatial resolutions there exists a functional organization of tuning properties. Anatomical microcolumns of interconnected neurons have been described in visual cortex with diameters on the order of tens of micrometers. It is likely that such microcolumns (Jones, 2000) are also present in auditory cortex and give rise to the micro-organization we observe here. Our results suggest that mouse auditory cortex might consist of a spatially intermingled assembly of such micro-columns. Our results also demonstrate that the functional organization of A1 can be orderly or disorderly depending on the spatial scale of observation.

929 Cooling and Lidocaine Inactivation of the Auditory Cortex Modulate Cochlear Responses in Chinchillas

Alex Leon¹, Diego Elgueda¹, Paul H Delano^{1,2} ¹Fisiología y Biofísica, ICBM, Universidad de Chile, ²Servicio Otorrinolaringología, Hospital Clínico Universidad de Chile

The auditory efferent system comprises the auditory cortex, inferior colliculus and olivocochlear neurons. Auditory-cortex descending projections are constituted by pyramidal neurons which somas are located in cortical layer V and VI. These neurons project to the inferior colliculus and also to the superior olivary complex. Medial olivocochlear neurons innervate outer hair cells in the cochlear receptor. The functional role of the efferent system remains unclear. We hypothesized that the auditory-cortex activity regulates cochlear afferent responses through the efferent system. We used two different methods to deactivate the left auditory cortex of 18 anesthetized chinchillas: (i) lidocaine cortical microinjections (3 µl at 1 µl/min rate) and (ii), cooling (2-8 °C) of the auditory cortex by cold methanol using cryoloops (Lomber et al., J Neurosci Methods, 86:179-194, 1999). We recorded cochlear microphonic potentials (CM) and the compound action potential of the auditory nerve (CAP) by positioning an electrode in the right round window. Middleear muscles were sectioned in all chinchillas. We found that cortical inactivation produced significant changes in the amplitude of CM in all chinchillas. The main observed effect was CM decreases (-4.9 ± 1.5 dB; mean + SEM), found in 12 chinchillas; however we also observed CM increases in 6 animals (2.2 \pm 0.5 dB). CAP decreases were obtained in 11 chinchillas (-5.0 \pm 1.1 dB), while CAP increases were found in six animals (3.4 \pm 0.6 dB). Sixty minutes after lidocaine microinjection or cooling of the auditory cortex, amplitudes of cortical potentials were completely recovered, however only partial recovery was observed in cochlear responses. These results show modulation of auditory periphery by the cerebral cortex. The diversity of effects suggests that there are several (at least two) functional pathways from cortex to cochlea.

930 Effects of Cortical Cooling on Single Unit Responses in Auditory Thalamus of Awake Marmosets

Marcus Jeschke^{1,2}, Frank W. Ohl^{2,3}, Xiaoqin Wang¹ ¹Johns Hopkins University, School of Medicine, Baltimore, Maryland, ²BioFuture Res. Group, Leibniz Institute for Neurobiology, Magdeburg, Germany, ³Institute for Biology, Otto-von-Guericke Univ. Magdeburg

A number of anatomical studies have shown that auditory cortex sends massive feedback connections to the auditory thalamus. Based on their microstructural appearance most of these connections have been believed to have a modulatory role on thalamic processing. How this suggested modulation manifests itself has not been fully explored. Few experiments have investigated the nature of corticothalamic modulation in awake animals. We used a small cooling probe to inactivate the auditory cortex of awake common marmosets (Callithrix jacchus) while recording single-unit activity in the auditory thalamus. In the present study, we investigated the effects of corticofugal feedback on the processing of time-varying sounds and spatial slectivity in auditory thalamus.

The maximum stimulus evoked firing rate was mostly reduced as a result of cooling the auditory cortex. Spatial receptive fields of thalamic neurons generally became narrower when auditory cortex was inactivated by cooling. Best azimuths mainly stayed within the same hemifield while best elevations tended to shift towards 45 degree elevation. Using temporally modulated stimuli we observed reduced synchronization in the thalamus especially at lower modulation frequencies, coinciding with the frequency range in which cortical neurons synchronize their firing to temporally modulated stimuli. In addition, cooling-induced changes in synchronization of thalamic neurons appeared to occur largely independent of firing rate changes. Our findings suggest that the processing of spatial locations as well as temporal modulations in auditory thalamus is regulated by the corticofugal feedback.

This work was supported by National Institutes of Health grant R01 DC003180 to X.W. and a grant from the Deutsche Forschungsgemeinschaft (DFG; SFB-TR 31, Project A3) to F.W.O.

931 Functional Microcircuitry of Spectral Integration and Perceptual Relevance of Recurrent Corticothalamic Loops in Primary Auditory Cortex

Max Happel^{1,2}, Marcus Jeschke¹, Juliane Handschuh¹, Matthias Deliano¹, Frank Ohl^{1,2}

¹Leibniz-Institute for Neurobiology, ²Otto-von-Guericke University

Local processing of feedforward input in sensory cortex strongly depends on different short- and long-range intracortical pathways, as well as on corticofugal pathways. Though various functions have been attributed to these pathways, their specific roles for representation of physical stimulus features, as well as perception are still under debate. By a combination of methods, including currentsource-density (CSD) analysis, pharmacological deactivation, and layer-specific intracortical microstimulation (ICMS) in primary auditory cortex of Mongolian gerbils, as well as by behavioral signal detection analysis, we dissociated different functional roles of the aforementioned pathways in spectral integration and perception in general.

We found a temporally highly precise integration of thalamocortical inputs and intracortical horizontal inputs when the stimulation frequency was in close spectral neighborhood of the best frequency, where the overlap between both inputs is maximal. Local horizontal connections provide both, directly feedforward excitatory and modulatory input from adjacent cortical sites, which determine how concurrent afferent inputs are integrated (Happel et al., 2010, J.Neurosci.). Further, we differentially activated the aforementioned subsystems using layerspecific ICMS. Analysis of detection performance showed that behaviorally interpretable percepts were caused by driving recurrent corticothalamic feedback loops, whereas wide-spread activations across cortical columns per se had no perceptual impact.

Our data suggest a conceptual framework of information flow in primary auditory cortex based on temporally precise interactions of afferent inputs and different short- and longrange intracortical networks and a local recurrent excitatory loop in the cortico-thalamocortical circuitry, which serves as a re-entrant loop of input information, which provided neural signals suitable for a "read-out" by horizontal cortical processing.

932 Genetic Dissection of Corticothalamic and Corticocollicular Axon Targeting

Masaaki Torii¹, Troy A. Hackett², Pat Levitt³, **Daniel B. Polley**^{4,5}

¹Yale University School of Medicine, ²Vanderbilt University School of Medicine, ³Keck School of Medicine, USC, ⁴Eaton-Peabody Laboratory, Mass Eye & Ear Infirmary, ⁵Harvard Medical School

Auditory stimulus representations are dynamically maintained by ascending and descending projections linking the auditory cortex (Actx), medial geniculate body (MGB) and inferior colliculus (IC). The mechanisms governing feedforward projections to the Actx are far better understood than those regulating feedback from the Actx. In this study, we characterize the role of EphA/ephrin-A signaling in the establishment of corticofugal connections from Actx to MGB and IC. Comparison of endogenous gradients for the ephrin-A5 ligand and EphA7 receptor confirmed that EphA7-positive cortical axons are repelled by ephrin-A5 to achieve their final position in the MGB and The importance of EphA7 in corticofugal axon IC. guidance was further tested by transfecting Actx neurons in living mouse embryos with genes for green fluorescent protein (GFP) and the EphA7 receptor via electroporationmediated gene transfer. Analysis of corticofugal connectivity in control mice electroporated with GFP alone revealed a relatively uniform distribution of Actx projections throughout the dorsal (d) and ventral (v) divisions of MGB, but far denser projections to the dorsal and lateral nucleus of the IC compared to the central nucleus of the IC. Overexpression of EphA7 in Actx had little impact on the distribution of corticocollicular projections, but substantially altered the pattern of corticothalamic (CT) connectivity. GFP-positive CT axons in EphA7 overexpressing mice shifted away from MGBv, terminating instead at the border between MGBv and MGBd. Additional studies using Dil labeling and neurophysiological recordings from MGBv of EphA7 overexpressing mice demonstrate that thalamocortical projections and sensory-evoked responses were grossly normal. These data identify a molecular mechanism to dissociate feedforward and feedback connections in collicular-thalamic-cortical circuits and provide a method to specifically reduce CT feedback without silencing the Actx.

933 Glutamatergic Pathway Distinctions Between Primary and Ventral Auditory Cortical Fields

Douglas Storace¹, Jennifer Chikar², Douglas Oliver², Heather Read^{1,3}

¹Department of Psychology, University of Connecticut, ²Department of Neuroscience, University of Connecticut Health Center, ³Department of Biomedical Engineering, University of Connecticut

Primary auditory cortex (A1), ventral auditory field (VAF) and suprarhinal auditory field (SRAF) in the rat are cochleotopically organized and process sound in complementary ways. At present there is no unified anatomic or physiologic model to explain the neuronal response property differences in neighboring regions. The simplest explanation would be that these differences are inherited from ascending thalamocortical pathways. Projections to A1 and VAF originate in rostral and caudal halves of the medial geniculate body (MGB), respectively, however no studies to date have identified the inputs to SRAF. Cell populations can also be distinguished based on complementary expression of vesicular glutamate transporter subtypes (VGLUT1-3). For example, VGLUT1 is found in rostral, but not caudal MGB. In the present study, we identified the thalamic inputs to A1 and the caudal half of SRAF (cSRAF) in terms of physical location and expression of VGLUT1 mRNA. Cochleotopic organization was mapped in multiple auditory fields with high resolution intrinsic optical imaging. Retrograde tracer Cholera toxin B subunit (CTb) and its gold conjugated form (CTbG) were injected into cSRAF and A1, respectively. Expression of VGLUT1 was identified via in situ hybridization. cSRAF and A1 projections originated in nonoverlapping distributions in caudal and rostral MGB. respectively. VGLUT1 was not found in the most caudal part of MGB that projects to cSRAF, increased in a gradient rostrally, and was found co-localized in most A1 projecting neurons. The results suggest primary and ventral auditory cortical fields can be distinguished based on origins of thalamic projections, and colocalized expression of VGLUT1.

Supported by: NIDCD HD2080 and R01 DC000189

934 Revisiting Subdivisions of the Ferret Auditory Cortex – New Insights from Immunohistochemical and Cytochemical Studies

Susanne Radtke-Schuller¹, Jonathan B Fritz²¹

Division of Neurobiology Department Biology II, University of Munich, ²Institute for Systems Research, University of Maryland, College Park

The auditory cortex (AC) of the ferret (*Mustela putorius*) is located in the ectosylvian gyrus of the temporal lobe. Studies utilizing neurophysiological and neuroanatomical methods have lead to proposals of multiple subdivisions, based on the presence of at least four, separate tonotopic areas and several non-tonotopic areas. However, limited information is available on the detailed cytoarchitectural and immunohistochemical features of these proposed subdivisions.

In order to more fully characterize ferret AC, we mapped the ectosylvian gyrus using a broad array of histological stains including cell- (Nissl), myelo- (Gallyas), chemo-(zinc - Timm-method, acetylcholinesterase, cytochrome oxidase), and immunohistochemical stains for calciumbinding proteins, perineuronal nets (Cat-301 chondroitin sulfate proteoglycan, CSPG), and VGlut2 (a vesicular glutamate transporter). To integrate our findings with existing data, we aligned our results to a reference coronal series consecutively stained for cells and myelin in alternate sections. Areal boundaries and cortical maps on the brain surface were reconstructed from results from the new stains, and tested for their congruency with existing maps from previous studies.

Based on the criterion that a border between different areas is reliable if and only if it can be confirmed by consistent tracing using at least three different stains, we defined seven subdivisions in the ferret AC. These corresponded subdivisions well to the electrophysiologically defined AC fields of Bizley et al. (2005) and are in accordance with the 2-deoxyglucose autoradiography data of Wallace et al. (1997) and connectional data and cytoarchitectural observations of Bajo et al. (2007; 2010). In conclusion, the utilization of different stains in a consistent set of data vielded a refined view of the ferret AC. The identified subdivisions are compared with the AC subdivisions in other mammals, especially cat, and the issue of homology is discussed.

935 A Three-Dimensional Atlas of the Brain (And Head) of the Mongolian Gerbil Based on Magnetic Resonance Microscopy and Cytochrome Oxidase Histochemistry

Nell Cant¹, Alexandra Badea¹, Douglas Fitzpatrick², Alisa Ray¹, Joseph Corless¹, Allan Johnson¹

¹Duke University, ²University of North Carolina

We will present an overview of an atlas of the gerbil brain based on magnetic resonance (MR) microscopy and cytochrome oxidase histochemistry. For the MR imaging, anesthetized gerbils were perfused with a mixture of formalin and a gadolinium compound (ProHance) to enhance tissue contrast. Images of the head were acquired with three different MR protocols. Two of these protocols yielding contrast dependent on spin lattice relaxation (T1) and magnetic susceptibility (T2*) resulted in a spatial resolution of 21.5 microns (isotropic). A third protocol was dependent on spin spin relaxation (T2) and yielded a spatial resolution of 90 microns (isotropic). Sections from some of the brains were cut at 40 microns on a freezing microtome and processed for cytochrome oxidase histochemistry. The MR images were viewed and manipulated in Image J (NIH) and Adobe Photoshop. We will demonstrate the utility of the atlas developed based on these images for 1) locating brain structures using reference points on the skull and head and 2) for mapping data from experimental brains cut in any plane of section onto a standard plane, allowing direct comparisons of data across cases. We will emphasize the use of the atlas for locating and analyzing components of the central auditory system, but the atlas can be used for visualizing any part of the gerbil brain and head, including the remarkable middle ear.

Grant support: All MR imaging was performed at the Duke Center for In Vivo Microscopy, an NCRR National Biomedical Technology Research Center (P41 RR005959) and NCI Small Animal Imaging Resource Program (U24 CA092656). Also supported by NIDCD grant RO1DC000135 (NBC).

936 Neural Correlates of Musical Scale Perception

Stephen Dunlap^{1,2}, Patpong Jiradejvong¹, Iwen Wu¹, Charles Limb^{1,2}

¹Johns Hopkins University School of Medicine, ²Peabody Conservatory of Music

The Western major (Ionian) scale plays a fundamental role in music. In this functional MRI study, we sought to identify neural substrates implicated in major scale perception in comparison to other musical scales. As a comparison scale, we used the Locrian scale, which is acoustically similar to the major scale while being generally regarded as a purely theoretical mode that rarely appears in either classical or popular musical genres. In addition, we examined the effect of presentation order for all scale tones. Ten non-musicians with normal hearing participated in the study. All musical stimuli were presented using piano tones. Major and Locrian scales tones were presented both sequentially (ascending and descending) and randomly, in all twelve musical keys. A control stimulus of white noise with a matching temporal envelope and rootmean square energy to the piano stimuli was also presented. During scanning and after stimulus presentation, subjects were asked to rate the pleasantness/unpleasantness of each condition on a Likert scale that ranged from 1 (very unpleasant) to 5 (very pleasant). Functional MRI data analysis revealed intense activation of visual cortex (calcarine gyrus) during major scale presentation in comparison to both randomized major scale tones and ascending/descending Locrian scale tones. Contrast analysis of sequential major vs. randomized major scale revealed left precuneus, inferior occipital gyrus and cerebellar activation. We found no limbic activation particular to the major scale, which corresponds to the finding that subjects showed no preference for Ionian or Locrian modes in this study. These data suggest that a multimodal functional network involving auditory, visual and cerebellar regions of the brain is involved in perception of the major scale.

937 Behavioral and Neurophysiological Indices of Speech Processing in Noise in Adults and in Children

Brett Martin¹, Wen Jie Wang¹, Lee Jung An¹ ¹Graduate Center of CUNY

The purpose of this study was to compare the behavioral and electrophysiological processing of speech in background noise in adults and in children. This study is part of a larger body of work evaluating speech in noise processing in adults and in children from 6 months through 12 years of age. This presentation will focus on the results from adults, 3-5 year old children, and 6-12 month old infants. The 65 dB SPL naturally-produced stimulus /ui/ was presented in a quiet listening condition and also in broadband noise presented at two signal-to-noise ratios (SNR = +6 and 0). The neurophysiologic measure used was the acoustic change complex. Behavioral discrimination of the /u/-/i/ contrast was evaluated using a button press task or a conditioned head turn task. Preliminary results indicate that broadband noise masking increased response latencies and decreased response amplitudes relative to the quiet condition despite high behavioral discrimination performance. Noise had a greater effect on the latencies and amplitudes of the acoustic change complex in children relative to adults and in younger children relative to older children. Results have implications for children's speech processing in degraded listening situations such as in typical classrooms.

[Work supported by the National Organization for Hearing Research and by PSC-CUNY].

938 Behavioral and Physiologic Measurements of Spectral-Ripple Discrimination

Christopher Clinard¹, Jong Ho Won^{2,3}, Seeyoun Kwon⁴, Vasant Dasika³, Kaibao Nie³, Ward Drennan³, Kelly Tremblay², Jay Rubinstein³

¹Department of Communication Sciences and Disorders, James Madison University, ²Department of Speech and Hearing Sciences, University of Washington, ³Virginia Merrill Bloedel Hearing Research Center, University of Washington, ⁴Department of Otorhinolaryngology-Head and Neck Surgery, Samsung Medical Institute

Spectral-ripple discrimination has been widely used in psychophysical studies with normal-hearing, hearingimpaired, and cochlear implant (CI) listeners. It is yet unknown how ripple stimuli are processed in the human and central auditory system how their neural representations relate to behavioral performance. For this reason, a single-interval, yes/no paradigm was developed that can be used to obtain behavioral and electrophysiologic spectral-ripple discrimination thresholds

using the same stimuli. Cortical P1-N1-P2 change responses were elicited by a spectral-ripple phase inversion occurring at the midpoint of the spectral-ripple stimuli. In Experiment 1, the effect of the number of vocoder channels on the behavioral discrimination thresholds and the physiologic responses was determined in three normal-hearing listeners. Behavioral thresholds as well as cortical P1-N1-P2 responses improved as the number of channels increased. In Experiment 2, the relationship between behavioral and physiologic data was further examined in the same subjects to see how closely the amplitudes of the change responses were related to d' from the behavioral task. Amplitudes of the P1-N1-P2 change responses were significantly correlated with d' values from the behavioral procedure. Results suggest that the single-interval procedure with spectral-ripple phase inversion occurring within ongoing stimuli is a viable approach for measuring behavioral or physiologic spectralripple discrimination and their relationship.

[Work supported by NIH-NIDCD grants R01-DC007525, P30-DC04661, R01-DC007705, T32-DC000033, F31-DC009755, F31-DC010553, F32-DC008238, L30-DC008490, as well as KRF-2006-612-D00106 and an educational fellowship from Advanced Bionics Corporation.]

939 Sustained BOLD Enhancement for Pitch Is Observed for Iterated-Rippled-Noise But Not for Click-Train Stimuli

Iris Steinmann¹, Alexander Gutschalk¹ ¹*Heidelberg University Hospital*

Human imaging studies have suggested that activity in lateral Heschl's gyrus, lateral to the primary auditory cortex, increases with pitch strengths. Stimuli used in these studies include iterated rippled noise (IRN), click trains, and harmonic complexes. While MEG results appear to be rather consistent across different stimulus types, the fMRI evidence for pitch specificity in Heschl's gyrus was not reproduced consistently by studies using harmonic complexes.

Here we compared pitch-specific activity induced by IRN (16 iterations) and click trains in fMRI and MEG (n=12). In contrast to previous studies, we used a paradigm where transient and sustained responses evoked by the pitch stimulus could separately be evaluated in both modalities. As non-pitch control, noise was used for comparison with IRN and jittered click-trains for comparison with periodic click trains. The f0 was 200 Hz; all stimuli were low-pass filtered at 4000 Hz. The sounds were presented continuously in 24-s long blocks at the same sound intensity. The baseline was either silence or the non-pitch control.

MEG revealed qualitatively similar waveforms for the IRN and the click train condition, with dipolar sources in lateral Heschl's gyrus. However, the sustained pitch response was larger for click trains than IRN. In contrast, fMRI revealed very different response patterns for IRN and click trains: First, only IRN versus noise revealed sustained activation of Heschl's gyrus. Second, the IRN produced a sustained BOLD timecourse across the 24 second stimulus, whereas the click train response was phasic with an onset and (larger) offset peak.

These results support earlier evidence, indicating that sustained MEG (near DC) and BOLD activity in auditory cortex are not directly coupled. Moreover, the results question if sustained BOLD activity evoked by IRN fulfill the criteria for a general pitch response.

940 The Human Cortical Response to Iterated Ripple Noise Is Largely Driven by Stimulus Features Unrelated to Pitch

Daphne Barker^{1,2}, **Christopher Plack**¹, Deborah Hall^{3,4} ¹The University of Manchester, ²MRC Institute of Hearing Research, ³Nottingham Trent University, ⁴National Biomedical Research Unit in Hearing

Human neuroimaging studies have identified a region of auditory cortex that consistently responds more strongly to iterated ripple noise (IRN) than to Gaussian noise. The IRN-sensitive region is located on the postero-lateral border of primary auditory cortex, on the border between lateral Heschl's gyrus and planum temporale. Based in part on these results, this region has been described by some researchers as the human 'pitch center'. Recent evidence, however, suggests that the IRN response is more likely to be driven by slowly-varying spectro-temporal modulations in the signal that are not related to pitch. IRN is created by generating a sample of Gaussian noise, delaying it and adding back to the original. The more times this delay-and-add process is repeated, the more salient the pitch becomes, but the depth of the slowly-varying modulations also increases. Two recent functional magnetic resonance imaging studies have used a novel type of stimulus, IRNo (no-pitch IRN), which is created by processing IRN in a way that removes the fine temporal structure responsible for the pitch percept, whilst leaving the slowly-varying modulations intact. The first study revealed that the response to IRNo was similar to the IRN response, with little differential activation that could be ascribed to pitch. In the second study, a factorial analysis of the effects of pitch and modulation in the region previously identified as 'pitch-responsive' did not find evidence for an interaction between the two effects. Furthermore, direct comparisons between IRN and IRNo with different numbers of iterations failed to provide conclusive evidence for an effect of salience for IRN or for IRNo, although an effect of pitch salience was found for an unresolved harmonic complex in planum temporale. Our findings raise the possibility that the response to sound features in IRN unrelated to pitch could previously have been erroneously attributed to pitch coding.

941 Age Differences in the Purr Call Distinguished by Units in the Guinea Pig Primary Auditory Cortex

Mark Wallace¹, Jasmine Grimsley¹, Alan Palmer¹ ¹*MRC Institute of Hearing Research*

Some communication calls contain information about the physical and emotional characteristics of the caller. We investigated how this information might be coded in the

auditory cortex of the guinea pig. The short purr call is an alarm/warning call that can be easily elicited from guinea pigs of all ages. The fundamental frequency of this call progressively decreases from 476 to 261Hz during development, but the repetition rate of the individual acoustic elements of the call remains the same. To reflect age-related acoustic changes, four pitch-shifted versions of a single call were used as stimuli while recording from units in the primary auditory cortex (AI). Almost half of our sampled units (43%, 79/182) responded to the purr call with an increase in firing rate. These responsive units had characteristic frequencies ≤5 kHz (mean 1.81 kHz). Responsive units were recorded at depths from 100 to 1025 μ m (mean 534 μ m). Non-responsive units were recorded over the same range of depths as we mainly recorded from the upper layers. Units responded either at the onset or had multiple response peaks in their peri stimulus time histograms. Both types of units showed differences in their firing rate in response to pitch-shifted versions of the call. Of the responsive units, 41% had a correlated firing rate that was at least 50% higher for one version of the call than any other. Our results suggest that both onset and multi-peaked responses may code information about the caller size in their firing rate and that many cells at the low-frequency end of AI are very sensitive to age-related changes in the purr. The multipeaked responses may contain additional temporal information that would be particularly relevant to the long version of purr that has a role in mating behaviour.

942 Responses to Repetitive Transients Within Human Lateral Superior Temporal Gyrus: An Intracranial Electrophysiology Study

Kirill Nourski¹, John Brugge^{1,2}, Richard Reale^{1,2}, Hiroto Kawasaki¹, Hiroyuki Oya¹, Christopher Kovach^{1,3}, Matthew Howard¹

¹The University of Iowa, ²University of Wisconsin -Madison, ³California Institute of Technology

Auditory cortex in humans, located on the superior temporal gyrus (STG), has been hypothesized to carry out sound processing as an interconnected system of core, belt and parabelt fields. The place of non-primary auditory cortex on the lateral STG within this hierarchy and its parcellation are not yet clear. Better understanding of cortical temporal processing may aid delineation of auditory fields on physiological grounds. This study investigated spatiotemporal properties of responses to acoustic click trains of varying rates within lateral STG in humans.

Subjects were neurosurgical patients undergoing chronic invasive monitoring for refractory epilepsy. Stimuli were trains of broadband acoustic clicks (duration 160 or 1000 ms, rates 4-500 Hz), delivered diotically via insert earphones. Recordings were made using high-density subdural grids placed over the temporal lobe. Local field potentials were analyzed as averaged evoked potentials (AEPs) and high gamma (70-170 Hz) non-phase-locked event-related band power (ERBP). Responses were localized to lateral STG, adjacent to the Heschl's sulcus/Sylvian fissure junction. The magnitude of AEPs and ERBP increased with click rate. Responses to 1000 ms trains presented at rates \geq 16 Hz featured onset and offset AEP complexes. Frequency-following responses (FFRs), measured in the AEP spectra as power increases at driving frequency, were detected at rates \leq 64 Hz. Spatial distribution of onset AEPs and FFRs did not reveal patterns consistent with a periodotopic map. Foci of largest ERBP changes tended to expand anteriorly within lateral STG with stimulus rate, for rates \geq 25 Hz.

The results indicate explicit temporal representation of periodicity within lateral STG extending to at least 64 Hz. Rate-dependent spatial distribution of ERBP may be related to tonotopic organization of lateral STG or represent a rate-place code for sound periodicity.

Supported by NIH RO1-DC004290, UL1RR024979, GCRC MO1-RR-59 and the Hoover Fund.

943 Neural Responses to Cochlear Implant Stimulation in Auditory Cortex of Awake Marmoset

Luke Johnson¹, Charles Della Santina^{1,2}, Xiaoqin Wang¹ ¹Johns Hopkins University Dept of Biomedical Engineering, ²Johns Hopkins Dept of Otolaryngology-Head & Neck Surgery

The success and limitations of a cochlear implant depends on the central auditory system's ability to adequately process and interpret the electric stimuli delivered to the cochlea. Such mechanisms are not vet fully understood. We have developed a new non-human primate model for cochlear implant (CI) research, the common marmoset (Callithrix jacchus), to study cortical processing of cochlear A limitation of previous cortical stimulation. neurophysiology studies of cochlear stimulation has been the use of anesthetized preparations, which has been shown to alter auditory cortex responses. In the present study, we investigated single-unit responses to timevarying signals via CI stimulation in the primary auditory cortex (A1) of the awake marmoset and compared the responses recorded from same neurons to acoustic stimulation. A multi-contact CI electrode was chronically implanted in one cochlea while the other cochlea remained acoustically intact. This enabled us to record responses to both acoustic and electric stimuli in each individual unit. Electric current pulses and acoustic clicks were delivered at repetition rates of 2-256 pulses per second (pps). Consistent with earlier CI studies, some cortical neurons had stimulus-synchronized discharges to individual electric pulses delivered at slow electric pulse rates (<64 pps), but poor synchronization or only transient onset responses at high pulse rates. Interestingly, we found another population of neurons that had significant increases in firing rate to rapid electric pulse trains (>64 pps) that was sustained throughout the stimulus duration. Often these neurons showed little synchronization in response to slow electric pulse trains. These results parallel findings from previous studies in awake normal hearing marmosets which show that A1 neurons utilize both temporal and firing rate-based representations to encode time-varying acoustic signals (Lu et al 2001), and suggest that A1 neurons utilize similar coding schemes to represent time-varying CI stimulation.

Supported by: NIH grant F31DC010321 (L.J.) and a Kleberg Foundation grant (X.W.)

944 Neural Activity in the Pre-Motor Cortex of Freely Vocalizing Marmosets Is Associated with Vocal Production

Sabyasachi Roy¹, Xiaoqin Wang¹

¹Johns Hopkins University, Biomedical Engineering

Neural activity in the primate pre-motor cortex has been linked to voluntary movement control and sensory guidance, yet we know little about its role in vocal production and feedback-dependant vocal control. Research in this area has been hampered because vocal activity of non-human primates typically diminishes if an animal's movement is restrained. We have developed a wireless neural recording system capable of recording 16channels of single-unit neural data via a chronically implanted electrode array in the common marmoset (Callithrix jacchus), a highly vocal New World primate. Using this system, we studied neural activity in pre-motor cortex of freely roaming and vocalizing marmosets. Singleunit activity in the pre-motor cortex was recorded from multiple electrodes while the marmosets produced phee calls in a custom designed RF / EMI and acoustically shielded chamber. Our preliminary results have revealed increased firing rate preceding the onset of self-produced vocalizations in a subpopulation of neurons in the premotor cortex. This increase in firing rate was observed at time periods immediately preceding a call $(100 \sim 500 \text{ ms})$ and within the inter phrase intervals of multi-phrased calls. The firing rate of the pre-motor neurons typically reduced to spontaneous levels during the individual phrases of a call. These observations suggest an important role of the pre-motor cortex of the marmoset in vocal production and feedback control. [Research supported by NIH grants DC005808, DC008578 (X.W.)]

945 Symmetric and Asymmetric Phantom Electrodes in Cochlear Implants: Stimulating "Very Apical" Regions of the Cochlea

Olivier Macherey¹, Robert P. Carlyon¹

¹MRC Cognition and Brain Sciences Unit

Two techniques have recently been proposed to shift the locus of excitation toward a more apical region of the cochlea, thereby partially overcoming the limited insertion depths of cochlear implants (CIs). The "phantom electrode" (Saoji and Litvak, Ear & Hearing, 2010) consists of injecting current through the most apical electrode and returning a portion σ of it to a neighbouring electrode and the rest to the extracochlear ground. For each subject, there was a σ for which the pitch was lower than for monopolar stimulation of the most apical electrode. Another method that we have tested consists of using asymmetric pulses having a short, high-amplitude phase followed by a longer and lower amplitude phase of opposite polarity. When presented in bipolar mode on the

most apical channel of the implant and with the effective short phase anodic relative to the most apical electrode, we have also found the pitch to be lower than that of monopolar or bipolar symmetric pulses. The present experiment was designed to compare and combine these two techniques. Seven Advanced Bionics subjects ranked the pitches of ten stimuli presented on electrode 1. The stimuli differed in their shape (symmetric or asymmetric) and in the ratio of current returning to electrode 3 (five ratios creating a continuum between monopolar (σ =0) and bipolar (σ =1) in steps of 0.25). At a pulse rate of 12 pps asymmetric phantom pulses produced, overall, a lower pitch than symmetric ones. For both shapes, the lowest pitch was usually obtained at σ =0.75, and, at this ratio, the pitch rank did not differ significantly between pulse shapes. At a pulse rate of 1031 pps the results were more variable, and possible reasons for this will be discussed.

This research was supported by the Wellcome Trust (Grant 080216).

946 Relating Loudness Growth to Virtual Channel Discrimination

Arthi G. Srinivasan^{1,2}, David M. Landsberger¹, Robert V. Shannon^{1,2}

¹*House Ear Institute,* ²*Univ. of Southern California* We have previously collected data which showed that dynamic range (DR) in µA has an effect on virtual channel (VC) discrimination ability. CI users had worse performance with electrode pairs with small and large DRs

than with electrode pairs with medium DRs. We hypothesized that loudness grows differently for stimulation on electrodes with different DRs, possibly indicating differences in the underlying physiology of the stimulated neural population (e.g. degree of spiral ganglion or dendritic survival). In this study, we correlated characteristics of the loudness growth functions with dynamic range and with VC discrimination scores.

Stimuli consisted of 300 msec biphasic pulse trains (on a single electrode) with a pulse train frequency of 550 pulses per second and a phase duration of 226 µsec. Stimuli were presented at amplitudes ranging from 5-100% of the DR in μ A, in 5% steps. For each presentation, subjects were instructed to click on a bar to indicate how loud the stimulus was. The loudness estimates of 15 presentations were averaged to obtain a single loudness estimate for each presentation level.

Preliminary data suggests that loudness grows linearly for stimulation on electrodes with small DRs when amplitude is normalized to percent DR. Loudness growth for stimulation on electrodes with medium and large DRs typically has slow and steep components (non-linear). If the slow and steep components of loudness growth reflect stimulation from different processes, i.e. dendritic and axonal stimulation respectively, the characteristics of the loudness growth curves might indicate why VC discrimination is worse for subjects with narrow DRs.

947 Improved Spectral Resolution with Focused Electrical Stimulation of the Cochlea

Zachary Smith¹, Christopher Long¹, Chris van den Honert¹

¹Research & Technology Labs, Cochlear Ltd.

Cochlear implants convey sound to the auditory nerve by delivering electric currents via intracochlear electrodes placed along the scala tympani. Typically, interleaved stimulation of multiple monopolar channels is used to convey acoustic energy from different bands in the frequency spectrum. One of the potential drawbacks of this type of stimulation is that longitudinal spread of current may lead to undesired overlap-of-excitation between adiacent channels and thereby reduce channel independence. Current focusing, using multi-polar electrode channels, is one technique that attempts to improve the electrode-neural interface by reducing spreadof-excitation of individual channels. In this study we compared the effectiveness of monopolar stimulation versus focused stimulation with phased array channels (van den Honert and Kelsall 2007). We assessed spectral resolution by finding the minimum ripple depth that subjects could discriminate out-of-phase spectral ripples at various ripple densities. Since spectral resolution has been shown to be correlated to speech perception by several labs (e.g. Henry et al. 2005), we also conducted tests of speech understanding, comparing the two conditions. Subjects used monopolar stimulation on a daily basis in their clinical processor but only had limited exposure to focused stimulation during testing sessions. Results from the psychophysical tests show that with focused stimulation subjects significantly improved in their ability to discriminate spectral ripples at the highest spectral-ripple frequency tested (2 cycles/octave) compared to monopolar stimulation. This suggests that phased array channels may successfully reduce the spread-of-excitation associated with monopolar stimulation of scala tympani electrodes. However, there was no corresponding increase in the level of speech understanding with current focusing observed in the speech tests. Potential explanations as to why spectral resolution improved without an increase in speech scores will be discussed.

948 Impact of Early Reflections on Binaural Cues in Small Mammals

Boris Gourévitch^{1,2}, Romain Brette¹

¹LPP, Univ. Paris Descartes, UMR CNRS 8158, Ecole Normale Superieure, ²CNPS, Univ. Paris Sud, UMR CNRS 8195

When a sound is followed by an echo with a delay of 1 to 10 ms, the echo is perceptually suppressed by the auditory system. In humans, this "precedence effect" is thought to underlie sound localization in echoic environments. Several animals also show behavioral correlates of the precedence effect in the same range of delays. For this reason, most work on sound localization has considered binaural cues in anechoic environments, implicitly assuming that reflections are suppressed or separately processed by the auditory system. However, the ears of small mammals (rodents, cats) are close to the ground, which means that for most sound sources, the reflection on the ground arrives too early to be suppressed by the precedence effect, and therefore could impact binaural cues.

To study the impact on binaural cues of reflecting surfaces, we use a geometrical model of reflection on a plane finiteimpedance surface and perceived interaural time (ITD) and level (ILD) differences estimated from spherical head models as well as real HRTF recordings from gerbil. We observe that for small mammals: 1) many reflections are too short to be suppressed, and should impact the perceived ITDs/ILDs, especially in low frequencies, where there is little absorption by natural materials; 2) direct and reflected sounds interfere and produce large oscillations in ILDs and smaller but substantial variations in ITDs. These oscillations provide an acoustical cue to distance and elevation.

We conclude that the description of natural ITDs and ILDs, especially in small mammals, should include ground reflections. One consequence is to extend the range of natural ITDs and ILDs, which casts new light on earlier results showing surprisingly large best delays in binaural neurons of small mammals. We also found a reliable binaural cue to elevation and distance, which should be investigated with further psychophysical studies.

949 Buildup, Breakdown, and Re-Buildup of the Precedence Effect: ITD Versus ILD

Andrew D. Brown¹, G. Christopher Stecker¹

¹University of Washington

Normal-hearing listeners effectively localize sounds in echoic environments by responding to the early-arriving spatial cues carried by the direct signal over the spurious later-arriving cues carried by its reflected copies. The temporal extent of this "precedence effect" has been shown to strongly depend on prior stimulation (e.g., "buildup" and "breakdown" effects). In the present study we characterized the effects of prior stimulation on normalhearing listeners' sensitivity to simulated echoes using click pairs and slow trains of click pairs (4/s) carrying interaural time differences (ITD), interaural level differences (ILD), and combinations of ITD and ILD presented over headphones. Echo thresholds were measured adaptively in four stimulus conditions: (1) Baseline trials consisted of a single "source-echo" click pair, (2) Buildup trials consisted of 12 "conditioner" sourceecho click pairs and a final test pair identical to the conditioner pairs, (3) Breakdown trials consisted of 12 conditioner pairs and a "switched" test pair in which the interaural cues were swapped between the "source" and "echo" clicks, and 4) Re-buildup trials consisted of 11 conditioner pairs, an intervening switched pair, and a final test pair identical to the 11 conditioner pairs. Results suggest a stronger precedence effect for ITD than ILD, but also that the two cues contribute complementarily to "dynamic" aspects of the precedence effect.

950 Temporal Weighting Functions for Lateralization by Interaural Time and Level Differences

G. Christopher Stecker¹, Jennifer D. Ostreicher¹, Andrew

D. Brown¹, Julie Stecker¹

¹University of Washington

Localization of real sounds in azimuth involves the integration of acoustic spatial cues over time. Dynamic variations in listeners' sensitivity to these cues can be characterized by temporal weighting functions (TWFs) for localization, discrimination, or lateralization of spatial cues carried by brief sounds. This study measured TWFs for ITD- and ILD-based lateralization of filtered-impulse trains (4 kHz Gabor click trains, 30-150 ms in duration). On each of many trials, listeners judged the apparent lateral position of a stimulus, responding either by head turn toward the perceived direction (in one response condition), or by indication along a horizontal scale displayed on a touchsensitive device (in another). Lateral positions varied from trial to trial consequent to overall interaural differences, which varied +/-500 µs ITD or +/-5 dB ILD across trials. Interaural differences carried by individual clicks in each train received additional random variation (ranging +/-100 µs or +/-2 dB) to allow calculation of TWFs by multiple linear regression of normalized responses onto the perclick ITD and ILD values. In separate conditions, TWFs were measured for (1) ITD alone, (2) ILD alone, (3) ITD and ILD covarying ("in agreement"), and (4) ITD and ILD varying independently across clicks. Consistent with past studies, TWFs demonstrated strong onset dominance (high weight on the first click and reduced weight thereafter) for stimuli with short interclick interval (ICI = 2 ms) but flatter weighting for longer ICI (5-10 ms). In some cases, TWFs additionally demonstrated upweighting [Stecker and Hafter 2009. JASA 125:3914-24], with greater weight for clicks near the offset than near the middle of the train. The latter result was observed only when stimuli carried ILD, and appeared more reliably for 5 ms than for 2 or 10 ms ICI.

951 Visual Influences on Echo Suppression

Christopher Bishop¹, Sam London¹, Lee Miller¹

¹University of California, Davis Center for Mind and Brain Auditory localization is challenging due to imprecise spatial acoustic estimates and distracting echoes. Fortunately, listeners can improve localization by perceptually suppressing the reverberations, a phenomenon called the "precedence effect", and by integrating sounds with spatially precise visual cues. Although multisensory integration and echo suppression are each known to improve performance independently, it is not clear if these mechanisms can cooperate or interfere with each other. We directly tested the visual contribution to the precedence effect in human listeners. Our data demonstrate that vision can both enhance and inhibit echo suppression depending on its spatiotemporal relationship to the primary (leading) or secondary (lagging or echo) sound. These data show that the brain's effort to suppress echoes is a fundamentally multisensory process, where

vision modulates even this largely automatic auditory mechanism to organize our spatial environment.

952 An Efficient and Robust Model of the Precedence Effect

Tom Goeckel¹, Gerhard Lakemeyer¹, Hermann Wagner¹, ¹*RWTH Aachen*

Binaural sound source localization systems based on simple interaural time difference models have significant problems when confronted with echoes. These algorithms are often unable to distinguish between the actual sources and their reflection sites. Humans resolve this problem with mechanisms that are subsumed under the term of precedence effect, which masks the directional information coming from the reflection sites. Our goal was to find a model of the precedence effect that is both efficient and reliable in reverberant environments. We based our algorithm on the idea of the interaural coherence value as a reliability measure. Interaural time difference values weighted by interaural coherence were accumulated over a time window of up to 100ms and a peak detector and time integration process determined the most reliable source directions. With the aid of auralization software, impulse responses of different simulated echoic environments with a white noise sound source have been generated to test the localization capabilities of the algorithm. The results showed a very good localization performance even under the influence of reverberances and signal-to-noise ratios of as low as -15dB. The measured localization errors, with an average of 1.3°, were mainly caused by the restricted time resolution of the digital input signal. Further tests on a mobile robot in a reverberant room vielded similar results with the exception of 2 lateral sound source positions in which the localizer turned to virtual sources. In all other test cases, the reflection sites of the sound sources were suppressed.

953 ITD Discrimination Performance and Optimal Coding

David Greenberg¹, David McAlpine¹, Torsten Marquardt¹ ¹University College London

The optimal coding model (Harper and McAlpine, 2004) established from theoretical principles that head-size and the frequency range over which interaural time differences (ITDs) are extracted are critical in determining the neural representation of ITD. This model accounts for the observation (McAlpine et al 2001) that the distribution of preferred ITDs is dependent on neural tuning for sound frequency such that within each frequency band the distribution peaks at ITDs equal to approximately 45° interaural phase difference (IPD). The consequence of this is that the sensitive slopes of ITD functions are positioned across the range of ITDs encompassed by the head-width, and directed towards frontal space. How relevant are such considerations for human spatial hearing? We measured just-noticeable-differences (inds) for ITD as a function of reference ITD in human listeners for tones and 50-Hz bands of noise as a function of frequency (or centre frequency of noise). Consistent with previous reports, for a reference ITD of zero, thresholds were lowest at 200 Hz and generally increased with increasing frequency, suggesting that very low-frequencies of sound provides for best interaural temporal resolution. We also observed a frequency-dependent change in threshold consistent with the periodicity reported in the physiological data. The rate at which performance deteriorated increased with increasing frequency, consistent with the interpretation that the underlying neural representation of ITD is frequency dependent. There was no apparent relationship between performance and the human range of ITDs. These data are consistent with a recent study (Dietz et al, 2009) reporting an apparent over-representation of ITD detectors tuned to 45° IPD in the human brain.

Harper NS, McAlpine D (2004) Nature 430, 682-6

McAlpine D, Jiang D, Palmer AR (2001) Nat Neurosci 4,396-401

Dietz M, Ewert SD, Hohmann V (2009) J Acoust Soc Am 125,1622-35

954 Lateralization of Envelope-Based Interaural Temporal Disparities of High-Frequency, Raised-Sine Stimuli: Empirical Data and Mathematical Modeling

Leslie Bernstein¹, Constantine Trahiotis⁷ ¹University of Connecticut Health Center

An acoustic pointing task was used to measure extents of laterality produced by ongoing interaural temporal disparities (ITDs) within the envelopes of 4-kHz-centered raised-sine stimuli while varying, parametrically, their peakedness, depth of modulation, and frequency of modulation. One purpose was to determine whether such manipulations would produce changes in laterality paralleling those found for ITD-discrimination thresholds reported by Bernstein and Trahiotis [(2009). J. Acoust. Soc. Am. 125, 3234-3242]. The data obtained revealed that they did in that: 1) increasing depth of modulation, peakedness, or frequency of modulation between 32 Hz to 128 Hz produced smaller threshold-ITDs and greater laterality and 2) increasing frequency of modulation to 256 Hz produced modest increases in threshold-ITDs and modest decreases in laterality. The extents of laterality measured were successfully accounted for via an augmentation of the cross-correlation-based "positionvariable" modeling approach developed by Stern and Shear [(1996). J. Acoust. Soc. Am. 100, 2278-22881 to account for ITD-based extents of laterality obtained at low spectral frequencies. [Work supported by research grant NIH DC-04147 from the National Institute on Deafness and Other Communication Disorders, National Institutes of Health.]

955 The Effects of Overall Level on Sensitivity to Interaural Time Differences

Mathias Dietz¹, Leslie Bernstein², Constantin Trahiotis², Stephan Ewert¹, Volker Hohmann¹

¹Universität Oldenburg, ²University of Connecticut Health Center

Data from several psychoacoustic investigations reveal that sensitivity to interaural time differences (ITDs)

conveyed by the envelopes of high-frequency stimuli depends on overall level. The results of those studies are, however, somewhat heterogeneous with regard to the degree to which overall level appears to have influenced threshold-ITDs. The diverse outcomes may have resulted from the use, across studies of: 1) different accompanying low-frequency noises for the purpose of masking distortion products, 2) high-frequency waveforms having different types of envelopes conveying the ITDs, and 3) highfrequency waveforms having different rates of modulation. The current study investigated the potential influence of those three factors on the degree to which overall level influences sensitivity to ITDs within high-frequency waveforms. To that end, threshold-ITDs were measured for high-frequency "signal" waveforms spanning overall levels of 30, 45, 60, and 75 dB SPL in the presence of either diotic or interaurally uncorrelated low-frequency masking noises that were (i) continuous, (ii) pulsed synchronously with the signal, or (iii) pulsed on 50 ms prior to the signal and gated off synchronously. Threshold-ITDs as a function of the overall level of the signal were also evaluated for several different absolute and relative levels of the low-frequency masking noises. Results showed that, in general, the overall level of the signal had a modest influence on threshold-ITD with substantial elevations occurring once its level was reduced below about 45 dB. The presence of different types of low-frequency maskers was, indeed, found to alter the form of the function relating threshold-ITD to overall level. The influences of envelope type (sinusoidally amplitude-modulated and "transposed") rate of modulation were also investigated. Results will be discussed in terms of modern models and theories of binaural processing.

956 Sound Localization in Mice: The Relative Importance of Binaural and Monaural Cues Amanda Lauer¹, Bradford May¹

¹Johns Hopkins School of Medicine

Mice have been increasingly used in studies of sound localization pathways, yet little is known about localization behavior in this species. Insensitivity to low frequencies suggests that mice localize sound source azimuth based on interaural level differences and not interaural time differences. Nothing is known about the localization of sound source elevation, although monaural spectral cues appear to exist in the head-related transfer functions (HRTFs) of the mouse (Chen et al. 1995). To explore the acoustic basis of sound localization in greater detail, we used a conditioned lick suppression paradigm to measure the spatial acuity of the mouse under stimulus conditions designed to separate the relative importance of binaural disparity cues and monaural spectral cues. Consistent with previous results, presentations of broadband noise from azimuths greater than 20° elicited significant suppression. Pure tones presented at 90° azimuth produced weak lick suppression. The enhanced directionality of broadband sounds suggests that binaural cues are reinforced by an increase in stimulus bandwidth or that monaural spectral cues dominate the discrimination. These opposing interpretations were tested by measuring spatial acuity in

the median vertical plane, where binaural disparities are minimized. The failure of broadband noise to elicit strong suppression under these conditions suggests that optimal localization is not based exclusively on monaural spectral cues. As a further argument against spectral processing, the shape of the mouse pinna was manipulated to distort HRTFs. This had little effect on suppression rates that were elicited by broadband noise in the interaural horizontal plane. By contrast, the disruption of binaural cues by plugging one ear severely disrupted performance, even when placement of the plug in the remote ear had no effect on monaural spectral cues that were produced by the ear closest to the speaker array. Support: DC009353, DC005211, DC000954

957 Spatial Hearing Acuity of the Common Marmoset Monkey

Evan Remington¹, Xiaoqin Wang¹

¹Johns Hopkins University School of Medicine

The common marmoset (Callithrix jacchus) is an attractive model system for studying sound processing and vocal communication due to its easily accessible auditory cortex and its tendency to vocalize in captivity. However, little is known about the perceptual abilities of marmosets. As a tropical arboreal species, marmosets need to to navigate their environment using acoustic spatial cues. Spatial processing is therefore an important function performed by the marmoset's auditory system. We have developed an operant conditioning task in which marmosets are trained to lick at a feeding tube with a photo-beam for a reward when a change in a particular sound parameter is detected. With this task, we investigated the ability of marmosets to discriminate sound location, measuring the minimum audible angle (MAA) of Gaussian noise, tone complexes, and pure tones for azimuth discrimination, and Gaussian noise and tone complexes for elevation discrimination. Preliminary data indicate that while tone discrimination thresholds are on par with what would be expected given the marmoset's head size in relation to previously studied mammals and their acuities, broad-band discrimination thresholds are lower, consistent with some other mammals. These observations suggest that marmosets have a highly developed sound localization system which is adapted to life in a visually occluded environment. [Supported by NIH Grant R01-DC03180 (X.W.)].

958 Behavioral and Neural Correlates of Auditory Distance Perception

Norbert Kopco^{1,2}, Samantha Huang¹, Chinmayi Tengshe¹, Tommi Raij¹, John W. Belliveau¹, Jyrki Ahveninen¹

¹Harvard Medical School – Martinos Center for Biomedical Imaging, Massachusetts General Hospital, ²Technical University of Kosice, Kosice, Slovakia

The mechanisms and cortical structures underlying human auditory spatial processing are not well understood. For the horizontal localization, the basic perceptual cues have been identified, while functional Magnetic Resonance Imaging (fMRI) studies suggest that posterior aspects of

non-primary auditory cortex (AC) areas are the main processing structures. However, very little is known about the mechanisms and structures responsible for sound source distance processing. Here, we present a framework that combines behavioral experiments with fMRI to directly examine both the mechanisms and structures of auditory distance processing. We illustrate the approach on the results of an experiment that studied auditory distance perception for nearby sources in virtual auditory environment. The combined approach allowed us to identify the processing regions and to separate the contribution of individual distance cues to the processing. Regions of most significant activation were found in nonprimary AC areas posterior to the AC when contrasting stimuli that varied in distance to stimuli varying in intensity, suggesting that level-independent cortical distance processing occurs in the regions close to the horizontal spatial maps. This result illustrates the potential of our framework for future examination of the three-dimensional representation of auditory space in the human brain.

[Supported by NIH awards R21DC010060, R01MH083744, R01HD040712, and P41RR14075, and the European Community's 7FP/2007-13 grant no PIRSES-GA-2009-247543]

959 Characterizing the Benefit of Residual Acoustic Hearing to Auditory and Auditory-Visual Cochlear-Implant Consonant Perception

Benjamin Sheffield¹, Joshua Bernstein¹, Gerald Schuchman¹

¹Walter Reed Army Medical Center

As cochlear-implant (CI) acceptance increases and the candidacy criteria are relaxed, these devices are increasingly recommended for patients with less than profound hearing loss. As a result, many patients who receive a CI also retain some residual hearing in the nonimplanted ear (i.e., bimodal hearing). The additional acoustic information provided by the non-implanted ear has proven useful for everyday listening. However, guidelines for the clinical decisions pertaining to cochlear implantation are largely based on expectations for postsurgical performance with the CI alone in auditory-alone conditions. A more comprehensive prediction of postimplant performance would include the expected effects of residual acoustic hearing and visual cues on speech reception performance. An evaluation of auditory-visual performance might be particularly important due to the between speech complementary interaction the information relayed by visual cues and that contained in the low frequency auditory signal. The goal of this study was to refine expectations for post-surgical speech reception performance of bimodal CI listeners by characterizing the benefit provided by residual acoustic hearing to consonant identification under auditory and auditory-visual conditions. Consonant identification was measured for conditions involving combinations of electric hearing (via the CI), acoustic hearing (via the nonimplanted ear) and lipreading (visual cues). The identification data are expressed in the form of

stimulus/response confusion matrices and analyzed to determine how consonant features are relayed and combined across stimulus modalities.

960 Co-Modulation Masking Release in Cochlear Implant Listening

Robert H. Pierzycki¹, Bernhard U. Seeber¹ ¹*MRC Institute of Hearing Research*

In normal hearing, detection of a signal in an on-frequency noise band (OFB) improves after adding flanking bands (FBs) of noise at frequencies remote from the OFB. This release from masking requires common envelope modulations in the OFB and FBs and is called comodulation masking release (CMR). As current cochlear implant (CI) processors transmit the sound envelope, comodulation might also be beneficial for signal detection in CI listening.

The FB CMR paradigm was adapted for CIs by modulating electric pulse trains on chosen OFB and FB electrodes with envelopes extracted from narrow-band OFB and FB noises. The noise bands were sinusoidally amplitudemodulated at fm=20 or 8 Hz. In signal intervals, pulse trains on the OFB electrode were modulated with the envelope of a tone added to the OFB noise. Two conditions were tested: 1) a FB at a basal and an apical electrode, each 4 electrodes away from a mid-array OFB electrode or 2) one FB placed 9 electrodes away from a basal OFB electrode. In a further condition the same noises were used as OFB and FBs to assess the impact of correlation. CMR was defined as a positive difference between thresholds for: 1) OFB only vs. OFB with comodulated FBs (OFB-CM=CMR 1), or 2) OFB with anti- vs. co-modulated FBs (AntiM-CM=CMR 2).

The addition of co-modulated FBs did not lead to a reduction of tone thresholds in any CI subject (N=5), i.e. CMR 1 was absent. For some subjects for fm=8 Hz, CM thresholds were lower than the AntiM thresholds, indicating CMR 2. However, this was unlikely a true CMR effect since both CM and AntiM thresholds were larger than the thresholds for the OFB alone. For large OFB and FB electrode separations, CM thresholds tended to decrease, attributed to reduced current spread. In none of the test conditions did CMR reach significance. The failure to observe CMR may be due to insufficient spectral and temporal cues in CI listening which precludes signal/masker segregation or grouping of the OFB with FBs.

961 Investigating the Impact of Mismatched Electrode Pairs in Simulated Bilateral Cochlear Implants on Binaural Sensitivity

Alan Kan¹, Corey Stoelb¹, Matthew Goupell¹, Ruth Litovsky¹

¹University of Wisconsin-Madison

In bilateral cochlear implant (CI) users, interaural mismatch in tonotopic stimulation is likely to occur, but the impact of this mismatch is poorly understood. As a first step, this issue was investigated in normal-hearing listeners using vocoder simulations of CIs. Subjects listened to 500 ms, band-pass filtered pulse trains presented over

headphones. The bandwidth of the pulse train was designed to mimic the effect of current spread along the basilar membrane resulting from electrical stimulation. In the reference condition, pulse trains centered at 4 kHz were presented to both ears. In the mismatched conditions, a pulse train centered at 4 kHz was presented at one ear and a pulse train centered at either 4.95, 6.13, 7.57, 9.35 or 11.54 kHz (representing mismatches of 1.5, 3, 4.5, 6 and 7.5 mm respectively) was presented to the other ear. In the first experiment, subjects provided a subjective description of the perceived sound image from a list of options that varied by intracranial locations and degree of fusion. Results indicate that there are substantial inter-subject differences in the perceived sound image when there is a high amount of mismatch. For some subjects, the sound image was always lateralized to the side of the mismatched electrode (higher frequency). For others it was to the reference electrode (lower frequency). In other subjects, two distinct sound images were heard at two different frequencies. In a second experiment, the ability of subjects to discriminate interaural time differences was investigated. Preliminary results showed degraded sensitivity with increased amounts of mismatch in all subjects. However, subjects who heard two distinct sound images showed a slower rate of degradation as a function of mismatch. These findings may have implications for understanding binaural listening in bilateral CI users. [Work funded by NIH-NIDCD R01003083]

962 Effects of the Envelope Shape on Interaural Envelope Delay Sensitivity in Acoustic and Electric Hearing

Bernhard Laback¹, Inge Zimmermann¹, Piotr Majdak¹ ¹Austrian Academy of Sciences

The importance of the envelope shape for the perception of interaural time differences (ITD) in the envelope has been demonstrated by showing improved sensitivity for transposed tones compared to sinusoidally amplitudemodulated (SAM) tones. The present study investigated the effects of different envelope parameters determining the envelope shape in nine normal-hearing (NH) and seven cochlear-implant (CI) listeners.

In NH listeners, the stimuli were 8727-Hz sinusoids with 27-Hz trapezoidal modulation. The stimuli had either constant rms-level or constant peak level. The results showed that increasing the off time (the silent interval in each modulation cycle) up to 12 ms, increasing the envelope slope, and increasing the peak level improved ITD sensitivity. There was no interaction between the effects of the off time and slope. The combined effect of the off time and slope seems to account for the gain in sensitivity for transposed relative to SAM tones.

In CI listeners, the stimuli were 1515-pulse/s pulse trains with envelopes corresponding to those of the acoustic stimuli. The peak levels were adjusted for constant loudness across conditions. Increasing the off time up to 20 ms improved sensitivity, but increasing the slope showed no systematic effect. An additional condition involved a 27-pulse/s electric pulse train, representing a special case of modulation with infinitely steep slopes and maximum possible off time. The sensitivity was considerably higher than for the best condition with trapezoidal modulation, which we attribute to the larger peak level. The CI results indicate that envelope-ITD sensitivity of CI listeners could be improved by using CI processing schemes which increase the sharpness of the signal envelope.

963 Comparison of Psychophysical and Clinical Performance with Cochlear Implants Between Prelingually Deafened Children and Postlingually Deafened Adults

Kyu Hwan Jung¹, Jong Ho Won², Ward Drennan², Elyse Jameyson², Gary Miyasaki², Susan Norton², Jay Rubinstein²

¹Haeundae Paik Hospital, Inje University, ²Virginia Merrill Bloedel Hearing Research Center, University of Washington

Because of the growing desire for improved perception of music and speech in noise of cochlear implant (CI) users, many psychophysical, music, and speech outcome measures have been developed. However, these measures were originally developed for adult CI users. In this study, psychophysical measures of spectral-ripple and Schroeder-phase discrimination tests, the clinical assessment of music perception (CAMP), consonantnucleus vowel-consonant (CNC) word recognition in quiet and speech reception thresholds (SRT) in noise were evaluated in 11 prelingually deafened CI users who were 8-16 years of age and had at least 5 years of CI experience. The children's performance was compared to the previously reported results of postlingually deafened adult CI users. The average spectral-ripple threshold (N=10) was 2.08 ripples/octave. Schroeder-phase discrimination average score for 50-Hz Schroeder-phase discrimination was 67.3% and for 200-Hz Schroeder-phase discrimination (N=9) was 56.5% . The CAMP test showed average complex pitch direction discrimination of 2.98 semitones. The mean melody score (10.61 %) was at a chance level and timbre scores averaged 34.09% correct. The mean CNC word recognition score was 68.6 % and the mean SRT in steady noise was - 8.5 dB SNR. When compared to the postlingually deafened adults, prelingually deafened CI users showed poor musical and Schroederphase performance in spite of their identical spectralripple, CNC word, and SRT in noise performance. In addition, these pediatric CI users could attend to the psychophysical and clinical tests well when they were appropriately instructed and encouraged.

Supported by NIDCD R01-DC007525, P30-DC04661, L30-DC008490, and F31-DC009755.'

964 Influence of Number of Harmonics, Intensity, Stimulation Place and Stimulation Pattern on Temporal Pitch Discrimination in Cochlear Implant Users

Lisette Harting-Oshovsky¹, Wiebe Horst¹, Deniz Baskent¹, Pim van Dijk¹

¹Department of Otorhinolaryngology / Head and Neck Surgery, University Medical Center Groningen

The ability of cochlear implant users to discriminate the rate of electrical pulse trains has been well described. However, the effect of harmonics is not clear, although they are extensively present in real-life sounds. The frequency discrimination of harmonic sounds could have an important contribution to the cocktail party effect.

Here, we study the influence of the *number of harmonics* (1 to 5) on rate discrimination. The harmonics were played on consecutive basal electrodes (e.g.: 200 Hz at electrode (EL) 1, 400 Hz at EL 2, 600 Hz at EL 3 etc.). We chose *fref* = 100 Hz or 200 Hz as reference frequencies, because these correspond to the fundamental frequency of typical human speech. We added the parameter *'place of stimulation'* (apical or basal). We used two methods of stimulus coding: constant amplitude pulse trains at the rate of the harmonic, and fast pulse trains (2.9 kHz), modulated by a half-wave rectified sinusoid at the rate of the harmonic.

We used an unforced-weighted up-down paradigm (Kaernbach, 2001) to determine the 67%-correct level. Every trial consisted of three tone bursts of 1 second each. Two of these sounds had the same *fref*, while the target had a higher frequency, *fref* + Δf . Current levels roved between -10%, 0% and +10% relative to M-level. Participants identified the sound with the highest pitch. The average Δf of the last 6 reversals (out of 10) was the just noticeable difference in frequency (JNDF).

Preliminary results (n=2) showed no conspicuous effect of the number of harmonics on JNDF. As for reference frequency, JNDFs were much higher for 200 Hz (up to 1000 Hz) than for 100 Hz. This might be explained by the occurrence of *octave errors* at 200 Hz: When Δf was between half an octave and a full octave, both subjects identified the lower-frequency tone as having the higher pitch. These preliminary results show that complicated mechanisms underlie rate pitch discrimination in CI-users. Work supported by Technology Foundation STW. Equipment provided by Advanced Bionics.

965 Pitch Ranking Focused and Unfocused Cochlear Implant Virtual Channels

David Landsberger¹, **Monica Padilla**¹, Arthi Srinivasan^{1,2}, Robert Shannon^{1,2}

¹*House Ear Institute,* ²*University of Southern California* We have been investigating the use of current focused virtual channels (Quadrupolar Virtual Channels or QPVCs) to improve spectral resolution in a cochlear implant (CI) sound processor. QPVCs are created by stimulating simultaneously on four intra-cochlear electrodes. Two adjacent electrodes provide in-phase stimulation to create a virtual channel while two flanking electrodes provide out of phase stimulation to reduce spread of excitation. The proportion of current on the apical electrode of the virtual channel is designated α . QPVCs allow current steering (like a Monopolar Virtual Channel or MPVC) and current focusing (similar to Tripolar stimulation). If QPVCs are to be useful in a speech processing strategy, then a change in QPVC location should correspond to a change in place pitch. However, with QPVCs, stimulation on a physical electrode X can be created with α =0 (and electrodes X-1 and X+2 as grounds) or α =1 (and electrodes X-2 and X+1). It is unknown if these two QPVC structures differ in pitch and current field.

A pitch ranking task was performed for MPVCs and QPVCs ranging from electrode 3 to 5 in α =0.5 steps to determine if pitch ranking is similar for MPVCs and QPVCs and if there is a pitch difference between α =0 and α =1 QPVCs. Data from 7 CI users suggest that QPVC and MPVC pitch discrimination is similar. Pitch ranking for QPVCs centered on a fixed electrode indicates that α =1 could be perceived as higher, lower or equal in pitch to α =0 stimulation, depending on the subject.

A follow up forward masking experiment measured the spread of excitation of QPVCs on electrode 4 with α =0 or α =1. Preliminary data on four subjects suggest that the shape and position of the forward masked curves differ across subjects but accurately predict which QPVC has a higher pitch. It is hoped that a full set of forward masking curves will reveal insight into the relative importance of the peak of stimulation and centroid of current spread on pitch perception.

966 Current Steering with Tripolar Stimulation Mode in Cochlear Implants

Ching-Chih Wu¹, Xin Luo¹

¹Purdue University

In current cochlear implant (CI), spectral resolution is limited by the large current spread of electrical stimulation. Tripolar (TP) stimulation mode has been proposed to reduce current spread and increase neural selectivity by using two adjacent flanking electrodes for current return. The degree of current focusing can be controlled by a TP compensation coefficient σ , which governs the fraction of current that is returned to the two flanking electrodes and has a value between 0 (monopolar mode) and 1 (TP mode). By introducing a steering coefficient α , which controls the proportion of return current on the basal flanking electrode, current steering can be incorporated into partial TP mode. This study investigated loudness and pitch perception with different steering coefficients for partial TP mode.

Adult CI users were tested on apical, medial, and basal electrode pairs. The maximum σ value that allowed for full loudness growth within the safety current limit was chosen for each subject. Different α values ranging from 0 to 1 with a step of 0.1 were tested, and the resulting stimulation mode was switched between partial bipolar ($\alpha = 0$ or 1) and partial TP modes ($\alpha = 0.5$). After obtaining the dynamic range for each α value, stimuli with different α values were loudness balanced to the most comfortable

level. Pitch discrimination was then measured between adjacent α values with a 1-dB amplitude roving.

Results showed that higher current levels were required for α around 0.5 to achieve equal loudness, due to more focused excitation patterns. As α was increased from 0 to 1, subjects perceived decreasing pitches, consistent with the hypothesis that the main peak of excitation pattern was shifted towards the apical end. Furthermore, pitch discrimination was significantly better for α around 0.5, for which the excitation pattern was more focused. These findings suggest that current steering with TP mode may greatly improve spectral resolution and pitch perception with CI.

967 How Good Is Your Cochlear Implant Simulator?

Daniel Aguiar¹, Thomas Talavage¹

¹Purdue University

Evaluation of novel cochlear implant (CI) signal processing strategies is often first done using a simulator that produces auditory stimuli for use with normal hearing (NH) listeners, increasing the size of the subject pool. Ideally, NH listeners using the simulator would have performance levels and behavior similar to those of CI subjects. In order to predict how CI subjects will perform based on data from simulator users, it is useful for researchers to have quantitative and qualitative measures comparing the performance of CI subjects and simulator users in psychophysical tasks.

Our goal is to compare the performance of NH listeners using an 8-channel noise-band vocoder to the performance of CI users in a 9-alternative forced-choice vowel identification experiment. We presented CI subjects with phonemes of the form H/vowel/d and asked them to identify the phoneme that was presented. We presented NH listeners the outputs of the noise-band vocoder of the same phoneme stimuli under 4 conditions: the combinations of with and without feedback, and for a simulated 0mm and 6mm basalward electrode array shift. We then computed a number of metrics from the resulting confusion matrices, including correct identification rates, rates of information transfer, Kullback-Leibler Distances, and vowel formant shifts.

968 Auditory Perceived Continuity and Masking Revisited: Evidence for an Illusory Tone Percept Through a Noise-Burst Containing a Brief Silence

Nicholas Haywood¹, Valter Ciocca¹

¹School of Audiology and Speech Sciences, University of British Columbia

Two tones separated by a silent interval can be heard as one continuous tone if the silence is filled with a louder sound. It has been proposed that continuity is heard only if the louder sound is capable of masking the tone, if the tone was present physically [Warren et al., 1972; Science, 176: 1149-1151]. Three experiments measured the perceived continuity of two flankers (300-ms, 1 kHz pure tones; 43 dBA) through a noise-burst segment (NB; 300ms, low-pass filtered at 10 kHz; 80 dBA). The NB contained a single interruption (NBI); either a silence (NBI-S) or a tone (NBI-T; a 1-kHz, 43 dBA pure-tone).

Expt. 1 used a 2I-2AFC procedure; listeners identified which interval contained NBI-T rather than NBI-S (feedback was provided). For both intervals, NBI had the same duration (20, 40, or 60 ms), and the same position after NB onset (75, 150, or 225 ms). Performance was very accurate without the flankers. Therefore, evidence of flanker continuity through NBI-S would demonstrate an illusory percept in the absence of a masking sound. Perceived flanker-tone continuity through NBI-S was expected to produce poor discrimination between NBI-T and NBI-S. As expected, performance decreased significantly for all NBI durations when the flankers were present, and was close to chance for the 20-ms case. NBI position had no significant effect on performance.

In Expt. 2, NBI occurred only at 150 ms after NB onset. Flankers were frequency glides that either changed along a common log-frequency trajectory (762 to 906 Hz prior to NB: 1103 to 1311 Hz following NB: "same-trajectory") or changed from 1103 to 906 Hz both prior and following NB ("different-trajectory"). Performance was overall poor for the same-trajectory condition, but significantly improved in the different-trajectory condition. In Expt. 3 listeners rated directly their perception of flanker continuity for the same flanker conditions of Expt. 2. Listeners perceived strong continuity in NBI-S conditions in which poor performance had been observed in the previous experiment. Overall, these results suggest that illusory continuity can occur through the NBI-S, even though the NB does not produce enough masking during the interruption for it to mask a physically-present intervening tone (NBI-T, no-flankers condition).

969 Frequency Change Aftereffect by Adaptation to Real and Illusory Frequency Sweeps

Keiko Masutomi¹, Makio Kashino^{1,2}

¹Tokyo Institute of Technology, ²NTT Communication Science Laboratories

The auditory continuity illusion is a compelling perceptual effect in which a sound is perceived as continuous even though parts of it have been replaced by an extraneous sound. Under appropriate conditions, the illusion is so powerful that it is difficult for the listener to distinguish illusory and real continuities. Here we examined whether the illusory and real continuities are processed by the same mechanism, using the frequency change aftereffect. The frequency change aftereffect is a phenomenon in which repeated exposure, or adaptation, to a frequency sweep results in a shift in the perceived frequency change direction of a subsequent test sound in a direction away from that of the adapting stimulus. The aftereffect is supposed to be mediated by neural mechanisms sensitive to frequency change. If the illusory and real frequency sweeps are processed by the same neural mechanisms, the adaptation to illusory sweeps is expected to produce the frequency change aftereffect for a real test sound. We compared the magnitude of aftereffect among different

types of adaptors, namely, 'real sweep' (i.e., six repetitions of a continuous sweep traversing 1/2 octave centered at 1000 Hz in 800 ms either upward or downward), 'illusory sweep' (i.e., the same as 'real sweep' except that a 200ms portion in the middle of it was replaced by a louder bandpass noise), and 'sweep with gap' (i.e., the same as 'illusory sweep' except that the 200-ms portion was replaced by silence). The test sound was an 800-ms tone having a frequency change of $\pm 1/8$ octave or less centered at 1000 Hz. Listeners judged whether the direction of frequency change of the test sound was upward or downward, and the points of subjective equality to no frequency change were obtained by the constant method. Eight listeners with normal hearing showed a significant aftereffect only for the 'real sweep' adaptors, suggesting that the illusory and real sweeps are processed by different neural mechanisms.

970 Sound Texture Perception Via Statistics of Peripheral Auditory Representations

Josh McDermott^{1,2}, Eero Simoncelli^{1,2}

¹New York University, ²Howard Hughes Medical Institute The sounds of rainstorms, fires, swarms of insects, and galloping horses result from the superposition of many acoustic events. A defining characteristic of these "auditory textures" is stationarity, and this reduction in complexity makes them a useful starting point for understanding sound representation. We have previously proposed (McDermott, Oxenham, & Simoncelli, 2009) that the auditory system encodes and recognizes sound textures using statistics - time-averages of the simple acoustic measurements made in the early auditory system. We have explored this hypothesis with synthesis algorithms, on the grounds that statistics responsible for perception should be sufficient to synthesize realistic sounding signals. Here we extend our statistical model to be compatible with the known structure of the auditory system, and test the role of different statistics and representational properties with experiments on human listeners.

Natural sounds were processed with a cascade of two filter banks, representing cochlear channels and modulation frequency bands. We measured marginal moments and pair-wise correlations of these filter responses, capturing spectral and temporal structure, and sparsity. Our synthesis algorithm then imposed these statistics on samples of noise. Although the statistics in our model were not hand-tuned to specific natural sounds, their imposition produced compelling synthetic examples of a large set of real-world sound textures. Omitting any individual class of statistics audibly impaired the results. Moreover, sounds synthesized using filters qualitatively distinct from those in the auditory system generally did not resemble their realworld counterparts, indicating that successful synthesis depends on, and reflects, the use of a biologically plausible representation. The results show that simple statistics can underlie sound texture percepts, and illustrate how sound textures and their synthesis can serve as engines for investigations of audition.

971 Contextual Effects in the Identification of Nonspeech Auditory Patterns in Random Maskers

Gerald Kidd Jr¹, Virginia Richards², Timothy Streeter¹, Christine Mason¹, Rong Huang²

¹Boston University, ²Univ of Calif Irvine

This study investigated the benefit of cuing for the identification of nonspeech auditory patterns in masked conditions. Six target patterns were formed by sequences of four brief sinusoidal tones drawn from narrow frequency bands. Maskers were also four-tone sequences in narrow bands with the individual tones chosen randomly on every trial. The frequency range from 200 to 6540 Hz was divided into 16 equally spaced bands. On any trial, the target occupied one of four possible bands and the maskers occupied eight others. The masker bands were randomized on every trial excluding the target band and the two bands adjacent to the target.

In a block of trials, the target pattern was presented in either the same frequency band (fixed) throughout, or was randomized among the four possible bands (random). No significant difference in performance was found for fixed versus random target frequency (with no cues). In three other conditions with random target frequency, various cues were presented just prior to the target-plus-masker interval. The presentation of an exact copy of the masker to the same ear provided the greatest benefit. The other two cues were an ipsilateral notched noise that spanned the range of potential masker frequencies excluding the target region, and an exact copy of the masker presented contralaterally. Both of these resulted in smaller, but significant benefits.

One likely mechanism underlying these findings is spectrotemporal "enhancement" which results from differential prior stimulation of target and masker frequency regions. Another factor is the correspondence of the cue to the subsequent masker which exerts a beneficial effect for either ipsilateral or contralateral presentation and may help to reduce masker uncertainty.

[Supported by NIDCD and AFOSR]

972 Remembering Content vs. Remembering Order of Auditory Sequences

Lenny Varghese¹, Virginia Best¹, Barbara G. Shinn-Cunningham¹

Boston Universitv

When abstract auditory sequences (e.g., sequences of non-verbal sounds) are stored in memory, encoding and recall mechanisms may differ depending on the perceptual relationship amongst the components of the sequence. If sequences are perceived as a connected stream, individual components are likely hard to identify, but the full sequence may be recalled, in order, relatively easily. However, if the components are dissimilar and therefore perceived as discrete, disconnected items, it should be relatively easy to recall any individual item, but difficult to recall the components in order. We tested this hypothesis by conducting a short-term memory experiment in which subjects were asked to remember either sequences of tones or sequences of "natural" sounds (e.g., a ferry horn,

a cell phone ringing, or a person coughing). Subjects heard a target sequence (tones or natural sounds) of 4-10 components in length. After the presentation of the target sequence, listeners either had to report whether or not a subsequent, single probe component was present in the target (present/absent condition), or to report whether a probe sequence (composed of the same components as the original target sequence) was identical in order to the target or had two components switched in order (same/different condition). Subjects performed better on the present/absent condition when natural sound sequences were heard, and better on the same/different condition when pitch sequences were heard. These results indicate that when subjects hear a sequence of perceptually connected components (such as pitched tones), the contour of the sequence is stored in memory, not the identity of individual components; serial ordering is encoded as a "feature" of the perceptual stream. However, when components are perceptually disconnected (such as for natural sounds), subjects store the identity of individual components without the serial ordering information. [Work supported by NSSEFF fellowship to BGSC.1

973 Adaptive Sonar and Flight Behavior in the Echolocating Bat, *Eptesicus Fuscus*

Benjamin Falk¹, Lasse Jakobsen², Delphia Varadarajan¹, Cynthia Moss¹

¹University of Maryland, ²University of Southern Denmark Echolocating bats emit ultrasonic pulses and listen for the returning echoes to gain information about their Bats use echolocation for navigation, environment. obstacle avoidance, and pursuit of prey. In this study, we examined how adaptive sonar and flight behaviors change with experience in a complex environment. We recorded the navigation behavior of the big brown bat, Eptesicus fuscus, in a laboratory flight room at the University of Maryland. The flight room was equipped with high-speed video cameras that permitted three-dimensional reconstruction of flight trajectories. Full-bandwidth acoustic recordings allowed characterization of the spectral and temporal content of sonar vocalizations. A microphone array along the walls of the flight room permitted reconstruction of the sonar beam axis, indicating acoustic gaze of the bat. Bats were trained to capture tethered mealworms located in the midst of an artificial forest, comprised of obstacles, which were constructed to resemble trees. The position of the tethered mealworm was changed between trials. We found that the bat initially directed its sonar beam axis repeatedly towards each obstacle (tree) that it encountered as it flew through the forest, but after experience with the obstacles, the bat modified its behavior and shortened inspection time of the trees. The results of this study suggest the role of spatial attention and memory in navigation by echolocating bats.

974 Social Vocalizations of Big Brown Bats: An Analysis of Call Structure Across Behavioral Contexts

Marie Gadziola^{1,2}, Paul Faure³, Jeffrey Wenstrup^{1,2} ¹NE Ohio Universities College of Medicine, ²Kent State University, ³McMaster University

We recorded and analyzed social vocalizations and associated behaviors of big brown bats (*Eptesicus fuscus*) in defined social interactions. Vocalizations were categorized into 4 behavioral contexts: low aggression, medium aggression, high aggression, and appeasement. We identified 23 syllables with unique spectral-temporal features, and examined how calls varied across the behavioral contexts. We describe the calls in terms of syllable acoustics, temporal emission patterns, and most typical syllable sequence. Low aggression calls were multisyllabic and composed of a single syllable type, a short downward FM sweep (bDFM). This syllable was rapidly repeated at an average rate of 78 Hz. The bDFM syllable was produced in low and medium aggression contexts. There were no context-dependent differences in syllable duration or spectral features, but a large difference in the temporal emission pattern was evident. As a bat's aggression level changed from low to medium, it increased both the average number of syllables per call (5.4 vs 8.7, p<0.01) and the repetition rate (78 vs 110 Hz, p<0.001), and was more likely to include an additional syllable type. High aggression calls included 10 additional syllable types and rarely included the bDFM syllable. The most common high aggression syllable was a broadband noise syllable. High aggression calls were most likely to be complex (69%), with 2-4 distinct syllable types per call. Nonlinear phenomena did not occur in low and medium aggression, but were common in high aggression, occurring in 23% of the syllables. Appeasement vocalizations were mono- or multi-syllabic, and composed of 3 common syllables. The calls typically transitioned to a different syllable at the end of the call (79%). The results demonstrate that big brown bats possess a diverse repertoire of social vocalizations and that emotion-related acoustic cues are evident in the call structure. Supported by NIH R01-DC000937-20 and DC000937-18S1, and NSERC.

975 Developmental Changes in Mouse Calls: Evidence for Vocal Learning

Jasmine Grimsley¹, Jessica Monaghan², Jeffrey Wenstrup¹

¹Northeastern Ohio Univ Coll Med & Pharm, ²MRC Institute of Hearing Research

Mice are highly vocal animals; adult males and females vocalize in same sex and cross sex social encounters. Mouse pups are also highly vocal, producing isolation calls when they are removed from the nest. This study characterized the developmental changes in pup isolation calls, and compared these to adult calls. We recorded isolation calls from three litters of CBA/CaJ mice, at ages postnatal day 4 (p4), p6, p8, p10, and p12. Adult calls were obtained in a variety of social situations from p90+. Altogether, over 28,000 calls were recorded using highly sensitive ultrasonic recording equipment. We analyzed the

types of calls, their spectral and temporal features, and the temporal sequencing of calls within bouts. We found that pups produced all but one of the 11 call types given by The proportions of call types changed adults. developmentally, but even the youngest pups produced complex calls with frequency-time variations. When all call types were pooled together for analysis, we observed only small changes in the peak frequency and call durations from p4 through p12. However, adult calls were significantly lower in frequency and shorter in duration. Individual call types showed different patterns of change over development, requiring analysis of each call type separately. As pups aged, the complexity of call bouts increased, with a greater tendency to switch between call types within a bout. Call bouts from hearing animals, p12 and adult, had a significantly more organized sequential structure than pre-hearing mice. The data indicate that several characteristics of mouse calls change over development, and these changes may reflect vocal learning. To provide age-appropriate vocal stimuli in behavioral and neurophysiological experiments, we developed a "Virtual Mouse Vocal Organ", a program that creates bouts of vocalizations based on the spectrotemporal properties of calls and their pattern within bouts.

Supported by NIH R01-DC000937-20 and DC000937-18S1.

976 Behavioral Discrimination of Ultrasonic Vocalizations in CBA/CaJ Mice

Erikson Neilans¹, Kelly Radziwon¹, Micheal Dent¹

¹University at Buffalo

Previous studies have shown that both male and female mice produce ultrasonic vocalizations (USVs) under a variety of circumstances, but the function of these USVs remains unclear. In addition to emitting many calls, mice also produce a wide array of call types, hinting that unique information is conveyed to listeners with each call type. At this time, it is not clear whether mice can actually discriminate amongst USVs, and if so, what characteristics are important for discriminations. The present study sought to determine the acoustic cues most salient to mice when discriminating vocalizations. CBA/CaJ mice were trained using operant conditioning procedures for reinforcement to discriminate targets calls from a repeating background call. Within a session, the repeating background was one of several different call types that were previously recorded from two female mice and one male mouse. The targets were manipulations of these background calls, different calls from the same mouse, different calls from other mice. and pure tones. Some of the features of calls that were manipulated included changing the average frequency, altering the frequency contour, inserting gaps, and reversing the entire call. The results indicated that the mice were affected by some of the manipulations more than others, suggesting that, as in the discrimination of vocalizations by many other animals, certain call features are more important than others in the perception of acoustic stimuli. Supported by NIH DC009483.

977 Perceptual Recognition and Identification of Conspecific Calls by Budgerigars (Melopsittacus Undulatus)

Camille Toarmino¹, Erikson Neilans¹, Thomas Welch¹, Micheal Dent¹

¹University at Buffalo

Previous experiments have shown that budgerigars are able to discriminate between calls emitted by conspecifics. However, the significance that each part of a call holds for the budgerigar is unknown. This experiment seeks to investigate which parts of a call are important for recognition. Using operant conditioning techniques, four budgerigars (two females and two males) were trained to identify two disparate conspecific calls. Once a bird reached 80% identification accuracy in the training phase, it moved on to the testing phase. For the testing phase, each call was cut into four pieces of equal length (0-25%, 25-50%, 50-75%, 75-100%), each representing 25% of the overall duration of the call. Each piece was also combined into larger chunks of the call (0-50%, 0-75%, 25%-100%, 50-100%). These "probe stimuli" were presented randomly on 20% of the trials, while the original (whole) calls continued to be presented on the remaining 80% of the trials. If the birds correctly assigned the piece of the call to the appropriate category, it suggests that the piece is sufficient for vocal recognition. Otherwise, performance would be at chance levels. The birds showed poor performance in identifying the small pieces of the calls where only 25% of vocal material was presented, but the performance improved as more of the call was presented. These results suggest that the birds may have difficulty communicating in noisy environments where parts of the calls are obscured. However, it may also be advantageous to have a recognition system that does not require 100% of a call to be heard for identification.

978 Detecting Time Shifts of Sounds in an ABA-Streaming Paradigm by the European Starling

Naoya Itatani¹, Imke Cordes¹, Georg M. Klump¹

¹Institute for Biology and Environmental Science, Carl-von-Ossietzky University Oldenburg

How sounds from multiple sources separated by the auditory system is one of the most important questions that need to be answered for understanding auditory scene analysis. Sequences of two alternating tones presented with a specific duration and rate are perceived as one stream (fusion) or two separate streams (fission) depending on their difference in tone frequency (van Noorden 1975). van Noorden (1975) observed that the time shift of the middle B tone in a sequence of triplet sounds (ABA-, A and B being different tones, - indicating a longer temporal gap) was more easily detected if the sounds in the triplet were perceived as one stream than if perceived as two streams.

. Here we present data on behavioral thresholds (d'=1.8) for detecting the time shift of B tones in ABA- tone triplet stimuli in the European starling (Sturnus vulgaris), a bird species in which auditory streaming of tone sequences has

previously been demonstrated (MacDougall-Shackleton et al. 1998). We varied the frequency separation between the A and B tones to elicit a one-stream, ambiguous or twostream percept in the starlings. They were trained in an operant Go-NoGo paradigm with food rewards to respond to the time shift of the B tone in ABA- triplets. The frequency separation between A and B tones was varied between 0 and 12 semitones. The duration of each tone in the triplet was 40 or 125 ms, and the inter-tone interval within a triplet was 40, 80 or 120 ms for 40 ms tones and 50 ms for 125 ms tones. The amount of time shift was randomly chosen being 10, 30, 50, 70 or 90% of the intertone interval. In agreement with human psychophysical observations, the starlings' threshold for detecting the time shift was raised as the frequency separation between A and B tones increased. This task allows determining the streaming percept of the birds instantaneously and can be combined with a study of the neural activity underlying auditory streaming.

(Supported by the DFG, SFB/TRR 31)

979 Detection of Tones in Noise by Nonhuman Primates: Effects of Time-Varying Signals or Noise

Margit Dylla¹, Andrew Hrnicek¹, Christopher Rice¹, Ramnarayan Ramachandran¹

¹Wake Forest University School of Medicine

A fundamental function of the auditory system is the detection of sounds – in quiet or mixed in with distractors. We have previously shown that the effects of continuous broadband noise on detection of tones is to shift tone thresholds to higher levels by about 1 dB/dB of noise. Our previous experiments in passively listening monkeys suggests that such detection performance may not be supported by the responses single units in the cochlear nucleus, but rather by the responses of a specific type of units in the inferior colliculus. However, these experiments were done with static stimuli; natural stimuli are not static, rather they show temporal fluctuations. Our goal was to assess the effects of noise on the detection of tones in more naturalistic circumstances, when either the tone, or the noise was temporally modulated.

Two nonhuman primates (Macaca mulatta) were trained to report detection of a tone by means of a lever release in a reaction time task. Appropriate catch trials were used to ensure that the release of the lever was specific to the presence of the tone. Temporal fluctuations were introduced by sinusoidal amplitude modulation of the tone or the noise at 10 Hz. Amplitude modulation of the noise resulted in a reduction of tone thresholds by 5-15 dB relative to thresholds in static noise of equivalent mean amplitude. Surprisingly, amplitude modulation of the tone resulted in only small changes in threshold for detection in static noise, and these changes were restricted mainly to low frequencies (< 4 kHz). In both cases, improvements in detection performance beyond threshold were associated with reductions in reaction times, similar to trends observed in the detection of static tones in static noise. These results suggest differential mechanisms for processing foreground and background stimuli, and will form the basis of future investigations of the neuronal basis of detection in noisy environments. Support: NIH RO3 DC9338, RO3 DC9338-02S1 & RO1 DC11092

980 Dip-Listening and Modulation Masking in Animal Social Aggregations Alejandro Vélez¹, Mark Bee¹

¹University of Minnesota - Twin Cities

Humans and other animals communicate using vocal signals in noisy social groups. A prominent feature of the background noise generated in these natural soundscapes is that it fluctuates in amplitude over time. In the presence of fluctuating speech-shaped noise, humans can better recognize speech at times when the amplitude of the noise dips to a low level, a general result consistent with "diplistening." Amplitude fluctuations, however, can also hinder speech perception when maskers are modulated at rates similar to those in speech, a phenomenon known as "modulation masking." We presently know very little about how other nonhuman vertebrates perceive their own vocal communication signals in the presence of naturally fluctuating background noise characteristic of social aggregations. In this study, we asked whether amplitude fluctuations in the simulated noise of a breeding chorus affect the ability of female gray treefrogs (Hyla chrysoscelis) to recognize male mating calls. We used phonotaxis experiments to test the hypothesis that thresholds for eliciting responses to mating calls are influenced by the presence of amplitude modulations in noise with the long-term spectrum of a breeding chorus. This "chorus-shaped" noise was either unmodulated or sinusoidally amplitude modulated (SAM) between 0.625 Hz and 80 Hz (1-octave steps). Compared to the unmodulated control, thresholds were ≈4dB lower at low SAM rates (0.625 Hz – 2.5 Hz) and \approx 6dB higher at high SAM rates (40 Hz and 80 Hz). Because the sounds of grav treefrog choruses are modulated both at slow rates (< ≈ 2 Hz) and at a faster rate characteristic of the pulsed structure of conspecific mating calls (≈45 Hz), female frogs might experience a combination of dip-listening and modulation masking in natural environments. Taken together with other studies, our results suggest that both dip-listening and modulation masking may be widespread phenomena in vertebrate vocal communication.

981 Neural Correlates of the Detection of Concurrent, Spatially-Separated Sound Sources in the Inferior Colliculus Mitchell Day^{1,2}, Bertrand Delgutte^{1,3}

¹Eaton-Peabody Laboratories, Massachusetts Eye and Ear Infirmary, ²Dept. of Otolaryngology, Harvard Medical School, ³Research Laboratory of Electronics, MIT The mammalian auditory system uses interaural time and

I he mammalian auditory system uses interaural time and level differences (ITD and ILD) to compute the location of a sound source in the horizontal plane. In the presence of multiple, spatially-separated sources these binaural cues are also used for perceptual segregation of the sources. In order to study the neural coding of the respective locations of separate sound sources, we measured the responses of single units in the inferior colliculus (IC) of awake rabbit to

two concurrent stimuli presented at different azimuths in virtual auditory space (VAS). Both stimuli were broadband noise with similar spectral and temporal properties, differing only in their binaural cues. Target stimuli were presented at 13 different azimuths in the frontal horizontal plane, while interferer stimuli were presented at 0°, +90°, or -90°. Although target azimuth tuning could differ dramatically in the presence of an interferer as compared to the single-source condition, significant rate coding of target azimuth remained even in the two-source condition. Minimum angles of separation for detecting the target in the presence of each interferer were calculated using an ideal observer analysis of rate responses. Minimum angles were smaller for the midline interferer than for the lateral interferers. consistent with human psychophysics regarding the perception of multiple sound sources. Similar minimum angles for the midline interferer were also observed for modified VAS stimuli in which only ITD varied with azimuth, but not for stimuli in which only ILD varied, even though most of our neurons were tuned to highfrequencies (> 2 kHz). Moreover, the azimuth tuning around the midline was similar for the two-source, full-cue condition as for the ITD-only condition. Thus, highfrequency neurons are highly sensitive to the spatial separation of sounds differing in ITD, possibly due to the decorrelation of the cochlear filter-induced envelopes. Supported by NIH grants RO1 DC002258 and P30 DC005209

982 Source Segregation Based on Frequency Differences Facilitates Vocal Communication in Frog Choruses Vivek Nityananda¹, Mark Bee¹

¹University of Minnesota

Source segregation contributes to our abilities to solve a fundamental problem in speech communication: difficulty following one conversation in noisy, multi-talker settings. Humans assign concurrent sounds to different sources based on a relatively small number of acoustic cues. One of the best studied cues is that of frequency differences. While previous studies of fish, songbirds, ferrets, and monkeys indicate that these vertebrate models can also assign concurrent sounds to different sources based on spectral differences, we have no knowledge about how these abilities function in the natural communication behaviors of these animals. We tested the hypothesis that female gray treefrogs (Hyla chrysoscelis) use spectral cues to segregate the pulsed mating calls of conspecific males from the overlapping, pulsatile calls of other frogs in mixed-species choruses. The task required females to segregate an attractive target signal comprising a discrete pulse train (50 Hz) simulating conspecific calls from a concurrent and unattractive background of continuous "distractor" pulses (also 50 Hz). Target and background pulses were temporally interleaved, so that the composite pulse rate was 100 Hz each time the signal was presented. If spectral cues promoted the segregation of concurrent pulsed sounds, we predicted that females, which are selective for conspecific pulse rates (50 Hz), would be more responsive to the signal as a function of increasing frequency difference between the signal and background ($\Delta F = 0, 3, 6, 9, 12$, or 15 semitones across different trials). As predicted, the proportion of subjects responding increased, and response latencies decreased, as a function of increasing ΔF . We suggest source segregation based on frequency differences may be an ancient evolutionary hearing mechanism that has been exploited by frogs to facilitate vocal communication in noisy social environments. [Supported by NIH RO1-DC009582]

983 Effect of Environmental Noise on the Discrimination of Bird Song Types

Nina U. Pohl¹, Hans Slabbekoorn², Georg M. Klump¹, Ulrike Langemann¹

¹Carl-von-Ossietzky University Oldenburg, ²Leiden University

Recent studies in great tits (Parus major) and other birds have shown that in urban environments birds produce on average higher pitched songs than in nearby woodland habitats (e.g., Slabbekoorn & den Boer-Visser, 2006, Curr. Biol., 16, 2326-2331). This change in song frequency has been interpreted as a counter strategy to avoid masking by low frequency traffic noise present in cities. Urban great tits react stronger to songs recorded in urban sites compared to songs recorded in woodland sites, and the opposite is found in woodlands (e.g., Mockford & Marshall, 2009, Proc. R. Soc. B, 276, 2979–2985).

In the present study we evaluate under controlled laboratory conditions how the ability of the great tits to discriminate in a Go/NoGo procedure between songs differing in duration (phrases of 2 or 3 elements) and pitch (low or high) is affected by urban and woodland noise with noise level and spectrum typical for the natural environment. The birds' response latencies for the discrimination between test and reference songs were analvzed using multidimensional scaling (MDS. PROXSCAL). The latencies are inversely related to the salience of the perceptual differences and MDS visualizes these as a "perceptual map" in which the distances between data points correspond to the perceived similarity of the songs. In a regression analysis we evaluated which physical features of the songs accounted for the perceptual distances. The results indicate that the birds used different features to discriminate the songs in the urban and in the woodland noise conditions. In woodland noise, frequency and duration of all song elements were used for the discrimination, whereas in the urban noise only features of the high frequency elements were used. The results emphasize the role of high frequencies for the birds' communication in urban environments and indicate that the frequency shift observed in urban songs is an adaptive modification of song structure.

(Supported by the DFG, SFB/TRR 31)

984 Preservation of Rhythmic Clocking in Cochlear Implant Users: A Study of Isochronous vs. Anisochronous Beat Detection

Irene Kim¹, Eunice Yang¹, Patrick Donnelly¹, Charles Limb^{1,2}

¹Johns Hopkins University School of Medicine, ²Peabody Conservatory of Music

The capacity for internal rhythmic clocking involves a relationship between perceived auditory input and subsequent cognitive processing, by which isochronous auditory stimuli induce a temporal beat expectancy in a listener. While rhythm perception has previously been examined in cochlear implant (CI) users through various tasks based primarily on rhythm pattern identification, such tasks may not have been sufficiently nuanced to detect defects in internal rhythmic clocking, which requires temporal integration on a scale of milliseconds. The present study investigated the preservation of such rhythmic clocking in twelve CI subjects, twelve normal hearing (NH) controls, and seven trained musicians. The subjects performed a task requiring detection of isochronicity in the final beat of a four beat series presented at different tempos. Our results show that CI users performed comparably to NH participants in all isochronous rhythm detection tasks, but that professionally trained musicians significantly outperformed both NH and CI subjects. These results suggest that CI users have intact rhythm perception even on a temporally demanding task that requires tight preservation of timing differences between a series of auditory events. Also, these results suggest that musical training might improve rhythmic clocking in CI users beyond normal hearing levels, which may be useful in light of the deficits in spectral processing commonly observed in CI users.

985 Perceptual Learning Using a Portable Real-Time Cochlear Implant Simulator on the iPhone

Christopher J. Smalt¹, Thomas M. Talavage¹, Mario A. Svirsky², David B. Pisoni³

¹School of Electrical and Computer Engineering, Purdue University, ²Department of Otolaryngology, New York University School of Medicine, ³Department of Psychology, Indiana University

Using a portable real-time speech processor that implements an acoustic simulation model of a cochlear implant (CI), we examined the nature of perceptual learning by assessing how speech intelligibility improves after training. Since it is widely recognized that there are many advantages to testing speech processing and learning approaches using a normal hearing population, experiments with vocoded speech are often conducted in the laboratory. However, it is desirable and more realistic to conduct tests that better model the real life perceptual learning experience that users of cochlear implants and hearing aids undergo. We have developed a software application for the Apple iPhone / iPod Touch that presents a vocoded CI simulation in real-time, allowing for a variable shift and number of noise bands. The device was worn by participants over a two week chronic exposure period in conjunction with isolating insert earphones and a microphone to capture environment sounds. 8 un-shifted noise band channels were used in this study. After exposure, using the simulator each day for 2+ hours, participants improved in word and sentence recognition. Participants' also underwent fMRI before and after exposure, performing an auditory sentence comprehension task while listening to normal and vocoded speech (generated using the same settings as the device). Changes in neural activation after perceptual learning under real-time CI simulation are consistent with the behavioral data, showing a shift in processing mode from nonspeech auditory pattern perception to speech perception of meaningful isolated words and words in sentences. These findings suggest that the human brain is able to adapt in a short period of time to a degraded auditory signal. Utilizing this portable CI simulator, it would be possible to test the effect of different processing strategies in normal hearing users and how they play a role in perceptual learning.

986 Sequential Stream Segregation by Cochlear Implant and Normally Hearing Listeners

Viral Tejani¹, Kara Schvartz¹, Monita Chatteriee¹ ¹Cochlear Implants and Psychophysics Lab, Dept. of Hearing and Speech Sciences, University of Maryland Sequential stream segregation was measured using a twointerval forced-choice, adaptive, irregular rhythm detection task in younger (19 to 22 yrs.) and older (66 to 75 yrs.) normal hearing listeners (YNH, ONH) and in cochlear implant (CI) listeners (27 to 67 yrs.). An alternating 4.4s A_B_ sequence was presented: in the interval to be detected, the delay between A and B was increased linearly for 1.00s, resulting in an irregular rhythm that was most perceptible when A and B fell into one stream. The stimuli were 60ms, equal-r.m.s, pure tones or 0.5, 0.33. and 0.2 octave-wide noisebands (simulating spectral degradation). The center frequency of A was fixed at 2 kHz; B varied from 0.793 to 5.039 kHz. CI users heard the sequences through their everyday speech processor, or as loudness-balanced pulse trains delivered via a custom research interface. In the latter case, A was presented to a fixed central electrode (approx. 2 kHz in the frequencyelectrode map) and B varied in electrode location from base to apex. ONH and YNH listeners showed less streaming as bandwidth increased. Both groups displayed similar performance when A and B were identical (reducing the task to simple rhythm discrimination), suggesting that known age-related declines in temporal processing were not a limiting factor. CI listeners showed the least streaming of the three groups, both with electric and acoustic stimuli. Relative to acoustic stimuli (in both CI and NH listeners), electric stimuli evoked the lowest thresholds for irregularity detection when A and B were identical. Though overall patterns of irregularity detection were similar in CI listeners across electric and acoustic stimulation, individual variations were observed that likely

stemmed from differences in parameters/features of the speech processor. Initial analyses suggest that electrode discrimination thresholds do not readily predict stream segregation abilities. [Work supported by NIH grant no. R01-DC00486].

987 Assessment of Musical Sound Quality Perception in Cochlear Implant Users

Alexis T. Roy¹, Patpong Jiradejvong¹, Courtney Carver¹, Charles J. Limb^{1,2}

¹Johns Hopkins School of Medicine, ²Peabody Conservatory of Music

Cochlear implant (CI) users commonly report poor sound quality (SQ) during music perception, but objective measurements of SQ are difficult to obtain due to its subjective nature. The aim of this experiment was to design a standardized method to assess the perception of musical SQ in CI users. We focused here on measuring limitations in CI users' perception of bass frequencies in music. The MUltiple Stimulus with Hidden Reference and Anchor method was modified for use with CI subjects (CI-MUSHRA). This method allows for a comparative evaluation of an original stimulus ("reference"), a highly altered version ("anchor"), and a series of related stimuli. We hypothesized that limitations in SQ perception would minimize the ability of CI users to discriminate between original and degraded stimuli. Eleven CI users and ten normal hearing subjects participated in the study. Subjects listened to seven randomly presented versions of 25 musical excerpts that included the reference, anchor (1000-1200Hz band-pass filtered), and five high-pass filtered versions (200-, 400-, 600-, 800-, and 1000-Hz cutoff). Subjects assigned a quality rating score between 0 (very poor) and 100 (excellent) for each stimulus. Overall mean quality rating assignments for the stimuli differed significantly between CI users and NH listeners (p<0.001, one-way ANOVA). NH controls displayed significant differences in quality ratings for all 21 possible contrasts (p<0.001 Tukey's pairwise comparison), while CI users demonstrated similar quality ratings for most stimuli. NH controls demonstrated an inverse correlation between cutoff frequency and SQ rating (r²=0.96, m=-0.065, linear regression); whereas CI users demonstrated a significantly weaker correlation (r²=0.95, m=-0.031, linear regression). These results provide evidence indicative of severe limitations in bass frequency perception in CI users during music perception. Furthermore, they support the use of the CI-MUSHRA as an objective method to assess perception of SQ in CI users.

988 Music Perception in Children with Cochlear Implants

Lindsay Scattergood^{1,2}, Patpong Jiradejvong¹, Courtney Carver¹, Caty Butler¹, Charles Limb^{1,2}

¹Johns Hopkins University School of Medicine, ²Peabody Conservatory of Music

Music perception is difficult for adult cochlear implant (CI) users, who struggle with pitch and timbre discrimination. However, relatively little is known about music perception in prelingually deaf children with CIs. To address this gap

in our knowledge, we developed a child-friendly test battery of music perception based on Gordon's Primary Measures of Music Audiation, The test, referred to as the Music in Kids with CIs (MiKCI), consists of 5 sections (Intervals, Rhythms, Melodies, Harmony and Timbre) with 10 questions in each section. For each question, two musical stimuli were presented sequentially. The subject was asked to identify whether the stimuli were identical or different. Intervals ranged from unison to octave and were presented using piano tones. Rhythm stimuli consisted of snare drum patterns presented over one four-beat measure at a fixed tempo. Melodies consisted of one-bar novel melodic fragments of decreasing interval distance presented with piano tones. Harmonic stimuli consisted of three-note chords presented using piano tones in a threechord sequence. Stimuli for timbre testing consisted of five instruments from different families playing identical melodic fragments. Ten normal hearing children and ten children with cochlear implants between the ages of 5-8 (p=0.11 unpaired t-test for age differences) were studied. Overall, CI and normal hearing participants scored above chance level on all sections. There was no statistical difference in performance scores between CI users and controls (p=0.22, intervals; p=0.58 rhythms; p=0.20, melodies; p=0.87, harmony; p=0.14, timbre). Moreover, children with CI scored surprisingly well in pitch and timbre perception (84±11.7%, intervals; 80±16.9%, timbre). These results suggest that children with cochlear implants may perform better than expected for music perception. These data indicate a potentially significant effect of brain plasticity on complex auditory perception in prelingually implanted children with cochlear implants.

989 Attention/Memory Training Does Not Improve Auditory Performance for Cochlear Implant Users

Sandra I. Oba¹, Qian-Jie Fu¹, John J. Galvin III¹ ¹House Ear Institute

Our previous research has shown that auditory training can significantly improve cochlear implant (CI) users' speech recognition (in guiet or in noise) and music perception. However, it is unclear whether such training improves listeners' auditory perception or general attention. In this study, speech and music perception, as well as auditory and visual memory, were assessed in ten CI users before, during, and after training with a nonauditory, attention/memory task - forward visual digit span (VDS), i.e., recall of visually presented sequences of digits. Prior to training, baseline recognition performance was obtained for IEEE sentences in quiet. HINT sentences in noise, digits in noise, vowels, consonants, voice gender, vocal emotion, melodic contour identification, auditory digit span (similar to VDS, but auditory-only) and VDS (same as the trained task). After completing baseline measures, subjects trained with VDS at home on their personal computers using custom software (Sound Express) for 1/2 hour per day, five days a week, for four weeks. During the VDS training, a sequence of digits flashed on the computer screen; subjects were asked to type in the sequence. Visual feedback was provided and the level of difficulty

was adjusted according to subject response. Performance on all test measures was re-measured following the 2nd and 4th weeks of training. Training was stopped after the 4th week and subjects returned to the lab one month later for follow-up measures. Preliminary results showed that after training with VDS, mean VDS test scores significantly improved from 6.8 to 8.0 digits. However, there were no significant improvements observed for auditory digit span, melodic contour identification or any of the speech recognition tasks. These results suggest that the posttraining performance gains observed in previous studies were due to improved auditory perception rather than improved memory or attention.

990 Brain Plasticity and Cochlear Implant Outcome in Adult-Onset Deafness

Seung Ha Oh^{1,2}, Hyo-Jeong Lee³, Hyejin Kang^{4,5}, Jeong Hun Jang¹, Jun Ho Lee^{1,2}, Dong Soo Lee^{4,5} ¹Department of Otorhinolaryngology, Seoul National University College of Medicine, ²Sensory Organ Research Institute, Seoul National University Medical Research Center, ³Department of Otorhinolaryngology-Head and Neck Surgery, Hallym University College of Medicine, ⁴Department of Nuclear Medicine, Seoul National University College of Medicine, ⁵Institute of Radiation Medicine, Medical Research Center, Seoul National University

Sensory plasticity in adults with mature brain has not been thoroughly investigated compared to that in developing brain, such as congenital deafness. In this study, we probed brain reorganization related to auditory deprivation in adult-onset deafness and its clinical relevance by metabolism measuring alucose before cochlear implantation (CI). 18F-FDG-PET scans were performed in 37 postlingually deaf patients (13 men and 24 women, duration of deafness: 2 months - 36 years 8 months) during the preoperative work-up period and 39 hearing controls (15 men and 24 women). Cl outcome was measured at 1 year using a phoneme identification test with auditory cue only. During and after FDG injection, subjects stayed in a waiting room of ambient light and noise with no specific instruction given. To examine deafness-induced metabolic change, the preprocessed PET images were compared between patients and controls. Correlation analyses were performed having the durationf of deafness and CI speech outcome as covariates. Hypo-metabolism found in deaf auditory cortices gradually returned to levels similar to the controls as the deafness duration increased. However, such metabolic recovery failed to prove significant prognostic effect, suggesting a relative resilience against the crossmodal plasticity in adults. Instead, individual traits in late stage visual processing and cognitive control seem to be more reliable prognostic markers in deaf patients of adultonset. In the medial frontal cortices, metabolism decreased either rapidly or gradually during the period of deafness and those patients who preserved metabolic activity as high as possible became the best CI performers.

Korea government (MOST) [Korea Science and Engineering Foundation (KOSEF) (No. 2006-05090)].

991 Vestibulo-Autonomic Reflex Mediates the Translation of Vestibular Deficit to Elevated Anxiety

Matti Mintz¹, Shahar Shefer¹, Tal Elkan-Miller², Joram Feldon³, Karen B. Avraham²

¹Psychobiology Research Unit, Tel Aviv University, ²Sackler Faculty of Medicine, Tel Aviv University, ³Laboratory of Behavioural Neurobiology, Federal Institute of Technology

Comorbidity of anxiety and vestibular disorders is a prevalent clinical entity. We developed a mouse model to study the mechanisms and causality factors in this form of comorbidity. First, we demonstrated the presence of comorbidity between progressive vestibular deficits and elevated levels of anxiety (Shefer et al, Brain Res, 2010) in Headbanger (Hdb) mice with an ENU-induced mutation in the Mvo7a gene (Rhodes et al. Mamm Genome, 2004). Secondly, Hdb mice were subjected at a young age to intensive behavioral training with the aim of improving their balance skills, and showed that improved balance alleviates symptoms of anxiety. These findings support the hypothesis that vestibular deficits may predispose or cause some forms of anxiety. Our goal is to decipher the mechanism that transforms the vestibular deficit to elevated expressions of anxiety. The Hdb vestibular phenotype is characterized by significant elongation of the stereocilia in the otolith organs. We predict that this form of structural phenotype distorts the translation of movement to neuronal information, and therefore may induce abnormal brain responses to vestibular stimulation. To verify the mechanism, we tested the vestibulo-autonomic reflex in *Hdb* and wild-type (wt) mice. Mice were rotated for 2.5 min on a plate that was tilted at 30 degrees in reference to the horizontal plane, with speed alternating every 10 sec to induce 2 to 6 G centrifugal force. With such manipulation, we intended to maximally activate the otoliths, as well as the semicircular canals. Autonomic response was measured as a change in the core temperature. Results demonstrated a drop in the core temperature in wt mice with an average of about 1.5°C at 10 min after the rotation offset. Hdb mice showed no reduction in core temperature as measured up to 20 min after the rotation offset. These findings suggest that the abnormal vestibulo-autonomic reflex mediates the transformation of the vestibular deficit to elevated anxiety.

992 Response Properties of Central Vestibular Neurons to Yaw Rotation

Shawn D. Newlands¹, Min Wei¹, Daniel J. Barbash¹, Laurel H. Carney¹

¹University of Rochester

The vestibular system responds to an array of stimuli that vary over a wide range of direction, frequency and amplitude. One vestibular response, the vestibulo-ocular reflex (VOR), responds linearly over a wide range of stimulus frequencies and amplitudes of rotation. Vestibular signals are carried from the vestibular end organs throughout the central nervous system in the form of neuronal responses that have limited dynamic ranges due to silencing over portions of the stimulus cycle and

due to saturation of discharge rate. We have previously shown that non-eye movement (NEM) neurons in the vestibular nuclei, which respond to yaw rotation but not eve movements, do not increase discharge rate linearly with increasing amplitude from 30 to 210 °/sec peak velocity of stimulation at frequencies between 0.1 and 2 Hz. In the current experiments, we also examined the linearity of eye-head velocity (EHV) and positionvestibular-pause (PVP) neurons in the rostral vestibular nuclei; both of these neuronal types have eve-movement sensitivity. EHV, PVP, and NEM were recorded during vaw rotations ranging from 0.5 to 80 °/sec at frequencies of 0.2, 0.5 and 1.0 Hz. Data was analyzed off-line. Evemovement influences on neuronal firing were removed by linearly subtracting the influence of eye position and velocity based on the responses of these neurons with fixation of static targets and with smooth pursuit of sinusoidally moving targets in the horizontal plane, respectively. We found that for all three types of neurons, sensitivity was higher to lower peak velocities of rotation than to higher peak velocities. Further analysis examined the relationship between the instantaneous velocity of rotation and discharge rate. We found that the instantaneous firing rate (IFR) of a neuron was dependent not only on the velocity of the stimulus at that moment, but on the peak velocity of rotation of the stimulus. Thus, the responses of central vestibular neurons adapt to changes of peak velocities of rotation. To assess this adaptation, we examined discharge rates as we transitioned between stimuli that had the same frequency but changed abruptly in peak velocity between 2.5 and 80 °/sec. Our data suggest that vestibular neurons rapidly adapt their responses to changing velocities of rotation.

993 Effects of Core Body Temperature on the Horizontal Angular Vestibulo-Ocular Reflex in Mice

Patrick Huebner¹, David Lasker², Americo Migliaccio^{1,3} ¹Neuroscience Research Australia, ²Johns Hopkins University, USA, ³University of New South Wales The aim of this study was to determine whether changes in core body temperature preferentially affect the sensitivity of irregular vestibular afferents enough to alter the properties of the angular vestibulo-ocular reflex (aVOR). A previous mouse study investigating extracellular recordings of vestibular-nerve afferents showed that the 'resting discharge rate' / sensitivity rose by ~50% / 18% for regular afferents and by ~90% / 113% for irregular afferents when temperature was increased from 32C to 37C. In this study we measured the horizontal aVOR of 9 normal adult C57BI6 mice maintained at core body temperatures of 32C and 37C. The vestibular stimuli consisted of whole-body sinusoidal rotations across frequencies ranging from 0.5 to 12Hz (peak velocity 50 or 100deg/s) and acceleration steps (acceleration 3000 or 6000deg/s²; velocity plateau 150 or 300deg/s). Binocular 3D eye position was measured using video-oculography. We calculated the aVOR gain (eye/head velocity), and phase or latency. The aVOR gain during sinusoidal rotations was ~13% lower at 32C than at 37C. However, the aVOR gain and phase lead did not increase more with velocity and frequency (both of which increase stimulus acceleration) at 37C. AVOR gains calculated during the constant acceleration portion, and velocity plateau portion, of the acceleration step paradigm slightly increased at 37C. Temperature did not affect the latency of the VOR. These results indicate that core body temperature does affect the aVOR response; however, the change is mostly due to changes in the contribution of regular afferents. The majority (~70%) of vestibular afferents are regular in their discharge, so changes in their sensitivity and resting rate will affect the overall vestibular signal more so than changes in irregular afferents. Our results also suggest that temperature effects on the resting rate, not sensitivity, are mediating the changes we measured in aVOR response.

994 Repeated Transtympanic Kainate Injections as a Model of Excitotoxic Vestibular Insult

Jonas Dyhrfjeld-Johnsen^{1,2}, Audrey Broussey², Sophie Gaboyard^{1,2}, Christian Chabbert^{1,2}, Aurore Brugeaud² ¹INSERM U583, ²Sensorion Pharmaceuticals

Excitotoxic injury to primary vestibular neurons is believed to underlie induction of permanent vestibular deficits, but lack of a simple, reliable animal model hampers investigations of specific mechanisms. A previous study using release from chronically implanted, kainate loaded gel-foam produced only modest vestibular deficits (Brugeaud et al., 2007). We here present a novel approach using behavioral testing and videooculography following repeated transtympanic kainate injections for evaluation of acute and persistent vestibular deficits.

Headposts containing 3 mm bolts were surgically fixed to the skull of Female Long-Evans rats (175-200 g) under ketamine-xylazine anesthesia using dental acrylic, surgical screws and cyanoacrylate. Each rat was trained 4 times on the videooculography stage following surgery, before receiving 100 μ L transtympanic injections of physiological solution with kainate at 1 hour intervals under isoflurane anesthesia. After 2 injections, and each hour after the last injection, spontaneous eye-movements were recorded and vestibular dysfunction scored for each of 5 criteria on a scale from 0-4: Circling, head-bobbing, lateral head tilt as well as tail-hanging and air-righting reflexes.

Initial mean combined vestibular deficit scores of ~10 (scale of 0-20) increased up to 15 over the course of 6 hours and spontaneous, lasting nystagmus was recorded in most animals. The nystagmus disappeared 24h after the initial injection while significant behavioral vestibular deficits persisted up to 1 week.

We conclude that repeated, transtympanic kainate injections provide a simple and consistent model for studying excitotoxicity in vivo in the vestibule. Combining this model with histological and electrophysiological assessments of the lesion induced at the first sensoryneural synapse will provide a powerful tool for enhancing our understanding of the neurophysiological mechanisms underlying acute vertigo crisis and ensuing vestibular deficits.

995 Can Antidepressant Facilitate the Recovery of Peripheral Vestibular Function from Inner Ear Damage?

Hiroaki Shimogori¹, Hideki Toyota¹, Kazuma Sugahara¹, Makoto Hashimoto¹, Takefumi Mikuriya¹, Hiroshi Yamashita¹

¹Yamaguchi University Graduate School of Medicine Phosphorvlation of the transcription factor cAMP responsive element-binding protein (CREB) is thought to play a key role in neurogenesis. In our previous study, phosphprvlated form of CREB (p-CREB) –like immunoreactivities were observed in vestibular ganglion cells after unilateral surgical labyrinthectomy and unilateral TTX infusion. These results indicate that vestibular ganglion cells may have a potential of neuronal plasticity. We thought the possibility that up-regulation of p-CREB might facilitate neuronal plasticity. Rolipram, а phosphodiesterase (PDE) 4 inhibitor, increases cAMP levels and leads to up-regulate the phosphorylation of CREB. We reported that inner ear application of rolipram induced continuous phosphprylation of CREB in vestibular ganglion cells. While, some damages were also observed in vestibular ganglion cells. Recently, it has been indicated that antidepressants induce acute CREB phosphorylation and regulate neurotrophic factors, such as brain derived neurotrophic factor. The aim of the present study was to evaluate the effects of general application of amytriptyline, a tricyclic antidepressant, on vestibular functional recovery after vestibular damage.

Hartley white guinea pigs with normal tympanic membranes and normal Preyer reflexes were used in this study. Vestibular lesion was made by injection of chloroform into the guinea pig right middle ear. Sinusoidal rotation tests were performed before chloroform injection, and 3, 7 days, and 1 month after injection. Vestibulooccular reflexes (VOR) were observed and VOR gains were calculated.

996 Modeling the Effects of Large Amplitude Gravity-Dependent Gain Adaptation of the Angular Vestibulo-Ocular Reflex (AVOR)

Yongqing Xiang¹, Sergei B. Yakushin², Bernard Cohen², Theodore Raphan¹

¹Dept of CIS, Brooklyn College of the CUNY, ²Dept of Neurology, Mt. Sinai School of Medicine, New York Gravity-dependent adaptation of the yaw aVOR gain using visual-vestibular mismatch can be modeled by a biologically-based neural network (Xiang et al 2006). When the amplitude of the sinusoidal oscillation during adaptation is small (±6°), the maximal gain changes occur when the head is at the position of adaptation, and the gain changes decline as the head is moved away from this position. When the amplitude of rotation during the adaptation is large (±90°, ±135°, ±180°), the positions in which the largest gain changes occur are spread over a wide angle and approach a uniform distribution after adaptation with the largest angles of rotation (±180°). We have postulated that there are both gravity dependent and gravity independent components for small angles of aVOR gain adaptation, and that a network of canal-otolith convergent neurons drives the gravity dependent component. The function of these canal-otolith convergent neurons was effectively implemented as a group of polarization vectors that adapted to a particular spatial distribution within the three canal planes. To explain the spread in distribution as a function of angular width during adaptation, we hypothesize that, the tuning is broader for wider angles of adaptation. The model accepts the center position and the amplitude/velocity of the adaptation, and after learning, it predicted the gain changes re gravity in three dimensions of the experimental data reasonably well. The model is also consistent with recent findings that orientation of polarization vectors of some central vestibular neurons is tuned to gravity in the position of adaptation (Eron et al 2008; Kolesnikova et al 2010, SFN). Thus, it is now possible to predict experimental data from adaptation experiments with narrow and wide angles. This could be useful to verify how the vestibular system implements the gravity-dependent adaptation of the aVOR in single unit recording experiments. SUPPORT: DC04996, DC05204, EY01867

997 Vestibulo-Ocular Reflex Function Analysis in Mice

Patrick Armstrong¹, Scott Wood², Tomoko Makishima¹ ¹University of Texas Medical Branch, ²2. Universities Space Research Association, NASA Johnson Space Center

Our goal is to establish the diagnostic performance of a battery of functional tests in mice to assess vestibular organ function involved in linear and angular acceleration input.

As a start, we used caspase-3 knockout mice as a model animal for vestibular dysfunction. Caspase-3 is a cysteine protease integral for programmed cell death. Caspase-3 knockout mice exhibit deafness and circling behavior, suggestive of inner ear dysfunction. Unlike the auditory dysfunction, the details of the vestibular dysfunction are unknown.

The vestibulo-ocular reflex (VOR) using videooculography is a non-invasive method to test vestibular function in mice. Five mice each of Caspase-3 knockout-, heterozygous-, and C57BL6 wild type mice were tested at 3 months of age. The frequency response of the VOR in darkness for each group was characterized during horizontal rotation at 5 frequencies ranging from 0.05Hz to 0.8Hz, with peak velocity of 60 deg/sec. The linearity of the VOR was tested at 0.2 Hz using peak velocities ranging from 30 to 120 deg/sec.

No response at any frequency or velocity was recorded for caspase-3 knockout mice. The VOR appeared linear at 0.2Hz for all three groups. However, the sensitivity was reduced for the heterozygote group, and negligible for the knockout group. Rapid frequencies produced significant differences between heterozygous and wild type mice, suggesting that adequate vestibular development has not occurred. We are now in the process of evaluating wild type mice at older ages as another model for vestibular dysfunction, as well as establishing other vestibular function tests.

998 Coding Of Gravity-Dependent and – Independent Adaptation of the Angular Vestibulo-Ocular Reflex (AVOR) By Central Vestibular Eye Movement-Related Neurons

Olga Kolesnikova¹, Theodore Raphan², Bernard Cohen¹, Sergei Yakushin¹

¹Dept. Neurology, Mt. Sinai School of Medicine, ²Dept. CIS, Brooklyn College, CUNY

When the aVOR is adapted in specific head orientations relative to gravity, the gain changes are maximal in the position of adaptation (Yakushin et al. 2000, 2005). The gain changes are comprised of gravity-dependent and gravity-independent components. Some positionvestibular-pause (PVP) and eye-head velocity (EHV) neurons are likely to be the excitatory neurons that drive oculomotor neurons. PVP neurons do not receive floccular inhibition, while EHV neurons that receive flocculus input are likely play a critical role in aVOR gain adaptation (Lisberger, 1994; Zhang et al., 1995). The role of PVP and EHV neurons in gravity-dependent adaptation is unknown. Here, we recorded from PVP and EHV neurons in the rostral medial and superior vestibular nuclei before and after aVOR gain adaptation. While holding single neurons, the aVOR gains were decreased for 2 hr with cynomolgus monkeys in a side-down position, and the yaw or pitch aVOR gains were adapted, depending on the origin of the canal-convergent input to particular neurons. Most PVP neurons with otolith polarization vectors that were nonorthogonal to orientation of gravity in the position of adaptation, had changes in firing rates associated with both gravity-dependent and -independent components. Some PVP neurons coded only gravity-independent components regardless of orientation of the convergent otolith input. That is, the changes in sensitivity were the same in all tested head orientations. None of three recorded EHV neurons coded the gravity-dependent component. Thus, some PVP neurons code both gravitydependent and gravity-independent components, but only when the otolith input is not orthogonal to gravity in the position of adaptation. The gravity-independent component of gain adaptation, however, was coded by both PVP and EHV neurons. These data provide a mechanism whereby activity related to gravity-dependent and gravityindependent adaptation of the aVOR in the vestibular nuclei reach the eye muscle motoneurons that implement these changes in gain.

999 Adaptation of the Cervico-Ocular and Angular Vestibulo-Ocular Reflexes (COR and AVOR) by Visual-Cervical Mismatch in Rhesus and Cynomolgus Monkeys After Canal Plugging

Sergei B Yakushin¹, Olga V Kolesnikova¹, Dmitri A Ogorodnokov¹, Charles C Della Santina², Lloyd B Minor², Theodore Raphan³, Bernard Cohen¹

¹Mount Sinai School of Medicine, ²Johns Hopkins University School of Medicine, ³Brooklyn College The gain of the COR in normal animals is 0.1-0.2 at frequencies below ~0.3Hz and is negligible at higher frequencies. However, the gain of the COR can be modified by visual-cervical mismatch (Rijkaart et al., 2004). Animals with plugged semicircular canals can provide a good model to study increases in COR gains that compensate for loss of the canal responses at low frequencies (Yakushin et al., 2009). Specifically, the gain of the COR in canal-plugged animals is $\approx 0.4-0.6$ at frequencies below 0.3 Hz and gradually decreases to 0.2 at 2-3 Hz. Here we studied whether COR gains could be adaptively increased and decreased and how such gain changes affect COR-aVOR interactions. Yaw COR and aVOR gains were tested at frequencies ranging from 0.02 to 6 Hz in two cynomolgus and one rhesus monkey. All six semicircular canals were plugged one year or more prior to the adaptive experiments. Gains and phases of the aVOR and COR responses were fit with corresponding transfer functions (Yakushin et al., 2009), and summated as phasors. The combined COR-aVOR gains were ≈0.4-0.7, and the phase of eye velocity relative to head velocity was ≈180°. After adaptation, COR gains were modified by 20-40%, mostly at low frequencies, affecting the summated response gains. The phases of the summated responses remained compensatory, regardless of the amount and the direction of the COR gain changes. This study confirms our previous findings in showing the compensatory action of the COR gain after canal plugging. It also suggests that adaptation of the COR gain can make an important contribution by expediting the rehabilitation process after vestibular injuries.

Supported by NIH Grants: DC04996, DC2390 ,DC9255, EY04148, DC05204

1000 Quiet Stance Study of Rhesus Posture

Lara Thompson¹, Richard Lewis^{1,2}, David Balkwill², Conrad Wall III^{1,2}

¹Massachusetts Institute of Technology and Harvard University, ²Massachusetts Eye and Ear Infirmary

Postural imbalance is a major concern for the elderly, as well as patients suffering from vestibular (equilibrium) and balance disorders. In order to improve postural stability for both elderly and vestibulopathic patients, vestibular balance prostheses are needed. However, animal models must first validate the implantable vestibular prosthesis.

The purpose of this research is to characterize postural responses for a Rhesus monkey animal model under three sensory states: normal, bilateral vestibular hypofunction, and bilateral vestibular hypofunction aided by prototype implant. The goal of implementing the implant in the Rhesus is to improve the balance of the ablated, vestibular loss animal and restore postural responses to normal.

In order to observe and quantify quiet stance of a normal Rhesus, a stationary balance platform that consisted of four footplates, each equipped with force sensors, was used in conjunction with position sensors located on the and hindtrunk of the head. foretrunk, animal. Somatosensory footplate cues were varied such that they were either optimal (gum rubber) or minimal (foam). Mediolateral base of support stance was varied to be either optimal (wide) or minimal (narrow). Four test conditions of varying levels of task difficulty were utilized to inspect the Rhesus' posture. The gum-wide condition was hypothesized to be the least challenging and narrow-foam to be the most challenging. The center-of-pressure time series trace was extracted from the force data and characterized in terms of sway measures (e.g. root-meansquare distance, maximum distance, etc) to inspect differences between significant test conditions. Furthermore, this method will be applied to vestibular hypofunctioned Rhesus to compare significant differences between each sensory state. Once the Rhesus is implanted, the goal would be to compare results to those seen in the normal and hypofunctioned states and ultimately draw conclusions about human implementation.

1001 Retinal Position Error Is Sufficient for Driving Vestibulo-Ocular Reflex Adaptation

David Lasker¹, Munetaka Ushio², Charley Della Santina¹, Lloyd Minor¹

¹Johns Hopkins University, ²University of Tokyo To examine the role of retinal position error in vestibulo-ocular reflex (VOR) adaptation, we rotated three macagues in the vaw plane for three hours with a sum-of-sines stimulus (0.5. 1.1, 2.3, 3.7, 4.9 and 5.7 Hz) during stroboscopic illumination (SI) at 2 and 8Hz with and without 1.7X magnifying spectacles. VOR gain was measured in the dark at frequencies from 0.2-8 Hz before and after each adaptation session. When animals viewed a background with horizontal stripes during 8 Hz stroboscopic lighting, there was no change in VOR gain at any frequency after the sum-of-sines stimulation. In contrast, viewing a patterned background with 8 Hz SI yielded a constant reduction in gain at all frequencies of rotation (17 ± 3 %). When animals wore magnifying spectacles during 8 Hz stroboscopic illumination, VOR gain increased at low frequencies (11 ± 3 % at 0.2, 0.5 and 2 Hz) but did not change at the higher frequencies of rotation (4-8 Hz). Gains at all frequencies after 8 Hz stroboscopic illumination were greater with magnifying spectacles than without (p < 0.001). When animals wore magnifying spectacles during 2 Hz stroboscopic illumination, gain did not change for 0.2-2 Hz but decreased at the higher frequencies (12 ± 4 % at 4-8 Hz). Gains at low frequencies (.2-2 Hz) were greater than gains after 8 Hz SI without magnifying spectacles (p < 0.01). Increased gain during SI while wearing magnifying spectacles shows that retinal position error can drive VOR adaptation. Support: NIDCD R01DC2390

1002 Noise Induced Vestibular Dysfunction of Eye Movement (VOR) and Head Postural Control in Guinea Pigs

Jonie Dye^{1,2}, W. Michael King^{1,2} ¹University of Michigan, ²Kresge Hearing Research Institute

Intense or repetitive noise exposure damages cochlear hair cells and produces hearing loss but has not been shown to produce damage to the vestibular system.Clinical data are controversial but animal studies show the saccular epithelium is disrupted by intense, prolonged noise exposure. These data confirm the possibility of noise induced vestibular loss, but do not address if damage is limited to the sacculus and what behavioral consequences result from prolonged noise exposure.

To address these questions, we examined eye and head reflexes in guinea pigs exposed to noise. Four animals were exposed on 5 occasions to 5 hours of 120 dB SPL noise, spaced 2 weeks apart (octave band centered at 4 kHz). ABR testing was performed prior to noise exposure and after the final exposure. Vestibular function was evaluated prior to, 3, 7, and 13, days after each noise exposure. Vestibular function was assessed by measuring the vestibular function was assessed by measuring the vestibulor reflex (VOR) and compensatory head responses during rotational testing about an earth vertical axis in the dark. Eye and head movement were measured using a search coil implanted in one eye and another coil mounted on the head. During testing, the animal's body was restrained on a computer-controlled turntable, but its head was free to move. Methodological details and analysis are described in Shanidze et al. 2010.

All animals exhibited post noise exposure changes in head stability and VOR. After noise exposure, oscillatory head movements in response to abrupt body angular acceleration increased consistent with reduced neck stiffness. We hypothesize that that change might reflect damage to the sacculus and reduced vestibular inflow to neck anti-gravity muscles. The observed changes were most pronounced after the third noise exposure. Subsequently, the neck stiffened suggesting а compensatory process of either vestibular or spinal origin. Following the second noise exposure, we documented a progressive decrease in VOR gain . Although changes in VOR gain may reflect a change in semicircular canal function, canal and otolith signals must be centrally combined to produce accurate responses. In the headunrestrained animal, otolith signals would be needed to correctly interpret the axis of rotation; thus we cannot conclude that the changes in VOR gain imply a change in semicircular canal function alone.

1003 The Impact of External Noise Perception on Sway in Normal Individuals Michael Hoffer¹, Ali Hoffer², Carey Balaban³

¹Naval Medical Center San Diego, ²SRHS, ³University of Pittsburgh

Background:

Balance and stability are complex activities that utilize inputs from a variety of different sources. The organs responsible for hearing are co-located in the inner ear with the balance organ which has led investigators to question weather hearing has any impact on balance function Methods

Healthy adolescents with no history of ear disease or balance disorders were utilized as test subjects. Individuals were instructed to stand as steady as possible on a force plate for twenty seconds while their sway was recorded. Individuals were tested under four conditions as follows: 1) Control condition: eyes closed, staggered stance (right foot forward), head rotation from side to side at 60-120 Hz; 2) external noise condition: Same parameters except with external orienting noise (a song played in speakers that were five feet in front of the subject and at head height); 3) No noise condition: Same parameters while wearing ear plugs; and 4) Head fixed noise: Same parameters while listening to music (the same song as before) with head phones.

Results:

Group mean sway analysis demonstrated that sway was significantly less in both the lateral and AP plane for external orienting noise as compared to the control condition of room noise. Conversely, elimination of all noise significantly worsened balance function. In single subject design comparisons approximately one-third of individuals had improved balance less sway in both the lateral and AP directions with external orienting noise as compared to the room noise control condition whereas approximately one-half of the group showed significant worsening of balance function with the elimination of noise. Conclusions:

In otherwise healthy individuals the external noise environment has a significant affect on balance function. We demonstrated that external noise that is in a fixed location (orienting noise) decreases sway in a challenging balance task whereas the elimination of external noise worsens balance.

1004 Optimization of Stimulus Characteristics for Vestibular Stochastic Resonance to Improve Balance Function

Ajitkumar Mulavara¹, Matthew Fiedler², Erin Heap³, Keena Acock², Yiri De Dios², Igor Kofman², Brian Peters², Scott Wood¹, Jorge Serrador⁴, Helen Cohen⁵, Millard Reschke³, Jacob Bloomberg³

¹Universities Space Research Association, ²Wyle Integrated Science and Engineering Group, ³NASA Johnson Space Center, ⁴Dept of Veterans Affairs NJ Healthcare System, ⁵Baylor College of Medicine,

Stochastic resonance (SR) is a mechanism by which noise can assist and enhance the response of neural systems to relevant sensory signals. Recent studies have shown that applying imperceptible stochastic noise electrical stimulation to the vestibular system significantly improved balance and ocular motor responses. The goal of this study was to optimize the amplitude of the stochastic vestibular signals for balance performance during standing on an unstable surface.

Fifteen subjects performed a standardized balance task of standing on a block of 10-cm-thick medium-density foam with their eyes closed. Balance performance was measured using a force plate under the foam block and using inertial motion sensors placed on the torso and head segments. Stochastic electrical stimulation was applied using a bipolar constant current stimulator to the vestibular system through electrodes placed over the mastoid process. Stimulus signals in the 0.01-30Hz frequency range were used to test subjects at seven amplitudes in the current range of 0-700 microamperes. Six balance parameters were calculated to characterize the performance of subjects during the baseline and the stimulus periods for all seven amplitudes. Optimal stimulus amplitude was determined as the one at which the ratio of parameters from the stimulus period to the baseline period for any amplitude range showed the most improvement than that for the no stimulus condition on a minimum of four of six parameters. Ten of the fifteen subjects showed an improvement in balance performance. Results from this study showed that balance performance at the optimal stimulus amplitude improved significantly with the application of the vestibular SR stimulation. The amplitude of optimal stimulus for improving balance performance in 8 subjects was in the range of 100-300 microamperes.

This study was supported in part by a grant from the National Space Biomedical Research Institute through NASA NCC 9-58 (SA02001)

1005 Temporal Integration of Vestibular and Auditory Stimuli

Nick N-Y Chang¹, Mark Sanders², Meghan Hiss³, Rosalie Uchanski¹, Timothy Hullar¹

¹Washington University in St. Louis, ²Arizona State University, ³The Ohio State University

Multisensory integration is critical to our ability to evaluate the world around us. Sensory inputs must be perceived as aligned in time and space in order to be integrated appropriately. Because individual inputs are perceived at different delays following a stimulus, central processes must act to synchronize them into a single percept. Our ability to synchronize vestibular and other stimuli in normal and pathologic conditions is not known.

We tested the hypothesis that the perception of vestibular stimuli is delayed compared to auditory stimuli. We used the method of constant stimuli to determine the point of subjective simultaneity (PSS) for auditory and vestibular stimuli presented to normal young subjects. The PSS represents the difference in time between the presentations of two stimuli at which the stimuli are perceived as synchronized. Each trial consisted of a 10millisecond, 800 Hz beep presented at a range of times before or after the onset of a whole-body earth-vertical rotation along a raised cosine trajectory (0.5 Hz) to peak velocities from 5 to 180 deg/sec.

We found that the perception of vestibular stimuli is delayed between 30 and 120 ms compared to simultaneous auditory stimuli in normal young subjects. In comparison, the perceptual delay between visual and auditory stimulus may be lower than 10 ms. This suggests that the brain is particularly tolerant of temporal mismatches between vestibular and other sensory stimuli. An inability to synchronize vestibular input with other sensory modalities may help explain imbalance in some patients.

Supported by NIH K08 DC006869 (TEH)

1006 Why Does the Trip Back Seem Longer: Order Dependence of Supra-Threshold Human Vestibular Perception

Benjamin Crane¹, Rachel Roditi¹

¹University of Rochester

Introduction: We previously found that healthy human subjects without vestibular disease frequently have significant asymmetries in their vestibular perception thresholds. The current study attempts to determine if such asymmetries extend into suprathreshold perception.

Methods: Seven subjects were tested using two types of motion: sway (right-left motion) and vaw (vertical-axis rotation). Two stimulation paradigms were used, an "opposite" stimulus consisting of motion in one direction followed by a motion in the opposite direction-each of which lasted 1.5 s, but with variable velocity. After the stimuli were delivered, the subject pushed a button to report if they felt their final position was to the left or right of the starting position, and subsequent stimuli were adjusted accordingly. A second stimulus paradigm (double) consisted of two movements of 1.5 s duration in the same direction and subjects determined which was smaller. Trials were conducted with actual motion in darkness (vestibular), and with a visual stimulus that stimulated a similar motion while the subject remained stationary (visual).

Results: The results were independent of if the stimulus type (visual, vestibular, sway, or yaw). With the "reverse" protocol the average outbound stimulus had to be $15 \pm 20\%$ (mean \pm SD, range -4 to 66%) faster than the return to be perceived as equal. This order asymmetry was independent of initial stimulus direction (p>0.1). For the "double" stimuli, the first stimulus had to be only $2 \pm 3\%$ larger than the second for them to be perceived as equal.

Conclusions: Motion perception is order dependent when comparing stimuli in different directions, with almost all subjects perceiving the second (return) motion larger than it actually was. These asymmetries are diminished when comparing stimuli in the same direction. Because the results did not depend on whether the stimulus was visual, vestibular, sway, or yaw, a central mechanism is likely.

1007 Asymmetries in Human Vestibular Perception Thresholds

Rachel Roditi¹, Benjamin Crane¹

¹University of Rochester-Strong Memorial Hospital

Introduction: Dizziness is a common clinical problem, but currently available tests of vestibular function do not assess motion perception. Vestibular reflexes are frequently asymmetric, but the possibility of asymmetric vestibular perception has not previously been investigated. The current study presents a method for measuring direction specific vestibular perception and normative data. Methods: Single-center prospective cohort study. Twentythree subjects (aged 21- 68 years) with normal caloric testing were included. A motion platform was used to generate sway, surge, heave, and yaw rotation at 0.5 and 1 Hz in darkness with noise masking. After movement, subjects pushed one of two buttons to report the perceived direction. Perceptual thresholds were determined using a novel method, which allowed independent determination of thresholds in each direction. An asymmetry index (AI) was calculated, and the correlation with age was analyzed using a Student's t-test.

Results: Thresholds for sway, surge, heave were 2.3 \pm 1.3 (mean \pm SD), 2.3 \pm 1.4, 6.3 \pm 3.5 cm/s, respectively, and yaw was 1.3 \pm 0.7 deg/s for stimuli presented at 0.5 Hz. For 1 Hz stimuli, the thresholds were 0.86 \pm 0.47, 0.78 \pm 0.38, 2.6 \pm 2.3 cm/s, and 0.87 \pm 0.67 deg/s. Subjects frequently had directionally asymmetric thresholds. The mean AI was highest for heave and lowest for yaw (4.45 \pm 3.09 vs. 1.62 \pm 0.56 at 0.5Hz) Asymmetries remained stable over multiple testing sessions. Although thresholds were frequently asymmetric. Older subjects, population averages were symmetric. Older subjects (\geq 45 years) had increased thresholds at 0.5 Hz when compared to subjects <45 yo for sway, surge, and heave (p<0.01 for all). In yaw, thresholds did not differ with age (p>0.1).

Conclusions: Healthy subjects frequently have significant directional asymmetry in motion perception thresholds. Otolith based vestibular perception thresholds were higher with advanced age and demonstrated the greatest degree of asymmetry.

1008 Computer Model of the Information Processes in the Vertical Semicircular Canals Vladimir Alexandrov^{1,2}, Tamara Alexandrova^{1,2}, Rosario Vega¹, Maribel Reyes Romero¹, Galina Sidorenko²,

Enrique Soto¹

¹Universidad Autónoma de Puebla, México, ²Moscow State University

We have developed a mathematical model of the information process in the lateral semicircular canals (ARO 33th Midwinter Meeting). Now we present a computer model of the information processes in the vertical semicircular canals in extreme situations (during a fall). The model has been created on the basis of the mathematical model of the vestibular mechanoreceptor that we developed. The functional and numerical parameters were obtained from the morphological measurements and dynamic experiments. This model is necessary because for design and testing of vestibular prosthetic devices, it is required to carry out the comparative analysis of the output signals of the prototype and information processes in the computer model of the vestibular apparatus with the same mechanical stimulus, corresponding to the first stage of the falling (0,1-0,2 s), for this purpose the computer model of the vertical semicircular canals was elaborated.

In particular, prototypes of the vestibular prostheses for persons with vestibular dysfunctions have been proposed and preclinical tests are needed for defining the quality of the prototypes. In 2010, we developed a vertical posture simulator (patent No 2379007, Russian Federation) for the development and testing of proposed vestibular devices. The results of the computer simulation showed that there is an essential difference in the output information between the right anterior and left posterior semicircular canals to the same mechanical stimulus (the difference in the output information in the left anterior and in the right posterior semicircular canals occurs analogously). When the mechanical stimulus corresponds to the first stage of falling, the vestibular canals provide information about the angular velocity, but not about the angular acceleration. In connection with this we conclude that it is an absolute requisite to include an accelerometer in the prototype in order for the device to detect the initial phase of a fall.

Supported by goscontract 01.740.11.0300 and RFFI grant 10-01-00182, Russia.

1009 Spatial Shaping of Inner Ear Innervation by Slitrk6 Expression

Azel Zine¹, Kei-ichi Katayama², Bernd Fritzsch³, Jun Aruga²

¹Institute of Neurosciences, University of Montpellier, France, ²Laboratory for Behavioral and Developmental Disorders, RIKEN Brain Science Institute (BSI), Wako-Shi, ³Department of Biology, College of Liberal Arts and Sciences, University of Iowa

Slitrks are type I transmembrane proteins that share conserved leucine-rich repeat domains similar to those in the secreted axonal guidance molecule Slit. They also show similarities to Ntrk neurotrophin receptors in their carboxy-termini, sharing a conserved tyrosine residue. Slitrk6 is strongly expressed in the sensory epithelia of the inner ear. We generated Slitrk6-knockout mice and investigated the development of the innervation of their auditory and vestibular sensory organs. Slitrk6-deficient mice showed pronounced reduction in the cochlear innervation. In the vestibule, the innervation to the posterior crista was often lost, reduced, or sometimes misquided. These defects were accompanied by the loss of neurons in the spiral and vestibular ganglia. Cochlear sensory epithelia from Slitrk6-knockout mice had reduced ability in promoting neurite outgrowth of spiral ganglion neurons. Furthermore, the Slitrk6-deficient inner ear showed a mild but significant decrease in the expression of Bdnf and Ntf3, both of which are essential for the innervation and survival of sensory neurons. In addition, the expression of Ntrk receptors, including their phosphorylated forms was decreased in Slitrk6-knockout cochlea. These results suggest that Slitrk6 promotes innervation and survival of inner ear sensory neurons by regulating the expression of trophic and/or tropic factors including neurotrophins from sensory epithelia.

Supported by the Japan Society For the Promotion of Science (JSPS)

1010 The Role of NeuroD in the Cell Fate Choice of Auditory Versus Vestibular Ganglion Neurons in the Chick Inner Ear

Jennifer Jones¹, Mark Warchol¹

¹Washington University

NeuroD is a bHLH transcription factor that is necessary for neuronal development. In mice, deletion of NeuroD results in deafness and head tilting/circling behavior due to the loss of cochlear and vestibular neurons, respectively (Liu et al., 2000; Kim et. al., 2001). We are examining the role of NeuroD in the development of afferent neurons of the avian cochlea and vestibular organs. Expression studies show that NeuroD is expressed in delaminating neuroblasts within the otic epithelium. It becomes downregulated in presumptive auditory neurons at ~E4.5, but is maintained in vestibular neurons until ~ E6.5. Ectopic expression of NeuroD in Xenopus is capable of converting epidermal cells into neurons (Lee et al., 1995), but the ability of this gene to specify a specific type of neuron is unknown. We are currently over-expressing NeuroD in the developing chick otocyst in ovo. Initial observations show that cells transfected with a PMES-NeuroD-GFP plasmid develop into neurons within the auditory and vestibular ganglia as well as ectopic neurons in the surrounding mesenchyme. In contrast, cells transfected with a PMES-GFP (control) plasmid acquire numerous phenotypes within the otic region. These data suggest that NeuroD directs cells to develop as neurons. Additional studies have focused on whether the peripheral projections of NeuroD-transfected cells innervate appropriate targets. Preliminary data show that peripheral projections of PMES-NeuroD-GFP and PMES-GFP transfected cells within the vestibular ganglion terminate in the vestibular sensory organs. Interestingly, the majority of PMES-NeuroD-GFP transfected cells within the auditory ganglion send peripheral projections toward the lagena, but not the basilar papilla. In contrast, the projections of PMES-GFP transfected cells innervate both the lagena and basilar papilla. These data suggest that ectopic expression of NeuroD influences progenitor cells to develop as vestibular neurons.

1011 Pou3f4 in the Otic Mesenchyme Regulates EphA4 to Promote the Fasciculation of Inner Spiral Ganglion Axon Bundles

Thomas M. Coate¹, E. Bryan Crenshaw², Matthew W. Kelley¹

¹Laboratory of Cochlear Development, NIDCD/National Institutes of Health, ²Children's Hospital of Philadelphia, U. of Pennsylvania

During development of the cochlea, spiral ganglion neurons (SGNs) form regularly spaced arrays of fascicles (the inner spiral bundles) that are partitioned from one another by bands of otic mesenchymal cells. The factors that mediate the formation of these bundles, as well as their role in normal auditory function, are unknown. In the present study, we demonstrate that expression of the transcription factor Pou3F4 (the mouse ortholog of DFN3) is restricted to otic mesenchyme cells during periods of SGN delamination and outgrowth. In Pou3f4 null mice SGN peripheral axons fail to properly fasciculate, and aberrantly disperse into the adjacent mesenchyme. In addition, preliminarily results indicate diminished ribbon synapse formation between SGNs and inner hair cells, likely as a consequence of impaired fasciculation. To elucidate possible guidance factors that may be altered in the absence of Pou3f4, mRNA from control and Pou3f4

null mesenchyme was compared by microarray. The classic chemo-repellant EphA4 was among a group of candidates that were down-regulated in the absence of *Pou3f4*. EphA4 protein is expressed by otic mesenchyme cells located at the boundary of spiral ganglion fascicles and this expression was found to be lost in Pou3f4 null mice. Moreover, similar defects in SGN fasciculation are present in EphA4 null mice, suggesting that the defects in Pou3f4 nulls are mediated through EphA4. These results suggest that some auditory deficits in Pou3f4 mutants may be a result of defects in SGN outgrowth and fasciculation that occur when the EphA4 inhibitory cue is lost from the surrounding otic mesenchyme. We are presently conducting chromatin immunoprecipitation (ChIP) assays to investigate whether Pou3f4 directly targets EphA4 regulatory elements, as well as rescue experiments to determine whether expression of EphA4 is sufficient to restore SGN fasciculation in Pou3f4 null mice.

1012 Role of Sox E Genes in the Development of the Auditory Portion of the Inner Ear

Ingrid Breuskin¹, Morgan Bodson¹, Nicolas Thelen¹, marc thiry¹, Laurence Borgs¹, Philippe Lefebvre^{1,2}, Laurent Nguyen¹, **Brigitte Malgrange**¹

¹University of Liege, ²Department of ENT

The transcription factors of the soxE family, including sox8, sox9 and sox10 play important roles in diverse developmental processes. However little is known about their function during inner ear development. In the developing inner ear we detected sox9 and sox10 in the sensory epithelia since the formation of the otic placode. As the organ of Corti begins to differentiate, sox9 and sox10 expression are progressively restricted to supporting cells. To elucidate the role of sox10, we first analysed sox10 knockout mice. Using sox2 as a molecular marker of the prosensory domain, we showed that sox 10 is not required for its formation but is necessary for its maintenance. Indeed, we observed a significant shortening of the cochlear duct. Interestingly, expression of the notch ligand Jagged 1, which plays a crucial role during cochlear development, is decreased in the prosensory area of sox10-deficient mice. In parallel, using both gain- and lossof function approaches, we showed that sox9 is required for cell patterning in the organ of Corti. Taken together, these results demonstrate diverse roles of soxE genes during the inner ear development, specification and maintenance of differentiated cells within the cochlea.

1013 Testin Genetically Interacts with Planar Cell Polarity Gene Vangl2 and Is Required for Normal Development of the Inner Ear and the Female Reproductive Organs

Dongdong Ren^{1,2}, Michael Kelly¹, Alessandra Drusco³, Carlo M. Croce³, Fang-Lu Chi², Ping Chen¹ ¹Emory University, Dept. of Cell Biology, ²Department of Otolaryngology, Eye, Ear, Nose, and Throat Hospital, Fudan University, ³Comprehensive Cancer Center, Ohio State University

During terminal differentiation, the mouse hearing organ, the organ of Corti, undergoes cellular rearrangements characteristic of convergent extension (CE) and generates precise arrays of sensory hair cells with uniform orientation. Both CE and uniform orientation of hair cells are manifestations of a type of tissue polarity, known as planar cell polarity (PCP). Mutations in a conserved PCP gene, Vangl2, result in CE defects, a shorter and wider organ of Corti, and randomization of hair cell orientation in the cochlea. To further explore the PCP pathway, we used C-termial cytoplasmic domain of the transmembrane protein Vangl2 and performed a two-hybrid screen with a cDNA library built from embryonic day 15 (E15) mouse cochleae. We identified Testin as one of the Vangl2interacting proteins. Testin is a member of the PET-LIM family that includes protein Prickle (Pk), a known PCP component interacting with Vangl2. We confirmed the expression of Testin in the cochlea during terminal differentiation. Gene mutations in the Testin cause patterning defects in the cochlea and abnormal morphology of the vestibular organs. Furthermore, Testin genetically interacts with Vangl2 to regulate the extension and formation of the opening of female vaginal track. Together, these findings implicate that Testin is a Vangl2interacting protein and regulates PCP processes in mice.

1014 FGFR1 Functions in Inner Ear Hair Cell Morphogenesis

Akira Honda¹, Tomoko Kita¹, **Raj Ladher¹** ¹*RIKEN CDB*

The ciliated mechanoreceptors of the vertebrate inner ear possess several structural features that enable detection of sound or balance. Key amongst these are the kinocilia, a single microtubule based cilium, and the stereocilia, actinbased villi that extend beyond the apical surface of the hair cell. The mechanisms that cause the elongation of the kinocilia and the specialization of stereocilia are unknown. FGF signalling is deployed at multiple steps during the formation of the inner ear and we have found that it is also involved in the structural specialization of the inner ear hair cells. Immunolocalisation revealed that FGFR1 is localized to the kinocilia during its development, in both vestibular and cochlear organs in mammals and birds. Reduction of FGFR1 activity using the FGF inhibitor SU5402 or using hypomorphic mouse mutants result in a reduction of kinocilia length and thus a perturbation in the polarity of hair cells. Studies are ongoing to determine the mechanism by which FGFR1 function can control kinocilia lenath.

1015 Thyroid Hormone Mediates Fgfr3 Signaling and Cellular Mechanics in the Developing Organ of Corti

Katherine B. Szarama^{1,2}, Núria Gavara², Ronald S. Petralia³, Richard S. Chadwick², Matthew W. Kelley¹ ¹Section on Developmental Neuroscience, NIH-NIDCD, ²Section on Auditory Mechanics, NIH-NIDCD, ³Section on Neurotransmitter Receptor Biology, NIH-NIDCD

Ligand-mediated activation of thyroid hormone receptors (TR) is required for development of the organ of Corti (OC) and the onset of auditory function. While functional consequences of hypothyroidism have been documented, little is known of the underlying molecular and morphological basis of these consequences. Previous studies demonstrated that Fibroblast growth factor receptor 3 (Fqfr3) is expressed in the OC in a pattern that could be consistent with a TR target gene. Also, Fgfr3 knockout mice are deaf and have similar pillar cell morphology to those of hypothyroid cochleae. To determine whether Fgfr3 could be a target of TR, gPCR was used to determine that hyperthyroidism leads to a premature down-regulation of Fgfr3, while Fgfr3 persists abnormally in hypothyroidism. In situ hybridization confirms qPCR results and localizes the persistence of Fgfr3 in outer hair cells of hypothyroid cochleae.

Previous research has also shown that hypothyroidism decreases microtubules in the OC. To determine whether defects in the formation of microtubules, or other cytoskeleton elements, could play a role in hypothyroidinduced auditory deficits, components of the cytoskeleton were compared in hair cells and supporting cells from control and hypothyroid animals. Marked differences in the assembly of microtubules in supporting cells of hypothyroid mice were observed; suggesting a potential alteration in cellular mechanics. To examine this, Atomic Force Microscopy was used to measure the mechanical properties of hair cells and supporting cells. It was found that hypothyroid cochleae at postnatal day 0 have a Young's Modulus (E) significantly increased in both hair cells and supporting cells relative to controls. However, by postnatal day 5, hypothyroid cochleae have a decreased E relative to control conditions. Taken together, these results suggest that thyroid signaling affects the gene expression, cell structure and mechanics of the OC.

1016 Overexpression of Wnt9a Interferes with Short Hair Cell Differentiation in the Embryonic Chicken Basilar Papilla

Donna M. Fekete¹, Deborah J. Biesemeier¹ ¹*Purdue University*

The chicken basilar papilla (BP) has two morphological classes of hair cells (HCs): tall and short. Tall HCs are located on the neural side and receive robust afferent innervation and modest efferent innervation. Short HCs are located on the abneural side, have broad apical surfaces and receive robust efferent innervation. There is a systematic shift from one type to the other across the neural-abneural axis of the BP. The molecular mechanisms that underlie variation across this axis are

beginning to be explored: specifically, dose-dependent BMP signaling plays a role in establishing sensory vs. nonsensory compartments across mouse cochlea (Ohyama et al., J. Neurosci., in press). The Wnts are another morphogen family whose members are expressed in locations that could generate gradients and influence cell fates across the neural-abneural axis. For example, as early as stage 27 in the chicken BP, Wnt9a expression is localized to the non-sensory domain along the neural border of the BP (Sienknecht and Fekete, 2009). This region continues to express Wnt9a through stage 36 as it differentiates into homogene cells (Sienknecht and Fekete, 2008). To determine whether Wnt9a acts cellautonomously to specify homogene cells, or non-cell autonomously to influence HC differentiation across sensory epithelium, we generated ectopic sources of Wnt9a using retroviral gene transfer. Otocysts were injected with RCAS(A)/Wnt9a virus on embryonic day 3 (E3; stages 15-18) and processed on E8 or E16-E18. Infected BPs were much wider than controls and their abneural halves did not assume the expected morphology. Rather, across the entire width, both the HCs and the innervation density were consistent with the morphology of the neural half of the BP, with its tall HCs. In some heavily infected regions, a second phenotype was seen: the organ assumed a vestibular sensory identity, similar to that seen in response to the forced expression of canonical Wnt signaling (Stevens et al., 2003).

1017 Live Imaging of Cell Movement in the Developing Cochlea Indicates Periods of Convergence and Extension

Elizabeth Carroll Driver¹, Zoë Mann¹, Matthew W. Kelley¹ ¹Laboratory of Cochlear Development, NIDCD, NIH

The mammalian organ of Corti (OC) is comprised of a mosaic of hair cells and supporting cells that extends along the entire length of the cochlear duct, and is organized into four rows of hair cells surrounded by several specific types of supporting cells. The proper formation of this mosaic of cells is critical for normal auditory function. At early stages of cochlear development, the cells of the prospective OC, identified by expression of the cell-cycle regulator p27^{kip1} are distributed in a domain that is much shorter and broader than is found in the mature OC. As the cochlear duct grows and extends, the domain of p27kip1-positive cells becomes progressively longer and narrower. This type of cellular rearrangement has been observed in diverse tissues and developmental contexts, and is usually achieved via a process known as convergence and extension. It has been suggested that cellular rearrangements in the cochlear duct also occur through convergence and extension, but the movement of cells within the embryonic cochlear epithelium has never been directly observed. Using cochlear explant cultures and individual fluorescently labeled cells expressing the hair cell gene Atoh1, we have been able to visualize the movements of cells within the developing epithelium in vitro. Time-lapse videos generated over several hours from approximately embryonic day 15 to 16 show movements of cells that are consistent with convergence and extension.

Moreover, migrating cells exhibit protrusive activity, suggesting that this movement is an active process. Observations of cell movements over several days indicate that most convergent cell migration occurs prior to embryonic day 16, but that the cochlear epithelium continues to extend until at least the equivalent of postnatal day 1. This study is the first to visualize the migration of living cells within the developing cochlea and indicates that active cell movements are necessary for cochlear development.

1018 The BHLH Transcription Factor Scleraxis Is Required for Auditory Function

Zoe Mann¹, Kyu Yup Lee¹, Weise Chang¹, Matthew Kelley¹

¹NIDCD, NIH

Normal auditory function relies on the precise patterning and specification of multiple cell types within the exquisite cellular mosaic of the organ of Corti. In addition to this precise organization, auditory function also requires the development of a tonotopic map along the length of the cochlea, such that basal hair cells transduce highfrequency sounds and apical cells encode low frequencies. Little is known regarding the developmental cues and/or signalling pathways that govern establishment of the inner ear frequency map. To identify possible candidate molecules involved in the establishment of tonotopy, we used Affymetrix chip arrays to compare gene expression between basal and apical ends of the chick basilar papilla (BP) at E6.5. One of the differentially expressed genes identified from this screen was scleraxis (Scx), a basic helix-loop-helix transcription factor that is necessary for patterning and differentiation of developing tendons and ligaments. To examine the potential role of Scx in cochlear development, expression was examined in both developing chick BP and mouse cochlea. In mouse, Scx was broadly expressed throughout the cochlear duct from E13.5-E15.5 but became restricted to the interdental cells, Deiters' cells, Claudius/Hensen cell region and the inner hair cells between E15.5-P0. The mature expression pattern was present by P0 and remained unchanged through at least P25. To determine whether Scx plays a role in auditory function, ABRs and DPOAEs were determined for Scx null animals and controls. Preliminary data suggest a 20dB threshold shift at 8, 16 and 32 Hz and absence of DPOAEs in Scx null animals, indicating an important role for Scx in cochlear development. The precise signaling pathways associated with Scx are poorly characterized, but recent studies have demonstrated an ability to regulate expression of Col1, Sox9 and BMP4. Considering the role of Scx in formation of tendons and ligaments it seems possible that it could regulate formation of extracellular matrixes, such as the basilar or tectorial membranes within the developing cochlea.

1019 In Vivo Visualization of Notch1 Proteolysis Reveals the Heterogeneity of Notch1 Signaling Activity in the Mouse Cochlea

Zhiyong Liu^{1,2}, Zhenyi Liu³, Thomas Owen^{1,4}, Raphael Kopan³, Jian Zuo¹

¹St. Jude Children's Research Hospital, ²University of Tennessee Health Science Center, ³Washington University at St.louis, ⁴University of Bath

Mechanosensory hair cells (HCs) and surrounding supporting cells (SCs) in mouse inner ear cochleae are important for hearing and are believed to derive from the same prosensory progenitors. Notch1 signaling plays dual but contrasting age-dependent roles in mouse cochlear development: it likely generates prosensory progenitors by subsequently lateral induction and blocks HC differentiation while promoting SC differentiation by lateral inhibition. However, directly visualizing mouse cochlear cells experiencing Notch1 proteolysis (or Notch1 signaling) at single cell resolution is not studied before. Also, whether levels of Notch1 activity differ between lateral induction and inhibition is unknown. In this study, we characterized two Notch1Cre/+ knock-in mouse lines, Notch1 Cre(Low)/+ and Notch1 ^{>Cre(High)/+}, in which the Notch1 intracellular domain (NICD) is replaced by 6×Myc-tagged Cre and Cre. respectively. Cre-mediated genetic lineage tracing analysis of either line crossed with Rosa26-EYFP loxp. mice strikingly labeled only SCs in the cochlea with the reporter EYFP. The number of EYFP+ cochlear SCs was substantially higher in Notch1 ^{Cre(High)/+}; Rosa26-EYFP ^{loxp/+} than Notch1 ^{Cre (Low)/+}; Rosa26-EYFP ^{loxp/+} mice, highlighting that level of Notch1 activity among cochlear SCs is heterogeneous. However, neither cochlear prosensory progenitors nor HCs were traced with EYFP, showing that levels of Notch1 activity differ between lateral induction and inhibition. To explain how the Notch1 activity evokes dual contrasting effects, we propose a model according to which low levels of Notch1 signaling lead to generation of cochlear prosensory progenitors whereas medium or high levels promote SC but block HC commitment and differentiation.

1020 A Role for EphrinB2 in Ossicular Chain Development

Steven Raft¹, Doris Wu¹

¹National Institutes of Health

In humans, ossicular fixation (ankylosis) is a cause of conductive hearing loss and may present as an isolated entity or as one feature of a number of congenital syndromes. Stapes ankylosis of young adult onset also occurs in otosclerosis, a disorder of temporal bone remodeling. Syndromes defined by ossicular ankyloses and appendicular joint fusions are associated with NOGGIN mutations and some genetic evidence exists for TGF-beta family member involvement in otosclerosis. However, genetic heterogeneity is thought to underlie all these clinical entities. We have therefore employed a reverse genetic strategy using the mouse to identify genes required for development and maintenance of a normally compliant ossicular chain. Transcriptional profiling identified the Eph receptor ligand ephrinB2 as a candidate, as previous studies suggest roles for Eph-ephrin signaling in endochondral skeletal development and adult bone We find ephrinB2 to be expressed in remodeling. mesenchyme surrounding the developing ossicles during early fetal stages, enriched in the maturing joint spaces and perichondrium of the late fetal middle ear, and restricted to temporal bone marrow spaces, the tympanic membrane, ligaments, tendons, and periostium of the adult middle ear cavity. Tissue-specific inactivation of ephrinB2 using a series of different Cre recombinase drivers causes various types of ossicular ankyloses in both the endochondral cartilage model and mature bone. These anomalies phenocopy those described in the human literature, including stapedial footplate fusion to the otic capsule and bony fusion of the dorsal crus of the stapes to Ongoing studies are aimed at the epitympanum. understanding how Eph-ephrin signaling contributes to the development and, perhaps, the maintenance of a properly compliant ossicular chain.

1021 Interactions Between an Usher Synaptic Complex and SNAP25 Possible Role in Hair Cell Synaptic Maturation

Marisa Zallocchi¹, Daniel Meehan¹, Duane Delimont¹, Joseph Rutledge², Michael Anne Gratton², Dominic Cosgrove^{1,3}

¹Boys Town National Research Hospital, ²Otolaryngology-Head, Neck Surgery, St Louis University, ³University of Nebraska Medical Center

The molecular mechanisms underlying hair cell synaptic maturation are not well understood. Cadherin-23 (CDH23, USH1D), protocadherin-15 (PCDH15, USH1F) and the very large G-protein coupled receptor 1 (VLGR1, USH2C) have been implicated in hair cell development, while clarin-1 (USH3A) has been suggested to play a role in synaptogenesis. Mutations in their genes cause Usher syndrome, characterized by congenital deafness, imbalance and retinitis pigmentosa. We observed that specific isoforms of these Usher proteins are developmentally expressed at the base of cochlear hair cells between P1 and P6. This spatiotemporal pattern coincides with the final steps in hair cell synaptic maturation, where there is a retraction and pruning of the type I afferent synapses from the base of the outer hair cells and a neurite outgrowth of the efferent fibers. We identify a synaptic Usher complex(es) comprised of specific isoforms of CDH23, PCDH15, VLGR1 and clarin-1 that associates with the t-SNARE (target-Soluble N-Attachment ethylmaleimide-sensitive factor Protein Receptor), SNAP25 (Synaptosomal-associated protein 25). The formation of the Usher/SNAP25 complex most likely occurs via the VLGR1 EAR domain that is involved in neurogenesis in brain. To establish the in vivo relevance of this complex, we performed morphological analysis of the synapses in the Clrn1-/- mouse. These mice showed defective synaptic maturation by both immunostaining and electron microscopy. Collectively, our results show that, in addition to the well documented role for usher proteins in stereocilia development, specific usher proteins complexes likely function in cochlear hair cell synaptic maturation as well.

NIH grants R01 DC004844 to DC, DC006442 to MAG

1022 Activity of Neuronal Ensembles During Development of Hearing: Evidence for Clusters of Co-Active Neurons in the Auditory Brainstem of Rats Adrián Rodríguez-Contreras¹

¹Biology Department, The City College of New York During early stages of development until the onset of hearing, cells in the auditory brainstem exhibit spontaneous patterns of electrical activity that originate in the cochlea (Tritsch et al., 2010). However, little is known about the patterns of activity in larger groups of auditory neurons, partly due to the difficulty of obtaining large-scale simultaneous neuronal recordings in neonate animals. We used silicon probes to record multi-unit activity simultaneously across sixteen distinct locations in the medial nucleus of the trapezoid body (MNTB) and neighboring regions in the superior olivary complex (SOC) of anesthetized rat pups between birth (P0) and P17. In P0-P5 rats (n = 18), we observed spatially sparse multiunit activity that resembled the bursts of action potentials described previously for single neurons. Such recordings were highly localized to medial or lateral MNTB regions and did not follow any consistent pattern across different animals. In some recordings, we noted transitions from quiescence to spiking activity and vice versa, suggesting that clusters of auditory brainstem neurons are independent, and that cells within clusters switch between spiking and silent modes, and/or comprise mixtures of spiking and silent cells. Using in vivo whole cell recordings we confirmed that 13 of 35 morphologically identified MNTB and SOC neurons were non-spiking cells. In P6-P10 (n = 15), and P11-P17 rats (n = 21), spontaneous bursts of multi-unit activity were observed more frequently and, in some instances, occurred in synchrony among different recording sites. Overall, these results provide evidence for the existence of spontaneously co-active clusters of cells in the auditory brainstem, and suggest that the coordinated activity of neuronal ensembles in the auditory system is subject to developmental regulation. (Supported by The Deafness Research Foundation and NIH grants G12-RR03060 and 1SC1HD068129-01.)

1023 Gene Expression Profiles in the Developing SOC Reveal Molecular Pathways Associated with Deafness Genes

Hans Nothwang¹, Heike Ehmann², Christian Salzig³, Satheesh Somisetty¹, Bohumila Tarabova², Mathieu Clément-Ziza⁴, Olaf Bininda-Emonds¹, Patrick Lang³, Marlies Knipper⁵, Dusan Bartsch⁶, Eckhard Friauf² ¹Carl von Ossietzkv Universität Oldenburg. ²TU Kaiserslautern, ³Fraunhofer Institute for Industrial Mathematics, Kaiserslautern, ⁴TU Dresden, ⁵Universität Tübingen, ⁶Central Institute of Mental Health, Mannheim The superior olivary complex (SOC) is an important auditory processing center and a model system to study basic neurotransmission and neuronal circuit formation. To identify the genetic program underlying postnatal development and functional maturation, we profiled gene transcription in the rat SOC at postnatal days P4 and P25, i.e. before and after hearing onset. Profiling was performed using genome-wide microarrays encompassing 41,000 probes. 1,319 oligos (3.2%) were up-regulated and 1,777 oligos (4.3%) were down-regulated. The molecular repertoire of mature SOC neurons was sculpted by extensive changes in several protein categories, among which K+ channels, myelination, and G-proteins were prominent. To identify SOC-related genetic programs, we also profiled the brain at P4 and P25. Differentially expressed sequences between SOC and brain almost doubled from P4 (4.4%) to P25 (7.6%). This implies considerable molecular specification around hearing-onset. 453 (1.1%) oligos were higher expressed in the SOC than in the brain at both P4 and P25. They may hence represent a genetic signature of the postnatal SOC. 'Regulation of action potential' was the most enriched gene ontology term in this gene list. In SOC-related gene sets, deafness-associated genes were enriched, pointing to their importance in the central auditory system. Among them were the transcription factors Gata3, Sox10, Hoxa2, Mitf, and Esrrb, which may ensure coordinated development and function of the peripheral and central auditory system. Furthermore, CaV1.3, previously associated with peripheral deafness, was demonstrated to be functionally expressed also in the SOC. Finally, we observed a trend of SOC-related genes to be overrepresented in human deafness loci. The enrichment of deafness-related genes in the SOC may have implications for restoring hearing, as central auditory structures might be more severely affected by mutation of these genes than previously appreciated.

1024 The Effects of Stimulus Uncertainty and Musical Experience on Auditory Temporal Interval Discrimination

Karen Banai¹, Shirley Fisher¹, Ron Ganot¹ ¹University of Haifa

Both musical experience and stimulus uncertainty are known to influence frequency discrimination, but whether these non-sensory effects are specific to the frequency domain or extend to auditory processing in general remains unclear. Our current goal was therefore to investigate the effects of stimulus uncertainty and musical experience on auditory temporal processing. In experiment 1 (n=34), temporal interval discrimination was compared between conditions in which a single base temporal interval (50, 100, 200 or 350 ms) was presented repeatedly across all trials and conditions in which one of two base intervals (100 and 350 or 50 and 200 ms) was randomly selected to be presented on each trial. Discrimination of naïve listeners was significantly poorer in the random compared with the single interval conditions for all base intervals and irrespective of whether the randomly mixed intervals were marked with tones of the same (1kHz) or of different (1 and 4 kHz) frequencies. In experiment 2 (n=24), discrimination thresholds of musicians and non musicians on a target temporal interval (100ms, 1kHz) were compared across 3 conditions: a single interval condition in which the target interval was presented repeatedly across trials, a random condition in which the target was randomly interleaved with a second interval (350 ms, 1kHz) and a random condition in which the second interval was marked with a different frequency (350ms, 4kHz). Musicians outperformed non-musicians on all 3 conditions, but the effects of randomization were similar in the two groups. Taken together, it appears that discrimination. like freauencv temporal interval discrimination also benefits from the opportunity to anchor to a repeated reference tone. Musical experience, while improving performance, did not seem to alter the anchoring effect suggesting that improved discrimination skills among musicians are not likely an outcome of more sensitive anchoring or predictive coding mechanisms.

1025 The Effect of Context in the Perception of an Ambiguous Pitch Stimulus

Claire Chambers¹, Daniel Pressnitzer¹ ¹*Ecole Normale Supérieure*

We investigated hysteresis and context effects in the pitch perception of Shepard tones (Shepard, J Acoust Soc Am, 1964). Hysteresis is a memory-like phenomenon which occurs in systems whose present state depends on recent history. Shepard tones are complexes of sinusoidal components with an octave relationship, filtered by a fixed Gaussian envelope. When two such tones with different fundamental frequencies (F0) are presented successively, the dominant cue for judging pitch direction is the logfrequency proximity between components. At an FOinterval of a half-octave (6 semitones, or a tritone), the pitch direction heard is ambiguous. We investigated hysteresis in Shepard tones in several different conditions, which were presented to subjects as series of trials. In the first condition, Shepard tone pairs were presented with a fixed F0-interval of 6 semitones. The order of standard and test tones within each trial was random. Subjects indicated whether they heard upward or downward pitch change. Perception was ambiguous across subjects and series, but remarkably stable within series. In a second condition, F0intervals (from 1 to 11 semitones) were presented in random order. Hysteresis was observed: the percept in a given trial was biased by the percept in the previous trial. Hysteresis was confirmed in additional conditions where F0-intervals were presented in increasing or decreasing

series. Unlike previous investigations, hysteresis is observed with an equivalent number of upward or downward responses. Thus, the biases observed cannot be attributed to response perseverance and are likely to be perceptual in origin. It is possible to produce strong hysteresis in pitch perception by using ambiguous stimuli. Additional results will be presented pertaining to the underlying mechanisms of the effect observed. Our method creates possibilities for future investigations of the neural bases of pitch as activity may be recorded for different subjective percepts caused by the same stimulus.

1026 Frequency Specificity of Auditory Stream Biasing

David Weintraub¹, Joel Snyder¹

¹University of Nevada

During repeating sequences of low (A) and high (B) tones in an ABAB pattern, the likelihood of hearing two separate streams ("streaming") increases with more repetitions of the patterns, a phenomenon referred to as "buildup". Previous studies have shown that buildup is frequency specific (Anstis & Saida, 1985) and that its biasing effects decays over several seconds (Beauvouis & Meddis, 1997). But no study has examined whether the frequency specificity of buildup persists for such a long duration. Previous studies have also not determined whether buildup completely decays over this duration. To address these issues, we presented trials in which variable context sequences were always followed by a constant test sequence of 4 repeating ABAB patterns, with A and B tones separated in frequency by 6 semitones. Context sequences consisted of a 10-sec silence or a 10-sec sequence of 111 repetitive tones of constant frequency that differed from the B-tone frequency of the test sequence by 0, 3, or 12 semitones. The delay interval between context and test sequences was 0, 1, 4, or 8 sec long. The results showed that (1) when the context tone matched the B-tone of the test, buildup was strongest at the 0-sec interval and declined with longer intervals, (2) for non-matching context tones, smaller buildup effects occurred at the 0-sec interval and showed less decay with longer intervals, and (3) non-silent contexts resulted in more buildup compared to silent contexts even at the longest intervals. These results confirm the presence of a frequency-specific component of buildup that may be longer-lasting than previously recognized and further supports the presence of a non-frequency-specific component that is also long-lasting.

Supported by NSF grant BCS-1026023.

1027 Informational Masking Paradigm Reveals Auditory Stream Segregation in Gerbils (Meriones Unguiculatus)

Lena-Vanessa Dollezal¹, Georg M. Klump¹ ¹Animal Physiology & Behavior Group, IBU, Carl-von-Ossietzky University

The process of segregation and grouping of sounds in forming auditory objects is advantageous for survival in the acoustic world. The sequential grouping of sounds in perception is called auditory streaming (Bregman 1990). Many studies in humans applying a range of paradigms have evaluated the sound characteristics that influence the auditory streaming effect. Unfortunately, only in few cases these paradigms could be transferred to animal experiments offering the opportunity to study the neural correlates of streaming on a cellular basis.

Ideally, the same paradigm would be applied both in humans and the animal models. Here we demonstrate that an informational masking paradigm developed by Winkler et al. (2003) allows comparing directly auditory streaming in humans and gerbils, an animal model well established in auditory research. Gerbils and humans were trained with the method of operant conditioning using positive reinforcement (gerbils - food reward, humans - visual feedback) in a Go/NoGo procedure. The task of the subjects was to report an increase in level of a deviant tone in a sequence of standard tones. Intervening tones varying in level were either presented with frequencies close to the frequency of the standard (one-stream condition) or with remote frequencies (two-stream condition). The resulting intensity discrimination thresholds were significantly higher in the one-stream condition than in the two-stream condition. The threshold values in humans and in gerbils were similar. The results demonstrate the suitability of the informational masking paradigm to study auditory stream segregation in the gerbil also offering the possibility to evaluate its underlying physiological basis.

Supported by the DFG (SFB TRR 31), the EU project Scandle, and by a Georg Christoph Lichtenberg stipend of Lower Saxony to L.-V. Dollezal.

1028 Substrates of Spatial Stream Segregation

John Middlebrooks¹, Chen-Chung Lee¹, Lauren Javier¹ ¹UC Irvine

In a complex auditory scene, listeners can assign multiple interleaved sequences of sounds ("streams") to discrete auditory sources. The physical locations of sources contribute strongly to such stream segregation. In some conditions, a separation of as little as 5° can permit nearly perfect segregation of two interleaved pulse trains by a human listener. We are examining stream segregation by neurons in the primary auditory cortex of anesthetized cats. We present alternating noise bursts from two speakers and quantify the spikes synchronized to one or the other speaker. Single neurons show prominent stream segregation in the sense that neurons can synchronize exclusively to one or the other sound source when the sources are separated by as little as 10°. Differences in proximal sound levels introduced by head and pinna acoustics contribute to spatial streaming, but the resulting "better ear effect" is not sufficient to account for the results. Ongoing experiments are quantifying the relative importance of high frequencies, which provide spatial cues in the form of interaural level differences, and low frequencies, which provide interaural phase differences. Ongoing study of differences among spatial streaming in various cortical lamina is intended to identify intra-corticalversus-sub-cortical contributions to spatial stream segregation.

supported by NIH grant RO1 DC00420

1029 Localization of Two Simultaneous Sound Sources: The Role of Amplitude Modulation

William A. Yost¹, **Christopher A. Brown**¹, Farris M. Walling¹

¹Arizona State University

When two spatially-separated sources produce sound at the same time, the resulting interaural time and level differences (ITD, ILD) can vary between those associated with each of the individual sound sources (thereby producing reliable interaural cues indicating the position of one or the other source) and spurious ITDs and ILDs not indicating the position of either source. The instantaneous variation in the ITD and ILD cues depends on changes in the relative levels of the two sound sources. That is, reliable ILD and ITD cues are modulated in concert with the amplitude modulation occurring for each sound source. In the current study, listeners participated in three experiments design to measure sound localization of two sources producing independent broadband noises at the same time. The noises were sinusoidally amplitude modulated (SAM) either in phase at the two sources or 180-degrees out of phase. In Exp. I, listeners were asked to judge the location of each of the two sound sources producing independent noises. Performance was more accurate for the out-of-phase conditions than for the inphase conditions even at high modulation rates. At low modulation rates, the out-of-phase condition produced the percept of a noise that appeared to oscillate between the two source locations. In Exp. II, listeners indicated that they perceived a change in source position when the SAM rate was less than approximately 20 Hz. In Exp. III, listeners were able to discriminate between the in-phase and out-of-phase SAM noise conditions up to rates as high as 200 Hz. The results will be discussed in terms of how interaural cues may be used in judging the location of two (or more) sources producing sound at the same time. [Work supported by NIDCD grants R01-DC01376 and R01-DC008329]

1030 The Role of Spectro-Temporal Continuity for Spatial Release from Masking Antje Ihlefeld¹, Ruth Y. Litovsky¹

¹University of Wisconsin-Madison

For normal-hearing (NH) listeners, target-masker spatial separation can improve speech intelligibility, a benefit known as spatial release from masking (SRM); this effect is considerably reduced for bilateral cochlear implant (CI) users. Because SRM can occur in vocode simulations with NH listeners even when only envelope cues are being transmitted, the lack of temporal fine structure cues and impoverished binaural sensitivity in CIs can only partially predict poor SRM. This study investigated potential contributions to SRM of two factors: energetic masking, i.e., access to speech segments with a sufficiently high target-to-masker energy ratio, and spectro-temporal

continuity. To simulate CIs in NH listeners, speech was band-pass filtered into eight linearly spaced spectral bands, their envelopes multiplied with low-noise noise carriers and summed to create noise-vocoded speech. Target and masker energy overlapped either strongly or weakly in time and frequency. Spectro-temporal continuity was manipulated: target and masker bands were either temporally gated in alternating 10-ms cycles, such that the odd frequency bands were gated on while the even bands were gated off, followed by gating off the odd and gating on the even bands, or target and masker were temporally continuous and co-gated, such that each source consisted of either the odd or the even bands only. SRM was somewhat smaller when target and masker energy had strong overlap than when the overlap was weak. Moreover, conditions with high spectro-temporal continuity had smaller SRM than those with low continuity, regardless of amounts of energetic overlap. We consider the hypothesis that continuity provides cues that are redundant with spatial cues for selecting the target. [supported by NIH DC003083]

1031 Temporal Interactions Between Speech and Masker Leading to Masking Release or Modulation Interference in Cochlear Implant and Normal Hearing Listeners

Bomjun J Kwon¹, Cassie Wilhelm¹, Eric W Healy¹ ¹The Ohio State University

Normal hearing (NH) listeners maintain speech understanding in fluctuating noise through masking release (MR), in which the speech is revealed during momentary minima of the masker. Cochlear implant (CI) listeners, however, do not typically show such resiliency. In fact, modulation interference (MI) has been sometimes observed, in which speech understanding is poorer in fluctuating than steady noise. In the present study, it was hypothesized that the amount of temporal overlap between speech and masker determined whether the masker produced either MR or MI. Speech Recognition Thresholds (SNR at 50% sentence recognition) were assessed under the following conditions: 1) max-MR (the instantaneous amplitude of the noise masker was opposite of the speech envelope), 2) min-MR (the noise envelope was correlated with the speech envelope), and 3) steady noise. Because SNR was the dependent variable, only differences in temporal overlap were examined. Preliminary results indicate that NH listeners demonstrate substantial MR, as expected, as large as -20 dB SNR in the max-MR condition, while the difference between the min-MR and steady conditions is not significant. Results obtained from 6 CI subjects to date are diverse. Two subjects show a pattern very similar to NH, with clear evidence of MR (max-MR versus steady). In another two subjects, while the effect of MR disappears, the differential effect between max- and min-MR remains. For the other two, the performance degrades with fluctuating envelope noise relative to steady noise, i.e., MI is in effect, regardless of temporal overlap. Thus, temporal interactions between speech and noise play an important role in both NH and CI users and deserve careful consideration. The results

indicating MI in some CI users and MR in others suggest that CI users might have access to mechanisms of speech understanding different from one another and in some cases different from NH listeners [study supported by NIH—R03DC009061, R01DC008594].

1032 The Role of Upward Spread of Masking in the Ability to Benefit from Asynchronous Glimpsing of Masked Speech

Erol J. Ozmeral¹, Emily Buss¹, Joseph W. Hall, III¹ ¹Department of Otolaryngology/Head and Neck Surgery, University of North Carolina at Chapel Hill

Masked speech perception can be improved with the introduction of amplitude modulation (AM) applied to the masker. Howard-Jones and Rosen [1993, JASA 93, 2915-2922] tested whether asynchronous AM of neighboring masker bands also confers some degree of advantage. A benefit of asynchronous masker AM was observed in that study, but only when the masker bands were spectrally wide. The goal of the present study is to determine whether upward spread of masking (USM) at the periphery plays a role in the failure to benefit from asynchronous AM with narrow masker bands. The target speech was a set of 12 VCVs, and the masker was a pink noise. Speech and noise stimuli were filtered into 2, 4, 8, or 16 nonoverlapping log-spaced frequency bands spanning 0.1 to 10 kHz. In AM conditions, the noise bands were then modulated via multiplication with a smoothed 10-Hz square wave, with modulation either coherent or 180° out-ofphase in neighboring bands. To determine the effects of USM, speech and noise bands were either presented diotically or dichotically, with odd and even numbered bands presented to opposite ears. Speech reception thresholds (SRTs) were measured, and unmasking was calculated as the difference in SRT between the AM and steady noise cases. In the mean data, masking release was 5-8 dB larger in the dichotic than the diotic asynchronous AM conditions, a result that is consistent with detrimental effects of USM in the diotic condition. These results demonstrate that listeners are able to benefit from non-comodulated glimpses of speech cues distributed across frequency and across ears, even for relatively narrow masker bands. Bandwidth effects previously observed can be partly but not entirely attributed to USM. [Work supported by NIH R01 DC000418]

1033 Beyond Normal Hearing: The Importance of Supra-Threshold Temporal Fine Structure Processing

Dorea Ruggles¹, Barbara Shinn-Cunningham¹ ¹Boston University

Most young and middle-aged listeners have "normal" hearing, which simply means that quiet sounds in a standard range of frequencies are audible to them. In complex settings, however, background noise and multiple talkers pose a greater challenge to some normal listeners than to others, even if they have normal pure-tone detection thresholds. We tested 50 normal hearing adults aged 18 - 55 on a taxing, spatial selective auditory

attention task that required them to report a stream of digits spoken from a source simulated from directly ahead (azimuth 0°) while ignoring competing digit streams spoken by the same male talker from simulated locations 15° to the left and 15° to the right. Subjects showed large individual differences in performance on this task, and the variability was not related to age or working memory span. Frequency modulation (FM) and interaural time difference (ITD) detection tasks were completed by the top and bottom guartiles of performers in the spatial attention task; these measures correlated with performance on the original task, implicating temporal fine structure processing. The same subjects completed a complex auditory brainstem recording EEG session, which showed that brainstem encoding of a speech sound presented in noise is also related to scores in the spatial selective attention task. These relationships show that the ability to direct spatial selective attention (a high-level cognitive task) is dependent on peripheral coding of supra-threshold timing information. NIDCD, ONR, and NSF provided funding to support this work.

1034 Predicting Spatial Benefit in Older Listeners

Frederick Gallun¹, Anna Diedesch¹

¹National Center for Rehabilitative Auditory Research, Portland VA Medical Center

The benefit of spatial separation in a multi-talker environment was assessed for listeners varying in age and degree of hearing loss. Subjects were recruited such that a range of ages was represented, pure-tone sensitivity ranged from normal to mild losses, and age and pure-tone sensitivity were largely uncorrelated. Speech recognition ability was measured for targets masked by two competing talkers, using recordings from the Coordinate Response Spatial benefit was examined by Measure corpus. comparing performance for co-located and spatiallyseparated target and masking talkers. Spatial separation involved symmetrical loudspeaker placement in an anechoic chamber, resulting in no changes in target-tomasker ratio at either ear based on spatial configuration. Age, pure-tone sensitivity, and sensitivity to interaural differences in time all correlated with spatial benefit. Multiple linear regression demonstrated independent contributions of aging and hearing loss to reduced spatial benefit, mediated by reduced sensitivity to interaural differences in time. Results suggest that accurate prediction of spatial benefit, and therefore success in multitalker environments, requires taking into account the age of the listener, especially when hearing sensitivity is normal or only mildly impaired. [Supported by VA RR&D CDA2 C4963W]

1035 Intra- And Inter-Modal Spatial Attention: A Case of Counting Flashes 'n Beeps

Jennifer Bizley^{1,2}, Barbara Shinn-Cunningham^{3,4}, Adrian KC Lee^{5,6}

¹Department of Physiology, Anatomy and Genetics, University of Oxford, ²Departments of Cognitive & Neural Systems Boston University, ³Hearing Research Center, Boston University, ⁴Departments of Cognitive & Neural Systems and Biomedical Engineering, Boston University, ⁵Department of Speech & Hearing Sciences, University of Washington, ⁶Intitute for Learning and Brain Sciences, University of Washington

In the "flash-beep" illusion, observers report seeing two light flashes when a single flash is presented with two brief sounds. Correspondingly, flash "fusion" may occur when two light flashes are paired with a single sound, causing listeners to report one flash. Here we explored whether spatial attention influences these effects by presenting two competing auditory-visual (A-V) stimulus pairs, one from the left and one from the right. Each A-V pair could contain either one or two beeps and either one or two flashes. We asked observers to direct attention to either left or right and to report both the number of beeps and the number of flashes from that location. As a control, we also tested unisensory stimuli. To aid source separation, the competing simultaneous sounds from left and right differed in timbre and spectral content and the flashes varied in color (in both cases counter balanced for side of presentation). Unisensory results in both the auditory and visual tasks showed that subjects were unable to ignore the unattended stream; responses were biased by the number of events in the unattended direction. When subjects were presented with combined auditory-visual stimuli, we observed sound-induced illusions (consistent with those previously reported in the literature) that were similar in magnitude to the 'confusions' observed in the unisensory visual conditions. The probability of a subject reporting a sound-induced illusion was greater when the illusion-inducing sound was presented from the attended location than from the unattended location. Observers were better able to ignore the unattended location when the auditory-visual stimuli at the attended location were congruent than when they had a different number of events. Together, these results reveal an influence of spatial congruence in determining how multi-sensory inputs combine to elicit sensory percepts.

Funded by L'Oreal-UNESCO, the Royal Society [JB], NSF-CELEST [BGS-C] and NIH-K99DC010196 [AKCL].

1036 Auditory-Tactile Integration in Musical Meter Perception

Juan Huang^{1,2}, Darik Gamble¹, Kristine Sarnlertsophon¹, Xiaoqin Wang¹, Steven Hsiao¹

¹The Johns Hopkins University, ²Beijing University

Music is not only heard by our ears, but also felt through the tactile system. To explore how auditory and tactile inputs are combined during musical meter perception, we studied how human subjects perceive 'duple-tending' (march-like rhythms) and 'triple-tending' (waltz-like rhythms) music note sequences. Subjects were given these music sequences under three conditions, 1) Unimodal, 2) Bimodal (auditory and tactile channels were each assigned interleaved parts of a sequence), and 3) Matched and Unmatched meter (meter cues in the two channels either agreed or conflicted). Results show that human subjects perceive meter equally well when presented with unimodal tactile or unimodal auditory cues (percent correct = 75%). We further show in bimodal experiments that auditory and tactile cues are integrated to produce coherent meter percepts. In these experiments, meter perception performance is between 70% and 90% when metrically important notes are assigned to the auditory and tactile channels respectively while the other channel contains the remaining notes. Performance is reduced to 60% when half the metrically important notes are assigned to one channel while half remain in the other channel. When presented simultaneously, matched meter cues from auditory and tactile channels enhance meter recognition to around 90%. Performance drops to 10% when subjects are presented with auditory conflicting cues and 60% with tactile conflicting cues. These findings show that the perception of music meter in human subjects involves both auditory and tactile information. demonstrating that meter and music perception is a cross modal percept and is not isolated to the auditory system. Supported by a JHU Brain Science Initiative grant (X.W. and S.H.), NIH grants DC03180 (X.W.).

1037 Empirical Derivation of Acoustic Grouping Cues from Natural Sound Statistics Josh McDermott^{1,2}, Dan Ellis³, Eero Simoncelli^{1,2}

¹New York University, ²Howard Hughes Medical Institute, ³Columbia University

The ear typically receives mixtures of sounds, from which listeners perceive individual sound sources of interest. Many sets of sound signals are physically consistent with the mixture that enters the ear, and the brain must use its knowledge of natural sounds to infer which set actually occurred in the world. Certain sound properties have long been viewed as grouping cues – frequencies with concurrent onsets or offsets, for instance, seem likely to be due to the same source, and are heard as such. Natural sounds could potentially contain many such cues, some of which might not be intuitively obvious. Here we propose an empirical framework for investigating the cues that could underlie sound segregation.

Our approach stems from the observation that the signals in incorrect mixture decompositions will themselves tend to be partial mixtures of the true sources. Grouping cues might thus be sound properties that have different values for individual sources compared to mixtures. Using databases of natural sound source recordings, we can evaluate sound statistics of individual sources and their mixtures, and search for statistics that should be useful for segregation.

We processed thousands of speech excerpts and their mixtures with an auditory model – a cochlear filter bank followed by a modulation filter bank. From these filter responses we measured a large set of simple statistics that we have shown to be perceptually relevant in the analysis and synthesis of natural sound textures (McDermott & Simoncelli). The statistics included marginal statistics, capturing sparsity and modulation power, and correlations between filter responses. We found that most statistics, some of which relate to conventional grouping cues, helped to discriminate sources from mixtures. The results suggest that acoustic grouping cues are more diverse than has previously been suspected, and point the way to new perceptual experiments and machine algorithms for sound segregation.

1038 Brain Bases of Auditory Stimulus-Driven, Figure-Ground Segregation

Sundeep Teki^{1,2}, Maria Chait³, Sukhbinder Kumar^{1,2}, Katharina von Kriegstein⁴, Timothy D. Griffiths^{1,2} ¹Wellcome Trust Centre for Neuroimaging, University College London, ²Newcastle University Medical School, ³UCL Ear Institute, University College London, ⁴Max Planck Institute for Human Cognitive and Brain Sciences Auditory figure-ground segregation, listeners' ability to selectively hear out a sound of interest from a background of competing sounds, is a fundamental aspect of scene analysis.

In contrast to the disordered acoustic environment we experience during everyday listening, most studies of

auditory segregation have used relatively simple, temporally regular signals. We developed a new figureground stimulus which incorporates stochastic variation of the figure and background that capture the rich spectrotemporal complexity of natural acoustic scenes. Figure and background signals overlap in spectrotemporal space, but vary in the statistics of fluctuation and the only way to extract the figure is by integrating the patterns over time and frequency. Our behavioral results demonstrate that human listeners are remarkably sensitive to the appearance of such figures.

In a functional magnetic resonance imaging experiment, aimed at investigating pre-attentive, stimulus-driven, auditory segregation mechanisms, naïve subjects listened to these stimuli while performing an irrelevant task. Results demonstrate significant activations in the intraparietal sulcus (IPS) and the superior temporal sulcus related to bottom-up, stimulus-driven, figure-ground decomposition. We did not observe any significant activation in the primary auditory cortex. The IPS activation is consistent with accumulating evidence suggesting a role for the IPS in structuring sensory input and perceptual organization. Our results support a role for automatic, bottom-up mechanisms in the IPS in mediating stimulus-driven, auditory figure-ground segregation

Author Index (Indexed by abstract number)

Abbas, Paul, 424 Abdala, Carolina, 101, 369, 376 Abe, Yasuhiro, 753 Abrams, Kristina S., 480 Acker, Leah, 484 Acock, Keena, 1004 Adams, Joe, 121, 859 Adams, Meredith E., 134 Adelman, Cahtia, 603 Adjamian, Peyman, 159 Admiraal, Ronald, 805 Aernouts, Jef, 49, 50 Afram, Renee K., 699 Agrawal, Sumit K., 56 Aguiar, Daniel, 967 Aguilar, Enzo, 182 Ahmad, Faisal I., 478 Ahmad, Iram, 426 Ahmad, Shoeb, 109, 112, 332 Ahmed, Zubair, 815 Ahmed, Zubair, 815 Ahn, Joong Ho, 209, 415 Ahn, Jungho, 264 Ahveninen, Jyrki, 958 Aizenman, Elias, 434 Akeroyd, Michael, 191, 193, 744 Akil, Omar, 403, 618, 636, 820 Akiyama, Takuya, 635 Alagrama Kumar, 549, 821 Alagramam, Kumar, 549, 821 Alamilla, Javier, 698 Albert, Sandrine, 764 Alexandrov, Vladimir, 1008 Alexandrova, Olga, 697 Alexandrova, Tamara, 1008 Ali, Hesham, 69, 78 Allen, Daniel, 291 Allen, Paul, 192, 889 Alliston, Tamara, 618 Allman, Brian L., 163, 164, 456, 459, 460 Almonte, Felix, 897 Alsaffar, Hussain A., 56 Altschuler, Richard A., 7, 149, 151, 152, 419, 848 Alves-Pinto, Ana, 482 Amatuzzi Monica 384 An, Lee Jung, 937 Ananthakrishnan, Saradha, 918 Anastas, Sara B., 63 Andeol, Guillaume, 181 Anderson, Kevin, 437 Anderson, Lucy, 172, 290, 724 Anderson, Samira, 142, 921 Ando, Takahiro, 635 André, Michel, 609 Andreou, Andreas, 264 Angeli, Simon, 643 Antunes, Flora, 278 Anvari, Bahman, 366 Aoyagi, Masaru, 221, 752, 753 Apostolides, Pierre, 10 Appelbaum, Meghan, 503 Applegate, Brian, 610 Appler, Jessica, 318, 530 Aranyosi, Alexander J., 84 Armstrong, Patrick, 997 Arnold, Rosemarie, 168 Aronoff, Justin, 494 Arotsker, Natan, 434 Arshed, Arslaan, 679 Arslan, Edoardo, 127 Arts, H Alexander, 388 Aruga, Jun, 1009 Ash, Megan, 676, 830 Ashmore, Jonathan, 575 Asp, Filip, 736 Assmann, Peter, 224 Atkinson, Patrick, 637 Augustine, George, 483, 541 Auth, Tanja, 132 Avenarius, Matthew, 136, 817 Avraham, Karen B., 808, 810, 991 Axe, David R., 480 Azem, Rami, 340 Baasov, Timor, 905

Back, Sang A., 403 Badea, Alexandra, 935 Bae, Ji Hye, 516, 774 Baek, Jeong-In, 135 Báez, Adriana, 763 Bahmer, Andreas, 680 Bai, Jun-Ping, 568, 569 Bailey, Erin, 393, 424 Baizer, Joan S., 431 Bajo Lorenzana, Victoria M, 732 Baker, Tiffany, 624 Balaban, Carey, 412, 1003 Balachandra, Ramya, 234 Balaker, Ashley, 864 Bali, Sulzhan, 811 Balkany, Thomas, 643, 644 Balkwill, David, 1000 Ballestero, Jimena, 582 Balough, Ben, 412 Bamberg, Ernst, 541 Bamiou, Doris-Eva, 379 Banai, Karen, 1024 Banakis, Renee, 489 Band, Hamid, 822 Bandyopadhyay, Sharba, 715. 927 Bao, Jianxin, 428, 654 Barbash, Daniel J., 992 Barbour, Dennis, 667, 741 Bardin, Fabrice, 764 Barhanin, Jacques, 246 Barker, Daphne, 940 Barker, Matt, 908 Barlow, Linda, 272 Barral, Jeremie, 347 Barria, Andres, 694 Bartles, James, 550 Bartlett, Edward, 143 Bartolami, Sylvain, 246 Barton, Matthew, 33 Bartsch, Dusan, 1023 Baskent, Deniz, 964 Basta, Dietmar, 215, 289, 913, 923 Batezati, Silvia, 376 Battey, Jr., James, 1 Batts, Shelley, 558 Baumann, Simon, 704 Baylan, Muzeyyen, 383 Bec, Jean Michel, 764 Bee, Mark, 980, 982 Behniwal, Gurbir, 249 Behra, Martine, 309 Behroozmand, Roozbeh, 747 Beisel, Kirk, 39, 67, 76, 313 Békésy, Georg von, 29 Belliveau, John W., 958 Belyantseva, Inna A., 275, 815 Belzner, Katharine, 104 Benedict-Alderfer, Cindy, 339, 814 Benson, Chelsea, 177 Benson, Thane, 881 Bergevin, Christopher, 371, 372, 373, 797 Bergles, Dwight, 418 Berman, Daniel, 317 Bernardeschi, Daniele, 505 Berninger, Erik, 736 Bernstein, Joshua, 751, 959 Bernstein, Leslie, 954, 955 Berrebi, Albert, 888 Best, Virginia, 497, 972 Beurg, Maryline, 345, 579, 581 Beyer, Lisa, 14, 134, 136, 427 Bhatt, Shrutee, 671 Bhutta, Mahmood F., 811 Bian, Lin, 368, 602 Bian, Shumin, 72, 80 Bibas, Athanasios, 379, 780 Bidelman, Gavin, 669, 918, 919 Bierer, Julie, 292 Bierer, Steven, 266, 267 Bierman, Hilary, 468 Biesemeier, Deborah J., 1016

Billings, Curtis, 220 Bininda-Emonds, Olaf, 1023 Bird, Jonathan, 65 Bishop, Brian, 464 Bishop, Christopher, 951 Bizaki, Argryo, 422 Bizley, Jennifer, 713, 1035 Blachon, Gregoire, 234 Blasbalg, Samantha, 707 Blatt, Melissa, 506 Bleser, Tana, 514 Blevins, Nikolas, 558 Bloomberg, Jacob, 504, 1004 Bodson, Morgan, 1012 Boerboom, Ralf, 178 Boesen, Michael, 887 Boettger, Thomas, 862 Bohorquez, Jorge, 643, 644 Bologna, William, 375 Bonham, Ben, 216, 703 Bonine, Kevin, 373 Bonnard, Åsa, 328 Bonneux, Sarah, 815 Borecki, Alexander, 692 Borecki, Alexander, 692 Boren, Aaron, 291 Borenstein, Jeffrey, 855, 856 Borgs, Laurence, 1012 Borst, J. Gerard G., 300, 321, 686, 695, 876 Bosen, Felicitas, 132 Bouleau, Yohan, 579, 581 Boutet de Monvel, Jacques, 575 Boyden, Ed, 484 Boyden, Edward, 537 Boyen, Kristiana, 158 Boyle, Patrick, 215 Bozorg Grayeli, Alexis, 389, 505, 642 Bozovic, Dolores, 350, 351, 352, 354, 559 Brandon, Carlene, 624, 904 Brandt, Christian, 373, 468 Brandt, Niels, 316, 656 Braun, Nadine, 887 Braun, Thomas, 862 Bremen, Peter, 701 Bremer, Tristan, 502 Brenowitz, Stephan, 11, 429, 432, 433 Bretan, P. Mason, 853, 854 Brette, Romain, 948 Breuskin, Ingrid, 1012 Brewer, Carmen, 217 Brigitte, Malgrange, 34 Brimijoin, W. Owen, 193 Brookes, Matthew, 159 Broussey, Audrey, 994 Broussy, Audrey, 247 Brown, Andrew D., 949, 950 Brown, Christopher, 293, 1029 Brown, David, 757 Brown, M. Christian, 484, 539. 881 oo 1 Brown, Nadean, 273 Brown, Steve D.M., 811 Browne, Cherylea, 457, 458 Brownell, William, 70, 73, 75, 77, 355, 356, 366 Brownstein, Zippora, 810 Brubaker, Donald, 447 Bruce, Ian, 678, 742 Brugeaud, Aurore, 247, 762, 846, 994 Brugge, John, 942 Brungart, Douglas S., 743 Brunner, Daniel, 598 Bryan, Keith E., 120 Budenz, Cameron Lind, 838 Bures, Zbynek, 446 Burger, R. Michael, 878, 879, 880 Burgess, Shawn, 43, 309 Burke, David T., 151, 152 Burkitt, Anthony, 678 Burns, Joseph, 22

Burnside, Beth, 551 Buss, Emily, 1032 Butcher, Stephen, 424 Butler, Caty, 988 Butts, Daniel, 443 Buytaert, Jan, 45 Cagaanan, Alain, 424 Cai, Hongxue, 53 Cai, Qunfeng, 404, 410 Calixto, Roger, 277, 450 Calzada, Audrey, 113 Camarena, Vladimir, 241, 760 Campagnola, Luke, 689 Campbell, Courtney, 162 Campbell, Dean, 33 Campbell, Kathleen, 786 Canlon, Barbara, 27, 124, 416, 911 Cant. Nell. 935 Cao, Lin, 599 Cao, Xiao-Jie, 681 Carey, John, 507, 512 Carey, Thomas E., 388 Carlin, Michael, 283 Carlyon, Robert, 295, 917, 945 Carney, Laurel, 480, 891, 992 Capelle, Vincent, 591 Carolyne, Garnham, 483 Carr, Catherine, 44, 463, 468 Carver, Courtney, 987, 988 Case, Daniel, 324 Caspary, Donald, 525 Castellano-Munoz, Manuel, 585 Castiglioni, Andrew, 552 Cazevieille, Chantal, 609 Cediel, Rafael, 147 Celik, Seymanur, 493 Cepko, Connie, 305 Cervantes, Vanessa, 212 Ceschi, Piera, 645 Cha, Kiweon, 865 Chabbert, Christian, 128, 246, 247, 762, 764, 994 Chadwick, Richard, 87, 346, 1015 Chai, Renjie, 21, 35, 310, 594 Chait, Maria, 1038 Chalfie, Martin, 2 Chamberlain, Kelly, 447 Chambers, Anna, 620 Chambers, Claire, 1025 Champneys, Alan R., 89 Chan, Siaw-Lin, 307 Chanda, Soham, 690 Chang, Brian, 858 Chang, Nick N-Y, 1005 Chang, Qing, 112, 816 Chang, Weise, 1018 Chao, Moses, 241, 760 Chapman, Edwin R., 579 Charitidi, Konstantina, 124 Charizopoulou, Nikoletta, 805 Charziak, Karolina, 186 Chatterjee, Monita, 375, 476, 750, 986 Cheatham, Mary Ann, 68, 103 Cheeseman, Michael T., 811 Chekroud, Karim, 764 Chen, Chen, 892 Chen, Daniel, 821 Chen, Fangyi, 360, 365 Chen, Fuquan, 905 Chen, Guang-Di, 131, 133, 144, 163, 395 Chen, Hui E, 814 Chen, Jessie, 71 Chen, Jing, 807, 812, 825 Chen, Joseph, 141 Chen, Kejian, 647, 909, 912 Chen, Lin, 716 Chen, Ping, 15, 36, 1013 Chen, Qingguo, 573 Chen, Shiuhwei, 545 Chen, Shu, 149, 151, 152 Chen, Spencer, 457

Chen, Wei Chun, 660 Chen, Yan, 560 Chen, Zheng-Yi, 20, 40, 139, 589 Cheng, Alan, 21, 35, 310, 594 Cheng, Christie, 214 Cheng, Jeffrey, 51 Cheng, Weihua, 909, 912 Cheon Lee, Byung, 815 Cheon, Jinwoo, 559 Cherniavsky, Marina, 905 Chertoff, Mark, 602, 676, 830 Cheung, Eunice, 558 Cheung, Linda, 137 Chevallier, Keely, 61, 733 Chhan, David, 47 Chi, Fanglu, 561, 845, 1013 Chiang, Bryce, 264, 509, 510 Chiba, Hiroyuki, 752, 753 Chidavaenzi, Robstein, 828 Chikar, Jennifer, 440, 933 Chintanpalli, Ananthakrishna, 668 Chiu, llene, 411 Cho, Edward, 513 Cho, Soyoun, 583 Cho, Yang-Sun, 755 Choi, Yang-Sun, 755 Choi, Byung Yoon, 806, 809 Choi, Chul-Hee, 602, 648, 909 Choi, Dongseok, 829 Choi, Eun-Young, 866 Chei, Hansel, 201 Choi, Hoseok, 391 Choi, Jae Young, 230, 336, 341, 382, 866 Choi, Jeong-Seok, 518 Choi, Seong Jun, 613 Choi, Seung Hyo, 415 Choi, Su-Jin, 135 Chole, Richard, 547 Chonko, Kurt, 840 Choo, Daniel, 640 Chou, Shih-Wei, 551 Choudhury, Baishakhi, 478 Choudhury, Niloy, 360 Choudnury, Niloy, 360 Choung, Yun-Hoon, 613, 902 Chow, Cynthia, 598 Christensen-Dalsgaard, Jakob, 44, 373, 463, 468 Christianson, G. Bjorn, 290, 724 Chumak, Tetyana, 446 Chuna Bom Xi, 407 Chung, Bom Yi, 407 Chung, Jong Woo, 209, 407, 415, 619 Chung, Won-Ho, 755 Chung, Yoojin, 707 Cimerman, Jelka, 593 Ciocca, Valter, 968 Clark, Emily, 192 Clark, Jason, 426, 849 Clarke, Aaron, 863 Clarke, Joseph C., 849 Clément-Ziza, Mathieu, 1023 Clifton, William, 411 Clinard, Christopher, 938 Clinger, John D., 849 Coate, Thomas M., 1011 Coffin, Allison, 785 Cohen, Bernard, 261, 773, 996, 998, 999 Cohen, Helen, 504, 1004 Cohen, Jeremiah, 620 Cohn, Samuel, 238 Colburn, H. Steven, 707 Cole, Stephanie, 519 Coleman, William, 878, 879 Coling, Donald, 130, 144, 404, 410, 784 Conde de Felipe, Magnolia, 597 Cone, Barbara, 280 Connelly, Catherine, 436, 871 Contreras, Melissa, 842 Cooper, Alan, 323 Cooper, Kathryn, 738 Cooper, Morris, 786 Cooper, Nigel, 359 Coordes, Annekatrin, 913

Corbetta, Maurizio, 804 Cordero, Ana, 333 Cordery, Patricia M., 732 Cordes, Imke, 978 Corey, David, 555 Corfas, Gabriel, 315 Corless, Joseph, 935 Corwin, Jeffrey, 22, 827 Cosgrove, Dominic, 137, 1021 Cotanche, Douglas, 834 Cote, Emily, 872 Cowan, Devon, 447 Cramer, Karina, 532 Crane, Benjamin, 1006, 1007 Crenshaw, E. Bryan, 238, 1011 Crieghton, Francis, 235 Crins, Tom, 300, 321 Croce, Carlo, 1013 Crumling, Mark A., 14, 634 Cullen, Kathleen, 264, 265 Cunningham, Lisa, 624, 904 Cunningham, Paul, 143 Cureoglu, Sebahattin, 383 Currall, Benjamin, 69, 78 Cyr, Janet, 257 Dabin, Willy, 609 Dai, Chenkai, 59, 264, 509, 510, 511 Dai, Chunfu, 770 Dai, Huanping, 479 Dai, Min, 119, 397, 408, 409 Dalamon, Viviana, 326 Dalhoff, Ernst, 64 Dallos, Peter, 68, 71, 103 Daniel, Sam, 46 Darrow, Keith, 881 Dasika, Vasant, 938 David, Larry, 397, 633, 829 David, Stephen, 175, 729 Davidovics, Natan, 264, 508, 509, 510, 511 Davis, Kevin, 705 Davis, Matthew, 748 Davis, Rickie, 658 Davis, Robin, 423, 660, 661, 662 Dawant, Benoit, 234 Day, Mitchell, 981 Dazert, Stefan, 614 de Boer, Egbert, 95 De Dios, Yiri, 503, 1004 de Kleine, Emile, 158, 160 Dean, Isabel, 664 Deans, Michael, 245 Decker, Jennifer, 485 Decker, Margaret, 848 Decraemer, Willem, 46, 52 Deegan, Brian, 506 Deeks, John, 295 Deerinck, Tom, 314 Degen, Joachim, 132 Degollada, Eduard, 609 Dehmel, Susanne, 437 Del Castillo, Ignacio, 127 Del Rio, Tony, 317 Delaney, Katherine, 343 Delano, Paul H., 929 Delgutte, Bertrand, 664, 706, 707, 870, 981 Deliano, Matthias, 931 Delimont, Duane, 137, 1021 Della Santina, Charles, 259, 264, 265, 508, 509, 510, 511, 943, 999, 1001 Dellamary, Luis, 638 Delprat, Benjamin, 128 Demason, Christine, 478 Dempsey, Kate, 69, 78 Dent, Micheal, 976, 977 Denu, John M., 145 Depireux, Didier, 175, 709, 719 Deroche, Mickael, 476 Deroy, Kristina, 184 Deshpande, Aniruddha, 177 Desmadryl, Gilles, 762 Dettling, Juliane, 316, 656

Deveze, Arnaud, 206 Dewey, James, 377 Dhar, Sumitrajit, 101, 104, 377 Di Fiore, Pier Paolo, 819 Diaz Santaella, Francisco, 922 Dicke, Nikolai, 132 Dickey, Thomas, 627 Diedesch, Anna, 1034 Dierick, Manuel, 45 Dietz, Beatrice, 884 Dietz, Mathias, 955 Digilio, Laura, 564 Dimitriadis, Panagiotis, 379 Ding, Dalian, 161, 460, 621, 622, 625, 629, 784, 900, 910 Ding, Nai, 723 Dinh, Christine, 643, 823, 835 Dinh, John, 823, 835 Dirckx, Joris, 45, 49, 50, 52 Dittami, Gregory, 269, 540 Do, Christina, 375 Dobreva, Marina, 192 Doetzlhofer, Angelika, 33 Dolan, David, 134, 136, 149, 151, 152 Doll, Sara, 236 Dollezal, Lena-Vanessa, 1027 Donato, Roberta, 466 Dong, Wei, 364 Donnelly, Patrick, 984 Dorrn, Anja L., 173 Dottori, Mirella, 25 Doucet, John, 258 Doyle, Philip C., 56 Drayna, Dennis, 135 Drennan, Ward, 198, 199, 938, 963 Drescher, Dennis, 572, 574, 584 Drescher, Marian, 572, 574, 584 Driver, Elizabeth Carroll, 1017 Druckenbrod, Noah, 530 Drusco, Alessandra, 1013 Du. Lilin. 327 Du, Xiaoping, 647, 648, 909, 912 Duan, Chongwen, 71 Dubno, Judy, 425, 524 Duifhuis, Hendrikus, 92 Dulon, Didier, 579, 581 Dumas, Michel, 764 Duncan, Jeremy, 38 Duncan, R. Keith, 419, 565, 567, 848 Dunlap, Myles, 86 Dunlap, Stephen, 936 Dunlap, Tareishap, 71 Dupanovic, Vedran, 710 Duque, Daniel, 895 Duran Alonso, Beatriz, 597 Duran, Daniel, 280 Durham, Dianne, 710 During, Matthew, 820 Dye, Jonie, 1002 Dyhrfjeld-Johnsen, Jonas, 994 Dylla, Margit, 979 Earl, Brian, 676, 830 Eastwood, Hayden, 852 Eatock, Ruth Anne, 250, 251, 344 Eberl, Dan, 270 Ebmeyer, Jorg, 338 Eckrich, Tobias, 562, 563 Eddington, Donald K., 496, 675 Edge, Albert, 19, 20, 25, 406, 846 Edlund, Renee, 31 Edwards, Robert, 636, 820 Egami, Naoya, 867 Eggermont, Jos J., 718, 725 Egner, Alexander, 120 Ehmann, Heike, 1023 Ehret, Günter, 173 Eisenman, David, 307 Elgoyhen, A. Bélen, 326, 566, 582, 606 Elgueda, Diego, 929

Elhilali, Mounya, 283 Eliades, Steven, 731 Eliassen, James, 177 Elkan-Miller, Tal, 991 El-Kashlan, Hussam K., 388 Elkon, Rani, 307, 810 Ellis, Dan, 1037 Ellisman, Mark, 314 Ellis-Weismer, Susan, 492 El-Zonkoly, Mai, 443 Engel, Jutta, 316, 656 Englitz, Bernhard, 175, 322, 688 Epp, Bastian, 89, 91 Erben, Ulrike, 913 Erfkemper, Pia, 614 Ernst, Arne, 215, 289, 913, 923 Ernst, Bamberg, 483 Escabi, Monty, 174, 892 Escera, Carles, 922 Eshraghi, Adrien, 643, 644 Eskilsson, Gunnar, 736 Etheredge, Jack, 36 Eustaquio-Martin, Almudena, 183 Evans, Michael G., 570 Evans, Steven, 196 Ewert, Stephan, 955 Fakler, Bernd, 83 Falk, Benjamin, 973 Fallon, James, 296 Falvo, Michael, 506 Fang, Jie, 66 Fantetti, Kristen, 42 Farahbakhsh, Nasser, 571 Farhangi Oskuei, Peyman, 571 Fasquelle, Lydie, 128 Faure, Paul, 974 Fayad, Jose N., 333 Feeney, Patrick, 757 Feijoo Redondo, Ana, 597 Feil, Robert, 316, 656 Feil, Susanne, 656 Fekete, Donna, 42, 1016 Feld, Julia, 741 Feldon, Joram, 991 Feldon, Joram, 991 Felix, Richard, 888 Felmy, Felix, 700, 702 Feng, Albert, 420 Feng, Lei, 728 Ferguson, Melanie, 222 Fernandez, Rayne, 638 Fernando, Carol, 551 Ferrary, Evelyne, 389, 642 Ferreira, Marisa, 609 Ferrucci, Luigi, 140 Fetjova, Anna, 120 Fetoni, Anna Rita, 395 Fettiplace, Robert, 82, 345, 573 Fiedler, Matthew, 1004 Fiering, Jason, 855 Finley, Charles C., 478 Fischl, Matthew, 880 Fisher, Shirley, 1024 Fishman, Andrew, 486, 488 Fishman, Yonatan, 726, 727 Fitzakerley, Janet, 218, 863 Fitzgerald, Tracy, 375 Fitzgleaud, 1racy, 375 Fitzglibbons, Peter, 526 Fitzpatrick, Douglas, 478, 935 Fitzpatrick, J. Michael, 234 Flamant, Frederic, 316 Flores, Emma, 552 Flores, Kate C., 674 Floyd, Robert, 647, 648, 909, 912 Flynn, Brianna, 637 Fontecha Santos, Azucena, 597 Formby, Craig, 228 Forsythe, Ian D., 877, 908 Fortuño, José-Manuel, 609 Foust, Kevin D., 634 Fox, Daniel, 786 Francis, Howard W., 868 Francis, Nikolas A., 180 Francis, Shimon, 624, 904 Frank, Thomas, 120 Fransson, Anette, 328

Franz, Christoph, 316, 563, 819 Fredrickson-Hemsing, Lea, 350, 351, 352, 354 Freeman, Dennis. M., 84 Freeman, Dennis, M., 34 Freeman, Nancy, 257 Friauf, Eckhard, 886, 887, 1023 Fridberger, Anders, 66, 75, 355, 360, 769, 888 Fridman, Gene, 264, 508, 509, 510, 511 Friedland, David, 500 Friedman, Thomas, 135, 275, 806, 809, 815 Friedrich Jr., Victor L., 772 Friesen, Lendra, 141 Frisina, Robert, 521 Fritsch, Michael, 26 Fritz, Jonathan, 802, 934 Fritzsch, Bernd, 38, 39, 41, 313, 417, 824, 839, 840, 1009 Froehlich, Henning, 862 Froemke, Robert, 302 Frolenkov, Gregory, 349, 390, 394 Frucht, Corey, 23 Fu, Qian-Jie, 177, 201, 203, 494, 989 Fuchs, Albert, 267 Fuchs, Paul, 554, 566, 576, 577, 578, 582 Fuente, Adrian, 219 Fuhrman, Susan, 515 Fujii, Masato, 312 Fujioka, Takako, 141 Fujita, Takeshi, 386, 650 Fukui, Hideto, 14, 427 Fukushima, Hisaki, 383 Fullarton, Lynne, 149 Funnell, Robert, 46, 52 Furlong, Cosme, 51 Furman, Adam, 400 Furman, Gabriel, 520 Furman, Joseph, 515 Furness, David, 125, 549, 573, 819, 825 Furst, Miriam, 470, 477 Furuya, Nobuhiko, 768, 771 Fuzessery, Zoltan, 444, 448 Fyk-Kolodziej, Bozena, 699, 874 Gaboyard, Sophie, 128, 246, 247, 762, 764, 994 Gabriele, Mark, 447 Gadziola, Marie, 974 Gaese, Bernhard, 188 Gahlen, Felix, 310 Galano, Maria M., 388 Galazyuk, Alexander, 167 Galecki, Andrzej, 149, 151, 152 Gallardo Mendieta, Viviana, 43, 309 Gallun, Frederick, 1034 Galvin, John, 203, 989 Gamble, Darik, 1036 Gan, Rong Z., 55, 59, 60, 342 Gandour, Jackson, 918, 919 Gannon, Richard, 260 Ganot, Ron, 1024 Gantz, Bruce, 673 Gao, Simon, 610, 615 Gao, Xiang, 303 Gao, Yan, 240 Garadat, Soha, 213 García-Añoveros, Jaime, 552 Garcia-Pino, Elisabet, 883 Gardner, James, 241, 760 Garnham, Carolyn, 643 Gassner, Davina, 710 Gavara, Núria, 1015 Geffen, Maria, 282 Gehrt, Anna, 132 Gellibolian, Robert, 333 Geng, Ruishuang, 549, 821 George, Manju, 822 Gerhard, Hoch, 483

Gerling, Andrea, 656 Germiller, John, 238 Geven, Leontien, 160 Ghaffari, Roozbeh, 84 Gharibian, Lucy, 369 Gibson, Brittany, 456 Giersch, Anne, 130 Gill, Ruth M., 853, 854 Gillespie, Deda, 323, 324, 534, 698 Gillespie, Peter, 397, 557, 607, 818, 829 Gittelman, Joshua, 708 Gladyshev, Vadim N., 815 Gleichman, Julia, 834 Glowatzki, Elisabeth, 250, 554, 578, 765 Glowina, Michaela, 173 Gockel, Hedwig, 917 Godar, Shelly, 492, 495 Goeckel, Tom, 952 Gob, Eui-Kyung, 857 Gohlke, Henning, 593 Goico, Brian, 488 Gold, Susan, 228 Golden, Erin, 33 Golding, Nace, 696 Goldstein, David B., 4 Golub, Justin, 17, 596 Gomez, Gustavo, 551 Gomez-Casati, Maria, 315 Gong, Tzy-Wen, 149 Gong, Wangsong, 262, 263 Goodrich, Lisa, 317, 318, 530 Goodyear, Richard, 549, 616 Gopal, Kamakshi, 453 Gorbunov, Dmitry, 83 Gordon-Salant, Sandra, 528 Gorga, Michael P., 98 Gotoh, Norimoto, 809 Gotze, Romy, 289 Goulding, David, 807 Goupell, Matthew, 493, 961 Gourévitch, Boris, 948 Graham, Christine, 114 Grande, Emilie, 591 Granham, Carolyn, 644 Grant, Ken W., 751 Grant, Wally, 86, 248 Grason, Gregory, 550 Grassi, Elena, 751 Gratton, Michael Anne, 137, 617, 1021 Gray, Lincoln, 104, 196 Grayden, David, 678 Grecova, Jolana, 446 Green, Glenn, 237 Green, Steven, 392, 393, 398, 424 Greenberg, David, 953 Greene, Nathaniel, 705 Greger, Bradley, 279 Gregg, Melissa, 721 Griesemer, Désirée, 886 Griffith, Andrew, 806 Griffiths, Timothy, 704, 1038 Grimm, Sabine, 922 Grimsley, Jasmine, 941, 975 Groeger, Nicole, 862 Groeschel, Moritz, 215 Grollich, Katja, 913 Gröschel, Moritz, 289, 913, 923 Grosh, Karl, 93, 94 Gross, Guenter, 453 Grothe, Benedikt, 443, 697, 700, 702 Grove, Andy, 31 Grover, Mary, 421 Groves, Andrew, 18, 411 Gu, Rende, 851 Guan, Xiying, 59, 342 Gubbels, Samuel P., 598 Gubelt, Martin, 656 Guillaume, Anne, 181 Guinan, John, 96, 180, 367

Gummer, Anthony W., 64 Gundelfinger, Eckart, 120 Guo, Wei, 926 Gupta, Chhavi, 644 Gupta, Sharad, 366 Gutschalk, Alexander, 722, 939 Guymon, Allan, 849 Guyot, Jean-Philippe, 268 Haburcakova, Csilla, 262, 263 Hackett, Troy, 932 Hackney, Carole, 573, 819, 825 Hainrichson, Mariana, 905 Hakizimana, Pierre, 75, 355 Halaszovich, Christian R., 83, 115 Hall, Deborah, 159, 229, 940 Hall, III, Joseph W., 1032 Hallman, Timothy, 601 Hallows, William C., 145 Hallworth, Richard, 27, 69, 78 Halpin, Christopher, 57, 58 Halsey, Karin, 146 Hamade, Mohamad, 51, 57, 58 Hamaguchi, Kiyomi, 387, 657 Hamann, Martine, 908 Hamel, Christian, 764 Han, Chang-Duk, 518 Han, Don Yi, 327 Han, Fengchan, 339, 340, 814 Han, Gyu, 516, 774 Han, Harrison, 332 Han, Lijuan, 353 Han, Xu, 814 Han, Zhao, 561 Hancock, Kenneth, 484, 539, 620, 707, 926 Handschuh, Juliane, 931 Hansen, Marlan, 426, 673, 849 Hansen, Stefan, 126, 614 Happel, Max, 931 Hara, Akira, 652, 791 Hara, Hirotaka, 903 Harada, Tatsuhiko, 107 Harke, Benjamin, 120 Harland, Ben, 73 Harper, Nicol, 737 Harrington, Ellery, 51 Harrop, Anne, 638 Harting-Oshovsky, Lisette, 964 Hartmann, Tanja, 450 Hartsock, Jared J., 853, 854 Harvey, Margaret, 330 Hasegawa, Shingo, 386, 650 Hashimoto, Kaori, 337 Hashimoto, Makoto, 223, 995 Hashino, Eri, 26, 847 Hatfield, James, 574 Hatzopoulos, Stavros, 370 Hausman, Fran, 334, 385 Hauswirth, William, 484 Hawley, Monica, 228 Hayasaka, Takahiro, 612 Hayashi, Kentaro, 652, 791 Hayashi, Yushi, 600 Hayden, Russell, 264 Hayes, Sarah, 431, 459 Haywood, Nicholas, 968 Hazrati, Oldooz, 749 He, David, 67, 76 He, Jiao, 643 He, Shouhuan, 399 He, Wenxuan, 102, 607 Healy, Eric W., 1031 Heap, Erin, 1004 Heeren, Wiebke, 473 Hegner, Erin, 841 Heil, Peter, 469, 586 Heinz, Michael, 414, 668, 669, 670 Heller, Stefan, 21, 310, 592, 594 Helms, Cynthia, 24 Hemmert, Werner, 205, 687 Henderson, Donald, 144 Henin, Simon, 99, 100 Henry, Kenneth S., 414

Herget, Meike, 310 Herisanu, Ioana, 236 Hernandez, Victor, 483, 541 Hershfinkel, Michal, 434 Hertzano, Ronna, 304, 307 Hess, Christi, 492 Hessler, Roland, 643, 644 Hetherington, Alexander, 216, 703 Heuschen, Sylvie, 505 Heyd, Julia, 720 Hickman, Tyler, 315 Hickox, Ann E., 187 Hidaka, Hiroshi, 233 Hiel, Hakim, 577 Higgins, Nathan, 174, 285 Highstein, Stephen, 269, 540 Hill, III, Gerhard, 419 Hill, Jessica A., 877 Hilton, Helen, 811 Hilton, Jennifer, 812, 825 Hinduja, Sneha, 161, 452, 784 Hiraumi, Harukazu, 639 Hiraumi, Harukazu, bos Hirose, Keiko, 783 Hirose, Yoshinobu, 402, 626 Hirsch, June, 766 Hirsch-Shell, Dylan, 761 Hirtz, Jan, 886, 887 Hiss, Meghan, 1005 Hittner, Emily, 142, 921 Hixon, Alison, 320 Hnizda, Kristyna, 436 Ho, Andrew K., 56 Hoang Dinh, Emilie, 691 Hoare, Derek, 229 Hoch, Gerhard, 541 Hoffer, Ali, 1003 Hoffer, Michael, 412, 1003 Hoffman, Howard J., 259 Hoffman, Larry, 249, 255, 761 Hoffpauir, Brian, 314, 533 Hoffpault, Briati, 314, 355 Hohmann, Volker, 955 Holley, Matthew C., 819, 825 Holstein, Gay, 772, 773 Holt, Avril Genene, 699, 874 Holt, Jeffrey, 553, 564, 659, 805 Holt, Joseph, 243, 244 Holz, Nina, 863 Homer, Martin, 89 Homma, Kazuaki, 68 Honda, Akira, 1014 Hong, Amy, 734, 739 Hong, Bo, 777 Hong, Qi, 240 Hong, Sung Hwa, 755 Horst, Wiebe, 964 Horwitz, Geoffrey C., 553, 659 Hoshino, Tomofumi, 652, 791 Hosoi, Hiroshi, 194 Hosono, Katsuhiro, 325 Hotta, Yoshihiro, 325 Hough, Tertius A., 811 Howard, Matthew, 942 Hradek, Gary, 216 Hrnicek, Andrew, 979 Hsiao, Steven, 1036 Hsieh, Wu-Shiun, 239 Hsu, Chuan-Jen, 138, 239 Hsu, Chuan-Jen, 138, 239 Hu, Bo Hua, 144, 404, 410 Hu, Ning, 648, 909 Hu, Yi, 500 Hu, Zhengqing, 850 Huang, Bernice, 484 Huang, Juan, 1036 Huang, Mingqian, 20, 139, 589 Huang, Rong, 971 Huang, Samantha, 958 Huang, Taosheng, 127 Huang, Yibo, 15 Hubbard, Allyn, 90 Hubka, Peter, 288 Huebner, Patrick, 993 Huganir, Richard, 13 Hughes, Hilary, 111 Hugnot, Jean-Philippe, 591

Hullar, Timothy, 547, 1005 Hultcrantz, Malou, 328 Hume, Cliff, 637, 836 Hume, Clifford, 17, 587 Humphrey, Mary Beth, 618 Hung, Chia-Cheng, 239 Hungerford, Michelle, 654 Hunker, Kristina, 817 Hunter, Lisa, 757 Hurd, Elizabeth A., 134 Hurley, Laura, 451 Husnain, Tayyab, 815 Hütter, Joachim, 656 Huwe, Janice, 253 Hwang, Margaret, 491 Hwang, Phil Sang, 551 Hwang, Semi, 745 Hyde, Blake J., 62, 207 Ibrahim, Rasha, 742 Idsardi, William, 750 Ihlefeld, Antje, 1030 lizuka, Takashi, 256 Ikeda, Katsuhisa, 256 Ikeda, Ryoukichi, 605 Im, Gi Jung, 566 Imig, Thomas, 710 Indzhykulian, Artur, 349, 390, 394 Ingham, Neil, 331, 807, 812, 825 Inoshita, Ayako, 256 Inui, Ken-Ichi, 639 Isaacson, Brandon, 231 Ishiyama, Akira, 113, 851, 864 Ishiyama, Gail, 113, 851, 864 Ison, James, 889 Ison, Matias, 908 Italia, Michael, 238 Itatani, Naoya, 978 Ito, Juichi, 387, 600, 639, 657, 844, 911 Ito, Tsukasa, 221, 752, 753 Ives, David, 481 Iwasa, Kuni, 65 Iwasaki, Satoshi, 325 lver, Nandini, 743 Izumi, Chisako, 65 Izzo-Matic, Agnella, 489 Jackson, Ronald, 412 Jackson, Ryan, 53 Jacob, Michele, 315, 567 Jacob, Stefan, 75, 355 Jacobs, Peter G., 374 Jacques, Steven, 360 Jagger, Dan, 663 Jahan, Israt, 39, 839 Jajoo, Sarvesh, 788, 794, 795 Jakobsen, Lasse, 973 Jamesdaniel, Samson, 130, 784 Jameson, Elyse, 266 Jameyson, Elyse, 199, 963 Jan, Taha, 21, 35, 310, 594 Jang, Jeong Hun, 454, 990 Janky, Kristen, 507, 512 Jansen, E. Ducco, 536 Jansen, Sebastian, 215, 289, 923 Janz, Katrin, 886 Jasien, Jessica, 506 Jaumann, Mirko, 656 Jauniaux, Thierry, 609 Javier, Lauren, 1028 Jayaram, Aditi, 456 Jedrzejczak, Wiktor, 370, 920 Jenkins, Herman A., 206, 207, 297 Jennings, J. Richard, 515 Jennings, Skyler, 179 Jensen-Smith, Heather, 824 Jeon, Ju Hyun, 341 Jeon, Yuyong, 745 Jeschke, Marcus, 930, 931 Jesteadt, Eric, 137 Jesteadt, Walt, 472 Ji, Hye-Min, 831, 833 Jiang, Haiyan, 161, 621, 625, 900, 910

Jiang, Hui, 850 Jiang, Kevin, 406 Jiang, Tao-Tao, 240 Jiang, Zhi-Gen, 118, 623, 628 Jiao, Yu, 885 Jin, Yan, 240 Jing, Zhizi, 120, 483, 541 Jiradejvong, Patpong, 936, 987, 988 Joachimsthaler, Bettina, 173 Johannesen, Peter T., 182 Johnson, Allan, 935 Johnson, Luke, 943 Johnson, Shane, 544 Johnson, Stuart, 345, 562, 563, 819, 825 Johnsrude, Ingrid, 748 Jokwitz, Melanie, 132 Jolly, Claude, 643, 644 Jones, Gareth, 85 Jones, Gary, 198 Jones, Heath, 465 Jones, Jennifer, 1010 Jones, Noble, 264 Jones, Sherri, 154, 254, 519, 553.821 Jones, Simon, 898 Jones, Timothy A., 519 Joo, Hyun Suk, 415 Jordan, Paivi, 243 Joris, Philip, 665, 666, 677, 701 Joseph, Debbie, 655 Joshi, Suyash, 472 Jovanovic, Sasa, 884 Juiz, Jose M., 890 Jung, Kyu Hwan, 963 Jung, Michael J., 490 Kagen, David, 374 Kaiser, Alexander, 697 Kajikawa, Yoshinao, 176 Kajikawa, Yoshinao, 176 Kakehata, Seiji, 74 Kakigi, Akinobu, 649, 793, 867 Kalantar, Nader, 655 Kalayjian, Zaven, 264 Kale, Sushrut, 414, 670 Kalinec, Federico, 348, 787 Kalinec, Gilda, 787 Kalluri, Radha, 101, 369 Kaltenbach, James, 896, 906 Kamar, Ramsy, 79 Kamide, Daisuke, 611, 635 Kamiya, Kazusaku, 256 Kan, Alan, 961 Kanagawa, Eiju, 402, 651, 899 Kandler, Karl, 883 Kane, Catherine, 398 Kaneko, Chris, 267 Kang, Hyejin, 990 Kang, Tong-Ho, 833 Kang, Woo Seok, 209, 619 Kanicki, Ariane, 146 Kanold, Patrick, 715, 719, 927, 928 Kantardzhieva, Albena, 20, 122, 139, 556 Kanzaki, Sho, 635 Kao, Albert, 352, 354 Kao, Chung-Lan, 517 Kao, Shyan-Yuan, 422 Karasawa, Takatoshi, 628, 633 Karcz, Anita, 889 Karg, Sonja, 205 Kariya, Shin, 337, 383 Karlén, Alexandra, 885 Karpenkopf, Pablo, 477 Kasagi, Hiromi, 256 Kashino, Makio, 969 Kashio, Akinori, 649, 793 Kaspar, Brian K., 634 Katayama, Kei-Ichi, 1009 Katsunuma, Sayaka, 386 Katsuyama, Shigemi, 714 Katz, Eleonora, 566, 582 Katz, Josh, 557 Kaur, Tejbeer, 788, 794, 795

Kavianpour, Sarah, 447 Kawasaki, Hiroto, 942 Kawase, Tetsuaki, 233, 605 Kawauchi, Satoko, 611 Kazmitcheff, Guillaume, 389, 642 Keating, Sarah, 901 Keefe, Douglas, 757 Keller, James, 813 Kelley, Matthew, 30, 274, 809, 1011, 1015, 1017, 1018 Kelly, Michael, 15, 1013 Kemp, David, 102 Kempfle, Judith, 19, 20, 406 Kempton, Beth, 334, 385 Kennedy, Helen J., 570 Kersigo, Jennifer, 39, 839 Ketten, Darlene R., 924 Khan, Khalid, 572, 574 Khan, Shaheen, 815 Khardori, Nancy, 786 Khatibzadeh, Nima, 366 Khatri, Safia, 31 Khimich, Darina, 120 Khurana, Sukant, 696 Kidd, Jr., Gerald, 190, 971 Kietzmann, Manfred, 645 Kikkawa, Yayoi, 639 Kikuchi, Makoto, 611 Kim, Dongwook, 195 Kim, Duck O., 464 Kim, Duk Joong, 90 Kim, Ernest, 855 Kim, Harry, 415, 619 Kim, Hong Lim, 403 Kim, Hongsig, 195 Kim, Hun Young, 833 Kim, Hyo Jeong, 129, 861 Kim, Hyoung-Mi, 150, 311, 806 Kim, Hyung-Jin, 832 Kim, Irene, 984 Kim, Jin Su, 454 Kim, Jinna, 382 Kim, Kun Woo, 225 Kim, Kyunghee X., 150, 860 Kim, Kyu-Sung, 518, 745 Kim, Mi Joo, 516, 774 Kim, Minbum, 382 Kim, Sang Cheol, 336 Kim, Se Jin, 831, 832, 833 Kim, Seung Won, 613, 902 Kim, Soo-Chan, 516 Kim, Sung Huhn, 336, 341, 382, 866 Kim, Sun-Gui, 335 Kim, Un-Kyung, 135, 866 Kim, Ye-Hyun, 659 Kim, Younju, 613, 902 Kim, Yuil, 10 King, Andrew, 713, 732 King, Kelly, 217 King, Mary-Claire, 5 King, W. Michael, 1002 Kirig, W. Michael, 1002 Kirby, Alana, 204 Kishon-Rabin, Liat, 779 Kita, Tomoko, 1014 Kitani, Rei, 74, 348 Klap, Tal, 470 Klimek, John, 397, 829 Klinge, Astrid, 893 Kloostra, Francka, 168 Klump, Georg, 893, 898, 978, 983, 1027 Knipper, Marlies, 316, 396, 562, 563, 641, 656, 819, 1023 Knox, Glenn, 208 Knudson, Inge, 156, 157 Kobayashi, Mariko, 241 Kobayashi, Toshimitsu, 233, 605 Kochanek, Krzysztof, 370, 920 Kodali, Vikas N., 436 Koehler, Karl, 26, 847 Koehler, Seth, 438 Koeppl, Christine, 48, 608 Kofman, Igor, 1004 Kohrman, David, 136, 149, 817

ARO Abstracts

354

Koistinen, Sonja, 287 Koka, Kanthaiah, 61, 62, 206, 207, 297, 465, 733 Kokal, Rachel, 447 Kokkinakis, Kostas, 749 Kolesnikova, Olga, 998, 999 Kollmar, Richard, 420 Kommareddi, Pavan K., 388, 632 Kondo, Kenji, 793, 837 Kondo, Takako, 847 Kong, Jee Hyun, 576, 585 Kong, Lingqiang, 286 Kong, Ling-Xuan, 501 Kong, Soo-Keun, 857 Konrad-Martin, Dawn, 374 Kontorinis, Georgios, 210 Koo, Jawon, 630, 789 Kopan, Raphael, 1019 Kopco, Norbert, 958 Kopecky, Benjamin, 41 Kopelovich, Jonathan, 393, 424, 673 Kopke, Richard, 647, 648, 909, 912 Kopp-Scheinpflug, Cornelia, 877, 889 Köpschall, Iris, 656 Kopun, Judy, 98 Körber, Inken, 132 Korte, Megan, 824, 842 Korzyukov, Oleg, 747 Kos, Izabel, 268 Kossl, Manfred, 188 Kostin, Sawa, 862 Kotak, Vibhakar, 319, 455 Kotlikoff, Michael, 769 Koulich, Elena, 231, 232 Kovach, Christopher, 942 Kowalkowski, Victoria, 229 Kral, Andrej, 288, 450 Kramarenko, Inga, 624, 904 Kramer, Florian, 887 Kramer, Matthew, 834 Krantz, Ian, 238 Kraus, Johanna, 608 Kraus, Kari Suzanne, 452 Kraus, Nina, 142, 921 Kraus, Suzanne, 161, 910 Kreeger, Lauren, 679 Kremer, Hannie, 805 Krishnamoorthy, Gayathri, 117 Krishnan, Ananthanarayan, 915, 916, 918, 919 Kristiansen, Arthur G., 422 Kros, Cornelis, 549, 563 Kruger, Pamela, 231 Ku, Yuan-Chieh, 24 Kubota, Toshinori, 221, 752, 753 Kuenzel, Thomas, 300, 686 Kugler, Sebastian, 83 Kühn, Anja, 913 Kuhn, Maggie, 241 Kuhn, Stephanie, 562, 563, 656, 825 Kujawa, Sharon G., 400, 401, 653 Kulecz, Walter, 503 Kumar, Sukhbinder, 1038 Kumei, Yasuhiro, 714 Kurima, Kiyoto, 806 Kurioka, Takaomi, 611, 635 Kurita, Akihiro, 611, 635 Kurt, Simone, 173 Kushmerick, Christopher, 300, 876 Kuwada, Shigeyuki, 464 Kwak, Eunyee, 754 Kwak, Sangyeop, 754 Kwon, Bomjun J., 202, 1031 Kwon, See Youn, 755 Kwon, Seeyoun, 938 Laback, Bernhard, 497, 735, 962 Labadie, Robert, 234 Lackner, Christina, 205 Ladak, Hanif M., 56

Ladher, Raj, 1014 Lakemeyer, Gerhard, 952 Lamb, Jessica S., 87 Landa, Melissa, 122, 123 Landsberger, David, 200, 946, 965 Lang, Dustin, 655 Lang, Hainan, 425 Lang, Patrick, 1023 Langemann, Ulrike, 983 Langers, Dave, 158, 281 Langner, Gerald, 680 Large, Charles H., 908 Large, Edward, 897 Lark, Arianna, 392 Larsen, Deb, 166 Larson, Charles, 747 Laske, Roman D., 594 Lasker, David, 993, 1001 Latoche, Joseph, 805 Lau, Bonnie K., 475 Lauer, Amanda, 871, 882, 956 Laurer, Amanda, 871, 882, 9 Laurent, Nguyen, 34 Lawrence, Josh, 320 Layman, Wanda S., 134 Le Prell, Colleen, 237, 655 Leach, Nicholas D., 732 Leake, Patricia, 211, 216, 703 Lebel, Carl, 638 Lee, Adrian KC, 796, 803, 1035 Lee, Amy, 120 Lee, Chen-Chung, 1028 Lee, Chien-Nan, 239 Lee, Daniel, 263, 484, 539 Lee, Dong Soo, 454, 990 Lee, Edmund, 661 Lee, Eun, 516, 774 Lee, Fu-Shing, 624, 904 Lee, Hae Kyung, 613, 902 Lee, Hyo-Jeong, 454, 990 Lee, II-Woo, 857 Lee, Jae Sung, 454 Lee, Jaebeom, 857 Lee, Jae-Hyun, 559 Lee, Jasmine, 338 Lee, Jeong-Han, 831, 832, 833 Lee, Jong Bin, 613, 902 Lee, Ju Hyoung, 426 Lee, Jun Ho, 990 Lee, Junghak, 195 Lee, Jungmee, 377 Lee, Kwang-Sun, 209 Lee, Kyu Yup, 806, 1018 Lee, Kyungwon, 195 Lee, Kyu-Yup, 135 Lee, Roger, 709 Lee, Sang Goo, 589 Lee, Sang-Heon, 831 Lee, Sangmin, 745 Lee, Sue, 815 Lee, Sung Min, 755 Lee, Wen-Han, 73 Lee, Won-Sang, 866 Lee, Yong-Won, 226 Leeuwenburgh, Christiaan, 145 Lefebvre, Philippe, 1012 Legan, Kevin, 616, 822 Léger, Agnès, 189 Lehar, Mohamed, 577, 871 Lei, Debin, 654 Leichtle, Anke, 338 Leijon, Sara, 769, 888 Leitner, Michael G., 115 Lelli, Andrea, 805 Lenarz, Minoo, 277, 450 Lenarz, Thomas, 210, 277, 450, 645, 646 Lenoir, Marc, 128, 609 Lenz, Danielle R., 808 Leon, Alex, 929 Lesica, Nicholas, 443 Levic, Snezana, 581 Levin, Jared R., 21 Levin, Michaela E., 564 Levine, Robert, 156, 157, 165

Levitt, Pat, 932 Lewicki, Laura, 452, 460 Lewis, Morag, 825 Lewis, Rebecca, 587 Lewis, Richard, 262, 263, 1000 Li, Daliang, 545 Li, Feipeng, 371 Li, Gang, 252 Li, Geng-Lin, 580, 583 Li, Hongzhe, 630, 790 Li, Huawei, 332, 560 Li, Kevin, 640 Li, Na, 301, 708 Li, Shuang, 907 Li, Song Zhe, 783 Li, Tianhao, 201 Li, Wei, 647, 912 Li, Wen-Hong, 545 Li, Yang, 430 Li, Yizeng, 93 Li, Yongqi, 900 Li, Yuhua, 112 Liang, Chun, 110, 111, 131, 133, 240 Liberman, M. Charles, 116, 120, 139, 187, 317, 384, 400, 401, 606, 620 Licari, Frank, 896, 906 Lichtenhan, Jeffery, 96 Lichter, Jay, 638 Lie, Michaela, 421 Lie, Tjensin, 264 Lim, David, 27, 865 Lim, Hubert, 277, 450 Lim, Hyun Woo, 209, 619 Limb, Charles, 548, 674, 871, 936, 984, 987, 988 Lin, Chia-Cheng, 520 Lin, Frank, 140 Lin, Harrison, 400 Lin, Shin-Yu, 239 Lin, Shuh-Yow, 555 Lin, Vincent, 17 Lin, Xi, 109, 112, 332, 816 Lin, Ying, 649 Lin, Yu-Pai, 517 Lin, Zhaoyu, 428, 654 Lina, Ioan, 882 Linden, Jennifer, 172, 290, 724 Ling, Leo, 266, 267 Lin-Jones, Jennifer, 551 Linthicum, Jr., Fred H., 333 Lipovsek, Marcela, 566 Litovsky, Ruth, 294, 492, 493, 495, 961, 1030 Liu, Baohua, 299 Liu, Christopher, 615 Liu, Haiying, 70 Liu, Hong, 621, 622, 625, 629 Liu, Jie, 545 Liu, Ligian, 565, 848 Liu, Qing, 660, 661 Liu, Wenke, 662 Liu, Xiuping, 717 Liu, Xue Zhong, 327 Liu, Zhenyi, 1019 Liu, Zhiyong, 16, 1019 Lobarinas, Edward, 161, 162, 395, 460, 910 Löhrke, Stefan, 887 Loizou, Philipos, 500, 749 Lomax, Margaret, 149 London, Sam, 951 Long, Christopher, 947 Long, Glenis, 99, 100 Longenecker, Ryan, 167 Lopata, Christopher, 740 Lopez, Ivan, 113, 851, 864 Lopez-Poveda, Enrique A., 182, 183 Lorente, Beatriz, 329 Lorenzi, Christian, 189, 481 Lorteije, Jeannette, 300, 695 Lovas, Sándor, 76 Lovett, Michael, 24

Löwenheim, Hubert, 593 Lu, Cindy, 530 Lu, Guang-Jin, 240 Lu, Jianzhong, 647, 912 Lu, Na, 40 Lu, Sandy, 872 Lu, Ying-Chang, 138 Lu, Yong, 462, 685, 691 Luckovich, Shannon, 101 Luebke, Anne, 746 Lujan, Rafael, 890 Lukashkin, Andrei, 85, 357, 604, 616 Lukashkina, Victoria, 357, 616 Lundeberg, Megan, 818 Luo, Bin, 716 Luo, Xiao-Xing, 240 Luo, Xin, 200, 966 Lupo, Eric, 61, 62, 207, 733 Lurie, Diana, 320 Lustig, Lawrence, 211, 403, 618, 636. 820 Luxford, William, 787 Lv, Ping, 129 Lynch, Eric, 851 Lysakowski, Anna, 828 Ma, Ke-Tao, 118 Ma, Wei-Li, 429 Macarthur, Carol, 334 Macchiarini, Paolo, 781 Macherey, Olivier, 295, 945 Macleod, Katrina, 679 Maestre, Iranzu, 609 Maftoon, Nima, 46, 52 Magnusson, Anna, 769, 888 Mahendrasingam, Shanthini, 125 Mahfoud, Lorice, 57, 58 Mahoney Rogers, Amanda, 32 Maier, Hannes, 862 Maison, Stéphane F., 116, 606, 620 Majdak, Piotr, 497, 735, 962 Makishima, Tomoko, 997 Malgrange, Brigitte, 1012 Malmierca Manuel 278 895 Manak, John, 424 Manis, Paul, 9, 684, 689 Manley, Geoffrey, 608 Mann, Zoë, 1017, 1018 Manohar, Senthilvelan, 144, 431, 452, 459, 460 Marc, Isabelle, 764 Marchetti, Gregory, 520 Marcotti, Walter, 345, 549, 562, 563, 819, 825 Marcus, Daniel C., 150, 860 Maricich, Stephen, 531, 840 Marie Laure, Volvert, 34 Marks, Kendra, 378 Marguardt, Torsten, 953 Marrs, Glen, 533 Marsh, Roger, 238 Martin, Brett, 937 Martin, Donna M., 134 Martin, Pascal, 347 Martinelli, Giorgio, 772, 773 Martinez-Monedero, Rodrigo, 554 Martinez-Vega, Raquel, 147 Martz, Ashlee, 676, 830 Masetto, Sergio, 563, 819, 825 Mason, Christine, 971 Massing, Thomas, 126 Massoudi, Roohollah, 712 Masutomi, Keiko, 969 Matassa, Keith, 924 Matic, Agnella, 486, 487, 488, 491, 535, 538 Matsui, Jonathan, 834 Matsumoto, Masahiro, 396 Matsunaga, Tatsuo, 312, 650 Matsunobu, Takeshi, 611, 635 Matsuoka, Akihiro, 26 Mattox, Douglas, 332 Mauermann, Manfred, 91

Mausset-Bonnefont, Anne-Laure, 128 May, Bradford, 682, 868, 882, 956 Mayko, Zachary, 445 Mayle, Ryan, 31 May-Simera, Helen, 809 Mc Laughlin, Myles, 666 McAlpine, David, 466, 663, 672, 953 McBride, Ethan, 875 McDermott, Daniel, 374 McDermott, Josh, 371, 970, 1037 McDermott, Jr., Brian, 551 McGee, Joann, 372, 824, 841, 842 McIntosh, Michael, 578 McKenna, Michael J., 422 McLean, Will J., 250 McMillan, Erin, 598 McMillan, Garnett, 374 McMillan, Nadia F., 436 McRackan, Theodore, 234 McShefferty, David, 193 Meaud, Julien, 94 Meech, Robert, 786 Meehan, Daniel, 137, 1021 Meenderink, Sebastiaan W.F., 106 Meffin, Hamish, 678 Megason, Sean, 589 Mehta, Swapnil, 392 Melcher, Jennifer, 156, 157 Melki, Sami, 821 Mellado-Lagarde, Marcia, 357 Mellott, Jeffrey, 441 Meltser, Inna, 124, 416 Melvin, Thuy-Anh, 264 Meng, Xiangying, 461 Merchant, Gabrielle, 57, 58 Merchant, Saumil, 51, 57, 58, 363, 381, 859 Meredith, Andrea L., 116 Meredith, Frances, 252 Merfeld, Daniel, 262, 263 Merkison, Marquitta, 375 Mescher, Mark, 855 Mesgarani, Nima, 729 Metter, E. Jeffrey, 140 Meyer, Elisabeth, 700, 702 Meyer, Michaela, 251 Meyer, Thomas, 644 Meyer-Zum-Gottesberge, Angela-Maria, 126 Michaels, Leslie, 380 Michalski, Nicolas, 579 Michelet, Pascal, 666 Micheyl, Christophe, 181, 479, 727 Micucci, Steven, 401 Middlebrooks, John, 204, 1028 Migliaccio, Americo, 264, 993 Mikiel-Hunter, Jason, 466 Mikuriya, Takefumi, 223, 402, 651, 995 Milenkovic, Ivan, 884 Miles, Ronald, 54 Miller, Brooke, 196 Miller, Christopher, 504 Miller, David, 847 Miller, Frank, 173 Miller, Josef, 237 Miller, Lee, 951 Miller, Matthew, 631 Miller, Megan, 440 Miller, Richard A., 151, 152 Miller, Roger, 258 Mills, John, 425 Mills, Kristal N., 519 Min, Jiyoung, 613, 902 Mineta, Hiroyuki, 325, 612 Minor, Lloyd, 999, 1001 Minoshima, Shinsei, 325 Mintz, Matti, 991 Miroir, Mathieu, 389, 642

ARO Abstracts

Mishina, Masayoshi, 418 Mishra, Srikantha, 369, 376 Mistrik, Pavel, 663 Misurelli, Sara, 492, 495 Mitchell, Diana, 264, 265 Mitchell, Jason, 234 Miyasaki, Gary, 963 Miyazaki, Makiko, 233 Mizuta, Kunihiro, 325, 612 Mizutari, Kunio, 406 Mohr, Ian, 241, 760 Molitor, Scott C., 874 Mollendorf, Joseph, 460 Momin, Suhael, 821 Monaghan, Jessica, 975 Monahan, Kelly, 806 Monfared, Ashkan, 558 Montey, Karen L., 868 Moon, Il Joon, 755 Moon, In Seok, 230 Moon, Sung, 865 Mooney, T. Aran, 924 Moore, Brian C.J., 189 Moore, Christopher, 257 Moore, David, 222 Moore, Ernest, 453 Moran, John, 155 Morell, Maria, 609 Moreno, Laura, 487 Morgan, Bodson, 34 Morita, Norimasa, 383 Morley, John, 457, 458 Morris, Ken A, 39 Morrison, Annie, 307 Morton, Cynthia C., 130 Moser, Tobias, 120, 132, 541 Moss, Cynthia, 973 Motts, Susan, 441 Moulin, Annie, 181 Mountain, David, 88, 90, 358 Mueller, Melissa, 834 Mueller, Susanne, 215 Muhr, Jonas, 885 Mukerji, Sudeep, 539 Mukherjea, Debashree, 788, 794, 795 Mulavara, Ajitkumar, 504, 1004 Mulheran, Mike, 908 Muller, Agnes, 764 Müller, Britta, 887 Müller, Marcus, 593 Munguia, Raymundo, 718 Muniak, Michael A., 436, 868 Murakoshi, Michio, 74 Murillo-Cuesta, Silvia, 147 Mutai, Hideki, 312 Myung, Nam-Suk, 857 N. Darrow, Keith, 926 Nachtigall, Paul E., 924 Nadol, Joseph B., 675 Nagaki, Takahiko, 74 Nagaraj, Aaditya, 696 Naghibolhosseini, Maryam, 99 Nagura, Mitsuyoshi, 865 Naik, Khurram, 68, 103 Nair, Thankam S., 388 Nakagawa, Susumu, 312 Nakagawa, Takayuki, 387, 600, 639, 657, 844, 911 Nakajima, Hideko, 58, 363 Nakajima, Hideko H., 57 Nakamagoe, Mariko, 652, 791 Nakamoto, Kyle, 442 Nakanishi, Hiroshi, 325, 612 Nakaya, Kazuhiro, 605 Nakayama, Masahiro, 791 Nakmali, Don, 55, 59, 648 Nam, Hui, 367 Nam, Jong-Hoon, 82 Nam, Sungil, 381, 859 Namba, Kazunori, 312 Nambiar, Shruti, 46 Namdaran, Parhum, 590 Narins, Peter, 571 Nation, Javan, 214

Navaratnam, Dahsakumar, 23, 72, 80, 568, 569 Nayagam, Bryony, 25, 637 Nayak, Gowri, 822 Nayak, Shruti, 760 Neef, Andreas, 120 Neely, Harold, 805 Neely, Stephen, 97, 98, 756 Neggers, Bas, 178 Neidhart, Elizabeth, 128 Neilans, Erikson, 740, 976, 977 Neiman, Alexander, 353 Nerlich, Jana, 884 Neubauer, Heinrich, 469, 586 Neuheiser, Anke, 277 Neuman, Arlene, 499 Newlands, Shawn D., 992 Newman, A. Jensen, 460 Nguyen, Laurent, 1012 Nguyen, Tot Bui, 17, 596 Nguyen, Yann, 389, 642 Nibu, Ken-Ichi, 386, 650 NIDU, KER-ICHI, 386, 650 Nichols, David, 313 Nicolau, Joel C., 890 Nicoucar, Keyvan, 262 Nie, Kaibao, 199, 266, 267, 938 Nilsen, Natalie, 77 Nishimura, Bungo, 652, 791 Nishimura, Koji, 844 Nishimura, Tadashi, 194 Nishioka, Rie, 867 Nishizaki, Kazunori, 337, 383 Nityananda, Vivek, 982 Niwa, Katsuki, 611 Noben-Trauth, Konrad, 805, 813 Noble, Jack, 234 Nodal, Fernando, 713, 732 Noel, Victor A., 496 Nordehn, Glenn, 218 Northrop, Clarinda, 384 Northup, John, 805 Norton, Susan, 963 Nothwang, Hans, 887, 1023 Nouaille, Sylvie, 575 Nourski, Kirill, 942 Novozhilova, Ekaterina, 885 Nowack, Amy, 267 Nowotny, Manuela, 188 Nudelman, Igor, 905 Nusse, Roel, 21 Nuttall, Alfred, 95, 102, 118, 119, 360, 361, 362, 365, 397, 408 Oba, Sandra I., 989 Obholzer, Nikolaus, 589 O'Brien, Richard, 140 Oertel, Donata, 681 Oesterle, Elizabeth, 17 Offenhauser, Nina, 819 Oghalai, John, 356, 411, 610, 615 Ogorodnokov, Dmitri A., 773, 999 Oh, Gi-Su, 832 Oh, Seung Ha, 225, 454, 990 Ohl, Frank, 930, 931 Ohlemiller, Kevin K., 522 Ohtsubo, Masafumi, 325 Ojima, Hisayuki, 714 Okada, Hiroko, 256 Okamura, Jun, 612 Okano, Mitsuhiro, 337 Okano, Takayuki, 30 Okoruwa, Oseremen, 76 O'Leary, Stephen, 852, 853 Oleskevich, Sharon, 692 Oline, Stefan, 880 Oliver, Dominik, 83, 115 Oliver, Douglas, 440, 933 Olivius, Petri, 885 Olshausen, Bruno, 737 Olson, Elizabeth, 212, 364 Omelchenko, Irina, 397, 408 O'Neil, Jahn N., 674 O'Neill, William, 192, 738 Ortega, Aída, 763

Orton, Llwyd, 449 O'Shea, K. Sue, 419 Oshima, Kazuo, 592, 594 Oshima, Takeshi, 605 Osmanski, Michael, 474 Ostreicher, Jennifer D., 950 Ou, Henry, 391, 626, 901 Ouyang, Jessica, 925 Ouyang, Xiaomei, 327 Owen, Thomas, 16, 1019 Owens, Kelly, 590, 792 Oxenham, Andrew J., 185, 479 Oxford, Trey, 266, 267 Oya, Hiroyuki, 942 Ozmeral, Erol J., 1032 Paans, Anne, 160 Paasche, Gerrit, 210, 645, 646 Pace, Edward, 169 Padilla, Monica, 200, 965 Paige, Gary, 192, 738, 889 Pak, Jhang Ho, 407 Palmer, Alan, 159, 941 Palmiter, Richard, 596, 836 Paludetti, Gaetano, 395 Pan, Alex, 15 Pan, Ning, 39, 839 Pangršic, Tina, 120 Paolone, Nicholas, 431 Paparella, Michael, 383 Pararas, Erin, 855, 856 Parbery-Clark, Alexandra, 142, 921 Parham, Kourosh, 148 Parikh, Malav, 437 Park, Channy, 831, 832, 833 Park, Heonjin, 745 Park, Hong-Joon, 135 Park, II-Yong, 225 Park, Judy, 882 Park, Keehyun, 902 Park, Kyoung Ho, 403 Park, Kyungjoon, 135 Park, Min-Hyun, 454 Park, Raekil, 831, 832, 833 Park, Shi-Nae, 403 Park, Sung-Hwan, 857 Park, Yong-Ho, 226, 335 Parker, Andrew, 811 Parker, Mark, 406 Parsons, Carl, 457, 458 Parthasarathy, Aravindakshan, 143 Patel, Chirag, 894 Patel, Shail, 660 Paulin, Michael, 761 Pawlowski, Karen, 231, 232 Paz, Arnon, 810 Pearson, Selina, 329, 331, 807, 812 Pecka, Jason, 67, 76 Pedersen, Courtney, 907 Peelle, Jonathan, 748 Pelizzone, Marco, 268 Pellieux, Lionel, 181 Peña, Jose Luis, 467 Pendola, Martin, 319 Pennington, Jeffrey, 238 Peppi, Marcello, 122, 123, 556, 653 Pereria, Fred, 70, 411 Perez, Ronen, 603 Perez-Castro, Rosalia, 241 Perez-Gonzalez, David, 895 Perez-Rosello, Tamara, 434 Perkins, Guy, 314 Perry, Trevor, 202 Peters, Brian, 503, 504, 1004 Peterson, Ellengene, 253 Peterson, Jonathan, 245 Peterson, Joy, 238 Petit, Christine, 575, 579, 616 Petkov, Christopher, 704 Petralia, Ronald, 11, 806, 1015 Petrillo, Marco, 20, 589 Peusner, Kenna, 766, 767

Pfingst, Bryan, 213 Philippe, Lefebvre, 34 Phillips, Amanda, 627 Phillips, James, 266, 267 Piao, Wenxue, 832 Pienkowski, Martin, 718, 725 Pierce, Jessica, 154 Pierce, Marsha, 824, 826 Pierzycki, Robert H., 960 Pilati, Nadia, 908 Pilka, Edyta, 920 Pisano, Dominic, 212 Pisoni, David B., 985 Piu, Fabrice, 638 Plack, Christopher, 916, 917, 940 Platt, Christopher, 258 Plinkert, Peter K., 236 Poeppel, David, 711 Pohl, Nina U., 983 Pollak, George, 301, 708 Polley, Daniel B., 63, 620, 926, 932 Pollock, Lana, 551 Pongstaporn, Katanyu, 871 Pongstaporn, Tan, 436, 692 Poon, Paul, 449 Popelar, Jiri, 446 Popelka, Gerald, 558 Popratiloff, Anastas, 767 Porres, Christian P., 702 Porsov, Edward, 102 Porter, Forbes, 217 Portfors, Christine, 445, 451 Potter, Kimberlee, 44 Potter, Paul, 811 Pradhan, Shashwati, 437 Praetorius, Mark, 236 Pressnitzer, Daniel, 1025 Price, Steven, 828 Probst, Rudolf, 752 Profant, Oliver, 170 Protant, Oliver, 170 Prolla, Tomas A., 145 Puel, Jean-Luc, 128, 609 Purcell, Erin, 419, 565, 848 Purdy Drew, Kirstin, 550 Puria, Sunil, 53, 615 Purnell, Tom, 811 Putnam, Susan K., 740 Pylaeva, Olga, 250 Pyott, Sonja, 116, 250 Pysanenko, Kateryna, 170 Qian, Dong, 36, 332 Qing, Chang, 109 Quinones, Patricia, 255 Rabbitt, Richard, 54, 269, 540 Rachel, Rivka, 809 Radtke-Schuller, Susanne, 934 Radziwon, Kelly, 976 Raft, Steven, 1020 Rahman, Mehdi, 264, 509 Raible, David, 391, 590, 626, 785, 792, 901 Raij, Tommi, 958 Rajagopalan, Lavanya, 70 Rajguru, Suhrud, 269, 485, 486, 487, 488, 489, 490, 491, 535, 540 Ralle, Martina, 627 Ralli, Massimo, 395 Ramachandran, Ramnarayan, 979 Ramage, Erin, 291 Ramakrishnan, Neeliyath, 574, 584 Ramamoorthy, Sripriya, 361, 362 Ramkumar, Vickram, 788, 794, 795 Ramsey, Nick, 178 Ramunno-Johnson, Damien, 559 Ranatunga, Kishani, 563 Raphael, Patrick, 610 Raphael, Robert, 79, 858 Raphael, Yehoash, 14, 134, 136, 427, 543, 634, 817, 838

999 Rask-Andersen, Helge, 865 Ratnam, Rama, 105 Ravicz, Michael, 47, 51 Rawool, Vishakha, 227 Ray, Alisa, 935 Ray, Kausik, 805 Read, Heather, 174, 285, 892, 933 Reale, Richard, 942 Rebillard, Guy, 128 Rebscher, Steve, 703 Redfern, Mark, 515 Redhead, Carmela, 894 Reece, Alisa, 640 Reed, Randall, 271 Rees, Adrian, 449, 704 Rehman, Atteeg Ur, 815 Reimann, Katrin, 117 Reinders, Megan, 238 Reitano, Melissa, 447 Remington, Evan, 957 Remis, Natalie, 552 Remme, Michiel, 466 Remus, Martina, 188 Ren, Chongyu, 683 Ren, Dongdong, 1013 Ren, Tianying, 102, 607 Renaud, Nicole, 24 Rennie, Katie, 252 Rennies, Jan, 473 Reschke, Millard, 1004 Resnick, Susan, 140 Reyes Romero, Maribel, 1008 Rhim, Johng, 865 Riazuddin, Saima, 815 Riazuddin, Sheikh, 815 Ricci, Anthony, 585 Rice, Christopher, 979 Richards, Virginia, 971 Richardson, Guy, 84, 549, 616, 822 Richardson, Rachael, 637 Richter, Claus-Peter, 269, 485, 486, 487, 488, 489, 490, 491, 535, 540 Riedel, Dietmar, 120 Riesenberg, Amy N., 273 Ringdahl, Erik, 291 Rinne, Teemu, 287 Rinzel, John, 461, 466 Risner-Janiczek, Jessica R., 553 Rivas, Alejandro, 868 Robbins, Carol, 792 Robenstine, Jacinta, 617 Roberston, Nahid G., 130 Roberts, Michael, 10 Roberts, Patrick, 445, 451 Robinson, Alan, 485, 491 Robinson, Barbara, 673 Robles, Luis, 665 Rocha-Sanchez, Sonia, 824, 826, 841, 842, 843 Roche, Jennica, 520 Roche, Katherine, 12 Rode, Thilo, 450 Rodgers, Jonathan D., 740 Roditi, Rachel, 1006, 1007 Rodriguez, Joyce, 97 Rodríguez-Contreras, Adrián, 319, 1022 Rodriguez-de la Rosa, Lourdes, 147 Roehm, Pamela, 241, 241, 760 Rogers, Abigail, 101 Rohbock, Karin, 656 Rohde, Stefan, 236 Rohm, Henning, 645 Roland, Peter, 231 Romero, Maria R., 811 Roongthumskul, Yuttana, 354 Roos, Matthew, 682 Ropp, Tessa-Jonne, 430 Rosalie, Sacheli, 34

Raphan, Theodore, 996, 998,

Rosenblatt, Adam, 674 Rosowski, John, 47, 51, 57, 58, 363 Roux, Isabelle, 578 Rowe, Michael, 253 Rowland, David, 559 Roy, Alexis T., 987 Roy, Sabyasachi, 371, 944 Rubel, Edwin, 391, 529, 590, 596, 626, 693, 694, 785, 792, 836, 875, 877, 878, 901 Ruben, Robert, 759 Rubinstein, Jay, 198, 199, 266, 267, 938, 963 Rubio, Maria, 8, 872 Rübsamen, Rudolf, 322, 688, 884, 889 Rudnicki, Marek, 687 Ruettiger, Lukas, 316, 641 Ruggles, Dorea, 1033 Ruhland, Janet, 734, 739 Runge-Samuelson, Christina, 500 Rupprecht, Laura, 358 Russell, Ian, 85, 357, 604, 616 Rusu, Silviu, 300, 321, 876 Ruth, Byron, 238 Rutherford, Mark A., 120 Rutledge, Joseph, 617, 1021 Rüttiger, Lukas, 396, 656, 819 Ryals, Brenda, 104 Ryan, Allen F., 338 Rybak, Leonard, 788, 794, 795 Ryu, Ara, 831, 833 Ryugo, David, 436, 674, 692, 868, 871 Sadeghi, Soroush, 265, 765 Sadighi Akha, Amir A., 151 Saeed, Shakeel, 778 Safieddine, Saaid, 575, 579 Sahani, Maneesh, 724 Sakai, Yoshihisa, 330 Sakamoto, Takashi, 649, 793 Sakamoto, Tatsunori, 639, 911 Saleur, Aurélie, 247 Salih, Wasil, 45 Salt, Alec, 413, 852, 853, 854 Salvi, Richard, 130, 144, 161, 162, 163, 164, 395, 431, 452, 459, 460, 621, 622, 625, 629, 784, 900, 910 Salzig, Christian, 1023 Samie, Sina, 617 Sams, Mikko, 801 Sanchez, Jason, 694 Sanchez, Sonia, 822 Sanders, Mark, 1005 Sandner, Peter, 656 Sanes, Dan, 455 Sangi-Haghpeykar, Haleh, 504 Sanneman, Joel D., 150 Santarelli, Rosamaria, 127 Santi, Peter, 544 Santos-Sacchi, Joseph, 23, 72, 80, 81, 585 Sarnlertsophon, Kristine, 1036 Sarshar, Mohammad, 366 Sato, Shunichi, 611, 635 Satoh, Yasushi, 635 Saunders, Thomas, 136, 806 Sautter, Nathan, 343 Savary, Etienne, 591 Savel, Sophie, 181 Saylor, Kate, 818 Sayyid, Zahra N., 21 Scacheri, Peter, 339 Scattergood, Lindsay, 988 Schacht, Jochen, 146, 151, 152, 543, 632, 905 Schacht, Peter, 544 Schaechinger, Thorsten J., 83 Schaette, Roland, 672 Schatz, Daniel, 889 Scheetz, Laura, 822, 842, 843

Scheidt, Ryan E., 414 Scheper, Verena, 645, 646 Schilp, Soeren, 643 Schimmang, Thomas, 597 Schinkel-Bielefeld, Nadja, 443 Schipper, Joerg, 614 Schmiedt, Richard, 425, 523 Schmitz, Heather, 544 Schmitz, Klaus-Peter, 645 Schnee, Michael, 585 Schneggenburger, Ralf, 579 Schneider, David M., 284 Schnitzer, Mark, 546, 558 Schnupp, Jan, 713 Schoenecker, Matthew, 703 Schofield, Brett, 441, 442, 869 Scholl, Ben, 303 Schraders, Margit, 805 Schramm, Jordan, 746 Schreiber, Daniela N., 115 Schroeder, Charles, 176, 799 Schubert, Michael, 507, 512 Schuchman, Gerald, 959 Schulte, Bradley, 425 Schulz, Kristine, 242 Schurman, Jaclyn, 476 Schurzig, Daniel, 234 Schütz, Melanie, 132 Schvartz, Kara, 986 Schweizer, Felix, 255 Scott, Hamish, 128 Scully, Peter, 356 Seal, Rebecca, 636, 820 Sedlacek, Miloslav, 433 Seeber, Bernhard U., 960 Segil, Neil, 18, 304 Seidl, Armin, 694 Seidman, Aaron, 14 Sekerkova, Gabriella, 550 Sekiya, Tetsuji, 911 Selvakumar, Dakshnamurthy, 572 Sereda, Magdalena, 159 Serrador, Jorge, 506, 1004 Setou, Mitsutoshi, 612 Setsompop, Kawin, 156 Sewell, William, 122, 123, 556, 653, 856 Seymour, Kelen, 786 Seymour, Michelle L., 70 Seyyedi, Mohammad, 675 Sha, Su-Hua, 146, 405 Shah, Samit, 420 Shamir, Ron, 810 Shamma, Shihab, 175, 715, 729, 927 Shanbhag, Sharad, 467 Shannon, Robert, 298, 775, 946, 965 Shao, Mei, 766 Sheehan, Kelly, 788, 794, 795 Shefer, Shahar, 991 Sheffield, Benjamin, 959 Sheffield, Isaac, 426 Sheffeld, Isaac, 426 Shelton, Ryan, 610 Shen, Aihua, 831 Shen, Wen-Sheng, 138 Shepherd, Robert, 296 Shera, Christopher, 96, 371, 372 Sherlock, Laguinn, 228 Shi, Fuxin, 19 Shi, Xiaorui, 119, 397, 408, 409 Shibata, Seiji, 14, 427, 838 Shillitoe, Caroline, 162 Shilnikov, Andrey, 353 Shiloh, Yosef, 810 Shim, Katherine, 32 Shimano, Takashi, 699 Shimogori, Hiroaki, 223, 402, 651, 899, 903, 995 Shimokura, Ryota, 194 Shin, Homin, 550 Shin, Jung-Bum, 557, 829 Shin Ki Soon 135 Shinkawa, Hideichi, 74

Shinn-Cunningham, Barbara, 286, 798, 926, 972, 1033, 1035 Shino, Masato, 768, 771 Shiotani, Akihiro, 611, 635 Shivatzki, Shaked, 808 Shore, Susan, 437, 438, 914 Shrestha, Bibesh, 453 Shreve, Lauren, 914 Shub, Daniel E., 197 Sibrian-Vazquez, Martha, 627, 631 Sidorenko, Galina, 1008 Siegel, Jonathan, 54, 103, 186, 378, 756 Sienknecht, Ulrike, 37 Sigrist, Alain, 268 Sihn, Choong-Ryoul, 129, 861 Simmons, Caitlin, 406 Simmons, Dwayne, 249, 571 Simon, Jonathan Z., 723 Simon, Julian, 626, 792, 901 Simoncelli, Eero, 970, 1037 Simonoska, Rusana, 328 Simpson, Brian D., 743 Singer, Wibke, 396, 562 Singh, Harmann, 452 Singh, Harmann, 452 Sinkkonen, Saku T., 21, 310, 594 Skarzynski, Henryk, 370, 920 Skopin, Mark D., 874 Slabbekoorn, Hans, 983 Slabu, Lavinia, 922 Slama, Michael, 706 Slattery, Eric, 592 Sliwa, Lech, 370 Smalt, Christopher, 915, 918, 985 Smati, Ibtihel, 591 Smith, Elliot, 279 Smith, Felicia L., 423 Smith, Heather, 69, 78 Smith, Mathew, 177 Smith, Michael E., 588 Smith, Philip H., 677 Smith, Richard J., 6 Smith, Sonya, 346 Smith, Zachary, 947 Snyder, Joel, 291, 721, 1026 Snyder, Russell, 703 So, Hong-Seob, 831, 832, 833 Sohmer, Haim, 603 Sohn, Junil, 195 Sokolowski, Bernd, 330 Soleimani, Manoocher, 150 Sollini, Joseph, 482 Somers, David C., 286 Someya, Shinichi, 145 Somisetty, Satheesh, 1023 Sommers, Mitchell, 741 Song, Lei, 81 Songer, Jocelyn, 344 Sonntag, Mandy, 322, 688 Soto, Enrique, 763, 1008 Soucek, Sava, 380 Soukup, Garrett, 601, 824, 826 Souza, Natalie, 54 Souza, Pamela, 186 Spector, Alexander, 73, 77 Spencer, Martin, 678 Spinelli, Kateri, 829 Spirou, George, 314, 533 Spoon, Corrie, 86 Srinivasan, Arthi, 946, 965 Stacey, Paula, 229 Staecker, Hinrich, 710 Stakhovskaya, Olga, 211, 216, 703 Stankovic, Konstantina M., 422 Starr, Arnold, 127, 671 Starzynski, Christian, 722 Stecker, G. Christopher, 949, 950 Stecker, Julie, 950 Steel, Karen, 3, 329, 331, 807, 812, 825 Steele, Charles, 53, 615

Steffes, Georg, 825 Stehr, Anne, 289 Steinmann, Iris, 939 Steinschneider, Mitchell, 726, 727 Stenberg, Annika, 328 Stepanyan, Ruben, 349, 390, 394 Sterkers, Olivier, 389, 642 Sternberg, Katrin, 645 Stewart, Charles, 647, 909 Steyger, Peter, 623, 627, 628, 630, 631, 633, 770, 789, 790 Stoelb, Corey, 961 Stoever, Timo, 210 Stolzberg, Daniel, 163, 164 Stone, Jennifer, 17, 18, 276, 587, 590.596 Storace, Douglas, 174, 285, 933 Storer, Elizabeth K., 567 Stöver, Timo, 645, 646 Stover, Timo, 040, 040 Strait, Dana, 142 Streeter, Timothy, 971 Strenzke, Nicola, 120, 132, 483, 541 Strickland, Elizabeth, 179, 184 Striessnig, Jörg, 887 Strimbu, C. Elliott, 350, 351, 352 Strome, Scott, 307 Strongin, Robert, 627, 631 Stuart, Andrew, 519 Sturm, Carly, 758 Stuyvenberg, Jessica, 882 Su, Yi-Ning, 239 Sugahara, Kazuma, 223, 402, 651, 899, 903, 995 Suh, Jin Kyung, 415, 619 Suh, Myung-Whan, 225 Suller, Sharon, 191 Sullivan, Jeremy, 692 Sullivan, Jeremy, 692 Sullivan, Jessica, 224 Sullivan-Mahoney, Maureen, 757 Sultemeier, David, 249, 255 Sumner, Chris, 482 Sun, Daniel, 264 Sun. Haoxin. 667 Sun, Huifang, 588 Sun, Li, 704 Sun, Sean, 73, 77 Sun, Wei, 161, 456, 910 Sun, Xiao-Ming, 758 Sun, Yujiao, 171 Surguchev, Alexei, 569 Sutton, Griffin, 291 Sutton, Zachary, 137 Suzukawa, Keigo, 649, 837 Svirsky, Mario, 499, 985 Swaroop, Anand, 809 Swisher, Jascha D., 286 Syka, Josef, 170, 446, 527 Szalai, Robert, 89, 359 Szarama, Katherine B., 1015 Tabata, Yasuhiko, 639 Tabor, Kathryn, 878 Tabuchi, Keiji, 652, 791 Taira, Masato, 714 Takago, Hideki, 483, 541 Takaki, Yuya, 194 Takayasu, Yukihiro, 768, 771 Takeda, Setsuko, 867 Takeda, Taizo, 867 Takeno, Kenji, 651 Takesian, Anne, 455 Takizawa, Yoshinori, 325, 612 Talamo, Maria Victoria, 644 Talavage, Thomas, 967, 985 Tallini, Yvonne, 769 Talmadge, Carrick, 100 Tan, Hongyang, 98 Tan, Xiaodong, 67, 76 Tanaka, Chiemi, 144 Tanaka, Shiro, 639 Tananka, Syuhou, 652 Tang, Jie, 67, 76

Tang, Wenxue, 109, 112, 332 Tang, Yong, 40 Tang, Yong, 40 Tang, Zheng-Quan, 462, 685 Tanigawa, Makoto, 436 Tanokura, Masaru, 145 Tao, Huizhong, 299 Tao, Yuan, 615 Tarabova, Bohumila, 1023 Taiapi Viral, 986 Tejani, Viral, 986 Teki, Sundeep, 1038 Telian, Stevan A., 388 Telischi, Fred, 643, 644 Tempel, Bruce, 877, 889 Tengshe, Chinmayi, 958 Teramukai, Satoru, 639 Thaler, Nick, 291 Thein, Pru, 787 Thelen, Nicolas, 1012 Thibodeau, Linda, 224 Thiede, Benjamin, 827 Thiele, Alexander, 704 Thielk, Marvin, 858 Thiry, Marc, 1012 Thomas, Elisha, 852, 853 Thomas, Lenarz, 542 Thomas, Paul, 565 Thomas, Steven A., 606 Thomeer, Marcus L., 740 Thompson, Eric, 190 Thompson, Jennifer, 710 Thompson, John H., 63 Thompson, Lara, 1000 Thornton, Jennifer, 61, 465, 733 Tian, Chunjie, 613, 902 Tian, Cong, 339, 340, 814 Tickle, Jaqueline, 573 Tillein, Jochen, 288 Tipton, Philip, 432 Toarmino, Camille, 977 Todd, Dylan, 392 Todd, N. Wendell, 235, 332 Tollin, Daniel J., 61, 62, 206, 207, 297, 465, 733 Tong, Ling, 596, 836 Tong, Mingjie, 846 Tonndorf, Jürgen, 28 Toomey, Jennifer A., 740 Torii, Masaaki, 932 Toupet, Michel, 505 Toyota, Hideki, 651, 899, 903, 995 Trachte, George, 863 Trahiotis, Constantine, 954, 955 Tran, Quy, 425 Travo, Cécile, 247, 764 Tremblay, Kelly, 220, 938 Tridane, Zohra, 218 Trimarchi, Jeffrey, 305 Tringali, Stephane, 206 Trivedi, Parul, 598 Troiani, Diana, 395 Trune, Dennis, 334, 343, 385 Trussell, Larry, 10 Trzaskowski, Bartosz, 920 Tsai, Betty, 618 Tsao, Po-Nien, 239 Tu, Tian, 637 Tucci, Debara, 242 Tuft, Bradley, 849 Turcanu, Diana, 64 Turecek, Rostislav, 170 Turner, Jeremy, 166 Typlt, Marei, 322, 688 Tyrer, Hayley E., 811 Tzounopoulos, Thanos, 434, 439, 90Ż Uchanski, Rosalie, 1005 Uemaedomari, Isao, 652, 791 Ugoeke, Nene, 478 Uhler, Kristin, 61 Ulfendahl, Mats, 75 Ushio, Munetaka, 1001 Usubuchi, Hajime, 116, 606 Uziel, Alain, 591 Valente, Daniel, 472

Valentin, Nicholas, 264 Valerino, Orlando, 333 Valero, Michelle, 105 van Aken, Alexander, 549 Van Camp, Guy, 815 Van De Water, Thomas, 643, 644, 823, 835 van de Weyer, Philipp, 236 Van den Ackerveken, Priscilla, 34 van den Honert, Chris, 947 van der Heijden, Marcel, 106, 300, 666, 686, 695 van Dijk, Pim, 158, 160, 168, 281, 964 Van Nechel, Christian, 505 van Opstal, John, 712 van Wanrooij, Marc, 712 van Wetter, Sigrid, 712 Van Zanten, Bert, 178 Vanderniepen, Pieter, 45 VandeVord, Pamela, 925 Vann. James M., 145 Varadarajan, Delphia, 973 Varavva, Polina, 364 Varela-Nieto, Isabel, 147 Varghese, Lenny, 972 Vater, Marianne, 720 Vega, Rosario, 763, 1008 Veile, Rose, 24 Velenovsky, David, 373 Veleri, Shobi, 809 Vélez, Alejandro, 980 Vélez-Ortega, A. Catalina, 394 Velkey, J. Matthew, 419 Vendrell Laguna, Victor, 597 Verhey, Jesko, 91, 473 Verhoef, Rianne, 178 Verhulst, Steven, 786 Verma, Rohit, 539 Verschooten, Eric, 665 Versnel, Huib, 178, 712 Vetter, Douglas, 114, 606 Viberg, Agneta, 911 Vijayakumar, Sarath, 154, 254 Vizor, Lucie, 811 Voelker, Courtney, 595 Vogt, Gerhard, 483 Volk, Matthew J., 70 Volker, Martin A., 740 Vollmer, Maike, 502 Vollrath, Melissa, 555 von Gersdorff, Henrique, 580, 583 von Kriegstein, Katharina, 1038 von Trapp, Gardiner, 711 Vowell, Kate, 811 Vranceanu, Florin, 828 Vu, Ly, 823, 835 Wada, Hiroshi, 74 Wagner, Hermann, 952 Wagner, Jan, 923 Walder, Thomas, 735 Waldhaus, Jörg, 593

Walker, Claire, 889 Walker, Edgar, 667 Walker, Kerry, 713 Wall, Conrad, 268, 1000 Wallace, Mark, 941 Wallace, Matthew, 447 Walling, Farris M., 1029 Walsh, Edward, 372, 824, 841, 842 Waltzman, Susan, 499 Wan, Eric A., 374 Wang, Carol Peiyi, 717 Wang, Chuansong, 820 Wang, Grace, 664, 870 Wang, Hai-Tao, 716 Wang, Hongning, 872 Wang, Hui, 399 Wang, Jian, 399 Wang, Jing, 128 Wang, Liecheng, 685 Wang, Liecneng, 665 Wang, Philip Y., 11 Wang, Qi, 623, 627, 628, 631, 633, 789, 790 Wang, Qiong, 392, 398 Wang, Qiuju, 814 Wang, Ruikang, 360 Wang, Tian, 21, 623, 628 Wang, Wen Jie, 937 Wang, Xiaobo, 638 Wang, Xiao-Hui, 110 Wang, Xiaoqin, 371, 474, 728, 730, 731, 776, 930, 943, 944, 957, 1036 Wang, Yajie, 588 Wang, Ya-Xian, 11 Wang, Yong, 683 Wang, Yongmin, 428 Wang, Yuan, 693, 875, 877 Wang, Yunfeng, 109, 112 Wang, Yunyan, 467 Wangemann, Philine, 117, 150, 311, 806 Warchol, Mark, 24, 592, 595, 783, 1010 Ward, Jonette, 640 Wasserman, Stephen I., 338 Watanabe, Tomoo, 221, 752, 753 Watkins, Paul, 928 Wearne, Kimberly, 146 Webster, Paul, 865 Weddell, Thomas, 357, 604, 616 Wehr, Michael, 303 Wei, Dongguang, 599 Wei, Min, 992 Wei, Shun-Hwa, 517 Weimann, Sonia R., 879 Weintraub, David, 291, 1026 Weisz, Catherine, 554 Welch, Thomas, 977 Welker, Joseph, 248 Wells, Sara, 811 Welstead, Lindsev, 616 Wen, Bo, 664

Wen, Yaqing, 806 Wenstrup, Jeffrey, 974, 975 Wenthold, Robert J., 11 Wenzel, Gentiana I., 542 Werner, Lynne A., 475 Wernert, Maria Florencia, 326 Wess, Jessica, 719 West, Megan, 551 Weston, Michael, 824, 826, 842, 843 White, Judith, 513 White, Keith, 514 White, Patricia, 18, 308 White, Peter, 238 Whitehurst, Heather, 43 Whitlon, Donna S., 421 Whitney, Susan, 520 Whitton, Jonathon, 63 Wier, Withrow Gil, 117 Wikman, Patrik, 287 Wild, Conor, 748 Wiley, Jacque, 376 Wilhelm, Cassie, 202, 1031 Willecke, Klaus, 132 Willemsen, Antoon, 160 Williams, Anthony, 444, 448 Williams, Barbara, 253 Williams, C. Rogers, 924 Williams, Debbie, 811 Williams, Rich, 782 Williamson, Ross S, 724 Willis, Katie, 44 Wilmarth, Phillip, 397, 829 Wilson, Angus, 241, 760 Wilson, Daryl, 748 Wilson, Elizabeth, 806 Wilson, Teresa, 397, 408, 409 Winkowski, Daniel, 715 Winn, Matthew, 750 Wise, Andrew, 637 Witsell, David, 242 Wojtczak, Magdalena, 185 Wolpert, Stephan, 656 Wong, Chelsea, 338 Wong, G. William, 245 Wong, Gerard, 550 Wong, Hiu-Tung, 14 Woo, Jeong-Im, 865 Wood, Scott, 503, 506, 997, 1004 Woodfield, Alexandra, 744 Woolley, Sarah M.N., 284 Wright, Beverly A., 711 Wright, Kevin, 32 Wright, Samantha, 681 Wu, Calvin, 453 Wu, Chen-Chi, 138, 239 Wu, Ching-Chih, 966 Wu, Doris, 1020 Wu, Guangying, 171, 299 Wu, Iwen, 936 Wu, Tao, 119 Wu, Xuewen, 621, 622, 625, 629

Wynne, Dwight, 671 Xia, Anping, 21, 35, 610, 615 Xiang, Yongqing, 996 Xie, Ruili, 684 Xiong, Hao, 641, 819 Xu, Jie, 150 Xu, Jinze, 145 Xu, Li, 498 Xu, Linjing, 673 Xue, Hui Zhong, 660 Xu-Friedman, Matthew, 690 Yakushin, Sergei B., 773, 996, 998, 999 Yamamoto, Norio, 387, 600, 639, 657, 844 Yamashita, Daisuke, 386, 650 Yamashita, Hiroshi, 223, 402, 651, 899, 903, 995 Yamashita, Tetsuji, 66 Yamasoba, Tatsuya, 649, 793, 837.867 Yamazaki, Muneharu, 860 Yamoah, Ebenezer, 129, 561, 599, 861 Yan, Denise, 327 Yan, Jun, 717 Yang, Aizhen, 428 Yang, Bin, 339, 340 Yang, Eunice, 984 Yang, Hsin-I, 501 Yang, Juanmei, 561 Yang, Shiguang, 257 Yang, Tian, 417 Yang, Won Sun, 230 Yang, Yue, 397 Yang, Yuqin, 118, 623, 628 Yang, Ziheng, 914 Yanjanin, Nicole, 217 Yantis, Steven, 800 Yao, Xiao-Fang, 240 Ye, Qiang, 638 Yee, Kathleen, 435 Yeo, Sang Won, 403 Yi, Jee Hyun, 135 Yin, Shankai, 399 Yin, Tom, 734, 739 Yorgason, Joshua, 787 Yoshida, Shuhei, 899 Yoshida, Syuhei, 402, 903 Yost, William A., 1029 Young, Bruce, 468 Young, Eric, 430 Yousaf, Rizwan, 815 Yu, Heping, 339, 340, 814 Yu, Wei, 145 Yu, Wei-Ming, 318, 530 Yu, Xun, 218 Yuan, Hui Jun, 327 Yuan, Tao, 610 Yuan, Yasheng, 845 Yusuf, Afiqah, 748 Zalewski, Chris, 217 Zallocchi, Marisa, 137, 1021

Zampini, Valeria, 563, 819, 825 Zeng, Chunhua, 914 Zeng, Fan-Gang, 501, 671 Zeng, Yaguang, 360 Zeng, Yi Arial, 21 Zens, Bettina, 692 Zettler, Cynthia, 492 Zha, Dingjun, 360, 362, 365 Zhang, Fawen, 177 Zhang, Huiming, 894 Zhang, Jian, 32 Zhang, Jinsheng, 155, 169, 214, 925 Zhang, Lei, 850 Zhang, Li, 171, 299 Zhang, Ming, 153 Zhang, Suchun, 598 Zhang, Xiangming, 55, 60 Zhang, Xuego, 214 Zhang, Xueguo, 214 Zhang, Xueguo, 155, 169, 925 Zhang, Yibo, 770 Zhang, Yingxin, 418 Zhang, Yupeng, 169 Zhao, Hong-Bo, 108, 110, 111, 131, 133, 240 Zhao, Min, 599 Zhao, Wei, 377 Zhao, Xiwu, 324 Zhao, Yanjun, 439 Zheng, Jing, 71 Zheng, Qing Yin, 339, 340, 814 Zheng, Yuxi, 814 Zhong, Sheng, 72 Zhou, Binfei, 109, 112 Zhou, Mu, 299 Zhou, Ning, 498 Zhou, Xue Jun, 327 Zhou, Yi, 730 Zhu, Juhong, 425 Zhu, Yan, 108, 110, 111, 131, 133 Zhuo, Xiu-Hui, 240 Zilany, Muhammad, 891 Zimmermann, Inge, 962 Zimmermann Ulrike 316 656 Zine, Azel, 591, 1009 Zion, Danielle, 476 Zirkle, Whitney, 486 Zobay, Oliver, 222 Zonderman, Alan, 140 Zong, Liang, 110, 111, 131, 133 Zorrilla de San Martin, Javier, 582 Zosuls, Aleks, 358 Zuccotti, Annalisa, 396 Zuckerman, Emily, 338 Zumer, Johanna, 159 Zumsteg, Terese, 448 Zuniga, M. Geraldine, 507, 512 Zuo, Jian, 16, 66, 306, 316, 357, 1019 Zwolan, Teresa, 213

Association for Research in Otolaryngology

Executive Offices 19 Mantua Road Mt. Royal, NJ 08061

Phone: (856) 423-0041

Fax: (856) 423-3420

E-mail: headquarters@aro.org

Website: www.aro.org